ÉCOLE POLYTECHNIQUE
FÉDÉRALE DE LAUSANNE

11

CISBAT

CLEANTECH FOR SUSTAINABLE BUILDINGS

From Nano to Urban Scale

PROCEEDINGS VOL. I


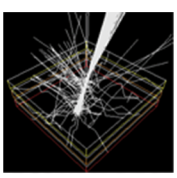

International Scientific Conference
Lausanne, 14-16 September 2011

LESO-PB
LABORATOIRE D'ENERGIE SOLAIRE
PHYSIQUE DU BÂTIMENT

Cambridge University
MIT
IBPSA - CH

LABORATOIRE D'ENERGIE SOLAIRE
PHYSIQUE DU BÂTIMENT

ÉCOLE POLYTECHNIQUE
FÉDÉRALE DE LAUSANNE

CISBAT 2011

PROCEEDINGS VOL. I

CLEANTECH FOR SUSTAINABLE BUILDINGS
From Nano to Urban Scale

14-16 September 2011
EPFL, Lausanne, Switzerland

cisbat

Schweizerische Eidgenossenschaft
Confédération suisse
Confederazione Svizzera
Confederaziun svizra

Swiss Federal Office of Energy SFOE

IBPSA-CH

Cambridge University

MIT

CISBAT 2011

International Conference
14-16 September 2011, EPFL, Lausanne, Switzerland

CLEANTECH FOR SUSTAINABLE BUILDINGS –
FROM NANO TO URBAN SCALE

ISBN Print-version: Vol.I: 978-2-8399-0907-5 Vol.II: 978-2-8399-0918-1
ISBN CD-ROM version: 978-2-8399-0906-8

Conference Host / Editor
Solar Energy and Building Physics Laboratory (LESO-PB)
Ecole Polytechnique Fédérale de Lausanne (EPFL)
Station 18, CH-1015 Lausanne / Switzerland
leso@epfl.ch
http://leso.epfl.ch
Conference Chair: Prof. J.-L. Scartezzini
Conference administration: Barbara Smith

Scientific partners:
Cambridge University, UK
Massachusetts Institute of Technology, USA
IBPSA-CH, Switzerland

Scientific committee:
Chairman:
Prof. J.-L. Scartezzini, EPFL, Switzerland
Members:
Prof. Derek Clements-Croome, Reading Univ., UK
Prof. Leon Glicksmann, MIT, USA
Prof. Anne Grete Hestnes, NTNU, Norway
Prof. Hansjürg Leibundgut, ETHZ, Switzerland
Prof. Hans Martin Henning, FhG-ISE, Germany
Dr Nicolas Morel, EPFL, Switzerland
Prof. Brian Norton, DIT, Ireland
Prof. Christoph Reinhart, Harvard University, USA
Dr Darren Robinson, EPFL, Switzerland
Christian Roecker, EPFL, Switzerland
Prof. Claude Roulet, EPFL, Switzerland
Dr Andreas Schueler, EPFL, Switzerland
Prof. Koen Steemers, Cambridge University, UK
Dr Jacques Teller, Univ. of Liège, Belgium

Members IBPSA Switzerland:
Prof. Gerhard Zweifel, HSLU, Lucerne
Prof. Thomas Afjei, FHNW, Muttenz
Prof. Stéphane Citherlet, HES-SO Yverdon
Dr Darren Robinson, EPFL, Lausanne

With the support of
Ecole Polytechnique Fédérale de Lausanne
Swiss Federal Office of Energy (SFOE)

Private sponsors:
Romande Energie
Julius Bär Swiss Private Banking group

PREFACE

The vocation of the CISBAT international conference cycle is to present new perspectives offered by renewable energies in the built environment as well as the latest results of research and development in sustainable building technology in a setting that encourages interdisciplinary dialogue and networking at the international level. The 2011 edition gathered on the EPFL campus the largest number of scientists, engineers and architects of its 20 year long history. Travelled from all over the World in an effort to promote clean technologies for sustainable buildings and cities, the participants presented 171 scientific papers during three intense days of conference.

Major international events, such as the “Deepwater Horizon” oil spill in the Gulf of Mexico and the Fukushima-Daiichi nuclear accident, which occurred in the last few years, certainly account for the growing interest of the scientific community - as well as the interest of stakeholders - for energy efficient technologies and decentralized energy systems in the built environment, such as promoted by the conference.

CISBAT was organized for the fourth consecutive time in scientific partnership with the Massachusetts Institute of Technology (MIT) and Cambridge University. Furthermore, the organizing committee is proud to have been supported again by a renowned international team of scientists in order to ensure the scientific quality and rigor expected from the conference. CISBAT 2011 also teamed up with the Swiss Chapter of the International Building Performance Simulation Association (IBPSA-CH) to strengthen the subject of “Building and Urban Simulation”, one of the conference's leading topics.

Thanks to the financial support of a growing number of institutional and private partners, such as the Swiss federal Office of Energy (SFOE), Bank Julius Bär and the public utility Romande Energie, the CISBAT international conference cycle has undoubtedly gained maturity and recognition on the international scene for its 20th Birthday Anniversary, and deserves a promising sunny future.

Prof. Dr Jean-Louis Scartezzini
Conference Chairman
Solar Energy and Building Physics Laboratory
Swiss Federal Institute of Technology Lausanne

CONTENTS VOL. I

Author index at the back.

Keynotes

Nanostructured Materials for Renewable Energies

Sustainable Building Envelopes

Solar Active and Passive Cooling

Daylighting and Electric Lighting

Indoor Environment Quality and Health

CONTENTS VOL. II

Advanced Building Control Systems

Urban Ecology and Metabolism

Integration of Renewables in the Built Environment

Building and Urban Simulation

Information Technologies and Software

KEYNOTES

THE IPCC SPECIAL REPORT ON RENEWABLES AND CLIMATE CHANGE

Summary of Keynote Lecture of Professor Dr Olav Hohmeyer

Zentrum für nachhaltige Energiesysteme, Universität Flensburg, Auf dem Campus , D-24937 Flensburg, Germany
Phone: ++49-461-805-2533
Mail: hohmeyer@uni-flensburg.de

SUMMARY

In May 2011 the plenary of the Intergovernmental Panel on Climate Change (IPCC) accepted the final version of the Special Report on Renewable Energy Sources and Climate Change Mitigation. This comprehensive report, which was written by more than one hundred experts from all parts of the world set out to highlight the possible contribution of the use of renewable energy sources to the mitigation of climate change.

In its Fourth Assessment Report the IPCC had come to the conclusion that a successful mitigation of climate change will require a global reduction of anthropogenic greenhouse gas (GHG) emissions by about 50% by the year 2050 to avoid the most drastic impacts of climate change (see: IPCC 2007, p. TS 39). As the CO_2 emissions from fossil fuel combustion for the supply of energy caused about 60% of the human induced GHG emissions world wide by 2004, with an ever growing share, the anthropogenic greenhouse effect can only be mitigated successfully, if these CO_2 emissions from our energy system are reduced drastically.

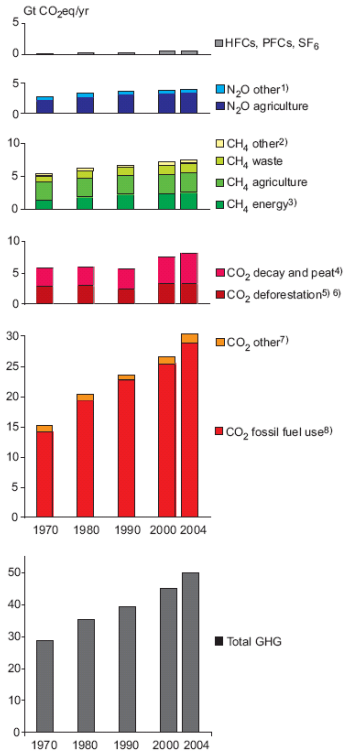

Figure 1: The development of global greenhouse gas emissions and the emissions of CO2 since 1970 in Gt of CO_{2eq}/a (source: IPCC 2007, p. TS 28)

For the necessary 'decarbonisation' of our energy supply four major options are available. These are the capture and underground storage of CO_2 from combustion processes, the increased use of nuclear energy, the more efficient conversion and use of energy and the use of renewable energy sources. As the accidents of Harrisburg, Chernobyl and Fukushima have shown nuclear energy has other massive problems, which disqualify it as a major future source of energy. The possible contribution of carbon dioxide capture and storage (CCS) to the reduction of CO_2 emissions have already been dealt with by the IPCC in its Special Report on Carbon Dioxide Capture and Storage, which was published in 2005 (IPCC 2005). The possible contribution will be limited by available save storage volumes as well as by public acceptance of such storage. While the possibilities for improved efficiency in the conversion and use of energy have been dealt with at length in the Contribution of Working Group III to the Fourth Assessment Report of the IPCC published in 2007 (IPCC 2007) the possible contribution of an increased use of renewable energy sources had not received an extensive treatment by the IPCC. Thus, the 192 member countries of the IPCC unanimously decided in April 2008 to order the preparation of a special report on the possible contribution of the increased use of renewable energy sources to the mitigation of climate change. At the same time the plenary decided on the structure of the report based on a comprehensive scoping document prepared by a group of more than one hundred international experts.

After about 400 scientists were nominated by the member countries of the IPCC about 120 lead authors from all parts of the world were selected to write the report. The writing process started in January 2009 and went through a five stage internal and external scientific and government review process of all written texts. After all comments from the scientific review and the government review were considered in the development of the final text the Summary for Policy Makers (SPM) of the Special Report was scrutinized in a one week line by line discussion and approval process by the IPCC plenary in Abu Dhabi in May 2011. On this basis first the SPM and thereafter the full report was accepted unanimously by all member states of the IPCC. Thus, it can be claimed that the Special Report on Renewable Energy Sources and Climate Change Mitigation (SRREN in the following) is one of the most widely accepted documents on the possible future role of renewable energy sources for the mitigation of climate change.

As Figure 2 shows, the Special Report covers the six major renewable energy sources, puts the use of renewables into the context of climate change and deals with issues of integration into the energy system, the overall mitigation potentials and costs as well as with questions pertaining to sustainable development, policies, financing and implementation.

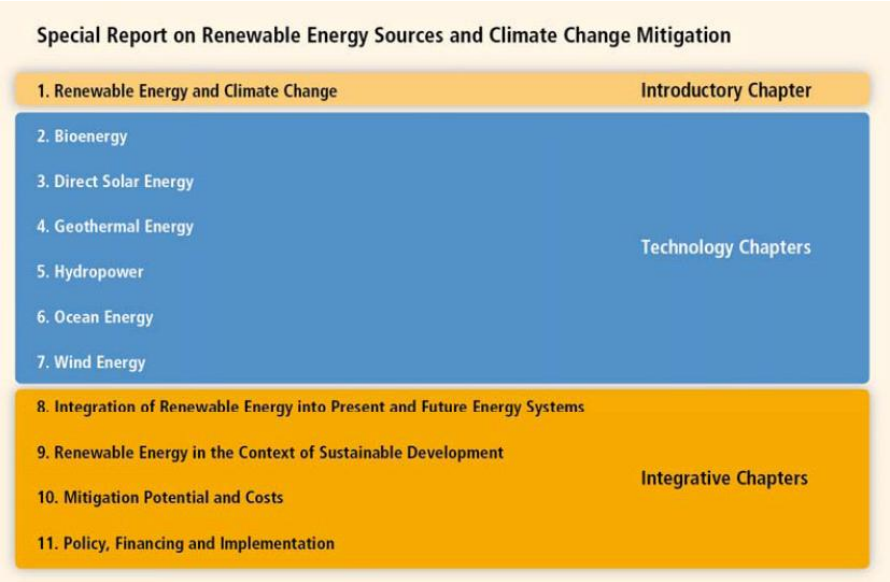

Figure 2: Structure of the IPCC Special Report (source: IPCC 2011, p.2)

Based on the available scientific assessment literature the IPCC concludes that the global technical potential of renewable energy sources is many times larger than the present global primary energy supply (492 EJ/a in 2008) and the present global electricity demand of 61 EJ (2008). With 85 EJ/a even the lowest estimate of the global wind energy potential alone is higher than the total global electricity demand, while the technical potential of solar energy is 3 to 100 times as large as the global primary energy supply of 2008 (see IPCC 2011, p. 8). Figure 3 summarizes the findings of the IPCC on the ranges of technical potentials of the different renewable energy sources.

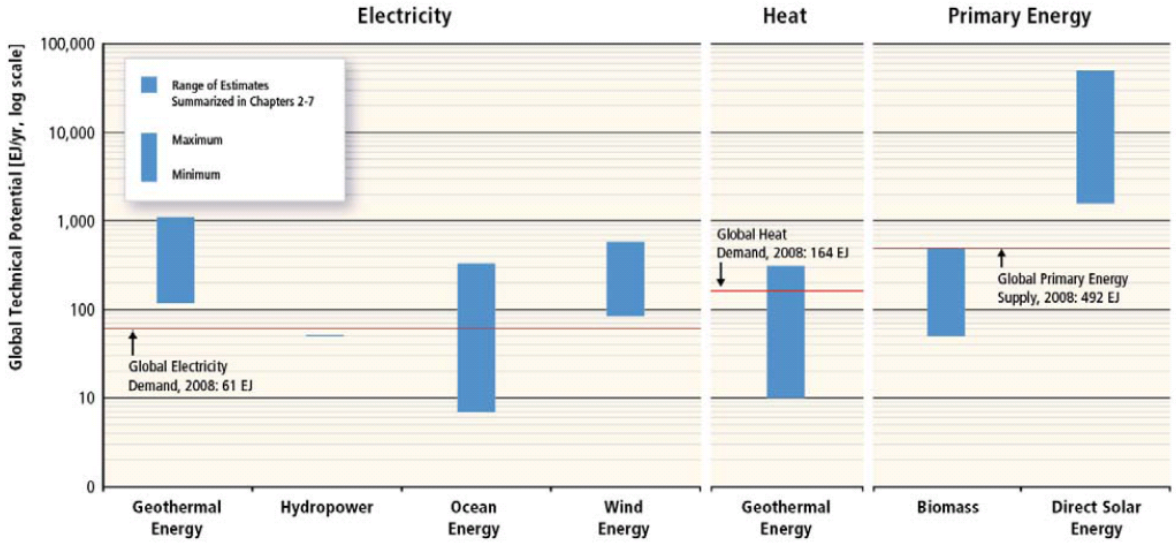

Range of Estimates of Global Technical Potentials

Max (in EJ/yr)	1109	52	331	580	312	500	49837
Min (in EJ/yr)	118	50	7	85	10	50	1575

Figure 3: Ranges of global technical potentials of renewable energy sources given in the IPCC SRREN (source: IPCC 2011, p. 8)

At the same time the IPCC points out that the energy costs of renewable energy sources vary widely. While in some cases some renewable energy sources may be competitive to non-renewable energy sources in most cases the electricity, heat or fuels generated or produced from renewable energy sources are more expensive than their non-renewable competitors, as Figure 4 shows. Nevertheless, the cost of energy based on renewable energy sources has decreased quite substantially over the last decade as the cumulated global capacity has increased. This is shown in the form of logarithmic experience curves for the price of silicon photovoltaic modules and for onshore wind power plants in Figure 5.

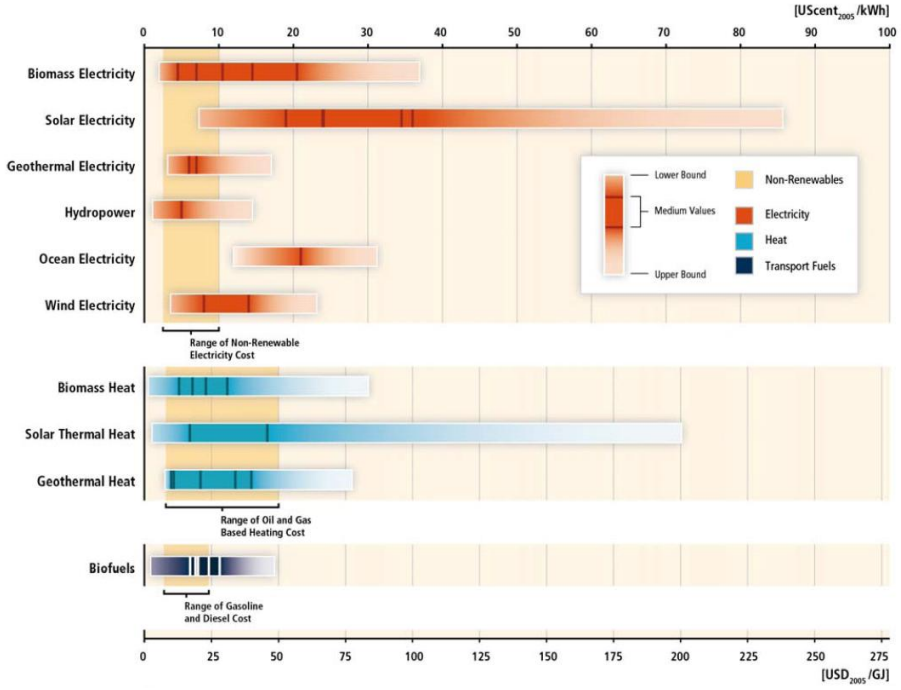

Figure 4: *Range of levelized cost of energy for selected commercially available renewable energy technologies in comparison to recent non-renewable energy costs (source: IPCC 2011, p. 10)*

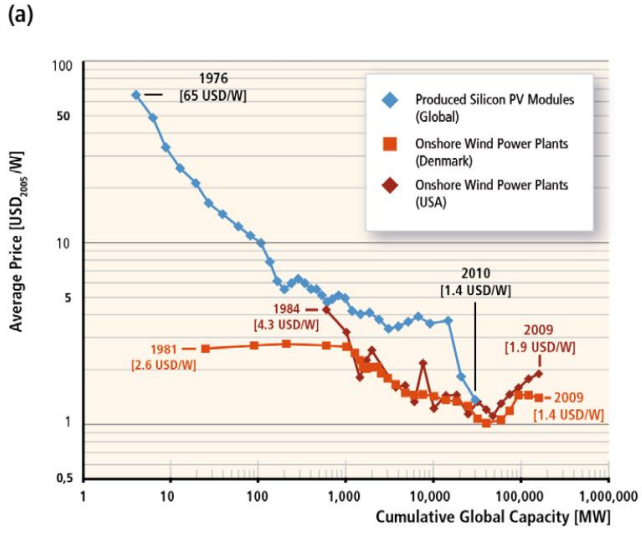

Figure 5: *Selected experience curves in logarithmic scale for the price of silicon PV modules and onshore wind power plants per unit of capacity (source: IPCC 2011, p. 12)*

Besides their almost unlimited availability over time the major advantage of renewable energy sources are their comparatively low direct and indirect greenhouse gas emissions. Although biomass may have comparatively high net CO_2 emissions as compared to wind or solar energy, it offers the unique advantage to combine it with CCS technologies to create substantial negative CO_2 emissions. While fossil fuels still have substantial CO_2 emissions, even if they are combined with CCS, biomass can have negative CO_2 emissions reducing the atmospheric CO_2 balance by up to 1.4 kg CO_2/kWh of electricity produced from biomass, as Figure 6 shows.

Figure 6: Estimates of lifecycle GHG emissions (g CO_{2eq}/kWh) for broad categories of electricity generation technologies, plus some technologies integrated with CCS (source: IPCC 2011, p. 17)

The IPCC comes to the conclusion that ambitious greenhouse gas stabilization targets in the range of 400 ppm CO_{2eq} can not be attained without a substantial use or renewable energy sources (see IPCC 2011a, p. 147). The IPCC SRREN shows that the lower the targeted GHG stabilization level, the larger will be necessary contributions of renewable energy sources. This is shown in Figure 7, which gives the renewable primary energy supply in EJ/yr depending on the allowed CO_2 emissions from fossil fuels in different scenarios. Especially for the longer range scenarios until 2050 there is a clear correlation between the contribution of renewable energy sources and the targeted GHG stabilization level. In the highest scenarios the global share of energy from renewable sources reaches 43% in 2030 and 77% of the global energy supply in 2050 (IPCC 2011, p. 19).

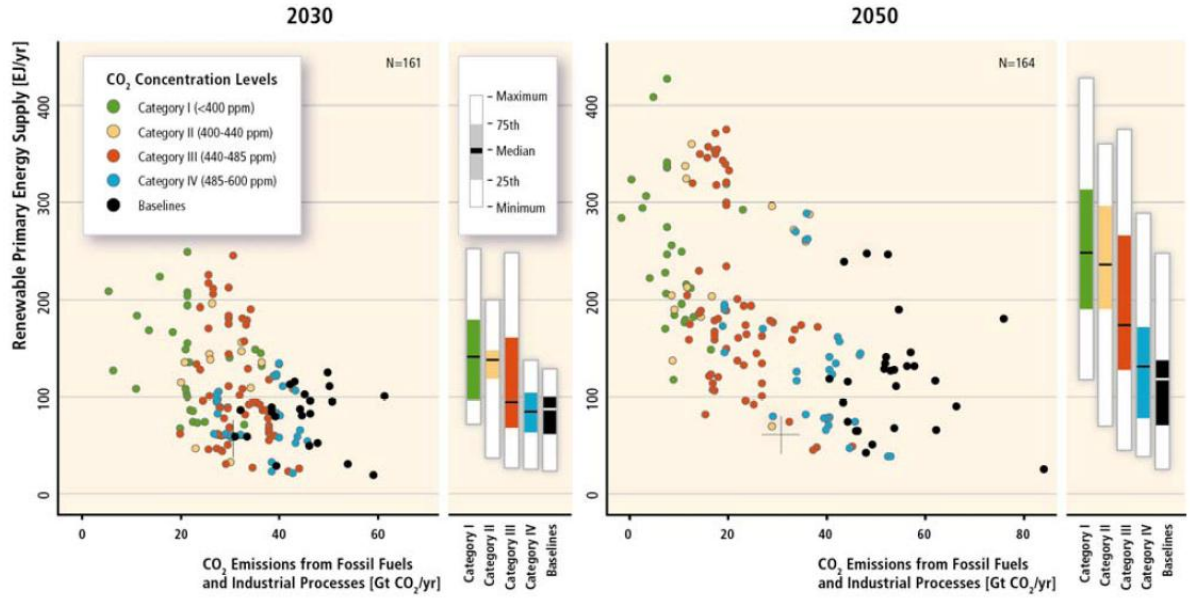

Figure 7: Global primary energy supply from renewable energy sources from 164 long-term scenarios versus fossil and industrial CO2 emissions in 2030 and 2050. (source: IPCC 2011, p. 19)

The IPCC Special Report shows that renewable energy sources can and most likely will play a central role for the mitigation of climate change. Their massively increased use can supply a major share of the global energy demand in all different sectors and uses. Nevertheless, this will require enabling policy support to further reduce costs and to help overcome various barriers (see IPCC 2011, p. 23).

In the most advanced countries renewable energy sources may supply 100% of the national electricity demand by 2050, if the necessary grid infrastructure and storage capacities are build on time, as a report by the German Council of Environmental Advisors shows (Sachverständigenrat für Umweltfragen 2011).

REFERENCES

Intergovernmental Panel on Climate Change (IPCC) (2005):
Carbon Dioxide Capture and Storage. Bert Metz, Ogunlade Davidson, Leo Meyer (Eds.). Cambridge, United Kingdom

Intergovernmental Panel on Climate Change (IPCC) (2007):
Contribution of Working Group III to the Fourth Assessment Report of the Intergovernmental Panel on Climate Change, 2007. B. Metz, O.R. Davidson, P.R. Bosch, R. Dave, L.A. Meyer (eds). Cambridge, United Kingdom

Intergovernmental Panel on Climate Change (IPCC) (2011):
Special Report on Renewable Energy Sources and Climate Change Mitigation. Summary for Policy Makers. Final release as approved at the 11th Session of the Working Group III of the IPCC, Abu Dhabi, United Arab Emirates. 5-8 Mai 2011

Intergovernmental Panel on Climate Change (IPCC) (2011b):
Special Report on Renewable Energy Sources and Climate Change Mitigation. Technical Summary. Final release as approved at the 11th Session of the Working Group III of the IPCC, Abu Dhabi, United Arab Emirates. 5-8 Mai 2011

Sachverständigenrat für Umweltfragen (SRU) (2011):
Wege zur 100% erneuerbaren Stromversorgung. Sondergutachten. Berlin

FIVE EASY PIECES – TOWARDS ZERO EMISSIONS ARCHITECTURE

Summary of Keynote Presentation by Professor Dr arch. Marc Angélil

Dean, Department of Architecture of the Swiss Federal Institute of Technology Zurich (ETHZ), Partner of agps architecture, Zurich

ETH Hönggerberg, Wolfgang-Pauli-Str. 15, 8093 Zurich, Switzerland

With the title quoting from the alternative 1970's Hollywood movie starring Jack Nicholson, a series of five projects will demonstrate the development of alternative energy concepts in the work of *agps architecture*.

Our first design project involving sustainability was the Esslingen Town Center project in the early 1990's. At the time, the term was sufficiently new that research was conducted as to what it meant. Our definition of sustainable design became efficiency in land use, materials use, and energy use – which has held up over time, involving a series of research investigations in building construction.

1) Almost ten years later, the competition brief for the Midfield Terminal at the Zurich International Airport asked for the most progressive environmentally designed airport terminal in Europe. Our proposal, in collaboration with Martin Spühler and Amstein + Walthert Engineers, incorporated geothermal heating and cooling with imbedded tubes in the 250 structural foundation piles. Tempered air is distributed vertically, not requiring horizontal ducts in the 500 meter long building. The long north and south walls are thermally protected by glazed buffer zones, providing maximum day lighting and views out to the airfield and landscape beyond. Photovoltaic panels are incorporated into glazed louver shade screens on the accessible rooftop, which with a planted landscape and wood deck becomes the fifth facade for the building.

2) The Zürich International School was configured as a dense bar, demonstrating efficiency in land use to the extent that space on the site could be given back to the community as a public park. The building itself is a campus, a dense block with flexible spaces that can be reconfigured over time. In terms of energy, heat pumps are fed by 30 borehole heat exchangers 150 meters deep. In ZIS, the air-box was developed, a decentralized system of fresh air supply tempered by the heat pump system. Ceiling panels provide additional thermal and acoustic control with integrated lighting and sprinklers. Structural concrete is exposed, industrial materials are used as cladding, and additional layers are minimized. This allowed the school's construction costs to be significantly lower than standard while the flexibility for future needs is far greater.

3) IUCN, or the International Union for Conservation of Nature, in Gland near Geneva, is the largest and oldest conservation network in the world. Philosophically, their new headquarters addition needed to be sustainably progressive, while their funds were limited. The design concept expanded upon the previous buildings' approach of reducing to the max in order to afford new systems. The 14 geothermal boreholes for IUCN are 250 meters deep, being fewer but deeper than before; air-boxes have been relocated to the floor to reduce conflicts with various trades during construction, and the ceiling panels are thermo-active acoustic with integrated lighting, sprinklers, CO2 sensors, and air returns: all a further level of development. Exposed concrete, including insulated concrete, and anhydrite floors – usually used as a leveling compound – generate the

language of minimal construction. Whatever could be avoided was cut but flexibility is inherent with non-structural interior walls and open plan spaces.

4) The housing project B35 continues the exploration of geothermal to a new level. Only two boreholes have been dug to 380 meters in depth. The boreholes are insulated to 150 meters, and uninsulated below. Heat from rooftop hybrid solar/water collectors will gather the heat from the summer sun and store it below ground for use throughout the year, with the deeper depth yielding hotter temperatures for winter use. With this project, it became clear that energy from the sun and the earth are abundant and free, and therefore it can be wasted – with the result that building envelopes can be lighter and consume fewer materials. This also means that all current energy codes are out of date, in an evolving process of research and development.

5) The Esslingen Town Center, the first project referred to at the beginning of this talk, has continued in its development for over 20 years. The most recent component, now in design, is housing with 40 apartments. Here we are taking the concepts of B35 even further with geothermal storage of heat using a swarm of earth piles. This allows for significant material savings due to less insulation - reducing "grey energy".

These “5 Easy Projects” together make up a series of explorations involving heating and cooling buildings from the sun and the earth. Except that they are not always so easy. This brings me to another figure, this time in physics: Richard Feynman. I want to conclude with a final project inspired by his book *6 Not So Easy Pieces*.

As sustainability includes social and financial as well as environmental sustainability, our “From the Ground Up” project addresses the synthesis of the three. Located in upstate New York, which has been hit hard by the recent economic downturn, the project proposes revitalized urbanism by recycling abandoned buildings. The generic housing stock is wood framed houses that can be relocated, re-wrapped, re-powered, and re-stored based on community needs and empowered stakeholders. This project was developed with the logic of “Why not?” which is how we are approaching our continuing work toward zero emissions architecture.

SUSTAINABLE LIGHTING: LET'S TALK ABOUT VALUE

Keynote Presentation of Professor Mark S. Rea, Ph.D

Director, Lighting Research Center, Rensselaer Polytechnic Institute, Troy, NY

INTRODUCTION

Sustainability has various meanings, but often the word is associated with reducing negative impacts on the Earth, either through limiting energy use, limiting entry of waste products or hazardous materials into the environment, or limiting negative health or economic impacts on other humans or on other species [1]. These are important and laudable goals; indeed, they are essential objectives for achieving a sustainable planet. But if these were the only objectives for sustainability, we would simply close our factories, shops, schools, and offices. By closing them, we would no longer need electric energy and we would no longer produce or consume manufactured products, thereby reducing the emission of mercury and acid rain into our water and air. This approach would be an unacceptable and, indeed, an unsustainable strategy. In that light, sustainability must not simply be about the elimination or reduction of the negative impacts, or *costs*, but sustainability must also be about the creation or improvement of the positive impacts, or *benefits*. Thus, sustainability should be considered a *value* proposition, whereby both the costs to the environment and society are reduced and the benefits to the environment and society are increased.

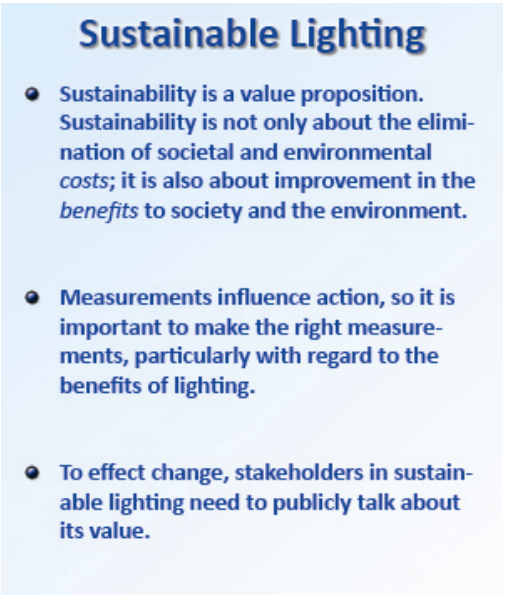

This is a logical conclusion to which most people would agree, even though the *value* of sustainability has been much more closely associated with reducing the costs than with increasing the benefits. This focus on the denominator of the value ratio for sustainability is a result, at least in part, of the fact that it is often easier to measure costs than it is to measure benefits. We can measure energy consumption of a building, a cost, but it is much more difficult to measure worker productivity in that building, a benefit. To be fair, regulators interested in sustainability do try to use measurable surrogates for the benefits of energy use, but these measures are often poor or incomplete characterizations of expected benefits. For example, illuminance level is used almost exclusively in building standards as a surrogate for the benefits of lighting [2-4], even though many studies have shown that illuminance level can be a poor predictor of visibility, preference, and comfort [5,6]. Because illuminance level is such a poor predictor of the benefits of lighting, we waste electric energy, put more toxins into the environment, and compromise health and productivity. Therefore, we formally institutionalize unsustainable lighting systems day after day.

The present paper is based upon a simple, three-part logical framework for sustainable lighting. First, we do what gets measured; second, we need new measures for the benefits of lighting; and third, we need to create a stakeholder-wide, public discussion about the value of lighting.

WE DO WHAT GETS MEASURED

Constructs like security, safety, and health are often reduced to surrogate metrics.

- We do not directly measure national economic security; we measure trade balance ($). Many believe that for a country to be successful, a positive trade balance is essential.
- We do not directly measure roadway safety; we measure and enforce driving speeds (km/h). It is generally believed that enforcing speed limits has led to lower traffic fatalities.
- We do not directly measure personal health; we measure blood pressure (mmHg) and cholesterol (mg/dL) levels. Many believe that the drugs commonly prescribed by physicians to reduce blood pressure and cholesterol levels will extend life expectancy.

These example measures ($, km/h, mmHg, and mg/dL) of important constructs (economic security, roadway safety, and personal health) have a very large impact on our political and personal actions because we believe these measures gauge our quality of life and our lifespan. But do they?

Figure 1: Trade balance is often thought to be a measure of economic security.

National competitiveness in the world economy has been used by politicians and economists alike as a measure of prosperity and social well-being. Although we often measure trade balance, it is largely unrelated to social well-being. Mexico, for example, ran a very large trade surplus in the 1980s, but the standard of living for its citizens was not better than it was in the 1990s when it ran a very large trade deficit [7]. Labor prices are often blamed for uncompetitive trade balance, but Sweden, Germany, and Switzerland have very high labor rates while still enjoying a high standard of living [8]. The reason that trade balance has little to do with social well-being appears to be a result of the fact that most products produced by a country are consumed within that country. In the United States, for example, 90% of its production goes to the United States. Productivity (price of the output produced divided by cost of labor or capital input [8,9]) appears to be more aligned with national prosperity [7,9], and is largely determined by domestic policies, not whether there is a positive or negative trade balance. If people within a country produce value-added products, that is, they are productive, they tend to prosper. Trade balance is largely the wrong measure of economic security of nations.

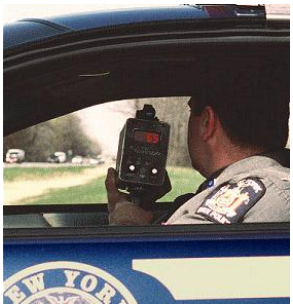

Figure 2: Many believe that enforcing lower speed limits can save lives.

Many believe that lower speed limits save lives. Indeed, after speed limits on interstate highways were increased from 55 mph to 65 mph in 24 of the United States in 1987, there was an increase in fatalities on interstate highways of approximately 15% [10]. This would seem to indicate that measuring and enforcing lower speed limits saves lives and therefore is good social policy. A study by Lave and Elias, however, argued that this view on the social good derived from lower speed limits was much too narrow [11]. They showed that in those states where speed limits had increased, there was actually a 3 to 5% reduction in statewide fatalities of all kinds, arguing that this was the result of shifting police resources from enforcing speed limits to other safety activities, such as truck safety inspections or drunk driving checkpoints. Furthermore, they argued that with an increase in speed limit, traffic on a road will increase as well, naturally leading to an increase in the number of fatalities. Lave and Elias suggested that the rate of fatalities, or fatalities per vehicle mile traveled, is a more appropriate measure, which can account for the change in traffic patterns and can more appropriately compare

fatalities before and after the change. Measuring and enforcing speed limits can improve roadway safety, but the study by Lave and Elias demonstrates that reliance on one measure may mislead and misinform social policy.

Figure 3: Blood pressure is considered to be a reliable measure of health.

Many of us are on blood pressure and cholesterol medicine with the implicit belief that our life span will be extended. In fact, lower cholesterol is associated with reduced mortality, but apparently primarily in those under 50 years of age [12]. The impact of lower cholesterol decreases with age, and, interestingly enough, high cholesterol is associated with longevity over 85 years of age [13]. Among the general population, the interaction between cholesterol levels and type of illness is critical to understanding the health impact of cholesterol medicine. There was an improvement from cholesterol reduction in longevity for those diagnosed with heart disease but there was actually an inverse relationship between cholesterol-reducing medicine and longevity in those with illnesses unrelated to heart disease [14]. With regard to blood pressure, a different picture emerges. The evidence supports the conclusion that antihypertensive drugs provide a clear benefit for reducing stroke and major coronary events for those diagnosed with those diseases, thereby increasing longevity [15-17]. So, making the appropriate measurements for a given application can make a real difference.

Figure 4: The benefits of lighting are currently measured in terms of illuminance levels on work surfaces.

In terms of lighting, we primarily measure and regulate illuminance (lm/m^2) and luminous efficacy (lm/W). Indeed, these measures drive our lighting designs. As a result of societal emphasis on sustainability, illuminance levels have been reduced [18] and light sources have been made more efficacious [19]. Less efficacious light sources, such as incandescent lamps, are even being banned [20-23]. These measures are commonly believed to improve sustainability. But do they?

WE NEED NEW MEASURES FOR THE BENEFITS OF LIGHTING

Illuminance and luminous efficacy are both based upon the photopic luminous efficiency function institutionalized in 1924 by the International Lighting Commission (Commission Internationale de l'Éclairage, CIE). The photopic luminous efficiency function (Figure 5) weights the spectral irradiance distribution of any light sources to characterize the "visual" effect of the light. As visual science has progressed, however, the photopic luminous efficiency function is now known to be based upon only two of the three cone types in the retina [24], so it is inherently incapable of capturing the effectiveness of different light sources for many applications. Importantly, $V\{\lambda\}$ *does* adequately represent the effect of light on the speed and accuracy of reading achromatic tasks (e.g., newspaper print), but it does not characterize the perceived brightness of an indoor or outdoor space, the sense of discomfort glare from windows and headlights, the ability to discriminate between subtle hues, or the effectiveness of light for regulating our biological rhythms. It is remarkable then that illuminance level is the *sole* lighting application criterion for many national standards when it has such narrow relevance to the luminous environment.

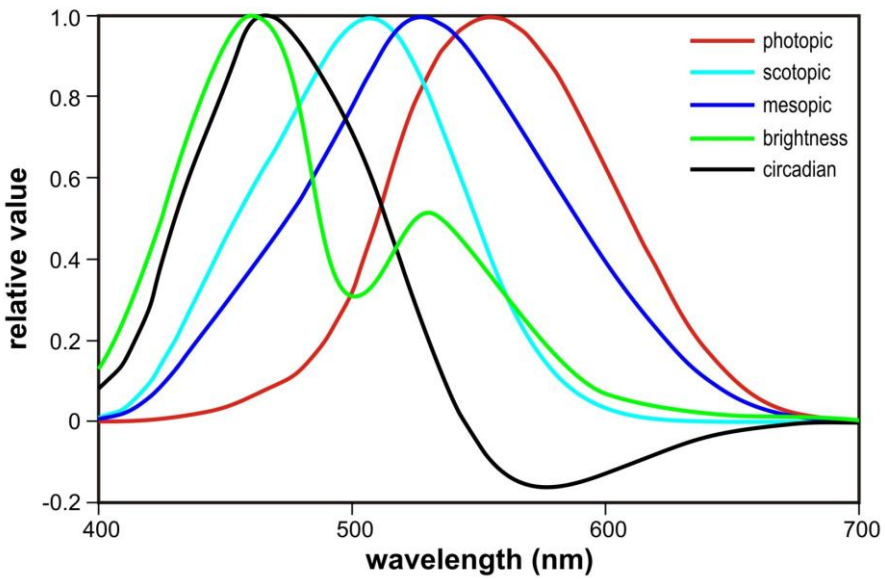

Figure 5: A wide variety of spectral weighting functions could be used to measure the benefits of lighting; see text for explanations of each function. Presently we rely almost solely on one function, the photopic luminous efficiency function. Doing so compromises sustainable lighting.

What is needed for sustainable buildings are new and better metrics for the benefits, and therefore the value, of lighting. As with illuminance and luminous efficacy, these new metrics must be quantifiable and easily measured. Without convenient and consistent measurement technologies and techniques, any new metric will have very limited effect on building practice and therefore building sustainability - again, we do what we measure, but we should be measuring the right things.

The metrics discussed briefly below reflect the fact that the visual system is not a monolithic, single-dimension system, as implied with our focus on illuminance level and luminous efficacy. Rather, we use multiple, parallel channels to process different kinds of visual information important for performance, comfort, and aesthetics. Among the many pathways in the visual system, we have different neural channels to compute color, detect movement, discriminate fine detail, and make an overall assessment of how much light is present in the environment. Each of these channels weights the electromagnetic spectrum differently because different combinations of photoreceptors provide input to these channels. Defining "good" lighting in terms of illuminance levels or luminous efficacy diminishes, and even compromises, the benefits that lighting can produce. Discussed below are some practical metrics researched in our laboratory that better characterize the response characteristics of these visual channels.

Color rendering

After illuminance, color rendering index (CRI) is the most commonly used criterion for characterizing the benefits of lighting, although it is not regulated. In simple terms, CRI reflects how different the color rendering properties of a light source are from the reference light sources, natural daylight or incandescent light. The higher the CRI value, the closer the lamp is to revealing colors as they would appear under a reference light source (Figure 6).

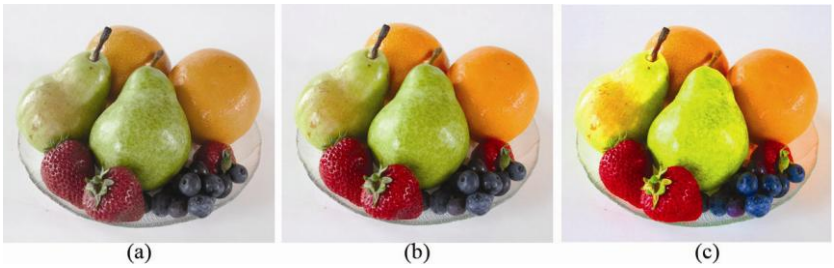

Figure 6: Good color rendering by a light source depends upon providing an optimum amount of color saturation. Panel (a) renders the fruit pale and desaturated, while panel (c) makes the fruit appear unnaturally vivid. By using both color rendering index (CRI) and gamut area index (GAI) to measure the color rendering properties of a light source, a color balance can be achieved, making natural objects like fruit appear appealing, as shown in panel (b).

CRI, developed in the early 1960s [25,26], has been particularly important as a metric in retail applications, such as groceries and cosmetic stores, where colors are important for sales. It is considered to be the most commonly used criterion for color rendering, and is recognized internationally [27]. A number of recent studies have shown, however, that CRI is not a completely satisfactory measure of people's perception of the color rendering properties of a light source. Indeed, some studies have shown that CRI is *negatively* correlated with color preference [28] and the perceived "naturalness" of fruits and vegetables [29]. These results suggest that electric energy (and money) may be wasted on light sources that are intended to provide good color rendering, but in fact do not. Thus, CRI alone is an unsatisfactory metric for accurately characterizing the color benefits of lighting under some conditions.

A new adjunct metric, Gamut Area Index (GAI), was recently developed to address these documented limitations to CRI. In simple terms, GAI is a measure of the vividness of colors provided by a light source. GAI is very easy to determine because it relies on the very same measurement methods employed in the CRI calculation, but the GAI calculation utilizes the data in a slightly different way. Research has shown that when used together, light sources associated with high CRI *and* optimal GAI (high, but not too high) provide colors that look more natural and are generally more acceptable in a retail application [30,31]. Interestingly, reliance on a single metric, either CRI or GAI alone, leads to less acceptable color rendering. Importantly, many commercially available light sources provide suitable values of both CRI and GAI, and these sources are not more expensive, in terms of both initial and operating (energy and maintenance) costs.

Mesopic Vision

The human visual system is often referred to as having a duplex retina because it contains two different classes of photoreceptors, rods for night-time vision and cones for day-time vision. Photometry is the internationally accepted system for the measurement of light, and two spectral response functions, the scotopic (night-time) and photopic (day-time) luminous efficiency functions, are formally recognized by the CIE (Figure 5) [32,33]. The scotopic function is intended to be applied when rod-only vision is considered and the photopic function is to be applied when cone-only vision is of relevance. No photometric system has been formally adopted for roadway lighting recommendations, under mesopic (i.e., "middle") conditions when *both* rods and cones are operating, as is the case for most outdoor lighting applications [34]. In practice, the photopic luminous efficiency function underlies *all* formal electric lighting recommendations, including mesopic conditions.

Figure 7: Most night-time outdoor lighting provides illumination in the mesopic region where both rods and cones provide visual information.

A reliance only on the photopic luminous efficiency function for outdoor applications can be a problem for maximizing visibility as well as for minimizing electric energy use from a light source. Since the spectral weighting function, $V(\lambda)$, does not match the spectral sensitivity of the visual system under mesopic conditions, both visibility and energy efficiency are compromised. The rods are sensitive to shorter wavelengths than is measured by the photopic luminous efficiency function, so outdoor light sources that emit energy at shorter wavelengths will stimulate the visual system more under mesopic conditions than is being measured by a light meter that has been calibrated in terms of the photopic luminous efficiency function. In other words, two light sources at the same measured (photopic) light level will be differentially effective for visibility under outdoor lighting if they differ in terms of their short-wavelength emission spectra.

A unified system photometry was developed [35,36] to bridge the CIE scotopic and photopic luminous efficiency functions throughout the mesopic region of visual response, where both rods and cones are functioning. One of the many mesopic luminous efficiency functions is shown in Figure 5. The foundation of this unified system is based upon studies of the speed of visual processing [34]. This is generally considered a suitable response criterion for roadway applications because the speed of visual processing should be related to driving safety; the faster one can see a hazard, the faster one can make an appropriate response. Since outdoor lighting applications are commonly in the mesopic region, the application of a unified system of photometry should help ensure that the visual benefits (and presumably safety) of the light source are maximized while the electric energy needed to operate the lamp is minimized [37]. A version of the unified system of photometry has recently been adopted by the CIE [38] and is being considered by some countries as a basis for prescribing roadway lighting.

Apparent Brightness

The apparent brightness of a visual scene changes with light level; as the light level increases from scotopic, through mesopic, to photopic conditions, the world looks increasingly brighter. The unified system of photometry tracks the spectral sensitivity of the speed of visual processing, but research shows that combinations of the scotopic and photopic luminous efficiency functions in the unified system of photometry do not track the change in apparent brightness. Physiologically, a different combination of visual channels is used to assess apparent brightness than is used to react quickly to a hazard. In particular, the short-wavelength S-cone mechanisms that contribute to color are also very important to perceptions of brightness [39], even though this mechanism does not contribute significantly to the speed of visual processing. Consequently, brightness cannot be measured appropriately with illuminance level, even if based upon a unified system of photometry. Also, recent data suggest that the contribution from the S-cone mechanisms to brightness differentially increases with light level [37]. At low, mesopic levels the S-cone mechanisms play a minor role in brightness perception, but at higher, photopic levels this system begins to dominate. A brightness response function at high levels is shown in Figure 5. At office lighting levels (300-1000 lx) a room illuminated with “cool lamps” (e.g., 6500 K) that look bluish white will appear brighter than a room illuminated with “warm lamps” (e.g., 2800 K) at the same measured illuminance level (lm/m^2). Lighting standards based upon providing equal apparent brightness rather than equal illuminance on the work plane could provide significant energy savings.

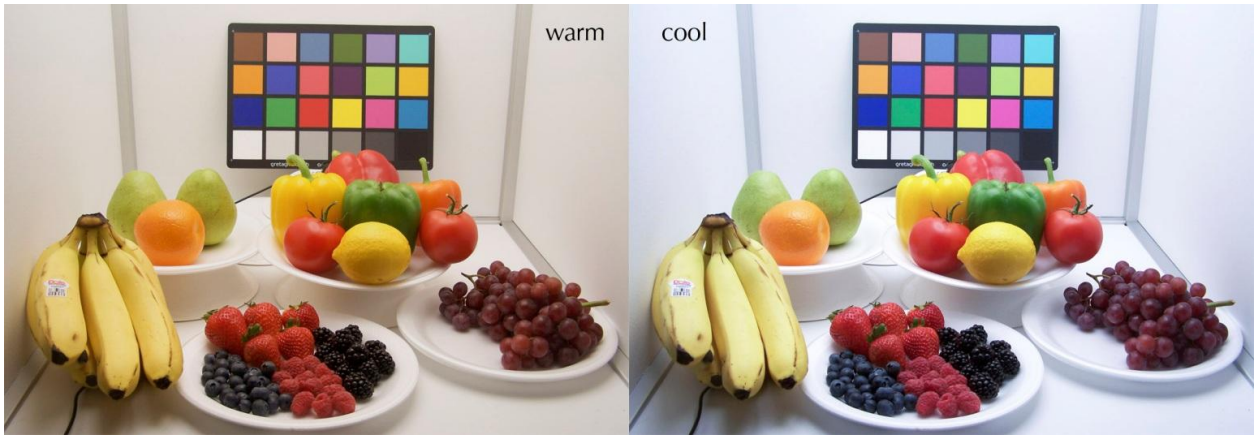

Figure 8: Two boxes illuminated to the same photopic light level. The box on the right illuminated with a blue-white "cool" light source (6500 K) appears brighter than the box on the left illuminated with a yellow-white "warm" light source (2800 K).

Circadian Light

In effect, the retina is a triplex retina, not a duplex retina, because it contains rods, cones, and a non-visual photoreceptor system that regulates the timing of our biological rhythms. An intrinsically photosensitive retinal ganglion cell (ipRGC) was recently discovered [40], which plays the central role in converting light into neural signals to the superchiasmaitic nuclei (SCN) in the brain, which contain our master circadian (circa one day) clock. This clock orchestrates control over almost every aspect of our physiology, including production of hormones such as melatonin and cortisol, glucose metabolism, body temperature, blood pressure, sleep, and cognitive functions such as learning and memory consolidation [41].

Figure 9: The circadian system is effectively a "blue sky detector," with peak sensitivities at short wavelengths.

Like the visual channels, this neural channel formed in the retina has a unique spectral response. The human circadian system exhibits a non-linear characteristic known as "subadditivity," illustrated by the positive and negative regions of the spectral response function in Figure 5. In effect it is a "blue sky detector" with a peak sensitivity at short-wavelengths. Interestingly, it is essentially blind to long-wavelength light to which our visual system is quite sensitive [43]. This non-visual, but light-sensitive, system is responsive to the oscillations in the natural, 24-hour light-dark cycle. Disruption of this daily cycle, as with shift work or rapid trans-longitudinal travel, may result in a wide variety of maladies from sleep disturbances to diabetes to cancer [44]. Modern architecture has created deep-core buildings with electric lights that can shield us from the bright daytime and extend night into day, both of which provide the potential to disrupt the regular 24-hour pattern of light and dark needed to maintain circadian timing and, consequently, good health.

Would adopting these additional lighting metrics make any real difference? For outdoor lighting where a unified luminance, rather than photopic illuminance on the roadway, is the design criterion, switching from the mainstay lighting system of high-pressure sodium (HPS) to, for example, white light-emitting diodes (LEDs), the energy savings can be as much as 40% [45]. In principle too, the safety benefits of the outdoor lighting system can be increased while energy use can be held constant [46,47]. In either case the value ratio, and therefore sustainability, of the outdoor lighting system has been increased by using a new and better metric to design outdoor lighting.

For indoor lighting, apparent brightness of the visual environment is often more important than photopic illuminance on the workplane [48]. Where apparent brightness is the design criterion, energy savings of 20% to 30% can be readily achieved with existing technologies. Similarly, where color rendering is important, existing technologies can be used to achieve high CRI and optimal GAI. This change will have little or no impact on energy use, but would improve the benefits, and therefore the value, of the lighting system. By joining the new apparent brightness and color rendering criteria into standards, the sustainability of the lighting system will be increased because both the cost denominator has decreased and the benefit numerator has increased in the value ratio.

To promote the regulation of biological rhythms in buildings, daytime lighting energy use might increase by 20% because circadian light levels are probably too low in existing buildings that have used workplane illuminance as the sole design criterion. Lighting controls become critical in this value proposition because high circadian light levels are not needed all day long. Rather, it seems that high circadian light levels are primarily effective for regulating biological rhythms in the early morning, and high light levels have little or no effect on the circadian system in the afternoon. It is beyond the scope of this paper to discuss lighting control strategies for buildings operated at night or over the full 24-hours with multiple shifts, but such strategies based upon the evolving science of circadian rhythms are beginning to be discussed more widely among application engineers [49].

WE NEED TO DISCUSS THE MEASURABLE BENEFITS, AND THEREFORE THE VALUE, OF LIGHTING

Unfortunately, logical, evidence-based arguments do not necessarily persuade. We have already seen that commonly held beliefs about trade balance, speed limits, and cholesterol levels are not necessarily valid. Yet, many of us believe they are. J. Edward Russo and Paul Schoemaker make a very strong argument that we believe what we hear, and the more we hear it, the more we believe it, *whether or not what we hear is true* [50]. They compared peoples' beliefs about health risks with what was published in newspapers about health risks. What they found was that peoples' beliefs were not based upon the facts, but rather, on the frequency of newspaper reports devoted to a topic. For example, stomach cancer is a greater killer than all motor vehicle accidents combined, but stomach cancer is not covered by the newspapers, while motor vehicle accidents are (Table 1). Consequently the majority of us believe that more people die from motor vehicle accidents than from stomach cancer. The Lighting Research Center (LRC) performed a similar study comparing the amount of press coverage devoted to different outdoor light sources with what was actually specified, and found a nearly perfect correlation between what was talked about in the trade press and what got applied in practice, despite clear evidence that, objectively, the least specified technology was superior to all others based on existing lighting design criteria [51].

Cause of Death	People's Choice in Each Pair	Annual U.S. Total (in 1,000s)	[Typical] Newspaper Reports Per Year
Stomach Cancer	14%	95	1
Motor Vehicle Accidents	86%	46	137
Emphysema	45%	22	1
Homicide	55%	19	264
Tuberculosis	23%	4	0
Fire and Flames	77%	5	24

Table 1: Russo and Schoemaker compared what people believe with what was true and what was covered in the press [50].

If we are going to improve sustainability of lighting, we must publically talk about the *value* of lighting. Evidence-based results are not going to be effective on their own. We must therefore draw attention to the fact that the benefits of lighting go well beyond workplane illuminance and luminous efficacy. Current lighting recommendations and standards based on illuminance and luminous efficacy may, in fact, compromise health, well-being, productivity, and energy efficiency; in other words, existing standards based upon illuminance and luminous efficacy likely compromise sustainability. Talk is cheap, so we have to agree on quantifiable metrics on which to base new recommendations and standards. These ideas must be broadly discussed and resolved if we are to make real strides in developing sustainable lighting practices.

Figure 10: To achieve sustainable lighting we must talk about its benefits as well as its costs, that is, its value.

CONCLUSION

In sum then, we do not have sustainable lighting practices today because we are focused on inadequate metrics, illuminance and luminous efficacy. We can change that for the better by defining, measuring, and specifying metrics that better characterize the benefits as well as the costs of lighting. Perhaps most importantly, we must also begin to publically talk about the *value* of lighting so that new and better metrics can be accepted and used by regulators and lighting practitioners.

ACKNOWLEDGMENTS

Sincerest thanks are given to Ines Martinović for her editing and background research used in this manuscript. Thanks are also given to Dennis Guyon for his assistance in producing the graphics for this manuscript, and to Mariana Figueiro and Russ Leslie for their helpful suggestions on an earlier draft.

REFERENCES

[1] United Nations General Assembly. 2005. *2005 World Summit Outcome, Resolution A/60/1*.

[2] Commission Internationale de l'Éclairage. 1975. *Guide on interior lighting.* CIE Committee TC-4.1. Paris: Bureau Central de la CIE: CIE Publication No. 29.10

[3] IES Committee on Recommendations for Quality and Quantity of Illumination. 1980. Selection of illuminance values for interior lighting design (RQQ Report No. 6). *J Illum Eng*, 9:188-189.

[4] Rea MS, (ed.). 2000. *The IESNA Lighting Handbook Reference and Application*, 9th Edition. New York: IESNA.

[5] Boyce PR, Eklund NH, Hamilton BJ, Bruno LD. 2000. Perceptions of safety at night in different lighting conditions. *Light Res Tech*, 32(2):79-91.

[6] Bodmann HW. 1962. Illumination levels and visual performance. *Int Light Rev*, 13:41-47.

[7] Krugman P. 2001. Competitiveness: A dangerous obsession. *Foreign Affairs*, 73:28-44.

[8] Porter ME. 1990. What is national competitiveness? *Harvard Business Review*, March-April:84-85.

[9] Field, AJ. 2008. Productivity. *The Concise Encyclopedia of Economics*. [Online] Library of Economics and Liberty, 2008. [Cited: July 8, 2011.] http://www.econlib.org/library/Enc/Productivity.html.

[10] Farmer CM, Retting RA, Lund AK. 1999. Changes in motor vehicle occupant fatalities after repeal of the national maximum speed limit. *Accident Analysis & Prevention*, 31(5):537-543.

[11] Lave C, Elias PI. 1994. Did the 65 mph speed limit save lives? *Accident Analysis & Prevention*, 26(1):49-62.

[12] Anderson KM, Castelli WP, Levy D. 1987. Cholesterol and Mortality: 30 years of follow-up from the Framingham study. *Journal of the American Medical Association*, 257(16):2176-2180.

[13] Weverling-Rijnsburger AWE, Blauw GJ, Lagaay AM, Knock DL, Meinders AE, Westendorp RGJ. 1997. Total cholesterol and risk of mortality in the oldest old. *Lancet*, 350(9085):1119-1123.

[14] Muldoon MF, Manuck SB, Matthews KA. 1990. Lowering cholesterol concentrations and mortality: A quantitative review of primary prevention trials. *BMJ*, 301.

[15] Robinson SC, Brucer M. 1939. Range of normal blood pressure. *Archives of Internal Medicine*, 64(3):409-444.

[16] Pearce KA, Furberg CD, Rushing J. 1995. Does antihypertensive treatment of the elderly prevent cardiovascular events or prolong life? A meta-analysis of hypertension treatment trials. *Archives of Family Medicine*, 4(11):943-949.

[17] Mulrow CD, Cornell JA, Herrera CR, Kadri A, Farnett L, Aguilar C. 1994. Hypertension in the elderly. *Journal of the American Medical Association*, 272:1932-1938.

[18] Mills E, Borg N. 1999. Trends in recommended illuminance levels: An international comparison. *Journal of the Illuminating Engineering Society*, Winter:155-163.

[19] Rea MS, Bullough JD. 2000. Application Efficacy. *Proceedings of the Illuminating Engineering Society of North America Annual Conference*, 485-516. New York: Illuminating Engineering Society of North America.

[20] Kanter, J. Europes Ban on Old-Style Bulbs Begins. *New York Times*, August 31, 2009.

[21] Anonymous. Canada to ban incandescent light bulbs by 2012. *Reuters*. April 25, 2007.

[22] Europa. Member States approve the phasing-out of incandescent bulbs by 2012. *Europa Press Release*. Brussels: December 8, 2008.

[23] Australia Government - Department of Climate Change and Energy Efficiency. Lighting: Phase out of inefficient incandescent bulbs. [Online] 2010. [Cited: July 21, 2011.] http://www.climatechange.gov.au/what-you-need-to-know/lighting.aspx.

[24] Lennie P, Pokorny J, Smith VC. 1993. Luminance. *J Opt Soc Am*, 10:1283-1293.

[25] Nickerson D. 1960. Light sources and color rendering. *J Opt Soc Am*, 50:57-69.

[26] Judd, D. 1967. A flattery index for artificial illuminants. *Illum Eng*, 62:593-598.

[27] Rea MS, Deng L, Wolsey R. 2005. Light Sources and Color. *NLPIP Lighting Answers*, 8(1).

[28] Narendran N, Deng L. 2002. Light Sources and Color. *Solid State Lighting II: Proceedings of SPIE*.

[29] Jost-Boissard S, Fontoynont M, Blanc-Gonnet J. 2009. Perceived lighting quality of LED sources for the presentation of fruit and vegetables. *Journal of Modern Optics*, 56(13):1420-1432.

[30] Rea MS, Freyssinier-Nova JP. 2008. Color Rendering: A Tale of Two Metrics. *Color Research and Application*, 33:192-202.

[31] Rea MS, Freyssinier JP. 2010. Color Rendering: Beyond Pride and Prejudice. *Color Research and Application*, 35:401-409.

[32] Commission Internationale de l'Éclairage. 1926. CIE Proceedings, 1924. Cabridge: Cambridge University Press.

[33] Commission Internationale de l'Éclairage. 1951. Recueil des travaux et comptes rendus des séances: Douzième Session, Stockholm. New York: Bureau Central de la C.I.E., 1951.

[34] He Y, Rea MS, Bierman A, Bullough J. 1996. Evaluating light source efficacy under mesopic conditions using reaction times. *Journal of the Illuminating Engineering Society*, Winter:236-257.

[35] Rea MS, Bullough JD, Freyssinier-Nova JP, Bierman A. 2004. A proposed unified system of photometry. *Light Res Tech*, 36(2):85-111.

[36] Rea MS, Bullough JD. 2007. Making the move to a unified system of photometry. *Light Res Tech*, 39(4):393-408:12

[37] Rea MS, Radetsky LC, Bullough JD. 2010. Toward a model of outdoor lighting scene brightness. *Light Res Tech*, 43(1):7-30.

[38] Commission Internationale de l'Éclairage. 2005. *CIE 10 Degree Photopic Photometric Observer*. Vienna: CIE.

[39] Guth S, Graham B. 1975. Heterochromatic additivity and the acuity response. *Vision Research*,15:317-319.

[40] Berson DM, Dunn FA, Takao M. 2002. Phototransduction by retinal ganglion cells that set the circadian clock. *Science*, 295:1070-1073.

[41] Foster RG, Wulff K. 2005. The rhythm of rest and excess. *Nature Reviews Neuroscience*, 6:407-414.

[42] Figueiro MG, Bullough JD, Bierman A, Rea MS. 2005. Demonstration of additivity failure in human circadian phototransduction. *Neuro Endocrinol Lett*, 26(5):493-498.

[43] Rea MS, Figueiro MG, Bierman A, Bullough JD. 2010. Circadian light. *Journal of Circadian Rhythms*, 8(2).

[44] Figueiro MG, Rea MS, Bullough JD. 2006. Does architectural lighting contribute to breast cancer? *Journal of Carcinogenesis*, 5(1):20.

[45] Radetsky LC. 2011. Streetlights for Local Roads. *NLPIP Specifier Reports*. 14(1).

[46] Rea MS, Bullough JD, Akashi Y. 2009. Several views of metal halide and high-pressure sodium lighting for outdoor applications. *Light Res Tech*, 41:297-320.

[47] Bullough JD, Rea MS. 2011. Intelligent control of roadway lighting to optimize safety benefits per overall costs. *IEEE Intelligent Transportation Systems Conference*, Washington, D.C.

[48] Cuttle C. 2010. Towards the third stage of the lighting profession. *Light Res Tech*, 42:173- 193.

[49] Figueiro MG. 2008. A proposed 24 h lighting scheme for older adults. *Light Res Tech*, 40:153-160.

[50] Russo JE, Schoemaker PJH. 1989. *Decision Traps: Ten barriers to brilliant decision-making and how to overcome them*. New York: Doubleday.

[51] Rea MS, Bullough JD. 2004. In defense of LPS. *Lighting Design and Application*, 34(9):51-55.

Nanostructured Materials for Renewable Energies

FLEXIBLE AND LIGHTWEIGHT SOLAR MODULES FOR NEW CONCEPTS IN BUILDING INTEGRATED PHOTOVOLTAICS

S. Buecheler, A. Chirilă, J. Perrenoud, L. Kranz, C. Gretener, P. Blösch, F. Pianezzi, S. Seyrling, A.N. Tiwari

Laboratory for Thin Films and Photovoltaics, Empa – Swiss Federal Laboratories for Materials Science and Technology, Überlandstr. 129, 8600 Dübendorf, Switzerland

ABSTRACT

Most promising technology for cost-effective decentralized solar electricity production is based on thin film photovoltaics. Lowest production costs per output power are reached with thin film solar modules based on the inorganic compound semiconductors CdTe and $Cu(In,Ga)Se_2$ (CIGS). The high conversion efficiency potential of these two technologies has been demonstrated on laboratory scale solar cells reaching 16.5% and 20.3%, respectively, resulting in high power output per installed area. Substituting the commonly used rigid glass substrate by flexible and lightweight materials such as polyimide films or metal foils will further reduce production costs due to the possibility of fast roll-to-roll manufacturing and will also open new markets and enable advanced applications. In addition to mobile solar energy production in consumable electronics as well as in vehicles on land, on sea, in air, and in space, the flexibility and lightweight of this technology allows new concepts for solar electricity sources integrated in facades or roofs of sustainable buildings in future.

Latest results on the development of flexible thin film solar cells and monolithically interconnected modules based on CdTe and CIGS absorber materials are presented in this paper. The concept of coloured solar cells for architectural glazing or shading elements will also be presented. CdTe and CIGS devices are multilayer stacks of thin films and precise structuring on nanometre scale is essential to obtain high efficiencies. We focus on low-temperature deposition processes for both technologies which allow exact control of required nanostructure at the interfaces and grain boundaries of the polycrystalline layers. For CIGS we developed an innovative multi-stage deposition process yielding an optimized energy band gap profile across the absorber layer thickness in order to reduce recombination losses in the device. We present conversion efficiencies for flexible CdTe solar cells exceeding 13% and for flexible CIGS solar cells crossing 18%. We also demonstrate the feasibility of up-scaling of the processes and fully laser based monolithically interconnected mini-modules with conversion efficiency towards 10% for CdTe and 15% for CIGS.

INTRODUCTION

Inorganic thin film photovoltaics based on chalcogenide semiconductors such as $Cu(In,Ga)Se_2$ (CIGS) and CdTe proved high potential as the most cost-effective PV technology in the near future. This is due to the lower production costs compared to wafer based PV technologies and higher achievable conversion efficiencies compared to other thin film approaches like amorphous/micromorph silicon, dye sensitised, or organic solar cells. The latter two might, however, become even more cost-effective in remote future.

In this paper we present the latest achievements in the development of flexible and lightweight CIGS and CdTe solar cells and modules. We discuss the feasibility of up scaling of these technologies and the impact on sustainable building development.

METHOD

The CIGS and CdTe solar cells and modules presented in this paper are grown by low temperature processes on polyimide films.

For CIGS solar cells a Molybdenum based metal layer structure is deposited as back contact by dc-sputtering onto the flexible polyimide substrate. The p-type CIGS absorber layer is grown by a multi-stage co-evaporation process in high-vacuum. The maximum substrate temperature during the evaporation process is in the nominal range between 450-500°C as measured contactless with a k-type thermocouple behind the substrate. The n-type CdS buffer layer is grown by chemical bath deposition followed by a transparent i-ZnO/ZnO:Al bi-layer front contact. The solar cells are finished with Ni/Al/Ni fork-shaped grid fingers and separated by mechanical scribing to nominal 0.6 cm^2 device area. Details of the fabrication process can be found elsewhere [1,2].

CdTe solar cells are fabricated in the superstrate configuration where the choice of substrates is limited to transparent materials since the light enters the solar cell through the substrate. In the superstrate configuration a transparent conductive oxide (TCO) front contact ZnO:Al layer and a highly transparent and resistive i-ZnO layer are grown by rf-magnetron sputtering on the polyimide substrate. The n-type CdS and p-type CdTe layer stack is deposited by high vacuum thermal evaporation from the compounds and subsequently annealed at 420°C in a chlorine and oxygen containing ambient. The solar cells are finished by evaporation of a Cu/Au bilayer onto Te enriched CdTe surface. The solar cell area of 0.15 cm^2 is defined by the back contact geometry. More details of the process can be found elsewhere [3].

The photovoltaic properties of the flexible solar cells are measured by current-voltage characteristics at standard test conditions under simulated AM1.5G illumination at 1000 W/m^2 irradiation intensity and 25°C device temperature following the international standard IEC 60904-1 Ed.2.

RESULTS AND DISCUSSION

The chalcopyrite thin film solar cells are multilayer devices which can be grown on large area substrates. Figure 1 illustrates schematically the built-up of the layers of the two devices discussed in this paper. In both technologies the core of the device is a pn-junction formed between the p-type absorber layer CIGS or CdTe, respectively, and the n-type CdS layer. In this system the incoming light is absorbed and free charge carriers are generated which are then separated by the built-in electrical field in the pn-junction. The charge carriers are extracted by two electrical contacts, a transparent conductor at the front which is commonly made of a transparent conductive oxide (TCO) and a metallic structure at the back.

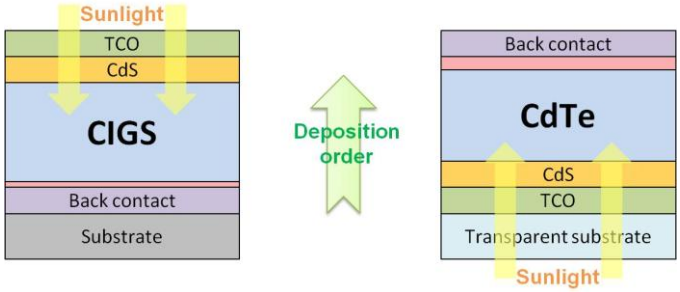

Figure 1: Schematic built-up of the CIGS and CdTe thin film solar cells. CIGS devices are commonly grown in the illustrated substrate configuration while highly efficient CdTe devices are achieved in the superstrate configuration. In the superstrate configuration the choice of substrates is limited to transparent materials because the light enters the solar cell through the substrate.

Conversion efficiencies of 20.3% for CIGS and 16.5% for CdTe are reported for solar cells on glass substrate fabricated with high temperature deposition methods (>600°C) [4-6].

Low temperature deposition processes for both the CIGS (<500°C) and CdTe (<450°C) technology were developed in our laboratory. These processes allow the utilization of a larger variety of substrate materials. This includes polyimide films, stainless steel and mild steel foils as well as aluminium foils for the CIGS process and transparent materials such as soda lime glass and polyimide film for the CdTe process.

Figure 2 shows the conversion efficiency values achieved for flexible CIGS and CdTe solar cells within the last decade. The photovoltaic performance continually increased due to improved understanding of material synthesis and interface engineering. For CIGS technology the most recent advancement was achieved by optimization of the CIGS composition grading, the sodium doping and the microstructure. This led to reduced recombination losses in the device and to a solar energy conversion efficiency of 18.7% for a flexible CIGS solar cell. This is the highest reported efficiency for any flexible and lightweight technology [7]. In case of CdTe the most recent improvement was achieved by reducing the parasitic light absorption in the substrate material. With a clear polyimide film the conversion efficiency was increased to 13.8% [8].

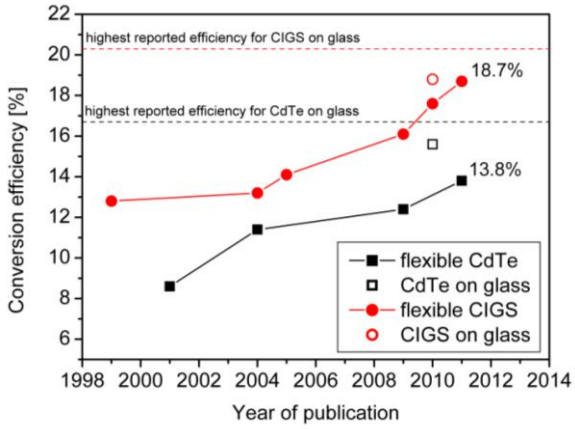

Figure 2: Conversion efficiencies of flexible CdTe and CIGS solar cells fabricated by low temperature processes. Also shown is the in-house reference on glass and the highest reported efficiency for each technology.

Photographs of flexible CIGS and CdTe solar cells on polyimide substrate are shown in figure 3. The solar devices have a critical radius of curvature below 1 cm and a power density without lamination of >2.3 kWp/kg and >1.7 kWp/kg for CIGS and CdTe, respectively.

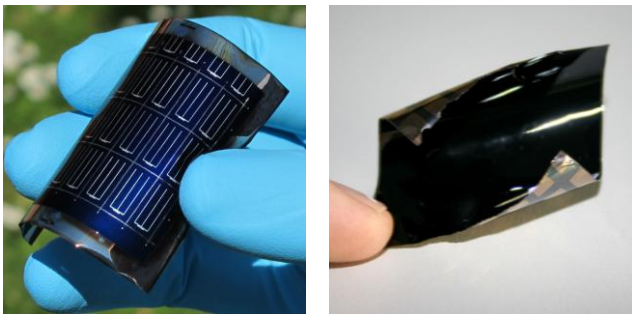

Figure 3: Photographs of flexible CIGS (left) and CdTe (right) solar cells on polyimide substrates.

In operating conditions (maximum power point) CIGS and CdTe solar cells have a typical voltage of about 0.6 V and 0.7 V, respectively. This voltage is too small for most applications and also would result in major resistive losses in the cabling. The device voltage is increased by serial interconnection of the solar cells to solar modules. A key advantage of thin film photovoltaics is the possibility for monolithical interconnection. The flexible solar modules presented in this paper are monolithically interconnected using laser scribing technique for all patterning steps [9].

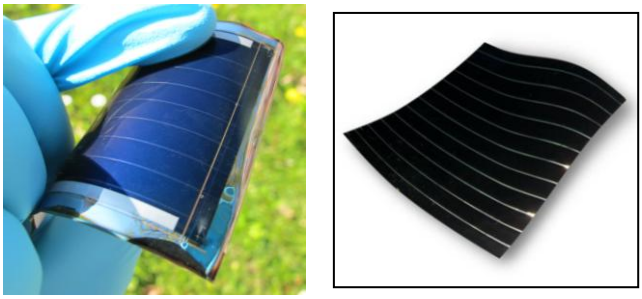

Figure 4: Flexible and lightweight CIGS (left) and CdTe (right) solar modules.

Figure 4 shows photographs of flexible CIGS and CdTe solar modules where all patterning steps are performed with laser scribing. For the CIGS solar module with an aperture area of 13 cm^2 eight cells are connected in series yielding a device voltage of 5.22 V and an active area efficiency of 14.7%. For the first time we proofed the concept of flexible CdTe solar modules. Eleven cells are connected to a module with an aperture area of 32 cm^2 yielding a voltage of 8.35 V and an active area efficiency of 9.4% [9].

The flexibility and lightweight of the highly efficient CIGS and CdTe solar devices allow building integration (and also building application) in structures which can not take the additional load of heavy and rigid glass laminated solar modules. Flexible photovoltaics can be integrated in light constructions in order to reduce the overall footprint. The flexible solar modules can be laminated to building elements such as flat roof membranes, tiles or metallic covers without adding weight and thus, the installation costs can be reduced significantly. Furthermore, the flexibility and lightweight allows for new concepts in design oriented PV application.

For optimized light absorption an additional optical coating is applied in order to match the refractive index at the interface and reduce reflection losses over a broad wavelength

spectrum. Furthermore, the additional optical coating can be used to engineer constructive and destructive interference effects. By changing the thickness of the optical coating the narrow wavelength region for constructive reflection can be tuned, i.e. the colour of the thin film PV devices can be selected (fig. 5).

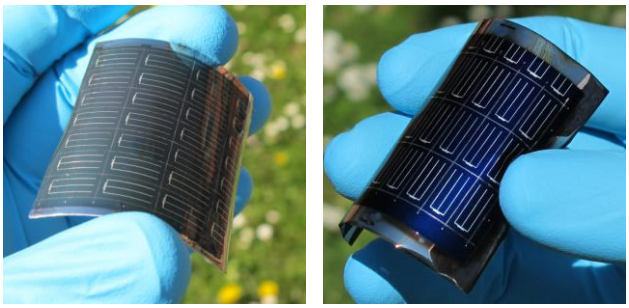

Figure 5: Illustration of the effect of constructive interference for colour selection. Choosing the colour of the PV devices for architectural glazing is possible.

Beside the advantages of flexibility and lightweight of the finished product the rollable substrate material enables the use of cost-efficient and fast roll-to-roll production methods which proofed very high throughput in applications like food packing or newspaper printing. With the roll-to-roll technology not only a higher throughput but also lower investment costs for the equipment are expected. Currently several companies such as Global Solar (USA), Ascent Solar (USA), Odersun (Ger), Solarion (Ger) or Flisom (CH) are developing or ramping up production facilities using roll-to-roll based manufacturing.

The high efficiency, flexibility, and lightweight of the presented thin film PV technologies have significant advantages and allow new concepts in PV application:

- Smaller surface area for same output power
- Lower balance of system costs
- Application on windows, roofs, and facades possible also in light constructions and curved surfaces
- Customizable for design oriented PV applications

These results show that conversion efficiencies of flexible and lightweight inorganic thin film photovoltaics are approaching the values achieved on rigid glass substrate yet with additional advantages not only of the product but also during manufacturing. The flexibility and the lightweight of the CIGS and CdTe thin film devices as well as the projected low production costs make the application in new concepts for building integrated photovoltaics possible.

ACKNOWLEDGEMENTS

This work was supported by the Swiss National Science Foundation, the Swiss Federal Office of Energy, the Commission for Technology and Innovation and the European FP7 Project hipo-CIGS. The Authors would like to thank Flisom AG, Switzerland for performing laser scribing and helping in mini-module development.

REFERENCES

1. Chirilă, A., et al.: Optimization of composition grading in CIGS for flexible solar cells and modules, Proc. of the 35th IEEE Photovoltaic Specialist Conference Honolulu, 2010.
2. Chirilă, A., et al.: Cu(In,Ga)Se2 solar cells grown on flexible polymer substrate with efficiencies exceeding 17%.
3. Perrenoud, J., et al.: Flexible CdTe solar cells and modules: challenges and prospects, Proc. of SPIE, Vol 7409, pp. 74090L-1–74090L-5, 2009.
4. Jackson, P., et al.: High Quality Baseline for High Efficiency Cu(In1-x,Gax)Se2 Solar Cells, Prog. Photovolt. Res. Appl., Vol 15, pp 507-519, 2007.
5. Jackson, P., et al.: New world record efficiency for Cu(In,Ga)Se2 thin film solar cells beyond 20%, Prog. Photovolt. Res. Appl., DOI: 10.1002/pip.1078, 2011.
6. Wu, X.: High efficiency polycrystalline CdTe thin film solar cells, Solar Energy, Vol 77, pp 803-814, 2004.
7. Empa: Record efficiency of 18.7% for flexible CIGS solar cells on plastics, Empa Press Release, http://www.empa.ch/plugin/template/empa/1256/107447/---/l=1, Duebendorf, St. Gall, Thun, 19 May 2011.
8. Empa: Efficiency record for flexible CdTe solar cell due to novel polyimide film, Empa Press Release, http://www.empa.ch/plugin/template/empa/1256/108288/---/l=1, Duebendorf, St. Gall, Thun, 9 June 2011.
9. Perrenoud, J., et al.: Fabrication of flexible CdTe solar modules with monolithic cell interconnection, Solar Energy Materials & Solar Cells, Vol 95, pp 8-12, 2011.

COLOURED COATINGS FOR GLAZING OF ACTIVE SOLAR THERMAL FAÇADES BY REACTIVE MAGNETRON SPUTTERING

S. Mertin, V. Hody-Le Caër, M. Joly, J.-L. Scartezzini, A. Schüler

Solar Energy and Building Physics Laboratory, EPFL – ENAC – IIC LESO-PB, Station 18, Bâtiment LE, 1015 Lausanne, Switzerland

ABSTRACT

For building integration of solar-powered energy systems, aesthetic aspects play an important role. Covering a standard solar collector with a coloured glazing, opaque to the human eye but highly transparent to solar energy, permits a perfect architectural integration of solar thermal panels into glazed building façades. The thermal energy produced can be used for both solar heating and cooling, as well as for domestic hot water. The principle of the coloured appearance is based on interference in the thin-film coating on the reverse side of the cover glass. Different interference filters based on nano-composite materials deposited by the sol-gel method were presented at CISBAT 2007 [1].

Currently, we are developing new plasma-deposition processes, which are more suitable for industrial large-scale production. A new state-of-the-art ultra-high vacuum (UHV) system for magnetron sputtering deposition of novel nano-composite solar coatings has recently been designed, constructed, and installed at the Solar Energy and Building Physics Laboratory (LESO-PB). Up to five different magnetron sources can be used simultaneously, in reactive and non-reactive mode. The geometric configuration of the chamber has been optimised for best film homogeneity and allows the deposition on substrates up to 100 mm in diameter.

The optical and electronic properties of thin films are closely interrelated and highly relevant for solar coatings. Photoelectron spectroscopy provides information on the coating structure, the deposited material and its chemical state inside the coating, as well as the nature of the interface between different layers. A system for ESCA analysis (Electron Spectroscopy for Chemical Analysis) has recently been installed and put into operation at LESO-PB. By ellipsometry and spectrophotometry, we can determine exactly the different optical properties of the coating, such as layer thickness, refractive index, or absorption coefficient. This provides best conditions for highly efficient research and development on new materials for further optimisation of the coloured interference filters.

First results have been obtained with our new experimental infrastructure and will be presented in this contribution.

INTRODUCTION

A perfect architectural integration of standard solar thermal collectors, which are either glazed or unglazed, is difficult to obtain. Perfect building integration means that the collector is part of the building's envelope or an architectural design element and can therefore not be recognised immediately as solar collector [2,3]. Nowadays, most thermal collectors are installed on rooftops and produce domestic hot water or heat swimming pools. Very rarely one finds collectors mounted on the façades of buildings [3]. The main reason for this is the black or dark bluish colour of the selective absorber, which is highly visible through a standard cover glass. However, associating the visible and exposed part of the collector with a colour would grant architects complete freedom for a perfect architectural integration into the

building's envelope [2,4]. By using not only the roof but also the façade, a much larger surface will be available for active solar energy conversion and will enable the possibility of solar cooling for commercial buildings with limited space on their rooftops [5].

At the Solar Energy and Building Physics Laboratory (LESO-PB) of the École Polytechnique Fédérale de Lausanne (EPFL) several coloured filters based on thin-film nanotechnology were developed [6-8]. Those filters combine a visible coloured reflection with a very high transmittance of solar radiation. The work benefitted considerably from the collaboration with the Physics Department of the University of Basel.

For the thin-film deposition we work with reactive magnetron sputtering, which is today the state-of-the-art coating technique used for a wide range of optical applications going from thin-film photovoltaic cells to precision optical filters and large area window glass. A new ultra high vacuum (UHV) deposition system for magnetron sputtering was recently designed, constructed and installed in our brand-new NanoSolar Lab. For physical and chemical analysis of the coating we use a UHV system for ESCA analysis (Electron Spectroscopy for Chemical Analysis), which was installed and put into operation recently. Furthermore, we perform spectrophotometry and ellipsometry measurements for the optical characterisation of the deposited thin films.

This paper reports on recent developments and results obtained within the scope of a technology transfer to our industrial partner SwissINSO SA. The energetic performance of the coloured filters was improved in comparison to the real-size collector glasses at the LESO-PB and we obtained in our new deposition chamber a seven times larger homogenous zone for laboratory samples. Additionally, the possibility of matching the reflection colour with the colours of commercial window glasses was demonstrated. Another contribution to this conference will present the recent status in application and building services [5].

METHODS

Photoelectron Spectroscopy (PES, ESCA) is a powerful analysis method for measuring the elemental composition and the chemical state of the elements in a coating, as well as its electronic properties, which are directly linked to its optical properties [9,10]. In PES measurements the sample is exited with energetic photons. Due to the external photo effect, electrons are ejected from the sample. Depending on the different energy of the photoelectrons leaving the sample, the chemical composition of the surface of a sample and the chemical status of the atoms can be determined. Since the electron escape depth is only a few Å, which corresponds to several monolayers of atoms, this method is very surface sensitive.

Our ESCA system, shown in figure 1a, is equipped with X-ray and monochromatic X-ray sources for quantification of the elements and their chemical state on the sample. For the characterisation of the valence band and the metallic properties of a material our spectrometer has additionally a UV source [11,12].

Thin-film deposition by magnetron sputtering is a high-tech and complex state-of-the-art plasma process for a large variety of coatings on glass. For our research on novel nanostructured materials we use a very flexible and modular deposition chamber, which is equipped with five magnetrons positions, which allows us to deposit different materials simultaneously by co-sputtering on substrates up to 100 mm in diameter.

The plasma based sputtering process is schematically shown in figure 1b, as well as a photograph of the chamber with an on-going co-sputtering process in figure 1c. Already without any bake-out of the chamber, the background pressure obtained is in the range of

10^{-8} mbar. The geometry of the chamber and the process parameters were optimised in order to achieve a large homogenous deposition zone across the substrates.

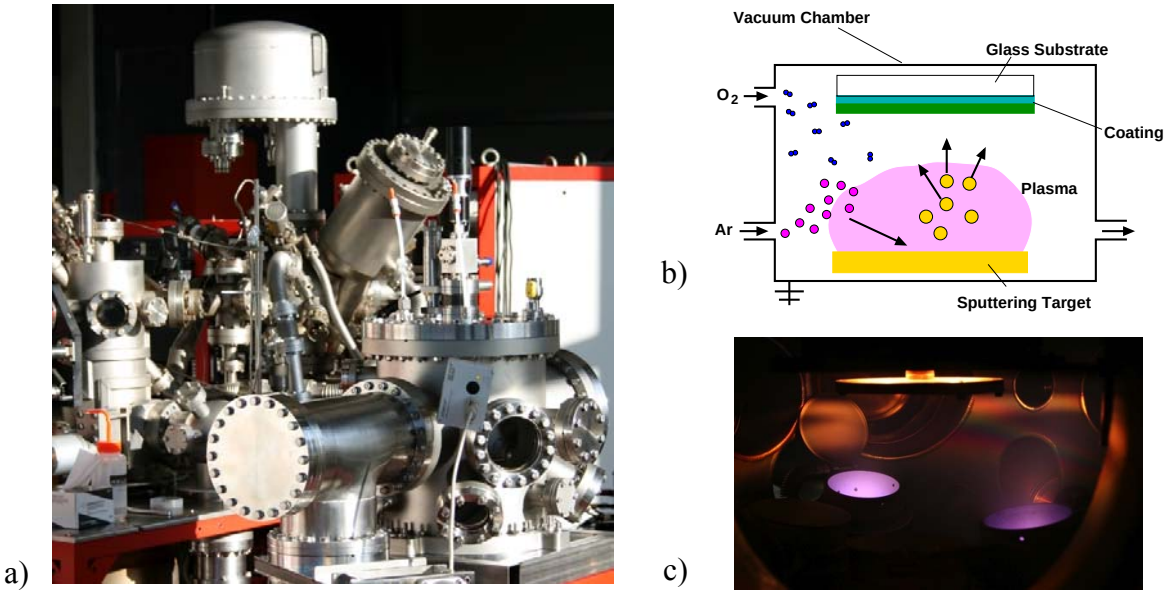

Figure 1: a) The UHV deposition chamber for magnetron sputtering and the ESCA analysis system of the NanoSolar Lab. b) Schematic drawing of the reactive sputtering process in our chamber. The magnetron with the target is located underneath the rotating substrate. c) Photograph of chamber during co-sputtering: By using two magnetrons with different target materials, nanostructured optical thin-film coatings are obtained.

Experiments for optimising the sputtering parameters to achieve good material properties and at the same time a large homogenous zone were performed. A suitable gas flow for the sputtering gas (argon) was determined to obtain a stable plasma with a RF power of 100 W at 13.56 MHz. By using the hysteresis of the self-bias voltage for Si and TiO targets versus the Ar:O_2 ratio, we obtained a first indication for the argon-oxygen ratio suitable for the deposition of completely oxidised SiO_2 and TiO_2 layers. To ensure that we reached the correct stoichiometry of the oxides, we worked in the stable reactive deposition regime of the hysteresis. XPS measurements support finding optimised sputtering conditions at higher deposition rates with the intended film stoichiometry.

RESULTS

Homogeneous laboratory samples of 70x60 mm^2 with highly transparent coloured filters are shown in figure 2. The interference filters, based on multilayers of nanostructured oxidic materials, consist of silicon dioxide (SiO_2), titanium dioxide (TiO_2), and compounds $Ti_xSi_{1-x}O_y$ with y close to 2. The homogeneity was achieved by rotating the substrate during deposition, after optimising the target-substrate distance. The layer designs are scope of the technology transfer, and therefore confidential.

For a good solar performance of the solar thermal collector glazing a direct solar transmittance τ_{sol} greater than 85% was envisaged to have nearly the same performance as a standard collector with an extra-white solar glass (τ_{sol} = 91%). Several coloured samples with colours from blue to green to yellow with a total solar transmittance from 88% up to 91% have been produced. A selection of the produced coloured samples is shown in figure 2. For the reddish and orange-reddish (brick red) coloured samples we achieved a performance of 83% of solar transmittance.

Figure 2: Demonstration boxes with eight homogenous coloured thin-film filters on 4-mm-thick extra white glass samples (70x60 mm^2) with front surface treatment by chemical etching. The coloured filters hide perfectly the parts of a real solar thermal absorber mounted at the bottom of the demo boxes.

Depending on their colour the coatings consists of different multilayer stacks. The stacks were designed with the method of the characteristic matrices for thin films by multiplication of their mathematically complex components starting from the multilayer design types presented by Schüler et al. in 2005 [8,13]. The measured optical data is in good agreement with the fit-curves (see the spectral reflectance of selected design types in figure 3b). The optical constants n(λ) and k(λ) used for fitting the data were determined by ellipsometry measurements. The high accuracy and reproducibility of the multilayer stacks offer the possibility of refinement of colours. Due to this we could match the interference filters with colours of existing commercial glazing (see figure 3a).

a)

b)

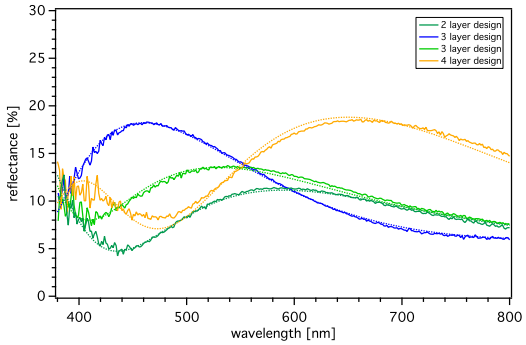

Figure 3: a) Photograph of green and blue coloured samples (middle) which match to given commercial sun protection glasses. b) Reflectance curves of sputtered samples with different layer design and colours are presented. The measured data are in good agreement with the fit-curves (dotted lines). The colours in the graph indicate approximately the reflection colours of the samples.

The presented greenish and bluish samples match the colours of the commercial sun protection glasses shown in the same photograph. For the colour matching the commercial glasses were investigated with the Window Stand, with which reflectance and transmittance spectra of real-size glazing can be measured angular depended [14]. The colours of the samples were optimised for an angle of incidence of 15°, the smallest angle for the reflectance measurements of the glazing.

DISCUSSION AND OUTLOOK

Homogeneous coloured samples for solar thermal collectors were successfully produced by magnetron sputtering. The samples are very promising, as they can have a high solar transmittance τ_{sol} greater than 88%, which is close to the one of standard collector cover glass ($\tau_{sol} \approx 91\%$), and at the same time they are completely opaque to the human eye. Furthermore, we achieved for laboratory samples an outstanding homogeneity in layer thickness and therefore in their colour reflection. By fine-tuning of the coloured filters the reflection colour of the cover glass for the collector can be matched with the colour appearance of commercial products. As bluish and greenish colours are widely used for glazing on façades, we demonstrated it for a dark blue and a green-bluish commercial sun protection glass.

Those coloured filters, by accepting 3% of energy loss, will grant all flexibility for building and façade integration and therefore will increase the accessible surface used for solar thermal energy tremendously, especially on high-rise buildings. Since the interference colour can be varied, it is also possible to re-produce colours of existing commercial sun protection glasses to provide a completely uniform colour appearance on a façade of a building.

So far, the deposition parameters for the reactive sputtering with oxygen, determined with the characteristic hysteresis, were chosen conservatively for depositing in a stable sputtering regime with high oxygen content in the gas mixture. The advantage of this was to achieve a good layer quality with the correct stoichiometry inside the coating. However, high oxygen content is reducing the deposition speed, which limits the flexibility in layer thicknesses. In order to increase the sputtering yield without altering the coating stoichiometry, we will use a lambda probe for controlling more precisely the partial oxygen pressure during film deposition. With transmittance measurements by spectrophotometry the film stoichiometry is verified and ESCA analysis supports the research for new suitable coating materials for advanced interference filters.

The requirements for physical, chemical, and optical properties of those materials are:

- Transparency: Near-zero absorption over a wide range of the solar spectrum.
- Durability: The coating must be chemically stable and must stick to the glass for the lifetime (~20 years) of the collector itself.
- Tempering stability: Heating and shock cooling persistence, to be able to integrate the coloured glass in façades.
- Hardness: For handling and mechanical resistivity the coating material has to be hard and scratch resistant.
- Tuneable refractive index n for high-index layers and a very low n for low-index layers.

The current results and the gained experience, in combination with our brand-new NanoSolar Lab will support the development of those novel nanostructured materials. They will grand more flexibility in the multilayer design of the interference filters and with it in the reflection colour of the solar panels. As already now architects show a large interest in building integration of solar energy devices, a free choice of their colours combined with a good energetic performance will promote the usage of the building's façade for solar energy conversion.

ACKNOWLEDGEMENTS

The authors are grateful to the Swiss Federal Office of Energy SFOE and to our industrial partner SwissINSO SA for their financial support, and to Pierre Loesch for his technical support. For advice with respect to architectural questions we thank Christian Roecker, Marja Edelman, and Dr Maria Cristina Munari Probst. Finally, we would also like to thank Professor Peter Oelhafen and Roland Steiner, Physics department of the University of Basel, for great support and fruitful discussions.

REFERENCES

[1] E de Chambrier, D Dutta, C Roecker, M C Munari Probst, J-L Scartezzini, and A Schüler, in *Cisbat 2007* (2007), pp. 527-532.

[2] M C Munari Probst, Architectural Integration and Design of Solar Thermal Systems, École Polytechnique Fédérale de Lausanne, 2009.

[3] edited by Werner Weiss, *Solar Heating Systems for Houses: A Design Handbook for Solar Combisystems* (James & James (Science Publisher) Ltd, London, 2003).

[4] M C Munari Probst and C Roecker, Solar Energy **81**, 1104-1116 (2007).

[5] I Mack, S Mertin, V Hody-Le Caër, A Schüler, and Y Ducommun, in *Cisbat 2011* (2011).

[6] P Oelhafen and A Schüler, Solar Energy **79**, 110-121 (2005).

[7] A Schüler, C Roecker, J-L Scartezzini, J Boudaden, I R Videnovic, R S-C Ho, and P Oelhafen, Solar Energy Materials and Solar Cells **84**, 241-254 (2004).

[8] A Schüler, J Boudaden, P Oelhafen, E de Chambrier, C Roecker, and J-L Scartezzini, Solar Energy Materials and Solar Cells **89**, 219-231 (2005).

[9] H Tomaszewski, H Poelman, D Depla, D Poelman, R De Gryse, G Heynderickx, and G B Marin, Vacuum **68**, 31-38 (2002).

[10] D Guerin and S Ismat Shah, Journal of Vacuum Science & Technology A: Vacuum, Surfaces, and Films **15**, 712 (1997).

[11] A Schüler and P Oelhafen, Physical Review B **63**, 1-8 (2001).

[12] S Jeong, J Kim, B Kim, S Shim, and B Lee, Vacuum **76**, 507-515 (2004).

[13] A Schüler, C Roecker, J Boudaden, P Oelhafen, and J-L Scartezzini, Solar Energy **79**, 122-130 (2005).

[14] R Steiner, P Oelhafen, G Reber, and A Romanyuk, in *Cisbat 2005* (2005), pp. 441 - 446.

EFFICIENCY OF SILICON THIN-FILM PHOTOVOLTAIC MODULES WITH A FRONT COLOURED GLASS

S. Pélisset[1]; M. Joly[2]; V. Chapuis[1]; A. Schüler[2]; S. Mertin[2] ; V. Hody-Le Caër[2]; C. Ballif[1]; L.-E. Perret-Aebi[1]

1: Ecole Polytechnique Fédérale de Lausanne (EPFL), Institute of Microengineering (IMT), Photovoltaics and thin film electronics laboratory, Breguet 2, 2000 Neuchâtel, Switzerland, e-mail : segolene.pelisset@epfl.ch

2: Ecole Polytechnique Fédérale de Lausanne (EPFL), Solar Energy and Building Physics Laboratory, EPFL-ENAC-IIC-LESO-PB, Station 18, 1015 Lausanne, Switzerland.

ABSTRACT

Photovoltaic electricity has already proven its ability to compete with other well established technologies for energy production. The abundant and non-toxic raw materials, the yearly increasing efficiency as well as the production cost of silicon thin-film solar cells getting lower and lower make this technology always more interesting for a wide spread use.

Beside the functional features, the size, colour and glass texture of a PV module determine its appearance and aesthetics. In order to be more compliant with the built environment, photovoltaic installations have to be improved in terms of visual rendering, matching of colour of the existing roof-tops and parasitic reflections. The crystalline technology already offers various types of systems with a large choice of shapes, textures and colours as well as "semi-transparent" modules more easily integrated in the roof-tops or facade. By changing the anti-reflective coating (ARC) of a crystalline solar cell, it is possible to modify their colour [1]. However, for thin-film silicon technology the challenge is completely different, and up to now, the only way to modify the module colour is to reduce the thickness of the active layer and consequently its efficiency. Therefore new ways to enhance the visual rendering of the thin-film modules have to be explored. A study led in the frame of the ArchinSolar project [2] has shown that architects are ready to integrate PV modules with enhanced aesthetic aspect, even though there was a 10 % loss in efficiency.

The present study shows how new coloured filters can be used to enhance PV modules' appearance while minimizing power loss, to achieve a better integration in the traditional urban or rural environment.

INTRODUCTION

The enhancement of aesthetics for a better building integration of solar thermal collectors has already been developed by the use of coloured filters [3]. The challenge of the ArchinSolar project is to develop further these techniques and adapt them to PV modules, for which the requirements concerning the range of light transmission are completely different [4]. In this purpose, a special chemical treatment of the outer side of the novel glass element shall produce a textured or matt appearance while decreasing light reflection. In order to vary the module's colour, an optically selective filter is applied on the inner side. Minimizing energetic losses, this filter should only reflect a selected part of the incoming radiation. The coloured filters have to be optimized to combine an intense colour with a good light transmission.

A first version of these selective filters was tested on amorphous silicon (a-Si:H) thin-film modules. Each combination of cell, filters, back-reflector and texturized glass was characterized optically and electrically. Transmission and reflection spectra were recorded in the UV-Visible-NIR range by spectrophotometry and the quantum efficiency and the current-voltage characteristic were measured.

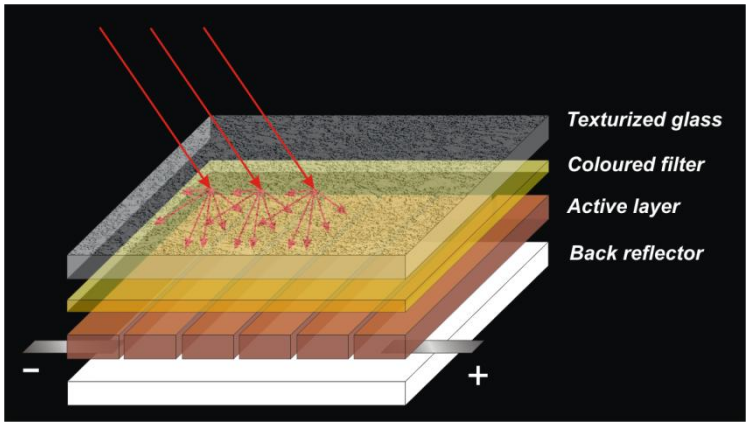

Figure 1: Sketch of the measured stack

METHOD

Two different selective filters, reported hereafter as Filter 1 and Filter 2 were tested. They were both orange, filter 1 having a low reflection, while filter 2 was more reflective and its colour appeared more intense. Commercially available a-Si:H mini-modules were used for the measurements. The modules were monolithically inter-connected; therefore, to connect one cell, wires were soldered at the back of the cell n^{th} and $n+1^{st}$. To get an as low as possible contact resistance with the back ZnO, the wires were soldered with the USS9200 ultra-sonic soldering station from MBR Electronics. The filters were placed on top of the cell covered with an index matching liquid, Immersol 518N from Zeiss, corresponding to the glass and encapsulant indices, to avoid the presence of air between the filters and the glass of the modules. Between the measurements, the different parts of the stack were cleaned in an ultra-sonic bath filled with isopropanol.

External quantum efficiency was measured with an in-house setup, current-voltage characteristics was measured with a Wacom sun simulator and the transmission and reflection spectra were recorded using a Lambda 900 spectrometer from Perkin-Elmer, with an integrating sphere.

RESULTS

External Quantum Efficiency measurements

External quantum efficiency (EQE) setup allows measuring the amount of charge carrier created at each wavelength with the cell in short circuit. A grating selects the wavelength of the light illuminating the cell and the current is collected through two wires directly soldered on the zinc oxide electrodes. The incident power at each wavelength is reported to the solar spectrum AM1.5, in order to determine the current density in short circuit J_{sc}, at 1000 $W.m^{-2}$.

Only a small area of the cell was illuminated ($2mm^2$), therefore 3-5 measurements were made for each conditions, moving the sample each time, in order to average the values. The standard deviation of the short circuit current density measured with EQE was below 1% for each sample. For each cell, the measurements were done under 6 different conditions (bare

cell, cell with white back-reflector (BR) on the back, cell + filter 1 on top, cell + filter 2 on top, cell + BR + filter 1, cell + BR + filter 2). Due to the design of the EQE setup, it was not possible to include the texturized glass in the set of samples.

A higher loss due to reflection was observed for the cell + filter condition (see Figure 2) in the blue part of the spectrum as compared to the bare cell condition. The reflection in this region did not participate to the colour of the stack and therefore this part would have to be optimized. The amount of current lost in the blue region was only 0.5% for the filter 1 whereas it was 2.5% for the filter 2. By reducing the reflection of the filter 2 in the blue region, the loss in current density could be reduced to a value around 10%.

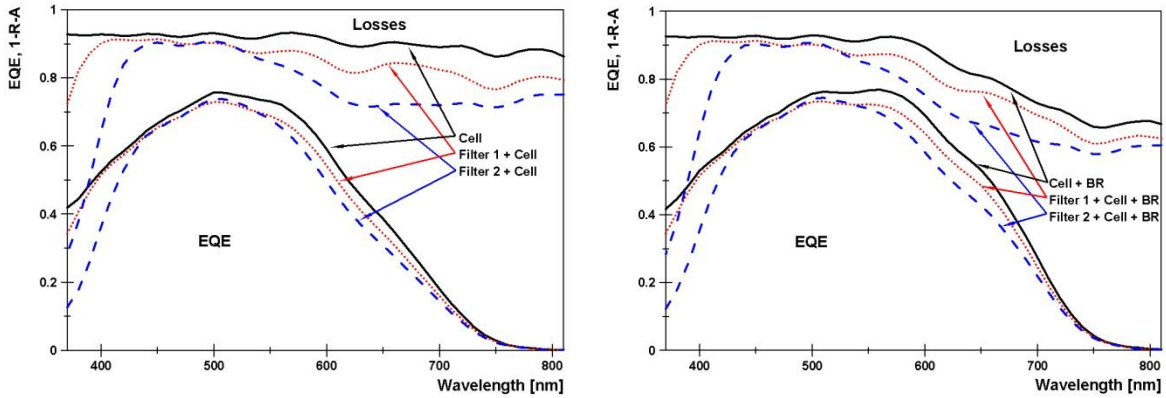

Figure 2: Measurements of the EQE and the losses due to reflection and absorption in the front part of the cell (glass and filters), for the bare cell (plain curves), the cell with the filter 1 (dotted curves) and the cell with filter 2 (dashed curves). Plot on the left corresponds to the cell without back-reflector; plot on the right corresponds to cell with white reflector.

Optical simulation of EQE

1-dimension optical simulations of a-Si:H solar cells with filters were performed using the Sunshine software [5] developed by the University of Ljubljana, Slovenia. Simulations allowed us to avoid taking into consideration the power loss due to the module quality and other parasitic electrical effects present in the measurements. Simulation of the bare cell fitted well the measured EQE (see Figure 3).

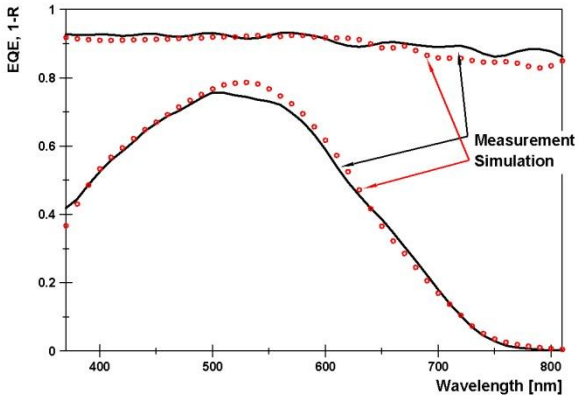

Figure 3: EQE and 1-R curves for the a-Si:H cell measured (plain curves) and simulated (circles)

Based on the transmission measurements of the filters, the solar spectrum AM1.5 was transformed and inserted in the simulator. Conditions with and without back-reflector were considered.

Due to some imprecision in the calculation, this method overestimated the loss in current. The loss was found to be 3.6 to 4.4% higher than the one measured with EQE (see Table 1 and Table 2). But when those simulated losses were compared to I-V data, the difference was found to be below 3.5%. Even though the losses were different, the trends remained the same; therefore Sunshine could be an interesting tool for the optimization of the filters, before manufacturing.

Current-Voltage measurements

The I-V characteristics were recorded for the same combinations as described above. The texturized glass was also placed on top of the stack.

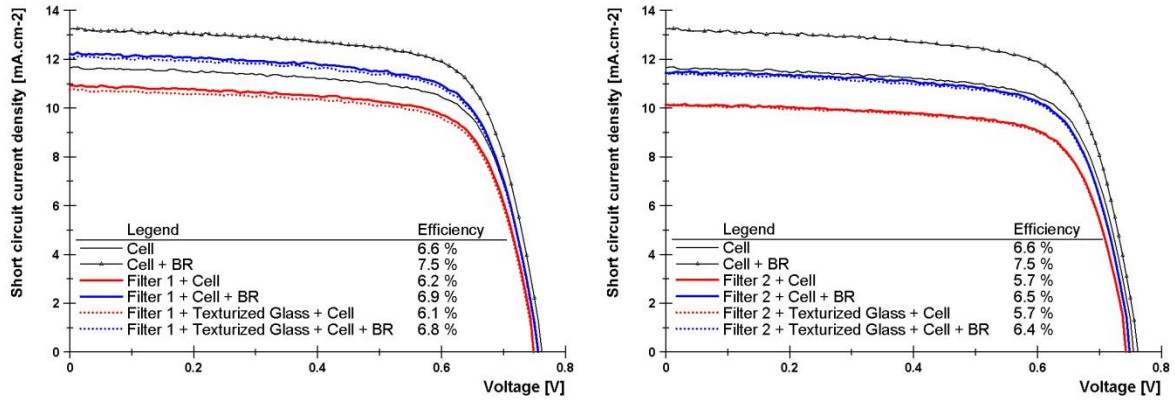

Figure 4: I-V curves of a mini-module with filters, back-reflector and texturized glass. The voltage was divided by the number of cells connected.

Introducing an additional textured glass on the top of the stack should lead to a decrease in reflection and though an increase in efficiency. However, during the measurements, there was light leakage, due to the thickness of the glass, on the edges of the cell. This was the reason why the loss in current was higher for the I-V measurements than for the EQE measurements. This leakage will be reduced by increasing the area of the module.

The relative efficiency loss was below 9.1% for the cell with filter 1 and below 14.4% for the cell with filter 2 (see Figure 4).

	Loss in Jsc from EQE (%)	Loss in Jsc from IV (%)	Loss in Jsc from Simulation (%)
Cell + Filter 1	5.4	6.2	9.6
Cell + Filter 1 + Texturized glass		7.7	
Cell + Filter 2	11.0	12.9	15.4
Cell + Filter 2 + Texturized Glass		13.4	

Table 1: Loss in short circuit current when filters and texturized glass are placed on top the cell. The reference is the bare cell.

	Loss in Jsc from EQE (%)	Loss in Jsc from IV (%)	Loss in Jsc from Simulation (%)
Cell + Filter 1	6.3	7.8	9.9
Cell + Filter 1 + Texturized glass		9.0	
Cell + Filter 2	11.8	13.5	16.0
Cell + Filter 2 + Texturized Glass		13.8	

Table 2: Loss in short circuit current when filters and texturized glass are placed on top the cell with back-reflector. The reference is the bare cell with back-reflector.

Colour determination

The aim of this study was to show the colour changes when adding coloured filters on modules. The CIE (International Commission on Illumination) Yxy colorimetric co-ordinates shown in Figure 5 were evaluated from the pictures of each element, under standard illuminant D65 and standard observer 1931.

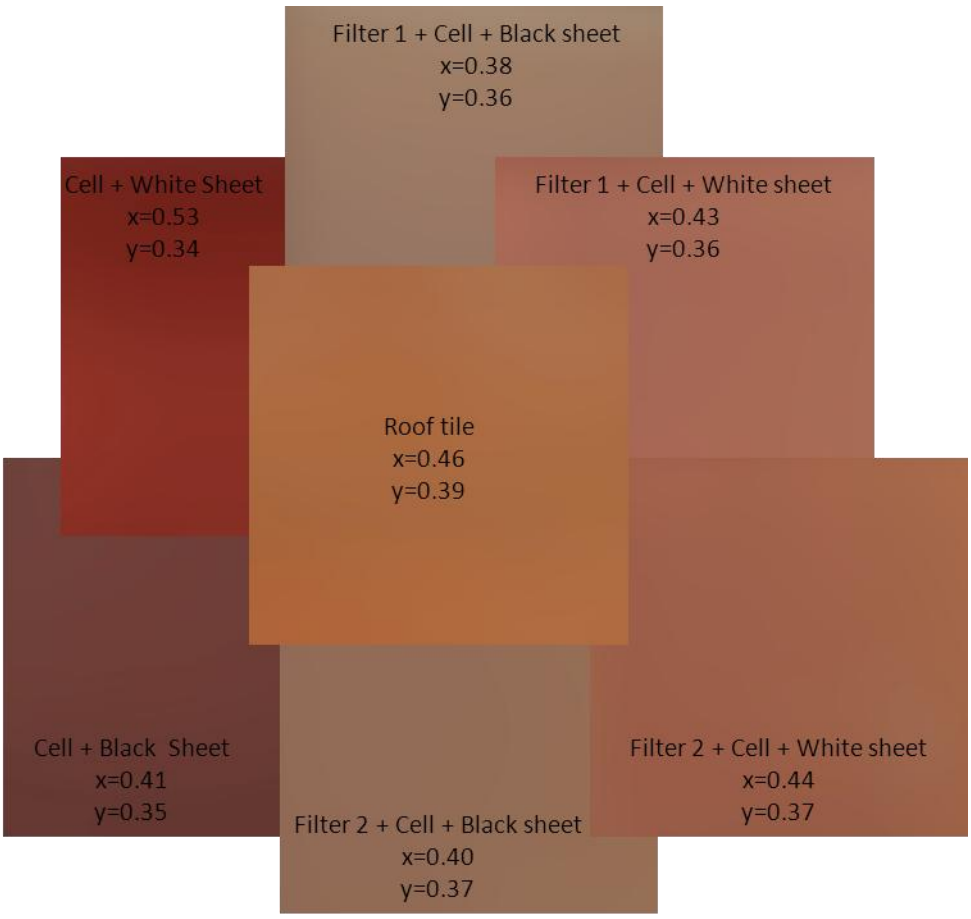

Figure 5: Blurred picture and CIE xy co-ordinates of each stack

xy values of the different stacks showed that adding the filters allowed to tune the tint to get closer to the colour of a typical roof tile and that the role of the white reflector could also help for a better visual rendering.

CONCLUSION

This study shows clearly that by using filters 1 and 2, the loss of efficiency is lower than 16%, which is much lower than the 33% considered in the work of Selj et al. for crystalline technology [1]. A module with the filter 1 would be in the acceptable range of efficiency, if we consider the limit of 10% loss in efficiency the architects would accept. For the filter 2, it has been shown above that reducing the reflection in the blue range of the spectrum could reduce the loss in current (and therefore in efficiency) to a value closer to the 10%. For both filters, any absorption will be avoided by tuning finely the deposition parameters. The present study shows us the importance, for a better precision, to consider the simulation of the whole stack instead of combining spectrophotometry measurements and simulation of the cell only. Despite the filters optimization is still needed for better performances as well as the design of others colours, our results are really promising for designing more esthetical modules better adapted for a respectful architectural integration.

REFERENCES

1. J.H. Selj, T.T. Mongstad, R. Søndenå, E.S. Marstein. Reduction of optical losses in colored solar cells with multilayer antireflection coatings. Solar Energy Materials and Solar Cells, In Press, Corrected Proof, 2011.
2. Archinsolar: "Unique and innovative building integration solution", demonstration project financed by Swiss Electric Research (SER), Competence Center Energy and Mobility (CCEM.CH), Services Industriels Genevois (SIG), Office Fédérale de l' Energie (OFEN), 04.2010-04.2013.
3. Andreas Schüler, Deepanshu Dutta, Estelle de Chambrier, Christian Roecker, Gregory De Temmerman, Peter Oelhafen, and Jean-Louis Scartezzini. Sol-gel deposition and optical characterization of multilayered $SiO_2/Ti_{1-X}Si_XO_2$ coatings on solar collector glasses. Solar Energy Materials and Solar Cells, 90(17):2894-2907, 2006.
4. A. Shah (2010, 1st edition). Thin-film Silicon solar cells, EPFL Press isbn 1420066749.
5. Janez Krc, Franc Smole, and Marko Topic. Analysis of light scattering in amorphous a-Si:H solar cells by a one-dimensional semi-coherent optical model. Progress in Photovoltaics: Research and Applications, 11(1):15_26, 2003.

CHARACTERISATION OF $CuInSe_2$ THIN FILMS

O. Aissaoui[1], S. Mehdaoui[1], M. Benabdeslem[1], L. Bechiri[1], N. Benslim[1], M. Morales[2], X. Portier[2], A. Ihlal[3].

1 : LESIMS, Département de physique Université de Annaba, BP. 12, 23200 Sidi Amar, Algérie

2 : CIMAP – Centre de recherche sur les ions, les matériaux et la photonique, UMR 7176 CNRS, ENSICAEN, 6 Boulevard du Maréchal Juin, 14050 Caen cedex (France) Phone: 33 2 31 45 26 54, Fax: 33 2 31 45 26 60

3 : Laboratoire Matériaux et Energies Renouvelables (LMER) Faculté des sciences BP 8106 hay Dakhla 80 000 Agadir, Maroc.

ABSTRACT

$CuInSe_2$ thin films have been grown on Corning glass and Si (100) substrates by a modified substrate temperature. X-ray diffraction and SEM measurements show that the films have an excellent crystallinity and crystallize in a tetragonal structure. Scanning electron microscopy investigations show that the films have a structure with large grains of 80 – 200 nm in diameter. An increase of the deposition temperature from room temperature to 300 °C leads to a change in the composition and morphology after annealing at 450°C. In the X-ray diffraction pattern of the $CuInSe_2$ on Si (100) sample prepared by SEL technique, characteristic peaks of the chalcopyrite structure such as (101), (211) and (311) were clearly observed for a both layers. The determined lattice parameters were a = 0.57725 (6) nm, b = 1.1621 (2) nm for sample prepared at room temperature and a = 0.57770 (4) nm, b = 1.1602 (1) nm for Ts = 300°C. The crystallographic structure of the $CuInSe_2$ sample was analyzed by Rietveld analysis using X-ray powder diffraction data.
Spectrophotometer was used to measure the optical characteristics of different Cu/In/Se/Se thin layers the spectral range between 300 – 2000 nm, and the band-gap energy of the material increases from 0.95 to 1.01 eV.

INTRODUCTION

$CuInSe_2$ (CIS) compounds have been some of the most extensively studied photovoltaic materials due to their a high value of absorption coefficient (10^4-10^5 cm^{-1}) within the visible and near infra-read, its near-optimum band gap Eg and a excellent outdoor stability [1]. Thin film solar cells have produced using this material or quaternary alloy of I-III-VI_2 group, with a record efficiency of 19.5% [2, 3]. $CuInSe_2$ thin films can be prepared by various techniques including, three source evaporation, flash evaporation, rapid thermal processing, radio-frequency magnetron sputtering, pulse laser deposition, metalorganic chemical vapor deposition molecular beam epitaxy and spin coating technique. The best results were obtained only for the layers grown using the coevaporation technique, which uses sophisticated technology so it needs high fabrication costs. Studies were undertaken to deposit films by a lower costs deposition technique such as stacked elemental layer (SEL) processing and selenization of stacked metallic precursor layers [4]. Compared to other deposition methods, SEL offer some advantages, such as a precise control of the composition, a high homogeneity, and the ability to deposit large area films on complex substrates. Here, we report the synthesis, structure, and optical properties of the semiconductor $CuInSe_2$ thin films as well as the results of effect of substrate temperature and substrate on these properties.

EXPERIMENTAL

Elemental layers of copper, indium and selenium were thermally evaporated sequentially onto 7059 glass and on Si (100) substrates at room temperature and at T_S = 300°C under high vacuum conditions (~ 10^{-3}Pa). Cu, In were evaporated from W boats, while Se was evaporated from a graphite effusion source. The Cu, In and Se thickness were chosen of about 14nm, 28nm and 63nm respectively. After a heat treatment of these films at 250°C for 30min, we have deposed a layer of Se (30nm) (figure 1). The selenium was used in excess to be sure to obtain p-type material. The thickness of these elemental layers were controlled by a quartz crystal monitor. Samples were then subjected to annealing at 450°C under Ar flow. This second annealing step transforms the elemental layers into a polycrystalline CIS films.

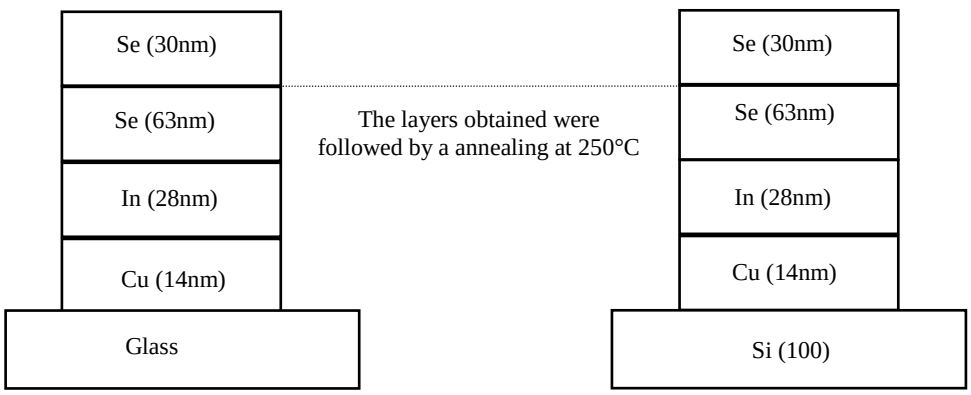

Figure 1: Schematic diagram of the elemental layers.

In this work, structural analysis of the samples has been done by grazing incidence X-Ray diffraction (GIXRD), XRD, scanning Electron Microscopy (SEM) and Transmission Electron Microscopy (TEM). Compositional analysis was made by Energy Dispersive X-Ray Spectroscopy (EDS) line scan of Cu/In/Se/Se and optical properties were studied with UV-VIS- NIR Spectrometer (Perkin Elmer λ 9). For electron microscopy investigation, the starting materials were evaporated directly on carbon film supported by Ni grids (3mm, 200mesh). The data were obtained at incident electron energy of 200kV using Jeol 200CX transmission microscopy.

RESULTS

Cu/In/Se/Se on glass substrat

The SEM photograph of the CIS produced by SEL technique, with Cu/In ratio of (a) 1.16, (b) 0.82, is shown in figure 2. The TEM photographs of the starting elements Cu, In and Se on Ni grids are also shown for reference (figure 3). SEM studies (figure 2a) revealed smooth amorphous-like structures with an almost complete absence of defined grain structure. An increase in growth temperature to 300°C resulted in a significant improvement in crystalline quality on a morphological level. SEM studies (see figure 2b) revealed a dense and compact structure of well-defined grains with typical sizes between 0.4 and 1.6μm. This morphology was also observed by several authors [5, 6] and photomicrographs similar to theirs are not produced here. Many studies have investigated the effect of temperature substrate and have suggested that increasing the substrate temperature during film growth increases the grain sizes [7] and reduces the number of defects inside the CIS grains [8].

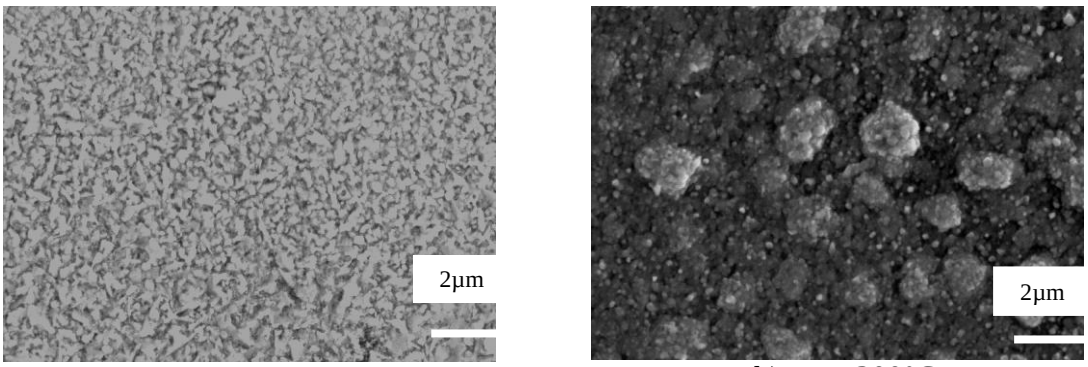

2a) Room temperature 2b) Ts = 300°C

Figure 2: SEM micrographs, illustrating the surface morphology of Cu/In/Se/Se film produced by the SEL technique at different substrate temperature after annealing.

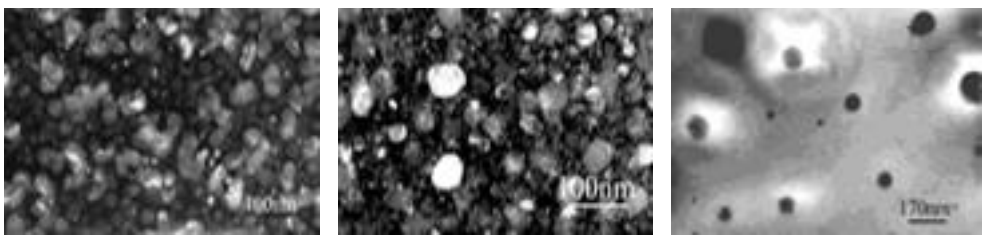

Cu on Ni In on Ni Se on Ni

Figure 3: TEM photographs of the starting materials Cu, In, and Se.

The Cu/In/Se/Se films were examined using X-ray diffraction (XRD) to check the structure in the overall samples. It revealed that the thin films grown by SEL process are of the chalcopyrite structure. This is confirmed by the presence of the main diffraction peaks in their XRD spectra: (112), (211), (220/204) and (312/116).

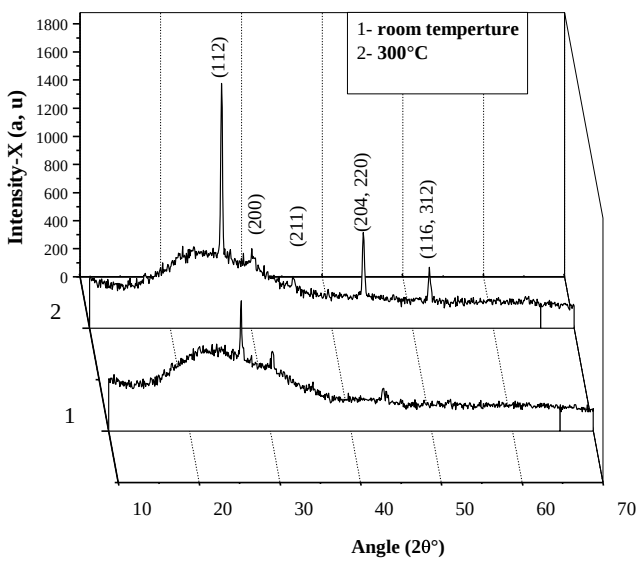

Figure 4: XRD 2θ/θ scan of a $CuInS_2$ film grown on glass substrate after annealing.

Thus, XRD indicates that the film contains no secondary phase. Although substrate temperature had a dramatic influence over morphology as described above, it had little impact on the underlying orientation. Both samples were polycrystalline and displayed a high degree

of (112) orientation. At the temperature of 300°C the FWHM becomes smaller and the signal from the (112) orientation is the strongest as shown in figure 4. The broadening of the XRD peaks is mainly related to the size of grains. Because the grain size is of the order of nanometers, its effect on peak broadening obscures the much smaller broadening effect because of the size of the starting material, which is in the micron range. Hence, XRD broadening was not used to measure the grain size; instead, direct measurements were made from SEM graphs.

Figure 5 depicts the glancing incident x-ray diffraction (GIXRD) scans at incident angles of 0.2º, 0.5° and 1.5º for the best layer. Figure 5 show GIXRD measurements of the diffraction patterns of (112) peak of the sample deposited at 300°C. The set of GIXRD patterns reflect the uniformity of the film. The scattering volume decreases with decreasing incidence angle. The main feature in the patterns is therefore a decreasing intensity for smaller incidence angle, besides these, no significant changes and no additional peak are found in the scans.

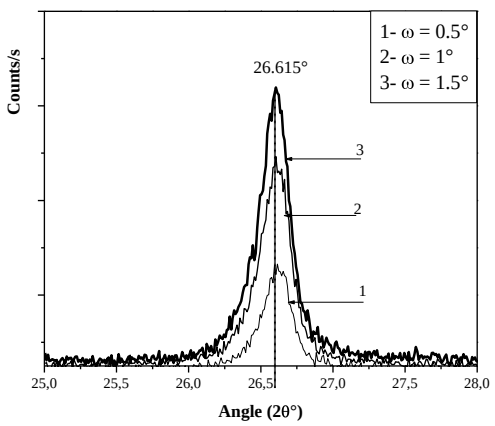

Figure 5: Grazing-Incidence X-Ray Diffraction (GIXRD) patterns of the (112) peak of sample prepared by SEL method at Ts= 300°C.

The optical characteristics of the layers were obtained by means of transmittance measurements at room temperature. To estimate the energy gap Eg we have plotted $(\alpha h\nu)^2$ versus hν and extrapolated the linear part of the curves to an intercept on a photon energy axis, yielding the band gap of CIS layer crystals. Figure 6 shows the variation of band gaps with the substrate temperature onto glass. The figure depicts that values increase with increasing substrate temperature. The values obtained for $CuInSe_2$ films at room temperature (empty triangles) and T_S = 300°C (empty squares) are 0.95 and 1.01 eV, respectively, which lie in the reported range of values for $CuInSe_2$ [9, 10].

Cu/In/Se/Se on Si (100) substrat

The X-ray diffraction pattern of the CIS sample prepared by the conventional SEL method on Si (100) substrate is shown in figure 7. Phase identification in thin films can be accomplished by determining the d-spacings of the phases present in the film and comparing them with the d spacings of the known phases compiled by the Joint Council for Powder Diffraction Studies (JCPDS). X-ray patterns were analysed by MAUD program [11], which is based on the Rietveld method [12] combined with a Fourier analysis. This method thus allows the refinement of the structural and microstructural parameters, the lattice parameters and the size of crystalline domains.

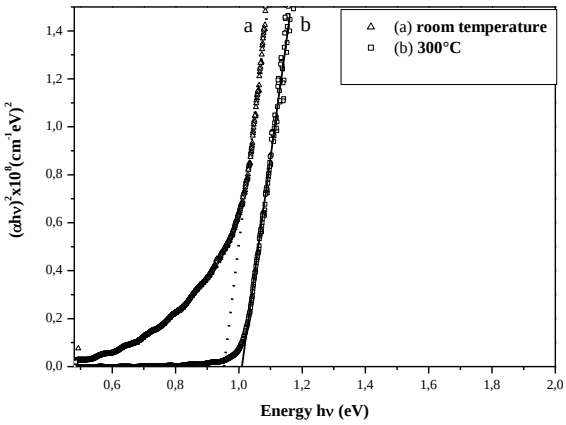

Figure 6: Plot of $(\alpha h\nu)^2$ vs photon energy hν of $CuInSe_2$ layers: (a) at room temperature and (b) at 300°C after annealing at 450°C.

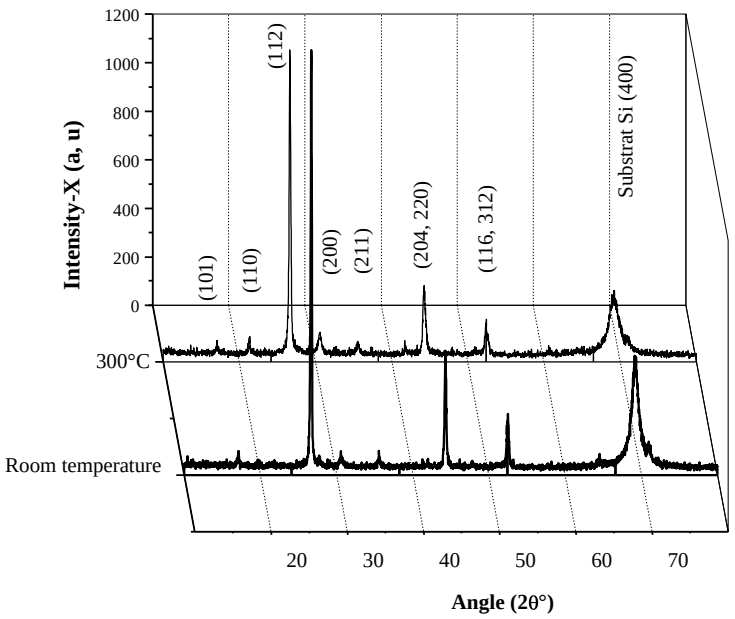

Figure 7: XRD 2θ/θ scan of a $CuInSe_2$ epitaxial film grown on [100] oriented Si Substrate.

The principal peak of $CuInSe_2$ phases in thin films is the (112) peak. The (204) and (220) peaks are the next strongest peaks, followed by (312) and (116). All of these peaks and with (101), (211), (105) and (301) characteristic peaks which they had low intensity, of the CIS prepared by the SEL can be indexed on a basis of a tetragonal unit cell having lattice parameters listed in table I.

Sample	a(nm)	b(nm)	c/a	Thickness (nm)	Structural formula	Grain size(nm)	Cu/In
Room temperature	0.5772	1.1621	2.0132	609.0	$Cu_{0.73(7)}In_{0.85(5)}Se_{2.34(7)}$	37.5	0.64
T_S=300°C	0.5777	1.1602	2.0083	946.8	$Cu_{0.80(4)}In_{0.85(3)}Se_{2.50(7)}$	78.5	0.91

Table I: Crystallographic parameters of CIS on Si (100) substrate from the Rietveld analysis (Maud program).

These values are a little smaller than the reported lattice constants of a chalcopyrite-type CIS of JCPDS number 40 - 1487, a_c=0.5782(1) nm and c_c=1.1619(1) nm. As expected, the substrate temperature during evaporation critically influenced the structural properties (morphological features and formation of crystalline phases) of the thin film and showed that the annealing process reduced the full width at half-maximum (FWHM) value from 0.24 to 0.16° indicating a change in both film composition and microstructure.

If we compare RX results obtained from comparable Cu/In/Se/Se on different substrates. We remark that there is a striking difference between the XRD of non stœchiometric CIS layers grown on Si (figure 7) and those ones CIS (figure 4) on glass substrate. Additionally, the XRD spectra observed from CIS on Si substrate is practical identical to those reported in [13, 14] prepared with the same technique and without excess of Se.

CONCLUSION

We have shown in this work that the control of substrate temperature T_s can be used to obtain $CuInSe_2$ thin films after annealing, produced by SEL technique, with suitable properties: formation of Chalcopyrite structure with big grains and preferentially oriented [112] and with direct band gap.

The result indicates also that the CIS sample prepared by the SEL method on Si (100) has the good crystallinity as well as the sample synthesized by the conventional methods (cooevaporation or flash). The crystallographic parameters and chemical formula of the CIS on Si substrate prepared by the SEL technique were determined by the Rietveld analysis using X-ray diffraction data. From the analysis of chemical composition, the $CuInSe_2$ crystals were found non-stoichiometric compounds

REFERENCES

1. Ran, U, Schock, W: Appl. Phys., A Mater. Sci. Process. 69 (1999) 131.
2. Contreras, M.A. et al. : Prog. Photovolt: Res. Appl. 13, (2005) 209.
3. Ramanathan, K.R, Contreras, M.A,. Perkins, C.L, Asher, S, Hasoon, F.S, Noufi, R: Prog. Photovolt. Res. Appl. 11 (2003) 225.
4. Mitchel, K: In Soar Cells and their applications, Edited by L. D. Partain, Wiley, New York 1995, p.1995.
5. Neelkanth, G, Dhere, M, Lourenco, C and Dhere, R.G: Solar Sells, 13, (1984) 59.
6. Benslim, N, Maasmi, A, Mahdjoubi, L and Gouskov, L: 11th European Photovoltaic Solar Energy Conference, Switzerland , Montreux, 12-16 0ctober 1992, p. 890.
7. Don, E. R, Hill, R and Russell, G. J: Solar Cells 15, (1986) 131.
8. Shafarman, W. N. and Zhu, J: in Mat. Res. Soc. Symp. Proc., 668, H2. (2001) 3.
9. Jaffe, J.E, Zunger, A: Phys. Rev. B 29 (1984) 1882.
10. Zhang, S.B, Wei, Su-Huai,Zunger, A, Katayama-Yoshida,H: Phys. Rev. B 57 (1998) 9642
11. Lutterotti, L: MAUD CPD, Newsletter (IUCr) 24 (2000).
12. Rietveld, H.M: *J. Appl. Cryst.* (1969). **2**, 65-71
13. Bechiri, L, Benabdeslem, M, Benslim, N, Djekoun, A, Otmani, A, Mahdjoubi, L, Madelon, R, Ruterana, P and Nouet, G: Catalysis Today, Volume: 113, Issue: 3-4, April 15, 2006.
14. Merdes, S, Bechiri, L, Benabdeslem, M, Benslim, N, Madelon, R, Nouet, G, Sano, M, and Ando, S: Japanese Journal of Applied Physics Vol. 45, No. 3A, 2006, pp. 1495-1499

FORMATION OF BALL MILLED $CuIn_{0.25}Ga_{0.75}Se_2$ NANOPARTICLES. MICROSTRUCTURAL CHARACTERISATION USING X-RAY DIFFRACTION LINE BROADENING

M. Benabdeslem[1], F. Hamida[1], A. Bouasla[1], S. Mehdaoui[1], N. Benslim[1], O. Aissaoui[1], L. Bechiri[1], A. Djekoun[2], X. Portier[3]

1: Laboratoire d'Etude des Surfaces et Interfaces de la Matière Solide (LESIMS), Université Annaba 23000, Algérie

2: Laboratoire LM2S, Université Annaba 23000, Algérie

3: ENSICAEN/SIFCOM. UMR CNRS 6176, Université, 6-Boulevard du Maréchal Juin 14050, Caen, France

ABSTRACT

Nanocrystalline $CuIn_{0.25}Ga_{0.75}Se_2$ alloy powders have been prepared by mechanical alloying using high-energy ball milling. The formation and the structural properties have been investigated by X-ray peak broadening analysis. In the XRD patterns, characteristic peaks similar to that of tetragonal chalcopyrite are observed. The crystallite size and lattice strain, for $CuIn_{0.25}Ga_{0.75}Se_2$ nanoparticles have been estimated by Scherrer's equation and by Williamson–Hall (W–H) plot from powder X-ray diffraction data. It is found that the average crystallite size measured by W–H plot method is in good agreement with TEM results. The scanning electron microscopy (SEM), show that for short milling times, the welding effect overrides the fracture phenomenon and by increasing milling time, the refinement of the structure continues. The TEM results confirm the nanometric nature of $CuIn_{0.25}Ga_{0.75}Se_2$ powders with an average size in the range [50-100] nm.

INTRODUCTION

Ternary and quaternary semiconductors are promising as absorber materials because of their high-efficiency and potential for low-cost production. Solar cells utilizing $Cu(In,Ga)Se_2$ (CIGS) have recently reached 20.3% efficiency, which is the highest efficiency ever reported for a thin film solar cell [1]. Of additional importance, solar cells based on CIGS absorber material are sufficiently stable to radiation exposures without ant degradation problems [2]. Many kinds of processes have proven their suitability for large-scale $Cu(In,Ga)Se_2$ deposition including the coevaporation from individual sources [3], physical vapour deposition [4], electrodeposition [5], selenization of metallic Cu/In layers [6] and by flash evaporation [7]. In recent years, much attention has been paid to the synthesis and investigation of nanoparticles. The controlled particle size and morphology facilitate the desired characteristics in the materials. A non vacuum technique called mechanical alloying (MA) has received considerable interest in material science. This technique has been used by several research groups to synthesize $CuInSe_2$ [8-10], $CuIn_{0.7}Ga_{0.3}Se_2$ [11], $CuIn_{1-x}Al_xSe_2$-$CuInS_2$ and ZnS [12] powders. Mechanical alloying is a processing technique adapted to form nanostructured materials from blended elemental powder mixtures. This technique is considered as a solid-state powder processing involving repeated fracturing and welding of powder particles in a high-energy ball mill. The present work describes the experimental results obtained on the $CuIn_{0.25}Ga_{0.75}Se_2$ powders prepared by mechanical alloying. A comparative evaluation of the mean particle size of nanoparticles obtained from direct TEM measurements and from powder XRD procedures is been reported. The strain associated with the as-prepared $CuIn_{0.25}Ga_{0.75}Se_2$ powders has been estimated by Williamson-Hall model.

EXPERIMENTAL

Polycrystalline ingot of $CuIn_{0.25}Ga_{0.75}Se_2$ has been grown by vacuum fusion of stoichiometric mixture of elemental starting materials Cu, In, Ga and Se. The product has been introduced into a specially cleaned and prepared quartz tube and pumped down to a vacuum of 4.10^{-6} Torr and sealed off to form an ampoule, closed at both ends. The sealed ampoule with its charge of

elements has been placed in a resistance .furnace where the temperature has been first increased to 220°C at the rate of 20°C/h to allow the selenium and indium to react together exothermically. The temperature has been then raised to 1100 °C above the melting point of the compound to be grown. The melt has been then maintained for 24 h with mechanical vibrating to enable the compound synthesis to be completed and to ensure compositional homogeneity of the mixture. At the end of the process, the ampoule has been cooled by decreasing the lower furnace temperature at a controlled rate of approximately 4°C/h. Crystals intended for mechanical alloying have been extracted from the central zone of the ingot which is considered as the best zone. The starting powders and 12 mm diameter steel balls have been loaded into steel container inside an argon gas filled in glove box. The ratio of the weight of the balls to the powder has been maintained at 20:1. The milling process has been conducted in a planetary ball mill (Fritsch P-7) under a rotational speed of 250 tr/mn and milling periods of 1h and 3h. The structural state of the as-milled powders have been given by X-ray diffraction measurements (XRD) by means of a Philips diffractometer with a Cu K_α radiation (λ = 1.541837Å) at 40 kV and 40 mA settings. The crystallite size and lattice strain in the powder particles can be determined .from peaks broadening. As milled powder particles were cold-pressed in the form of circular wafers of 10 cm in diameter and 0.5 mm in thickness by isostatic pressing at 7tn/cm^2. The compacted samples have been characterized by energy dispersive spectroscopy (EDS) for the chemical composition and scanning electron microscopy (SEM) for surface observation at incident electron energy of 20 kV using a JSM Jeol 6400-scanning microscope. Transmission electron microscopy (TEM) image has been taken on a JEOL 2010 transmission electron microscope at 200 kV accelerating voltage.

RESULTS

Structural analysis

Figure 1 shows the X-ray diffraction patterns of the unmilled mixture and ball milled samples recorded by the XRD method. All of the peaks of the $Cu_{0.25}Ga_{0.75}Se_2$ corresponding powders have been indexed on a basis of a tetragonal unit cell in comparison with JCPDS cards. The main characteristic peaks (112), (204/220) and (116/312) reported in the diffraction patterns, confirm the chalcopyrite-type structure of the Cu(In,Ga)Se_2 material. Secondary phase ascribed to InSe has been also detected. During the early stage of milling, the characteristic peak of InSe gradually decreases in amplitude and after 3 h of milling there is no trace of reflections of InSe. It is also observed from figure 1, that XRD patterns of the milled powders show a broadening of the diffraction peaks and a decrease of their intensities. This type of observation is quite common in mechanosynthesized nanomaterials and may be attributed to the reduction in crystallite size and to the internal stresses induced by the mechanical milling. With increasing milling times, the evolution of the (112) lines show a shift towards lower angles and this is due to the expansion of the lattice on CIGS alloy formation.

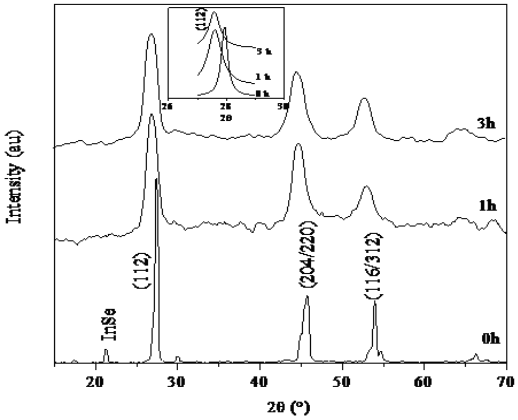

Figure 1: Experimental XRD diffraction patterns of $CuIn_{0.25}Ga_{0.75}Se_2$ for various milling times

Taking into account the quadratic form for the tetragonal system, the lattice constants a and c of $CuIn_{0.25}Ga_{0.75}Se_2$ unit cell, have been determined from:

$$\frac{1}{d^2} = \frac{h^2 + k^2}{a^2} + \frac{l^2}{c^2} \quad (1)$$

h, k, and l are the Miller indices corresponding to a particular diffraction peak at an X-ray incident angle θ. The results obtained are a little smaller than the reported lattice constants of a chalcopyrite-type $CuInGaSe_2$ [13-14]. The relationship between the lattice constants and the milling time in the $CuIn_{0.25}Ga_{0.75}Se_2$ alloy is shown in figure 2. It is observed that milling gives rise to larger lattice parameters. The expansion of lattice parameters with milling time is due to the disordering of the alloy and can also be explained by the increase of internal strain induced by ball milling. For long milling period, the observed plateau can be attributed to a solubility limit and therefore crystallite size become less dependent on milling time.

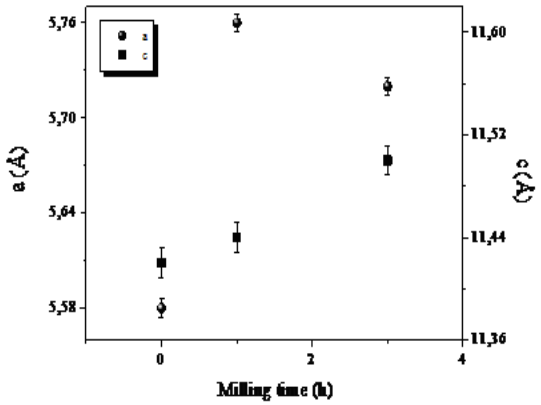

Figure 2: Milling time dependence of the $CuIn_{0.25}Ga_{0.75}Se_2$ lattice parameters.

The crystallite size D for the intense peak (112) was first estimated using the Scherer equation as follows:

$$D = \frac{k.\lambda}{\beta.\cos\theta} \quad (2)$$

where k = 0.9 (assuming the particles are spherical in shape), λ, ß and θ are the X-ray wavelength, Bragg diffraction angle, and the full width at half maximum (FWHM) of the diffraction peak, respectively. In the Scherrer's formula, large crystallite size values are obtained as a result of neglecting the microstrain components in the Scherrer equation. There is a significant difference between crystallite sizes obtained by the Scherrer analysis and the TEM analysis. The crystallite size values were then compared with those deduced from the Williamson–Hall model and TEM analysis results. Furthermore, it is known that FWHM is represented by the sum of the contributions of crystallite size and strain present in the compound. Assuming that the strain present in the material is uniform, thus considering the isotropic nature of the crystal, the average crystallite size and lattice strain were calculated using the Williamson–Hall (W-H) equation [15] for the total peak broadening:

$$\beta.\cos\theta = \frac{k\lambda}{D} + 4\varepsilon\sin\theta \quad (3)$$

where ε is the average internal strain

In both methods, the lines broadening are assumed to be Lorentzian profile. In W-H method, the effective particle size taking strain into account is estimated by plotting β.cosθ vs. 4.sinθ. For the experiment, the plot was drawn only for the (112), (204) and (116) planes. The curve β.cosθ vs. 4sinθ shows approximately a linear variation as seen in figure 3.

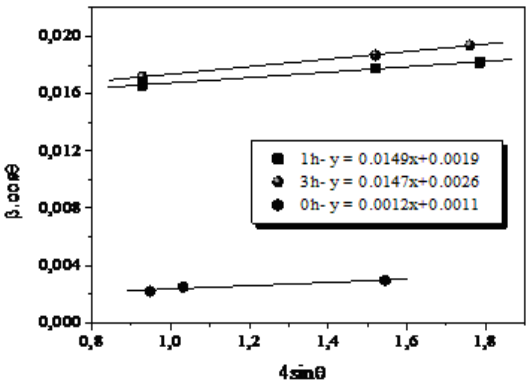

Figure 3: William-Hall plots of nanocrystalline $CuIn_{0.25}Ga_{0.75}Se_2$

The crystallite size and strain are calculated using a linear equation y=εx+1/D. The strain may be estimated from the slope of the line and the crystallite size from the intersection with the vertical axis. The average crystallite size obtained from Scherrer's formula and W–H analysis shows a variation, this is because of the difference in averaging the particle size distribution. In comparison, there is a good agreement between the crystallite size values obtained by W–H model and that obtained by TEM analysis. Figure 4 shows that with increasing milling time, the crystallite size decreases, while the internal strain increases (figure 5).

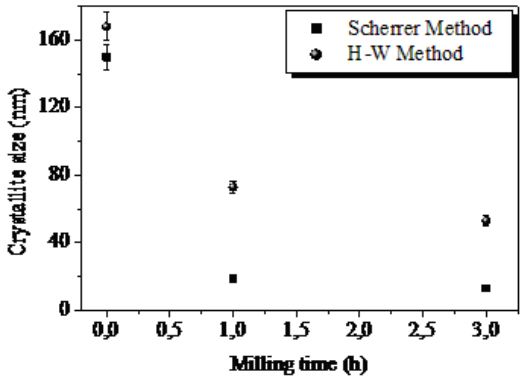

Figure 4: The variation of average crystallite size obtained by Williamson-Hall and Scherrer method at different milling times

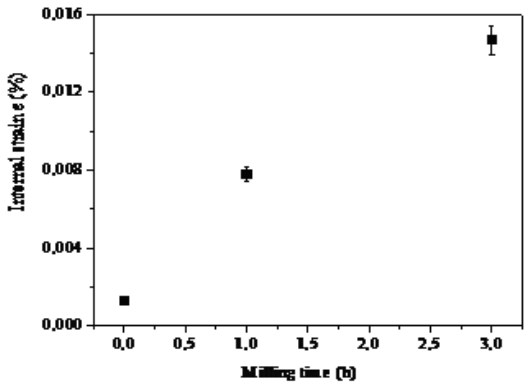

Figure 5: The variation of internal strain of $CuIn_{0.25}Ga_{0.75}Se_2$

This behaviour is explained by the formation of defects during the milling process. The positive slopes for the milled powders indicate the presence of tensile strain in the crystal lattice. From the W–H plots, it is observed that the better fit of the experimental data points confirms the uniformity of the lattice strain. Current analysis demonstrates that the Williamson- Hall formula is the most suitable to determine the size of crystallite and strain variance in the CIGS powders.

Morphological analysis

During the initial stage of ball milling, particles are formed for short milling time as shown in figure 6a. At this stage, the fracture process result in fragmentation particle fracture. The mixture is composed of dispersed particles with a size in the range [0.05-10]µm. Some particles are composed of large agglomerate states of crystallites as shown in figure 6b. With increasing milling time, welding becomes the predominant mechanism. The particles change into a large platelet shape as seen in figure 6c. For milling period of 3h, the large amount of fine particles is reduced and their agglomeration leads to the formation of particles with a wider size distribution as a consequence of a better weldability.

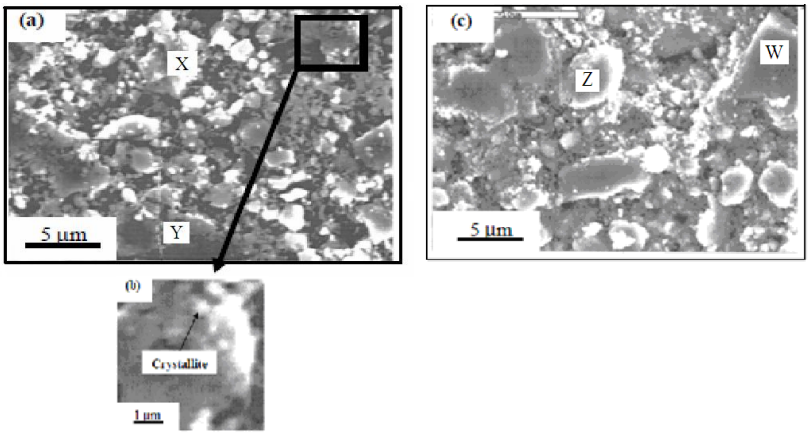

Figure 6. SEM micrographs of the $CuIn_{0.25}Ga_{0.75}Se_2$ powder for different milling times.

TEM observations

Bright field TEM has been employed to further examine the nanocrystalline nature crystal of the produced powders. The TEM micrographs reported in figure 7 show the aggregated nature of nanoparticles with size [50-100] nm and an average lattice parameter of 0.58 nm.

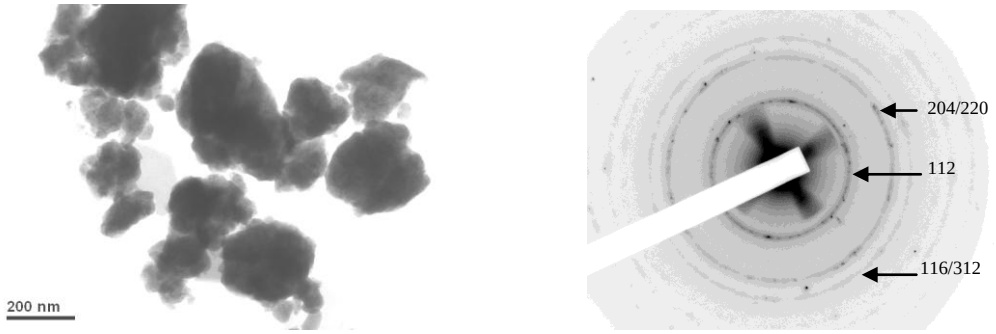

Figure 7 : TEM images of $CuIn_{0.25}Ga_{0.75}Se_2$ nanoparticles.

Composition analysis

The global chemical composition of $CuIn_{0.25}Ga_{0.75}Se_2$ powder milled for 1h is Cu: In: Ga: Se: O = 31.06 at.%: 15.64 at.%: 5.02 at.%: 37.75 at.%: 10.53 at.% whereas for 3h this composition is Cu: In: Ga: Se: O = 36.57 at.%: 15.09 at.%:5.65 at.%: 35.18 at.%: 7.51 at.% and correspond respectively to the chemical formula $Cu_{124}In_{0.62}Ga_{0.2}Se_{1.40}$ and $Cu_{1.46}In_{0.6}Ga_{0.22}Se_{1.40}$. Both powders showed deviation from the ideal stoichiometry. The sticking to the stainless vial wall of selenium and indium could explain their amounts decrease. To check the homogeneity of the composition, different selected particles labeled X, Y, Z and W have been analyzed as shown in

figure 6. As reported in table I, the elemental composition reported differs from a particle to another. To complete the refinement of the powders and to form chalcopyrite structure with the desired properties more milling times are required to achieve a steady state between the fracturing and cold welding mechanisms. Chemical analysis of the mechanically alloyed powders shows also the presence of oxygen. The presence of this element is due to the oxidation of the starting ingot. The composition analysis shows that the oxygen content decreases for long period milling as well for the global composition as for the particles.

Table I: Results of local composition analysis

	1h – Composition (at.%)						3h – Composition (at.%)				
	[Cu]	[In]	[Ga]	[Se]	[O]		[Cu]	[In]	[Ga]	[Se]	[O]
X	30.02	20.56	4.06	45.36	-	Z	27.31	13.85	6.45	40.68	11.71
Y	28.06	15.64	5.02	37.75	13.53	W	50.23	18.08	2.96	24.43	4.30

CONCLUSION

Nanocrystalline $CuIn_{0.25}Ga_{0.75}Se_2$ in the range of 50–70 nm has been prepared by dry mechanical alloying technique in a high energy planetary ball mill. XRD diffraction patterns of the as milled powders show that the main phase is the chalcopyrite. Ball milling process leads to an expansion of the tetragonal unit cell and a decrease in crystallite size. Williamson–Hall model results in more accurate estimation of crystallite size compared to Scherrer analysis. The crystallite size and the lattice strain values obtained from the Williamson–Hall model can be further extended to estimate the dislocation densities present in the material. Composition measurements reveal a deviation from the ideal stoichiometry and on the other hand inhomogeneous distribution of the elemental constituents has been detected in individual grain.

REFERENCES

1. New world record with efficient CIGS solar cell, Zentrum für Sonnenenergie-und Wasserstoff-Forschung, Stuttgart, Press release, 2010
2. Rau, U, Jasenek, A., Shock, H. W, Werner, J. H., LaRoche, G, Robben, A, Bogus, K: Proceedings. 28th Photo. Spectr. Conference, pp 1032, 2000
3. M. Powalla and B. Dimmler: Proceedings of the 3rd World Conference on Photovoltaic Energy Conversion, Vol 11–18, pp 566, May, 2003
4. Hashimoto, Y, Kohara, N, Negami, T, Nishitani, M, Takahiro, T, , Jpn. J. Appl. Phys, Vol 35, pp. 4760- 4764, 1996
5. Guimard, D, Bodereau, N, Kurdi, J, Guillemoles, J.F, Lincot D, Grand, P.P, BenFarrah, M, Taunier, S, Kerrec, O, Mogensen, P: Proceedings of the 3rd World Conference on Photovoltaic Energy Conversiom, Vol 11–18, pp 515, May, 2003
6. Kushiya, K, Yamase, O: Jpn. J. Appl. Phys, Vol 39, pp 2577- 2582, 2000
7. Klenk, M, Schenker, O, Alberts, V, Bucher, E: Thin Solid Films, Vol 387, pp 47-49, 2001
8. Otani, T, Motoki, M, Koh, K, Ohshima, K,. Mater. Res. Bull, Vol 30, pp 1495-1504, 1995
9. Wu, S, Xue, Y, Zhang, Z: Journal of Alloys and Compounds, Vol 491, pp 456-459, 2010
10. Wada, T, Kinoshita, H, Kawata, S: Thin Solid Films, Vol 431/432, pp 11-15, 2003
11. Suryanarayana, C, Ivanov, E, Noufi, R, Contreras, M. A, Moore : J. J, Mater. Res, Vol 14, pp 377-383, 1999
12. Abdel Rafea, M, Roushdy, N,: Chalcogenide Letters, Vol 5/10, pp 219-227, 2008
13. Deeva, A. N, Valeeva, R. G, Gil'Mutdinova, F. Z, Gaia, D. E: Journal of Surface Investigation, X-ray, Synchrotron and Neutron Techniques, Vol 1, pp 40–43, 2007
14. Mansour, B. A, El Zawwawi, I. K, Shaban,: H. Journal of Materials Science: Materials in Electronics, Vol 14, pp 63-68, 2003
15. Williamson, G. K, Hall, W. H, J.: Acta Metall, Vol 1, pp 22–31, 1953

NANOMATERIALS FOR ADVANCED GLAZING TECHNOLOGIES

Tao Gao[1]; Bjørn Petter Jelle[2,3]; Arild Gustavsen[1]

1: Department of Architectural Design, History and Technology, Norwegian University of Science and Technology, NO-7491 Trondheim, Norway.

2: Department of Materials and Structures, SINTEF Building and Infrastructure, NO-7465 Trondheim, Norway.

3:Department of Civil and Transport Engineering, Norwegian University of Science and Technology, NO-7491 Trondheim, Norway.

ABSTRACT

As the interest increases in the concept of zero energy buildings that do not consume any non-renewable energy from the utility grid, improving the energy efficiency of buildings has been attracting great attention. Windows may constitute some 50% of the total energy loss through the building envelope due to their poor thermal insulation property, and may, therefore represent a crucial bottleneck in this field. Several technologies are currently being researched to improve the energy efficiency of windows, including low-emissivity coatings, vacuum windows, aerogel windows, and gas-filled windows. However, the properties of these window products are static and can not change according to seasonal and daily solar radiation and temperature variations. One way to improve the energy efficiency of buildings would be to develop dynamic glazing systems such as electrochromic (EC) smart windows, which can change the solar radiation throughput (both visible and near infrared) by application of an external voltage, e.g. taking advantage of passive solar heat gain in winter and rejecting unwanted solar radiation in summer. The application of EC smart windows may provide opportunities to maximize energy efficiency of buildings by reducing a certain amount of heating, cooling, and lighting loads.

The success of EC smart windows and also other highly insulating window products depends not only on the potential benefit that will be realized by the end user, but also by a sophisticated design and selection of materials to make the device durable and affordable. So far, the manufacture cost associated with some of these high performance windows is high and appears to be an inhibiting factor for their large-scale applications. The past couple of decades have witnessed an exponential growth of activities in nanotechnology, which contribute to a variety of technical applications ranging from microelectronics to constructions. We address here the recent progress on advanced glazing technologies for energy efficient buildings, with emphasis being given to the application of nanomaterials in low-emissivity coatings and EC smart windows.

KEYWORDS: Glazings, Energy Efficiency, Nanotechnology, Electrochromism

1. INTRODUCTION

In recent years, there is an ever increasing interest in zero energy buildings—a residential or commercial building with greatly reduced energy needs through efficiency gains such that the balance of energy needs can be supplied with renewable technologies. Obviously, improving the energy efficiency of buildings is very important. Buildings consist of various structural or functional materials and components, such as windows, walls, and roofs; each of them has rather different energy features and plays different but important roles on the overall energy efficiency of the buildings.

Windows as a building element allow light, solar energy and fresh air to promulgate the living area and offer an indoor–outdoor interaction, thus having a large impact on occupant comfort. Windows have also an impact on the energy efficiency of buildings, e.g., up to about 50% of the total energy loss through the building envelope coming from its windows. The thermal insulation of windows remains a bottleneck compared with walls and roofs in the building envelope. For example, walls have a typical U-value (a measure of the heat lost due to indoor-outdoor temperature differences) of about 0.1–0.2 W/(m^2K), whereas today's efficient double-glazed windows with low emissivity (low-e) coatings have a U-value of about 1.2 W/(m^2K) [1]. So far, several window innovations have been developed to produce highly insulating window glazings [2]; many efforts have been dedicated to the development of an insulating glass unit with a U-value of 0.5–0.7 W/(m^2K) to meet the requirement of zero energy buildings. Such windows can now be achieved with multilayered gas-filled low-e windows [2] or aerogel glazings [3]. However, these window products are costly for most applications.

Recent research has indicated the promising potential of dynamic window systems (i.e. smart windows) [4]. A smart window may optimize its solar-gain characteristics according to ambient conditions, e.g., taking advantage of passive solar heat gain in winter (or cold weather) and rejecting unwanted solar radiation in summer (or hot weather). Smart windows may also control glare and improve the indoor thermal and visual comfort. Various materials and technologies have so far been tried for smart windows, where electrochromic (EC) materials that exhibit a reversible color change induced by an externally applied electric voltage probably represent the most promising candidate [4]. Many industrial institutions have been investigating EC smart windows, and commercial products are starting to emerge. However, most EC smart windows on the market are still rather small in size compared to most glazing requirements and are also quite expensive.

Though not specifically analyzed in this paper, we believe that high performance window systems, i.e., highly insulating windows and dynamic glazing systems are helpful for fulfilling the vision of zero energy buildings. In this paper, we outline the status of current window innovations and address the applications of nanomaterials in high performance windows.

2. NANOTECHNOLOGY AND NANOMATERIALS

The past couple of decades have witnessed an exponential growth of activities in nanotechnology dealing with small-sized materials with typical dimensions of 0.1–100 nm. Due to their small size and large surface area, nanomaterials usually exhibit new or improved properties that are different from those seen in the corresponding bulk counterparts, hence contributing to a variety of technical applications ranging from microelectronics to constructions [5].

The majority of nanotechnology research in construction has been focused on cement-based materials, although a variety of nanomaterials may have beneficial applications in high performance windows that encompass various functional coatings (Table 1). Despite the relatively high cost of nanomaterials, their applications in high performance windows—and elsewhere in the construction sector—is likely to increase because of (1) highly valuable properties can be achieved at relatively low dosage of nanomaterials and (2) decreasing cost of nanomaterials as they are produced in larger quantities. Moreover, nanomaterials with small featured sizes are ideal for large-area and large-scale window applications, where many cost-effective wet chemical approaches such as dip coating and layer-by-layer assembly can be employed.

Table 1: Selected examples of nanomaterials for window glazings.

Nanomaterials	Expected Benefits	Ref
SiO_2 nanoparticles	anti-reflection coatings	[6]
TiO_2 nanoparticles	self-cleaning coatings	[7]
WO_3 nanoparticles	chromogenic films	[8]
SnO_2(F) nanoparticles	low-e coatings	[9]
Aerogel	thermal insulating glass	[3]

Since the applications of nanomaterials are mostly dependent on their properties, the research dedicated to fundamental issues such as the structure-property relationship is of importance. It is worth pointing out that the control of composition, size and morphology at nanometer scale may lead to a myriad of possibilities (Figure 1), whereas it also results in a certain complexity in understanding the involved thermodynamics and/or kinetics [10]. Note that the small sizes and large surface area of nanomaterials may endanger their durability/stability during the operation. This is of primary concern because windows are intended to last for 20–50 years. Moreover, the safety and environmental effects of nanomaterials need to be evaluated. Obviously, there are many opportunities and challenges for the application of nanomaterials in the window sector.

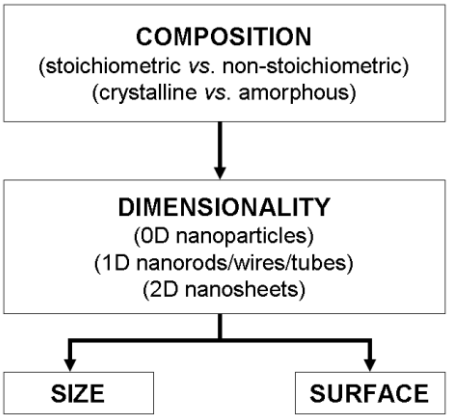

Figure 1: Properties of nanomaterials depend on various parameters, among others, composition, dimensionality, size, and surface.

3. ADVANCED WINDOW TECHNOLOGIES

3.1 Low-Emissivity Windows

Developed during the 1970s and 1980s, low-emissivity (low-e) windows have significantly reduced window-related energy use and peak demand [11]. Windows with low-e coatings typically cost about 10–15% more than regular windows, but they can reduce energy loss by as much as 30–50%. By reflecting long-wave radiant energy, low-e glazings can reduce the radiative heat transfer, thereby reducing the windows' U-values. Although valuable in all climates, low-e windows with reduced U-values are most useful in cold climates where the heating load dominates the energy use.

Low-e coatings must have low emissivity in the infrared wavelength range and high transmittance in the visible range; moreover, the coatings should have a low luminous reflectance and preferable be essentially colorless (for most applications, but wishes from the architect may result in other specifications). Low-e coatings in practice generally comprise an ultrathin metallic layer, in particular Ag, for infrared reflectance and low emissivity, sandwiched between dielectric layers of metal oxides to reduce the visible reflectance. Adhesion layers and/or protection layers are also commonly applied to ensure the durability of the coatings. A typical multilayered structure of low-e coatings is illustrated in Figure 2.

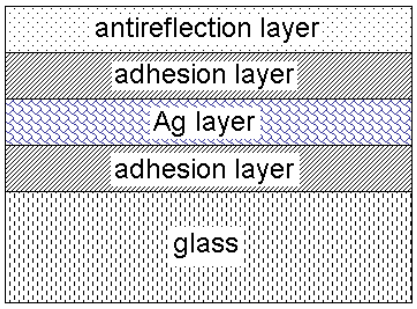

Figure 2: Multilayered structure of low-e coating on glass.

The multilayered low-e coatings are usually prepared by sputtering or chemical vapor deposition, which can be performed with either online process with flat-glass production or offline coating with more possibilities, such as the use of new materials or the formation of new structures. The use of nanoparticles as low-e and/or dielectric layers may open possibilities for high performance and cost-effective products. For example, recent progress indicates the excellent antireflection properties of mesoporous SiO_2 nanoparticles [6]. We are currently investigating the application of Ag nanoparticles as low-e layer and the results will be reported in subsequent work.

3.2 Gas-filled Low-Emissivity Windows

Gas-filled low-e highly insulating windows have usually three glazing panes. These windows are available today and can reach an insulation value of insulating glass unit with a U-value of 0.5–0.7 W/(m^2K) [2]. Challenges in this field include increased costs, increased weight and thickness, and the leakage of gas fillings as the cavities between two layers of glass are usually filled with low conductivity gases such as argon (Ar) or krypton (Kr) instead of air.

3.3 Vacuum Windows

Since vacuum can eliminate all conduction/convection between two layers of glass, vacuum windows may offer theoretically high insulating glazings. In practice, however, the performance of vacuum windows is compromised by various parameters, such as the thermal bridge through the frames/spacers and the gas (water and air) diffusion. Vacuum glazings are commercially available in Japan and a U-value of about 1 W/(m^2K) for the centre-of-glass area has been reported [2].

3.4 Aerogel Windows

Aerogel is a porous solid consisting of SiO_2 matrix and nanopores of diameters about 20 nm. Aerogel is a very low-density silica-based solid (2-3 mg/cm^3) composed of up to 99.8% air. It has high compressive strength and very low thermal conductivity (~ 0.01 W/mK). Moreover, aerogels can be produced as either opaque, translucent, or transparent materials, thereby enabling a wide range of building applications.

Aerogel windows consisting of a 15-mm-thick aerogel layer sandwiched between two glass panes has been reported [3], where the windows transmit 76% of the visible light and have an average U-value of about 0.72 W/(m^2K), which is very promising compared to multilayered low-e windows. In this field, minimizing manufacturing costs remains a major challenge. Aerogel windows in some/most cases have a translucent appearance, which may represent an excellent way to reduce direct light transmission and glare, dispersing natural full spectrum light evenly within a space, e.g., classroom (Figure 3). However, such window glazings may show limitation when a clear view is required.

Figure 3: A comparison between clear windows (left) and translucent aerogel windows (right).

3.5 Electrochromic Smart Windows

The properties of highly insulating glazings such as aerogel windows are static and usually provide less-than-optimal performance. For example, an insulating window that reduces solar gain will lower summer cooling energy consumption but also reduce the solar gain that can significantly offset wintertime heating costs. In this regard, dynamic glazing systems such as electrochromic (EC) smart windows offer obvious advantages [2,4,11].

An EC smart window is an electrochemical cell integrated in or attached to a window glazing and consists of various functional components (Figure 4). The optical switching part has an EC layer, an electrolyte, and an ion storage layer that can also be another EC material. Under an external voltage of the order of 1 V, an electrochemical reaction cycles between the EC layer and the ion storage media, thereby changing the overall optical properties by forming colored compounds; a voltage pulse with opposite polarity makes the device regain its original state [10].

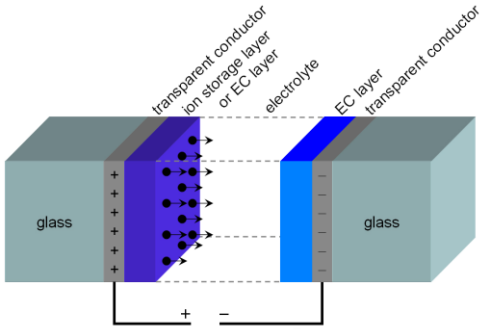

Figure 4: Architecture of an EC smart window, showing the transport of cations under an external electrical field.

For window applications, many EC materials, both organic and inorganic compounds, have been reported, where WO_3 represents the most studied compound [4]. Usually, the amorphous WO_3 have better EC performance than the crystalline ones, though their durability/stability remains problematic. Recent studies have demonstrated that, due to the improved crystallinity, WO_3 nanoparticles have excellent cycling stabilities compared to amorphous WO_3 [12]. Moreover, the application of WO_3 nanoparticles can lead to improved EC performance such as high coloration efficiency, high color contrast, and fast switching, indicating a promising potential for the assembly of high performance windows by using EC nanomaterials [10].

4. CONCLUDING REMARKS

The application of high performance window systems, i.e., highly insulating windows and/or EC smart windows, is helpful for fulfilling the vision of zero energy buildings. The progress depends on not only the potential benefit that will be realized by the end user, but also a sophisticated design and selection of materials to make these window systems durable and affordable. Nanotechnology in this regard may offer the possibilities for high performance and cost-effective products.

ACKNOWLEDGEMENTS

This work has been supported by the Research Council of Norway and several partners through the NTNU and SINTEF *Research Centre on Zero Emission Buildings* (ZEB).

REFERENCES

1. Gustavsen, A.; Jelle, B.P.; Arasteh, D.; Kohler, C.: State-of-the-art highly insulating window frames–research and market review. Project Report 6, SINTEF Building and Infrastructure, 2007.
2. Arasteh, D.; Selkowitz, S.; Apte, J.; LaFrance, M.: Zero energy windows. Lawrence Berkeley National Laboratory: LBNL-60049, Berkeley, 2006.
3. Schultz, J.M.; Jensen, K.I.; Kristiansen, F.H.: Super insulating aerogel glazing. Solar Energy Materials and Solar Cells 89 (2005) 275–285.
4. Baetens, R.; Jelle, B.P.; Gustavsen, A.: Properties, requirements and possibilities of smart windows for dynamic daylight and solar energy control in buildings: A state-of-the-art review, Solar Energy Materials & Solar Cells, 94 (2010) 87–105.
5. Lee, J.; Mahendra, S.; Alvarez, P.J.J.: Nanomaterials in the construction industry: a review of their applications and environmental health and safety considerations. ACS Nano 4 (2010) 3580–3590.
6. Li, X.; Du, X.; He, J.: Self-cleaning antireflective coatings assembled from peculiar mesoporous silica nanoparticles. Langmuir 26 (2010) 13528–13534.
7. Paz, Y.; Luo, Z.; Rabenberg, L.; Heller, A.: Photooxidative self-cleaning transparent titanium-dioxide films on glass. Journal of Materials Research 10 (1995) 2842–2848.
8. Baeck, S.H.; Choi, K.S.; Jaramillo, T.E.; Stucky, G.D.; McFarland, E.W.: Enhancement of photocatalytic and electrochromic properties of electrochemically fabricated mesoporous WO_3 thin films. Advanced Materials 15 (2003) 1269–1273.
9. Rajala, M.; Pimenoff, J.; Hovinen, A.; Vainio, T.: Rapid growth nanoparticle low-e coating. Glass Performance Days (2007) 477–479.
10. Gao, T.; Gustavsen, A.; Jelle, B.P.: Nanoelectrochromics with applied materials and methodologies. Zero Emission Buildings–Proceedings of the Renewable Energy Research Conference, Trondheim, Norway, (2010) 61–71
11. Apte, J.; Arasteh, D.; Huang, Y.J.: Future advanced windows for zero-energy homes. ASHRAE Transactions v. 109, 2003.
12. Park, S.Y.; Lee, J.M.; Noh, C.; Son, S.U.: Colloidal approach for tungsten oxide nanorod-based electrochromic systems with highly improved response times and color efficiencies. Journal of Material Chemistry 19 (2009) 7959–7964.

THIN FILM SILICON TECHNOLOGY AND BIPV APPLICATIONS

V. Terrazzoni-Daudrix, S. Pelisset, F. Sculatti Meillaud, M. Despeisse, L. Ding, S. Nicolay, L.- E Perret-Aebi, C. Ballif

Ecole Polytechnique Fédérale de Lausanne (EPFL), Institute of Microengineering IMT, Photovoltaics and thin film electronics laboratory, Breguet 2, 2000 Neuchâtel, Switzerland

ABSTRACT

Buildings use 40% of the energy consumed in the EU and in order to reduce this consumption, the building energy standards are becoming stricter in many countries, leading to the integration of thermal insulating elements, temperature regulation systems, shading and glare protection and micro generation technologies such as photovoltaic collectors.
Many different photovoltaic technologies are available on the market. Among them, thin film silicon presents many advantages for building integration, especially for a large scale integration of photovoltaics in the future energy mix.

- No use of toxic materials,
- Low process temperature and material consumption,
- Better usage of solar spectrum than c-Si, due to multiple absorbers,
- Higher kWh/kWp output performance, due to the small temperature coefficient (-0.30 %/K) and the lower sensitivity to the angle of installation,
- No feedstock limitation,
- Aesthetic aspects,
- Compatibility with flexible substrates. (See www.uni-solar.com and www.flexcell.com in Switzerland)

The technology has the advantage to be less expensive than crystalline Si in euro/m^2, reaching already today production costs around 50€/m2.

10% stable efficiency modules are available on the market with promising perspectives demonstrated in laboratories; Record lab cells reaching 12.5% stable efficiency have been demonstrated by United Solar [1] and calculations predicting efficiencies up to 17% were presented by Krc et al at the 21st EU-PVSEC [2].

In this paper, the authors present the state of the art of thin film photovoltaics, focusing more specifically on thin film silicon. Then, some of the most important research topics on thin film silicon are discussed, as well as the latest results achieved at EPFL:

- Latest developments and results on advanced nano-structured substrates and Transparent Conductive Oxide layers,
- Some investigations and results on newly developed cell designs and deposition regimes,
- Some reliability tests performed in our laboratory, and perspective towards new encapsulation solutions.

These topics are addressed in the frame of many different projects, including two collaborative projects financed by the European Commission and involving EPFL:
- PEPPER project (http://pepper.epfl.ch/),
- The silicon-light project (http://www.silicon-light.eu/).

INTRODUCTION

PV market has become more and more important over the last decade; the awareness about the PV's capabilities grows in the public opinion and PV appears now on the energy map of several countries. According to the European Photovoltaic Industry Association (EPIA), penetration in Spain went up to 4% of the electricity production during 2010 summer and prices for large systems decreased as low as 2.5 Eur/Wp in some countries.

The total of newly installed capacity added in 2010 represents in average the electricity production of two large coal-fired power plants. In several countries, grid parity for residential systems is reachable in the coming years. In some specific cases in countries or regions with very high electricity prices, PV could already become competitive very soon.

Several photovoltaic technologies are currently investigated and developed, including crystalline silicon and various thin film approaches like CIGS, CdTe and thin film silicon.

In this paper we report on thin film photovoltaic technologies with a special focus on thin film silicon.

THIN FILM SILICON TECHNOLOGY OVERVIEW

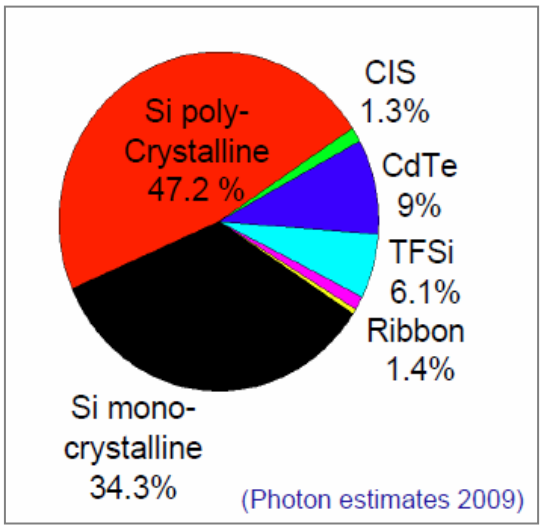

Fig. 1 : Market share of the different photovoltaic technologies

As shown on Fig. 1, crystalline silicon dominates the market. Nevertheless, three thin film technologies have become between 15 and 20% of the market in 2009 (Photon estimate 2009).

Thin film approaches are particularly attractive because they offer the prospect of low material usage, low production cost and high production throughput. Until recently, they have suffered from their relative immaturity and the lack of dedicated equipment suppliers in contrast to the well established crystalline silicon technology case but the situation is now changing.

Today, CdTe technology is the most dynamic on the market, due to the success of the American company First Solar with manufacturing costs below 0.7€/Wp.

Thin film silicon is in second position. Production costs around 0.5€/Wp were announced by the Swiss production line manufacturer Oerlikon Solar in 2010 and the technology presents many advantages such as:

- No use of toxic materials,
- Low process temperature and material consumption,
- Better usage of solar spectrum than c-Si, due to multiple absorbers,
- Higher kWh/kWp output performance, due to the small temperature coefficient (-0.30 %/K) and the lower sensitivity to the angle of installation,
- No feedstock limitation,
- Aesthetic aspects (See contribution to CISBAT 11 from Dr. L.-E. Perret-Aebi et al),
- Compatibility with flexible substrates (United Solar or Flexcell)

Several tens companies started the production of single junction and multiple junctions amorphous and microcrystalline silicon modules (over 80 worldwide and more than 25 in Europe). Among these companies Pramac Solar, Inventux Solar Technologies, Bosch Solar or

Gadir Solar in Europe commercialize amorphous or tandem microcrystalline/amorphous silicon modules reaching up to 10% efficiency (see X3-140 series from Inventux Solar Technologies). Sharp in Japan announced also 10% stable efficiency; United Solar in the US, Flexcell in Switzerland and Fuji in Japan commercialize thin film silicon flexible panels.

The challenges faced now by these companies are to prove the technologies as reliable and cost competitive when compared to the mature crystalline silicon market, to follow the aggressive cost reduction route and to resist the competition of other technology routes.

The state of the art of thin film technologies is presented in the table below.

Table 1: State of the art of thin film photovoltaics

	CdTe	CIGS	TFSi
Record lab efficiency (>1cm2)	16.7% (1cm2)	19.4% (1 cm2)	12.5% triple junction 11.9% micromorph on glass, 10% micromorph on flexible substrates
Commercial module efficiency	8-11%	8-12%	6-10%
Production quantity 2009	1140 MW	150 MW	750 MW
Main producers 2009	First Solar, (Abound Solar)	Würth Solar, Showa Shell	Unisolar, Kaneka, Sharp, MHI,, Trony, Bosch, SCHOTT, Gadir Solar, Pramac, Flexcell
Strength	Fast and « easy process » for absorber deposition	Efficiency close to c-Si	Synergy with flat panel display sectors, ressources unlimited
Weakness	Concern on Te availability, reliability of back contact, acceptance linked to Cd	Concern on In availability, sensitive process for absorber deposition	Medium efficiency

PVLAB ACTIVITIES TOWARDS HIGHER EFFICIENCY, LOWER PRICE AND BUILDING INTEGRATION

The PVLab at the EPFL represents at the international level one of the main driving forces in the field of photovoltaic energy. The PV-Lab introduced several breakthrough innovations during the last 20 years, holds several patents and has triggered the creation or development of many companies such as Oerlikon Solar (Leading European supplier of production equipments for thin film silicon modules), Flexcell (flexible panels), Indeotec (Chemical vapor Deposition Clusters for laboratories), or R&R Switzerland (equipment manufacturer for heterojunction modules).

The activities in BIPV are focused on the idea that BIPV products have to become “commodity objects”, which color, shape and function can be chosen depending on the client and application. In addition it should be cost effective, reliable, easy to install and respect the historic traditions, architecture and geographic situations.

Fig. 2: Examples of thin film silicon module integration; (left) Demonstrator realized at the PVLab of EPFL, (right) Flexible modules produced and commercialized by Flexcell on the roof of an industrial building.

On thin film silicon, the PVLab's projects are focused on the development of:

- Thin film silicon solar cells deposited on glass, light trapping optimization and plasma processing,
- Thin film silicon solar cells deposited on flexible low cost plastic substrates,
- Module integration and reliability testing

Today, 1m2 of thin film silicon module produces 100-220kWh annually depending on the average annual illumination, corresponding to 2500-5500kWh over the 25-year lifetime.

LATEST DEVELOPMENTS AND RESULTS ON ADVANCED NANO-STRUCTURED TRANSPARENT CONDUCTIVE OXIDE LAYERS

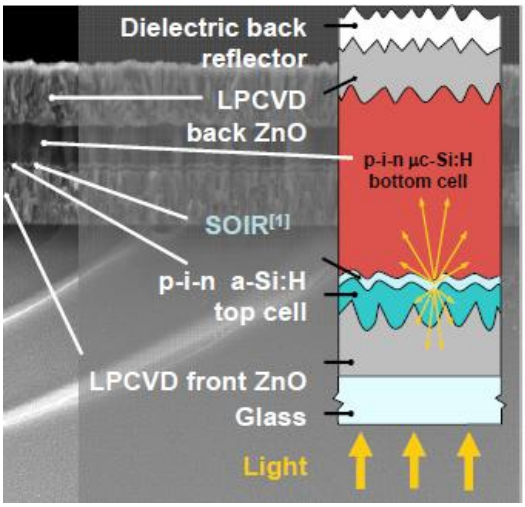

Fig. 3: SEM image and scheme of amorphous /microcrystalline silicon tandem cell

Amorphous and microcrystalline thin film silicon modules

Thin Film silicon modules are made from extremely thin layers of photosensitive materials (amorphous and microcrystalline silicon) and Transparent Conductive Oxide (TCO) on glass, stainless steel or plastic substrates. Once deposited, the thin layers are cut into solar cells with a laser and connected together. Thin Film modules are most often enclosed between two sheets of glass and frameless. If the photosensitive material is deposited on a thin plastic foils, the module becomes flexible and offers unique possibilities for building integration. Figure 3 presents the typical design of a tandem junction thin film Si module.

Latest developments and results on light trapping management

One important research topic towards higher efficiency and lower production costs is the optimization of the interface roughness in order to simultaneously enhance the light trapping in the active layer and ensure the growth of high quality active layers. A way to achieve optimal properties is to control and optimize the surface roughness of the substrate, either by replication of a suitable roughness in a lacquer previously spread on the substrate [4] or using rough TCO layers.

The recent work published by Dr. S. Nicolay and L. Ding has shown that the roughness shape and size of the surface features at the TCO surface can be tuned by using multi-layers processes or by varying the deposition regime. Detailed information is published in recent papers [3].

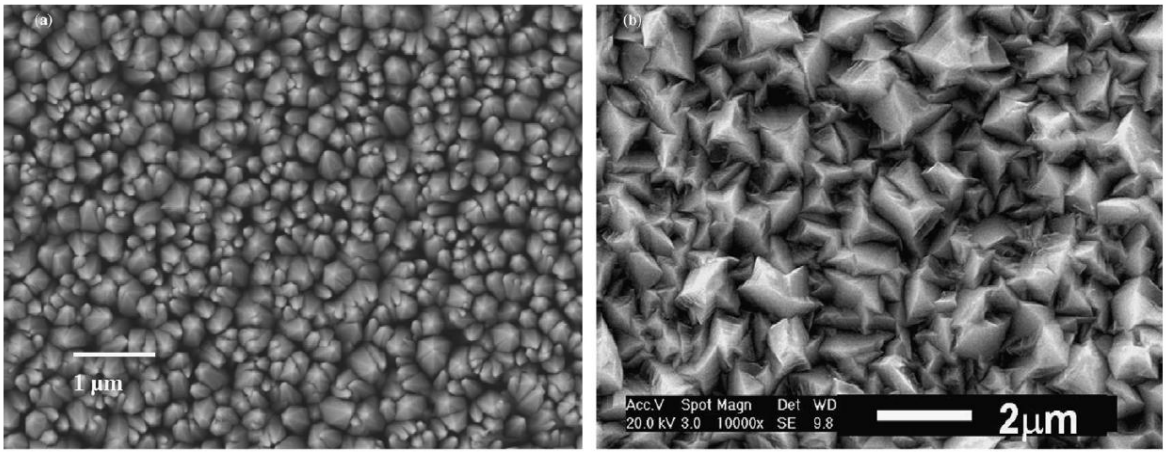

Fig. 4: Different surface roughness obtained by varying the LPCVD-ZnO deposition parameters

Investigations on new deposition regimes and cell designs

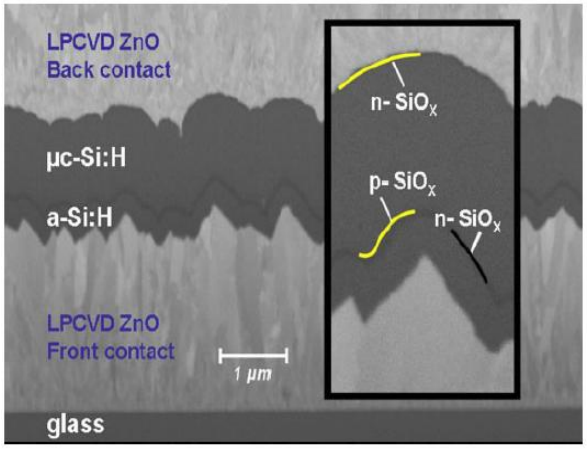

Fig. 5: FIB cut imaged by SEM of the amorphous silicon/microcrystalline silicon tandem cell: Zoom in the cell structure to illustrate the implementation of the doped nanostructured silicon rich silicon oxide layers used for the top cell and the bottom cell.

In order to use the best compromise between efficient substrate roughness for light trapping (see above) and high quality active layers which are more difficult to obtain on very rough substrates, many investigations have been realised on the effect of the deposition parameters, the thickness and exact chemical composition of the silicon layers. The doped layers were shown particularly important for the solar cell and module performances on rough substrates.

In his work, Dr. M. Despeisse [5] studied the effect of doped layers obtained from nano-structured silicon phases embedded in a silicon oxide matrix implemented in thin film silicon solar cells. Their combination with optimized deposition processes for the silicon intrinsic layers is shown to allow for an increased resilience of the cell design to the substrate texture, with high electrical properties conserved on very rough substrates.

The optimizations presented in this work permit turning the efficient light trapping provided by highly textured substrates into increased cell efficiencies. Stabilized efficiencies up to 11.3% were reported for thin tandem cells with only 1.1µm thick microcrystalline silicon bottom cell.

Module reliability

Most of thin film silicon modules available today on the market are fully glass encapsulated and 80% of their initial performances are guarantied over typically 25 years.
Nevertheless, in order to develop new flexible products and reduce the weight and production costs of today standard thin film silicon modules, the trend is to replace at least one of the two glass sheets by a polymer foil.
Towards this goal, the mechanisms and environmental influences that cause photovoltaic modules performance degradation are intensively investigated. A recent study published by S. Pelisset et all [6] has show that the gases permeation of the polymer is not the only important criterion, but that the components and by-products coming from the polymer degradation are probably also directly involved in the degradation process of thin film silicon solar cells.
Investigations are ongoing on the introduction of dielectric layers such as SiO_x or SiN_x between the device and the polymer foils in order to minimize the degradation effect.
These experiments have shown that the optimization of the interaction between the active layers and the dielectric/polymer stack is the most important and that high performance polymers are not compulsory for a good protection of the solar cells.

CONCLUSION

Thin film silicon photovoltaics is well established on the market, with the presence of many module suppliers in Europe and worldwide.

Today modules have typical efficiencies between 7% for single amorphous silicon modules to 10% for tandem amorphous and microcrystalline silicon modules.

The technology offers the advantage to use small amounts of material, promising perspectives in term of production costs and efficiency, as well as nice homogeneous appearance for building integration.

The main research axes are basically focussed on:

- Flexible technology,
- Light management in the device,
- Best compromise between the active layers quality and the interface roughness necessary for light trapping,
- Innovative and lower cost encapsulation processes.

At the PVLab of EPFL, two European funded projects are currently ongoing on this technology: PEPPER and Silicon-Light projects (http://pepper.epfl.ch/ and http://www.silicon-light.eu/)

REFERENCES

[1] M. Green et al, Prog. Photovolt: Res. Appl. 2011; 19:84–92
[2] J. Krc et al, Proceedings of the 21st EU-PVSEC, Dresden 2006
[3] J. Escarré Palou et al, Solar Energy Materials and Solar Cells, Vol. 95, pp. 881-886, 2011.
[4] S. Nicolay et al, Solar Energy Materials And Solar Cells, vol. 95, 2011, p. 1031-1034
[5] M. Despeisse et al, Phys. Status Solidi A, 1–6 (2011)
[6] S. Pelisset et al, Proceedings of the 25th EU-PVSEC conference, 2010

Sustainable Building Envelopes

DEVELOPMENT OF A CO_2 ACCOUNTING METHOD FOR NORWEGIAN ZERO EMISSIONS BUILDINGS (ZEB)

A.A-M. Houlihan Wiberg[1]; A.G. Hestnes[2]

1, 2: Zero Emissions Research Centre (ZEB), The Faculty of Architecture and Fine Art, NTNU, Alfred Getz vei 3, Trondheim, Norway.

ABSTRACT

Energy-plus, zero energy and zero emission buildings denote some of the best buildings of today and the future with respect to energy efficiency and environmental impact. A zero emission building might be defined in different ways. Nevertheless, the main concept is that renewable energy sources produced or transformed at the building site have to compensate for CO_2 emissions from operation of the building and for production, transport and demolition of all the building materials and components during the life cycle of the building. In order to fulfill this, CO_2 emission data has to be made available and verified for traditional building materials (e.g. concrete, wood and mineral wool), new 'state-of-the-art' building materials (e.g. vacuum insulation panels, VIPs) and the active elements used to produce renewable energy (e.g. photovoltaic panels).

An initial literature review found that although there are databases of embodied carbon values for most building materials, the range in results for various materials are varied and inconsistent. This paper presents the first stage of development of a transparent and robust method to calculate CO_{2eq} emissions from materials use in future ZEB buildings at all stages of design. This is underpinned by the development of a materials database containing a list emission factors ($kgCO_{2eq}/kg$) which should be flexible enough to add and evaluate new 'state of the art' materials for ZEB. The method should also make it easy for the user to visualize the impact on CO_{2eq} emissions of their choice of material. Emission factors ($kgCO_{2eq}/kg$) for use in the ZEB database are sourced and compared from three existing databases including Klimagassregneskap.no, Version 3.0 [1], Ecoinvent (Althaus & Ökobilanzdaten and Bauteilkatalog) [2], Inventory of Carbon & Energy Version 2.0 (ICE) [3] and published Norwegian Environmental Product Declarations (*epd-norge.no*) where available.

INTRODUCTION

In order to assess the performance of ZEB pilot projects, an accurate, transparent and robust method of emissions accounting in terms of embodied carbon is needed. Embodied carbon can only be used in the context of materials, for example, activities related to the construction and demolition of a building, including the production of materials. [4] Current options to assess emissions are numerous including (but not limited to) at one level conducting a full Life Cycle Assessments (LCA) and at the other, using green house gas accounting tools or manual calculations using published materials databases. An initial literature review by the authors found that although there are existing databases of embodied carbon values for most building materials, the range in results are varied and inconsistent. Discrepancies amongst existing databases can arise from the choice of system boundaries and the emission factor used for electricity production in the country where the material is produced. Recent studies stress that the year of construction of the building, hence year of production of the material, will have an impact on the choice of emission factor due to future changes in the energy mix of the European grid. This has particular relevance for emissions calculations of future Zero Emissions Buildings in Norway due to the existence of cross border trade of electricity with

the continental European grid. The emissions from the different energy mixes vary considerably, for example, the Norwegian energy mix is approx. (50-100gCO_{2eq}/kWh), Nordic in excess of (200gCO_{2eq}/kWh) and European (400 - 500gCO_{2eq}/kWh) depending on the number of countries included e.g. EU15 (450gCO_{2eq}/kWh) and EU27 (500gCO_{2eq}/kWh). Advanced and comprehensive simulations of the European electricity system towards 2050, have been undertaken by SINTEF Energy. [5] The simulations show that the proposed measures together with a large increase in transmission capacity between countries and regions will reduce the European average specific emission to 31 g/kWh. This is a reduction by more than 90 % compared to the 2010 level. If we assume a linear development, we get a CO_2-factor trend which when extrapolated beyond 2050 leads to a zero emission level in 2054. [6] This is corroborated by Jones [4] who points out that a failure to consider a year on year improvement in electricity will result in an over-estimation of the total GHG emissions of electricity by as much as 270% between now and 2050 which is clearly significant. This point has also been addressed in the new version 3.0 of Klimagassregnskap.no where they have replaced the European figure by a function based on the gradual reduction in emissions from electricity generation European. [7] As a result the emission factor used in the emissions calculation will then be determined by year of construction.

For example, the boundary conditions within the ICE database are ‘cradle to gate’ for most but not all materials. However, even within these boundaries there are many possible variations that affect the absolute boundaries of the study. One of the main problems of using secondary data resources is variable boundaries which can be responsible for large differences in results. Transport is included within specific boundaries i.e. typically cradle to gate. In klimagassregnskap.no, the boundary conditions are cradle to gate and include extraction & transport of raw materials, refinery& production of basic materials and in some cases further production to an end use product (depends on the complexity of the end-use product). Transport from gate to building site is not included and demolition and “grave” is not included. These two last steps have to be site-specific and calculated as such. In Ecoinvent (used by Althaus/Ökobilanz/Simapro databases and Bauteilkatalog) the boundary conditions are not explicitly stated or defined and therefore require some interpretation. The input categories (modules/materials) normally give an indication of the boundary condition, for example ‘at plant’ which for this study can be interpreted as ‘to gate’ for the purposes of consistent terminology for the development of the database. Transport for materials to the plant is included while the transport to site is not included in ‘cradle to gate’. Direct emissions (production) should be included in ‘cradle to gate’ but it was noted that it is often not included. Demolition is only included in a ‘cradle to grave’ while reuse would be included in ‘cradle to cradle’. An exact method for allocating offsets (inputs) to the next phase/generation is a classic dilemma in LCA-making and is not included in the ‘cradle to gate’ scenario.

Another limitation was the use of a ‘black box’ method of emissions calculation in some cases. In general, LCA methods were found to be complex and too time consuming for the average user. A more specific problem for Norwegian ZEBs is that some materials or components will be produced in Norway and would therefore not be included in the European/Swiss based databases. A particular limitation for ZEB was the lack of flexibility in existing online accounting tools and databases to add and assess the impact on emissions of ‘state of the art’ materials where a full LCA would not be yet available nor would their emission factors be included in any databases. It was concluded that currently none of these methods are suitable to assess ZEBs in the Norwegian context and underlines the need for the development of an accurate, transparent and robust method to calculate CO_{2eq} emissions from materials use for future ZEB buildings at all stages of design.

METHOD

The database and calculations are made using Excel for transparency and flexibility and to ensure that it can be easily updated as and when new 'state of the art' materials become available. To ensure simplicity, the selection of emission factors ($kgCO_{2eq}/kg$) has been limited to those used in an existing ZEB case study project in the first instance due to the vast amount materials available in the databases. The boundary conditions, reference sources and specific comments are also carefully recorded to ensure transparency in the database. The basic principle for the calculations of emissions from material use is:

Quantity of Materials (kg) x Emissions Factor ($kgCO_{2eq}$ /kg) = CO_2 Emissions ($kgCO_{2eq}$)

To demonstrate the application of the accounting method, to test its robustness and rigorousness and whether the results are credible, this method has been used to calculate and compare the CO_{2eq} emissions from materials use for an existing ZEB case study project in Løvåshagen, Bergen. The project comprises 80 apartments, of which 52 are low energy units and 28 built to Passive House standards. A materials inventory is created from the existing Bills of Quantities for the Løvåshagen project and includes a list of materials and quantities used for the project. The input for quantities of materials is (kg) which in some cases requires additional information about the density of the materials for conversion. The results confirm the findings of the literature review that the most significant impact on the resulting emissions is caused by the choice of boundary conditions *i.e. cradle to gate or cradle to grave* and emission factor for electricity mix in the material production. It was also found that in further development of the database for other project using 'state of art' materials that the choice of density of material is particularly significant as seen in phase change materials (PCM).

ZEB Database

The database contains a list of emission factors for selected materials specified in an existing ZEB case study project. Emission factors ($kgCO_{2eq}/kg$) for use in the ZEB database are sourced and compared from the three existing databases previously referred to. The inputs for each reference database include information on the emission factor used, boundary conditions and other relevant comments that impact the calculation. For example, it is important to know the country of the production of the material and which emission factor was used for electricity production i.e. European, Nordic (regional) or Norwegian (national). The Swiss databases Althaus & Ökobilanzdaten, which underpin the Ecoinvent database, contain additional emission factors for materials to those found in Ecoinvent and are included for reference in the ZEB database.

Material	Klimagassregnskap ($kgCO_2eq/kg$)	Boundary Conditions	Comments	Ecoinvent ($kgCO_2eq/kg$)	Boundary Conditions	Comments	ICE ($kgCO2eq/kg$)	Boundary Conditions	Comments
Steel/Iron	**3,22**	**Cradle to gate**	European avg, not Fossdal el quantity!	**1,94**		UCTE el mix, Swiss techn	**2,89**		World Steel Association data, UK average mix of steel products
Concrete	**0,19**	**Cradle to site**	Production and forming on site (EPD), Fossdal gives el req	**0,13**		Swiss el mix, German technology	**0,11**		Assumed use of UK weighted average
Alu	**10,63**	**Not defined**	European industry avg, EEA 2000, Fossdal el data	**12,40**		European alu ind el mix and technology	**12,79**		IAI data, average UK mix of aluminium
Wood laths/massive	**0,45**	**Cradle to gate**	Wood taken as proxi, Fossdal el data	**0,09**		Hardwood taken as proxi, UCTE el mix, german technology	**0,24**		Sawn hardwood used as proxi, high uncertainty stated by ICE, plus 0,63 in biocarbon
Wood parquet	**0,44**	**Cradle to gate**	Wood taken as proxi, Fossdal el data	**0,07**		Scandinavian softwood as proxi (no parquet module), UCTE el mix, german technology	**0,24**		Sawn hardwood used as proxi, high uncertainty stated by ICE, plus 0,63 in biocarbon
Glulam wood	**0,34**	**Cradle to gate**	No el data, Puettmann and Wilson 2005	**0,46**		UCTE el mix, German technology	**0,42**		Plus 0,45 in biocarbon
OSB-plate	**0,64**	**Cradle to gate**	board used as proxi, Fossdal el data	**0,64**	**Cradle to gate**	UCTE el mix, German technology	**0,45**	**Cradle to gate**	Plus 0,54 in biovarbon
Glass	**1,56**	**Cradle to gate**	Pilkington Fasadeglass, Fossdal el data	**0,98**		Coated flat glass, UCTE el mix, German technology	**0,85**		Average UK mix of glas, 38 % recycled
Insulation - EPS	**10,35**	**Not defined**	Plastics Europe, Fossdal el data	**4,26**		European technology	**3,29**		APME data
Insulation - mineral	**2,34**	**Cradle to site**	Incl. Tranport to site, Fossdal el data	**1,50**		Swiss el mix	**1,28**		No comment
Damp proof layer plastic	**8,30**	**Gate to gate?**	PVC membrane, Production, AMPE, European data, Fossdal el data	**2,70**		No documentation found	**2,60**		LDPE film, APME data
Wind proof layer plastic?	**8,30**	**Gate to gate?**	PVC membrane, Production, AMPE, European data, Fossdal el data	**2,70**		No documentation found	**2,60**		LDPE film, APME data
Plasterboard 13 mm 9 mm	**2,13**	**Cradle to site (gate?)**	Fossdal el data	**0,35**		German el mix, Swiss technology	**0,39**		Data from WRAP, incl disposal
Ceramic tiles	**1,68**	**Gate to gate?**	Porsgrunn bad data, not well defined reference, Fossdal el data	**0,78**		UCTE el mix, Italian large scale plant	**0,78**		Ceramic cladding element EPD, ref 292
			NB: Fossdal el data means that the total energy has been used for calculating new GHG emissions from el generation (358 g/kWh)						

Table 2. Summary table extracted from the emerging ZEB database showing emission factors, boundary conditions and other comments for selected materials used in ZEB case study project. (Note: Detailed inputs for each material are not shown in this paper, for example, there are different emission factors for different types of concrete.)

RESULTS

The results show the range in resulting emissions for the same materials vary depending on the database used as seen in Figure 1. It should be noted that these emissions do not include emissions for window, door and balcony railing components due to, in some cases, insufficient information or in other cases, lack of published data.

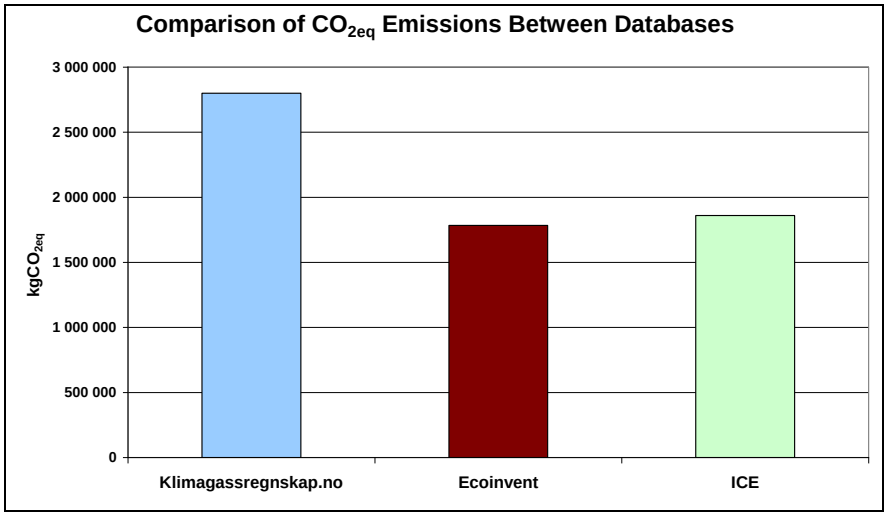

Figure 1: Comparison of total CO_{2eq} emissions for materials use for the ZEB case study project.

From Figure 1, it can be seen that there is almost a two fold difference in resulting emissions between databases. Furthermore, the three materials responsible for most of the emissions include concrete, steel/iron and aluminium as seen in Figure 2. It can be seen that the emissions from concrete, using the ICE database, are approximately 10% higher than the other two databases whereas those for aluminium, using the Ecoinvent database, are three times those calculated using Klimagassregnskap.no database. It was found that the most significant impact on the resulting emissions are the choice of boundary conditions i.e. cradle to gate or cradle to grave and emission factor for electricity mix in the material production which explains the difference in resulting emissions shown in Figure 1.

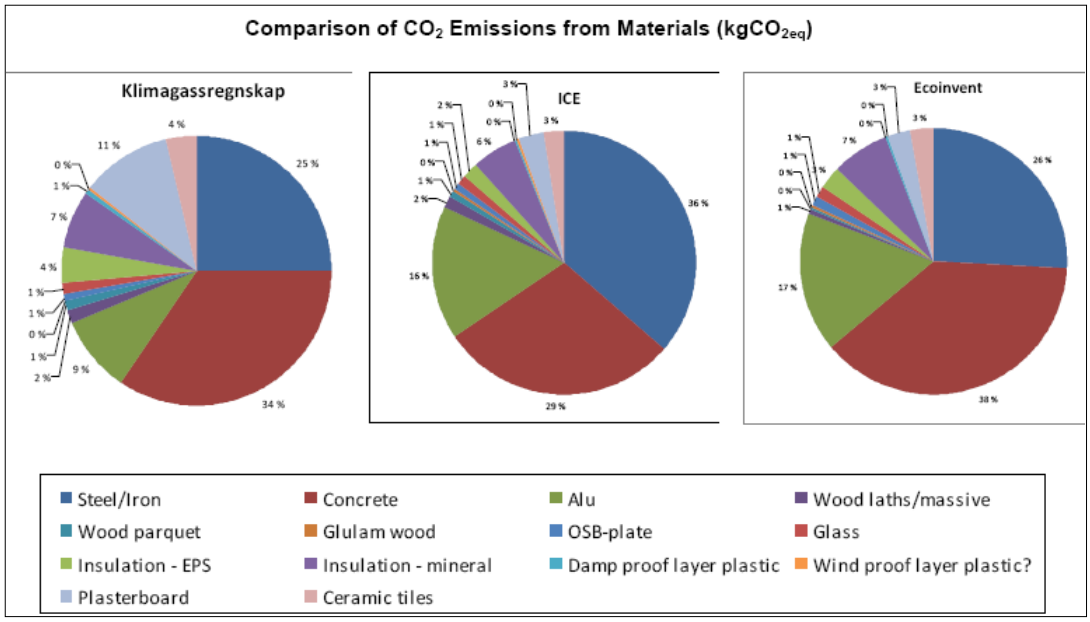

Figure 2: Comparison of total emissions for materials use for ZEB case study project.

DISCUSSION

This paper presents the first stage of development of an accounting method which provides the reliability, transparency and flexibility required by ZEB to add and assess the CO_2 performance of emerging 'state of the art' materials to be used in future pilot projects. Moreover, it provides an easy-to-use method for use in the early design stage when feedback to the designer on the impact on emissions of different choices of materials is most critical.

At the outset of this research, it was envisaged that a single column of emission factors could be developed for each material if there was correlation between the emissions factors sourced from the three databases. However, as shown in this paper there is much complexity in the calculation of these factors which vary depending on the year of data, choice of boundary conditions and fuel mix in the country of production. Moreover, information on the density of material was also found to be a significant factor particularly in the case of phase change materials. As a result, the proposed accounting method instead provides a 'palette' of transparent, reliable emission factors sourced from three existing databases from which the user can select the most appropriate emission factor for the selected material. However, a current limitation to introducing such a 'palette' of emission factors is that there are differences between the boundary conditions used in different databases. In addition, further work on the development of the database will need to address the fact that different emission factors are used for the electricity production depending on the country of production. Further work should also clearly define what is included/excluded for example, extraction, transport, refinery & production in the definition of cradle to gate, cradle to grave etc. until such time that consistent terminology is mandatory in any future standardization of emissions accounting methodology. To conclude, the key requirement of this accounting method is that it is flexible enough to add, edit and evaluate new 'state of the art' materials using a simple, standard, transparent and above all accurate method. The method makes it easy for the user to assess and visualize the impact on emissions of their materials choice at all stages of design.

ACKNOWLEDGEMENTS

The authors wish to acknowledge the significant work of Ms. Karin Sjöstrand, M.Sc. student Industrial Ecology at NTNU, Norway in the development of the ZEB database and for providing information and data from the Ecoinvent database referred to in this paper.

REFERENCES

1. Statsbygg/Civitas (2011). *Klimagassregnskap.no Version 3.0.* Online GHG accounting tool. Statsbygg/Civitas. March 2011
2. Ecoinvent . *Ecoinvent v2.2.* Online Life Cycle Inventory Data (LCI). Swiss Centre for Life Cycle Inventories, Dübendorf, CH.
3. Hammond GP, Jones CI: (2011) *Inventory of Carbon & Energy (ICE) Version 2.0.* University of Bath, Bath. 2011
4. Jones, CI (2011*). Embodied Carbon: A Look Forward*. Sustain Insight Article: Volume I.
5. Graabak, I., Feilberg, N. (2011) *CO_2 emissions in different scenarios of electricity generation in Europe.* Report TR A7058. SINTEF Energy Research, January 2011.
6. Dokka, T.H. (2011) *Proposal for CO_2-factor for electricity and outline of a full ZEB-definition.* Published Memo. ZEB Zero Emissions Research Centre. May 2011.
7. Statsbygg/Civitas (2011). *Utslippsfaktorer for elektrisitetsbruk Hvordan er dette implementert i klimagassregnskap.no versjon 3.* Statsbygg/Civitas, 3. March 2011.

ENERGY EFFICIENT BUILDING ENVELOPES

THE ROLE OF THE PERIODIC THERMAL TRANSMITTANCE AND THE INTERNAL AREAL HEAT CAPACITY TO REACH A HIGH LEVEL OF INDOOR COMFORT

M. Rossi[1]; V. M. Rocco[2]

1: Università degli Studi di Camerino, School of Architecture and Design "Eduardo Vittoria", Viale della Rimembranza, 63100 Ascoli Piceno, Italy.

2: Politecnico di Torino, DICAS - Department of Housing and City, Viale Mattioli n.39, 10125 Torino, Italy.

ABSTRACT

The necessity to decrease the building energy demand for heating and for cooling and to reach a high level of indoor thermal comfort in summertime is the subject of many current scientific researches. In particular, a recent study, carried out by *Università Politecnica delle Marche* (UNVPM), has shown that considering the values of superficial mass (M_s) and periodic transmittance (Y_{mn}) of external walls is not sufficient in order to achieve energy savings and a high level indoor comfort in the summer period. For this reason experimental reference values for the parameter of internal areal heat capacity (k_1) were introduced. The aim of this study is to understand the interdependencies between some thermal parameters (U, M_s, φ, F_a, Y_{mn} and k_1) of massive and lightweight external walls with respect to their summer energy performance in use. The study analyses in a first step eight external walls with good values of U and Y_{mn}. Then the same selected walls have been modified in order to reach an average k1-value. The energy demand for heating and for cooling, necessary to ensure a defined level of indoor thermal comfort, has been verified by means of thermodynamic simulations applied to a virtual test room localized in two different Italian cities: Milano and Catania. The results of this research are: to show the relationship between the Y_{mn} and k_1 values of the selected external walls; to demonstrate that for both types of external walls, massive and lightweight, it is possible to obtain good k_1 values, with easy and often economic building envelope design solutions; to describe some design solutions for external walls to improve their thermal performance and the level of indoor thermal comfort; and to quantify the energy demand for heating and cooling of the improved walls in comparison to the selected walls.

INTRODUCTION AND METHODOLOGY

Several studies have demonstrated the importance of having a building envelope with a high thermal inertia, both for saving energy and for indoor comfort. Some authors have particularly pointed out the importance of preferentially choosing building envelopes with an external insulation and a high density rather than a thermal insulation on the inner side, in order to save energy for heating and cooling [1]. Furthermore, the new European regulation [2] and the Italian legislations [3] [4] [5] have introduced other parameters and have defined their reference values - in addition to the thermal transmittance (U in W/m²K) and the superficial mass (M_s in kg/m²) - for the evaluation of the thermal inertia and the summer thermal performance of building envelopes. These parameters are: thermal time shift (φ in hours),

thermal decrement factor (F_a, dimensionless) and periodic thermal transmittance (Y_{mn} in W/m² K). The periodic thermal transmittance incorporates the concepts of thermal transmittance, time shift and decrement factor. Recent research [6] has also demonstrated that a low value of Y_{mn} of building envelopes is not sufficient to realize energy savings and a high level indoor comfort during the summer period. In fact a low Y_{mn} -value leads to a reduction of the impact of thermal loads from outside, particularly from direct sunlight irradiation on the external walls, but it is not able to reduce the contribution of the internal thermal loads. Internal heat loads are however the main cause of excessive indoor temperatures in office buildings during the summertime. For this reason the UNI EN ISO 13786/2008 have introduced a new parameter: the internal areal heat capacity (k_1 in kJ/m²K). This parameter describes the actual capacity to accumulate heat on the inner side of a building element and characterizes the internal thermal mass. An envelope with a high potential for heat accumulation on the inner side has a high k_1 value. Whereas the European Regulation [2] doesn't define a minimum value for k_1, recent research, carried out by UNIVPM [6], has defined minimum values for k_1 depending on the values of Y_{mn}. Our study is organized in three steps and analyzes the influence that the values of thermal parameters of external walls have on the thermal comfort level of rooms with high internal thermal loads (e.g. office buildings).

FIRST STEP: ENERGY PERFORMANCE OF THE SELECTED EXTERNAL WALLS

In order to evaluate the relation between thermal transmittance (U), superficial mass (M_s), time shift (φ), decrement factor (F_a), periodic thermal transmittance (Y_{mn}) and internal areal heat capacity (k_1) of external walls, 8 massive and lightweight walls (fig 1), commonly used or available in Europe, have been selected. The selected walls are characterized by different layers, materials and thickness. The first step has been to analyze and compare - conforming to the Italian legislation (tab.1) - the above mentioned parameters of the selected walls (tab.2).

	Legislation	**Reference value**
U	D.Lgs. 311/2006	$U <$ 0,34 W/m²K - climate zone E (a cold Italian zone)
M_s	D.Lgs. 311/2006	$M_s >$ 230 kg/m² (exception to zone F, the coldest one)
φ	D.M.- 26th June 09	8h $\geq \varphi >$ 6h average - $\varphi >$ 12h excellent
F_a	D.M.- 26th June 09	0,40 $\leq F_a <$ 0,60 average - $F_a <$ 0,15 excellent
Y_{mn}	DPR 59/2009	$Y_{mn} <$ 0,12 W/m²K
k_1	-	$k_1 \geq$ 50 if $Y_{mn} \leq$ 0,04 / $k_1 \geq$ 70 if 0,04 $\leq Y_{mn} \leq$ 0,08 / $k_1 \geq$ 90 if 0,08 $\leq Y_{mn}$ n $\leq$ 0,1

Table 1: Thermal parameters of external walls according to the Italian law.

External walls	**s** [cm]	**U** [W/m²K]	**M_s** [kg/m²]	**F_a** [-]	**φ** [h]	**Y_{mn}** [W/m²K]	**k_1** [kJ/m²K]	**Min. k_1 value** [kJ/m²K]
M - 01	32,50	0,34	240	0,123	12,39	0,04	14,70	50
M - 02	34,50	0,34	252	0,367	9,55	0,12	49,50	90
M - 03	31,50	0,34	239	0,356	9,32	0,12	38,90	90
M - 04	33,00	0,34	542	0,253	8,61	0,09	24,70	90
L - 01	23,25	0,34	141	0,350	9,62	0,12	37,30	90
L - 02	15,40	0,33	83	0,370	7,88	0,12	41,40	90
L - 03	24,50	0,34	146	0,200	11,13	0,07	27,50	70
L - 04	24,80	0,23	55	0,499	6,80	0,12	12,00	90

Table 2: Thermal parameters of the selected external wall and minimum k_1-values that should be achieved in relation to the value of Y_{mn}.

Table 2 shows that all the selected walls do not have a k_1-value corresponding to the reported minimum values although they meet the current European and Italian regulation on the summer thermal performance for external walls. Hence they do not reach good thermal performance in relation to the internal heat loads, which are extremely relevant in office buildings, generally characterized by a high demand of cooling energy during summer. Therefore, to improve the level of indoor comfort during summer it is suggested [6] to allot modifications to the selected external walls in order to increase their k_1-values above the limits specified in Tab.1, or to reduce the value of Y_{mn}. The reduction of Y_{mn} implies in fact a lowering of the minimum value of k_1 (Tab.1), making it in this way easier to reach the minimum value of this parameter.

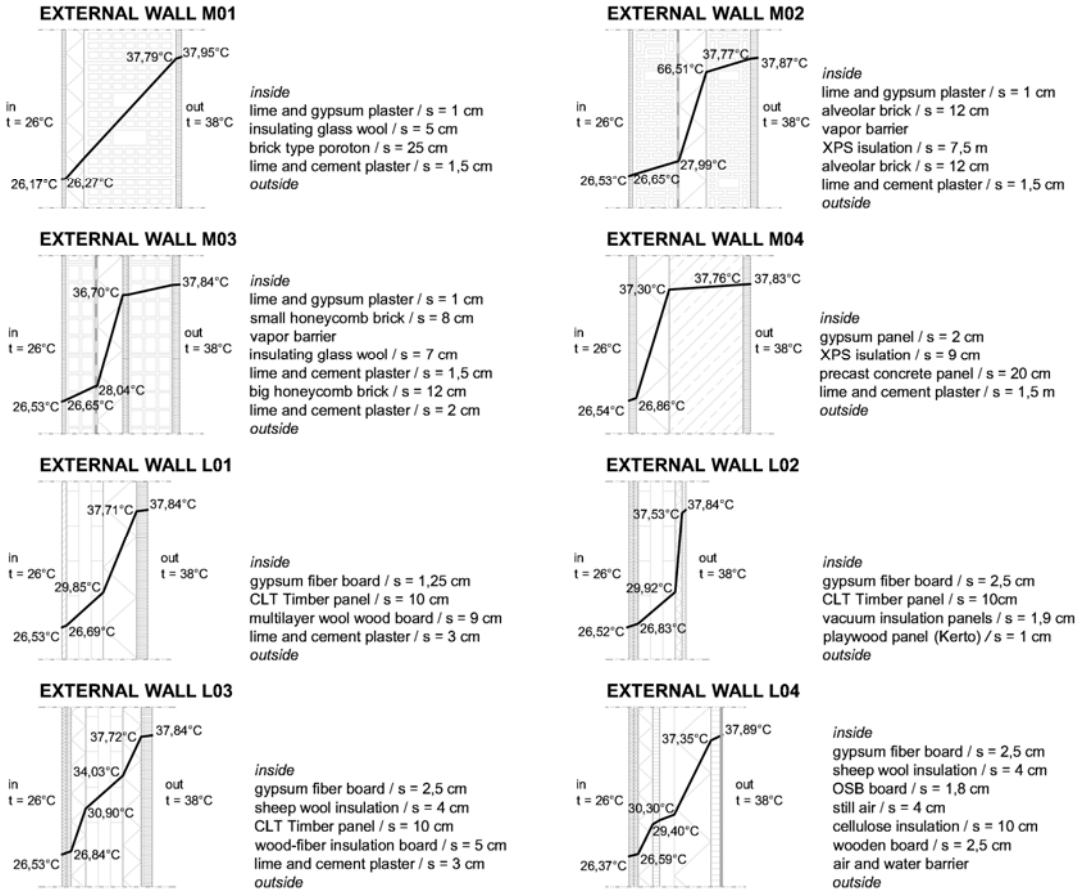

Figure 1: Description of the selected external walls (M01-M04 massive walls and L01-L04 lightweight walls).

SECOND STEP: IMPROVING THE EXTERNAL WALLS

Analyzing one by one the selected walls and making changes to their layers characteristics and layers sequence in order to achieve an adequate k_1-value (in relation to the Y_{mn}-value) it has been noticed that it is possible to identify similar strategies of improving the values of their thermal parameters. Two possible amendments to decrease the value of Y_{mn} and to increase the value of k_1 have shown to be most efficient. The first one is moving the layers with a higher value of specific weight (ρ) towards the inner side and the insulation towards the outer side of the wall. The position of layers is irrelevant for the U-value and it has a only a light influence on F_a, φ, Y_{mn}, but it has a high influence on the k_1-value. The inner side layer density influences the wall capacity of absorbing the internal thermal loads more than the density of the rest of the external wall. The second one is choosing for the internal lining a

material characterised not only by high density but also by high specific heat and low value of periodic penetration depth of heat (δ in m), such as clay plaster instead of gypsum plaster (tab.3). The δ (which depends on the density and specific heat) shows the thickness of the wall that is affected by a temperature increase and hence by the internal thermal load. The bigger wall material mass and thickness affected by the internal thermal loads are, the higher capacity of the wall to absorb heat from internal thermal loads resulting in a positive contribution to the indoor comfort is.

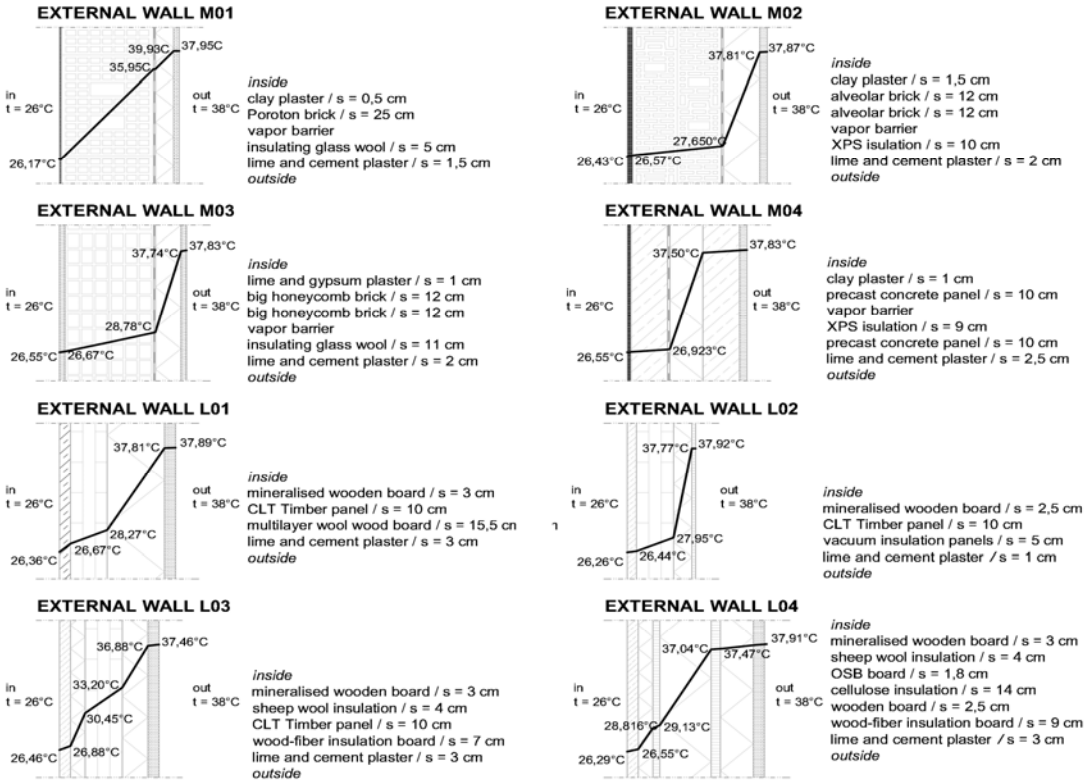

Figure 2: Description of the improved external walls.

Based on these considerations, the selected external walls have been improved (fig.2) in order to obtain good k_1-values in relation to the Y_{mn}-value (tab.4).

External walls	**S** [cm]	**U** [W/m²K]	**M_s** [kg/m^2]	**F_a** [-]	**φ** [h]	**Y_{mn}** [W/m²K]	**k_1** [kJ/m²K]	**Min. k_1 value** [kJ/m²K]
M – 01	34,00	0,33	305	0,055	15,97	0,02	76,60	> 50
M – 02	37,50	0,29	286	0,222	9,44	0,06	70,20	> 50
M – 03	34,00	0,25	328	0,172	9,71	0,04	51,60	> 50
M – 04	32,00	0,34	537	0,180	10,34	0,06	85,40	> 70
L – 01	31,50	0,23	179	0,162	14,69	0,04	55,00	> 50
L – 02	18,50	0,16	96	0,235	11,39	0,04	54,30	> 50
L – 03	27,00	0,30	163	0,122	14,30	0,04	53,40	> 50
L – 04	37,30	0,19	148	0,205	14,40	0,04	54,30	> 50

Table 4: Thermal *parameters of the* improved *external wall and minimum k_1-values that should be achieved in relation to the value of Y_{mn}.*

Materials	λ [W/mK]	c [J/kgK]	ρ [kg/m^3]	δ [m]
thin clay plaster	0,350	2100	3000	0,039
mineralised wooden board	0,260	2100	1800	0,052
clay plaster	0,900	2100	1800	0,081
gypsum fiber board	0,320	1100	1000	0,089
lime and gypsum plaster	0,350	1000	1200	0,090

Table 3: Comparison between some characteristics of the different interior lining materials.

THIRD STEP: THERMODYNAMIC SIMULATIONS

In the third step the energy demand for heating and for cooling [kWh, €, kg of CO_2] - necessary to ensure good indoor thermal comfort (21°C in winter and 26°C in summer) - has been verified by means of thermodynamic simulations, using the software package "Energy Plus", applied to a virtual test room localized in two different Italian cities characterized by different climatic conditions: tempered continental for Milano and Mediterranean for Catania. Tab.5 shows the methodology of the thermodynamic simulations.

Test room characteristics	Office space 5,0 x 4,5 x 3,0 m. Walls, floor and roof are adiabatic, except the south oriented wall with a window = 3,00 x 1,35m, no solar shading.				
Locations	Latitude	Longitude	Altitude a.s.l.	Max temp.	Min temp.
MILANO (MI)	45°27' E	9°11' N	122 m	29 °C	-2 °C
CATANIA (CT)	37°30' E	10°05' N	7 m	33,6 °C	5 °C
Internal heat loads		2 people + 2 computers + 1 lamp			180 + 150 + 50 W
Ventilation	Natural vent. rate in air changes = 0,6 h^{-1}. Mechanical vent. = not exist				
Heating	Fuel = gas. Temp. set point of heating device < 20°C Milano: October 15th – April 15th / Catania December 1st – March 15th				
Cooling	Energy source = electric power. Temp. set point of cooling device >26°C. Milano and Catania May 1st – September 30th				
Schedules of heat loads, heating and cooling			9 a.m.- 1 p.m. & 3 - 7 p.m. (Mo.- Fr.)		
Output simulation	Heating, cooling, total annual energy demand [kWh, €, kg of CO_2]				

Table 5: Simulation methodology: input and output.

RESULTS AND CONCLUSIONS

This study has demonstrated how the achievement of certain values of k_1 –corresponding to the standard defined by the above mentioned study [6]– can effectively reduce the energy demand necessary to ensure good indoor thermal comfort. The analysis of the walls and the proposal for improving them have shown that a good design (reachable with some simple changes) can enable massive and lightweight external walls with good values of k_1 (in relation to the value of Y_{mn}). If the value of Y_{mn} is already fairly low, it is possible to obtain significant results modifying the inner layer of the wall (choosing materials with high ρ and c and a low δ) without changing the thickness or the type of the insulating material. If the Y_{mn}-value is quite high, increasing the thermal insulation is necessary in order to reduce the value of Y_{mn} (which also depends on U) and therefore decreasing the minimum value of k_1. In massive walls it is usually enough to modify the inner layer; on the other hand the improving of lightweight walls, characterized by many layers, is more complex and it is necessary to know the physical properties of each layer to be able to determine its correct position and thickness. The design strategy for lightweight walls (Ms < 230 kg/m^2) is to reduce the Y_{mn} value below 0,04 W/m^{2}K in order to have 50 kJ/m^{2}K as limit for k_1.

Furthermore the results of the thermodynamic simulation in 2 Italian cities have demonstrated that the same improved walls give different results: in Catania cooling energy savings have been higher than in Milano; in Milano the heating energy savings have been higher than in Catania. This result has confirmed the necessity to design the envelope building according to the climate conditions. In addition, tab. 6 shows that there isn't a direct proportionality between costs for improving the walls and the consequent energy saving (kWh/m^2 year, €, kg of CO_2). Walls M-01, M-04 and L-03 allow for the lowest cost variation of building materials. Of these, the massive ones also allow for cost savings, since the improved walls have less thickness of inner lining materials. The very expensive changes to improve the wall's thermal performance are related to the use of the VIP panels (L-02) and to the necessity to increase the thickness of the insulation materials (L-01 and L-04) of more than 6 cm.
In conclusion this study has demonstrated that: 1) in massive and lightweight external walls it is possible to get a good *k1* value in relation to Y_{mn} making cheap changes; 2) the improving of the *k1*-value doesn't always lead to a reduction of the energy demand for cooling or heating; 3) the improving of the k_1 value allows for energy and cost saving only in the walls characterized by a low Y_{mn}-value; 4) it isn't possible just introducing lower values of Y_{mn} to obtain improvements for indoor comfort: low Y_{mn} values don't necessary corresponding to appropriate *k1*-values (tab.2). In fact, in these walls it is possible to get an improvement of the k_1, a reduction of the energy demand and a better level of thermal comfort indoor thanks to economic and easy modifications: e.g. choosing a different type of inner plaster.

external wall	cost for wall improving [€]	MILANO					CATANIA				
		energy saving [kWh/m^2 year]			fuel cost savings [€]	kg of CO_2 saving	energy demand [kWh/m^2 year]			fuel cost savings [€]	kg of CO_2 saving
		heating	cooling	total	total	total	heating	cooling	total	total	total
M-01	-1,37 €	- 9,01	- 2,60	- 11,61	- 0,74 €	- 2,46	- 1,30	- 2,36	- 3,65	- 0,21 €	- 0,71
M-02	65,91 €	- 9,04	- 1,43	- 10,47	- 0,69 €	- 2,26	- 1,39	- 2,52	- 3,91	- 0,21 €	- 0,75
M-03	41,34 €	- 33,89	- 1,55	- 35,44	- 2,39 €	- 7,80	- 3,15	- 4,87	- 8,02	- 0,45 €	- 1,55
M-04	-1,42 €	- 4,63	- 6,25	- 10,88	- 0,62 €	- 2,13	- 2,61	- 5,01	- 7,62	- 0,42 €	- 1,47
L - 01	196,84 €	- 19,93	0,49	- 19,43	- 1,34 €	- 4,34	- 1,58	- 0,79	- 2,37	- 0,15 €	- 0,49
L - 02	575,36 €	- 37,65	7,33	- 30,31	- 2,22 €	- 7,07	- 1,80	- 11,21	-12,27	- 0,67 €	- 2,38
L - 03	32,79 €	- 16,74	- 1,59	- 18,33	- 1,22 €	- 4,00	- 1,70	- 2,97	- 4,67	- 0,26 €	- 0,90
L - 04	377,06 €	- 39,74	1,82	- 37,92	- 2,63 €	- 8,51	- 5,69	- 3,12	- 8,72	0,27 €	1,02

Table 6: Materials cost for improving the thermal performance of the selected walls, and saving of energy demand, fuel cost and CO_2 emission after the improving.

REFERENCES

1. Aste, N., Angelotti, A., Buzzetti M.: The influence of external walls thermal inertia on the energy performance of well insulated buildings, Energy and Buildings, n. 41, pp. 1181-1187, 2009.
2. UNI EN ISO 13786:2008 - Thermal performance of building components.
3. DECRETO LEGISLATIVO 29 dicembre 2006, n.311.
4. DECRETO MINISTERIALE 26/6/2009.
5. DECRETO DEL PRESIDENTE DELLA REPUBBLICA 2 aprile 2009, n. 59.
6. Di Perna, C., Stazi, F., Ursini Casalena, A. and D'Orazio, M.: Influence of the internal inertia of the building envelope on summertime comfort in buildings with high internal heat loads, *Energy and Buildings*, n. 43, pp. 200-206, 2011.

DReSS: A Climate and Occupant Responsive Residential Envelope System

Geoffrey Thün[1], Kathy Velikov[1] Ivan YT Lee[2], Bartosz A. Lomanowski[2], Lynn Bartram [5]

1: Taubman College of Architecture and Urban Planning, University of Michigan, Partner RVTR, Ann Arbor, MI USA gthun@umich.edu, kvelikov@umich.edu

2: University of Waterloo, Department Civil and Environmental Engineering, Waterloo, Ontario, Canada iytlee@engmail.uwaterloo.ca, blomanow@engmail.uwaterloo.ca

3: Assistant Professor, Simon Fraser University, School of Interactive Art and Technology, Surrey, BC Canada lyn@sfu.ca

Abstract

Dynamic, responsive facades - especially ones that target energy use optimization, energy production and climate adaptive automation - are currently at the forefront of architectural research for commercial buildings. Yet the questions surrounding such technology uptake for residential building design are often quite different, and include the incorporation of appropriate technologies, functions and interfaces, as well as issues of individual comfort and expectations of building/inhabitant relationships. Performance of residential buildings also varies by use, with differences in individual behaviour producing up to 300% variation in energy consumption [1]. If we consider that the domestic realm as a territory where behaviours are conditioned and developed, the relationship between the physical components of a responsive façade and the associated user interface are positioned as a critical site of design intervention and research, where such systems may play a key role in fostering sustainable behaviour. The North House Project [2] is utilized as a case study The North House Project operates within a paradigm of high-performance housing that embraces advanced integrated technologies to develop dwellings that reconfigure occupant's sustainable behaviour in relation to their surroundings. North House was developed to perform beyond net-zero energy consumption/production and produce a net energy *positive* dwelling. Such homes are capable of annually producing more energy than they consume, and contributing to a distributed grid-tied energy infrastructure thus rendering each homeowner and domicile an energy producer. North House prioritized design strategies tailored to address issues specific to near northern climates (42° – 55° Latitude) where heating loads are often significant relative to annual energy use. These climates are further characterized by wide annual fluctuations in temperature and humidity, and during much of the annual cycle, periods of available daylight are short, placing special emphasis on maximizing available daylight to the project's interior.

Introduction

A goal specific to the North House as a research undertaking was to challenge the dominant 'best practice' paradigms projected by benchmark and measurement metrics such as LEED, which assume that buildings with high window-wall ratios are considered to be energy inefficient. Low-energy and passive buildings, particularly in northern climates are often designed to minimize glazing areas, in response to traditional glazing design that contribute the smallest insulation value and the highest air leakage coefficient relative to opaque insulated assemblies. Most energy standards restrict the window-wall ratio to 40% or less as a result. This paper discusses a tripartite interdependent suite of technologies utilized within the

North House characterized by three primary systems that, in aggregate, constitute a climate and occupant responsive net energy-producing residential envelope system: (i) DReSS: Distributed Responsive System of Skins, (ii) CHAS: Central Home Automation Server, and (iii) ALIS: Adaptive Living Interface System.

I DReSS: Distributed Responsive System of Skins

In order to respond to the broad spectrum of seasonal climate extremes characteristic of near northern regions, and to achieve environmentally responsive envelope performance, the overall project design was based on an ecological systems approach, wherein the building skin was composed of performative and interdependent layers. Like the body's epidermis, these layers serve individual as well as cumulative environmental functions and are capable of automated modification in response to external conditions and internal demand.

The schematic design of the opaque components of the envelope (walls, roof and floor) deployed building simulations to determine high thermal resistance values targets for the design, which are typical of cold-climate, low-energy design. Hygrothermal analysis performed with WUFI suggested that a fully vented rainscreen wall system should be used for the vertical faces of the assembly. Each of the opaque components of this system are developed as engineered wood structural panel assemblies utilizing offset framing to create a continuous thick assembly eliminating direct thermal bridges. Cavities are filled with R-7.2/inch soy-based polyisocyanurate foam insulation to produce an airtight enclosure varying across assembly type from R72-R60. Exterior and interior 5/8" MDO panel skins manage shear and face-related forces while providing continuous anchorage support. These are finished on the exterior face with a liquid applied air barrier system over which subsequent assemblies are added as a rainscreen.

Above the roof membrane of the project, a system of 8.3 kWp Building Applied Photovoltaic (BAPV) modules are horizontally arrayed (capturing high summer sun). This PV array also integrates solar thermal evacuated tube collectors (4 kWp) tied to domestic hot water and supplementary space heating. A 600mm airspace between roof and the underside of the modules assists in mediating heat gain beneath panels, which enables optimum performance during periods of intensive solar exposure. Vertical exterior surfaces on the east and west, combined with the southern facing fascia, are clad with a glass encapsulated 5.3 kWp Building Integrated Photovoltaic (BIPV) dry-jointed façade system anchored to extruded aluminum face-mounted rails, integrating electrical power generation with the building envelope system. These active vertical BIPV facades extend the daytime electrical power generation period and are intended to capture low incidence solar energy typical of winter and shoulder seasons. Transparent assembly components for the project infill all remaining spaces on the east, south and west facades, and are comprised of a number of distinct layers to enable its performance as a net-energy producing assembly [3]. Active exterior shading capacity is delivered via a motorized horizontal aluminum venetian shading system aligned by vertical tension members to the structural ordinance of the façade. Primary glazed assemblies consist of a custom designed quad-glazed wood curtainwall system with a very high thermal resistance. Inboard of the primary envelope, a proprietary system of motorized interior blinds deliver daylight diffusion on demand and a custom fabricated interior soffit distributes light deep into the space. The final layer of performance in this system is delivered via Phase Change Materials (PCM) embedded in the floor assembly to chemically provide the performance of thermal mass within the prefabricated wood framing system. *(see Fig. 1)*

Figure 1: (top left) North House completed façade detail at BIPV cladding and exterior dynamic shading; (top right) User interface components and embedded design; (bottom left) DReSS components diagram; (bottom right) Exterior shade configurations based on climatic and solar data and as prioritized in CHAS logic controls.

Early energy models using customized ESP-r and TRYNSIS determined that the use of exterior shading could significantly lower the cooling load, while allowing the glazed areas to take advantage of passive solar radiation during the heating months. Venetian exterior shades were selected and offered two significant advantages over other formats: (i) the shades can easily and automatically be fully retracted from the face of the building behind its fascia to admit maximum solar penetration, daylight, and views; and (ii) the individual slats are capable of a rotational range of almost 180° allowing for extremely high fidelity solar control. The field of shades was divided to enable individual rotational control of an upper clerestory zone and a lower zone. Shade location on the exterior of the envelope is critical to overall system performance by allowing solar block to prevent energy entry and impact on the envelope. Roof mounted daylight and wind sensors provide primary data regarding exterior resource availability to this system. Blind controllers are actuated to retract below exterior lighting levels of 100 lux and at wind speeds over 12 m/s. The use of this active shading system on the outside of the house is expected to reduce cooling load by as much as 46%.

Given that cooling is managed by the exterior shading, the glazing system is designed to provide maximum thermal resistance combined with optimized passive solar heat gain. Based on extensive energy modelling and constraints related to product availability and constructability the chosen IGU was a Quad-Glazed Krypton-filled unit comprised of two 6.5 mm sheets of clear low-iron glass sandwiching two sheets of Heat Mirror 88 (HM-88) mylar films with low-emissivity (low-E) coatings on glazing surfaces 3, 5, and 7. The coatings are a softcoat low-E with emissivities on the order of 0.004, 21 times lower than clear glass [4]. Low-E coatings minimize long-wave thermal radiation transfer across the cavity which typically accounts for about 60% of the thermal transmission in typical IGUs [5]. To optimize the balance between thermal resistance and solar heat transmission, HM-88 was chosen over films with lower emissivities for its clarity and solar transmittance while a lower emissivity

was chosen for surface seven. Krypton gas fill further reduced convective heat transfer across the IGU. Krypton is a denser noble gas with lower convective heat transfer properties compared to air, and it has an optimal cavity width of 9mm, as opposed to 12.7mm, resulting in a reduced overall IGU thickness with increased overall thermal resistance. This Quad-Glazed IGU has a Centre-Glass insulating value of R12 (U-value of 0.474 W/m2K), a Solar Heat Gain Co-efficient of 0.404, and a Visual Transmittance of 0.5434. The overall design of the glazing system first minimized locations of edge and mullion incidence by developing an uninterrupted floor to ceiling frame with large areas of individual IGU panels (nom. 3'-8"x9'-6") which reduce the ratio of centre of glass (highest resistance) to frame (lowest resistance), resulting in a performance of R8 across the whole assembly. In order to improve the thermal resistance of the spacer, the team worked directly with the manufacturer to integrate a proprietary low conductance material for all perimeter spacer locations.

Solar heat gained throughout the day is not only used to passively serve immediate heating requirements but can be stored for use as latent heat throughout the night through the use of Phase Change Materials (PCMs) embedded in the floor assembly directly underneath 5/8" engineered hardwood flooring, where they absorb thermal energy from the sunlight falling directly on the floor. The large heat storage capacity and specifiable temperature of the PCM helps to reduce both total heating and cooling loads, by storing heat when there is an excess and releasing it when there is a deficit, as well as peak heating and cooling loads by mitigating the daily variations in interior temperatures. The PCM selected for application in the North House is a proprietary salt-hydrate solution encapsulated in 15 mm thick polypropylene panels. This particular PCM is engineered to melt at 24°C (76°F) and solidify at 22°C (72°F). A total of 62.1 m2 of PCM panels were installed under the finished floor. With a latent heat capacity of 158 kJ/kg, the panels have an approximate heat storage capacity of 62.6 kWh [6]. Because the PCM is not directly exposed to the interior space, the resulting assembly will experience a 15 minute delay in the absorption and release of heat. The PCM contribute significantly to the overall energy performance of the home, and ESP-r simulations predicted the overall space conditioning load of the home is reduced from approximately 2800 kWh/yr to less than 2000kWh/yr through their contribution.

II CHAS: CENTRAL HOME AUTOMATION SERVER

In order to manage the high degree of building adaptability, Team North developed a customized Central Home Automation Server (CHAS). CHAS is a computerized controls architecture that manages all of the systems and subsystems of the house and is designed to make high-level decisions to enhance energy performance by continually optimizing available energy flows. For example, the CHAS will determine the operation of the external shading system depending on the internal air temperature of the home, the amount of incoming solar radiation, the exterior wind speeds, and the detected position of the sun. Based on these conditions the system will determine if the house should go into solar heat harvest mode to save on heating energy or solar heat rejection mode to save on cooling energy. Similarly, the CHAS also controls the HVAC system in conjunction with the operation of the exterior shades to ensure thermal comfort while maximizing energy efficiency. Throughout most of the year the house's heating and cooling needs can be managed and delivered by the exterior shades and passive building envelope assembly. As this is the more energy efficient strategy, the CHAS privileges this method of thermal management whenever possible, reserving the HVAC system as a backup. This integrated approach offers significant savings in operational energy as well as capital costs, since the majority of the HVAC equipment can be significantly downsized and in some cases completely eliminated. The team developed a customized solar domestic hot water and HVAC system comprised of a three-tank system combined with one variable capacity heat pump. Because of the unique way in which the

system was implemented, it is estimated to provide on average 65% of the required hot water for space heating, cooling and domestic uses with collected solar thermal energy alone.

Embedded sensors on the interior ceiling and exterior sensors located on a rooftop weather station provide continuous real time data to the CHAS system. For all system components that would operate in different states depending on conditions, such as the interior temperature, relative humidity, and exterior shading, a hysteresis control algorithm allows the CHAS to make intelligent decisions based on real-time inputs and the previous state of the system. This ensures smooth transitions between states and avoids frequent chattering between different settings. In total, the CHAS provides interface with and co-ordinates seven systems, including the HVAC, domestic hot water production, exterior shades, interior blinds, lighting, bed retraction, energy monitoring, and the ALIS. The CHAS system performed well during initial testing, and during the period of the Solar Decathlon competition produced a net energy positive performance. While the hysteresis control algorithm developed for CHAS was based on design logics prioritizing energy performance, system logistics were pre-determined relative to a range of anticipated scenarios.

III ALIS: ADAPTIVE LIVING INTERFACE SYSTEM

Although all of North House's building envelope and engineering systems are automated through the CHAS, the ALIS interface gives inhabitants the ability to set predefined modes, to override the system and to operate the home as meets their needs and lifestyles through an intuitive graphical touch screen interface. The broad intent of this system is to provide meaningful feedback to the user around the home's systems without requiring expert knowledge regarding any one of the specific components of the house. A great deal of the operational energy consumed by a typical building is dedicated to the provision of comfort: heating, cooling, ventilation, humidity control, and lighting. While efficient equipment and advanced building envelope technologies can reduce this energy load, further energy conservation can be achieved by involving the inhabitant directly in the control of comfort provisioning [7].

The ALIS moves beyond automated controls to directly address the needs of inhabitants by providing an easy-to-use ubiquitous interface and supporting tasks that help the inhabitant control the systems of the house. It is integrated with the house design and inhabitant lifestyle and delivers meaningful performance feedback across a range of didactic, haptic and ambient formats. As such it is intended to support long term behavioural transformation towards energy-saving living patterns. Three types of user interface components comprise the ALIS. These include (i) active touchscreen control panels distributed throughout the house; (ii) a web application, extended to a smartphone application for providing detailed graphic information feedback and advanced control options; and (iii) an ambient display that provides user feedback in subtle, haptic formats.

The touchscreen control panels are located at central and convenient locations throughout the house so that both control and feedback is easily accessible and can help the inhabitant sustain energy conscious living practices. A large touchscreen panel PC located in the kitchen provides access to fine grained control of all home systems, while a small touchscreen is positioned at each entrance to offer control of local lights. A similar smartphone application allows ubiquitous access to home monitoring and control. The web-application provides the inhabitants with an array of features, including visualizing resource usage, managing house settings according to 'modes' and schedules, and accessing community networks. Operational modes can be scheduled through the house calendar within the web-application, which can import common calendaring applications such as Google Calendar™ and iCal™ so that the house settings can be easily integrated with the inhabitant's personal schedule. When

inhabitant preset overrides compromise energy use optimization, the system informs the inhabitant so that they have the opportunity to choose a setting that does not compromise energy usage.

The 'Community Network' feature is a platform that recognizes the potential agency of online communities toward education and motivation for energy and resource use reduction. This application encourages personal and communal goal setting, friendly competition, and community information and resource sharing. Lastly, the Ambient Canvas illuminated backsplash subtly delivers visual cues pertaining to the performance of the house in real-time, while also acting as an aesthetic element in its own right. It is comprised of a series of LED rope lights mounted behind a translucent Corian™ surface. The LEDs glow with varying intensity in different zones according to net-energy consumption/production and water consumption, and their appearance can be customized through the ALIS relative to other formats of user-related goals. The intent of this haptic feedback is to provide a continuous non-quantitative yet sensorially available registration of the home's performance that compliments the other forms of didactic feedback comprising the ALIS system. In aggregate, the overall intent of ALIS is to address through design the social and occupancy related potential of sustainable buildings as active agents in a dynamic relationship, and to educate inhabitants about energy efficient practices to support intelligent home use.

REFERENCES

1. Janda, Kathryn B. 2009. "Buildings Don't Use Energy: People Do," in *Architecture, Energy and the Occupant's Perspective - Proceedings of the 26th conference on Passive and Low Energy in Architecture (PLEA)*, eds. Claude Demers and Andre Potvin. Quebec, Canada: Les Presses de l'Universite Laval: 22-27.

2 for a comprehensive list of Team North project credits, see: http://www.rvtr.com/rvtrWeb/TEAM_NORTH_CREDITS.pdf

3 see Thun, G. 2009. "Latitude Housing | North House Prototype: Prefabricating Building Integrated Phototvoltaic Envelopes for Energy Positive Housing Design in Northern Climates": *Solar Architecture and Urban Planning, Conference Proceedings of the 4th Energy Forum*, Bressanone, IT: Economic Forum

4 for a detailed discussion of envelope modeling glazing design, see Lee, I.Y.T. et al. (2010). "High Performance Facades for Heating and Cooling in Northern Climates", *International High Performance Buildings Conference*, West Lafayette, IN, July 12-15

5 Hollands, T.K.G., Wright, J.L., Granqvist, C.G., (2001), *Glazing and Coatings, Solar Energy The State of the Art* ISES Position Papers, ISES, (London, UK: James & James (Science Publishers) Ltd): .29-107

6 "Delta PCM Smart Temperature Management," in Cosella Dorkin Products [database online]. [cited 2010]. http://www.cosella-dorken.com/bvf-ca-en/products/pcm/index.php.

7 for further details on the principles behind the development of the ALIS system, see Velikov, K. and Bartram, L. 2009. "North House: Developing Intelligent Building Technology and User Interface in Energy Independent domestic Environments", *PLEA 2009 – 26th Conference on Passive and Low energy Architecture*, Andre Potvin ed. Quebec City: 22-24

SOLAR THERMAL ENERGY CONVERSION AND PHOTOVOLTAICS IN A MULTIFUNCTIONAL FAÇADE

Bernd Windholz[1]; Christoph Zauner[1]; Marcus Rennhofer[1]; Hermann Schranzhofer[2]

1: AIT – Austrian Institute of Technology, Giefinggasse 2, A-1210 Vienna, Austria

2: Institute of Thermal Engineering, University of Technology Graz, Inffeldgasse 25/B, A-8010 Graz, Austria

ABSTRACT

Beyond constructing buildings with very small demands of energy out of non-renewable sources, cf. passive house standard, more and more buildings with even no demand of these sources are erected, so-called energy-plus-buildings. Therefore, renewable energy sources, such as biomass, geothermal, solar thermal or photovoltaics are directly used in family houses, offices and industrial buildings, thus converting more renewable energy than consumed for heating, cooling and electricity. By integrating renewable energy systems into buildings requirements of architects, system planners, manufacturers, building companies and end-users must be taken into consideration. Sound energetic design, ease of fabrication, proper functionality and architectural quality must be ensured over the whole life-span of decades.

The Austrian research project "Multifunctional Plug & Play Façade" (MPPF) treats the building envelope as an active part of the building. The conversion of various renewable energy sources is integrated directly into the façade. In addition, heating and cooling out of the façade as well as ensuring a suitable indoor climate is developed. Our consortium, consisting of façade builders, system planners and manufacturers as well as research institutes, entangles the various interest groups right from the beginning.

In the second year of the five years lasting MPPF-project the first demonstration façade was installed in Stallhofen near Graz (Austria) including innovative solar thermal collectors (ST) and photovoltaic modules (PV).

In order to study the energetic behaviour of the various technologies as well as the influence of single functional façade elements on the building core an intensive monitoring was set up. Important building physical aspects, such as temperature loads, moisture content, and heat transfer were recorded via temperature, humidity and heat flux sensors at various positions. Analysis of the energy yield of ST collectors was done via mass flow meters and temperature sensors, the energy yield of PV modules was detected by their short circuit current. Measurements of the ambient conditions, such as solar radiation, wind speed, wind direction and outside temperature complemented the monitoring.

In addition to the very concept as well as the installed demonstration façade itself we show continuous monitoring results starting from June 2010 covering the periods of low-standing sun, most important for these façade modules.

INTRODUCTION

Beyond constructing buildings with very small demands of energy out of non-renewable sources, cf. passive house standard, more and more buildings with even no demand of these

Modules 1-3, 7-15, 17 facing southwards
Modules 4-6, 16, 18 facing westwards

1-3	opaque polycrystalline PV
4-5	opaque polycrystalline PV
7	amorphous semi-transparent (10%) PV
8	amorphous semi-transparent (20%) PV
9	daylight photovoltaics module
10-12	solar thermal collectors
13-15	solar thermal collectors
16	HVAC module
17, 18	electrochromic windows

Figure 1: First demonstration façade at FIBAG façade test building (Stallhofen, Austria)

sources are erected, so-called energy-plus-buildings. Therefore, renewable energy sources, such as biomass, geothermal, solar thermal or photovoltaics are directly used in family houses, offices and industrial buildings, thus converting more renewable energy than consumed for heating, cooling and electricity [1]. By integrating renewable energy systems into buildings requirements of architects, system planners, manufacturers, building companies and end-users must be taken into consideration. Sound energetic design, ease of fabrication, proper functionality and architectural quality must be ensured over the whole life-span of decades [2, 3].

The Austrian research project "Multifunctional Plug & Play Façade" (MPPF) treats the building envelope as an active part of the building. The conversion of various renewable energy sources is integrated directly into the façade. In addition, heating and cooling out of the façade as well as ensuring a suitable indoor climate is developed. Our consortium, consisting of façade builders, system planners and manufacturers as well as research institutes, entangles the various interest groups right from the beginning.

METHOD

Demonstration façade

After a literature study and a development phase the first demonstration façade including innovative solar thermal collectors (ST) and photovoltaic modules (PV) was installed in Stallhofen near Graz (Austria), see figure 1.

In the opaque fields 1 to 3 (southward facing) and 4 to 6 (westward facing) of the demonstration façade the outer end panels were replaced by polycrystalline glass-glass modules with an anthracite enamelling. Instead of the original fixed glazing in the modules 7 and 8, fixed glazing with integrated amorphous semi-transparent silicon thin-film modules was installed. Module 9 intented for combining shading and photovoltaics is still in the development phase. Two solar thermal collector fields (10 to 12 and 13 to 15) are integrated into the south facing façade and are connected in parallel to charge a hot water tank (500 litre) via a controlled solar pump group. The tank provides hot water for the façade-integrated module for heating, ventilation and air conditioning (module 16). To investigate several technologies the two collector fields have different glazing, different selectively coated absorber materials (copper / aluminum) and different insulation, see figure 2. The modules 17 and 18 are prototypes of electro chromic windows for controlling the radiation input into the building by changing their light transmissibility.

Monitoring

An intensive monitoring was set up in order to study the energetic behaviour of the various technologies as well as the influence of single functional façade elements on the building core. Important building physical aspects, such as temperature loads, moisture content and heat transfer were recorded via temperature, humidity and heat flux sensors at various positions in the solar thermal collectors, the HVAC module and the photovoltaic modules (cell and glass temperatures), see figure 2.

Measuring of the fluid temperatures and volume flows through the solar thermal collectors as well as the hot water tank temperatures allow for energy balancing. Short circuit measurements were taken in order to characterize the performance of the photovoltaic modules.

The ambient conditions have been characterized by monitoring solar radiation, wind speed, wind direction and outside temperature.

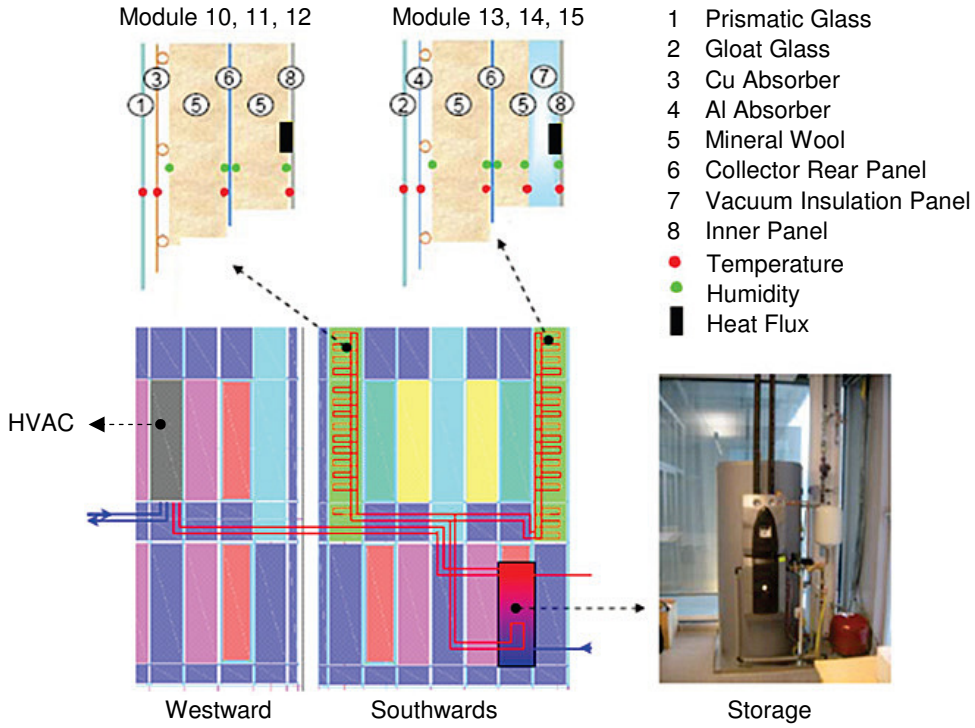

Figure 2: Lower left: demonstration façade with hydraulic scheme of the solar thermal energy system (collectors, hot water tank and HVAC module). Upper picture: sectional view of solar thermal collectors with sensors.

RESULTS

Solar thermal façade collectors

The weather conditions and the behaviour of the solar thermal system in 2010 are shown exemplarily for one week at the beginning of autumn (calendar week 38), see figure 3. The controlled solar pump group keeps the temperature difference between the inlet and outlet of the collector field equipped with copper absorbers in the range of 10 to 15 Kelvin. The calculated thermal output of the two different collector fields is nearly the same – peaks range from 1.5 kW to 1.8 kW at a global radiation of about 800 W/m². Figure 4 shows the current efficiencies calculated out of the mean values of 2.5 minutes intervals (referring to absorber

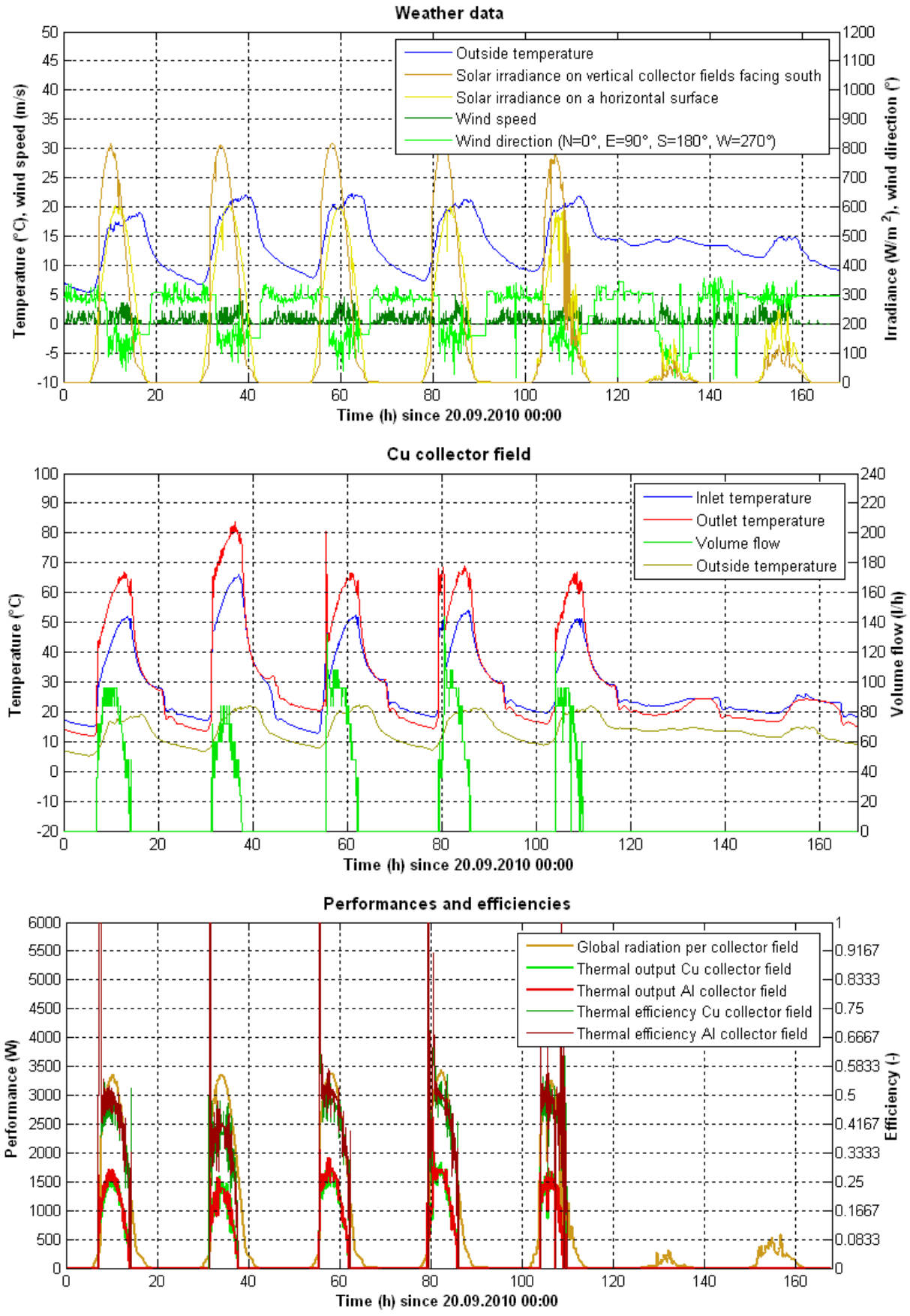

Figure 3: Weather conditions and behaviour of the solar thermal system in calender week 38/2010. (For better legibility see colour version on CD-ROM of CISBAT 2011 Proceedings)

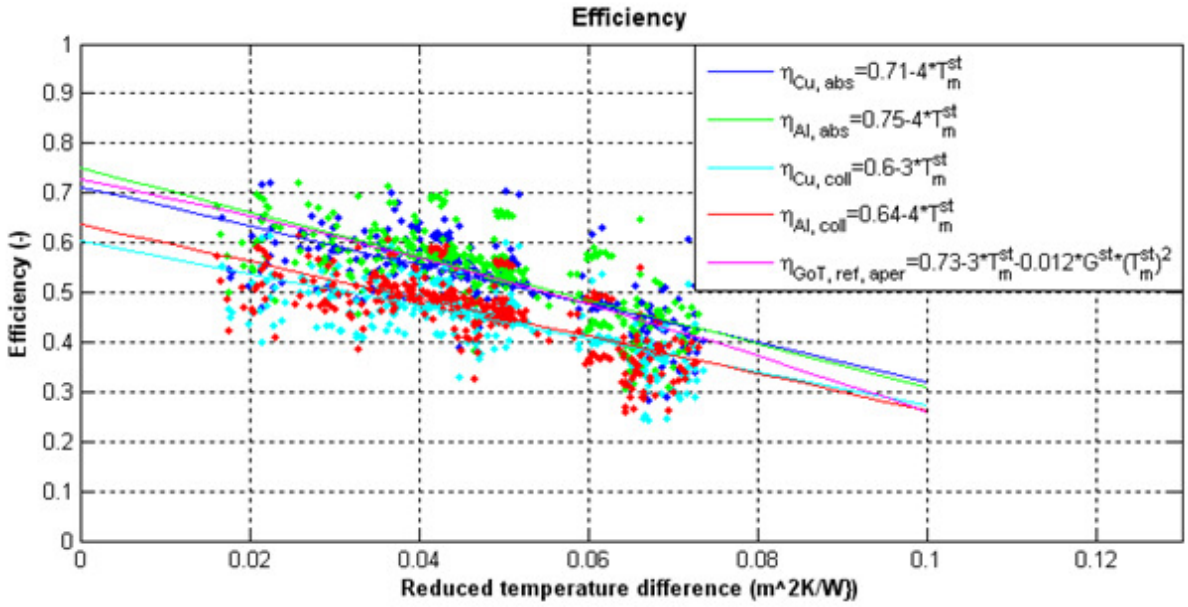

Figure 4: Efficiency of the façade modules referring to absorber area and gross area respectively in periods of fine weather in 2010. (For better legibility see colour version on CD-ROM of CISBAT 2011 Proceedings)

area and gross area respectively) over the reduced temperature difference (i. e. the difference of the mean temperature of the collector and the ambient temperature divided by the global radiation) in chosen periods of fine weather in 2010. In order to compare the monitoring results of the two collector fields with results of common laboratory tests one can calculate fitting lines. It turns out that the efficiency of the collector field equipped with aluminum absorbers is slightly higher and that both collector fields have efficiencies like the reference product of our collector manufacturer.

Photovoltaic Façade Elements

By reference to one sunny day in summer 2010 performance and temperatures inside the photovoltaic modules can be shown, see figure 5.

As expected, the short circuit current of the polycrystalline façade elements is higher than that of the amorphous semitransparent photovoltaic modules. A temperature difference of up to 20 Kelvin in vertical direction have occured inside the polycrystalline PV module on the south façade. Since higher temperatures reduce the efficiency of the modules, reasons for this behaviour have to be found. On the one hand it is possible that the lower cells are cooled by natural convection. On the other hand shading due to a ledge at the top of the façade element could alter the upper cells into ohmic resistors which heat up while they are current-carrying. Further investigations are necessary to exactly identify the reasons for this problem.

CFD simulations of the façade-integrated solar thermal collectors

It has turned out that the temperature of the inner wall of the façade elements is too high in terms of comfort. This is a crucial problem in particular in times of stagnation of the solar thermal system. In order to investigate and optimise the physical processes inside the façade elements, CFD simulations are used. At the beginning radiative heat transfer has been neglected and temperature boundary conditions have been chosen. The results have been satisfying.

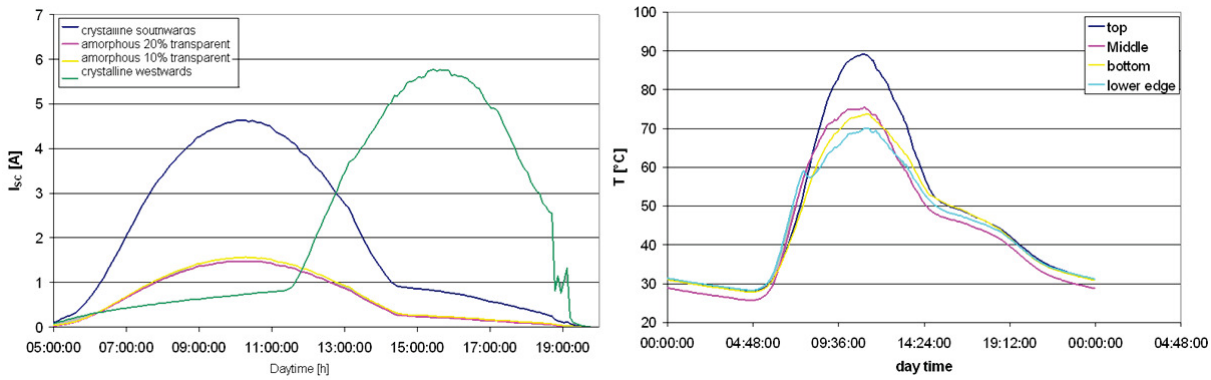

Figure 5: Left graph: Short Circuit Current of PV modules. Right graph: vertical temperature distribution of the southward facing polycrystalline PV module for a sunny day (19.7.2010).

Modelling of the solar thermal façade collectors by means of Dymola and Genopt

The parameters of simulation models of the two collector fields were determined via Dymola-simulations combined with Genopt-optimisation on the basis of the monitoring data collected in calendar week 26/2010. The types provide the medium-temperature on the outlet port of the respective collector field, as a function of volume flow, inlet temperature, global radiation, outside temperature and wind speed. The type only provides reasonable results if the flow in the respective collector field is different from null. Therefore, results in standstill periods of the equipment must be filtered out of the simulation. It turns out that the simulation results largely meet the monitored values.

SUMMARY AND OUTLOOK

On the basis of the operating data collected in the first operating year characteristics of the solar thermal system, building physical aspects of the façade-integrated collector fields and the behaviour of the photovoltaic modules have been found out. Based upon that CFD as well as Dymola simulations have been started, which allow for further characterisation and optimisation of the ST modules as well as for the complete solar thermal system. Further development of the St collectors will lead to the next prototypes which will be equipped with new insulation materials (e. g. Aerogel) in order to reduce the temperatures on the inner walls of the façade modules. Some of the insulation materials to be considered have already been characterised by thermo physical measurements.

ACKNOWLEDGEMENTS

The authors wish to thank all MPPF team members for their individual contributions and valuable discussions in the course of the project.

This work was financially supported by the Österreichische Forschungsförderungsgesellschaft (FFG, COMET project no. 815075), Steirische Forschungsförderungsgesellschaft (SFG), tecnet and Kärntner Wirtschaftsförderungsfonds (KWF).

REFERENCES

1. Kalogirou S. A., Solar Energy Engineering – Processes and Systems, Oxford,UK, Elsevier Inc., 2009.
2. Matuska T., Sourek B., Façade solar collectors, Solar Energy 2006, 80(11): 1443-1452
3. Roberts S., Building Integrated Photovoltaics, Basel, CH, Birkhäuser, 2005

THE IMPACT OF CLIMATE ON MOISTURE WITHIN NON-VENTILATED FLAT ROOFS IN TIMBER FRAME CONSTRUCTION

J. Bachinger[1,2]; K. Krec[1]
1: Vienna University of Technology, Faculty for Architecture and Regional Planning, Institute of Architecture and Design, Karlsplatz 13, A-1040 Vienna, Austria
2: Gartenmann Engineering SA, Av. d'Ouchy 4, 1006 Lausanne, Switzerland

ABSTRACT

After the development of prefabricated elements in timber frame construction and their common application for non-ventilated flat roofs (the so called "Multibox" flat roof), the instances of reported damage to these flat roofs increased in Vorarlberg (Austria).

Due to the lack of investigations into the factors influencing the moisture behaviour of non-ventilated flat roofs the reasons for damage are often difficult to determine [1]. The present study investigates the influence of climate conditions on the hygrothermal behaviour of "Multibox" flat roof systems. For this purpose, data of realized flat roofs was collected in the Vorarlberg region in order to base the investigation on realistic assemblies. 25 flat roof types were examined by both calculation according to Glaser and through dynamical simulation. Both calculation methods were applied to three different climate locations in the Vorarlberg region.

The analysis of the results of these comparative studies reveals the influence of climate conditions on the hygrothermal behaviour of "Multibox" flat-roof systems.

Firstly, it turns out that a Glaser calculation based on Austrian standards is inadequate to reproduce realistic results for these constructional elements.

Moreover, a Glaser-calculation based on radiant air temperature values discloses the inadequacy of this calculation method to provide realistic data for the moisture behaviour of non-ventilated flat roofs.

Furthermore climate conditions are proven to have a significant influence on the total amount of moisture within the Multibox flat-roof systems. One major factor highly influencing the process is solar radiation. To add further support to this discovery, a hygrothermal simulation of varying absorptivity for solar radiation of the outer surface was carried out.

INTRODUCTION

In the late 1990s prefabricated flat roof timber-frame construction (the so called "Multibox-Element") was developed in Vorarlberg, a region in Austria where timber frame construction is commonplace.

As beam and insulation are arranged on one common level between vapour-barrier or vapour-brake and roof membrane, the height of the element is reduced compared with the traditional arrangement of insulation on top of the beam. Therefore this box-section element responds perfectly to the aesthetical demands of architects and allows, at the same time, a better insulation performance and shorter construction time.

However, regarding their moisture behaviour, these building elements do show some disadvantages. Professionals in Vorarlberg are nowadays aware of the sensitivity of these constructional elements and try to avoid them particularly in regions with high altitudes, because simple calculations according to Glaser show more problems for non-ventilated flat roofs if realized in severe climates [1].

But do climate conditions at high altitudes really have a worse influence on the moisture behaviour of "Multibox" flat roofs than mild climates at lower altitudes? And is the influence of climate conditions on the non-ventilated flat roof significant? And moreover, which parameters (temperature, humidity, radiation) show the most significant impact on moisture behaviour for these roof systems?

In the present investigation 25 elements constructed in Vorarlberg are examined using three different climate conditions. Thus, the impact of solar radiation on the moisture behaviour of the "Multibox" flat roofs can be deduced.

In addition, the ability of the Glaser-calculation to produce realistic results is examined. For this purpose, the influence of solar radiation on the outer surface of the assembly is integrated into the ambient air temperature values used for the calculation.

METHODS

Description of the "Multibox" flat roof

In principle, the "Mulitbox-Element" consists of beams arranged between an upper and a lower board of plywood (figure 1).

Some flat roofs in timber frame construction are constructed with a ventilation zone between the roof membrane and the insulation. Roofs with ventilation like this do not form part of this investigation.

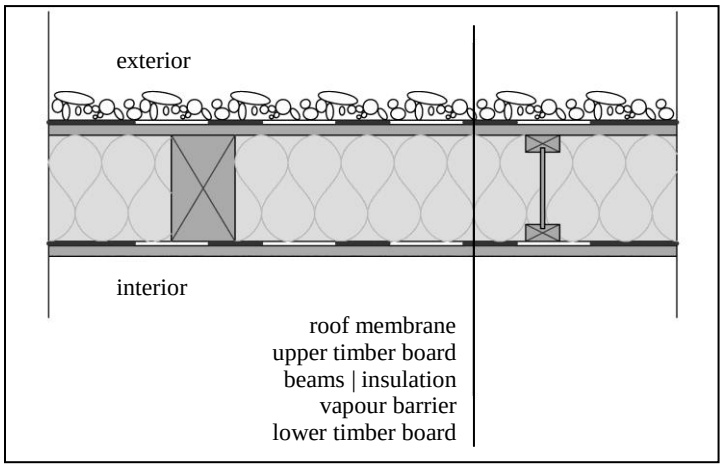

Figure 1. Schematic illustration of a "Multibox" flat roof

Data of "Multibox" flat roofs

Existing flat roofs in the Vorarlberg region were examined, thus grounding this research on realistic construction methods. In order to collect information about flat roofs, several architects, carpenters and claim experts have been consulted. Among the examined flat roofs, 25 assemblies met the criteria for a "Multibox" flat roof as shown in figure 1 and were chosen for this study.

In general, the exterior layer of a flat roof can consist of a membrane, gravel, concrete slab or a green covering. This study is solely based on cases for which the roof membrane is the exterior layer.

Calculation methods and climate data

Moisture behaviour for the 25 construction elements was calculated using the Glaser-method as is set out in EN ISO 13788 [2] in the first instance and using the moisture transfer simulation program WUFI [7] in the second. In both methods, the location in the Vorarlberg region was introduced as an additional variable of the cities of either Bregenz, Bürs or Schröcken.

Their climate can be characterized as follows:

Bregenz (Br): altitude 400 m. Situated in the Rhine Valley riparian to Lake Constance, Br has a mild climate that is rather humid with frequently overcast sky and fog in spring and autumn.

Bürs (Bü): altitude 570 m. Bü is situated in the southern Rhine Valley in Vorarlberg. Its climate is dryer and cooler than the climate of Br: The monthly average ambient air temperature in Bü is in December 2.9 K cooler than in Br.

Schröcken (Schr): altitude 1269 m. Schr is a village in the mountains where winter can be very cold and dry with little cloud.

The climate data of the three cities are taken from different data-bases:

climate data set 1 (Glaser-calculation): Monthly average ambient air temperature and relative humidity pursuant to Austrian standard ÖNORM B 8110-5 [5].

climate data set 2 (Glaser-calculation): Radiant air temperature values based on long-term monthly average values of ambient air temperature and relative humidity recorded by the Austrian Central Institute for Meteorology and Geodynamics [8, 9, 10]. The influence of solar radiation on the outer surface of the construction element was integrated into the ambient air temperature values as shown by Koch & Pechinger [4]. Solar radiation data was taken from PVGIS [6].

climate data set 3 (dynamical simulation): Semi-synthesised climate data records (German: HSDK = halbsynthetische Klimadatensätze) were created using the method according to Heindl et al. [3]. Long-term monthly average values of climate data for the three locations (Br, Bü, Schr) were converted into hourly data based on recorded hourly data of the climate station Vienna, "Hohe Warte" between January 1, 1951 and December 31, 1988 [6, 8, 9, 10].

For each city three different sets of climate data were applied in the calculations.

CLIMATE INFLUENCE ON THE MOISTURE BEHAVIOUR OF "MULTIBOX" FLAT ROOFS

Glaser-calculation based on climate data set 1

For the city Schr formation of condensate can be observed for more flat roof systems than for Br and Bü, especially in the beam layer. Moreover, the evaporation of the accumulated condensate during summer months is higher in Br and Bü than in Schr. When comparing the two, more condensate can be detected in Bü than in Br [1].

As the only difference between the calculations for the three locations is given by the climate data, the inhomogeneity of the calculation results is affected by the ambient air temperature and relative humidity.

According to the Austrian standard ÖNORM B 8110-5 [5] the monthly average ambient air temperature is determined by the region and the altitude of the location. Since pursuant to ÖNORM B 8110-5 [5] all three positions are located in the same region, the only variable is the altitude. The higher the altitude of the location, the lower is the average ambient air temperature. And as a consequence, more condensation in winter and less evaporation during summer months appears according to the Glaser-method.

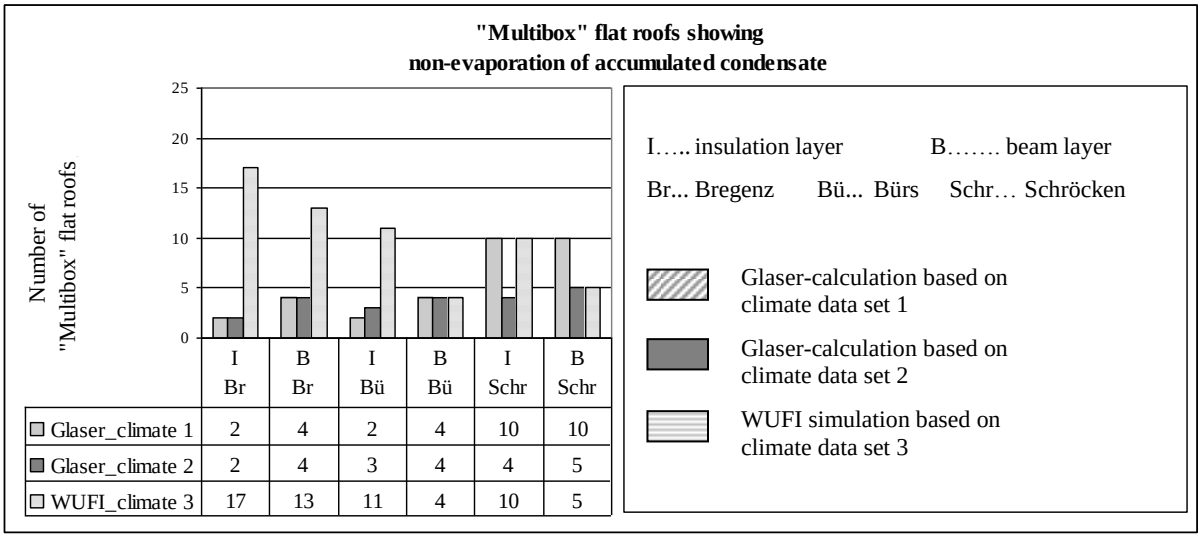

Figure 2. Number of "Multibox" flat roof systems showing non-evaporation of accumulated condensate for the Glaser-calculations based on climate data set 1 and climate data set 2 and elements showing increase of the total moisture content for the WUFI-simulation based on climate data set 3.

Dynamical simulation and comparison of climate conditions

Dynamical simulation based on climate data set 3

In Br, 52 % (insulation layer) or 68 % (beam layer) of the "Multibox" roof systems shows increase in total moisture content. In Bü and Schr fewer elements are exposed increasing the total moisture content: In the insulation layer 40 % (Schr) to 44 % (Bü); in the beam layer 16 % (Bü) to 20 % (Schr). Moreover, more flat roof systems show an increase of total moisture content in Br than in Bü and Schr.

The results of the Glaser-calculation based on climate data set 1 shows the opposite tendency. Whereas the Glaser-calculation determined Schr to be the least favourable place for the flat roof system, the output of the WUFI simulation identifies Schr as the most suitable of the three cities.

What is the difference between the climates of the three cities?

The components of climate data set 3 are: ambient air temperature; relative humidity; global radiation; diffuse solar radiation; wind velocity; wind direction; rainfall. As the WUFI simulation was established without an exterior heat transfer coefficient - dependent on wind and without absorption of rain - the data of wind velocity, wind direction and rainfall do not affect the simulation results.

Comparing ambient air temperature and relative humidity of climate data set 3 for Br, Bü and Schr to those of climate data set 1, no discrepancy can be detected that would serve to explain the opposed outcome of the investigation. In Br, the monthly average of ambient air temperature of climate data set 3 is higher than the monthly average of climate data set 1. In Bü, climate data set 3 shows for winter months cooler monthly averages of ambient air temperature than climate data set 1. Only in Schr could ambient air temperature be a factor of influence on the moisture behaviour of the flat roofs: In December, January and February the monthly average of ambient air temperatures is about 1.0 K higher than the monthly average of climate data set 1.

When comparing the data of global radiation and diffuse solar radiation of climate data set 3 for Br, Bü and Schr, radiation turns out to be the main influence on the varied simulation results. The sum of the monthly averages of the daily totals of both global radiation and diffuse solar radiation is every month higher in Bü than in Br. Even though the disparity between the radiation in Br and Schr is less important than between Br and Bü, the city Schr always shows higher radiation sums than Br (with the exception of global radiation in August).

This explains why more "Multibox" flat roofs show decreasing total moisture content in Bü and Schr than in Br, despite a higher altitude and lower ambient air temperatures. The influence of radiation on the roofs contributes to the drying-out of accumulated moisture.

Simulation results with differing radiation absorptivity

A second WUFI simulation (simulation **b**) was carried out for "Mulibox" flat roof number 3 in order to prove the influence of radiation on these roof systems. For this purpose, the absorptivity for solar radiation and the emissivity for long wave radiation of the outer surface were modified compared to the first dynamical simulation (simulation **a**) thus:

Coefficients used for simulation **a**:
- Absorptivity for solar radiation: 0.4
- Emissivity for long wave radiation: 0.9

Coefficients used for simulation **b**:
- Absorptivity for solar radiation: 0.8
- Emissivity for long wave radiation: 0.97

The modification of these values is indicated by a different colour of the roof membrane. While simulation **a** assumes a light-grey colour of the membrane, simulation **b** adopts a dark-grey membrane colour.

The results for the total moisture content of simulation **a** and simulation **b** are compared in figure 6. For simulation **b** total moisture content is decreasing in all three climate locations. Even

in Br a decreasing Δu'm can be observed for simulation **b**, although simulation a showed little decrease in the insulation layer and even an increase of total moisture content in the beam layer.

No variation was applied in the investigation except of the radiation coefficients, which determines the effect of global and diffuse solar radiation on the construction element. Therefore, this study highlights that radiation has a major influence on the moisture content of "Multibox" flat roofs.

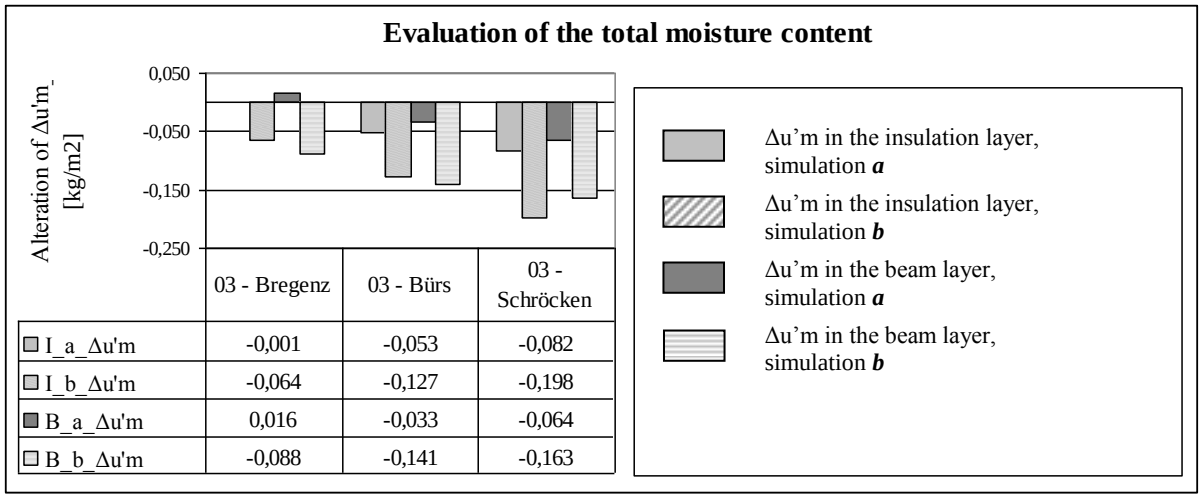

	03 - Bregenz	03 - Bürs	03 - Schröcken
I_a_Δu'm	-0,001	-0,053	-0,082
I_b_Δu'm	-0,064	-0,127	-0,198
B_a_Δu'm	0,016	-0,033	-0,064
B_b_Δu'm	-0,088	-0,141	-0,163

Figure 3. Evaluation of the total moisture content for simulation a and b for "Multibox" flat roof no.3 (dynamical simulation, climate data set 3).

Glaser-calulation with inclusion of the influence of solar radiation (climate data set 2)

A second calculation according to Glaser was carried out based on climate data set 2 to examine the suitability of a Glaser-calculation to display the moisture behaviour of "Multibox" flat roof systems.

In Br no accordance can be detected comparing the results of this Glaser-calculation to the results of the dynamical simulation. The same observation can be made for the insulation layer in Bü. In the beam layer, the same number of construction elements show non-evaporation of condensate and increase of total moisture content in Bü. In Schr, the calculation based on climate data set 1 determines the same number of construction elements showing non-evaporation in the insulation layer as the WUFI simulation. However, the results of the Glaser-calculation based on radiant air temperatures do not correspond to the WUFI simulation results. In the beam layer, the Glaser-calculation based on climate data set 2 for Schr is able to produce results corresponding to the dynamical simulation.

Thus, the inclusion of radiation in ambient air temperatures for a Glaser-calculation only for the beam layer in Schr produces similar results to the output of a dynamical simulation.

Furthermore, the amount of condensate was also compared. In Br and Bü, the roof elements show more condensate with the Glaser-calculation based on climate data set 2 than with climate data set 1. In Schr, the calculation based on radiant air temperatures determines less condensate and more evaporation than the calculation based on climate data set 1. The application of radiant air temperatures contributed to higher evaporation in Schr, which accords better with the dynamical simulation than the results of the calculation based on climate conditions according to Austrian standards. However, it is not possible to reproduce a realistic output by employing radiant air temperatures in a Glaser calculation corresponding to the standard EN ISO 13788 [2].

Hence, there is no satisfying accordance between a Glaser-calculation based on radiant air temperatures and the increase of total moisture content after the dynamical simulation.

CONCLUSION

The present study shows the high impact of climate conditions on the moisture behaviour of "Multibox" flat roof systems. In particular solar radiation was identified as the main factor of influence on the total moisture content of non-ventilated flat roofs. Thus, the current philosophy to not use "Multibox" flat roofs in high altitudes appears to be problematic. The opposite can be advisable as there is often more solar radiation in such locations than in valleys with predominantly mild but humid conditions and frequent fog. Therefore the climate conditions of locations situated on the mountainside can be more appropriate for non-ventilated flat roofs.

Furthermore, the important contribution of solar radiation to achieve a stable value of the total moisture content shows clearly that the construction of these roofs should be avoided in places where exposition to sufficient solar radiation cannot be guaranteed.

Moreover, the present study shows the impact of solar radiation on the moisture evaluation of flat roofs and it delivers useful advice for future dynamical simulations. The selection of climate data for such dynamical simulation is limited. Frequently, data is not available for the location under investigation. For this reason, data for sites with similar or more severe climate conditions are often used as substitutes. When choosing the appropriate climate for an investigation of non-ventilated flat roofs the impact of radiation should be considered. Thus, colder climates could even lead to more favourable climate conditions for these construction elements.

In addition, it was shown that calculations according to Austrian standards are not appropriate to predict the moisture behaviour of non-ventilated flat roofs. Even Glaser-calculation based on radiant air temperatures fails to generate realistic data.

REFERENCES

1. Bachinger, Julia. 2010. Moisture behaviour of flat roofs in timber-frame construction. Particularly of non-ventilated flat roofs, whose insulation and beam layer are situated between vapour barrier / vapour brake and roof membrane. Doctoral thesis. Vienna University of Technology.
2. EN ISO 13788. 2001. Hygrothermal performance of building components and building elements – Internal surface temperature to avoid critical surface humidity and interstitial condensation – Calculation methods. Brussels: European Committee for Standardization
3. Heindl, W. Kornicki, T. Sigmund, A. 1990. Creation of semi-synthesized climate data sets for meteorological stations (Erstellung halbsynthetischer Klimadatensätze für meteorologische Messstationen). Forschungsbericht im Auftrag des Bundesministeriums für Wissenschaft und Forschung (GZ. 70.630/18-25/88) und des Amtes der NÖ - Landesregierung (Zl. NC 23-1988/1989). Vienna:
4. Koch, H.A. Pechinger, U. 1977. Options to incorporate the influence of solar and heat radiation on surfaces of buildings. (Möglichkeiten zur Berücksichtigung von Sonnen- und Wärmestrahlungseinflüssen auf Gebäudeoberflächen). Gesundheits-Ingenieur 98. No. 10. 265-280.
5. ÖNORM B 8110–5. 2007. Thermal insulation in building construction – Part 5: Model of climate and user profiles. Vienna: Österreichisches Normeninstitut.
6. PVGIS, Solar Irradiation Data, © European Communities, 2001 – 2007, http://re.jrc.europa.eu/pvgis
7. WUFI Pro. 2005. Version 4.0. Release 4.0.0.190.DB.23.10. PC-Program for calculating the coupled heat and moisture transfer in building components. Holzkirchen: Fraunhofer Institut Bauphysik.
8. ZAMG = Zentralanstalt für Meteorologie und Geodynamik (Central Institute for Meteorology and Geodynamics). 2006. Funished climate data set for Bregenz on 30.08.2006. Average determination for the period between 01.01.1976 and 31.12.2005. Vienna – Hohe Warte
9. ZAMG. 2006. Statistical monthly average values for Schröcken. Climate data of Austria 1971 – 2000. Vienna – Hohe Warte: Central Institute for Meteorology and Geodynamics www.zmag.ac.at. Sector „langjährige Klimadaten"
10. ZAMG. 2006. Furnished climate data set for Bürs on 30.08.2006. Average determination fort he period between 01.01.1971 and 31.12.2000. Vienna – Hohe Warte

BUILDING SIMULATION STUDY OF A RESIDENTIAL DOUBLE-ROW HOUSE WITH SEASONAL PCM-TRANSLUCENT FAÇADE

Francesco Frontini[1,2],*, Jens Pfafferott[1], Sebastian Herkel[1], Dietrich Schwarz[3]

1:Fraunhofer Institute for Solar Energy Systems ISE, Heidenhofstr. 2, 79110 Freiburg, Germany.

2: Institute for Applied Sustainability to the Built Environment (ISAAC-SUPSI), campus Trevano, CH-6952, Canobbio-Lugano

2: GlassX AG, Technoparkstrasse 1, CH-8005 Zürich

*: main author email: francesco.frontini@supsi.ch

ABSTRACT

Natural sources of energy exist in many forms and in adequate quantities on Earth, but they are not always available when needed. How can we take advantage of the warm daytime during the night or, vice versa, exploit the cool night temperatures far into the day? One traditional measure is the use of the thermal storage capacity of solid materials, such as timber, stone, bricks or concrete. In lightweight forms of construction building elements of great mass are not used. In such situations, thermal-storage media offer new possibility for storing heat Thermal energy storage (TES) systems using phase change material (PCM) have been recognized as one of advanced energy technologies in enhancing energy efficiency and sustainability of buildings. The use of PCMs in buildings provide the potential for a better indoor thermal comfort for occupants due to the reduced indoor temperature fluctuations, and lower energy consumption due to the load reduction/shifting.

This paper presents a retrofitting study of a residential double-row house based on dynamic simulation. The existing light-weight façade will be replaced by an air-tight high-performance construction with an increased transparent area using a translucent panel with phase change material.

The innovative component, X-comfort, is a translucent wall element without any mechanical components or electronic devices. It consists of a triple glaze unit (TGU) with a hydrate of salt sealed in polycarbonate hollow cellular slabs in the inner gap. These cells are coloured grey to improve the heat absorption. The thickness of such PCM hollow is about 25mm. The glazing can be equipped in the outer side with a prismatic-glass skin that reflects the high-angle rays of the sun away from the building.

INTRODUCTION

Buildings account for almost 40% of overall energy consumption both in Europe and USA. The majority of this demand is due to the energy needed to provide sufficient indoor comfort. The majority of the existing building stock has to be renovated in order to reduce the energy consumption both for heating and cooling. This paper presents a dynamic simulation for an innovative façade concept which can be used for standardised refurbishment.

The simulations demonstrate that the use of a PCM wall (X-comfort) in the parapet area the heating energy demand can be reduced of about 20% and in summer the indoor temperature can be decreased by 2K.

METHOD

In order to define the best façade design and to investigate the influence of the new PCM glazing system (X-comfort) on comfort and energy demand a three step method is applied.

In the first step, the X-comfort system is measured in the laboratory of Fraunhofer ISE. The direct transmission and the g-value (total solar energy transmittance) were evaluated for different incident angle in order to assess the angle dependency of the transparent façade and to model it correctly in the building simulation software (ESP-r).

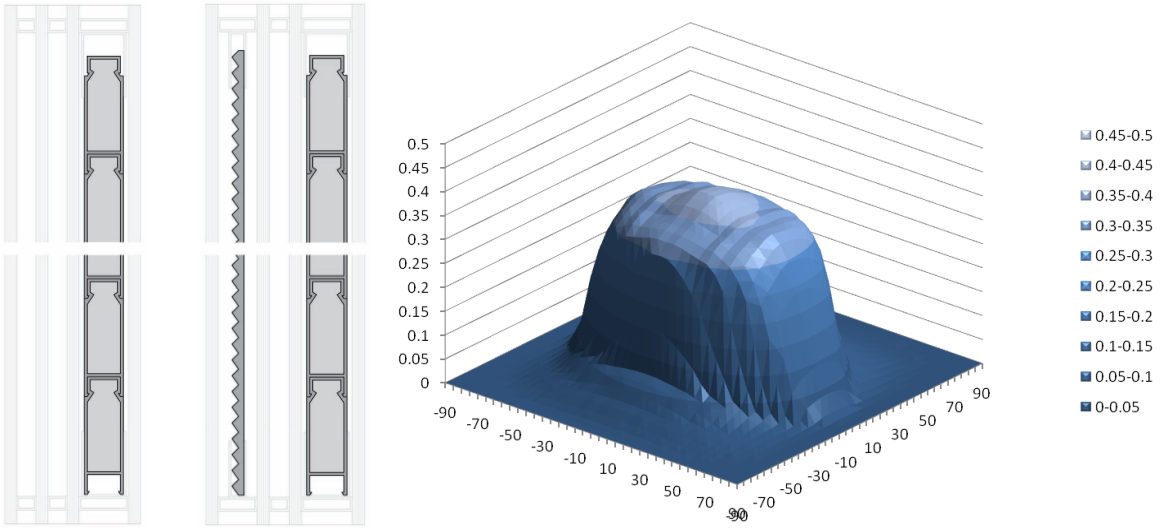

Figure 1: The seasonal PCM translucent façade with and without prismatic skin. The solar transmission of the whole system is pre-calculated with a bi-directional description (5° step).

The second step interpolates the measurement to get the complete angles spectrum of $\tau_{solar}, \rho_{solar}$ (solar transmittance and reflectance) and the g-value, Fig. 1.

In the final step dynamic building simulations with ESP-r [1] are performed for different situations in order to assess the internal temperature and the energy demand for heating and cooling.

The behaviour of PCMs is modelled using ESP-r's special materials facility according to the Heim model [3]. The effect of phase transition is added to the energy balance equation as a latent heat generation term according to the so-called effective heat capacity method.

MODEL SETUP

The ESP-r simulation programme has been modified to allow the modelling of such complex system, see [1], [2] and [5]. Thermal simulations were performed to evaluate the effect of the proposed design on the thermal behaviour and the energy demand of a residential building.

The simulated building is modelled with four different rooms. The zones are considered to be surrounded on the West and on the East site by similar zones (no heat flux is considered through the partition walls). The basement of the zone is linked to the ground and the roof to the external air. The building is South West oriented. To leave the model simple no transversal ventilation is considered between the north and the south zones.

Both the heating energy demand and the room temperature are investigated in order to assess the impact of changing the external glazing façade. The parapet area is changed in order to have four different façade configurations.

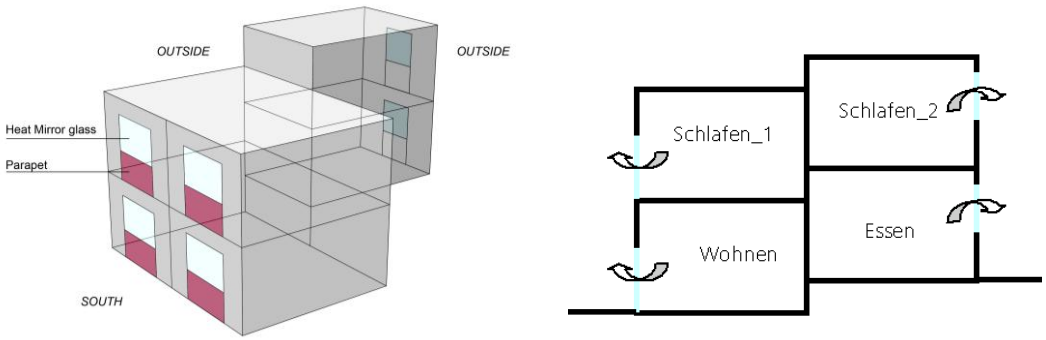

Figure 2: Representation of the simulated model. The model consists of four zones.

Occupants, light and equipment are considered as internal loads. During the whole year the internal gains are 2.1W/m^2. The construction is described in Table 1

Construction	U-value [W/m²K]	Boundary condition
External wall (Sandwich element)	0,18	Facing outside
Partition (plasterboard with insulation)	0,7	adiabatic (no heat flux just thermal mass)
Internal floor	2,8	adiabatic (no heat flux just thermal mass)
Roof	0,17	Facing outside

Table 1: Building Constructions properties

The air exchange between indoor climate and outside is simulated via air change rate which is varied according to the seasons (winter and summer) and to the temperature difference between inside and outside regarding window opening.

The simulations are carried out during winter period to assess the energy demand for the heating system and during summer period to assess the cooling energy demand and to evaluate the indoor air temperature. The heating set point is 20°C and the cooling set point is 26°C.

Two different climates are considered: Stockholm and Frankfurt. Both weather files are generated with Meteonorm.

Façade design

Four façade concepts are simulated for different parapet areas facing South West (respectively in the *Wohnen* and *Schlafen_1* zones, see Figure 2). One configuration has an external shading device to protect the PCM parapet during summer and is activated only during cooling period (Table 2).

concept	window	parapet technology	PCM
V01	Heat mirror Glass	Opaque wall	Without
V02	Heat mirror Glass	Solar Control Glazing	Without
V03	Heat mirror Glass	X comfort	With
V04	Heat mirror Glass	X comfort with external shading	With

Table 2: Four different concepts.

RESULT

A 6 minute time step was used within the simulations. The values of the resultant temperature, PCM node temperature and energy demand for cooling and heating were saved at each time step and evaluated in monthly time periods. The energy demand is also presented for the whole year.

Energy demand

The latent heat stored in the PCM panel is expected to partially cover the heating energy demand at the beginning and end of the heating season. The most important feature of the material is the solidification temperature. The solidification point should be above, but relatively close to, the required internal air temperature. Therefore, a material with a solidification temperature of 22 °C is the most suitable.

The results obtained for concepts V03 and V04 reveal the importance of considering a seasonal shading device in front of the PCM parapet in order to reduce the cooling energy demand in summer (see Figure 3 and Figure 4).

	Frankfurt		**Stockholm**	
	Heating	Cooling	Heating	Cooling
	kWhr/m^2 a	kWhr/m^2 a	kWhr/m^2 a	kWhr/m^2 a
v01	18.74	4.34	60.52	0.57
v02	17.75	11.16	60.41	0.91
v03	14.64	26.51	47.18	3.70
v04	14.92	4.72	48.12	0.67

Table 3: Annual energy demand for Frankfurt and Stockholm.

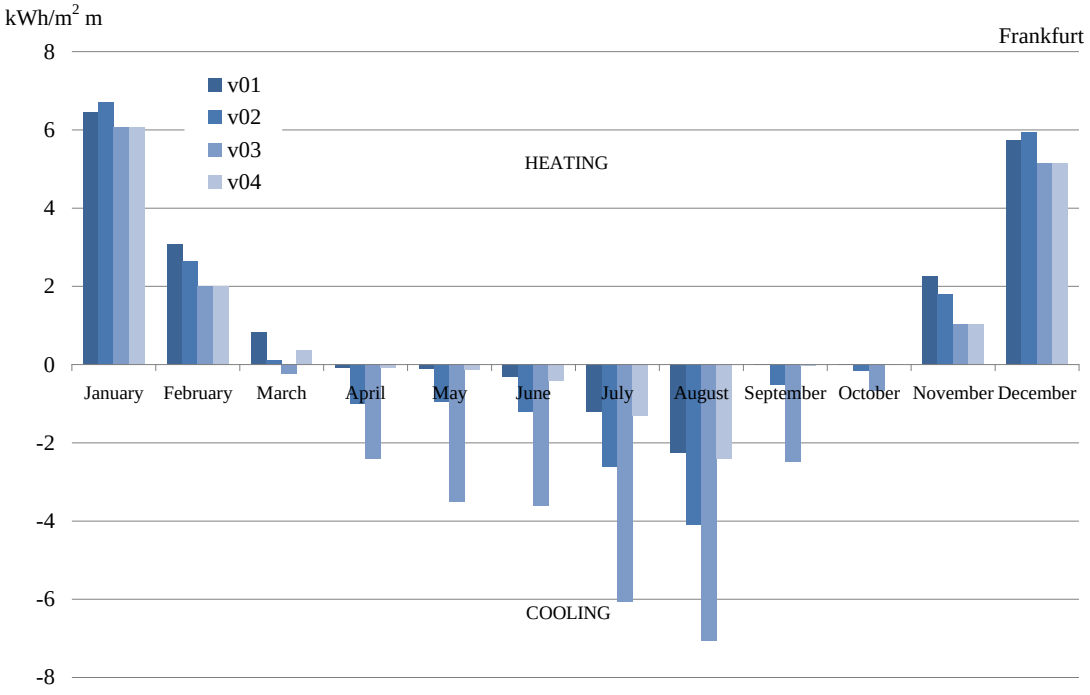

Figure 3: Monthly energy demand for the Frankfurt situation.

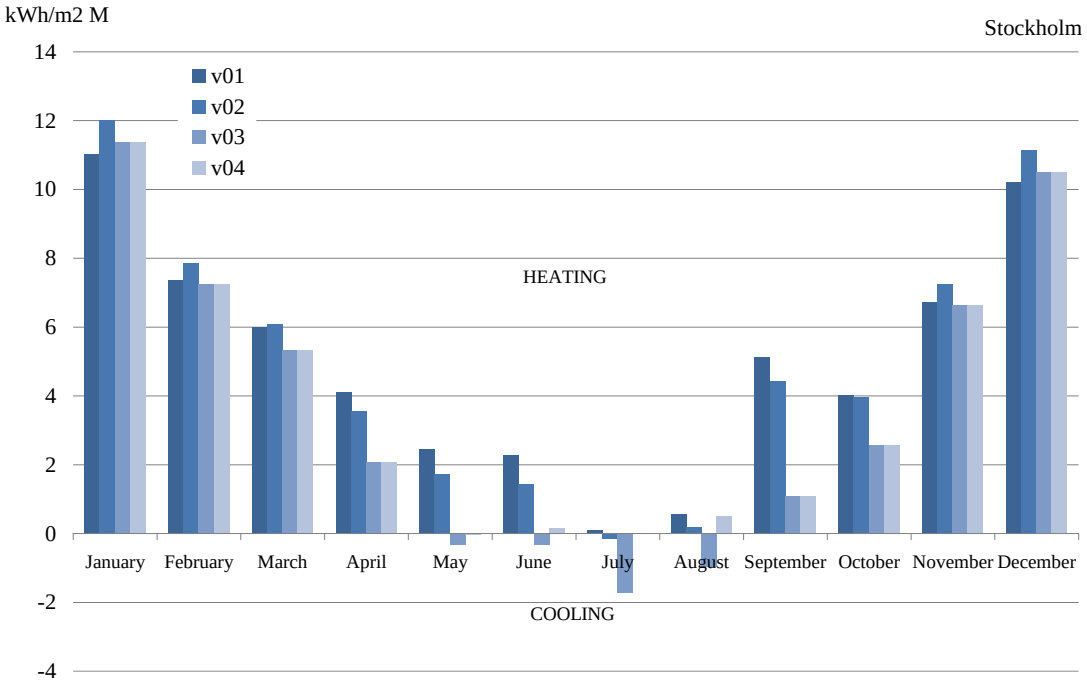

Figure 4: Monthly energy demand for the Stockholm situation.

Operative room temperature

The thermal behavior of the PCM glazing façade affects the operative room temperature. Figure 5 shows the profiles over a selected winter period periods in Frankfurt. It can be shown that due to the latent heat capacity of the X-comfort parapet the system can store heat energy during the day and release it during the late afternoon / night. The summer situation for case v02 is worse because the parapet inside temperature can reach 40°C during summer.

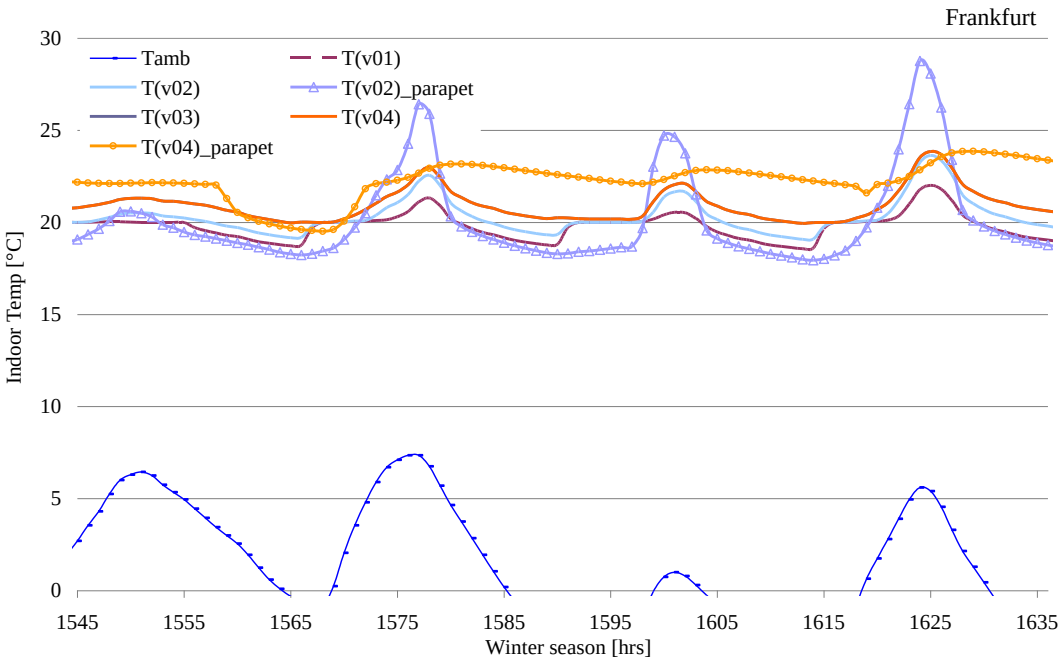

Figure 5: Indoor temperature for a typical winter week in Frankfurt. The inside surface temperature of the parapet for v02 (solar control glazing) and for v04 (X-comfort) is also plotted.

CONCLUSION

The obtained results show the effect of latent heat storage on the thermal behaviour of the building. While this effect does not cause a considerable reduction in diurnal temperature fluctuation, it decreases the internal air temperature in the seasonal transitions periods when the solar energy can effectively be stored. The energy for heating and cooling can also be reduced both in Stockholm and in Frankfurt.

In winter solar thermal gains are optimally attained, stored and released over a long period of time (more than a conventional concrete wall). Due to the high thermal capacity of the PCM the system can increase the thermal mass of the building with a minimum volume.

The software ESP-r is used for the thermal simulations and the solar processing routine is used for the direct transmittance and to calculate the absorptivity of each façade layer.

The simulations demonstrate that the use of a PCM wall (X-comfort) in the parapet area the heating energy demand can be reduced of about 20% and in summer the indoor temperature can be decreased by 2K.

Used properly, PCMs can increase the thermal comfort in lightweight structures and allow service installations to be dimensioned more economically.

The system guide carefully metered daylight into the interior of the building independently of the season in order to guarantee a good daylight performance during the whole year.

Further analysis have to be done in order to enhance the daylighting and to reduce the artificial lighting. Additionally, a more accurate description of the PCM structure with variable density and conductivity is planned.

REFERENCES

[1] Clarke J., Energy Simulation in Buiding Design, second ed., Butterworth-Heinemann, 2001.

[2] Frontini F., T.E Kuhn, S. Herkel, P. Strachan, G. Kokogiannakis, Implementation of a new bi-directional solar modelling method for complex façades within the ESP-r building simulation program and its application, 11th International Building Performance Simulation Association Conference and Exhibition in 2009. Glasgow.

[3] Heim D., Clark J.A., Numerical modelling and thermal simulation of PCM–gypsum, Energy and Buidlings, 2004, n36

[4] Strachan P.. Addition of Blind/Shutter Control to Transparent Multi-Layer Constructions and Other Improvements to the Solar Routines of ESPsim, ESRU Occasional Paper, 1990.

[5] Kuhn, T.E., Herkel, S., Frontini, F., Strachan, P., Kokogiannakis, G., Hand, J. 2009. ESP-r: Implementation of a General Method for the Modelling of Solar Gains through Complex Façades, Energy and Buildings, 2010.

[6] Wienold, J. Daylight Glare in Offices. PhD Thesis, Fraunhofer ISE, 2009.

[7] Wienold, J., Christoffersen, J. Evaluation methods and development of a new glare protection model for daylight environments with the use of CCD cameras, Energy and Buildings, 2008.

[8] EN410: Glass in building - Determination of luminous and solar characteristics of glazing, March 2000.

A STUDY ON HEAT AND MOISTURE BALANCE OF A SUSTAINABLE BUILDING ENVELOPE FOR SUBTROPICAL REGIONS

Y.Goto[1,2]; Th.Frank[2]; K.Ghazi Wakili[2]; Y.Ostermeyer[1]; Th.Stahl[2]; H.Wallbaum[1]

1: ETH Zurich, Swiss Federal Institute of Technology Zurich, Wolfgang-Pauli Strasse 15, CH8093 Zurich, Switzerland

2: EMPA, Swiss Federal Laboratories for Material Science and Technology, Ueberlandstrasse 129, CH8600 Duebendorf, Switzerland

ABSTRACT

Concerning the resource depletion and global warming, the realization of sustainable constructions is crucial because the building industry has a big impact on the greenhouse gas emission. Recently the interest in the buildings in subtropical regions has been growing due to the high growth rate of their urbanized areas. From the view point of building physics, those regions are challenging because they have both heating and cooling demands. Also the prediction of indoor air humidity is acquiring a greater interest concerning the envelope durability, the comfort and the energy consumption. Authors developed a new building envelope system for subtropical regions. This envelope is a vapor-open and sorption-active system which allows the moderate transfer of the water vapor in both directions i.e. from exterior to interior and from interior to exterior. It consists of hygroscopic materials such as wood and clay, and its design system enables the make-up of the envelope to be flexibly changed according to the individual design conditions such as local climate, preferred room temperature and humidity and so on. The wall make-up is optimized so that no occurrence of interstitial condensation is predicted by transient heat and moisture transfer simulations.

The energy consumption and the comfort of the building with this system, which will be built in central Japan, was analyzed. The dynamic energy simulation on hourly basis of an example case was carried out by means of a simulation program in accordance with ISO 13790. Based on the heat balance simulation, the indoor humidity of the living room was predicted by means of a simplified moisture balance equation. This equation included the ventilation rate, the internal moisture load and the moisture buffering by the interior materials. The result of the heating and cooling energy need was 13.9 kWh/m^2 and 9.8 kWh/m^2 respectively. The moisture buffering by the interior finishing reduced the fluctuations of the humidity and the acceptability of the room air. As a result, it was concluded that the utilization of the building envelope system has a high potential to provide the low-energy-consuming and durable houses in subtropical regions. However, there still remains a need to improve the indoor comfort situation in summer. The model will be validated by the in-situ measurement in the test house in the near future.

INTRODUCTION

Concerning the resource depletion and global warming, the realization of sustainable constructions is crucial because the building industry has a big impact on the greenhouse gas emission [1]. Especially, the interest in the buildings in subtropical regions has been growing due to the high growth rate of their urbanized areas in the last decades. It is also worth noting that subtropical area could be geographically extended due to the global warming.

From the view point of building physics, those regions are challenging because they have both heating and cooling period which creates the vapor pressure difference between interior and exterior. The direction of the moisture transfer across building envelopes changes throughout the year. In hot and humid summer, the moisture transfer happens from exterior to interior, and vice versa in cold and dry winter. There already are solutions for cold regions to make buildings more energy efficient and more comfortable dealing with the moisture transfer in winter. However it is inappropriate to implement such design methods to subtropical regions since they are not taking into account the moisture transfer in hot and humid summer. There is a need of new building envelope which can deal with the moisture transfer in both directions.

Also the prediction of indoor air humidity is acquiring a greater interest concerning the envelope durability, the comfort and the energy consumption. Inappropriate design of envelopes results in the interstitial condensation in the envelopes which eventually causes biological deteriorations such as mold growth. This makes the longevity of the building shorter and causes health problems of the inhabitants. Thus it is very important to ensure by building physical means that there is no condensation taking into account the local climatic conditions and the user behavior such as preferred temperature and humidity.

In this study a newly developed building envelope for subtropical regions, which is vapor-open and sorption-active, is introduced. The indoor humidity prediction is carried out using an example case of a building with this system which will be realized in central Japan. In the end the energy consumption and the comfort of the building with this system is analyzed.

METHOD

Vapor-open and sorption-active building envelope

Figure 1 shows the newly developed envelope which is vapor-open and sorption-active allowing the moderate transfer of the vapor in both directions. It consists of hygroscopic materials such as wood and clay, and its design system enables the make-up of the wall to be flexibly changed according to the individual design conditions such as local climate, preferred room temperature and humidity and so on. The sustainability aspect of this system is also of major concern. The materials used for this system contain no substances which are harmful to the humans and the environment, and they have the potential to be produced locally since the basic materials are common materials. The wall make-up is optimized so that no occurrence of interstitial condensation is predicted by transient heat and moisture transfer simulations. The detailed design concept, the prediction of its hygrothermal property and its validation is described in [2].

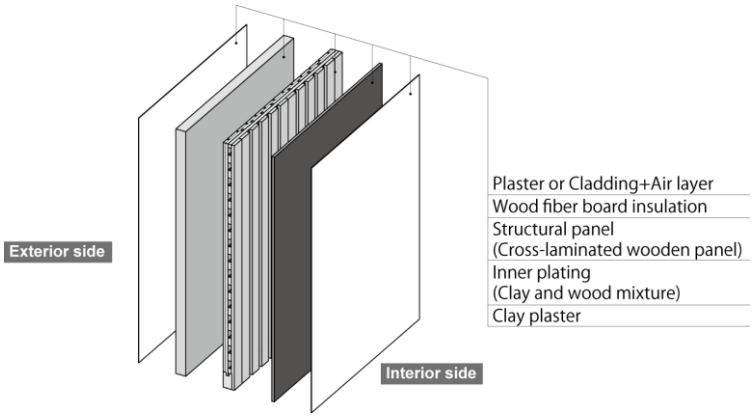

Figure 1: The illustration of the vapour-open and sorption-active building envelope.

Example case

Within this project, several test houses are planned to be erected in central Japan whose climatic condition is subtropical. In the present study, one of those test houses whose gross floor area is 58.7 m^2 (hereafter called "Test House") was chosen for carrying out the in-situ measurement of the room climate (Figure 2). Test House will be located in Ohmihachiman city (at latitude 35.13 degree north and longitude 136.08 degree east), and two inhabitants will be living in it. The wall make-up consists of external finishing with wooden cladding, 18 mm thick air layer, 180 mm thick wood fiber insulation, wind-tight and vapor-open membrane, structural wooden panel, 14mm thick clay board and thin layer of plaster as interior finishing.

Figure 2: The drawings of Test House (floor plans, elevation plans).

Heat and moisture balance simulation

The heat balance simulation of the whole Test House throughout one year was carried out using the simulation program Helios which was developed by EMPA [3]. Helios is able to perform dynamic energy simulations on hourly basis in accordance with ISO 13790 [4]. For the energy calculation, a one zone building model was used. The thermal property of the envelope was defined according to the actual layer design of the building. The corresponding U-value of the wall and roof was 0.20 W/m^2K and that of the windows was 1.3-1.5 W/m^2K. The heating and cooling set-point temperature was 20 °C (maximum heating power: 3.0 kW) and 27 °C (maximum cooling power: 1.5 kW). Regarding the solar gains, it was modeled that movable shading is activated when the room temperature is 25 °C or higher. The daily schedule of the internal heat gain due to the human activities and the appliances were defined in accordance with the Swiss energy standard SIA 380/1 [5] (yearly mean value per floor area: 3.15 W/m^2). Regarding the ventilation, the mechanical ventilation with heat recovery was translated into a reduction of ventilation rate considering the actual efficiency of the heat

exchanger. The input of the modified ventilation rate was 0.14 1/h. The climatic conditions at this site were generated with METEONORM 6.1 (©Meteotest, Bern, 2010) for Hikone city where there is the nearest weather station around Ohmihachiman city. Its temperature and absolute humidity is shown in Figure 3.

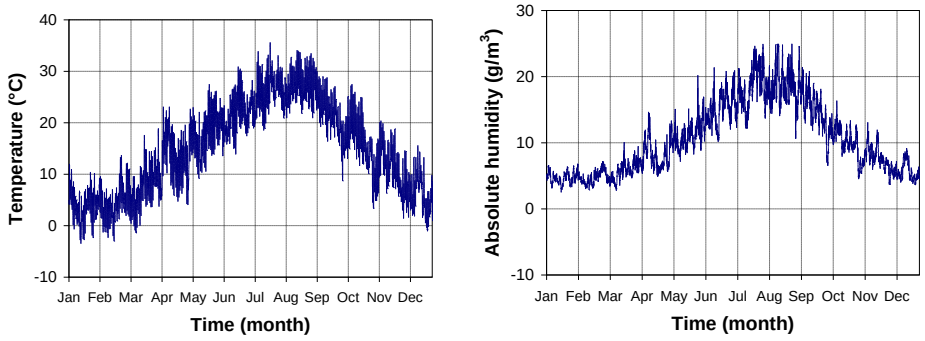

Temperature Absolute humidity

Figure 3: Exterior temperature and absolute humidity of Hikone city.

From the heat balance simulation, one can acquire the predicted indoor temperature throughout the year in addition to the heating and cooling load. Using this predicted room temperature, the indoor humidity of the living room was calculated by means of a simplified moisture balance equation [6] (equation (1)) which includes the ventilation rate, the internal moisture load due to human activities and the moisture buffering by the interior materials.

$$V_R + V_{sor} \cdot \frac{dv_i}{dt} = q_v \cdot \left(v_i - v_e \right) + G_{\text{int}} \tag{1}$$

Where V_R (m^3) is the volume of the room, V_{sor} (m^3) is the equivalent volume of air representing the sorption capacity of the interior surfaces, v_i (g/m^3) is the absolute humidity of the room, q_v (m^3/h) is the exchanged airflow rate, v_e (g/m^3) is the absolute humidity of the supply air, G_{int} (g/h) is the resulting internal moisture load. V_{sor} is calculated by equation (2).

$$V_{sor} = \frac{\sum A_k \cdot MBV_k \cdot 100\% RH}{v_{i,sat}} \tag{2}$$

Where A (m^2) is the area of the sorption-active interior surface, MBV ($g/m^2\%RH$) is the moisture buffer value which was defined in NORDTEST project [7] and $v_{i,sat}$ (g/m^3) is the humidity of the room air by volume at saturation.

By solving equation (1), the absolute humidity of the room air can be given as a function of time as shown by equation (3).

$$v_i(t) = v_e + \frac{G_{\text{int}}}{q_v} \cdot \left(1 - e^{-\frac{n_L}{1+V_{sor}/V_R} \cdot t} \right) \tag{3}$$

Where n_L (1/h) is the ventilation rate.

In the present study, two MBVs were used. One was the MBV of untreated wood which covers the large percentage of the ceiling. The actual experimental MBV was 1.2 $g/m^2\%RH$ which is given in [7] as the value of untreated spruce wood. The other one was the MBV of

the finishing of the walls with clay and plaster. For getting more reliable simulation results, the measurement of its MBV was carried out in accordance with the NORDTEST protocol. The actual experimental MBV was 1.5 g/(m^2%RH). The daily schedule of the internal moisture load of the living room was defined according to the inhabitants' behavior. The input of occupancy of the living room (30m^2) was as follows: 1 hour by two persons in the morning, one hour at noon by one person and 6 hours in the evening by two persons resulting in a daily mean moisture load per floor area of 2.0 g/(h·m^2). The supply air flow rate was 50 m^3/h. For taking into account the dehumidification in summer, the moisture load was reduced assuming a radiator type dehumidifier with the surface area of 4.6 m^2. It was modeled that this equipment was activated giving the surface temperature of 18 °C when the room air was 25°C or higher.

RESULTS

The result of the heating and cooling energy need was 13.9 kWh/m^2 and 9.8 kWh/m^2 respectively. The predicted room air temperature and the relative humidity which took into account the moisture buffering throughout the year is shown in Figure 4 (a) for the living room. The relative humidity was calculated in two cases, namely one case which takes into account the moisture buffering by the interior and the other case which does not. Those results in a humid period (from 22.08 to 01.09) are shown in Figure 4 (b).

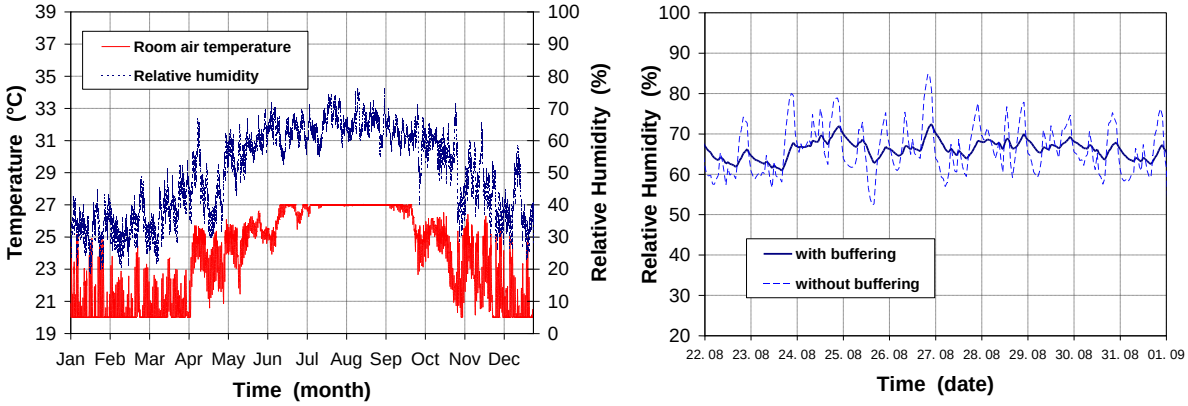

(a) The predicted room temperature (b) Comparison of with/without buffering

Figure 4: The predicted air temperature and relative humidity for the living room

DISCUSSION

The energy consumption for both heating and cooling is fairly low. This is because of the sufficient amount of the insulation and the design considering the solar gains in winter. Over heating in summer can be avoided by implementing an appropriate shading system.

From Figure 4 (b), it is shown that the moisture buffering by the interior finishing reduced the humidity fluctuations. According to Fang et al. [8], the indoor air quality can be predicted with an acceptability-index (Acc), based on the air temperature, humidity and the pollution level. Acc. is given between 1.0 and -1.0. The higher the value is, the more comfortable the air is. Figure 5 (a) shows the predicted acceptability-index in the living room throughout the year for clean air. Figure 5 (b) shows the comparison with the two cases, namely with and without buffering. The mean values of the Acc. did not change with the buffering function. However it is worth noting that the fluctuation of the Acc. was reduced by significant level. For the summer period, there is a need to improve the acceptability-index.

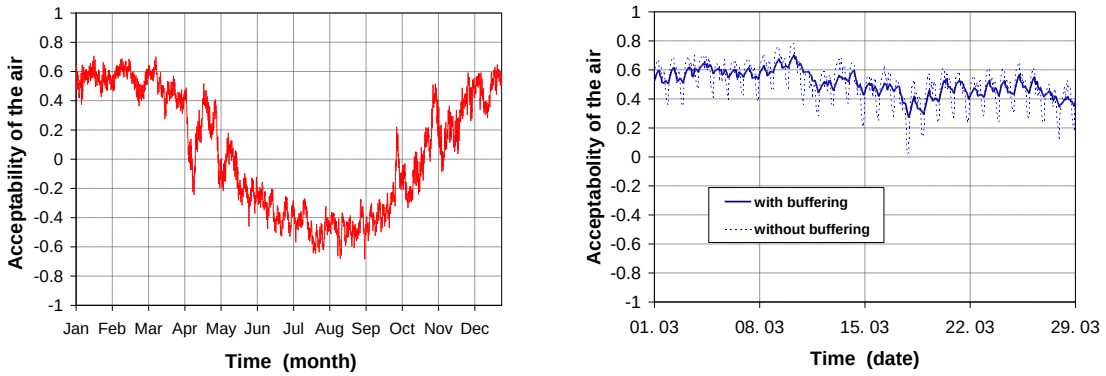

(a) Acc. Throughout the year (b) Acc. Comparison between with/without buffering

Figure 5: The predicted acceptability of air quality in the living room.

In the end, the transient heat moisture transfer simulation across the envelope described in [2] was carried out using the temperature and the humidity obtained in the present study. The result showed that there was no interstitial condensation inside the envelope.

As a result, it was concluded that the utilization of the building envelope system introduced in this study has a high potential to provide the low-energy-consuming and durable houses in subtropical regions. However, there still remains a need to optimize shading, ventilation and cooling strategy in summer to improve the indoor comfort situation. This should be considering the preferred way of living. The present model will be validated by the in-situ measurement in Test House in the near future.

ACKNOWLEDGEMENTS

The authors express the gratitude to Mr. and Mrs. Iida for there cooperation for the realization of the test house. The innovation promotion agency CTI of the Swiss Confederation is also acknowledged for the financial support (grant 9755.1 PFIW-IW).

REFERENCES

[1] CIB: AGENDA 21 on sustainable construction (1999).

[2] Goto, Y. et al.: Preliminary investigation of a vapor-open envelope tailored for subtropical climate; Building and Environment 46, pp. 719-728 (2011).

[3] Frank, Th., Carl, S.: Ueberarbeitung Programm Helios Helios-XP Schlussbericht (in German); Swiss Federal Office of Energy (2006).

[4] ISO 13790:2007. Energy performance of buildings – Calculation of energy use for space heating and cooling.

[5] SIA 380/1: Thermische Energie im Hochbau (2009).

[6] Zuercher, Ch., Frank, Th.: Bauphysik – Bau & Energie (in German), vdf Zuerich (2010).

[7] Rode, C. et al.: Moisture Buffering of Building Materials; Report BYG-DTU R-126, Department of Civil Engineering, Technical University of Denmark (2005).

[8] Fang, L. et al.: Impact of temperature and Humidity on the Perception of Indoor Air Quality, Indoor Air 8, pp.80-90 (1998).

COMPARISON OF SAMPLING METHODS FOR AIR TIGHTNESS MEASURMENTS IN NEW FRENCH RESIDENTIAL BUILDINGS

B. Moujalled[1]; F. Richieri[1]; R. Carrié[2]; A. Litvak[3].

1: CETE du Sud-Ouest, Rue Pierre Ramond, CS 60013, 33166 Saint-Médard-en-Jalles Cedex

2: INIVE, Lozenberg 7, BE-1932 Sint-Stevens-Woluwe

3: CDPEA, 58 rue Jean Duvert, Ecoparc, Le Fiducia, 33295 Blanquefort Cedex – andres.litvak@cdpea.fr

ABSTRACT

With the increasing need for higher energy efficiency in buildings, thermal regulations are evolving toward more stringent rules in buildings at the European and national level. In France, new constructed buildings will have to comply with mandatory regulations that promote low-energy buildings from 2012 and positive-energy at the horizon of 2020.

In this context, air tightness becomes a major performance issue in buildings. In fact, the part of heat loss due to air leakage in well insulated buildings becomes more important. Besides, air leakage can lead to cold draught and construction pathologies.

The French thermal regulation sets a compliance scheme to guaranty good air tightness in new constructed buildings based on the evaluation of the overall building air tightness, through field measurements. However, there are often practical, technical and economical limitations to measure the global air tightness in large or multi-family buildings. In this case, building air tightness is evaluated through partial measurements in few apartments of the building using a sampling method. This method does not account for the leakages in the untested zones, including other apartments, halls, stairwells, etc.

Actually, a research project (MININFIL) associating national institutions, research laboratories, resource centres and building professionals is conducted in France in order to enhance the knowledge on the air tightness and its impact on the energy performance in buildings, and to support building professionals to achieve much better envelope air tightness. MININFIL includes a campaign of air tightness measurements in ten residential buildings in order to identify the sampling methods that characterize the air tightness of a whole building through limited set of measurements in apartments, hall, stairway, etc.

This paper presents a bibliographical review of the sampling methods followed by the measurement campaign that was carried out in ten new buildings. In each building, the air tightness was measured on the whole building and in each apartment of the building. The results have served to identify the typical air leakage paths, and the appropriate sampling method for the air tightness evaluation in large residential buildings.

INTRODUCTION

As recommended by the EPBD, the new French thermal regulation imposes that new constructed buildings must be low energy buildings from 2012. Different studies have shown that the impact of the infiltration losses becomes more important on the energy efficiency in the case of high performance buildings [1, 2]. Therefore, air tightness requirements have been included in the French regulation with an obligation for air tightness measurements in residential buildings, especially in multi-family buildings.

The European standard EN ISO 13829 [3] describes the measurement method of air permeability of buildings. This measurement is planned to be done on the whole building. In the case of multi-family buildings, there are often practical limitations to measure the air permeability of the whole building (main reasons: building is too large, floors are not connected with an internal airflow path, or very leaky elements in the stairway). For these buildings, the standard allows separate measurements on individual parts of the building; e.g. apartments of multi-family buildings can be measured individually. In many European countries, the measurement is done on a sample of apartments for practical and technical reasons. A sampling method is given to specify the sample size, the selection criteria, and the airtightness requirements for the sample. Walther [2] has presented a review of the different sampling methods in Europe. Table 1 gives the German, UK, and French methods. The French sampling method has been included in the EN ISO 13829 implementation guide [4].

Sampling Method	Sample size	Selection criteria	Extrapolation method for the whole building
Germany	At least 20% of the total number of apartments	Apartments located at the top, in-between and ground floor.	1. The weighted average based on the volume must be lower than the limit value. 2. Air permeability of tested apartments can be 30% greater than the limit value.
UK	At least 20 % of the buildings envelope area	Areas representative of the whole envelope construction.	1. Air permeability of tested apartments must be 10% smaller than the limit value. 2. No requirements for the whole building.
France (GA P50-824)	= 3 apartments if the building has 30 units or less = 6 apartments otherwise	1. Apartments with the largest length of floors and windows. AND 2. Apartments located at the top, in-between and ground floor.	1. The weighted average based on the envelope area must be lower than the limit value. 2. No requirements for the tested apartments.

Table 1: The sampling methods for the air tightness measurements in multi-family buildings.

In France, the research project MININFIL has been conducted since 2008 in order to enhance the knowledge of professionals on the air tightness and its impact on the energy performance in buildings. Under the task 3 of the project, an extensive campaign of airtightness field measurements has been carried out in ten new multi-family buildings. In each building, the air tightness was measured for all the apartments and for the whole building. The results have enabled the evaluation of the sampling methods for the measurement of airtightness in muti-family buildings. This paper presents the results of this work.

METHOD

The air permeability measurements have been realised with the fan pressurisation method according to the standard EN ISO 13829 [3] using Minneapolis Blower Door systems. The aim of the measurements is to identify separately the air permeability of each apartment, the common areas, and the whole building. Therefore, three types of air permeability measurements have been carried out in each building:

1. Individual measurements of each apartment of the building with a blower door positioned on the entrance door of the apartment. The entrance door of the building is fully opened.
2. A global measurement of the whole building, including leakages in apartments and common areas. This measurement is realised with a blower door using a single or double fans. The blower door is positioned on the entrance door of the building. The doors between apartments and common areas are fully opened
3. A measurement of the common areas. This measurement is similar to the previous, but this time the doors between apartments and common areas are closed, in order to eliminate the leakage in apartments from the measurement. This requires that the doors are air-tight.

Table 2 presents the multi-family buildings characteristics. The number of apartments per building varies between 12 and 38, and the number of the levels between 2 and 7. The volume of buildings varies between 2365 m^3 and 5704 m^3, with 2 buildings larger than 4000 m^3.

Building code	**B01**	**B02**	**B03***	**B04**	**B05***	**B06**	**B07**	**B08**	**B09**	**B10**
# of levels	4	3	2	4	3	5	5	4	7	5
# of flats	17	12	17	20	16	17	17	16	38	36
Area (m^2)	1325	956	1266	1486	1150	1455	1248	1375	2256	2246
Volume (m^3)	3280	2365	3150	3700	2893	3544	3446	3031	5704	5175

Table 2: The description of the assessed buildings.

The measurements have been done at the end of the building construction. All apartments were unoccupied, in order to facilitate the access to all the parts of the building. However, the global measurements of buildings B03* and B05* have been disturbed by the presence of workmen during the tests. The global measurements for these building will not be considered in the analysis.

RESULTS

In France, the air permeability ($Q_{4Pa\text{-}Surf}$) is calculated as the ratio between the infiltration airflow rate at 4 Pa with the envelope area of the building except the floors area ($A_{T\ bat}$). The new thermal regulation sets the limit value required of air permeability to 1.0 $m^3/h/m^2$ for the case of multi-family buildings. This value is based on the French low-energy building standard. In this paper, the results will be presented with the French air permeability indicator.

The ten buildings represent a total of 208 apartments. For the individual measurements, more than half of the apartments (52%) show lower results than the limit value 1.0 $m^3/h/m^2$. For the global measurement of the whole buildings, only three buildings (over eight) are lower than the limit value. The major part of the leakage in the apartments (40%) has occurred across the fenestration (joints at window sash, window sill, and shutter box), while 30% of the leakage occurs at the joints of hatch and ducts, and 25% across the electricity plugging. The leakage across the joints between walls and slabs are negligible.

Figure 1 presents the results of the individual and global measurements for each building. We can observe that the individual measurements of air permeability are very heterogeneous between buildings, and between apartments in the same building in some cases. The buildings can be classified into two categories:

– Buildings B05*****, B06, B07 and B08 having the global measurement and the individual measurements globally below the required limit value (1.0 $m^3/h/m^2$). For these buildings, the individual measurements are uniform and vary in a narrow range.

– For the other buildings, both the global measurement and the median of the individual measurements are greater than the limit value. The individual measurements in each building are very heterogeneous and vary in a wide range. In B09, the upper value of the individual measurements is almost ten times greater than the lower value.

Figure 1: Box plot of the measured air permeability values in each building: the box lines indicate the statistic results of individual measurements and the red marks indicate the global measurement of the whole building in each case. The global measurements of B03 and B05*have been excluded.*

In order to evaluate the sampling methods, the GA P50-784 method has been tested and compared to the results of the measurements. Table 3 presents a comparison of the GA P50-784 method with other methods in terms of the sample size criterion. Only one building has a sample with more than 20% of the total number of apartments as required by the German method [2]. Whereas, 7 buildings have samples with more than 20% of the building envelope as required by the UK method. This can be explained by the fact that the selection criterion of the GA P50-784 method privileges the apartments with the largest envelope areas.

Building code	**B01**	**B02**	**B03***	**B04**	**B05***	**B06**	**B07**	**B08**	**B09**	**B10**
# of flats	17	12	17	20	16	17	17	16	38	36
# of tested flats	3	3	3	3	3	3	3	3	6	6
% of tested flats	*18%*	25%	*18%*	*15%*	*19%*	*18%*	*18%*	*19%*	*16%*	*17%*
% of tested $A_{T\ bat}$	20%	22%	22%	20%	29%	21%	*18%*	24%	*19%*	*16%*

Table 3: Comparison of the GA P50-784 sampling method against the other methods.

The left panel of Figure 2 presents a comparison between the weighted average air permeability of the sample of apartments and the weighted average of all the apartments for each building. For the buildings with uniform individual measurements lower than the limit value (B05*****, B06, B07, and B08), the results of the samples are very close to those obtained with all the apartments. For the other buildings, the difference is more significant.

This figure gives also the statistical values of the weighted average air permeability that can be obtained with the different possible random samples of apartments for each building. The

random samples are selected according to the required size of the sampling method with the apartments being at the top, in-between and ground floors. The median values are globally close to the weighted average of all the apartments. For buildings B01, B02, B04, B09 and B10, the difference between the minimal and maximal values that can be obtained with a random sample is very important. The minimal values can be as low as the half of all the apartments in the case of B10. The sample size and the selection criterion are critical for the sampling method.

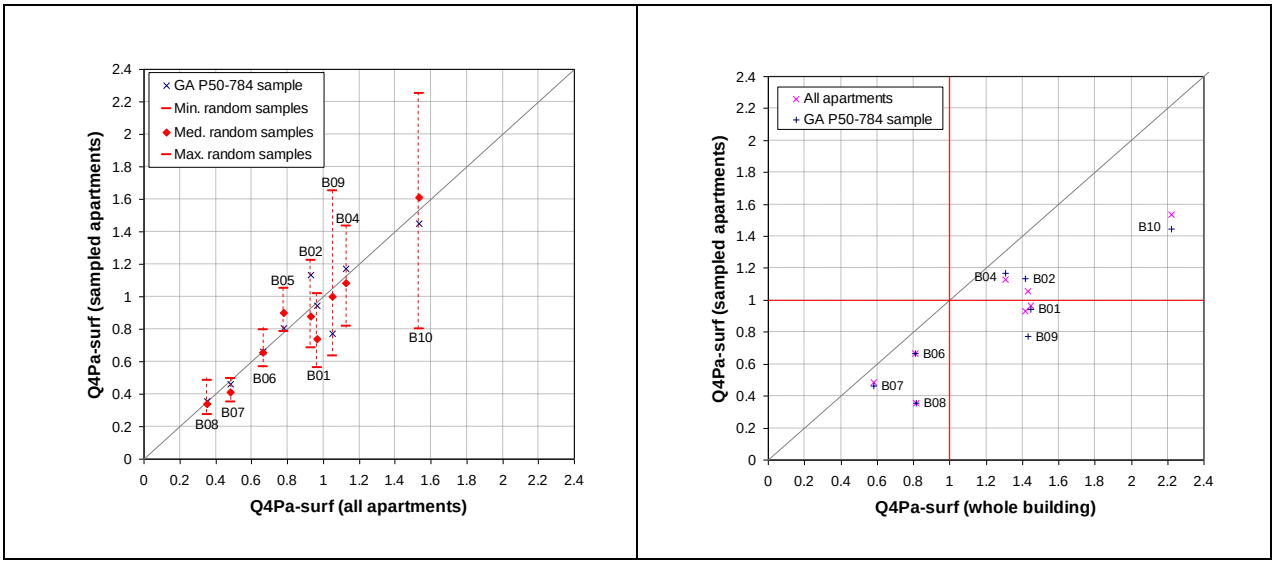

Figure 2: Comparison of the weighted average air permeability of the samples of apartments against the weighted average air permeability of all apartments on the left panel, and against the global measurement of whole building on the right panel.

The GA P50-784 method evaluates the air permeability of the whole building through the weighted average of the sample of apartments. Besides it doesn't impose any requirement on the individual measurements. The use of a selection criterion is important to guarantee that the air permeability of the sample is at least equivalent to all the apartments. The GA P50-784 method uses the ratio of the length of floor and windows per unit of floor area as a selection criterion. The method selects the apartments with the largest value of this ratio, as they are considered to be potentially the leakiest apartments. Figure 3 shows on the right panel the variation of the air leakage rates at 4 Pa against this ratio. As we can see, there is no correlation between these two parameters, and besides the air leakage rate shows a decreasing tendency with this ratio. The correlation is more significant with the envelope area as we can see on the right panel of figure 3. The envelope area seems to bee more relevant as a selection criterion than the ratio of the length of floor and windows per unit of floor area.

Now we will compare the results of individual measurements against the global measurement. The right panel of Figure 2 presents the comparison of the weighted average air permeability of the samples of apartments (the sample of GA P50-784 method, and the sample of all the apartments) against the global measurement of the whole building. For both samples, the weighted average air permeability of apartments is always lower than the air permeability of the whole building as it doesn't account for the leakage in the common areas caused by the lift shaft, the parking basement and other shafts and hatches. The greatest difference was found in the case of buildings B08, B09 and B10 with lift shaft and basement parking in the common areas.

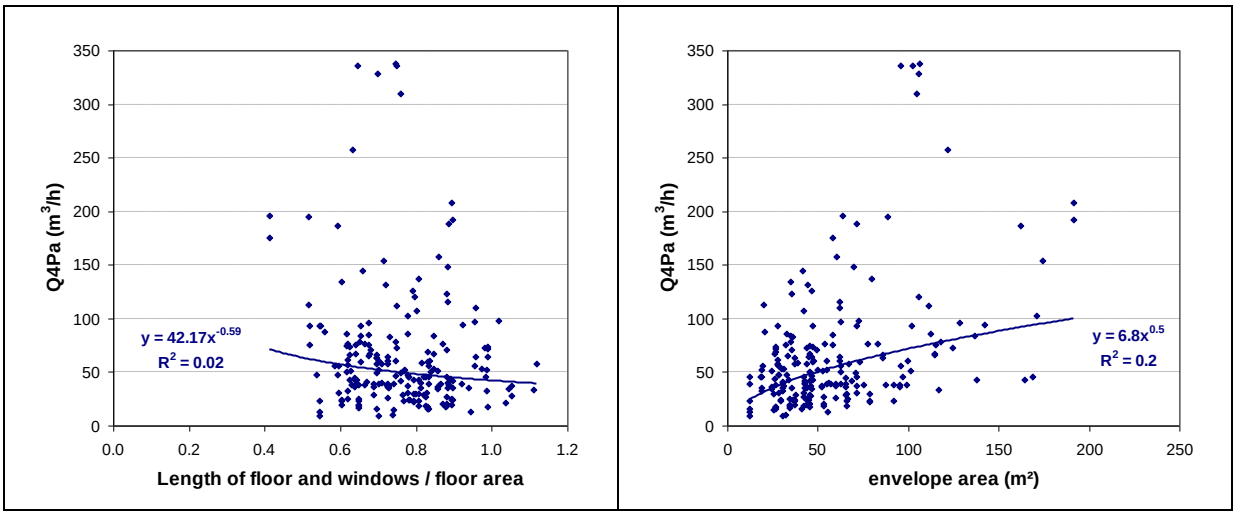

Figure 3: The variation of the measured air leakage rates at 4 Pa as a function of the sampling criteria (the GA P50-784 sampling criteria on the left panel and the envelope area excluding floor on the right panel).

CONCLUSION

A detailed campaign of air permeability measurements has been carried out in ten multi-family buildings in France. For each building, the air permeability of individual apartments and the whole building have been measured, and the sampling method of the implementation guide GA P50-784 has been evaluated. The results showed that the sampling method gives good results only in the case of buildings with uniform individual measurements. The method is as good as a random sampling. Nevertheless, in the case of buildings with heterogeneous individual measurements, the result of a random sampling varies in a very wide range. The selection criterion of the GA P50-784 sampling method doesn't identify the apartments with greater risk of leakage. The use of another criterion based on the envelope area can be more relevant. The results have shown that the leakage in the common areas are significant and can have an important impact on the air permeability of the whole building in the case of common areas with lift shaft and basement parking. These leakages should be considered in the measurement method if it extrapolates the individual measurements to the whole buildings.

ACKNOWLEDGEMENTS

This work has been conducted under the task 3 of the research project MININFIL that is financed by the French Mininstry of Housing and the French Agency for the Energy Efficiency and the Environment ADEME.

REFERENCES

1. Erhorn-Kluttig, H, Erhorn, H, Lahmidi, H: Airthightness requirements for high performance building envelopes. ASIEPI information paper #157, 2009.
2. Walther, W, Rosenthal, B: Airtightness testing of large multi-family buildings in an energy performance regulation context. ASIEPI information paper #165, 2009.
3. NF EN 13829 : February 2001 - Thermal performance of buildings - Determination of air permeability of buildings - Fan pressurization method.
4. GA P50-784 : February 2010 – Thermal performance of Buildings – Implementation guide for NF EN 13829 : 2001.

WHAT IS A "NATURAL INSULATION MATERIAL"? ASSESSMENT MODEL BASED ON THE LIFE CYCLE

Sophie Trachte, Arnaud Evrard, Valentine Regniers and Cécile Aubecq

Architecture et Climat, Université catholique de Louvain (UCL),
Place du Levant, 1, B-1348, Louvain-la-Neuve, Belgium.
E-mail : sophie.trachte@uclouvain.be
Phone: +32/10.47.26.36

ABSTRACT

So far, strategies to reduce the environmental impact of buildings focused on lowering the energy needs. Improving the characteristics of the building leads to a lower heating energy demand but also needs more construction materials to be used, especially insulation and airtightness materials. In the Walloon Region, a system of financial subsidies for envelope insulation has been implemented. In addition to the basic subsidy, an additional one of 3€/m² is granted if a «natural insulation material» is used. « Natural insulation material » is currently defined by the Ministerial Decree of the Walloon Government as a material containing 85% or more fibers originating from plants or animals, or cellulose.

The present contribution aims to analyse and improve this current definition. The authors show that a pertinent choice cannot only be based on raw materials composition but must refer to many other criteria, taking into account the whole life cycle of the material. An assessment model and a weighting of the criteria were developed and tested on 39 generic materials based on the data coming from available database and scientific literature.

INTRODUCTION

In the Belgian building sector, during the last ten years, a will to significantly reduce the building heating energy requirement has appeared. It is undoubtedly related to the increasing price of fossil fuels but also increased awareness of some environmental impacts such as climate change, natural resources depletion and biodiversity decrease. Reduction of heating energy requirement in Belgian houses is essentially reached by higher performance of the envelope, and more specifically by higher insulation and airtightness.

With the objective of promoting the renovation of low energy houses, the Walloon Government, has implemented a system of financial subsidies for building envelope insulation. Based on a mandatory energy audit, this system offers subsidies from 10€/m² to 30€/m² of insulated area, according to the type of walls and the insulation system (outside, inside...). Moreover, an additional subsidy of 3€/m² is granted if a «natural insulation material» is used. « Natural insulation material » has been defined by the Ministerial Decree of the Walloon Government voted on March 2010 and adapted on January 2011 as insulation material containing 85% or more fibers originating from plants or animals, or cellulose.

Nevertheless, when improving the energy performance of houses more materials and components are applied. The environmental impact of building materials becomes then proportionally very important in the context of very well insulated buildings. Environmental impact of building could be currently assessed by a lot of LCA tools, over its lifespan, taking into account the building materials, components and systems. But none of those tools presents

specific analysis on the "natural character" of building products, considering the nature and characteristics of materials used, the processing undergone by raw materials, the additives used for implementation, the emission of pollutants during the life and treatment opportunities at the end of life. On the other hand, "natural" insulation material based on plant or animal fibers have more and more success though they are not as thermally efficient as minerals or synthetic insulation materials. But do these insulation materials actually have a lower environmental and health impact due to their raw materials?

The paper presents a proposal that the authors submitted to Walloon Government, showing that this definition still does not guarantee a pertinent choice of materials. The authors showed that some insulation with mineral base could also be regarded as « natural ». This pertinent choice cannot be only based on raw materials composition but must refer to many other criteria, taking into account the whole life cycle of the material.

This paper introduces an assessment and a weighting model tested on 39 generic insulation materials. Firstly, the paper describes the life cycle steps and considered criteria, the data collection and the boundaries of the study. The assessment model and the weighting are subsequently presented. Finally the results of the study are discussed.

METHOD

Goal and scope of the research

Regarding the current definition, the goal of this study is to assess the "natural "character of insulation materials over the whole life cycle and to propose to the Walloon Government a more accurate definition of "natural insulation material".

Two steps were proposed but the paper only presents the second one (more complete): the Decree definition will be refined through a set of criteria based on the insulation material life cycle. This definition involves a full analysis of the environmental and health impacts of the proposed materials and a requirement on their treatment at the end of life. The "natural" insulation material is defined as *a material coming from nature, without any impact on nature nor health and returning to nature.*

The environmental impact were calculated for 1m² of insulation layer with an equivalent thermal resistance R = 2 m²K/W. This value is the minimum required by the Walloon Decree to obtain the basic subsidy for wall and floor insulation. For roof insulation, the Decree requires a value $R \geq 3.5$ m²K/W.

Life cycle analysis and selection of criteria

The authors have divided the life cycle of material into five steps. For each step, some criteria were selected:

→ **Raw material (non-energy resources):** some raw materials provide the insulating character; others are additives that provide additional properties. Each of those materials is characterized by its nature, its place of extraction, its environmental impact (culture, extraction); its health impact (hazardous matters), its availability and its intrinsic qualities.

Criteria: nature of resources (main and additional raw material), geographical origin (main raw material), resource availability (main and additional raw material), impact of culture, farming or mining on the environment (main raw material), natural resistance (main raw material), environmental impact (additional raw material), impact on worker's health (additional raw material)

→ **Production process:** the production process can involve different types of processing: change of t°, form, physical or chemical state. The energy used and the environmental impact are assessed.

Criteria: type of transformation, embodied energy (total and Non Renewable Energy), environmental impact (Global Warming Potential, Acidification Potential, Photochemical Ozone Creation Potential)

→ **Implementation process:** according to the type of assembly, the material can be reused or recycled, or not. Some insulating materials are implemented with an additive: glue or binder. This additive must also be evaluated. The implementation of the building materials may cause nuisances to workers, due to the texture of the material, its emission or its additives (toxic substances).

Criteria: reversibility of assemblies, additive required for assembly, noxiousness related to the implementation

→ **Life in use:** most of toxic emissions occur when materials are handled or in direct contact with the indoor air. Moisture in the building is a significant health problem. It can promote mould growth, degradation of surface materials and a decrease of the indoor air quality.

Criteria: pollutants emission, hazardous substances, humidity and thermal inertia

→ **End of life / elimination:** some materials are reusable, some may be used in a new cycle of production, while others are destined to be incinerated or landfilled. The ability of a material to be recycled or treated is not enough: the recycling or the treatment must really exist and perform (market demand). The lifespan of material is also important to assess the number of replacements needed on the buildings lifespan.

Criteria: type of treatment/elimination, existing treatment processes, material lifespan

Data collection and collaboration with manufacturers

Unlike other European countries, Belgium does not have database related to the environmental impact of construction materials. Considering the difficulty of obtaining complete and valid data for all insulation products, the authors have used several databases [9 to 16]. These databases have been established by independent organizations and are based on life cycle analysis.

To assess the health impact, the authors have considered the "hazard phrases (EUHxxx)" of each of the components present in the insulation material, according to the Regulation CLP on the classification, labelling and packaging of substances and mixtures but also precautions according to the risks incurred by workers during the implementation. These are indicated in precautionary statements issued by manufacturers of substances, according to the Regulation CLP.

Moreover, the authors developed a direct cooperation with manufacturers of insulation materials. The aim was firstly to collect data on materials, secondly to initiate a substantive debate on the topic of natural insulation. An online questionnaire was implemented in December 2010. Manufacturers were invited to complete it in order to make available the necessary data. This approach has been well received by most manufacturers, but only a few gave complete information.

Systems boundaries

Due to the lack of relevant data, some insulation materials such as straw, reeds, duck feathers and seashells were not included in the study.

Due to the time allotted to this study, the authors have voluntarily limited the quantitative criteria of environmental impact to a "cradle to gate" scheme taking into account only embodied energy, Global Warming Potential, Acidification Potential and Photochemical Ozone Creation Potential. Other criteria are more qualitative, except the availability of resources, moisture behaviour and thermal inertia of insulation material. In the assessment model, the authors have also considered others certifications or environmental labels such as Natureplus, FSC, PEFC, Der Blaue Engel, Öko Plus AG.

Performance evaluation and weighting

With the objective of defining insulation material as "natural" or not following the previously detailed definition, the evaluation of criteria needs to be done, in a quantitative manner, on the five steps of life cycle. To compare the criteria that are expressed with completely different units, the authors developed a weighting system that is divided into three levels: first, each criterium is evaluated individually, then the criteria of a single stage are weighted, and finally the five phases of the life cycle are weighted together. For the individual evaluation (according to each criterium), the authors have proposed to work with a scale of 1 to 5. This choice of weighting makes the definition of categories sufficiently accurate but also simple to understand:

Weighting	**Qualitative criteria**	**Quantitative criteria:** the limit values between levels (X1, X2…) are determined by dividing the difference between worst and best value on the market.
1	Very bad	from [**worst value** on market] to X1 [unit];
2	Bad	from X1 to X2 [unit];
3	Average/ neutral	from X2 to X3 [unit] –including **average value**;
4	Good	from X3 to X4 [unit];
5	Very good	from X4 to [**best value** on market] [unit].

Table 1: Weighting system for each criterium

RESULTS

The authors have worked on a baseline scenario and five specific scenarios, each testing a different version of "natural insulation material" definition : (0) Baseline scenario, (1) "Main raw material" Scenario, (2) "Additional raw material" Scenario, (3) "Environmental impact on the all life cycle" Scenario, (4) "Insulation material close to nature" Scenario, and (5) "Production with a low environmental impact" Scenario. A last scenario was defined to quantify the impact on health. Due to the lack of available data and information - the classification and labeling of chemicals being done on voluntary basis until December 2010 - the authors chose not to include it in the study.

The scenarios were tested using an excel tool and a list of 39 generic materials. Most of insulation materials were analysed in various forms or products: rigid or semi-rigid panels, mattress or roll and in bulk. The list was compiled based on manufacturer's technical information and on the reference [1] for the following values: embodied energy, NRE, GWP, AP and POCP.

For all scenarios, the authors have proposed to consider the score of 3.5 as the minimum to achieve in order that insulation material could be regarded as "natural". A score of 3 corresponds to a neutral result (average value), but a score higher than 3.5 seems too severe. It is clear that this threshold should be chosen according to the accuracy with which the values obtained by insulation materials have been determined.

WEIGHTING FACTORS	Scen (0)	Scen (1)	Scen (2)	Scen (3)	Scen (4)	Scen (5)
RESOURCES						
MAIN RAW MATERIAL	1	1	0	1	1	0
Nature of resource	0	0	0	0	1	0
Resource availability	1	1	1	1	0	1
Impact on environment	1	1	1	1	0	1
Natural resistance	1	1	1	1	0	1
Geographical origin	1	1	1	1	0	1
ADDITIONAL RAW MATERIAL	1	0	1	1	1	0
Nature of resource	0	0	0	0	1	0
Resource availability	1	1	1	1	0	1
Impact on environment	1	1	1	1	0	1
PRODUCTION PROCESS	1	0	0	1	1	1
Nbr of transformation places	0	0	0	0	0	0
Transportation	1	1	1	1	0	0
Production process	1	1	1	1	1	0
Embodied energy (total)	1	1	1	1	0	1
%NRE	1	1	1	1	0	1
GWP	1	1	1	1	0	1
AP	1	1	1	1	0	1
PCOP	1	1	1	1	0	1
IMPLEMENTATION	1	0	0	1	1	0
Reversibility of assembly	1	1	1	1	1	1
Toxicity of additive	0	0	0	0	0	0
Protection required	1	1	1	0	0	1
LIFE (USE) IN BUILDING	1	0	1	0	0	0
Oral toxicity	1	1	1	1	1	1
Ocular toxicity	1	1	1	1	1	1
Dermal toxicity	1	1	1	1	1	1
Respiratory toxicity	1	1	1	1	1	1
Specific organ toxicity	1	1	1	1	1	1
END OF LIFE	1	0	0	1	1	0
Possible treatment	1	1	1	1	1	1
Existing treatment system	0	0	0	0	0	0
Lifespan	0	0	0	0	0	0
MIN. to be considered as "natural"	3,5	3,5	3,5	3,5	3,5	3,5
Nbr of accepted products (tot 39)	29	26	29	32	24	20
	74%	67%	74%	82%	62%	51%

hemp with polyester (mattress)	1
hemp with starch (mattress)	2
hemp in bulk	3
flax with polyester (mattress)	4
flax with starch (mattress)	5
coconut with polyester	6
coconut with natural latex	7
wood fibers - wet process	8
wood fibers - dry process - polyester	9
wood fibers - dry process - parafin	10
wood fibers in bulk	11
cork - panel	12
cork in bulk	13
sheep wool with polyester	14
sheep wool with starch	15
sheep wool in bulk	16
cellulose - panel with polyester	17
cellulose - panel with polyester 2	18
cellulose in bulk	19
rock wool 200kg/m³	20
rock wool 20kg/m³	21
rock wool without formaldehyde	22
glass wool	23
glass wool	24
glass wool	25
cellular glass - panel	26
cellular glass in bulk	27
cellular glass in bulk, recycled glass	28
expanded clay in bulk	29
perlite - panel	30
perlite in bulk	31
vermiculite - panel	32
vermuculite in bulk	33
expanded polystyrene	34
extruded polystyrene	35
polyurethane	36
expanded polystyrene	37
extruded polystyrene	38
polyurethane	39

Figure 1: Various scenarios, weighting factors and insulation materials analysed

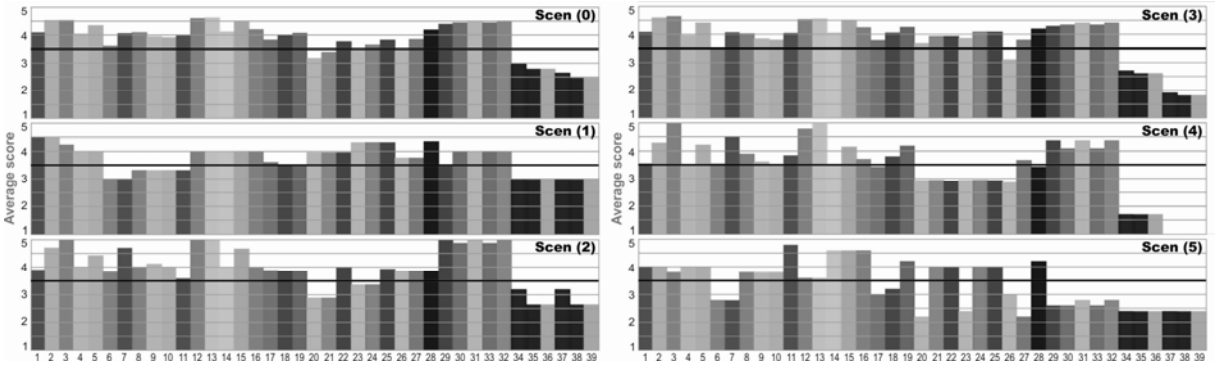

Figure 2: Results obtained by all insulation materials according to each scenario

DISCUSSION

Considering the 6 scenarios as a whole defining the "natural" character of a insulation material, some conclusions can be drawn:

- Generally speaking, insulation material "in bulk", based on plant, animal or mineral achieve good results (n°3,11,16,19, 27, 31);
- Synthetic insulation (n° 34 to 39) materials cannot be considered "natural" because they get a result between around 1.5 and 3 for all the scenario;
- Mineral-based insulation materials, that have not undergone chemical processing, such as expanded clay, perlite or vermiculite get a very good score (> 4) for all the scenario except the scenario 5;
- Results for mineral wool (n°20 to 25) fluctuate around 3.5 depending on the scenario. Generally wool without formaldehyde obtain higher scores;
- Insulation materials based on plant, animal and/or recycled fibers get higher scores (> 4) for all scenarios except the coconut fibers materials

The results obtained by the 39 analysed insulation materials show that it is insufficient to provide a subsidy for insulation based exclusively on the composition of the insulation material. For example, according to the definition of the Walloon Decree, insulation material

like perlite or vermiculite is rejected. According to the new accurate definition, it is accepted. Integration of environmental and health impact in the material assessment, throughout the whole life cycle, is essential to ensure a sustainable renewal and improvement of the housing stock in Wallonia.

ACKNOWLEDGEMENTS

Having worked together with a similar involvement, the four authors are to be considered alike for this presentation. This research was funded by the Walloon Government through the SPW – DGO4, "Département de l'Energie et du Bâtiment durable". The authors also thank all the manufacturers that participated to the study.

REFERENCES

1. Trachte S., De Herde A. : Choix des matériaux, écobilan de parois, Architecture et Climat, Louvain la Neuve, 2010
2. Pfundstein M., Gellert R., Spitzner MH., Rudolphi A.: Insulating Materials, principles, materials, applications, Edition Detail, 2008
3. Hegger M., Auch-Schwelk V., Fuchs M., Rosenkranz T., Construire, Atlas des Matériaux, Presses polytechniques et universitaires Romandes, Lausanne, 2009
4. Oliva JP, L'isolation écologique, conception, matériaux et mise en œuvre, Terre Vivante, Mens, 2001
5. Leitfaden für nachhaltiges Bauen und Renovieren, Centre de Ressources des Technologies pour l'Environnement(CRTE), Luxembourg, 2008, disponible sur www.crte.lu
6. Regulation EC n°1272/2008 on classification, labelling and packaging of substances and mixtures (CLP Regulation)
7. NORME NBN B 62-002, Annexe A - Tableaux de valeurs de calcul pour la conductivité thermique des matériaux de construction, 2008.
8. NORME NBN EN 12524, Matériaux et produits pour le bâtiment - Propriétés hygrothermiques - Valeurs utiles tabulées, 2000.
9. EPD database INIES : http://www.inies.fr
10. EPD database BRE : http://www.bre.co.uk
11. EPD database SIA : http://www.sia.ch
12. Database Ecoinvent : http://www.ecoinvent.ch
13. Ecobau : http://www.eco-bau.ch.
14. Database KBOB : http://www.bbl.admin.ch/kbob.
15. Database Ecosoft : http://www.ibo.at/de/oekokennzahlen.htm
16. Catalogue d'éléments de construction : http://www.catalogueconstruction.ch
17. Label Natureplus – http://www.natureplus.org
18. Label Der Blaue Angel – http://www.blauer-engel.de
19. Marking ÖkoPlus – http://www.oekoplus.de
20. European Chemical Agency (Echa) – http://echa.cdt.europa.eu

THE CARBON NEGATIVE BUILDING FAÇADE

R. Boyd[1]; M. Overend[1]; Q. Jin.[1]

1: Department of Engineering, University of Cambridge, Trumpington Street, Cambridge, CB2 1PZ

ABSTRACT

Glass is a valuable building material: it is strong, durable, easily maintained, and most importantly, transparent. This transparency reduces artificial lighting loads and heating loads in the heating season, but results in undesirable solar heat gain in the cooling season. As a result a design compromise exists between high and low window-to-wall ratios, in terms of energy used in heating, cooling and lighting. Buildings with a high window-to-wall ratio are generally unable to maintain a comfortable and temperate internal environment in the cooling season without the use of energy-intensive HVAC systems; those with a low window-to-wall ratio do not exploit the potential solar hear gain in winter and require more artificial lighting. Smart glazing units, which can alter their optical properties through a reversible reaction, allow energy savings to be made, but typically have greater embodied energy than their static competitors.

This paper considers how current state-of-the-art glazing technologies might be used to create a carbon negative building envelope. Following a literature review, the decision is made to compare electrochromic (EC) glazing with a high performance static solar-control (SC) glazing. Figures for embodied energy of these technologies are quoted. The energy demand of a typical office room is assessed using building simulation software. This simulation is evaluated for an office facing north, south, east and west. The locations of London, Abu Dhabi and Singapore are considered to evaluate the effect of local climate. The window-to-wall ratio that delivers the lowest energy use is chosen for each location. The office is subsequently tested with each technology and the energy demand calculated. The sensitivity of the results to the size of the office is evaluated. The EC glazing is defined as carbon neutral if it delivers a greater reduction in carbon emissions through its use than are emitted in its production. The findings are considered in the context of a high profile highly glazed building to evaluate their relevance with regards façade design decisions. A façade life of 25 years is assumed.

It is found that EC glazing delivers net lifetime carbon savings of 13.0% in London, 10.8% in Abu Dhabi and 7.6% in Singapore, averaged across the four orientations, when compared to SC glazing. It is thus found that EC glazing is carbon negative. The maximum net carbon saving of 329 $kgCO_2$ per square metre of office floor space was realised for a south facing façade in Abu Dhabi. The greatest relative reduction is 20.5% for a south facing façade in London. It is found that potential savings reduce with room depth. When considered in the context of the construction of the Shard, London, the cash value of the savings at the current carbon price is found to be negligible.

INTRODUCTION

The building envelope is arguably the most important factor in determining the energy use of a building. The properties of a façade, for example the window-to-wall ratio or G-value, are variables in complex non-linear relationships that relate building energy use and occupant

comfort to the transient external environment. This complexity is difficult to deal with in the early design stages. Aesthetic considerations tend to dominate the design of many façades, with occupant comfort provided through the extensive use of building services, often at the expense of energy efficiency.

Glass is a building material that has the potential to create a façade that satisfies the conflicting requirements of aesthetic demands, energy efficiency and occupant comfort. Its transparency is architecturally attractive and can be used to create dramatic spaces. The flow of radiation through a façade can be harnessed to reduce energy demand, but excessive solar gain will create energy demand through a need for cooling. Thus for a transient external environment, there is a set of optimum façades, as defined by their window-to-wall ratios, G-values, U-values and visible transmittances, which deliver the lowest building energy loads. The energy loads mainly depend on the type of building, its location, the geometry of the internal space, and the orientation of the façade in question. Energy savings are possible if a façade that can dynamically alter its properties to match the varying external boundary conditions to deliver the lowest energy loads. Several technologies exist to create this "Wall for all Seasons" [1]. They are evaluated below.

One tool that could be used to rationalise the design process is Life Cycle Analysis (LCA). It divides the life cycle of any product into four phases: raw materials, production, use and disposal [2]. For façade components, the use-phase can be evaluated using building energy simulation. LCAs are greatly simplified when used to compare two similar products, as the common aspects of each can be neglected.

Building energy simulation also represents a powerful tool for the designer. This paper uses a small, simple model of a typical office room to compare the energy loads placed on building services by façades comprising of the static and dynamic technologies.

Technology Review

Four dynamic glazing technologies were considered, as shown in Table 1.

Technology	Advantages	Disadvantages
Liquid Crystal	Proven technology widely used as privacy glass.	Consumes energy to maintain clear state.
Thermotropic	No energy input required.	No occupant control
Gasochromic	Can control large uninterrupted areas of glazed.	Liquid system give rise to a risk of leaks.
Electrochromic	Energy only consumed when changing state.	Effective only for limited size glazing.

Table 1: Summary of Technology Review [3].

Electrochromic (EC) glazing was chosen for this study. Research has found it capable of delivering significant energy reductions [4]. Papaefthimiou et al. [5] conducted an LCA to calculate the embodied energy of materials used in EC glazing manufacture. A market-leading static solar control (SC) glazing was chosen as the comparison.

METHOD

Building Energy Simulation

A typical rectangular office room was constructed using EnergyPlus Version 6.0.0. London, Abu Dhabi and Singapore were chosen as three locations spread over a range of latitudes with

a high demand for commercial office space. A preliminary investigation was used to find the optimal window-to-wall ratio in a range from 50% to 99% for each location. 99% was considered the maximum feasible and 50% the minimum acceptable window area for a commercial office. The aim was to find a window-to-wall ratio that gave the lowest energy use, assuming that a designer would aim to use a geometry that minimised energy use before then deciding the glazing specification. The glazing units used in the simulation were uncoated double-glazing and the default switchable glazing defined within EnergyPlus. The results were the same for all four façade orientations. The window-to-wall ratio that resulted in the lowest office energy use was 99% in London and 50% in Abu Dhabi and Singapore.

The heating system was fuelled by natural gas with an overall system efficiency of 76.5%. The cooling system was an electrically powered heat pump with a seasonal energy efficiency ratio of 3. The heating and cooling setpoint temperatures were 19.9°C and 23.9°C respectively. The lighting and electrical equipment loads were set to be 15W/m^2 each, and the required work plane illumination was 500 lux. Occupation density was 10 m^2/person and ventilation provision was 8 litre/s/person [6]. Electricity for cooling, lighting and equipment was based on the UK National Grid [7], with average emissions of 0.125 $kgCO_2$ per MJ. The generation and transmission efficiency of the grid were assumed to be 40%.

The simulation was extended to consider offices of different sizes but each with the same floor plan aspect ratio. The offices considered are shown in Table 2.

	Width (m)	**Depth (m)**	**Floor Area (m^2)**	**Façade Area (m^2)**
Office 1	3	4.68	14.05	6.82
Office 2	6.65	10.38	69.07	15.14
Office 3	9.34	14.61	136.8	21.31
Office 4	12.47	19.46	242.7	28.36

Table 2: Offices considered in the study of room depth.

Life Cycle Analysis

It was assumed that the EC and the SC glazing units use the same amount of glass, sealants and frames, manufactured with the same processes. If the embodied energy due to the components is the same, then in a comparative study they can be neglected. The static SC glazing consisted of a double-glazed insulated glass unit (IGU), with a thin-film coating applied to surface two of the unit. The process energy of the coating process was the most significant component of the embodied energy of the SC glazing.

The EC glazing included materials and processes not found in the SC glazing. Papaefthimiou et al. [5] accounted for the production and preparation of the EC glazing polymer electrolyte. The manufacture of the EC film was counted, but the embodied energy of the material used in the layer is small and was therefore neglected. Values of 2.25 $kgCO_2$ and 120.1 $kgCO_2$ per square metre of façade are found for SC glazing and EC glazing respectively.

The values from the building energy simulation and life cycle analysis were combined as follows. The above-mentioned efficiencies for the office building services were used to convert the energy loads into kilograms of carbon dioxide emitted due to primary energy consumption each year. This is factored for an assumed 25-year service life, and then normalised per square metre of office floor space. This was added to the normalised embodied energy to find the total carbon footprint for each technology. The net carbon savings were then found by calculating the difference between EC glazing and SC glazing in total carbon footprint.

Case Study

The office room simulation was subsequently altered to match the floor to ceiling height and façade tilt of the Shard, which is currently under construction in London. This building has a complex façade shape formed of seven facets or "Shards". Offices 2, 3 and 4 have depths chosen to represent "Shards" 8, 1 and 3 respectively. The carbon savings due to an EC façade are calculated as before, and are converted into a cash value by adjusting the savings in kilograms into pounds sterling using a carbon price of £15.80/tonne [8].

RESULTS

Life Cycle Analysis

The highest magnitude net lifetime carbon saving of 329 kg CO_2 / m^2 was achieved for a south facing façade in Abu Dhabi. The greatest relative net saving was 20.5% for a south facing façade in London. Figures 1, 2, 3 and 4 show the results of the LCA.

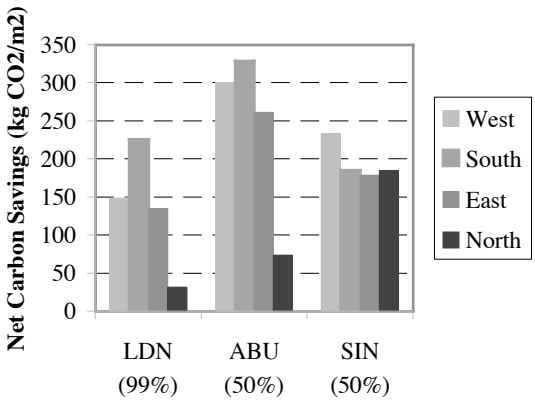

Figure 1: Net Lifetime Carbon Savings for EC Glazing with respect to SC Glazing for Office 1 at different orientations (window-to-wall ratios in parentheses).

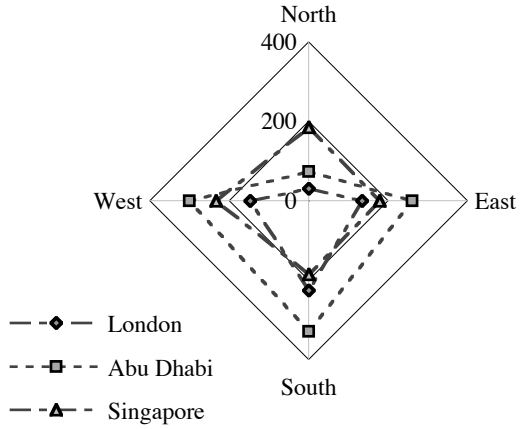

Figure 2: Geometric view of Net Lifetime Carbon Savings for EC Glazing with respect to SC Glazing for Office 1 at different orientations.

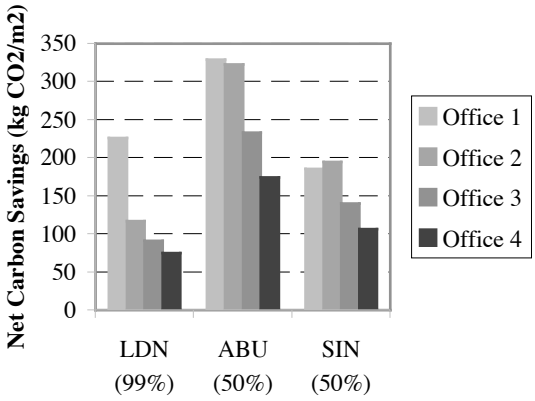

Figure 3: Net Lifetime Carbon Savings for EC Glazing over SC Glazing for Offices 1, 2, 3 and 4 facing south (window-to-wall ratios in parentheses).

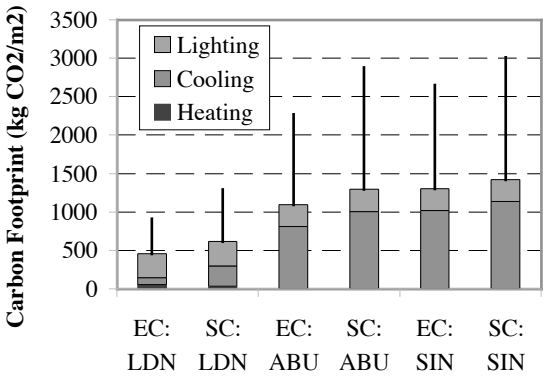

Figure 4: Carbon footprint, as the sum of lighting, cooling and heating, for the best-case window-to-wall ratios for office 1 facing south. Error bars represent carbon total for worst-case window-to-wall ratio.

Case Study

Shard Number:	**1**	**3**	**8**
Cash Value of Savings (£) per m^2	0.53	0.54	1.89

Table 3: Lifetime Cash Value of Carbon Savings per metre square of office floor space, based on a carbon price of £15.80 per tonne [8].

DISCUSSION

The carbon saving potential of EC glazing for different façade orientations in the three locations considered in this study is shown in Figure 1. This figure shows that EC glazing, despite its higher embodied energy, can deliver net carbon savings over its lifetime when compared with SC glazing. By the definition set out in this paper, EC glazing is carbon negative. The greatest potential carbon saving was achieved for a south facing façade in Abu Dhabi, showing that EC is particularly effective in locations with high peak temperatures and intermediate sun angles.

The change in potential savings with orientation shown in Figure 1 follows a similar pattern for London and Abu Dhabi, both of which lie in the Northern Hemisphere. The behaviour is different in Singapore, which lies on the Equator. The energy loads vary depending on east/west orientation rather than north/south, due to the high sun angle. The office is occupied for longer in the afternoon than in the morning, so the west facing office offers greater savings than the east facing one. For a location in the southern hemisphere, a reflection in the east/west plane of the pattern of behaviour for London and Abu Dhabi would be expected.

Referring again to Figure 1, it is perhaps surprising that the savings potential of EC glazing on a south facing façade in London exceeds that for all the orientation in Singapore other than west. In addition, from Figure 1 the average relative carbon saving of 13.0% achieved in London is the highest of the three locations. The high sun angle and consistent high air temperature throughout the year in Singapore means that the performance improvement of EC over SC glazing is less significant. This is reinforced by Figure 4, which shows that in Singapore EC glazing reduces total energy loads while maintaining the proportions of cooling and lighting energy. In contrast, EC glazing in London reduces the cooling load with respect to the total energy demand from 24.1% to 19.7%. These cooling loads are associated by high solar gains that occur at low sun angles.

Figure 3 shows the change in potential carbon savings with room depth for south facing façades. In London and Abu Dhabi the net benefit of EC glazing falls consistently with increased depth. The capacity of the façade to influence the internal conditions reduces with depth, and this is reflected in the reduced performance enhancement offered by EC glazing. The behaviour of offices 1 to 4 in Singapore is different, with the greatest savings achieved for Office 2. At this depth the proportion of the energy use due to lighting falls to a minimum of 16%. Artificial lighting is more carbon intensive than cooling, and so this minimum value for the proportion of energy use required for lighting coincides with greater carbon savings.

Table 3 shows the cash value of the net lifetime carbon savings per square metre of floor space for offices modelled with ceiling height, room depth and orientation to match three of the façade facets of the Shard, London Bridge. This assumes a carbon price of £15.80 per tonne [8], over a service life of twenty-five years. It is evident that at the current carbon price, the cash value of the carbon savings due to EC is negligible. The carbon price would need to be orders of magnitude higher to become pay back the capital cost of upgrading from SC glazing to EC glazing, based on the value of the carbon savings alone.

Conclusions and Future Work

This study has shown how a simplified life-cycle analysis that includes the building energy simulation of a typical office can be used to calculate the net lifetime carbon savings of one glazing technology over another. Compared to SC glazing, EC glazing offers greater potential savings in locations and at orientations that experience the greatest variation in external boundary conditions, including specifically peak air temperatures and incident solar radiation from low sun angles. These conditions are found on south facing façades in Abu Dhabi and London respectively.

Offices with greater floor depths benefit less from the added performance of EC glazing. At the current carbon price, however, the cash value of even the greatest potential carbon savings is insignificant. The reduction in the operating energy costs resulting from the use of EC glazing and the potential increase in occupant comfort and performance would have a more significant impact on the whole life cost.

Acknowledgements

The authors wish to express their gratitude to Will Stevens of Ramboll London, Helen Sanders of SAGE Electrochromics Inc, David Healy of Arup London and Giampiero Manara of Permasteelisa Italy for their help and advice at crucial stages of the project.

References

1. Davies, M.: A Wall for all Seasons, RIBA Journal – Royal Institute of British Architects, Vol. 88, Issue 2, 1981 p. 55-57.
2. ISO 14040:2006, Environmental Management, Life Cycle Analysis, Principles and Framework, International Organisation for Standardisation, Geneva, Switzerland.
3. Baetens, R., Jelle, B. P., Gustavsen, A.: Properties, requirements and possibilities of smart windows for dynamic daylight and solar energy control in buildings: A state-of-the-art review. Solar Energy Materials & Solar Cells, Vol. 94, 2010 p. 87-105.
4. Sullivan, R., Rubin, M., Selkowitz, S.: Energy Performance Analysis of Prototype Electrochromic Windows, LBNL-39905, 1996.
5. Papaefthimiou, S., Syrrakou E., Yianoulis, P.: Energy Performance Assessment of an Electrochromic Window, Thin Solid Films, Vol. 502, 2006 p. 257 – 264.
6. CIBSE Guide F: Energy Efficiency in Buildings, Chartered Institute of Building Service Engineers, 2004.
7. Annex B & E, Energy and Emissions Projections, Department of Energy and Climate Change, 2010.
8. ETFS Carbon, ETF Securities [Online]. Available from: www.etfsecurities.com, [accessed 12/05/2011]

GLAZING STRUCTURES WITH A MAXIMUM SEASONAL CONTRAST RATIO AND THE SIMULATION OF SUCH BUILDING ENVELOPES

Stephan A. Mathez[1], Walter Sachs[1]

1: Solar Campus GmbH, Technologiepark Wetzikon, Buchgrindelstr. 13, CH-8620 Wetzikon, e-mail: info@solarcampus.ch, phone: +41 (0)43 495 21 00

ABSTRACT

For well insulated buildings the annual solar irradiance onto the building facades exceeds the buildings energy demand by a multiple. Even for Central European climate conditions the irradiance in the winter season is about two to three times higher than the buildings energy demand. In order to make this irradiance available, a glazing of the façades is necessary on the one hand, on the other hand at least a short-time storage that is able to effectuate a day-night phase shift is required. As the investigations with the simulation framework *Tachion* show, an entirely solar façade heated building is within reach.

However, glazed façades have as well as transparent insulations the problem of overheating in the summer. This can be defused either by means of active measures, such as shading elements (shutters) in front of or inside the façade and/or by ventilating the absorbed heat away, or by means of passive measures, such as particularly shaped lamellas, prisms or other geometrical forms with seasonally variable transmission.

In this paper, a passive method is presented that achieves solely with the help of a particularly configured glazing the desired effect in a very efficient way. The contrast ratios, i.e. the ratio of maximum to minimum transmission of direct solar irradiance depending to the season, of up to 10:1 are possible. Compared to present-day systems, the winter/summer transmission ratio is improved substantially. If the glazing configuration is tailored individually to the specific situation of the building, even higher values can be obtained. Moreover, the diffuse part of the irradiance is used more effectively than with present-day setups. Thanks to all of these advantages, further overheating measures can in most cases be omitted. In the last section we shall present an effective and environmentally friendly way for a short-term storage of the gained irradiance energy. Investigations with the elaborated physical and mathematical simulation framework *Tachion* are promising for the design of an entirely self-supplied building solely based on façade irradiance.

INTRODUCTION

Covering the energy demand of well insulated buildings for Central European climate conditions without seasonal storage of solar thermal energy and without overemphasizing the envelope insulation (“passive house”) is a major challenge in the development of self-sufficient buildings. Detailed irradiance simulation of the diffuse and direct irradiance onto a building’s façade show good evidence that this goal can be reached provided the irradiance can be absorbed and stored to a certain extend.

Since sunlight as heating energy source is considered and used, overheating has become a sincere problem of comfort in summer time. Several strategies to handle this problem have since been developed: active system to prevent irradiance when it is not needed work well as long as they operate accordingly, in general they are rather laborious in handling and maintaining, and prone for malfunctions. Passive systems have less problems of this kind, but they

are less sensitive to the building's energy needs. In order to establish the desired properties, an accurate planning of such elements is necessary. Especially for renovations, adapted solutions are a necessity to obtain good results.

Our search for an adaptive, flexible, cost and power effective and purely passive concept led us to the glazing structure called *SunPattern*[1] whose characteristics shall be presented in the following.

As a realistic example we shall consider a square, two floor, single family building of (merely) Swiss Minergie standard with an energy reference area of 200 m^2 with exterior dimensions of 10 x 10 x 6 meters (façade height 5.5 m). The annual heating energy demand equals Q_h = 4500 kWh. As meteorological data, the Meteonorm dataset for Wetzikon (near Zurich) is used. Wetzikon, located 532 meter above sea level, has a yearly global irradiance of G_h = 1108 kWh/m^2 and a mean ambient temperature of 9.7 °C. The façades are assumed to be oriented exactly towards north, east, south and west. The Perez model[1] is applied to compute the distribution of the hemispheric diffuse irradiance, partitioned into isotropic sky, horizon ribbon and a contribution for ground reflection. The albedo model, also applied in Meteonorm, considers albedo variations on a daily basis[2] which is quite crucial for a reliable façade irradiance model. Based on this simulation setup, the monthly façade irradiance looks as follows:

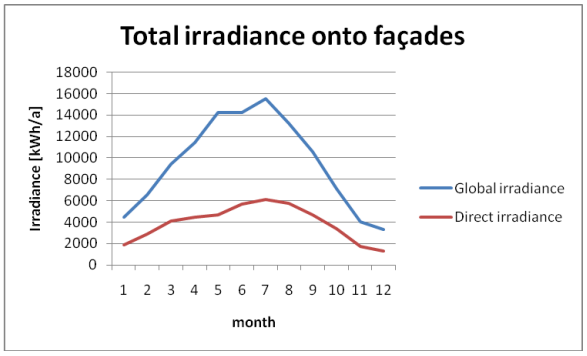

Fig. 1: Specific monthly irradiance onto all façades where the window fraction is 30 % for the south façade, 20 % for the east and west façade and 10 % for the north façade. The direct radiation amounts to 40.8 % of the global irradiance.

The annual irradiance onto the building's façade amounts to 114'250 kWh for global and 46'670 kWh for direct irradiance, which is more than an order of magnitude above the heating energy demand.

To compare façade irradiance with the buildings energy demand, we make use of the building simulation within the *Tachion framework* on the basis of the hourly R5C1 model from the ISO EN 13790[3] which has been upgraded by a strongly improved irradiance routine. The window area fractions are assumed to be 30% on the south, 20% on the east and west, and 10% on the north side. Internal loads contribute with constant power of 600 Watt. Mechanical ventilation, heat recovery, standard values for infiltration and transmission losses for different parts of the building envelope are defined in detail. For the above described building with a specific heating demand of 22.5 kWh/m^2 of the energy reference area, the comparison of the total irradiance onto the entire façade and the required heating energy yields the following graph:

From figure 2 we conclude that if a building concept is able to transform 30-50 % of the façade and window irradiance into usable heat and if that heat is available for one to five days

[1] The patent for the corresponding glazing structure is applied for. Please contact Solar Campus for details.

that this kind of (passive) heating system would able to keep the temperature setting without supplementary energy.

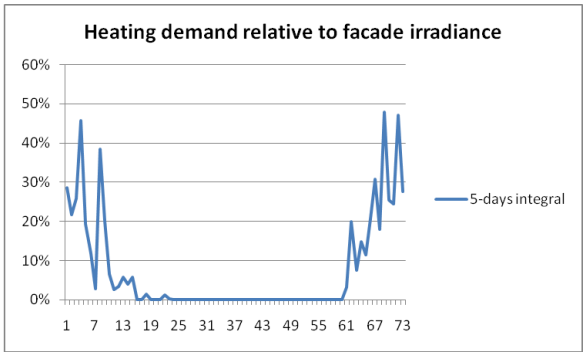

Fig. 2: Relative heating demand as a 5-days integral compared to the total façade (and window) irradiance for the same time intervals for the entire year. Already on this time basis (not only a monthly integral) the required irradiance for heating need not even be 50% of the available irradiance.

ANGEL SENSITIVE STRUCTURE

Covering the energy demands in winter is certainly the main task for our climate zone. More details about the constructive aspects are given in the second last paragraph of this paper. Another crucial aspect of using the building's envelope as source of energy is the problem of overheating in summer. The energy savings during the cold season should not be made up by an air conditioning demand during the summer. In order to solve this problem, a number of concepts have been developed in the past and are applied in many existing building. A common aspect in all these overheating preventers is the angle dependent transmission properties according to high sun elevation in summer and low elevation in winter. An illustrative example is the following sketch of such an angle selective blind:

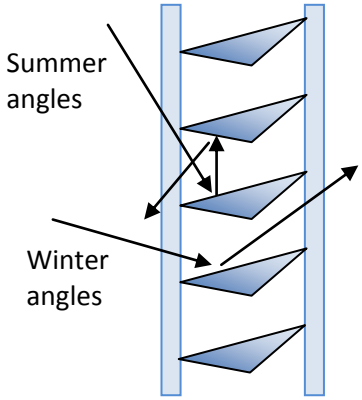

Fig. 3: Schematic sketch of an angle selective façade glazing as it is used to control the seasonal irradiance transmission. On the south façade, in summer, the steeply incoming irradiance is reflected back to the ambient, in winter, the flat angles of the sun elevation allow a transition through the structure. This sketch represents a reference case of an angle selective construction, hence referred to as "standard structure".

The setup in figure 3, hence referred to as "standard structure", represents a typical construction with an angle sensitive behavior in order to have high transmission rates in winter and low transmission rates in summer. The reflecting lamellas in this example are enclosed between two glasses. In the following we will present the energetic properties of the standard structure and of *SunPattern*.

ENERGY GAINS

The ability to control the seasonal irradiance or energy flow is of course only one aspect in covering the heating demands of the building under consideration. In order to obtain the actual energy gains, the direct and diffuse irradiance values have to be integrated, as shown in the following figure:

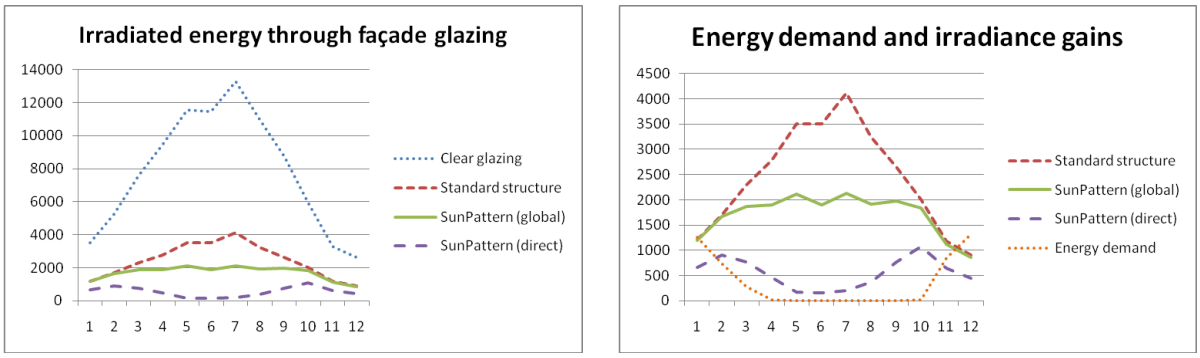

Fig. 4: Monthly energy transmission for a clear glazing (left diagram dotted line), for the standard structure (narrow dashed line) and for SunPattern (solid line). The dotted line in the right diagram represents the buildings energy demand. The difference between standard structure and SunPattern in summer with respect to overheating is evident. Furthermore, the direct irradiance for SunPattern is almost suppressed completely during summer. Both scalings are in kWh/a.

The annual, transmitted irradiance values in case of the left diagram amount for the entire building to 93'670, 29'080, 20'490, resp. 6'640 kWh. The comparison of the standard structure and *SunPattern* shows especially in the summer a substantial lowering of the irradiance of approximately 50 %. In the winter time, both structures have similar transition rates. Furthermore, the left diagram shows the energy gain due to direct irradiance (wide dashed line). As can be seen from this curve, almost all of the summer gains in case of *SunPattern* arise from diffuse irradiance, whereas the standard structure is equivalently transparent also for direct sunlight. This aspect points at another advantage of the *SunPattern* concept: for Central European climate conditions, buildings often require heating energy also during the summer half-year when bad weather periods occur with sparse direct sunlight. Under these conditions, the exploitation of this source of energy is reasonable and helpful in the substitution of supplementary energy.

The right diagram in figure 4 relates the monthly irradiance integrals of *SunPattern* with the buildings energy demand. The demand could just be covered by irradiated when the entire absorbed energy could be used for heating purposes. In the next chapter, we will present a possible solution to handle the temperature shift problem between day and night by using a short-term storage concept.

STORAGE CONCEPT

Storing the irradiated energy is not easy for a couple of reasons. First, the building envelope is well separated from the buildings core and thermal mass. Any means of energy transportation like fans offer potential wickets of loss and require mechanical equipment and electricity supply. Another aspect is the thermal mass to store the energy.

Since the temperature level should be kept low in order to have small losses when collecting the irradiance energy, the corresponding mass should be large. And finally, the temperature level should be possibly the lowest in the system, also to obtain high solar yields. To this situation described, a known concept of placing exterior thermal masses used as secondary building skin is able to decouple the interior from the façade processes.

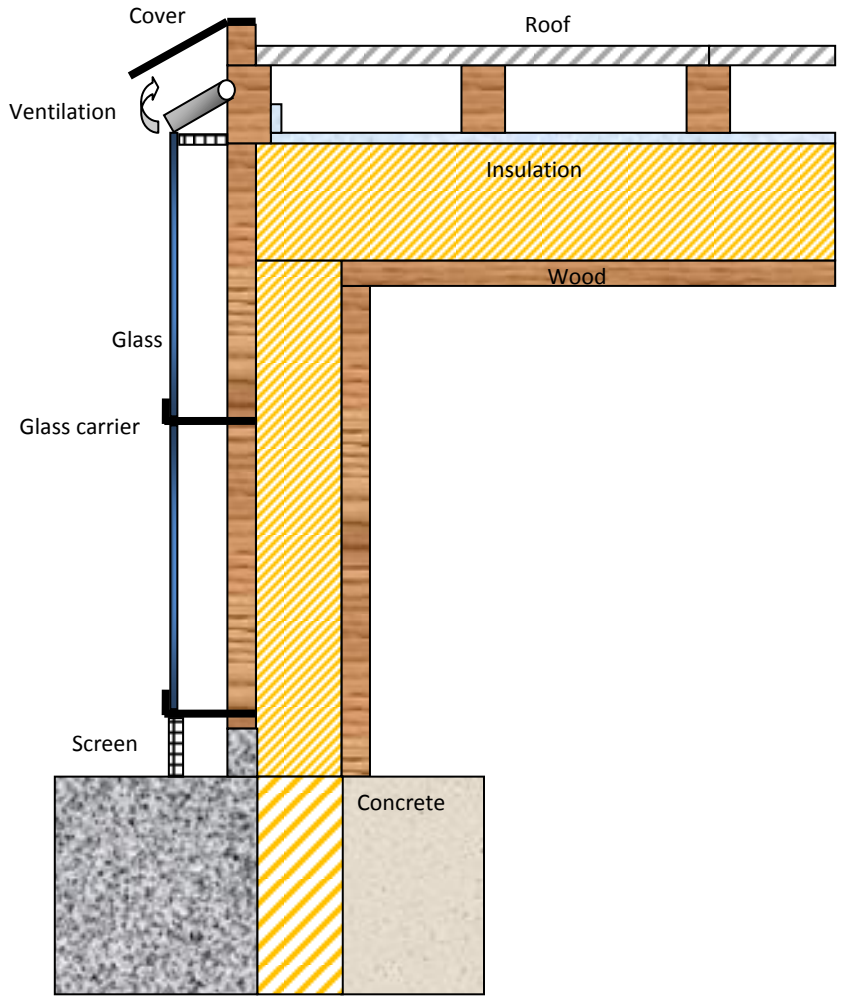

Fig. 5: Constructive setup of a glazed façade, using an exterior capacity made with wood in that example. The carriers of the glazing are solely hold by the exterior construction, preventing heat bridges to the interior construction. In order to ventilate surplus energy away in summer, the construction can be passively air conditioned by natural convection which occurs as soon as the ventilation lid on top of the glazing is opened. This needs only be opened or closed once in a year.

Since irradiance reliably occurs during day time, even if it is only diffuse light of 100 W/m^2 and the transmission rate is assumed to be 50 %, a temperature difference of 10 K can be established after some time, reducing the transmission energy loss from the building substantially and accumulating energy for the evening and night which lowers the façade's energy loss also during night. Due to the low temperature level, the energy losses when gaining the radiation energy are minimal. As a well suited material for this outer mass, wood brings interesting properties with respect to its thermal capacity, low heat conductivity, and of course its tremendous processing and static properties.

The façade's glazing allows for temperature differences of 20 – 30 K in case of direct irradiance shining onto the façade. But dynamically, this temperature is achieved only after some hours the corresponding energy is stored within the wood's capacity.
In summer, if an almost perpendicular irradiance of 800 W/m^2 enters the façade, the actually transmitted irradiance only comes from diffuse irradiance which is of order 100 W/m^2. So

also in this case, the temperature difference will not exceed 10 K, or even less, since the heated air can escape the air gap through the ventilation lid. The left diagram in figure 4 shows a reduction of the summer irradiance of a factor 6 in case of *SunPattern* with respect to a clear glazing. From these considerations it is clear that the presented building envelope helps in a very effective way to keep the inside temperature on a comfortable level (as long as the energy flow through windows is well controlled). And no need for electric air conditioning arises.

CONCLUSION

The art of designing buildings for an optimal environmental energy supply is characterized by the intensive interaction of geometrical, material property, heating installation and controlling aspects, and need to be tailored to the users heating and cooling demands. The geometrical nature of direct and diffuse solar irradiance is still a challenge to incorporate into a project in a beneficial way. Material and component properties are subject of a rapid development. Long, middle and short term heat storage, the control of energy flows and forecasting the availability of irradiance and the varying demand of energy is another player in this complex game.

SunPattern brings in a highly differentiating element for all kind of façade, roof and other glazed building parts. It is clear that this broad spectrum of requirements with competing aspects, cannot be handled with a simple recipe, but require a comprehensive simulation handling high temporal and spatial resolutions. In order to analyze waste fields of variations and to follow the path of improvement with thousands of iterations, preferment algorithms need to be developed and proven in practice.

REFERENCES

1. Perez, R., P. Ineichen, E. Maxwell, R. Seals and A. Zelenka (1991): Dynamic Models for hourly global-to-direct irradiance conversion. Edited in: Solar World Congress 1991. Volume 1, Part II. Proceedings of the Biennial Congress of the International Solar Energy Society, Denver, Colorado, USA, 19-23 August 1991.
2. Remund, J. and J. Page (2002): Chain of algorithms: short- and longwave radiation with associated temperature prediction resources. SoDa Deliverable D5-2-2/3. Internal document.
3. EN ISO 13790:2008, Energy performance of buildings - Calculation of energy use for space heating and cooling (ISO 13790:2008)

THERMAL EVALUATION OF ENVELOPES OF NON AIR-CONDITIONED BUILDINGS

G. Barrios, G. Huelsz, J. Rojas

Centro de Investigación en Energía, Universidad Nacional Autónoma de México, A.P. 34 Temixco, Centro, 62580, Morelos, México. Tel/fax 52+55-56-22-97-57

ABSTRACT

Most of the studies on the thermal evaluation of building envelopes have been done for air-conditioned buildings. For that condition, the total energy per unit area consumed to maintain the indoor temperature constant at the comfort temperature is the evaluation parameter most used. In this study, three thermal performance indexes for building envelopes are proposed as parameters for their evaluation in non air-conditioned buildings. The envelope thermal performance index (ETPI), the hot thermal performance index (HTPI) and the cold thermal performance index (CTPI). The three indexes give a number from 0 to 100, a higher number means a better thermal performance. The ETPI is the average of HTPI and CTPI. HTPI quantify the ability of the envelope to avoid overheating and CTPI to avoid overcooling, both with respect to a comfort temperature. A one dimensional heat transfer model for periodic outdoor conditions for a typical day of a month is used to simulate heat transfer through the envelope. The effect of solar radiation, convection and infrared emission on the outdoor envelope surface is included via the sol-air temperature and the outdoor film heat transfer coefficient. The indoor film heat transfer coefficient is used to account for the effect of radiative and convective heat transfer on the indoor envelope surface. Four monolayered and three multilayered envelopes are tested. The four monolayered envelopes are made of high density concrete (HDC), aerated concrete (AeC), expanded polystyrene foam (EPS), and zinc (Zinc). The multilayered envelopes are made of HDC and of EPS, with different locations of the EPS: in the exterior side, in the middle, and in the interior side. The envelope performance of air-conditioned buildings is also evaluated using the total energy per unit area.

INTRODUCTION

Walls and roofs of the building envelope play an important role in the heat transfer between the exterior and interior of the building. From the thermal point of view a good wall/roof keeps the interior temperature as close as possible to the comfort temperature without the use of an air-conditioning system or minimizes the energy consumption if an air-conditioning system is used.

For air-conditioned buildings (A/C), parameters such as the total energy per unit area or the decrement factor with the time lag have been used to evaluate an envelope wall/roof [1], the decrement factor with the time lag has also been used to evaluate envelopes in non-air conditioned buildings (nA/C). In a previous work, the authors have used the decrement factor to evaluate six roof configurations in non-air conditioned buildings [2].

In this work, thermal indexes to evaluate the thermal performance of a wall/roof are proposed for nA/C. These indexes are used to evaluate the performance of seven roofs, these roofs are also evaluated in A/C buildings using the total energy as the performance parameter.

MODEL

The heat transfer equation through a roof/wall composed by N layers of different materials, with a total width L, is [3]

$$\frac{\partial T_j}{\partial t} - \alpha_j \frac{\partial^2 T_j}{\partial x^2} = 0 \tag{1}$$

This equation describes the temperature inside the *j*th layer, *Tj* as a function of time and position *x*. The coefficient α_j is the thermal diffusivity of the corresponding material. Given energy conservation, between layers the following condition must be satisfied

$$-k_j \left.\frac{dT}{dx}\right|_{j,j+1} = -k_{j+1} \left.\frac{dT}{dx}\right|_{j,j+1} \tag{2}$$

and in the exterior and interior surfaces

$$-k_1 \left.\frac{dT}{dx}\right|_{wo} = ho(To - Two) \qquad -k_N \left.\frac{dT}{dx}\right|_{wi} = hi(Twi - Ti) \tag{3}$$

where k_1 and k_N are the thermal conductivity of the first and last layer (from exterior to interior), and h_o and h_i are the film heat transfer coefficients for the exterior and interior, respectively. T_o and T_i are the outside and indoor air temperatures T_{wo} and T_{wi} are the surface wall temperatures at the outside and inside side of the wall/roof.

When simulating an air-conditioned room (A/C), the indoor temperature is kept constant and known. For non air-conditioned rooms (nA/C), the indoor temperature is assumed to be only a function of the heat transfer through the wall [3]

$$d\rho_a c_a \left(\frac{\partial Ti}{\partial t}\right) = hi(Ti - Twi) \tag{4}$$

where ρ_a and c_a are the density and specific heat of the air, *d* is a distance where the heat transfer is assumed to be zero.

ENVELOPE THERMAL PERFORMANCE INDEXES

The proposed indexes qualify the thermal performance of an envelope wall/roof. The indexes are scaled with the worst configuration. The indexes have values from 0 to 100 and the wall/roof is better as the value approaches to 100.

The hot thermal performance index (HTPI) evaluates the ability of the wall/roof to avoid overheating respect to the comfort temperature and is scaled with the maximum possible overheating, given by the sol-air temperature considering an absorptivity equal one. It is defined as

$$HTPI = \left[1 - \frac{\sum_j (Ti_j - Tc)}{\sum_j (Tsa(1)_j - Tc)}\right] \times 100 \tag{5}$$

such as $Ti_j > Tc$ and $Tsa(1)_j > Tc$. Where *Tsa(1)* is the sol-air temperature [1] for an absorptivity *a=1* and *Tc* is the comfort temperature [5]. The subindex *j* indicates the discretization of time.

The cold thermal performance index (CTPI) evaluates the ability of the wall/roof to avoid overcooling respect to the comfort temperature and is scaled with the maximum possible overcooling, given by the sol-air-temperature considering an absorptivity equal zero. Thus, it is given as

$$CTPI = \left[1 - \frac{\sum_j (Tc - Ti_j)}{\sum_j (Tc - Tsa(0)_j)} \right] \times 100 \quad (6)$$

such as $Ti_j < Tc$ and $Tsa(0) < Tc$.

The envelope thermal performance index (ETPI) is defined as the average of the hot thermal performance index and the cold thermal performance index,

$$ETPI = \frac{HTPI + CTPI}{2} \quad . \quad (7)$$

RESULTS

For all simulations the outdoor temperature was calculated using the equation proposed by Chow and Levermore [6], the solar radiation was approximated by a sinusoidal with the day duration according to the place and the month. The weather data needed to calculate the ambient temperature correspond to Torreon, Mexico, for the month of June. Roofs are evaluated considering *d=2.5m* and the values for the film coefficients for the exterior and interior are *ho*=13W/m^2 ^{o}C y *hi*=6.6W/m^2 ^{o}C.

Seven roof configurations were chosen to prove the utility of the indexes. The configurations are described in Table 1 and all of them are evaluated considering A/C and nA/C rooms. The properties of the materials used are presented in Table 2. In all roofs the absorptivity was *a=0.2* but for Zinc a=*0.8*, also all roofs have a total thickness of 0.10m, but Zinc is 0.01m. The first six configurations are the same than the ones used in [2].

EPS	Expanded Polystyrene Foam 0.10 m
AeC	Aereated Concrete 0.10 m
HDC	High Density Concrete 0.10 m
EPS_ext	EPS 0.02m + HDC 0.10 m
EPS_int	HDC 0.08 m + EPS 0.02 m
EPS_mid	HDC 0.04 m + EPS 0.02 m + HDC 0.04 m
Zinc	Zinc 0.01m

Table 1: Configurations described from the outside to inside.

Material	k $[W/m^oC]$	ρ $[kg/m^3]$	c $[J/kg^oC]$
AeC	0.12	550	1004
HDC	2.00	2400	1000
EPS	0.04	15	1400
Zinc	110	7130	390

Table 2: Properties of the materials, k thermal conductivity, xxx density and xxx specific heat.

The total energy per unit area used in A/C buildings for the seven configurations is presented in Figure 1. The EPS is the best configuration, followed by the EPS_ext. In this case, the roof made of Zinc is the configuration that has the largest energy consumption, almost 32 times more than the EPS, and the HDC is the second worst, using more than 6 times the energy needed by the EPS.

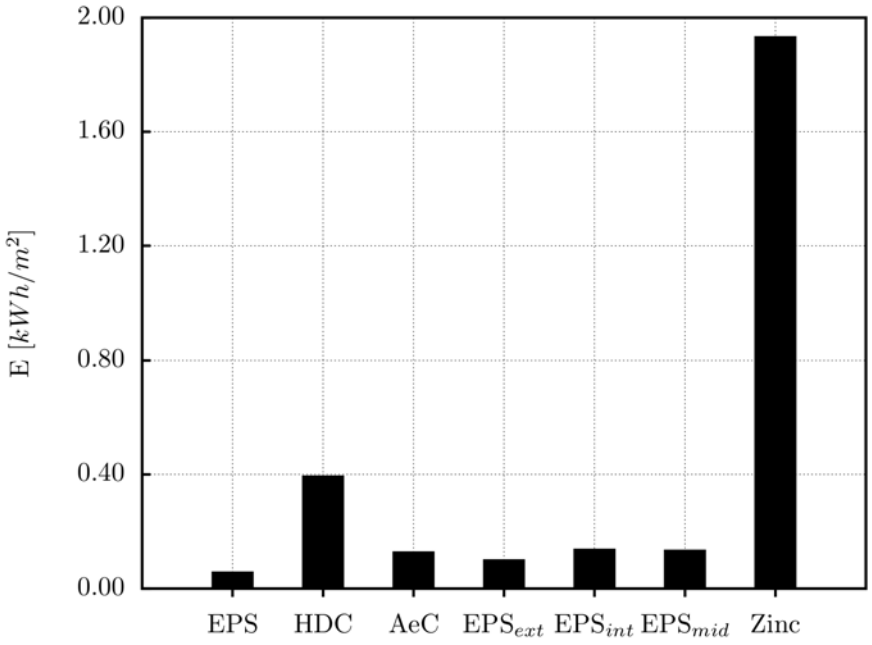

Figure 1: Energy per unit area used in A/C buildings .

In Figure 2, the three indexes are presented (CTPI, HTPI and ETPI) for the seven configurations in nA/C buildings. The best configuration according to the ETPI is EPS_ext (94), followed by EPS_mid (91), AeC (79), HDC (77), EPS_int (74), EPS (65), and Zinc (32). The HTPI and CTPI give the same order. This order is the same as obtained using the decrement factor as the parameter [2]. The Zinc was not considered in that work.

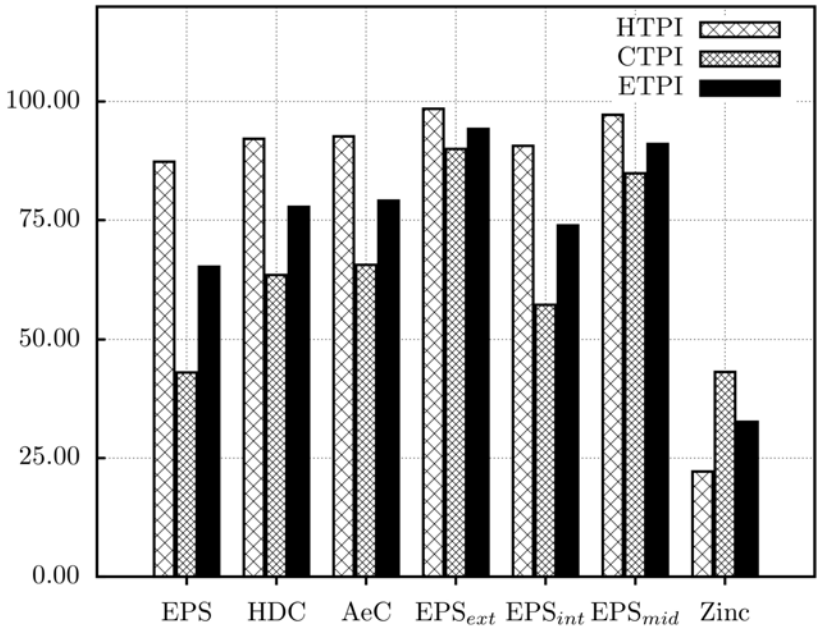

Figure 2: Thermal performance indexes for the six configurations.

CONCLUSIONS

The main conclusion of this work is that the use of the envelope thermal performance index (ETPI), as a parameter to evaluate the thermal performance of an envelope wall/roof in non air conditioned buildings orders the configurations in the same way than the decrement factor. The advantage of the ETPI is that it gives a grade ranging from 0 to 100, which is simpler to interpret than the value of the decrement factor. The results show that the best envelope for air-conditioned buildings (EPS) can be not suitable for non air-conditioned buildings.

ACKNOWLEDGEMENTS

Partial economic support from CONACYT and from CONACYT-SENER 118665 projects is acknowledged.

REFERENCES

1. Givoni B. Man, climate and architecture. Applied Science Publishers, London, 1981.
2. G. Barrios, G. Huelsz, R. Rechtman and J. Rojas. Wall/roof thermal performance differences between air-conditioned and non air-conditioned rooms. Energy and Buildings 43, pp 219-223, 2011.
3. Incropera, F. P. and De Witt, D. P. *Fundamentals of Heat and Mass Transfer*, pp 88-93 and 239-324, John Wiley & Sons, New York, 2002.
4. ASHRAE. SI Edition , American Society of Heating, Refrigerating and Air-Conditioning Engineers, 1997.

5. M. A. Humphreys, F. J. Nicol, Outdoor temperature and indoor thermal comfort-raising the precision of the relationship for the 1998 ASHRAE database files studies, ASHRAE Transactions 106, 2000.
6. Chow D. H. C., Levermore G. J. New algorithm for generating hourly temperature values using daily maximum, minimum and average values from climate model. Building Serv. Eng. Res. Technol., 28(3), 237–248, 2007.

ENERGY PERFORMANCES OF AN ETFE ROOF APPLIED TO A SWIMMING POOL

A. Bellazzi[1], S.Galli[1]

[1]*ITC-CNR, Construction Technologies Institute – National Research Council*

Via Lombardia 49, 20098 San Giuliano Milanese - Italy

ABSTRACT

The forward-looking analysis of the energy demand plays a key role in the design of sustainable buildings in terms of energy consumption and impact on the environment; in particular, the use of new materials and advanced architectural solutions needs to be taken into account also while calculating the building envelope efficiency. This research aims to evaluate the performances of an innovative material, such as ETFE (Ethylene Tetrafluoroethylene), using dynamic simulation tools, applied to the case study of a swimming pool, a scenario which is very far from a traditional building because of the presence of water in a confined environment.
The building modelling process is particularly complex with regard to the roof of the swimming pool zone, both due to its complex shape and geometry and to the peculiar envelope stratigraphy. The roof is composed of two different types of ETFE, an innovative high performance material. The roof surface is constituted by "cushions" of different shapes, which are built up by laying a different number of polymeric sheets one upon the other, with an air gap in between.

All the internal gains have been introduced in the model, which include gains linked to the presence of people in the building, those due to the lighting system and to the presence of water in the pool, which considerably affects the energy demand in terms of latent load.

The energy demand has been evaluated both through the monthly net energy demand, which is indicative of the envelope's performances, both in terms of monthly energy consumption for heating and cooling: these last data take into account also the energy need due to the air treatment, which is necessary in order to satisfy the thermo-hygrometric comfort and to ensure the internal target values of temperature and relative humidity. The achievement of comfort conditions is verified by analysing the detailed data of internal air temperature and operative temperature in the different building zones, in particular the daily data related to the most critical months, especially July for the cooling period and January for the heating season, as well as the hourly data of the coldest and the warmest days of the year. The results analysis allowed to confirm that the design solution using the ETFE roof is able to satisfy the desired internal conditions, avoiding overheating during summer, which could affect a building using a roof with similar characteristics but made with traditional materials.

INTRODUCTION

The use of new materials and innovative architectural solutions should be considered in terms of energy efficiency. The aim of the research, carried out by ITC-CNR of San Giuliano Milanese, was the evaluation of the energy performances of an innovative roofing material such as ETFE (Ethylene Tetrafluoroethylene) through the use of dynamic simulation tools

applied to a swimming pool case-study, a context which is very different from a normal building due to the presence of water in a closed environment
The research is a part of an agreement with Tekser Srl, focused on the study of the energy and environmental impact of the ETFE, used as roofing for an aquatic park which is on the cutting edge as far as structural, architectural and plant solutions are concerned.
The target of the project managers (Sering Srl) was the realization of an aquatic centre to be used all over the year, giving the visitors the feeling of being in an open-air space even when they are in the internal swimming pools. The roofing material of the internal pool area had to permit the maximum entry of daylight and the maximum visibility towards the outside, without increasing the energy consumption related to both summer and winter air conditioning. The EFTE option was chosen for the reasons above.
The aquatic park consists of 12 swimming pools, some of which are located under the ETFE roof. The construction of the dynamic simulation model was focused on the area of the internal pools, named "dome area", consisting of two basement floors and one floor above ground, which has a mezzanine floor with a refreshment bar that faces the pools area.

Description of the roofing material - ETFE

Multiple layers of Ethylene Tetrafluoroethylene can be composed in order to build "air cushions" that can be used as envelope components. The sheets are 50-150 mm thick and they form a set of air cushions, fixed by aluminium extruded bars and sustained by a light structure. The standard component, made of three layers separated by two air gaps, can reach a thermal transmittance of 1,96 W/m2K and a solar factor of 78,4%. The solar factor, which represents the ratio between transmitted solar energy and incident solar energy , can be reduced by using graphic patterns made by opaque or translucent fluorine-polymers, or using variable patterns which can be modified if necessary. Light transmission varies from 97% of a single sheet to lower values according to the number of layers and their composition. ETFE allows the transmission of UV rays and facilitates photosynthesis phenomena in indoor environments. The material, developed for the aerospace industry, has excellent performances in terms of resistance to UV rays and pollutant agents in the atmosphere. Its resistance facilitates the construction of complex structures and its smooth surface requires little maintenance.

METHOD

Description of the design approach

The project management group was assisted in choosing the roofing material, in order to grant a high level of thermo-hygrometric comfort, without increasing energy consumptions for heating and cooling purposes. The evaluation of energy performances of the ETFE roof has been structured in the following steps:

- gathering of information about the building and setting the input data;
- realization of the model through the dynamic simulation software Energy Plus and the GUI Design Builder;
- implementation of energy simulations in winter and summer seasons, with a more thorough analysis on the most critical days;
- results analysis.

The dynamic simulation model

Dynamic simulations allow to perform very accurate analysis of the building's energy performances and can produce a great amount of output data; for these reasons, a very deep knowledge of the case-study building's characteristics is required, as well as the definition of

many input data, in order to put up an adequate building model. Simulations can calculate thermal balances even at very short time intervals; hourly time steps are typically used, but some software give the opportunity to use even hour fractions as time steps.

During the simulation of the energy performances, the real building's envelope behaviour is represented (heat storage and transfer, thermal losses, infiltrations) according to climatic conditions and heat gains due to sunlight or internal loads, and the HVAC plant operation is reproduced, taking account of transient periods. This last aspect is fundamental when simulations are used for plant dimensioning, as it allows to choose the solutions that can best be integrated into the building, while ensuring optimal conditions in terms of indoor comfort.

The realization of the simulations model of the "dome area" faced many difficulties in reproducing the complex morphology of the structure and in defining the physical characteristics (both thermal and visual) of the innovative roofing material. The ETFE sheets are separated by air gaps and they assume a peculiar "cushion" shape, and it was therefore extremely important to reproduce their average performance when calculating the global roof performance. Another critical situation was represented by the simulation of the internal latent load due to the high occupancy and to the presence of water pools at different temperature levels which change according to the season and to the people's activity.

The climatic data used in the model are referred to the Energy Plus database, of the "International Weather for Energy Calculation" (IWEC). The "dome area" has been divided in thermal zones which are homogeneous in terms of internal gains, design temperatures and occupancy profiles: due to the complexity of the building's geometry, only four thermal zones have been defined in order to avoid excessive extensions of the simulation's duration and to prevent any distortion of the expected results:

- thermal zone 1, "Swimming pool", which represents the zones of the water pools;
- thermal zone 2, "Sunbeds", representative of the relax areas near the swimming pools;
- thermal zone 3, "Plants", including the whole second underground level and some parts of the first underground level;
- thermal zone 4, "Refreshment bar", representative of the bar zone located on the mezzanine floor.

Particular attention has been paid to transposing" the shape of ETFE "cushions" into the simulation software. The performances of two different types of roofs have been analysed: the former, named "ETFE clear", made of three layers separated by two air gaps, allows the maximum visibility towards the exterior, and has a solar factor of 0,784 and a light transmission of 75%. The latter, "ETFE white", which is used in order to create an acoustic barrier towards the residential area near the aquatic park, is made of just two ETFE sheets, separated by an air gap, and by a layer of internal acoustic panels.

Solar Heat Gain Coefficient (SHGC)	0,784
Direct Solar Transmission	0,776
Light Transmission	0,751

Table 1. ETFE Clear technical characteristics (data provided by the manufacturer)

Latent load calculation

Internal gains of the "dome area", apart from solar gains, are caused by people, lighting system and equipment. In swimming pools, more than 50-60% of heat transmission is related to evaporation phenomena (ASHRAE, 1999), so it is fundamental to calculate latent loads. Evaporation depends on several factors, such as pools surface, water temperature, relative humidity, number of occupants in the area and their type of physical activity, difference of

vapour pressure. Evaporation increases as air temperatures increase or as relative humidity decreases. In literature, many studies have been carried out in order to calculate latent loads of indoor and outdoor swimming pools: the calculated value for the global latent load for the internal swimming pool is 665 kW. The internal pool has a maximum occupancy of 1200 people, divided into four thermal zones. The internal gains due to the lighting plant and to the equipment are illustrated in Table 2, divided by thermal zone.

Thermal zone	**Lighting and equipment (W/m^2)**	**Weekdays**	**Weekends**
SWIMMING POOL	40	9:00-23:00	9:00-1:00
SUNBEDS	40	9:00-23:00	9:00-1:00
REFRESHMENT BAR	100	9:00-23:00	9:00-1:00

Table 2. Internal loads due to lighting and equipment

The internal load of 100 W/m2 calculated for the refreshment bar zone has been divided in 40 W/m2 of sensible load and 60 W/m2 of latent load. People in the Sunbeds zone are assumed to be sitting, while people in the Swimming pools zone are assumed to be doing some physical activity. Metabolic rates (met) and the clothing insulation degree (clo) are defined according to the standards presented in ISO 7730. Input data about ventilation and internal design temperatures have been taken from the design data.

Thermal zone	**Setpoint temperature (°C)**		**RH (%)**	**Air change l/sp**	**$T_{inlet\ air}$ °C**	
	Summer	**Winter**			**Summer**	**Winter**
SWIMMING POOL	29	29	65	6,5	21	35
SUNBEDS	29	29	65	6,5	21	35
REFRESHMENT BAR	28	28	55	10	20	32

Table 3. Indoor design temperature and air changes per person

RESULTS

Energy analyses have been first carried out on a whole year period with a daily time step, in order to point out the most critical months and days, both in winter and summer period. Then, more exhaustive analyses have been carried out for the most significant periods, through hourly simulations whose aim was to analyse the energy consumption and the comfort indexes in the most critical days of winter and summer. Energy analyses have considered the consumption of the whole building, while comfort analyses have been detailed independently for each thermal zone, in order to verify any anomalous result in any part of the building. The simulation produced the following output data: energy consumption for heating and cooling (kWh), indoor air temperature (°C), operative temperature (°C) and internal surface temperature of the roofing (°C).

Comfort analysis

The simulation has been used also for the verification of the design indoor comfort conditions. Analysis have been carried out independently for each thermal zone, in order to verify that the different boundary conditions (type of envelope, presence of water, internal gains due to occupancy) did not cause any considerable difference in the correct operation of the building. The analysis considered daily internal mean temperature in the opening hours, during the months of January and July, and focused on:

- air temperature (°C);

- operative temperature (°C)
- radiant temperature (°C).

Following the identification of the most significant days corresponding to the peak values of energy consumption, the temperature hourly data have been analysed to verify that there were no excessive deviations from the design values and no discomfort situations.

		Opening hours		Closing hours	
		Air temp	Operative temp	Air temp	Operative temp
18th January: minimum value	°C	29,0	25,0	18,0	17,9
	Hour	-	10:00	24-1:00	8:00
18th January: maximum value	°C	29,0	26,0	27,8	23,5
	Hour	-	13-14:00	9.00	9:00

Table 4. Hourly temperature values – Sunbeds zone, 18th January

		Opening hours		Closing hours	
		Air temp	Operative temp	Air temp	Operative temp
15th July: minimum value	°C	29,0	29,6	18,7	21,8
	Hour	-	10:00	2:00	2:00
15th July: maximum value	°C	29,0	31,8	29,0	28,9
	Hour	-	14:00	9:00	9:00

Table 5. Hourly temperature values – Sunbeds zone, 15th July

At the end of the study, specific analyses have been conducted on the surface temperatures of the roofing elements with the acoustic insulation. The inner and outer surface temperatures have been calculated during the months of January and July and then, the temperature trends in the coldest and in the hottest days of the year have also been calculated into detail.

During winter, the internal surface temperature is quite constant, while the external surface temperature varies according to the variation of the external temperature. Some variations related to the HVAC plant operation can be noticed over the course of the day.

In summer, the daily average internal surface temperature follows the external temperature. A daily analysis shows that there are strong variations between day and night (up to 35°C of temperature range throughout the day), with peaks over 55°C. The internal surface temperature shows a softened behaviour, keeping the temperature range within 20°C, but it reaches values up to 45°C. Such high values of surface temperature justify the maximum operative temperature calculated during summer simulations.

DISCUSSION

Verification of preliminary plant design

The first analysis carried out on the simulation model was the verification of the preliminary design of the HVAC plants. The total heating power needed for the "dome area" has been then calculated at winter design conditions (outdoor temperature of –5°C). It is a nearly steady-state analysis where the worst possible conditions are considered, thus excluding any external and internal gain, related to solar radiation and to electrical equipment or occupancy. Thermal losses due to ventilation and transmission through the envelope are considered; the sum of these components is then multiplied by an adequate safety factor, obtaining a final value of 834 kW.

HEATING	
Maximum loss due to ventilation (kW)	464
Maximum loss through the envelope (kW)	370
Total losses (kW)	834

Table 6. Heating design power

The simulation software Design Builder calculates the cooling power by considering the day with the highest external temperatures throughout the year (named "Summer Design Day"). A new nearly steady-state analysis is carried out, considering also all the internal gains, which represent an additional load during the cooling period. The energy consumption for cooling is analysed during the day, in order to determine the time of the peak load, considering both losses due to transmittance through the envelope and ventilation. Taking into account also the internal and solar gains helps to determine the real peak value of the cooling demand, which is used to calculate the design cooling power, always considering the safety factor. The load is divided into latent and sensible, in order to underline the importance of the load related on the one hand to the presence of people, and on the other hand to the mass of water contained in the pools: the total value is 1.512 kW.

COOLING	
Sensible load (kW)	560
Latent load (kW)	665
Maximum loss due to ventilation (kW)	287
Total load (kW)	1.512

Table 7. Cooling design power

Both values are very similar to the design values calculated by the project managers in designing the HVAC plant: this is an important confirmation concerning the accuracy of such a complex simulation model.

Calculation of energy requirements

The energy consumption has been calculated with daily time step and monthly values have been analysed in order to determine the consumption trend over the whole year. The results analysis shows that there is always a cooling consumption, even in winter. This can be explained through the analysis of the software's calculation model: the air treatment needed to achieve the desired humidity level is included in the cooling consumption. A dehumidification process is always active in order to maintain relative humidity at 55-65%, because of the presence of water within the structure. This causes a considerable energy consumption which is included in the cooling load (because this energy is used to eliminate the latent load). Similarly, heating consumption is always greater than zero because of the treatment of the fresh air entering the building all the year round. The net energy consumption represents the thermal losses related to the building envelope, without considering any air treatment process. The calculated values are 915.000 kWh for heating and 2.110.000 kWh for cooling. The analysis has been carried out with daily detail both in January and July in order to determine the days with the highest energy demand. The daily analysis shows that during the weekends there are higher consumptions because the swimming pool opening period is longer. The hottest day in July and the coldest day in January have been analysed into further detail, with a hourly time step, which allowed to estimate the simulated peak loads and compare them with the values calculated during the plant design stage.

SUSTAINABLE RETROFIT OF A SOCIAL HOUSING BUILDING SUPPORTED BY AN ASSESSMENT TOOL

A.Devitofrancesco[1], M.Ghellere[1], I.Meroni[1]
[1]*ITC-CNR, Construction Technologies Institute – National Research Council*
Via Lombardia 49, 20098 San Giuliano Milanese - Italy
devitofrancesco@itc.cnr.it, ghellere@itc.cnr.it, meroni@itc.cnr.it

ABSTRACT

New buildings and the retrofit of existing buildings must comply with indications and rules concerning specific environmental requirements focused on the improvement of the quality of the building context and of the areas used by occupants.

ITC-CNR carried out a specific energy retrofit case-study which includes the assessment of the environmental sustainability of a building and the definition of construction and technological solutions with low environmental impact involving the application of renewable energy sources systems integrated into the building. The purpose of the work was to verify the possibility of bringing a non-sustainable building close to the best practice level of sustainability by applying efficient and effective technical and economic solutions, managed through the use of the national sustainability assessment tool: "Protocollo ITACA".

"Protocollo ITACA" consists of a set of evaluation criteria used to assess issues such as Quality of the site, Resources Consumption, Environmental Loadings, Indoor Environment Quality and Service Quality. Starting from the performance of each criterion, the tool provides a concise final score about the overall performance of the building.

The methodological approach used in this study involves the assessment of the actual energy and environmental performances of a social housing building located in Southern Italy, conducted by means of "Protocollo ITACA" contextualized to the regional characteristics ("Protocollo ITACA Puglia").

This analysis allowed to point out the building's most critical aspects and to set performance targets to be achieved by each assessment criterion. Afterwards, several design solutions were identified and validated with the "Protocollo ITACA" tool in terms of technical feasibility, energy and environmental efficiency, local availability, cost-effectiveness and with respect to the targets set. The case study building was finally reassessed using the tool after the application of the most efficient configuration of design solutions.

The result of the experimentation allowed to provide the Region with feasible technical directions, justifying the cost/benefits of a design that would reach at least a level of environmental and energy sustainability better than that achieved by the standard construction practice.

INTRODUCTION

The environmental sustainability-based approach to constructions is focused on the definition and aware management of a healthy built-up environment, making an effective and ecological use of resources. It takes into account environmental issues and the quality of life, social equity, cultural characteristics and economic constraints. The evaluation of the environmental sustainability needs a general framework to gather the different criteria under examination subdivided into main themes and categories. During the different life phases of a building, the evaluation approaches range from the simulation of the behaviour of the building and its components to the verification of their actual performances under real working conditions.

Through such evaluation the level of environmental performance of a construction can be objectively measured by assigning a score, then classifying it according to a quality scale.

The aim of this research, carried out by ITC-CNR, is to define efficient and effective technical and economic solutions with a low environmental impact for a social housing building, located in Southern Italy, managed with the use of the sustainability assessment tool "Protocollo ITACA".

METHOD

The methodological approach used in this study consists of the following activities:

1. Identification of the case study building and definition of the performances targets.
2. Analysis of the actual state of the building, which includes the energy evaluation, the calculation of the mean environmental indicators and the evaluation of the energy and environmental sustainability.
3. Definition of the optimal energy and environmental improvement strategies, related to the technical feasibility, the energy and environmental efficiency, the cost-effectiveness, the local available technologies and performance targets.
4. Energy diagnosis and evaluation of the energy and environmental sustainability (with the same tools used to analyse the actual state of the building) following up the identified improvement strategies.
5. Financial sustainability, cost-effectiveness and sensitivity analyses.

Identification of the case study and definition of performance targets

The first step of this study focused on the choice of a case study related to the real relevance of the Puglia territory through the selection of a public residential building with reinforced concrete load-bearing structure and horizontal distribution.

The reference performances targets were then defined, that is the performances levels that the "Protocollo ITACA Puglia" criteria have to achieve after the utilization of the improvement strategies.

In particular, the sustainability levels to achieve using the improvement strategies are:

- CASE A: average score of 0/5 with "Protocollo ITACA Puglia", representing the minimum acceptable performance defined by national laws and/or regulations or, in the absence of a specific requirement, the standard practice;
- CASE B: average score of 2/5 with "Protocollo ITACA Puglia", representing a significant improvement of the performance compared with national laws and regulations or, in the absence of specific requirements, the standard practice.

Figure 1. View of the case study building

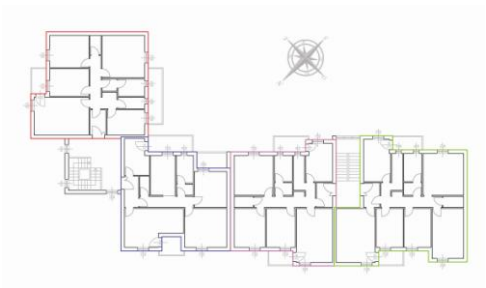

Figure 2. Plan of the standard floor

Analysis of the actual state of the building

Energy audit and assessment of environmental sustainability

The analysis of the energy performance of the current state of the building and the energy simulations concerning design alternatives are carried out using DOCET^{pro}, a diagnosis and energy certification software developed by ITC-CNR, on a web platform in accordance with the calculation methodology of standard UNI EN 13790 and series UNI TS 11300 1 and 2, the Presidential Decree 59/09 and Italian national guidelines for energy certification.

The analysis of the environmental sustainability of buildings before and after the application of design improvement strategies is carried out with the energy and environmental sustainability assessment tool "Protocollo ITACA Puglia".

In order to support the calculation of the performance indicators of the Protocol criteria, independent tools have been developed and contextualized to the specific climate context of the Puglia Region implementing the procedures for the calculation of "quantitative" indicators.

"Protocollo ITACA Puglia", contextualized to the regional characteristics allows to evaluate the level of environmental sustainability of new residential constructions and retrofit buildings. It consists of a set of evaluation criteria which assess issues such as Quality of the site, Resources Consumption, Environmental Loadings, Indoor Environment Quality and Service Quality. Starting from the performance of each criterion, the tool provides a concise final score about the overall performance of the building.

Characterization of design strategies

The methodological approach used to define the technical characteristics of different design strategies involves the following activities:

- Analysis of the results obtained with the "Protocol ITACA Puglia" that is a critical analysis of the performance achieved with the goal of determining the priorities of the redevelopment. The priority interventions are those that improve the performance of the building below the minimum level of sustainability and then those that affect the criteria with progressively higher scores.
- Optimization of performance targets in relation to the case study building: detection of the "target performances" for each criterion testing the room for improvement of the performance of the as-built building in relation to technical feasibility and cost effectiveness.
- Filing of technology solutions: development of the sheets of technological solutions in relation to performance targets and to specific areas of intervention. (Table 1). Each sheets contains:
  - *Description* of the technological solutions identified to achieve the predetermined performance level;
  - *Criteria* of "Protocollo ITACA Puglia" influenced by the application of each intervention with the respective performance indicators that measure the performance of each evaluation criterion influenced by the interventions,
  - *Analysis tools* that is software, spreadsheets, databases, etc.., useful for the calculation of the indicators,
  - *Technical feasibility* that is the technical constraints affecting the application of each intervention,
  - description of the *Application methodology* of each intervention

- *Assessment of environmental sustainability* that is the description of energy-environmental effects produced by the interventions on the whole building and in relation to all assessment criteria.

1. Envelope (opaque and transparent)
2. Heating system and DHW
3. Renewable energy systems
4. Environmentally-compatible materials
5. Water system
6. Layout of indoor common areas
7. Layout of outdoor areas
8. Telecommunication and management control system
9. Development and implementation of a maintenance management plan and building log.

Table 1. Areas of intervention

Assessment of environmental sustainability after the application of strategies

After the design strategies are characterized, the analysis of the environmental compatibility after application of the design strategies to the building, is carried out with the same procedure adopted for the as-built building. The building is assessed with the "Protocollo ITACA Puglia" getting the scores for each criterion and the overall score for environmental sustainability. (Table 2)

Protocollo ITACA 2009 PUGLIA Qualilty energy tool		CASE A		CASE B	
		SCORE	WEIGHTED SCORE	SCORE	WEIGHTED SCORE
CRITERIA					
Energy quality		2.15		2.45	
1. Heating		0.83	0.25	0.87	0.26
1.1	Thermal transmittance	2.03	0.51	1.62	0.41
1.2	Energy need for heating	0.15	0.04	0.45	0.11
1.3	Annual non-renewable primary energy used for facility operations (for heating)	0.75	0.28	0.94	0.35
1.4	Direct penetration of solar radiation	0.04	0.00	0.04	0.00
2. Cooling		3.43	1.71	2.96	1.48
2.1	Solar radiation control	3.46	0.94	3.46	0.94
2.2	Thermal wave reduction and phase-shift	4.99	1.35	3.28	0.89
2.3	Energy need for cooling	3.40	1.01	3.37	1.00
2.5	Natural ventilation efficiency	0.81	0.13	0.81	0.13
3. Renewable Energy		0.07	0.01	3.10	0.46
3.1	Thermal energy for DHW	0.00	0.00	2.00	0.67
3.2	Provision of on-site renewable energy systems (electric).	0.11	0.07	3.64	2.43
4. Other Primary Energy		3.50	0.18	5.00	0.25
4.1	Annual non-renewable primary energy used for DHW	3.50	3.50	5.00	5.00

Table 2. Score report of energy performances CASE A and CASE B after the application of design strategies

Financial sustainability, cost-effectiveness and sensitivity analyses

When the planning solutions are finally defined, the analysis of the financial sustainability and of the social cost-effectiveness of each CASE is carried out.

The financial sustainability analysis includes:

1. Evaluation of the financial situation related to the actual state of the building that includes the operating costs (fuel and electric consumption for heating, domestic hot water, other electric uses and potable water)
2. Evaluation of the financial situation related to the intervention that includes the intervention costs, the operating costs (fuel and electric consumption for heating, domestic hot water, other electric uses and water) and the applicable incentives.
3. Summary of the financial results: the benefits/cost analysis is made on the basis of the financial values (difference between costs and credits with or without intervention) calculating the economic feasibility indexes. The financial parameters used in the calculation are the inflation and discount rate and the life of the project The economic feasibility and the social cost-effectiveness indexes calculated are:
    - **NPV**: Net Present Value
    - **IRR:** Internal Rate of Return
    - **B/C Index**: Benefit/Costs Index

In parallel with the financial analysis a sensitivity analysis is also carried out. This analysis consists of the study of the variation of the financial and economic results related to the change of the costs and credits: the aim is to verify the validity and the stability of the hypotheses and of the financial values assumed and to identify the most uncertain areas.

RESULTS

The energy and environmental improvement hypotheses have led to different conclusions and the results show that the performance improvement is not always proportional to the financial benefits.

In order to assume interventions that are cost-effective and non-invasive (to limit users discomfort during the intervention operating phase), design actions involving the modification of the exterior facades and of the internal arrangement of the residential units have been avoided. These choices have limited the improvement of the environmental performances in particular those that are related to the indoor environmental quality, which has achieved, in all the cases, the lowest score.

The strategies are in the first instance applied to CASE A (lowest targets) and primarily involved the thermal envelope performances (i.e. thermal transmittance, solar radiation control) and the energy systems (reduction of the primary energy and CO2 emission and increase in the production of renewable energy); subsequently the interventions involved the less relevant criteria (i.e. highly environmentally-compatible materials, layout of indoor common *areas* and layout of the outdoor areas.

The economic benefits related to envelope and systems interventions have effects only on the operating costs savings (use of energy and water) except for the photovoltaic system that is related, in addition, to the Italian “Conto Energia” grants program. The financial sustainability analysis shows that all interventions are cost-effective (all the financial indicators are positive) and so the choice of the best case of intervention could be based on sensitivity and risk analysis.

The analysis of the results obtained shows that it is more convenient to achieve standard performances (CASE A intervention) than advanced performances (CASE B intervention). The reason of this result is due to the absence of financial risks, also in case of a parallel increase of investment and operation costs within the specific analysis range (Table 3).

Case study	Score	Initial costs (euro)	Initial costs (euro/m²)	NPV (euro)	IRR	B/C index	Intervention risk[1]
A	1.31 / 5	300000	318.5	137698	9.5%	1.45	0% (0/50)
B	1.98 / 5	530000	552.0	29481	5.6%	1.06	28% (14/50)

Table 3. Environmental and financial scores' analysis - CASE A and B

DISCUSSION

The result of the experimentation allowed to provide the Region with feasible technical directions, justifying the cost/benefits of a design that would reach at least a level of environmental and energy sustainability better than the standard construction practice.

The performance-based approach and the structuring of the requirements system into various stages make "Protocollo ITACA" a tool that helps checking the conformity of design choices in relation to the objectives defined by the benchmarks set according to the specific features of the local context of reference, managing the whole process of selection of the alternative solutions and design with an integrated approach.

REFERENCES

1. "Protocollo ITACA Puglia": http://www.regione.puglia.it/index.php?page=lr1409&opz=getdoc&id=427
2. B. Barozzi, A. Devitofrancesco, M. Ghellere, P. Lassandro, A. Lerario, R. Lollini: Schedatura di soluzioni tecnologiche per conseguire l'efficienza energetica in edilizia residenziale, http://www.arti.puglia.it/index.php?id=506, 2009
3. A. Devitofrancesco, M. Ghellere, I. Meroni: Sistemi di valutazione della sostenibilità ambientale degli edifici: esperienze nazionali ed internazionali, Edilizia, Speciale ITC-CNR, 2009
4. A. Devitofrancesco, M. Ghellere, I. Meroni: Sostenibilità energetico ambientale: ESIT – Edilizia Sostenibile Italia, Edilizia, Speciale ITC-CNR, 2010

[1] Calculated for a maximum variation of investment and operation costs of 10%. It represents the percent ratio of cases with negative financial indices that are calculated by 5% steps of costs variation. Round brackets indicate the number of risky combinations compared to all the combinations analyzed.

SUSTAINABLE IMPACTS BETWEEN CONVENTIONAL BUILDINGS AND VERNACULAR ARCHITECTURE: COMPARATIVE ANALYSIS METHODOLOGY

Elizondo, M.F. [1]; Guerrero, L.F.[2]; Mendoza, L.A.[1]

1: [1]Facultad de Arquitectura y Diseño, Universidad de Colima, México.
Cuerpo Académico Arquitectura y Patrimonio.

2: División de Ciencias y Artes para el Diseño. Universidad Autónoma Metropolitana-Xochimilco, México.

ABSTRACT

The road to sustainable development, more than ever must ensuring the welfare of people, without compromising the availability of natural resources for future generations. The exploitation of these resources in some places, has implications for other parts of the planet. Considering this, the modification of the environment to create the human habitat is no exception. The daily work of designers and builders, positively or negatively affect the sustainability of human settlements, and therefore affects the quality of life for its inhabitants. It is urgent that experts in the human habitat, have a vision of sustainable development.

This paper shows the comparative analysis of the impact caused by conventional buildings and vernacular architecture. We understand conventional architecture, when the works made primarily with industrial materials such as steel, aluminum and cement. As vernacular architecture, we consider traditional buildings made without architects, mainly earthen architecture. We propose a simplified method of qualitative analysis, which detect impacts generally at sustainability. At the end we present the results, and suggests corrective actions leading, which may be of mitigation, compensation and restoration.

Keywords: impact on sustainability, sustainable construction, conventional construction, vernacular architecture.

INTRODUCTION

Reference so, mention that the results of several studies, data that ensure that residential and trade buildings, consume 20 to 40 percent of total energy contributing 9.9 and 5.4 percent, respectively, at global emission CO2, and specifically in Mexico, the total emissions of CO2 of the building industry, contribute with 7.6 and 3.5 percent, respectively (Del Toro, M.R., 2009).

For the analysis of architectural phenomenon from the perspective of sustainability, we must consider the cultural axis, in addition to the traditional three: the environment, the economic and the social axis.

This paper presents partial results of the research project entitled "Characterization of the bullring La Petatera of Colima, Mexico, with criteria of sustainability." In particular, it describes the methodological approach used in this research project, for the comparative analysis between the conventional architecture (which involves the use of cement, steel and other industrial materials) and vernacular architecture, in the Mexico western. Yet, it is intended that this methodology, once developed, can be applied in other geographic contexts for the analysis of impacts on the sustainability of the architecture heritage.

We present a preliminary version of the proposed methodological framework, which has its starting point in methods of assessing environmental impacts of common use, but including the analysis of social impacts, cultural impacts and economic impacts. With the analysis of the impacts of the four axes, it is intended to determine the impacts to the sustainability of the building.

We need to measure the real impact of both the traditional and the conventional construction systems to define a decision-making basis for designing truly sustainable buildings. We should not romanticize buildings made of traditional materials as if "the past was better". We should weigh actual operating conditions from both systems and use the best of each to suit present and future requirements.

Earthen architecture is habitable constructions made of soaked natural soil, molded into bricks and sun dried. This technological process lies in the solidity and stability of molded natural soil.

We compare the environmental impact caused by conventional architecture with use cement, steel and cement-sand brick, and traditional architecture which includes the use of different natural soils: adobe, compressed clay brick (BTC), wall daub, or bajareque, techno-daub, and rammed earth.

VERNACULAR CONSTRUCTION SYSTEMS

Traditional construction techniques can be grouped into five categories:

Adobe: Bricks are popular for their similarity to masonry construction systems in terms of having the possibility to store prefabricated pieces for later use. The use of geometric patterns, leads to increased production of handmade bricks.

Compressed Clay Bricks (BTC): Compressed clay bricks are Similar to Those of traditional adobe, but hand pressed Into a mold, or with Specialized machinery. The Bricks Are Often mixed with Small Amounts of lime.

Rammed earth: Earth-wall or tapia is also known as mud, cob, or rammed earth. It is a single process where the soil handling and the dwelling construction happen at the same time. Soil selection and work organization are key components in this process. Evidence of walls built using this technique thousands of years ago are in places as far apart as India, China, Egypt, Syria, Lebanon, Bolivia and Peru. In China the use of this technique to make forts and palaces are found during the Shang Dynasty, dating from the period between 1766 and 1045 B.C. The technique was also found in various sections of the Great Wall built between the fifth and third centuries B.C.

Wall daub, or bajareque: The system is a moist soil mix and plant material. Possible origin of this material dates back to the days of settled communities over seven thousand years, when primitive man had to hunt animals for food, temporary shelters were built with materials made in motion as mats, skins and parts plants such as poles, straw and leaves. Gradually, when evolved basketry, the construction technology improved cabins with woven materials.

Techno-daub, or Tecno-bajareque, or Quincha Metalica: Is a mixture of moist soil with a three-dimensional structure of steel. We propose the use of this material as a viable alternative for contemporary use in the construction of affordable housing. This material has a high sustainable yield when considering environmental issues, economic, social and cultural rights.

METHOD

In another development, the formulation of indicators and benchmarks to "measure" the transition towards sustainability, has advanced significantly in the international arena, however, requires the development of methodological tools in several application areas as in the case of overall architecture and architectural heritage in particular. Current indicators are not applicable in the case of architectural phenomenon.

Consequently, we need a qualitative methodological tool, which is rather general, to determine trends of architecture under sustainability criteria, considering its four pillars: environmental, economic, social and cultural. This tool is not to be used by experts in sustainability, is designed to be used by any professional involved in the design, construction and management of human habitat.

Recent visions vinculated to sustainable development through a process of sustained and equitable improvement of quality of life of people, based on appropriate conservation measures and environmental protection. The fundamental principle is not to exceed the resilience of their surroundings: environmental, economic, social and cultural.

This is a transit rich and poor countries should do together to succeed, the transition to sustainability. Thus sustainable development considered economic growth, social equity, cultural roots and environmental protection. In this context, the environmental impact assessment (EIA), contributes to this transition to sustainable development, and can help to guide responsible decision making in that route.

Among the various methodological approaches and systems proposed so far by various authors, we cite the following: Canter (1977), Holling (1978), Munn (1979), PADC (1983), Westman (1985), Alberti (1988); Estevan Bolea (1989), Gómez Orea (1992); ITGE (1992), Conesa (1993), Bettini (1995), Morris et Therivel (1995), Canter (1996), Gómez Orea (1999), Nixon et Harrop (1999). In principle, the EIA for the construction, can be used the combination between two or more of them. As in other areas of knowledge, the claim that the EIA for the building are completely objective is impossible, since this is not a precise science, according Beder (1993), but this also occurs in disciplines such as law, economics or medicine.

The construction of indicators allows for greater certainty in the EIA, so it is convenient, as pointed out by Schneider (1997), differentiate in each case the reading more objective, measurable, testable, for those data that come from value judgments or more subjective assessments. This observation is consistent with the more human side of environmental science, which is considered inseparable from the objective data measured environmental parameters and how they view themselves, not only scientists and technicians, and the rest of the people and groups related to or involved with these environmental elements.

In this sense, the incorporation into the EIA for the construction of impact indicators, as well as life cycle analysis of buildings, the concept of EIPRO Study (Environmental Impact of Products), and the determination of the ecological footprint materials and processes associated with the implementation stages, construction, operation and abandonment of buildings, is inescapable. This encourages a more objective analysis of information in the EIA, and reduces subjective valuations, leading to more consistent performances.

The work with indicators required to reduce the large amount of scientific information related to the environment to a manageable number of appropriate parameters for these processes of decision making and public information, Environment Canada (1991). For the construction of indicators on environmental issues. For purposes of this research, we opted for a Type PSR (Pressure-State-Response), which is based on human actions that create pressure on the

environment, which changes the quality and quantity of natural resources (State). The company responds to these changes by adopting measures environmental and economic policy (Response). This model studies the interactions between human actions and the environment.

The Scope of study, you should consider not only the site where the building, also the origin and pre-processing of building materials and the different stages of the work:

- Site preparation,
- Preliminary maneuvers,
- Construction
- Occupation
- Abandonment

It is considered that the interactions at territorial level, mainly at three levels:

- Interactions of the building with its immediate surroundings.
- Interactions of the building to its surroundings.
- Interactions of regional capacity.

The intention is that the method is useful to reflect on existing cases, and above all serve as a prevention tool that is useful in planning and decision making.

RESULTS

Once the analysis by comparing the vernacular architecture and the conventional architecture, through the detection and characterization of the sustainability impacts were grouped in each of the four pillars of sustainability (look Table 1):

ENVIRONMENTAL SUSTAINABILITY AXIS IMPACT.

When considering the impacts in terms of energy conservation and reduced use of non-renewables materials, reuse and recycling and resource management, then definitely earthen architecture generates the least amount of negative impacts of the environment, is more sustainable than conventional building systems, with use of industrial materials.

ECONOMIC SUSTAINABILITY AXIS IMPACT.

Efficiency and economic performance are critical in terms of sustainability, have a positive impact on employment generation, in the extraction and material processing, and implementation of construction and preparation site. There are also other positive effects of conventional construction, especially in industrialized country, the modular building systems that enable faster construction process, and this results, reduce costs. In contrast, cause a reduction in the workforce, creating a negative impact in terms of equitable distribution of wealth. This situation does not exist in earthen architecture, because when the material removal takes place near the land where construction takes place, costs are considerably lower.

Environmental Axis	Economic Axis	Social Axis	Cultural Axis
Vernacular Architecture: Generates the least amount of negative impacts of the environment.	**Vernacular Architecture:** Efficiency and economic performance are critical in terms of sustainability, have a positive impact on employment generation, in the extraction and material processing, and implementation of construction and preparation site. In vernacular architecture, because when the material removal takes place near the land where construction takes place, costs are considerably lower.	**Vernacular Architecture:** Each person can build your own home with raw earth, since most people live in the architecture without architects. Earthen architecture does not require the transfer of technology on a large scale.	**Vernacular Architecture:** Cultural sustainability is directly related to the demystification of scientific knowledge as the only knowledge and try to recover some of the traditional wisdom.
Conventional Construction: is more in-sustainable, with use of industrial materials, generating waste and contamination.	**Conventional Construction:** Efficiency and economic performance are critical in terms of sustainability, have a positive impact on employment generation, in the extraction and material processing, and implementation of construction and preparation site. There are also other positive effects of conventional construction, especially in industrialized country, the modular building systems that enable faster construction process, and this results, reducing costs.	**Conventional Construction:** is also affected by the phenomena of self-construction, but the formal and informal builders are captives of the use of certain building systems as a result of the need to acquire the materials provided with the same supplier and are also dependent on technology transfer.	**Conventional Construction:** Identity loss, globalization and distortion of the attributes the building materials, due to marketing.

Table 1: Synthesis of detected impacts. Source: Own authors.

SOCIAL SUSTAINABILITY AXIS IMPACT.

Each person can build your own home with raw earth, since most people live in the architecture without architects. Earthen architecture does not require the transfer of technology on a large scale. This also makes possible social equity, which is another requirement for sustainability. Conventional construction is also affected by the phenomena of self-construction, but the formal and informal builders are captives of the use of certain building systems as a result of the need to acquire the materials provided with the same supplier and are also dependent on technology transfer.

CULTURAL SUSTAINABILITY AXIS IMPACT.

Cultural sustainability is directly related to the demystification of scientific knowledge as the only knowledge and try to recover some of the traditional wisdom. That is, with the traditional wisdom of each part of the world related to the resources available for the creation of human habitats, this is a trait of cultural identity. In these terms, earthen architecture is much more sustainable than conventional construction. In Mexico, there has been a cultural phenomenon: the substantial reduction of the building with raw earth, due to the emergence of construction materials like steel and cement.

DISCUSSION

The starting point of this work deals with a comprehensive view of vernacular architecture, the building systems, their structural relationship, their behavior on an urban scale and harmony with the natural and cultural environment that surrounds it. This way of thinking helps to explain some concepts related to holistic perception of the building systems,

preservation of architectural heritage, through appropriate and ongoing maintenance of the vernacular buildings and its study as a source for contemporary design of houses.

Lot of buildings of raw land in countries like Mexico, are not monumental, most are houses in rural or suburban areas, which remain unprotected by the laws of conservation of existing architectural heritage. Today interventions should take into account the earthen architecture and its relation to new buildings that surround, built with other materials and other building systems, looking for proper integration. We must promote a balance between past and future, respecting the natural environment, economic development and social and cultural development to which they belong.

REFERENCES

[1] Arenas, F., Ed. Edisofer, *El impacto ambiental en la edificación. Criterios para una construcción sostenible*, Buenos Aires, 2007.

[2] Elizondo, M.F., Gobierno del Estado de Jalisco, *Los Impactos Ambientales por la Edificación en Asentamientos Humanos; una aproximación,* (Chapter 3). *Edificación Sustentable en Jalisco*, Gobierno de Jalisco, pp. 110-125, 2009.

[3] Elizondo, M.F., Universidad de Colima, *Impacto Ambiental por la Edificación en Asentamientos Humano,* Thesis Degree, Ed. Own, 1990.

[4] Espinoza, G., CED-BID, *Fundamentos de Evaluación de Impacto Ambiental.* Santiago de Chile, 2001.

[5] Gómez, D., Ed. Mundiprensa, *Evaluación de Impacto Ambiental, Madrid, 2002*.

[6] Guerrero, L.F., Universidad Xaveriana, *Hacia la recuperación de una cultura constructiva* Arquitectura en tierra (Chapter 1). *Apuntes,* Bogotá, Colombia, Vol. 20, No.2, pp. 182-201, 2007.

[7] Montero, J.M., Fernández–Avilés, G., Mateu, J. & Porcu, E., *The Use of Environmental Quality Indexes for the Estimation of Housing Prices*, in "Impacto ambiental de las actividades económicas", Septem Ediciones, 2009.

[8] Reyes, J.C., Gobierno del Estado de Colima, *La Antigua Provincia de Colima, Siglos XVI al XVIII. Colima, Mexico*, pp. 270-272, 1995.

[9] Schneider, M. & Spitzer, M., WP/89, *Forecasting Austrian GDP using the generalized dynamic factor model*. Oesterreichische National bank (Austrian Central Bank), 2004.

[10]Schumacher, C., Journal of Forecasting, 26(4), *Forecasting German GDP using alternative factor models based on large dataset*, 2007.

[11] Zarnowitz, V., y Ozyildirim, A., NBER. Paper w8736, *Time series decomposition and measurement of business cycles, trends and growth cycles*. 2002.

DYNAMIC THERMAL BEHAVIOR OF VENTILATED WOODEN ROOFS

F. Fantozzi, F. Leccese, G. Salvadori

Dept. of Energy and Systems Engineering (DESE), University of Pisa
Faculty of Engineering, Largo L. Lazzarino, 56122 Pisa (Italy)

ABSTRACT

In this paper, by using a calculation code developed by the Authors, an analysis of the dynamic thermal behavior of some Ventilated Wooden Roofs (VWRs), lightweight building structures characterized by different stratigraphies which are currently used in Italy, is shown. From the results of the analysis carried out, some general criteria required for the right design and sizing of this type of ventilated structures are obtained and discussed.

1. INTRODUCTION

The use of passive cooling systems, in particular the use of ventilated roofs and walls, has recently been subject of remarkable development, especially after the adoption of the European Directive 2002/91/EC (EPBD), which recommends the use of these systems in order to increase the energy efficiency of buildings. The Ventilated Wooden Roofs (VWRs), lightweight building structures characterized by low and very low values of surface mass, are undoubtedly one of the most widespread example of passive cooling systems [1-4]. In the last few years, to improve the summer indoor thermal comfort, the analysis of thermal behavior of opaque building envelope under dynamic thermal conditions has become very important [5-6], even from the standpoint of European and national legislation. In Italy, for instance, limit values of the dynamic thermal transmittance (Y_{IE}, $W \cdot m^{-2} \cdot K^{-1}$), decrement factor ($f_a$, dimensionless) and time lag (φ, h) have been fixed for the opaque building structures of new realization [7].
In this paper, by using a calculation code developed by the Authors [8-10], an analysis of the dynamic thermal behavior of some VWRs, characterized by different stratigraphies which are currently used in Italy, is shown. In particular for each VWR analyzed, the parameters Y_{IE} and φ are evaluated in function of a dimensionless parameter γ, proportional to the air mass flow rate into the duct.

2. DYNAMIC THERMAL BEHAVIOUR: PERFORMANCE PARAMETERS

The dynamic thermal behavior of a VWR can be characterized by the same parameters used for non-ventilated walls [5, 8]: Y_{IE}, f_a and φ. Considering the external thermal field oscillating with amplitude T_E and period P and assuming the indoor air temperature to be constant, the heat flux Q exchanged through the VWR is given by [8]:

$$Q = A\, T_E \tag{1}$$

with:

$$A = (c\,\Delta/\Gamma)\,(1 - e^{-\Gamma/c\Delta})\left[(1/\Gamma) - (R/\Delta)\right] - (1/\Gamma) \tag{2}$$

The following has been stated:

$$\Gamma = Z_{2,11}\, Z_{1,12} + Z_{2,12}\, Z_{1,22} \quad , \quad \Delta = R\,\Gamma + Z_{1,12}\, Z_{2,12} \tag{3}$$

In the Eqs. (2) and (3) it has been indicated with:

- $Z_{i,11}$, $Z_{i,12}$, $Z_{i,21}$, $Z_{i,22}$ (i=1, 2), the elements of the transfer matrix of the outer slab (i=1) and of the inner one (i=2) composing the VWR (see Fig. 1);

- $c=Gc_p/\ell L$, the heat capacity rate ($W\cdot m^{-2}\cdot K^{-1}$) of the air flowing into the duct, referred to the roof surface unit, where G ($kg\cdot s^{-1}$) is the mass flow rate into the duct, c_p ($kJ\cdot kg^{-1}\cdot K^{-1}$) is the specific heat at constant pressure (mean value among the temperatures of interest), ℓ (m) and L (m) are, respectively, the duct width and length (in the direction of the air flow);
- $R=r_{01}r_{02}/(r_{01}+r_{02}+R_0)$ the thermal resistance ($m^2\cdot K\cdot W^{-1}$) due to convective and radiative heat transfer within the duct, where r_{01} and r_{02} are the convective resistances of the air flowing in the duct, related respectively to the heat transfer toward the inner face of the outer slab and toward the inner face of the inner slab, R_0 is the radiative thermal resistance between the two slabs.

The parameters Y_{IE}, f_a and φ, for each VWR, can be wrote as:

$$Y_{IE} = |A| \tag{4}$$

$$f_a = Y_{IE} / U_0 \tag{5}$$

$$\varphi = (P / 2\pi)\arg(1/A) \tag{6}$$

having indicated with: U_0 ($W\cdot m^{-2}\cdot K^{-1}$) the overall thermal transmittance of the VWR in case of closed air duct (under steady state thermal conditions) and with arg(1/A) the argument of the complex quantity 1/A. For general purpose can be considered $0\leq\arg(1/A)\leq 2\pi$ so that it results: $0\leq\varphi\leq P$.
From what has been explained above, for a given VWR, the parameters Y_{IE}, f_a and φ turn out to be dependent on: the wall overall thermal resistance and thermal capacity, the sequence of the layers, the air mass flow rate within the duct and the period P of the outdoor temperature oscillation. In absence of air flow into the duct (c=0), Eq. (2) gives: $A=-1/\Gamma$ and, according to Eq. (4), it results:

$$Y_{IE} = 1/|\Gamma| \tag{7}$$

The dynamic thermal transmittance Y_{IE} is given by the modulus of the reciprocal of the first-line, second-column element of the wall transfer matrix (EN ISO 13792/2005).

3. DYNAMIC THERMAL BEHAVIOUR: NATIONAL TECHNICAL RULES

In Italy, with a Decree of the President of the Republic [11], for the Italian municipalities in which the maximum intensity of the solar radiation on a horizontal plane is higher than 290 $W\cdot m^{-2}$, the following requisites have been imposed:

- for the vertical opaque walls (facing South, South-West and South-East), the value of the surface mass M should be higher than $M_{lim}=230$ $kg\cdot m^{-2}$ otherwise the value of the dynamic thermal transmittance Y_{IE} should be lower than $(Y_{IE})_{lim}=0.12$ $W\cdot m^{-2}\cdot K^{-1}$;
- for the horizontal and tilted opaque walls (e.g. roofs), the dynamic thermal transmittance Y_{IE} should be lower than $(Y_{IE})_{lim}=0.20$ $W\cdot m^{-2}\cdot K^{-1}$.

In a companion Ministerial Decree [12], on the national guidelines for energy certification of buildings, in order to rate the "performance level" on summer of the opaque building envelope, two methods valid for all building's uses are indicated: one based on the evaluation of a performance indicator for summer cooling (EP_E) suitably defined, the other based on the parameters f_a and φ (see Tab. 1). In [12] is also specified that, in the cases where values of f_a and φ do not belong to the same performance level (see Tab. 1), the assignation of the building performance level is based on the value of the time lag. Note that the parameters f_a and φ are used in the Guidelines for Sustainable Building of the Tuscany Region (April 2006). It is also important to remember that, in Italy, as European Directive EPBD implementation, limit values (U_{lim}) of the overall thermal transmittance for the external walls of buildings have

been fixed for each of the six climate zones (A÷F) in which the Italian territory is split up [11-12]. In particular, the more stringent limit values (Italian colder climate zone F) are: U_{lim}=0.33 $W \cdot m^{-2} \cdot K^{-1}$ and U_{lim}=0.29 $W \cdot m^{-2} \cdot K^{-1}$ for vertical walls and roofs respectively. Building structures with values of the overall thermal transmittance lower than the previous limits can therefore be used throughout the Italian territory.

Table 1 – Performance level attribution for opaque building envelope.

Performance		Decrement Factor	Time Lag
Level	**Description**	**f_a (-)**	**φ (h)**
I	Excellent	$f_a < 0.15$	$\varphi > 12$
II	Good	$0.15 \leq f_a < 0.30$	$12 \geq \varphi > 10$
III	Medium	$0.30 \leq f_a < 0.40$	$10 \geq \varphi > 8$
IV	Sufficient	$0.40 \leq f_a < 0.60$	$8 \geq \varphi > 6$
V	Poor	$f_a \geq 0.60$	$\varphi \leq 6$

4. CALCULATION EXAMPLES

Two different examples of ventilated roofs VWR1 and VWR2, representing common types of ventilated wooden roofs, have been analyzed. The stratigraphies of the roofs are shown in Fig. 1 and in Tab. 2.

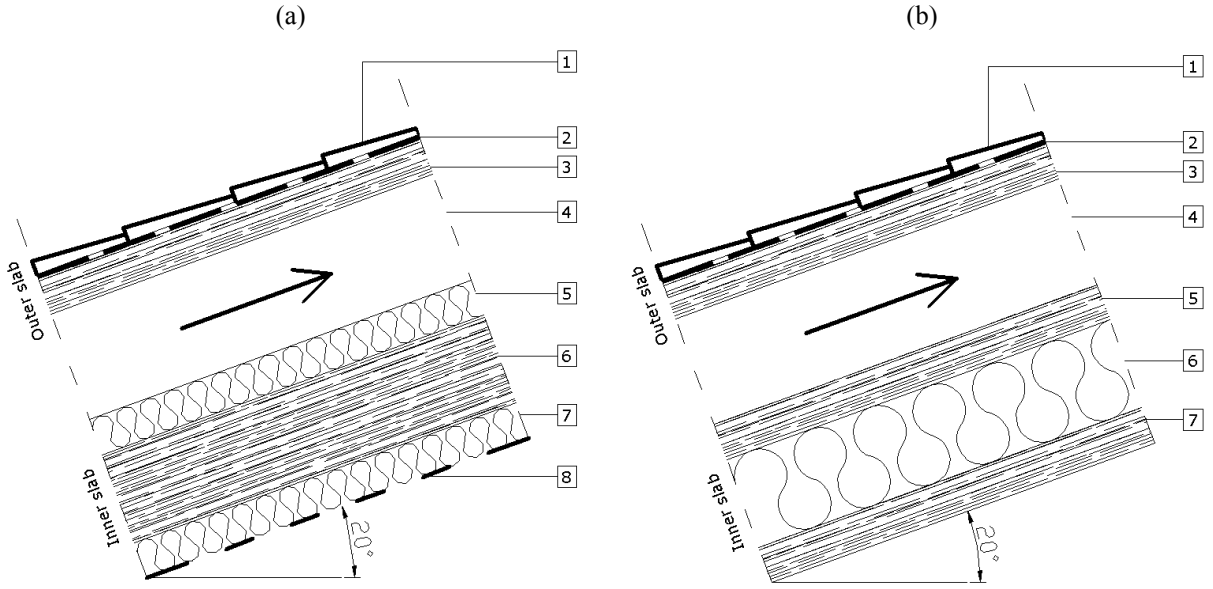

Figure 1: Stratigraphies of analyzed roofs: (a) VWR1, (b)VWR2 (see also Tab. 2).

Both the roofs have an outer slab realized with terracotta tiles layer placed on a continuous layer (properly waterproofed) in Oriented Strand Board OSB panels (VWR1) or in spruce wood panels (VWR2). The VWR1 has an inner slab realized with two layers of thermal insulation panels in wood fiber with a OSB panel interposed and plasterboard panels are facing toward the interior environment. The inner slab of VWR2 consists of two layers of continuous spruce wood panels with interposed an insulating layer in wood fiber, in this latter case one of the two spruce layers is facing towards the interior environment. Both roofs can be considered as lightweight building structures and can be realized completely with "dry technique".

In Tab. 2 the materials composing the various layers, of the roofs VWR1 and VWR2, with the respective thicknesses (d) and thermophysical properties (density ρ, thermal conductivity k, and specific heat at constant pressure c_p) are specified. In Tab. 2 the following values are also reported for each VWR: the overall thickness d_T, the surface mass M, the overall thermal resistance R_{T0}, the thermal transmittance $U_0=1/R_{T0}$ and the overall thermal capacity C. In the calculations the standard values for inner (r_i) and outer (r_e) surface thermal resistances and for thermal resistance (r_0) of the closed air duct have been assumed (EN ISO 6946/2003 and EN ISO 13792/2005): $r_i=0.13$ m^2·K·W^{-1}, $r_e=0.07$ m^2·K·W^{-1}, $r_0=0.21$ m^2·K·W^{-1}.

Table 2: Thermophysical properties of different layers for VWR1 and VWR2.

Roof	Layer	Material		d (cm)	ρ (kg·m^{-3})	k (W·m^{-1}·K^{-1})	c_P (kJ·kg^{-1}·K^{-1})
VWR1	1	(outer slab)	Terracotta tiles	2.0	2000	1.0	0.8
	2		Waterproofing	0.5	1100	0.23	1.0
	3		Oriented Strand Board (OSB)	5.0	650	0.13	1.7
d_T=39 cm	4	Air (ventilation duct)		12.0			
M=171 kg·m^{-2}	5	(inner slab)	Wood fiber	4.0	160	0.040	2.1
R_{T0}=3.6 m^2·K·W^{-1}	6		Oriented Strand Board (OSB)	10.0	650	0.13	1.7
U_0=0.28 W·m^{-2}·K^{-1}	7		Wood fiber	4.0	160	0.040	2.1
C=245 kJ·m^{-2}·K^{-1}	8		Plasterboard	1.5	1000	0.47	1.0
VWR2	1	(outer slab)	Terracotta tiles	2.0	2000	1.0	0.80
	2		Waterproofing	0.5	1100	0.23	1.0
d_T=34 cm	3		Spruce wood	2.5	450	0.12	1.4
M=97 kg·m^{-2}	4	Air (ventilation duct)		12.0			
R_{T0}=3.6 m^2·K·W^{-1}	5	(inner slab)	Spruce wood	4.0	450	0.12	1.4
U_0=0.28 W·m^{-2}·K^{-1}	6		Wood fiber	9.0	50	0.040	2.1
C=113 kJ·m^{-2}·K^{-1}	7		Spruce wood	4.0	450	0.12	1.4

Both the analyzed roofs are characterized by the same value of overall thermal transmittance (U_0) with closed air duct. The value of U_0 is lower than the limit value $U_{lim}=0.29$ W·m^{-2}·K^{-1}, the analyzed roofs can be hence realized in all the Italian climate zones (see Section 3).

5. CALCULATION RESULTS

For the analyzed VWRs, the following reference values for the air duct have been assumed: thickness d=0.12 m, width ℓ=10 m, length L=10 m. The roofs have been considered with a pitch inclination angle θ≅20° (pitch inclination percentage of 40%), as usual in Italy.
The modeling of the air flow inside the air duct has been carried out as described in [8-10]. The following has been considered: the friction factor of the heat losses localized on the inlet section $\lambda'_i=1/2$ and the friction factors on the outlet section $\lambda'_u=1$. For the evaluation of the friction factor λ along the duct the Haaland's equation has been used [9-10]. For the relative roughness of internal surfaces inside the air duct, the value β=0.050 has been considered, such a value is equivalent to a roughness of about 0.01 m, considering for example the presence of the support structures [9]. The convective heat transfer coefficients inside the air duct have been evaluated with the Gnielinski's equation [9-10]. For a typical summer situation the following reference climatic conditions have been assumed: air temperature in the shade $T_0=28$°C, indoor air temperature $T_i=24$°C and incident solar radiation intensity I=400 W·m^{-2} (with a=0.85 the absorption coefficient to solar radiation). All the calculations have been performed by using an iterative calculation procedure implemented on *MAPLE* software.
In Tab. 3, for the analyzed VWRs, the values of the thermal dynamic parameters f_a, φ and Y_{IE} have been shown, with reference to a time period P=24 h and in case of closed air duct (c=0). In Tab. 3, the values of M, R_{T0} and C are also indicated for each VWR.

Table 3: Comparison between the dynamic thermal performance of VWR1 and VWR2 (case of closed air duct and P=24 h).

Roof	M ($kg \cdot m^{-2}$)	R_{T0} ($m^2 \cdot K \cdot W^{-1}$)	C ($kJ \cdot m^{-2} \cdot K^{-1}$)	f_a (-)	φ (h)	Y_{IE} ($W \cdot m^{-2} \cdot K^{-1}$)
VWR1	171	3.6	245	0.081	15.6	0.023
VWR2	97		113	0.54	8.1	0.15

From Tab. 3 it is clear that, for the analyzed roofs, the values of Y_{IE} largely satisfy the limit values set out in the Italian legislation, $Y_{IE}<(Y_{IE})_{lim}=0.20$ $W \cdot m^{-2} \cdot K^{-1}$ (see Section 3). The VWR1 has a very high value of φ, this value allows the attribution of "excellent" performance level (see Tab. 1), unlike the VWR2 has a value of φ that leads to "medium" performance level (see Tab. 1). The VWR2 could reach the "excellent" performance level (φ>12 h) for example by increasing the thickness of the thermal insulation layer (wood fiber, layer 6) up to 20 cm or doubling the thickness of the spruce wood panels (layers 5 and 7) constituting the inner slab of the roof (see Tab. 2).
For the VWR1 and the VWR2 the trend of the parameters Y_{IE} and φ (in the case of P=24 h) with the dimensionless quantity $\gamma=cR_{T0}$, proportional to the air mass flow rate and, then, to the velocity of the air flowing into the duct, are shown in the Figs. 2a and 2b. For values of γ lower than 50, the air flow in the ventilation duct can be considered as natural (head pressure generated by stack effect), while for values of γ higher than 100 the air flow can be considered as forced (head pressure generated thanks to the presence of a fan with low electric power consumption). For the analyzed roofs, characterized by the indicated values of geometrical and physical parameters, the values of γ turn out about 20. The dependence of Y_{IE} and φ on β ($0 \le \beta \le 0.050$), for a given value of γ, has been verified to be small and negligible [8].

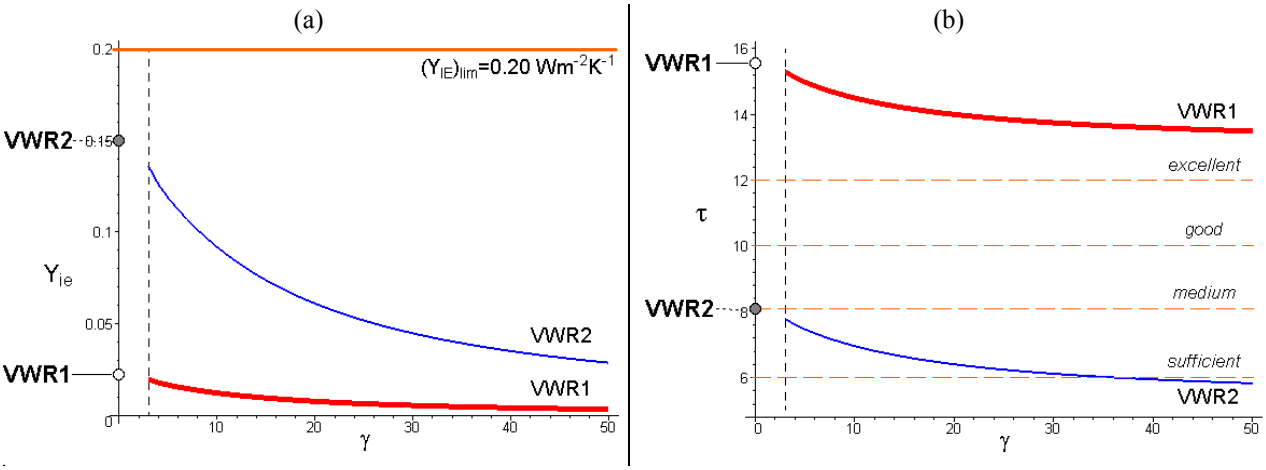

Figure 2: (a) Trend of the dynamic thermal transmittance Y_{IE} (W/m^2K) as a function of the dimensionless quantity γ; (b) trend of the time lag φ (h) as a function of the dimensionless quantity γ. In the Fig. 2a the horizontal line represents the $(Y_{IE})_{lim}$ value, in the Fig. 2b the horizontal dashed lines represent the performance levels, based on the time lag, as described in Tab. 1.

In the Figs. 2a and 2b, on the ordinates axis the values assumed by Y_{IE} and φ, in case of closed air duct (see Tab. 3), are pointed out with a circle. In the area included between the ordinates axis and the dashed vertical line, the air flow within the duct is laminar and thus not suitable for the used relations [8-9].

From the trends shown in Figs. 2a and 2b, Y_{IE} and φ turn out to decrease as γ increases. The remarkable reduction of Y_{IE} (80% for the VWR1 and the VWR2) is to be considered as a positive effect (see Fig. 2a). The small decrease of φ is a negative effect (see Fig. 2b); the reduction of φ is moderate and keeps, for the considered values of γ, lower than 12% for the VWR1 and lower than 26% for the VWR2.
Moreover analyzing the graphs of Figs. 2a and 2b it can be state that lightweight ventilated roofs with $M<M_{lim}$, which are designed to meet the requirements imposed by the Italian legislation on the parameter Y_{IE} ($Y_{IE}<0.20$ $W \cdot m^{-2} \cdot K^{-1}$) in case of closed air duct, are able to satisfy this limitation also in case of open air duct.

6. CONCLUSIVE REMARKS

The results obtained from the analysis carried out by the Authors show in particular, from both qualitative and quantitative point of view, how:

- the parameters Y_{IE}, f_a and φ, can be considered as characterizing to the thermal behavior of VWR under dynamic conditions;
- lightweight building roofs (e.g. VWR), if carefully designed, can satisfy the most recent Italian legislation concerning the energy performance of building, especially in terms of limit values fixed for Y_{IE} (and f_a) and φ;
- the ventilation air mass flow rate influences the parameters Y_{IE} and φ, in particular Y_{IE} (and f_a) decreases as the air mass flow rate increases, also φ decreases as the air mass flow rate increases but this decrease is moderate and turns out to be, generally, acceptable.

This analysis carried out by the Authors can be used as a tool for designers and building constructors in order to obtain the indication of general criteria required for the right design and sizing of this type of ventilated structures of building envelope.

REFERENCES

1. Straube J., Wood Pitched Roof Construction, *Building Science Digest*, 2006, 115, pp. 1-10.
2. Villi G., Pasut W., De Carli M., CFD modelling and thermal performance analysis of a wooden ventilated roof structure, *Building Simulation*, 2009, 2, pp. 215-228.
3. Prada A., Pancheri P., Baggio P., Baratieri M., Libardoni G., Experimental analysis and modeling of the thermal performance of ventilated roofs, *CLIMA 2010 – 10th REHVA World Congress*, Antalya (Turkey), 2010, CD-Rom, paper n° R8-TS8-OP05, p.1-8.
4. Catalogue of timber building materials, components and component connections, http://www.dataholz.com.
5. Tuoni G., Ciampi M., Leccese F., Caruso G., On the parameters characterizing the thermal transient behavior of the external walls of buildings, *CISBAT 2009 – International Scientific Conference*, Lausanne (CH), 2009, CD-Rom, pp.155-160.
6. Ciampi, M., Leccese, F., Tuoni, G., On the thermal design of the external walls in buildings, *CLIMA 2005 – 8th REHVA World Congress*, Lausanne (CH), 2005, CD-Rom, pp. 1-8.
7. Ciampi M., Leccese F., Tuoni G., Salvadori G., The use of light walls in buildings as a consequence of the most recent European regulations, *CISBAT 2009 – International Scientific Conference*, Lausanne (CH), 2009, CD-Rom, pp. 161-166.
8. Tuoni G., Ciampi M., Leccese F., Salvadori G., Passive cooling of buildings: ventilated facades and roofs, *CLIMA 2010 – 10th REHVA World Congress*, Antalya (Turkey), 2010, CD-Rom, paper n° R3-TS51-OP03, p.1-8.
9. Ciampi M., Leccese F., Tuoni G., Energy analysis of ventilated and microventilated roofs, *Solar Energy*, 2005, 79 (2), pp.183-192.
10. Ciampi M., Leccese F., Tuoni G., Ventilated facades energy performance in summer cooling of buildings, *Solar Energy*, 2003, 75 (6), pp.491-502.
11. D.P.R. n. 59 del 2 aprile 2009, *Regolamento di attuazione dell'articolo 4, comma 1, lettere a) e b) del D. Lgs.vo n. 192 del 19 agosto 2005, concernente attuazione della direttiva 2002/91/CE sul rendimento energetico in edilizia*.
12. D.M. Sviluppo Economico del 26 giugno 2009, *Linee guida nazionali per la certificazione energetica degli edifici*.

ENERGY PERFORMANCE ASSESSMENT OF A RESPONSIVE BUILDING ENVELOPE COMPONENT: RESULTS FROM A NUMERICAL ANALYSIS

F. Favoino[1]; F. Goia[1,2]; M. Perino[1]; V. Serra[1].

1: TEBE Research Group, Department of Energetics, Politecnico di Torino, C.so Duca degli Abruzzi 24, 10129 Torino (Italy).

2: Research Centre on Zero Emission Buildings, Faculty of Architecture and Fine Art, Norwegian University of Science and Technology, Alfred Getz vei 3, 7491 Trondheim (Norway).

ABSTRACT

Responsive Building Elements (RBEs) are technologies for the exploitation of the environmental and renewable energy sources. Their aim is to achieve optimal environmental performances with minimum fossil fuel consumption. Their implementation in buildings is considered a crucial step towards the nearly Zero Energy/Emission Building target.

Among the RBE concepts investigated by the IEA-ECBCS Annex 44, Advanced Integrated Façades (AIFs) are probably one of the most promising technologies. The growing interest towards these systems is demonstrated by the fact that some of the most important manufacturers in the field of façade technology have started to develop integrated modular façade solutions that show an active and dynamic behaviour, that incorporates various components for environmental control and solar energy exploitation, and that can be connected with the building services network. In the framework of a decade-long research activity on AIFs, a new Multifunctional Façade Module (MFM) has been conceived and a prototype realized to test the performance of this type of technology. During the design phase of such a multifunctional façade module (MFM) called ACTRESS (ACTive, RESponsive and Solar), different numerical analyses were performed to simulate the behaviour of the system and to find the optimal combinations/specifications for the module subsystems.

The paper briefly illustrates the ACTRESS MFM concept and its functional strategies, which have been designed to suit various boundary conditions and to allow different actions to be performed according to the different season. The paper focuses on some numerical analyses that were conducted to select the components' features and to size a particular subsystem of the façade module (i.e. a Phase Change Material layer coupled with an electric heated foil and PV panels). The numerical simulations allowed the optimal amount of PCM and the PCM nominal melting temperature to be determined. The annual total energy performance of the façade module was also assessed and compared against the one of a reference façade. The proposed MFM allows the total energy consumption to be reduced by more than 50%.

INTRODUCTION

The key role that the building envelope plays in managing the energy fluxes between the indoor environment and the exterior is both a crucial issue and a great challenge. Within the IEA Annex 44 research activity [1], devoted to study the most promising Responsive Building Elements (RBEs), dynamic building envelope systems (also known under the name AIFs) have been widely investigated and the huge potentiality of such a kind of technology has been outlined. Although it is not correct to state that the dynamic building envelope alone should

represent the only solution to reach the Zero Emission/Energy Building target, it is expected that advanced integrated façade systems should provide a substantial contribution, if coherently integrated with the other building components and services, to a drastic increase in the energy efficiency of the building.

A Multifunctional Façade Module (MFM) is a concrete solution to realize an almost "self-sufficient" building skin that presents a dynamic behaviour, incorporates different technologies (e.g. ventilation systems, decentralized heating/cooling units, heat exchangers, energy supply/conversion devices, energy storage, lighting equipments, shading devices, ventilated cavities, *et cetera*) and interacts with the other building services, with the ultimate goal of reducing the energy consumption and maximizing the indoor comfort conditions. Even if MFMs are at the present not a reference solution in the market, but the leading-edge products of the industrial and academic research, it is relevant to notice that some of the most important players in the field of the façade technology (e.g. Schüco, Wicona) have put remarkable efforts on developing and manufacturing integrated modular façade systems.

The ACTRESS façade module

The concept of the ACTive, RESponsive and Solar (ACTRESS) façade module has been developed to overcome some of the limitations given by present-day AIFs. For the sake of brevity, only a short description of the façade module technology and functional strategies is herewith given, but a more detailed explanation and artworks can be found in [2, 3, 4].

The façade module (frontal area: 1.5m (w) x 3.5m (h)) is divided into two sub-modules of equal size: a transparent one and an opaque one. The transparent sub-module is made of two different glazing systems (triple-pane glazing with low-e coating and argon gas), incorporating in one of the two cavities either a granular aerogel layer or a high-reflective and low-e coated venetian blind. The other half of the façade module is an Opaque Ventilated Façade (OPV), which outdoor surface is made of aSi PV panels. A 120mm cavity (fan-assisted ventilated) separates the outer PV layer from the inner sandwich wall panel. The structure of this component is (moving from the outer to the inner layer): a gypsum-board layer, a Vacuum Insulation Panel (VIP) layer, a gypsum-board layer, a Phase Change Material (PCM) layer that incorporates an electric heating foil (to activate the PCM on demand).

As far as the functional strategies are concerned, the module has been design to enable different level of integration with the centralized HVAC systems. The OVF shall be operated in exhaust air façade mode, supply air façade mode or outdoor air curtain mode, according to the season and to the desired level of integration with the building services and ventilation strategies. Electrical power generated by the PV layer can be used to power the hybrid (fan-assisted) ventilation of the OVF, to move the shading devices and to activate (to heat up) the PCM layer for Latent Heat Thermal Energy Storage (LHTES) purpose. A detailed description of the functional strategies and ventilation issues can be found in [3].

Aims of the paper

During the design phase of the ACTRESS MFM, numerical models have been developed and simulations performed, making use of various software products. The aims of the activity was to size the façade module's components, to foresee the overall behaviour of the MFM, and lastly to test the limitations and potentials of using commercial codes to model complex building technologies such as AIFs. The overall energy performance of the façade module is presented. For the lack of space, the paper then focuses on the sizing and on the assessment of only one component: i.e. the PCM layer combined with the PV layer. Additional and more detailed information about the entire modelling activity can be found in [3, 4].

METHODS

The commercial software IES VE has been used to assess the total energy performance of the ACTRESS façade module. Given its different sub-modules, IES VE can be used to evaluate not only the behaviour of a single component, but above all to assess the whole building energy performance. As far as the ACTRESS energy modelling activity is concerned, the main restrains of the software are related to the OVF sub-system, in particular to the hybrid ventilated cavity and to the PCM layer facing the indoor environment.

Modelling the total Energy Performance (EP)

The overall building energy demand of an office equipped with the ACTRESS façade module was estimated and compared against the one of a reference office. The two identical 30 m^2 office rooms (6m x 5m x 3,5m) were located in Turin (Lat.45°N, Long. 7.65°E), Italy. The ACTRESS façade (4 modules are used to cover the entire office room elevation) faces south and the other walls are adiabatic. The façade of the reference office room was made of a massive wall and presented the same glazed area as the ACTRESS one. The main physical properties of the reference envelope were such to comply with present day building regulations (U_{op} = 0,35 W/m^2K, U_w = 1,97 W/m^2K, g = 0,64). The internal heating loads were 20 W/m^2 (people and appliances) and 2 Wm^{-2} in non occupation period. The occupation period was 8:30-6:30 pm, Mon. to Fri. The indoor temperature set-point was 21 °C during winter and 26 °C in summer, with two ACH from the HVAC system as auxiliary ventilation.

Modelling the PCM performance assessment

Few commercially available software products permit, as part of the standard routine, to model directly a PCM. Additional modelling tricks are then often required to assess the behaviour of a PCM layer. The key feature of PCM is to absorb energy as latent heat rather than sensible heat over a small range of temperatures; hence, a PCM exhibits no sensible temperature rise within the melting range. In many commercial software products, it is not possible to set the specific heat capacity of a material as a function of the temperature, and the latent heat storage of the PCM can't be modelled unless simplifying assumptions are done.

The "conditioned cavity method" [5] has been adopted to model the PCM layer in IES VE. In this method, a virtual cavity, that simulates the PCM layer, is maintained at a set-point temperature (which corresponds to the nominal melting temperature of the chosen PCM) by means of an ideal HVAC system[1]. When this method is applied, an infinite latent heat storage capacity is thus assumed for the PCM layer; this implies a further verification to be performed to properly adopt the method: i.e. the sum on a daily base of the cavity's heating and cooling loads needs to be equal or lower than the actual latent heat storage capacity of the PCM. This verification can be also used as a design tool to estimate the optimal quantity of PCM to be used. The proper approach that provides the foundation of the conditioned cavity method implies the modelling of an infinitesimal volume cavity which wall surfaces have an (almost) null thermal resistance (at least lower than 10^{-4} m^2K/W) and no heat capacity (the sensible heat capacity is neglected and the entire latent heat capacity is accounted for in the cavity loads); the cavity itself exhibits a thermal resistance equal to the one of the PCM layer.

Within the ACTRESS module, the PCM layer is coupled with an Electric Heating Foil (EHF) in order to activate "on-demand" the PCM (i.e. to store energy within the PCM layer). The

[1] The virtual HVAC heating and cooling loads to maintain the virtual cavity at the desired set-point are not accounted for in the overall building performance (provided that their daily sum does not exceed the latent heat storage capacity of the PCM).

EHF can be powered either from the grid or (primarily) from the PV panels placed on the outer surface of the OPV. A complete evaluation of the system PV-EHF-PCM is therefore needed to assess the efficiency of the system. Tests were carried out in order to evaluate the optimal design of the solar power system (PV-EHF), to characterize the system in terms of circuit working point (according to the PV MPP with high and low solar irradiance), and to provide an uniform power distribution within the PCM layer. The evaluation of the PV-EHF-PCM system has been done by accounting the amount of the energy produced by the PV that covers the conditioned cavity heating loads during the occupation period in winter.

RESULTS AND DISCUSSION

Total Energy Performance (EP)

The EP indexes of the office equipped with the ACTRESS façade and the reference one are compared in Figure 1. In the Outdoor Air Curtain mode, the overall reduction of the primary energy demand EE_{tot} is 52%, i.e. from 19,1 kWh/m^{3}y to 9.1 kWh/m^{3}y. A considerable decrease in heating loads EE_h is also observed; this can be associated to the use of PV energy to activate the PCM in the OVF (almost 53%). Furthermore, it is remarkable that the electric consumption for lighting and appliances, on an annual basis, can be almost covered (ca. 95%) by the PV power production (the energy released into the PCM layer and the power to feed the fans are already included in this calculation). The possibility to exploit the air that is preheated by the OVF cavity as a supply air for the HVAC system (during winter and mid season) was assessed by means of a dedicated simulation. With this configuration, a further reduction in the EE_{tot} can be achieved (from 9.1 kWh/m^{3}y to 8.5 kWh/m^{3}y), resulting in a total energy conservation of about 55% in comparison to the reference building envelope.

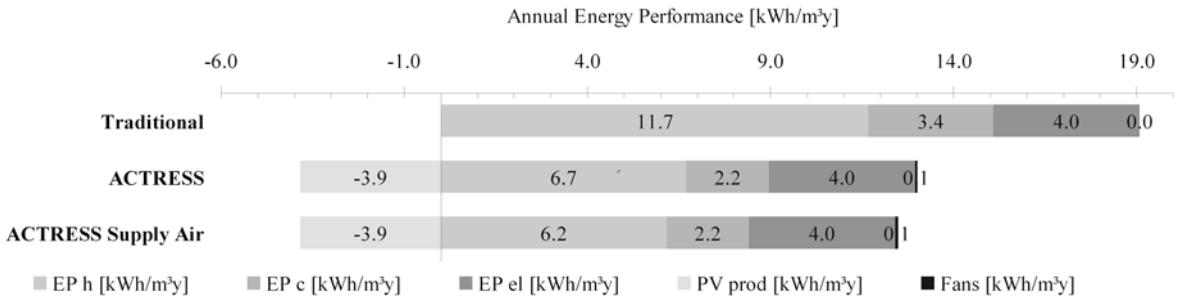

Figure 1: Annual total Energy Performance of the office equipped with the ACTRESS façade module (Outdoor Air Curtain or Supply Air mode) and the reference office equipped with a conventional façade system (Traditional).

PCM performance and component design

In order to select the optimal quantity and type (nominal melting temperature, T_{PCM}) of the PCM to be used in the ACTRESS façade module, several simulations where run to perform a parametric analysis. In particular, the following nominal melting temperatures were tested: T_{PCM} = 23 °C, 25 °C, 26 °C and 27 °C; the influence of the different amount of PCM (D_{PCM}) was investigated too: i.e. D_{PCM} from 0.5 kg/m^2 to 4 kg/m^2 (in steps of 0.5 kg/m^2), in combination with three possible PV panel surfaces (i.e. S_{PV} = 1.67 m^2, 2.50 m^2, 3.34 m^2). The optimal combination of the three parameters (T_{PCM}, D_{PCM} and S_{PV}) is affected, among the others, by three main variables (i.e. daily latent heat storage capacity, daily solar energy, heating degree-days) which correlations may not be linear.

The results of the simulations performed to select the proper amount and the nominal melting temperature of the optimal PCM (and to test the model reliability) are shown in Figure 2 (cooling season, "passive" use of PCM). The PCM with T_{PCM} = 25 °C is able to completely absorb (nearly 100% of the time) the virtual heating/cooling load of the virtual cavity, if at least 2-2.5 kg/m^2 are used. This combination represents the optimal configuration of the system, since a PCM with a higher T_{PCM} has a worse behaviour than the optimal solution (it is not fully activated for a longer period); a PCM with a lower T_{PCM} is always activated and the sum of the heating/cooling load exceeds the latent heat storage capacity of such a PCM. In Figure 3, a detailed analysis on the behaviour of the optimal solution is illustrated. It can be noticed that, during the occupational period, the PCM is maintained within the melting range for about 91%, 95% and 97% of the time in summer, midseason and winter, respectively.

The coupling between the PCM layer and the PV power production has been investigated during the winter season only, since the aim of this system is to store a certain amount of energy available during the daytime for heating purpose (heating season, "active" use of PCM). Considering the optimal design solution (PCM with T_m = 25 °C, D_{PCM} = 2 kg/m^2), on seasonal basis, it can be noticed that the PCM layer is able to store only 76% of the energy produced by a 1.67 m^2 PV surface (Figure 4). If the PV surface were increased (i.e. S_{PV} = 2.50 m^2, or 3.34 m^2), a lower percentage of the PV-generated energy could be stored within the PCM layer (nearly 60% and 20%, respectively). If D_{PCM} = 4 kg/m^2 were used instead, the entire amount of energy generated by the 1.67 m^2 PV surface could be stored. On seasonal basis, with D_{PCM} = 2 kg/m^2 and S_{PV} = 1.67m^2, the operation time of the heating system can be reduced by an average of about 2.5 h (Figure 5).

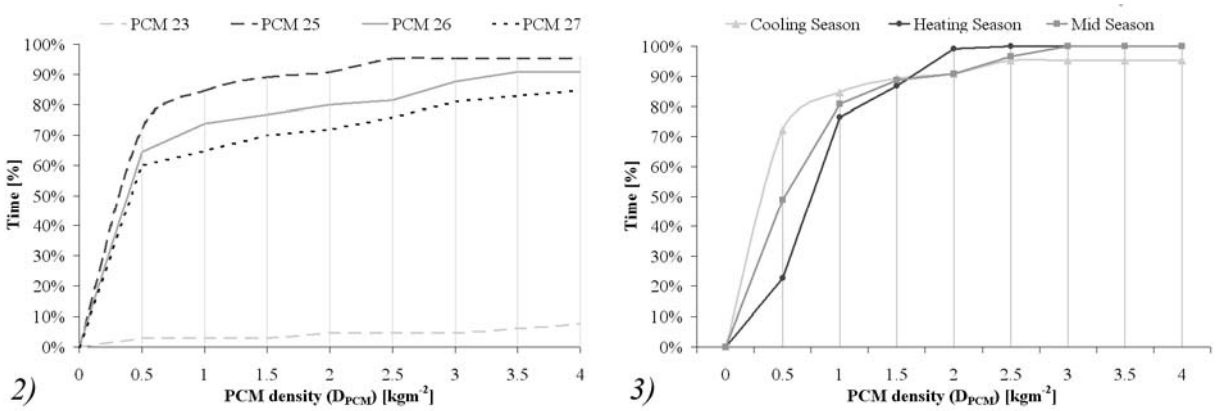

Figure 2. Time percentage in which the PCM is within the melting range (cooling season).
Figure 3. Time percentage in which the T_{PCM} = 25 °C PCM is within the melting range.

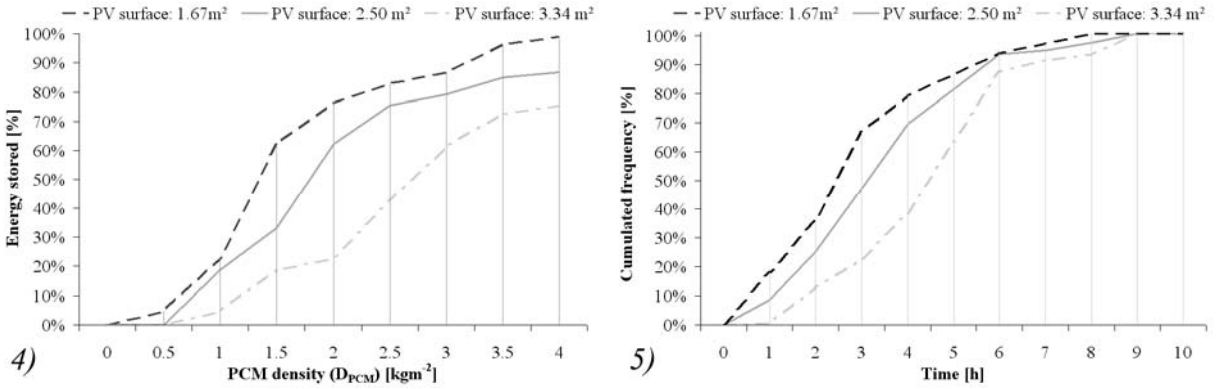

Figure 4. Percentage of the energy produced by the PV panel that is stored in the PCM layer.
Figure 5. Cumulated frequency of the winter night hours during which the PCM is within the melting range.

For the record, the actual specifications adopted in the ACTRESS façade module prototype (which is currently tested in a Test Cell apparatus) are: two layers of PCMs, where the outer one has T_{PCM} = 27 °C and the inner one has T_{PCM} = 23 °C; D_{PCM} = 1 kg/m^2 each layer, for a total D_{PCM} = 2 kg/m^2; S_{PV} = 1.67 m^2. The EHF is placed between the two PCM layers. The double layer with different T_{PCM} is aimed to further enhance the performance of the PCM system (due to considerations on the use of multiple PMCs in LHTES system [6]).

CONCLUSION

Together with the RBE concepts, Advanced Integrated Façades are expected to contribute significantly to the reduction of the energy demand in buildings. A new façade module called ACTRESS has been conceived and a prototype realized for experimental measurements. During the design phase of the façade module, numerical simulations were performed to size the module's subsystems. A numerical analysis performed with IES VE allowed the optimal configuration of a PCM layer, coupled with a PV layer, to be determined. The PCM layer is designed to work "passively" in summer, and "actively" in winter, when energy is stored during the daytime by means of an EHF that is directly powered by the PV system. The annual total energy performance was assessed by means of the numerical analysis too. It was estimated that, in an office building, the façade module is able to reduce the energy consumption by more than 50% with respect to a traditional building envelope configuration. Comparison between simulations and experimental data will be performed in the future to assess the reliability of the software product in simulating advanced building components.

ACKNOWLEDGEMENTS

The ACTRESS façade concept has been conceived in the framework of the PRIN 2007. The development of some sub-components (advanced glazings and PCM panels) has been and still is carried out in the framework of the Polight 2010 projects "SMARTGLASS" and SI^2. Authors are grateful to Skyline Srl, Pellini S.p.A. and DuPont for supporting the research in the supply of components and construction of the façade module prototype.

REFERENCES

1. IEA – ECBCS Annex 44, Integrating Environmentally Responsive Elements in Buildings, Design Guide – Vol II, 2010.
2. Goia F., Perino M., Serra V., Zanghirella F. Towards an Active, Responsive, and Solar Building Envelope. Journal of Green Building, College Publication, 5 (4), 2010, pp. 121-136, DOI: 10.3992/jgb.5.4.121
3. Favoino F, Goia F., Perino M., Serra V. The ACTRESS Concept: a new façade module for low energy buildings. Proceedings of RoomVent Conference 2011, Trondheim, June 2011 (in press)
4. Favoino F. Zero Energy Building: Evaluation of innovative ACTRESS façade through dynamic energy simulation. MSc thesis in Building Engineering, Polytechnic of Turin, 2010.
5. Kendrick C., and Walliman N. Removing unwanted heat in lightweight buildings using phase change materials in building components: simulation modelling for PCM plasterboard. Architectural Science Review, 50 (3), 2007, pp. 265-273.
6. Kousksou T., Strub F., Castaing Lasvignottes J., Jamil A., Bedecarrats J.P. Second law analysis of latent thermal storage for solar system. Solar Energy Materials and Solar Cells 91(14), 2007, pp. 1275-1281, DOI: 10.1016/j.solmat.2007.04.029

NUMERICAL ASSESSMENT OF VARIOUS PCM GLAZING SYSTEM CONFIGURATIONS

F. Goia[1,2]; M. Perino[1]; M. Haase[2].

1: TEBE Research Group, Department of Energetics, Politecnico di Torino, C.so Duca degli Abruzzi 24, 10129 Torino (Italy).

2: Research Centre on Zero Emission Buildings, Faculty of Architecture and Fine Art, Norwegian University of Science and Technology, Alfred Getz vei 3, 7491 Trondheim (Norway).

ABSTRACT

Glazing systems are probably among the most interesting and investigated element of the building envelope. Together with several positive features, they still show a poor thermal inertia, which reduces the efficiency of these systems in controlling the energy flows between outdoor and indoor. As far as the heat capacity of the glazing systems is concerned, the adoption of Phase Change Materials (PCM) has been proposed to increase the ability of the glazing to store (and later, to release) energy. One of the main advantages of these materials is their partial transparency to visible radiation that makes them particularly suitable for the use in transparent/translucent building envelope components.

The aim of the PCM glazing concept is to let the visible part of solar radiation enter the indoor environment while absorbing the infrared radiation and storing it within the PCM layer as latent heat. PCM glazing systems can therefore exploit solar energy in a more efficient way than the conventional glazing systems and at the same time provide daylight for the interior. The first concepts and assessments of PCM glazing systems were developed for cold climates, but this technology presents interesting features for warmer climates too.

The purpose of the whole research activity, which is partially presented in this paper, is to analyze different configurations of PCM glazing systems in various climates by means of experimental campaigns and numerical simulations, as well as to find optimal solutions for each climate and building type. A dedicated physical-mathematical model has been developed to simulate the behaviour of these glazing systems and the first version of the physical-mathematical model has been validated with data derived from a previous experimental activity. The work presented in this paper focuses on a numerical analysis of various triple glazing configurations, where one of the two cavities is filled with a PCM. Different layout and PCM melting temperatures were investigated, and the simulated glazing systems show promising features both in terms of thermal comfort and energy performance.

INTRODUCTION

During the last decades, highly glazed façades have been widely adopted in commercial and office building envelopes. Although considerable improvements have occurred in the field of glazing technology, especially as far as thermal resistance and solar control are concerned, the use of large glazed surface often poses significant problems of overheating and thermal discomfort. The positive features of a conventional transparent building envelope (i.e. visual contact with the outdoor, exploitation of daylight and passive solar heating) are counterbalanced by very little thermal inertia and its capability of acting as an energy buffer is

extremely low. A high coupling between indoor and outdoor environment may thus occurs in buildings characterized by large transparent, which results in high energy consumption.

The adoption of Phase Change Materials (PCM) in combination with transparent elements has first appeared in the 1990s and some works concerning transparent building envelope components filled with PCM can be found in literature [1-4]. The PCM layer is used to absorb and store (thanks to the latent heat) the largest part of the solar infrared (IR) radiation, and to let part of the solar visible (VIS) radiation enter the indoor environment in order to provide daylighting. The aim of this technology is therefore to minimize the unwanted heat loss and solar gain due to the buffer effect provided by the PCM layer, but still allowing the utilization of natural light. While the first concepts of PCM glazing systems have been developed for continental and cold climates, a more recent experimental activity [5-6] has proved the potentials of these systems in warm climates too.

The optimal configuration of a PCM glazing system is a complex issue, since different variables (e.g. the multi-layer structure, the PCM thickness, the PCM temperature range, etc) are involved and non-linear phenomena often occur. The aim of the work presented here is to deepen the knowledge with respect to two of the main variables that influence the problem: the location of the PCM layer and the melting temperature of the PCM. The results reported in this paper concern the numerical analysis of south facing PCM glazing systems with a southern exposure in a humid subtropical climate (Cfa - Köppen climate classification).

METHOD

Physical-mathematical model

For the sake of brevity, the detailed description of the physical-mathematical model is not given, but a short overview of the model structure and of some relevant assumptions is presented. The comparison between the simulations of a simple PCM glazing system (a double glazed unit with the cavity filled with PCM) and experimental data [5-6] of the same PCM glazing configuration has been carried out to validate the model under dynamic conditions and in different seasons.

The model is a 1D nodal model (heat and light transmission along x-y axes is not considered). Three nodes are associated to each glass pane, while the PCM layer is represented by five nodes. Heat and light transport equations are implemented for the glass panes and the PCM layer. Energy conservation equations are written for each node and numerically solved to obtain the heat transfer process. The heat capacity of both the glass panes and the PCM is taken into account, so that the model can simulate the behaviour of the PCM glazing system under dynamic conditions. The following hypotheses have been adopted for the model development: each node represents a layers that is supposed to be homogeneous; the glass surface is considered a grey body (for IR heat exchange with the surrounding environments); the surfaces of the outdoor and indoor environment are considered as black and/or gray body; the convection within the PCM layer (when in liquid state) is neglected; the radiative exchange between the two glass surfaces facing the cavity filled with PCM is also neglected; the optical properties of the glass panes are only function of the incidence angle of solar radiation; the thermal properties of the glass are temperature independent; the optical and thermal properties of the PCM depend on the temperature (state of the PCM) [6].

Numerical simulations and boundary conditions

The behaviours of the various PCM glazing configurations have been simulated in two seasons (summer and winter). The indoor air temperature is supposed to be maintained at the desired set point (26°C in summer, 20°C in winter). The simulated environment has five

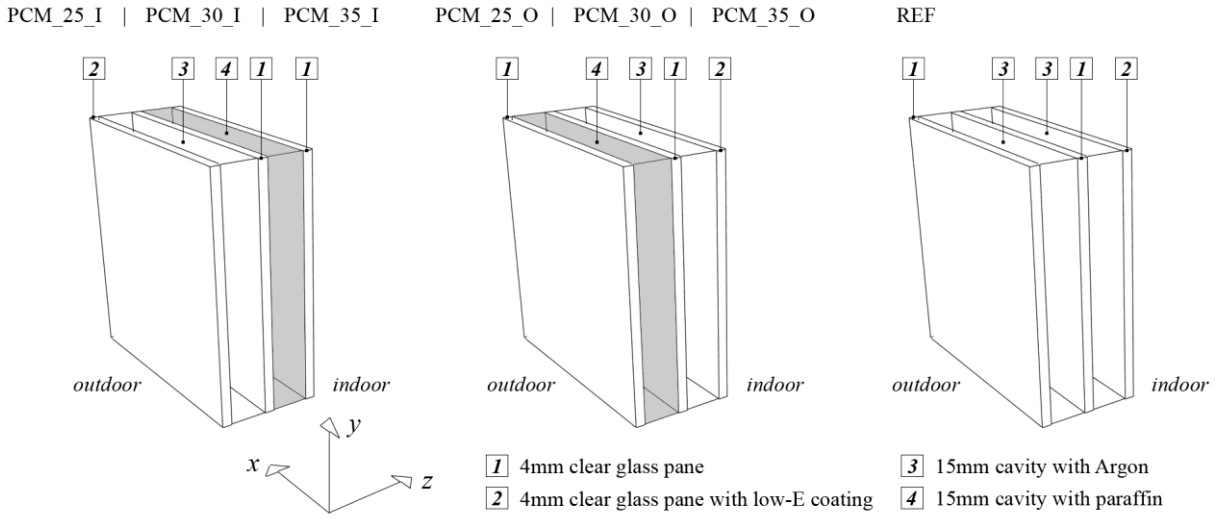

Figure 1: Scheme of the simulated triple-pane PCM glazing systems and reference glazing.

adiabatic surfaces (three walls, the floor and the ceiling) that are at the same temperature of the indoor air. The façade (equipped with a different PCM glazing system for each simulation) is the only non adiabatic surface and faces south. Outdoor air temperature profile and sun irradiance profile (on the vertical plan) used in the simulation derive from actual measurements [6] and are not reported here for the sake of brevity.

PCM glazing system configurations

As far as the multi-layer structure is concerned, two different configurations have been tested: a triple glazing with the outer cavity filled with PCM (codes: PCM_xx_O) and a triple glazing with the inner cavity filled with PCM (codes: PCM_xx_I). The cavity that does not contain the PCM layer is filled with Argon instead. All the cavities (filled with PCM or Argon) are 15mm thick, the glass panes are all made of a 4mm thick clear glass and a low-E coating (ε = 0.1) is always applied on one of the surface that faces the Argon-filled gap (see Figure 2). Three different PCM have been considered: a paraffin whose nominal melting temperature is 35°C (codes: PCM_35_y), a 30°C paraffin (codes: PCM_30_y) and a 25°C paraffin (codes: PCM_25_y). The three paraffin materials share the same optical and thermal properties, with the exception of the nominal melting temperature, that obviously changes from paraffin to paraffin. A 10°C melting range is maintained constant for the three paraffin waxes. The latent heat associated to the phase change is also a constant value for the three materials (i.e. 140 kJ/kg). Combining the two different multi-layer structures and the three paraffin materials, a total of 6 different PCM glazing system configurations were simulated[1] (Figure 1). A triple-pane glazing (4/15/4/15/4) with the two cavities filled with Argon and a low-E coated surface (ε = 0.1) is also simulated for reference purpose (code: REF).

Data analysis procedure

The behaviour of the glazing system with respect to both energy and thermal comfort performance has been analyzed considering two "typical" days each season: a sunny day and a cloudy day (solar irradiance is by far the main driving force that influences the behaviour of these systems [5]). The performance with respect to thermal comfort issues has been assessed by comparing the hourly profiles of the indoor surface temperature of the different glazing

[1] A PCM glazing system that hosts the 35°C paraffin layer on the outer cavity is named PCM_35_O, while the ones that contains the 25°C paraffin layer on the inner cavity is named PCM_25_I, and so on.

systems[2]. The energy efficiency evaluation has been carried out considering the energy that, on a daily base, enters (E^+) (1) and leaves (E^-) (2) the indoor environment through the glazing. In particular, it holds:

$$E^+ = \int_{24h} \dot{q}^+_{surf}(\tau) + I(\tau) d\tau \qquad (1)$$

$$E^- = \int_{24h} \dot{q}^-_{surf}(\tau) d\tau \qquad (2)$$

where $I(\tau)$ is the transmitted solar irradiance, $\dot{q}^+_{surf}(\tau)$ and $\dot{q}^-_{surf}(\tau)$ are the positive (entering the indoor) and negative (leaving the indoor) *surface* heat fluxes[3], respectively.

RESULTS AND DISCUSSION

Thermal comfort performance

Hourly profiles of the surface temperatures of the 7 glazing systems are illustrated in Figure 2. It can be observed that the position of the PCM layer (inside the inner or the outer cavity) affects to a great extend the behaviour of the system.

The PCM_xx_I configurations show always during the daytime a higher surface temperature than the reference. This behaviour may have a positive influence on the indoor thermal environment during the winter season (increasing the global comfort condition and, above all, avoiding local discomfort due to cold vertical surfaces, especially from 17:00 to 24:00). On the other hand, the indoor surface temperature drops approx. 5°C lower than the reference during the winter nights, because of the position of the low-E coating, with a negative impact on the thermal comfort. The various PCMs show different dynamics (the lower the melting temperature, the faster the melting process and the slower the re-solidification process), but the behaviour is very similar. In summer, the temperature profile is always higher than the reference one, for all cases regardless the PCM used, with unfavourable consequences on the thermal comfort. Even if the PCM_xx_I configurations may present some advantages in winter daytime, they pose considerable drawbacks in summer and during cold winter nights.

The PCM_xx_O configurations show a better performance, thanks to their ability to reduce the fluctuations in the surface temperature profile and to provide a more stable environment. In particular, during the summer days, these configurations are able to smoothen (especially in

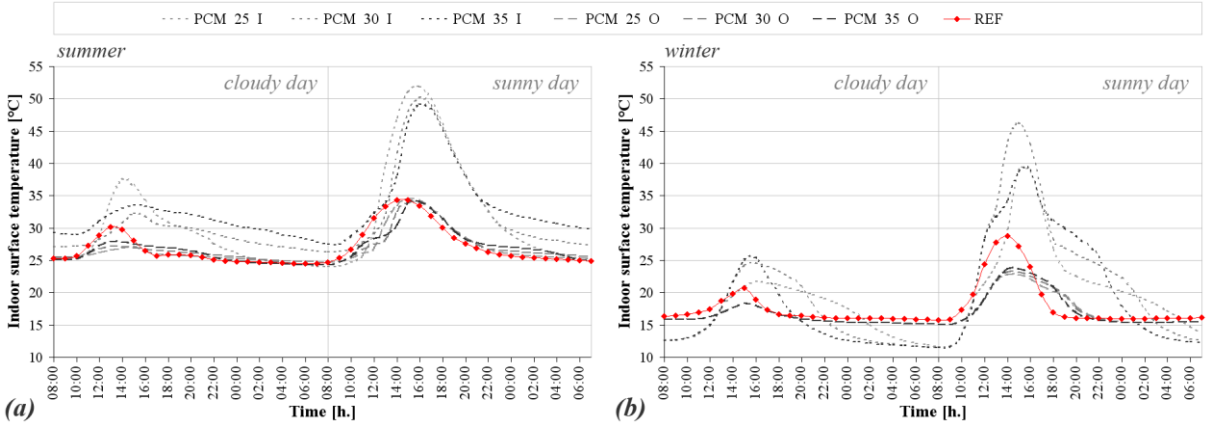

Figure 2: Hourly profile of the indoor surface temperature of the glazing systems.

[2] A more comprehensive analysis, which would have involved the evaluation of more complex parameters, such as PMV and PPD (see [6]), is on the way and cannot be here reported for the sake of brevity.

[3] The term *surface* designates the heat flux exchanged between the indoor surface of the glazing and the indoor environment. It includes the long-wave radiative heat flux and the convective heat flux.

cloudy days) and delay (especially in sunny days) the peak of the surface temperature profile and to maintain a more comfortable indoor surface temperature. In winter time, problems may arise during cloudy days, when the PCM layer is scarcely activated and it acts mainly as a shading device; however, the performance during sunny days is still appreciable. If compared to the reference, a slightly lower surface temperature is observed during the winter night time; it is probably due to the thermal conductivity of the PCM ($\lambda = 0.2$ $Wm^{-1}K^{-1}$) that determines a lower thermal resistance than the one that occurs within the cavity filled with Argon.

Energy efficiency performance

The energies that flow through the PCM_xx_I and PCM_xx_O glazing systems are reported in Table 1 and Table 2, respectively. As for the thermal comfort performance, the layer structure has a wide impact on the behaviour of the glazing system, but the adopted PCM melting temperature affects the performance of the system too.

As far as the PCM_xx_I configurations are concerned, the following observations can be made. In summer, during the cloudy day, the E^+ is reduced by more than 50% with the 30°C paraffin and by about one third if the 35°C paraffin is used instead. In sunny days, both the 30°C and 35°C paraffin waxes reduce by about 15% the E^+. The E^- is always zero, because of the discharge phase of the PCM that keeps on releasing heat towards the indoor environment even during the nigh (cf. Fig. 2a). The PCM_25_I system shows a behaviour that is similar to the reference glazing one, since the indoor/outdoor air temperatures are always within the melting range of the PCM or higher, and the PCM is hence activated most of the time.

In sunny winter days, it is remarkable how the PCM_xx_I configurations are able to reduce the energy losses E^- (PCM_25_I: more than -70%; PCM_30_I: more than -60%; PCM_35_I: about -50%), by converting and storing part of the income solar radiation during the daytime. In fact, the E^+ is also reduced of more than 40% (PCM_25_I and PCM_35_I). The same behaviour can be noticed for the cloudy days too, but with lower values. The systems show a good performance if it is desired to lower the solar gain during the daytime and to reduce the energy losses during the nigh.

The PCM_xx_O configurations show a notable performance in summer when, in sunny days, they are able to reduce of about one third (PCM_30_O and PCM_35_O) and of about one fourth (PCM_25_O) the E^+. In cloudy days, the reduction is in the range of -70÷75%.

		REF		**PCM_25_I**		**PCM_30_I**		**PCM_35_I**	
		E^+ [Wh m^{-2}]	E^- [Wh m^{-2}]	E^+ [Wh m^{-2}]	E^- [Wh m^{-2}]	E^+ [Wh m^{-2}]	E^- [Wh m^{-2}]	E^+ [Wh m^{-2}]	E^- [Wh m^{-2}]
Summer	*cloudy*	782	-85	735	-21	357	0	521	0
	sunny	2043	-38	2049	-5	1761	0	1793	0
Winter	*cloudy*	411	-446	93	-240	139	-321	122	-379
	sunny	2207	-432	1258	-115	1810	-163	1231	-210

Table 1: Transmitted energy through the PCM glazing systems (PCM_xx_I) and reference.

		REF		**PCM_25_O**		**PCM_30_O**		**PCM_35_O**	
		E^+ [Wh m^{-2}]	E^- [Wh m^{-2}]	E^+ [Wh m^{-2}]	E^- [Wh m^{-2}]	E^+ [Wh m^{-2}]	E^- [Wh m^{-2}]	E^+ [Wh m^{-2}]	E^- [Wh m^{-2}]
Summer	*cloudy*	782	-85	196	-65	205	-66	239	-97
	sunny	2043	-38	1553	-28	1376	-13	1356	-24
Winter	*cloudy*	411	-446	30	-586	30	-584	30	-584
	sunny	2207	-432	452	-440	469	-445	485	-463

Table 2: Transmitted energy through the PCM glazing systems (PCM_xx_O) and reference.

The E^- is generally reduced too, both on sunny and cloudy day (with the exception of PCM_35_O under cloudy weather conditions), due to the discharge phase of the paraffin. However, this issue seems not to be of particular relevance.

A more complex behaviour occurs during winter, when the PCM_xx_O systems are able to lower the solar gain during the daytime (as happened with the PCM_xx_I configurations), but do not reduce the energy loss E^- during the night This is due to the position of the PCM layer (that faces the outdoor), which increases the dissipation towards the outdoor environment of the heat stored during the daytime within the PCM layer. In cloudy days, because of the lower thermal resistance of the PCM glazing and the poor activation of the PCM layer, the heat loss through the PCM_xx_O systems is higher than through the reference (about +30%). In sunny days, the E^- is slightly increased in the case of the PCM glazing, but E^+ and E^- are of the same order, so that these configurations can be virtually considered a "nearly adiabatic" surface (due to the facts that the magnitude of the positive and negative energy flows is low and that the positive energy flow is equivalent to the negative one).

CONCLUSION

Different PCM glazing configurations have been tested by means of a numerical analysis to assess their behaviours with respect to the energy efficiency and thermal performance in a humid subtropical climate. These glazing systems (especially the ones with the PCM layer that faces the outdoor) can be beneficial in terms of thermal behaviour. A more complex evaluation is needed when the energy performance is addressed instead. All the systems are able to reduce the solar gain during the daytime, acting like solar shading device, and to store a certain amount of heat within the paraffin layer. The release of this energy is only driven by the boundary conditions, so a limited active control over this process is possible, and sometimes the behaviour of the system is less efficient than the reference one.

ACKNOWLEDGEMENTS

The research is part of the project "SMARTglass", co-financed by Regione Piemonte, Skyline – Strutture per l'Architettura srl and MBT srl, in the framework of Polight 2010 activity.

REFERENCES

1. Manz H, Egolf P.W, Suter P, Goetzberger A. TIM-PCM external wall system for solar space heating and daylighting. Solar Energy 1997;61:369–379
2. Ismail K.A.R, Henríquez J.R. Parametric study on composite and PCM glass system. Energy Conversion and Management 2002; 43:973–993.
3. Ismail K.A.R, Salinas C.T, Henriquez J.R. Comparison between PCM filled glass windows and absorbing gas filled windows. Energy and Buildings 2008; 40:710–719 (doi:10.1016/j.enbuild.2007.05.005).
4. Weinläder H, Beck A, Fricke J. PCM-facade-panel for daylighting and room heating. Solar Energy 2005; 78:177–186 (doi:10.1016/j.solener.2004.04.013).
5. Goia F, Perino M, Serra V, Zanghirella F. Experimental assessment of the thermal behaviour of a PCM grazing. In: Proceedings of IAQVEC 2010 – The 7th International Conference on Indoor Air Quality, Ventilation and Energy Conservation in Buildings (Syracuse, New York, USA) 15-18, August 2010, 2010, Paper Ref. 21-34, 1-8.
6. Goia F, Perino M, Serra V, Zanghirella F. Experimental analysis of a prototype PCM glazing: measurement system and thermal comfort performance, Building and Environment, Submitted for publication.

ZERO EMISSION BUILDING ENVELOPES - COMPARISON OF FLOOR CONSTRUCTIONS WITH PCM, WOOD AND CONCRETE IN A LIFE CYCLE PERSPECTIVE

Thomas Haavi[1,2,*]; Arild Gustavsen[1]

1: Department of Architectural Design, History and Technology, Norwegian University of Science and Technology (NTNU), NO 7491 Trondheim, Norway.

2: Department of Materials and Structures, SINTEF Building and Infrastructure, NO 7465 Trondheim, Norway.

**: Corresponding author, Phone +47 98230442, Thomas.Haavi@sintef.no.*

ABSTRACT

This paper presents a case study of a single-family house, where the effect of using thermal energy storage integrated in the floor is evaluated regarding GHG-emissions during the life cycle. The house has a lightweight wood frame construction, is well insulated, and fulfils the Norwegian energy regulations from 2010. Different floor configurations have been studied, both regarding energy demand and emissions. Floors with PCM panels have been compared with a reference case without thermal energy storage integrated in the floor, and have also been compared with concrete and wood as replacement for the PCM panels. The effect of changing the thickness of the PCM, concrete and wood has also been investigated (5 mm, 25 mm and 50 mm), as well as the effect of changing the emission factor of the energy supply to the building. The simulations have been carried out with three different climates: Oslo in Norway, Prague in the Czech Republic and Rome in Italy. The conclusions are:

- PCM gives the highest energy savings, compared with concrete and wood, but have also significantly higher GHG-emissions related to production of the materials. Due to this, the total GHG-emissions is very dependant on the emission factor for the energy supply to the building.
- When the emission factor of the energy supply is 0.050 kg CO_2 eq/kWh, the PCM causes increased GHG-emissions at 25 mm and 50 mm thickness. The wood and the concrete give only small reductions in emissions at all thicknesses.
- When the energy supply to the building is 0.500 kg CO_2 eq/kWh, the PCM causes the highest reduction in GHG-emissions at 5 mm and 25 mm thickness, and concrete causes the highest reduction at 50 mm thickness.
- The reduction in energy demand and emissions is slightly higher in Prague than in Oslo, but significantly higher in the hot climate in Rome.

INTRODUCTION

It is well known that a large share of the global energy consumption and the greenhouse gas (GHG) emissions is related to the building sector. Due to this, there has been a lot of focus on low energy buildings and passive houses, i.e. buildings with low energy consumption during the operational phase of the life cycle. Lately, the new focus has become Zero Emission Buildings (ZEB), i.e. buildings with "zero emissions" during the life cycle.

Energy efficient buildings often have a cooling demand, especially during the summer season. Phase change materials (PCMs) have introduced a new way of reducing the cooling and heating demand of buildings, due to the effective thermal energy storage and release capabilities of PCMs [1,2,8]. One of the products that have found their way to the market is DuPont™ Energain®, which is PCM panels with a mixture of ethylene based polymer and paraffin wax laminated on both sides with an aluminium sheet [3].

This paper presents a case study, where the effect of using thermal energy storage integrated in the floor is evaluated regarding GHG-emissions during the life cycle. A well insulated building with different floor configurations have been studied, both regarding energy demand and emissions. Floors with PCM panels have been compared with a reference case without thermal energy storage integrated in the floor, and have also been compared with concrete and wood as replacement for the PCM panels. The effect of changing the thickness of the PCM, concrete and wood has also been investigated, as well as the effect of changing the climate and the emission factor of the energy supply to the building.

DESCRIPTION OF THE BUILDING

The building is a single-family house with a lightweight wood frame construction. The heated floor area is 160 m^2, divided on two floors. The house fulfils the Norwegian energy regulations from 2010 [9]. Input parameters were taken from NS3031 [10, 11]. The building energy simulations were carried out with the software TRNSYS version 17.00.0019 [6, 7]. The main input parameters are summarized in Table 1.

Dimensions (internal)	Length x Width: 10 m x 8 m
	Height: 5 m (2 floors)
	Heated floor area: A_{BRA} = 160 m²
	Heated air volume: V = 384 m³
External walls	Internal area including windows and door: A_{wall} = 180 m²
	Internal area excluding windows and door: $A_{wall\ net}$ = 148 m²
	Thermal transmittance: U_{wall} = 0.18 W/(m²K)
Windows and door	Total area of windows and door: A_{wd} = 32 m² (A_{wd}/A_{BRA} = 20 %)
	Thermal transmittance of windows and door: U_{wd} < 1.2 W/(m²K)
Roof	Internal area: A_{roof} = 80 m²
	Thermal transmittance: U_{roof} = 0.13 W/(m²K)
Floor	Internal area: A_{floor} = 80 m²
	Thermal transmittance: U_{floor} = 0.15 W/(m²K)
Thermal bridges	Normalized thermal bridge value: ψ'' = 0,03 W/(m^2_{BRA}K)
Air tightness	Air changes at 50 Pa: n_{50} = 2.5 h^{-1}
Ventilation system	CAV ventilation (operating hours 24/7/52)
	Heat exchanger efficiency: γ_{he} = 80 %
	Ventilation rate: V_V = 192 m³/ h
	Specific Fan Power: SFP = 2.5 kW/(m³s)
Heating and cooling	Electrical heating and cooling system
	Heating and cooling efficiency: γ_{hc} = 100 %
Internal loads	Lighting (operating hours 16/7/52): P_l = 312 W (312 W heat gain)
	Technical equipment (op. hours 16/7/52): P_t = 480 W (288 W heat gain)
	Domestic hot water: P_{dhw} = 544 W (0 W heat gain)
	Heat gain due to people: 240 W

Table 1: Main input parameters for building energy simulations.

METHODOLOGY

In order to obtain a zero emission building, it is necessary to consider the emissions throughout the whole life cycle, i.e. GHG-emissions with CO_2-equivalents as the environmental indicator. The reduction in GHG emissions related to the energy savings during operation can be calculated on basis of the energy source(s) being used in the building. The GHG-emissions related to the additional use of materials, should consider the emissions related to production, transportation, construction, maintenance and disposal. If the materials can be recycled, this should also be taken into account.

In this case study, identical buildings with 10 different floor constructions were compared. The reference case was a lightweight wood frame construction insulated with glass wool, which was 300 mm thick, i.e. there was no layer for thermal energy storage. The remaining 9 configurations were modelled with one additional layer on the inside:

- 5 mm, 25 mm and 50 mm layer of concrete
- 5 mm, 25 mm and 50 mm layer of wood
- 5 mm, 25 mm and 50 mm layer of PCM

The thickness of the wood frame with glass wool was adjusted for each configuration, to get identical thermal transmittance (U_{floor} = 0.15 W/(m²K)), i.e. only the thermal energy storage and release capacity is changed.

All the buildings, i.e. with the 10 different floor constructions, were simulated with weather data for three different climates, extracted from the software Meteonorm version 6.1.0.20:

- Northern European – Oslo in Norway
- Central European – Prague in Czech Republic
- Southern European – Rome in Italy

The reduction in GHG-emissions was calculated according to the formula:

$$\Delta GHG_{Total} = \Delta GHG_{Operation} - \Delta GHG_{Materials} \quad (1)$$

The reduction of GHG-emissions, related to reduced heating and cooling demand:

$$\Delta GHG_{Operation} = \frac{(E_{ref} - E_i)KT}{A_{floor}} \quad (2)$$

The increase of GHG-emissions, related to increased use of materials:

$$\Delta GHG_{Materials} = \frac{GHG_{Materials\,i} - GHG_{Materials\,ref}}{A_{floor}} \quad (3)$$

E_{ref}	total energy demand for the building with the reference floor (kWh/year)
E_i	total energy demand for the building with alternative floor *i* (kWh/year)
K	GHG emission factor for energy, including emissions related to building of the transformation and transportation systems for the transformation of the primary energy to delivered energy (kg CO_2 eq/kWh)
T	life cycle of the building (years)
A_{floor}	internal floor area (m^2)
$GHG_{Materials\ ref}$	life cycle emissions related to the materials in the reference floor (kg CO_2 eq)
$GHG_{Materials\ i}$	life cycle emissions related to the materials in alternative floor *i* (kg CO_2 eq)

LIFE CYCLE ASSESSMENT

System boundaries

In this simplified life cycle assessment, only the following processes were included:

1. Production of the materials which were used in the initial construction of the floor
2. Transportation of the materials from the manufacturer to the building site
3. Operational energy use

Item 1 and 2 is the basis for the calculation of $\Delta GHG_{Materials}$, while item 3 is the basis for the calculation of $\Delta GHG_{Operation}$.

Data collection

Emission data for production of the PCM was received from DuPont [4]. Emission data for the remaining materials and emission factor for transportation was taken from Klimagassregnskap.no version 2 [14], which is a Norwegian tool for calculation of building related GHG-emissions. The electricity specific part of the emissions related to production of the materials can be adjusted according to a user specified emission factor for electricity in Klimagassregnskap.no. It was decided to use the emission factor for low voltage electricity in Luxembourg, 0.597 kg CO_2 eq/kWh [15], to make the results as comparable as possible to the PCM which is produced in Luxembourg. The life cycle of all the materials and the building was assumed to be 60 years, and the transportation distance of all the materials was assumed to be 1000 km.

Thermal conductivity, density and specific heat capacity was taken from NS-EN ISO 10456 [12], product data sheets [3, 5] and a test report from CSTB [13].

NOTE: The DuPont™ Energain® PCM panels is only 5.26 mm thick. Since this is a theoretical study, the material properties have been assumed to be applicable for different thicknesses. E.g. the emission for 50 mm thickness is calculated as: 50 mm/5.26 mm = 9.5 layers of PCM, although one thick layer sealed with aluminium may have given less emission.

RESULTS

Figure 1 shows the total reduction in heating and cooling demand (left side), and the increase of GHG-emissions related to the materials (right side). Figure 2 shows the total reduction in GHG-emissions with emission factor 0.050 and 0.500 kg CO_2 eq/kWh for the energy supply.

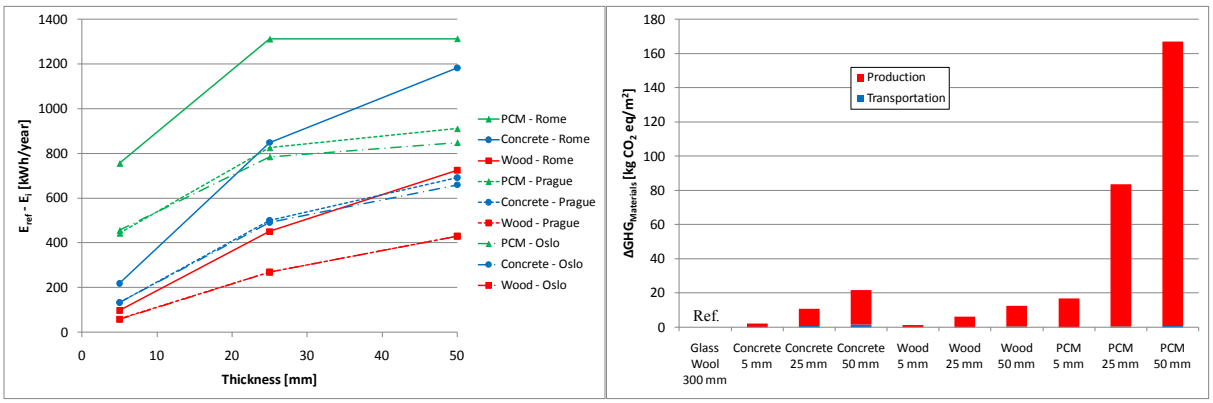

Figure 1: Left side: Reduction in energy demand due to the added thermal mass ($E_{ref} - E_i$). Right side: The increase of GHG-emissions, due to increased use of materials ($\Delta GHG_{Materials}$).

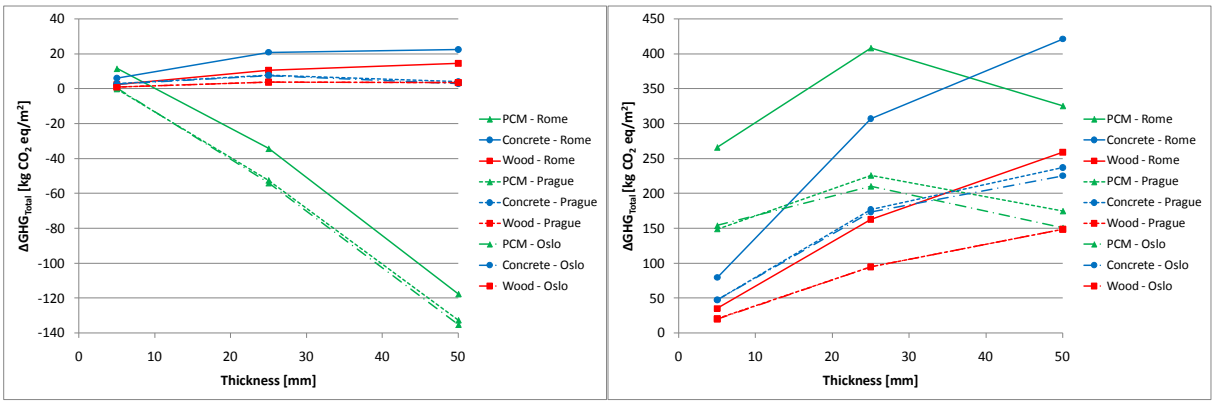

Figure 2: Left side: Reduction in emissions with factor K = 0.050 kg CO_2 eq/kWh for energy. Right side: Reduction in emissions with factor K = 0.500 kg CO_2 eq/kWh for energy.

DISCUSSION

The results on the left side in Figure 1 show that the PCM gives the highest energy savings, but the effect flattens out when the thickness is increased from 25 mm to 50 mm. When the thickness of the concrete is increased to 50 mm, the energy savings is almost as high as with PCM. The energy savings is only slightly higher in Prague than in Oslo, but significantly higher in the hot climate in Rome.

The results on the right side in Figure 1 show that wood causes the lowest increase in GHG-emissions due to the increased use of materials. The emissions related to concrete is slightly higher than wood, while PCM causes significantly higher emissions than wood and concrete.

The results on the left side in Figure 2 show that the PCM with 25 mm and 50 mm thickness causes increased emissions when the emission factor for the energy supply to the building is 0.050 kg CO_2 eq/kWh. The wood and the concrete give only small reductions in emissions.

The results on the right side in Figure 2 show that the PCM causes a large reduction in emissions when the emission factor for the energy supply to the building is 0.500 kg CO_2 eq/kWh. PCM gives the highest reductions when the thickness is 5 mm and 25 mm, but concrete with 50 mm thickness gives slightly higher reductions than PCM with 25 mm thickness. The reduction in emissions is only slightly higher in Prague than in Oslo, but significantly higher in the hot climate in Rome.

CONCLUSIONS

- PCM gives the highest energy savings, compared with concrete and wood, but have also significantly higher GHG-emissions related to production of the materials. Due to this, the total GHG-emissions is very dependant on the emission factor for the energy supply to the building.
- When the emission factor of the energy supply is 0.050 kg CO_2 eq/kWh, the PCM causes increased GHG-emissions at 25 mm and 50 mm thickness. The wood and the concrete give only small reductions in emissions at all thicknesses.
- When the energy supply to the building is 0.500 kg CO_2 eq/kWh, the PCM causes the highest reduction in GHG-emissions at 5 mm and 25 mm thickness, and concrete causes the highest reduction at 50 mm thickness.
- The reduction in energy demand and emissions is slightly higher in Prague than in Oslo, but significantly higher in the hot climate in Rome.

ACKNOWLEDGEMENTS

This work has been supported by the Research Council of Norway, AF Gruppen, Glava, Hunton Fiber as, Icopal, Isola, Jackon, Maxit, Moelven ByggModul, Rambøll, Skanska, Statsbygg and Takprodusentenes forskningsgruppe through the SINTEF/NTNU research project "Robust Envelope Construction Details for Buildings of the 21st Century" (ROBUST). Université de Lyon, by Frédéric Kuznik, is acknowledged for supplying the TRNSYS Type 260.

REFERENCES

1. Baetens, R., Jelle, B. P., Gustavsen, A.: Phase Change Materials for Building Applications: A State-of-the-art Review, Energy and Buildings 42, 1361-1368, 2010.
2. Cao, S.: State of the Art – Thermal Energy Storage Solutions for High Performance Buildings, Master Thesis, Norwegian University of Science and Technology/University of Jyväskylä/SINTEF Building and Intrastructure, Norway/Finland, 2010.
3. DuPont: DuPont™ Energain® Energy-Saving Thermal Mass Systems, Data Sheet – Measured Properties, DuPont de Nemours, Luxembourg, 2007.
4. Gilbert, J.: E-mail regarding the global warming potential of DuPont™ Energain® panels. 2011-01-18.
5. Glava: FDV-documentation (in Norwegian), Glava Plate A 37, Norway, 2010.
6. Klein, S. A., et al.: TRNSYS 17 - A TRaNsient SYstem Simulation Program, User Manual, Solar Energy Laboratory, University of Wisconsin-Madison, Madison, USA, 2010.
7. Kuznik, F., Virgone, J., Johannes, K.: Development and Validation of a new TRNSYS Type for the Simulation of External Building Walls Containing PCM, Energy and Buildings 42, 1004-1009, 2010.
8. Kuznik, F., David, D., Johannes, K., Roux, J-J.: A Review on Phase Change Materials Integrated in Building Walls. Renewable and Sustainable Energy Reviews 15, 379-391, 2011.
9. Ministry of local government and regional development (KRD): FOR 2010-03-26 no. 489: Regulations on Technical Requirements for Construction (in Norwegian). Norway, 2010.
10. NS 3031:2007: Calculation of Energy Performance of Buildings - Method and Data, Norway, 2007.
11. NS 3031:2007/A1:2010: Amendment A1 - Calculation of Energy Performance of Buildings - Method and Data, Norway, 2010.
12. NS-EN ISO 10456:2007: Building Materials and Products - Hygrothermal Properties – Tabulated Design Values and Procedures for Determining Declared and Design Thermal Values, Norway, 2007.
13. Sallee, H.: Thermal Characterization, Before and After Ageing of DuPont™ Energain® Panels, CSTB, N/Réf. CPM/09-035/HS/MLE/, Saint Martin d'Hères, France, 2008.
14. Selvig E.: Greenhouse gas accounting for development projects (in Norwegian). Civitas, Norway, 2007.
15. Ecoinvent: www.ecoinvent.com

AL-BAHR TOWERS SOLAR ADAPTIVE FAÇADE

Abdulmajid Karanouh[1], Pablo Miranda[2], John Lyle[3]

1: AK, Associate – Aedas R&D System Design
BSc Architecture, MSc Architecture; Computing & Design, MSc Façade Engineering
Aedas, 5-8 Hardwick Street, London, EC1R 4RG, United Kingdom

2: PM, Computational Designer & Architect – Aedas R&D
Diploma Architecture, MSc Architecture; Computing & Design
Aedas, 5-8 Hardwick Street, London, EC1R 4RG, United Kingdom

3: JL, Director of Advanced Technology and Research Engineer
Arup, 13 Fitzroy Street, London, W1T 4BQ, United Kingdom

ABSTRACT

This paper discusses using adaptive kinetic shading screens as a solution to ubiquitous glass facades when dealing with excessive solar exposure. The paper is based on case study – an international competition won by Aedas Architects in 2007 to design a landmark development for the Abu Dhabi Investment Council New Headquarters (Al-Bahr Towers) in Abu Dhabi, United Arab Emirates. The office twin towers will stand 150 meters high and are due to completion in 2012.

Islamic & Regional Architecture, Sustainable Technology and Inspiration from Nature form the triangular foundation of the design concept. For centuries, local Middle Eastern architecture has been well known for its sustainable features like wind catchers, solar screens, ventilation domes, and many others. The philosophy aims at recapturing some of those features used in the past coupled along with deriving bio-inspired design methodologies to enhance the performance of contemporary buildings in humid sunny regions. The power of the concept lies in the algorithmic rules developed via computation merging the design principles and translating them into a performance oriented form and integrated mechanized system able to adapt to the changing environment. The building comprises of many novel features including a secondary shading screen which comprises of 1049 automate units linked to a computerized control system that simulates the path of the sun. The shading screen acts like a dynamic 'Mashrabiya' (a traditional lattice shading screen particular to the Middle East) which fold/unfold like an umbrella/origami – driven by central linear actuators.

The concept is inspired from natural adaptive systems like leaves and flowers that open/close in response to the changing environment to overcome limitations of traditional vertical/horizontal louvers especially when applied to geometrically complex buildings reacting to the sun's changing location.

The dynamic screen will reduce solar gain and solar glare while providing better visibility by avoiding dark tinted glass and blinds distorting the appearance of the surrounding view. This intelligent system will better distribute natural diffused light and optimize the use of artificial lighting and reduce air cooling loads. The system will help reducing the overall energy consumption, carbon emission, and plant room size.

The Al-Bahr ICHQ Towers are currently under construction. The unique form, kinetic façade solution, and added value they bring to the towers will place the building as worldwide benchmark for performance oriented design and adaptive architecture.

INTRODUCTION

A major challenge that designers/engineers always face is meeting the required energy performance and user comfort in a changing environment. In nature we may find many solutions to similar problems; 'natural systems' are anything but static as they constantly adapt to their changing environment between day and night and from season to season. This was one of the major inspirations behind the concept design of the case study presented in this paper and which comprises of a novel smart adaptive façade following the sun path.

THE PROJECT; AL-BAHR TOWERS, ABU DHABI INVESTMENT COUNCIL

Aedas won an international competition in 2007 to design a worldwide unique landmark development for the Abu Dhabi Investment Council New Headquarters (Al-Bahr Towers) in Abu Dhabi – United Arab Emirates (Figure 01). The office twin towers will stand 150 meters high and are due to completion in 2012.

KEY ELEMENTS

***Geometric Composition**:* The intersection of the infinite arrangements and populations of circles (2D) & spheres (3D) generate infinite arrangements of nodes that – when connected following a mathematical logic – generate the famous Islamic patterns and forms.

***Main Form**:* All floor-plates and vertical profiles of each tower – made of tangential arcs following specially devised mathematical rules – generate an intelligent fluid form that maximizes volume to envelope ratio and natural lighting distribution while minimizing wind-load impact on the building skin and structure.

***Main Structure**:* An intelligent honeycomb formation – inspired from beehives and uniquely applied to towers – provides a highly efficient and redundant structure.

Figure 01. Al-Bahr ICHQ Towers; Emerging from the landscape, the energy and structural performance driven design dictated the organic form and geometric formation of the surrounding kinetic shading components.

Façade: a series of smart folding kinetic shading components generate a screening layer to the weathering glass skin protecting the building from excessive solar gain.

The design brief was based on the desire to create a building which would represent the ethos of the Investment Council, while relating to the context and also reflecting the underlying cultural tradition of Abu Dhabi in a contemporary idiom.

CONCEPT & PHILOSOPHY

Islamic & Regional Architecture, Sustainable Technology and Inspiration from Nature form the triangular foundation of the design concept of the ICHQ towers (figure 02). For centuries, buildings in the Middle East have been well known for their sustainable features like wind catchers and solar screens. While carefully avoiding mocking traditional styles or directly mimicking systems in nature, the philosophy aims at recapturing some of those features used in the past and deriving bio-inspired methodologies to enhance the performance of the building under similar weather conditions. The power of the concept lies in the algorithmic rules developed via computation transforming the design principles into performance oriented form and integrated mechanized system able to adjust and adapt to the changing environment.

FAÇADE DESIGN

A relatively clear glass curtain-wall forms the weather-tight layer of the towers' skin. A secondary layer comprises of intelligent automated shading components – opening/closing via centrally located linear actuators – linked back to a computerized control system that follows the sun path. The shading screen acts as a dynamic 'Mashrabiya' (Wooden lattice shading screen particular to the Middle East - Figure 03). The screen will reduce solar gain and glare while providing better visibility by avoiding dark tinted glass and blinds distorting the appearance of the surrounding view. This system will better distribute natural diffused light and optimize the use of artificial lighting through dimmers linked to sensors and reduce air cooling loads. The system will help reducing the overall energy consumption, carbon emission, and plant room size.

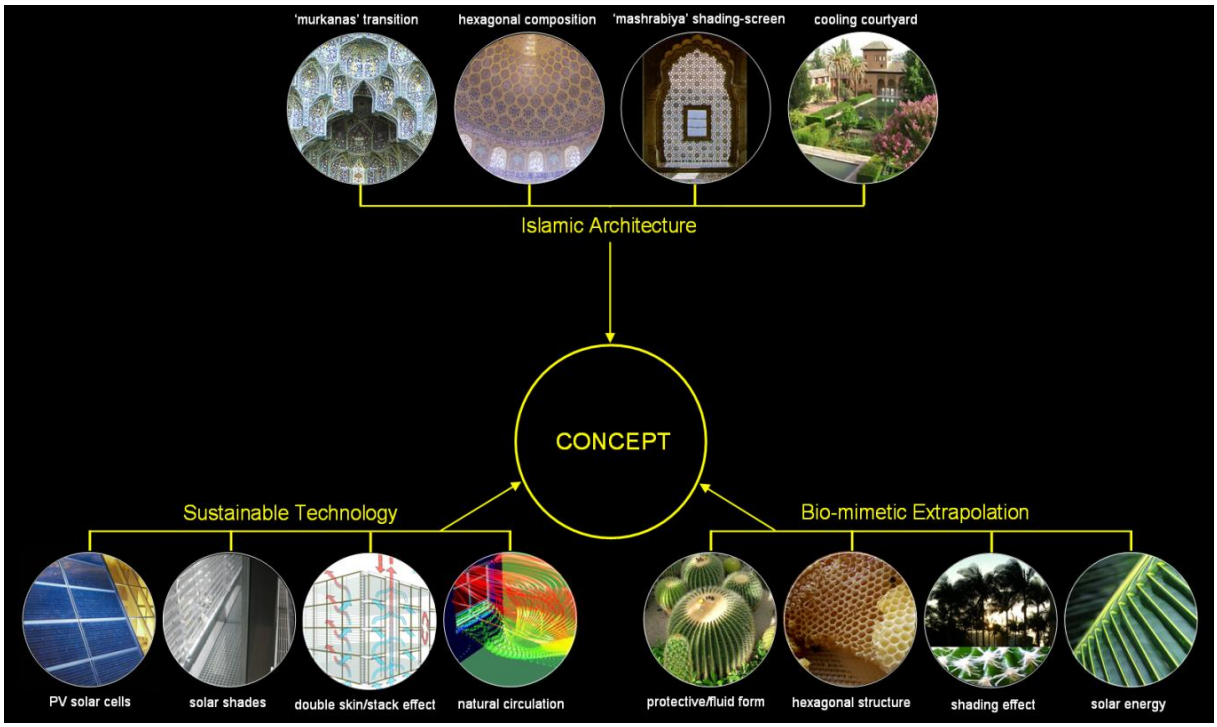

Figure 02. ADIC Concept & Philosophy displaying the key design drivers

THE CHALLENGE; WHY GLASS?

For the past two decades, 'naked' glass facades have dominated the vast majority of buildings in general and iconic office towers in particular in the Gulf Region becoming the norm in terms of clients and users expectations – mainly sponsored and encouraged by local governments. Therefore, it will take some time to re-educate the market and gradually re-orient expectations accordingly and introducing the dynamic Mashrabiya shading screen was viewed by the Design Team as step forward towards moving away from completely 'naked' glass facades. It is also becoming more encouraging now that the authorities in Abu Dhabi for example are rethinking this devotion to the transparent and issuing new regulations that may limit glass to no more than 30% of the façade.

THE RESPONSE; MASHRABIYA - DYNAMIC SHADING SCREEN

Concept: The Dynamic Mashrabiya is a kinetic shading system that comprises of triangular units that fold like an umbrella at various angles providing shading surfaces in various angles. The design concept was inspired by natural adaptive systems like leaves and flowers that open and close in response to the changing environment. The flexible smart folding geometry was carefully worked out to overcome the limitations of traditional vertical and horizontal louvers especially when applied on geometrically complex buildings.

Distribution: There are 1049 units fitted to each of the towers covering the East, South and West zones leaving the North face exposed (Figure 01) where there is no exposure to direct sunlight. When a façade zone is subjected to direct sunlight, the Mashrabiya units in that zone will deploy into their unfolded - closed state providing shading to the inner glazing skin. As the sun moves around the building each Mashrabiya unit will progressively open (Figure 04).

Building Management System: The Mashrabiya system will be automatically controlled from a BMS central control room with capability to control individual units or move groups of Mashrabiya for servicing purposes or special events. The main control system is based on a program pre-set to follow the sun path that will update the position / opening of each shading unit three times per day. The control system will be linked to an anemometer situated at that will send feedback to a wind-speed graph. In the event of excessive wind-speeds, the safety control system will override the pre-set system and fold the Mashrabiya units at their most robust positions. The system also links to a light sensor that detects unusual conditions (cloudy day) hence overriding the pre-set program and operates the shading units in real time.

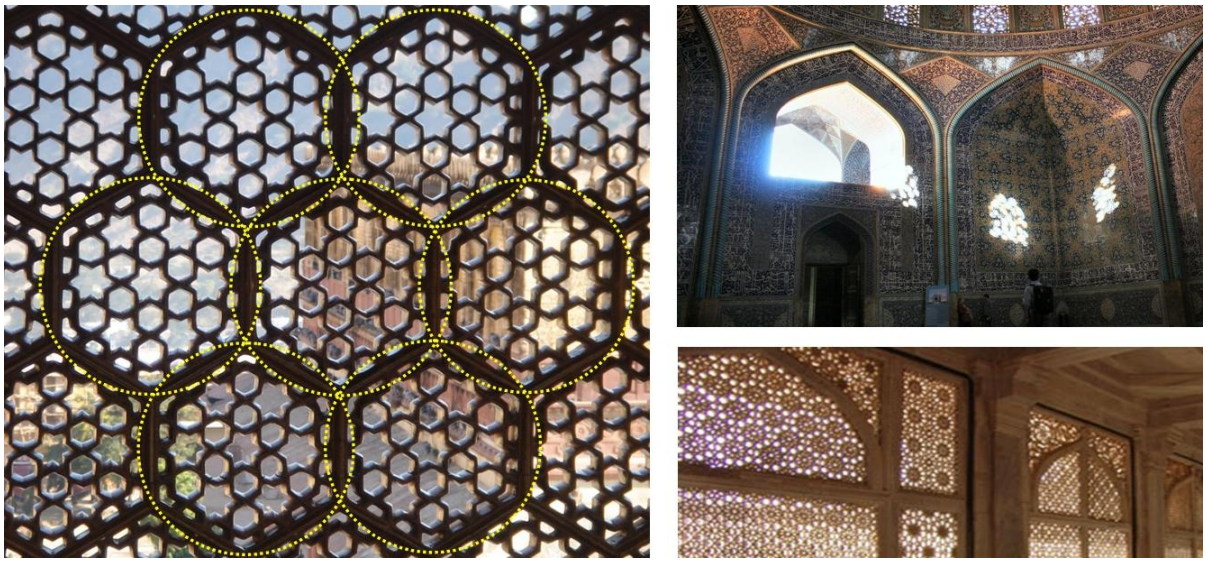

Figure 03. Traditional Mashrabiya Shading Screen and Geometry Derivation.

Hardware: The mechanism is driven by a centrally located electric screw-jack linear actuator. The actuator strokes up to 1000mm folding the mechanism up to 80% open area.

Materials: The supporting structure is made of duplex stainless steel, the shading mesh is made of FTPE coated fibre glass and the fabric frames are made of PVDF coated aluminium.

Power & Data Supply: Electrical outlets are provided at each floor to power the actuators and controllers. Data transmission from control room to actuators is via a dedicated Ethernet to PLC controllers using SCADA protocols.

Software: during the competition stage, the Aedas R&D team collaborated to produce a bespoke program using a Java stand-alone applet which simulated the path of the sun. Siemens control system will be utilized to program the actuators' operation.

Key Qualitative Benefits – User Comfort & Psychology: the responsive façade will provide many advantages to the occupants by offering better naturally lit spaces and external natural views, less use of obstructive blinds, reducing AC flow & drag.

Key Quantitative Benefits – Energy Performance: In addition to the advantages stated above, the Mashrabiya system will provide further benefits such as 20% energy saving (up to 40% to the offices), 20% reduction in carbon emission, and 15% reduction in plant capital cost

Testing and Verification: Regimes included a wind load (up to 90m/s) testing where a one-to-one Mashrabiya unit was built in a wind tunnel at the CSTB facilities in Nantes – France (figure 05). Another was carried out in Basel – Switzerland in order to test the mechanisms long term durability where a unit was built in a special chamber controlling temperature and humidity up to 60 degrees Celsius and 100% consecutively (figure 06). The Mashrabiya unit was sprayed with salty water, sand, and dust particles on a regular basis and was left to operate for 30,000 cycles – roughly equating 80 years of performance.

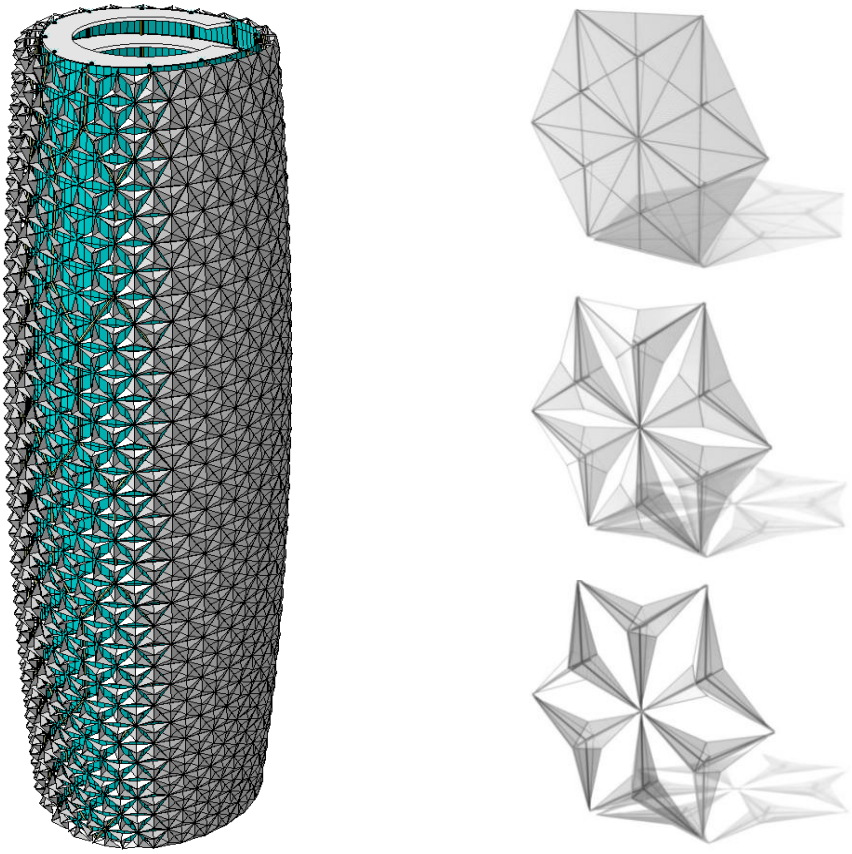

Figure 04: Mashrabiya grouped in six units at unfold, mid, & maximum fold (right).

LOOKING FORWARD

If the dynamic Mashrabiya shading screen of Al-Bahr Towers is successfully delivered and meets the performance criteria projected by the Design Team and Client's aspiration, it may present new standards to follow and will allow for others to build upon the current solution and improve it. Just like other technologies, the more it becomes more popular and common, the more it becomes reliable and affordable…

ACKNOWLEDGEMENTS:

Peter Oborn – Deputy Chairman at Aedas

Aedas R&D Group

Advanced Technology & Research at Arup

Ghery Technologies

Yuanda Europe

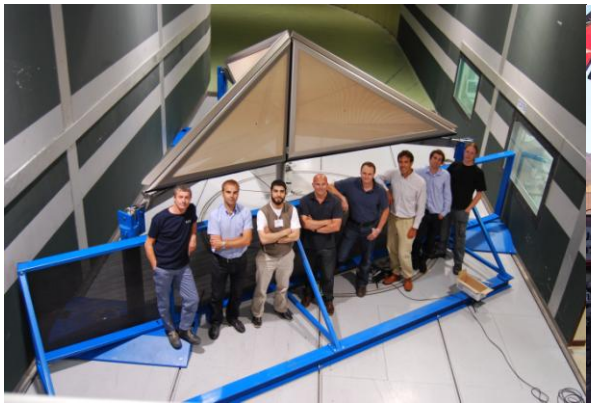

Figure 05: Wind-tunnel test at CSTB.

Figure 06: Durability test in Basel

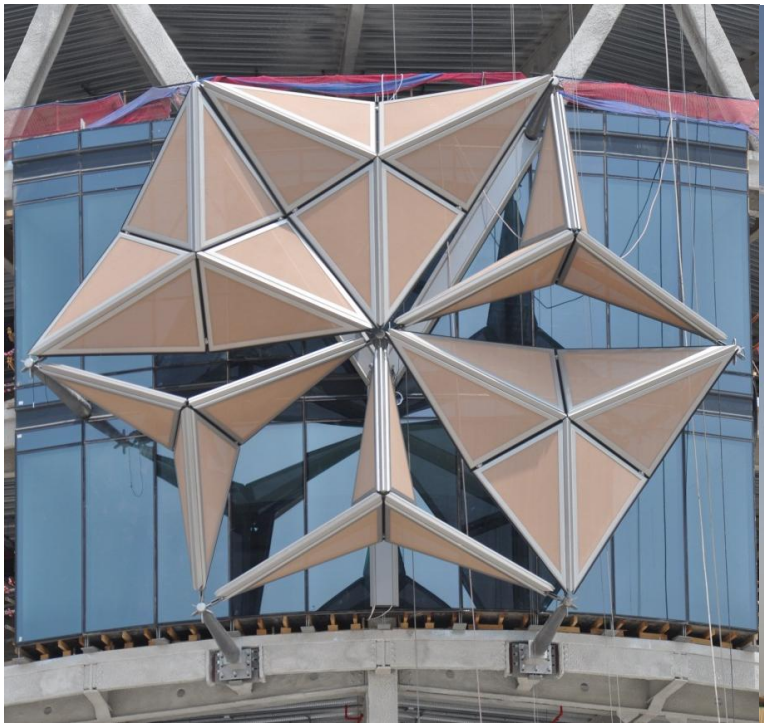

Figure 07: Six Mashrabiya units in operation, Figure 08: Al-Bahr Towers under construction

OVERCOMING THE ADDITIVE-INTEGRATIVE PARADOX: USING RESPONSIVE BUILDING MODELING TO CONCEIVE NEW APPROACHES TO THE INTEGRATED FAÇADE

J. Ko[1]; L. Widder[2]
1, 2: Department of Architecture, Rhode Island School of Design; 2 College Street Providence, RI 02906 USA

ABSTRACT

Integrated Design is defined by the multi-functionality of each architectural element and its capacity to serve structural, thermal, building physical and spatial mandates. For both engineers and architects, this degree of resolution has enormous intellectual appeal; for low-exergy approaches to the built environment, it means optimized performance. In practice, however, integrated design has meant a struggle to frame information appropriately so as to support the simultaneous resolution of structural, mechanical, building physical, fabricational and architectural problems. The quest for building systems and knowledge integration has often devolved into a series of add-ons chosen from market-available products.

The increased focus on energy efficiency and human comfort has driven the development of many computational building envelope assessment software tools. Yet the promise of computational analysis to contribute significantly to a truly integrative, rather than additive, design process for the detailing architect is far from realized. This paper builds on the premise that the detail scale is well-suited to a truly integrative approach to building systems if it is paired with analytic software that gives early performance feedback to detail considerations. To gauge the appropriate range of values and to map the process of resolution for envelope design as a support to more appropriate collaborative software interface, this paper considers detailed wall sections at the juncture of wall and a window, assuming a low-exergy model of acclimatization. It also applies a similar approach to a "ground-up" study of envelope-integrated acclimatization in which building components respond symbiotically to technical and architectural requirements.

This paper's contribution to the additive-integrative dilemma is two-fold: analytic, addressing the need to define the benchmarks and appropriate capacity for dynamism upon which relevant software in support of systems integration at the detail scale might be based; and creative, testing instances in which materials and design approaches both within and outside of the traditional repertoire of small-scale residential construction might realize better-integrated envelope systems.

INTRODUCTION

Integrated Design is defined by the multi-functionality of each architectural element and its capacity to serve structural, thermal, building physical and spatial mandates. For both engineers and architects, this degree of resolution has enormous intellectual appeal; for low-exergy approaches to the built environment, it is paramount to optimized performance. In practice, however, integrated design has meant a struggle to frame information appropriately so as to support the simultaneous resolution of structural, mechanical, building physical, fabricational and architectural problems.

The January 2011 issue of *Architect* Magazine, the official publication of the American Institute of Architects, may be a bell weather of the status of integrated design as it is currently practiced in the US. It featured an article by Kiel Moe, entitled 'Do More With

Less: Double-glazing vs. masonry', in which his diagnosis of the double glazed curtain wall's "cascade of compensations" for its environmental inadequacies is predicated on the insight that "the linear model of progress in architecture is invariably additive. When architects encounter new problems and obligations, they often respond by layering materials, technologies, consultants, software." The quest for building systems and knowledge integration has devolved into a series of add-ons: an "integrated" wall as an assembly of exterior shading devices, user-operable shades, multiple glazing layers, air gaps, cleaning mechanisms and other gadgets.

The building envelope is a site for the integration of technologies, which advance human comfort while also supporting optimal building performance. The building envelope is also the locus of enormous effort and activity on the part of the architect as he or she negotiates these demands and translates a design idea into reality via the detailing process. The detailing process has generally been an empirical one, reliant on good practice, precedent study and ratiocination. While not inherently incorrect, this has proven increasingly inadequate to meet the current need for building envelope innovation. The increased focus on energy efficiency and human comfort has driven the development of many computational building envelope assessment software tools. Yet the promise of computational analysis to contribute significantly to a truly integrative, rather than additive, design process for the detailing architect is far from realized.

In [2,3], a parametric approach to the detailing process is proposed, designed to bridge the gap between current practices and computational analysis at early stages of design detailing. This approach is captured by the following steps:

1. *Benchmarking*: In this initial step, typical cases of assemblies are identified as cases from which other versions can be derived. The criteria for benchmarking should consider best practice for thermal and building physical performance while architectural expression may be neutral or conventional.
2. *Formulating the problem parametrically to facilitate subsequent iterations*: Rules that govern the detailing decisions for these benchmark cases are extracted to create a framework for systematic variation. Positioning benchmarks as a part of a continuum typically requires a clear articulation of desired architectural expression, but also lightens the iterative process since considerable investment at this stage is placed on understanding relationships and anticipating potential trade-offs as a parameter is varied.
3. *Establishing a dynamic link to existing computational tools*: The analytical software appropriate to the particular focus of study is sought, its efficacy tested and recommendations for more interactive modes of operation shared. Applied to the parametric model, these computational tools are used to compare energy performance as parameters vary. An analysis at each iteration is used to refine the rules that govern the parametric formulation and as a basis to propose changes in detail strategy.

This paper considers a case study of systems incorporation at the juncture of wall and a window, assuming a low-exergy model of acclimatization. It also applies a similar approach to a "ground-up" study of envelope-integrated acclimatization in which building components respond symbiotically to technical and architectural requirements.

CASE STUDY: INTEGRATED HEAT EXCHANGERS FOR VENTILATION IN SOLID CONCRETE CONSTRUCTION

This approach can be demonstrated on a simplified design problem of incorporating a heat air exchanger in concrete wall construction with exterior insulation and rain screen. From an exergy standpoint, the choice of concrete wall construction offers an extensive, thermally stable wall surface for low temperature heating. From a low energy need and

building physical standpoint, the exterior insulation and rain screen construction represent proven methods of mitigating thermal transmission and both ultraviolet and water-based degradation of the insulating layer.

In a previous study, benchmark cases at the window were developed for typical locations of the window in the depth of such a wall construction [3]. To test the potential of the proposed parametric approach to envelope detailing for the promotion of systems integrated design, the problem here focuses on the location and detailing of a heat-pump-based air exchanger (BS2's Airbox[1]) relative to localized thermal performance in the window-to-wall assembly as the window position moves in the depth of the wall. Based upon the manufacturer's recommendations for the installation of the heat recovery ventilation unit, benchmarks for this augmented problem were devised relative to the different opportunities afforded by the window location.

In the construction details of the benchmarks in Fig 2, the location of a through-wall vent line is held constant, assuming a horizontal penetration below the windowsill behind the windscreen cladding.

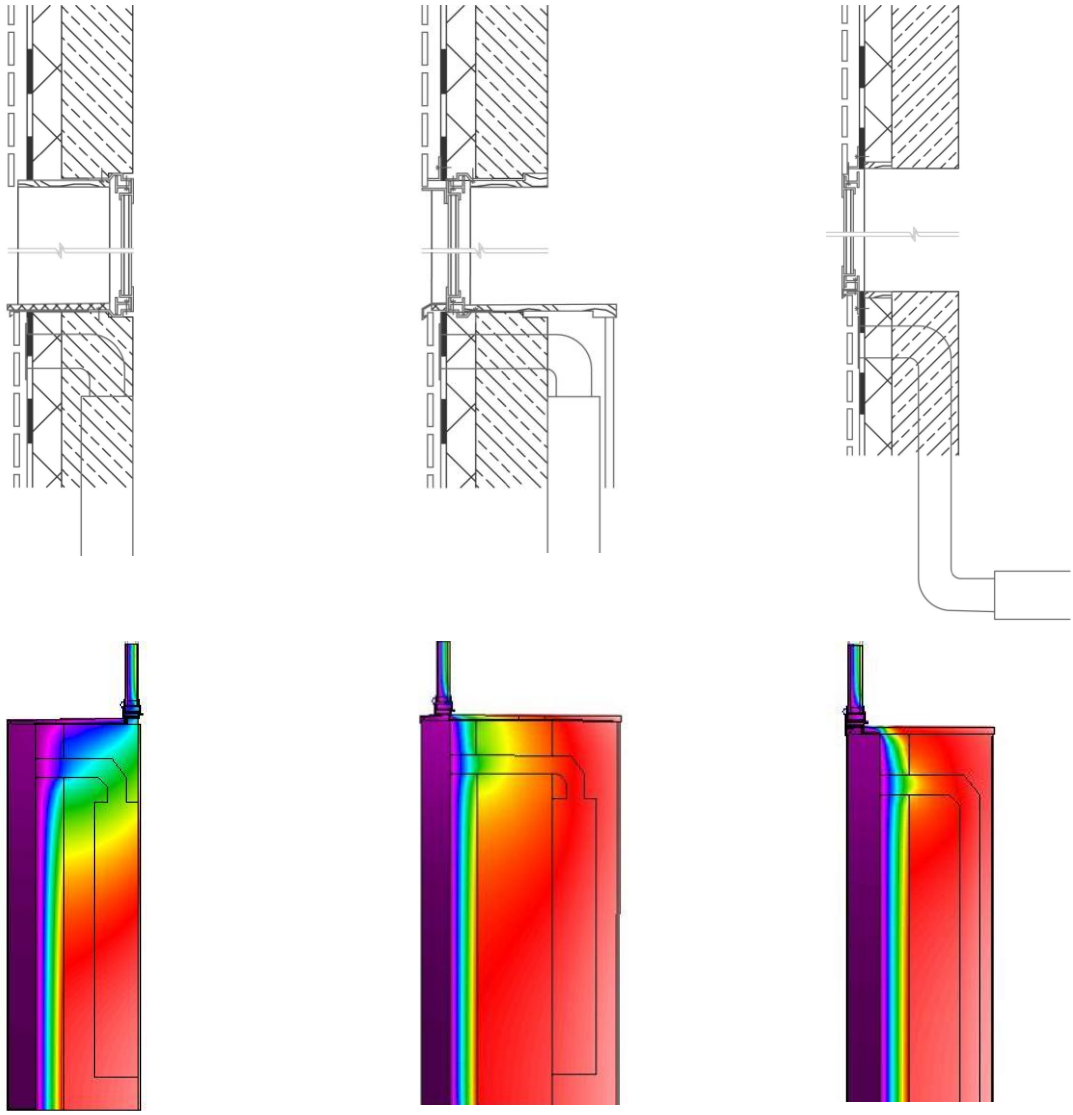

Figure 2: Construction details and THERM analysis for heat recovery unit locations as window position varies; from left to right: interior flush; thermal neutral axis and *exterior flush*

[1] See http://bs2.ch/de/products/airbox.php

In the interior flush case, the ventilation line could be routed horizontally, as depicted, or vertically to emerge beneath the sill, both suggested positions given by the manufacturer. In keeping with architectural merits of the interior flush window, its capacity to emphasize the interior surface of the room as a continuous, unbroken plane, the logical installation point for the heat recovery unit would be a niche below the window, in front of which an access panel that could be installed in plane with the finish wall surface. When the window is located in the neutral axis (within the insulating layer), the use of a wood casing on the interior is used to conceal the insulation layer and the installation brackets which hold the window in place. It is logical to imagine the extension of that casing as a cover for the heat recovery unit, which could then be located adjacent to the wall inside the tempered space rather than requiring a niche in the wall. Such casework details are a commonplace feature in the location and integration of conventional radiators. For an exterior flush window installation, which in architectural terms would allow the full expression of the concrete wall as both finish surface and deep envelope. Since no casing is foreseen at the window and the continuity of the concrete surface would be undermined by an access panel as foreseen as in either of the two cases to be described below, the heat recovery unit is located in the floor slab, one of the installation solutions suggested by the manufacturer.

Despite their substantial differences in appearance, this series of details represents a continuum as the parameter of window position varies. The advantage of conceiving of this problem parametrically is that it allows for comparative studies to be conducted at the early stages of the design detailing process during which a primary role is to support a detailing architect to distinguish competing alternatives, rather than to quantify absolute performance. The infrared color maps shown in Fig. 2 are appropriate for early stage evaluative response in the detailing process, and can be useful to draw initial conclusions that might affect detailing choices. Tradeoffs in architectural expression and thermal performance, for example, can be articulated in a way that would be difficult to do using empirical or typological approaches.

For all cases, the vent line perforation distends the isotherms, showing far greater thermal transmissivity near the window aperture. The better thermal performance of the exterior flush window installation is negatively impacted directly at the site of the perforation and in the sill area. Some loss of thermal capacity results from the displacement of solid concrete in the wall surface by the conduit, and colder surface temperatures are indicated from the sill downward but the lower portion of the wall appears to perform fairly consistently along its length. The trade-off for better localized performance at the window is the much longer conduit run to the heat recovery unit located somewhere in the floor slab and the reduced accessibility of the floor-based unit. In comparison to the exterior flush case, the neutral axis case displays similar thermal impact at the perforation, which is amplified by the greater transmissivity in the sill area associated with this window location. Loss of thermal performance along the length of the wall is, on the other hand, mitigated by placing the heat recovery unit on the warm side of the concrete wall. This case demonstrates superior thermal performance based upon surface temperature at the interior plane of enclosure, the trade-off being the need for an ancillary enclosure around the heat recovery unit, which protrudes into the interior space. The extent to which this solution is actually necessary depends on the ingenuity of the architectural design and its capacity to understand the enclosure box as, for example, contributing to furnishing. At first glance, the interior flush case could be discounted at the outset because of its poor thermal performance; from the perspective of architectural design and expedient installation, however, the preservation of the continuous wall plane and the short conduit run and easy accessibility of the heat exchange unit, it is the most plausible of the three installations. The ability to be able to do a quick performance study at this early stage of

design allows the detailing designer to anticipate conflicts that might arise despite an initial decision in favor of a construction strategy amenable to systems integration.

ALTERNATIVE PREMISES: SYSTEMS INTEGRATED DESIGN FROM THE GROUND UP

Even with the simple example just discussed, it is clear that choices made at a building-wide scale about systems and assemblies cannot guarantee truly integrative approaches to thermal performance. In fact, if one adds the mandates of reusability/recyclability, lower material intensity and an envelope balance point approach which takes into account the human desire for certain fluctuations in interior climate (as in opening a window), this goal is only rarely achieved by the assembly of available building products outside of an additive mode of working. Ultimately, by identifying these requirements and testing their interplay at detail scale, it may be possible to conceive of new families of assemblies and components that account for perforations, wall depth, fasteners and finish surfaces on a specific, as-needed basis. This approach to building components would start from the exceptions – windows, doors, parapets – rather than the typical approach, in which the standard envelope assembly is given primacy.

For illustrative purposes, we will consider the potentials of new families of materials relative to the demands of integrative design, for example, such high-strength, light-weight freely formable materials as natural fiber reinforced epoxy composites. Given their material and fabrication qualities, the means to address distributed building systems, structural capacity, low thermal transmissivity and architectural expression could be resolved in an integrated way rather than by the addition of components as the list of requirements grows. One example based upon the preceding exercise of locating a heat recovery ventilation system relative to a window appears in the speculative project for a thin wall house illustrated in Fig 3.

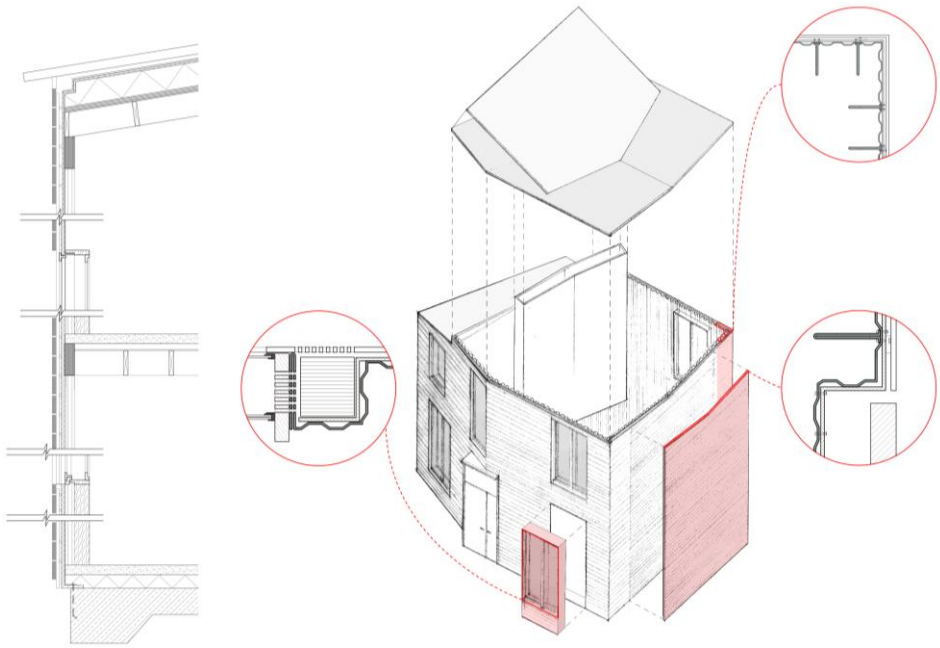

Figure 3: Study for a natural fiber reinforced low-rise house with integral structural, thermal, spatial and envelope considerations (Project: L.Widder, J.Ko, E.Nelson with J.Atkins, J.Honsa, T.Sheridan)

Inherently water and air infiltration resistant fiber reinforced walls, crenellated at two different scales for local bending and lateral/gravitational loading, comprise a thin, light exterior wall given thermal resistance by vacuum insulation and UV protection by a shorter-lived rainscreen façade. At the windows, however, the material efficiency of the thin shell defers to a deep, hollow wall construction, which would facilitate the installation of heat recovery ventilation, accommodate deeper operable window components and can provide additional lateral stability [4]. At a detail scale, the material's formability is exploited to create fasteners and brackets with reduced thermal transmissivity; this limits building physical problems from thermal transmission and the combination of unlike materials.

Without early-stage evaluation, the application of these new materials to the built environment is difficult to conceive at a detail scale. There can be no reliance on precedent or good practice, nor can manufacturer testing and specs be presumed. The prospect of working in a material in which any number of formal possibilities exist can much more productively translate into a collaborative, iterative process when quick, visually-couched feedback is available. Furthermore, the holistic development of a building assembly approach can model an integrative, rather than an additive, method of working which could be transposed to other assemblies. The transfer of emergent building materials and systems technologies to built environment implementation can be facilitated by the use of detail-scale feedback, accelerating industry uptake and leading the way out of the additive/integrative dilemma.

CONCLUSION

Many valuable modeling and visualization tools already exist at site, building and systems scale to aid in the prediction and realization of the most intelligent resolution of the energy needs accruing to human habitation. By complimenting these scales of inquiry with responsive tools at detail scale, the basis for true symbiosis in systems integration can be accelerated.

REFERENCES

1. Moe, Kiel 'Do Less With More' in: Architect Magazine January 2011 (web-based edition, http://www.architectmagazine.com/high-performance-building/do-more-with-less-lower-tech-higher-performance.aspx)

2. Ko, J. and Widder, L., Engineers/Architects: Defining Collaboration Bases for Improved Use of Parametric Software in Integrated Design, 2nd International Exergy, Life Cycle Assessment, and Sustainability Workshop & Symposium (ELCAS) Conference Proceedings, Nisyros, Greece, June, 2011, *forthcoming*.

3. Ko, J. and Widder, L., 'Building Envelope Assessment Tool for Systems Integrated Design: Understanding and Using the Reciprocity Between Parametric Analysis and the Architectural Construction Detailing Process', Proceedings of PLEA 2011, Louvain-la-Neuve, Belgium, July 2011, *forthcoming*.

4. Sauerbruch, M. and Hutton, L., www.sauerbruchhutton.de. A similar approach to double-glazed apertures has been used to good effect by, among others, Sauerbruch Hutton in their university buildings at Jessop West in Sheffield, England, and their office building Maciachini in Milan. See http://www.sauerbruchhutton.de/#projekte

TOWARDS A MINERGIE®-STANDARD FOR TROPICAL CLIMATES

Ruedi Kriesi[1] ; Fouad Aabid[2]; Claude-Alain Roulet[2]; Franco Vigliotti[3], Jean-Louis Scartezzini[2];

1: Kriesi Energie GmbH, Meierhofrain 42, CH-8820 Wädenswil, Consultant, Vice-President of Minergie®-Association

2: Solar Energy and Building Physics Laboratory (LESO-PB), Ecole Polytechnique Fédérale de Lausanne, CH-1015 Lausanne

3: EPFL Midlle East, Ras al Kaimah, United Arab Emirates (UAE)

ABSTRACT

The Swiss Minergie®-standard is, by the number of labelled buildings (> 20'000) one of the most successful building energy labels in the world. It is obviously a strong incentive for designing comfortable, low energy buildings. This standard is now valid for temperate - cold climates only. There is therefore a need for a similar standard for buildings dominated by cooling loads, as it is common in the tropical and sub-tropical climates of the world. Since the new EPFL campus planned in Ras al Kaimah (United Arab Emirates) should be exemplary, a project was launched by the Dean of EPFL Middle East, together with Minergie®-Association and the Solar Energy and Building Physics Laboratory of EPFL, aiming to set-up such a standard. In order to initiate this project, two buildings (a single family dwelling and an office building) were chosen. The single-family dwelling was simulated at an hourly time step using a detailed dynamic thermal model based on the computer simulation programme *Energy plus* issued from LBNL. The monthly energy consumption of the dwelling shows a good correlation with the monitored data. In addition to that, both energy consumptions, calculated with the dynamic and the simplified models are close to each other, giving confidence to the predictions of the latter. Therefore, both buildings were assessed using a simplified monthly energy balance method. Starting from the current buildings configurations, several variants implementing various improvements towards energy efficiency were considered. These simulations show that considerable energy saving (up to a factor 5) can be achieved by implementing together several improvements to these buildings. In addition, the building reaches a higher level of users comfort.

INTRODUCTION

The Minergie®-standard [1] is among the most applied building energy label in the world (about 20’000 labelled buildings in Switzerland by the end of 2010). It is obviously a strong incentive for designing low energy buildings in a perspective of climate change, as the standard not only asks for low energy consumption, but for above average comfort and competitive cost. It has even been extended by “Minergie®-Eco” (low environmental impact buildings) and “Minergie®-P” (optimized for passive solar gain). However, the methodology applied to evaluate the building energy performance and the conditions for getting the label are yet valid for temperate - cold climates only, where buildings are dominated by space heating and domestic hot water production and where cooling is only a minor issue. For hot and humid areas, a Minergie®-standard exists for villas in southern Japan only, where heating, cooling and dehumidification are equally required. There is therefore a need for a similar standard that can be applied to different types of buildings in areas dominated by cooling loads, as it is common in the tropical and sub-tropical climates of the world.

The new EPFL campus planned in Ras al Kaimah (United Arab Emirates) should be exemplary and gather buildings with high user comfort and top energy performance. Therefore, a project was launched by the Dean of EPFL Middle East, together with Minergie®-Association and the Solar Energy and Building Physics Laboratory of EPFL, in order to set-up a new Minergie®-standard for tropical climates.

METHOD

The Minergie® label is awarded to buildings that achieve the largestpossible energy performance with an optimal comfort at a competitive cost. These limits depend on local climate, building habits, available materials, etc. Therefore, we intended to simulate buildings in the climate of Ras-al-Khaimah for exploring various ways for reaching the goals. Passive ways such as thermal insulation, sun shadings, free cooling, as well as improvement of active ways such as artificial cooling, dehumidification or solar water heating should be explored.

Starting from typical local buildings, computer simulations using acknowledged and validated models allow estimating the effect of any energy saving measure applied to these buildings. Impacts on cost and comfort can be also assessed this way. A series of simulations of different types of buildings should provide the precise criteria for labelling buildings.

In order to initiate this project, a single-family dwelling was simulated both at an hourly time step using a detailed dynamic thermal model based on the computer simulation programme *Energy plus* issued from LBNL [2], as well as by a simplified model using monthly mean values [3]. The monthly energy consumption of the dwelling shows an excellentcorrelation with the actual energy use of the single family home, carefully monitored (Figure 1). In addition to that, both annual energy consumptions, calculated with the dynamic and the simplified models are close to each other (divergences lower than 10%), giving confidence to the predictions of the building models used in the simulation.

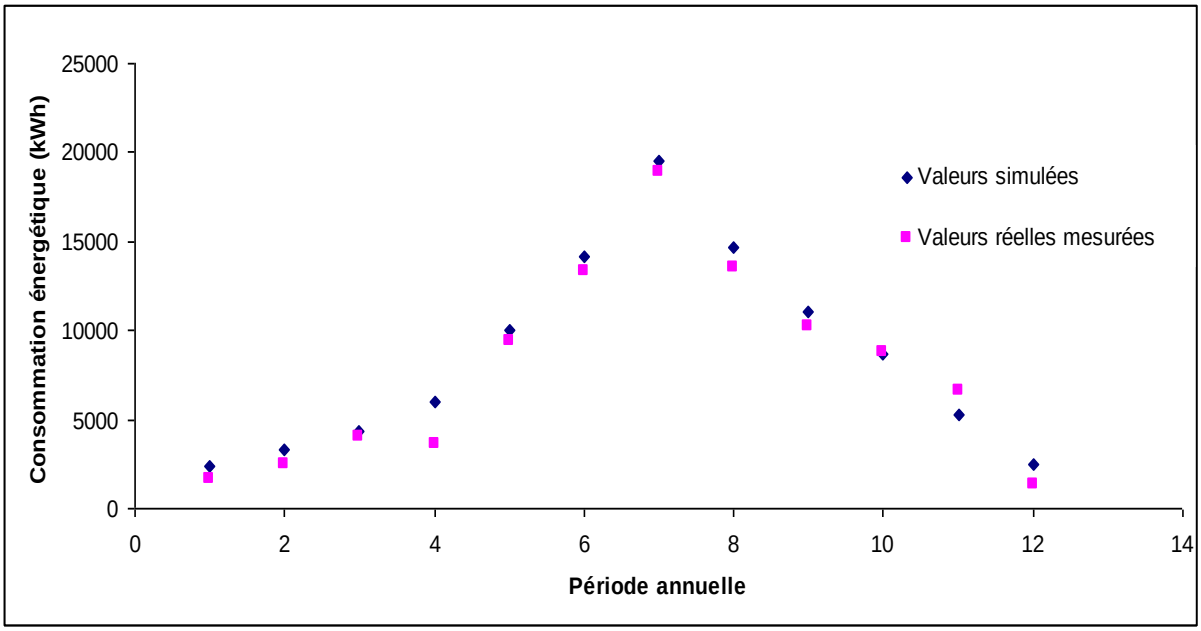

Figure 1: Measured monthly energy use and results of dynamic simulation of the family house.

The same technical improvements towards comfort and energy efficiency were considered for the calculation of an office building, assessed by the simplified monthly energy balance method, again starting from the current buildings configurations [4]. Only the results for the single family building are presented here.

RESULTS

Energy savings

The simulated home is an existing building for which annual energy use is known. Its actual view and model are shown on Figure 2. Its basic thermal characteristics are given in Table 1.

Figure 2: The modelled single family home in Raz al Khaimah. To the right is the 3-D model used for calculations.

Table 1: Characteristics of the reference building.

- Heated/cooled gross floor area:	437	m^2
- Surface of envelope to cooled floor area ratio:	2.1	-
- Cooled floor area per number of inhabitants:	73	m^2/p
- Set point room temperature winter:	22	°C
- Set point room temperature summer:	25	°C
- Window area:	103	m^2
- Window ratio per cooled floor area: $103m^2/498m^2$ =	0.24	
- Windows ratio of total walls area:	17	%
- Glass ratio of total window area:	80	%

The simulated improvement measures include, namely:

- Thermal insulation of the building envelope (walls, roof and windows)
- Efficient adjustable solar shadings
- Airtight envelope and enthalpy recovery through efficient HVAC systems
- Efficient appliances and lighting
- Improvement of the cooling quipment
- Solar hot water heater.

Typical values for these improvements are listed in Table 2, resulting energy use is given in Table 3 and illustrated in Figure 3, showing a dramatic reduction of electrical energy use.

Table 2: Reference characteristics and Minergie® improvements.

		Existing	Minergie®	
1.	U-Value roof	1.8	0.2	W/m^2K
2.	U-values walls	1.3	0.2	W/m^2K
3.	U-value windows:	2.8	1.0	W/m^2K
4.	g-value windows:	0.6	0.5	
	shading factor	0.3	0.8	
5.	air infiltration through cracks, open windows	0.6	0.1	h^{-1}
	air exchange by HRV/ERV:	-	0.46	m^3/m^2h
	efficiency of heat recovery:	-	0.85	
	efficiency of enthalpy recovery:	-	0.6	
	annual electricity use for ventilation	-	1.4	kWh/m^2
6.	annual electricity use for lights, appliances:	34	14	kWh/m^2
7.	domestic hot water, 300 l/day, 60°C	electric	solar	
8.	EER of cooling machine	3	4	

Table 3: Energy use for all purposes in the existing home and in the optimised one.

	Existing		Optimised	
Energy user	Load	Electricity use	Load	Electricity use
Transmission through envelope	195.0	65.0	27.6	6.9
Solar radiation through windows	61.5	20.5	17.6	4.4
Air infiltration	131.2	43.7	24.8	6.2
Enthalpy losses through heat recovery			19.3	4.8
Appliances		34.0		14.0
Load from appliances	34.0	11.3	14.0	3.5
Domestic hot water	13.0	13.0	13.0	0
Fan for ventilation			1.5	1.5
Total	**434.7**	**187.5**	**117.8**	**41.3**

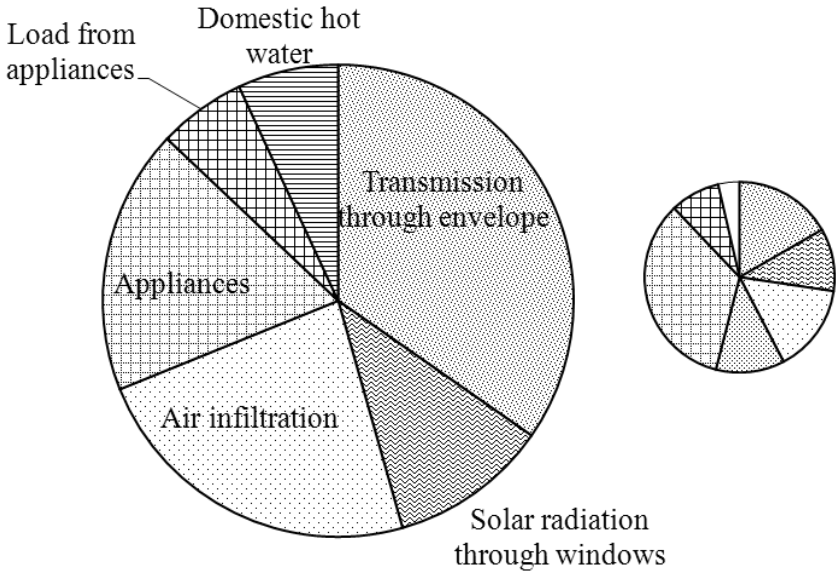

Figure 3: Representation of the energy use of the existing building (left) and the optimised one (right). Energy amounts are proportional to areas.

Cost

An important requirement of the Minergie® standard is that improvements shall be obtained at a reasonable cost. The estimated costs of recommended measures are listed in Table 4.

Table 4: Estimated cost of measure to reduce the energy use.

	Measure, description	Cost
1.	Roof insulation, 226m^2	100 CHF/m^2; (equal to wall); 23'000.-
2.	Wall insulation, 494m^2	140-170 CHF/m^2; 70'000.-
3.	Window insulation, triple heat mirror glazing instead of ordinary double glazing, 103m^2	double glazing: 350 CHF/m^2; triple glazing heat mirror: 400 CHF/m^2
4.	Shading between window panes, approx. 90m^2	Cost difference of internal to inter-glazing shading: 300 CHF/m^2;
5.	Air tight envelope, Enthalpy recovery ventilation in all rooms, type ComfoAir 550, ComfoFresh	5000 CHF for air tightness 20'000 CHF for Comfort Ventilation
6.	Optimized appliances and lights	5000 CHF (rough estimation),
7.	Hot water by unglazed solar collector	5000 CHF (rough estimation),
8.	Highly efficient cooling machine, oversized for exclusively night time use, distribution of cooling water in radiant ceiling	15000 CHF (rough estimation),

At electricity cost of 0.20 CHF/kWh, a life span of 20 years and an interest rate of 6%, investments of up to 2.50 CHF/kWh are economically interesting, if energy savings are the only one gain. With this point of view, wall insulation, insulating glazing and solar protection, which costs are between 3 and 4 CHF/kWh are not cost-effective. However, a well-insulated and air tight building envelope has many additional advantages related to comfort and hence building-value: avoid sand infiltration, better thermal comfort, lower cooling power, hence less draft and smaller cooling system, better acoustic insulation, less noise, no mould growth risk. Moreover, such investments fall below the short time economic limit if the life span is expanded to 40 years.

DISCUSSION

The energy consumption in this climate is mainly determined by space cooling. If the domestic hot water is heated by solar thermal collectors (preferably unglazed to avoid overheating), the demand is reduced to cooling and ventilation only. The load can be reduced to low values by :

- thermal insulation of roof and walls to U-values of 0.2 - 0.3 W/m^{2}K
- air-tight envelope (leakage rate at 50 Pa less than1/h) to reduce uncontrolled infiltration of hot, humid ambient air
- high efficiency enthalpy recovery ventilation to reduce the cooling needs for the required fresh air and to improve dramatically indoor comfort (no mould, no sand, no bad odours, no humid air)
- adjustable shading to reduce radiation through windows, while allowing for day-light on windows not hit by the sun (systems mounted between window panes exist)
- double or triple heat mirror inner glazing to reduce heat transmission

- highly efficient cooling machine, thanks to radiant cooling with water loop, over-sizing and enlarging heat exchangers. Oversizing allows using the cooling machine at night only, when outdoor air is cooler, thus improving its COP.

Photovoltaic system could provide electricity at reasonable cost, thanks to the 2100 sunshine hours of peak power per year. It is also a perfect means to reduce electricity demand, since the sun is available every month. However, according to users of the dwelling, PV absorbers have to be cleaned weekly from sand, to maintain a good efficiency. It must be assumed that this would not be done by average local users. It therefore makes less sense to include PV as a mandatory means of the standard.

A first draft of the definition of a Minergie® standard for the tropics is as follows

Maximum annual use of electricity 30 kWh/m^2 for space cooling and heating, domestic hot water and ventilation. This is close to twice the value in Switzerland, as a result of the difficult climate conditions.

Primary requirements:
- Air tightness of building envelope: $n_{L50} < 0.6h^{-1}$
- Automatic ventilation with heat recovery
- Minimal level of thermal insulation: U_{walls} and $U_{roof} < 0.3$ W/m^{2}K, $U_{windows} < 1.5$ W/m^{2}K
- Shading of windows with g < 0.15, for all windows receiving direct sun-light
- water consumption:
  - dishwasher < 7 l/use for 12 standard covers
  - washing machine < 45 l/use per 7 kg of laundry
  - shower heads < 12 l/min
  - water heads on sinks < 9 l/min
  - toilet flush < 6/3 l/use with choice of flush amount
  - only traditional plants in garden, to avoid or strongly reduce watering

ACKNOWLEDGEMENTS

The authors cheerfully thank the Ras Al Khaimah Investment Authority and Al Hambra Construction who provided the drawings, characteristics and data of the buildings.

REFERENCES

1. Minergie: T*he MINERGIE®-Standard for Buildings- Information for architects*. http://www.minergie.ch/publications.478.html
2. Aabid Fouad: *Standards Minergie® dans les pays à climat tropical humide*.Projet de semestre – Master en Mécanique, LESO-PB/EPFL, Juin, 2011.
3. Ruedi Kriesi: *Minergie® standard for single family home in the climate of Ras Al Khaimah.* Personal communication, 2011.
4. Ruedi Kriesi: *Minergie® standard for office building in the climate of Ras Al Khaimah.* Personal communication, 2011.

OPTIMIZATION OF INDOOR DAYLIGHT QUALITIES AND THERMAL COMFORT: A CASE STUDY OF EDUCATIONAL BUILDING ENVELOPE DESIGN UNDER TROPICAL SAVANNA CLIMATE

N. Liu[1*]; N. Jobard[2]

1: Laboratory of Urban Sociology, Doctoral Program Architecture & City Sciences, School of Architecture, Civil and Environmental Engineering, Swiss Federal Institute of Technology Lausanne-EPFL, Switzerland

2: Master of Advanced Studies Architecture & Sustainable Development, EPFL-LESOBP, Building For Climate, associated architects-urbanists, Paris, France

** Corresponding author: phone: +41 21 693 3232, fax: +41 21 693 3840,*

Email: ning.liu@epfl.ch

ABSTRACT

Under the global challenges of climate change, it becomes necessary to integrate the developing countries into the improvement of the environmental footprints of the built forms. Based on a PhD thesis on sustainable architecture and on the professional field studies carried out in Africa, this research aims to optimize the performances of educational spaces under tropical climates. The main goal is to develop innovative, adapted and yet simple systems for the building envelopes under the developing context.

The study is located under the tropical savanna climate in Ouagadougou, Burkina Faso. Until very recently, the realized models of schools are not scientifically optimized, in regard to the environmental performances as well as to the thermal & visual comforts. The used materials do not necessarily correspond to the economic and climatic realities of the countries in the South. In 2010, a pilot project, supported by governmental funds, is dedicated to the education of children affected by muscular dystrophy. The paper's authors are commissioned to its realization.

First, the study identifies a grid of major criteria on visual and thermal ergonomics within the educational spaces. Second, by measures and simulations, the performances of some existing best practices such as the Center for the women's well-being Gisèle Kambou in Ouagadougou are evaluated. Third, the paper proposes three guidelines to optimize the conventional roof structures in educational buildings. The priority is given to the passive means but the building's capacity to integrate active systems such as solar PVs is also considered.

This research participates to the development of new constructive models for the educational spaces under tropical climates. The optimization strategies are tested and applied to the pilot project, currently under construction. These built examples will constitute a pool of reliable references useful to the developing world. The envelope typologies proposed by the paper can be reproduced under similar climatic and economic contexts. In this process, the collaboration of local institutions and NGOs is indispensable to further adapt the models into different applicable variants.

INTRODUCTION

Ouagadougou, the capital city of Burkina Faso, is situated at the 12.37° north to the Equator and 1.52° west to the Greenwich Meridian line. The location of the city makes it still belongs to the most southern part of the Sahel belt. Sahel, means in Arab “coast”, “border” referring to the Sahara desert. In fact, even though Ouagadougou is situated far from the real desert border, the climate is still much affected by the Sahara. This typical savanna climate translates into a short rain period during summer followed by a hot period and a very hot and very dry period until the next year summer’s rain time. Each year from November to March, the Harmattan blows from the Sahara to the Gulf of Guinea bringing dust and epidemics through the African continent with it. In Ouagadougou, the relative humidity is often insufficient for comfort during the hot and arid period but too important during the rainy season. The outdoor temperature is very high except in December and in January. These climatic specificities require constructions to provide sunlight shadings to human activities in both outdoor and indoor situations. On the street, the sun path plays a definitive role in shaping the use of the public spaces through the daytime and the shadows are looked for in most of the outdoor activities. In addition, from the inside, ventilation is necessary to evacuate the heat. Furthermore, the humidity difference between the hot seasons and the raining season should also be controlled and regulated. Mechanical system such as the air-conditioning is expensive and energy consuming. Electric fans are more used to improve the indoor thermal comfort but the electricity provision is still very unstable in the capital city even today.

After the old city being burnt out by the European colonials in 1870s, Ouagadougou became “Bancoville”. With the typical building material made of the local red lateritic earth, Ouagadougou was populated over the years by typologies of houses very similar to the rural dwellings. The density of the city centre is relatively low. After the country’s independence in 1960, the new leaders have sought deliberately for a more modern image of the capital city built with more “noble” materials such as concrete and steel. Traditional materials such as adobe for walls and thatch for roofs are progressively abandoned. During the 1970s and 1980s, important research studies and field works on traditional building skills have been carried out in West Africa by academic researchers, architects and engineers such as CraTerre (Hugo Houben, Patrice Doat, Hubert Guillaud) and ADAUA (Atelier pour le Développement naturel d’une Architecture et d’un Urbanisme Africains) [1,2,3]. However, because of political turmoil and African elite’s aspirations for modernism, these models have not been applied. Very recently in Ouagadougou, the adobe constructions have even been more disregarded because of the damage cause to the unprotected earth walls during the flooding happened in September 2009. The AT technology, meant to the African context, developed and promoted by the French School of architects since the 1970s, has failed to be institutionalized in the end.

Today, all the self-constructed households in Ouagadougou are legally counted on the number of iron sheets covering the indoor spaces and built on an empty plot [3]. Currently, the school construction models in use by the Ministry of Education (MENA) in Burkina Faso are also based on the use of single iron roof sheet. The functional scheme of this model is also very basic. Each time, classrooms are juxtaposed one after the other in a linear form. The most used model is the three-class model without dedicated latrine. This model was applicable to the rural context because in a village, little space was required due to the small number of children. But in Ouagadougou, simple multiplication of the basic three-class models produces very poor urban configurations for playgrounds and even to the surrounding neighbourhood. Overheating and discomforts both in exterior and interior spaces are the serious problems everywhere these models are applied. Despite of this general phenomenon of poor performances, some exceptional buildings have been achieved in West Africa since the last

ten years. They have been mostly conceived by European educated architects and financed by international funding. The results show spectacular improvements on both building qualities and environmental performances. But because of their specific imported characters in terms of expertise, investment and material provision, there has been by so far very few if not at all impacts on the rest of building practices.

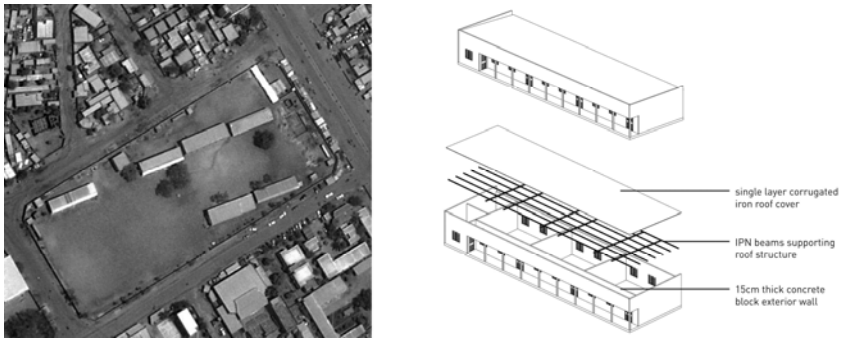

Figure 1: The existing basic model of schools applied by the Ministry of Education in Burkina Faso, aerial photo of a school in Ouagadougou and 3D scheme of the model's composition

This research, inspired by the low-tech and the light-tech thinking (K. Daniels, 1998) [4,5], defines its objective as to theorize the conceptual milestones settled by these recent projects, to seek for further maximal optimization from these existing built examples and to propose simplified building prototypes in order to have wider applications in the future.

Figure 2: The case study - CBF centre for the well-being of women, a European Commission financed and NGO supported educational building located in the northern suburb of Ouagadougou, aerial photo of the project, the exterior view and its roofing system

The main idea is to investigate in the first place some recently built educational buildings after several years of occupancy period. From the comparison between the initial intentions of the architects and the real state of use, the research attempts to find out how well each building serves the local users and whether the designed structure in use fits completely the comfort requirements. And in the second place, this research aims to propose simple procedures about enquiries and measures that could be taken later on by local actors to evaluate other educational buildings. The weak point of the basic school models built all over the country is above all the simple sheeted iron roof which is exposed to very important solar radiation. Therefore, the study finds necessary to summarize in a simple way a few guidelines on optimization principles for the roofing.

These guidelines enable the roof of an educational building to evolve from a single layered structure to a more complex system. They are applied in the construction example of the Fitima center of reference for handicapped children in Ouagadougou. At the beginning of 2010, the NGO Fitima has commissioned the authors as architects of this project. In phase with the research steps, the Fitima center offers ideal conditions to test locally different prototypes of roofing in coherence with local constraints such as feasibility and cost issues.

METHOD

The research project aims to improve the existing educational building models in Burkina Faso by new prototypes of roof systems capable of providing sufficient indoor comfort for studying activities under very hot outdoor temperature. The following steps are conducted to pursue this general objective:

- Identification of the key indoor comfort criteria

  This process consists of studying the geographical and climatic conditions of the region of Ouagadougou in order to establish a simplified check-list mainly focused on thermal and visual comforts. The high air temperature due to the excessive solar exposure is the main issue for the thermal discomfort. In traditional buildings, high inertia heavy masonry walls are used and only small openings are allowed. As consequence, only small amount of daylight comes into the rooms. This is understandable: as an important adaptation to the local climate, most Burkinabe only come back to the "case" for sleep at night. However, in the case of schools and more extensively to all educational buildings, lecture rooms and assembly rooms need reasonable amount of daylight. There is a trade-off to be found between the allowed amount of incoming daylight and the wished freshness inside without overheating by the sun. European standards of illumination in working and educational spaces (325-425 lux in French regulation of lighting for example) can obviously not be met if no additional lighting is used. The thermal comfort standard of 26°C is very difficult to achieve without mechanical systems such as air-conditioning. By discussions with the local users, consensus is established as to the acceptable temperature, the relative humidity and the lighting conditions in the study cases.

- Making software simulations by modeling the case study building envelopes using Google sketch-up, Autodesk Ecotect and Daysim dynamic daylight simulation tool

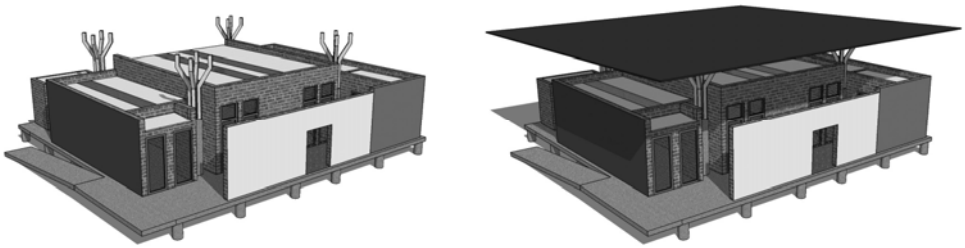

Figure 3: The case study - CBF centre for the well-being of women, 3D modelling of the educational block and daylight evaluations

The set of 3D modeling and daylight simulation tools are available to architects and relatively simple to use. The climate data are provided by Meteonorm 6.1. Further information on climate variations comes from the onsite enquiries with the inhabitants. Within the 3D models, indoors areas directly exposed to the sunlight at one moment during the day time can be easily identified by running the solar course at the typical periods of the year. These areas are minimized thanks to the large covering roof in the case of the CBF centre. However, some peripheral working spaces are still exposed to the afternoon sun, which means the risk of overheating. By simulations with the Daysim modules, the outline of lighting conditions in the main studying spaces can be evaluated. Furthermore, insolation analysis is made by month and through the year to optimize the shape of the zenithal openings in the experimental project of Fitima reference center. The best orientation for the solar PVs is also studied.

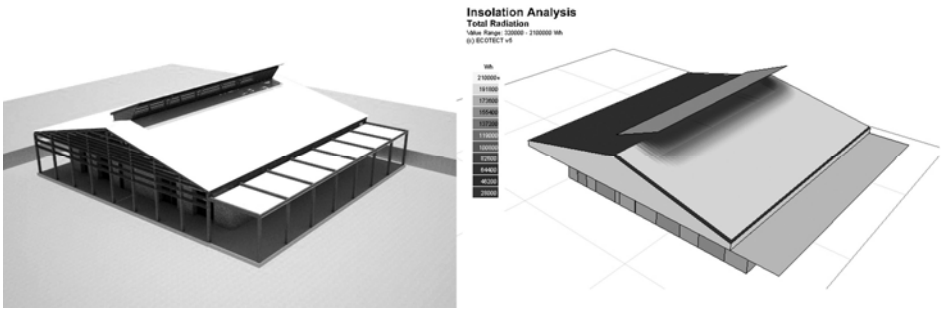

Figure 4: The experimental project - FITIMA centre of reference for handicapped children in Ouaga2000. The roof shape studies on 3D modelling and solar simulation

- Conducting field studies

  The onsite visits are necessary to truly understand the climatic constraints and to gather the occupants' points of view. With rather simple and portable instruments, temperature and humidity are measured several times a day during the visit. The daylight conditions are evaluated both by direct observation and by a light meter. The authors found out that the light contrast is important between the covered spaces and the exterior in the case of the CBF centre. Inside the working spaces, despite of zenithal openings, the light conditions at the table level are not optimized mainly because with the dust covering the flat plastic ceiling, there is no sufficient reflected sunlight coming into the room. All the observations and measures are listed in details in a written report apart. Several study trips are scheduled at different moments of the year to better understand the seasonal variations.

RESULTS

Figure 5: FITIMA centre: the aerial view of the neighbourhood, the construction site on February 2011 and the proposed optimized roof model for the educational block

As synthesis to this comparative study, three guidelines are proposed to optimize the existing conventional roof in the basic school model used today by the Ministry of Education (MENA):

- Double structure is needed; the separation of roof and ceiling is useful to avoid the direct overheating by the sun in the indoor spaces;
- Natural cross ventilation can be worked out together with optimized zenithal openings in the roof structure;
- Good inertia of walls should be obtained and lateral vertical openings on the walls should be shaded to minimize the direct sun glare.

The roof can be multifunctional by laying solar PVs with optimized orientation. In this case, the solidity of the roof and the complementary cost issues need to be studied during the conceptual stage.

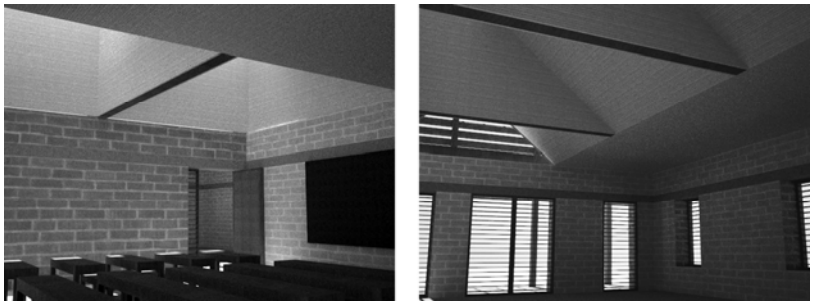

Figure 6: optimized indoor light conditions in the educational block of Fitima centre

DISCUSSION

The sustainable construction principles are currently totally absent from the construction legislation of the country of Burkina Faso. The urban regulation tools and competencies are also still very limited. The authors find out that a European Commission financed and NGO supported project like CBF centre for the women's well being is an "avant-garde" case in terms of technology input, construction know-how and work organization. On the aspect of the trade-off between the visual comfort and the thermal comfort, there is certainly still space for innovation and optimization. However, this building's global standard (study cost, expertise requirement and construction investment) is too demanding for further extensive local applications. Some materials used such as the umbrella shaped steel beams and the glass louvers are exceptional products for Ouagadougou and therefore they are not directly available on the market for other educational buildings. The other problem is if one of the parameters required for the sustainable architecture is missing during the conception and the construction process, there is no guaranty of the results at the end. For this reason, single realizations are not sufficient to improve the overall mean qualities of the constructions, guidelines should exist and simple prototypes such as a ventilated roofing system could also be alternatives. The construction case of Fitima centre of reference is an example to use at the maximum potential the available products on the market like the small section wood beams, the corrugated steel roof, the woven panels and the compressed earth bricks. Furthermore, to seek for possible ways on building innovation under the developing context, legislative insufficiency and local bureaucracy should also be taken into account.

REFERENCES

1. CraTerre in collaboration with Bureau du Projet Education III, MEBA - Ministère de l'Enseignement de base et de l'Alphabétisation de masse, Burkina Faso : Etudes sur les savoirs constructifs au Burkina Faso. CraTerre, EAG, Grenoble, 1991.
2. Houben, H., Guillaud, H.: Traité de construction en terre. Editions Parenthèses, Marseille, 1989, 1995, 2006.
3. Folkers, A.: Modern Architecture in Africa. Sun Architecture, Amsterdam, 2010.
4. Daniels, K.: Low Tech-Light Tech-High Tech, Bauen in der Informationsgesellschaft. Ed. Birkhaüser, Basel, 1998.
5. Hindrichs, D.H., Daniels, K., Eds: Plus minus 20°/40° latitude, Sustainable building design in tropical and subtropical regions. Ed. Axel Menges, Stuttgart/London, 2007.

PHENOMENOLOGICAL AND LITERAL TRANSPARENCY IN THE BUILDING ENVELOPES: THE ENVIRONMENTAL CONTRIBUTION OF THE VERANDA IN HOT HUMID CLIMATES.

G. V. Maragno[1]; H. Coch[2].

1: Federal University of Mato Grosso do Sul (UFMS). Cidade Universitária, C. Postal 549, 79070-900 - Phone: (55)6733457476 - Campo Grande, MS – Brazil.

2: School of Architecture of Barcelona - Polytechnic University of Catalonia (ETSAB-UPC). Av. Diagonal, 649, 08028 – Phone: (34)934010868- Barcelona – Spain.

ABSTRACT

The building envelope is a dynamic and selective limit between interior and exterior and may be made of opaque or transparent surfaces. Adopting the distinction described by Rowe and Slutzky, transparency can occur in a literal manner, through the physical characteristics of glass that interfere with reflections and other lighting effects; or in a phenomenological manner, through the creation of intermediate spaces that provide three-dimensionality to the envelope. Since the introduction of modern architecture, glass has been used very dominantly in architecture all over the world providing lightness and transparency. In hot climates, however, it causes problems like overheating and unwanted glare. The shading seemed to be the logical solution to these environmental problems, thus avoiding the negative effects of the incidence of direct solar radiation on the glass and maintaining its advantages by providing daylight, integrating interior and surroundings and offering endless possibilities of forms. This confirmed the importance of sun protection as one of the main bioclimatic strategies in hot climates. The envelope shading occurs through the phenomenological transparency represented by covered transitional spaces identified in the architecture of different countries over time. These spaces have the advantage of functioning as both environmental barriers and connectors working as environmental filters. In Brazil a significant number of residential projects use the solution with verandas, a kind of transitional space that provides three-dimensional transparency. The presence of a veranda has impact not only on the creation of shaded areas and sun protection of exterior walls, but also in other areas, such as daylight and natural ventilation. This paper studies the solutions of residential building envelopes distinguishing those with physical (literal) from those with phenomenological transparency (three-dimensional). Software Heliodon 2 compares the thermal radiation accumulated in the two types of solution and shows the contribution of transition spaces in hot humid climates, preserving the desirable transparency and contributing to more comfortable energy-efficient and therefore more sustainable solutions.

INTRODUCTION

The building envelopes are a dynamic and selective limit between interior and exterior and may be made of opaque or transparent surfaces (1). Since the introduction of modern architecture, glass has been used very dominantly in architecture all over the world providing lightness and transparency.

Glass is often exposed entirely, but in some cases it receives some type of solar protection. Many houses in the early twentieth century, for various reasons, were eventually fitted with glass windows protected by upper horizontal planes, like Frank Lloyd Wright houses, partly

in the Schröder House of Rietveld and even Mies' Barcelona Pavilion, which synthesizes the solution of one junction of vertical and horizontal planes. Le Corbusier, in some of his projects, protects the long window on a higher plane, but in others, as Villa Savoye, the windows are exposed despite the shaded sites in the *pilotis* and part of the terrace. Uzon (2007) notes that three of the five points of architecture described by Corbusier – the free design of the ground plan, the free design of façade and the horizontal window - were related to the façade transparency. In turn, architects such as Gropius and others influenced by the Bauhaus have continued to seek for the devices of transparency and maximum use of radiation in their projects (2).

If on the one hand the glass provided transparency and lightness for architecture, on the other, it was the source of serious environmental problems as overheating and unwanted glare. Facing some problems caused by these aspects, Le Corbusier later led architects to (re)discover the logical solution already used by the traditional architecture: the shadow (3). By avoiding direct sun on the glass, they could maintain their functional advantages of good lighting interiors and integrate the surrounding environment without losing the formal possibilities.

Regarding this issue, Rowe and Slutzky distinguished and described two forms of transparency in modern architecture: literal and phenomenological (4). The literal transparency is directly related to the physical characteristics of the material, which interfere with the reflections and other effects of light. The phenomenological transparency is related to the spatial organization and composition of solids and voids, and provides three-dimensionality to the envelope. Transparency can be an inherent quality of the material used in construction, a wall of glass or metal mesh, as well as a quality inherent to the spatial organization. Both options can work in the field of the aesthetic dimension of architecture, but with different answers. Rowe and Slutzky compare projects and attitudes of Gropius (Bauhaus, 1925-26) and Le Corbusier (Villa Stein in Garches, 1927); while Gropius was spatially aware of the nature of light and visual transparency of the glass, Le Cobusier devoted attention to flatness.

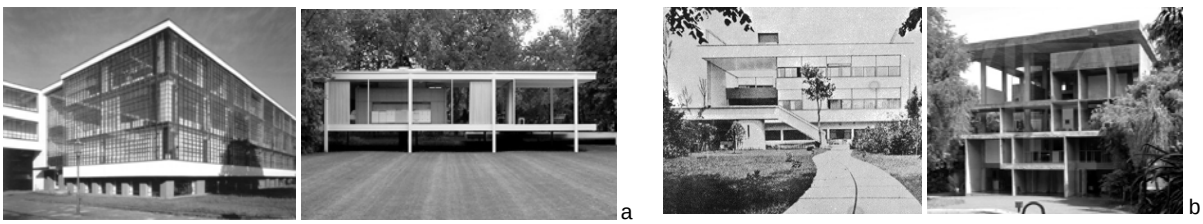

Figure 1. Examples of literal (a) and phenomenal (b) transparency on Modern Architecture.

In addition to the aesthetic dimension, the understanding of the two concepts of transparency can also be used to study environmental repercussions. This can be illustrated by the comparison of two works: the Farnsworth House by Mies (Illinois, 1946-51), considered the paradigm of transparency; and Le Corbusier´s La Villa Shodan (Ahmedabad, 1956) (4). Mies's house is a completely transparent glass box where all nature is seen from within and around, often reflecting the view from the outside, located in a temperate site, with temperatures ranging from -6 in the winter to 25ºC in the summer. La Villa Shodan, on the other hand, is characterized by a volume surrounded by a concrete structure forming a large brise-soleil, which provides shade in spaces and enclosing surfaces. It is situated in a tropical climate with temperatures ranging between 25 and 33 º C.

In the first example, with a physical transparency, the vertical glass almost disappears, giving the impression that there are only floor and ceiling, even more because the floor is lifted off the ground and enhances the image of transparency and lightness. Depth is mainly perceived because furniture and wooden inner planes exist; depending on the angle, it may reflect the interior or landscape. In the second instance, with phenomenological transparency, light and shade graduation through holes of sunscreen change image and depth throughout the day. Depending on the angle, the planes are opaque or review fragments of the landscape. The free visual and spatial organization of the three-dimensional façade is accentuated by the dynamism of the shadows.

Besides the visual effects, transparency in modern architecture has provided a symbolic character. One meaning is a result of the trend of Hegelian thought seeking for the ethereal dimension of buildings. There has also been the intention to express the ideology of progress and the ideas of hygienist principles of the early twentieth century, considering the axiom of the healthy (5). Transparency is materialized by two different aspects; one is material, the glass itself, and the other is spatially represented by the permeability and ability to visually scroll through the space.

The strength of the solutions of physical transparency, with the indiscriminate spread of glass curtain walls all over the world, under the most diverse and unsuitable weather conditions, may be found stamped on the covers of architectural publications. The phenomenological transparency, with the help of solar protection, is mainly present in the architecture more sensitive to regional and environmental values, especially in places with climates different from the cold characteristic of northern and central Europe.

From the moment the search of transparency began to be assumed in tropical and temperate climates, the need to simultaneously consider the protection of the transparent planes became clear (6). In hot climates long unprotected exposure of glass causes problems like overheating and unwanted glare. The shading seemed to be the logical solution to these environmental problems by avoiding the negative effects of the incidence of direct solar radiation on the glass and maintaining its advantages providing daylight, integrating interior and the surroundings and offering endless possibilities of forms. The *brise-soleil*, in particular, but also transitional shaded spaces were being pointed out as a strategy to obtain shading, conferring depth to the façades while shading the vertical glass surfaces.

In Brazil, a country with a predominantly warm-humid or semi-humid climate, the most common transitional space in architecture is the veranda, which has the special possibility to provide a three-dimensional transparency to the building envelope. In addition to acting as a filter between indoors and outdoors of countless environmental conditions, they represent a specific place in the dwellings (7). Although verandas are not an architectural element unique to Brazil, their considerable presence in the buildings of almost all Brazilian regions and periods of history has had a significant impact on Brazilian architecture. From an environmental perspective, the veranda can be summed up as a habitable, covered transitional space that is added to a building and open to the exterior on one or more sides. It protects both the building envelope and the space itself from rain and unwanted radiation. The veranda is ventilated with fresh outside air and illuminated with less intense light than the exterior. (8)

METHOD

The first step was to draw a comparison between the residential projects with literal transparency and phenomenological transparency in Brazil in two representative periods: the former 25 years of introduction of modern architecture in the country (1930-1955) and the

latter 25 years (1994-2009). The objects were selected from relevant architectural publications on the national scene in each period.

We developed some simulations in order to determine solar radiation impacts according to the existence or not of a veranda, the existence of the literal or the phenomenological transparency. We used a veranda model with dimensions 6.0x3.5x2.5m protruding from the building façade and without columns. In order to check its impact, this model was compared with two others: one without a veranda and another with an inserted veranda. The model was tested at different latitudes intended to represent the situations found in Brazil (0o, 15oS and 30oS, corresponding to the northern, central and southern regions). Moreover, the model was tested at summer solstice on three different periods of the day (8 h, 12 h and 16 h) and with different orientations (north, south and west). The variations were analyzed at 15oS, the average of the country, and the typical model and all the other situations of hours and orientations were compared.orientations.

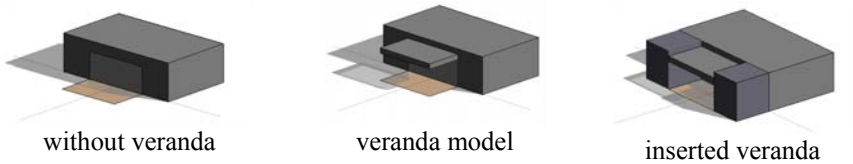

without veranda | veranda model | inserted veranda

Figure 2. The model and its variations

The model and its variations were analyzed with program Heliodon 2, version 2009, used to construct the sun paths at different latitudes and to analyze the impact of direct and diffuse solar radiation, taking into account the masking of the veranda produced by the model and its variations. The program proved to be useful in studying variations with different projections (shaded plan, stereograph, isochronous) and graphs. As it is easy to use and offers many options for analysis (an attribute highlighted by architects), it is complementary to other programs such as those used for ray tracing and radiosity (9). The calculations were carried out on two selected surfaces: the vertical surface immediately below the veranda (6x2.5 m) and the horizontal surface formed by the horizontal projection of the veranda (6x3.5 m); one representing the windows or walls, and the other representing the floor protected by the veranda. The latitudes considered for simulations are equivalent to the cities of Boa Vista (on the equator), Brasília and Porto Alegre. Figure 3 show examples of the simulation results.

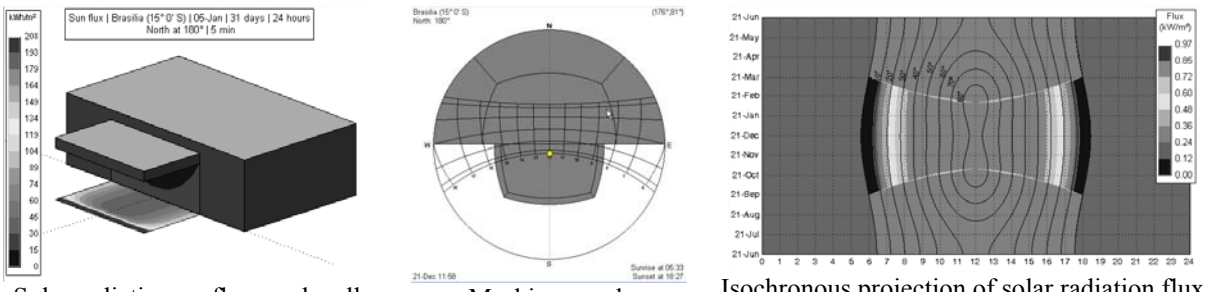

Solar radiation on floor and wall from Dec. to Jan. | Masking graph | Isochronous projection of solar radiation flux during one year

Figure 3. Examples of the solar radiation simulations on the veranda.

RESULTS

Research has suggested that the veranda is the main strategy used in the Brazilian architecture to obtain shadow on the glass surfaces, resulting in the use of phenomenological transparency on the envelopes. The veranda could be said to hold three-dimensional transparency by the depth of shaded space, by its deep shadows that protect the envelope, then allowing the use of physical transparency of a glass wall. There are not many projects with physical transparency. The most common is the veranda, but some projects studied in the research show ambiguous solutions, exemplified mainly by the outcome of the *pilotis* with deep shadows on the ground floor topped by unprotected glass boxes.

Figure 4. Examples of different models of transparencies on Brazilian architecture.

The results obtained by the simulation with Heliodon 2 (Fig. 5) show the variation of the accumulated solar radiation in a model without veranda (maximum values) to the model with an inserted veranda, passing by other types: shorter, less deep, normal model and with columns.

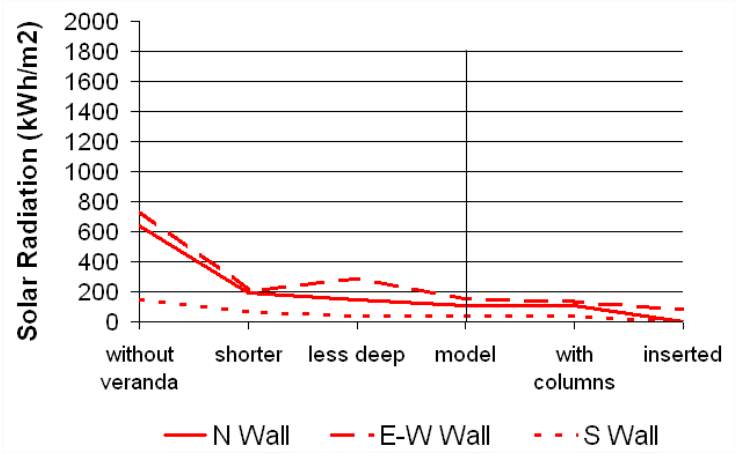

Figure 5. Overall comparison of total annual incidence of solar radiation at 15ºS on simulated verandas.

DISCUSSION

In tropical climates, warmth is usually due to a combination of high air temperature, humidity and rainfall combined with a considerable action of solar radiation. The general term "tropical" is used to describe a range of situations, as tropical climates are not homogeneous. However, in tropical zones, seasons with the aforementioned characteristics predominate. The rigorous climate of the tropics can be mitigated by two essential strategies: blocking solar radiation and ensuring air movement; in other words, by providing shade and fresh air (7). If we remember that the most significant energy input into a building is solar radiation (10), and that unshadow glass surfaces are the most vulnerable to direct sun beams, we see the reason

why the shading devices and therefore the phenomenological transparency are the primary strategy to obtain comfort in hot climates: by reducing the accumulated solar radiation.

It is possible to observe that the environmental efficiency (with respect to sun protection and consequent reduction of radiation gains) through the use of phenomenological transparency was confirmed by the simulations. We saw that the reduction of accumulated solar radiation incident on a transparent surface in comparison to a shaded surface can be approximately 75 to 100% northwards (protruding and inserted verandas, respectively); from 72 to 85% eastwards and westwards; and 90 to 100% southwards − very significant values. Thus, without compromising the transparency of the building envelopes aimed at by a considerable number of architects – and using the phenomenological transparency instead of physical transparency in hot climates, we can get more luminous and thermal comfort, more energetic efficiency, and contribute to a more sustainable architecture.

ACKNOWLEDGEMENTS

This paper was supported by the Spanish MICINN under project ENE2009-11540. The first author also thanks CAPES-MEC/Brazil (Coordenação de Aperfeiçoamento de Pessoal de Nível Superior) for supporting his doctoral research at UPC.

REFERENCES

1. Ganem, C.; Coch, H. Building envelope design for a zero energy response. A: "PLEA 2004 Proceedings: Built environtments and environmental buildings". M de Witt / Technische Universiteit Eindhoven, 2004, p. 867-872.
2. USÓN GUARDIOLA, E. *La Nueva Sensibilidad Ambiental en la Arquitectura Española*. Barcelona: Clipmedia, 2007.
3. ROTH, L. M. Entender la Arquitectura. Barcelona: Gustavo Gili, 1999.
4. SUAREZ, M. Límites: transparencias y espacios intermedios. Documento electrónico. Disponible en: http://issuu.com/mayasuarez/docs/limites. Consulted in October 2009.
5. DUARTE, R. “Sentido y Significado de las Transparencias en la Arquitectura”. In: NEVES, J. M. (dir.). Transparências = Transparências. Casal de Cambra: Caleidoscópio, 2006.
6. MAHFUZ, E. Transparência e sombra: O plano horizontal na arquitetura paulista. *Arquitextos*, São Paulo, 07.079, Vitruvius, dez 2006 <http://www.vitruvius.com.br/revistas/read/arquitextos/07.079/284>. Consulted in september 2009.
7. MARAGNO, G.; COCH, H. Impacts of form-design in shading transitional spaces: the Brazilian veranda. Proc. of the CESB 10 Conference, pp 01-07, Prague, 2010.
8. MARAGNO, G.; COCH, H. Integrated environmental response of shaded transitional spaces in hot climates: the design of the Brazilian veranda. Proc. of the PALENC 2010. p. 1-8, Rhodes Island, 2010.
9. BECKERS, B.; MASSET, L. Heliodon 2: Guía del usuario. Liege: Barcelona: 2009. Disponible en: www.heliodon.net. Consulted in october 2009.
10. SZOKOLAY, S. Introduction to Architectural Science: the basis of sustainable design. Oxford: Elsevier: Architectural Press, 2008.

TEXTILE MEMBRANES AS BUILDING ENVELOPE

Leonardo Marques Monteiro, Marcia Peinado Alucci

Department of Technology, Faculty of Architecture and Urbanism, University of Sao Paulo, Rua do Lago, 876, Cidade Universitaria, 05508-080, Sao Paulo, Brazil, leo4mm@gmail.com

ABSTRACT

The objective of this research was to verify which textile membrane would give better environmental performance, in terms of thermal comfort, as an envelope of an exposition building in the city of Sao Paulo, the greatest Brazilian metropolitan area with over eighteen million inhabitants. The method adopted was based on simulations using a computational application that allows choosing membranes and sizing them for tensioned structures in order to provide thermal comfort. The computational modeling consists of: thermo-physiological balance; radiation model; calculation of sky temperature following the Bliss model; calculation of surface temperatures of ground, vegetation and membrane. The Heat Load index was adopted for assessing thermal comfort. The model validation was done through positive comparisons with results of empirical data gathered in field research. The membrane database was developed through: field researches of solar transmittance using Kipp & Zonen CM6B piranometer; field researches of solar absorption using Type J thermo couples and globe thermometers; and lab researches using Cary 500 UV-Vis-NIR spectrophotometer. Different configurations with single and double membranes, of different types, were tested. The assessments are done hourly for a typical day of each month of the year, for thermal performance. The process of simulation assessed the comfort in the environment and aided choosing and designing the membrane solution for the envelope of the building.

INTRODUCTION

This study verified two office buildings in the metropolitan area of the city of São Paulo, Brazil. Both of them have the same plate and number of stories, but one is oriented north-south, whilst the other is east-west. The main façades are all glazed without any kind of solar protection. Considering that glazed façades are responsible for solar heat gain and penetration of direct sun radiation on people, work plan and equipment, this study was performed in order to obtain the design of a system of sun protection and its check in terms of reducing heat load and its possible effects in the energy consumption of air conditioning system. Different solutions were checked and compared, including coated film, screen and brise-soleil. In order to perform simulations of thermal energy, an annual weather database on hourly basis was used. Given the lack of specific data on the place where the buildings are under study, the availability of existing data was considered, focusing on their reliability and proximity to place of study. Thus, the database project Solar and Wind Energy Assessment Resource [1] was chosen to be used. The database refers to the meteorological station of Congonhas [2], S23°37',W46°39',GMT-3.0,803M above sea level, standard atmospheric pressure of 92043Pa. Data were collected from 1973 to 2002, having been treated statistically to the creation of one year from the months typically representative of climatic conditions of the period.

SOLAR ANALYSIS

In the solar analysis, firstly, the need for masking the sky was determined, for each of the façades involved, in order to take advantage of daylighting and preserve the maximum possible visibility to the outside, determining the dimensions of the brise-soleils.

The mask proposed for the south façade allows the penetration of sun in the summer solstice after 18:30. Considering the conditions of the surroundings (other buildings), a considerable part of the building will not even receive this incidence. Moreover, that time is outside the period of

occupation provided by the client (Monday to Friday, from 8:00 to 18:00). In geometric terms, we have then an angle β = 55 ° (angle of vertical brise protection in relation to the normal of the facade) and about an angle α = 75° (angle of protection of the brise horizontal to the horizon). In fact, the solution of brise-soleil in the south façade, as will be seen, needs no horizontal plates, only one grid for each floor, which serves as the "closure" to the vertical brise and allows the maintenance of the façade. As can still be seen from Figure 1, the mask proposed for the north facade allows the entrance of the solar rays especially during the fall and winter. In the limit of the winter solstice (22/06), the penetration of direct solar radiation is from 6:45 until 12:30. In the months before and after (from early April until mid-September) the period that receives direct solar radiation decreases, to the extent that it penetrates only a small slit for a moment at 8:20. In geometric terms, it has remained the same angle β = 55° (angle of vertical brise protection in relation to the normal of the facade) in order to standardize the two solutions brises in the north and south facades, also using the same solution grid to maintain the facades. However, due to higher solar incidence, an angle α = 75° (angle of protection of the horizontal brise to the horizon) was determined. Thus, in the south façade vertical brises are enough for solar protection, whilst in the north facade horizontal brises are also required.

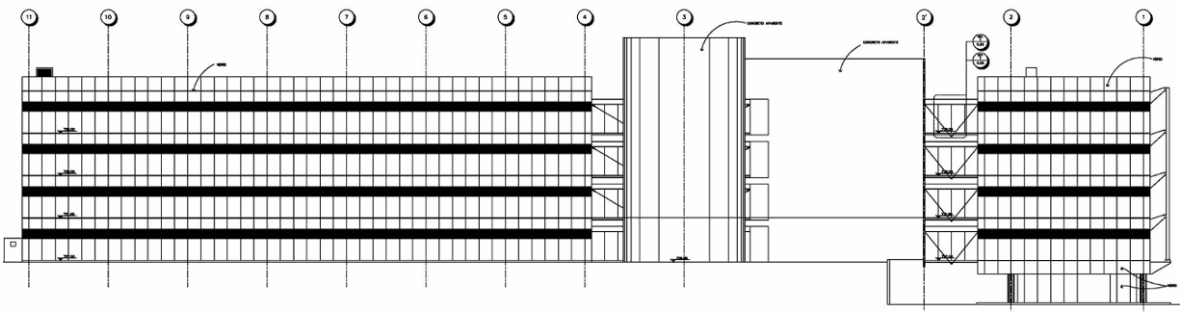

Figure 1. Elevation of North Façades, with Horizontal Brise-Soleil (black stripes) and Vertical-Brise Soleil (thin vertical lines)

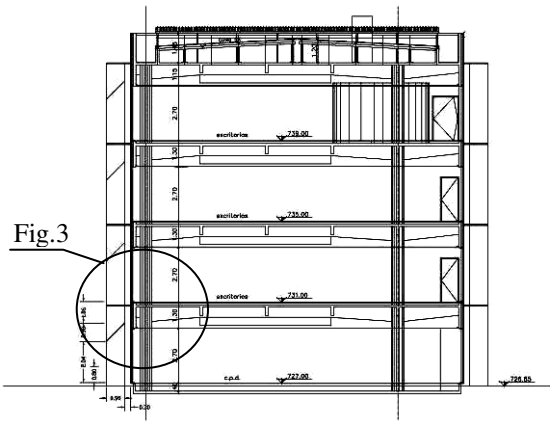

Figure 2. Section with the brise-soleil solution Façade)

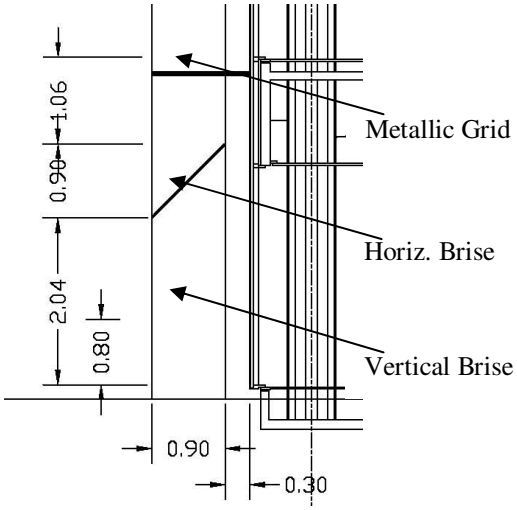

Figure 3. Detail with the brise-soleil (North

The next studies aim to check the penetration of direct solar radiation in the openings of different façades, respectively for the case of winter and summer. The goal was to compare the penetration of direct sun penetration to the current situation and the situation with the use of the proposed systems of brise-soleils. Figure 4 shows the results.

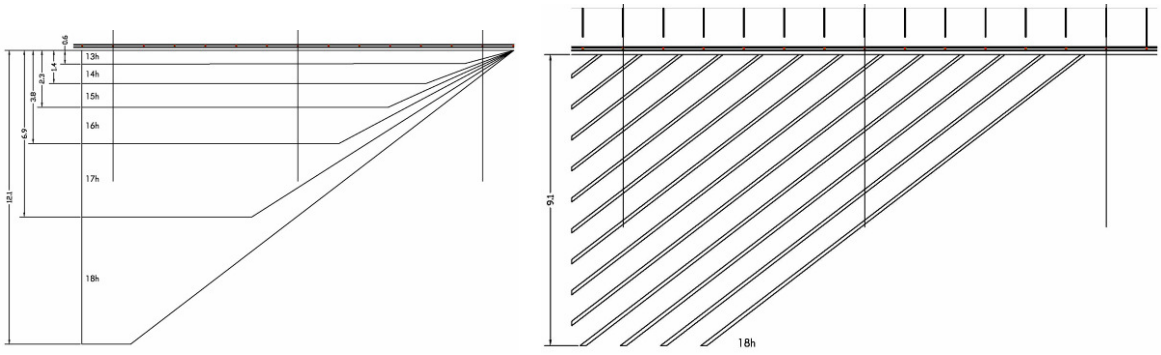

Figure 4. Solar penetration in the summer (South Façade) without brise-soleil (from 13h to 18h) and with brise soleil (only at 18h).

DAYLIGHTING ANALYSIS

For the quantification of the daylighting system, the availability of daylight was considered in the order of 20,000 lux for the frequency of occurrence of 67% of daylight hours of the year in the city of São Paulo. To calculate the Daylight Factor (DF), the celestial component was considered, the external and internal reflection components being the sum of these components weighted by frame, maintenance and the light transmission of glazing coefficients [3]. The following spots (see Table 1) were studied to determine the values of sky component and availability of daylight.

Table 1: Results of Daylight Factor and iluminance in different spots of the two buildings

	North Façade (2m from façade)		North and South Façades (8,2m from façades)		South Façade (2m from façade)	
Building A	DF	Ep	DF	Ep	DF	Ep
Actual	5,7%	1140 lx	3,3%	660 lx	-	-
Film	3,8%	760 lx	2,2%	440 lx	-	-
Screen	3,0%	600 lx	1,7%	340 lx	-	-
Brise-Soleil	2,8%	560 lx	2,0%	400 lx	-	-
Building B						
Actual	5,2%	1040 lx	1,6%	320 lx	4,7%	940 lx
Film	3,5%	700 lx	1,1%	220 lx	3,1%	620 lx
Screen	2,6%	520 lx	0,8%	160 lx	2,3%	460 lx
Brise-Soleil	1,5%	300 lx	1,1%	220 lx	1,9%	380 lx

As can be seen, in building A, the three solutions provide sufficient daylight, for office activities, considering the NBR 5413[4], which recommends values between 300 and 700 lx, and one may note that the three solutions satisfactorily meet this criterion in situations of the studied sky conditions. With respect to Building B, the three solutions also comply with that in the facades, with values between 300 and 700 lx. Note that the dimensioning of horizontal plates in the previous topic was done exactly based on meeting the criterion of 300 lx in this situation. Regarding the situation of the inner situation in building B, it should be noted that the results have been between 160 and 220 lx. They appear quite favourable since, although not sufficient for the practice of labour activities, they are sufficient for general lighting or for lighting for circulation. Finally, we emphasize once again that the adoption of the value of 20,000 lx refers to a situation of overcast or partly cloudy skies and when there is sun exposure, the availability of daylight will be up to five times greater than that shown in the results. Thus it is considered that the intensity and distribution of solutions of daylighting proposals are appropriate, but may reach values much higher than necessary on a clear day. Thus, the brises solution proved to be more advantageous to minimize the situations of glare by blocking the direct solar radiation, as shown earlier in this article.

EXTERIOR VISUAL ACCESS

Among the three solutions under verification, the application of coated film is the one that least affects the visibility of the exterior, just causing some changes in terms of tone colours. The use of the screen remains visible outside, but its quality is impaired, reducing, for example, recognition of details of the external environment. The option of brise soleil also significantly alters the

external visibility, but in a different manner. The visibility is reduced vertically by the lower horizontal edge of the plates (which is above the eye level of people), while the presence of vertical elements segments the visual as a whole. These consequences can be seen in the drawings presented earlier in this article, when considering the solutions proposed for the brise soleil.

THERMAL ENERGY ANALYSIS

Thermal energy simulations, based on the annual climate database, aimed to compare the reduction in heat load, and thus the energy consumption of the system of artificial air conditioning, for different interventions in the buildings (Table 2).The internal heat sources considered were: A) Occupation: According to data supplied by the client, Building A has capacity for 362 people and Building B for 370 people. Thus, considering the activity of office, which has metabolic rate of 130W, in which 65W are sensible heat and 65W are latent heat, the internal heat load factor was calculated, resulting in the 7W/m^2 for sensible heat and 7W/m^2 for latent heat. B) Equipment: Specific data regarding the thermal loads of equipment were provided only to a lab of the 4th floor of Building A. Thus, for the generalization to other environments, it was assumed that each user has a computer, with an estimated load of 120W, resulting in 13W/m^2 sensible heat. C) Lighting: considering all the fixtures, lamps and their powers, it resulted in 13.5 W/m^2; considering the whole lighting system, ie, the power of the lamps, plus their control equipment used in conjunction (ballast, ignitor, transformer, etc), it resulted in 21W/m^2. Once the computer simulations finalized, considering all the hygrothermal trades of energy balance, Tables 4 and 5 show the thermal loads to be removed respectively from Building A and B, considering the system of artificial air conditioning operating in a way to provide environmental conditions with an air temperature at 24°C, relative humidity 50%, Monday to Friday, from 8h to 18h, with a total of 2.600 conditioning hours per year (approximately 60% of daylight hours of the year).

Table 2: Material properties used for the annual hourly basis thermal energy simulations

Components: façades, ceilings, and pavements	Thermal conductibility λ (W/mºC)	Density d (kg/m^3)	Specific heat c(J/kg^{o}C)	Global Heat transmission U (W/mºC)	Solar absorption α	Emissivity ε
Exposed concrete	1,65	2200	1005	3,196 (↔)	0,65	0,90
Structured concrete	1,75	2400	1005	3,226 (↔)	-	-
Corrugated metal roof	43	7800	500	4,759 (↓) 7,137 (↑)	0,53	0,25
Epoxy	0,31	1381	1600		0,60	0,90
Concrete	1,28	2000	1005		-	-
Air layer	-	-	-	0,391 (↓) 0,413 (↑)	-	-
Glassfiber	0,04	64	754		-	-
Veil of white glass	-	-	-		0,40	0,90
Carpet	0,06	186	1360		0,60	0,90
Felt	0,04	150	754		-	-
Concrete	1,28	2000	1005	0,384 (↓)	-	-
Air layer	-	-	-	0,405 (↑)	-	-
Glassfiber	0,04	64	754		-	-
Veil of white glass	-	-	-		0,40	0,90

ENERGY SAVINGS

In order to verify the savings in the consumption of air conditioning the coefficient of performance (COP) of air conditioning system and the pricing adopted by the energy supplier are required. According to available data, the value of the contract price is R$0.256/kWh. (1R$=0.54US$= 0.37 EURO, in Nov 10th 2010). The HVAC in Buildings A and B is composed of a central chilled water of 360 TRs, supplied by 4 refrigeration units (chillers) with air condensers and scroll type compressors. The expansion system is indirect, by cold water and fancoils, with no cooling towers. The chillers are Trane, model CGAD090-90TR. The cold water at 5°C is pumped to the buildings for bombs with spin control to keep the pressure at 6 kg/cm². Each floor has two fancoils, except the ground floor of Building A and the 1st floor of Building B that have only one each. Adjustment of temperature environments is done by controlling the volume of air blown by

flow control valve installed in the distribution pipeline. The return air is full of the liner, or without ducts to the fancoil. Considering the description provided by the client, a coefficient of performance of the system COP = 3.0 was adopted.Considering an area of 3500m^2 per building, the values, presented before in this article, can be applied to forecast electricity consumption for artificial lighting system and equipment, considering the period from 8 to 18h from Monday to Friday throughout the year. Tables 3 and 4 present the results.

Table 3. Annual Energy Costs and Savings for Building A (1R$=0.56US$=0.39EURO, in Dec 15th 2009)

	Actual	%	Film	%	Screen	%	Brise	%
HVAC	R$ 79.226	33,3	R$ 78.020	33,0	R$ 77.381	32,8	R$ 76.403	32,5
Lighting	R$ 97.844	41,2	R$ 97.844	41,4	R$ 97.844	41,5	R$ 97.844	41,7
Equipments	R$ 60.570	25,5	R$ 60.570	25,6	R$ 60.570	25,7	R$ 60.570	25,8
TOTAL	R$ 237.640		R$ 236.434		R$ 235.795		R$ 234.817	
Reduction	-		0,5%		0,8%		1,2%	
Savings			R$ 1.205		R$ 1.845		R$ 2.823	

Table 4. Annual Energy Costs and Savings for Building B (1R$=0.56US$=0.39EURO, in Dec 15th 2009)

	Actual	%	Film	%	Screen	%	Brise	%
HVAC	R$ 79.894	33,5	R$ 73.508	31,7	R$ 70.181	30,7	R$ 67.038	29,7
Lighting	R$ 97.844	41,1	R$ 97.844	42,2	R$ 97.844	42,8	R$ 97.844	43,4
Equipments	R$ 60.570	25,4	R$ 60.570	26,1	R$ 60.570	26,5	R$ 60.570	26,9
TOTAL	R$ 238.308		R$ 231.922		R$ 228.595		R$ 225.452	
Reduction	-		2,7%		4,1%		5,4%	
Savings			R$ 6.386		R$ 9.714		R$ 12.856	

THERMAL COMFORT ANALYSIS

For the evaluation of thermal comfort, ASHRAE 55 [5] was used. Thus, considering the climate-controlled environments, PMV model was applied, which considers the air temperature, relative humidity, air velocity, mean radiant temperature, user activity and type of clothing. Considering the studies that were conducted, the following variables were considered for verification of thermal comfort: air temperature = 24°C (kept constant by the system of artificial air conditioning); Relative humidity = 50% (kept constant by the system of artificial air conditioning); Air velocity <0.2 m/s (at the user level, given the conditions of system); metabolic rate = 1.3 Met (rate of metabolic heat on the daily activities of office); clothing insulation = 0.5 clo (summer clothing: pants and social shirt). Therefore, the mean radiant temperature remains to be determined to see if the conditions are, or not, providing comfort. These values were obtained by the performed thermal energy simulations. As a result, the curves of mean radiant temperature for the first and fourth floor of each building proved to have lowest and highest values, whilst the results of the second and third floors are intermediate to the previous curves. Thus, the results are going to be considered in terms of the extreme cases. For the given conditions was calculated the operative temperature, which, for the typical situation in question, was estimated from average of the mean air temperature and mean radiant temperature, as recommended by the standard. Performing the procedures prescribed by the standard, it is observed that for the conditions listed above, the operative temperature which provides comfort conditions (percentage of people dissatisfied with the environment in general, considering the criteria of less than 10%) is ≤ 27.2ºC (represented by the strong black line in graphics of operative temperature).

SUMMARY

Table 5 presents a synthesis of the results found considering the solar and daylighting analysis, exterior visibility, energy saving and thermal comfort for different solutions (coated film, screen and brise-soleil) for the façades of the two different studied buildings. Considering the results presented, the solutions found to the first building (facing mainly North and South) show results with small reductions in energy consumption for air conditioning, respectively 1.5%, 2.3% and

3.6% for solutions with coated film, screen and brise-soleil, whereas estimates total energy reduction in respectively of 0.5%, 0.8% and 1.2%. When considering the results for the second building (facing mainly East and West), the results show more significant reductions in energy consumptions for air conditioning: 8.0%, 12.2% and 16.1%, estimating total energy reduction for respectively of 2.7%, 4.1% and 5.4%. Considering the results presented, the coated film solution provided an excessive daylight penetration, although it does not alter the exterior visibility. On the other hand, it provides very low to low energy savings and worse thermal comfort conditions than the actual ones. The screen solution provides satisfactory illuminance levels and reasonable homogeneity, but with some alterations in the exterior visibility. Energy savings can be very low to considerable, providing better thermal comfort conditions than the current ones.

Table 5. Final results for solar, daylighting, exterior visibility, energy saving and thermal comfort (R$=0.54US$=0.37EURO, in Nov 10th 2010)

	Film	Screen	Brise-Soleil
Solutions	Prestige Line Model P70 Brand 3M	Generic (to be produced) Luminuous transmission and solar transmission: 50%	According to drawings presented in this article
Daylighting	Satisfactory to excessive Reasonable homogeneity Façade: North, Centre, South Bldg.A: 760, 440, - lx Bldg.B: 700, 220, 620 lx	Satisfactory Reasonable homogeneity Façade: North, Centre, South Bldg.A: 600, 340, - lx Bldg.B: 520, 160, 460 lx	Satisfactory Adequated homogeneity Façade: North, Centre, South BlocoA: 560, 400, - lx BlocoB: 300, 220, 380 lx
Exterior Visibility	Practically no alteration	Alteration in quality	Alteration in quantity
Energy Saving	Bldg.A: Very Low Bldg.B: Low HVAC Energy Saving Bl.A: 1,5% Bl.B: 8,0% Total Energy Saving Bl.A: 0,5% Bl.B: 2,7% Annual Financial Saving Bl.A:R$1.205 Bl.B:R$6.386	Bldg.A: Very Low Bldg.B: Considerable HVAC Energy Saving Bl.A: 2,3% Bl.B: 12,2% Total Energy Saving Bl.A: 0,8% Bl.B: 4,1% Annual Saving Bl.A:R$1.845 Bl.B:R$9.714	Bldg.A: Very Low Bldg.B: Considerable HVAC Energy Saving Bl.A: 3,6% Bl.B: 16,1% Total Energy Saving Bl.A: 1,2% Bl.B: 5,4% Annual Financial Saving Bl.A:R$2.823 Bl.B:R$12.856
Thermal Comfort	Worse than actual (heating of glasses due to greater solar absorption of the film) Discomfort (hot summer): Bldg.A Pav1: 16h Bldg.B Pav4: 13h to 18h	Better than actual (cooling of glasses due to their partial shading by the screen) Desconforto (hot summer): Bldg.A Pav1: None Bldg.B Pav4: 14h	Far better than actual (better cooling of glasses due to their shading by the brises-soleil) Discomfort (hot summer): Bldg.A Pav1: None Bldg.B Pav4: None

Finally, the brise-soleil solution proved to be the most adequate one in the relation between energy and environment. It provides satisfactory illuminance levels and adequate homogeneity, although reduction in exterior visibility. Energy savings vary as well from very low to considerable, but are the most significant among the three studied solutions and, considering thermal comfort, it provides the better results. As a conclusion, based on the results found for the specific case studies, despite the difference in the amount of energy savings in each building, in both of them the results point to the coated film as the weakest solution, the screen as a quite good one, and the brise as the most adequate of them.

REFERENCES

1. SWERA 2004. Solar and Wind Energy Assessment Resourse. Available at: http://swera.unep.net.
2. IAG-USP. 2007 Laboratório de Micrometeorologia. São Paulo: IAGUSP, Available at: www.iag.usp.br/meteo/labmicro.
3. ALUCCI, M. P. 2007. Manual para dimensionamento de aberturas e otimização da iluminação natural na arquitetura. 1. ed. São Paulo: FAUUSP.
4. ABNT 1992. NBR 5413. Interior lighting. Associação Brasileira de Normas Técnicas.
5. ASHRAE. 2004. *ASHRAE 55-2004* Thermal Environmental Conditions for Human Occupancy. Atlanta.

THERMAL EFFECTS OF CREEPERS AND TURFGRASS WALL CLADDING ON BUILDING ENVELOPE

U. Mazzali[1]; M. Olivieri[2]; F. Peron[1]; V. Tatano[1];

1: Università IUAV di Venezia, ex Convento Terese, Dorsoduro 2206, I-30123 Venezia, Italy

2: Faculty of Architecture, University of Ferrara, Italy

ABSTRACT

Climate is getting hotter over the last two decades over Europe and North America. Especially in the urban area the air temperature has been growing at a faster rate (Urban Heat Island UHI) leading to greater use of air-conditioning and energy demand. One possible strategy to lower ambient temperature is to increase the amount of greenery in the city. In this context we have assisted recently to a rediscovering of covering of buildings envelopes by green facades and green roof. Actually green facades may consist in traditional creepers or in more technological green vertical claddings. In this paper the authors report the results of two monitoring campaigns, carried out in Italy in 2009 on a traditional greenery covering and on a vertical modular turf cladding .The aim was to better understand the thermal effect of the green cover on walls and be the starting point for a more detailed investigation on the effects on energy consumptions for summer air conditioning.

Two monitoring campaigns have been performed during warm summer periods and show that relevant decreases in surface temperatures can be reached by the use of creepers and vertical turf claddings as shading devices for building surfaces. In the first case-study located in Venice (Veneto, North Italy) were studied two external surfaces West and South oriented covered by Parthenocissus and Jasminum. The external surface temperature of the bare wall was 11°C higher than the covered one for the south oriented wall, during a sunny day. The second case-study was located in Pisa (Tuscany, Central Italy) concerns a SouthEast oriented test wall with turfgrass cladding. Reductions of around 10°C on building surface temperatures have been measured also in this test facility confirming the huge shading effect of the green covers directly related with high values of solar radiation during sunny days. A specific simplified index called Green Factor has been assessed and validated for the natural creeper covered wall, in order to foresee surface temperatures of the green wall.

INTRODUCTION

The aim of this work is to provide field measurement data about thermal behaviour of building envelopes covered by green facades. Actually green facades may consist in traditional creepers [1] [2] [3] or in vertical green technological claddings [4] [5]. The two monitoring campaigns have been performed in 2009 in order to better understand the effect of the green cover by a traditional greenery and by a innovative vertical turf cladding. The first field measurement concerns a residential building in Venice with two external surfaces covered by creepers. The second field measurement, located in Pisa, concerns a test wall with turfgrass cladding. Both the monitoring campaigns used the same instruments. For surface temperature measurement were utilized platinum resistance sensor (PT100) with an accuracy of 0,15°C. Air conditions indoor and outdoor were recorded by mini-dataloggers (TinyTag Ultra) with temperature and humidity sensors. Total irradiance on a plane surface was recorded by Kipp&Zonen CM6B Pyranomter with a spectral range from 305nm to 2800nm. After the monitoring campaign, the result's analysis has started and some key days have been

identified during the monitoring period, to better understand the green facade thermal performance related to the climatic variable course, e.g. during the day with the strongest solar radiation. Some interesting considerations have been carried out about surface temperature reduction during sunniest and cloudiest day for both residential building surfaces and test wall surfaces.

FIELD MONITORING: CASE STUDY ONE

The first field campaign in Venice regarded the surface temperature monitoring of a West oriented wall covered by Parthenocissus tricuspidata and a South oriented wall covered by Jasminum. Each one are very common greenery at Italian latitudes, they have a deciduos seasonal cycle and are suitable for covering half sun exposed and sun exposed walls respectively. Building walls are made up of an internal plaster layer 1cm thick, and of a brick external layer of 25cm. The monitoring period go on from 17th of July to 31st of August. Four temperature probes on each wall are coupled as follows: the first couple has been positioned on the inside surface and on the outside surface of the bare portion (without creeper cover) of the wall and the other couple has been positioned on the inside surface and on the outside surface of the creeper covered portion of the wall. Were also monitored internal and external air temperature and humidity. Some key days have been selected to better understand thermal behaviour of the covered walls under strong climatic conditions. The identified key days are: the day with the highest irradiation values (August, 5th), the day with the lowest irradiation values (August, 3rd). It is evident, from the graph in figure 1 (on the left), that, during the day with highest irradiation, the external surface temperature of the South bare wall reaches 11°C higher than the covered portion. The internal surface temperatures behaviour is similar between the bare portion and the covered portion, with the bare surface temperature slightly higher, 1,8°C, than the covered one during the night. The time lag of the building walls is 4 hours for the bare one and 7 hours for the covered one. Similar considerations could be done about West oriented wall surface temperatures, shown in figure 1, on the right. During the day the external surface temperature of the West bare wall is 5°C higher than the covered portion. During the night the external surface temperature of the bare wall is lower than the temperature of the covered one. Probably this is related to radiative heat transfer with the sky.

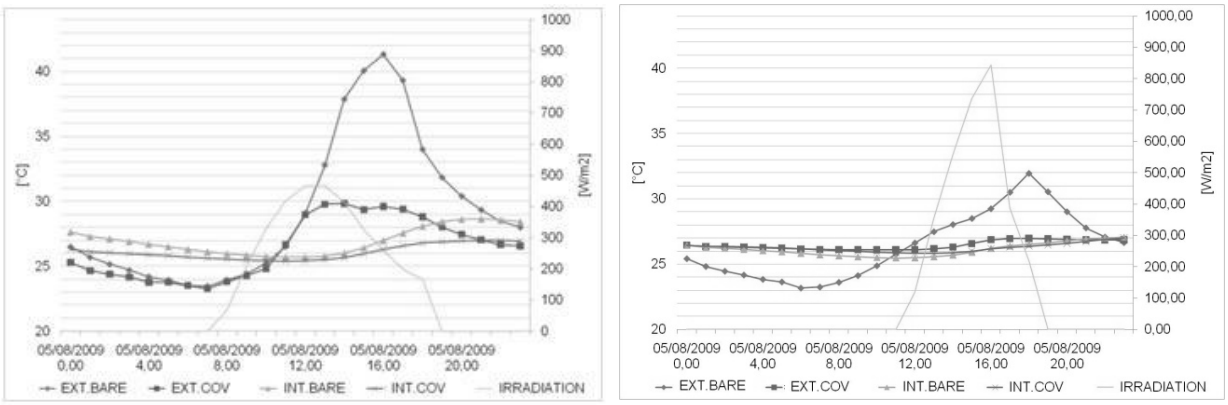

Figure 1: sunniest day surface temperatures on the South wall (left) and West wall (right)

Again, internal surface temperatures are very similar both for bare portion of the wall and the covered portion of the wall. A similar behaviour is confirmed also for the day with the lowest irradiance. External surface temperature differences between the bare portion and the covered portion are shown in figure 2 for the South wall (left) and for the West wall (right). A positive value of the temperature difference means that the external surface temperature of the bare wall is higher than the external surface temperature of the covered one, being $\Delta T = T_{eb} - T_{ec}$

with T_{eb} = surface external temperature of the bare wall and T_{ec} = surface external temperature of the covered one. The south wall shows an external surface temperature of the bare wall always higher than the covered one. The only ΔT negative value is during the day with the lowest level of irradiation, in which the radiation collected by the wall is not enough to significantly heat the wall. Thus, during night, the bare portion cooled itself by radiation towards the sky more than the covered one. ΔT values reach 12°C 13°C during days with high values of irradiation. This means a very high level of shading of the wall by the green cover. On the West wall the ΔT behaviour is different from the South one. The external surface temperature of the bare wall is always higher during the day. However, during night, the surface temperature of the bare wall is always lower than the covered one. This behaviour is confirmed both in sunny and cloudy days, this means that it is not related with solar irradiation. This particular behaviour of the West wall could be explained through an obstruction analysis of the measurement field near the probes.

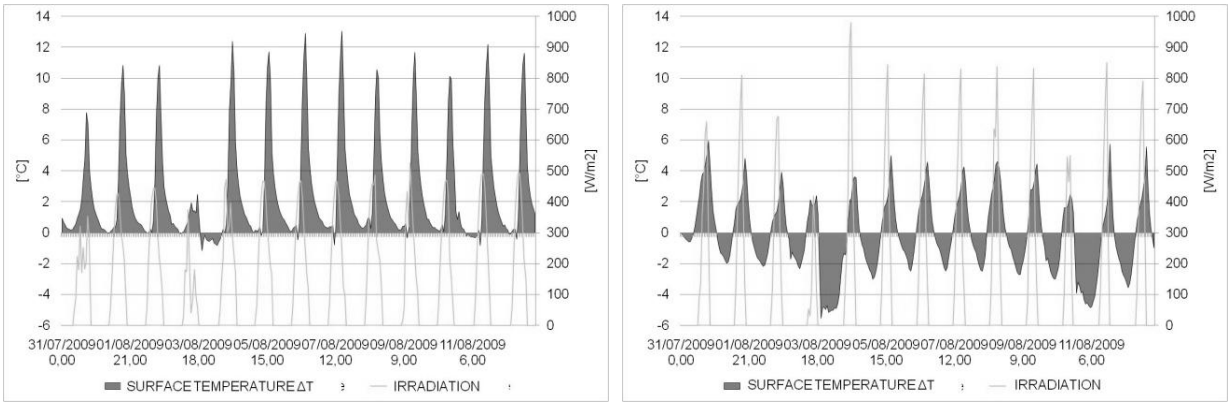

Figure 2: external surface temperature difference on South wall (left) and West wall (right)

It is possible that the presence of buildings or trees near the West wall reduces the possibility for the wall to heat itself during the day. This lower heat absorption allows to the bare wall to cool itself by radiation during night reaching temperature values lower than the covered wall. From another point of view the lower bare wall surface temperatures show that the covered portion has a limited heat transfer by radiation. This could be due to a higher density of the shading creeper on the west wall.

FIELD MONITORING: CASE STUDY TWO

The second monitoring campaign concerns a SouthEast oriented test wall located in San Giuliano Terme (Pisa, Italy), at Pacini nursery, with a turfgrass architectural wall cladding, as shown in figure 3, on the left. The test facility is 10,80 m long, 2,80 m high and is made up of 126 recycled polypropylene panels in which many type of turf grasses are pre-sown. The different kind of turf are: Zoysia matrella 'Zeon', Zoysia tenuifolia, Zoysia japonica 'El Toro', Cynodon dactylon X Cynodon trasvalensis 'Patriot', Stenotaphrum secondatum, Dicondra, Paspalum vaginatum, Cynodon transvalensis. The temperature monitoring for the covered portion of the test wall has been performed just next to the Dicondra turfgrass. Dicondra is an herbaceous plant suitable to all Mediterranean latitudes. It prefers warm climate and it is much in demand for low maintenance turf-grasses, thanks to its characteristics of low growth, and low irrigation demand, it doesn't grow above 4cm – 5cm. Monitoring campaign has lasted 4 weeks from September 5th, to October 2nd. The South-East orientation doesn't offer the best irradiance conditions, but relatively to the site availabilities, it was the best solution. Four probes have been positioned on the bare wall side of the test wall, with probe T3 on the internal wall surface, and probe T1 on the external wall surface (figure 4). Other six probes

have been positioned on the Dicondra covered side of the test wall, and precisely on the internal surface (probe T9), inside the cavity, as shown in figure 3 (on the right), between the wall and the polypropylene panel (probes T5,T6,T7), and just next the Dicondra under the turfgrass (probe T8). The T4 probe has been positioned to monitor internal air temperature.

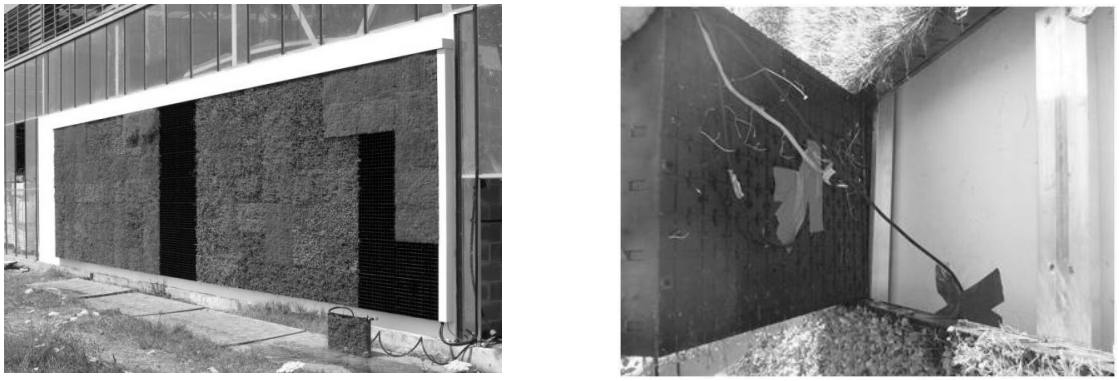

Figure 3: turf cladding system and probes positioning

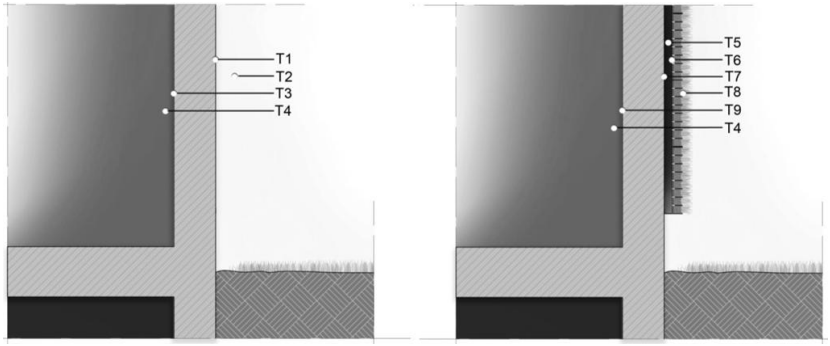

Figure 4: PT100 probes positioning. Bare wall section(left), covered wall section (righ).

Also in this case, as key days were selected the highest irradiation (September, 12nd) and the the lowest irradiation day (September, 14th). In figure 5 on the left is shown the day with the highest values of irradiation, it is clear that external surface temperature of the bare wall depends on solar irradiation. The higher the value of irradiation the higher the external surface temperature. Moreover, during night the external bare surface temperature is lower than the covered one. This is probably due to the protection effect of the polypropylene panel which reduce the possibility of the wall to loose heat by radiation towards the night sky. The time lag of the bare wall is 10 hours and the time leg of the covered wall is 5 hours. During the day with the lowest value of solar irradiation the external surface temperature of the bare wall is always lowest than the covered one. A reduced irradiation doesn't allow the bare wall to heat enough itself, thus the surface temperature of the covered side of the test wall is warmer. This happens also to internal surface temperatures which are higher for the covered portion of the wall. The internal and external surface temperature trend is very clear if related to solar irradiation during an entire week. During the hottest week, from 21st to 27th of September, as shown in figure 6, it is evident that the external surface temperature of the bare wall is always higher, during the day, than the covered portion of the wall. The ΔT reaches values of 10°C – 12°C. This temperature behaviour reverses its trend during night when the ΔT value is negative. This means that the covered wall keeps its temperature at higher values. A similar trend could be seen for internal surface temperature values with a time lag of 6 hours and with ΔT reduced at 0,5°C 1,5°C. During the coldest week, from 14th to 20th of September, the

temperature trend doesn't change and during diurnal hours the surface external value of the bare wall is higher.

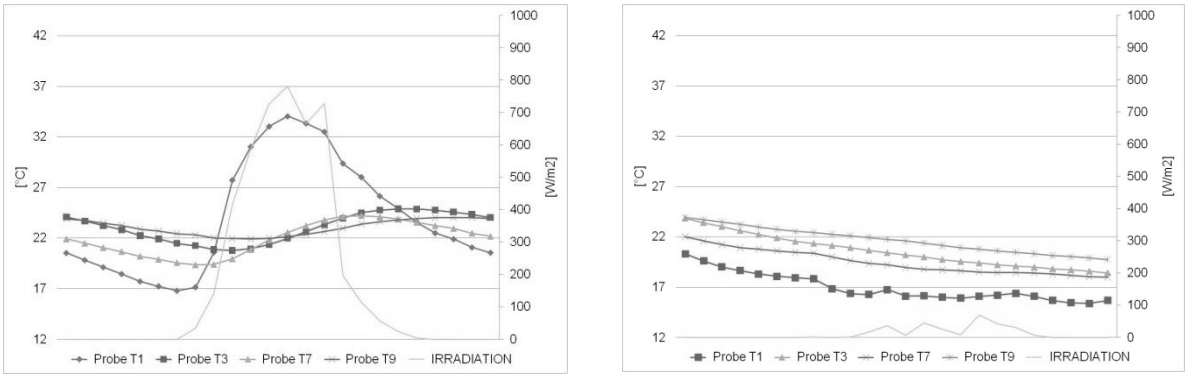

Figure 5: Surface temperatures with highest irradiation (left) and lowest irradiation (right)

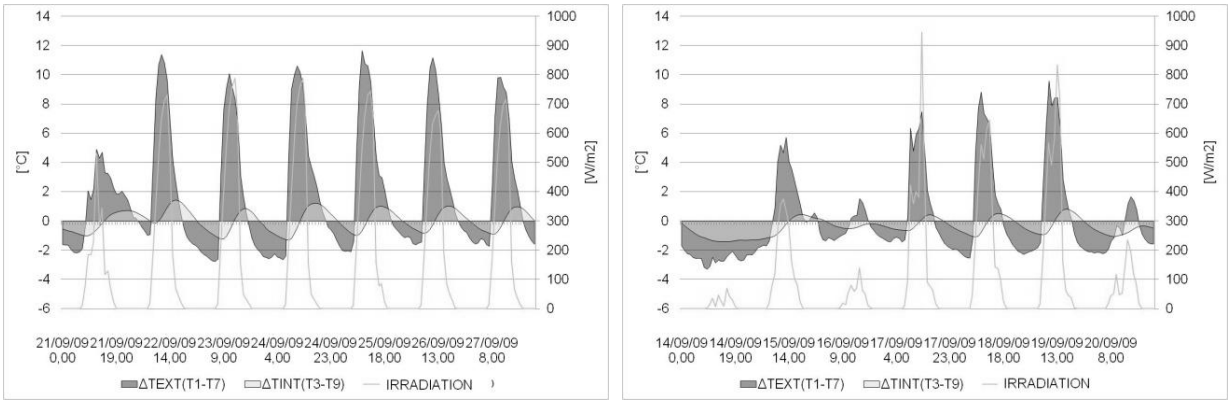

Figure 6: bare wall and covered wall ΔT during hottest week (left) and coldest week (right).

An exception is during the day with the lowest value of irradiation in which the bare wall surface temperature keeps its value lower than the covered one all day long. The direct relation with the solar irradiation is again clear and evident. During days with low irradiation, the green cladding protects the wall keeping temperatures high. During sunny days the shading effect of the green cladding is very useful to maintain lower surface temperatures. During the coldest week the ΔT reaches values of 5 – 8°C on external surfaces and 0,5 -1°C on internal ones.

THE GREEN FACTOR

For the first case study, the natural creeper one, also the green factor K_V [2] has been calculated. This synthetic simplified index is able to characterize the performance of the traditional green walls in reducing summer cooling loads by predicting surface temperatures. The green factor could be expressed as:

$$K_V = \frac{T_{se} - T_{sev}}{T_{se} - T_{ae}} \quad (1)$$

With T_{se}= external surface bare wall temperature, T_{sev} = external surface green wall temperature and T_{ae} = ambient temperature. The green factor for the South wall covered with Jasminum is 0,77 and the green factor for the West wall covered with Parthenocissus is 0,73. With these values is now possible to predict the external surface green wall temperature behavior as shown in figure 7. It is clear that the South orientation is the best situation to

predict surface temperatures because of the strong solar radiation and the lack of obstructions. In this case the K_V and the related calculated temperatures are close to real ones. West wall case, because of obstructions and reduced solar radiation is not representative.

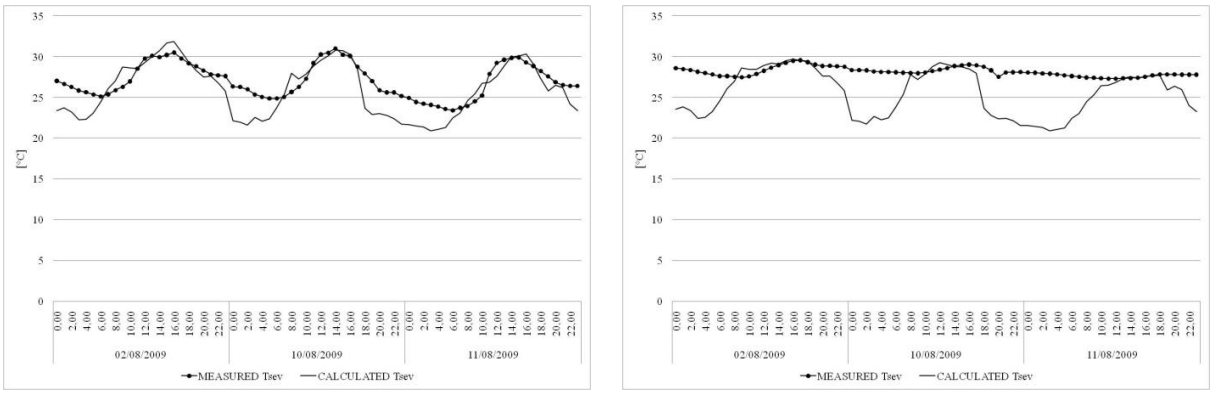

Figure 7: surface temperatures of the South green wall (left) and West green wall (right)

CONCLUSIONS

The two monitoring campaigns have pointed out the extremely useful shading effect of green facades both with natural creepers or artificial claddings. The surface temperature reduction due to the shading effect could be summarized in 10°C – 12°C of temperature difference between a bare wall, and a covered one with natural creeper or turfgrass sown on polypropylene claddings. A clear relation between solar irradiation and external surface temperatures has came out. During days with highest values of solar irradiation the external surface temperature of the bare wall is always higher than the covered one. During days with lowest values of solar irradiation the external bare wall temperature tends to reduce its values and during night the surface temperature is lower than the covered surface. Thus, the shading effect of the green cover is clear and effective during sunny days and the protection effect from heat loss is helpful during cloudy days. Also the green factor has been assessed for the natural creeper and for the south wall has been validated with experimental results.

AKNOLEDGEMENTS

The authors are very grateful to G. Carnevale and M. Montuori family and to Tecology srl who have done possible the access to the monitoring areas. Moreover are in debt with M. De Bei and A. Casalin for the precious collaboration in the monitoring campaigns.

REFERENCES

1. Di, H.F., Wang, D.N.: Cooling effect of ivy on a wall. Experimental Heat Transfer, Vol 12, pp 235-245, 1999.
2. Ariaudo, F., Corgnati, S.P., Fracastoro, G.V., Raimondo, D.: Cooling load reduction by green walls: results from an experimental campaign. 4th International Building Physics Conference, Istanbul, 2009.
3. Sandifer, S., Givoni, B.: Thermal Effects of Vines on Wall Surfaces. Proceedings of the 25th National Passive Solar Conference, American Solar Energy Society, 2000.
4. Lam, M., Ip, K., Miller, A.: Vegetation on building facades: "Bioshader", Case Study Report. Durabuild Project, Brighton, 2000.
5. Alexandri, E., Jones, P.: Temperature decreases in an urban canyon due to green walls and green roofs in diverse climates. Building and Environment, Vol 43, pp 480–493, 2008.

IMPACT OF BUILDING COMPONENT LIFESPAN ON THE ENERGY INDICATOR ACCORDING TO THE CHOICE OF TECHNICAL SOLUTIONS

M. Méquignon[(a) (b)] , H. Ait Haddou[(b)], L. Adolphe[(a)] , F. Bonneaud[(b)],
(a) LMDC- INSA, 135, Avenue de Rangueil - 31077 - France
(b) LRA- ENSAT, 83 rue Aristide Maillol – BP 10629 – 31106 Toulouse

ABSTRACT

Buildings represent one of the basic components of a city. Yet, walls are one of the basic elements of a building. From a metabolic perspective of building, we consider the energy consumption of the wall on his full life cycle. This article focuses on the assessment of the energy required by buildings during their building process. We separate the energy consumption deriving from the use of the building from the one depending on the choice of the technical solutions. We study the result considering the entire life cycle. All the technical solutions studied have an equivalent thermal performance.

First, the principal components analysis (PCA) was used to prove that « nonrenewable energy" is the most representative indicator in the data set. Second, we consider a wall area unit (i.e. 1 sqm) and we determine a long time span of service function. Third, we choose technical solutions in agreement with the specifications. Fourth, we determine the expected lifespan of each technical solution. Fifth, we find the corresponding energy's indicator value through appropriate database. Sixth, we simulate the time evolution of the indicator defined previously. Several technical solutions based on concrete, brick, stone and aerated concrete were tested under lifespan ranging from a few years up to centuries. The results suggest that lifespan has a significant impact over the value of the energy's indicator. The best technical solution considered on a short time span may be worst on a longer duration or vice versa. In order to make these results understandable to anyone, they are translated into the equivalent distance traveled by car in a year. We then consider each technical solution with different lifespans to observe the evolution of the energy consumed. We show that equivalent energy consumptions may be found among different technical solutions but under different lifespans.

Keywords: sustainability - lifespan – buildings – energy - decision making

1. INTRODUCTION

In recent decades, many studies have addressed the issues of energy consumption by buildings while in phase of use. They provided knowledge that lead to the production of many tools. The energy consumption by buildings has actually decreased. Thus, the relative share of the energy needed to achieve the buildings, as well as the associated environmental impacts, have increased. Studies for the production stage are few and the durations of the building's function are short [1], [2] or there is no neutralization of the energy consumption for the use phase [3]. The European Committee for Standardization has established sizing and justification standards for building structures and civil engineering. In its EUROCODE 0 edition, the committee recommends ordinary lifespans for ordinary buildings according to use. The specified lifespan for the calculation of sizing for ordinary buildings such as housing is 50 years. Moreover, in the very interesting Environmental and Health Declaration Notes (FDES) of INIES building products database, « typical » lifespans are used to define the impacts of the Functional Unit (UF). These lifespans, are identical by definition whatever the product in the same function of use, do not allow to measure the impact of lifespan in the performance comparison.

First, we study the sensitivity of the available data to determine the number of indicators that best represent the environmental impact indicators. To do this, we use the principal components analysis to reduce the amount of data to representative indicators. The result of the PCA show that « nonrenewable energy" is the most representative indicator [4]. Next, regarding the choice of technical solutions for the manufacture of building, the aim of this study is to highlight the impact of their lifespan on « nonrenewable energy and to measure their importance. We propose in this paper to study the impact of lifespan of a bearing wall facade unit of a building housing, or 1 sqm, on energy. The span of the function to fill in by our wall area unit is fixed. In order to compare different technical solutions, the method has been to characterize the need through functions that must be met by the wall with the help of the development of synthetic functional specifications. This document allows us to propose different technical solutions satisfying all the desired functions with the same rigor. To assess the nonrenewable energy consumption, we use the information provided in the base FDES. In a first phase, we will fix on a hypothetical basis the lifespans of various options and we will evaluate the cumulative energy over the life of the desired function. In a second phase, we will seek to provide a size scale of the impact from the choice of the technical solution. Finally, these livespans being not very « objectivable » considering our present means, we present for each of the solutions, changes in nonrenewable energy consumption based on changes in their own lifespan.

2. STUDY METHODOLOGY

2.1. The principal components analysis (PCA) and energy

First, for external supporting wall, we select multiple products and FDES. These products are listed in Table 1 below.

Concrete block	Mineral coating	Multi cell brick	Plasterboard
Aerated concrete	Insulator LV	Stone	Shuttered concrete

2.2 From the lifespan of building to "nonrenewable energy".

2.2.1. Conditions

The studied object is an outside bearing wall unit from a home style detached house. Location and environmental constraints are considered average. They are the same whatever the evaluated technical solution.

Span of the evaluated function:

The evolution of the nonrenewable energy consumption emissions of this wall unit is measured for a function of use of 300 years. This may seem a long time. However, this choice reflects both the problem and the large number of century-old homes in our cities. Whereas the function of accommodation, a duration of 300 years does not seem so extravagant as the needs may be considered temporally unlimited. It seems that no cause is likely to remove the physiological needs, of security, belonging and esteem in Maslow's sense, whatever the time scale considered. Qualitatively, the needs met by the function are changing but the old homes, sometimes several centuries old, seem to adapt to the changing original needs or to meet new needs [5]. In 2006, in France, more than 5.33 million housing units were over a century old. When the lifespan of the proposed technical solution is less than that of the function, the assumption is identical reconstruction and identical accounted data from those used originally. This hypothesis is simplistic because technological developments and means of producing energy are important. Nevertheless, the results produced in this article are determined considering current knowledge and practice. When lifespan is longer than the remaining term of the function, the respect of equity will lead us to include the last index to the "prorata temporis".

Wall unit study – Exerpt from simplified Functional Specifications

The various solutions that are proposed, must meet the same functional specifications based on the NF X50-151 standard. The element must be able to bear structural and operating loads of another level while protecting the interior space and its occupants from external disturbances. Elements of specifications are regular carrying function, insulation coefficient R=3.7, regular interior and exterior finishing

Solutions adopted

Different solutions meeting the specifications in the same way are available. These solutions are described in the Table 1. The outside finishing is mineral coating. The inside finishing is plasterboard

Data gathering and critics

The data used are provided by the INIES database within the Environmental and Health Declaration Notes (FDES) conducted within the frame of the NF P01-010 standard. The latter is established on the basis of the ISO standard 14040 series fixing the conditions of the life cycle analysis. These are the values established throughout all the product life cycle (LCA). These values result from the addition of emissions through all stages from raw material extraction to demolition. Only the impacts related to production facilities are neglected. We can not use established values of functional units (FU). Typical lifespans, by definition are identical whatever the product with the same function, and do not allow a comparison of performances of different technical solutions throughout time. How could one imagine that a solid wood frame has the same lifespan as a frame made out with trusses? With the objective of evaluating the impact of lifespan of different technical solutions on environmental performance and enable comparison, we use values of the entire cycle.

The index values of "nonrenewable energy" of products, thus retained for full life cycle, are considered constant over the period of 300 years. This hypothesis is simplistic because changing technology and modes of energy production are important. However, as explained in the paragraph about the lifespan of the function, the results found in this article are determined taking into account current knowledge and practice.

Note: - Since there is no FDES reference in INIES for structural wood, the impact of the wood solution is assessed on the basis of other "wood" products. In this database, the "nonrenewable energy indicator of wood product account the internal energy product. The other databases, such as KBOB, provide the value with just energy necessary to made it. We keep the two indicators.

Development

1st phase: Simulation of "nonrenewable energy" based on lifespan of solutions accepted as hypothetical

During this first phase, lifespans are determined as hypothesis according to expert opinions.

Evaluation of lifespans of the proposed solutions

This evaluation of lifespan may be the result of method called « according to expert » [6]. This method, used within a first approach based on intervals, allows simulation that provides approximate results. These lifespan are described in the Table 1.

Type of wall	Insulator	Lifespan	Sources
Stone	190 mm insulator LV	500-1500	On existing
Wood frame	190 mm insulator LV	60-80	Chief of mission cultural Quebec
Shuttered concrete	80mm PSE + 50mm LV	180- 200	Concrete engineer
Concrete blocks	170 mm insulator LV	100	Industrials
Aerated concrete	20 mm insulator LV	100	Industrials
Multi cell bricks	40mm insulator LV	100	Industrials
Insulator LV		40-60	Industrials and scientists
mineral coating		25-35	Technical Director HLM

Table 1: Technical solutions used and estimated lifespan

Data processing

The technique used is cumulative index values, established in the LCA, during the function of 300 years. This simple technique allows for the results on span and for observation on the changes in time accordingly.

2nd phase: variable lifespans

Lifespan of a product is difficult to be objectified. For this reason, during this phase, lifespans of the different solutions are variables. Evaluation is performed without any a priori on product lifespans. This phase assesses the impact of lifespan of the solution itself on its own results but also allows to compare the solutions to each other.

3. RESULTS

Result 1 : The principal components analysis (PCA) and energy

By using the PCA, we establish a relationship between values of nine environmental indicators and the matrix reveals strong correlations for the 8 products. The correlations are with nonrenewable energy and primary energy, energy process, GHG, resource depletion, acidification, water, radioactive waste, ozone photochemical, inert waste. The correlation coefficients are 0.87 to 1.

Result 2 : Processed data in determined conditions give these results:

The variations of "nonrenewable energy" overtime are represented in Chart 1 below.

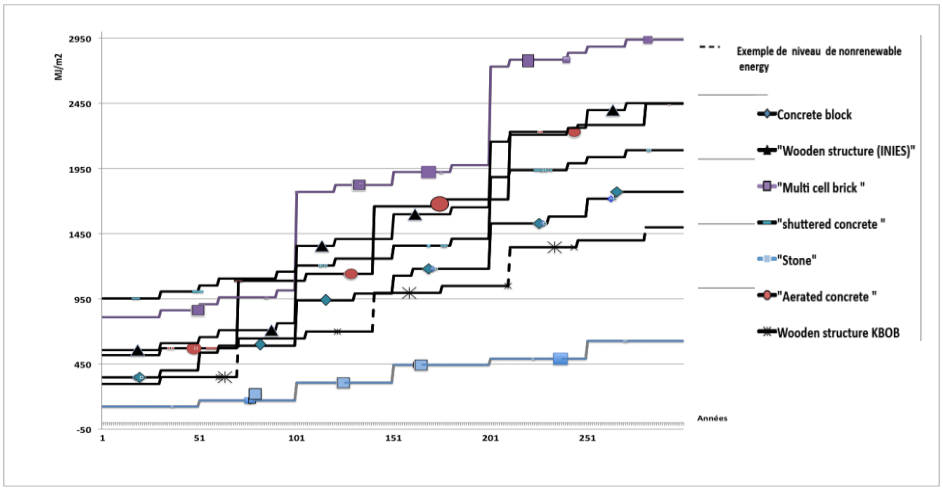

Chart 1 : Sum of nonrenewable energy to answer the function

Result 3 : Impact of lifespan of technical solutions on "nonrenewable energy"
In this second phase, we calculated the level of "nonrenewable energy" to meet the public use for 300 years, depending on lifespan of the technical solutions chosen. Changes in emissions are represented by the curves in Chart 2. The results show profiles of type of the inverted function « y=1/x ». We can notice :1) Significant reductions in emissions for extensions from 50 to 100 years or 150 years 2). The curve of the solution « wood INIES index », curves on an inverted trend compared to the others.

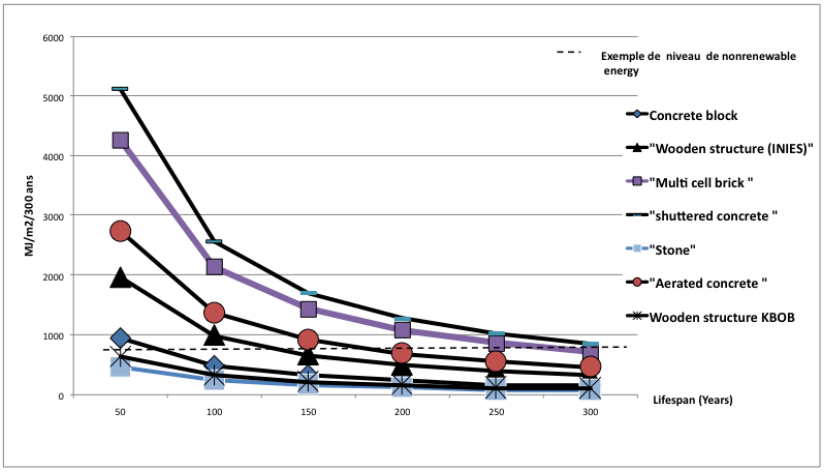

Chart 2: Changing of emissions according to lifespan

4 . DISCUSSION

4 .1 PCA and energy

Analyze the behavior of the indicator "nonrenewable energy" statistically allows to observe the behavior typically 9 of 16 environmental indicators maps Product with a sensitivity very correct.

4.2 Cumulative emissions.

We can see several observations about chart 1. The « stone » solution is effective whatever the considered lifespan for our wall unit. This solution allows a significant reduction of between 40 and 74% emission for a period of 300 years compared to other solutions. This performance is achieved through the extremely long lifespan found, energy requirement restricted and finally with the absence of coating. In the case of building rapid obsolescence, the stone can be easily reused. Overall, the « wood » solution, combined with "KBOB", seems to be a successful solution, whatever the lifespan. There is a paradox. These two solutions of stone and wood which are the most effective because they do not use energy for their transformation are the least ones used, at least in France. Since the life of a wall is never known in advance with certainty, this solution limits the consequences of an « early » demolition and deals with uncertainty based on the precautionary principle. The solution of block concrete block is just after. The solution "aerated concrete" relatively efficient for a period of 70 years, became one of the worst solution to the "multi cell brig. The solution "Shuttered concrete" was less well for a period of 100 years. After this period, it is more efficient than the solution "multi cell brig" and becomes more efficient than the solution "aerated concrete" the past 140 years.

We can assess the significance of the difference of impacts between the choices of extreme performance solutions. The average surface of a home in France is 91 sqm in 2006 (source: INSEE). This represents a typical example, about 78 sqm of bearing wall. The difference in consumption between the extreme solutions for a home represents an annual motor vehicle travel of 449 km.

4.3 Impact of lifespan of technical solutions on “nonrenewable energy”

This third result allows for more analysis. The interest of extending lifespan is obvious. Like shown in chart 2, whatever the solution, to extend lifespan from 50 to 100 years or 300 years can reduce emissions respectively by 50% and 83%. It is also established that a solution presented as less performing may be just as good if lifespan is proportionately longer (dashed black marker). For example, a wood structure built (KBOB index source) for 45 years has a similar impact as a wall made of stone if kept for about 40 years, hollow concrete blocks for 140 years or aerated concrete for 180 years, multi cell brick for 250 and shuttered concrete for 300 years. cellular concrete for 225 years. What is required from these observations is :

- to obtain scientifically based assessments of product lifespans ;
- to choose products in order to maximize the impacts of “nonrenewable energy” while taking into account the wanted lifespan of buildings;
- To design the buildings so that they give the best answer best to changing needs thus timing away obsolescence and educate the contractor in his choices during construction or in his decisions between potential renovation or demolition.

5. CONCLUSION

The study of the impact of the lifespan of a bearing wall unit outside on the indicator "nonrenewable energy", is equivalent to the study of nine among fourting initial environmental indicators exist. This study demonstrates the importance of lifespan of a building component on “nonrenewable energy”. To extend lifespan reduce the energy consumption. Whatever the level of energy consumption allowed, there are equivalents on the basis of different lifespans. By indicating lifespans of 50 years for current buildings, and although the objective is a design based on a calculation of failure probability, this European standard will result in the building industry to try to nearer the value for economy reasons. It is shown that it would not favor an optimization in terms of “nonrenewable energy”. This implies lifespan indications from EUROCODE to be reviewed. The FDES provide on the LCA basis a lot of useful information. However, the index values of functional units cannot be used as is. The qualities of the products and technical solutions chosen have obviously an impact on decisions to keep or demolish a building. How can one imagine that a frame of trusses has the same lifespan as the solid wood solution? It is necessary that manufacturers specify lifespan of their products by using scientifically established existing assessment tools. Designers and builders will then be able to adapt their choice and the quality of their project to the desired durability. Decisions for renovation or demolition should also consider the materials that were used originally. To design and build in a responsible way, designer and contractor should be able to better understand these lifespan issues and their consequences. The difficult assessment of wood products requires a quick consensus that allows to provide usable data. These initial results encourage us to examine the consequences on other themes: the impact of lifespan on the impact of lifespan on the other component and entire building.

BIBLIOGRAPHY

[1] Thormark, C. 2006. « The effect of material choice on the total energy need and recycling potential of a building ». *Building and Environment* 41 (8): 1019–1026.

[2] Junnila S, Saari A. « Material and energy flowestimation for building elements in the context of LCA ». Helsinki University of Technology, Report 150; 1997.

[3] Haapio, A., et P. Viitaniemi. 2008. « Environmental effect of structural solutions and building materials to a building ». *Environmental Impact Assessment Review* 28 (8): 587–600.

[4] Lebart, L. 1982, « traitement des données staistiques », 2d ed., Bordas Ed ., Dunod, Paris.

[5] Simon, Philippe (1997) *Architectures transformée: Réhabilitations et reconversions à Paris*. Paris: pavillon de l’Arsenal

[6] Talon A. (2006), *Evaluation des scénarii de dégradation des produits de construction*. Thèse de doctorat : Génie civil : Université Blaise Pascal – Clermont 2

A TOOL TO CHOOSE ENVIRONMENTALLY-FRIENDLY FINISHING PRODUCTS

Ilaria Oberti, Adriana Baglioni, Francesca Plantamura

Dept. Building Environment Science and Technology (BEST) - Politecnico di Milano, Via Bonardi 3 – 20133, Milano, Italy

ABSTRACT

This paper reports a part of a research, commissioned by the Lombardy Region with regard to the preparation of a guide for the public housing development, where our contribution is focused on developing a decision-making tool, that support in the choice of building products. Although the proposed method is valid in order to make a responsible choice of any product involved in building construction, nevertheless here we intend to focus on finishing products, due to their high responsibility to create conditions of safety and health of indoor environments. The tool offers various decision-making steps that highlight and prioritize the critical moments during the choice of building materials and, through a series of cards requirements/criteria, helps the designer in the selection of materials with more environmentally-friendly features.

INTRODUCTION

The choice of building products, taking into consideration the heavy impacts related to all stages of life cycle, is a decisive moment in a perspective of building sustainability, which doesn't match the appropriate awareness of how to make that choice. The eco-friendly product for excellence doesn't exist, rather, more realistically, it refers to a series of products with their environmental, technical, aesthetic and economic features, that may influence the various environmental components along the product life cycle. Therefore the designer must choose mediating between advantages and disadvantages. In the absence of an open and impartial guidance to lead the designer towards sustainability criteria in the selection of building products, the role is partly covered by the methods of environmental assessment of buildings, such as LEED (Leadership in Energy and Environmental Design). It's important to note that a building product that can be considered eco-friendly should be checked not only by the environmental impact indicators that assess environmental aspects, but also through indicators related to all those aspects that characterize the topic of Indoor Air Quality (IAQ).

METHOD AND RESULTS

The research work has been carried out in two work-packages (WP), with related but distinct aims.

WP1 – Decision-making tools

Decision-making tools have been developed to support the identification, through the design process, of the most significant environmental guidelines to be used as a guide for the choice of building products, for the specific building project.

At first, the path of choice for building products has been analyzed in the different phases of the project process and in reference to the specific features of the building project. The path has been viewed through flow charts.

The following is the proposed diagram for the choice of finishing products (fig.1).

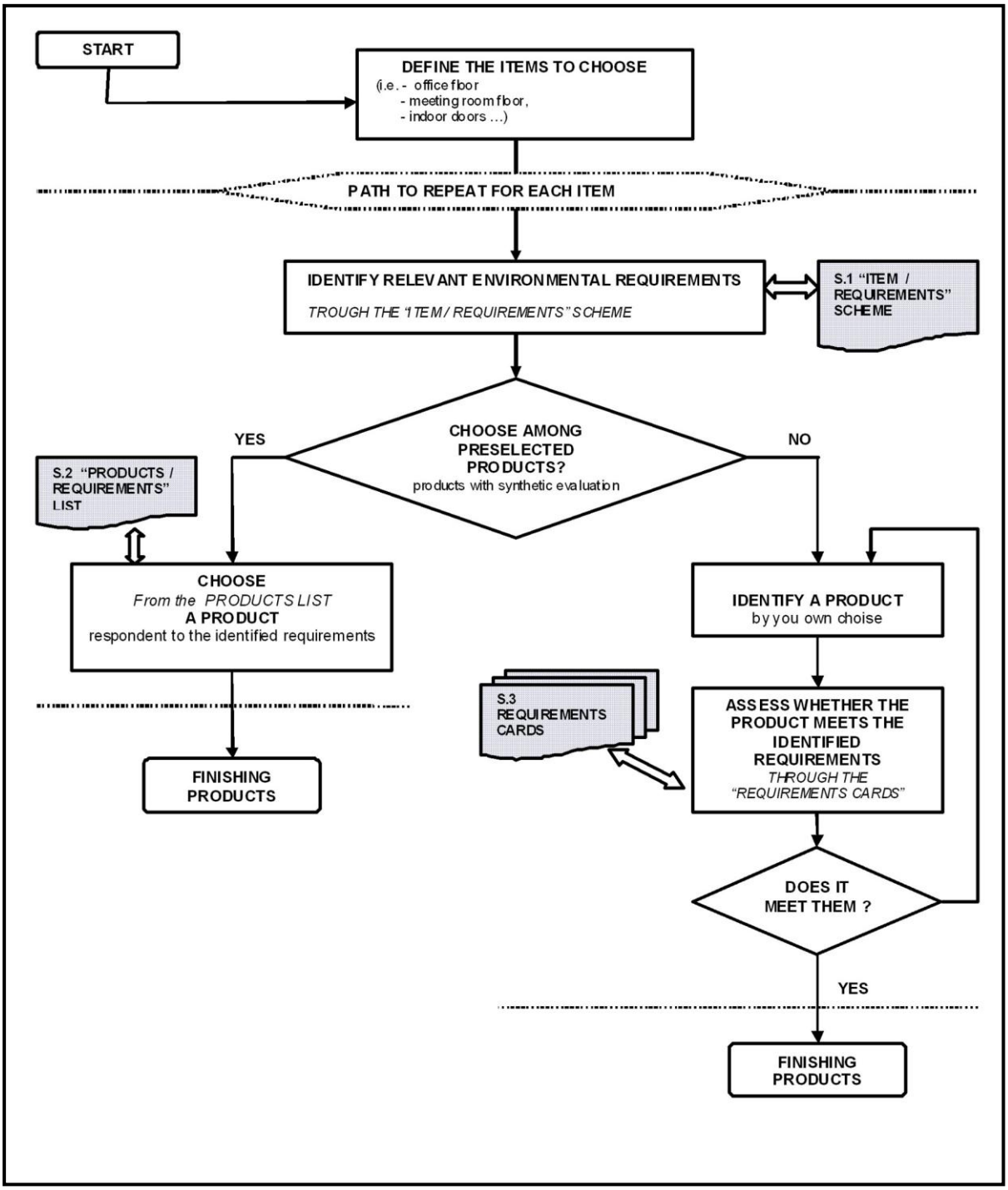

Fig. 1- Diagram for the choice of finishing products.

The path starts by identifying the most significant environmental requirements for each product to choose. Therefore, to help the designer to decide, it was developed a selection tool in order to identify those requirements according to the elements of the specific project.

This tool, formalized in "Item / Requirements Scheme", is shown below (fig.2):

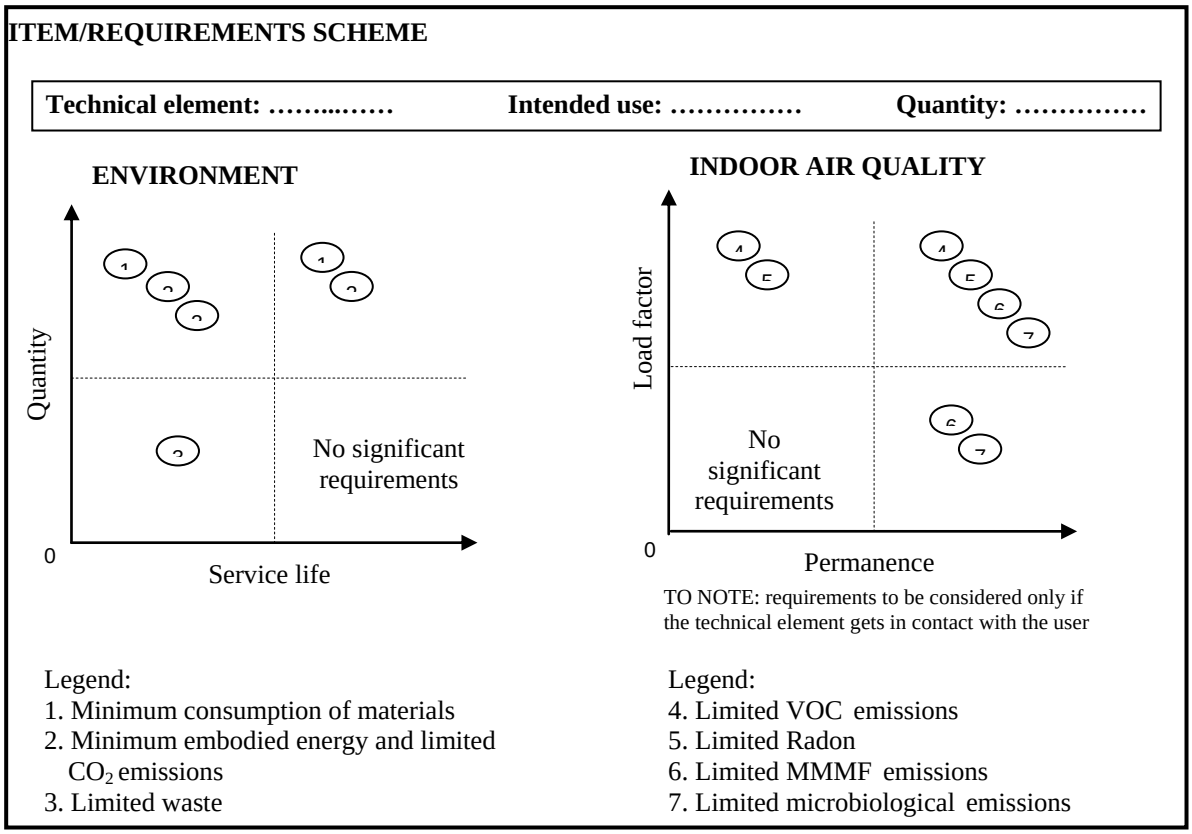

Fig. 2 - Item / Requirements Scheme.

WP2 – Information tools

In parallel, the information about the environmental aspects related to building products were systematized in form of "Requirements Card" and, for finishing products, also as preselected list of building products with a synthetic assessment of the requirements for IAQ.
Made an initial choice of the building products, the designer can verify their compliance with the requirements identified as significant by the guidelines proposed in "Requirements Card", preceded by a short thematic framework of reference. The cards are provided for requirements related to the main potential environmental impacts of building products at different stages of life cycle (tab.1).

Topic	Specific subject	Requirement
Environment preservation		
	Consumption of resources	Minimum consumption of materials
	Emissions	Minimum embodied energy and limited CO_2 emissions
	Waste	Limited waste (of production, construction and demolition)
Indoor air quality		
	Indoor emissions	Limited VOC emissions
		Limited Radon
		Limited MMMF emissions
		Limited microbiological emissions

Tab.1- The main potential environmental impacts of building products.

The considered requirements can find references in the most common methods of environmental assessment of buildings such as the Itaca Protocol, adopted in some italian regions, the international system LEED, the French HQE method.
For finishing products, the path of choice also indicates a more direct procedure; this procedure uses a list of products with a concise environmental assessment. The following is an example of "Products / Requirements" List for flooring systems (tab.2).

Finishes		**Products assessment**		
Flooring systems	**Materials & Products**	**Occupants**	**Environment**	**Building performances**
Ceramic tiles	Cotto	☺	☹	😐
	Glazed ceramics	☺☺	☹	☺
	Grès	☺	☹	☺
Parquet	Wood mosaic	😐	☺☺ **1)**	☺
	Solid wood	☺	☺☺ **1)**	☺
	Solid bamboo	☺	☺☺ **1)**	☺
	Solid plank wood	☺	☺☺ **1)**	☺
Stone	Marble	☺	☹	☺
	Granite	☹	☹	☺
	Marble with resin	😐	☺☺	☺
Carpet	Wool	😐	☺☺	😐
	Coconut fibres	😐	☺☺	😐
	Polyamide fibres	😐	☺	😐
	Synthetic fibres	😐	☺	😐
Resilient	Rubber	😐	☺	😐
	Rubber-PVC	😐	☺	😐
	PVC	☹	☺	😐
	Linoleum	😐	☺	😐

1) The problems are negligible if the wood comes from managed sources**.**

Tab.2 - Example of "Products / Requirements" List for flooring systems.

The classes of the materials or products are shown in the first two columns. The third column of the table gives information on possible effects on occupants.

As to environmental issues, which are also highly complex, assessments are made by taking note of the following: effect on air quality, effects on the environment (increase in the greenhouse effect, increase in acidity), quality of resources, possibility to recycle, energy consumption over the whole life of the product, that is, from the acquisition of the raw material to the elimination of a no longer used item.

The last column gives the effects of the material or product on the overall performance of the building. A series of factors, such as its contribution to the achievement of good heat/humidity, sound, visual, and tactile conditions. A material which, for example, does not make it possible for the building to breathe, is considered as negative with respect to another which is able to ensure good heat and humidity conditions inside the building. And we will

have a better assessment for a material which can be more easily cleaned or maintained or is durable.

The assessment ranges from unapproved to recommended, with intermediate levels, as shown below:

☹☹ unapproved; ☹ not recommended; 😐 neutral; ☺ acceptable; ☺☺ recommended.

CONCLUSION

To sustainable architecture, the impact of building products is widely recognized; at the same time, there is a lot of technical and environmental product information available to the designer.

The questions on the matter, however, are not completely solved, primarily because it can not be easy for the designer to navigate between information that is not always consistent or equally reliable.

Moreover, in the current technical and scientific context, generally, the environmental quality of a building is fragmented in a set of aspects and relative criteria/indicators and assessed by the sum of scores achieved for the various aspects. In this context the designer has to choose the environmental criteria to be taken as guide, sometime without considering the interaction among the assessed elements, the selected criteria and the whole project. To this issue, in particular, this paper has tried to give an initial answer, with this believe: if the environmental building quality can be measured as the sum of single quality aspects, it's essential to provide the designer with some tools to decide which are the most significant aspects and criteria to take in count, in order to guide the design process, in relation to the features of each project.

ACKNOWLEDGEMENTS

This paper is part of a research carried out within the "Convenzione tra Regione Lombardia e Fondazione Politecnico di Milano con il consorzio CIS-E per le costruzioni dell'ingegneria strutturale in Europa finalizzata alla predisposizione di una guida per l'edilizia pubblica sostenibile" (Scientific Chief Prof. A. Migliacci, 2010).

REFERENCES

1. Berge, B.: The Ecology of Building Materials, Elsevier, Oxford, 2009
2. Piardi, S., Carena, P., Oberti, I., Ratti, A.: Costruire edifici sani. Guida alla scelta dei prodotti, Maggioli, Rimini, 1999
3. Spiegel, R., Meadows, D.: Green Building Materials: A Guide to Product Selection and Specification, John Wiley & Sons, New York, 2006
4. Wilson, A., Piepkorn, M.: Green Building Products, New Society Publisher, Gabriola Island, Canada, 2008
5. Yudelson, J.: Green Building Through Integrated Design, McGraw-Hill, New York, 2008
6. Yudelson, J.: The Green Building Revolution, Island Press, Washington, 2008

DIFFERENT STRATEGIES FOR REFURBISHMENT

Dipl.-Ing. T. Osterhage [1], D. Calì M.Sc. [1] and Prof. Dr.-Ing. D. Müller [1]

RWTH Aachen University, E.ON Energy Research Center, Institute for Energy Efficient Buildings and Indoor Climate, Mathieustraße 6, 52074 Aachen

Corresponding email: tosterhage@eonerc.rwth-aachen.de

ABSTRACT

A large number of buildings constructed in the second half of the twentieth century consume a big amount of energy. The housing society "Volkswohnung Karlsruhe" has 35 residential buildings in the area of Karlsruhe-Rintheim with more than 1.000 apartments built in the 1950s and 1960s.

In cooperation with "Volkswohnung Karlsruhe" and the University of Applied Sciences Karlsruhe, a field test on energy modernization with different combinations of innovative solutions in the area of building's physics and technical installations, including a control system has been planned and realized, accompanied by extensive monitoring and simulations. Each building has a different retrofit scenario in terms of insulation, heat production and delivery, domestic hot water production and air-handling systems. In this case six different retrofit solutions are realized and compared to the standard retrofit model of the Volkswohnung. Each retrofit solution is realized for ten apartments, an adequate number to evaluate the user-behavior.

For the evaluation of the efficiency of each retrofit solution a high resolution monitoring system for rooms, apartments and engineering system (heat production, storage, distribution and delivery) has been installed. In each room, for example, a monitoring module collects the relative humidity, window opening, CO_2 and VOC, the temperature of the air inside the room, outside the room and supplied to the room.

The better the building envelope is insulated, the more it becomes important to realize a heat bridge reduction or even a heat bridge free building structure. For the analysis of the thermal and energetic performances of the buildings, the heat bridges of the buildings have been calculated through the Finite Element Method. All the results are published in a heat bridge atlas.

The preliminary analysis with Energy Saving Ordinance [EnEV] [4] has shown a potential for reducing the energy consumption up to 85%. However, first analyses of the monitoring data show that the heat consumption of the buildings is above the heat demand calculated following the EnEV procedure.

INTRODUCTION

Over the last years the federal government has greatly tightened the requirements for new buildings, in order to limit the primary energy demand as a way of conserving resources. In parallel, the Renewable Energy Law [EEG] [1] and the Renewable Energy Heat Law [EEWärmeG] [2] were created to promote the use of renewable energies. Most of these laws relate to new buildings and only in part to the retrofitting of old buildings. The energy consumption of households makes up about 29% of primary energy consumption. A closer analysis of the energy distribution shows that nearly 75% of the energy is consumed for space

heating. For existing residential buildings (detached single-family homes and small apartment buildings) it should be noted that the final energy demand has been decreasing significantly in recent decades, due to the new legislation. The biggest savings can be achieved for the building built between 1950 and 1960 [3]. In Germany, about 5 million residential units exist in this age group. To a large extent these buildings were built and administered by building societies and the classical housing floor plan is between 45 and 60 square meters [3].

The housing society "Volkswohnung Karlsruhe" owns approximately 20,000 apartments, which will gradually be refurbished. There are 35 residential buildings in the area of Karlsruhe-Rintheim with more than 1.000 apartments built in the 1950s and 1960s, 1.5 km from the city center. The particularity of this refurbishment project lies in the fact that it focuses on three identical blocks of flats with the same orientation.

A block consists of three buildings with separate entrances. Each entrance has 10 apartments. Per block there are 30 and in sum 90 identical apartments with same orientation available.

The west front of each building has a length of 52m and is aligned to the garden. The total floor space of each building is 721m²; the envelope-surface is 1,097m² for the frontage-buildings, 959m² for the buildings in the middle. Each apartment has a kitchen, a bathroom, a living room, two sleeping rooms and a small central corridor, for a total floor space of 72 m².

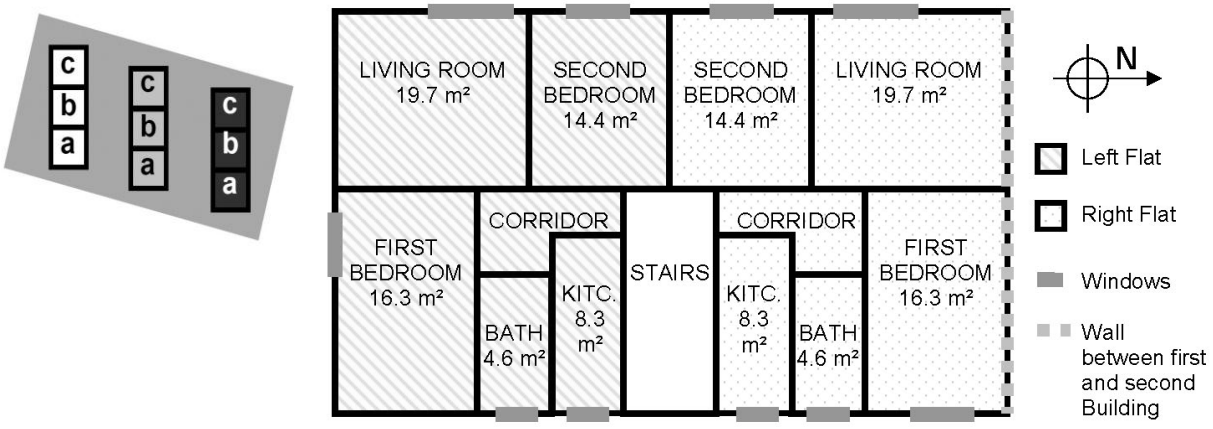

Figure 1: left: Building alignment / right: Qualitative layout of one floor of the first buildings of each block / KITC. is the Kitchen

Apart from the energetic redevelopment also a revaluation of the buildings` substance was made. The old inserted balconies were removed, and replaced with new thermally decoupled elements. Existing thermal bridges were reduced through this measure. Outside the area of the buildings a thermally decoupled elevator was set up, which facilitates the access to the floors.

In terms of technical building issues, the complete pipeline network was renewed and adapted to modern standards, with all the equipment to be replaced during the operation. The plant technology varies from building to building. In course of the project different process engineering approaches have been developed and implemented each retrofit solution is realized for ten apartments, an adequate number to evaluate the user-behavior.

The buildings were built in 1955, originally without insulation and with single glass windows. The heat was provided by a cackle stove installed in each living room, domestic hot water (DHW) was supplied by electrical or gas circulatory type water heater. In the course of time the buildings had been lightly refurbished. Before the first retrofit the buildings had double

glass windows with an overall heat transfer coefficient U equal to 3.1 W/(m²K), those windows have been installed during a previous refurbishment process in the eighties. In 1970 the south and the north façades were insulated with 4 cm insulation with λ=0.04 W/(mK). The U-values for the external walls were between 1.22 and 0.55 W/(m²K). The ceiling of the last floor, under the pitched roof space, had a U-value of 2.58 W/(m²K). There was no insulation between the basement and the ground floor, therefore the U-value amounted to 1.93 W/(m²K). The walls between the flats and the stairs had a U-value of 1.25 W/(m²K). The specific heat demand per year and square meter of floor space q_h amounted to 190 kWh/m²with small differences in the terms of each building. The cause of this are small geometric variations of the buildings, for example the windows orientation. The specific primary energy demand of the buildings per year and square meter floor space q_P amounts to 350 kWh/m². The heating system, as well as the domestic hot water (DHW) plant, is equal for each building: as consequence, q_h and q_P are proportional.

METHOD

The retrofit solutions are analysed and compared in order to better understand the importance of buildings' retrofits in terms of primary energy saving per year and square meters. In parallel, the aim is to comprehend which retrofit solution is more effective, in terms of heat consumption and primary energy savings.

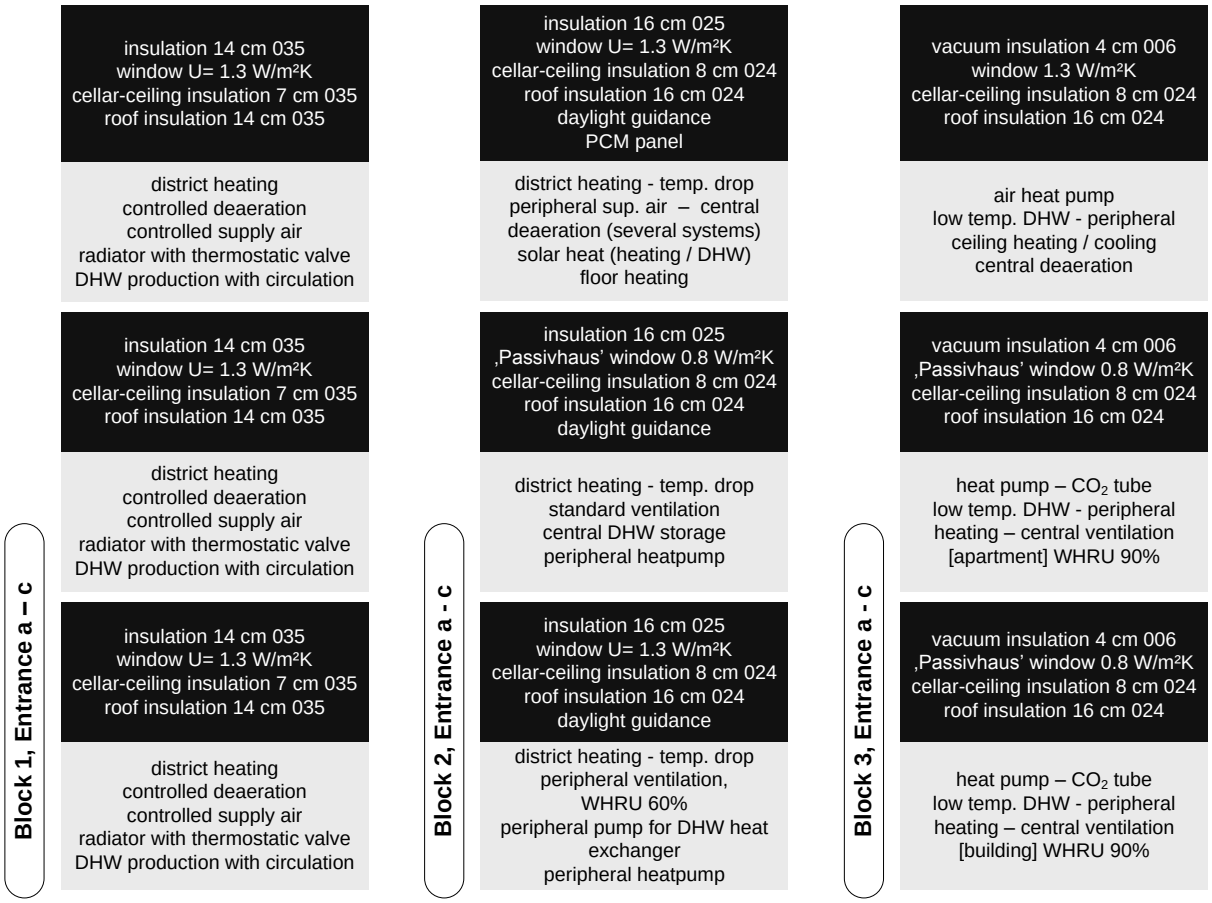

Figure 2: Refurbishment solutions: the white text on dark background is related to the thermal insulation, the dark text on the grey background is related to the engineering system solutions

The first block will be considered as reference case and represents the standard refurbishment solution of the Volkswohnung. This means that every entrance of the first building is equal in

terms of thermal insulation and engineering system with common standard products available on the market. The retrofit of the second block makes use of state of the art insulation and a more advanced engineering system technology, which are as well to be found on the market. The most advanced refurbishment solutions are realized for the third block with the use of vacuum panels together with high efficiency heat pumps and waste heat recovery units. The third block is designed to reach the lowest primary energy demand. In Figure 2 the refurbishment solutions are described. WHRU indicate waste heat recovery units, the number in percent next to WHRU is the efficiency of the heat exchange process. The thermal conductivity λ of the insulation is indicated by a number in each box, for example 035 means λ=0.035 W/(mK).

For the evaluation of the efficiency of each retrofit solution a high resolution monitoring system for rooms, apartments and engineering system (heat production, storage, distribution and delivery) has been installed. The installed measuring technique and the detectable measured variables were selected in such a way that the influence of the building construction and technical components on energy consumption and the space comfort can be determined. The collection of the room climate data in the apartment is made via a bus system (M2-Bus) developed at the University for Applied Sciences of Karlsruhe, with which the data of the individual apartment are obtained (The topology of the measurement system is described in Figure 3).

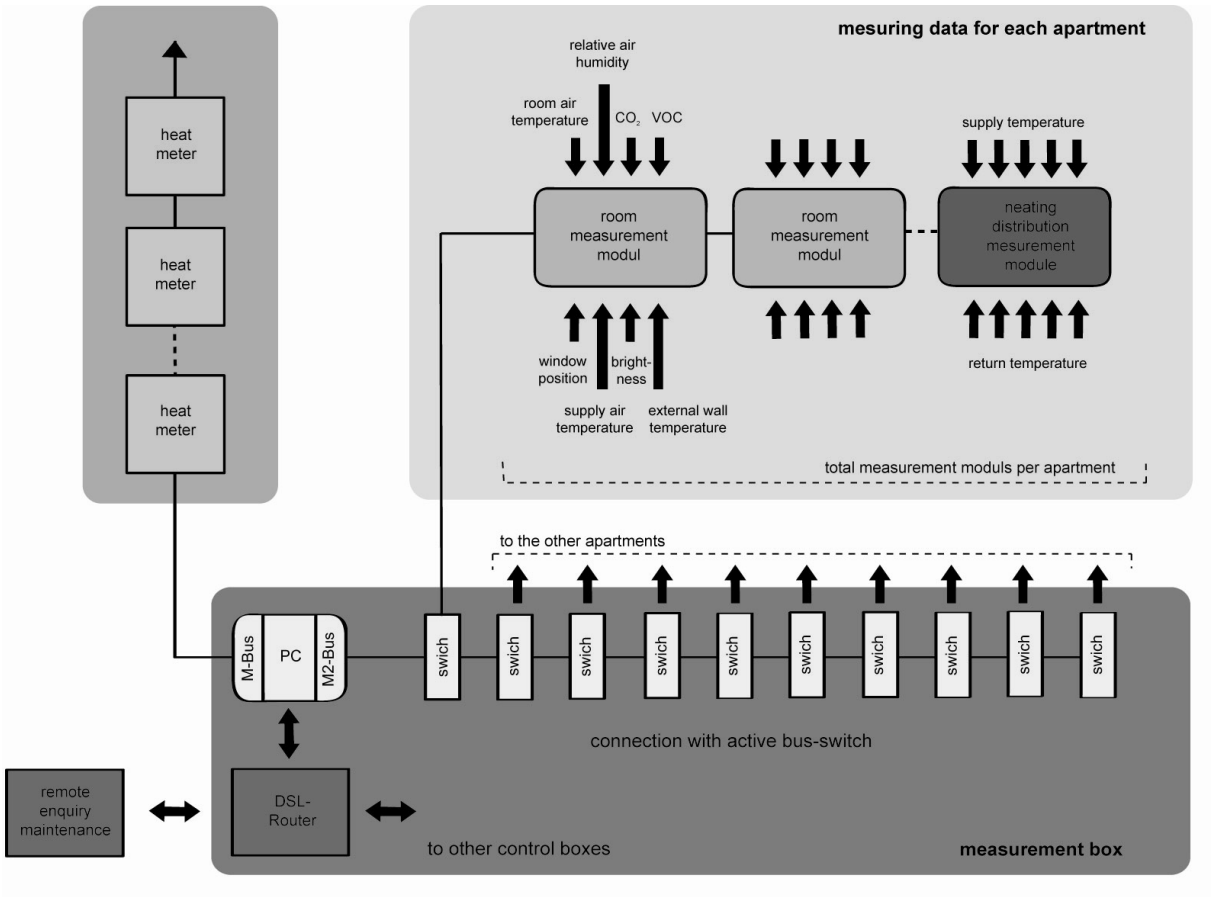

Figure 3: Overview of the topology of the measuring system

In each room a monitoring module collects the relative humidity, window opening position, CO_2 and VOC concentrations, the temperatures of the air inside the room, and supplied to the room. In each apartment (of the second and of the third building) a volume flow meter measures the volume flow through the heating system, flow and return water temperatures are

measured as well. Also the consumption of DHW is monitored through flow meters and temperature sensors. In four apartments per entrance a heat meter has been installed for each heating device.

CONCLUSION

One of the main tasks of this work is to outline the possible savings in terms of primary energy in the field of building refurbishment. The second main task is to evaluate which of the refurbishment measures is more effective.

The complete redevelopment of the buildings has been finalised. In the first block all three entrances are supplied by district heating and have exactly the same engineering system. All apartments of the second block have been occupied from February 2010 onwards. The third block presents the most advanced refurbishment solutions. Each entrance has a separate engineering system.

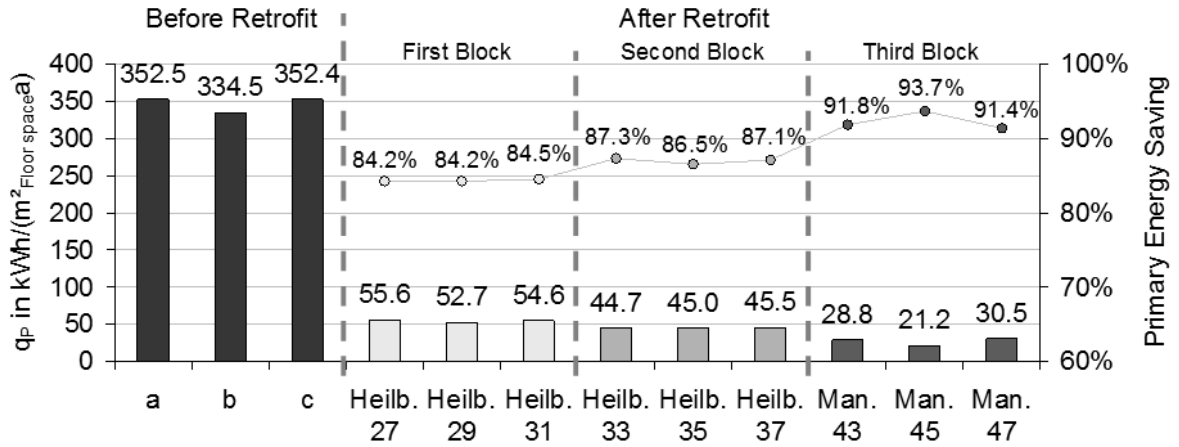

Figure 4: Primary Energy demand per square meter of floor space and year, for the blocks before and after refurbishment. In per cent, the primary energy saving of the retrofit solutions, compared to the primary energy demand of the buildings before the retrofit

Static calculation results [EnEV] [4] showing the q_P and the primary energy savings are presented in Figure 4. Before the redevelopment, the primary energy demand amounts to 350 kWh/m². After the renovation a significant reduction is observed. Compared to the stock an energy saving of about 80% is reflected to the standard redevelopment. In the third block with the most expensive retrofit solution a further reduction of 10% to only 20-30 kWh/m² is expected. As shown in Figure 4 the CO_2 ground heat exchanger installed in the first entrance and in the middle entrance ensure better energy performances than the air heat pump.

Figure 5 shows the comparison between the measured heat consumption and the calculated heat demand. The measured consumptions vary greatly. The average consumption of all apartments is 40% above the EnEV [4] calculation. It should be noted that the EnEV calculations used standard user profiles and therefore a deviation is to be expected, because no tenants behave according to standards. Because of the high deviation the emergence of a rebound effect can be concluded. Rebound effect describes in the energy economy the fact that the potential savings from increased efficiency is not or only partially met, as users tend to increase their consumption.

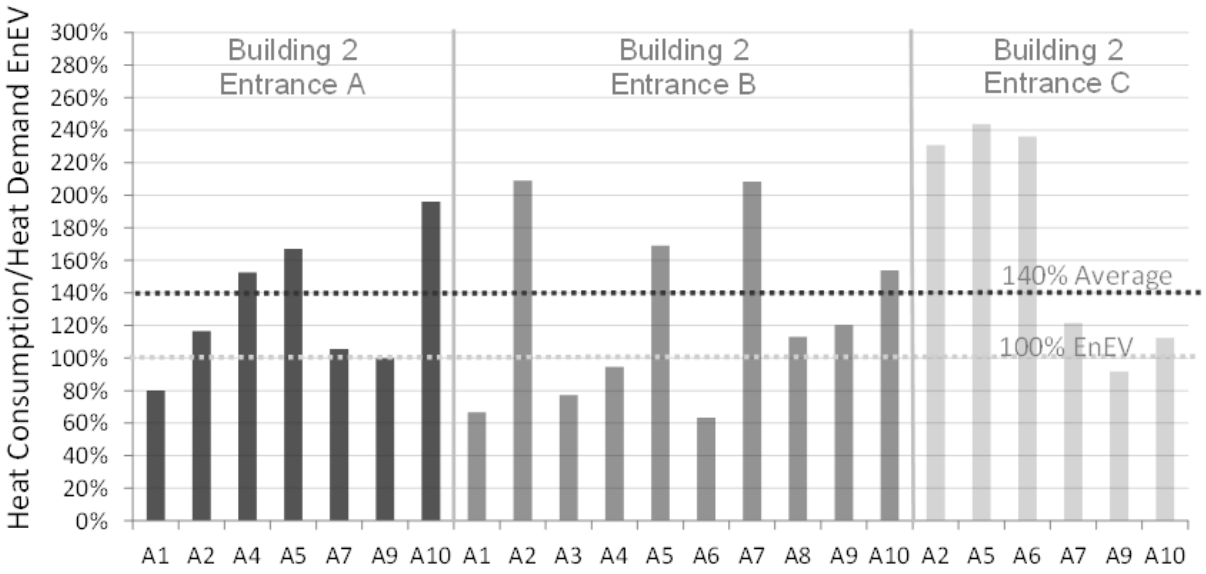

Figure 5: Comparison between measured heat consumption and calculated heat demand

After the completion of another measurement period we plan to further increase our understanding on the tenants' behavior and the technology acceptance. Parallel to the evaluation of the measurement technique a dynamic building and system simulation using Modelica is performed, in order to be able to test different control strategies and to evaluate the resulting system efficiency.

ACKNOWLEDGEMENTS

Special thanks to Dr. Reinhard Jank (Volkswohnung Karlsruhe) for the generous support of the project and to Prof. Klaus Wolfrum (Technical University Karlsruhe) for the realization of the high time resolution monitoring process.

Grateful acknowledgement is made for financial support by BMWi (German Federal Ministry of Economics and Technology), promotional reference 0327400G.

REFERENCES

1. Erneuerbare-Energien-Gesetz – EEG, (BGBl. I S. 2074), zuletzt geändert durch das Gesetz vom 11. August 2010 (BGBl. I S. 1170), EEG 2009.
2. Erneuerbare-Energien-Wärmegesetz – EEWärmeG, veröffentlicht im Bundesgesetzblatt Jahrgang 2008 Teil I Nr. 36 vom 18. August 2008, S. 1658, EEWärmeG 2008.
3. CO_2-Gebäudereport, im Auftrag des Bundesministeriums für Verkehr, Bau und Stadtentwicklung (BMVBS), co2online gemeinnützige GmbH und Fraunhofer-Institut für Bauphysik, 2007.
4. Energieeinsparverordnung für Gebäude – EnEV, Verordnung über energiesparenden Wärmeschutz und energiesparende Anlagentechnik bei Gebäuden, veröffentlicht im Bundesgesetzblatt Jahrgang 2009 Teil I Nr. 23 vom 30. April 2009, Seite 954, EnEV 2009.

LCA BASED COMPARATIVE EVALUATION OF BUILDING ENVELOPE SYSTEMS

F. Pittau[1]; E. De Angelis[1]; G. Masera[1]; G. Dotelli[2].

1: Politecnico di Milano, Dipartimento B.E.S.T. – Via Ponzio, 31 IT-20133 Milano

2: Politecnico di Milano, Dipartimento di Chimica, Materiali e Ingegneria Chimica "G.Natta" - P.za Leonardo da Vinci, 32 IT-20133 Milano

ABSTRACT

Issues about the evaluation of the environmental sustainability of products and industrial processes are slowly involving every industrial sector among which, building and construction sector. While National strategies are finally moving toward an agreement for the reduction of green-house gas emissions, in order to mitigate the global warming effects, buildings, which are also responsible for a significant share of non-renewable energy use, are not yet enough analyzed in every different life cycle phase: the discussion about the choice of environmental indicators to be considered [1], their computational methodology and the limits to be respected is still open.

Life Cycle Assessment (LCA), fully defined in a series of International Standards for industrial products, seems to be the only holistic tool able to give an objective measure of the environmental impact of a building and, from it, its sustainability. Nevertheless, its application in the building sector is particularly difficult, due to the intrinsic complexity of the building itself: the variety of products it is made of, the many impacts it generates during its life cycle, the length of its life and the difficulty to forecast its use and maintenance during its service life and disposal or reuse opportunities after more than fifty years. Different models and approaches have been developed and carried out, in the two last decades, by several authors [2], to cope with this complexity and the literature review shows that there are still different opened critical issues for the identification of a valid methodology [3].

The aim of the paper is to make the point of the environmental assessment of building envelope subsystems and to pave the way for a LCA-based measure of the environmental performances of the design solutions and the evaluation of the sustainability propensity of building technologies in general, as a tool to support not only detail design choices but also strategic choices. A preliminary environmental comparison of one technology against another, in fact, can be used to take decisions in the very first phases and to compare life cycle impacts to life cycle costs and performances.

INTRODUCTION

In the last decades, as a result of the community commitments to reduce the impacts of the built environment [4], the traditional design, by which for centuries buildings have been designed, has been integrated with other competences into a new design concept in order to reduce the energy consumption and the greenhouse gasses emissions. Although the energy performance improvement of the new constructions rose to higher limits, much more severe than in the recent past, the need for a holistic methodology to assess the sustainability of the built environment still remains [5], which often is not proportional to the reduction of energy consumption during the service life. In order to estimate how much a building or a particular design choice is or might be better than another one from the environmental prospective, the

analysis of the whole life cycle is strictly essential, from the extraction of the use of natural resources (cradle) to the end of the service life (grave) of the building.
Several authors already faced this issues. Kennedy [6], for example, investigated the critical issues about the environmental choices, nevertheless without proposing a specific model. Cole [7] discussed many LCA-based models to compare the sustainability of different design choices. Kohler [8] evaluated the need to set up a specific LCA approach for the selection of construction materials. Other fundamental contribution have come from Canadian Wood Council and Swedish Institute for Wood Technology Research (Trätek) published several studies about the inventory of building products and components. Other contributions [9] proposed a LCA-based model to evaluate the sustainability of different envelope systems.
The main problem that always arises from these experiences is the lack of inventory data or their poor reliability to give clear and doubtful results. In fact, although a large amount of data is available worldwide, their use needs systematic reviews in order to tune up them with the many differences encountered locally (e.g. the incidence of the transportation in the production process or the different mix energy for the different regions). Therefore an uncritical use of these data might compromise the effective measure of the sustainability and, eventually, its achievement. Another critical issue concerns the functional unit (F.U.) considered for the calculation of the various environmental indicators. Most of the material's data are reported to the mass or volume/area, and often the comparison of data measured with different F.U. is very difficult.

METHOD

In this paper a specific model for the comparative assessment of the environmental sustainability of vertical envelope systems and building components has been adjusted considering a F.U. that is linked to the measure of the extension of its surface but to its specific performance. In this case we tried the thermal resistance (R_T) of envelope components, because of its strong connection with for heating and cooling energy consumption, during the operating phase of the whole building, that is not the only but the most important parameter to be optimized, in the design phase of any envelope system design.

At first, four different envelope technologies have been considered, each one designed to assure a thermal resistance value of 4 m^2K/W. Each functional layer is codified, in reference to the main performance requested to provide a specific requirement.

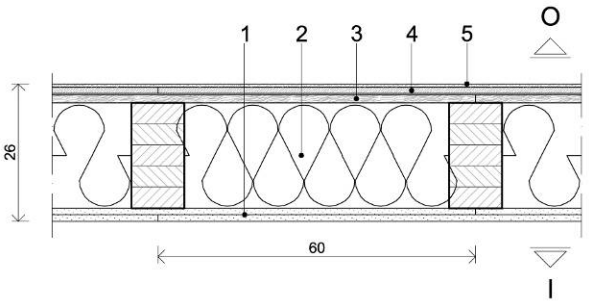

Figure 1: Type A – Lightweight wood-framed system (WFS).

N°	Cod.	Material description	t [m]	ρ [kg/m^3]	λ [W/mK]	$R_{t,i}$ [m^{2}K/W]
1	IFL	Gypsum plasterboard	0,025	900	0,21	0,12
2	IL	Woodwool + timber stucture	0,2	218	0,054	3,73
3	SL	Oriented strand board	0,015	650	0,13	0,12
4	LL	Fibre-reinforced cementboard	0,015	1150	0,32	0,04
5	EFL	Cement mortar	0,006	2000	1,40	0,004

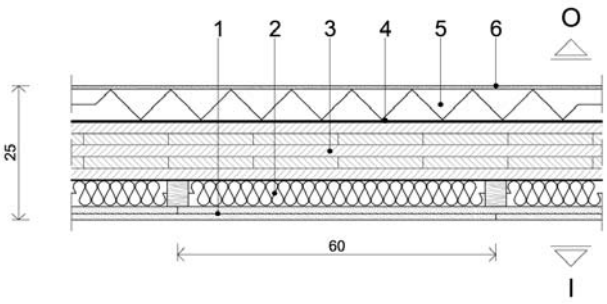

Figure 2: Type B – Wood-massive system (XLAM).

N°	Cod.	Material description	t [m]	ρ [kg/m^3]	λ [W/mK]	$R_{t,i}$ [m^{2}K/W]
1	IFL	Gypsum plasterboard	0,025	900	0,21	0,12
2	IL	Fibreglass	0,05	125	0,037	1,35
3	SL	Wood cross-laminated panels	0,11	450	0,12	0,92
4	AL	Cement-based adhesive	0,002	2000	1,40	0,001
5	IL	Cork	0,06	160	0,04	1,63
6	EFL	Cement mortar	0,006	2000	1,40	0,004

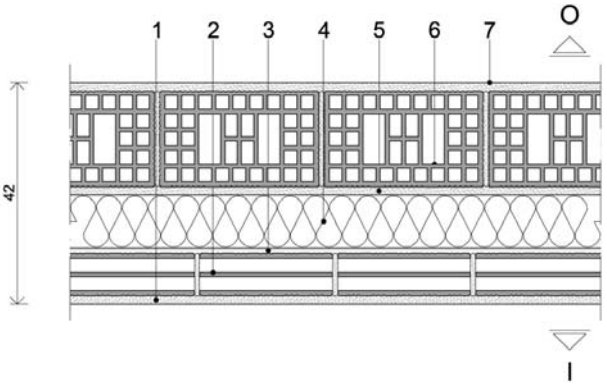

Figure 3: Type C – Masonry system (BRICK).

N°	Cod.	Material description	t [m]	ρ [kg/m^3]	λ [W/mK]	$R_{t,i}$ [m^{2}K/W]
1	IFL	Gypsum mortar	0,015	1400	0,70	0,02
2	EL	Light bricks	0,08	1088	0,30	0,27
3	IL	Non-ventilated air gap	0,01	0	0,067	0,15
4	IL	Rockwool	0,10	100	0,035	2,86
5	LL	Cement mortar	0,01	2000	1,40	0,01
6	SL	Light bricks	0,18	850	0,30	0,66
7	EFL	Cement mortar	0,015	2000	1,40	0,01

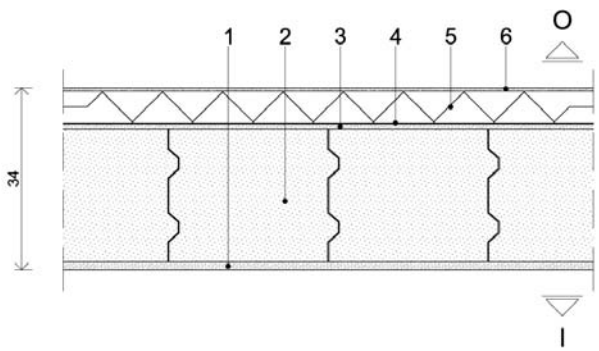

Figure 4: Type D – Aerated autoclaved concrete blocks system (AAC).

N°	Cod.	Material description	t [m]	ρ [kg/m^3]	λ [W/mK]	$R_{t,i}$ [m^{2}K/W]
1	IFL	Gypsum mortar	0,015	1400	0,70	0,02
2	SL	Autoclaved concrete blocks	0,24	450	0,101	2,38
3	LL	Cement mortar	0,01	2000	1,40	0,01
4	AL	Cement-based adhesive	0,002	2000	1,40	0,001
5	IL	EPS	0,06	80	0,038	1,58
6	EFL	Cement mortar	0,006	2000	1,40	0,004

For the inventory and the definition of the eco-profiles of the various materials, the *Inventory of Carbon & Energy* database (ICE v.2.0) [10] have been used assuming to operate in a British context. The only indicators that are considered in the model are the CO2 equivalent emissions (GWP) and the Embodied Energy (energy consumption during extraction/ production phases EE). Each value is calculated with boundaries of the system "from cradle to gate". The database does not consider the capacity of some materials to store carbon over its lifetime or, alternatively, the feedstock energy, typical of combustible materials. For the energy evaluation the values of non-renewable energy is considered, whereas the contribution of renewable energy resources is considered zero in terms of environmental impact. The impact indicator of each material $I_{m,i}$ is related to its mass, , a F.U. of 1 kg of product. From these elementary indicators for the materials used it is possible to define a performance indicator I_T of the envelope component, that comes out to be a simple function of the thickness of every layer, the ratio between the sum of the impact of every layer and the sum of their thermal resistance:

$$I_T = \frac{\sum_{i=1}^{N}\left(I_{m,i}\cdot\rho_i\cdot t_i\right)}{\sum_{i=1}^{N}\left(\frac{t_i}{\lambda_i}\right)} \qquad (1)$$

where: I_T is the impact indicator defined according to the requirement of thermal resistance [MJ/(m2K/W) o $kgCO_{2,eq}/(m^2K/W)$], $I_{m,i}$ is the impact indicator of the layer defined as function of the mass unit [MJ/kg o $kgCO_{2,eq}/kg$], ρ_i is the density of the considered layer [kg/m^3] and λ_i is the coefficient of thermal resistivity of the layer [W/mK]. These indicators, as seen from the equation, are functions independent from the thickness considered, therefore they can be considered as characteristics of the material.

RESULTS

Applying the equation (1) to the defined values of the individual functional layers for the four types of envelope systems, it is possible to calculate the impact in terms of CO2,eq emitted and non-renewable energy consumption.

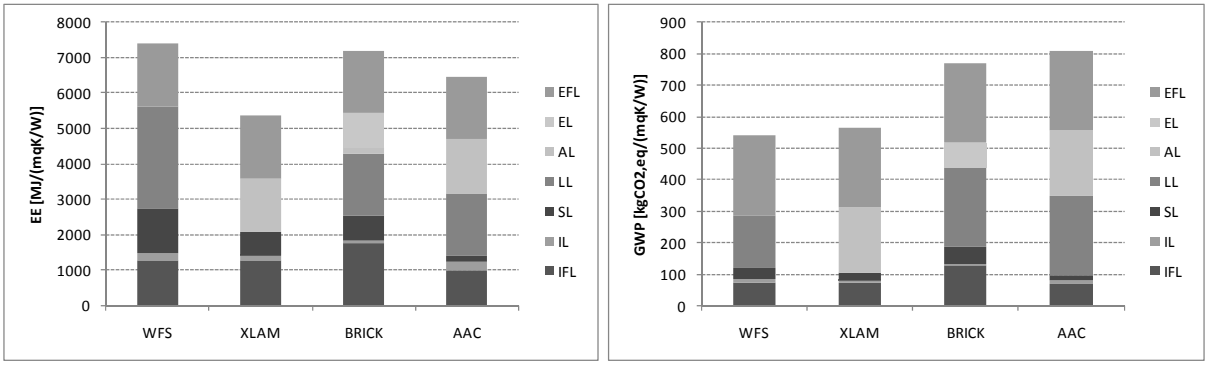

Figure 5: Total embodied energy and greenhouse gas emission for the "cradle to gate" phases for the four envelope systems analysed.

That approach, applied to the insulation layers, set up the scale of the impact levels of the considered different type of materials, defining in a more appropriate way the environmental qualities of the various solutions.

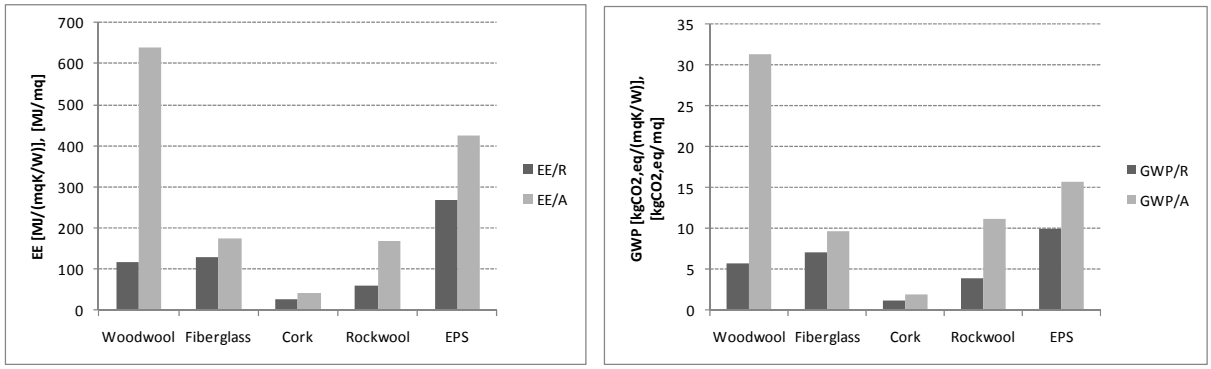

Figure 6: Comparison among the five different thermal insulation materials, considering as functional unit both the area and the thermal resistance.

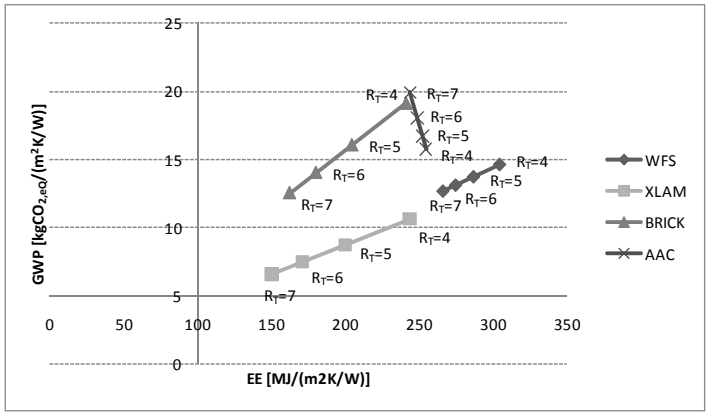

Figure 7: Total impact of the four envelope solutions considering the thermal resistance as functional unit and the variation of the insulation thickness.

Above the sensitivity analysis of the solutions considering a variation of the thermal insulation thickness to obtain consequentially an increment of a unit of thermal resistance from 4 m^2K/W to 7 m^2K/W.

DISCUSSION

From obtained results it can be seen that the proposed model is easily applicable for the comparison of the sustainability of envelope systems, resulting a practical support in the planning stage. As shown in Figure 7, the two wood-based solutions (WFS and XLAM) have a very low values of GWP than the other two traditional solutions, as well as a very low sensitivity to the increments of the insulation thickness. These values, if the capacity of wood-based materials to store the carbon is considered, would be even more lower.

However, many limitations still remain, including the limited boundaries of the analyzed system, with a condition "from cradle to gate" which does not allow to assess adequately the sensitivity of the solutions to reduce the consumption and emissions in every life stage (in particular in the stages of use & maintenance and end of life). In addition, the model considers only two indicators of environmental impact, probably the most important, but that does not give an exhaustive measure to evaluate the solutions' footprint on the ecosystems. Also the problem about the weighing of the impact indicators, in order to have only an indicative parameter for the comparison, is still open. This operation, however, is subjective and may provide very different results depending on the weight that is considered for one or another indicator. For this reason, in this text, none of weighing is considered.

REFERENCES

1. Alfsen, K., Greaker, M.: From natural resources and environmental accounting to construction of indicators for sustainable development. Ecological Economics, Vol. 61(4), pp 600–610, 2007.
2. Werner, F., Richter, K.: Wooden Building Products in Comparative LCA, Wood and Other Renewable Sources, Vol. 12(7), pp 470-479, 2007.
3. Malmqvist. T., et al.: Life cycle assessment in buildings: The ENSLIC simplified method and guidelines. Energy, 2010.
4. Various: Kyoto Protocol to the United Nations Framework Convention on Climate Change, United Nations Framework Convention on Climate Change *(UNFCCC)*, 1997.
5. Optis M., Wild P., Inadequate documentation in published life cycle energy reports on buildings, *International Journal of Life Cycle Assessment*, Vol. 15(7), 2010, pp 644-651.
6. Keeney, R.L.: Value Focused Thinking. Harvard University press, London, 1992.
7. Cole, R.J.,: Building environmental assessment methods: clarifying intentions. Building Research and Information, Vol. 27(4/5), 1999.
8. Kohler, N.: The Integration of Environmental Impact Assessment Methods in the Planning Process of Buildings. IEA-Future Buildings Forum, Wolfensberg-CH, 1995.
9. Hassan, O.A.B.: Application of value—focused thinking on the environmental selection of wall structures. Journal of Environmental Management, Vol. 70, pp 181–187, 2004.
10. Hammond, G., Jones, C., Inventory Of Carbon & Energy (ICE) Version 2.0. University of Bath, 2011.

Analysis of the Building Geometry Influence on Energy Efficient Integration of Small Wind Turbines in Building Envelopes

M. Popovac; R. Teppner; M. Rudolph;

AIT Austrian Institute of Technology, Energy Department, Sustainable Building Technologies Giefinggasse 2, 1210 Vienna, Austria.

Abstract

In an attempt to improve the overall energy sustainability in buildings, the idea of integrating Small Wind Turbines (SWT) in building envelopes is gaining popularity despite numerous practical problems. In addition to the safety and security issues, very important question is the energy efficient SWT integration in the building envelope, having in mind very limited energy potential of the wind in urban areas.

The present paper addresses this question by investigating the influence of the building geometry on the SWT energy potential. This investigation is performed by means of the Computational Fluid Dynamics (CFD), where the wind energy fluxes of the air flows around buildings in urban environments (obtained from numerical simulations) are compared for several different urban geometries.

Introduction

When analyzing energy efficient inclusion of Small Wind Turbines (SWT) in building envelopes it is very important to obtain accurate information about the actual velocity field in the building vicinity. On one hand, the wind energy flux that is available in urban flows is very limited due to strong influence of the flow effects (such as the air flow impingement, separation and its reattachment) which are related to the presence of the solid obstacles (buildings). And on the other hand, there is very strong dependency (power three) between the energy flux and the local velocity magnitude, hence the error in obtaining the actual velocity data leads to very high errors in the wind energy flux predictions.

This is why the Computational Fluid Dynamics (CFD) is appropriate engineering tool which can provide all information necessary for understanding the problems of energy efficient SWT building integration. Namely, on such a large scale it is practically impossible to acquire by means of field measurements sufficient amount of data necessary to reconstruct the urban flow field totality, whereas the laboratory measurements can hardly reproduce the actual wind characteristics in an urban environment. On the other hand, however, by solving the governing equations of fluid motion CFD provides a full insight into urban flow situation and all relevant flow characteristics. Still, the open issues for CFD predictions, such as the boundary conditions and wind characteristics, are best derived from the field measurements. In that respect the combination of numerical simulations supplied with the field data obtained from the on-site measurements is the best approach for the present analysis.

In the present paper the investigation of the energy efficient integration of SWT in building envelopes is organized as follows: in the first step the starting numerical setup is presented for the urban flow in a realistic residential neighborhood in Vienna (Austria), and the obtained results are compared with the measured values (averaged over main wind directions, according to the wind occurrence frequency), and in the second step this realistic geometry is slightly simplified and subsequently varied in order to test the influence of this geometry variation on the predicted wind energy flux around buildings.

NUMERICAL SIMULATIONS

For the present analysis, the numerical simulations are performed using commercial CFD package FLUENT [1]. Shown in Figure 1 is the realistic urban area, selected for these calculations in order to compare the obtained results with the available measurements [2]. The computational domain (commercial and residential neighborhood in Vienna, Austria) consists of several groups of residential buildings spread along the underground line and the underground station, several public buildings, as well as the shopping mall complex of a futuristic design (blue in Figure 1, the focal point of the investigation). For the flow simulations of such a developed urban organism it is important to have full geometrical representation in the numerical domain: exact building shape, bridges, and alike.

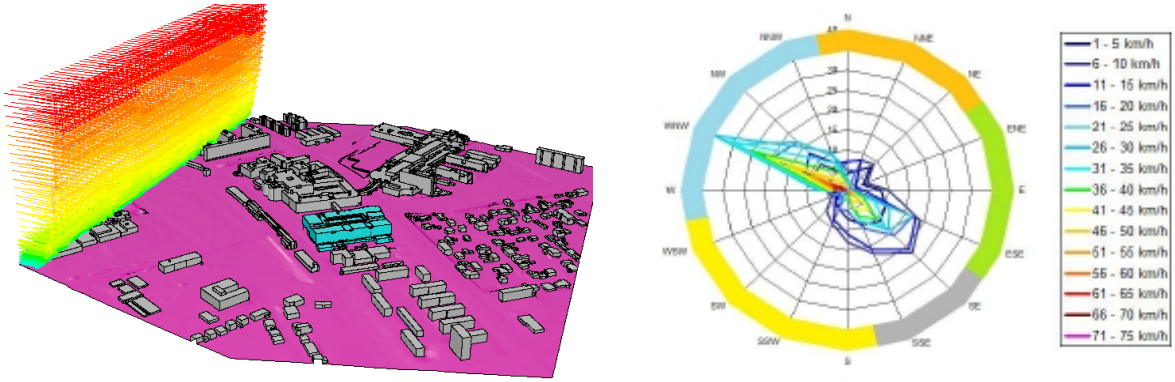

Figure 1: geometry of a developed urban organism, with exponential inlet wind velocity profile (left), and prevailing wind directions with their occurrence frequencies (right).

As shown in Figure 1 for a single wind flow direction, the wind was simulated by imposing the exponential velocity profile on the appropriate domain boundary faces. For assessing the entire flow situation a series of flow simulations is performed for all relevant wind directions, to include the spacial wind distribution following measured data at the given location. To this purpose the representative wind profile is imposed for each selected wind direction (prevailing wind directions), and the resulting wind velocity fields are then averaged according to the occurrence frequency of each wind direction (Figure 2). As for the wind speed distribution, a widely used approach for modeling the wind speed variations is two-parameter Weibull distribution [3], which can be written as:

$$f(U)=k(U^{k-1}/c^{k})e^{-(U/c)^{k}} \quad (1)$$

where U is the velocity magnitude, c and k are respectively the scale and shape parameters of the Weibull distribution, with $m_n=c^n\Gamma(1+n/k)$ being the n^{th} raw moment of this distribution.

With the wind speed variations modeled using Eq.(1), the *1st* raw moment (*n=1*) relates the velocity magnitude to the scale parameter ($m_1 = U = c\,\Gamma(1+1/k)$), while from the *3rd* raw moment (*n=3*) a rough but simple and fast estimation of the effective energy flux (in *W/m²*) at any specific SWT location can be estimated:

$$E_{eff} = \frac{1}{2}\rho\, m_3 = \frac{1}{2}\rho\left[c^3\,\Gamma\left(1+\frac{3}{k}\right)\right] \qquad (2)$$

where Γ denotes the Gamma function, and ρ is the density of the air. As the averaging procedure (depicted in Figure 2) is producing the representative velocity field, Eq.(2) can be used for the analysis of the energy efficient SWT integration in an urban environment.

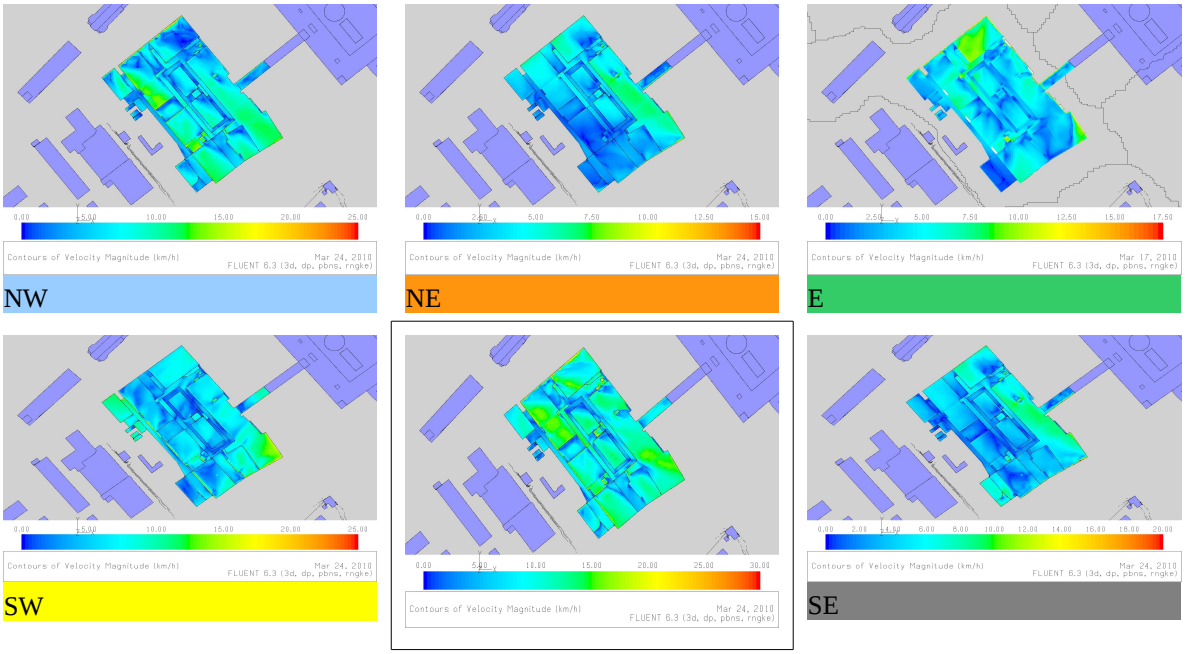

Figure 2: wind velocity in the roof vicinity – per direction (denoted by NW, NE, E, SW and SE, with appropriate colors) and the resulting averaged velocity field (in the box).

Results

The first numerical simulations are performed for a realistic geometry, in order to compare the simulations results with measurements. Four measurement masts are mounted on the roof of the central building, with two measurement points on each mast. The comparison between the averaged velocity field and the wind velocity measurements for the period June-September 2010 is presented in Figure 3.

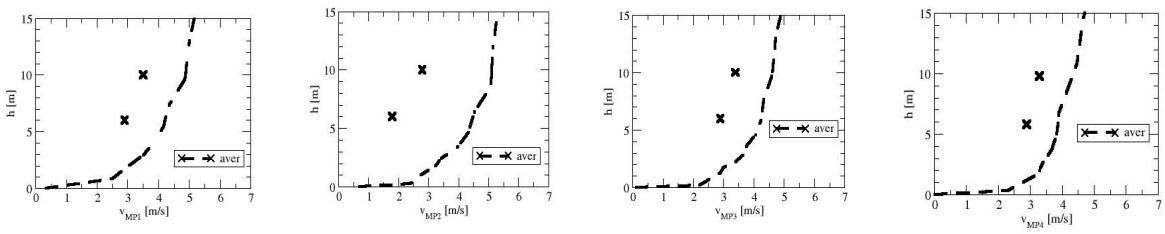

Figure 3: comparison between the wind measurement (symbols) and the velocity field predictions (lines), at four measurement points at the roof of the central building.

The overall flow pattern for this case can be identified from the flow path-lines around the buildings, shown in Figure 4. Clearly, urban environment flows are characterized by mutually interacting flow effects (separation, impingement etc.) which are typical for flows around bluff bodies. As the geometrical complexity increases the interaction between these effects becomes more complex, especially when the flow quantities in the near-wall region are considered (which is exactly where SWT are to be included in building envelopes).

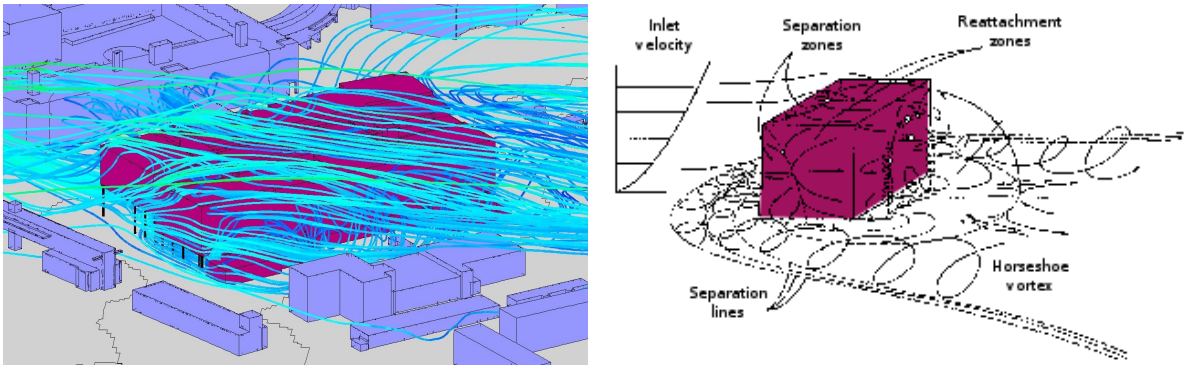

Figure 4: depicting an urban flow pattern, the path-lines of the flow around building (left) have the flow features characteristic for the flow around a bluff body (right).

In order to quantify the influence of the building geometry on the wind energy flux in an urban flow, this realistic geometry is simplified so that it can be easily varied and the obtained results compared. The geometry produced as the simplification of the realistic one, as shown in Figure 5, will be referred to as the basic case. The first variation includes the change of the horizontal disposition of buildings, where the central building is shifted successively for *10m* and *20m*, so that the space free of obstacles between the buildings is increased For the second variation, the height of the building previously shifted for *20m* is increased successively for *10m* and *20m*, and hence the wind from higher altitudes becomes more important in this case.

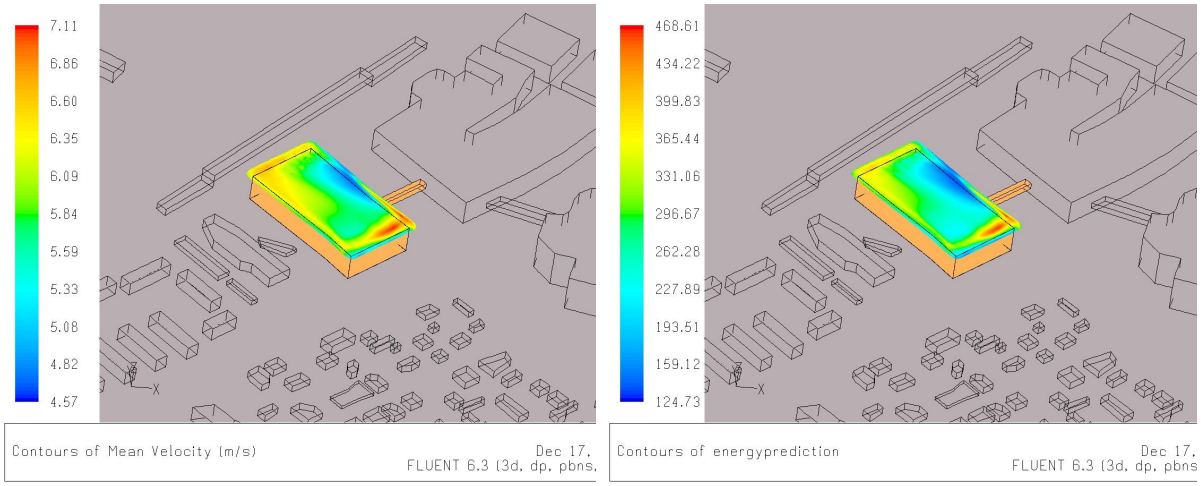

Figure 5: average velocity (left) and energy flux (right) for the basic case of the simplified geometry, in the cut-plane 6m above the building roof.

The results obtained for varied urban geometries are summarized in Figures 6 and 7, where the influence of different horizontal and vertical building disposition can be seen from the contour plots of the energy flux obtained from the averaged velocity magnitude, plotted in the cut-plane *6m* above the roof of the building under consideration. The regions of high energy flux can easily be identified (because in Eq.(2) the velocity comes to the power three), although some of the high energy flux regions are not practical for SWT building integration (e.g. chimneys). It should be noted that the Figures 6 and 7 show predicted energy fluxes that are based on the representative velocity field which is obtained by averaging the velocity fields from the prevailing wind directions (Figure 2), and by using the Weibull distribution defined by Eq.(1) for the wind speed distribution. Hence, the predicted energy fluxes should be understood as the expected values following these assumptions.

Finally, please note that the figures in this paper are provided in full color, and therefore they might not be legible in the black and white printed version. The full color version of this paper can be found on the CD-ROM issue of the CISBAT 2011 Proceedings.

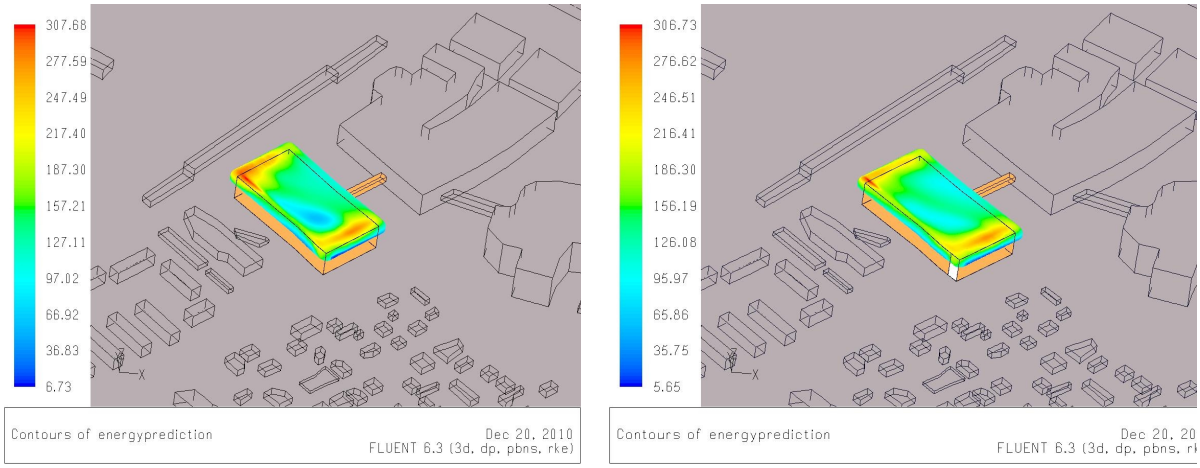

Figure 6: wind energy flux in the cut-plane 6m above the building roof, for the horizontal building disposition modified for 10m (left) and 20m (right).

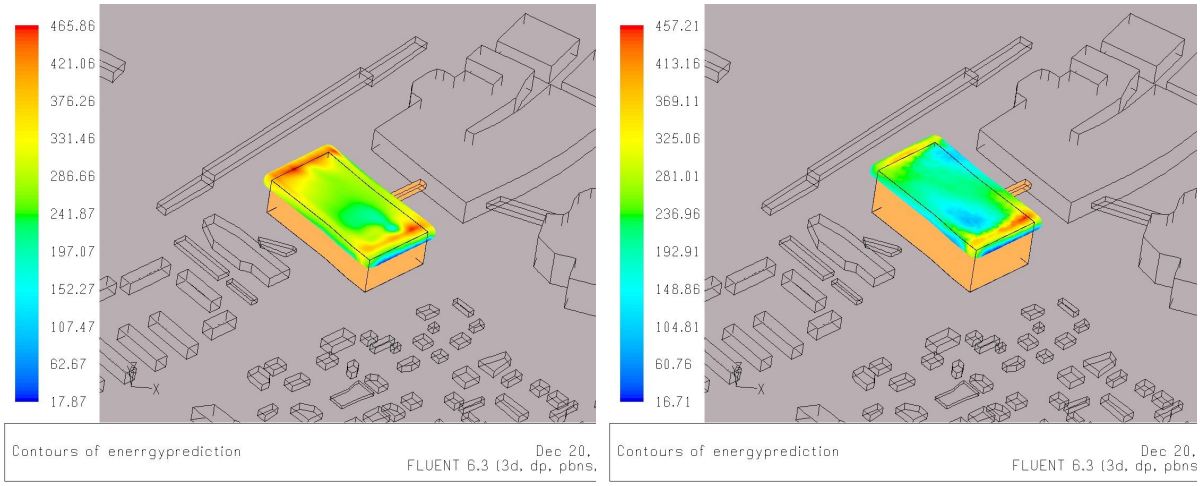

Figure 7: wind energy flux in the cut-plane 6m above the building roof, for the vertical building disposition modified for10m (left) and 20m (right).

Conclusions

In the wind energy flux expression given by Eq.(2) the velocity magnitude comes with the power three, hence for the accuracy of the wind energy flux predictions the wind velocity predictions accuracy is essential. Furthermore, as depicted in Figure 4, the velocity field in the urban environment is characterized by numerous flow effects (separation, impingement etc.) which are influencing one another. Naturally, as the geometrical complexity increases the interaction between these effects becomes more and more complex, and the resulting flow field is more difficult to predict in the near-wall region (which is exactly the region where SWT are to be installed in an urban context).

In the first part of performed numerical simulations, the flow field was analyzed for the exact geometry for which the measurements have been performed. For this case the imposed boundary conditions were resembling the realistic conditions as close as possible (Figure 1), however the perfect matching can hardly ever be reached. On the other hand, also the field measurements have a very large uncertainty factor, as they are very vulnerable to numerous external influences. The discrepancies between the measured values and the numerical results can be viewed from that perspective, and Figure 3 shows the difference of *20-30%* for the obtained velocity profiles, which can be acceptable. As for the wind energy flux predictions, however, from the velocity magnitude in the cut-plane *6m* above the roof of the building under consideration, shown in Figure 5, the regions of high energy flux can easily be identified (by virtue of the power three dependency). Some of the high energy flux regions, however, are not practical for installing SWT (e.g. the chimneys top, and similar protrusions), and therefore areas clear of obstacles have to be found for SWT building integration.

Finally, the analysis of the geometry variation (the difference between the base case, and the horizontal and vertical disposition) shows some tendencies which can be explained by the virtue of the urban flow pattern. Comparing the base case (Figure 5) with the geometries with different horizontal building disposition (Figures 6), one can see that for the geometries with the same height but with the difference in space in the immediate surrounding that is free of obstacles, the resulting velocity magnitude is not significantly changed. On the other hand, comparing the base case (Figure 5) with the geometries of changed vertical disposition (Figures 7), one can see that as the building height is increasing the resulting velocity magnitude (and corresponding energy flux) is increasing as well. However, the obtained increase is not as high as intuitively (or wishfully) expected, and the reason for such a behavior is the interaction of the complex flow phenomena that are taking place for the given flow situation. This interdependency of different factors makes difficult any generalization of the obtained results, and hence only this quantitative description is possible for a guideline for SWT building integration in an urban environment.

Acknowledgements

For the presented work the authors acknowledge the financial support from Österreichische Forschungsförderungsgesellschaft mbH – FFG (project “STEP-A“, project number 825371), and the weather data fron the Zentralanstalt für Meteorologie und Geodynamik – ZAMG.

References

1. FLUENT 6.3 User's Guide (2006). Fluent Inc, Lebanon, USA.
2. IPPONG project report, (2011). Österreichische Forschungsförderungsgesellschaft mbH (FFG), Wien, Austria.
3. Burton, Sharpe, Jenkins and Bossanyi, Wind Engineering Handbook (2001). John Wiley & Sons Lt. UK.

THE NEW INFORMATION COMMUNICATION TECHNOLOGY CENTRE OF LUCCA

Prof. Marco Sala[1], Arch. PhD. Rosa Romano[2]

1 ABITA Inter University Research Center Florence, Department of Architecture Technology and Design, University of Florence marco_sala@unifi.it, 2 ABITA Inter University Research Center Florence, Department of Architecture Technology and Design, University of Florence rosa.romano@taed.unifi.i

ABSTRACT

The Information Communication Technology Centre project was commissioned by the Chamber of Commerce of Lucca. The ABITA Centre was in charge of the green design of the project. This allowed us to test new technologies related to energy efficiency of the office building. The project focused on: the development of components and advanced energy saving systems, integration of dynamic facades to reduce heat loss through the building envelope, and energy production through renewable energy sources. Currently the building is under construction, and will be completed by the end of 2011.

Three buildings are connected by a central atrium, which is covered by a large glass and steel roof, (on the east-west axis), while the laboratories are covered by a green roof.

The project is focused on the adoption of intelligent facade systems to control the solar radiation in summer and heat loss in winter. All the windows have mobile aluminium shutters, which allow sun protection. The south facing glass roof of greenhouse is made of semi-transparent polycrystalline silicon photovoltaic panels. Those panels are integrated also on the south wall of building one. The selective low-E glass skylight and transparent surfaces have been designed to ensure excellent natural lighting inside the building. Solar pipes have been integrated in the roof of the laboratories. Air exchange is provided by a natural ventilation system.

The building will be certified – according to national legislation – as class A, thanks to the choice of materials. The materials are ecological and sourced from the project site. The choice of the building envelope uses a metal wall system with a low U value, thermal inertia and the integration on renewable energy system. In fact, the building's annual consumption is around 20 kWh/m^2 compared to 170kWh/m^2 in a traditional office building.

1. INTRODUCTION

The New ICT of Lucca project has been developed with the aim of spreading sustainable construction methodology in Italy. The aim is to reach the goals of 20/20/20 and to diffuse regulations that govern energy efficiency in buildings. The European Union established these regulation through the *Energy Performance Building 2002/91/CE* and *EU Directive 2010/31*. These aim to diffuse local and national regulations to guarantee high the efficient buildings, using appropriate policies which consider local climate conditions. From 31st December 2018, we must start building *zero energy* public buildings.

In Southern Europe, we must think about on winter and summer conditions and avoid copy in Northern Europe energy efficiency architectural solutions, to create appropriate solutions in energy efficient buildings. Southern Europe has specific climatic conditions, with the problems of indoor summer comfort, and the consumption of water resources and natural resources. Therefore it is necessary to improve research into new technologies for envelope solutions with regard to the energy consumption.

In Italy, the constant dependency on fossil fuels, oil and methane gas is still high in housing and office buildings sector. At a national level, Italy has adopted the European Directive 2002/91 with the dlgs 192/2005, that has been integrated and modified over the years. So, in 2009 the energy certification of buildings was made compulsory. In July 2009 the National Guide Lines, about the energy certification of buildings were issued. The *UNI TS 11300,* that follow the CEN regulations, were adopted. These propose a new and improved calculation method, including which incorporates energy consumption. The new regulation introduce new parameters of evaluation, like the periodic thermal transmittance or the indices of summer energy consumption.

In this paper we report on the strategies and technologies that we adopted to improve the energy performance of the new Lucca office building, to reduce the costs of heating, cooling and lighting, responding to national and international energy laws.

Fig. 1: East facade with Smart Skin Envelope

2. APPROACH

2.1 OFFICE IN ITALY: THE ENERGY SITUATION

The standard practice in Italian office buildings shows the following situation:

- full dependency on air conditioning systems to compensate deficiencies in the design's buildings
- high maintenance costs for the buildings and plants
- high electricity consumption
- an inexistent indoor environmental control system

Moreover it's important to note that energy consumption data is rarely available.

This is symptomatic of the lack of objectives to improve the quality of the environment:

- outdated environmental conditions in terms of air quality, visual quality and thermal performance
- environmentally-friendly and energy conscious design have been completely ignored due to a lack of knowledge about handling natural resources like natural day-light and ventilation;
- no environmental monitoring and control.

For these reasons this research needed project for a sustainable future in southern Europe, deals with successful solutions to decrease the growing effects of energy consumption trough air conditioning in urban buildings. In this contest, the ICT of Lucca offers great margins for energy improvement to promote a sustainable approach.

2.2 OBJECTIVES OF THE PROJECT

The reduction of energy consumption and the attention to environmental requirements are the main objectives of our project. The design concept of the building has been characterized by the adoption of solutions which improve solar gains and natural ventilation, and guarantee the integration of technologies to produce renewable energies with the building envelope. During the stage of design we simulated every energy performance of the building, choosing the system which would most reduce energy consumption. During the first design stage we employed an energy concept which corresponded to the features of the functional plan, the site, the local conditions weather and climate. On the basis of those parameters, the shape and consequently the structure were defined.

The project objectives of the new ICT Centre of Lucca are:

- To implement a concept design and a building construction based on technological solutions for passive cooling, natural lighting and ventilation, renewable energies, geothermal systems, greenhouses and a smart skin envelope
- To apply and test new and innovative energy saving technologies in order to improve the energy performance and the indoor environment of office buildings
- To realize a 50% reduction energy consumption and CO2 emissions
- To set a new standard for energy consumption and CO2 emissions in offices, while fully maintaining comfort conditions for workers
- To demonstrate, that energy efficient and sustainable office buildings can fully meet all the architectural, functional, comfort, control and safety features required, through the application of innovative and intelligent and integrated design. This demonstration could contribute to greater acceptance of innovative and renewable technologies in public buildings
- To diffuse and capitalize the results to increase the awareness of energy saving practices (in the medium and long term), and to integrate and improve policies for energy performance in buildings in Italy
- To use a monitoring system to compare the energy performance of buildings and define a new energy standard, in accordance with EU Energy Labels for the Mediterranean Area.

2.3 HOW CAN WE REDUCE ENERGY CONSUMPTION?

The construction of this new office building incorporates energy efficient measures, which are not only current innovations for the actual state of art but are also replicable in other offices in Italy. The importance of this project, with regards to our current situation, is the introduction of some specific, innovative, energy saving techniques, which set new energy, environmental and health standards for office buildings. In this framework, the following measures have been incorporated:

- An appropriate orientation of the building and envelope design.
- Smart façades and highly insulated building.
- Use of natural ventilation thought a good design.
- The sun space between the buildings acts as a buffer zone to reduce heat loss.
- Use of skylights for even distribution of daylight.
- Use of a geothermal system with a heat pump for cooling and heating.
- Integration of renewable energy, in the form of photovoltaic and solar thermal panels in the building envelope.

Thanks to its materials and innovative technologies, this building aims to spread the use of renewable resources and bio-architecture strategies.

3. SUSTAINABLE STRATEGIES

3.1 CLIMATIC ANALYSIS

Lucca is located at latitude 43° north and longitude 10° East, and has a typically Mediterranean climate with a cold winter (average temperatures ranging between -1.7-15.6°C) and hot summer (average temperatures ranging between 13-30°C), and rainfall mainly between November and March (precipitations of 125 mm/month).

Global radiation on a horizontal plane in summer may rise above 24 MJ/m^2day, while a winter value may rise above 4.5 MJ/m^2day. This data allows us to use active and passive strategies to reduce the energy consumption in the building. So, we have integrated PV panels in the roof of the big sun space and in the south façade.

The climate is dry with an average humidity in summer of about 70%, so we have adopted solutions about to control the humidity value inside the building in these months.

Finally, this climatic analysis has showed that the Lucca climate requires both heating (in December, January, February and March) and cooling (in June, July and August). Throughout the design process the aim has been to maximize heat gain in winter and minimize it in summer, and to encourage heat loss in the summer and limited in winter. In the intermediate months (April, May, September and October) the building won't be heated or cooled with artificial systems.

3.2 INTEGRATION OF PV SYSTEMS IN THE BUILDING ENVELOPE

In this project, to reduce the electricity needs, we integrated in the building envelope of a system:
- The sunspace roof; 48 glass PV panels integrated in half of the sunspace roof to improve the shading of the open space, this system produced 11.52 kWp.
- South façade; 84 opaque PV panels are integrated in the opaque modules of the vertical envelope (2.92 x 1.48 m), this system produced 15.96 kWp.
- The building roofs; this system is integrated in the roofs of buildings 1 and 3 and is made to 108 PV panels with amorphous cells, and it produced of 17.00 kWp

3.3 GEOTHERMAL HEATING AND COOLING

The ITC of Lucca is equipped with a geothermal system. The geothermal system is made to:
- 18 geothermal probes (90.00 m. Long).
- A heat pump with a cooling capacity about of 43.5 kw and heating capacity about of 45.00 kw.
- Radiant ceiling with an area of 5000.00 m^2.

The purpose of using the geothermal energy for cooling and heating ensure the decrease of the environmental impact of the building, in fact, this system produces renewable energy, it saves

about 50 % of the heating costs and supplies the energy needs for heating, cooling and water thought the year.
For energy consumption control, each office and laboratory is equipped with a heating, electricity and water meter so that the office user can see their energy consumption.

3.4 SUN SPACES

The sun space in the ICT Centre of Lucca has a surface of 1000,00 m^2, and was designed as an active roof, permitting the integration and flexible management of all mechanisms designed for heat and soundproofing, natural light and ventilation.

The design objective has considered not only the energy and environmental aspects but also the social impact: the primary objective is to create a pleasant, social atmosphere space which can be used for semi-outdoor activities through much of the year without any extra energy consumption.

Moreover, each office, is opens into the greenhouse, to improve daylight and to reduce the energy needs for lighting.

Particular attention was given to the design of the sun space envelope. The roof has a specific shape, with an angle of about 30% facing south, to ensure the integration of the PV panels, thus providing an overhanging surface which shadows the glazed roof from the sun. A motorized adjustable venetian blind is integrated in to the south and north façade, to improve ventilation in the summer. The main structure of the glass of the entrance hall as crescent shape, and is made of square steel beams, and tubular steel elements

4. FACADE ENGINEERING

The envelope of the building has two types of surface, according to the different orientation:

- Type 1 is the north and west façade, this uses a ventilated façade and has a U value of 0.28 W m^2
- Type 2 is the south and east façade, this is a smart façade with an internal transparent surface which has a U value of 1.2 W m^2 and a solar factor equal to 40%; the internal opaque model has a U value of 0.3 W m^2; external glazed surface has a U value of 4.00 W m^2 and solar factor equal to 57%; the PV cells are placed above the south façade, in front of the opaque module.

4.1 Smart facade

The south and the east façade have been designed as a smart skin that can change performance with the outdoor climatic conditions. The smart skin is a mobile double skin with a 50% opaque module, where a PV or solar thermal panel can be integrated, and a 50% transparent module. The façade consists of several parts assembled "dry" with a window frame whit an aluminum metal coating.

The modules are dynamic and can change configuration because the façade is integrated with two mobile pannels with a shading device and a glass pannel. In front of the trasparent module a metallic mosquito net is installated that allows the window of the transparent module to be opened at night to improvenight cooling in the building, in summer.

In winter a mobile glass panel is placed in front of the transparent module. So the smart facade will have the shape of double skin facade with a buffer zone that increase its U value to 0.8 W/m^2K.

In summer a panel with a shading device is placed in front of the transparent module, to regulate direct solar radiation and increase heat loss in the office.

5. CONCLUSION

The ICT Centre demonstrates that the energy efficient in the office buildings can fully meet all the requirements of the sustainability (architectural, functional, comfort and control) trough the application of innovative, intelligent and integrated design. This experimental project could contribute to a better dissemination of innovative and renewable technologies in public buildings in Italy.

Office 1		Office 2	
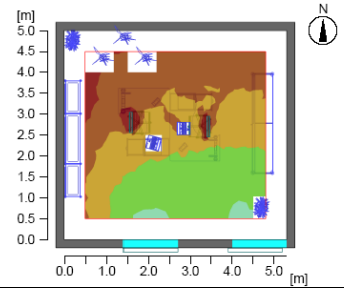		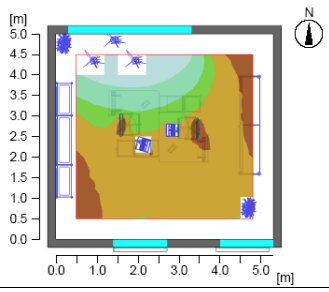	
		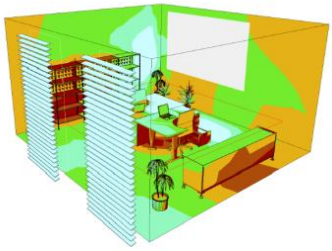	
E. Medium	267 lx	**E. Medium**	784 lx
E. Min	84 lx	**E. Min**	360 lx
E. Max	619 lx	**E. Max**	2450 lx

*Table 1: **Office Daylight Analysis.** We have integrated a window in the wall to the atrium to improve the natural lighting in the office.*

REFERENCES

1. Banham, R., The Architecture of the Well – Tempered Environment, Architectural Press, London, 1969
2. Hammad, F. Abu-Hijleh, B., The energy savings potential of using dynamic external louvers in an office building, in Energy and Buildings. An international journal devoted to investigations of energy use and efficiency in buildings, v. 42, p. 1888 1895, ELSEVIER, 2010
3. Hausladen, G., De Saldanha, M., Liedl, P., Sager, C., Climate Design: Solutions for Buildings that Can Do More with Less Technology, Hardcover, 2005
4. Jones D. L., Hudson, J., Architecture and the environment. Bioclimatic building design, Laurence King Publishing, London, 1998
5. Oesterle L., Lutz, H., Double-Skin facades: integrated planning, Prestel, Munich – London – New York, 2001

WIDE CONCEPTION OF «ZERO» ECOBUILDINGS AND ECOCITIES ON BASE OF ECOLOGICAL INFRASTRUCTURE

A. Tetior [1]

1: Professor of Moscow State University of Environmental Engineering, #19, Prjanishnicov St., Moscow, 127550, Russia

ABSTRACT

Wide conception of «zero» ecobuildings and of «zero» ecocities is based on three principles: «zero» interference in the nature, «zero» consumption of consumable resources from state networks, «zero» issue of pollution. «Zero» interference in the nature is the «zero» built-up area of buildings; it includes the minimal interference to natural circulation of matter, to migrations of animals; it signifies the sensory likeness to nature (use of sensory ecology – visual, odor and sound ecology); gardening of buildings, etc. «Zero» consumption of consumable resources includes: energy economy; renewable electric and thermal energy generation; natural ventilation and air-conditioning without energy consumption; decrease of expenses for internal illumination; reduction of water consumption, etc. «Zero» issue of pollution includes «zero» life cycle of buildings, recycling of waste products, use of ecological and recycled materials, the «zero» water drain, etc. The basis of «zero» ecobuildings and ecocities creation is new branch in building ecology - ecological infrastructure (it is complex of natural resources, constructions and systems, providing support of environment of human life at all levels - from the whole country up to cities and to separate buildings). Environment of life and environments of «zero» buildings and cities must be subject to all-embracing ecologization. All-embracing ecologization is system of upbringing of ecological thinking for respective activity and for use of ecological decisions based on ecological postulates, ecological philosophy and ethics, principles of sustainable building, adoption into account ethnical and geographical traits, social-psychological and social-economical features of inhabitants in city. This ecologization is the hierarchical system (from global up to local).

INTRODUCTION

Three principles of wide conception of «zero» ecobuildings and of «zero» ecocities creation include the following important parts of positive interaction of mankind with nature: «zero» interference in the nature; «zero» consumption of consumable resources from city networks; «zero» issue of pollution. Every part consists of several factors (tab. 1). One of the most important factors is preservation of landscapes with soil - vegetative layer from buildings and engineering structures. The surface of the ground in ecocity should be free; it may be filled by natural and cultural landscapes, and exempted from transport (fig. 1). This problem can be solved by overground and underground construction.

«Zero» ecocities with ecobuildings may include all components of natural landscapes; all complex of protected natural territories; all technosphere, all directions of human activity - architecture, construction, industry, power, transport, water supply, removal and processing of waste products; socio - psychological and socio - economic

environment; ecological satisfaction of needs of inhabitants. Ideological base of «zero» ecocities creation should be ecological postulates.

Three principles of creation of «zero» ecocities and ecobuildings		
«Zero» interference in the nature	«Zero» consumption of consumable resources from city networks	«Zero» issue of pollution
«Zero» built-up area of buildings	Use of natural technologies in lighting, ventilation, conditioning, etc.	Use of ecological life cycle by creation and maintenance of buildings and cities
Overground and underground buildings	Energy-active buildings	Use of ecological and recycled building materials
Sensory likeness of built-up territory to nature	Energy-efficient buildings	Use of systems of renewable energy from bio-waste
Minimal interference to natural circulation of matter	Reduction of water consumption	Use of systems of biological purification of waste
Planting of greenery of all artificial surfaces of buildings	Renewable thermal energy generation	«Zero» water drain
Support of being of small animals and birds	Utilization of thermal waste	Utilization of all waste
Creation of green corridors for support of biovariety	Use of intelligent (clever) systems in building and city for achievement of «zero» effect	

Table 1. Principles of creation of «zero» ecocities and ecobuildings

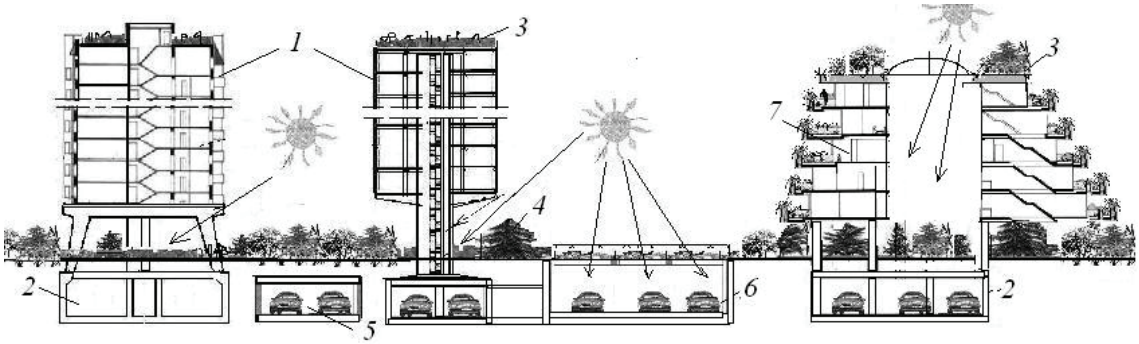

Figure 1. Scheme of "zero" ecocity with ecobuildings: 1 – overground buildings: 2 – underground parts of buildings; 3 – green roof; 4 – soil-vegetable layer; 5 – underground structures; 6 – underground street with sun lighting; 7 – "green hill"

Results

It is possible to believe, that the «zero» ecocities with ecobuildings with equality between their citizens can be created by help of new scientific complex inclusive urban ecology, architectural ecology, building ecology, ecological infrastructure, resilience of life in city, sensory ecology, ecological philosophy, ecological ethics, socio-psychological and socio-economic decisions [1-5]. This new scientific complex and its usage will allow creating ecological healthy cities and settlements, to stop retreat of nature, and to achieve a state of ecological equilibrium. Urban, architectural and building ecology is interconnected sciences about making of settlements and buildings, which are in balance with nature, and allow creating high-quality environment in region, cities and in buildings. These purposes are achieved by ecological decision of territorial, planning, geological, geographical, biological, hygienic, architectural, technical and aesthetic problems starting with general town planning scheme and ending with

construction of biopositive buildings. Solution set includes many directions of ecological construction, from biopositive buildings for preservation of soil-vegetable layer with flora and fauna, to backing of flora and fauna by help of creation of ecological framework, etc. (tab. 2) The new scientific complex should help to solve problems of «zero» ecocity and ecobuildings creation, including at gradual ecological reconstruction of any city. This complex consists of three principal directions: ecological environment, ecological activity, and ecological society. All these directions are equally important for forming of «zero» ecocity and ecobuildings.

Ecological environment	Ecological activity	Ecological society
All-embracing ecologization of environment	All-embracing ecologization of all activity	Support of equality
Support of ecological balance between city and nature	Resilience of socio-ecological system of city	Support of equal rights in free access to all world resources
Creation of ecological framework of city and region	Resilience of social component of system	Ecological upbringing and education
Creation and support of well-founded ecological infrastructure	Resilience of ecological component of city. Support of well-founded eco-footprint	Eco-philosophy, ecological ethics of inhabitants
Support of well-founded volume of nature	Urban ecology. Phyto-melioration.	Maintenance of ecological rights of inhabitants
Maintenance of flora and fauna by help of human activity	Architectural-constructive ecology. Sensory ecology (visual, smell, sound)	Ecological rights and duties. Participation in support of healthy environment
Restoration of all components of landscapes	All-embracing ecologization of industry, transport, etc.	Upbringing with help of beauty environment. Love to city

Table 2. Scientific complex for «zero» ecocity and ecobuildings creation

New complex of interconnected sciences for healthy cities creation includes the sciences about ecological, healthy, sustainable and beauty cities with high-quality environment of person's life and with environmental technologies: urban ecology, architectural ecology, building ecology, ecological infrastructure, sensory ecology, and ecological ethics. Creation of «zero» ecocity is based on inculcation of ecological thinking, ecological culture, eco-philosophy, and ecological ethics. It is possible to assert, that ecological compatibility, biopositivity of «zero» ecocity, their life in harmony with the natural environment as allied component is the good way of the development, allowing carrying out eternal mankind's dream of unity with nature.

The fundamental concept of ecocities will be invariable: they will be in ecological equilibrium with nature, and thus to create ecologically well-founded high quality environment life for inhabitants. But they will differ essentially from each other by set of individual decisions - from the size of city up to a degree of use of renewable resources, from a degree of preservation of the natural environment up to use of local materials, from a degree of equality of inhabitants up to a level of satisfaction of needs of inhabitants, etc. A base of new scientific complex is ecological infrastructure (tab. 3). Ecological infrastructure is complex of natural resources, constructions and systems, providing support of environment of human life at all levels - from the whole country up to cities and to separate buildings and engineering constructions. Ecological infrastructure includes interactive among themselves completely natural environment, quasi-natural cultural environment - cultural landscapes etc., artificial technical

environment of cities, socio - psychological and socio - economic medium (tab. 3). Ecological infrastructure is the interactive among themselves mastered and natural territories, ecological framework of city and green corridors, soil - vegetative layer, biopositive and «clever» buildings, systems of phyto-melioration and permaculture, ecologically restored landscapes and ecologically reconstructed buildings, favourable perceptible city environment, favourable conditions of life.

Artificial environment with all-embracing ecologization	Completely natural environment	Quasi-natural (cultural) environment
Technological systems with their ecologization	All natural territories with natural flora and fauna	Created by the person green areas
Traditional infrastructure with ecologization	All natural resources	Ecological built environment
Systems warning and liquidating adverse phenomena	Natural ecological framework with ecological corridors	Ecological cities and towns. Ecological buildings
Socio-economic and socio-psychological medium		

Table 3. Frame of ecological infrastructure

Urban ecology is most general science for ecological design of territories of cities and towns. It includes the decisions of ecological problems of big territories. The major problem of urban ecology is creation of the ecological framework of big territory. Ecological framework of Earth is system of large natural territories which are interconnected by ecological corridors, indissoluble interrelation of which allows supporting ecological equilibrium, environment of life, and biovariety.

Natural and improved cultural landscapes are the basis of ecological framework of city, united by "green corridors", “green wedges” sites of nature of various areas. The ideal ecological framework of city should look like a network with "cells" of nature including all components of natural and cultural landscapes in regular intervals distributed on the area - forests, parks, rivers, lakes, meadows, hollows, heights, squares, gardens and so forth. At their absence, it is necessary to create cultural green corridors that can be accompanied by formation of new "cells" of framework if their area on territory of city is small or if their number is insignificant.

Architecturally - constructive ecology contains two complexes of ecology knowledge’s: complex of general knowledge that allows forming the ecological thinking of builders, and complex of special ecology thinking for ecologization of building. Resilient environment of life of person presupposes a presence of conditions providing long, practically endless, satisfaction of essential (prime) and other ecologically well-founded needs necessary for human life, raising quality of the life, forming the harmonious social environment. For achievement of ecological equilibrium and high quality environment of life, it is necessary to keep ecologically well-founded territory of nature in all its biodiversity, to change interaction of person and technologies with nature.

«Zero» ecobuildings should be multifunctional, and alongside with the basic function (apartment house, industrial building, see shore construction etc.) can carry out one or several nature protection functions. «Zero» ecobuildings can use the renewable energy; they can clean polluted air and water through surfaces of buildings contacting with air and underground water by way of setting on all surfaces of walls of filters with compulsory circulation of polluted air and water(fig. 2).

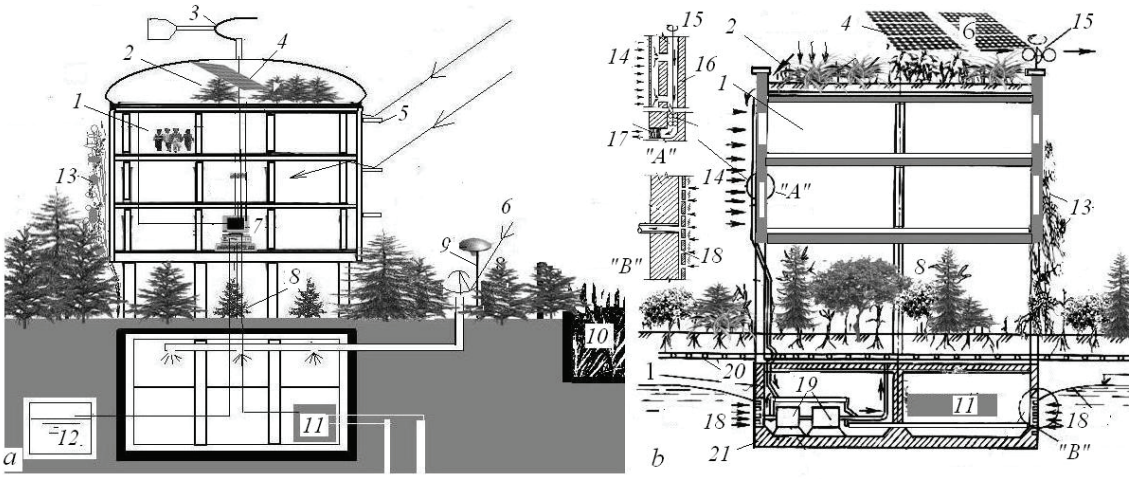

Figure 2. "Zero" buildings: a – with use of renewable energy; b – with cleaning of polluted air and water:1 – overground building;2 - winter garden; 3 - natural ventilation (such as a hood); 4 - solar battery; 5 - receipt of light due to reflecting a venetian blind; 6 - daylight into basement; 7 - computers for receipt of the data from devices (sensors); 8 - trees under building; 9 - solar energy for night illumination; 10 – "living machine" for black water cleaning; 11- thermal pump of system of geothermal heating; 12 - collection of "grey" water; 13 – vertical greenery; 14 – polluted air; 15 – wind turbine; 16 – canal for air;17 – filter; 18 – polluted water; 19 – pump; 20 - perforated pipe; 21 – underground part of building; "A", "B" - details

In «zero» ecocity may be used intelligent («clever») buildings. They supervise constantly through system of sensors the condition of the external and internal environment and at deviation of parameters from norm includes the effectors clearing, for example, environment from pollution, or improving other parameters. The «clever» building should create optimum conditions for people which are in it. Automatic sensors serve for support of normal physical and psychophysiological conditions of people environment. Such building contains sensors (converters), located in places of the best selection of the information on parameters of physical and psychophysiological conditions of people (they determine blood pressure, frequency of breath and heartbeat, a timbre and loudness of a voice, a condition and color of iris of the eyes, weight and growth of the person etc.). They transmit these parameters in the computer. The computer analyzes normal and current parameters on the basis of medical expert system (MES) and at deviation from norm, it signals about the beginning of illnesses. On the basis of the data incorporated in memory the computer gives out signals on the executive mechanisms giving in rooms medical aerosols and the appropriate additives for smells; in potable water, in water for douche or bath - medicinal additives; creating necessary (raised or lowered) temperature and humidity indoors; giving out on the monitor in kitchen of the recommendation for a meal; including appropriate (the soothing or stimulating music, appropriate holographic or other pictures on walls; it allows to support in due time health of the person and to remove a psychological pressure (fig. 3).

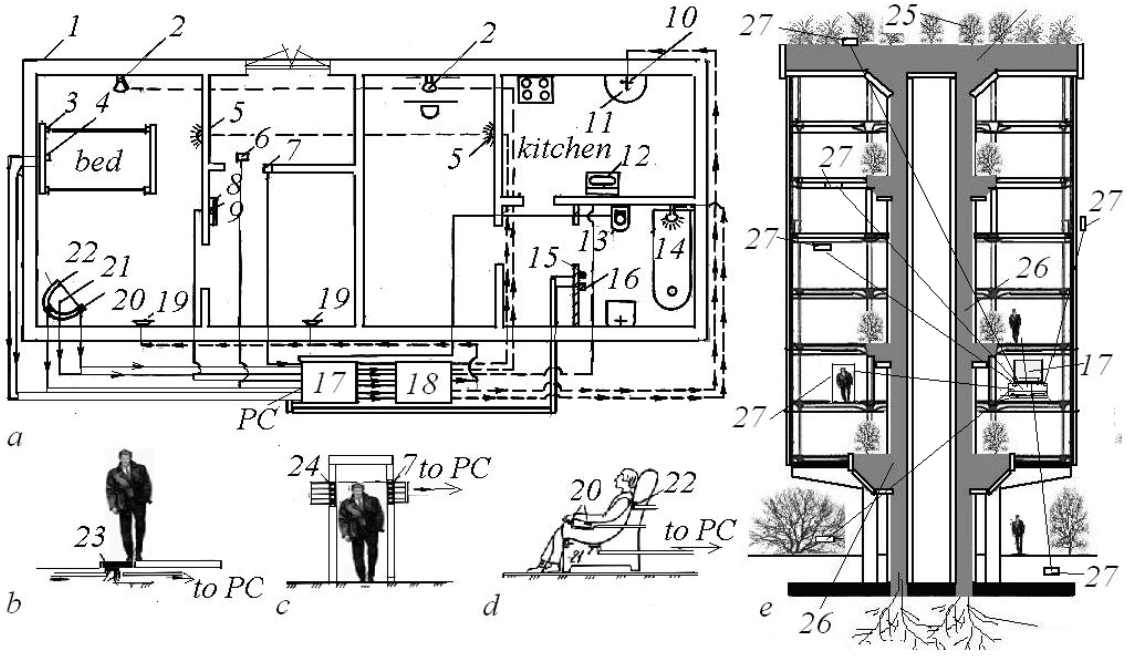

Figure 3. Plan of intellectual home with the indication of the locations of detectors (sensors) and effectors (executive mechanisms) (a); details (b-d); soil-filled building (e): 1 - external wall; 2 - spray for supply of aerosols; 3 - resistive-strain sensors on bed; 4 - sensor (receiver) of exhaled air; 5 - lighter with color filters; 6 - sensors of weight of body in floor; 7 - photo resistors in a jamb of door; 8 - mirror; 9 - transmitting color TV camera; 10 - supply of medicinal additives in potable water; 11 – wash-bowl; 12 - display with conclusion of the data on a recommended diet and a healthy way of life; 13 - the sensorы in «clever» toilet; 14 - tube for introduction of medicinal additives in water in douche and in bath; 15 - thermovision camera; 16 - equipment for control by method Kirlian - effect; 17 - system of executive mechanisms; 18 - microprocessor; 19 - loudspeaker; 20 - sensors of blood pressure and heartbeat; 21 - resistive-strain sensors in sitting of armchair; 22 – microphone; 23 – sensors of shuffling in floor; 24 - sources of light; 25 – green roof; 26 – soil in vertical canals; 27 - soil on floors

Conclusion. Undoubtedly, the «zero» ecocities and ecobuildings are the attractive future of mankind. New scientific complex may help to form new ecological thinking of future specialists – authors of «zero» ecocities. All-embracing ecologization of all directions of people activity may be the basis of creation of future realistic ecocities.

REFERENCES

1. Register R. Ecocities. – Berkeley: «Hills Books», 2002.
2. Kibert Ch. J., Sendzimir J., Guy G. B. Construction Ecology. – London: «Spon Press», 2001.
3. Tetior A. Ecological infrastructure. – Moscow: «Koloss», 2003.
4. Tetior A. «Zero» ecological home. – Moscow: «MSUEE», 2010.
5. Tetior A. Architectural-building ecology. – Moscow: «Academy», 2009.

TEENERGY SCHOOLS: HIGH ENERGY EFFICIENCY IN SCHOOL BUILDINGS IN THE MEDITERRANEAN AREA

Arch. Antonella Trombadore[1], Arch. Rainer Toshikazu Winter[1] Arch. Rosa Romano [1] ,

[1] *ABITA Inter University Research Center Florence, Department of Architecture Technology and Design, University of Florence*

ABSTRACT

TEENERGY SCHOOLS is a EU project co-financed by the MED programme which gathers 8 international partners operating in 4 strategic Mediterranean countries: Italy, Greece, Spain and Cyprus. The project aims at solving 2 common problems of the Mediterranean area: the lack of energy saving benchmarks targeted to south Europe climatic conditions and the low energy efficiency of existing school buildings. The project works on the improvement of existing Secondary Schools' energy efficiency by developing a Common Strategy, based on the 3 typical climatic models that characterize the MED area: coast, mountain and plain. An internet based Platform is helping to implement a strategic approach in benchmarking of the comparable energy data of the selected Schools.

The main activities are:

- the realisation of Energy Audits, Surveys and Benchmarks;
- the redaction of a common Action Plan throughout the international partnership;
- the elaboration of a Concept Design for 12 innovative Pilot Projects, also through the organisation of 3 thematic Workshops and 1 international Campus involving experts, designers, students and decision makers;
- the creation of an in ICT Platform that works as an interactive operational tool gathering audit data and cataloguing laws, best practises and existing technologies; it contains the Guidelines of the Common Strategy for energy management; it is addressed to local authorities and decision makers, schools, technicians, public and private operators and all citizens interested in the construction sector and energy related issues;
- the diffusion and capitalisation actions directed also to raise awareness on the use of new energy techniques and standards and – in medium long term – to integrate and improve the energies policies and rules in the MED area and Europe;

The Specific objectives of the project are:

- to create a trans-national network amongst partners, other Public Authorities, Universities or technical bodies and schools, involving students in the educational dimension of Teenergy Schools;
- to experiment Benchmark activities for comparing buildings energy performances and defining a MED Action Plan, useful also for new construction;
- to implement a Concept Design action based on technological solutions for (passive) cooling, natural lighting and ventilation, renewable energies, also through the organisation of international events (3 Workshops and 1 Week international Campus);
- to diffuse and capitalize the results with the aim of increasing the awareness on energy saving practises and standards and –in medium long term – integrating and improving the policies at MED level.

INTRODUCTION

Teenergy Schools has developed a Decalogue to meet the needs for the providing a Common Method of decisional support involving stakeholders to fulfill the challenge of improving the school environment of education for the next generation of pupils, by starting today. The Teenergy Schools Decalogue aims at giving the basic indications for the implementation of existing schools retrofitting action a process. It is targeted to all the actors, but particularly to the public authorities—who must set themselves up as promoters of the process—and the scientific experts in charge with the coordination and the management of its application.

This Decalogue aims to illustrate the way towards an appropriate energy efficient retrofitting of school buildings in the specific Mediterranean context, going beyond the usual isolated interventions and taking into account new aspects such as bio-climatic technologies: solar architecture, passive cooling, intelligent windows for natural ventilation, energy efficient facades including sun shading, cool or green roofs and the use of materials from natural local resources with positive LCA evaluation.

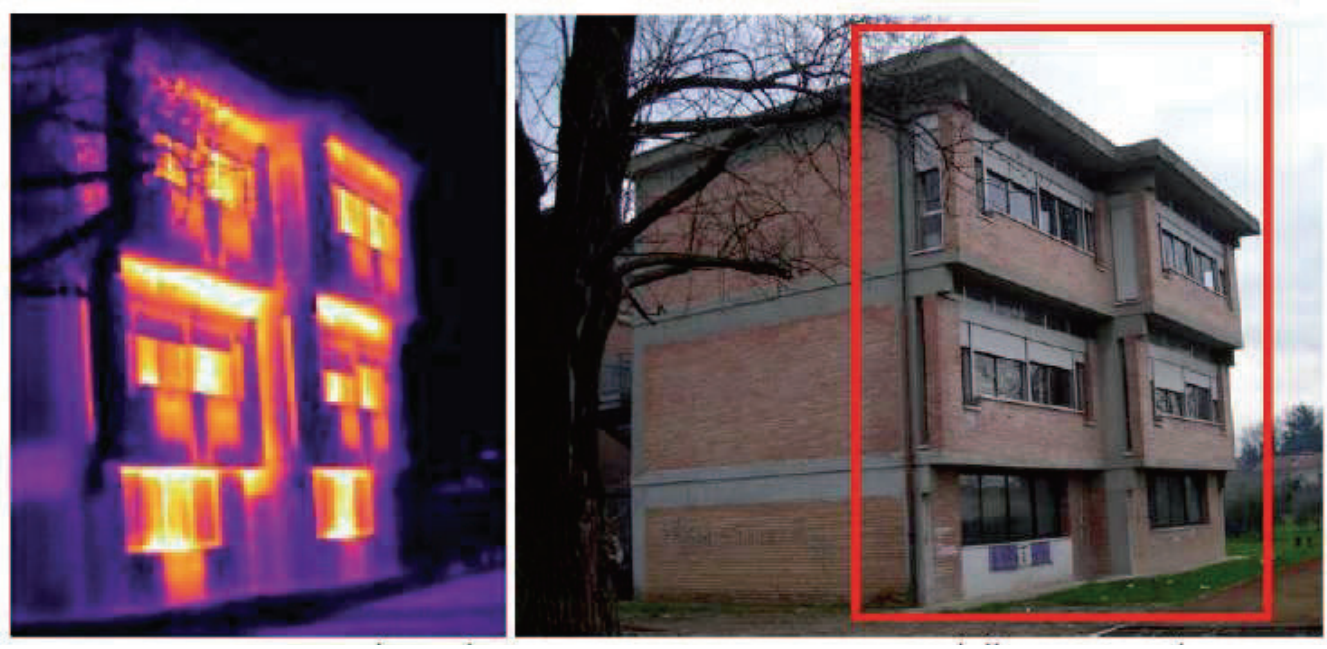

Figure1: Thermography has been a fundamental instrumenti in the diognosis fase: heat losses can be localized easily

METHOD

Teenergy Schools Decalogue for the Mediterranean Area

1. **Setting the targets:**
   definition of the Quality objectives to be reached in the retrofitting of existing schools and for the construction of new school buildings aiming at energetic efficiency and good indoor climate in all seasons
   - High Energy efficiency for heating and cooling
   - Efficient natural and artificial lighting
   - High standard of natural ventilation in classrooms guaranteeing low CO2 rate during the lessons ensuring good study conditions
   - Use of sustainable building material based on critical LCA analysis
   - Bioclimatic Strategies for energetic efficiency and good indoor climate in all seasons using Passive cooling (Ground Cooling/Night Cooling) Sun shading and Natural Ventilation systems against Summer overheating

- Correct Use and management of renewable resources: use of appropriate, cost- and energy-efficient technology
- Acoustic quality inside the building for good audio comfort in the classrooms
- High Outdoor Environmental Quality (outside microclimate)
- Good visibility and media communication to guarantee wide spreading of results
- Didactical aspect of the intervention as added value of retrofitting / new construction for the active involvement of pupils (change of mindset/behavior)

2. Energy Audit:

Checking the State of Art of the building and the energy performance of the envelope and energy consumption on HVAC (Heating, Ventilation and Air Conditioning) systems throughout data collection including bills, measurements and software simulations:

- energetic behavior of the building taking into account the real consumption, the simulations (expressed in kwh/a/m3)
- thermographic anaylis for the detection of heat losses for efficient problem solving
- Analysis of the functionality, occupancy (pupils/m2), use and costs for the running of the building (euro/pupil/year)
- Evaluation of the Security norms
- Evaluation of Level of maintenance
- Structural characteristics, anti-seismic aspects
- Sanitary equipment

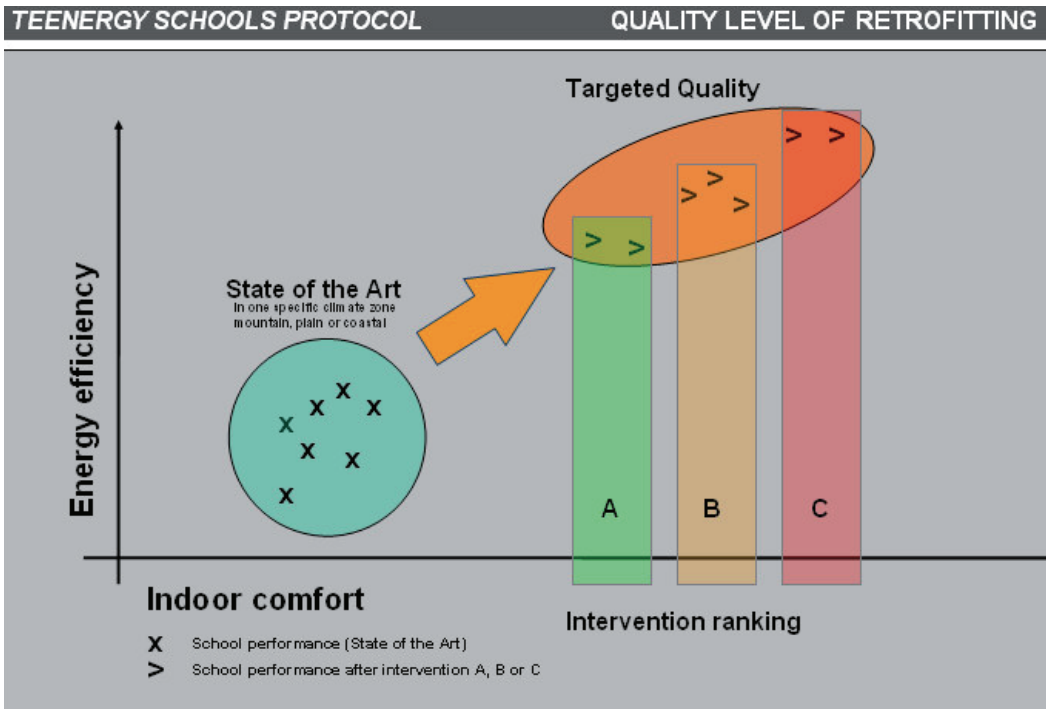

Figure 2: The definition of the Quality Objectives defined by energy efficiency AND indoor comfort in the school buildings within the Mediterranean climate context

3. End user feed-back questionnaire:

- Analysis of the feedback of pupils and teachers throughout a specific (anonymous) Questionnaire in order to define the psycho-physical aspects regarding the actual perception of indoor comfort by the end users
- Involvement of the students and end user to improve their awareness

- Evaluation of indoor quality
- Comparison between assessed performances of the e school building, the monitored use and occupancy and the satisfaction of the end users of the building in order to obtain a critical view of the actual situation.

4. Mapping and Evaluation

- Analysis and mapping the results with the support of adequate tool for the homogenization of the data at an appropriated decision scale (Municipality context, Provincial/Regional/National/ International) and Analysis and graphical visualization of the collected data from the Energy Audit, the End User Feedback Interpretation and graphical visualization of the collected data from the Energy Audit and the End User Feedback
- Evaluation of the gap between State of Art and Target,
- Analysis of the critical point where the data of energy performances of the school buildings are below the average (Mapping and Positioning of the results in a larger context (regional, national, European) taking into account specific 3 climatic sub areas: Coast, mountain and plain.

5. Benchmarking in the context :

- Comparison of the monitored school buildings to obtain a performance-ranking for the definition of preferences : which school building need to be refurbished first?
- Analysis throughout multi issue criteria: **what are the main criteria?**
- Definition of thresholds of energy performance, indoor quality level, available budget
- Definition of acceptable limits

6. BEST PATH Methodology

- The Best Path Methodology aims at defining the most adapted solution in terms of economical technical and human aspects following the elaborated quality criteria as indicated above. On administrative and political level a critical weighting of the importance of each of the following four main objective must be considered: energy efficiency B. indoor comfort C. quality of communication of the project, D. technical aspects (for instance obligatory issues such as anti-seismic norms, fire-security, sanitary aspects)
- Obviously each refurbishment or new construction of a school has an important mediatic value for the local administration, therefore the quality of the communication has to be considered an important issue. Building Sustainable Schools in the Mediterranean Area with bioclimatic principles in an energy efficient, socially and politically participated approach has a high value in terms of innovation.
- Each one of these aspects will have a weight expressed in % following the strategic decisions of each single administration.

7. Interdisciplinary involvement in the Participated Planning Process

- involving all the stakeholders of the school environment: pupils, parents and teachers, driven by the initiative of the administrational responsibles engaged in a transparent, participatory round table with the help of qualified technicians: the project bases for new schools or the refurbishment strategies for existing schools has to be elaborated in an interactive and interdisciplinary process involving all parts, taking into account the above mentioned ranking of priorities following the Best Path integrating previous analysis such as Energy Audit and the End User Satisfaction.

- The continuous illustration and monitoring of the proceedings of the process with is of great importance to guarantee satisfaction of all interests.

8. Concept Design Implementation of Architectural Solutions /Retrofitting strategies

- The Concept Design Solutions will be based on sustainable, energy efficient building technologies taking into account bio-climatical aspects in order to respond adequately in each single micro-climate area.
- High Indoor comfort is targeted by improving thermal, acoustic and visual comfort in the classrooms
- at least three scenarios with low medium and high outputs proportioned to the dedicated investment will be elaborated

9. Cost benefit evaluation

- Critical choice of the most suitable solution in terms of energy efficiency, satisfaction of the end users, economic context and communicational aspects for the local administrator's political targets

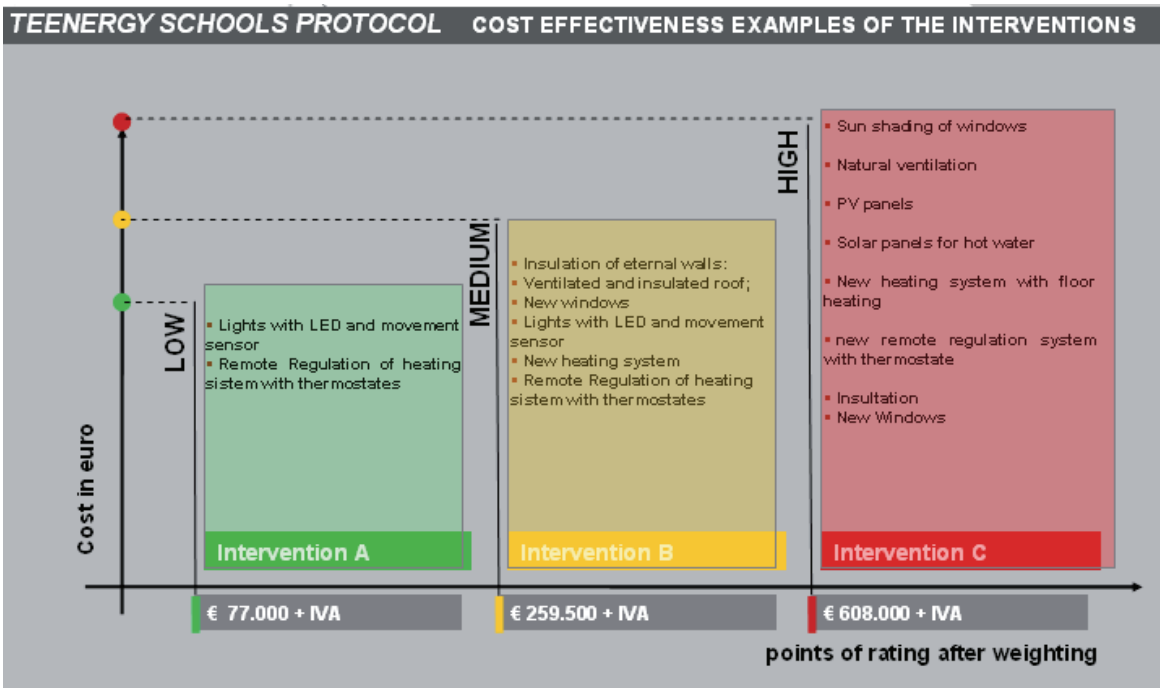

Figure 3: The three-scales scenario permits a ranking that takes into account energy performances of the proposed retrofitting solution, indoor comfort and economical aspects:

10. Diffusion and Communication of the results: towards Best Practice

- Constant monitoring of the feedback within the participated process
- Promotion of the results within the context of a Pilot Project that has a didactical vocation
- Networking of similar experiences in order to promote wide speading of the initiatives and guarantee efficient research results in collaboration with scientific institutions and exponents of the building industry.

RESULTS

A common Action Plan has been published gathering the obtained results of the project. It illustrates the partnership's methodology and shows tangible results by integrating the 12 Pilot Projects for retrofitting and new building of climate orientated, high energy performance

school building in the Mediterranean Area. The Projects have been developed in Mountain, Coast and Plain area in the 4 different partner countries: Italy, Spain , Greece and Cyprus.

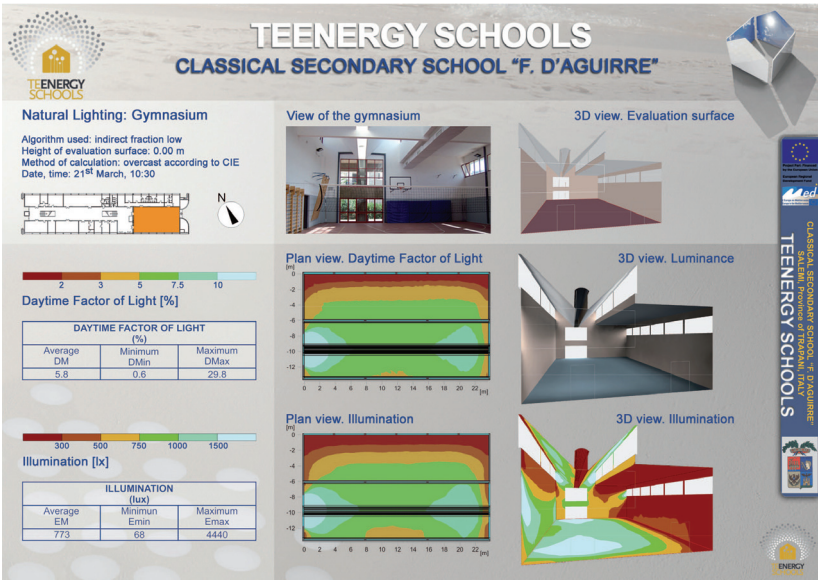

Figure 4: The 12 Pilot Projects have been elaborated by each territorial partner with the help of a scientific partner. The results take part in an international exhibitioni all partner countries.

REFERENCES

1. C.A. Roulet Ventilation and airflow in buildings Methods for diagnosis and evaluation. Ed. Earthscan Ltd., London, UK, 2007
2. F. Allard C. Ghiaus Natural ventilation in the urban environment Assessment and design. Ed. Earthscan Ltd., London, UK, 2005
3. M. Sala (a cura di) Integrazione Architettonica del Fotovoltaico Casi studio di Edifici Pubblici in Toscana. Alinea editrice, Firenze, 2003
4. M. Sala, a cura di, I percorsi della progettazione per la sostenibilità ambientale,Atti del Convegno Nazionale ABITA, Firenze, 20-21 ottobre 2004. Alinea editrice, Firenze, 2004.F. Sartogo M. Bastiani
5. P.F. Smith Building for a Changing Climate The Challenge for Construction, Planning and Energy. Ed. Earthscan Ltd., London, UK, 2009
6. Santamouris M. Energy Rating of Residential Buildings; Earhscan, London, 2005
7. Santamouris M, Mihalakakou G, Patargias P, Gaitani N, Sfakianaki K, Papaglastra M, et al. Using Intelligent Clustering Techniques to Classify the Energy Performance of School Buildings, Energy and Buildings, Vol. 39, Issue 1, January 2007, p.45-51.
8. S.Burton, M. Sala "Energy Retrofitting in office buildings" James&James, London, 2000
9. Serghides D., "Bioclimatic and Low Energy Buildings in the Mediterranean Region" Proceedings IAES & WREC, 2009, Sohar, Oman.

LIFE CYCLE ASSESSMENT (LCA) OF BUILDINGS APPLIED ON AN ITALIAN CONTEXT

N. Villa[1]; E. De Angelis[2]; G. Iannaccone[3]; L. Zampori[4]; G. Dotelli[5]

1: Politecnico di Milano, Dip. BEST, Milan, Italy - (nadia-villa@libero.it)

2: Politecnico di Milano, Dip. BEST, Milan, Italy - (enrico.deangelis@polimi.it)

3: Politecnico di Milano, Dip. BEST, Milan, Italy - (giuliana.iannaccone@gmail.com)

4: Politecnico di Milano, Dip. di Chimica, Materiali e Ingegneria Chimica "G.Natta", Milan, Italy - (luca.zampori@chem.polimi.it)

5: Politecnico di Milano, Dip. di Chimica, Materiali e Ingegneria Chimica "G.Natta", Milan, Italy - (giovanni.dotelli@polimi.it)

ABSTRACT

The present study is focused on the application of Life Cycle Assessment (LCA) in the design of residential buildings, in the Italian context. The aim of the analysis is to use LCA as a tool to compare design choices (for structures, envelope technologies, building services etc.) in term of environmental impacts.

Three different buildings, in different geographical localization but in a similar climate, characterized by different size, structure, and material used, were analyzed. The case studies focused their attention on the same environmental impacts: i) the embodied energy of the building materials, ii) the energy consumption of the operating phase and iii) the CO_2-equivalent emissions in the atmosphere during both phases. Transports, the energy involved during the construction operations, materials used to produce the components of the building services, maintenance operations, end of life (reuse or recycling) and disposal of the whole buildings, have not been analyzed, because of the lack of reliable primary data, either from each specific case or from databases.

The cases considered faced some different aspects connected to the LCA of buildings:

- *Case study A* analyzed a residential building realized in L'Aquila, after 2009 earthquake, made with prefabricated wood panels. The real building was compared with two traditional alternatives: loadbearing masonry and concrete frame. The analysis took into account both construction and operation phases of the three alternatives with the following databases: IBO (based on Austrian context), ICE (UK context), ITACA (Italian context);
- *Case study B* focused on two other residential buildings realized in L'Aquila with steel and prefabricated concrete technologies, following *Case study A* guideline;
- *Case study C* focused on a Class A residential house built near Milan in the same period. In this case, the building life have been analyzed on wider boundary conditions, i.e. including average value of transports, construction site energy consumption and maintenance phases.

A direct comparison of these cases was possible due to the similarity of the boundary conditions or to the adaptation of the existing boundaries condition to the most restrictive ones. Also, the choice of applying the same databases (i.e. IBO, ICE and ITACA) to the three case studies considered made the comparison possible, under the known hypothesis that each

database was built to respond to the production system and the energetic context of the country selected as reference and accordingly to the most applied technologies in the area.
As common baseline, the operational phase was found to have the highest environmental impacts, even when a significant reduction of the operation energy needs was reached by improving thermal insulation, air-tightness and ventilation heat recovery to a standard A-class value.

Due to the various possible applications of Life Cycle Assessment in the building sector, it would be highly desirable and useful for nowadays designer to have a univocal tool to support the design since the early phases of the building scheme, in order to reach the optimization of the process, starting from the choice of materials to the best suitable plants.

INTRODUCTION

Nowadays there is a growing concern about the environmental impact caused by buildings and following this trend the aim of this study is to perform a comparison among different residential buildings in the Italian context, using LCA methodology.
LCA application to buildings must deal with numerous variable parameters: lifetime, climatic conditions, assumed indoor air temperature, amount of hot water use, system boundaries of included building parts and processes, data on material production, production of electricity, rates of materials spread at the building site, transport distances, the most probable service life of components and elements, their maintenance treatments and frequency,...

For a reasonable comparison of design choices, the overall performance has to be considered, but this is not always possible due to the lack of data during the many phases of the long service life of a building. For this reason the energy and environmental evaluations of the case studies focus on values concerning material production and on the energy required during a standard 50 years long operational phase and similar climatic conditions.

METHOD

Three macro-case studies of residential buildings have been analyzed with a LCA method.

LCA consists in analyzing the entire life cycle of the object of the analysis (a building in this case), considering all phases, from the production to the end-of-life. For each phase, the various energy and materials flows are assessed and then various impact indicators can be computed.

Boundary conditions:

For each building an inventory of installed building materials is compiled and their operational energy requirement is evaluated (heating, domestic hot water and electrical devices) over 50 years. These restrict boundary conditions result from data fault related to transports, construction operations and maintenance plan.

Assumption and limitations:

It is assumed that the energy mix for electrical services will be the same over the entire life span of the building. The impacts for the facilities used for installation were not considered for the energy services and all the construction materials.

Functional unit

The functional unit used for the buildings considered is one square meter of floor area.

Buildings characteristics:
Each buildings is realized with different materials and technological solutions, as shown in *Table 1*:

	Case A1	Case A2	Case A3	Case B1	Case B2	Case C
Place	L'Aquila	L'Aquila	L'Aquila	L'Aquila	L'Aquila	Arluno, Milan
n° floor	3+ boxes	3+ boxes	3+ boxes	3+ boxes	3+ boxes	3+ boxes
Year of construction	2009	2009	2009	2009	2009	2009
Lifespan	50 years	50 years	50 years	50 years	50 years	50 years
n° apartment	27	27	27	25	24	12
Area [m^2]	1404	1404	1404	1453,16	1484,28	982
Loadbearing structure	Xlam panels	Loadbearing masonry	Concrete frame	Steel frame	Concrete frame	Concrete frame
Ufacade [W/m^2K]	0,3	0,3	0,3	0,34	0,34	0,29
Ufirst floor [W/m^2K]	0,23	0,23	0,23	0,33	0,33	0,26
Uroof [W/m^2K]	0,17	0,17	0,19	0,3	0,3	0,19 or 0,26
Window type	Double-glass filled with argon and metal frame (thermal edge)			Double-glass filled with argon and metal frame (thermal edge)		Double-glass filled with argon and wood frame
Building services	Condensation boiler and solar panels			Centralized condensation boiler and solar panels		Geotemic heat pump (for heating, DWH and cooling)and photovoltaic panels

Table 1: Case studies.

Case A:
A dwelling in L'Aquila built in 2009 after the earthquake, with a cross-lam, wooden panel structure (*Case A1*) and then hypothetically re-designed with a masonry (*Case A2*) and concrete (*Case A3*) structure, keeping the same U-value for the envelope solutions. The environmental impact of these case is studied applying three databases: IBO (based on Austrian context), ICE (UK context), ITACA (Italian context).

Case B:

Following Case A scheme of analysis, two other residential buildings realized in L'Aquila in 2009 are studied. These buildings have similar shape and a size to Case A, but with a steel (*Case B1*) and concrete (*Case B2*) structure.

Case C:
A building realized in Arluno, near Milan in 2009, on an area with the same climatic characteristics of L'Aquila, but with a lower size concrete frame.

The analysis of this building does not spread over three databases, but it is focused only on ITACA database, considering also an average value for transports, the construction site energy consumption and a maintenance program, as shown in *Table 2.*

CASE C	CO_2eq	Energy
Lifespan: 50 years	[kg CO_2eq/m^2]	[MJeq/m^2]
Materials	1064,3	14584,7
Plants materials	8,4	9,7
Construction site	33,6	6,4
Operational phase	1995,9	11243,6
Maintenance	144,5	1810,1

Table 2: Case C analyzed phases and impacts

Environmental impact categories:

There are a lot of environmental impacts that can be evaluated in a LCA scenario, but when buildings are considered, the two most important indicators are: i) global warming potential (GWP) [kg CO_2eq] and ii) energy, both embodied in materials and operational [MJeq].

RESULTS

Databases comparison

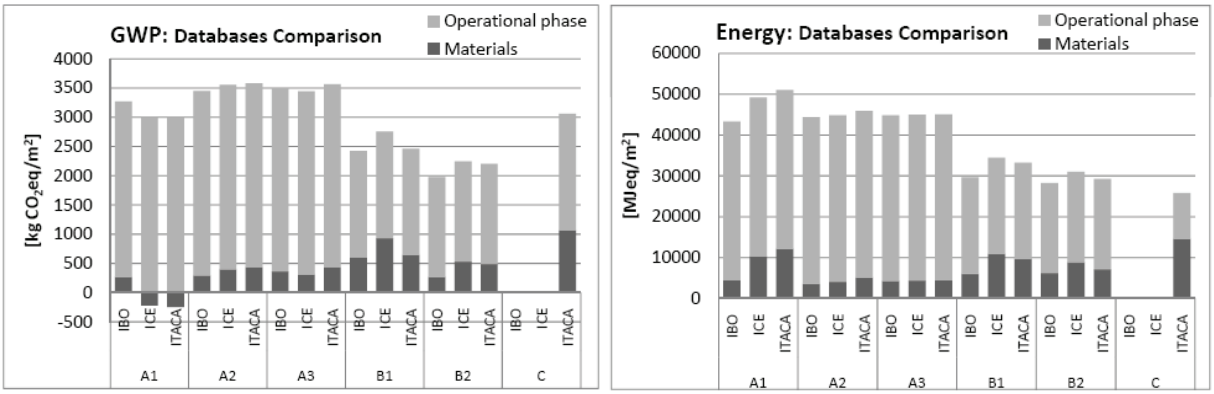

Graph 1 and Graph 2: Global Warming Potential and Energy of the case studies and their database comparison.

*Graph 1*and *Graph 2* show that the environmental impact of the same building can vary on the basis of the chosen database: every source of data is based on a defined scenario or specific equations that create the unitary impact values associated to materials and energy.

Each *Case* has its own operational energy, whose quantification depends on the software used for the thermal simulation and it does not vary when changing the database. For this reason the differences observed for GWP and energy values is due to the amount of the impact associated to each specific material and its quantity in the building.

The mean GWP value variation among the database considered is about 200-300 kg CO_2eq, but the greatest difference in GWP value reaches about 500 kg CO_2eq in *Case A1* because negative values are connected to the use of wood that has a positive contribution on the

environment, thanks to carbon storage characteristic of wood and the few manufacturing processes needed. It is important to underline that wood manufacturing industries could also be largely energy self-sufficient by using biomass residues as fuel.

From the energetic point of view the highest discrepancy is connected to *Case A1* where a gap of about 7500 MJeq was observed. This great gap is due to the different method considered by the three databases to quantify energy impact connected with wooden products.

Italian context: ITACA database

Focusing on the Italian database ITACA, a comparison among the cases is carried out considering only materials and operational energy requirement over 50 years.

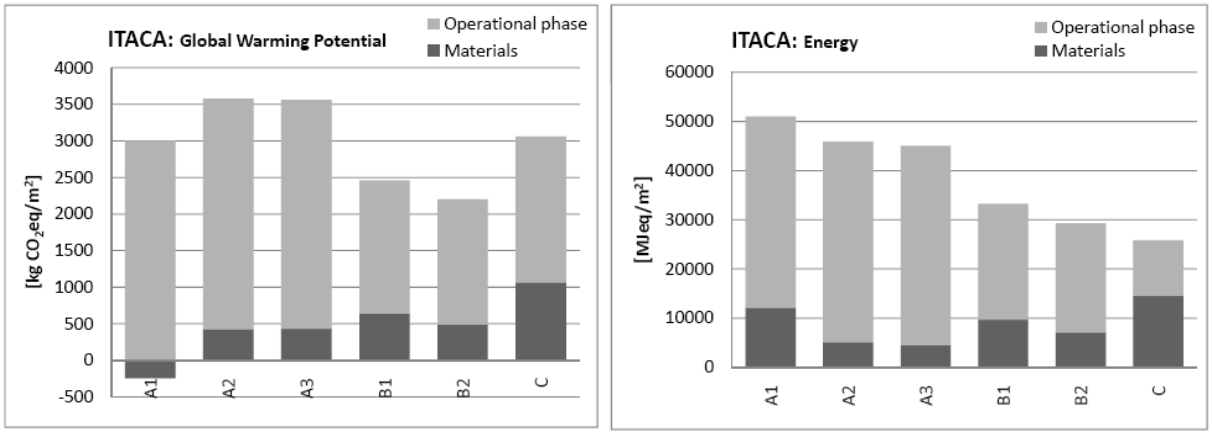

Graph 3 and Graph 4: Database ITACA - Global Warming Potential and Energy of the case studies.

As previously seen, the wooden building (*Case A1*) presents a CO_2 saving, on the contrary the one with a steel structure (*Case B1*) has the highest impact in term of GWP .

Considering *Case C* the embodied energy is higher than in the other cases, but its wooden frame demonstrate to be less energy intensive during the operational phase than other structural materials that fulfill the same function.

Even if the contribution of the building materials themselves is low compared to the values of the whole life cycle, their careful choice, together with an appropriate design of the building structure and orientation, can lead to important energy savings during the operation phase. So, the optimization of the operation phase is necessary starting from the initial design of a building, exploiting the use of renewable resources, making a rational use of energy (changes in consumption patterns) and focusing on technologies which require and consume less energy and have lower emissions.

The variability of the outputs, related to the dynamic behavior of a building and to the availability of different databases, makes the LCA a tool that should be carefully managed in order to obtain reliable data. In this scenario, a reliable and trustable comparison, in order to guarantee a competition to get the best performances (not only from an energetic point of view, but also environmental), is not easy to reach. To avoid the spreading of troubles connected to the large amount of databases available it is desirable to create a unique reference source with a large spread of materials, to cover the whole Life Cycle of a building.

REFERENCES

1. G.L. Baldo, M. Marino, S. Rossi, *Analisi del ciclo di vita LCA: gli strumenti per la progettazione sostenibile di materiali prodotti e processi*, Edizioni Ambiente, 2008.
2. C. Scheuer, G. A. Keoleian, P. Reppe , *Life cycle energy and environmental performance of a new university building: modeling challenges and design implications*, Energy and Buildings 35 (2003), pp.1049–1064.
3. S. Thiers, B. Peuportier, *Life cycle assessment of a positive energy house in France*, Centre for Energy and Processes, MINES ParisTech, Paris, CEDEX 06.
4. L. Itard, G. Klunder, *Comparing environmental impacts of renovated housing stock with new construction*, Building Research & Information (2007) 35(3), pp. 252-267.
5. I. Blom, L. Itard, A. Meijer, *Environmental impact of building-related energy consumption in dwellings*, Building and Environment 46 (2011), pp. 1657-1669.
6. S. Citherlet, T. Defaux, *Energy an environmental comparison of three variants of a family house during its whole life span*, Building and Environment 47 (2007), pp. 591-598.
7. N. Mithraratne, B. Vale, *Life cycle analysis model for New Zealand houses*, Building and Environment 39 (2004), pp. 483-492.
8. O. Otiz, C. Bonnet, J. C. Bruno, F. Castells, *Sustainability based on a LCM of residential dwellings: A case study in Catalonia, Spain*, Building and Environment 44 (2009), pp. 584-594.
9. L. Gustavsson, A. Joelsson, R. Sathre, *Life cycle primary energy use and carbon emission of an eight-storey wood-framed apartment building*, Energy and Buildings 42 (2010), pp. 230-242.
10. L. Gustavsson, A. Joelsson, R. Sathre, *Life cycle primary energy use and carbon emission of an eight-storey wood-framed apartment building*, Energy and Buildings 42 (2010), pp. 230-242.
11. M. Suzuki, T. Oka, K. Okada, *The estimation of energy consumption and CO_2 emission due to housing construction in Japan*, Energy and Buildings 22 (1995), pp. 165-169.

THE ENERGY EFFICIENCY OF AN ADVANCED SHADING ENVELOPE ELEMENT AND A TERRACOTTA SLAB: "SHADING SCREEN"

Arch. Villalta Begazo Milagros
ABITA Inter University Research Center Florence, via S. Niccolò 89/A, 50125 Firenze, Italy

ABSTRACT
The proposal of a multi-layer dry element will add a contribution to the research industry already developed by unprecedented project proposals in the field of ventilated building envelopes, with the new "shading screen", a slab designed to help improve the global facade performance with a reduced solar absorption, thermal insulation and rationalization of the components: the advanced screen with mechanical assembly, in fact, was created with a configuration capable of changing the values of the hygrothermal and environmental parameters of the internal microclimate, contributing to the improvement of savings and building energy efficiency.

INTRODUCTION
The advanced ventilated multilayer element[1] was created with the objective to investigate the systems of building envelopes designed as multilayer membranes, with high-energy performances and formed by the dry assembly of advanced facade components. The specific subject of the investigation were commercial buildings located in hot and humid climates.
The theme develops concepts related to product and process innovations, aimed at achieving greater levels of energy efficiency and, consequently, to methods and design tools essential to the introduction of these innovations. The validity of the project proposal has been confirmed by thermal and hygrometric tests (in static and dynamic conditions) using energy simulation software.

THE SYSTEM
The proposed multilayer ventilated envelope element is composed of two sub-systems: the first, the inner layer, is formed by a dry-mounted system, while the second, the external closing system, consists of a "ventilated wall package". Each of the two sub-systems is in turn divided into several functional layers. The external closing advanced screen system is composed of extruded brick slabs mounted - through mechanical anchor pins – on metal structure uprights (with a "groove" profile of 300 x 200 x 2 mm) anchored in turn, to the main structure of the building by "L" shaped brackets (around 500 x 500 x 5 mm). The stratigraphy of the screen is formed by:

- bearing facade substructure (columns, brackets, anchor elements);
- accessory elements and joints (PVC spacer pads with circular section and rectangular shading rods);
- insulating rock wool layer (density 50 kg/m^3);
- control layer;
- ventilation layer;
- brick slabs
  - Shading screen TR1 slab (tile used in two directions)
  - Shading screen TR2 slab (angular horizontal and/or vertical)
  - Shading screen TR3 slab (sill)
  - Shading screen TR4 slab (string course)
  - Shading screen TR5 slab (shading rods).

SHADING SCREEN SLAB
The "shading screen" slab was designed to create a self-shading ventilated facade cladding. The slab is obtained by optimizing the geometry of the outer surface, so that in itself it helps to reduce heat absorption through the creation of the largest possible dispersion area. The "shading screen" slab indeed has an outer surface which is 2,8 times the size of a normal dry curtain wall slab. The slab also features a design of the external surface which can be applied in two different directions (horizontal and vertical), both to suit aesthetic requirements and to ensure protection from the solar radiation under different orientation conditions. The choice of colour also contributes to the thermal improvement of the slab. Light colours are more reflective and less absorbent towards solar radiation, allowing the slab to cool down more easily; on the other hand, in the case of dark colours, the absorption of solar radiation is significantly higher.

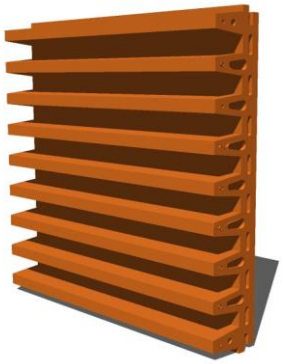

Fig.1 "Shading Screen" slab

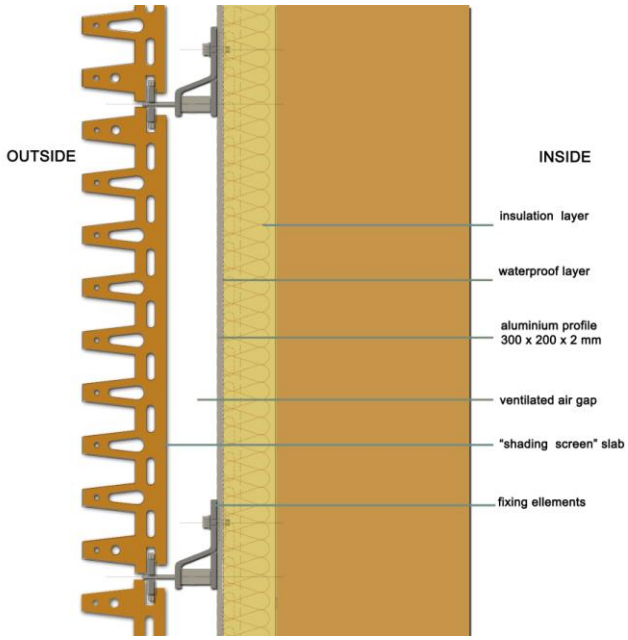

Fig 2. Stratification layer

TRANSMITTANCE CALCULATION

The calculation of transmittance[2] values was performed with the program CRTherm which complies with the requirements of UNI EN ISO 1745, Appendix D, using the finished elements method applied to a two-dimensional flat section of the slab parallel to the macroscopic direction of the heat flow.
The thermal resistance of the cavities of the slabs was evaluated following the method described in UNI EN ISO 6946-1996, Section 5.2.
The calculation was carried out on two specimens. The first with a slab of 400 x 400 mm, considering clay of 1800 Kg/m with a conductivity, increased for humidity, of 0.62 W/mK. There is the following data:

Conductivity	λ	1,080 W/mk
Conductance	C	14,994 W/m^{2}k
Resistance	R	0,067 W/m^{2}k
U-value	U	4,227 W/m^{2}k

The second slab of 500 x 500 mm, with the same input data, results in:

Conductivity	λ	1,26 W/mk
Conductance	C	13,44 W/m^{2}k
Resistance	R	0,074 W/m^{2}k
U-value	U	4,66 W/m^{2}k

During the calculation applied to the proposed slab an improvement of thermal behaviour was found (reduction of heat absorption), both because of the present air cavities and of the dispersant shape.

VERIFICATION OF THE ENERGY PERFORMANCE OF THE DRY ENVELOPE ELEMENT

The audit was performed[3] through the simulation carried out for a building located in Abu Dhabi (latitude 24.6°N); the choice of location was made to evaluate the system's behaviour under extreme conditions.
The audits of the energy performance of the dry multilayer casing element were conducted in three phases:

- hygrothermal tests;
- physical and thermal tests;
- energy consumption on a Test-Room with the application of the facade component.

The thermal tests were performed using the energy simulation program "Termus". Results show that under all weather conditions interstitial condensation problems do not occur. The thermal tests were conducted by considering the values of radiation on the surface of the claddings and the calculation of the heat flow by conduction and convection inside the wall in the direction from the outside towards the inside the building. The simulation was carried out using the energy simulation "TRNSYS" and calculating "ECS" programs. The initial conditions are:

- assessment of an area of 100 m^2 (10x10 m);
- slab colours: red and sand;

- size of air gap: 2.5 cm, 5 cm and 10 cm;
- horizontal arrangement of the corrugated outer surface of the slab;
- comparison was made with a terracotta slab with a constant section of 7 cm. This allows to evaluate the performance of the "shading screen" slab in relation to another component that has the best features of the considered range, and therefore the survey is carried out under the most disadvantageous conditions for the proposed slab.

In addition, the survey was developed with a progressive induction methodology of data values from a sequence of calculation steps on various parameters, such as:

- percentage of shaded area of the slab;
- average temperature of the outer surface of the slab;
- heat flow from the outer surface of the slab to the inner surface of the wall.

For the slab of red colour the diagrams reveal, however, an efficacious reduction of surface area exposed to radiation, showing that:

- in the case of eastern orientation[4], the shading of the surface of the slab reaches a maximum of 68.81%;
- in the case of western orientation, shading of the surface of the slab reaches a maximum of 71.51%;
- in the case of southern orientation, the shading of the surface of the slab reaches a maximum of 60.09%.

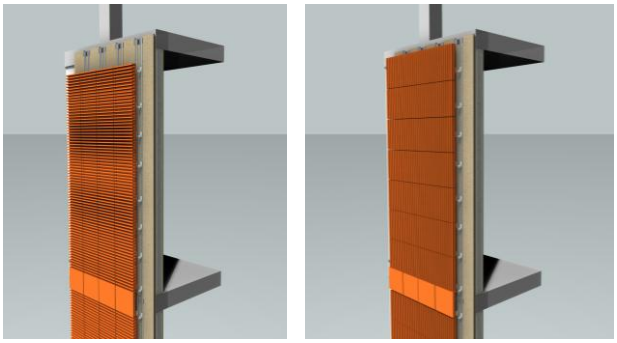

Fig 3. Horizontal and vertical orientation slab

EST FACADE SEASONAL AVERAGE BY MONTHS				SHADING SCREEN SLAB			FLAT SLAB		
	SOLAR RADIATION	λ sunny surface%	Λ shaded surface%	Wh/ (m^2*day) sunny	Wh/ (m^2*day) shadow	Wh/ (m^2*day) sum	Wh/ (m^2*day) flat slab	Dif	%
JANNUARY	317,4	33,38%	66,62%	84,18	-60,98	23,20	50,94	-27,74	-54%
FEBRUARY	314,2	34,21%	65,79%	84,44	-58,02	26,43	52,18	-25,76	-49%
MARCH	418,4	38,34%	61, 6%	113,58	-48,75	64,83	96,69	-31,86	-33%
APRIL	363,9	42,60%	57,40%	111,74	-42,24	69,50	82,94	-13,44	-16%
MAY	427,8	39,78%	60,22%	125,16	-36,46	88,70	117,49	-28,79	-25%
JUNE	402,1	38,81%	61,19%	118,49	-34,51	83,99	111,11	-27,12	-24%
JULY	354,8	39,97%	60,03%	110,92	-28,57	82,35	100,78	-18,42	-18%
AGOST	392,4	42,11%	57,89%	125,28	-28,25	97,03	112,83	-15,80	-14%
SEPTEMBER	387,6	42,77%	57,23%	125,08	-32,61	92,47	104,75	-12,29	-12%
OCTOBER	395,1	39,48%	60,52%	116,58	-39,51	77,07	97,90	-20,83	-21%
NOVEMBER	466,4	31,19%	68,81%	108,08	-58,27	49,81	109,56	-59,75	-55%
DECEMBER	330,0	31,81%	68,19%	84,08	-58,98	25,10	63,19	-38,09	-60%

WEST FACADE SEASONAL AVERAGE BY MONTHS				SHADING SCREEN SLAB			FLAT SLAB		
	SOLAR RADIATION	λ sunny surface%	Λ shaded surface%	Wh/ (m^2*day) sunny	Wh/ (m^2*day) shadow	Wh/ (m^2*day) sum	Wh/ (m^2*day) flat slab	Dif	%
JANNUARY	316,1	33,86%	66,14%	88,66	-47,53	41,12	63,39	-22,26	-35%
FEBRUARY	372,2	36,73%	63,27%	102,49	-43,24	59,25	86,65	-27,40	-32%
MARCH	425,2	37,40%	62,60%	119,37	-35,74	83,63	113,92	-30,29	-27%
APRIL	329,8	40,42%	59,58%	110,12	-26,62	83,49	89,32	-5,83	-7%
MAY	390,5	38,42%	61,58%	123,25	-18,81	104,44	122,15	-17,71	-14%
JUNE	354,1	36,69%	63,31%	113,31	-17,68	95,62	110,94	-15,31	-14%
JULY	312,4	36,78%	63,22%	105,58	-14,39	91,18	100,80	-9,62	-10%
AGOST	350,2	39,07%	60,93%	119,42	-12,26	107,16	114,64	-7,48	-7%
SEPTEMBER	386,7	39,05%	60,95%	125,22	-17,42	107,80	121,36	-13,56	-11%
OCTOBER	384,6	38,72%	61,28%	121,46	-22,81	98,65	113,88	-15,23	-13%
NOVEMBER	346,9	28,49%	71,51%	89,03	-44,61	44,42	86,12	-41,70	-48%
DECEMBER	290,5	30,03%	69,97%	79,72	-45,44	34,27	62,10	-27,82	-45%

SOUTH FACADE SEASONAL AVERAGE BY MONTHS			
	SOLAR RADIATION	λ sunny surface%	λ shaded surface %
JANNUARY	408,1	53,45%	46,55%
FEBRUARY	351,0	48,25%	51,75%
MARCH	318,9	44,39%	55,61%
APRIL	188,4	43,40%	56,60%
MAY	141,4	40,75%	59,25%
JUNE	123,6	39,91%	60,09%
JULY	123,9	40,23%	59,77%
AGOST	164,9	42,02%	57,98%
SEPTEMBER	258,8	43,90%	56,10%
OCTOBER	365,8	48,61%	51,39%
NOVEMBER	547,0	51,06%	48,94%
DECEMBER	420,7	53,61%	46,39%

SHADING SCREEN SLAB			FLAT SLAB		
Wh/ (m^2*day) sunny	Wh/ (m^2*day) shadow	Wh/ (m^2*day) sum	Wh/ (m^2*day) flat slab	Dif	%
111,53	-37,15	74,37	83,99	-9,62	-11%
99,74	-39,82	59,92	69,36	-9,43	-14%
101,93	-36,73	65,21	69,86	-4,65	-7%
72,24	-31,67	40,57	25,93	14,65	56%
61,85	-24,99	36,85	17,83	19,02	107%
54,82	-23,36	31,45	13,48	17,98	133%
57,68	-19,41	38,27	20,53	17,74	86%
74,35	-18,35	56,01	37,93	18,08	48%
98,92	-22,66	76,26	67,62	8,64	13%
120,45	-24,98	95,47	99,17	-3,70	-4%
146,93	-34,68	112,25	145,59	-33,34	-23%
117,68	-33,81	83,88	96,89	-13,01	-13%

During the calculation phase of the average temperature of the outer surface of the red slab, as in the following stages, comparison is made between the effects of radiation on the "red shading screen" slab and those on the flat slab.

The results show that even if on one hand the temperatures reached by the external surface of the slabs under consideration are very similar, despite the morphological diversity, on the other (as the next stage of calculation will show), the loss of heat by the "red shading screen" is greater than that of the flat slab, demonstrating not only the efficacy of the corrugated surface as a system of heat dissipation, but also that the performance of the corrugated sheet improves even more in the more extreme geographical contexts.

Regarding the stage of calculating the heat flow from the outer surface of the slab to the inner surface of the wall, the procedure sets a stable internal temperature of the surface of 20 °C and sets as input data the temperature change of the outer surface during the day, during every day of the year and the variation of the thermal resistance values of the entire wall package. The results show that:

- with the "red shading screen" applied on East orientation, the heat flow is equal to 23.20 Wh/m^2* day;
- with the flat slab, the heat flow entering the wall is at best 50.94 Wh/m^2 * day, not subtracting the value of any outgoing heat flow;
- in the comparison, the resulting heat flow entering the wall with the "red shading screen" is less than the flow into the wall with the flat slab, with a difference ranging from 12% to 60%, which represents the efficiency of the "red shading screen" versus the flat slab on the side facing east.

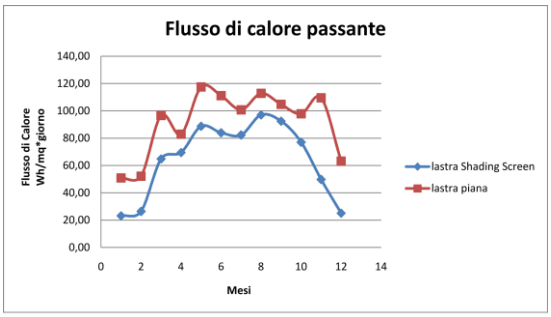

Fig 4. Heat flow- east orientation

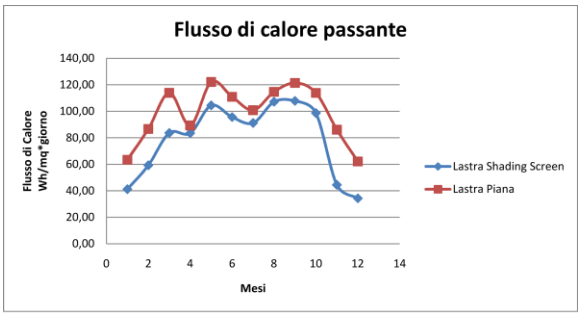

Fig 5. Heat flow west orientation

- with the "red shading screen" applied on the West face, the resulting heat flow is of 34.27 Wh/m^2* day;
- with the flat slab, the heat flow entering the wall is at best 62.10 Wh/m^2 * day, not subtracting the value of any outgoing heat flow;
- in the comparison, the resulting heat flow entering the wall with the "red shading screen" is less than the flow into the wall with the flat slab, with a difference ranging from 7% to 48%, which represents the efficiency of the "red shading screen" compared to the flat slab with the front facing west.
- with the "red shading screen" applied in a northern or southern direction, the resulting heat flow is of 83.88 Wh/m^2 * day;
- with the flat slab, the incoming heat flow on the wall at best is 96.89 Wh/m^2 * day;
- in the comparison, the resulting heat flow entering the wall with the "red shading screen" is less than the flow into the wall with the flat slab in the months with higher irradiance, with a difference ranging from 7% to 23%.

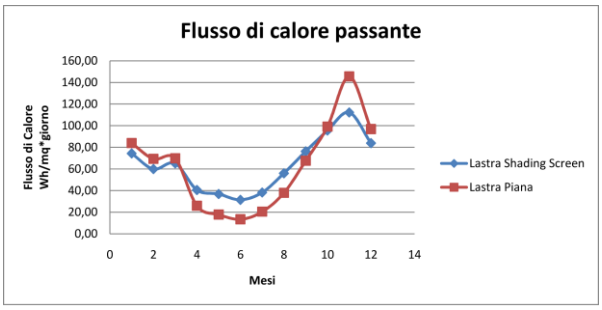

Fig 7. Heat flow – north-south orientation

The same procedures were followed for calculating the "sand shading screen" slab with an absorption value of 0.2 and the results reveal that the temperature reached by the outer surface of the slabs under consideration, despite the morphological diversity, are very similar, but the loss of heat by the "sand shading screen" is more or less identical to that of the flat slab, due to poor absorption of heat caused in turn by a strong reflection. In this case, the screen is not confirmed as a more effective system of heat dissipation for the corrugated surface versus the flat surface.

CASE STUDY RESULTS

The data which can express the amount of energy consumption for heating or cooling indoor air depending on the temperature difference between outdoor and indoor air set operating at 20 ° C, are expressed in Wh, and refer to a volume called "test room" of 10 m per side, allowing for a kind of spatial-energy unit represented by the perimeter of the 10x10x10 unit volume, comparable to the design of a building structure.

The calculation procedure allows detection of:

- average annual consumption of each of the sides of the test room, depending on their orientation;
- average annual consumption of the test room as a whole.

Consumption is obtained as a direct function of the factors considered in the previous stages and includes, as in these stages, the comparison between walls with shading screen slabs, divided into red and sand colour walls, and walls equipped with the reference flat slab.

As shown by the graphs in the case of Abu Dhabi, total energy consumption of the test room by applying the "sand shading screen" slab is higher (+8%) than with the flat slab. This allows us to understand that a light coloured shading screen is inefficient in the analysed context (considering however, as already mentioned, that the simulation is limited to the analysis of the passing heat flow and does not include fluid dynamics evaluations).

Applying instead the "red shading screen" slab the situation is reversed and the same consumption is significantly reduced (-16.1%) in comparison to that with the application of a flat slab, as there is a greater absorption and dispersion of heat. The best results (higher savings) occur on the eastern and western faces, while on the north and south sides, as can be imagined, benefits could be obtained by orienting the slab with vertical corrugations. These excellent results are even more encouraging, as:

- the simulation does not consider the needs of smaller indoor humidity control due to a lower inflow;
- the simulation provides the less advantageous "conditions" for the application of the shading screen, since the flat slab has a greater width (7 cm) compared to the thickness of the common wall slabs (3 cm).

ABU DHABI						
VENTILATED AIR GAP 2.5 cm - ABSORPTION 0.2						
	SHADING SCREEN SLAB		FLAT SLAB		DIFFERENCE	
EAST	144352	Wh	132319	Wh	12033,36	Wh
NORTH / SOUTH	280910	Wh	268438	Wh	12471,49	Wh
WEST	174691	Wh	153250	Wh	21440,58	Wh
TOTAL	599953	Wh	554007	Wh	45945,42	Wh
					8,3%	
VENTILATED AIR GAP 2.5 cm - ABSORPTION 0.5						
	SHADING SCREEN SLAB		FLAT SLAB		DIFFERENCE	
EAST	388603	Wh	491765	Wh	-103162	Wh
NORTH / SOUTH	637477	Wh	729577	Wh	-92099,2	Wh
WEST	466158	Wh	558244	Wh	-92085,4	Wh
TOTAL	1492238	Wh	1779585	Wh	-287346	Wh
					-16,1%	

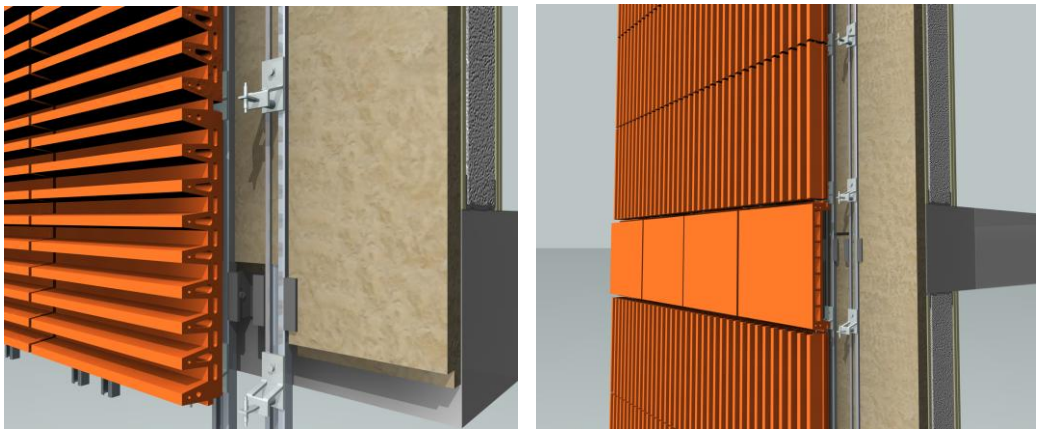

Fig 8. Construction details

CONCLUSIONS ON THE DESIGN OF THE SHADING SCREEN SLAB AND POSSIBLE DEVELOPMENTS

On the basis of the simulation tests results described above, it was possible to verify and validate the intuitive hypothesis that a component covering ventilated facades can have properties which reduce the absorption of solar energy in climates with high radiation. Test results not only validate the above assumptions, but envisage that the efficiency demonstrated by the proposed slab may help even in temperate climates, especially with regards to hot seasons.

The association between factors such as the heat resistance of brick, the design of a corrugated surface that can cast shadows on the surface, holes in the interior designed to improve the resistance to the passage of heat, seems therefore, on the basis of the obtained results, a "good optimization strategy of the outer skin" of a facade with advanced screening, as part of a systemic logic oriented towards sustainable development. The levels of reduction of the heat flow through the component that have been recorded in the tests are to be allocated only to the shape factor, and therefore future developments could be further in-depth studies that also consider the fluid dynamic aspects of the heat transfer flow, in order to have an even more accurate picture of the functioning and performance of the slab. These further investigations could also affect the cladding system with a slab placed horizontally and vertically, as it is expected that at the facades facing north and south the vertical arrangement can help to increase performance.

NOTES

1. The following paper will develop contents of PhD thesis in Architectural Tecnology and Design of University of Florence (XXI Cycle).Energy Efficiency of Building Envelope for Hot-Humid climate.
2. The calculation of slab's thermal properties was carried out in collaboration with Eng. G. Zanarini(Alveolater Gr.)
3. The energy performance of building envelope was developed in collaboration with the Department of Energy "S. Stecco" to University of Florence – prof. M. de Lucia and Ing. D. Fissi.
4. In locations close to equator, the east and west surfaces are subject to higher irradiation

BIBLIOGRAPHY

- AA.VV. *Pareti Ventilate*, edizione Graniti Fiandre, Ancona 2000
- Balocco, C. ; Mazzocchi, F. ; Nistri, P. *Facciate ventilate in laterizio: tecnologia e prestazioni* Costruire in laterizio, n. 83 (settembre-ottobre 2001), pp. 63-71
- Bazzocchi, F. *Facciate Ventilate, Architettura, Prestazione e Tecnologia*, Alinea, Firenze 2002
- Ciampi, M. ; leccese, F. ; Tuoni, G. *Sull'impiego delle pareti ventilate per la riduzione dei crichi estivi*, Costruire in Laterizio n 89 (2002), pp. 70-74
- Ciampi M., leccese F., Tuoni G., *Sul comportamento termico di facciate e coperture ventilate*, La Termotecnica, n. 89 (gennaio 2002), pp. 87-97
- Grassi E. *La sottostruttura meccanica: Il fissaggio degli elementi in cotto alla facciata, Atti di convegno "Il rivestimento ventilato in cotto delle pareti esterne*", Firenze 2001
- Kwork Aliso G., AIA, Grondzik Walter *T., PE, The green studio Handbook, Environmental Strategies for Schematic Design Elsevier Inc.,* Oxford (UK), 2007
- Lavagna M., *Sostenibilità e risparmio energetico. Soluzioni tecniche per involucri eco-efficienti, Clup* Milano 2006
- Lucchini, A. *Le pareti ventilate, Metodologia di progettazione e messa in opera di materiali e componenti*, Il Sole 24 Ore, S.p.A., Milano 2000
- Schittich C. (a cura di), *Involucri edilizi. Progetti, strati funzionali, material*, Detail, Birkhauser, Monaco-Basilea 2003
- Torricelli M.C, Marzi L., Le facciate ventilate in cotto di Renzo Piano, *Costruire in Laterizio*, 71(9/10 1999), pag.36-47
- Tucci, F. *Involucro Ben Temperato, Alinea Editrice*, Firenze 2006.

Solar Active and Passive Cooling

PASSIVE COOLING APPROACHES IN NET-ZERO ENERGY SOLAR BUILDINGS: LESSONS LEARNED FROM DEMONSTRATION BUILDINGS

L. E. Aelenei[1]; R. Lollini[2]; H. Gonçalves[1]; D. Aelenei[3]; M. Noguchi[4]; M. Donn[5]; F. Garde[6]

1: National Energy and Geology Laboratory, Paço do Lumiar 22, 1649-038 Lisboa, Portugal

2: Institute for Renewable Energy of EURAC research, Viale Druso1, I-39100 Bolzano, Italy

3: Faculty of Science and Technology, Universidade Nova de Lisboa, 2829-516, Caparica, Portugal

4: MEARU, Mackintosh School of Architecture, The Glasgow School of Art, Glasgow, United Kingdom

5: Victoria University of Wellington, 139 Vivian St. Wellington, New Zealand

6: University of La Réunion, 97430 Le Tampon, La Reunion, France

ABSTRACT

Zero Energy performance buildings have gained more attention since the publication in 2010 of the EPBD recast [1]. Meanwhile the USA promotes "marketable zero energy homes in 2020 and commercial zero energy buildings in 2025" [2]. Japan proposes "carbon neutralized buildings", including existing buildings, by 2050 [3]. The UK government aspires to achieve a zero carbon standard by 2016 [4]. With countries well on the way to putting this new standard into effect, worldwide around three hundred buildings are already claiming Zero Energy or similar performance [5]. Successful implementation of such an ambitious target depends on a great variety of factors. For designers and code writers these include: balancing climate driven-demand for space cooling with climate-driven supply for renewable energy resources and/or matching building design to shade from the sun in summer while providing for good daylight. With a literature full of theoretical advice and a building industry rife with myths about the value of technologies, the study of these existing buildings may be decisive in establishing the best strategies for achieving true Net Zero energy performance.

The authors of this paper, who are active participants in the IEA Task 40/Annex 52 ("Towards Net Zero Energy Solar Buildings") [6] intend to present and discuss the strategies used for cooling a number of selected buildings identified in the project database as zero-energy balance, with the aim of defining solution sets and indicators of relative performance. The buildings, which incorporate solutions for passive cooling, have been divided into three functional component sets: overheating prevention, heat rejection, and modulation and control. The IEA NZEB buildings demonstrate a range of passive solutions for both residential and non-residential situations to show that it is possible to reduce cooling loads through passive design. This has contributed to reduction of the size of the active systems with the aim to cover the residual energy demand through Renewable Energy Systems, getting the overall building energy balance to zero. This paper will review the insights that this classification process has revealed.

PASSIVE APPROACHES FOR COOLING IN NZEB DESIGN

Net Zero Energy Design

A Net Zero Energy Building (NZEB) is defined as a high energy performance building that over a year is energy neutral. In the international context, the most frequently cited definitions are “net zero site energy” and “net zero source energy” [7]. “Net zero site energy” means that the annual balance is based on the grid interaction at the boundary of the building site, i.e. the overall energy delivered to the building from the utility grid has to be offset by the overall energy feed in to the grid. In the “net zero source energy” definition, which is the one that matches the currently used by EPBD recast in a nearly zero-energy context [1], the energy (delivered from and feed into the grid) has to take into account primary energy conversion factors. Although there is no exact approach for designing and realizing a net-zero energy building (there are many different possible combination of building envelope, utility equipment and on-site energy production equipment able to achieve net-zero energy performance) there is some consensus that zero energy buildings design should start from passive sustainable design [8, 9]. It is in the line of this principle that most of the zero energy buildings are now designed [e.g. Enerpos building in cooling dominated climate]. According to this, the net zero-energy performance may be achieved as a result of executing two fundamental steps (Figure 1a): (a) reduce building energy demand - energy efficiency and (b) generate electricity or other energy carriers, to get enough credits to achieve the desired energy balance - energy generating.

As one can observe from Figure 1a, “energy saving” is the start-up step in NZEB design. Passive approaches play a fundamental role in addressing NZEB design as they affect directly the loads put on the buildings mechanical and electrical systems, and indirectly the strive for renewable energy generation. In general, in heating and cooling dominated climates, the passive heating solutions must be studied together with the cooling solutions in order to avoid undesired overheating and glaring by daylight. Passive cooling are pursued mainly by increasing building time constant through thermal inertia increasing, to allow a significant building cooling load reduction while the benefits of natural ventilation and daylighting are explored. On the other hand, in cooling dominated climates characterised by a high potential for natural ventilation, wall insulation should be avoided to allow an easier cooling of the house during the night (something that the insulation will prevent). Generally, the design of passive solutions of NZEB´s may be a challenging task given the constraints related to desired energy performance level/CO2 emission reduction target, climate, type of building, etc. Although the main principles applied in passive sustainable design are well known, the fundamental issue here is to find if the same can be applied in NZEB as well.

Passive Cooling Approaches

The passive approaches used for cooling the building usually is divided into three functional component sets: overheating prevention, heat rejection, and control. Whereas the purpose of the passive heating is to draw heat into the building, the purpose of a passive cooling is to prevent, remove or reject the heat from the building. Thermal insulation can work both ways – preventing building heat loss keeping the indoor warm, or preventing the heat transfer from outdoor to indoor, keeping indoor cold. The external shading devices (overhangs, screens), represent another effective passive cooling system reducing or preventing overheating on the building south and west oriented spaces. The rejection of the building heat gain from the external environment can be achieved by facilitating heat loss to the following natural sources of cooling: air movement, cooling breezes, evaporation and earth coupling. One of the most successful cooling strategies used to reduce the internal loads of the building, by means of

heat rejection, is natural ventilation. Natural ventilation relies on the natural airflow and breezes to reduce the need for mechanical cooling and to improve the indoor air velocity when the building is occupied. Ventilation coupled to an earth tube system that use the earth as the cold source, is another strategy often used to reduce the building internal loads by pre-cooling ventilation air and evacuation, rejection. In synthesis there are three categories of passive cooling systems which can prevent or disperse the heat reducing building cooling load: by radiation to the sky, convection to the air and conduction to the ground.

CASE STUDIES

In order to find out details and discuss the strategies used for cooling in NZEB design, twenty projects have been selected from the IEA Task 40 project data base for analysis. These case studies, which represent zero-energy/near zero-energy or plus-energy balance buildings, are well documented in terms of physical characteristics, monitored and/or simulated energy performance, as well as lessons learned about designing, operating, and post-evaluating processes. The twenty selected projects are of residential and non-residential type and correspond to three different categories of climates-heating dominated, heating and cooling dominated and cooling dominated, as it can be seen from Table 1.

Residential buildings				**Non-residential buildings**			
1 Le Soleil Canada		**2 Riehen** Switzerland		**11 Lajon** Italy		**12 Solar XXI** Portugal	
3 ÉcoTerra Canada		**4 Avalon** Canada		**13 Pixel** Australia		**14 Acciona** Spain	
5 Green tomorrow South Korea		**6 Blaue Heimat** Germany		**15 Benasque** Spain		**16 RSF** USA	
7 Leaf House Italy		**8 Little Greenie** New Zealand		**17 Solon** Germany		**18 Enerpos** France	
9 Robert Ryan UK		**10 Lima** Spain		**19 Solvis** Germany		**20 Oberlin** USA	

Table 1: Case studies

Energy Performance

The building design associated to 20 selected cases comprises a variety of energy-saving strategies able to provide an energy performance, at least 50% better than that of a standard building (a criterion used for selection). The energy performance of the selected buildings in terms of energy efficiency versus energy production can be seen in Figure 1b which clearly illustrates a number of 7 net zero-energy buildings, the remaining being either nearly zero-energy (6 buildings) or plus-energy balance (7 buildings). Primary energy is used as metrics for the annual energy balance.

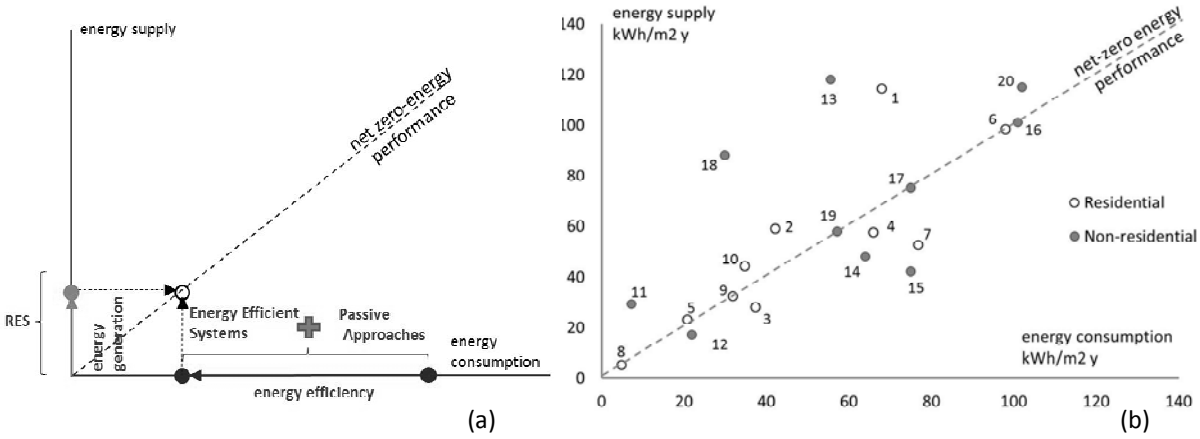

Figure 1: (a) NZEB fundamental steps; (b) Annual energy performance of 20 case studies estimated relative to "zero-energy"

Passive Cooling Approaches of 20 Case Studies

In order to have a clear picture of the cooling strategies adopted in the 20 case studies, the passive strategies were summarised and then ordinated according to relevance in Figure 2.

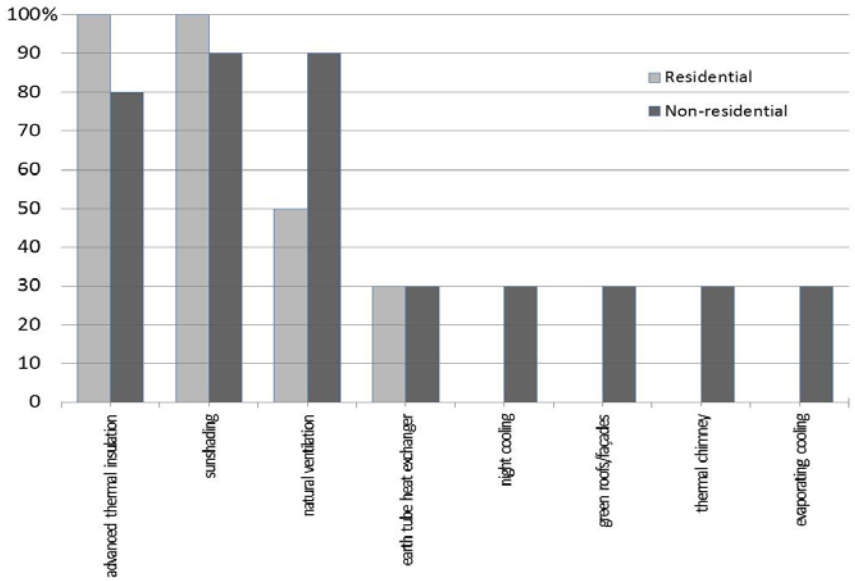

Figure 2: Relevance of passive cooling measures across 20 case study buildings according to building type (percentage)

As it can be seen in Figure 2, all residential buildings rely on thermal insulation and sunshading in terms of "prevention", whereas natural ventilation (50% share), followed closely by ground cooling (30% share), are applied for "rejection". To obtain a clearer picture on this issue, the passive cooling strategies adopted for each building were summarised according to climate and building type in Figure 3.

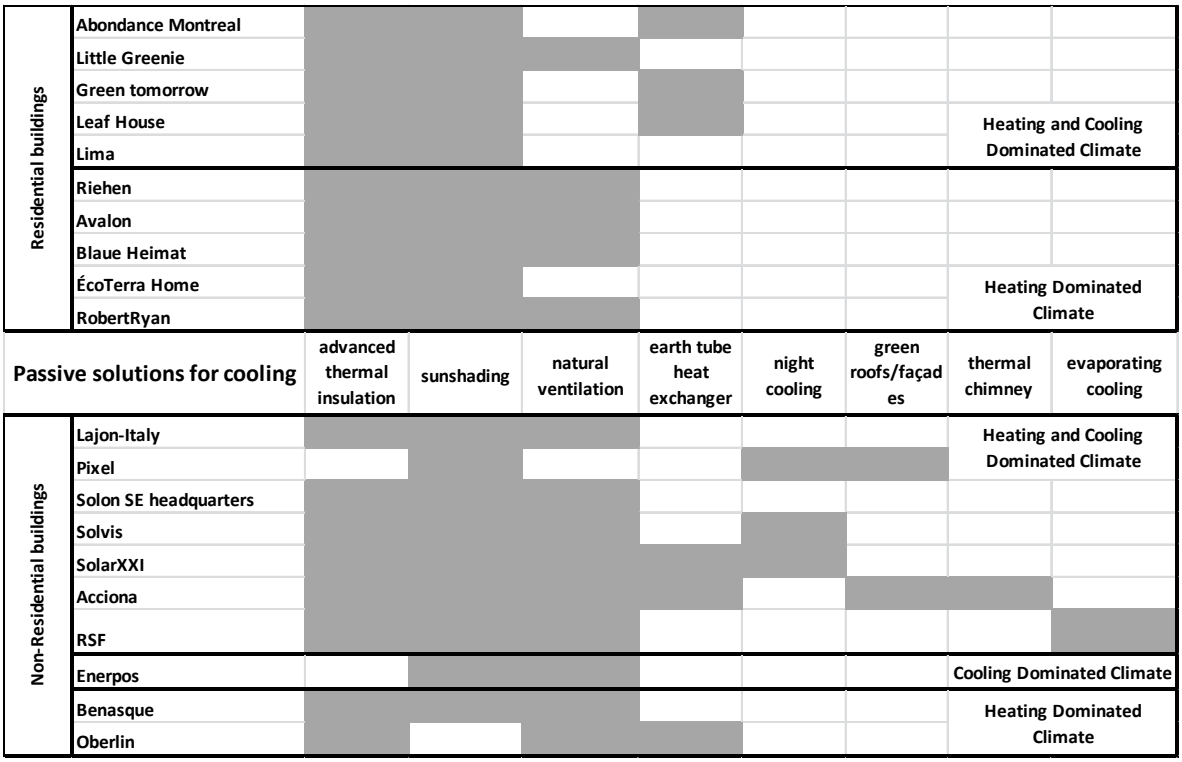

Figure 3: Passive cooling measures across 20 case study buildings according to building type

According to Figure 3, the most common heat rejection strategy used in heating dominated residential buildings is natural ventilation. Earth tube exchanger is mostly used in heating and cooling dominated climate, where natural ventilation is likely less effective during cooling season due to the high temperature during the night too.

A similar analysis applied to non-residential buildings (Figure 2 and 3) reveals that thermal insulation and sunshading are used as prevention measures, although not always. Natural ventilation appears as the most common strategy for heat rejection (90% share), whereas earth tube exchanger, night cooling green roofs/façades, thermal chimney and evaporative cooling come in second place with equal shares (Figure 2). Figure 3 shows that heat rejection strategies are usually applied in combinations higher or equal than 2 in order to reduce the building cooling loads. The exception to this rule is made by "Solar XXI" and "Acciona", with 3 and 4 rejection strategies applied at the same, respectively. This approach is likely to be due to lack of existence of HVAC equipment in both cases.

FINAL REMARKS

In order to present and discuss the strategies used for cooling in NZEB design, a number of 20 case studies have been selected from IEA Task 40/Annex 52 ("Towards Net Zero Energy Solar Buildings") project database.

The analyses carried out regarding the strategies and indicators of relative performance of 20 case studies revealed that it is possible to achieve zero-energy performance using well known passive cooling strategies, a fact which provides evidence in the support of the theory that zero-energy buildings design is a progression of passive sustainable design.

A close inspection on the results revealed that zero-energy performance of residential buildings can be properly addressed, in terms of passing cooling approaches, using thermal insulation in combination with either natural ventilation or earth tube exchanger, according to climate type. With regard of non-residential building types, the results shown that passive cooling approaches become more diverse, a fact easily explained by the greater cooling loads and different type of use.

Although the role played by each strategy individually remains to be demonstrated, it is believed that this paper presents useful insights into decisions relating to type of strategies likely to succeed in achieving a true zero-energy performance in a certain type of climate.

ACKNOWLEDGEMENTS

The authors of this paper gratefully acknowledge the contributions of IEA Task 40/Annex 52 members, as well as the support of all building professionals linked to case studies under discussion.

REFERENCES

1. The Directive 2010/31/EU of the European Parliament and of the Council of 19 May 2010 on the energy performance of buildings, Official Journal of the European Union, 53, 2010
2. DOE, Building Technologies Program, 2008 http://apps1.eere.energy.gov/buildings/publications/pdfs/corporate/myp08complete.pdf
3. N. Yokoo: Transition of Technology and Belief for Green Buildings in Japan, International Conference on Sustainable Integrated Design Process for Building and Construction, Hong Kong, 2009
4. Department for Communities and Local Government, Sustainable New Homes – The Road to Zero Carbon: Consultation on the Code for Sustainable Homes and the Energy Efficiency standard for Zero Carbon Homes, London: Department for Communities and Local, 2009
5. E. Musall, T. Weiss, A. Lenoir, K. Voss, F. Garde, M. Donn: Net Zero energy solar buildings: an overview and analysis on worldwide building projects, EuroSun conference, Graz, Austria, 2010
6. The IEA SHC Task 40 / ECBCS Annex 52 ‘Towards Net Zero Energy Solar Buildings (NZEBs); http://www.iea-shc.org/task40/index.html
7. Torcellini, P., Pless, S. & Deru, M.: Zero Energy Buildings: A Critical Look at the Definition. National Renewable Energy Laboratory (NREL), USA, 2006
8. Kolokotsa, D., Rovas, D., Kosmatopolous, E. and Kalaitzakis, K.: A roadmap towards intelligent net zero- and positive-energy buildings, Solar Energy (In Press), 2010
9. Sartori, I., Napolitano, A., Marszal, A.J., Pless, S., Torcellini, P., Voss, K.: Criteria for Definition of Net Zero Energy Buildings, EuroSun conference 2010, Graz, Austria, 2010.

USING SOLAR THERMAL FLAT PLATE COLLECTORS FOR ACTIVE SOLAR COOLING OF COMPUTER SERVER ROOMS

M. Brünig, T. Tschan, A. Haller

Ernst Schweizer AG, Bahnhofplatz 11, CH-8908 Hedingen, Switzerland

ABSTRACT

The year round operating safety of computer servers is evident in the day-to-day business. To reach stable climatic server room conditions the whole electric energy supplied the room plus the external heat load has to be removed via an air-conditioning system. To reduce the electric energy consumption for cooling of the server room a system for "free cooling" and "adsorption cooling" mode was installed. The first measurement data show the stable operation and a reduction of the electric energy consumption of this promising concept.

INTRODUCTION

Our enterprise has the ambitious goal of reducing the overall energy consumption while continuously growing its business. In 2009 a second server room for redundant data backup of the whole company was installed. For the cooling of this server room different cooling methods and systems were analyzed in depth. As compressor based air conditioning systems use a significant amount of electric energy and therefore well controlled and reliable computer server room cooling is very expensive. An air conditioning system using solar thermal energy looked highly promising since the cooling demand correlates also with the level of solar radiation.

To reduce the electric energy consumption level, we have realized an air cooling system combining an adsorption chiller with a solar thermal system using flat plate collectors [1]. The goal of this field experiment was to track, analyze and verify the cooling performance in a day to day operation of the computer server room under real weather and operation conditions throughout the summer 2010. In the following the schematic and photos of the installed system are presented and first results are discussed.

COOLING METHOD AND SYSTEM

The cooling system was designed for a yearly cooling energy demand of Q=70'080 kWh representing our enterprise's computer server room with a cooling power load of P_{cool}=8 kW and a coolant inlet temperature of T_{in}=20°C to the water-air cooling rack of the computer server. The cooling system has two operating modes - "free cooling" and "thermal driven adsorption cooling" - which are selected depending on the ambient temperature T_{amb}. The aim is of the concept is to keep the energy ratio in the modes of "free cooling" to "adsorption cooling" in the range of approx. 80% to 20%. Free cooling is activated if the outside temperature T_{amb} is below 18°C and for all other temperature levels the system operates in the adsorption cooling mode if the temperature in the hot water storage tank is above T=65°C. The target cooling temperature of the adsorption chiller is adjusted to T=15° (outlet temperature).

In Fig.1 a schematic of the cooling system is shown. The heat rejection subsystem for both modes is equipped with a re-cooler mounted on the roof top of the building in which the server room is located, Fig.2. To prevent freezing of the water coolant of the server a heat exchanger is installed to separate the indoor circuit from the outdoor circuit which is filled

with antifreeze liquid. So, the excessive heat of the server room is either directly transferred to the re-cooler (ambient) or through the adsorption machine. The adsorption machine is a P_{cool}=8kW SORTECH ACS08.

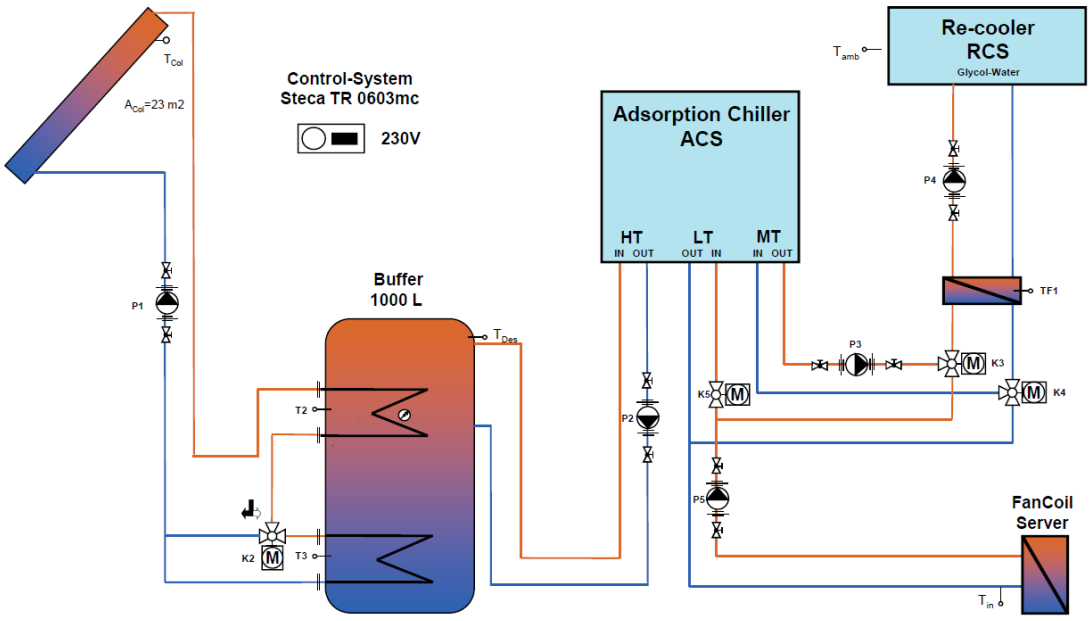

Figure 1: Schematic of the cooling system with an adsorption cooling chiller.

Figure 2: Photo of the flat plate collector field (back) and the heat rejection cooler (front right).

The ACS08 adsorption chiller consists of two separated chambers of which each has one integrated adsorption-desorption silica gel coated heat exchanger. For a quasi continuous

operation one chamber is in the desorption-mode and the other in the adsorption-mode [2]. In the adsorption machine the cooling effect is achieved through the evaporation of water out of the evaporator chamber into the adsorption chamber. The major advantage of adsorption chillers compared to absorption machine is that they run with a lower operation temperature range of T_{Des}=55° to 90°C. This was a very important consideration when using flat plat collectors as their working temperature matches quite well with that of the adsorption chillers. The thermal energy source of the adsorption cooling machine is a flat plat collector field with 10 collectors having a total absorber area of A_{Col}=23 m^2, see Fig.2. A conventional closed loop hydraulic pump system is installed to transport the solar energy from the collector field to a V=1000 liters hot water storage tank. This storage tank acts as a buffer for a certain sun less time.
All key data like temperature, fluid flow, valve positions and status of the pumps were acquired in a logging system. A conventional solar controller system was used to implement the above described trigger points.

RESULTS

A typical temperature profile of the outside temperature on a typical summer day in Hedingen (Switzerland) is shown in Fig. 3.

As it can be seen, the mode of free cooling alone cannot achieve the requested cooling temperature of maximum 20°. After 8 AM the outside temperature was already above 20°C. At around 11 AM the storage temperature exceeds the required 65°C and the adsorption cooling machine starts its operation. From this start on the fluid inlet temperature decreases from T_{in}=24°C down to T_{in}=15°C, it oscillates around this value with an amplitude of 1°C and increases from 6:30 PM on up to 25°C. The adsorption cooling machine ends its operation at 55°C.

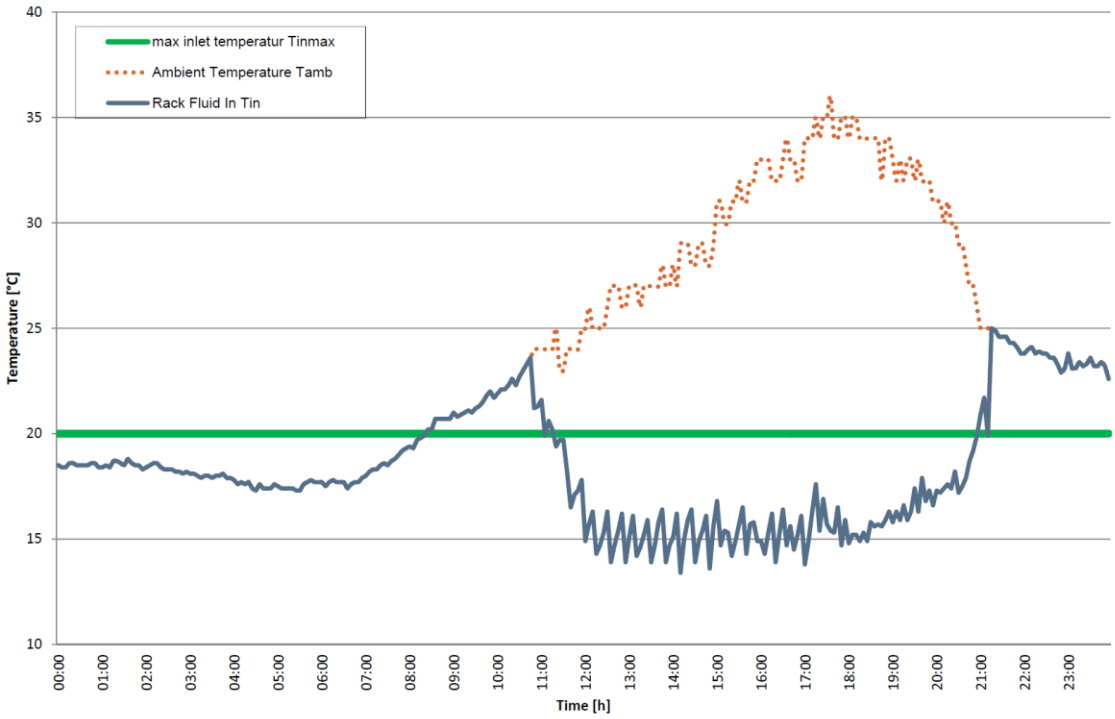

Figure 3: Typical temperature profile of the ambient temperature T_{amb} (roof top) and the fluid inlet temperature T_{in} (Rack Fluid In) in function of day time.

In Fig. 4, the curve shows the temperature in the cooling fluid circuit of the server room achieved with the combined modes of free cooling and adsorption cooling. The temperature peaks T_{in}>20°C in the morning was caused by the hot water temperature in the storage tank being below 65°C and so the operation temperature of the adsorption cooing machine was not reached and the adsorption process could not start yet while free cooling was continuously running. This behavior was also partially caused by the south orientation of the flat plate collectors. The cause of the temperature peak in the evening was from the hot water storage tank being depleted. Because the ambient temperature was higher than T_{amb}>18°C the system was running in the free cooling mode but could not match the necessary load.

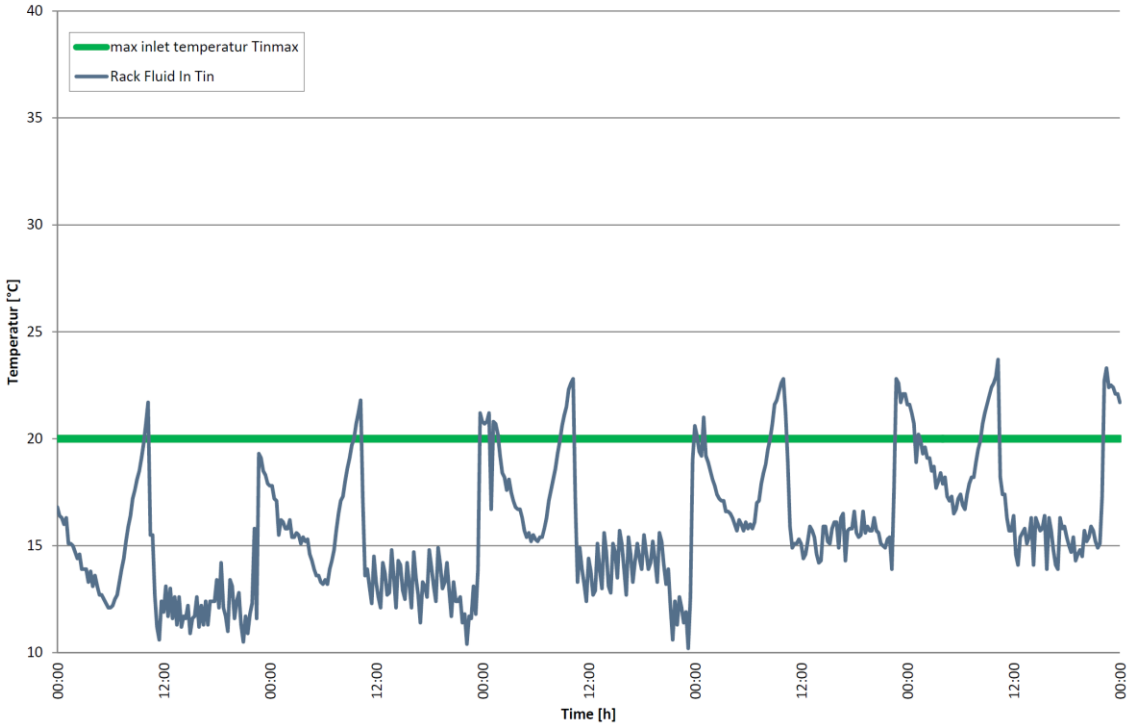

Figure 4: Temperature T_{in} by using combination of free cooling and adsorption cooling.

DISCUSSION

The combined solar thermal cooling and free cooling system proved to provide reliable cooling throughout the year. Especially during weeklong hot summer days the computer server room temperature was mainly in the defined temperature range and the server was 7x24h fully functional. The system has also shown that conventional flat plate collectors perform well even under a higher temperature application of 75°C and provide the thermal energy to the chiller when a higher load results. Nevertheless the morning and evening temperature peaks above T_{in}=20° are demanding for additional measures. One possible solution is the implementation of a cold storage tank. Thus providing not only a longer free cooling period in the morning because of heat rejection through the colder night time but also the storage of cold water from the adsorption machine throughout the day in order to support the free cooling in the evening. In our system setup we expect a V=1000 liter cold storage tank to be large enough to eliminate those server room temperature peaks even under most unfavorable ambient temperature conditions.

The analysis of the weather data are showing that at our geographical location in Hedingen / Switzerland the annual ambient temperature T_{amb} is approximately 20% above 18°C. Therefore 80% of the cooling demand can be provided by the free cooling circuit.

A drawback of our solar cooling system is its high investment cost. Further optimization potential lays in the heat rejection subsystem (re-cooler) where the highest part of the electrical energy consumption can be identified. The electric energy use of the various fluid pumps could in parts also be reduced by using other "Class A" pumps. All of them were operated in an ON / OFF modus but will be operated in a variable speed (0 - 10 V control) mode. The performance of the re-cooler can also be further optimized by relocating to a shadier and thus colder place to reduce the influence of the roof top sun heated ambient air.
The results are showing a good coincidence of high cooling demand and solar energy input to the solar thermal system i.e. to the adsorption cooling machine. The double use of the re-cooler in the two modes has shown to be a very efficient way to reduce the overall electric energy consumption. Calculations showed that an optimized system can reach a COP of 13, resulting in an energy reduction of more than 50% compared to conventional compressor based air conditioning systems. The results are reflecting the high potential of thermal solar energy for cooling application.

In a further project supported by the Federal Commission of Technology and Innovation (CTI) the planned system improvements will be tested in collaboration with the HSR Institute for Solar Technology SPF (HSR University of Applied Sciences of Rapperswil).

REFERENCES

[1] Solar-Assisted Air-Conditioning in Buildings. A Handbook for Planners. Hans Martin Henning (Ed.). ISBN 3-211-00647-8, Springer-Verlag, 2004.

[2] Development of an adsorption chiller and a heat pump for domestic heating and air-conditioning applications. T. Nunez et al.; Applied Thermal Engineering 27 (2007) 2205-2212.

IMPROVEMENT OF NATURAL VENTILATION AS PASSIVE DESIGN STRATEGY IN A SCHOOL BUILDING

U. Mazzali[1]; F. Peron[1]; P. Romagnoni[1]

1: Università IUAV di Venezia, ex Convento Terese, Dorsoduro 2206, I-30123 Venezia, Italy

ABSTRACT

School buildings in Italy traditionally haven't a cooling plant as during the peak summer period they are closed. Otherwise nowadays the teaching period has been expanded and the classrooms in many cases are used also for recreations of pupils free from school by local authorities. During months like June or September also in North Italy are present periods of high diurnal temperature and humidity. Consequently at least in the design of new school building some kind of cooling strategy is needed and considering the limited economic budget for functioning of this kind of institutions have to be low energy demanding. In this context night natural ventilation seems a promising solution able to provide cooling when requested. Even if its cooling capacity is limited, an optimized design process can lead to comfortable and controllable conditions for the occupants and can reach relevant decreases in energy consumption. As a case study the authors assumed the design of a new school building near Treviso in the North-East Italy. The purpose of the work is to analyse for northern Italian climate the performances of natural ventilation strategies such as stack chimney effect and wind induced cross ventilation by means of computational fluid dynamics simulation (CFD). Through a climatic analysis the mean wind directions and velocities and the mean ambient temperature fluctuations have been calculated. After the climatic analysis a urban CFD simulation has been performed to investigate wind behavior near the school building. A first design step was the sizing of openings and ventilation chimney by means of normographs and after that an internal CFD simulation has been performed with the aim of evaluate air flow patterns inside the classrooms. Vent placement and ventilation chimney shape and height have been verified and optimized considering a night ventilation flow pattern during summer. The internal analysis has highlighted that during a typical summer night the air moves across the school room entering from the bottom window and going out from the top chimney, providing an air changes value of 9 volumes per hour. This night summer air flow pattern lead to a surface temperatures reduction of about 2,2°C and to an air temperatures reduction of about 4,7°C.

INTRODUCTION

In recent years cool night air flow into the buildings has been rediscovered as one way to reduce energy consumptions for conditioned spaces and decrease air and building's structures temperatures. Many natural ventilation strategies have been developed and analysed for different climate. Wittchen [1] used local weather forecast to control the passive night cooling obtaining indications of improvements to the indoor climate. Macias [2] worked on solar chimneys with absorber and building shape to allow totally passive night time cross ventilation without window opening, obtaining night temperatures drop down to around 20°C starting from the 28°C of the reference case. Lomas [3] studied temperature reduction related with passive ventilation, pointing out that passive ventilation can reduce greatly mean radiant temperatures. Field experiments performed by Kubota [4] indicate that the cooling effect of night ventilation is larger than those of the other ventilation strategies during the day and night in hot humid climate; it was observed that the night ventilation technique lowered the

peak indoor air temperature by 2,5 °C and reduced nocturnal air temperature by 2,0 °C on average, compared with other ventilation patterns. The major obstacle, pointed out by Kubota in applying night ventilation is the high humidity values carried in. Other studies on reliability of the design of natural night ventilation have been performed from Breesch [5] considering a list of influencing input parameters for the building simulation in energy and airflow network simulation tools, and a suitable long term evaluation criterion. The analyses has pointed out that reliability of building simulation results depends on the accuracy of the input data and a practical guideline has been suggested. Related to night cooling efficiency Geros [6] studied urban microclimate and its influence on the performance of the passive cooling techniques. The result of the latter research shows that the use of the undisturbed climatic conditions dominant outside the urban context is not appropriate for the study of night ventilation; both temperatures and wind profiles are very different and using undisturbed climatic conditions passive cooling efficiency is overestimates. Concerning building energy simulation, an overview of pressure coefficient data has been done by Costola [7], in which the influence by a wide range of parameters on pressure coefficient has been highlighted and the lack of information about the uncertainty associated with the values, provided by each data source raises questions about the accuracy of building performance simulation based on these data. This paper presents a detailed study of natural ventilation contest for a primary school in Montebelluna near Treviso, Italy. During summer period, natural ventilation conveys, as much as possible, fresh external air inside the building. In many schools, where the occupational period is limited to diurnal hours, natural ventilation can be used to remove heat stored by the building structures and as pre-cooler system during the morning of the next day. However, it is important to put in evidence that the greater is the internal-external temperature difference, the higher natural ventilation effect. Thus, natural ventilation technology is particularly useful especially during summer nights when the above mentioned temperature conditions are satisfied [8]. The aim of this work is to verify and optimize natural ventilation strategies such as stack chimney effect and wind induced cross ventilation by means of computational fluid dynamics analysis. The results will be compared in terms of air temperatures, radiant temperatures and comfort indexes.

CLIMATIC ANALYSYS

As a starting point a local climatic analysis was performed. Direction and velocity of wind and air temperatures have been analyzed in order to evaluate if the local climate are suitable for the natural ventilation strategies. Successively an urban CFD study has been performed to understand the possible wind impact in terms of velocities and pressures, near the school openings. Finally, a CFD analysis, has been performed inside the school for the south oriented classrooms and the air and surfaces temperatures and comfort indexes have been analyzed before and after the natural ventilation process. The local meteorological service authority (ARPAV, Environmental Agency of Regione Veneto) was able to make available hourly the following variables: air temperature, air humidity, solar radiation, wind direction, wind velocity and rainfall. Since no climatic data was available for the design site (Montebelluna) weather data of three adjacent sites (Volpago, Maser and Castelfranco Veneto) with a maximum distance of 18 km, have been used. The data find out covered a time period from 2005 to 2009. As consequence a new weather file with averaged hourly values has been created for the climatic analysis and for the energy simulation process performed to calculate the boundary conditions for the CFD simulation. A wind analysis has been performed for the wind direction during summer nights for the three sites. In the city of Castelfranco, the wind blows mainly both from NorthWest and NorthEast, for the Maser climate, the wind blows mainly from North East, and in Volpago the wind blows mainly from North West and North during summer nights. It is reasonable to consider the wind in Montebelluna blowing, during

summer nights from North, North West and North East directions. A further study on mean wind velocity has been performed pointing out that the wind doesn't achieve significant velocities during summer nights and the velocity values are roughly 0,6 m/s. These values doesn't create high dynamic pressures on building facades, however a comparison with pressure gradient generated by temperature differences between inside and outside the school must be done, to avoid conflicts between the two pressure gradients and for a correct positioning of the natural ventilation openings. Another crucial parameter for natural ventilation analysis is the ambient air temperature. A basic condition for natural ventilation, used as passive environmental control technology, is that the ambient night summer air temperature is lower than the inside air temperature. This temperature difference contributes to create vertical pressure gradients which is partially responsible of the so called "stack effect" in which the higher the difference between the inside and outside air temperature, the greater the heat removed from the room. In figure 2 a typical temperature behavior in a summer month is shown. Low minimum temperatures corresponds to night period in which the air temperature values are between 15°C and 20°C. These ambient air temperature values are low enough for generating temperature differences of about 5°C – 6°C with the inside air temperature.

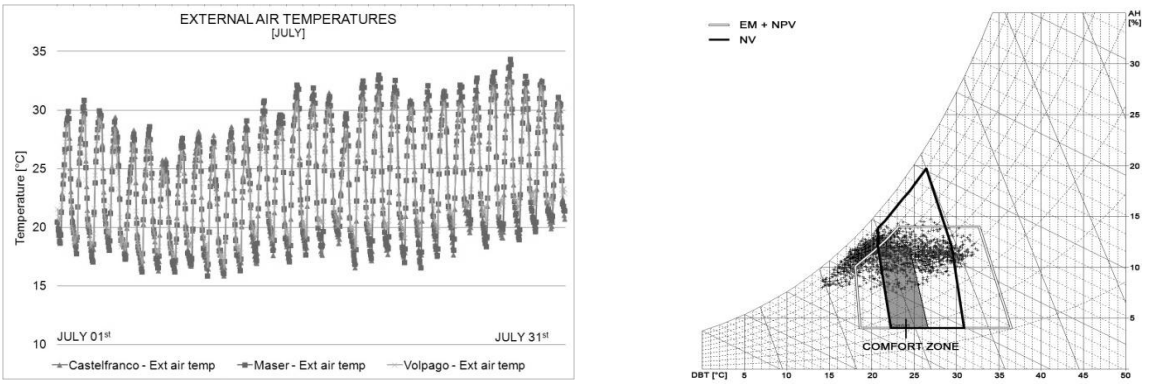

Figure 1: External air temperature fluctuation during the month of July (left). Givoni's chart for July with different comfort area: usual summer conditions, presence of exposed mass plus night purge ventilation (EM+NPV) and natural ventilation (NV) (right).

A Givoni's chart has been developed to support the natural ventilation approach at the design and is reported in figure 1. The two passive technologies connected with natural ventilation, exposed mass plus night purge ventilation (EM+NPV) and natural ventilation (NV) expand the comfort zone during summer night. Givoni's chart supports previous considerations about wind and ambient air temperatures, confirming that natural ventilation is a useful passive technique in this area that can contribute to cooling energy reduction.

URBAN AREA FLUID DYNAMICS ANALYSIS

On the basis of the climate analysis outputs a computational fluid dynamics (CFD) model was set up to study the wind velocities and pressures near the natural ventilation inlet and outlet openings using PHOENICS from CHAM [9]. It is based on the solution of the differential equations expressing the balances of mass, momentum and energy integrated in a finite volumes scheme [9]. A steady-state CFD analysis at an urban scale was performed. The simulation domain are 220 metres long, 220 metres large and 30 metres high. A 3D analysis grid has been specified with 2.282.280 cells. Two different scenario were set up considering the average summer night condition the two nearest cities, Maser (scenario A) and Volpago (scenario B). Specifically the air get in at the boundaries of the domain with mean velocity

and direction obtained from climatic analysis. It was assumed a logarithmic wind vertical velocity profile with an effective roughness height of 0.5 (because of the presence of numerous obstacles). The absolute wind speed at the reference height was 0.4 m/s for scenario A with reference height of 5 m, and 0,6 m/s for scenario B with reference height of 2 m. Air get in the numerical domain with a wind direction of (the wind direction in degrees relative to north, clockwise is positive): 45° (North-East) in scenario A and 337,5° (North-West) in scenario B. The velocity fields reported in figure 3, show that the wind velocity, initially not so strong, is further reduced by the effect of the ground roughness and the building obstructions in the neighbour area. In the two scenarios A and B respectively the mean velocity near school building are respectively 0,28 m/s and 0,44 m/s.

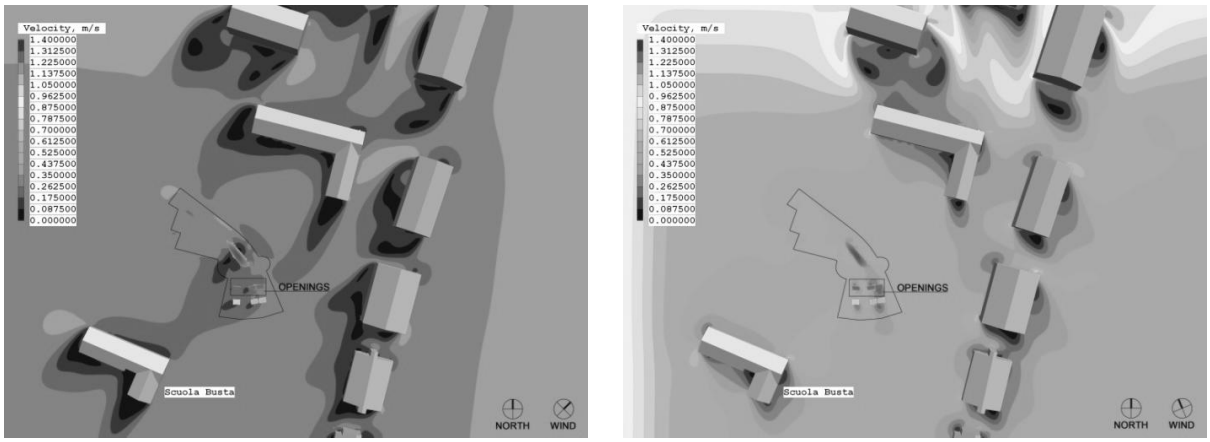

Figure 3: The computed velocities fields around school for scenario A on left and B on right

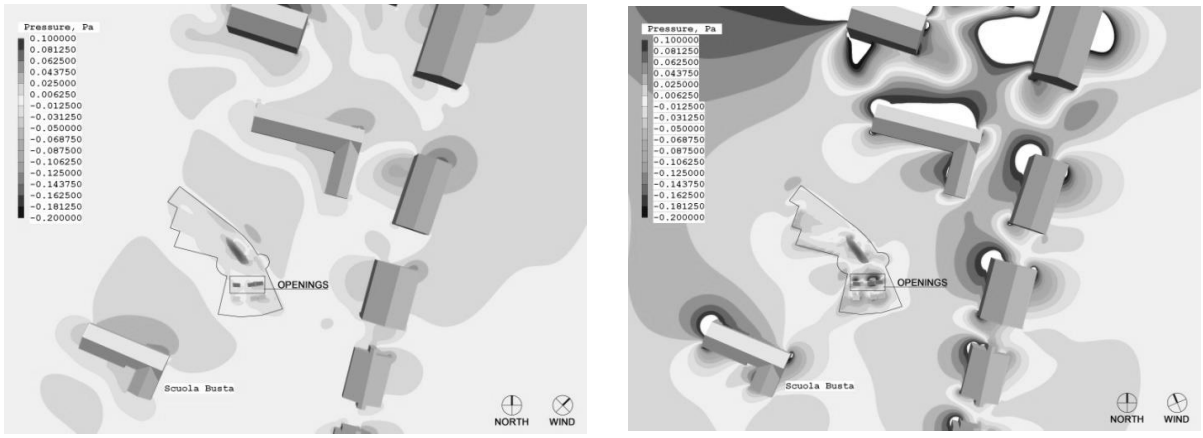

Figure 4: Wind pressures for scenario A on left and B on right

Further considerations could be done about wind pressures against the building. It is necessary to verify that the pressures generated by the wind are consistent with the ventilation openings position. A good practice [12] is design natural ventilation inlet openings in positive pressure conditions, i.e. windward side of the building, and design natural ventilation outlet openings in negative pressure conditions, i.e. leeward side of the building. This design technique assures that wind blows through the building entering from the windward side and going out from the leeward side of the building, assuming no obstruction inside the building. As shown in figure 4 the inlet openings of the building school are on the windward side of the building (positive pressure) for scenario A and the same conditions are verified for scenario B, also in this case a positive pressure value near the inlet opening is calculated by the CFD simulation.

CLASSROOM ENVIRONMENT ANALYSIS

A CFD and energy analysis has been performed also for indoor school's rooms; the energy simulation has been undertaken with EnergyPlus software [10] and the CFD simulation has been undertaken with DesignBuilder software [11]. The energy simulation results, in terms of surface temperatures and air flow rates through openings, have been used as boundary conditions for the CFD simulations. In the energy simulation vents have been considered opened during night hours from 23:00 to 6:00 and closed during day hours from 7:00 to 22.00. The energy simulation has been performed with one hour time-step during a representative day for the typical week during summer. The section of the typical classroom is shown in figure 5. The architect for ventilation considered the utilization of windows and the adoption of a chimney. There are 4 openings, two of them are at the top of the ventilation chimney and the others are in the south-exposed window. The double ventilation chimney's openings, towards the North and towards the South, is designed with the aim to promote natural ventilation both by means of temperature driving force and by means of wind driving force. If the wind driving force is stronger than the temperature one, the north chimney opening will let the wind enter the room. At the opposite, if the temperature driving force is stronger than the wind one, the north chimney opening will let the air go out the room.

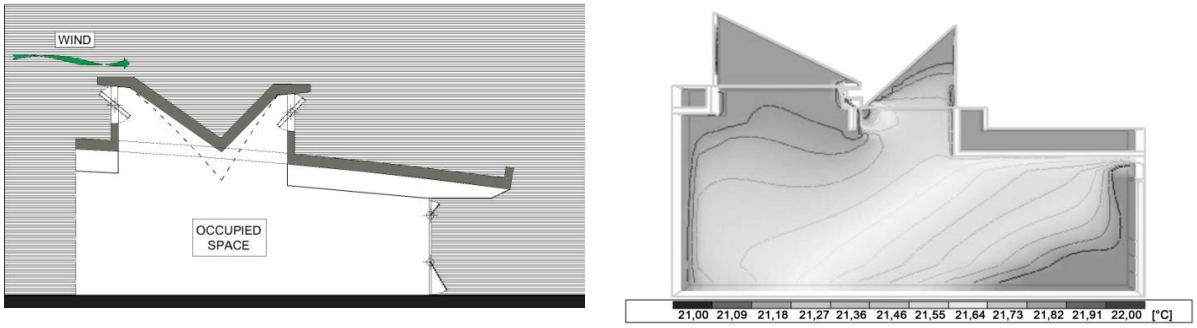

Figure 5: Typical school room section (left) and temperature distribution at 23:00 (right).

Figure 5 shows the results of CFD analysis in a section of the school's classroom. At 22:00 the school room air temperature, just before vents opening, is roughly 24°C. After one hour, figure 5 (left), the temperature falls down because of the effect of fresh air entering the room and at 1:00, the air temperature value is quite uniform and equal to 21°C. By the end of the night the air temperature goes down until its minimum value of 20,1°C at 5:00. Air velocities inside the room are under 0,25 m/s and the mean air changes rate is equal to 9 1/h. The air flows from the bottom openings to the upper openings towards the ventilation chimney. For this particular moment, in the summer night, the temperature driving forces are stronger than the wind driving forces, thus the air comes into the room from the south-exposed openings and goes out from the top of the chimney. The air movement during night hours affects both air temperature and radiant temperatures. During typical summer week, in night time, mean air temperature values are 24,2°C and 20,3°C and mean radiant temperature are 23,8°C and 22,7°C respectively before and after night cooling. Using environmental parameter values obtained from simulation (mean radiant temperature of surfaces, temperature, velocity and humidity ratio of the air) a further analysis has been performed on comfort inside the classroom. The comfort indexes (PMV "predicted mean vote" and PPD "percentage people dissatisfied during diurnal hours with and without night natural ventilation has been calculated assuming a clothing resistance of 0.5 clo and an activity level of 1.2 met. In typical summer conditions starting from not highly critical climate with a PMV around 0,3 (slightly warm) without natural ventilation, after the adoption of night ventilation strategy the index

resulted closer to 0 (thermal neutrality), during the central hours of the day. Regard to PPD index, values very close to 5%, essentially during week days, have been calculated after adoption of the night natural ventilation, in contrast with 7% or 8% of PPD values without the natural ventilation.

CONCLUSIONS

A natural ventilation strategy shall be adopted by means of a very integrated design process starting from a detailed climatic data analysis supported by CFD analysis. The climatic analysis is very useful to understand if the project location climate is really suitable for passive technologies like natural ventilation. In the case study the climatic and CFD analysis has pointed out that the local wind intensity are very low (0,2 m/s – 0,4 m/s). However the ambient night summer air temperatures, between 15°C and 20°C, are low enough to provide fresh air movement and recirculation inside the school room and natural ventilation benefits. The CFD urban analysis has pointed out that in the local urban context vent openings can receive a useful air flow. The next step in the design process is an indoor CFD analysis in order to evaluate the indoor air movements. This analysis in the case study has highlighted that the effect of the natural ventilation operating from 23:00 to 7:00 is to reduce air temperatures of 4°C - 5°C and radiant temperatures of 1°C - 2°C. This temperature reduction directly affects energy consumption for building conditioning by pre cooling structures during night. Finally a indoor comfort analysis has highlighted that, with night natural ventilation, PMV and PPD comfort indexes are very close to neutral sensation in typical summer conditions. PMV index is between -0,2 and 0,1 and PPD index is between 5% and 6%.

REFERENCES

1. Wittchen, K.B., Logberg, E., Pedersen, S., Djurtoft, R., Thiesen, J.: Use of weather forecast to control night cooling. 9th IBPSA Conference, Montreal, Canada, 2005.
2. Macias, M., Mateo, A., Schuler, M., Mitre, E.M.: Application of night cooling concept to social housing design in dry hot climate. Energy and Buildings, 38, pp 1104-1110, 2006.
3. Lomas, K., Cook, M.J., Fiala, D.: Low energy architecture for a severe US climate: design and evaluation of a hybrid ventilation strategy. Energy and Buildings, 39, pp 32-44, 2007.
4. Kubota, T., Toe Hooi Chyee, D., Ahmad, S.: The effects of night ventilation technique on indoor thermal environment for residential buildings in hot-humid climate of Malaysia. Energy and Buildings, 41, pp 829-839, 2009.
5. Breesch, H., Janssens, A.: Reliable design of natural night ventilation using building simulation. proceedings of ASHRAE THERM X, Clearwater, Florida, 2007.
6. Geros, V., Santamouris, M., Karatasou, S., Tsangrassoulis, A., Papanikolaou, N.: On the cooling potential of night ventilation techniques in the urban environment. Energy and Buildings, 37, pp 243-257, 2005.
7. Costola, D., Blocken, B., Hensen, J.L.M.: Overview of pressure coefficient data in building energy simulation and airflow network programs. Building and Environment, 44, pp 2027-2036, 2009.
8. Ashrae Handbook – Fundamentals 2009.
9. Flair user guide, CHAM Technical report TR 313, June 2010.
10. Energy Plus Documentation, Input/Output Reference, U.S. DOE, June 2010.
11. DesignBuilder EnergyPlus Simulation Documentation, Design Builder Software Ltd.
12. Brown, G.Z., DeKay, M., Sun, Wind and Light: Architectural design strategies, 2001.

FLUID DYNAMIC EFFICIENCY OF A DYNAMIC GLAZING SYSTEM

L.Danza; A.Bellazzi

ITC-CNR, Istituto per le Tecnologie della Costruzione del Consiglio Nazionale delle Ricerche (Construction Technologies Institute of the National Research Council)
Via Lombardia 49, 20098 San Giuliano Milanese
tel. 029806213
bellazzi@itc.cnr.it, danza@itc.cnr.it

ABSTRACT

The reduction of air-conditioning energy consumptions is one of the main indicators to act on when improving the energy efficiency in buildings.

In the case of advanced technological buildings, a meaningful contribution to the reduction of thermal loads and energy consumptions could depend on the correct configuration and management of the envelope systems. In recent years, the architectural trend toward highly-transparent all-glass buildings presents a unique challenge and opportunity to advance the market for emerging, smart, dynamic windows.

A prototype dynamic glazing system was developed and tested at ITC-CNR; it is designed to actively respond to the external environmental loads. Analyses by theoretical models were carried out, aimed at evaluating the possible configurations depending on different boundary conditions, such as weather conditions and airflow. Therefore, the analytical models of the building envelope were defined by using a software, called WIS, setting up physical models, calculating a solution and analyzing results.

The variables that determine the system performance, also influenced by the boundary conditions, were analysed, such as U and g value and surface temperature of the internal glazing; they concern the morphology of the envelope system, such as dimensions, shading and glazing type, gap airflow thickness, in-gap airflow rate, air path and management, in terms of control algorithm parameters tuning fan and shading systems, as a function of the weather conditions.

The configuration able to provide the best performances was finally identified by also assessing such performances, integrating the dynamic window in the heat recovery system.

The dynamic envelope system prototype has become a commercial product with some applications in façade systems, curtain walls and windows.

The paper describes the methodological approach to prototype development and the main results obtained.

CONTEXT

The building energy efficiency improvement should be pursued, first of all, by reducing the building net energy demand. This can be achieved through suitable architectural and constructive choices in order to control the energy fluxes induced by the weather conditions and building operation. A good building envelope allows the size of both HVAC and lighting systems to be reduced. These aspects are significant for office building design where wide transparent surfaces are used and the request for high performance components boosted the

façade market towards technologically improved products, without actual performances that could justify the high prices.

The phases of design, development, realization, commissioning and the management of a dynamic envelope component should be carried out by focusing on the needs of building typologies, not defining a close system, but an open one, able to be tailored to the specific building where it will be installed.

A dynamic glazing system prototype was studied at ITC-CNR to evaluate the performance and the capability of the system itself to fit all the possible working conditions.

SYSTEM DESCRIPTION

The analysed dynamic system is a double glazing. The system envisages internal blinds and the possibility to mechanically ventilate the inner gap by a fan.

Figure 1. Operation of VetroVentilato

The gaps' sizes, the panes typology, the shading component characteristics and the management of the whole system are defined and set in the design and commissioning phases, and the system can operate stand-alone or be integrated with the HVAC plants.

The control system allows the main operational parameters to be monitored and to actively drive the fan, in order to optimise the passive gains and the indoor environmental comfort.

Such versatility allows also the designers a broad freedom to refurbish energivorous buildings acting on the existing windows without replacing them, but by integrating the upper frame with the mechanical ventilation system, called VetroVentilato. The dynamic system performance was assessed in comparison with a reference glazing system with the same type of glass. The same type of windows were considered. The difference is that, regarding the dynamic system, the air is drawn from the indoor environment by a fan placed at the top of the internal gap and ejected in summer and winter, while in the reference glass there is no air change in the gap.

GLAZING ELEMENTS	Reference glass	VetroVentilato
Outside	Clear glass 4+4	Clear glass 4+4
	Air gap: 12 mm	Air gap: 12 mm
	Glass low-E 3+3	Glass low-E 3+3
	Air gap: 20 mm	Ventilated gap: 20 mm
Inside	Semi-transparent blind	Semi-transparent blind

Table 1. Glazing considered in the analysis

METHODOLOGICAL APPROACH

The dynamic system performance was assessed in comparison with a reference glazing system, both through an experimental campaign, using the methodological approach of the outdoor test cells, and analytically, using WIS, that is a tool to assess the performance of the glazing system with a given air flow inside the gap. The heat transfer coefficients were calculated by the software in compliance with ISO 15099.

The last stage of the analysis was aimed at generalising the experimental results, obviously dependent on some boundary conditions which were not controlled (e.g. weather conditions).

An experimental campaign foresees the analysis of the innovative envelope system and all of its characteristics for the purpose of identifying the independent and dependent variables.

Independent variables are: fan power; type of fan; difference between the air gap and the indoor air temperature. Dependent variables are: U-value, g-value, energy consumption; predicted percentage of dissatisfied (PPD); air change. Dynamic simulations were used, in order to generalize the experimental results, trying to apply the dynamic envelope system to a real building and in different climatic conditions.

Outdoor test-cells

The test cells at ITC-CNR allowed to compare the energy efficiency of different envelope systems. Throughout the experimental campaign the system operative parameters were directly measured, and then used as inputs for the simulations. In order to compare the measures obtained during the experimental campaign, two main parameters were used: energy consumption to maintain the set indoor comfort conditions and the air change rate (assessed through the tracer gas method).

Figure 2. Outdoor test-cells

RESULTS

The results obtained with the experimental campaign and the analytical analysis are illustrated below.

Experimental campaign

Energy consumptions were measured in active conditions by a thermostatic control of the two test cells at 20 °C. Such a comparison allowed the estimation of a mean energy saving of about 10% for the cell with the dynamic system compared with the standard one.

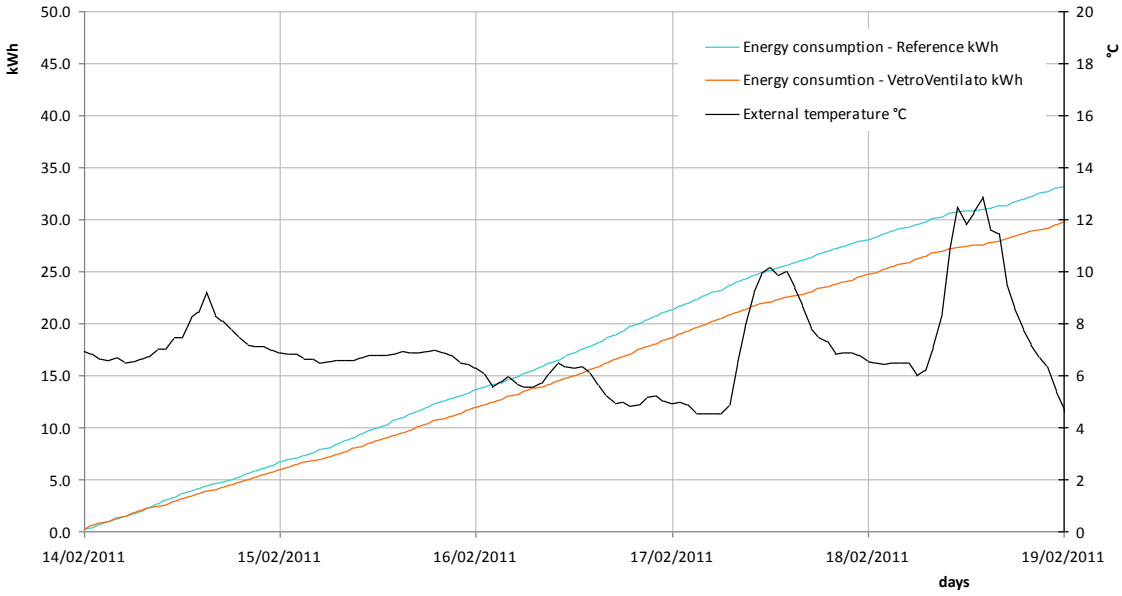

Figure 3. Energy consumption

In a steady operational mode, the dynamic system ensures a better comfort ($\Delta \approx 50\%$) when the external temperature reaches the maximum value ($T \approx 30°C$).

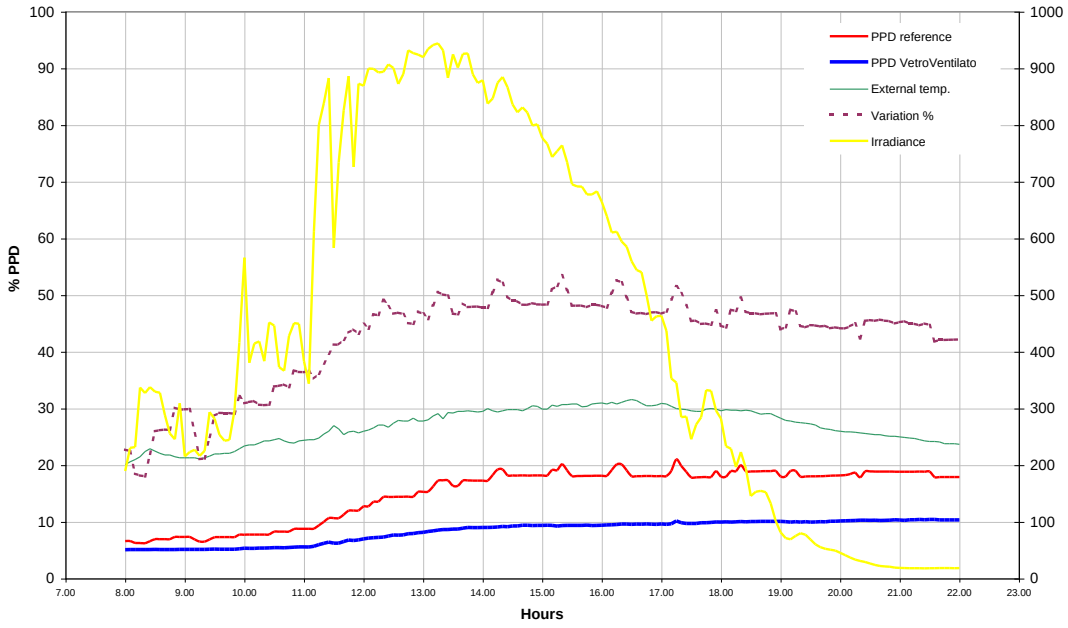

Figure 4. PPD comfort index in a spring day

Simulations

The analytical analysis carried out with WIS shows that in the case of ventilated gaps (from lower/in to upper/out in winter conditions and in summer conditions) short-cuts (pathways) are created for energy flows that would not be present in the case of non-ventilated gaps. Again, this will influence the U-value, but less strongly than with gaps ventilated from indoor to indoor.

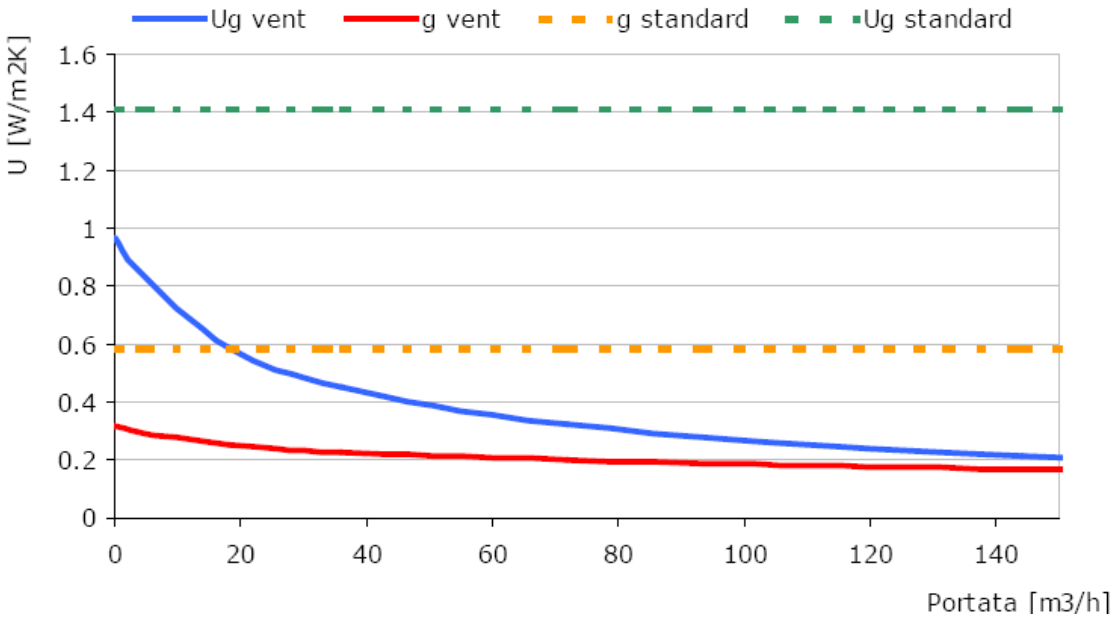

Figure 5. U-value pattern depending on the air change per hour

Figure 5 shows the curve fitting, in winter and summer conditions, describing the relationship between U-value and ventilation air flow rate; on the graph are also plotted the mean U-values of the same double pane glass, without ventilation (calculated in compliance with EN 673), of 1.4 W/m^{2}K. The asymptotic curve decreases as ventilation increases, starting from a U-value of about 1.0 W/m^{2}K (no ventilation), it goes down to 0.2 W/m^{2}K, with a hypothetic ventilation rate of 150 m^3/h.

CONCLUSIONS

The experimental campaign shows quite good energy saving and comfort performances. The analysis of the heat fluxes, and subsequently of the temperatures, allows the detection of a significant improvement of the internal environmental conditions between a double glazing and the analysed dynamic system, with more or less relevant variances according to the configurations. It is shown that the best thermal comfort condition is reached when the fan is activated.

Following the used methodological approach it is possible to handle a complete assessment of the component. In this way the choice of the best configuration of the dynamic system, in relation with planning requirements, can be carried out with full knowledge of all its capabilities and the requirements it can satisfy.

REFERENCES

1. http://www.windat.org/wis/html/
2. http://www.vetroventilato.it
3. ISO 15099 Thermal performance of windows, doors and shading devices - Detailed calculations.
4. [10] EN ISO 7730 Ergonomics of the thermal environment -- Analytical determination and interpretation of thermal comfort using calculation of the PMV and PPD indices and local thermal comfort criteria.

THE GENERATION OF SUBSURFACE TEMPERATURE PROFILES FOR YAZD

S.Z. Emadian Razavi (PHD student)[1], M.M. Fakhroddin Tafti(M.Arch)[2]

1: School of Architecture and Urban Planning, Shahid Beheshti University, Evin, Tehran, Iran,E-mail address: z_emadian@sbu.ac.ir
2: Architecture Faculty, Taft Branch, Islamic Azad University,Taft,Yazd,Iran

ABSTRACT

In hot-arid climate of Yazd, there is a great heritage of traditional underground structures. These undergrounds are considered as shelters against high temperature extremes and intense solar radiation. The earth mass can serve as a natural passive cooling source for these buildings. In summer the soil temperature, at a depth of a few meters, is always below the average ambient temperature, and is especially below the daytime air temperature. Due to its density and specific heat, it has a high heat capacity. The high heat capacity allows a damping of the aboveground temperature fluctuations at a rate exponential to soil depth. It thus has the potential to serve as a heat sink with either passive or active mechanisms of heat transfer from the building.

In order to gain an understanding of the subsurface climate, we should well document it. Unfortunately the subterranean climate in Yazd has not been studied over a long period of time. The subsurface environment is governed by a number of factors, including the prevailing climatic conditions of the locale and thermal and physical properties of the soil, such as density, thermal diffusivity and moisture content.

In this article, a predicted profile of the periodic variation of subsurface temperature with depth is presented for the soil conditions of Yazd. The generation of the profile is based on Lab's equation for subterranean temperatures, which takes into account the thermal and physical properties of the soil and the local climate. The equation makes use of a straightforward mathematical model, the soundness of which has been substantiated by sizeable empirical research at different locations. The accuracy of the equation depends on the accuracy of quantifying the thermal and physical properties of the soil and surface temperatures. The soil properties found in the literature have been measured locally and the surface temperatures have been estimated with reasonable accuracy. The subsurface temperatures are then compared with the ambient dry-bulb temperature. The profiles are then used to analyse the seasonal variations in subsurface temperatures at different depths compared with sol- air temperatures. The resulting charts and graphs should be a useful tool for those interested in the energy conversation potential of earth-sheltered and earth-bermed structures in Yazd.

INTRODUCTION

The city of Yazd is located in the central desert of Iran. It has a rich historical architecture that is built of heavy mass, thick adobe walls, and vaulted roofs. Almost all the buildings have basements that are considered as shelters against high summer temperature. Yazd's climate is characterized by high temperature extremes and intense solar radiation with little cloud cover. During the summer, maximum mean temperature is 37.2°C; minimum mean temperature is 21.2°C, and mean daily range is about 15 to 17°C. In winter, that is almost cold, maximum mean temperature is 16°C; minimum mean temperature is 2.6°C, and mean daily range is

about 13 to 13.5°C. Typical of dry regions, very little precipitation is observed. Average relative humidity ranges from 12 to 28% in summer and 25 to 73% in the winter. The amount of precipitation is about 61.5 mm in a year. The percent of sunshine hours is 63% in winter, 69% in spring, 83% in summer, and 75% in autumn [1].

From this data, it can be seen that Yazd has hot-dry summers. In regions with extreme climates such as Yazd, the underground environment will be noticeably less extreme, with relatively small temperature fluctuations. These fluctuations will also be seasonal, rather than the wide daily fluctuations of the aboveground environment, and will be subject to a large time lag. So, it would be advantageous to investigate the potential thermal benefits of the subterranean environment. In Yazd, the local climate is well documented, however, the subterranean climate is not. In order to gain an understanding of the subsurface climate, the soil must be characterized. Soil is a very good moderator of temperature. Due to its density and specific heat, it has a high heat capacity. The high heat capacity allows a damping of the aboveground temperature fluctuations at a rate exponential to soil depth [2]. The physical properties of soil differ from location to location. These properties and the local climate affect the subsurface temperature profiles of a particular location. A favourable subterranean environment has the energy conservation potential of reducing heat transfer between the surrounding earth and an earth-sheltered or earth-bermed building. Therefore, a prediction of subsurface temperature profile as a function of time and depth could be a useful tool. Such a profile for the city of Yazd will be presented here.

It will be shown here that compared with the aboveground climate in Yazd, the predicted subsurface environment is much milder.

METHOD

Soil temperature, as a function of depth and time, is usually expressed as a sum of one or more exponentially damped temperature waves. The formulae of the temperature waves are solutions to the heat equation in which the ground is considered to be a semi-infinite solid with a plane surface at a uniform temperature.

Moreland (1978), Kusuda (1975), and Labs (1989) have used models that incorporate surface temperature data [3]. Since their equations are similar, only Labs' model will be discussed here. His equation is:

$$T_{z,t} = T_m - A_s \exp\left[{}^{-z\sqrt{\pi/365\alpha}} \right] \times Cos\left\{ \left(\frac{2\pi}{365} \right) \left[t - t_o - (\frac{z}{2})(\sqrt{365/\pi\alpha}) \right] \right\} \quad (1)$$

Where: $T_{z,t}$ is the soil temperature at depth z and day t, T_m the mean annual ground temperature, A_s the annual surface temperature amplitude,t the time of the year(in days), t_o date of the minimum surface temperature, α soil thermal diffusivity (in m^2 per day).

In several studies the annual patterns of the earth's temperature have been measured at different depths. Givoni has compared the experimental data bringing to a common basis: the relative range, at a given depth, relative to the range of the surface temperature. On the basis of these experimental studies, which were conducted in regions with different climatic characteristics, the values in Table1 is suggested for the range damping factor (F) for soils in different climatic regions. The suppression of the annual temperature with depth, for intermediate soil in arid and in wet climates, is shown in Table2. [3]

Combining together the formulae for the range damping factor,F, and the time lag, L, a generalized formula estimating the soil temperature, $T_{z,t}$, for any depth and time is suggested by Givoni [3]:

$$T_{z,t} = T_m + A_s \exp^{(-F\times Z)} \times Sin\left(0.986 \times t - 125 - L \times z\right) \quad (2)$$

Where: $T_{z,t}$ is the soil temperature at depth z and day t (°C); T_m the mean annual ground temperature (°C); A_s the annual surface temperature amplitude; t the time of the year (in days); F, range damping factor, depends on climate and soil type; z, depth under the surface (in m); L, time lag per meter depth, depends on climate and soil type (in days)

Climate	**Soil type**		
	Loam/clay	Intermediate	Sandy
Desert	0.45	0.50	0.55
Arid	0.40	0.45	0.50
Intermediate	0.35	0.40	0.45
Humid	0.25	0.35	0.40
Wet	0.20	0.30	0.35

Table1: Damping factor (F) for different climates and soil types.

Climate	**Soil type**		
	Loam/clay	Mixed	Sandy
Desert	24	25	26
Arid	22.5	23.5	24.5
Intermediate	21	22	23
Humid	19.5	20.5	21.5
Wet	18	19	20

Table2: Time lag(L) for different climates and soil types.

Unfortunately, long-term experimental values for mean annual ground temperature in Yazd is not available. However, according to Watson and Labs [4], adding about 1.7°C to the average annual air temperature can approximate the mean annual ground temperature. In Yazd, the long-term average annual air temperature is 19.3°C, thus making mean annual ground temperature, T_m=21°C.

The annual temperature amplitude, A_s , corresponds to the maximum elevation temperature from annual mean of the soil surface. Since the ground temperature is not available, Watson and Labs[4] suggest A_s can be estimated by taking one-half the difference between the July and January monthly average air temperatures and adding 1.1°C. The July and January long-term monthly average temperatures, taken from 50 years of statistics, are 32.51 and 5.47, respectively[1]. This leads to a value for A_s of 14.62.

As Yazd is located in a desert region with desert climate, and its soil is mixed of loam and sand in defferent places, damping factor (F) of 0.50 and time lag(L) of 25 is suitable for it.

RESULTS

Eq. (2) can now be expressed for Yazd with variables that are based on long-term climatic and soil conditions. The resulting equation is:

$$T_{z,t} = 21 + 14.62 \exp^{(-0.5\times Z)} \times Sin\left(0.986 \times t - 125 - 25 \times z\right) \quad (3)$$

Eq. (3) can now be used to predict a subsurface temperature profile for Yazd at any depth. The results at different depths are graphed and compared to the annual average air temperatures in Fig.1. It can be seen that the average air temperature can reach as high as 32.5°C, whereas at a depth of only 1 m, the maximum temperature reaches about 29.5°C. At a depth of 7 m, the temperature is almost a constant 21°C, that is in summer and winter thermal comfort range.

Fig.2. compares subterranean temperatures to sol-air temperatures on south wall for a typical summer day(15 Aug.). Sol-air temperature is calculated for two different solar absorptivity (a=0.4 for cream bricks and a=0.7 for brown ones) that are common materials for external surfaces in Yazd.

Using this data in building heat- transfer applications will reveal the savings in energy.

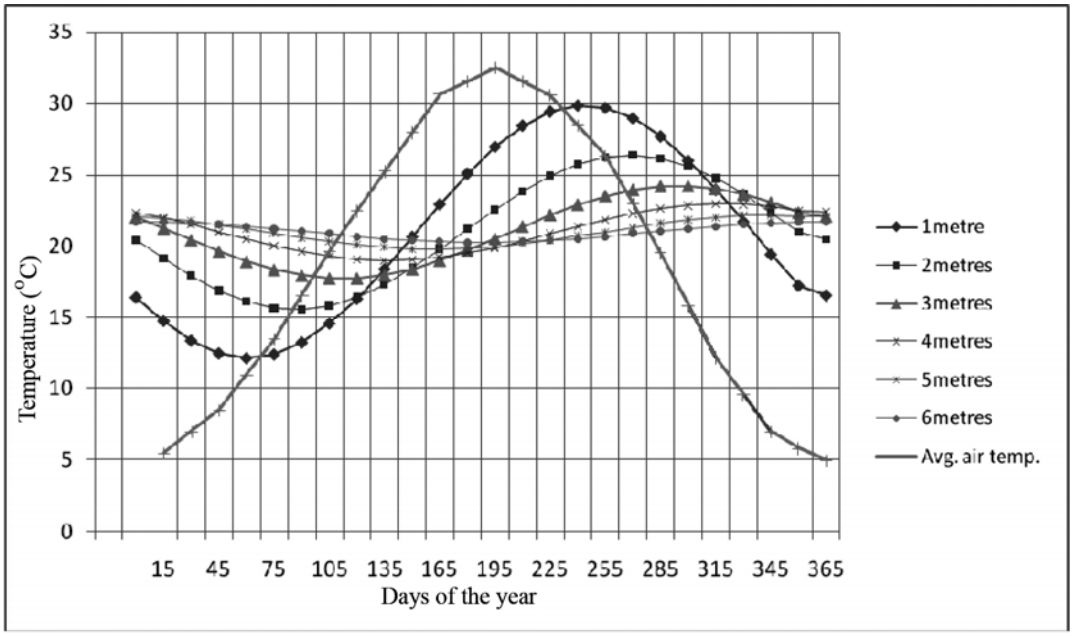

Figure1: Average daily air and subsurface temperature at various depths.

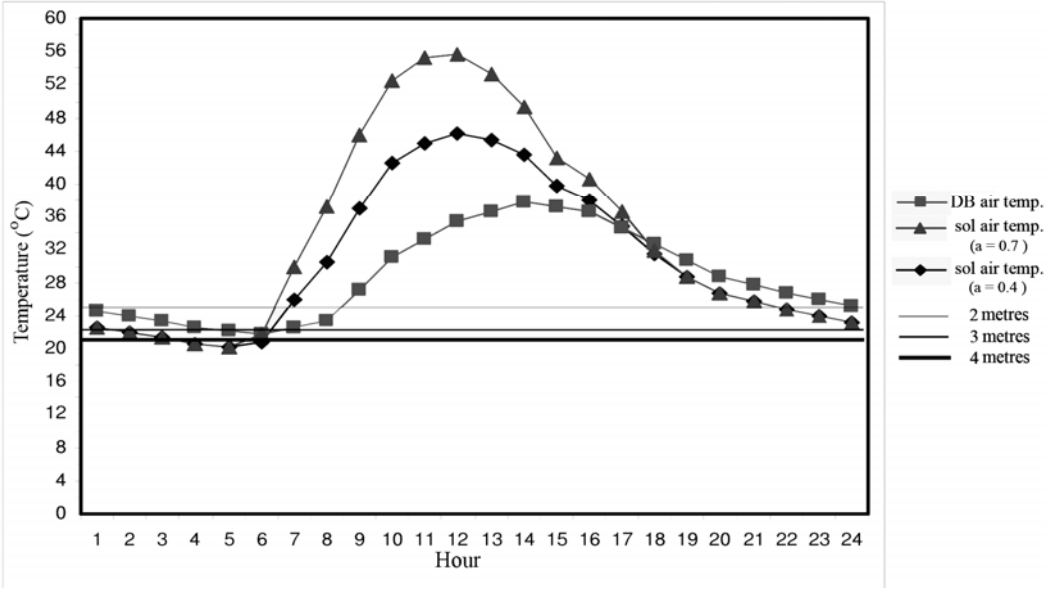

Figure 2: Air, sol-air(on south wall), and underground temperature for August 15.

DISCUSSION

It is obvious from Fig.1 that the subsurface cyclical temperature wave is considerably dampened when compared to the air temperature wave, especially at increasing depths. The subsurface temperatures are shown to be significantly lower when air temperatures are at their peak. This observation implies that structures sheltered by the earth will result in decreased energy consumption.

Close study of Fig.1 can give designers insight as to where the optimum depths a building should lie and how much of the building should be left exposed, if any.

Another comparison one could make is the difference in degree-days. When the total heat flow for a building envelope is known for a 1°C temperature difference, the degree-day concept can be used to find the total energy consumed for known outside temperatures at a specific locality. Summing the difference each day of external average temperature and a base temperature for days when the average external temperature is above the base temperature in summer or under the base temperature in winter, makes cooling and heating degree-day calculation. Using the data in Fig.1, with a base temperature of 21°C as an upper limit of thermal comfort, and 18°C as the lower limit of thermal comfort, the cooling and heating degree-days can be calculated and compared to aboveground. The results are given in Table3, which shows that at a depth of 3 m, there is a reduction of 68% in cooling degree-days compared with aboveground. At depths beyond 5 m, cooling degree days is almost zero. It must also be noted that the comparison is being made to outside air temperatures, neglecting the effects of solar radiation that an aboveground building will receive. Since heat-transfer calculations normally account for sol-air temperature, the difference between aboveground and underground degree days will be more.

	Cooling degree-days (base:21°C)	**Heating degree-days** (base:18°C)
Aboveground	1190.1	1337.4
Subsurface (m)		
1	1030.57	538.91
2	625.07	173.33
3	379.00	8.17
4	229.80	0
5	139.35	0

Table3: A comparison of above- and subsurface cooling and heating degree-days

Another obvious observation from Table3, shows that at a depth of 3 m, the temperature is above 18°C and the heating degree days is zero. So the underground structures can also benefit earth thermal stability during cold months of the year.

REFERENCES

1. www.irimet.net, Islamic Republic of Iran Meteorological Organization.
2. A.J. Davis, R.P. Schubert, Alternative Natural Energy Sources in Building Design, Van Nostrand Reinhold, New York, 1981.
3. Givoni, B: Climate Consideration in Buildings and Urban Design, New York, Van Nostrand Reinhold, 1998.
4. D. Watson, K. Labs: Climatic Buildings Design, McGraw-Hill, New York, 1983.

AIR COOLING POWERED BY FAÇADE INTEGRATED COLOURED OPAQUE SOLAR THERMAL PANELS

I. Mack[1]; S. Mertin[2]; V. Hody - Le Caër[2]; A. Schüler[2]; Y. Ducommun[1];

1: SwissINSO SA, EPFL – PSE (Parc Scientific), Bâtiment D, Av. J.-D. Colladon, CH-1015 Lausanne, Switzerland

2: Solar Energy and Building Physics Laboratory, EPFL-ENAC-IIC-LESO-PB, Station 18, CH-1015 Lausanne, Switzerland

ABSTRACT

Air conditioning is an important part in building services world-wide in both commercial and residential buildings. With the general attempt to reduce the usage of fossil fuels and increase the usage of green solutions, the market for solar air conditioning is growing rapidly.

Solar air conditioning combines solar thermal absorbers to transfer solar radiation into heat with heat-driven cooling technologies. Common heat-driven cooling technologies are absorption and adsorption chillers using heat to produce cold by a thermodynamic cycle.

However, solar thermal collectors are currently limited to roof applications, as their black surface with its tubing is not aesthetic. This limits the potential amount of possible heat gain, which could be used for solar air cooling or heating.

By using the Klymaa™ opaque coloured solar thermal collectors of SwissINSO, the solar coverage for air cooling and/or heating can be significantly increased, as they are aesthetically integrated into the façade. SwissINSO's coloured collectors use a cover glass with a thin coating developed by the Solar Energy and Building Physics Laboratory (LESO-PB) of the Ecole Polytechnique Fédérale de Lausanne (EPFL). The coating is a multilayer system deposited by magnetron sputtering on solar float glass. The solar transmittance τ_e of these coatings is high to assure a maximum efficiency of heat absorption by the black absorber behind the coloured cover glass. The absorber can be flat-plate or vacuum tubes, depending on the needs for the air conditioning, as the cover glass is opaque.

INTRODUCTION

Air conditioning in the commercial as well as in the residential building sector is nowadays becoming standard. The cooling power is generally provided by electrical-driven compressor cooling equipments with huge energy consumption, leading to an increased power demand during summer. This means in turn that the emission of greenhouse gasses increases, due to this energy demand, which contribute to climatic changes [1].

There is thus a desperate need to supplement or even better, to replace, the use of fossil energies by renewable energies to generate the power needed to control the temperature of public or commercial buildings, large residential complexes, educational institutions or hospitals. From the renewable energies - wind, sun, water or biogas - the solution of choice is the use of solar energy. Solar energy has the great advantage that the solar gains and the cooling loads of buildings occur at more or less the same time [1]. Furthermore, it can also be used for heating of the building as well as for providing the necessary domestic hot water.

The incoming solar radiation can be transformed by different processes into cold air to provide cooling for buildings. One possibility is the conversion to electricity by photovoltaic cells and the usage of a classical electrical-driven compressor cooling equipment. This concept is not highly considered, as the maximum use of photovoltaic is achieved by feeding the obtained electricity into the public grid [2,3]. The other possibility is to convert the solar radiation into heat by using solar thermal collectors, and to run thermal-driven chillers for providing the desired cooling [4].

Solar thermal collectors typically consist of a metallic absorber sheet, which is covered with a black optical selective coating, converting the incoming solar radiation into heat by absorption. However, the visibility of the unaesthetic inside of the thermal panels (tubes, corrugations of the metal sheet, etc.) has limited their acceptance as integrated elements of the building's envelope. "Integration" in conventional architecture is often considered synonymous to "invisible" [5].

Due to their unpleasant visual aspect, solar thermal collectors have been until now considered as technical components to be hidden and are confined to roof-top applications, where they are less visible and have less impact on the architectural design [6]. As a consequence, the surface available for collecting solar energy is very limited in most cases, and therefore the solar gain available to be used for the thermal control of a building is very low.

A solution to overcome this difficulty of aesthetic architectural integration is to use the Klymaa™ opaque coloured solar thermal collectors of SwissINSO. They use a front face cover glass with a thin coating developed by the Solar Energy and Building Physics Laboratory (LESO-PB) of the Ecole Polytechnique Fédérale de Lausanne (EPFL) [7-9]. The coloured collectors and their application for solar air cooling will be presented in this paper.

COLOURED COLLECTORS

SwissINSO's approach for the integration of the Klymaa™ solar thermal collectors is illustrated in Figure 1, which schematically shows a thermal solar collector with a coloured coating applied to the inner surface of the covering glass pane. This coating reflects only a very small part of the visible light giving the coloured impression of the collector [7,8]. The main part of the solar radiation passes the coating and is absorbed by the thermal absorber mounted behind the glass. The necessary spectral-reflection band needed for the coloured

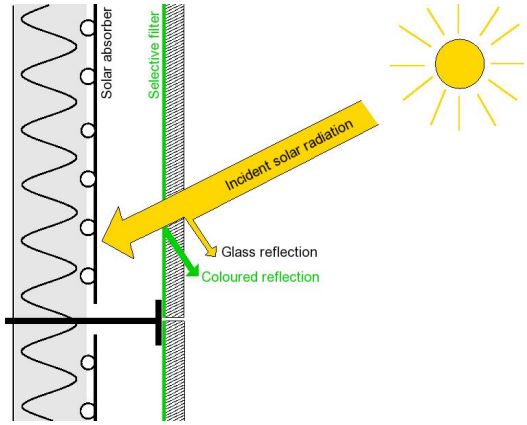

Figure 1: Principle of the SwissINSO coloured solar thermal panel indicating that most of the solar radiation is transmitted through the coating and only a few percent are reflected.

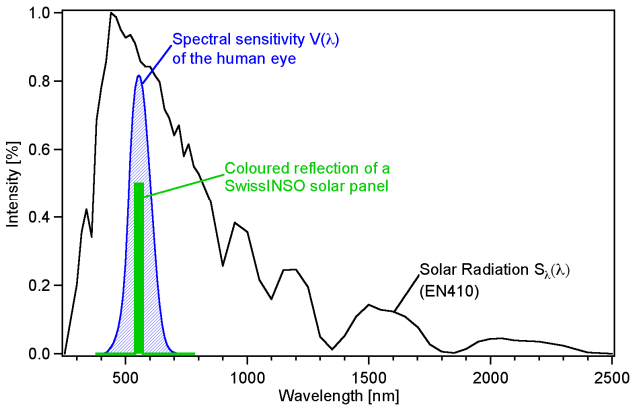

Figure 2: Showing the spectral distribution of the solar radiation in comparison to the spectral sensitivity of the human eye and the coloured reflection of a SwissINSO solar panel.

impression is very narrow compared to the spectral distribution of the incoming solar radiation, as can be seen in Figure 2 [10]. In this figure also the spectral sensitivity of the human eye is shown. This shows only a very small part of the solar spectrum is used for the coloured appearance of the collector, whereas most of the solar energy is transmitted through the glass.

The coloured coating is combined with a diffusing treatment on the outer surface of the cover glass to further enhance the amount of energy transmitted to the absorber. In combination with this surface treatment the energetic losses compared to a standard glass covered absorber are only a few percent [8]. The advantage of the coloured cover glass in comparison to a coloured absorber is that the function of optical selectivity and coloured reflection are separated, giving more freedom to coating optimisation [7].

The current development towards new colours and new materials for coloured coatings will be presented in another contribution of this conference [11].

SOLAR CURTAIN WALL SOLUTION

The overall aesthetics of the building's envelop can be kept uniform by SwissINSO's coloured solar thermal collectors. On the surfaces of a building exposed to solar radiation, the Klymaa™ solar collectors are installed as spandrel areas. Whereas in areas with low or no sun exposure, the cladding panels use the same coloured opaque glass not mounted on solar collectors but used simply as conventional glazed spandrels with isolation material behind them. This provides a homogeneous façade from the aesthetic point of view and on the same time the investment costs are kept low, as only the solar active parts of the façade are equipped with a solar thermal collector.

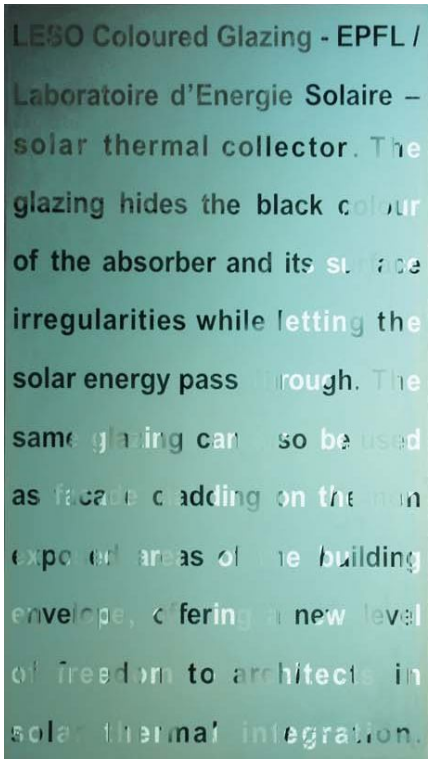

Figure 3: Klymaa™ coloured opaque solar thermal panel of SwissINSO.
Design: Munari-Probst

The configuration of the solar thermal collector can be adapted to the usage of the gained heat as well as to climatic conditions. For the solar collector in the SwissINSO's coloured panels it is possible to use flat-plate, evacuated tube as well as CPC (Compound Parabolic Concentrator) collectors [12-14]. The type of collector used is always adapted to the needs of each building, as a function of usage of the gained energy, climatic conditions, window to wall ratio or building usage. An advantage of evacuated tube collectors is that the solar gain can be increased by turning the individual tubes in such a way, that the absorber fines in each tube are optimal orientated towards the incidence angle of the solar radiation [15].

Besides providing the uniformity of the building envelope, the Klymaa™ solution renders the exact curtain wall expression sought by the architect, because the glass panes can be produced in colour shades and patterns designed to custom specifications. An example is shown in Figure 3.

SOLAR AIR COOLING

Air conditioning is the process of treating air to control simultaneously its temperature, humidity, distribution and cleanliness. Since cooling loads and solar gain occur at more or less the same time, it seems logical to use solar energy for cooling purposes. Solar cooling systems consist of the following main components: The solar collectors (flat-plate, evacuated tubes or CPC), a heat buffer storage, the heat distribution system, the thermally driven chiller, an optional cold storage, a cooling tower to remove auxiliary heat from the system, the air conditioning system, and a backup system.

In the following section only the thermally driven chillers, the cooling towers and the back-up heat source are described, as the collectors have already been described in the previous.

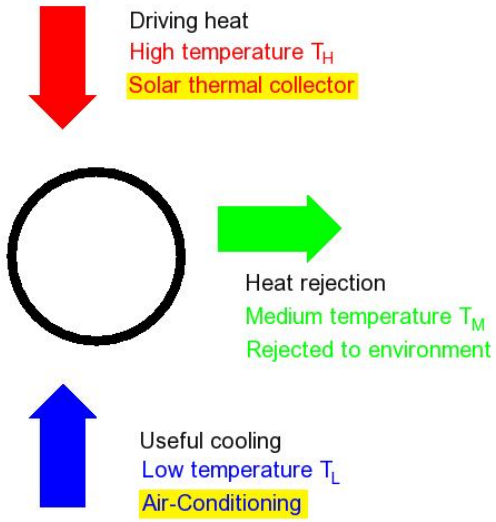

Figure 4: Schematic drawing of the energy flows and the temperature levels in a thermally driven chiller.

Chillers consume energy to transfer heat from a low temperature source to a sink at medium temperature. The necessary energy to run the chillers can be gained by SwissINSOs coloured solar thermal collectors by transferring solar radiation into heat. The principle and the different temperature levels are shown in Figure 4 for thermal-driven chillers.

Thermally driven chillers using the chemical process of absorption consist of two chemical components, one of them serving as sorbent and the other as refrigerant [2]. Absorption cycles are based on the fact that the boiling point of a mixture is higher than the corresponding boiling point of the pure liquid. The different operational steps of such systems are well documented and not described here [3].

An alternative to absorption is the physical process of adsorption, where the liquid sorbent is replaced by a highly porous solid adsorber. To obtain a quasi continuous operation with adsorption cycles it is necessary to have at least two compartments working parallel [3]. The advantages of those systems are, their simple mechanical construction and their very low electrical consumption, as no internal solution pump is required [1].

The operation temperature of the different chilling system as well as the desired temperature for the cooling system influence on one hand the chiller choice, and on the other the collector type [4,16]. The collector efficiency of flat-plate and evacuated tube over the generated temperature is shown in Figure 5. Furthermore, the working areas of the different sorption technologies are indicated, showing that it is crucial to choose the correct combination for a efficient cooling system. For absorption and adsorption systems it is therefore possible to use flat-plate, evacuated tube collectors and CPCs.

To complete the chilling system, a cooling tower is needed to remove extra heat at medium temperature. Hereby two possibilities exist; The open-circuit system, with direct contact between the primary cooling water and air, and the closed-circuit system, with only indirect contact between the two media across a heat-exchanger wall. Both systems use latent heat transfer where the coolant, which has to be water, is cooled by evaporating about 2-3 % of itself [3]. This is a very efficient method of cooling, but it is accompanied with significant water consumption. Therefore in areas of low water availability it is advisable to use closed-

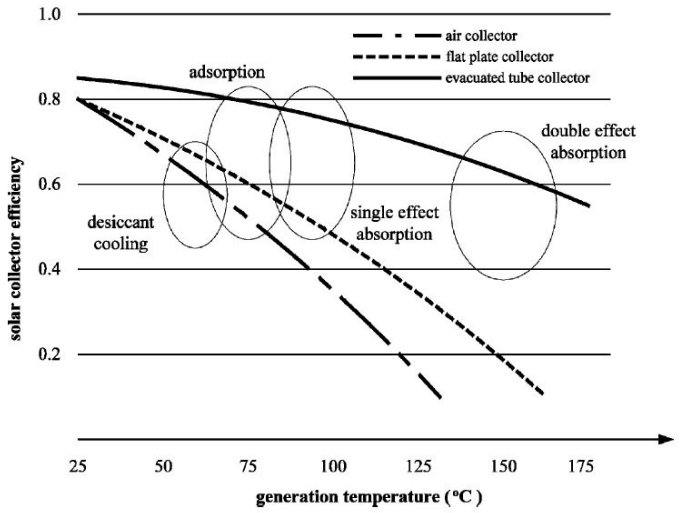

Figure 5: Possible combination of solar thermal and sorption refrigeration technologies (Source [16]*).*

circuits in combination with dry-air coolers which transfer just sensible heat and no water to the ambient air [3].

Additionally, back-up heaters are needed to assure that air conditioning is also provided at times when the solar energy is not sufficient (cloudy days, night time or exceptional internal loads).

CONCLUSIONS

Solar cooling is a clean, energy thrifty and sustainable solution for air conditioning of urban buildings. The demand of renewable energy sources for air conditioning is sharply increasing and the necessity to find sustainable solutions is becoming more and more important. To benefit from the available solar coverage for solar air conditioning, it is necessary to have a sufficient amount of collectors to gather the necessary solar energy and transform it into cold.

The Klymaa™ coloured solar thermal panels of SwissINSO provide the opportunity to aesthetically integrate solar thermal collectors into façades, thus offering much larger active surfaces for solar energy collection. This provides the possibility to increase the potential heat gain, which can be used for air conditioning or heating of the building. To provide the best solar coverage for each building it is necessary to adjust the components of the solar system to the building's character and to the occupants' behavioural pattern. The flexibility of SwissINSO's collector to use flat-plate, evacuated tube or CPC collectors is a large step towards this adjustment.

ACKNOWLEDGMENTS

The authors are grateful to Christian Roecker and Dr. Maria Cristina Munari-Probst for their support and good collaboration.

REFERENCES

[1] M. Delorme, R. Six, D. Mugnier, J.-Y. Quinette, N. Richler, E. Wiemken, H.-M. Henning, T. Tsoutsos, E. Korma, G. Dall'O, P. Fragnito, L. Piterà, P. Oliveira, J. Barroso, J. Ramòn-Lòpez, and S. Torre-Enciso, *Solar air conditioning*, 2004.

[2] H.-M. Henning, "Solar assisted air conditioning of buildings – an overview," *Applied Thermal Engineering*, vol. 27, Jul. 2007, pp. 1734-1749.

[3] H.-M. Henning, ed., *Solar-Assisted Air-Conditioning in Buildings: A Handbook for Planners*, Springer, 2007.

[4] A. Papadopoulos, "Perspectives of solar cooling in view of the developments in the air-conditioning sector," *Renewable and Sustainable Energy Reviews*, vol. 7, Oct. 2003, pp. 419-438.

[5] W. Weiss, ed., *Solar Heating Systems for Houses - A Design Handbook for Solar Combisystems*, James & James (Science Publisher) Ltd, 2003.

[6] M. Munari Probst and C. Roecker, "Towards an improved architectural quality of building integrated solar thermal systems (BIST)," *Solar Energy*, vol. 81, Sep. 2007, pp. 1104-1116.

[7] A. Schüler, C. Roecker, J.-L. Scartezzini, J. Boudaden, I.R. Videnovic, R.-C. Ho, and P. Oelhafen, "On the feasibility of colored glazed thermal solar collectors based on thin film interference filters," *Solar Energy Materials and Solar Cells*, vol. 84, Oct. 2004, pp. 241-254.

[8] A. Schüler, J. Boudaden, P. Oelhafen, E. de Chambrier, C. Roecker, and J.-L. Scartezzini, "Thin film multilayer design types for colored glazed thermal solar collectors," *Solar Energy Materials and Solar Cells*, vol. 89, Nov. 2005, pp. 219-231.

[9] A. Schüler, D. Dutta, E. de Chambrier, C. Roecker, G. de Temmerman, P. Oelhafen, and J.-L. Scartezzini, "Sol–gel deposition and optical characterization of multilayered SiO2/Ti1−xSixO2 coatings on solar collector glasses," *Solar Energy Materials and Solar Cells*, vol. 90, Nov. 2006, pp. 2894-2907.

[10] A. Schüler, C. Roecker, J. Boudaden, P. Oelhafen, and J.-L. Scartezzini, "Potential of quarterwave interference stacks for colored thermal solar collectors," *Solar Energy*, vol. 79, Aug. 2005, pp. 122-130.

[11] S. Mertin, V. Hody - Le Caër, M. Joly, J.-L. Scartezzini, and A. Schüler, "Coloured Coatings for Glazing of Active Solar Thermal Facades by Reactive Magnetron Sputtering," *CISBAT 2011*, 2011.

[12] E. Zambolin and D. Del Col, "Experimental analysis of thermal performance of flat plate and evacuated tube solar collectors in stationary standard and daily conditions," *Solar Energy*, vol. 84, Aug. 2010, pp. 1382-1396.

[13] C. Tíba and N. Fraidenraich, "Optical and thermal optimization of stationary non-evacuated CPC solar concentrator with fully illuminated wedge receivers," *Renewable Energy*, vol. 36, Sep. 2011, pp. 2547-2553.

[14] N. Fraidenraich, C. Tiba, B.B. Brandão, and O.C. Vilela, "Analytic solutions for the geometric and optical properties of stationary compound parabolic concentrators with fully illuminated inverted V receiver," *Solar Energy*, vol. 82, Feb. 2008, pp. 132-143.

[15] M. Munari Probst, "Architectural Integration and Design of Solar Thermal Systems," Ecole Polytechnique Federale de Lausanne, 2009.

[16] H.-M. Henning, "Air Conditioning with Solar Energy," *SERVITEC 2000*, Barcelona: 2000.

ANALYSIS OF PASSIVE COOLING AND HEATING POTENTIAL IN VIETNAM USING GRAPHICAL METHOD AND TYPICAL METEOROLOGICAL YEAR WEATHER FILE

Anh-Tuan Nguyen*, Sigrid Reiter
LEMA, University of Liège, Belgium
*Address: LEMA, Bât. B52/3, Chemin des Chevreuils 1 - 4000 Liège; Email: natuan@ud.edu.vn**

ABSTRACT

This paper studies the potential to improve thermal comfort in Vietnam thanks to passive strategies. First, a thermal comfort zone for the Vietnamese is proposed by using the PMV-PPD heat balance model of Fanger and the effects of adaptive mechanism of the people living in tropical hot humid region. Then, the comfort zone is enlarged using the algorithms proposed by the authors to calculate the effects of the passive heating and cooling strategies. Typical Meteorological Year (TMY) weather data are used for graphically printing of hourly environmental parameters on the psychrometric chart and for climate analysis, subsequently. The limitation and the scope of this method are also specified. Results of this study show that in all climatic zones of Vietnam, natural ventilation is an efficient cooling solution, low-cost and easy to apply. Thermal comfort improvement of natural ventilation strategy varies with the climatic zones, increasing from 17.1% in Hanoi, 21% in Danang to 31.4% in Hochiminh city. Meanwhile, passive solar heating is not really effective since winter in Vietnam is usually not too cold and the capacity of the passive solar collector system is usually limited. Direct evaporative cooling also has a great cooling effect compared with that of natural ventilation, but significant humidity augmentation in the air in hot and humid conditions may be inappropriate. Seasonal analysis reveals that natural ventilation gives higher performance than other methods and is particularly effective in mild seasons. During 12 months in Hanoi, the analysis clearly shows significant contribution of natural ventilation in the period from April to October during which comfort period achieved might vary from 30% to 81%. The combination of all passive strategies considerably improves thermal comfort: 22.6%, 31.7% and 47.6% of total time in Hanoi, Danang and Hochiminh city, respectively. Finally, the findings of this study indicate that conventional heating and cooling methods are also needed during extreme weather conditions in summer and winter, especially in Hanoi.

1. INTRODUCTION

A full understanding of local climate is the main requirement for the designs of climate responsive architecture towards sustainable development. There have recently been some weather tools developed for climate analysis, but they are usually aimed to the application on people living in temperate climate and thus inappropriate when being applied to people living in hot humid climate. This study proposes a simple method for hot humid climate analysis with which the potential of comfort improvement of passive cooling and heating strategies in many regions of Vietnam is examined. In this analysis three typical sites, including Hanoi *(21° North)*, Danang *(16° North)* and Hochiminh city *(11° North),* have been selected. They represent 3 climatic regions in the North, Centre and South of Vietnam.
The method proposed will be carried out through three steps: (1) proposition of an appropriate comfort zone for people living in hot humid climate; (2) printing of climate data and (3) quantitative analysis and assessment of heating and cooling potential of passive strategies.

2. COMFORT ZONE FOR PEOPLE LIVING IN HOT HUMID CLIMATE OF VIETNAM

There is still an argument that under a specific condition the comfort zone for different climatic regions is unchanged. Based on Fanger's study , ASHRAE [1] reported that under steady-state

condition, "people cannot *physiologically* adapt to preferring warmer or colder environments, and therefore the same comfort conditions can likely be applied throughout the world". However, the comfort zone proposed by ASHRAE standard [2] seems to be inappropriate for Vietnamese since it neglects the adaptation to the humidity of people living in hot humid climate. Some computer weather tools also failed to predict comfortable period for the climate of Vietnam since they used inappropriate comfort boundaries. The comfort zone for Hanoi proposed by Climate consultant software [3] (using comfort model of ASHRAE standard 55) gives that only 4.9% of total time in a year should be comfortable, which is extremely low. Also in Hanoi, Fig. 1 shows the comfort prediction of another weather tool [4] in which Szokolay's method [5] was adopted. The significant weakness of this method is that a steady-*state condition* was imposed, but the *adaptive comfort model* was employed to find neutral temperature. According to this prediction, only 2.5% of total time in a year is considered comfortable, extremely underestimating the real thermal environment.

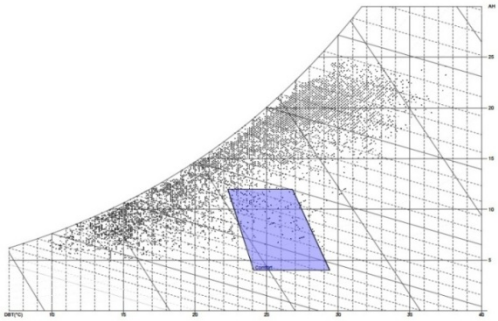

Figure 1: Incorrect prediction of comfort zone for Hanoi by weather tool [4]

The above analysis indicates that it is essential to create appropriate thermal comfort boundaries for Vietnamese considering the adaptation to humidity. This study proposes a thermal comfort zone for Vietnamese as shown in Fig. 2 using a steady-state thermal comfort model. This comfort zone, which is applied for a normal Vietnamese (height of 1.65m and weight of 60kg) in sedentary work (60W/m2 – 1 met) and in still air condition (0.15 m/s), is established for 90% occupant acceptability. Clothing insulation values may vary from 0.5 clo (summer) to 1 clo (winter), reflecting the change of clothing style to suit seasonal weather.

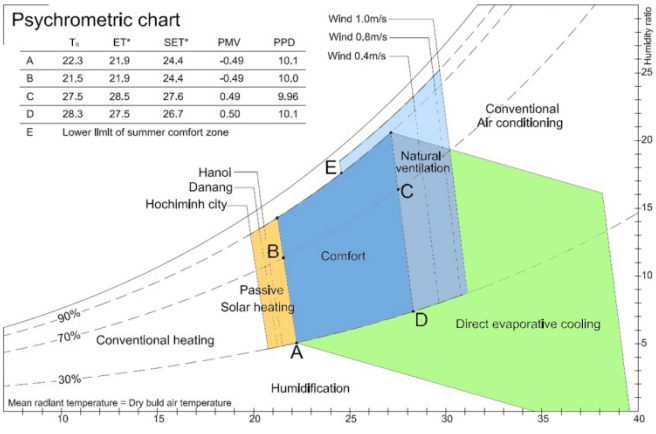

	T_o	ET*	SET*	PMV	PPD
A	22.3	21.9	24.4	-0.49	10.1
B	21.5	21.9	24.4	-0.49	10.0
C	27.5	28.5	27.6	0.49	9.96
D	28.3	27.5	26.7	0.50	10.1
E	Lower limit of summer comfort zone				

Figure 2: Comfort zone proposed for Vietnamese and its enlargements

The cooler and warmer boundaries of the comfort zone are defined by the PMV-PPD model (-0.5 ≤PMV≤0.5; PPD ≤ 10%). These boundaries are the lines AB and CD respectively (Fig. 2). Point B and C rely on 70% RH since PMV-PPD model is assumed to be inaccurate at RH higher than 70% [6]. These lines nearly coincide with the lines of constant ET*.

The lower humidity lever of the comfort zone was fixed at 30% relative humidity since it hardly falls below this value in humid climate and Vietnamese are not acquainted with dry nose, throat, eyes and skin caused by extremely dry air. The upper humidity limit is more complicated due to

lack of specific survey on this issue. ASHRAE [2] specifies an upper humidity ratio limit of 0.012 $kg_w/kg_{dry\ air}$. That is based on avoiding condensation and mold growth in the ducts of HVAC system [7] and hygienic conditions rather than on human thermal comfort requirements. Besides, in hot humid climate surface temperatures are closer to the ambient air temperature which is normally very high. This reduces the potential for condensation and mold growth, allowing the higher acceptable humidity limit in hot humid climate. Olgyay [8] proposed around 78% relative humidity as upper limit for U.S. moderate zones inhabitants. In his book, Givoni [9] suggested that upper limit could be enlarged to 90% relative humidity and up to 93% with ventilation. Pham [10] conducted a small comfort survey in Vietnam in 2002. His result revealed that over 80% of subjects found to be thermally comfortable at 28.5 – 29.5°C and 90% relative humidity. Adaptive comfort standards [2,11] even indicated that no humidity limit was required for thermal comfort. Based on above-mentioned studies and findings, the upper limit of comfort zone shown in Fig. 2 was fixed at 90% relative humidity. In summer, this humidity limit may be even enlarged to 95% under effect of a wind speed of 0.8 – 1m/s due to the effect of air change.

3. COMFORT CONTROL POTENTIAL ZONE BY USING PASSIVE COOLING AND HEATING STRATEGIES

3.1 Passive cooling by natural ventilation

Precise comfort improvement by elevated air speed has not been established. Both ASHRAE 55 [2] and ISO 7730 [6] recommend a maximum wind speed of 0.82 m/s for sedentary activity. However, this mainly bases on the requirement of stabilization of loose paper rather than human draught. It is not difficult to create thermal comfort for a person exposed to a wind velocity of 1 m/s [12] and under overheated conditions air velocities up to 2 m/s may be welcome [5]. The velocity of 1 m/s is, therefore, adopted in comfort enlargement shown in Fig. 2. Temperature offset above warmer limit of comfort zone by increased air velocity is strictly followed these two standards [2,6]. This enlargement neglects the effect of humidity on cooling potential of air movement since this effect is rather minor.

3.2 Passive cooling by Direct evaporative cooling

In direct evaporative cooling, water evaporates directly into the airstream, reducing the air's dry-bulb temperature and raising its humidity, but wet-bulb temperature is always unchanged. The total heat content of the system does not change, therefore it is said to be *adiabatic*. The cooling performance or leaving air temperature of the cooler may be determined:

$$T_{LA} = T_{DB} - (T_{DB} - T_{WB}) * \varepsilon \quad (1)$$

where

T_{LA} = Leaving air dry-bulb temp; T_{DB} = Inlet Dry-bulb temp; T_{WB} = Inlet Wet-bulb temp; ε = Efficiency of the evaporative cooler.

The cooler efficiency usually runs between 80% and 90%. Under typical operating conditions, an evaporative cooler will nearly always deliver the air cooler than 27°C. A typical residential 'swamp cooler' in good working order should cool the air to within 3°C – 4°C of the wet-bulb temperature [13]. Based primarily on previous experiment of other authors, Givoni [14] stated that ambient air can be cooled by 70–80% of the DBT-WBT difference. This observation led him to a comfort limit of ambient DBT of 42°C controlled by direct evaporative cooling. It is impractical to lower dry-bulb temperature more than 11°C by direct evaporative cooling [5], thus in Fig. 2, comfort zone was enlarged 11°C along wet-bulb temperature line.

3.3 Passive heating using Solar energy

This section will examine the lowest temperature at which the solar gain by the passive solar system (e.g. trombe wall system, massive masonry wall, south-facing glazing façade, sunspaces…) can match the heat losses of the building. Useful solar energy gained by a solar collector can be estimated on the following basis:

$$Q_u = A_c[I_t\tau\alpha - 24U_L(t_p - t_a)] \quad (2)$$

where
Q_u = useful energy delivered by solar collector in a day, Wh; A_c = solar collector area, m2; I_t = Global solar irradiance, Wh/m2.day; τ = transmittance, dimensionless; α = absorptance, dimensionless; U_L = overall heat loss coefficient, W/(m2·K); t_p = average temperature of absorbing surface, °C; t_a = atmospheric temperature, °C

Some parameters in equation (2) are very difficult to identify. For convenience, equation (2) is empirically simplified using solar collector efficiency η (the fraction between useful heat distributed and total solar radiation falling on a solar collector system):

$$Q_u = \eta A_c I_t \tag{3}$$

According to ASHRAE [15], η can theoretically achieve maximum value of 0.82. For preliminary calculation, η is about 0.5. The limiting condition will be when the solar heat input equals the heat loss (ignoring heat loss caused by ventilation and infiltration):

$$Q_u = UA\,(t_i - t_a)*24 \tag{4}$$

and then rearranging for t_a: $$t_a = t_i - \frac{Q_u}{UA*24} \tag{5}$$

where
U = building overall thermal transfer value (U-value), W/m^2.K; A = total building surface area, m^2; t_i = lower limit of comfort temperature - indoor, K; t_a = atmospheric temperature at which thermal balance is achieved, K

Assume a standard building of 4.0x4.0x3.6 m with overall thermal transfer value (U) of 1.58 W/m^2.K; solar collector area (A_c) of 2.0 m^2 on the roof; t_i = 22.3°C at RH = 30% (see Fig. 3); total solar irradiance (I_t) (coldest month) of Hanoi, Danang and Hochiminh city are 2678, 3718 and 5161 Wh/m2.day [16], respectively. Thus t_a for Hanoi, Danang and Hochiminh city are 21.51°C, 21.21°C and 20.78°C. These are lowest temperature at which heat delivered by a passive solar system can compensate for achieving comfort temperature.

4. CLIMATE ANALYSIS AND ASSESSMENT USING TYPICAL METEOROLOGICAL YEAR WEATHER DATA SET

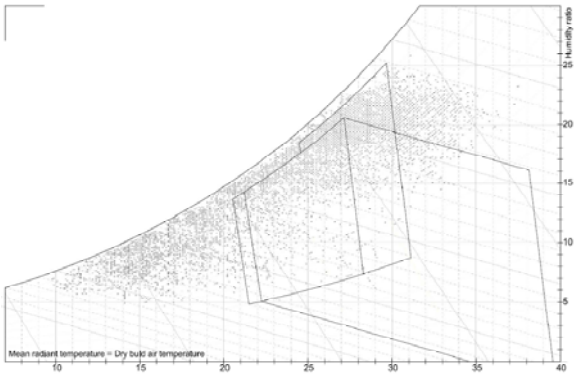

Figure 3: Hourly plot of Hanoi weather data on psychrometric chart

The TMY files for more than 2100 locations of the world can be obtained from the opened database of the U.S. Department of Energy [17]. A TMY data set provides users with a reasonably sized annual data set that holds hourly meteorological values for a one-year period that typify conditions at a specific location over a longer period of time, such as 30 years. Consequently, hourly weather data of any season, any month or any day can be separately printed out. In this step, hourly meteorological parameters of Hanoi, Danang, and Hochiminh city were graphically printed on the psychrometric chart (see Fig. 3) using TMY weather file. The comfort zone and its enlargements in Fig. 2 were then superimposed. All analysis and statistics were carried out on this two-layer psychrometric from which comfortable, potentially comfortable and uncomfortable period can be determined.

5. RESULTS

5.1 All year assessment

Fig. 4 shows the potential for comfort improvement of various passive cooling and heating strategies and their combinations. The weather in Hanoi is found to be naturally comfortable during only 23.6% of total time of a year whereas in Danang and Hochiminh city this value was around 32%, revealing that the climate of Hanoi seems more severe than the others.

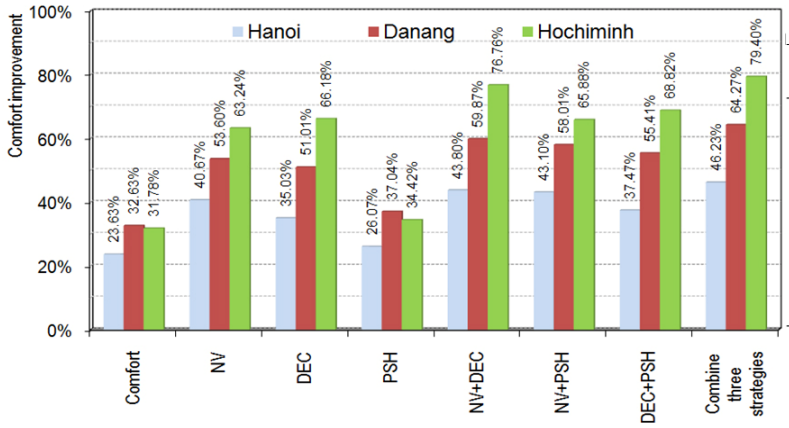

Comfort improvement

Passive strategies applied	Comfort improvement (%) Hanoi	Danang	Hochiminh
Natural ventilation (NV)	17.04	20.97	31.45
Direct evaporative cooling (DEC)	11.40	18.37	34.39
Passive solar heating (PSH)	2.44	4.40	2.64
NV + DEC	20.17	27.23	44.98
NV + PSH	19.47	25.37	34.09
DEC + PSH	13.84	22.78	37.03
Combine 3 strategies	22.60	31.64	47.62

Figure 4: Potential of comfort improvement using passive heating and cooling strategies

In Hanoi, natural ventilation proves to be the most effective strategy for comfort improvement (17.04%). The combination of all strategies does not give considerable further improvement (22.60%). Maximum potential of comfort is only 46.23%, revealing that Hanoi mainly rely on many other solutions to obtain all year comfort. In Hochiminh city, natural ventilation is an extremely effective solution by which the comfort period can be doubled. Direct evaporative cooling is also a good promise since it may provide comfort for over 66% of total time. Nearly 80% of total time would be thermally acceptable if all strategies were combined, revealing that passive solutions must be considered as the first choice in building design in Hochiminh city. Danang is geographically located in the centre of Vietnam, consequently its climate in Fig. 4 is intermediate compared to those of Hanoi and Hochiminh city. In all cities, passive solar heating is not effective (comfort improvements were minor - smaller than 4.4%) due to much cloud cover as well as high average temperature in Vietnam in winter.

5.2. Four-season and twelve-moth assessment in Hanoi

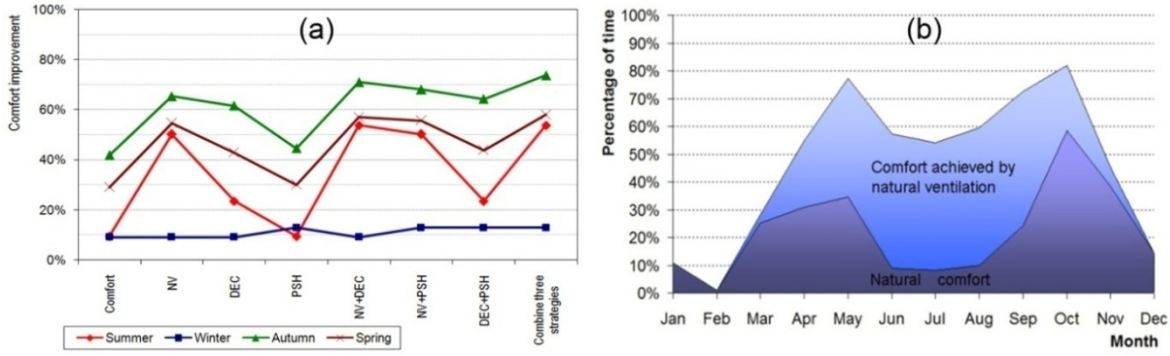

Figure 5: Comfort improvement (a) during 4 seasons and (b) during 12 months in Hanoi

A further analysis was carried out to examine the potential of comfort improvement of these strategies in each specific season and month in Hanoi. Fig. 5a shows that in winter, no strategy would be effective. In other seasons, natural ventilation would provide comfort at least of 50% of the total time. Combination of various strategies is not recommended as the effect is not noticeably higher. Comfort improvement during 12 months by natural ventilation is presented in Fig. 5b. According to this, natural ventilation is effective from April to the end

of September. The most effective period falls within summer (from June to the end of August), confirming that natural ventilation would significantly reduce cooling load. Maximum comfort occurs in mid-spring and mid-autumn. This figure also reveals that during winter natural comfort is extremely low (lower than 15%) due to the cold weather. Suitable heating solutions and building designs are therefore needed to keep indoor environment comfortable.

6. DISCUSSION AND CONCLUSION

In this study, natural ventilation and direct evaporative cooling almost have similar cooling effectiveness. Direct evaporative cooling requires sophisticated equipments and may raise the air humidity and mold growth on walls and clothes. Natural ventilation is low-cost, easy to apply and provides good indoor air quality but strongly relies on natural wind and building configuration as well as its location. Since Vietnam has hot and humid climate, natural ventilation in most cases would be the better choice for passive cooling because the increase of air humidity due to direct evaporative cooling is less appropriate for humid climates. The passive solar heating system does not have high efficiency since it can not store solar energy for nighttime heating. Active system with thermal energy storage and heat exchanger might perform better, even at night or under cloudy conditions. Relying completely on passive solutions to maintain human comfort is not feasible in Vietnam but there is a significant potential of comfort improvement.

This method has its own limitations as the TMY weather files are required for the analysis, but in current data resource they are available for only 2100 locations (1042 locations in the U.S.). For a certain location, weather file can be manually created using computer –aided tools (e.g. weather tool) with acceptable accuracy providing that sufficient input data exist. The method proposed in this paper can give reliable results and can be refined and applied by software programmers who focus on computer weather tools and building simulation tools.

REFERENCES

[1] ASHRAE handbook of Fundamentals 2009. ASHRAE, Inc. Atlanta, GS; 2009
[2] ASHRAE standard 55-2004: Thermal Environmental Conditions for Human Occupancy. ASHRAE, Inc, Atlanta, GS; 2004
[3] Climate consultant 5 (www.energy-design-tools.aud.ucla.edu) [Accessed 08 Feb 2011]
[4] Autodesk Ecotect Analysis 2011 (www.students.autodesk.com) [Accessed 01 Jun 2010]
[5] Szokolay, SV: Introduction to architectural science. Elsevier Science, Oxford, 2004
[6] ISO: ISO 7730-2005: Ergonomics of the thermal environment - Analytical determination and interpretation of thermal comfort using calculation of the PMV and PPD indices and local thermal comfort criteria. Geneva, 2005
[7] The US Department of Defense: Cooling buildings by natural ventilation. (UFC 3-440-06N), 2004
[8] Olgyay, V: Design with climate. Princeton University Press, New Jersey, 1963
[9] Givoni, B: Man climate and architecture. Elsevier publishing Co.Ltd, Oxford, 1969
[10] Pham, DN: Bioclimatic architecture. Construction publisher, Hanoi, 2002
[11] Comité Européen de Normalisation: CEN Standard EN15251: Indoor environmental input parameters for design and assessment of energy performance of buildings - addressing indoor air quality, thermal environment, lighting and acoustics. Brussels, 2007
[12] Fanger, PO: Thermal comfort. McGraw-Hill book company, the US, 1970. p.99
[13] Evaporative cooler (www.philippine-builder.com) [Accessed 27 Jan 2011]
[14] Givoni, B: Passive and low energy cooling of buildings. Van Nostrand Reinhold, New York, 1994
[15] ASHRAE HVAC Systems and Equipment 2008. ASHRAE, Inc. Atlanta, GS; 2008
[16] Ministry of Construction of Vietnam: Vietnam Building Code 2009 - QCVN 02: 2009/BXD - Natural Physical & Climatic Data for Construction. Hanoi, 2009
[17] U.S. Department of Energy (http://apps1.eere.energy.gov) [Accessed 07 Jan 2011]

SUMMER COMFORT IN A LOW INERTIA BUILDING WITH A NEW PASSIVE COOLING SYSTEM USING THERMAL PHASE-SHIFTING

Adrien Brun[1], Etienne Wurtz[1], Daniel Quenard[2] and Pierre Hollmuller[3]
[1]LOCIE,CNRS FRE 3220, INES-RDI, Université de Savoie, Le Bourget du Lac, France
[2]Centre Scientifique et Technique du Bâtiment (CSTB), 38400 St-Martin d'Hères, France
[3]Institut des Sciences de l'Environnement, Groupe Energie, Université de Genève

ABSTRACT

This study aims to evaluate the thermal behaviour of a new passive cooling system working with a non-continuous ventilation pattern. The research is based on numerical studies and experiments performed on the full-scale phase shifter which was designed and installed at CSTB (Scientific and Technical Centre for Building research), a French building research center. In the first part of this study, we describe a model implemented on the SimSpark simulation platform. The validation phase is in two parts: first, we validate the implementation against the analytical solution for constant airflow and harmonic temperature profile: then we use experimental data to assess its predictive capability with an intermittent airflow pattern. The second part focuses on the optimisation of the system considering the ventilation stop and start times and the quantity of storage material. To investigate its efficiency, two indexes were proposed and computed; one concerns the environment cooling potential and the other the energy storage efficiency which represents its capability to transfer nocturnal potential into daytime potential. The environmental evaluation shows an optimal relations between ventilation stop and start times start exist in order to maximise the mean cooling potential. For non-continuous airflow, the energy storage efficiency index shows that a reduction in the daily ventilation must be combined with a reduction in the material storage volume. Finally, simulations were done for an experimental building with very high energy efficiency (INCA, INES, le Bourget-du-lac, France) for several ventilation strategies. The results in terms of summer thermal comfort show that intermittent ventilation with optimised work periods is an interesting alternative to the more usual continuous ventilation. The choice of appropriate periods of operation permits a damping of the daily temperature swings so that the behaviour approaches one of a high-inertia building.

INTRODUCTION

Low inertia buildings are subject to internal higher daily temperature swings than more massive buildings and this usually leads to thermal discomfort. In the summer, the low thermal storage of these buildings makes passive cooling strategies such as nocturnal ventilation inappropriate, because they increase the day/night temperature difference. In order to use this free cooling potential, we propose the use of thermal mass by associating an air/mass storage system called *"phase-shifted ventilation"* to the HVAC building system[1]. The aim of the phase-shifted ventilation is to delay the input temperature signal without damping it[2]. Our work consists of reducing the system's size and electricity consumption to optimal levels.

NUMERICAL MODEL

The physical phenomena that take place in thermal phase-shifting are similar to those in a packed bed. A mechanically induced air flow passes through storage elements that are homogeneously distributed within a duct with cross section S and length L. The void fraction is defined as $\eta = (1 - V_b/V)$. The two-phase model is based on the following assumptions:

- Temperature in each storage element is homogeneous (lumped capacity models).
- The arrangement of the storage elements, air flow and convective coefficient are independent on the cross-section and along the length of the system.

- Axial heat transfer is negligible.
- The ducting is totally adiabatic.

These assumptions lead to the two-phase Schumann model [8] in which equations represent the energy balance on air and on material. This system is numerically solved using the finite volume method on a SimSpark platform [6]. Equations for the i^{th} control volume are presented below:

$$Cp_a\dot{m}_a\left(T_{e_i}-T_{s_i}\right)=A_{b_i}hc_i\left(T_{a_i}-T_{b_i}\right)+\rho_aCpaV_ad_tT_{a_i} \tag{1}$$

$$A_{b_i}hc_i\left(T_{a_i}-T_{b_i}\right)=\rho_bCpbV_bd_tT_{b_i} \tag{2}$$

$$T_{a_i}=\left(T_{e_i}+T_{s_i}\right)/2 \tag{3}$$

To confirm that the implementation is correct and the discretisation sufficient, the model was compared to the analytical solution of Zgraggen [9]. The validation concerns the air temperature outlet in the case of harmonic excitation ($T_a=\theta cos(wt)$) and constant air flow. Further investigation has been done on model validity with non-constant airflow using the prototype presented below.

PROTOTYPE DESCRIPTION AND EXPERIMENTAL VALIDATION

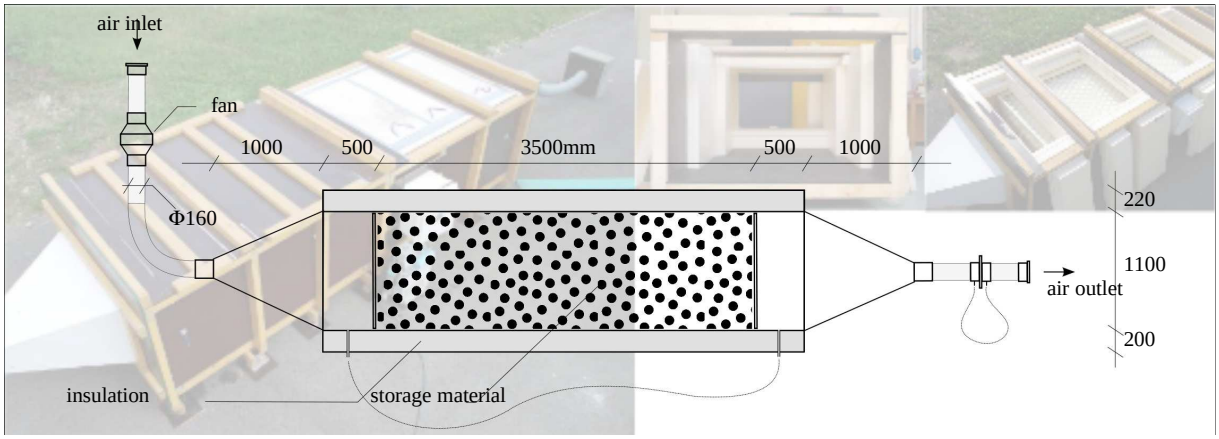

Figure 1: *Diagram and photo of the prototype.*

Our prototype differs from models of previous experiments [5] in three main ways. The first is that the airflow rate can be made time-dependent; the second concerns the structure and dimensions of the duct that allow the use of material in sufficient quantities to enable phase-shifting greater than $8h$, considering an air flow rate of $250m^3.h^{-1}$. Finally, the system is designed for external use and therefore it could be easily coupled to a small building or test cell. The prototype consists of a duct which is $4.5m$ in length and $1.1\times0.6m$ in cross-section with $20cm$ of polystyrene insulation around it. A fan provides the airflow and the rate can be controlled with a $0-10V$ controller. Water was chosen as the material due to its high sensible heat, which can reduce the required quantities by 40% [4]; water is held in $10cm$ diameter polyolefine ball (Cristopia nodules). The duct was filled with 2200 nodules in a compact hexagonal arrangement occupying $1.25m^3$, so the void fraction was approximately 0.34. We carried out experimentation over several weeks with an airflow of $380m^3.h^{-1}.m^{-2}$. There are temperature sensors along the channel (air and surface material) and measurements are made of the airflow rate at the outlet and of pressure losses in the packed bed. The analysis of these measurements was decomposed in Fourier series. Transmission and phase-shift were deduced from the component with the 24-hour periods. We obtained a transmission of 33% and a phase-shift of eleven hours. Compared to the 80% transmission obtained with the $16/13$ PVC tubes placed perpendicularly to the airflow, the 33% transmission is not

satisfactory. Reducing the diameter of the nodules may enhance the transmission by increasing the surface per volume unit but nodules are not produced in a smaller size. In spite of a transmission that was lower than expected, the experimental set-up could assess the validity of the numerical model for intermittent airflow circulation.

The first step consists of calibrating the model parameters for permanent airflow circulation. Two parameters were chosen - the convective heat transfer coefficient and the effective volume of material. Calibration is obtained by minimizing the quadratic error between experimental and numerical output temperature. The value of the convective heat transfer resulting from the optimisation is $11.8 W.m^{-2}.K$ and the volume is $0.92 m^3$ - a reduction of 27% as compared to the real volume. This difference could arise from the non-homogeneous airflow on the section and along the axis. Furthermore, the experimental result revealed that 24 hours are needed to initialise the dynamic variables, after which only small differences (of less than 0.5^oC) persist. In the second step, we were mainly interested in assessing the validity of our model for alternated airflow circulation (alternating 6-hour periods with and without ventilation). The previously calibrated model was used unchanged and the airflow pattern used was the same as the experimental one. The experimental and numerical comparison for this case is shown in FIGURE 2. In this case, it took approximately 48 hours to achieve an accurate result. The current model can be used with different ventilation patterns.

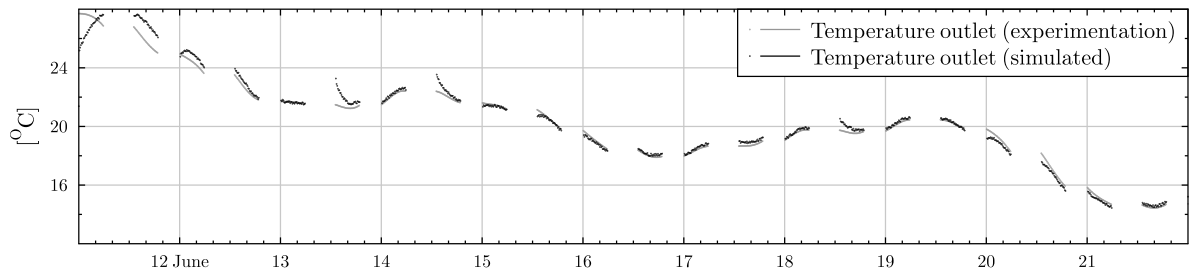

Figure 2: *Comparison of experimental and numerical output temperature in non-continuous airflow circulation.*

INTERESTS OF AN INTERMITTENT AIR FLOW PATTERN

For the moment, very few studies deal with the interest of linking a phase-shifter to building ventilation ([3], [7]) and, as far we know, none deal with its intermittent use. Since its only consumption is the electricity needed for ventilation, we are interested in optimising the period during which the storage material is cooled, as well as the capability of the system to store potential during the night and release it in the day.

The calculation presented in FIGURE 3a depicts, for the period of a day, the external air temperature and the mean temperature difference between external air and a reference (25.5^oC) depending on the periods considered (a combination of the ventilation start time and duration). The positions of the iso-values reveal an optimum start time for each ventilation period. Further work is needed to assess the constancy of this relation which could be useful in systems using air-cooling potential. After this brief analysis of the cooling source, we were interested in the effect of intermittent ventilation on the energy effectively transferred to the building. We have studied the thermal storage efficiency defined as the capacity of the system to transfer the cooling potential available at night to the day. The numerical model previously presented has been used to calculate the thermal storage efficiency of a system with 73% transmission and a 12 hour phase-shift and functioning $24h$ a day for variable material quantities and ventilation time lapses. The result (FIGURE 3b) indicates that storage efficiency could be optimised by combining shorter ventilation cycles with less storage material. For example, for $2 \times 8h$ cycles per day, the optimal efficiency is obtained with a reduction of 38% of the initial material quantities. While the functioning period is reduced by 34%, FIGURE 3c shows that the mean daily cooling potential of

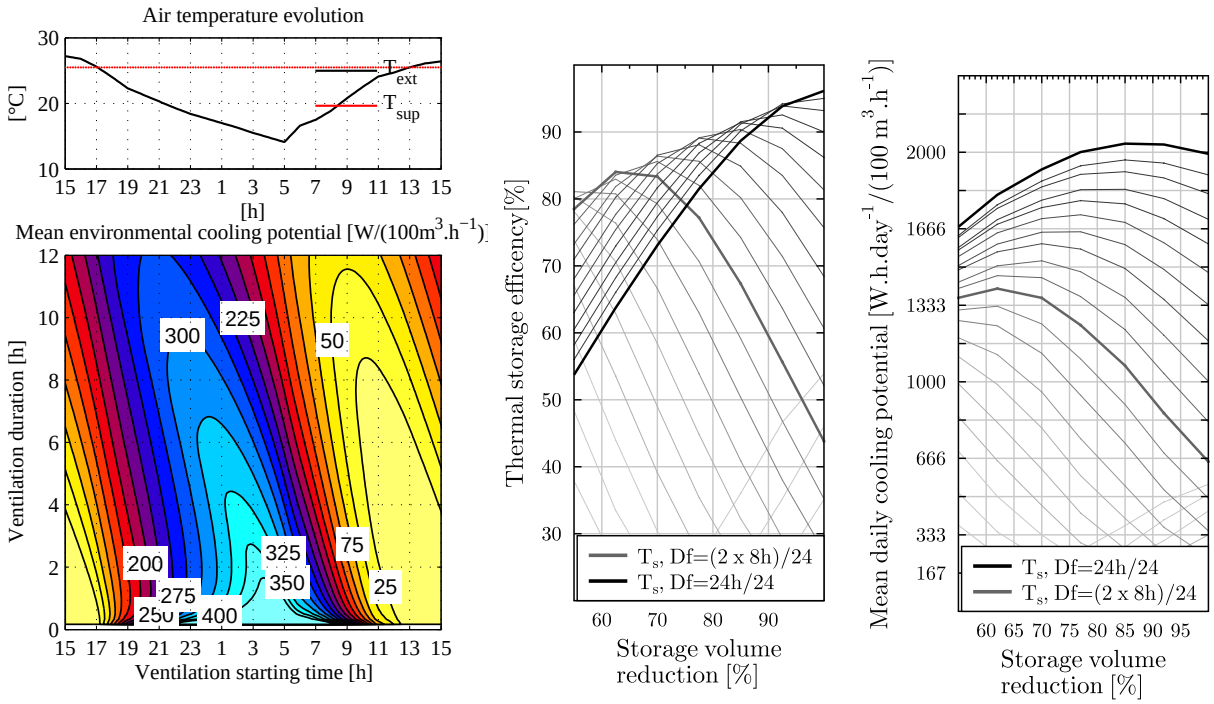

(a) *Typical daily environmental cooling potential, 5 August Marseille.*

(b) *Thermal storage efficiently of system.*

(c) *Calculation of the mean daily cooling load for a period of 4 days (30 June to 02 July 2010).*

Figure 3: *Environmental cooling potential, thermal efficiency and mean daily cooling load.*

the optimised system is reduced by about 29%. Nevertheless, intermittent functioning presents several advantages: the system is more compact, the energy consumption is reduced (less loss of pressure and shorter ventilation periods) and cold supplied by the system could be adapted to the cooling needs of the building.

EXAMPLES OF INTERGRATION

We propose to apply the system to the wood-framed building of the experimental platform INCAS (FIGURE 4) of the French National Institute of Solar Energy. This is a two-storey building with insulation ranging from 20*cm* (slab and vertical wall) to 40*cm* for the ceiling. Overhang size and south windows surfaces have been optimized to reduce heating consumption and heat gain during summer.

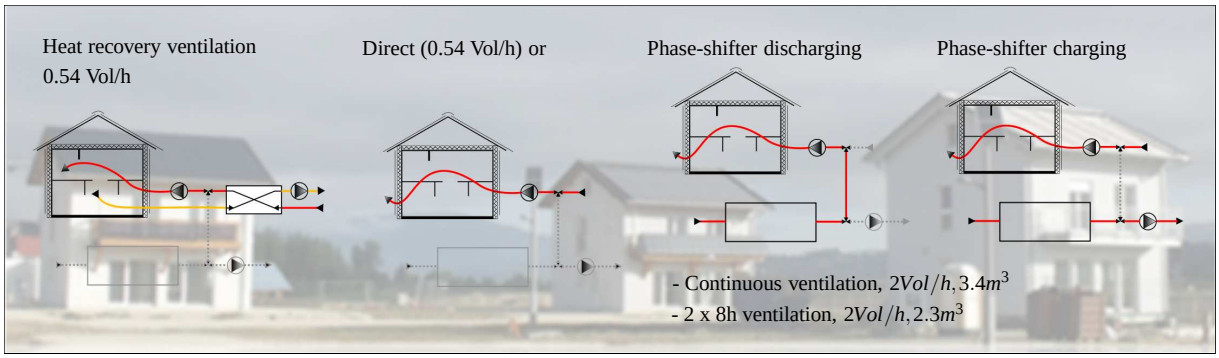

Figure 4: *Integration into the building ventilation system and INCAS Building experimental platform.*

We plan to test two thermal phase-shifting systems that deliver an air-flow rate of up to $2vol.h^{-1}$.

One is continually ventilated and requires $3.4m^3$ of storage material while the other ventilates $8h$ at night and $8h$ during the day and requires $2.3m^3$ of storage material. The analysis concerns the overheating duration and temperature change for a summer period. The latter system was compared with a wooden structure and with an externally insulated concrete structure which was not fitted with the system. The features common to these four configurations are: the Chambery meteorological data set, a direct night ventilation of $4vol.h^{-1}$ (period from 20 : 00 to 09 : 00), internal gains corresponding to those of a family of 4 people and a free floating summertime temperature. The airflow into the building is controlled via an algorithm which selects the best strategy in order to have the lowest temperature at the inlet. The different ventilation modes are presented in FIGURE 4. Simulations over the year were carried out with SimSpark in two steps. First, the storage system was pre-simulated and then the building response was simulated using system output as input for building ventilation. Building temperatures for each configuration are presented in FIGURE 5a and overheating duration for the year in FIGURE 5b. Our conclusions are as follows:

- Without the system, a low inertia building is subject to higher temperature swings than a more massive building. The number of hours when the temperature is over 27^oC is negligible in massive construction whereas it approaches $500h$ in low inertia buildings.
- The behaviour of the low-inertia building coupled to a phase-shifting system is similar to the high-inertia building.
- Considering cumulated temperatures higher than 27^oC, the distribution provided by the intermittent system is identical to that of the continuously ventilated system and contributes to a 38% reduction in electricity consumption and a 30% reduction in the size of the system.

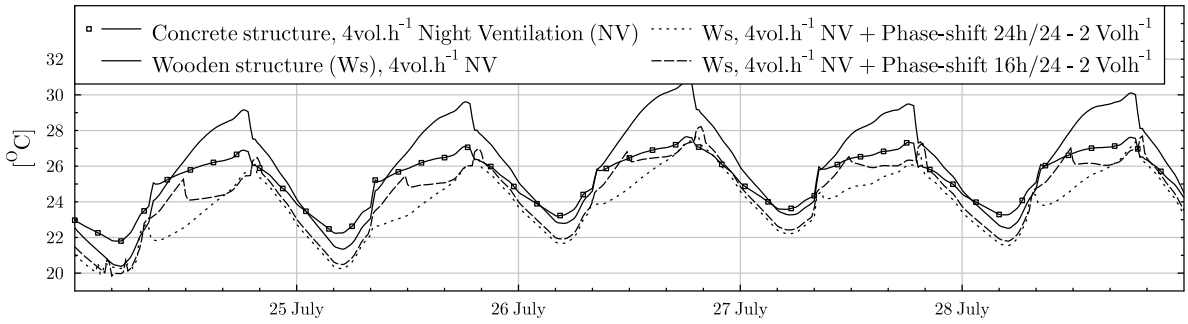

(a) *Internal temperature evolution during summer.*

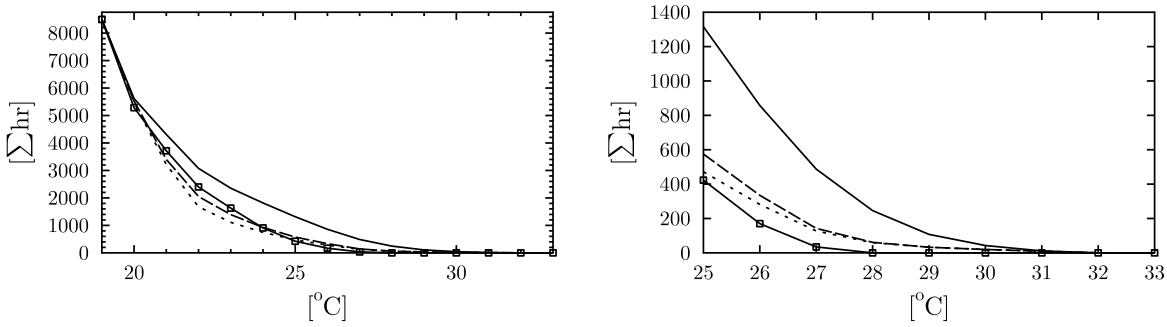

(b) *Overheating cumulated temperatures on a year simulation, overview and zoom on temperature higher than* 25^oC.

Figure 5: *Simulation results.*

To conclude, the thermal phase-shifter system significantly improves the summer thermal comfort of the low inertia building. Indeed, thanks to the adoption of the phase-shifter for ventilation (weighing $340 + 30kg.m^{-2}$), its performance is not so different from the one made of concrete (weighing $1300kg.m^{-2}$). Our proposition consists in limiting the use of the system to periods when environmental

potential and building cooling needs are at a maximum, which permits a considerable reduction (more than 30%) in the size and in the electricity consumption of the system.

ACKNOWLEDGEMENTS

This research was possible thanks to the contribution from the French Environment and Energy Management Energy Agency (ADEME) and the Scientific and Technical Centre for Building (CSTB).

References

[1] Adrien Brun. *Amélioration du confort d'été dans des bâtiments à ossature par ventilation de l'enveloppe et stockage thermique*. PhD thesis, Université de Grenoble, 2011.

[2] Pierre Hollmuller. *Utilisation des échangeurs air/sol pour le chauffage et le rafraîchissement des bâtiments*. PhD thesis, Université de Genève, 2002.

[3] Pierre Hollmuller, Peter Gallinelli, Bernard Lachal, and Willi Weber. Extensive sensitivity analysis of diverse ventilation cooling techniques for a typical administrative building in mid-european climate. In *Eurosun, 1st International Conference on Solar Heating, Cooling and Buildings*, 2008.

[4] Pierre Hollmuller, Bernard Lachal, and Jean-Marc Zgraggen. Phase-shifted ventilation, a new thermal storage technique for passive cooling of buildings: theoretical and experimental characterization. *Applied Energy (in review)*.

[5] Pierre Hollmuller, Bernard Lachal, and Jean-Marc Zgraggen. A new ventilation and thermal storage technique for passive cooling of buildings : thermal phase-shifting. In *PLEA*, 2006.

[6] Lawrence Berkeley National Laboratory. *SPARK 2.0 Reference Manual : Simulation problem analysis and research kernel*, 2000.

[7] M.Ordenes F.Westphal P Hollmuller, J Carlo and R.Lamberts. Potential of buried pipes systems and derived techniques for passive cooling of buildings in brazilian climates. In *Proceedings of the 10th International Building Performance Simulation Association Conference*, 2007.

[8] T.E.W. Schumann. Heat transfer: A liquid flowing through a porous prism. *Journal of the Franklin Institute*, 208(3):405 – 416, 1929.

[9] Jean-Marc Zgraggen. Etude d'un lit de shères pour le déphasage d'une onde thermique. Master's thesis, Université de Genève, 2003.

Daylighting and Electric Lighting

LIMITS AND POTENTIALS OF DIFFERENT DAYLIGHTING DESIGN APPROACHES BASED ON DYNAMIC SIMULATIONS

A. Pellegrino[1]; V.R.M. Lo Verso[1]; S. Cammarano[1]

1: Politecnico di Torino, Department of Energetics, TEBE Research Group, Turin, Italy

ABSTRACT

This paper presents the results of some daylighting design applications which were developed within courses and works of theses carried out at the Faculty of Architecture of the Politecnico di Torino. Different approaches were used depending on the characteristics and aims of the analyzed case-study: in particular physical models under a sun simulator facility and numerical tools such as Daysim and Lightsolve. Final goal of the paper is to show potentials and limits concerned with each approach in usefully analyzing and representing the results of a lighting analysis from a designer's point of view and in which stage of the design process its application is more appropriate.

1. INTRODUCTION

During the last decade a number of new metrics and numerical simulation tools have been developed and made available, which allowed passing from a static to a dynamic building modelling. The so-called Dynamic Daylight Performance Metrics DDPM [1] are parameters able to account for the dynamic variation of skylight and sunlight conditions during the course of the year as a function of the specific climate conditions of a site and of the orientation of the considered building. Although the higher level of advance in dynamically analyzing the overall performances of daylit spaces, current daylighting design practice still favors prior experiences and rules of thumbs during schematic design and largely relies on the daylight factor [2]. More over a methodological guideline for applying a dynamic daylighting design approach has not been standardized yet. Most of daylighting design tools presently available are based on Radiance, with the result that expert users are often needed to carry out simulations. As a result, designers still have troubles to adopt a dynamic approach since the early design stages and throughout the whole design process. In the following sections, some case-studies of architectural designs where daylighting was considered as one of the key design factors are presented together with a discussion of how the dynamic approach was addressed during each design stage through different design tools.

2. DAYLIGHTING DYNAMIC DESIGN APPROACHES IN ARCHITECTURAL DESIGN

The presented case-studies are concerned with redesigning a no longer used industrial building to be converted into a public library: this is a type of building for which daylight plays a crucial role with regard to both the visual tasks users have to carry out and their perception of visual comfort conditions. The existing building is characterized by large open-plan spaces which are both sidelit and toplit through large clerestory windows (figure 1). Two projects in particular are described in detail: these were both aimed at optimizing daylighting conditions within the redesigned building through a dynamic design approach, but different procedures and tools were used. Furthermore, different design concepts were assumed: in the first case, a 'conservative' approach was chosen, aimed at keeping the shape and the structure of the existing building, whilst in the second case the whole structure and the roof were completely redesigned. As a result, a totally new building was conceived.

Figure 1: Design site and images of the existing building

2.1 'Conservative' project

The design concept was based on taking advantage of the large open-plan toplit spaces the building offers. For this purpose, a dynamic daylighting design approach was adopted, consisting of the following phases:

1. analysis of direct sunlight penetration for some representative days and hours throughout the year (December 21st from 9 to 16, March 21st from 7 to 18, June 21st from 8 to 20), aimed at visualizing areas where glare/overheating problems due to sunlight might occur;
2. definition of spaces lay-out and first hypothesis for daylighting systems;
3. verification of resulting daylight availability through a Climate-Based Daylight Modeling, CBDM [3], and critical analysis of obtained values of Dynamic Daylight Performance Metrics, DDPM [1];
4. further analysis of direct sunlight penetration to better investigate the contribution of sunlight to DDPM values and to identify time-steps during the year with potential thermal/visual discomfort problems;
5. identification of solutions to correct problems which were observed, based on modifying daylighting systems' properties and on designing specific shading systems;
6. further analysis of daylighting results to verify the efficacy of defined daylighting and shading systems.

Different design tools were used throughout the design stages to achieve above design goals. For the analysis of direct sunlight penetration a 1:100 scale model under the sun simulator available at Politecnico di Torino was used: for each aisle of the building the images of direct sunlight penetration corresponding to different hours of the day and days of the year were superimposed, so as to identify which parts of the floor area may suffer from glare or overheating during the year due to direct sunlight (figure 2a). Architectural strategies in terms of space lay-out and transparent/opaque materials were set based on this analysis (figure 2b shows an example relative to the reading room). The resulting overall annual daylight availability was then verified through a CBDM by means of Daysim 2.1, a Radiance-based software which allows running a climate-based annual simulation (with a time-step down to 5 minutes) and provides with values of the Daylight Factor (DF), and of DDPM based on a user-defined occupancy profile and target illuminance. The results found for the reading room are shown in figure 2c: the average Daylight Factor over the room met the value prescribed by Italian standards (DF_{mean}>3%) but a non-uniform distribution of illuminances was highlighted. The average $UDI_{achieved}$ over the room yielded a high level for most of the reading area. Beside this, values of Maximum Daylight Autonomy over 5% were observed, which suggests a possible occurrence of direct sunlight or other potentially glary conditions [4]. It is important to stress out that DDPM values provide a synthesis of daylighting conditions occurring during a time interval: thanks to this synthesis, they can result useful to identify areas with good daylight potentials as well as areas with potential problems. On the other hand it's not possible to identify if sunlight or diffuse skylight is responsible of the obtained DDPM and for which time-step critic conditions appear. For this purpose, a further set of analyses of direct sunlight penetration was specifically carried out by using a virtual model in

Ecotect with the aim of detecting specific time-steps during the year with potential thermal/visual discomfort problems. Based on this analysis, new design solutions were defined: in particular, movable shading devices and opaque partitions plus fritted glazing were adopted respectively for the skylight clerestory windows and the west-facing windows to reduce sunlight penetration within the reading area. The resulting daylight availability was then calculated through Radiance simulations so as to verify the illuminance distribution within the space for specific time-steps identified through earlier sunlight analysis with Ecotect and for which movable shading devices resulted to be necessary. In this phase, Radiance was used as Daysim doesn't allow running a simulation for a period of time other then the full year and to simulate specifically designed movable shadings.

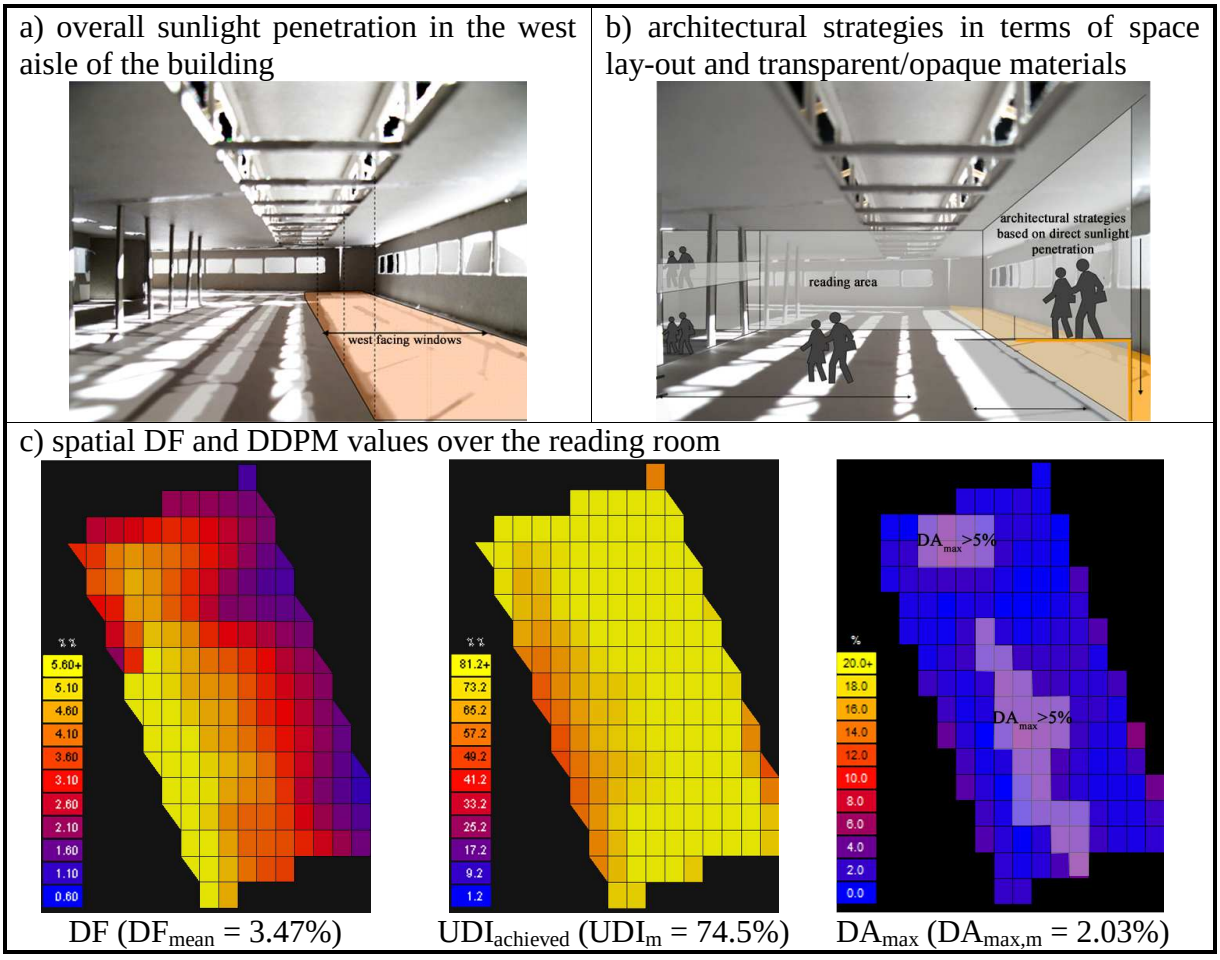

Figure 2: Results of the analyses carried out for the case of the 'conservative' project.

2.2 Design of a new building

The concept of the project was to design a new building with a public terrace on the roof for users of the library. As a consequence, the existing roof, with zenithal daylighting system, was completely redesigned. On this first design hypothesis a dynamic daylighting analysis was carried out to verify the annual daylight availability, and results were used to correct the preliminary project in order to optimize daylighting condition with respect to visual comfort. Unlike the previous example, in this case a single tool was used to study the interaction between daylight and the building, and the analysis was reiterated, modifying different building features such as internal partitions, openings dimension, shape and characteristics, until a satisfactory solution was achieved. The tool adopted for the lighting analysis is Lightsolve, a software developed by the M.I.T. Daylighting Lab, Department of Architecture,

Building Technology Program [5,6] whose aim is to support the daylighting design process using a goal-based approach. The tool proposed is a quickly calculating annual data sets for which temporal maps and spatial renderings are the graphical outputs. For user-defined illuminance thresholds, the temporal maps gives an outcome with different colors, based on the portions of the results that meet, overstep or don't reach the goals set by user. The annual data set is simplified splitting the year into 8 periods of similar season and 7 daily moments.

The first step of the daylighting design approach was to create a 3D model of the building and of the outdoor context using Sketch-up. The model was simplified as much as possible, taking care of reproducing all the building elements influencing daylight penetration while simplifying all other details. After preparing the 3D model a simulation with Lightsolve was carried out to evaluate both direct sunlight penetration and global illuminance in different building areas where daylighting was of particular importance, in some case for the need of maximizing its availability in other case for the need of reducing it (reading areas, conference room, multimedia areas, etc.). Results obtained from the first simulation for some representative areas are presented in figure 3a. Illuminance temporal maps pointed out an excessive amount of daylight in the reading areas compared to the designer illuminance requirements. Furthermore, as shown by internal renderings, direct solar radiation, penetrating through skylights and vertical east-facing windows, interested the reading area during most hours of the day and months of the year with high probability of glare and summer overheating occurrence. A number of changes were applied to the initial project on the basis of the daylighting results and new Lightsolve simulation were run until satisfactory results in terms of sunlight protection and daylight availability were achieved for the whole year and for the different library areas. In figure 3b the final solution and the corresponding daylighting results for the previously presented library areas are reported.

3. RESULTS

Applying a dynamic daylighting approach to the case-studies described earlier showed some main potentials and limits concerned with the design tools which were adopted, especially with regards to the different stages of the design process.
With regard to the *early daylighting design stage*, in the case of the 'conservative' project, an analysis of sunlight penetration into the building was carried out with a scale model under a sun simulator. This offered the advantage of a direct visualization of sun patches, but on the other hand evaluations were limited to a number of time-steps and days throughout the year, since an overall annual simulation would have been time-consuming. Furthermore, the analysis was qualitative, limited to the direct sunlight component only, thus without accounting for diffuse skylight, with a consequent lack of quantitative results. This implied to proceed to more detailed, software based, analysis to have an exhaustive description of dynamic daylight availability in indoor spaces. In the second case instead, the early daylighting design stage was addressed through Lightsolve. This produced fast climate-based annual analyses with reasonably comprehensive outputs, hence allowing the design team comparing different design solutions. Available outputs consisted of both quantitative and qualitative data, in terms of temporal maps of illuminances and spatial renderings. The temporal maps display the dynamic variation of illuminances averaged over the space: as a result, no quantitative information is given about the illuminance spatial distribution. This can be qualitatively assessed through rendered images. Moreover, the possibility for users to set the illuminance requirements offers a consistency with the objectives of daylighting design for the specific building usage. On the other hand, main drawbacks appeared to be concerned with some difficulties in setting up the model consistently (Lightsolve can hardly handle increased model complexities) and with the limited number of time-steps the program assumes to run the annual simulation.

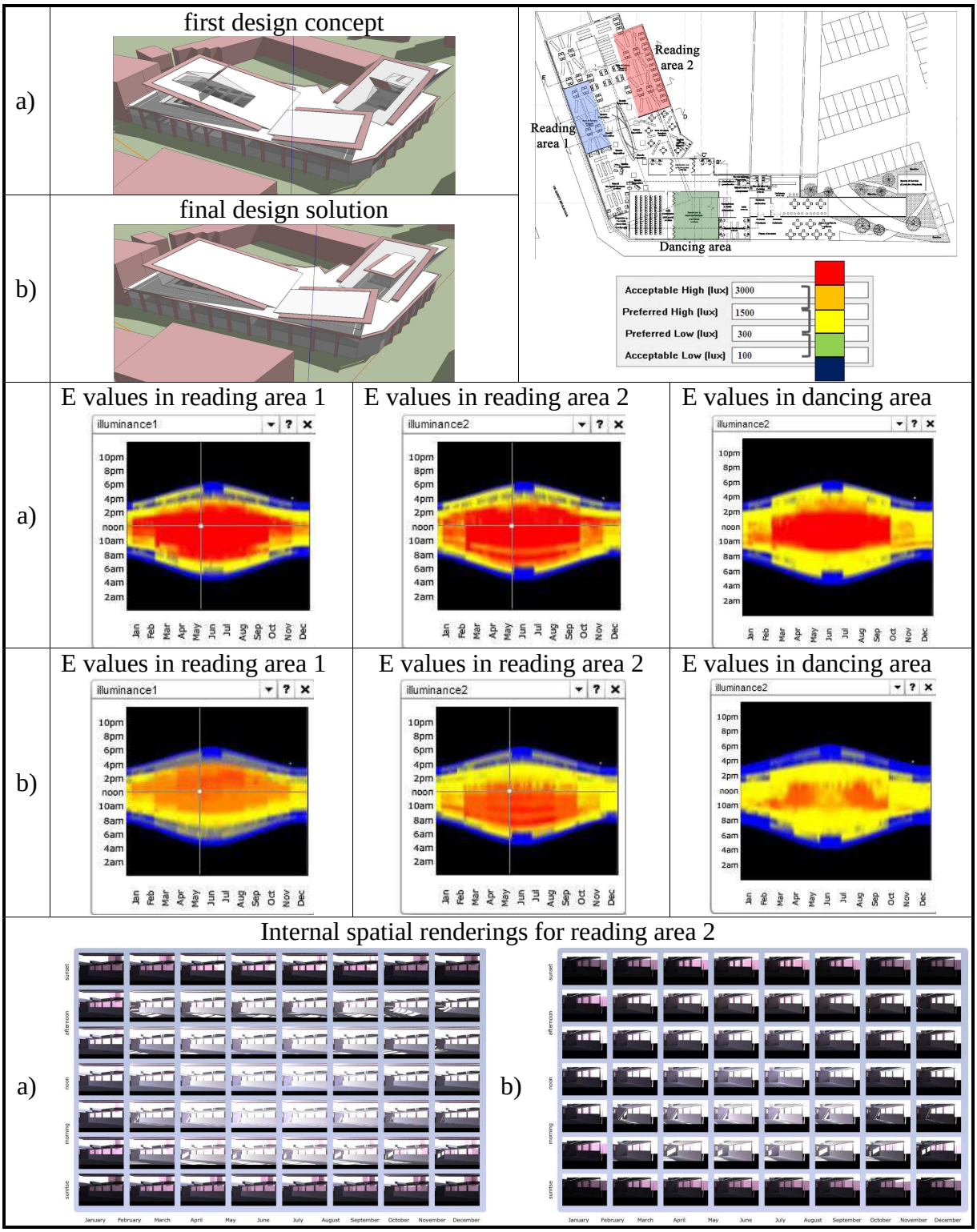

Figure 3: Lightsolve results referred to some of analyzed areas: first design concept (a) and final design solution (b)

In short, Lightsolve proved to be effective in assessing the dynamic annual daylight availability in the early design stage, whilst it appears to be somewhat limited to address a detailed annual analysis, in presence of complex daylighting systems (i.e. movable shadings).

As far as the *more advanced design stages* are concerned, these were addressed for the case of the 'conservative' project only, mainly through Daysim. This allowed running detailed annual

simulations taking advantage of short time-steps users can set (down to 5 minutes). The results available for the design team consist of a set of metrics which synthesize the daylight availability throughout the year, including potential occurrence of glary conditions. It is possible to observe the spatial distribution of daylight within a space, but it is not possible to identify the daylight levels which are available for desired time-steps. Other limits seem to be concerned with the impossibility for users to define the illuminance thresholds to which refer the UDI or the DA_{max} calculation and with long simulation times in presence of complex models. Furthermore, being a Radiance based calculation tool, it requires expertise on how to set the calculation parameters with respect to the desired results accuracy.

It is worth noticing that in the case of the design of a new building, the design team did not proceed to a 'detailed' daylighting design, as the information provided by Lightsolve during the early design stage was considered sufficient to prove the efficacy of the design solutions.

4. CONCLUSIONS

Addressing a daylighting design through a dynamic approach allows assessing daylight availability within a space with higher accuracy than an analysis based on the daylight factor only, in terms of both determining quantity and quality of daylight and of verifying potential visual and thermal discomfort problems due to direct sunlight penetrating into a room. A dynamic approach allows a more conscious architectural design which is integrated with the design site and its climate conditions, also accounting for the effect of the orientation. Nevertheless, it should be noted that, while the dynamic daylighting design approach is becoming more and more diffuse within the scientific community, it still results hard to be correctly understood and applied by the designers. Certainly as long as building standards and rating scheme have generally remained on static approach designers are not involved to move towards more advanced daylighting analysis [2]. Consequently, a more widespread knowledge of a dynamic daylighting approach is desirable to make accessible to practitioners.

ACKNOWLEDGEMENTS

Work carried out within the research program 'Daylighting design for energy saving and visual comfort purposes: climate-based daylight modeling, glare indices and integrated ventilation system performances' (http://www.polito.it/tebe). Projects developed respectively by Chiara Tamburini e Abel Silva Lizcano.

REFERENCES

1. Reinhart, CF, Mardaljevic, J, Rogers, Z: Dynamic daylight performance metrics for sustainable building design. Leukos, 3 (1), pp.1-25, 2006.
2. Reinhart, CF, Wienold, J: The daylighting dashboard – A simulation-based design analysis for daylit spaces. Building and Environment. 46(2), pp. 386-396, 2011.
3. CIE Division 3: Reportership R3-26. Climate-based daylight analysis. Vienna, 2008.
4. Rogers, Z: Daylighting Metric Development using Daylight Autonomy calculations in the Sensor Placement Optimization Tool: development report and case studies. Boulder, Colorado, USA: Architectural Energy Corporation, 2006. http://www.archenergy.com/SPOT/download.html (last retrieved: May 2011).
5. Andersen, M, Kleindienst, S, Yi, L, Lee, J, Bodart, M, Cutler, B: An intuitive daylighting performance analysis and optimization approach. Building Research and Information. 36 (6), pp. 593-607, 2008.
6. Kleindienst, S, Bodart, M, Andersen, M: Graphical representation of climate-based daylight performance to support architectural design. Leukos, 5 (1), pp. 39-61, 2008.

SUSTAINABLE LIGHTING: MORE THAN JUST LUMENS PER WATT

Mariana G. Figueiro, PhD and Mark S. Rea, PhD

Lighting Research Center, Rensselaer Polytechnic Institute, Troy, USA, figuem@rpi.edu

ABSTRACT

Patterns of light and dark in today's built environment are often inconsistent with the natural 24-hour rhythm of sunset and sunrise. Light exposures in buildings, with or without windows, may be low enough to induce "circadian darkness" during the day, but some sources of electric light in the evening may be bright enough to prolong daytime into the night. Weak or irregular light-dark patterns can induce circadian disruption, which, in turn, can have a negative effect on our health and well-being. In fact, recent studies using animal models showed that circadian disruption by irregular light/dark patterns are associated with increased mortality, higher risks for developing diabetes, obesity, cardiovascular disease, and even cancer [1].

Sustainable buildings must be able to minimize wasted energy while maximizing human benefits. Light obviously should be provided to occupants of sustainable buildings to see well, but light should also be provided to minimize circadian disruption. Exposure to weak or irregular light/dark patterns may be particularly prevalent in modern offices and schools. Because humans spend so much time indoors, we may be inadvertently creating "architectural jet lag" in our buildings that may result in chronic conditions such as sleep disorders and reduced performance.

Discussed here are laboratory and field studies investigating the impact of light and daylight on biomarkers and performance. In the field studies, which were performed in schools with teenagers, we examined how restriction of circadian-effective light exposures impacted dim light melatonin onset (DLMO), a marker of circadian time [2-4]. Since a regular, 24-hour pattern of light and dark appears essential for human health, the measurement of light as it affects circadian rhythms is at the very core of creating sustainable buildings. In these field studies, students wore a circadian light dosimeter, the Daysimeter, which measured actual circadian light exposures for the study weeks [5, 6].

In the laboratory studies, we investigated the impact of daylight exposure as well as intermittent blue light exposure on performance and feelings of sleepiness. Subjects were kept awake for 26 hours and performance was measured every 4 hours. Subjects either remained in a dimly illuminated room or sat in front of a window all day. During the performance tests, they were exposed to 40 lux of 470-nm (blue) light, which has been shown to increase alertness at night. Results suggest that nighttime performance is improved by light compared to darkness but that daylight exposure did not have a differential impact on performance compared to daytime darkness.

In summary, to help minimize sleep restriction and circadian disruption, and thereby increase human performance, health, and well-being, sustainable buildings should provide users with high levels of morning light and low levels of evening light. The present results demonstrate that, in both laboratory and real-life environments, light can impact humans in important ways that go beyond recommended levels of illumination based upon seeing. Therefore, sustainable buildings should be about more than lumens per watt.

BACKGROUND

Sustainable buildings should be able to minimize wasted energy while maximizing human benefits. The daylighting of buildings is often associated with sustainability and is seen as a technique for increasing energy efficiency. For daylighting to be a successful energy-saving technique, sophisticated lighting control systems must be used where the photoelectric control system is adaptable to local architectural elements, building orientation, seasons, and most of all, occupant preferences. Therefore, even though daylighting *can* save energy and expenses, implementing successful daylighting techniques is neither trivial nor common.

With regard to maximizing human benefit in sustainable buildings, it is often argued that daylight improves worker productivity. Although there is a wealth of studies showing that people *like* daylight, there is no compelling evidence that daylighting actually improves human performance [7-11]. Light can potentially affect human performance through three pathways: the visual system, the perceptual system, and the circadian system [2]. Lighting characteristics for stimulating the visual system is well understood and there is no reason to believe that daylight is a special light source to improve vision and, thus, improve performance through the visual system. Studies that have tried to show a reliable relationship between daylight and improved psychological well-being and, thus, improved performance through the perceptual system, have been consistently unsuccessful. Models that predict how light affects behaviour through the circadian system have not been developed; however, an understanding of how lighting characteristics affect the circadian system has been developed [12].

Daylight is an ideal light source for the circadian system. Thus, it is reasonable to pursue the hypothesis that daylight might improve performance through the circadian system. The human circadian system regulates the timing of all behavioral, physiological and cellular activities to a 24-hour cycle on Earth. The sleep-wake cycle is perhaps the most commonly observed circadian rhythm, but performance, digestion, hormone production, and cellular DNA repair also follow a regular 24-hour pattern. Light is the most important regulator of timing of circadian rhythms, and people across the entire surface of the Earth are able to coordinate their circadian cycles to the local times of sunrise and sunset.

Although light must enter the eye to stimulate both the visual and the circadian systems, the biophysics of activation for the two systems is quite different. In particular, the circadian system has a much higher threshold to light activation and is more sensitive to short-wavelength (blue) light than the visual system used for reading. Most importantly, it is differentially sensitive to the time when the light is presented to the retina; light incident on the retina in the morning will advance the circadian clock, whereas light in the late evening will delay it [13]. Exposure to weak or irregular light/dark patterns may pose an increased risk for circadian system disruption. Therefore, daylight through windows or skylights would seem to be an ideal source of light for circadian entrainment during the daytime, and could be particularly important in offices and schools where occupants have limited access to the outdoors. Often, however, access to sufficient levels of daylight for circadian entrainment are not available to building occupants, either because their activities are remote from windows or skylights or because occupants use window shading for visual comfort. This limited access to daylight may result in what we call “architectural jet lag,” with all the associated maladies of ordinary jet lag, such as poor sleep and digestion. Potentially more serious maladies may occur from circadian disruption, such as breast cancer [14].

Discussed here are one laboratory and two field studies investigating the impact of light and daylight on biomarkers and performance. In the field studies, which were performed in schools, we examined how restriction of short-wavelength, circadian light exposure in teenagers impacted performance and dim light melatonin onset (DLMO), a marker of circadian time

[2-4]. In both studies, students wore a circadian light dosimeter, the Daysimeter [5], which measured their personal circadian light exposures. In the laboratory study, we examined the acute effect of exposure to daylight as well as intermittent blue light exposures on performance.

METHODS AND RESULTS – FIELD STUDIES

In the first phase of the first field study we examined how restriction of short-wavelength, circadian-effective light impacted evening DLMO [2]. This field study was conducted at a middle school in North Carolina with unusually high levels of daylight in the classrooms. After 11 teenage subjects wore special orange glasses in the morning to remove short-wavelength, circadian light for five consecutive school days, their DLMO was delayed by about 30 minutes relative to the previous week when they did not wear the orange glasses. During the second week, when Daysimeter data were collected, the Daysimeter sensors were equipped with the same orange filter. Figure 1 shows the spectral transmittance of the glasses and Figure 2 shows the cumulative frequencies of the DLMO times the week before and the week after students wore the orange glasses. The orange glasses allowed them to see well enough to perform their visual tasks, but their circadian pacemaker was not receiving enough stimulation in the morning to advance its period.

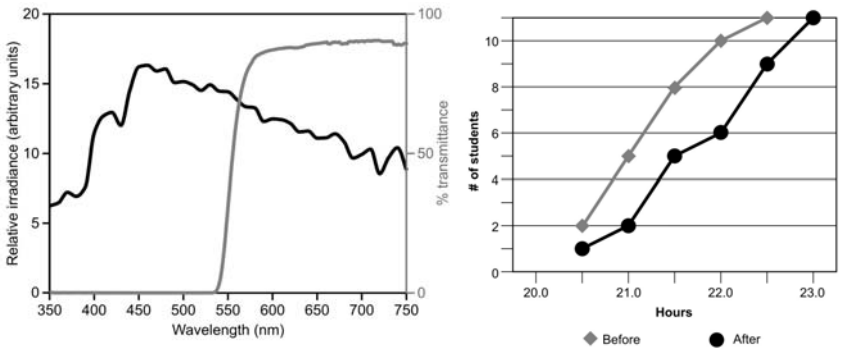

Figure 1 (left): The spectral irradiance distribution of a phase of daylight (6500 K) and the spectral transmittance of the orange glasses. Short wavelengths below approximately 540 nm are removed.

Figure 2 (right): Cumulative frequencies of DLMO times before and after students wore the orange glasses.

In the second phase of the study, 22 students participated in a 5-day field study conducted at the same North Carolina middle school [4]. Half of the students studied (n = 11) wore the orange glasses that removed short-wavelength, circadian light for five consecutive days, while the other half did not. Again, the Daysimeter was equipped with the orange filter for those students who wore the orange glasses. DLMO times were significantly delayed (approximately 30 minutes) for those students who wore orange glasses compared to the control group. Sleep durations were slightly, but not significantly, curtailed in the orange-glasses group.

In the second field study, DLMO was measured for 16 teenage students attending an upstate New York school one winter evening and one spring evening. Circadian light exposures in the evening were significantly greater in the spring than in the winter (Figure 3) and DLMO was delayed by about 20 minutes in the spring relative to that in winter (Figure 4). Sleep onset was also significantly delayed in the spring by about 16 minutes relative to that in the winter [3]. The delays in DLMO and in sleep onset shown in the studies were consistent with the measured differential circadian light exposures. Namely, restricting circadian light exposure in the morning and extending it in the evening can delay evening DLMO and sleep onset.

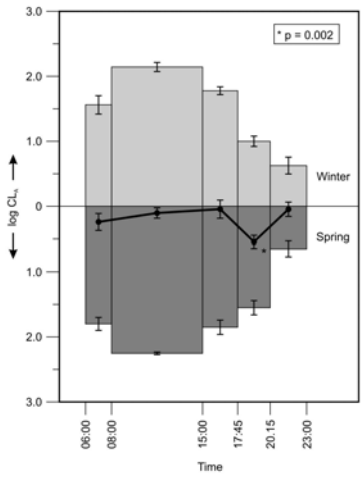

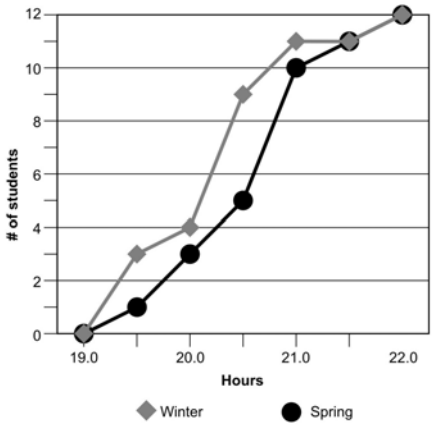

Figure 3 (left): Circadian light exposures (CL_A) in the evening were significantly greater in the spring than in the winter.

Figure 4 (right): Cumulative frequencies showing the number of students who reached DLMO between 19.0 and 22.0 hours. DLMO was delayed by about 20 minutes in the spring relative to the winter.

METHODS AND RESULTS – LABORATORY STUDY

Eight subjects, (2 females) participated in a 3-session, within-subjects study without sleep. Each session was separated by at least one week. Each 26-hour session began at 07:00 and concluded at 09:00 the following day. During the control session, subjects remained in continuous dim ambient light (< 3 lux) for 26 hours. For the other two sessions, conducted 7 months apart, the same lighting conditions were experienced by subjects. During these two sessions subjects were exposed to daylight and to 40 lux of 470-nm (blue) light for one hour every four hours starting at 08:00. During all three sessions subjects were seated at desks facing a window that was either covered or not with opaque black-out shades to occlude the natural daylight. During the blue-light exposure periods, performance was measured on the Multi-Attribute Task Battery (MAT) for Human Operator Workload and Strategic Behavior Research software program (NASA COSMIC collection, Open Channel Foundation). The 54-minute MAT Battery was comprised of (i) a monitoring task, (ii) a tracking task, (iii) a communication task, and (iv) a resource management task. Subjects were also asked to fill out the Karolinska Sleepiness Scale (KSS), a 9-point scale used to assess their subjective sleepiness; higher values of KSS indicate that subjects felt sleepier.

Figure 5 shows the KSS and tracking data for the three sessions. The KSS data represent the average responses from all eight subjects. For the tracking task, subjects used a joystick to maintain a moving circle on a fixed target presented at the center of a computer-generated display. Average deviation distances of the circle from the target for one minute were recorded. The root mean square (RMS) data from all eight subjects represent the one-minute average pixel deviations from the central target over six nine-minute epochs (i.e., over 54 minutes); higher values of the RMS deviations indicate poorer performance.

As shown in Figure 5, the rate of deterioration in self-reports of sleepiness and of performance becomes faster at normal sleep time. This deterioration probably reflects the physiological transition between the time for daytime wakefulness to the time for nighttime sleep [15]. The results also indicate that the rate of deterioration of self-reports of sleepiness is greater than the rate of deterioration of performance across 26-hours of wakefulness, suggesting that feelings of sleepiness can be overcome to improve performance. The exposure to daylight did not affect performance nor did it affect subjective sleepiness relative to continuous

dim ambient light exposure. Not only is this true during the daytime, but it is also true at night, indicating that there is no carryover effect of daylight into nighttime hours. Blue light exposure at night reduced subjective sleepiness and increased performance, but not during the day. It should be added that these results are for subjects who slept the night before and whose circadian systems were entrained to a regular light-dark cycle.

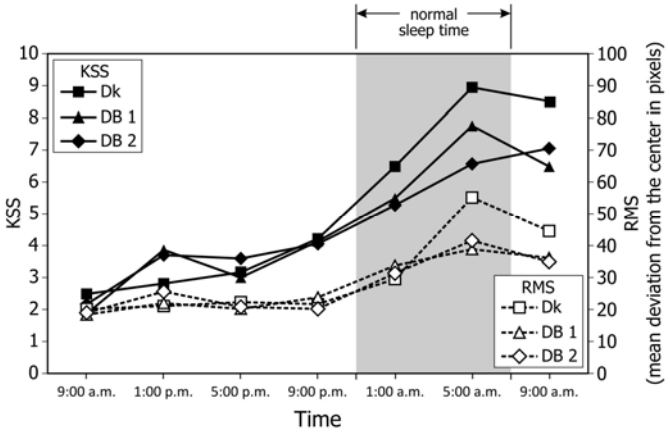

Figure 5: *Self-reports of sleepiness and performance for 26 hours; subjects were continuously awake during each of three sessions. The Karolinska Sleepiness Scale (KSS) was used to measure subjective sleepiness (solid symbols); higher values indicate greater feelings of sleepiness. Performance was measured using a computer-screen tracking task; larger root mean square (RMS) deviations between the circle and the target indicate higher tracking errors (open symbols). For one session subjects were in continuous dim ambient light (Dk). For the other two sessions (DB1 and DB2) subjects were exposed to 40 lux of blue light at the cornea for one hour every four hours and sat in front of an uncovered, west-facing window at all other times.*

DISCUSSION

Daylighting is often associated with sustainable buildings. The results presented here suggest that daylighting is important for maintaining our circadian rhythms, sleep and well-being, but that it has little if any effect on tracking performance and feelings of fatigue in the daytime, or later that night, despite some reports that daytime light exposures increase performance and alertness [15, 16, 17].

The field data presented here suggest, consistent with our collective understanding of the circadian system, that morning light can set and synchronize our circadian clocks to a common time. In situations where a strict schedule is necessary, as it is for school, restricting our evening light may be just as important for maintaining an entrained circadian clock. This has implications for modern electric display devices such as computers and tablets, which are often used late into the night [18]. In the laboratory study, blue light at night, known to be sufficient to suppress the nocturnal hormone melatonin [19], improved performance and feelings of sleepiness, suggesting that during normal sleep times light can have a positive alerting effect. Unpublished data from another study by the Lighting Research Center (LRC) suggest that red light exposures at night, ineffective for suppressing melatonin, has comparable effects on performance as blue light exposures. From a still different study, it was shown that caffeine has comparable effects on performance as blue light exposures at night. The long-term consequences of blue light exposure at night exposure (or caffeine) may, however, have untold consequences to health and well-being. Future research is aimed at understating how other colors of light impact acute performance and sleepiness as well as circadian disruption and health [15, 19, 20].

Acknowledgements: These studies were funded by the US Green Buildings Council, the Trans-National Institutes of Health Genes, Environment, and Health Initiative, and the National Science Foundation.

REFERENCES

1. Stevens, R. G., Blask, D. E., Brainard, G. C., et al.: Meeting report: The role of environmental lighting and circadian disruption in cancer and other diseases. Environmental Health Perspectives, Vol 115, pp 1357-1362, 2007.
2. Figueiro, M. G., Rea, M. S.: Lack of short-wavelength light during the school day delays dim light melatonin onset (DLMO) in middle school students. Neuroendocrinology Letters, Vol 31, No. 1, 2010.
3. Figueiro, M. G. Rea, M. S.: Evening daylight may cause adolescents to sleep less in spring than in winter. Chronobiology International, Vol 27, No. 6, pp 1242-1258, 2010.
4. Figueiro, M. G., Brons, J., Plitnick, B., Donlan, B., Leslie, R., Rea, M. S.: Measuring circadian light and its impact on adolescents. Lighting Research & Technology, 2010.
5. Bierman, A., Klein, T. R., Rea, M. S.: The Daysimeter: A device for measuring optical radiation as a stimulus for the human circadian system. Measurement Science and Technology, Vol 16, pp 2292-2299, 2005.
6. Miller, D., Bierman, A., Figueiro, M. G., Schernhammer, E., Rea, M. S.: Ecological measurements of light exposure, activity, and circadian disruption in real-world environments. Lighting Research & Technology, Vol 42, pp 271-284, 2010.
7. Boyce, P. R.: Human Factors in Lighting, 2nd Edition. London; New York: Taylor & Francis, 2003.
8. Cuttle, C.: People and windows in workplaces. Proceedings of the People and Physical Environment Research Conference, Wellington, New Zealand, 1983.
9. Hopkinson, R. G., Kay, J. D.: The Lighting of Buildings. Frederick A. Praeger: New York and Washington D. C., 1969.
10. Heerwagen, J., and Heerwagen, D.: Lighting and psychological comfort. Lighting Design and Application, Vol 6, pp 47-51, 1986.
11. Leslie, R. P.: Capturing the daylight dividend in buildings: Why and how? Building and Environment, Vol 38, pp 381-385, 1986.
12. Boyce, P. R., Rea, M. S.: Lighting and Human Performance II: Beyond Visibility Models Toward a Unified Human Factors Approach to Performance, Electric Power Research Institute, Palo Alto, CA, National Electrical.
13. Rea, M. S., Figueiro, M. G., Bullough, J. D.: Circadian photobiology: An emerging framework for lighting practice and research. Lighting Research Technology, Vol 34, No. 3, pp 177-190, 2002.
14. Stevens, R. G., Rea, M. S.: Light in the built environment: Potential role of circadian disruption in endocrine disruption and breast cancer. Cancer Cause Control, Vol 12, No. 3, pp 279-287, 2001.
15. Figueiro, M. G., Rea, M.S.: Sleep opportunities and periodic light exposures: impact on biomarkers, performance and sleepiness. *Lighting Research and Technology*, in press,2011.
16. Vandewalle, G., Gais, S., Schabus, M., Balteau, E., Carrier, J., Darsaud, A., Sterpenich, V., Albout, G., Dijk, D. J., Maquet, P.: Wavelength-dependent modulation of brain responses to a working memory task by daytime light exposure. Cerebral Cortex, Vol 17, pp 2788-2795, 2007.
17. Phipps-Nelson, J., Redman, J. R., Dijk, D. J., Rajaratnam, S. M.: Daytime exposure to bright light, as compared to dim light, decreases sleepiness and improves psychomotor vigilance performance. Sleep, Vol 26, pp 695-700, 2003.
18. Figueiro, M. G., Wood, B., Plitnick, B., Rea, M. S.: The impact of light from computer monitors on melatonin levels in college students. Neuroendocrinology Letters, Vol 32, No. 2, 2011.
19. Figueiro, M. G., Rea, M. S.: The effect of red and blue lights on circadian variations in cortisol, alpha amylase, and melatonin. International Journal of Endocrinology, 2010.
20. Figueiro, M. G., Bierman, A., Plitnick, B., Rea, M. S.: Preliminary evidence that both blue and red light can induce alertness at night. BMC Neuroscience, Vol 10, 2009.

RAY-TRACING SIMULATION OF COMPLEX FENESTRATION SYSTEMS BASED ON DIGITALLY PROCESSED BTDF DATA

J. H. Kämpf[1]; J.-L. Scartezzini[1]

1: Solar Energy and Building Physics Laboratory (LESO-PB), Ecole Polytechnique Federale de Lausanne (EPFL), CH-1015 Lausanne, Switzerland

ABSTRACT

The implementation of Complex Fenestration Systems (CFS) in the day-to-day life by practitioners, such as lighting designers, architects and façade makers is not an easy task. However, computer design tools can reinforce their usage through the determination of the luminous properties of a building interior prior to its construction or refurbishment. This paper presents a methodology based upon computer daylighting simulations carried out with RADIANCE in which the *mkillum* procedure was improved in order to render the light distribution due to diffuse daylight and sunlight on the inner surface of a fenestration system by the way of BTDF data. For the sake of standardization, the BTDF data accepted as input may be formatted according to the course of IEA Task 31 "Daylighting in Buildings" (e.g. following Tregenza format).

Keywords: Complex Fenestration Systems (CFS), Bi-directional Transmission Distribution Function (BTDF), RADIANCE software, backward ray-tracing, video-goniophotometer

INTRODUCTION

Complex Fenestration Systems (CFS) available today on the market are mainly constituted of solar shadings and light redirecting devices. They can contribute to substantial reduction of the heating and electricity loads in non-residential buildings through an optimal use of passive solar gains and daylighting [1]. Their implementation in the day-to-day life by practitioners, such as lighting designers, architects and façade makers is not an easy task, as long as the latter will be unable to: i) integrate and combine CFSs with efficient luminaries for the sake of energy savings (optimal use of daylighting and electric lighting) and ii) improve simultaneously the users' visual comfort and performance in computerized office spaces (avoiding glare risks and excessive task luminance). Computer simulation tools such as RADIANCE [2] can help to achieve these objectives through the determination of the luminous properties of a building interior prior to its construction or refurbishment.

Nowadays, new photometric equipments, such as bidirectional video-goniophotometer [3], can be used to assess the luminous transmission properties of CFSs, the so-called Bidirectional Transmission Distribution Function (BTDF). Measurements can be realized according to the sensitivity of the human eye V(λ) [4] and even in the near infrared [5]. A collection of measured BTDFs corresponding to a bunch of CFSs is available today at EPFL [6], but currently not sufficiently used in practice. The collection is stored in an international standard for BTDF data defined in the course of IEA Task 31 "Daylighting in Buildings" [7].

The first approach of CFS simulations with RADIANCE was carried out using an approximation of the measured BTDF data with the *prism2* primitive [8] and successfully applied for sharp redirecting CFS (Laser Cut Panel, Holographic Film and 3M Film) [9]. Recently, RADIANCE has been improved [10] to be able to render the light distribution due

to diffuse daylight and sunlight on the inner surface of a fenestration system by the way of BTDF data. The latter is stored in an XML file according to a data format defined at Lawrence Berkeley National Laboratory (e.g. suggested by Klems) [11].

The computer methodology presented in this paper aims at being a link between the international standard for BTDF data storage [7] and the improved RADIANCE version [10]. The paper describes the modifications brought in this prospect to the RADIANCE ray-tracing programme along with simulation results of a non-sharp redirecting CFS (Veglas Lumitop) whose BTDF data were monitored at EPFL.

METHODOLOGY

The RADIANCE *mkillum* routine in the official release 4.0 is able to read and use an XML file that contains BTDF data [10]. However, this XML file format has nothing to do with a prior defined BTDF data standard of goniophotometers such as the one defined in the course of IEA Task 31 "Daylighting in Buildings" [7]. In the latter, a text file is given for each pair of incoming angles (azimuth and elevation) according to the Tregenza subdivision of the hemisphere in 145 zones. In the case of symmetry of the sample (vertical and/or horizontal), the number of measured pairs of incoming angles may be reduced down to 42. The C++ programme *btdf2prism2* [8], that has already been developed by the authors to approximate a BTDF with two main redirecting components using the RADIANCE *prism2* routine, was used as a basis for reading the IEA 21 BTDF file format. The programme was renamed to *btdf2radiance* and modified to generate the BTDF data as a matrix of size (input directions) times (output directions) in the XML file format. As mentioned earlier, with EPFL's goniophotometer the input directions are the centroid of the 145 Tregenza zones, and the output directions are each 5° in azimuth and 5° in elevation leading to 1297 zones. This last number being equal to (90°/5°) times (360°/5°) plus the zenithal zone, the corresponding BTDF matrix is rectangular. Two steps were required to achieve the link between the measurements of EPFL's goniophotometer in IEA 21 format and the BTDF data usable by the RADIANCE routine *mkillum*:

1) Modify the RADIANCE *mkillum* routine to take into account the basis in which the 145 input Tregenza directions and the 1297 (5° by 5°) output directions are defined,
2) Write the *btdf2radiance* routine to convert the IEA 21 BTDF format in the XML file format usable by *mkillum*.

The following two paragraphs present the last points in details.

Modifications in the RADIANCE mkillum routine

The source code of RADIANCE is modular; all what concerns the basis of BTDF data is located in the file /common/bsdf.c. Three existing basis can be found in the latter: LBNL/Klems Full, LBNL/Klems Half and LBNL/Klems Quarter. Those are given by couples of inclination and number of subdivisions of the band that is in between the current and next inclinations. Symbolically the couples can be represented by:

$$\theta_1,1\ ,\ \theta_2,s_{2\to3}\ ,\ \theta_3,s_{3\to4}\ ,\ldots,\ \theta_n,0\ , \tag{1}$$

in which θ is the inclination angle (accounted for from the normal, see Figure 1) and $s_{a\to(a+1)}$ is the number of subdivisions between θ_a and θ_{a+1} for $a=1..(n-1)$. The first number of subdivisions is always 1 in common hemisphere subdivisions, e.g. the zenithal zone is unique. The last number of subdivisions on the other hand is always 0 to end the series. The Tregenza

basis, named in the modifications brought to *mkillum* “EPFL/Tregenza Full”, is thus given in this notation by:

$$-6,1\ ,\ 6,6\ ,\ 18,12\ ,\ 30,18\ ,\ 42,24\ ,\ 54,24\ ,\ 66,30\ ,\ 78,30\ ,\ 90,0\ \ , \qquad (2)$$

and the 5° by 5° basis, named in the modifications brought to *mkillum* “EPFL/5deg Full”, is given by:

$$-2.5,1\ ,\ 2.5,72\ ,\ 7.5,72\ ,\ 12.5,72\ ,\ 17.5,72\ ,\ldots,\ 87.5,72\ ,\ 90,0\ \ , \qquad (3)$$

in which we notice a fixed number of subdivisions of the bands and a fixed step increment of 5° in θ. The first inclination angle of each series is negative and equals in absolute value to the second inclination angle to indicate the extent of the unique zenithal zone. With the basis defined, each zone of the hemisphere is then identified by a unique number which starts by the zenithal zone and follows with the successive bands. The numbering goes according to the right-hand rule associated with the reference frame shown in Figure 1.

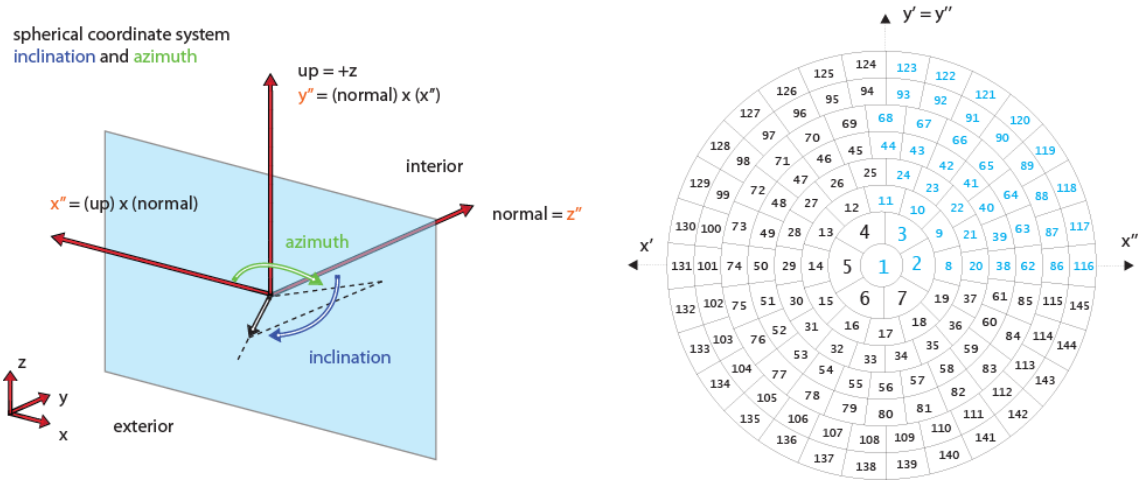

Figure 1: The coordinate system associated with the glazing used by default by mkillum (up=+Z) on the left-hand side, the numbering of the zones in the “EPFL/Tregenza Full” basis on the right-hand side (in blue the minimum of 42 zones for a complete set considering symmetries).

When defining a surface in RADIANCE to be represented by a BTDF, the user should define the vertex order to arrange for the normal of the surface to point inside the room. The *mkillum* routine then associates another reference frame to the surface: (x’’,y’’,z’’). The latter is defined by taking as default an “up” direction equals to the z-axis in the room’s Cartesian coordinate system (x,y,z): the vector product between “up” and the surface normal defines the x’’-axis, the vector product between the surface’s normal and x’’ defines y’’ and finally the normal itself defines the z’’-axis.

Remember that a fully transparent glazing represented by its BTDF matrix using the “EPFL/Tregenza Full” basis in input and output directions is diagonal.

Conversion of the IEA 21 BTDF file format to the *mkillum* XML file format

The programme *btdf2radiance* makes the link between the IEA 21 BTDF file format and the XML file format requested by *mkillum* after the previous modifications. The IEA 21 BTDF file format defines a separate file for each pair of incoming angles, each of which contains the BTDF values associated with a pairs of outgoing angles. Those angles (incoming and

outgoing) are measured in a reference frame attached to the considered CFS sample (x',y'.z'), that is different from the one used by *mkillum* (see Figure 2).

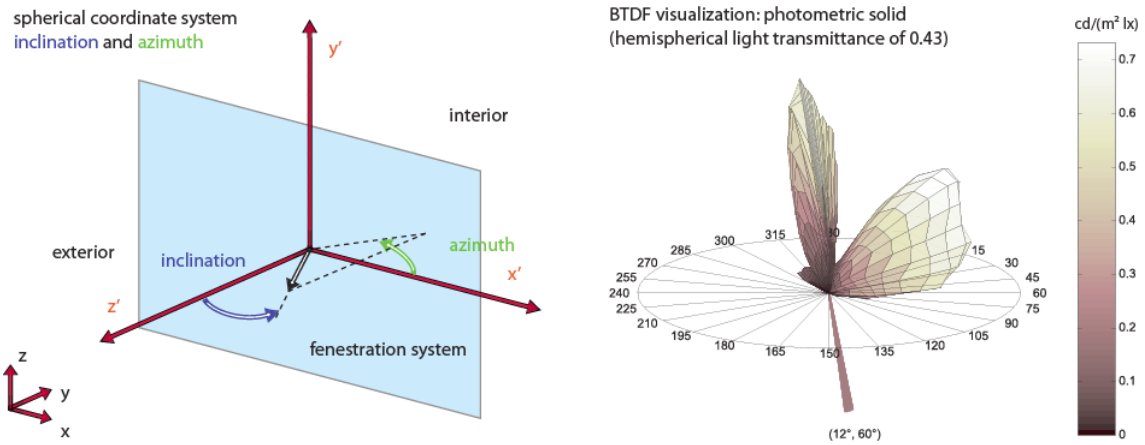

Figure 2: The coordinate system associated with the measured BTDF in the international standard IEA 21 and a visualization of the measured BTDF of Veglas Lumitop for impinging angles of 12° in inclination and 60° in azimuth (z'-axis goes downwards).

The transformation that goes from IEA 21 coordinate system (x',y',z') shown in Figure 2 to the *mkillum* coordinate system (x'',y'',z'') shown in Figure 1 can be written, in spherical coordinates, as:

$$\theta \mapsto \pi - \theta, \varphi \mapsto \pi - \varphi, \tag{4}$$

in which $\theta \in 0,\pi$ is the inclination angle and $\varphi \in 0,2\pi$ the azimuth angle in IEA 21 reference frame. The algorithm which produces an XML file usable by *mkillum* from IEA 21 BTDF files contains six steps: 1) transformation of the incoming angles in the *mkillum* reference frame, 2) identification of the incoming zone number (in the "EPFL/Tregenza Full" basis from 1 to 145), 3) transformation of all outgoing angles to the *mkillum* reference frame, 4) identification of the outgoing zone number (in the "EPFL/5deg Full" basis from 1 to 1297), 5) attribution of the BTDF values in the asymmetrical matrix (of size 145*1297) and 6) in case of symmetries defined, copy the values accordingly in the matrix. The final asymmetrical matrix is written in the form given by Table 1.

```
<?xml version="1.0" encoding="UTF-8"?>
<WindowElement>
 <Information Material="Lumitop" Source="btdf2radiance"/>
 <Optical>
  <Layer>
   <WavelengthData>
    <Wavelength>Visible</Wavelength>
    <WavelengthDataBlock>
     <WavelengthDataDirection>Transmission Front</WavelengthDataDirection>
     <ColumnAngleBasis>EPFL/Tregenza Full</ColumnAngleBasis>
     <RowAngleBasis>EPFL/5deg Full</RowAngleBasis>
     <ScatteringData>
      ... the asymmetrical BTDF data in 1297 rows of 145 columns ...
     </ScatteringData>
    </WavelengthDataBlock>
   </WavelengthData>
  </Layer>
 </Optical>
```

```
</WindowElement>
```

Table 1: The structure of the XML file for the simulation of BTDF data with mkillum.

As illustration of the matrix structure, the normal-hemispherical transmission of a monitored CFS sample can be computed using the first column of the matrix which corresponds to the incoming zone 1 (normal to the sample). Furthermore, the BTDF visualization in Figure 2 of Veglas Lumitop for incoming angles (12°,60°) corresponds to the incoming zone 4, in other words the 4th column of the matrix.

Usage of the resulting XML file with *mkillum*

The routine *mkillum* is used exactly in the same way as for any kind of glazing, except that one need to mention the name of the XML file to be used. Table 2 shows a RADIANCE file describing a surface that should behave in the same way as the XML file specified. For more details about RADIANCE simulations please refer to [2].

```
#@mkillum i=void c=d d=btdf2mkillum145x1297.xml s=40000 l+ u=+Z

void polygon upper_glazing
0
0
12
 0.1   0  2.7
 3.35  0  2.7
 3.35  0  2.1
 0.1   0  2.1
```

Table 2: The radiance description file (.rad) of a glazing with mention of the XML data file.

SIMULATION RESULTS

An office room in the LESO Solar Experimental Building located on the EPFL campus in Switzerland was chosen as virtual model for producing renderings (see Figure 3). The glazed facade faces south, with a standard double glazing in its lower part and a hypothetical installation of a Veglas Lumitop in its upper part. The device redirects the sun rays towards the ceiling in winter, spring and autumn; it blocks the sun rays in summer.

Figure 3: RADIANCE renderings of a virtual model of a simple room in LESO-PB office room (Switerland), from left to right: winter solstice, spring/autumn equinox and summer solstice at noon (local winter time).

These renderings give convincing results, which is not the case for the ones that can be realized with the *prism2* primitive in RADIANCE [8]. Indeed, the Lumitop has a diffuse directional redirection property (see Figure 2 for an illustration) that cannot be represented by two sharp directions.

CONCLUSION

The approximation of monitored BTDF data using the RADIANCE *prism2* primitive developed previously by the authors comes to a limit when considering CFS having a significant diffuse component. To overcome this and bring compatibility between the international standard IEA 21 for BTDF data storage and the recent improvement of the RADIANCE *mkillum* routine, a new C++ programme *btdf2radiance* was developed. The renderings are convincing so far; however a further verification procedure is foreseen for the next months.

ACKNOWLEDGEMENTS

The authors gratefully acknowledge the financial support of the Swiss Federal Office of Energy (SFOE) under the grant # 154 393.

REFERENCES

1. J.-L. Scartezzini et al., Daylighting design of European buildings, Technical Report, pp. 225, LESO-PB/EPFL, Lausanne, 1997.
2. G. W. Larson and R. Shakespeare. Rendering with Radiance: The Art and Science of Lighting Visualization. Morgan-Kaufmann, San Francisco, 1998.
3. M. Andersen. Light distribution through advanced fenestration systems, Building Research and Information, Volume 30, Issue 4, July 2002, Pages 264-281.
4. M. Andersen, L. Michel, C. Roecker and J.-L. Scartezzini. Experimental assessment of bi-directional transmission distribution functions using digital imaging techniques, Energy & Buildings, Vol. 33, N°5, p. 417-431, 2001.
5. M. Andersen, E. Stokes, N. Gayeski, C. Browne. Using digital imaging to assess spectral solar-optical properties of complex fenestration materials: A new approach in video-goniophotometry, Solar Energy 84 (4), pp. 549-562, 2010.
6. M. Andersen. Innovative bidirectional video-goniophotometer for advanced fenestration systems: List of BT(R)DF measurements. Internal Report, LESO-PB, EPFL, 2004.
7. International Energy Agency Task 21, Source Book on Daylighting Systems and Components, Chap. 8.3: Optical Characteristics of Daylighting Materials, pp. 8.16 - 8.22, Paris, July 2000.
8. J. Kaempf, J.-L. Scartezzini. Integration of BT(R)DF Data into Radiance Lighting Simulation Programme, Technical Report, CTI Project 4881.1 "Bidirectional Goniophotometer", LESO-PB/EPFL, Lausanne, 2004.
9. A. Thanachareonkit, J.-L. Scartezzini. Modelling Complex Fenestration Systems using physical and virtual models, Solar Energy 84 (4), pp. 563-586, 2010.
10. G. Ward, Radiance 4.0 Improvements, Radiance Workshop, Harvard University, Graduate School of Design, October 2009.
11. M. Konstantoglou. Radiance: Visualizing Daylight Impacts, Complex Fenestration Systems Workshop, LBNL, June 1-3, 2009.

REDIRECTION OF SUNLIGHT BY MICRO STRUCTURED COMPONENTS

S. Klammt [1], H.F.O. Müller [2], A. Neyer [1]

1: Arbeitsgebiet Mikrostrukturtechnik, TU Dortmund, Friedrich-Wöhler-Weg 5, D-44227 Dortmund, andreas,neyer@tu-dortmund.de

2: Green Building R&D, Graf-Adolf-Sr. 49, D-40210 Düsseldorf, helmut.mueller@greenbuilding-rd.com

ABSTRACT

Non tracking daylight systems, which redirect the light from solar altitudes between 15° and 65° deep into the room without causing glare effects, have been applied successfully in several office buildings recently. Based on these macro structured systems, fixed in the upper area of windows above eyelevel, advanced solutions with micro structures are developed now. Main objective is the reduction of material input (e.g. PMMA) and production costs. Additionally the optical properties and redirection performance are to be improved. Ray tracing calculations were carried out for principal solutions of micro structured optical systems capable of redirecting daylight with high and almost homogeneous efficiency over the relevant angular range of solar altitudes and not showing colour effects. The production process of hot embossing has been optimized and prototypes of PMMA panels with dimensions of 1400 mm x 400 mm x 4 mm were tested. Design principles for integration of the panel in triple glass units in windows are shown.

1. REQUIREMENTS OF COMBINED SOLAR CONTROL AND DAYLIGHTING

Windows have to control solar heat gains effectively in order to avoid uncomfortable room temperatures respectively high energy consumption for cooling. The main design parameters of the façade influencing this performance are window area and orientation as well as shading coefficient of glazing and additional shading facilities.

Simultaneously the façade has to provide a high daylighting performance, especially in non-residential buildings like offices, in order to create a high quality illumination as to visual tasks and biological (circadian) effects of the user as well as to reduce the electricity consumption for artificial lighting. Latest research results demand illuminances much higher than the standard (DIN EN 12464-1) values for artificial lighting (300 lx to 750 lx). Desirable values should be up to 2000 to 4000 lx [1-1 to 1-2], at least under daylight conditions. The main design parameters in addition to those of solar control are position and shape of window, light transmittance of glass and shading facility. A differentiation of sky conditions, i.e. diffuse and direct sunlight, has to be taken into account.

2. PRINCIPAL SOLUTIONS

Conventional solar control systems like external louvers or roller blinds have the side effect to reduce the daylight transmission strongly so that the minimum illumimance often can only be provided by artificial light. In order to utilize the available daylight but control the solar heat gains simultaneously, combined shading and daylighting solutions have been developed [2-1]. They improve the illuminance, as the comparison of conventional louvers, partly light directing louvers and light directing glass in Fig. 2.1 shows.

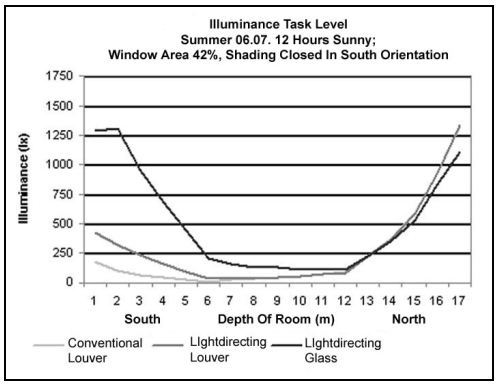

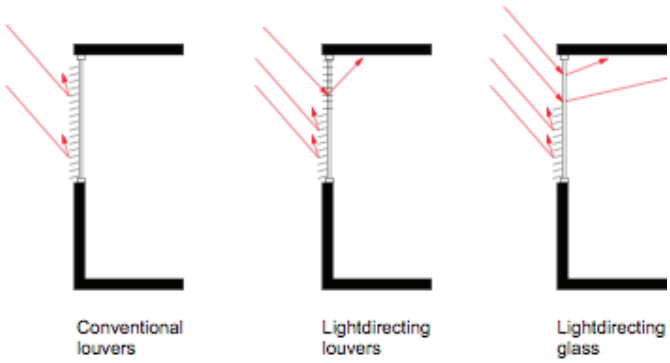

Fig. 2.1, left: Illuminance (lx) and distance from window (m), south / north orientation, shading device closed in south, opened in north [2-2], right: Three daylight and shading solutions: Conventional louvers, light directing louvers, light directing glass in upper and louvers in lower window area.

Physical effect	Principle solution	No.	Drawing	Aspects of selection
Reflection	Diffuse reflector (Lightshelf)	1		- limited reflection - limited trans-mission for covered sky conditions - glare for low solar altitudes
	Specular reflector (DLS-Fisch)	2	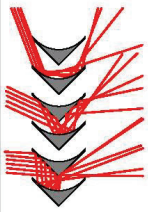	- limited reflection - limited trans-mission for covered sky conditions - dirt avoidance by enclosure in gap of double glazing - DLS-Fisch, Eckelt, [2-5]
Refraction (internal total reflection)	Light-conductor (Lumitop)	3		- reflection without loss - high transmission - dirt avoidance by enclosure in gap of double glazing - Lumitop, 11mm wide light con-ductors in gap, [2-5]
	Plane with two structured surfaces (Lumilight)	4	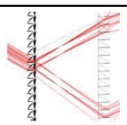	- reflection without loss - high transmission - dirt avoidance by enclosure in gap of double glazing - Lumilight, 4mm PMMA plane with micro structures, [2-3]

Table 2.1: Principle solutions for redirection of direct sunlight by fixed systems (no solar tracking)

Relatively small window areas are sufficient for redirecting sunlight to the depth of the room because of the intensity of direct solar light. In order to avoid glare only the upper part of the window above eye level should be used for sunlighting. If louver systems are used the lamellas have to be highly reflective, especially shaped and tracked according to the solar position. More robust are redirecting systems, which have not to be moved and which are protected against external impact like dust, wind and rain, e.g. in the gap of a double glass unit.

This study focuses on the fixed type of solar redirection with the following task: Redirection of direct sunlight in windows, facing east, south and west, from solar altitudes up to 65° in Middle Europe to the ceiling and depth of the room without causing glare. Because of reduced radiation intensity and obstructions close to the horizon a minimum solar altitude of 20° can be assumed. Most of the light has to be redirected above a horizontal level. The remainder of light with an emergent angle smaller 0° must be less than 10% to avoid glare. Principle solutions, all of which have a translucent image, are given in Table 2.1.

The systems based on refraction have a higher efficiency than those based on reflection, as total internal reflection works without losses. The protection against external impact and deposition of dirt helps to avoid performance losses, thus the encapsulation in a multilayer glass unit is recommended. Although principle No. 3 with light conductors has proved a good performance in numerous applications [2-2], it was taken as a challenge to reduce the complexity of the 11 mm PMMA profiles in the gap of a double glass unit. Solution No. 4 was chosen for an advanced approach, a simple pane of transparent material with optical surfaces to be placed in a glass unit [2-3]. The development of suitable surface structures and their production in micro dimensions is shown in chapter 4 to 6.

3. BOUNDARY CONDITIONS OF APPLICATION

Integration of light redirection	Fixed solar control	Movable solar- and glare control	No.	Drawing	Exemplary characteristics for: - Lightdirecting glass, LD-G - Glas with solar control, G-SC				
Upper window area separated by frame	None	Outside from above	1	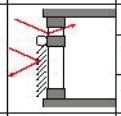		T_L	g	f_c	g*f_c
					LD-G	0,5	0,5	1	0,5
					G+SC	0,5	0,5	0,25	0,13
	Solar control glass, selective	Inside from above	2	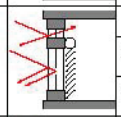		T_L	g	f_c	g*f_c
					LD-G	0,5	0,25	1	0,25
					G+SC	0,5	0,25	0,8	0,2
	External shading		3	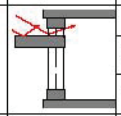		T_L	g	f_c	g*f_c
					LD-G	0,5	0,5	1	0,5
					G+SC	0,5	0,5	0,5	0,25
Without separating frame	None	Outside from down below	4	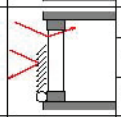		T_L	g	f_c	g*f_c
					LD-G	0,5	0,5	1	0,5
					G+SC	0,5	0,5	0,25	0,13
	Solar control glass, selective	Outside from down below	5	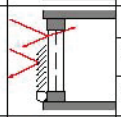		T_L	g	f_c	g*f_c
					LD-G	0,5	0,25	1	0,25
					G+SC	0,5	0,25	0,25	0,06
		Inside from down below	6	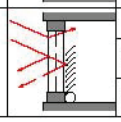		T_L	g	f_c	g*f_c
					LD-G	0,5	0,25	1	0,25
					G+SC	0,5	0,25	0,8	0,2

Table 3.1: Boundary conditions for light directing systems in side windows

The boundary conditions of architecture and building construction have to be considered for the development: Different kinds of facades with single windows or larger glazed areas have to be taken into account as well as various types of solar control, which can be fixed or movable. There can be continuous glazing or a separating frame between upper and lower window part. A survey is given in Table 3.1., including approximate performance characteristics for lighting and solar heat gain. For the time being a maximum dimension of 1500 mm x 400 mm for light directing panels was derived from existing buildings with state of the art daylight systems.

4. OPTICAL MICRO STRUCTURES AND RAY TRACING CALCULATIONS

Research work by the Institute of Solar Energy (ISE) in Freiburg on prismatic structures showed that micro prism arrays are principally suited for light redirection [4-1], however with the drawback that the redirection efficiency varies considerably over the angular range of the daily solar altitudes. In consequence, at certain hours of the day the light redirection works with high efficiency, while at other hours the incoming sunlight causes severe glare. In this work ray tracing has been employed to develop a micro structured optical system which is capable of redirecting light homogeneously over the whole angular range of the daily solar altitudes.

The ray tracing calculations lead to a double sided microstructure as optimized configuration. The system combines lens-like structures at the light incident and prismatic structures at the light redirection side (see Fig 4.1). The implementation of the lens-like microstructures at the light incident side leads to reasonably homogeneous angular redirection efficiencies and avoids colour effect which are generally present in pure prismatic systems.

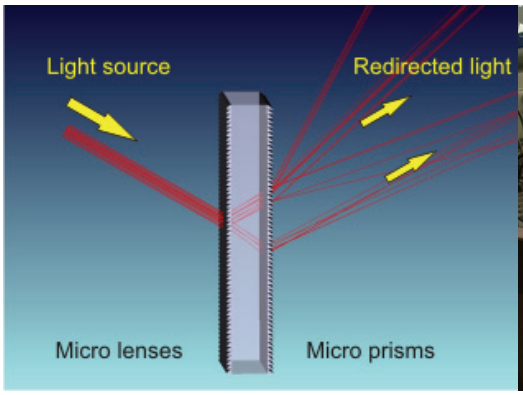

Fig. 4.1 Schematic configuration of light redirection by double sided micro structured surface

Fig. 5.1: First large-scale prototype with dimensions of 1500 mm x 300 mm x 4 mm for implementation in windows / skylights

5 PRODUCTION TECHNOLOGIES, PROTOTYPING, LARGE SCALE PRODUCTION

For the fabrication of micro optical elements a variety of high precision replication processes are available like precision injection moulding, hot or UV-embossing, or casting. All materials with high optical transparency are principally suited for the realization of such micro structured components, with preference of polymeric materials - due to their easier mass production capabilities.
In this work, the numerically optimized designs have been successfully implemented in casting and in hot embossing processes. Casted prototypes were fabricated by using PDMS (a highly transparent silicone polymer). The structure dimensions of the lenses and prisms were in the range of 250µm. After demonstrating experimentally the high light redirecting efficiency of PDMS prototypes (dimensions: 100mm x 100 mm) the technology has been transferred to large scale industrial production by hot embossing (Jungbecker Technology, Olpe, Germany). The size of the fabricated panels allows for 1500mm x 400 mm x 4 mm, which is a size well suited for implementation in standard windows or skylights.

In order to achieve a window image with continuous glazing (no separating frame between upper and lower part), two solutions are possible: Joint of PMMA and glass pane in the gap or continuous glass pane with micro structured plastic foils laminated at the desired position on a glass sheet. Fig. 5.2 shows the appearance of a window which has been laminated with a micro structured PDMS foil in the upper part.

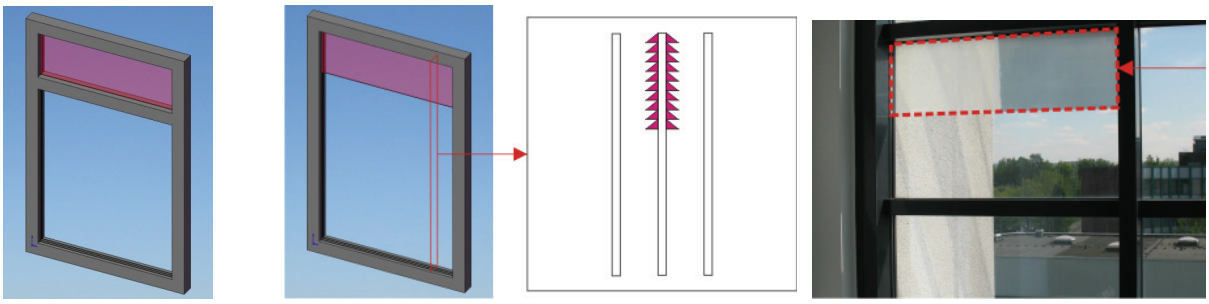

Fig. 5.2, left: Separating frame between upper and lower window area, right: Lamination of micro structured foils (900 mm x 300 mm x 1.5 mm) in the upper part of a continuous glass panel

6. EXPERIMENTAL TESTS, OPTIMIZATION PROCESS

While a simple test with a torch already demonstrates the systems efficiency (see Fig. 6.1), the redirection performance was also measured with a goniometrical setup. The obtained results prove the expected high efficiency in redirecting daylight without causing glare and confirm the estimated results of the numerical simulation. First samples achieve a redirecting overall efficiency which surpasses the values of existing commercial systems.

Fig. 6.1 Demonstration of light redirection performance: light distribution without (left) and with inserted daylighting system (right).

The diagram in Fig. 6.2 shows the percentage of transmitted light directed upwards (green line) and downwards (red line) over the solar altitude of the incident light. Overall, about 70% of the incident light (between solar altitudes of 15 to 60 degrees) is redirected and scattered to the ceiling. The remaining 10% of the transmitted light (red line) is diffusely scattered and may contribute to an additional illumination of the working area.

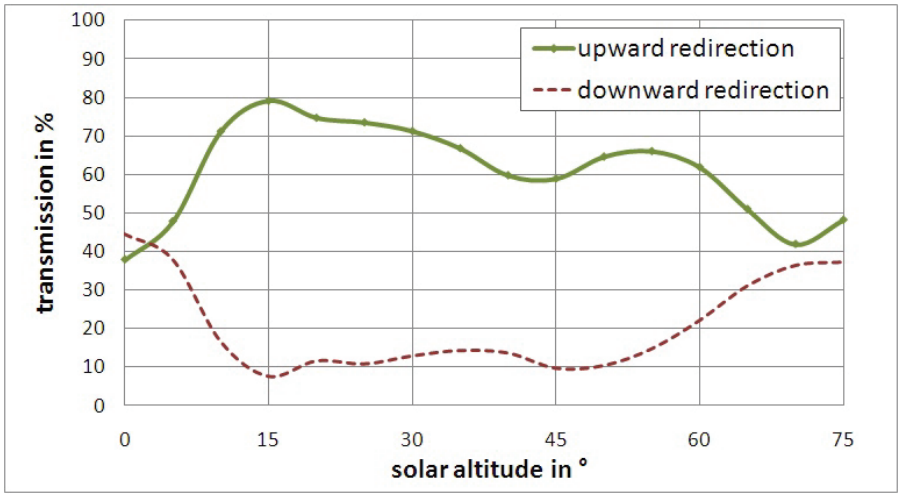

Fig. 6.2 Diagram of redirection performance (based on measurements of a PDMS prototype).

7. CONCLUSIONS

The development of non tracked, micro structured solar lighting systems has been successful as to large scale embossing technology in dimensions of 1500 mm x 400 mm as well as to prototype testing. By mounting the PMMA pane between two glass panels the characteristics of a triple glass unit, as shown in Fig. 7.1, can be achieved. Depending on dimensions, coating and gas fill the following characteristics are expected:

- U-value = 0.7 – 0,8 W/m² K (2 low-e coatings & argon)
- Solar heat gain g = 0,25 – 0,30 (selective coating)
- Light transmission T = 0,50 - 0.60

In comparison to state of the art solutions efficiency of redirection and light transmission could be improved and material input of PMMA as well as complexity of construction be reduced. Depending on the boundary conditions like room geometry, window size, orientation, solar and glare control, high daylight quality (illuminances > 1000 lx), and low annual lighting energy demand (reduction 20% to 40% compared to conventional systems) can be achieved [2-3].

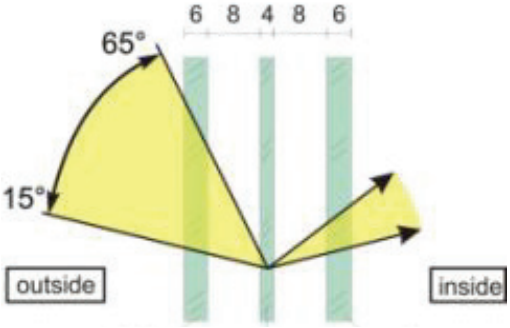

Figure 7.1: Example of micro structured light directing pane integrated in glass unit

The reported advanced micro structured daylighting system was designed to be manufactured by high-productivity processes. In addition, the slim design leads to a reduced material consumption and simplifies the assembly process of the final glass unit significantly. The resulting lower costs as well as the capability of integrating the system into windows with separate clerestory (frame) as well as without is considered a favourable pre-condition for a successful and deep market penetration.

REFERENCES

[1-1] W.J. M. van Bommel, G.J. van den Beld: Lighting for Work: Visual and Biological Effects, Philips Lighting, The Netherlands, April 2003.

[1-2] Berson, D.M., Dunn, F.A., Motoharu, Takao: Phototransduction by retinal ganglion cells that set the circadian clock, Science, February 8, (2002).

[2-1] IEA International Energy Agency: Daylight in Buildings, A Source Book on Daylighting and Systems and Components. A Report of IEA SHC Task 21, 2000.

[2-2] Müller, H.F.O., Emembolu, A., Oetzel, M., Schuster, H., Soylu, I.: Sonnenschutz und Tageslicht in Büroräumen, in: Bauphysik-Kalender 2005, Hrsg. E. Cziesielski, Ernst & Sohn, Berlin.

[2-3] Klammt, S., Müller, H., Neyer, A.: Advanced Daylighting by Micro Structured Components. Proceedings of PLDC, Berlin, 2009.

[2-4] Eckelt: Product information: DLC Day Light Systems: “Fisch, intelligent daylight by Barthenbach”

[2-5] Saint-Gobain Deutsche Glas: Product information “Lumitop”, Daylighting-Verglasung mit Lichtumlenkung

[4-1] P. Nitz, A. Gombert, B. Bläsi, G. Walze, 2007, „Verglasungen mit mikrostrukturierten optisch-funktionalen Komponenten“, Ostbayerisches Technologie-Transfer-Institut e.V. -OTTI-, Regensburg: 13.Symposium „Licht und Architektur“, 2007.

ACKNOWLEDGEMENT: Jungbecker GmbH, Olpe, has contributed know-how and services for large scale production of micro structured PMMA plates.

COMPARISON OF OBJECTIVE AND SUBJECTIVE VISUAL COMFORT AND ASSOCIATIONS WITH NON-VISUAL FUNCTIONS IN YOUNG SUBJECTS

Borisuit A[1], Linhart F[1], Kämpf J[1], Scartezzini J-L[1]* and Münch M[1]*

*1: Solar Energy and Building Physics Laboratory, School of Architecture, Civil and Environmental Engineering, Ecole Polytechnique Fédérale de Lausanne, Station 18, 1015 Lausanne, Switzerland, * common last authors*

ABSTRACT

Visual comfort is a key element at work places and at home. Besides task illuminance and color rendering it is the indoor light distribution, which strongly impacts visual comfort. We aimed to show possible relations between subjective and objective visual comfort and non-visual functions such as mood, alertness, and wellbeing.

Twenty-two healthy young volunteers were recruited to spend six hours in the afternoon in a testing room at our laboratory. They were exposed to daylight in the range between 1000 and 2000 lx. Artificial lighting was added when daylight illuminance decreased below this target range. In order to determine objective visual comfort, luminance ratios of the room were extracted from high dynamic range (HDR) images, taken three times during the afternoon. From these HDR images we calculated glare indexes by using specialized software (Evalglare v0.9, Fraunhofer ISE). Those glare indexes served as objective visual comfort assessments. At several occasions we asked subjects to assess their subjective visual comfort and glare as well as alertness, mood and well-being on visual analogue scales. We correlated objective and subjective glare assessments with those from alertness, mood and wellbeing.

We found that objective visual comfort exhibited a time of day-dependent positive or negative association with subjective physical wellbeing, visual comfort and alertness. Higher objective glare indexes at the beginning of the afternoon slightly correlated with greater physical wellbeing ($p<0.1$); whereas in the middle of the afternoon, higher objective glare indexes were significantly correlated with lower subjective visual comfort and lower alertness. Towards the end of the afternoon, we found that higher objective glare was associated with significantly lower physical wellbeing (for all significant results: $p<0.05$).

Taken together, our results show that objective glare indexes were associated not only with subjective visual comfort but also with non-visual functions such as subjective physical wellbeing and alertness. However, these assessments varied with the time of day, reflecting the effects of dynamic light conditions on subjective homeostatic and circadian functions. This might have implications on the lighting environment at many work places and homes in the future.

INTRODUCTION

Beyond vision, light influences many non-visual functions such as mood, alertness and wellbeing. It has recently been shown that visual and non-visual functions share common neuronal pathways which depend on photo biological properties, such as the lighting environment[1-2]. Light is the most important zeitgeber to synchronize the internal biological clock to the external 24-hours light-dark cycle [3-5]. Besides the spectral composition of visible light, light intensity (vertical illuminance, E_v) and the timing of light exposure play an important role in modulating these non-visual light effects in humans [3, 6-9].

To achieve an optimal visual comfort in a working environment, we have to take into account not only the task illuminance and color rendering, but also the luminance distribution. The avoidance of discomfort glare is one aspect of visual comfort which is used to assess optimal indoor light quality. Several glare indexes have been developed to evaluate discomfort glare [10-14]. High dynamic range imaging (HDR) techniques have been applied as a tool to capture a lit scene and to assess its luminance distribution [15-17]. In order to determine objective visual comfort, we can extract those luminance ratios from HDR images and calculate glare indexes, by using specialized software[18-19].

In this study, we aimed at investigating the associations between objective glare, visual comfort and non-visual functions, at different times of day. We assessed objective visual comfort from three different glare indexes by using HDR imaging techniques. We compared those objective glare indexes with subjective visual comfort, alertness, mood and well-being ratings in young subjects, who spend an afternoon in our laboratory under daylighting conditions.

METHODS

Study design

Twenty-two healthy young volunteers were recruited (14 men; 8 women; age 23.5 ± 2.4 years; mean ± SD). We only included healthy subjects without any medication (except for oral contraceptive). Seven days before the study started, subjects were asked to maintain a regular sleep-wake cycle. Compliance was controlled by a wrist activity monitor and sleep logs. All subjects were requested to spend two afternoons and evenings in a testing room at the Solar Energy and Building Physics Laboratory (LESO-PB) at the Swiss Federal Institute of Technology in Lausanne (Switzerland) under two different lighting conditions, in a balanced cross over design (between October and February). In this paper, we report results from the first six hours during the afternoon under daylighting conditions. Subjects were exposed to daylight with a vertical target illuminance between 1000 and 2000 lx (mean: 966 lx; SE±94.8 lx). The lower part of all windows was covered with translucent blinds in order to avoid vertical outside view. Artificial light (from six ceiling luminaires: 58W, 4000K) was added when vertical illuminance dropped below 1000 lx. Subjects came 4-5 hours after their habitual wake time to the laboratory and spent the afternoon (from noon to 6pm) in the testing room, in a steady sitting position. They were allowed to read, work or listen to music, (no computer work). In order to ensure vertical gazing, subjects worked on vertically tilted table boards. Study procedures were approved by the local ethical board and subjects gave their written informed consent before the study.

Objective & subjective assessments

Vertical illuminance was continuously recorded in 5 minutes intervals throughout the study by using a spectroradiometer (Specbos 1201, JETI, Germany). Three times during the study (at 12pm, 3pm and 5:30pm) a sequence of 14 photos was taken in vertical gaze direction of the subjects by using a camera with a fisheye lens (Nikon Coolpix 5400). From these photos we created HDR images and calculated glare indexes by using the software Photosphere [20] and Evalglare (Evalglare v0.9, Fraunhofer Institute, Germany) [14, 19]. Three different glare indexes served as objective visual comfort assessments: the Daylight Glare Probability (DGP) [14], the Daylight Glare Index (DGI) [10] and the Unified Glare Index (UGR) [21].

Subjective visual comfort, light preference and glare ratings as well as alertness, mood and well-being were estimated on visual analogue scales at the same clock times when the photos for the HDR calculation were taken. We finally correlated objective visual comfort assessments with subjective ratings.

RESULTS

Objective visual comfort

Vertical illuminance measured with the spectroradiometer and vertical illuminance calculated from the HDR images correlated well ($r = 0.84$; $p < 0.01$). Both, vertical illuminance and the calculated glare indexes (DGP, DGI and UGR) changed in the course of the afternoon (one-way repeated analysis of variance; ANOVA; $p < 0.001$; Figure 1). The change of objective glare over time was such that all glare indexes (DGI, UGR, DGP) were significantly lower at 5:30 pm when compared to those earlier in the afternoon (t-test for independent samples; $p < 0.05$).

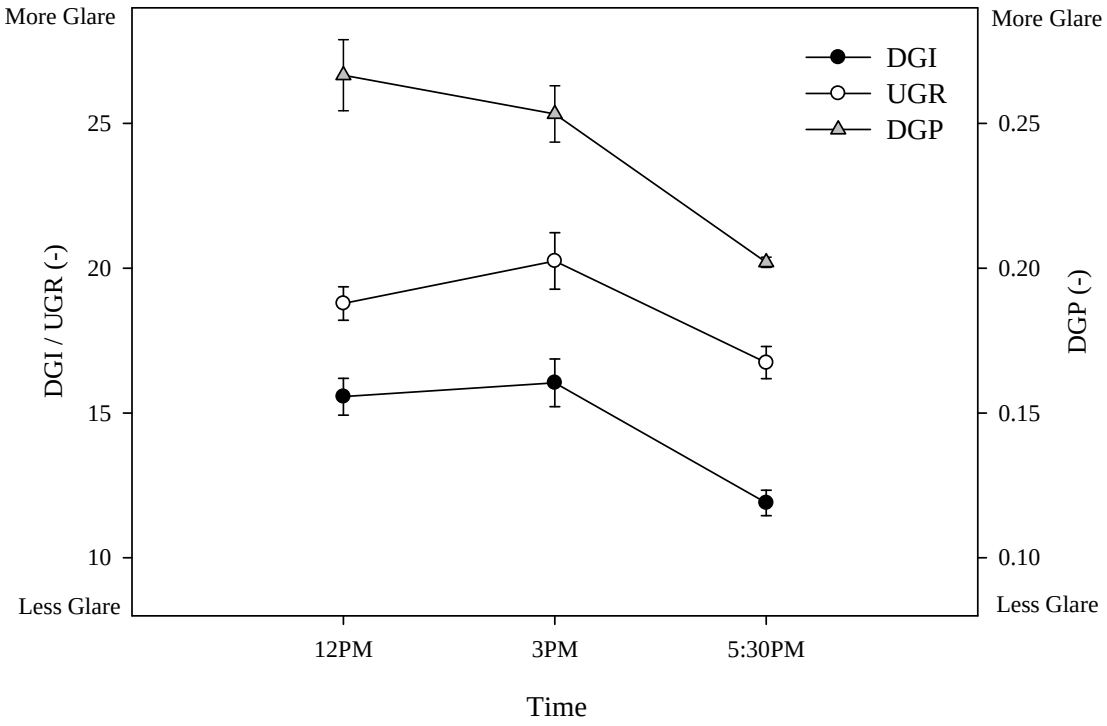

Figure 1: Dynamics of averaged glare indexes (mean of different days) in the course of the afternoon. DGP=Daylight Glare Probability, DGI=Daylight Glare Index, UGR=Unified Glare Index; mean ± SEM

Correlations of subjective and objective visual comfort

Lower subjective visual comfort was significantly correlated with greater objective discomfort (higher objective glare index) in the middle of the afternoon (3pm; $r = -0.44$ for DGI; $p < 0.05$) and was slightly associated with UGR at the same time ($r = -0.40$; $p < 0.1$; Table 1). Light preference had a slight relation with all glare indexes (DGP, DGI and UGR) at the beginning of the study, such that higher objective glare tended to be correlated with greater subjective preference of the lighting condition (Table 1; $r > 0.37$; $p < 0.1$). There was no correlation between objective and subjective glare assessments ($r < 0.28$; $p > 0.1$).

Subjective Assessments	Objective Glare Assessments 12:00 AM			Objective Glare Assessments 3:00 AM			Objective Glare Assessments 5:30 PM		
	DGP	DGI	UGR	DGP	DGI	UGR	DGP	DGI	UGR
Visual Comfort	-	-	-	-	−0.44*	−0.40†	-	-	-
					↑ glare ↓ comfort				
Light Preference	0.37†	0.40†	0.38†	-	-	-	-	-	-
	↑ glare ↑ preferred								
Relaxation	-	-	-	−0.60*	−0.46*	−0.47*	−0.41†	−0.36†	−0.48*
					↑ glare ↓ relaxed			↑ glare ↓ relaxed	
Physical Comfort	0.38†	-	0.40†	-	-	-	−0.50*	−0.48*	−0.59*
	↑ glare ↑ comfort							↑ glare ↓ comfort	
Alertness	-	-	-	−0.42*	−0.36†	−0.37†	-	-	-
					↑ glare ↓ alert				

*Table 1: Correlation coefficients (r) between objective glare indexes and subjective assessments (visual comfort, light preference, subjective wellbeing and alertness) at different times during the afternoon; * p< 0.05, † p< 0.1 and - p=ns. For significant values or tendencies, the direction from correlation coefficients is indicated with arrows.*

Associations of objective glare with non-visual functions

Higher objective glare was significantly associated with lower subjective relaxation at 3pm (r > -0.46; p< 0.05) and at 5:30pm (r= -48; p< 0.05 for UGR and r >-36; p< 0.1 for DGP and DGI; Table 1). For the relations between objective glare and physical comfort we found a slight positive correlation at the beginning of the afternoon (r > 0.38; p< 0.1) and a significant negative correlation at the end of the afternoon, such that at 5:30pm, subjects felt less comfortable, when there was greater objective glare (r > -0.48; p< 0.05). Subjective alertness was negatively correlated with objective glare indexes in the middle of the afternoon (3 pm), such that greater objective glare indexes (i.e. higher objective discomfort) were associated with lower subjective alertness (r = -0.42; p< 0.05 for DGP; r > -0.36 and p<0.1 for UGR and DGI). There was no significant correlation of objective glare indexes and mood assessments (r< 0.24; p> 0.1).

DISCUSSION

We investigated, whether objective visual comfort (via the calculation of glare indexes) correlated with simultaneously rated subjective visual comfort, wellbeing and alertness in young subjects at different times of day. Our results showed a time of day-dependent positive or negative association between objective visual comfort with subjective visual comfort and non-visual functions, such as subjective physical wellbeing and alertness.

Significant correlations between subjective visual comfort and objective glare assessments were only found at 3pm, even though objective glare indexes did not differ between 12pm and 3pm, indicating a certain dynamic in subjective assessments but not the indoor daylight distribution and glare sources. Similarly, we found slight positive correlations of subjective light preference and objective visual comfort at 12pm but not at 3pm.

The correlations of objective visual comfort with physical comfort and relaxation also showed a time of day dependency, such that at the beginning of the afternoon lower objective visual comfort (i.e. higher glare indexes) were slightly associated with higher physical comfort but significantly lower physical comfort at the end of the afternoon. This was the case even though absolute objective visual comfort (i.e. lower glare indexes) was better at 5:30 pm than before. Lower subjective relaxation and alertness were also associated with lower objective visual comfort, starting in the middle of the afternoon. From these results it seems that at the beginning of the afternoon absolutely higher glare indexes (i.e. higher objective visual discomfort) did not reveal negative repercussions on physical comfort, relaxation and alertness, only later in the afternoon those subjective variables went in the same less favorable direction. The change of subjective assessments in the course of a day was also shown by Boyce et al.[22], where subjects rated their lighting conditions poorer in the later afternoon than in the morning hours.

We did not find significant correlations with subjective and objective glare ratings as it was the case in a study reported by Wienold and colleagues, even though we used a similar glare assessment for the calculation of the DGP glare formula [23]. One explanation might be that we tried to avoid discomfort glare caused by direct sunlight during the entire study duration. We therefore had lowered the translucent blinds to prevent a vertical outside view but also to avoid direct sunlight. Secondly, we performed the study in a room which was equipped with anidolic daylighting systems [24-25]. These systems enable a more even light distribution even deeper in the room and reduce the glare risk[17].

In this study, we investigated rather the effects of indoor light distribution, not light intensity or the spectral composition of light per se. Lower objective visual comfort (i.e. higher glare index) does not necessarily mean a brighter light source but indicates a poorer distribution of the incoming daylight flux. One new finding from this study is that subjects felt significantly less comfortable, less relaxed and less alert under poorer indoor daylight distributions. However, these associations went not always in the same direction, depending on the time of day assessment and were not reflected in absolute values of glare indexes.

To conclude, we found that objectively assessed indoor light distributions by HDR imaging techniques led to correlations with time-dependent non-visual functions. Further investigations regarding the effects of indoor light distribution on non-visual functions are needed to quantify the latter in larger populations. We also need longer lasting studies in order to better understand the impact of light on visual comfort and non-visual homeostatic and circadian functions in humans.

ACKNOWLEDGEMENTS

AB and MM are supported by the VELUX Foundation (Switzerland). FL and JK are supported by the Swiss Federal Office of Energy (SFOE).

REFERENCES

1. Commission Internationale de l'Eclairage (CIE): Ocular lighting effects on human physiology and behaviour. in *CIE 158-2004*. Vienna, CIE, 2004.
2. Van Bommel W, Van den Beld G: Lighting for work : A review of visual and biological effects. *Lighting Research and Techonology.* 2004, *36*(4),255 - 69.

3. Cajochen C, Zeitzer J, Czeisler C, Dijk D: Dose-response relationship for light intensity and ocular and electroencephalographic correlates of human alertness. *Behavioural Brain Research.* 2000, *115*(1),75-83.
4. Czeisler C, Richardson G, Zimmerman J, Moore-Ede M, Weitzman E: Entrainment of human circadian rhythms by light-dark cycles: a reassessment. *Photochemistry and Photobiology.* 1981, *34*(2),239 - 247.
5. Roenneberg T, Daan S, Merrow M: The art of entrainment. *Jornal of Biological Rhythms.* 2003, *18*(3),183 - 94.
6. Daurat A, Aguirre A, Foret J, et al.: Bright light affects alertness and performane rhythms during a 24-hh constant routine. *Physiology & Behavior.* 1992, *53*(5),929-936.
7. Avery D, Kizer D, Bolte M, Hellekson C: Bright light therapy of subsyndromal seasonal affective disorder in the workplace: morning vs. afternoon exposure. *Acta Psychiatric Scandinevia.* 2001, *103*(4),267-74.
8. Bauer M, Kurtz J, Rubin L, Marcus J: Mood and behavioral effects of four-week light treatment in winter depressives and controls. *Journal of Psychiatry Research.* 1994, *28*(2),135-45.
9. Rosenthal N, Sack D, Gillin J, et al.: Seasonal affective disorder. A description of the syndrome and preliminary findings with light therapy. *Archives of General Psychiatry.* 1984, *41*(1),72-80.
10. Chauvel P, Collins J, Dogniaux R, Longmore J: Glare from windows: current views of the problem. *Lighting Research and Technology.* 1982, *14*(1),31 - 46.
11. Commission Internationale de l'Eclairage (CIE): Discomfort glare in the interior working environment. in *CIE 055-1983,Paris*, CIE, 1983.
12. Einhorn H: A new method for assessment of discomfort glare. *Lighting Research and Techonology.* 1969, *1*(4),235-47.
13. Commission Internationale de l'Eclairage (CIE): CIE Collection on glare, in *CIE 146-2002*. Vienna, CIE, 2002.
14. Wienold J, Christoffersen J: Evaluation methods and development of a new glare prediction model for daylight environments with the use of CCD cameras. *Energy and Buildings.* 2006, *38*(7),743-57.
15. Inanici M: Evaluation of high dynamic range photography as a luminance data acquisition system. *Lighting Research and Technology.* 2006, *38*(2),123 - 34.
16. Beltrán L, Mogo B: Assessment of luminance distribution using hdr photography. *ISES Solar World Congress.* Orlando FL (USA): 2005.
17. Borisuit A, Scartezzini J, Thanacharoenkit A: Visual comfort and glare risk assessment by HDR imaging technique. *Architectural Science Review.* 2010, *53*(4), 359-73.
18. Ward G, Shakespeare R: *Rendering with Radiance*. San Francisco, CA, Morgan Kaufmann Publishers, 1998.
19. Frauhofer I: *Evalglare v0.9.* Retrieved February, 2011 from http:// www.ise.fraunhofer.de/areas-of-business-and-market-areas/applied-optics-and-functional-surfaces/lighting-technology/lighting-simulations/radiance/radiance?set_language=en&cl=en
20. Ward G: *Anyhere.* 2011 from http://www.anyhere.com.
21. Commission Internationale de l'Eclairage (CIE): Discomfort Glare in the Interior Lighting. in *CIE 117-1995*. Vienna, 1995.
22. Boyce P, Veitch J, Newsham G, et al.: Lighting quality and office work: Two field simulation experiments. *Lighting Research and Technology.* 2006, *38*(3),191-223.
23. Wienold J: Daylight glare in offices. Universität Karlsruhe, Karlsruhe, 2009
24. Scartezzini J, Courret G: Anidolic daylighting systems. *Solar Energy.* 2002, *73*(2),123-35.
25. Courret G: Systèmes anidoliques d'éclairage naturel. Ecole Polytechnique Fédérale de Lausanne, Lausanne, 1999.

INTEGRATION OF EYE-TRACKING METHODS IN VISUAL COMFORT ASSESSMENTS

M. SareyKhanie[1], M. Andersen[1], B.M.'t Hart[2], J. Stoll[2], W. Einhäuser[2]

1: Interdisciplinary Laboratory of Performance-Integrated Design (LIPID), ENAC, École Polytechnique Fédérale de Lausanne (EPFL), Switzerland

2: Neurophysics Department, Philipps-Universität Marburg, Germany

ABSTRACT

Discomfort glare, among different aspects of visual discomfort is a phenomenon which is little understood and hard to quantify. As this phenomenon is dependent on the building occupant's view direction and on the relative position of the glare source, a deeper knowledge of one's visual behavior within a space could provide pertinent insights into better understanding glare. To address this need, we set up an experiment to investigate dependencies of view direction distribution to a selected range of brightness and contrast distributions in a standard office scenario. The participants were asked to perform a series of tasks including reading, thinking, filling in a questionnaire and waiting. The direction of their view was monitored by recording participants' eye movements using eye-tracking methods. Preliminary results show that different facade configurations have different effects on the eye movement patterns, with a strong dependency on the performed task. This pilot study will serve as a first step to integrate eye-tracking methods into visual comfort assessments and lead to a better understanding of the impact of discomfort glare on visual behavior.

INTRODUCTION

Daylight, while undeniably a desirable component in any working and living space [1, 2], can create uncomfortable situations that may reduce visibility and create dissatisfaction and visual discomfort. Among the different types of visual discomfort that can be caused by daylight in an indoor environment, a phenomenon known as discomfort glare is recognized as the most common problem; yet, despite years of study, it still has not been fully quantified and understood. The studies on discomfort glare are mainly subjective and based on light measurements combined with conventional psychophysical procedures [1]. They have resulted in a series of glare indices that predict the expected degree of discomfort an occupant will experience as caused by different light settings. These indices are in general drawn upon four physical quantities: the luminance, the size and the position index of the glare source, and the general field of luminance that the eye adapts to (cf. Fig. 1). The position index is a complex equation, which expresses the change in discomfort based on the angular displacement of the glare source from the line of sight [3, 4]. The main assumption in the definition of this index is that the line of sight is fixed and focused on a given point.

In a natural experience of a space, the view direction is not fixed but varies through time and space. To change their line of sight, humans move body, head and eyes. The hypothesis is that there might be clear relations between these movements and discomfort glare perception.

Eye-movement analysis is used in fields such as car safety, surgery, software usability, product design, and also in assessing glare from monitor screen. Very few studies so far have

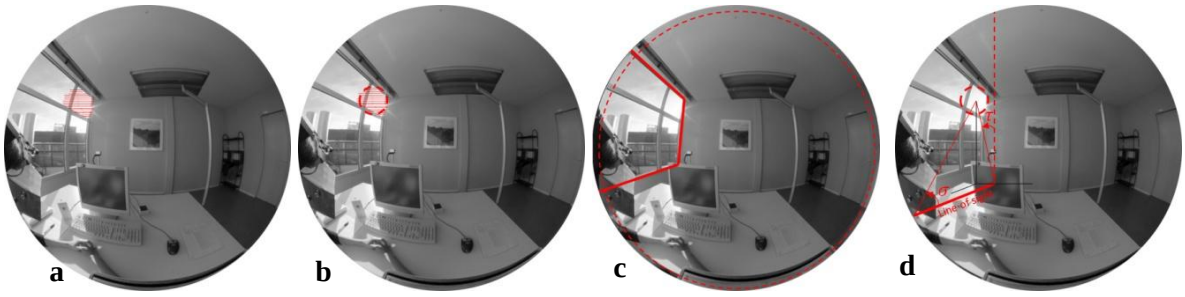

Figure 1: Discomfort glare depends on four general variables a) Luminance of glare source, b) Solid angle of source, c) Background luminance, and d) Position index

investigated the relationship between eye movements and building-induced visual context, such as a window [5, 6]. None went as far as connecting findings on eye-movements patterns to glare perception. The use of this new method can lead on one hand to novel and quantitative insights in the cognitive factors driving eye movements in natural settings, and on the other hand to objective measures of comfort and more reliable predictions of occupant response, that together contribute to support improved workplace design.

To investigate this, a pilot study was designed in a realistic scene using eye tracking methods. The experiment included five participants and was carried out in an office-like room where photometric quantities relevant to visual comfort were gathered. A sequence of four daylight conditions was created by changing the facade configuration, and a fifth light configuration was considered using artificial lighting. Eye movements were recorded for each light-condition sequence and task event by means of an eye-tracker.

This paper describes the overall methodology adopted to approach this problem and illustrates the potential for new insights offered by integrating eye-tracking methods in discomfort glare assessments. It also presents preliminary results of the pilot study conducted in the daylight test room at Fraunhofer-ISE, Freiburg, Germany.

METHODS

The method adopted for this study included measuring eye movements of human participants in an office-like environment. In natural visual behavior, we avoid the discomfort glare sensation changing our view direction and putting the source of glare out of our visual field. Looking into this behavior by means of objective measurements such as eye movements, can lead to a better understanding of this phenomenon in indoor spaces.

Eye-tracking

Using eye tracking has the potential to provide objective measures of comfort and more reliable predictions of a building occupant's response, which contributes to improved workplace design. Eye movements in general are divided into volitional and reflexive movements and in natural stimuli are driven by local features of visual stimuli [7], visual context [8] and task [9, 10, 11]. In addition to eye movements, humans may change their line of sight by head and body movements, which frequently interact with eye movements. For applicability to realistic scenarios, the eye-tracking method should not constrain the participant's movements. To monitor gaze and head movements simultaneously, we therefore employed the EyeSeeCam (Fig. 2), a mobile, state-of-the-art eye tracker [12] that performs binocular video oculography and records real-time head-centered and gaze-centered movies.

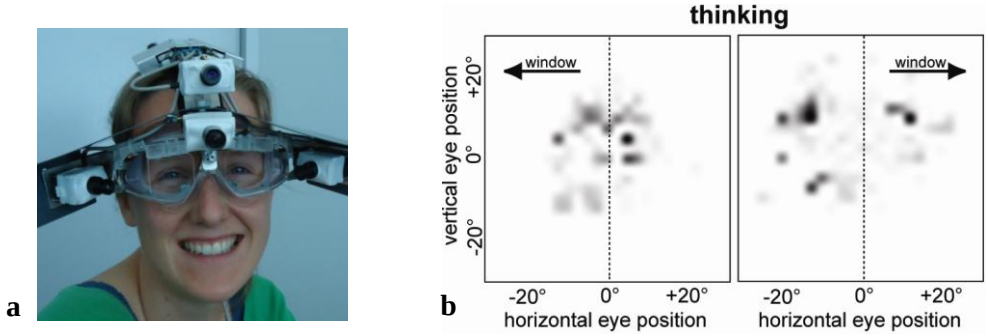

Figure 2: EyeSeeCam a) EyeSeeCam worn by a participant b) Eye-tracking analysis: Heat maps of eye positions recorded with the EyeSeeCam.

Because eye-tracking is an objective, quantifiable method, it provides a new perspective in visual discomfort glare assessment. It adds an objective measurement of occupant response through eye-movement recordings and moves beyond the conventional subjective assessment based on questionnaires.

Experimental setup

As a first step, a pilot study was conducted, whose objective was to investigate the possible relations between eye-movement patterns and light distribution in the room. The experiments were performed in an office-like side-lit module located on top of a four story building in the south-western part of Germany in Freiburg. The module is 360º rotatable so as to allow reasonably repeatable experiments for varying sun positions. The glazing type is a double glass with a light transmission of 54%, a U-value of 1.1 W/m²K, and a total solar energy transmission of 29%. The room is equipped with control systems such as interior venetian blinds, roller blinds, and covering sheets for reducing the glazing surface.

The sequence of light conditions ranging from dark and low contrast to bright and extreme contrast was determined through initial testing with different facade configurations compared in simulation using Radiance [13] and in the real space with the help of High Dynamic Range imaging techniques [14]. The main concern was to have different significant contrast conditions and glare situations in the room while maintaining the view contact to the outside and ensuring an easy flow of the measurement procedure. Based on this comparison, four daylight conditions were considered for the experiment (cf. Fig. 3). In addition, an artificial situation was also considered as the fifth light system.

Each task event started with the participant coming in from the outside, first to the neighbor module and then to the test scene so as to have a similar eye adaptation processes to indoor light. Light variations outdoors were monitored with a meteorological station that records the global, total and diffuse illuminance (lux), as well as the global horizontal irradiance (W/m^2) [15]. Indoor light distribution was monitored by lux meters and calibrated HDR cameras equipped with a fish-eye lens used as a multiple point luminance-meter. Eye-movements were recorded by means of the EyeSeeCam eye-tracker system. Photometric quantities relevant to visual comfort as well as subjective glare rating were gathered.

Test procedure

The test procedure consisted of five parts with five different light settings and included five task events: 1) reading from the monitor screen, 2) thinking/waiting, 3) answering one multiple choice question on the reading, 4) filling in the questionnaire, 5) pause.

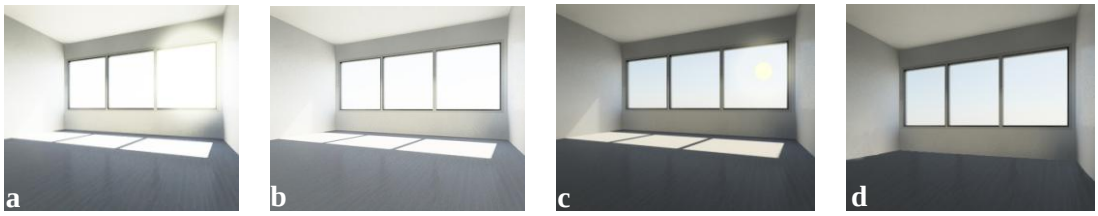

Figure 3: The visualization of the four daylight conditions: a) dark and low contrast, b) dark and high contrast c) bright and high contrast d) bright and extreme contrast (direct sun).

In order to ensure the homogeneity of the reading task for all participants, its appearance on the monitor screen was standardized based on ergonomics of human-system interaction (ISO 9241-303). To avoid uncontrolled skimming or skipping that occurs naturally when reading a continuous paragraph [16] the text was carefully adjusted and set to the center of the monitor. The texts were chosen with a text difficulty that could be read in 1 minute.

Five volunteers were recruited in the age group of 20 to 30 of native German speakers amongst the Fraunhofer-ISE staff. Participants wore the EyeSeeCam to measure eye movements, and performed one trial per facade condition. Each trial consisted of five one-minute tasks as described above. The reading text was chosen randomly among six different paragraphs and displayed on the monitor at the beginning of each trail. The order chosen for the lighting condition sequence was randomized across participants to avoid any order effects. For each task (except for the 3rd event), eye-tracking parameters and subjective comfort ratings were assessed as dependent variables, the overall luminance distribution (resulting from each facade configuration) being considered the independent variable. Photometric quantities relevant to visual comfort were recorded continuously during each task. These measured quantities included: work plane illuminance (lux), illuminance (lux) on the monitor plane, vertical illuminance (lux) at the participant's eye, and luminance distribution (cd/m^2).

RESULTS

The effect of light condition sequence and task was addressed in a preliminary analysis of the eye movement data. This analysis will be restricted to the two extreme facade configurations for glare, namely the dark and high contrast and the bright and extreme contrast, further discussed below. Variance over the horizontal eye-in-head position signal ('horizontal variance') is likely to measure behavior with some more sensitivity than radial variance or vertical variance as window is always to left.

The illuminance measure at the eye level of participants for each facade configuration, have created a good diversity of perceived light and have kept a reasonable consistency through each trail (cf. Fig. 4) .

Horizontal variance increased in the tasks that invite participants to explore the surroundings ('think' and 'pause') as compared to the two tasks where gaze is restricted to the monitor ('read' and 'question') (cf. Fig. 5a). During the 'think' phase of the trials this increase is lower for the bright and extreme contrast facade. This suggests that horizontal variance of eye-in-head orientation is sensitive to the effects of light conditions on comfort.

To quantify this, a three-way ANOVA was performed on horizontal variance. The factors used were facade ('2: dark and high contrast', '4: bright and extreme contrast'), task ('read', 'wait', 'question' or 'pause') and eye ('left' or 'right').

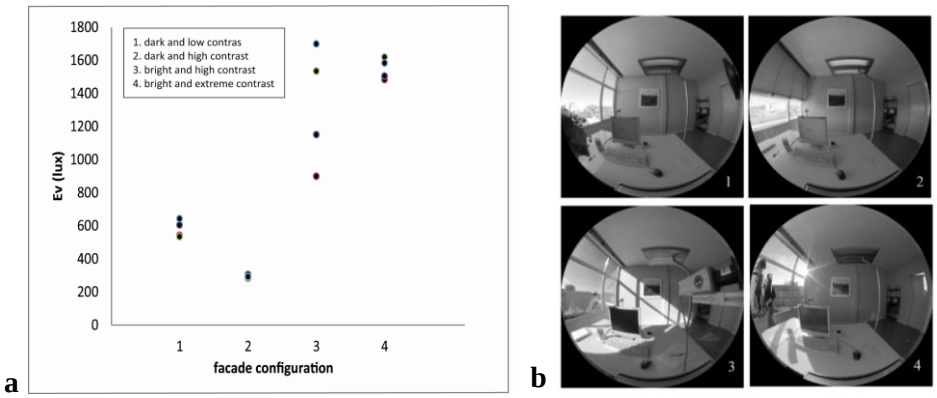

Figure 4: Measurement results a) Comparison between illuminance (lux) at the eye level of participants in all four facade configurations b) Representation of the four façade configurations

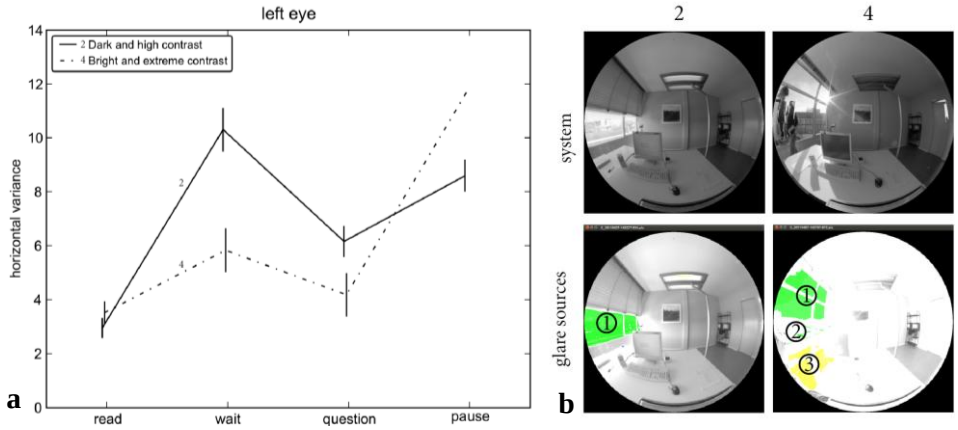

Figure 5: Analysis results a) Horizontal variance between two facade configurations: '2: dark and high contrast' '4: bright and extreme contrast' b) The two facade configurations and the glare sources within the field of view

There are main effects of facade ($F(1, 40) = 34.49$, $p<.001$) and task ($F(3, 40) = 70.94$, $p < .001$). There is no main effect of eye ($F(1, 40) = 3.04$, $p = .088$). There is a two-way three-way interactions (all $p > .643$). Interaction between facade and task ($F(12) = 17.99$, $p < .001$). There were no other two- or three-way interactions (all $p > .643$).

The effect of the facade means that eye-orientation varies depending on which system is used. A glare evaluation made by Evalglare, a Radiance-based tool [15], illustrates the distribution of glare sources in the field of view (cf. Fig. 5b) which shows that more glare sources in the field caused has created a different effect. The results also indicate that facade effect is different for different tasks. For example, when participants are reading, the variation of eye-orientation is mainly determined by the task, but when they are thinking or making a pause variation of eye-orientation is mainly determined by the facade.

DISCUSSION

This paper presents the preliminary results of a pilot study conducted to evaluate the potential of integrating eye-tracking methods as an objective insight to visual comfort assessment. An experiment was designed as a first step towards this end that demonstrated there are significant changes of eye movement behavior in different light settings. This method can reveal new perspectives in understanding discomfort glare.

The goal of this research is, ultimately, to refine our understanding of dependencies of view direction as a function of light distribution. To reach this goal, further detailed analysis needs to be done on the light distributions based on head-in-room orientation to allow for more precise assessment of comfort dependent gaze. Moreover, subjective glare ratings are also to be considered in order to have a better understanding of subjective assessments. The inclusion of measurable gaze in visual comfort studies creates a basis for identifying objective relationships between eye-movement patterns and perceived comfort, and between occupant response patterns and lighting conditions.

Findings will advance the state of the art in visual comfort assessment in interior spaces by providing new insights into the position index as a parameter that is - possibly - dependent on light distribution and forming a basis on which lighting conditions, glare perception and gaze patterns can be brought together.

ACKNOWLEDGEMENTS

The authors were supported by the Ecole Polytechnique Fédérale de Lausanne (EPFL), German Research Foundation (DFG) through grant EI 852/1 (WE) and research training unit GRK 885 (BMtH). The authors wish to thank Dr. Jan Wienold for his contribution and for granting access to the Fraunhofer ISE test modules and equipment.

REFERENCES

1. Boyce, P. R.: Human factors in lighting. London & New York: Taylor & Francis, 2004
2. Newsham, G., Arsenault, C., Veitch, J., Tosco, A., Duval, C.: Task lighting effects on office worker satisfaction and performance, and energy efficiency. LEUKOS, 1(4), 7-26, 2005
3. Guth: Brightness in Visual Field at Borderline between Comfort and Discomfort (BCD). National Technical Conference of the Illuminating Engineering Society, 1949
4. Wonwoo, K. H. H. : The position index of a glare source at the borderline between comfort and discomfort (BCD) in the whole visual field . Building and Environnent , 44, 1017-1023, 2009
5. Surry P. M., Hubalek S., Schierz, C.: A first step on eye movements in office settings.
6. Hubalek, S., Schierz, C.: LichtBlick – photometrical situation and eye movements at VDU work places. Lux Europa. Berlin, 2005
7. Itti L., Koch C., Niebur, E.: A model of saliency-based visual attention for rapid scene analysis. IEEE Transactions on Pattern Analysis and Machine Intelligence 20(11): pp. 1254-1259, 1998
8. Torralba, A., Oliva, A., Castelhano, M., Hendeson, J.M., Contextual guidance of eye movement and attention in real-world scenes: The role of global features in object search, Psychological Review 113, pp 766-786, 2006
9. Buswell, G. T.: How people look at pictures: A study of the psychology of perception in art. Chicago: University of Chicago Press, 1935
10. Yarbus, A. L.: Eye movements and vision. New York: Plenum Press, 1967
11. Einhäuser, W., Stout, J., Koch, C., Carter, O.: Pupil dilation reflects perceptual election and predicts subsequent stability in perceptual rivalry. Proceedings of the National Academy of Sciences USA (PNAS) 105(5), pp1704-1709, 2008
12. Schneider, E., Villgrattner, T., Vockeroth, J., Bartl, K., Kohlbecher, S., Bardins, S., Ulbrich, H., Brandt, T.: EyeSeeCam: an eye movement-driven head camera for the examination of natural visual exploration. Ann N Y Acad Sci 1164, pp 461-467, 2009
13. Ward, L., Shakespear, R.: Rendering with Radiance- The art of lighting visualization. Morgan kaufman Publishers, INC. , 1998
14. Inanichi, M.: Evaluation of high dynamic range photography as a luminance data acquisition system. Lighting research and Technology 38 (2), pp 123-136, 2006
15. Wienold, J., Christoferessen, J.: Evaluations methods and development of a new glare prediction model for daylight environments with the use of CCD cameras. Energy and Buildings, pp 743-757, 2006
16. Legge, G.E.: Psychophysics of reading in normal and low vision. Mahwah, New Jersey: Lawrence Erlbaum Associates. Inc., Publishers, 2006

GLAZING COLOUR TYPES, DAYLIGHT QUALITY, AROUSAL AND SWITCH-ON PATTERNS FOR ELECTRIC LIGHTS

H. Arsenault[1]; M. Hébert[2]; M.-C. Dubois[1]

1: Université Laval, École d'architecture, 1 Côte de la Fabrique, Québec (Québec), G1R 3V6, Canada, helene.arsenault.1@ulaval.ca, marie-claude.dubois@arc.ulaval.ca

2: Département ophtalmologie, d'oto-rhyno-laryngologie et chirurgie cervico-faciale, Faculté de Médecine, Université Laval, Québec (Québec), Canada, marc.hebert@crurlg.ulaval.ca

ABSTRACT

A study is presented about the effects of three glazing colour types (blue, neutral, bronze) of equal visual transmittance on daylight quality, self-reported arousal levels and switch-on patterns for electric lights. This study was carried out using a large scale model (1:4) of a typical office room where the luminous conditions were evaluated by subjective assessments of 36 participants (mean age 23.8 years), who had their upper body immersed in the model. The evaluation of daylight quality relied on a questionnaire assessing five key factors of light quality: 1) visual comfort; 2) naturality; 3) pleasantness; 4) precision and 5) light level. The questionnaire's oral and written questions were then analyzed using mixed model analyses, which revealed statistically significant higher scores for pleasantness (written questions p=0,003; combination of oral and written questions p=0,017), comfort (written questions p=0,015) and light level (written questions p=0,044) for the bronze glazing compared to the blue and neutral types. The neutral glazing was also preferred over the blue one for pleasantness (written questions p=0,021). The participants' arousal level was also evaluated at the beginning and end of each assessment session using the Karolinska Sleepiness Scale (KSS). A t-test performed on the KSS scores indicated that the level of arousal decreased in the presence of the blue glazing, which was contrary to the initial hypothesis. Finally, participants were also asked to switch-on the electric lights at the end of each assessment session and adjust the light level according to their own preference using a dimmer. This study did not reveal any significant effect of the glazing types on switch-on patterns and preferred illuminance level at this point, but this could be due to methodological limitations. Overall, the study shows that there is a preference for daylight filtered through bronze window glazing, confirming results of earlier research. The study also indicates that glazing colour type may have a significant effect on arousal with blue glass yielding a reduction in self-reported arousal level.

INTRODUCTION

In work environments, particularly in office buildings, one strong architectural trend of the last decades has been to design buildings with large glass facades. One consequence of this design trend is the wide spread of solar-protective glazing (reflective and tinted or heat-absorbing glass). Modern window glass is moreover nowadays coated with low-emissivity coatings in order to reduce radiative heat losses to the outside and the heating load of buildings. Coatings and tints distort the natural colour of daylight reaching the eye and skin of building inhabitants, which may have implications for the visual system's performance and perception, but also for all photobiology-related or so-called non-visual effects of light.

Earlier studies by Pineault et al [1] and Bülow-Hübe [2] have intended to measure the variation in visual comfort of occupants as well as the perceived light quality inside a room in

relation to glazing colour types. The rooms studied in those two cases were a living room and a bedroom. The present study considers instead an office space facing southeast. Earlier studies suggest that there is a preference for a warm shift [3, 4]. But the non visual photobiological effects of light on vigilance and performance are better achieved with cold light such as blue light [5]. Therefore, a colder (blue) and a warmer (bronze) shift were tested in the present research along with a neutral glazing which was slightly greenish in appearance.

METHOD

Experimental setting

The study was entirely carried out using a large scale model (1:4) of a typical office room with a single window facing southeast (Fig. 1). The 1:4 scale was selected in order to allow research participants to have their upper body completely immersed in the scaled room.

Figure 1: Photograph of the interior of the scaled office room taken from the viewpoint of the research participant. Starting from left to right: views with the blue, neutral and bronze glazing.

The scaled room was furnished as a typical office space. The walls and ceiling had a white mate finish that yielded to a surface reflectance of around 80%. The model was fixed on a table 86 cm high, which allowed the participants to be seated on a chair with only the upper body immersed (waist-height to head) while performing their evaluation. The model was also provided with a ceiling-mounted artificial lighting system consisting of six xenon lamps (serial number I-K303WH, CCT: 2700°K, 220 lumens per lamp using 20W xenon light bulbs) connected to a dimmer. The model's window, which measured 836 mm (width) by 465 mm (height) and was located at 230 mm from the floor, was divided into three sections surrounded by a white coloured 28 mm thick frame. The model box was inserted inside the opening of an existing window of the Architecture School building and directly exposed to the natural climate of Quebec City (46°48'N). The experiment was performed over a five-week period that was completed at the end of March 2010.

Glazing colour types

The three glass conditions that were evaluated had a similar visual transmittance but different dominant colours: blue (VT 0,526), neutral (VT 0,538) and bronze (VT 0,538) (see Fig. 2 for spectral transmittance properties). The three glass samples were provided by a local glass manufacturer, who certified that these were rather common glazing types often selected by architects in the region of Quebec City.

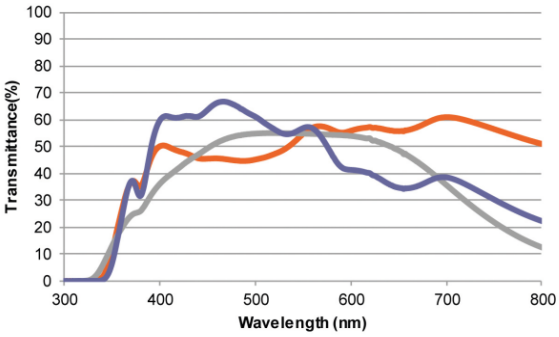

DESCRIPTION	U-VALUE (W/m²°K)	VISIBLE LIGHT Trans. %	Refl. Out %	Refl. In %
A- blue - single 6 mm	5,811	52,57	5,65	5,65
B- neutral - 4 mm+9 mm air gap+6 mm	1,65	53,75	12,98	18,05
C- mono - single 6 mm	5,822	53,82	5,46	5,3

Figure 2: Spectral transmittance of the glazing samples studied.

Experimental procedure

A total of 36 persons participated in the research (23 females, aged 18-45 years). They were recruited at Laval University during the months of February and March 2010. The participants did not present any major vision problems. They were all naive about the objectives of the study and were monetarily compensated for their participation.

Each experiment started with a verbal explanation of the procedures before the participant was instructed to sit in the model and assess subjectively its level of arousal using the validated 9 points Karolinska Sleepiness Scale (KSS [6]). Reading tasks were performed in order to allow the subject to adapt chromatically to the lighting conditions in the room for about five minutes. An oral questionnaire was then performed followed by a written questionnaire (see next section for details) before a second assessment of the level of arousal with the KSS scale was performed. At the end, the participant was instructed to adjust the electric lighting to the desired level using a dimmer. The same procedure was repeated, once with each glazing sample with the total experiment lasting 90 to 120 minutes including a 5 to 10 minutes pause between conditions to change the glazing samples while the participant was asked to go for a short walk indoors. The three glazing samples were evaluated by each participant using a counter balanced order of presentation (see [10] for details).

Oral and written questionnaires

The main interest of this research concerned the evaluation of light quality, as determined by five subjective factors such as: 1) visual comfort; 2) naturality; 3) pleasantness; 4) precision (of details and textures); 5) light level. Oral questions were used primarily to allow the participant to concentrate on the model's atmosphere without glancing back and forth at a questionnaire. The oral questionnaire focused on the ambient light conditions in the room, the general atmosphere of the room and finally, the perception of the environment as seen through the windows. Questions were answered out loud using a scale from 1 to 5, where 1 stands for "fully agree" (see [10] for details).

The written questionnaire contained a total of five groups of questions, which could be answered with five-degree Lickert scales with semantic opposites (Table 1). The participants had to circle a number from 1 to 5, where 1 corresponded to the most positive score and 5, to the most negative. Written questions concentrated on similar topics as the oral ones but were answered directly by the participants, in order to reconfirm their opinion. Opposite adjectives used in this exercise were selected from previous research in the field [2, 7, 8, 9]. Photometric measurements were also performed throughout the experiments (see [10] for details).

Factors related to each question	*Written questions and affirmations*						
	Question 1: Colors in the pictures appear to be :						
naturality	Natural	1	2	3	4	5	Artificial
precision	Precise	1	2	3	4	5	Blurry
pleasantness	Lively	1	2	3	4	5	Dull
	Question 2: Daylight in this office seams to be :						
naturality	Natural	1	2	3	4	5	Artificial
precision	Precise	1	2	3	4	5	Blurry
pleasentness	Pleasant	1	2	3	4	5	Unpleasant
visual comfort	Comfortable	1	2	3	4	5	Glaring
light level	Uniform	1	2	3	4	5	Variable
light level	Sufficient	1	2	3	4	5	Insufficient
visual comfort	Appropriate	1	2	3	4	5	Improper
	Question 3: Textures and appearances of objects in this office seam to be :						
naturality	Natural	1	2	3	4	5	Artificial
precision	Detailed	1	2	3	4	5	Undefined
naturality	True	1	2	3	4	5	Altered
precision	Precise	1	2	3	4	5	Blurry
precision	Visible	1	2	3	4	5	Invisible
	Question 4: Daylight's color appears:						
naturality	Natural	1	2	3	4	5	Artificial
pleasantness	Cheerful	1	2	3	4	5	Depressing
pleasantness	Welcoming	1	2	3	4	5	Drab
light level	Appropriate	1	2	3	4	5	Improper
	Question 5: In general, the ***ambiance created by the light*** in this office is :						
light level	Bright	1	2	3	4	5	Dark
visual comfort	Stimulating	1	2	3	4	5	Boring
pleasantness	Pleasant	1	2	3	4	5	Unpleasant
naturality	Natural	1	2	3	4	5	Artificial
pleasantness	Cheerful	1	2	3	4	5	Depressing
visual comfort	Comfortable	1	2	3	4	5	Glaring

Table 1: Written questionnaire (freely translated from French).

RESULTS

Mixed model analyses were used to compare groups of answers from the oral and written questions corresponding to the five qualitative factors (visual comfort; naturality; pleasantness; precision; light level). The results for the five factors are presented in Table 2.

Results corresponding to each factor were combined to obtain an average score for written questions, oral questions, and the two combined, for each of the glazing condition. A low mean score indicated that the participants were in favour of the affirmation, and a higher mean score indicated a tendency towards a negative opinion. Statistical analyses were performed using SPSS version 18.0.

Overall, the level of significance ended up to be higher for the written questions than for the oral questions. Significant results for the written questions were found for: visual comfort: p=0.015; pleasantness: p=0.003; light level: p=0.044 (Table 2). Since the oral and written questionnaires related to the same factors, the answers were combined and further analysed to validate the results. The combined answers remained significant for visual comfort (p=0.014) and pleasantness (p=0.015), see Table 2. In all cases, these results indicate that the bronze glass was perceived as being more comfortable for the eye and more pleasant than the two other samples.

Written questions regarding *pleasantness*					
glazing	compared with:	Mean Difference	Std. Error	df	Sig.a
blue glazing	neutral glazing	,264*	0,109	35,003	0,021
	bronze glazing	,410*	0,131	35,002	0,003
Written questions regarding *visual comfort*					
glazing	compared with:	Mean Difference	Std. Error	df	Sig.a
blue glazing	neutral glazing	0,16	0,12	35	0,192
	bronze glazing	,354*	0,139	35	0,015
Written questions regarding *light level*					
glazing	compared with:	Mean Difference	Std. Error	df	Sig.a
blue glazing	neutral glazing	0,111	0,109	35	0,314
	bronze glazing	,269*	0,129	35	0,044
Combined oral and written questions regarding *visual comfort*					
glazing	compared with:	Mean Difference	Std. Error	df	Sig.a
blue glazing	neutral glazing	0,158	0,119	35	0,192
	bronze glazing	,356*	0,137	35	0,014
Combined oral and written questions regarding *pleasantness*					
glazing	compared with:	Mean Difference	Std. Error	df	Sig.a
blue glazing	neutral glazing	0,172	0,097	34,997	0,084
	bronze glazing	,314*	0,122	34,998	0,015

Table 2: Results for the five factors analysis for the written questions and a combination of oral and written questions.

The average score from each of the five written questions (see Table 1), were further analyzed by comparing each group of questions (Q1 to Q5) performing Wilcox Son paired t-tests for each glazing type. Due to the multiple comparisons, significance was considered only with $p<0.017$. From these analyses, two groups of questions yielded to significant results in favor of the bronze glass. Those questions refer to the appearance and texture of the objects in the model (Q3, $p=0.013$) and to the general lighting ambiance inside the model (Q5, $p=0.004$). A trend was observed for two other questions; namely daylight color (Q4, $p=0.022$) and general daylight ambiance in the room (Q2, $p=0.02$), still favoring the bronze glazing (see Table 3).

pairs	glazing and questions (Q)	Mean	t	df	Sig. (2-tailed)	effect size
1	blue_Q1 - neutral_Q1	0,13806	1,385	35	0,175	0,052
2	blue_Q1 - bronze_Q1	0,29583	2,189	35	0,035	0,12
3	neutral_Q1 - bronze_Q1	0,15778	1,174	35	0,248	0,038
4	blue_Q2 - neutral_Q2	0,12583	1,196	35	0,24	0,039
5	blue_Q2 - bronze_Q2	0,29639	2,441	35	0,02	0,145
6	neutral_Q2 - bronze_Q2	0,17056	1,519	35	0,138	0,062
7	blue_Q3 - neutral_Q3	0,15	1,477	35	0,149	0,059
8	blue_Q3 - bronze_Q3	0,24571	2,628	34	0,013	0,165
9	neutral_Q3 - bronze_Q3	0,11429	1,451	34	0,156	0,057
10	blue_Q4 - neutral_Q4	0,23611	2,314	35	0,027	0,133
11	blue_Q4 - bronze_Q4	0,30714	2,399	34	0,022	0,141
12	neutral_Q4 - bronze_Q4	0,07857	0,578	34	0,567	0,009
13	blue_Q5 - neutral_Q5	0,17139	1,638	35	0,11	0,071
14	blue_Q5 - bronze_Q5	0,35139	3,052	35	0,004	0,21
15	neutral_Q5 - bronze_Q5	0,18	1,525	35	0,136	0,062

Table 3: T-test results from the five groups of written questions: Q1-color appearance; Q2-daylight in general; Q3- appearance & textures; Q4-daylight's colour; Q5-general ambiance.

The participant's level of arousal recorded at the beginning and end of each evaluation was compared using a paired t-test analysis. Significant results ($p<0,05$) indicate that when the blue glazing was being tested, the arousal level decreased slightly over the evaluation period ($p=0,042$), see Table 4.

Pair	glazing - time 1 and 2	Mean	t	df	Sig. (2-tailed)
1	blue_t1 - blue_t2	-0,389	-2,116	35	0,042
2	neutral_t1 - neutral_t2	0	0	35	1
3	bronze_t1 - bronze_t2	0,028	0,167	35	0,869

Table 4: Analysis of arousal level with KSS scale at time 1 and time 2 of the experiment.

The adjustment of electric lighting, recorded at the end of each glass evaluation, was analysed with a logistic regression, but no significant results were obtained.

DISCUSSION

Results for the qualitative factors analysis indicate a preference for the bronze glass, in terms of visual comfort, pleasantness and light level. Results from the grouped written questions indicate that in presence of the bronze glass, the appearance and textures of the objects in the room and the general lighting ambiance were perceived as more natural and pleasant. Other results from the written questions regarding daylight's colour and daylight presence in general indicate again a tendency in favour of the bronze glazing. Finally, the participant's self-reported level of arousal had a slight decrease with the blue glazing. We believe that the latter results could be related to the fact that the eye could perceive a bluish ambient environment as less bright and therefore less stimulating, since in daylight, the eye is most sensitive to green-yellow light but not much to blue light. But, in that case, we would have expected participants to increase the level of light at the end of the study, which was not the case: the adjustment of the lighting level was not significant during this research. An other explanation for this could be that visible light transmittance of the three glass samples was very similar; therefore the participants generally felt that the lighting was sufficient inside the model.

ACKNOWLEDGEMENTS

The authors thank the research participants as well as Luc Joubert, Quebec, Canada, for his precious financial contribution in this project.

REFERENCES

1. Pineault N, Dubois M-C, Demers CMH, Briche M (2008). Effect of coated and tinted glazing on daylight quality in a residential space: experimental study in a scale model. *Proc. of Challenging Glass Conference,* TU Delft, Holland, May 22nd 2008.
2. Bülow-Hübe H (1995). Subjective reactions to daylight in rooms: Effect of using low-emittance coatings on windows. *Lighting Res and Technol;* 27 (1):37-44.
3. Boyce PR, Beckstead JW, Gutkowski JM, Fan J, Strobel RW (1992). *Brightness-enhancing glazing: perception, performance and energy.* Report from MSR Scientific to Public Works Canada, Ottawa: Public Works Canada.
4. Cuttle K (1979). Subjective assessments of the appearance of special performance glazing in office. *Lighting Res and Technol;* 11 (3):140-149.
5. Brainard GC, Hanifin JP, Greeson JM, Byrne B, Glickman G, Gerner E, Rollag MD (2001). Action spectrum for melatonin regulation in humans: Evidence for a novel circadian photoreceptor. *Journal of Neuroscience*; 21:6405–6412.
6. Kaida K, Takahashi M, Akerstedt T, Nakata A, Otsuka Y, Haratani T, and Fukasawa K (2006). Validation of the Karolinska sleepiness scale against performance and EEG variables. *Clinical Neurophysiology;* 117:1574-1581.
7. Dubois M-C, Cantin F & Johnsen K (2007). The effect of coated glazing on visual perception: A pilot study using scale models. *Lighting Res and Technol;* 39 (3):283–304.
8. Pineault N & Dubois M-C (2008). Effect of Window Glazing Type on Daylight Quality: Scale Model Study of a Living Room under Natural Sky. *LEUKOS: Journal of the Illum. Eng. Soc. of N. America;* 5 (2). Online.
9. Küller R (1991). Environmental assessment from a neuropsychological perspective. In: T. Gärling T & Evans GW. (Eds). *Environment, cognition, and action: An integrated approach.* Oxford University Press: New York. pp. 111-147.
10. Arsenault H, Hébert M & Dubois M-C (2011). Effects of glazing colour types on daylight quality, arousal and switch-on patterns for electric lights in a scaled office room. *Glass Performance Days Conference,* Tampere (Finland), 17-20 June.

PROPERTIES AND PERFORMANCE INDICATORS OF VIRTUAL NATURAL LIGHTING SOLUTIONS

R.A. Mangkuto; M.B.C. Aries; E.J. van Loenen; J.L.M. Hensen

Eindhoven University of Technology, Department of the Built Environment

Den Dolech 2, 5612 AZ Eindhoven, the Netherlands

ABSTRACT

Several studies have shown that in the built environment, natural light is highly preferred over electrical lighting for its positive effects on user satisfaction, health, and the potential on saving electrical energy. However, natural light is highly variable and limited by time and space. For example, significant fractions of working population in the world do their work during nighttime. Shift workers experience various discomfort issues, and increased long-term risk of some types of cancer due to a lack of synchronisation between the shift work schedule and the worker's light-dark cycle. Many buildings also have several inside spaces, while admission of natural light into work places is strongly suggested.

A possible way to overcome this problem is to develop and apply a Virtual Natural Lighting Solution (VNLS), which is a system that provides virtual natural light, with all of its qualities, which can be integrated inside new and/or existing buildings. One of the first challenges in developing such solutions is modelling their behaviour and predicting their impact on spatial use and performance of buildings. In order to model a VNLS, it is necessary to understand the relevant properties that the solution itself should have, as well as the relevant performance indicators which show how the solution affects performance of buildings where it is applied.

For the case of VNLS, the performance indicators of a building will be described in terms of visual comfort, space availability, thermal comfort, and energy consumption. A study is presented, based on literature reviews, in which the properties of currently known artificial windows and skylights are compared to that of real ones. The comparison shows that each existing solutions addresses a subset of all aspects required for a VNLS. The paper concludes by summarising the relevant properties and performance indicators with their expected range of values, which will be the input for developing a computational model of VNLS.

INTRODUCTION

Human beings have a strong preference for natural light. Several studies have shown that natural light is highly preferred over electrical lighting in the built environment for its positive effects on user satisfaction and health, (e.g., [1, 2]); as well as for the potential to save on electrical energy by reducing artificial lighting consumption by 50% to 80% (e.g., [3, 4]).

However, natural light is highly variable and limited in time and space. For example, significant fractions of the working population in the world do their work during nighttime [5, 6]. Night shift workers experience various discomfort issues and even increased long-term risk of some types of cancer due to a lack of synchronisation between the shift work schedule and the worker's light–dark cycle [7]. Furthermore, many office buildings have inside spaces which cannot be used as working space, because, for example according to Dutch regulations, admission of natural light into work places is strongly recommended.

A possible way to overcome those problems is to develop and apply a Virtual Natural Lighting Solution (VNLS), which is a system that ideally has the possibility to provide virtual natural lighting, with all of its qualities, including a realistic outside scene view, which can be applied and integrated inside new and/or existing buildings. One of the first challenges in developing such solutions is modelling their behaviour, and predicting their impact on building performance. Therefore, it is necessary to understand two main ideas: (1) describing the relevant properties that the solution itself should have and (2) describing the relevant performance indicators which show how the solution affects performance of buildings where the solution is applied. The objective of this paper is to classify the relevant properties and performance indicators and their expected range of values, in relation with VNLS. The properties are also used as mean for comparison, based on literature reviews, of the currently known artificial light windows and artificial view windows and skylights.

PROPERTIES REQUIREMENT OF VNLS

In the design stage of VNLS, it is important for product designers and developers to know what properties are required to present in the solution. The properties can be determined from that of the real natural light solution (i.e., window). Related to daylight and view, Boerstra [8] and Hellinga and Bruin-Hordijk [9] proposed quality levels for themes that influence visual comfort. Depth perception cues, i.e., movement parallax, occlusion, and blur, are also taken into account based on experimental research of IJsstelsteijn et al. [10]. Some of the quality levels are given in A, B, C, and D, which respectively represents the best, good, sufficient, and insufficient choice.

Table 1 summarises the requirement of VNLS properties as follows. The requirement can be taken as a general guideline, and continuous improvements are consequently needed.

Properties	Symbol	Unit	Possible range	Target range
Light quality				
Surface luminance	L_s	cd/m^2	0 ~ 8000	125 ~ 6000
Correlated colour temperature	CCT	K	2600 ~ 12000	2700 ~ 12000
Colour quality scale	CQS	-	0 ~ 100	82 ~ 98
Directionality	DIR	-	A, B, C, D	A or B
View quality				
Presence of green, sky, distant objects [9]	GSD	-	A, B, C, D	A or B
Information [8, 9]	INF	-	A, B, C, D	A or B
Complexity and coherence [8, 9]	ORG	-	A, B, C, D	A or B
Depth perception cues [10]	DPC	-	A, B, C, D	A or B

Table 1: Requirement of VNLS properties.

PERFORMANCE INDICATORS OF A BUILDING WITH VNLS

In order to model VNLS in a building, it is necessary to gain a complete understanding of all indicators which are relevant to describe the performance of the system. The term performance indicator (PI) will be used, which is a quantified expression of performance, having a range, definition, unit and a direction of increasing or decreasing value, in order to enable more structured negotiation between stakeholders, so that the design task can be expressed in the same set of criteria [11]. The indicators can be based on the principles of physics (“hard” indicators) or on environmental psychology (“soft” indicators) [12].

In the case of natural light, Dubois [13] suggested a number of simple PIs, i.e. workplane illuminance, illuminance uniformity, and luminance ratios. For design purposes, Reinhart et

al. [14] suggested illuminance-based dynamic performance metrics such as daylight autonomy, continuous daylight autonomy, and useful daylight index. Pati et al. [12] suggested several PIs related to general work place lighting, which were classified in terms of energy efficacy, task lighting, view to outside, and visual comfort. Other aspects are also considered to describe indicators of the work environment, in terms of thermal comfort and energy.

For the case of a building with VNLS, the relevant PIs can be classified in the following terms.

1. Visual comfort: workplane or task illuminance, illuminance uniformity on the workplane, task-to-surround luminance ratios [14], task-to-wall luminance ratio, directional-to-diffuse luminance ratio [14], and unified glare rating [16].
2. Space availability: virtual criterion rating and space availability ratio (discussed below).
3. Thermal comfort: predicted mean vote, percentage people dissatisfied and summed weighted overheating hours [17].
4. Energy consumption: total annual electrical energy demand and total annual heating and cooling energy demands [8, 18].

PI	Symbol	Unit	Range	Target
Visual comfort				
Task illuminance	E_{task}	lx	0 ~ 25000	200 ~ 800
Illum. uniformity on workplane	U	-	0 ~ 1	≥ 0.6
Task-to-surround lum. ratio	$LR_{t\text{-}s}$	-	0 ~ ∞	1:20 ~ 20:1
Task-to-wall luminance ratio	$LR_{t\text{-}w}$	-	0 ~ ∞	10:1 ~ 40:1
Directional-to-diffuse lum. ratio	$LR_{d\text{-}d}$	-	0 ~ ∞	1.4:1 ~ 2.5:1
Unified glare rating	UGR	-	10 ~ 30	≤ 16
Space availability				
Virtual criterion rating	VCR	%	0 ~ 100	≥ 70
Space availability ratio	SAR	-	0 ~ ∞	*to be refined*
Thermal comfort				
Predicted mean vote	PMV	-	–3 ~ +3	–0.5 ~ +0.5
Predicted percentage of dissatisfied	PPD	%	0 ~ 100	5 ~ 10
Summed weighted overheating hours	WOH-∑	hrs	0 ~ 375	≤ 225
Energy consumption				
Total electrical energy demand	E_{ed}	kWh/m^2/yr	0 ~ 20	≤ 15
Total heating energy demand	E_{hd}	kWh/m^2/yr	50 ~ 500	≤ 325
Total cooling energy demand	E_{cd}	kWh/m^2/yr	50 ~ 250	≤ 60

Table 2: Performance indicators for a building with VNLS.

For visual comfort, an image-based lighting analysis procedure and tool called Virtual Lighting Laboratory (VLL) was introduced by Inanici and Navvab [15]. VLL is a computer environment where the user has been provided with matrices of per pixel data of luminance and illuminance values extracted from High Dynamic Range (HDR) images, processed through mathematical and statistical operations to perform more detail lighting analysis.

As suggested by Inanici [19], per pixel data analysis allows even more detailed study. For instance, it can be used to calculate a PI which quantifies the probability that a specific criterion (such as luminance, illuminance, and contrast) is met within a defined space or area [20]. The PI is called Virtual Criterion Rating (VCR), which is defined as:

$$\text{VCR} = \frac{\text{Number of pixels satisfying the criterion in a space / on a surface}}{\text{Total number of pixels}} \times 100\% \qquad (1)$$

As a guideline, it is suggested to study the task illuminance values to ensure that they are between 2/3 and 4/3 of the target values. It is suggested to aim for achieving the 2/3 to 4/3 range in 90 percent of the task locations [19].

Related to the VNLS application, the VCR can be applied to indicate how much additional space can be used for working (e.g. on paper or computer task), due to enhancement of the lighting and view quality, after installation of the VNLS in a given building space. The idea is to show the comparison between the VCR of the given space before and after the installation, in terms of task illuminance and surface luminance. Therefore, a new PI is proposed, namely Space Availability Ratio (SAR) in a given space at a given time, which is defined as:

$$\text{SAR} = \frac{\text{VCR in a space after the VNLS installation}}{\text{VCR in a space before the VNLS installation}} \quad (2)$$

PROPERTIES COMPARISON OF VNLS PRECURSORS

Several products have been developed to provide, or to mimic some aspects of real natural lighting solutions (e.g., windows and skylights). Based on their main function, the early attempts to approach VNLS (precursors) can be classified into two types: one that is dedicated mainly to provide "virtual" natural view (usually outdoor scenery); and one mainly to provide "virtual" natural light (for quality lighting or curing diseases).

Table 3 presents comparisons of some properties of some selected existing precursors of VNLS. The PIs presented in the Table 2 are not yet available to be compared for the precursors, since it requires a selected building case study followed by applications of modelling and simulation, which will be the next step to be taken.

Properties / Features	Light quality				View quality			
	L_s (cd/m^2)	CCT (K)	CQS	DIR	GSD	INF	ORG	DPC
Natural view								
Static, backlit transparent photos on lamp's surface	≤ 1200	2700 ~6500	64~80	C~D	A~C	B~D	A~C	B~C
Projection simulating sunlight and shadows	≤ 500	6500	64~80	A~C	B~C	D	C~D	C~D
Luminous / backlit translucent material	≤ 2500	2700 ~6500	82~92	A~D	C~D	D	D	C~D
Dynamic images on arrayed monitor	≤ 2500	2700 ~6500	82~92	D	A~B	B~D	A~C	B~C
Real-time dynamic images without parallax	≤ 1000	6500	82~92	D	A~B	A~B	A~B	B~C
Dynamic images with parallax	≤ 1000	6500	82~92	D	A~B	A~B	A~B	A~B
3D technique with parallax	≤ 1000	6500	82~92	D	A~B	A~B	A~B	A~B
Natural light								
No images, provide very bright light	≤ 8000	2700 ~6500	82~92	D	D	D	D	D
No images, provide enhanced blue light	≤ 250	6500	82~92	D	D	D	D	D

No images, provide gradual light levels	≤ 2500	2700 ~6500	82~92	D	D	D	D	D
LED light	≤ 50	2700	82~92	D	D	D	D	D
Fluorescent light	≤ 500	6500	64~80	C	D	D	D	D

Table 3: Comparison of properties of some VNLS precursors.

DISCUSSION

Based on the properties comparison in Table 3, it is clear that existing virtual natural view and light solutions have their own limitations. The virtual natural light solutions do not provide any viewed image, and therefore obtain the lowest score for the view quality properties. The virtual natural view solutions do provide viewed image with different levels of quality. The presence of green, sky, and distant object on the view can be provided either in static or dynamic solutions. For the information quality, the biggest challenge is to provide a constantly changing impression of the displayed information. The static solutions will mostly fail, since they only provide still image without any view variation. The dynamic solutions are also better in providing organisation (i.e., more detailed image) and depth perception cues.

The depth perception cues are determined by movement parallax, occlusion, and blur effects [10]. The movement parallax comes out as the hardest effect to imitate. The static solutions definitely cannot give any movement parallax; neither can the dynamic solutions which use normal large monitor display. The technique using head tracker for the viewer position and/or novel 3D television set should be applied to provide the effect, even though it seems to be still limited to one or two viewers.

For the lighting quality, it is very difficult to provide an artificial light source that can give 25000 lx of illuminance on workplane, without combining several sources. Most virtual windows or displays with light source can provide up to 5000 lx illuminance near the source, while most monitor display can provide up to 1000 lx. Virtual windows, which normally use lamps behind an image-covered translucent screen, generate light with CCT between 2700 and 6500 K. Typical monitor displays generate light with CCT of 6500 K.

Directionality of the incoming light (i.e., the balance between directional and diffuse component) is also an issue to be considered. Directionality can be evaluated by observing the light intensity polar diagram. Most virtual windows and large monitor displays will give almost only a diffuse light. Nevertheless, it is more meaningful to evaluate the effect on the luminous environment where the solution is placed, which will be discussed in later stages with the other performance indicators (PIs).

The PIs that belong to space availability, thermal comfort, and energy consumption are not yet available to be compared for the precursors, since they are very dependent on the building environment where the solutions are placed in. Therefore, to evaluate different PIs of the existing precursors and even non-existing solution, a building environment should be taken as case study. Again, comparisons are to be performed, with reference to the real windows. To this purpose, computational modeling and simulation will be used for steering the innovation process and early feasibility testing of the VNLS. Computational modeling is chosen since it comes with considerably lower required time and cost than real prototyping.

CONCLUSION

For the case of VNLS, the required properies can be given in terms of light and view quality. Performance indicators of a building with VNLS are currently classified in terms of: visual comfort (workplane or task illuminance, illuminance uniformity, task-to-surround luminance

ratios, directional-to-diffuse luminance ratio, and unified glare rating); space availability (virtual criterion rating and space availability ratio); thermal comfort (predicted mean vote, percentage people dissatisfied, and summed weighted overheating hours); and energy consumption (total annual electrical energy demand and total annual heating and cooling energy demands). Comparisons of some properties of some selected existing precursors of VNLS are presented. The completeness of the PIs for VNLS cannot be fully tested yet, since a specific architectural conditions is required. For further research, a building environment will be defined as a case study, to completely evaluate PIs of the existing precursors, and compare to the real windows. Computational modeling and simulation will be used for this purpose.

REFERENCES

1. Farley, K. M. J., Veitch, J. A.: A Room with a View: A Review of the Effects of Window on Work and Well-being. Rep. No. RR-136, IRC Research, 2001.
2. Aries, M.B.C., Veitch, J.A., Newsham, G.R.: Windows, View, and Office Characteristics Predict Physical and Psychological Discomfort. Journal of Environmental Psychology, 30(4), pp 533-541, 2010.
3. Bodart, M., De Herde, A.: Global energy savings in offices buildings by the use of daylighting. Energy and Buildings, Vol 34(5), pp 421-429, 2002.
4. Mardaljevic, J., Heschong, L., Lee, E.: Daylight metrics and energy savings. Lighting Research Technology, Vol 41(3), pp 261-283, 2009.
5. Lockley, S.W.: Circadian Rhythms: Influence of Light in Humans. Encyclopedia of Neuroscience, Vol 2, pp 971-988, 2009.
6. Stevens, R.G.: Working against our endogenous circadian clock: Breast cancer and electric lighting in the modern world. Journal of Mutation Research/Genetic Toxicology and Environmental Mutagenesis, Vol 680 (1-2), pp 106-108, 2009.
7. Blask, D.E.: Melatonin, sleep disturbance and cancer risk. Sleep Medicine Reviews, Vol 13 (2009), pp 257-264, 2009.
8. Boerstra, A.C.: Arbo-Informatieblad 24: Binnenmilieu. Den Haag: Sdu Uitgevers, 2006. [in Dutch: Recommendations for working condition: Indoor environment]
9. Hellinga H.Y., Bruin-Hordijk G.Y. de: A new method for the analysis of daylight access and view out. Proceedings of Lux Europa, Istanbul, Turkey, pp 1-8, 2009.
10. IJsstelsteijn W.A., Oosting W., Vogels I.M., de Kort Y.A.W., van Loenen E.: A room with a cue: The efficacy of movement parallax, occlusion, and blur in creating a virtual window. Presence: Teleoperators and Virtual Environments, Vol 17(3), pp 269-282, 2008.
11. Houben, J.H.V.: Computational Innovation Steering: Simulation-assisted performance improvement of innovative buildings and systems. MSc Thesis, Eindhoven University of Technology, 2010.
12. Pati, D., Park, C., Augenbroe, G.: Roles of quantified expressions of building performance assessment in facility procurement and management. Building and Environment, Vol 44(4), pp 773-784, 2009.
13. Dubois, M.: Shading devices and daylight quality: an evaluation based on simple performance. Lighting Research and Technology, Vol 35(1), pp 61-76, 2003.
14. Reinhart, C.F., Mardaljevic, J., Rogers, Z.: Dynamic daylight performance metrics for sustainable building design. Leukos, Vol 3(1), pp 1-25, 2006.
15. Inanici, M.N., Navvab, M.: The Virtual Lighting Laboratory: Per-pixel Luminance Data Analysis. Leukos, Vol 3(2), pp 89-104, 2006.
16. Commission Internationale de l'Éclairage (International Commission of Illumination): Discomfort Glare in the Interior Lighting. Technical committee TC-3.13, Division 4, Interior Environment and Lighting Design, Vienna, Austria, 1992.
17. Van der Linden, K., Boerstra, A.C., Raue, A.K., Kurvers, S.R: Thermal indoor climate building performance characterized by human comfort response. Energy and Buildings, Vol 34 (2002), pp 737-744, 2002.
18. Smaling, R., Weck, O.: Assessing risks and opportunities of technology infusion in systems design. Systems Engineering, Vol 10(1), pp 1-25, 2007.
19. Inanici, M.N.: Transformations of high dynamic images into virtual lighting laboratory. Proceedings 8th International IBPSA Conference, Eindhoven, the Netherlands, pp 539-546, 2003.
20. Rea, M. (editor): The IESNA Lighting Handbook, 9th ed. The Illuminating Engineering Society of North America, New York, USA, 2002.

CLIMATE-BASED DAYLIGHT PERFORMANCE: BALANCING VISUAL AND NON-VISUAL ASPECTS OF LIGHT INPUT

M. Andersen[1], J. Mardaljevic[2], Nicolas Roy[3], Jens Christoffersen[3]

1: Interdisciplinary Laboratory of Performance-Integrated Design (LIPID), Ecole Polytechnique Fédérale de Lausanne (EPFL), Lausanne, Switzerland

2: IESD, De Montfort University, Leicester, UK

3: VELUX A/S, Horsholm, Denmark

ABSTRACT

This study uses a domestic dwelling as the setting to investigate and explore the applicability of daylighting metrics for residential buildings, including the formulation of metrics for non-visual effects. The simulation approach used to generate the performance data from which the metrics are derived is called climate-based daylight modelling (CBDM). This approach delivers predictions of various luminous quantities using sun and sky conditions that are derived from standardised annual meteorological datasets.

Although there are uncertainties regarding the precise calibration, there is now sufficient empirical data to parameterise models that also simulate the non-visual aspects of daylight, e.g. for circadian entrainment and a general sense of 'alertness'. For these non-visual aspects, vertical illuminance at the eye was predicted using a modified climate-based daylight modelling approach. In the paper, we consider what relation there might be between the three aspects of daylight provision and if these relations appear to be complementary or conflicting in nature: for task; to reduce electric lighting usage; and, for non-visual effects. The implications for future building guidelines for daylighting are also discussed.

INTRODUCTION

It is now widely accepted that the standard method for daylighting evaluation - the daylight factor - is due for replacement with metrics founded on absolute values for luminous quantities predicted over the course of a full year using sun and sky conditions derived from standardised climate files [1]. The move to more realistic measures of daylighting introduces significant levels of additional complexity in both the simulation of the luminous quantities, and the reduction of the simulation data to readily intelligible metrics. The simulation component, at least for buildings with standard glazing materials, is now reasonably well understood and is widely known as climate-based daylight modelling (CBDM). Typically, these metrics address daylight provision for task and electric lighting usage [2,3]. There is no consensus however on the composition of the metrics, and their formulation is an ongoing area of active research.

This study uses a domestic dwelling as the setting to investigate and explore the applicability of daylighting metrics for residential buildings. In addition to daylighting provision for task and disclosing the potential for reducing electric lighting usage, we also investigate the formulation of metrics for non-visual effects such as entrainment of the circadian system, which is the focus for this paper. This fomulation is built upon a methodology developed by Pechacek, Andersen & Lockley [4].

Previously thought of mainly in terms of task illumination and aesthetics/design, it is now believed that daylight in buildings might serve another purpose through non-visual effects. In addition to building occupants having subjective preferences for daylit spaces, it has been firmly established that daylight has measurable biochemical effects on the human body, in particular with respect to maintaining a healthy sleep-wake cycle [5]. Recent findings on these non-visual aspects of occupant light exposure have led to a reconsideration of the function of daylight in buildings. Evidence is indeed suggestive of links between daylight exposure and both health and productivity. The duration, intensity and spectrum of the light received at the eye are the principal factors determining the suppression in the production of melatonin by the pineal gland (mostly during nightime), and thus a key component in the entrainment of the circadian cycle - the maintaining of which is believed to have significant short and long-term beneficial health effects [5]. Another important factor is the time of day when the light is applied. Compared to the luminous efficiency function of the eye, which has a peak value at 555nm, the action spectrum for the suppression of melatonin is known to be shifted to the blue end of the spectrum [6]. The body of empirical data from photobiology studies is now sufficient to elaborate preliminary non-visual lighting evaluation methods, which has become a relevant quantity to consider when assessing the overall performance of a space. The various modelling procedures and assumptions that were developed for this purpose are described in the paper, and a novel means of visualising the 'circadian potential' of a point in space is presented.

GENERAL METHODOLOGY

In this study, conventional climate-based daylight modelling [2] is combined with a refined approach for occupant exposure to non-visual effects. These refinements include accounting for the variation in spectrum between light from 'grey' overcast skies, 'clear blue' skies and 'warm' direct beam sunlight.

The setting, a residential building with and without skylights, was evaluated using climate-based daylight modelling for all 32 combinations of eight European climates (Hamburg (D), Madrid (E), Paris (F), London (UK), Rome (I), Warsaw (PL), Moscow (RU) and Ostersund (SE)) and four building orientations (N, S, E, W). Daylight for task was assessed using the Useful Daylight Illuminance (UDI) schema [7]. Electrical lighting usage was predicted on the basis of typical schedules and daylight availability using the RT 2005 switching model [8]. For non-visual effects, the eye-level vertical illuminance was predicted at sixteen locations, and at each one, for four cardinal view directions to account for the arbitrary nature of view direction in a residential space.

The CBDM approach used in this study delivers predictions of various luminous quantities using sun and sky conditions that are derived from standardised annual meteorological datasets. Thus the performance data accounts for the prevailing local climate, the building orientation and light from both the sun and the sky [2].

However, their application in a model for non-visual effects (N-VEs) requires that the spectral characteristics of the various sources (i.e. direct beam, overcast skylight and light from a clear blue sky) be inferred from values in the basic climate data. It also requires new threshold values to be determined, which would be relevant to generating non-visual effects yet would be based on traditional building simulation methods.

INCORPORATING NON-VISUAL EFFECTS

Overall, the proposed approach uses outcomes of photobiology research to define threshold values for illumination in terms of spectrum, intensity, and timing of light at the human eye, and translates these into goals for simulation and, ultimately, into goals for building design.

Relevant findings from the photobiology field

An action spectrum was determined for our non-visual circadian photoreceptor system (melanopsin) by Brainard et al in 2001 [6]. It led to the sensitivity curve illustrated in Figure 1(a) (for now called C(λ)) that peaks in the blue region of the spectrum and is represented alongside our well-known photopic curve V(λ).

On the other hand, threshold photon densities (photons/cm^2 s^{-1} on the retinal surface) have been found to be necessary to have a significant effect on circadian photoreception, and a dose-response curve was determined by Cajochen et al in 2000 for subjective alertness during a prolonged night-time exposure to polychromatic light [9]. This particular study found that a (visual) illuminance of about 300 lux[1] was required to achieve a 100% subjective alertness effect when the light source was fluorescent lighting (4100K) and exposure duration was 6.5 hours. As of yet, very few alertness studies for polychromatic light are available during daytime exposure and none provides a dose-response curve. One daytime study of reference is the one conducted by Phipps-Nelson et al in 2003 [10] that compares the effect on alertness of daytime exposure to bright (1000 lux) and dim (< 5 lux) light for 5 hours, for slightly sleep-deprived subjects and using fluorescent lighting. Unlike previous related studies [11,12] that used higher `dim' light levels (50 lux e.g.), this one reported a significant effect of bright light exposure during daytime, probably due to the combination of having particularly dim comparison levels and having sleep-deprived subjects.

Light timing and exposure history have a critical influence on how the circadian system is stimulated and how the circadian clock is reset or can be slightly shifted, such as to help combat jet-lag for example. Research in this area indicates that the above-mentioned thresholds will be strongly dependent on the duration of light exposure. This discussion being beyond the scope of the present paper and not advanced enough to provide more tangible hypotheses, we will use these thresholds as indicative exposure levels for which one might expect a non-visual effect (alertness increase e.g.) during nighttime and daytime, respectively.

The following sections will describe how these selected findings in the photobiology field can be applied to building simulation and the assessment of the `circadian potential' of a space.

Spectral properties and conversion factors

The spectral properties of the daylight are important because the action spectrum C(λ) for the non-visual photosensitive ganglion cells in the eye is different from the visual sensitivity curve V(λ). Thus, the vertical daylight illuminance assessed at the eye for a person inside a building has to be considered as a set of individual contributions from direct sunlight, diffuse daylight from the blue sky and diffuse daylight from an overcast sky, but also account for the spectral alteration of light when transmitted through glass and when reflected on internal & external surfaces before reaching the eye.

As a first approximation, we will consider that all surfaces and glazings that daylight will encounter are spectrally neutral (grey). While this is obviously a rough assumption, it becomes acceptable if the aim is – like here and in [4] where this point was discussed previously - to build a methodology rather than trying to get to quantitative conclusions. Thus, the calculated vertical illuminance only has to be split into the different daylight 'sources' involved because they have a distinct relative spectra. To convert climate-based vertical illuminance calculations into their equivalent 'circadian-lux' (based on the C(λ) action spectrum), we use the approach described [4] and illustrated in Figure 1(a). We can then use this relationship to derive preliminary 'circadian-lux' thresholds from photobiology findings.

[1] Based on a visual reading of Fig 5 (left), p. 81 in [10].

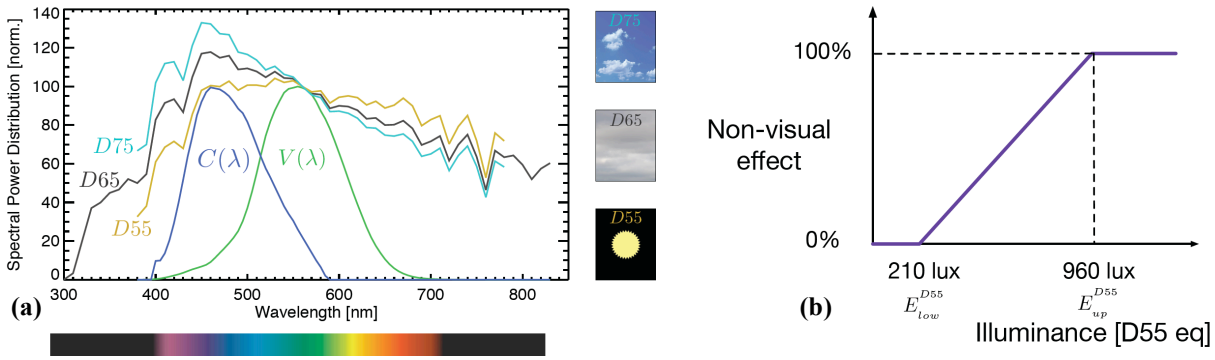

Figure 1: (a) Spectral power distribution for CIE daylight illuminants and sensitivity curves V(λ) and C(λ) (b) Ramp function for likelihood of non-visual effect.

Intensity of illumination

Until these more reliable thresholds are determined, and the duration of exposure is more reliably included, we can prospectively use the dose response curve from the night-time Cajochen study [9] in combination with the daytime Phipps-Nelson results [10] as a lower and an upper bound, respectively, for alertness effects: one can reasonably assume that the illuminance threshold required to have a significant effect on alertness during daytime will be at least as high as what was found out during night-time. On the other hand, one can also reasonably assume that if an effect was found during daytime with a given illuminance, those effects will also be observed with a higher illuminance. One should note that the Phipps-Nelson study was run with slightly sleep-deprived subjects but the argument for now is more on the method than the exact values. In both cases, fluorescent tubes were used as the light source (approximated as Illuminant F7), so we can determine that the threshold for a 100% alerting effect would be equivalent to an illuminance at the eye of 210 lux, 190 lux, and 180 lux for Illuminant D55 (used for sunlight), D65 (used for overcast sky light) and D75 (used for clear (blue) sky light) respectively, based on the 'circadian-equivalent' relationships discussed in [4]. As one would expect, the bluer spectrum corresponds to the lowest equivalent illuminance threshold.

We then have all the data necessary to determine the 'circadian' illuminance with daylight that would be equivalent to 1056 lux of fluorescent (F7) light [4]: we find 960 lux, 870 lux and 830 lux for Illuminants D55, D65 and D75. To avoid having to calculate the equivalent circadian illuminance, and then apply the relevant alertness thresholds independently for overcast sky light, clear sky light and sunlight, we will arbitrarily choose a single light source of reference, and thus consider 210 lux as the lower bound 'circadian' threshold and 960 lux as the upper bound 'circadian' threshold for the Illuminant D55 used to approximate sunlight.

Accounting for the noted uncertainties, a simple ramp-function appears as a reasonable proxy to represent the likelihood that the vertical illuminance at a given point in time and for a given view direction is sufficient to affect the circadian system and have either circadian entrainment and/or subjective alertness effects: low likelihood (0%) below 210 lux and high likelihood (100%) above 960 lux with a linear interpolation between these, as illustrated in Figure 1(b), expressed in terms of D55 equivalent. This and other parameters will be refined with advances in measurements from photobiology studies.

Timing of exposure

The timing of the exposure determines the type of effect and whether it is beneficial or detrimental. Given our incomplete knowledge, the boundaries are 'fuzzy', but nevertheless it is possible to delineate three distinct periods, illustrated in Figure 2(a): early to mid-morning

(where sufficient daylight illuminance can serve to 'lock' and maintain a preferred (i.e. healthy) sleep - wake cycle); mid-morning to early evening (where high levels of daylight illuminance may lead to increased levels of subjective alertness); and the rest as notional night-time (daylight exposure that might trigger the N-VE is to be avoided so as not to disrupt the natural wake-sleep cycle). The timing factor includes not only the duration and time of occurrence but also the history, i.e. recent exposure. However we do not know enough yet to warrant the additional complexity of including this factor, so we consider only time of occurrence in isolation of the duration and history of the exposure.

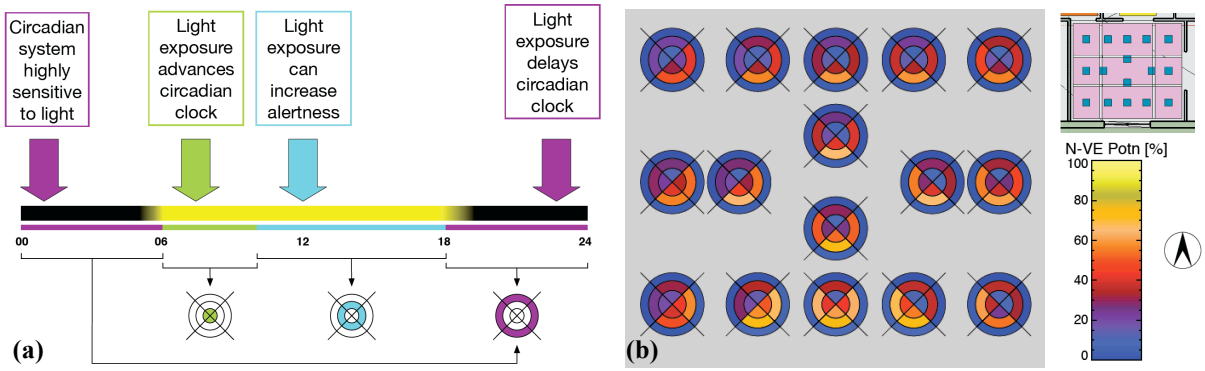

Figure 2: (a) Three day periods according to type of non-visual effect (b) Sombrero plot

Visualizing 'circadian potential'

We present the cumulative N-VE occurring in these three periods using a simple graphical device that we have called the 'sombrero', illustrated in Figure 2(b). The boundaries for the periods were set following the above-mentioned periods of the day: 06h00 to 10h00 (inner circle of the 'sombrero'); 10h00 to 18h00 (middle circle of the 'sombrero'); and, 18h00 to 06h00 (outer circle of the 'sombrero'). The cumulative effect of N-VE for these three periods is apportioned to the respective segments in the three circles according to view direction.

The four quarter-segments of the sombrero indicate the view direction, i.e. to the 'bottom', 'top', 'left' and 'right' according to the inset floor plan. Each ring segment gives the cumulated percentage of that time period across the year for which the circadian potential (likelihood of having an effect) would be achieved for that view direction and at that location.

Study Results

The resulting eye-level vertical illuminances predicted on a 15 minute time-step are shown using annual temporal maps in Figure 3(a). The four maps are for the four view directions. Illuminances of 960 lux or greater are shaded white (i.e. 100% likelihood of non-visual effect) and illuminances 210 lux or less are shaded black (i.e. 0% likelihood of effect). Hours of darkness are shaded grey. Although the quantities in the temporal maps and the sombrero are different, they share the same scale (i.e. 0-100%) and false-colour shading.

The lower and right-hand temporal maps represent views away from the corner and directed towards the opposing walls, i.e. 'right' and 'down'. These views look in part towards the window wall and the centre of the room, which, in this case is illuminated by a skylight. These directions show a much greater occurrence of N-VE than the other two view directions (which look away from the middle of the room and into one corner, 'up' not shown here). The pattern is what we might expect. The 'sombrero' plot shows the percentage of the cumulative occurrence of N-VE across the year for each of the three periods described in the previous section. Thus a cumulative value of 40% could represent a full N-VE occurring for 40% of the time, a 40% N-VE occurring for all of the time, or, as is more likely, something in between.

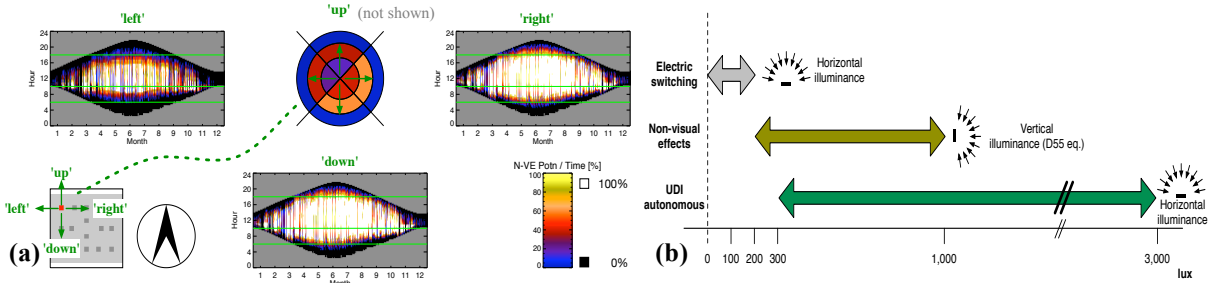

Figure 3: (a) Example time-series (temporal maps) and cumulative occurrence (sombrero) plot for skylit living room in Ostersund. (b) Application ranges for three lighting perspectives.

DISCUSSION

The methodology and initial findings from an exploratory study of three aspects of daylight in a residential building have been described in this paper, with a focus on non-visual effect evaluation that was an extension of the method proposed by Pechacek, Andersen & Lockley [4]. Key enhancements include the concept of a ramp-function from a lower to an upper vertical illuminance threshold, based on photobiology findings, that expresses the increasing potential for circadian effects. Another enhancement is the ability to treat independently light from the sun and sky, thereby accounting for the varying circadian efficiency of the light according to its spectral type, i.e. D55, D65 or D75. And, in terms of data visualization, we introduce the sombrero plot as a simple graphical device to display the cumulative non-visual effect at a point in space and as a function of view direction.

When considered in combination with the other two aspects of daylight – electric lighting savings and visual illumination – we realize that the electric light switching sensitivity is essentially contained within a 0 to 200 lux band, which makes it somewhat separate from UDI or N-VE considerations that both start around 200 lux or more (Figure 3(b)). Relations between UDI-a [7] and N-VE will probably depend on the nature of the daylight illumination (more likely for top-lit situations e.g.). One must however keep in mind that given the very early developmental stage of photobiology in this field, any finding has to be considered as a possible approach to solve the problem rather than as a design guideline.

ACKNOWLEDGEMENTS

The authors would like to acknowledge the support of the Velux Corporation who commissionned this study. M. Andersen was also supported by the Ecole Polytechnique Fédérale de Lausanne and John Mardaljevic by De Montfort University.

REFERENCES

1. Clarke, J. A. Energy Simulation in Building Design 2nd Edition. Butterworth-Heinemann, 2001.
2. Mardaljevic, J. Simulation of annual daylighting profiles for internal illuminance. Lighting Res. and Technology, 32(3):111–118, 2000.
3. Reinhart, CF, Mardaljevic, J., Rogers, Z. Dynamic daylight performance metrics for sustainable building design. Leukos, 3(1):7–31, 2006.
4. Pechacek, C.S., Andersen, M., Lockley, S.W. Preliminary method for prospective analysis of the circadian efficacy of (day) light with applications to healthcare architecture. Leukos, 5(1):1–26, 2008.
5. Lockley, S. Influence of light on circadian rhythmicity in humans. L. R. Squire (Ed.) Encyclopaedia of Neuroscience. Oxford, UK, 2008.
6. Brainard, G. C., Hanifin, J. P., Greeson, J. M., Byrne, B., Glickman, G., Gerner, E., Rollag, M. D. Action spectrum for melatonin regulation in humans: Evidence for a novel circadian photoreceptor. Journal of Neuroscience, 21(16):6405–6412, 2001.
7. Mardaljevic, J. and Nabil, A. The useful daylight illuminance paradigm: A replacement for daylight factors. Lux Europa, p.169–174, 2005.
8. Mardaljevic, M., Andersen, M., Roy, N., Christoffersen, J. Daylighting Metrics for Residential Buildings, In Proceedings of the 27th Session of the CIE, Sun City, South Africa, July 11-15, 2011.
9. Cajochen, C., Zeitzer, J., Czeisler, C., Dijk, D. Dose-response relationship for light intensity and ocular and electroencephalographic correlates of human alertness. Behavioral Brain Research, 115:75–83, 2000.
10. Phipps-Nelson, J., Redman, J., Dijk, D., Rajaratnam, S. Daytime exposure to bright light, as compared to dim light, decreases sleepiness and improves psychomotor vigilance performance. Sleep, 26(6):695–700, 2003.
11. Badia, P., Myers, B., Boecker, M., Culpepper, J., Harsh, J. Bright light effects on body temperature, alertness, eeg and behavior. Physiology & Behavior, 50:583–8, 1991.
12. Lafrance, C., Dumont, M., Lesperance, P., and Lambert, C. Daytime vigilance after morning bright light exposure in volunteers subjected to sleep restriction. Physiology & Behavior, 63:803–10, 1998.

INFORMING WELL-BALANCED DAYLIGHT DESIGN USING LIGHTSOLVE

M. Andersen[1], J.L. Gagne[2], S. Kleindienst[2]

1: Interdisciplinary Laboratory of Performance-Integrated Design (LIPID), School of Architecture Civil and Environmental Engineering (ENAC), Ecole Polytechnique Fédérale de Lausanne (EPFL), Switzerland

2: Building Technology Program, Department of Architecture, Massachusetts Institute of Technology (MIT) - USA

ABSTRACT

Designing spaces that are able to balance illumination, glare and solar gains over a whole year is a real challenge, yet a problem faced every day by building envelope designers. To assist them in this search, a full year, climate-based daylighting simulation method was developed, called Lightsolve, meant to be used early on in the design process when façade and space details have not yet been defined. It focuses on the variation of daylight performance over the day and the year, combining temporal performance visualization with spatial renderings, and including an expert system to support a guided search process.

This paper describes the foundations and set of innovative simulation resources that Lightsolve offers as a whole, and puts its different components - including a time reduction method, a set of three goal-based metrics and an expert system - back to Lightsolve's overall context aiming to an early stage, comprehensive, prospective support for daylighting design.

INTRODUCTION

Daylighting design is both highly relevant to cutting edge societal issues such as energy conservation, sustainability and health, and highly sensitive to careful planning and control. With lighting being responsible for the greatest energy requirements in commercial buildings [1] - that are also mostly used during daytime -, and with heating and cooling being the two second most energy-demanding building functions [2], it appears very clearly how efficient daylighting and solar control strategies can have a tremendous impact on energy use. Savings predictions for lighting can vary between 20% and 80% [3,4]; but these savings can only be effective if one also carefully accounts for our visual needs and our comfort and health criteria. The main challenge resides in the reconciliation of the many factors influencing how daylight and sunlight each interact with the built environment and in the great variations they show in intensity and distribution depending on location, weather and time.

If one wants to propose new methods to inform designers about daylighting management, these methods have to be developed in harmony with the way architects work and think. Today, simulation tools have become the dominant form of design support [5,6] but due to the large number of parameters involved and the need for detailed, climate-based analyses to be realistic about daylighting potential [7,8], evaluating annual daylighting performance of a schematic building project interactively and comprehensively is particularly challenging.

An innovative simulation project called Lightsolve has been initiated to address this challenge, that intends to inform the design process through a goal-driven, interactive guided search process. It is based on expert rules, and on combining an inverse (goal-based) approach with a simultaneous visualization of quantitative and qualitative aspects of space and of its annual, climate-based performance.

LIGHTSOLVE OVERALL CONCEPT

Lightsolve aims to provide building designers with the means necessary to assess critical parameters of a successful daylighting design by efficiently combining qualitative and quantitative criteria in the search process. The question of daylighting metrics has become a key design issue to solve in today's environmental context: what kind of metrics would be appropriate to provide a comprehensive yet condensed assessment of the daylighting performance of a space? The challenge is to approach this problem both from quantitative and qualitative perspectives, while still conveying enough information about the variability of daylight over time and space, and its dependence on location and climate. With so many parameters involved, it is essential to gauge the extent to which these metrics will still be able to inform design.

The general approach for Lightsolve is to inform well-balanced daylight design during early design stages through an interactive visualization and a pro-active, guided improvement of full-year time-varied daylighting performance [9]. One of the underlying principles in terms of how daylighting performance is evaluated is to make it specific to the user's own performance objectives and to his or her areas of interest, as well as to combine a synthetic perspective of full-year data with a visual impression of what the space looks like over time.

The metrics used in Lightsolve differ from most existing daylighting simulation programs in two ways: they are goal-based and they place emphasis on the variation of daylight performance over the day and the year. The temporal map [10] indeed appears as a form of graphical representation of performance that is particularly well suited to schematic design stages because it is able to inform designers at a glance about how a given metric of interest varies over time, daily and annually. The days/months of the year are plotted along the horizontal axis, and the times of day are plotted along the vertical axis (see Figure 1(b)).

In the Lightsolve framework, we use that representation to show how closely the users' current design fulfills their own (or standard-based) visual comfort, solar gain and light distribution goals, on an annual yet time-varied basis that accounts for weather conditions [11]. An intuitive color scale (Figure 1(a)) indicates how closely the goals are met over the year: yellow indicates that the goals were met for this sensor (or that solar gains are neither excessive nor insufficient), red indicates that values were too high, and blue that they were too low. The three Lightsolve metrics express the performance of each *entire* area of interest (big or small, defined by the user) rather than on a point per point basis, as discussed below.

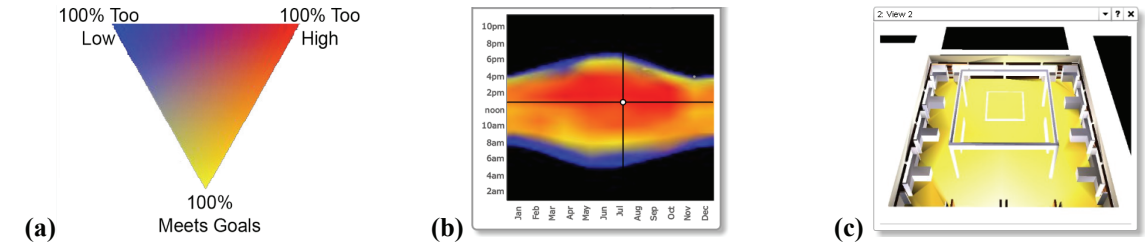

Figure 1: Reading Lightsolve Temporal Maps – (a) Color scale (b) Correlation of time/day with performance (color) and (c) with lighting distribution (renderings).

Year-representative series of renderings are also produced and associated to a given time of day/year and weather condition (the dominant one e.g., Fig 1(c)). In the Lightsolve interface (Figure 2(a)), these renderings (right + 2(b)) are interactively displayed together with sky type occurrence (2(a) upper left) as one moves a cursor over the temporal map (middle), and are combined with the goal-based visualizations of annual performance (temporal maps) for illumination (based on desired illuminance ranges), glare (based on desired glare tolerances) and solar gains (based on probable heating/cooling needs), whose basis is detailed below.

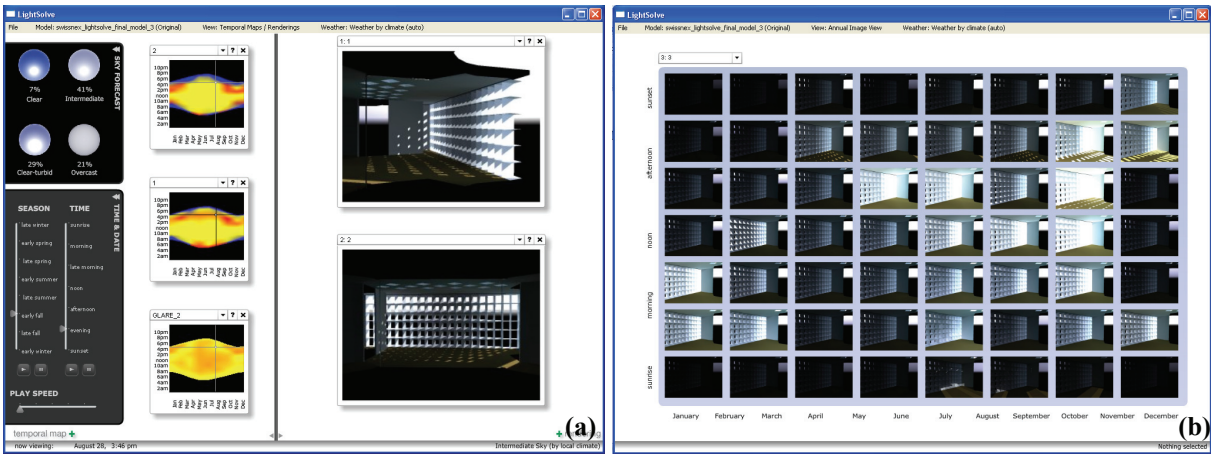

Figure 2: Lightsolve analysis interface – (a) Time-varied display of performance interactively linked to renderings of the space (b) Annual Image Map showing all renderings over time.

One of Lightsolve's major innovations also resides in its user-interactive expert system approach. The expert system allows designers to create a 3d model of their own design and to input project-specific performance goals for illuminance and glare within the space; it aims at providing performance-based decision support while respecting the role of the architect and his or her design intent and is described in further detail below.

FULL-YEAR, TIME-VARIED ANALYSIS

To allow for climate-specific calculations, illuminance and glare values are calculated for each sensor plane patch and for each of four sky types [12], ranging from overcast to clear. A climate-based representative value is then calculated as a weighted average from each sky type based on their respective occurrence during that time period. To make whole-year calculations more efficient, the year is split into 56 periods and climate-based data are calculated for each of them as far as the diffuse component of daylight is concerned [9]. The comparisons between temporal maps produced using the data reduction method and those produced using detailed illuminance data extracted from the program Daysim at 5 minute intervals showed a strong visual and numerical correlation [13], illustrated in the example shown on Figure 3. A separate calculation for zero-bounce direct sunlight is performed for 1200 sun positions (80 times of year and 15 times of day) and results are combined to the first (diffuse) set [14].

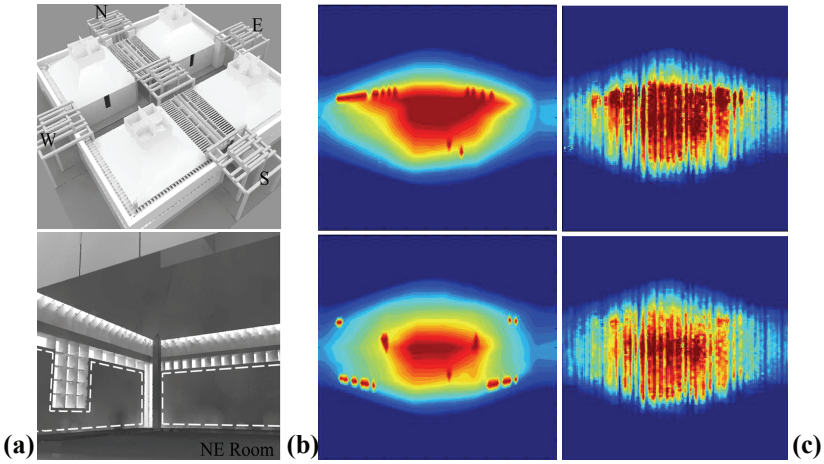

Figure 3: Condensing annual data. Museum case study (a) used to compare the 56 time period reduction method with sun overlay (b) against Daysim (shadow casting mode) (c).

RENDERING AND CALCULATION ENGINE

The overall intent of Lightsolve being to inform design in an exploratory way, there was a need for a quick calculation engine that could produce both numerical results (at the basis of temporal maps) and renderings over a whole year so that interactivity could be maintained. A hybrid global illumination method was developed for this purpose at the Rensselaer Polytechnic Institute, called the LightSolve Viewer or LSV [15]. It relies on patch-based radiosity for the sky and uses indirect illumination and shadow volumes for pixel-based shadows for direct illumination by the sun. This rendering system was validated through a set of qualitative and quantitative comparisons with Radiance and a pixel difference of less than 10% was found between LSV and Radiance for a variety of different scenes, camera positions, and daylighting conditions [15].

GOAL-BASED METRICS

Unlike most daylighting analysis tools, the three metrics that were developed for Lightsolve and are represented as colored temporal maps emphasize the time-variation of light over its detailed spatial distribution. They are also explicitly goal-based: performance objectives in daylighting can indeed vary greatly depending on the type of space and the intentions of the designer. A set of three metrics, whose underlying principles are illustrated in Figure 4, were developed to display goal-based performance information for a user-defined area of interest on a single temporal map and to offer a comprehensive and intuitive way to represent annual daylight performance of a design proposal; details can be found in [11]. A color scale - consistent amongst the three metrics - indicates how closely the goals are met over the year.

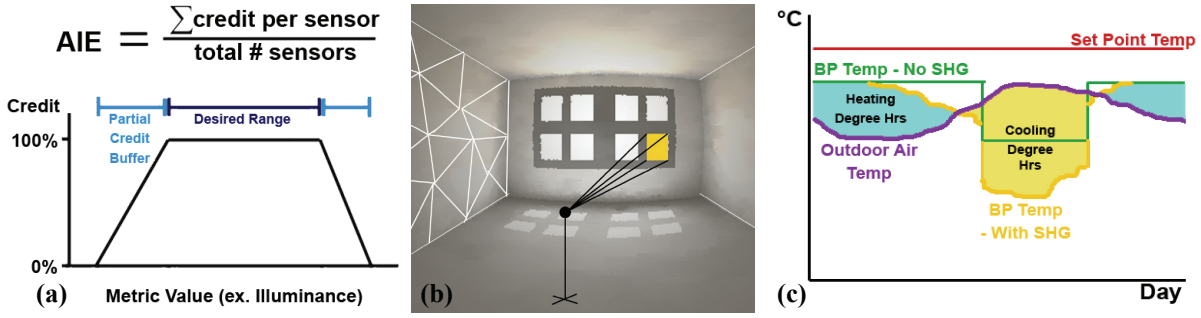

Figure 4: Lightsolve Metrics – (a) Acceptable Illuminance Extent (AIE) credit system (b) Glare Avoidance Extent (GAE) derived from DGP and based on window luminance and radiosity model (c) Solar Heat Surplus/Scarcity (SHS) based on cooling/heating daily totals.

Illumination

The illumination metric, called Acceptable Illuminance Extent (AIE), calculates how the portion of a user-defined area of interest in which the illuminance stays within a chosen range varies over time. In other words, this metric condenses the portion of a user-defined area of interest in which the illuminance stays within a chosen range to a single percent, and displays the variation of that percent over time. It assigns full credit to sensor portions within range, and partial credit to sensor portions out of range but within a user-defined 'buffer' interval. It is referred to as Acceptable Illuminance Extent (AIE), as shown in Figure 4(a).

Glare perception

Similarly, a single number representative of overall glare perception within an area of interest is introduced as Glare Avoidance Extent (GAE) and based on the Daylight Glare Probability (DGP) metric. The derived GAE metric used in Lightsolve indicates the proportion of the

glare zone or glare sensor area that falls above the glare threshold considered non-acceptable by the user. It can therefore represent the glare risk for a particular location and a particular viewpoint over the year (small unique glare sensor with its normal facing that direction) but can just as well indicate the overall glare risks for a space or a range of viewing locations (e.g. for all the students in a classroom). Because this glare analysis is run annually and often for multiple viewpoints, it required more efficient methods for computing glare, that were developed for that purpose and are schematically illustrated in Figure 4(b) [16]. It relies on threshold values suggested by the DGP author for glare tolerance.

Solar gains

Finally, a new solar gains metric called Solar Heat Scarcity/Surplus (SHS) is used to convey the urgency of either allowing more direct solar gain or avoiding it, based on revisited balance point calculations [17] (see Fig 4(c)). Although dynamic energy analyses should ultimately be used in determining energy loads, balance point can be as useful indicator in the earliest stages of design. The recently released 16 DOE Benchmark Commercial Buildings [18] was used to validate this approach. Within the Lightsolve environment, the Solar Heat Scarcity and Surplus metric requires additional input about the thermal properties of the envelope and building type and occupancy but is able to provide a good approximation of how much of a liability or benefit the daylight-associated solar gains are for the proposed designs.

Although the non-spatial aspect of solar heat gain usually makes it more difficult to analyze along side illuminance or glare, the value of resorting to time-variant graphics was made evident from its ability to provide a basis of comparison so that solar heat gain information can be comparable with location-based data.

EXPERT SYSTEM

The expert system consists of two major components: a daylighting knowledge-base which contains information regarding the effects of a variety of design conditions on resultant daylighting performance [19], and a fuzzy rule-based decision-making logic which is used to determine those design changes most likely to improve performance for a given design [20]. As in Lightsolve's analysis mode, the user starts with an initial design, and be guided towards improved performance like by a "virtual daylighting consultant. By involving the designer and utilizing his or her knowledge as well as the intelligence built-in the tool, the process is made more efficient while the exploration space is expanded.

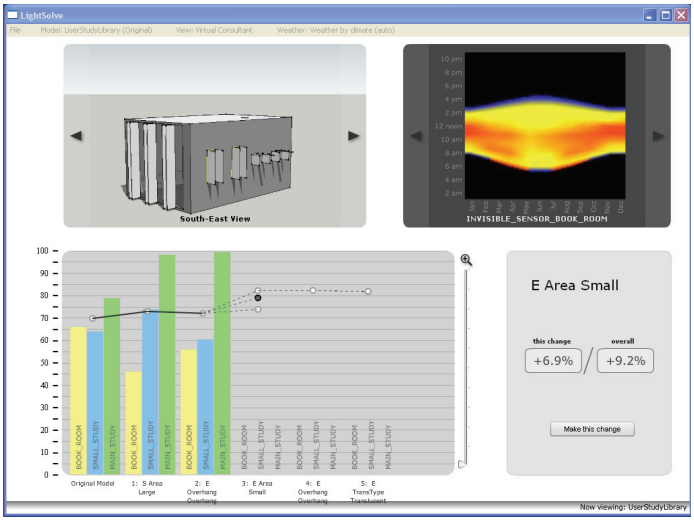

Figure 5: Lightsolve Expert System interface (Virtual Consultant) – Guided search to increase annual performance for all areas of interest and all and all performance objectives.

The expert system is currently implemented in Google SketchUp as a plug-in; its user interface, illustrated in Figure 5, displays the current performance of a given design and the list of design changes suggested to the user. The tool was evaluated against high performing benchmark designs generated with a genetic algorithm [21] and tested for varying levels of aesthetic constraints. The results of these studies indicated that the expert system was successful at finding designs with improved performance for a variety of initial geometries and daylighting performance goals [20]. It has also been tested by a group of designers who were asked to complete a design task with the system and to evaluate their experiences using the tool. These studies demonstrated a good acceptance by designers and demonstrated its ability to effectively guide a design process while offering an educational potential [22].

CONCLUSION

This paper discusses the underlying principles of the different components of a new approach in daylighting simulation named Lightsolve. The main innovations are pointed out, and brought together in a more holistic overview of the project. Lightsolve shows promise as a complementary method to daylighting performance evaluation: instead of summarizing time and emphasizing spatial light distribution, Lightsolve offers a way to evaluate broader areas within a space with an emphasis on how this performance varies over the seasons and time of day. This perspective thus seems particularly relevant to early design stages. The positive feedback received during the expert system user study [22] encourages the authors to pursue this development effort into a tool that could be used more broadly. Such resources could indeed enable a desirable shift in schematic stage design practices and move daylighting analysis one step closer to achieving “best practice” recognition.

ACKNOWLEDGEMENTS

The authors were supported by the Massachusetts Institute of Technology and would like to acknowledge additional support from the Ecole Polytechnique Fédérale de Lausanne (Prof. M. Andersen) and the Martin Family Society for Sustainability (Drs. Gagne and Kleindienst).

REFERENCES

1. Swiss Federal Office of Energy : Energieforschung 2009 – Ueberblicksberichte. Swiss Confederation, 2009.
2. US Deptartment of Energy: "Buildings Energy Data Book" (September 2007), sec. 1.3.3.
3. Bodart M., De Herde A. : Global energy savings in offices buildings by the use of daylighting. Energy & Buildgs 34(5), 421-429, 2002.
4. Ihm P., Nemri A., Krarti M.: Estimation of lighting energy savings from daylighting. Buildg and Envment 44 (3), pp. 509–514, 2009.
5. Reinhart C, Fitz A.: Findings from a survey on the current use of daylight simulations in building design. En.&Bldgs 38(7), 824-835, 2006.
6. Sarawgi T. : Survey on the use of lighting design software in architecture and interior design undergraduate education. International Journal of Architectural Computing 4(4): pp. 91-108, 2006.
7. Reinhart, C.F., Wienold, J.: The Daylighting Dashboard - A Simulation-Based Design Analysis for Daylit Spaces, Building and Environment, 46(2), pp. 386-396, 2011.
8. Mardaljevic, J., Heschong, L., Lee, E.: Daylight metrics and energy savings, Lighting Res. and Technology, 41(3), pp. 261-283, 2009.
9. Andersen, M., Kleindienst, S., Yi, L., Lee, J., Bodart, M., Cutler, B.: An intuitive daylighting performance analysis and optimization approach, Building Research and Information, 36 (6), pp. 593–607, 2008.
10. Mardaljevic, J.: Spatio-temporal dynamics of solar shading for a parametrically defined roof system, Energy & Bldg 36, 815-823, 2004.
11. Kleindienst, S., Andersen, M.: Comprehensive Annual Daylight Performance from Goal-Based Design Inputs, Bldg Res.&Inf, submitted
12. Perez R, Michalsky J, Seals R.: Modelling Sky Luminance Angular distribution for real sky conditions; Experimental evaluation of existing algorithms, Journal of the IES, 21(2), pp. 84-92, 1992.
13. Kleindienst, S., Bodart, M., Andersen, M.: Graphical Representation of Climate-Based Daylight Performance to Support Architectural Design, LEUKOS, 5(1), pp. 39-61, 2008.
14. Kleindienst, S.: Time-Varied Daylighting Performance to Enable a Goal-Driven Design Process, PhD thesis, MIT, 2010.
15. Cutler, B., Martin, S., Sheng, Y., Glaser, D., Andersen, M.: Interactive Selection of Optimal Fenestration Materials for Schematic Architectural Daylighting Design, Autom. in Construction, 17(7), 809-823, 2008.
16. Kleindienst, S., Andersen, M.: The Adaptation of Daylight Glare Probability to Dynamic Metrics in a Computational Setting, In Proceedings of Lux Europa 2009, Istanbul, September 9-11, 2009.
17. Kleindienst, S., Andersen, M.: Solar Heat Surplus and Solar Heat Scarcity: the Inclusion of Solar Heat Gain in a Dynamic and Holistic Daylight Analysis, Proc. IBPSA-USA SimBuild 2010, New York, August 2010.
18. Torcellini P., Deru M., Crawley D.B. et al.: DOE Commercial Building Benchmark Models, Proc. 2008 ACEEE Summer Study, 2009.
19. Gagne, J.L., Andersen, M.: A daylighting knowledge-base for performance-driven facade design exploration, accepted, LEUKOS.
20. Gagne, J.L., Andersen, M., Norford, L.K.: An Interactive Expert System for Daylighting Design Exploration, Bldg & Env, in press.
21. Gagne, J.L., Andersen, M.: A Generative Façade Design Method Based on Daylighting Performance Goals, J. Bldg Perf. Sim., in press.
22. Jaime L. Gagne, An Interactive Performance-Based Expert System for Daylighting in Architectural Design, PhD thesis, MIT, 2011.

DAYLIGHT OPTIMIZATION OF BUILDINGS AND APPLICATION OF ADVANCED DAYLIGHTING SYSTEMS IN CENTRAL MEXICO

Basurto C., Borisuit A., Kämpf J, Münch M and Scartezzini J-L
Solar Energy and Building Physics Laboratory (LESO-PB)
Ecole Polytechnique Fédérale de Lausanne, CH-1015 Lausanne, Switzerland

ABSTRACT

The intensive use of daylight in buildings is beneficial at many levels: it provides sufficient levels of illumination to perform working activities throughout the day and it reduces the use of artificial light, which in turn leads to lower electricity consumption [1-3]. The spectral composition of daylight often leads to higher visual comfort in humans, compared to electric lighting. There are also illuminance and spectrally-dependent light effects on the human circadian system, which regulate hormonal rhythms, alertness and (visual) performance across 24 hours [4-6]. The main objective of this work was to assess luminous performance in office buildings and to test optimizations by virtually applying different daylighting strategies by computer simulations.

We first assessed the daylight distribution in two different office rooms, set-up as test modules on the EPFL campus in Lausanne (46° 32'N, 6° 39'E). One of these test modules is equipped with a standard double-glazing; the second one comprises anidolic daylighting systems [7], which convey diffuse daylight and sunlight deeper in the room, and reduce glare risk. In both rooms, we also assessed vertical spectral irradiance in the visible range, which gave us additional information with respect to photo biological properties of the available daylight. We then measured the real daylighting situation in an office room located in the city of Zacatecas, Mexico (22°47'N 102°34'W), which is equipped with a standard double-glazing window. In a next step we tested, whether the daylight distribution for this room could be improved by virtually applying different complex fenestration systems (such as prismatic panels and laser cut panels) by using computer simulations. The results of these simulations showed higher indoor luminous performance with the two advanced daylighting systems. This new method may contribute to an improved and tailored design of daylight availability in real buildings at different geographical locations.

INTRODUCTION

Daylight in buildings often leads to benefits for energy efficiency and to positive effects on visual and non-visual functions in humans. Because of these benefits the efficient use of daylight has become more relevant recently [2]. Many strategies have been developed to effectively use this natural light source, including the development of advanced daylighting systems. Their common principle is the efficient collection of the exterior daylight (direct and indirect components) its redirection into the interior space and thereby improvement of light distribution in the room [7]. One of the main characteristics of daylight is its temporal variation caused by meteorological and seasonal parameters [8] and therefore, different types of advanced daylight systems were designed to fit the geographical location of a building. For example, at locations with predominantly overcast weather conditions, the main task of the advanced daylighting system is to collect and redistribute the diffuse daylight component inside the room. Different advanced daylighting systems, based on non-imaging optics (anidolic systems), were developed for this purpose. The physical principle of these non-imaging optics systems is an angular selection of the admitted light rays with a minimal number of inter-reflections so that the system efficiently collects diffuse daylight from the sky vault and re-distributes it in the interior space [7]. In the case of locations with predominantly clear sky conditions, the objective is not only to collect and re-distribute the daylight indoors but also to protect from the incidence of direct sunrays and to avoid overheating and the risk of discomfort glare. Therefore, for locations at low geographical latitudes different solutions are required and only few advanced systems have been implemented so far [9].

One of the objectives of this work was to analyse the performance of an already implemented advanced daylighting system in a real size test room, and to compare the distribution of daylight to a second test room with standard double glazing windows in Switzerland. A second aim was to evaluate the lui nous performance at low latitude locations with prevailing clear sky conditions (Zacatecas, Mexico 22°47'N 102°34'W). We finally simulated the efficiency of different complex fenestration systems (CFS) by using ray tracing simulation methods (Radiance-based, [10]). For the CFS, we used a laser-cut panel and a prismatic panel, which are recommended for prevailing clear sky conditions [2].

METHODOLOGY

1. Assessment of daylight availability in two test modules (with and without advanced daylighting systems)

The two test modules are located on the EPFL campus in Lausanne, Switzerland (46°32'N, 6°39'E Altitude: 410 m), with an equal size of 3.05 x 6.55 x 3.05 m and south orientated windows. One of these two modules is equipped with a standard double glazing window and serves as reference room, while the second module contains two different anidolic daylighting systems (ADS): an anidolic ceiling (AC) and an integrated anidolic system (IAS) [11]. Both modules have identical photometrical and geometrical features (Figures 1 and 2). For this work, we have chosen to compare the IAS to the standard double glazing window, because of its lower cost and presumably easier adaptation for potential building retrofits in México.

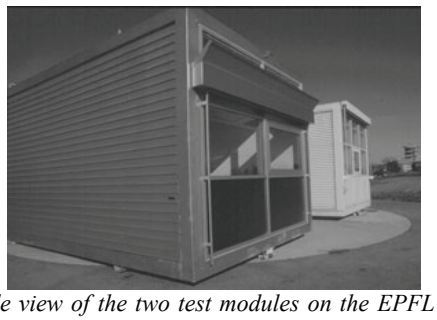

Fig.1 *Outside view of the two test modules on the EPFL campus. The test module on the left side contains integrated anidolic systems (IAS) and the test module on the right side is equipped with a standard glazing window.*

Fig.2 *Interior view of the standard double glazing module at the EPFL campus (Switzerland).*

In order to better understand the advantages of the IAS vs. the glazing system in the reference room, we conducted on-site monitoring: We first assessed the daylight distribution in both test modules by calculating their daylight factors (DF). The DF is defined as the ratio of indoor illuminance on a horizontal surface (E_i) and the simultaneously available outdoor iluminance (E_o) by using the formula: $DF=(E_i/E_o)$ x100 (%). [11, 12]. To account for the non-visual aspects of daylight, we also assessed the vertical C(λ)-weighted spectral irradiance [13] in the blue range of the visible light spectrum, using a portable digital spectroradiometer (Specbos 1201, JETI Technische Instrumente GmbH, Jena, Germany). The spectroradiometer was placed in the centre of the room, by directing the device on a vertical plane to the wall at 1.2 m height (i.e. at the approximate eye level of a sitting person). Measurements were taken every 15 minutes, alternating for both modules from 9am until 6pm, under intermediate sky conditions.

2. Luminous performance assessment in an office without advanced daylighting systems at a different geographical latitude

We selected an existing building in the city of Zacatecas, Mexico (22°47'N 102°34'W) and assessed its real luminous performance by performing illuminance and luminance measurements. We used two different illuminance meters (Chauvin Arnoux C.A. 811 Lightmeter) for interior and exterior measurements, which had prior been referenced to a calibrated device (Spectroradiometer, Specbos 1201, JETI Technische Instrumente GmbH Jena, Germany). For luminance measurements we used a special customized device made of a tube with an aperture of 3° (diameter of opening= 2 cm) covered inside with a black foil and placed on the illuminance sensor; the calibration of this device was made by using a luminance meter as reference (LS-110 Minolta).

The selected room was the Library's office of a private educational University (Tecnologico de Monterrey campus Zacatecas, México). The room showed poor availability of daylight due to the very low glazing transmittance of the tinted glass (31%) and a South-West orientation of the building. Two pictures taken at imes of day show the interior view of the Library's office in the morning (Figure 3) and in the evening hours (with direct sun shining on the working area; Figure 4).

Fig. 3. View of the Library's office under overcast sky conditions in the morning

Fig. 4. View of the Library's office under clear sky conditions in the evening

In order to perform a detailed analysis of the real luminous performance in the office showed on Figure 3 and 4, we carried out measurements under overcast and clear sky conditions, using the DF as a metric to assess the indoor daylight distribution.

3. Luminous performance optimization for an office with poor daylight availability

The optimization of daylight availability in buildings requires a strategy which includes early decisions in the architectural design, such as interior material properties, window configuration and glazing transmittance as well as the use of CFS. Different combinations of these previously mentioned parameters were virtually assessed and tested by using computer simulations, based on ray tracing software (Radiance [10]). In order to simulate the implementation of two different CFS [14], we used existing BTDF data (Bi-directional Transmittance Distribution Function[15]). Simulations with two different CFS, laser-cut panel and prismatic panels (3M Optical Lighting Film), were performed.

RESULTS

1. Assessment of daylight availability in two test modules

Overall, there was a significant difference of the DF's between both test modules ($p<0.05$). Morevover, the DF in in the middle of the room of the reference test module was only 2.5%, but 4% for the module equipped with the IAS, which suggests a different light distribution deeper in the room (Figure 5).

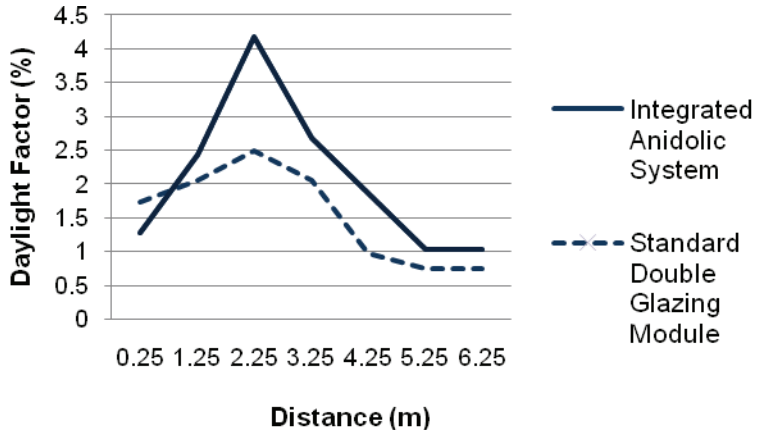

Fig. 5 Daylight Factor (%) in the test modules with the integrated anidolic system and the standard room.

The vertically C(λ)-weighted spectral irradiance of the visible light spectrum was significantly higher in the module with IAS compared to the reference test room with standard double glazed window (1.295 W/ m² vs. 0.5089 W m²; $p<0.05$, Figure 6).

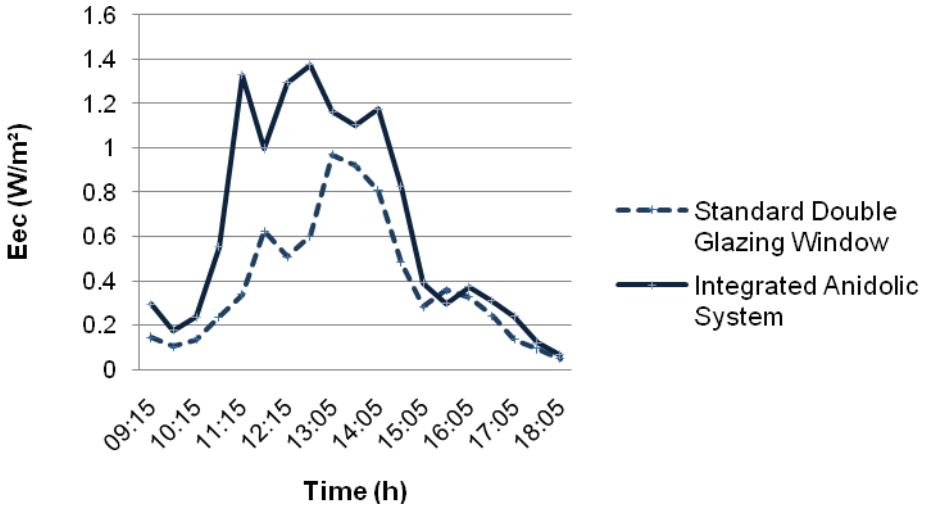

Fig.6. Spectral irradiance (W/m^2), measured in a vertical direction from the centre of the two test modules, across different times of day.

2. Luminous performance assessment in a real office without advanced daylighting systems

The calculation of the DF in the Library Office in México showed a rapid decrease deeper in the room. Starting with a DF of 5.9% at a distance of 0.4 m from the window, the DF gradually decreased and was only 0.9% in the back of the room (Figure 7). The luminance measurements further showed low levels and inadequate luminance-ratios between paper tasks, screen and walls, as well as a high contrast between the window and the surrounding areas (data not shown). These on-site measurements were used to compare the optimization strategies which we carried out with computer simulations.

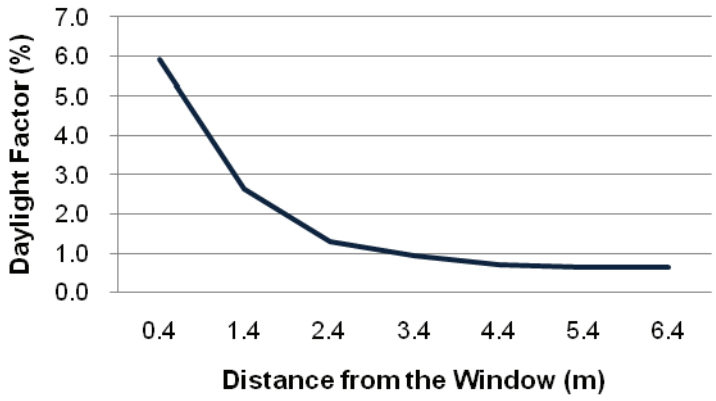

Fig.7. Daylight Factor measurements in the Library Office, México (measurements were taken every m)

3. Daylight simulation of a real office with and without complex fenestration systems

Figure 8 illustrates the simulated Library's office room situation in México, where we measured in average a minimum illuminance of 926 lx. After increasing the transmittance of the glazing up to 80% (Figure 9), the same room showed a minimum illuminance of 3451 lx. When we virtually applied a prismatic panel, a minimum illuminance of 3531 lx (Figure 10) was obtained, and with a laser-cut panel we reached a minimum illuminance of 3540 lx (Figure 11); all simulations were carried-out using BTDF data.

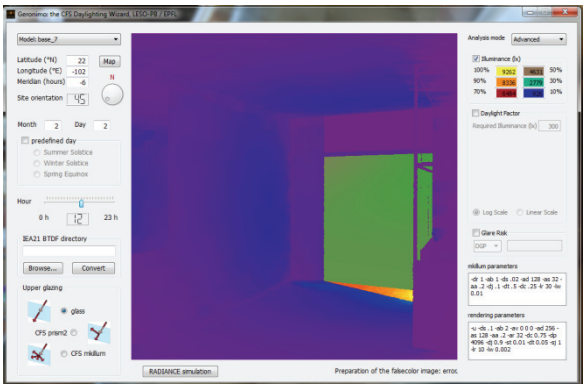

Fig. 8 Print screen of the simulated real illuminance situation in the office in Mexico, with South-West orientation of the building and a glazing transmittance of 31%.

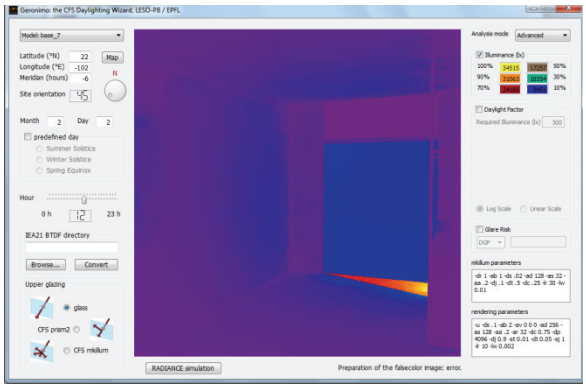

Fig. 9. Simulated higher illuminance in the same office room in Mexico when the glazing transmittance was increased to 80% (South-West orientation).

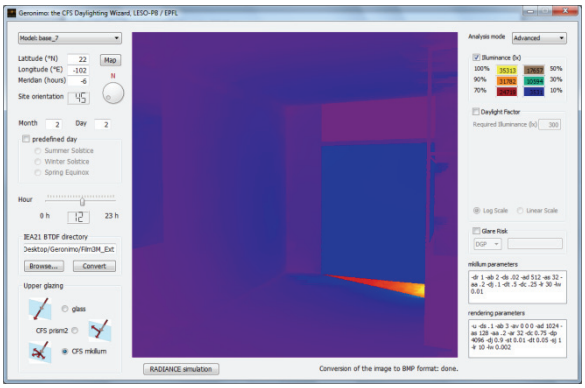

Fig.10.Simulated optimized illuminance situation by using a prismatic panel as a complex fenestration system (South-West orientation; Film 3M interior)

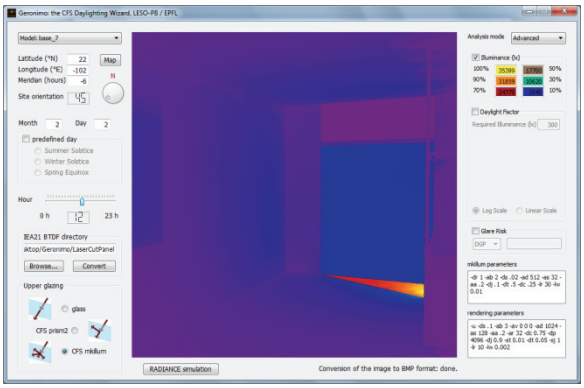

Fig.11. Optimized daylight situation by using a laser-cut panel as a complex fenestration system (South-West orientation).

DISCUSSION

We assessed the real daylighting situation by monitoring the daylight factor in two test modules in Switzerland and in an office room in Mexico. For the two test modules in Switzerland, we found a slightly better daylight distribution in the module equipped with the IAS, when compared to the module with the standard double-glazing window. The C(λ)-weighted spectral irradiance in the blue range of the visible spectrum was significantly higher in the module with the IAS, suggesting that the interior daylighting environment may be beneficial not only in terms of energy savings but also for visual and non-visual human functions. We also showed by computer simulations that the luminous daylight performance could be improved in real office rooms at low geographical latitudes (library office in México) by using different complex fenestration systems. Further studies are needed to investigate different daylighting metrics in order to also include time of day and year, weather conditions and local climates [16]. Future work should also address problems related to discomfort glare and thermal comfort, in order to avoid potential overheating due to excessive solar gains - both are non-negligible risks for buildings located at low geographical latitudes. To summarize, our results showed possible improvements for indoor daylight performance by virtual application of advanced daylighting systems, using computer simulations. This might be used to improve daylight performance in the design of new buildings or the retrofit of existing buildings at low geographical latitudes.

ACKNOWLEDGEMENTS

This study was supported by a grant of the Mexican National Council of Science and Technology (CONACYT), and by the Research Contract no. 154393 of the Swiss Federal Office of Energy (SFOE). M. Münch and A. Borisuit are supported by the VELUX Foundation (Switzerland).

REFERENCES

1. McHugh, J., P.J. Burns, and D.C. Hittle, *The Energy Impact of Daylighting.* Ashrae Journal, 1998. 40(5): p. 31-35.
2. Ruck, N., et al., *Daylight in Buildings*. 2000: International Energy Agency (IEA).
3. Bodart, M. and A.D. Herde, *Global energy savings in offices buildings by the use of daylighting.* Energy and Buildings, Elsevier, 2001. 34: p. 421-429.
4. Brainard, G.C. and J.P. Hanifin, *The effects of light on Human Health and behavior relevance to architectural lighting*, in *Simposium: Light and Health: non-visual effects. CIE*. 2004: Vienna, Au. p. 2-16.
5. Cajochen, C., *Alerting effects of light.* Sleep Medicine Reviews, Elsevier, 2007. 11: p. 453-464.
6. Bommel, W.J.M.v., *Non-visual biological effect of lighting and the practical meaning for lighting for work.* Elsevier, 2006. 37(4): p. 461-466.
7. Scartezzini, J.-L. and G. Courret, *Anidolic Daylight Systems.* Solar Energy, 2002. 73(2): p. 123-135.
8. Becchi, E., et al., *Daylighting in Architecture, A european reference book*, ed. N. Baker, A. Fanchiotti, and K. Steemers. 1993: James & James for the Comission of the European Communities, Directorate-General XII for Science, Research and Development.
9. Edmonds, I.R. and P.J. Greenup, *Daylighting in the tropics.* Solar Energy, 2002. 73(2): p. 111-121.
10. Larson, G.W. and R. Shakespeare, *Rendering with Radiance, The Art and Science of Lighting Visualization*. 1997: Morgan Kaufmann.
11. Thanachareonkit, A., *Comparing physical and virtual methods for daylight performance modelling including complex fenestration systems*, in *LESO-PB*. 2008, Ecole Polytecnique Féderale de Lausanne: Lausanne.
12. IESNA, *IES Lighting Handbook, Reference Volume*. 1984: Illuminating Engineering Society of North America (IESNA).
13. Gall, D. and K. Bieske, *Definition and measurement of circadian radiometric quantities*, in *Light and health- non-visual effects: proceedings of the CIE*. 2004: Vienna, Austria.
14. Kaempf, J. and J.-L. Scartezzini, *Integration of BT(R)DF data into Radiance Lighting Simulation Programme, Technical Report* 2004, EPFL: Lausanne.
15. Andersen, M., *Light distribution through advanced fenestration systems.* Builiding Research & Information, 2010. 30(4): p. 264-281.
16. Reinhart, C.F. and J. Mardaljevic, *Dynamic daylight performance metrics for sustainable building design.* Institute for Research in Construction NRC-CNRC, 2006. 3(1): p. 1-25.

REGULATION AND CONTROL OF INDOOR ENVIRONMENT DAYLIGHT QUALITY. A CASE STUDY.

A. Bellazzi[1], S.Galli[1], I. Meroni[1]

[1]*ITC-CNR, Construction Technologies Institute – National Research Council*

Via Lombardia 49, 20098 San Giuliano Milanese - Italy

INTRODUCTION

The proper entry of solar energy in an office should be carefully analysed as it affects both the visual, psychological and physiological well-being of users and the energy demand for heating, cooling and electrical requirements of a building. It is important to analyse whether it is useful to privilege heat gains during the winter as a function of the specific intended use of the building, the exposure and the climatic conditions, taking care to avoid overheating during the summer; the solar radiation in the visible field makes it possible to take advantage of daylighting to perform specific activities, reducing the use of artificial light, taking care to avoid glare; daylighting in working places influences the mood, the body and the working activity of the employees, with advantages in terms of productivity. The influence of solar radiation on the energy demand for heating, cooling and electrical requirements of a building produces two main effects: solar radiation can reduce energy demand for heating but can increase the one for cooling; the possibility to take advantage of daylighting instead of using artificial light can lead to energy and economic saving, reducing the impact on the environment. A holistic design approach is necessary when all these aspects are viewed as a whole.

Unfortunately European and Italian regulations tend to be sector-based and do not promote integrated design that should be able to evaluate more aspects at the same time, from visual and thermal comfort to energy saving. At the moment the benchmarks are either only about well-being or about consumption and they are often annual benchmarks which do not consider the cyclicality of seasons or the dynamicity of daylighting.

PERFORMANCE ANALYSES OF SHADING SYSTEMS THROUGH ANALYTIC CALCULATIONS

The performances of six different glazing systems of an office room in Milan were analysed using the Energy Plus software, developed at the Lawrence Berkeley National Laboratory of the University of California. The test room indoor dimensions are 2,80 x 5 x 2,80 metres and the south façade is completely glazed, in order to evaluate the real behaviour of the transparent system. The glass dimensions are 2,60 x 2,60 metres and the frame and dividers are made of aluminium without thermal break, as shown in Figure 1. Internal gains, occupancy and HVAC operation profiles were calculated using standard values defined by the regulations in force.

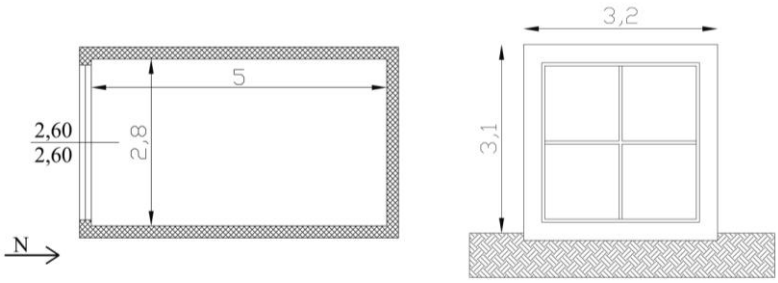

Figure 1. Layout and front view of the test room (south view)

The analysed situations are shown in Figure 2.

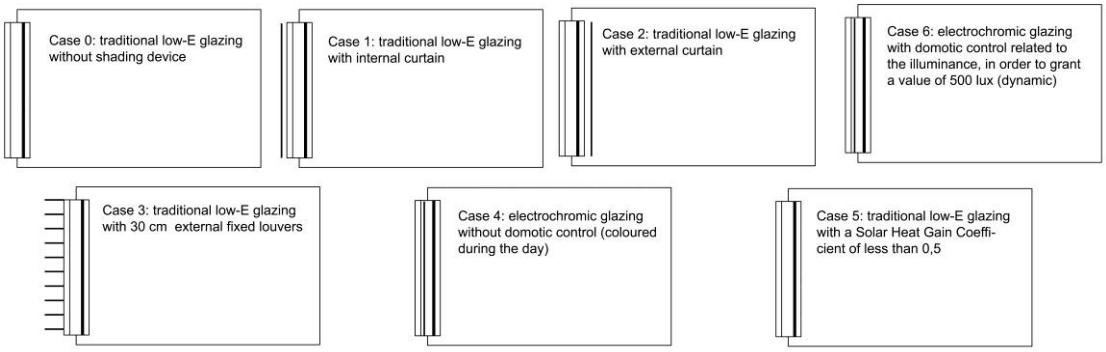

Figure 2. Shading systems to improve the thermal and visual performance of Case 0

The calculations of Solar Factor (g, expressed in percent) and thermal transmittance (U, expressed in W/m^2K) were carried out using the software Window 6.0 (developed at the Lawrence Berkeley National Laboratory of the University of California), in accordance with UNI 15099, which describes winter and summer climatic conditions, thus defining two different values for winter and summer performances. Case 6 uses the same electrochromic glazing as in case 4, but its visible transmittance coefficient is regulated by a control system depending on the internal illuminance value in the middle of the test cell in order to maintain a constant value of 500 lux. All glazed windows have the same U-value of 1,35 W/m^2K, while Solar Factor and Visible Transmittance Coefficient are variable, as shown in Table 1. The simulated space is provided with a control system which is capable to switch the lights on and off, depending on the illuminance value measured by the sensor placed in the middle of the room.

		Case						
		0	***1***	***2***	***3***	***4***	***5***	
g	Winter	0,53	0,375	0,162	0,541	0,075	0,401	Min 0,48
	Summer	0,544	0,40	0,172	0,545	0,121	0,418	Max 0,09
LT		65,6%	19,4%	16,9%	65,9%	2,9%	57,7%	62%-3,5%

Table 1. Solar Factor and visible transmittance coefficient in the analysed situations

RESULTS

The software EnergyPlus is able to evaluate both energy demand and visual comfort indicators at the same time. The most important values analysed are the primary energy

demand for heating, cooling and artificial lighting, the illuminance value, the glare index value, the number of hours in which the illuminance and the glare index threshold values of 500 lux and of 22 are exceeded respectively. The graph in Figure 3 shows the monthly primary energy demand of the simulated solutions: the value is the sum of energy demand for heating, cooling and artificial lighting in order to maintain a target illuminance of 500 lux.

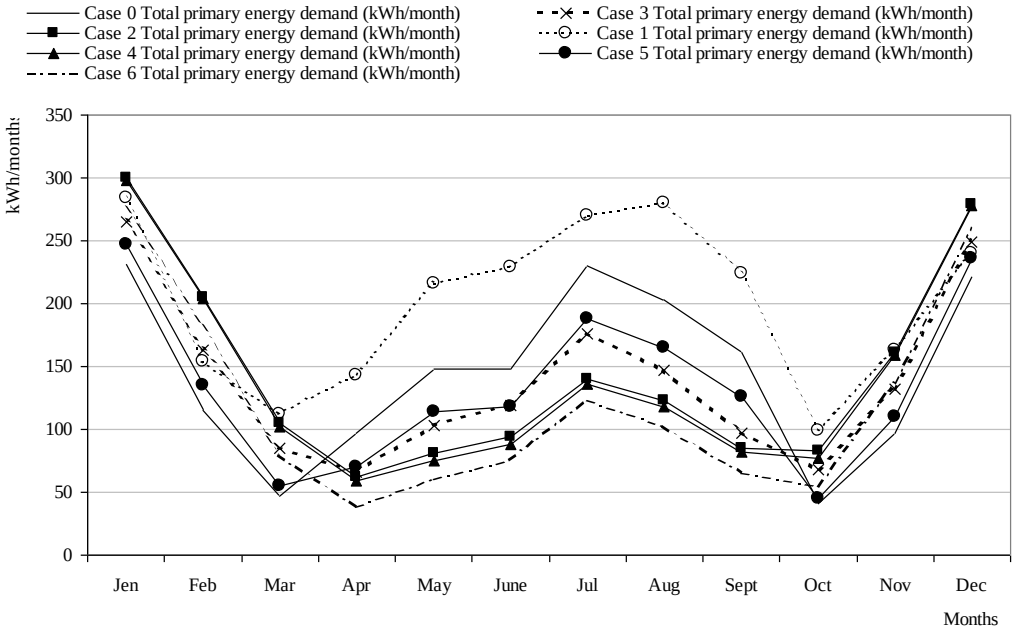

Figure 3. Annual Total Primary Energy demand (kWh/month)

The heating energy demand in Figure 4 does not show a linear trend: it decreases as the Solar Factor (g) increases, but it is also influenced by the Visible Transmittance Coefficient (VT), which acts as the control parameter for the operation of the artificial lighting system. Case 1, for example, has a smaller g-value than case 5, but the *VT* is very small and causes a considerable increase in the use of artificial lighting, with a consequent increase of internal gains and a decrease in the heating energy demand.

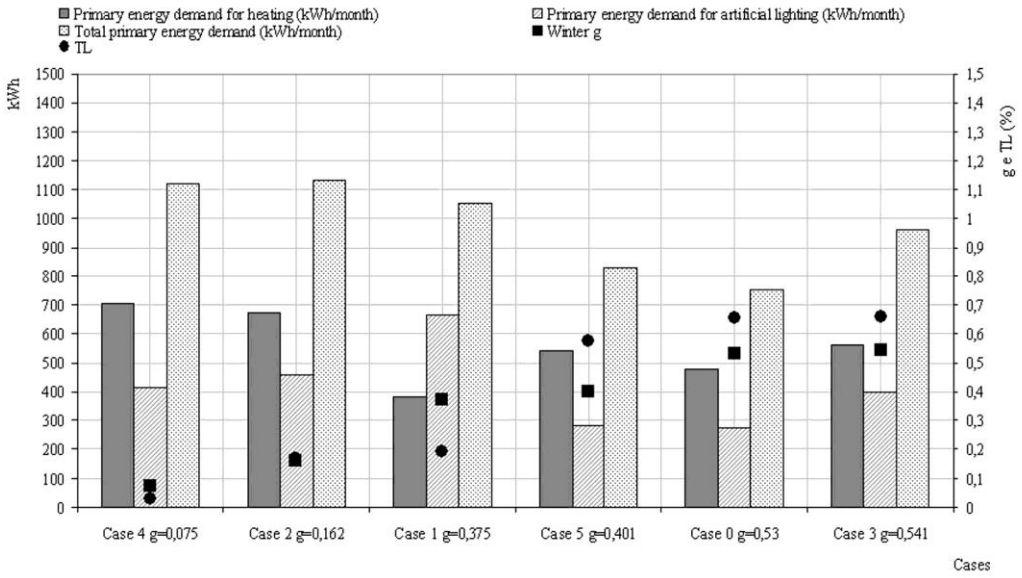

Figure 4. Primary energy demand related to winter Solar Factor

The increasing trend of g-value does not imply a linear growth of cooling primary energy demand (Figure 5), as it is influenced by the variation of *VT*: case 1, which has a high value of g-value and a low value of *VT* shows the highest result for cooling energy demand, which can be explained with the sum of solar radiation and high gain due to artificial lighting. When *VT* increases keeping a constant value of *g*, the variation of cooling energy demand is closely related to the entry of direct solar radiation: even if similar in cases 0 and 3, the cooling energy demand of the glazing system with external louvers, which facilitates the entry of diffuse solar radiation, is smaller by 30% with respect to the system with no shading device.

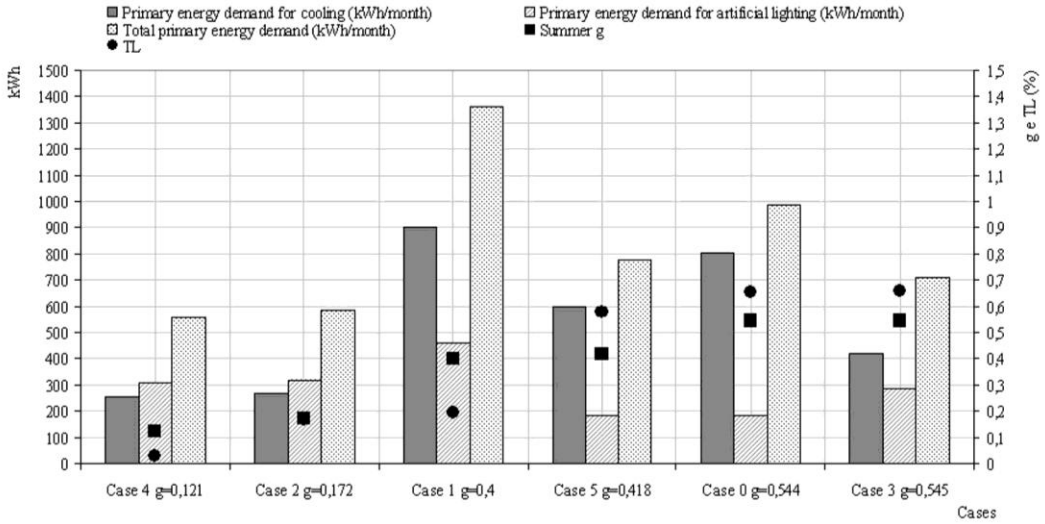

Figure 5. Primary energy demand related to summer Solar Factor

Also considering the visual comfort, graphs shown in Figure 6 and in Figure 7 point out how a small value of g-value is extremely limiting in terms of use of natural lighting provided by sunlight: higher values of g-value can frequently lead to glare-related problems. Cases 1, 2 and 4 show an excessive reduction of transmitted solar radiation, also outlined by the high energy demand for artificial lighting; cases 0, 3, 5 and 6 allow a better use of daylight for natural lighting of the indoor environment, even if only case 3 shows a good behaviour in reducing glare.

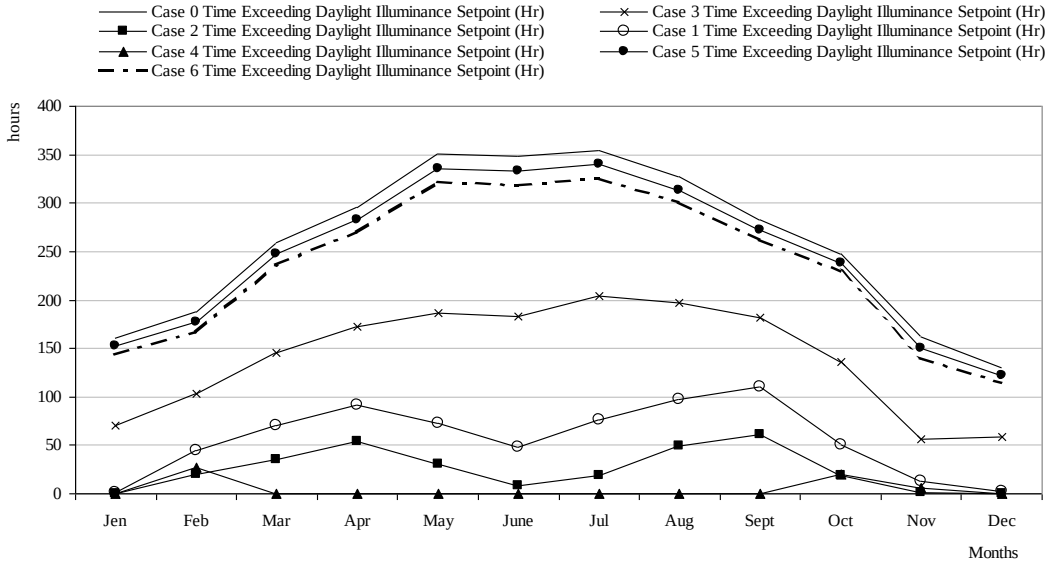

Figure 6. Time exceeding Daylight Illuminance set point at reference point in the middle of the room (hours/monthly)

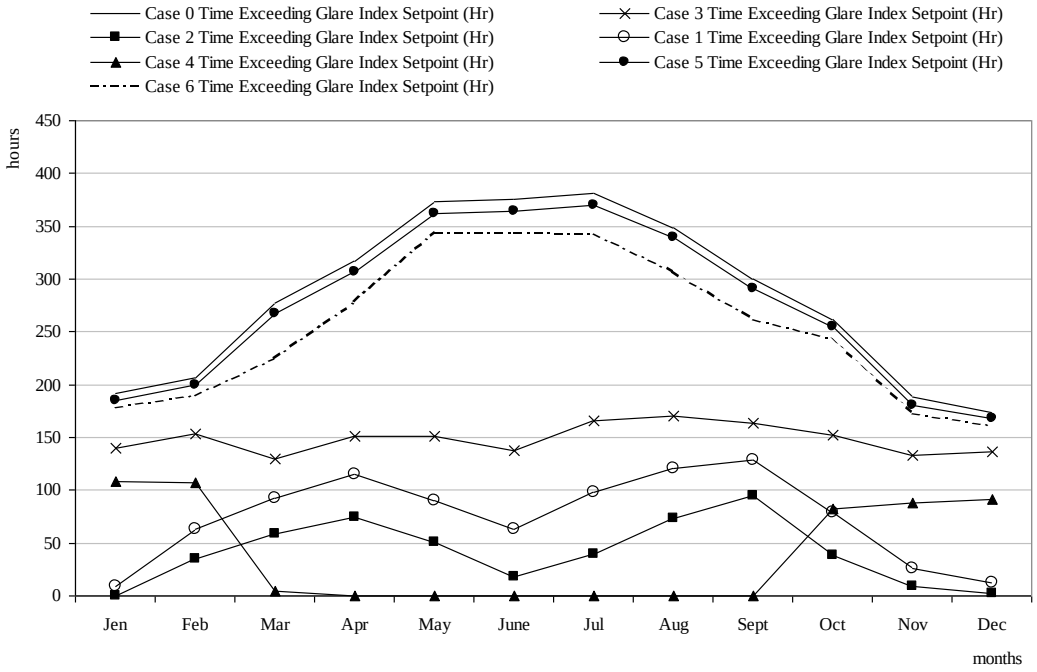

Figure 7. Time exceeding Daylight Glare Index set point at reference point in the middle of the room (hours/monthly)

The total primary energy demand of the electrochromic glass with the domotic control is the lowest among all the simulated solutions and the 500 lux illuminance is very often provided without resorting to artificial lighting. The monthly assessment shows a high percentage of hours during which the glare limit is exceeded; however, an analysis of hourly data shows that the limit value is exceeded by just a few points (Figure 8). The best situations as to the reduction of glare are those of cases 3 and 6; cases 1 and 2 show a very small value of glare index, but the use of natural lighting is also reduced. In cases 3 and 6 the 500 lux illuminance is often reached without using artificial lighting and the primary energy demand values are the lowest among the analysed solutions.

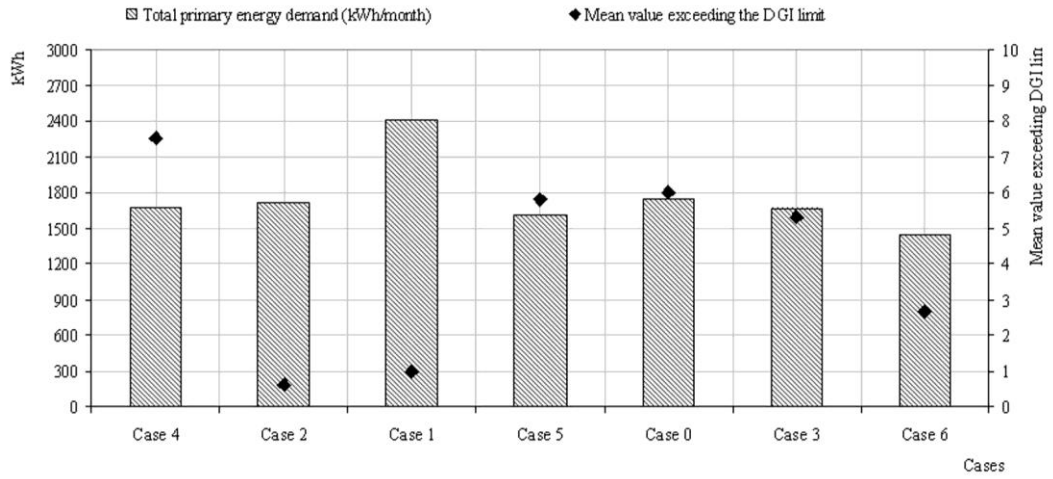

Figure 8. Total primary energy demand related to the mean value exceeding the DGI limit

The illuminance hourly trend in Figure 9 represents the trend on the central sensor and shows that case 6 reaches a constant value of 500 lux, while other cases denote a bell-shaped distribution. The domotic control is able to guarantee the desired minimum illuminance level

while reducing overheating and total primary energy requirements, which takes into account both cooling and artificial lighting consumption.

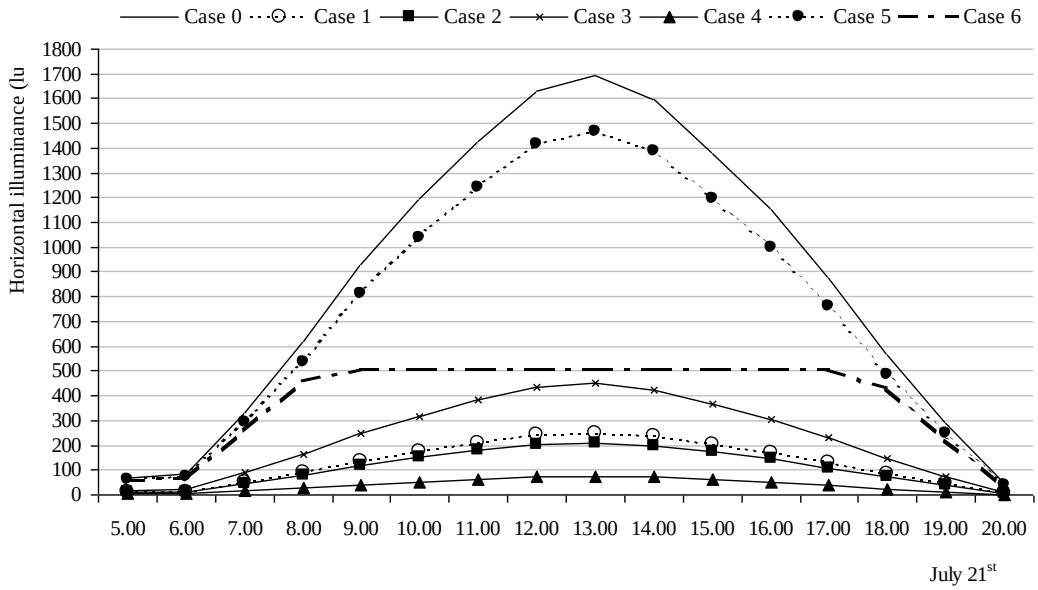

Figure 9. Illuminance in the middle of the room on July 21st

CONCLUSIONS

These studies emphasize the importance of a holistic design approach able to evaluate energy and comfort-related aspects at the same time. The paper outlines the importance of performing annual energy and comfort balances with monthly steps, as well as elaborating on the hourly trends in some days of the year. During the hourly analyses it is also important to examine the internal distribution of some indicators, such as illuminance.

In an office, where the internal gains are very high, the increasing of g-value influences more the glare effects than the reduction of the heating energy demand. Heating energy demand is influenced by g-value and indirectly by the VT which acts as the control parameter for the operation of the artificial lighting system. The regulations should give indications about g-value and VT at the same time: these are two indicators that need to be considered together. Considering the visual comfort, on the one hand a small value of g-value could limit the use of natural lighting provided by sunlight, while on the other hand higher values could lead to glare-related problems. Analysis results show that dynamic technologies are the most appropriate solutions for heterogeneous geographic contexts, while the usage of a unique g-value during the whole year can lead to poor results both concerning glare problems and energy consumption.

Each glazing system analysed during this research could be a good solution in a specific day or hour of the year, but it is important to consider the energy and comfort performance during the whole year. A domotic control of the shielding system is essential to guarantee both comfort and energy saving as a function of the climatic conditions and the room's intended use.

PLASMA LIGHTING TECHNOLOGY

Calame Laurent[1], Andreas Meyer[1], Courret Gilles[2]

1: Lumartix SA, Rue de l'Ouriette 131, 1170 Aubonne

2: *HEIG-VD, Institut MNT / Laboratoire de physique appliquée et des technologies émergentes, Avenue des sports 20, 1400 Yverdon-les-Bains, gilles.courret@heig-vd.ch*

ABSTRACT

The solar radiation is the main energy for the biosphere. During millions of years of evolution, living organisms have been adapting to the radiation that comes through the atmosphere. The Plasma Lighting Technology can reproduce the spectrum of this radiation like no other. As a psychological effect, a sense of summer day inside buildings is obtained at any time. The richness of the spectrum gives an impressive rendering of the indoor architecture, furniture and decoration.

The Plasma Lighting Technology reduces the environment footprints of buildings in two respects. The high luminous efficiency reduces the electricity consumption. Moreover, the design principle of this technology makes it suitable for intelligent heat management systems because most of the heat emission can be collected at its source.

In comparison to other discharge lamps, this technology offers a much longer lifetime. Substantial savings can be therefore expected on bulbs replacement and related maintenance operations.

Besides this technology is complementary to the LEDs, because the efficiency of the first increases as the bulb temperature increases, in opposite to the second. The today commercial offers of Plasma Lamps concerns mainly high power luminaires (700W and more). The LEDs are not competitive in this market segment.

This technology gives all its potential in the illumination of large volumes or large areas. It is particularly well suited for shopping centers, stadiums, halls, atriums, exhibition halls, television studios and theaters.

This innovative technology contributes to the CleanTech conversion for two reasons; it allows saving energy and stopping the release of mercury into the environment by lighting. She meets the new lighting standards set for 2016 by the European commission.

INTRODUCTION

The lamp is designed as a chain of modules going from the plug to the bulb (Figure 1). A power module outputs a direct voltage above 3 kV in order to supply a magnetron. This second component outputs microwaves at 2.45 GHz. The bulb, which is filled with a rare gas, is coupled to the magnetron so that a discharge appears at the electromagnetic resonance. Then the substance contained inside the bulb evaporates and heats up by induction, and as a result, a flux of light is produced. After a short warm-up, the light becomes very similar to the sunlight, as showed by spectral measurements.

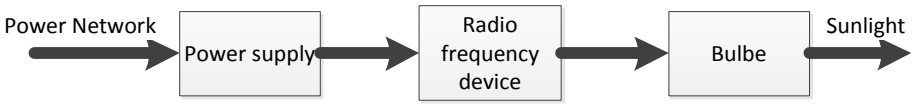

Figure 1: The design principle

SPECTRUMS

The light produced by the sun that comes through the atmosphere has a continuous spectrum in the visible (Figure 2). Most of its energy is spread from the UVB to the close infra-red.

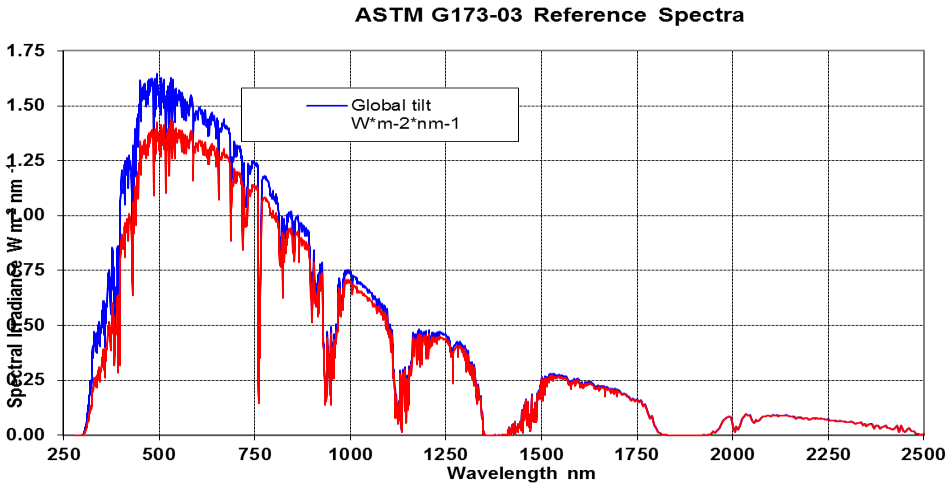

Figure 2: Solar spectrum on the earth [1]

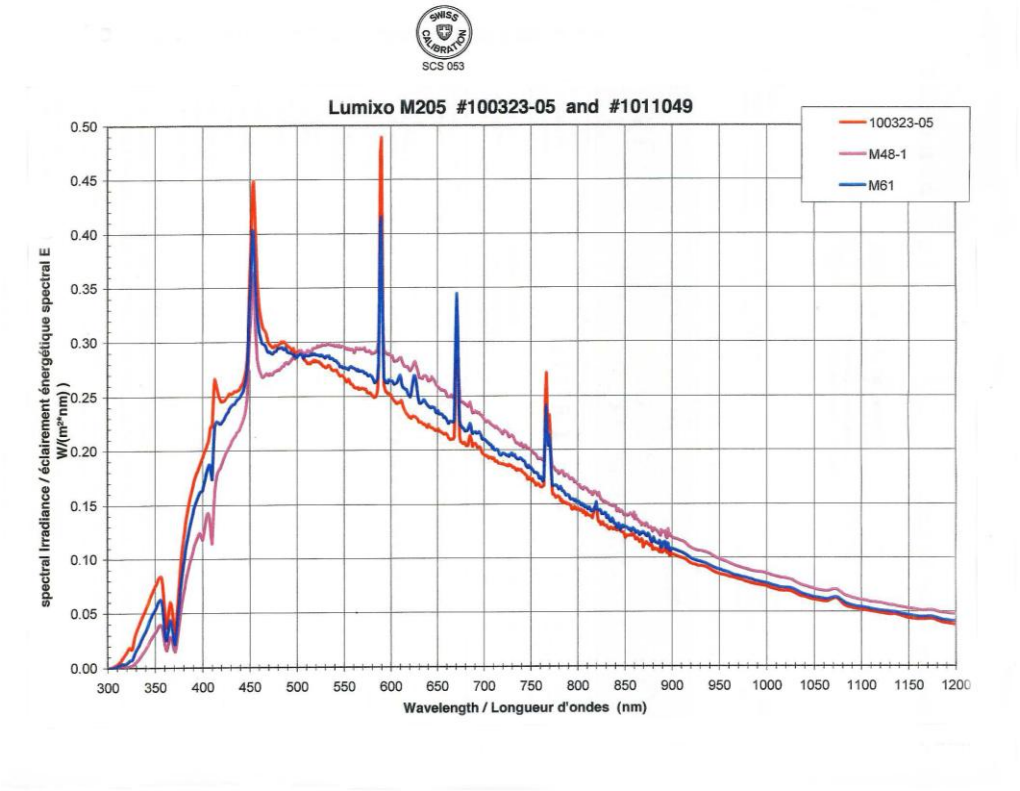

Figure 3: Spectrum of plasma lamps of the type "sunlight" of three different versions [2]

Comparing with the solar spectrum reveals an exceptional matching (Figure 4). We note however four peaks that rise above the solar spectrum, among which three are in the visible range. These peaks have no visible effect since they cover a neglectable area in respect to the total area covered in the visible range.

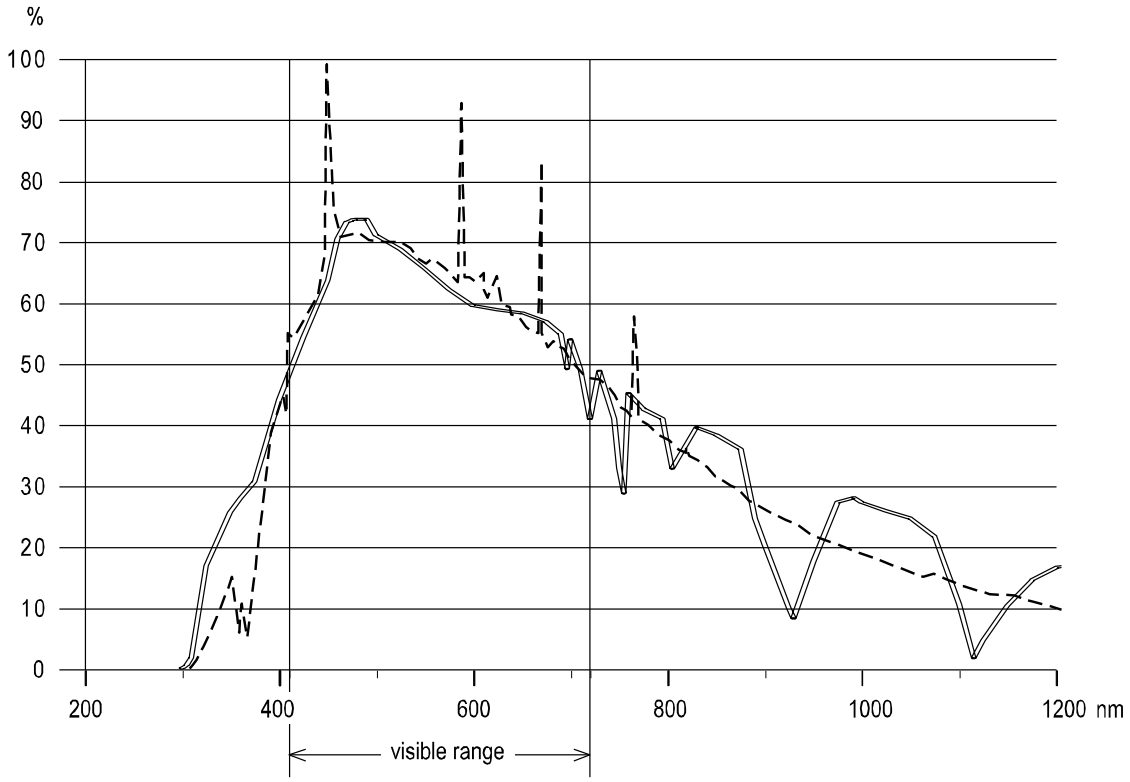

Figure 4 Comparison of the plasma lamp M61 (dash line) and the sunlight (double line)

SPECIFICATIONS

The light source has the following specifications:

- Solar spectrum or very high efficiency light (dependent of the bulb content)
- Lifetime : 40’000 h, 12h/day during 10 years
- Efficiency : 65 or 140 lm/W [2]
- Colour rendering : 98 (65 lm/W) or 80 (140 lm/W) [2]
- Colour temperature : 3500 K to 7000 K
- Power of light source : 1000W or 3000W
- CleanTech (without mercury or arsenic)

ADVANTAGES

The flow of energy comes into the bulb by induction. There is hence no electrode. This provides great advantages over standard discharge bulbs since electrodes suffer from erosion, and as a result, modify the content. Hence the light output fades continuously during

utilization and the spectrum changes as well (cf. Figure 5). With the Plasma Lamps, the quality and the quantity of light are preserved throughout the lifetime of the bulb.

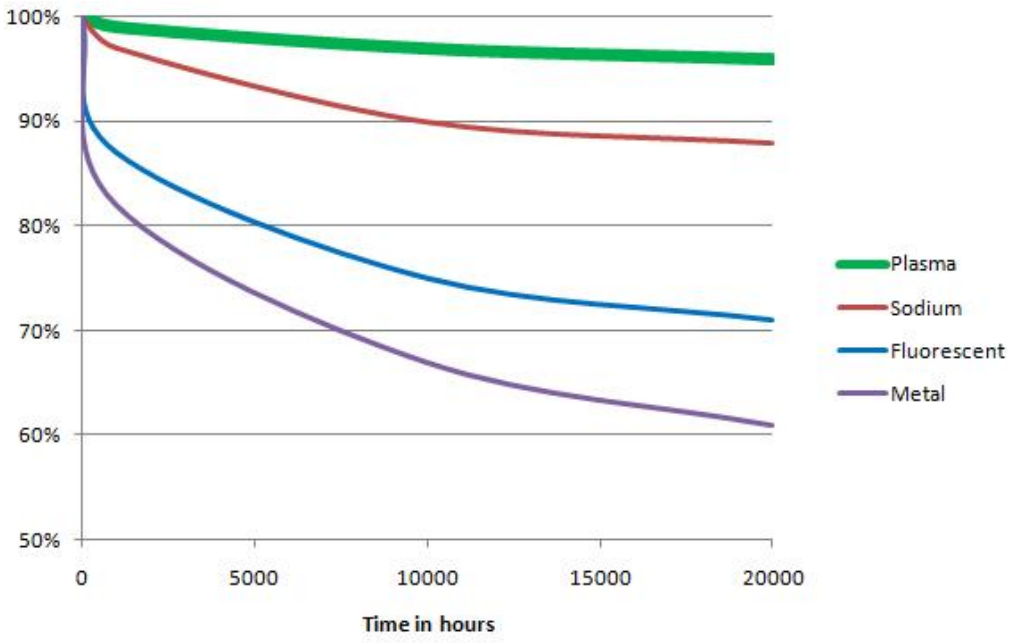

Figure 5: Output fading of the discharge lamps that meet indoor lighting requirements [3]

ENERGETIC RANKING

Plasma Lighting Technology is the best compromise in terms of energy efficiency, lighting quality and durability. It ranks among the Class A lighting technologies. It extends more than double the return sought by the class A in the configuration "energy efficiency".

Classe	Efficacité
A	> 50 lm/W
B	51< lm/W<21
C	20< lm/W<16
D	15< lm/W<13
E	13< lm/W<11
F	11< lm/W<9
G	< 9 lm/W

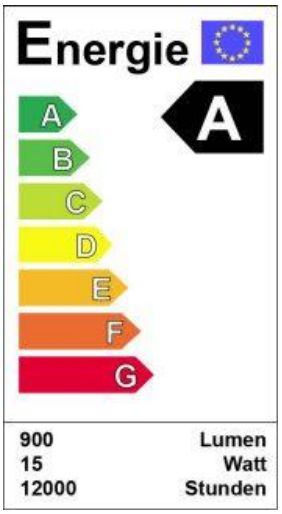

CLEANTECH

This technology is the only discharge lamp technology that meets the requirement of color rendering in building and that uses no harmful substance, unlike nowadays technologies which uses bulbs containing mercury.

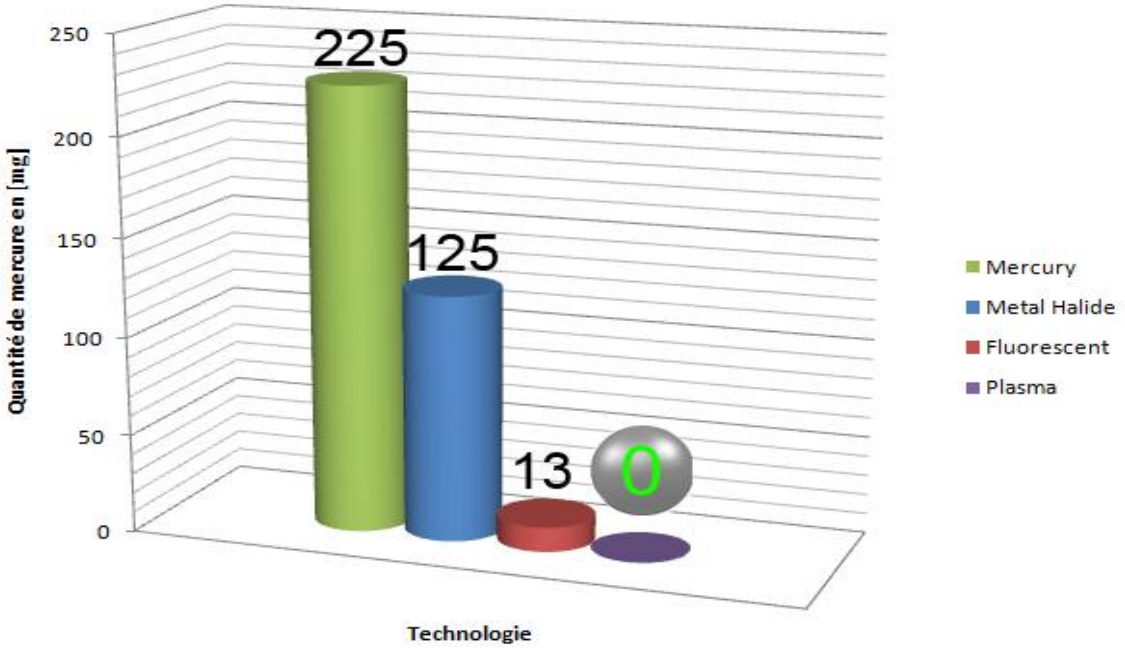

Figure 6: Mercury content of the discharge lamps that meet indoor lighting requirements [4]

The high efficiency and the reduction of consumable reduce the environmental footprint.

IMPACT ON AIR CONDITIONING

The design principle of the Plasma Lighting Technology makes it suitable for intelligent heat management systems. Indeed, almost half of the heat emission is localized in the power module and the magnetron. In operation, these modules are cooled by a forced air flow. Using a low speed fan the noise has been reduced below any perception for the users. If this air flow is extracted outside in the periods of cooling demand, the load of air conditioning due to lighting is then cut by half. Of course, in order to get even more energy savings, the air flow can be directed advantageously into the occupied volume in the periods of heat demand (Figure 7).

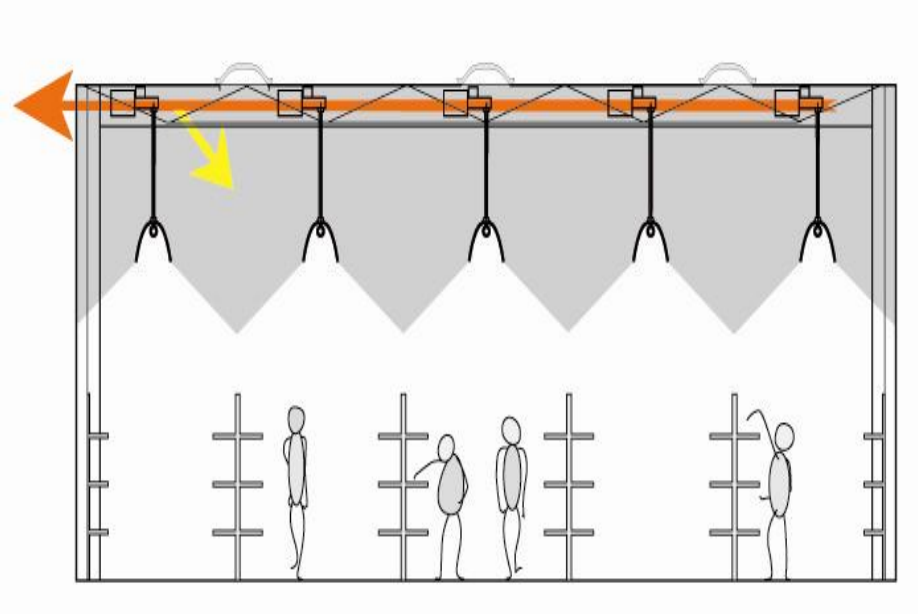

Figure 7: Heat management [5]

CONCLUSION

Thanks to their longer lifetime, nowadays Plasma Lamps are economically competitive. The today commercial offers concerns mainly high power luminaires (700W and more). This technology gives all its potential in the illumination of large volumes or large areas. It is particularly well suited for shopping centers, stadiums, halls, atriums, exhibition halls, television studios and theaters. Moreover, comparing to other discharge lamps that meet the indoor lighting requirements, this is the only available solution to prevent any risk of dissemination of toxics, as the competing discharge lamps use bulbs containing mercury. Plasma Lamps meet the new environmental standards, which will come into force in 2016 in Europe. LEDs do not contain mercury, but contain heavy metals. In addition LEDs are not suitable for luminaires of high power, the segment market addressed by the Plasma Lamps of nowadays.

The Plasma Lighting Technology is classified as Class A in the luminous efficiency ranking. It even exceeds the value of a factor two in its optimal configuration.

The Plasma Lighting Technology can reproduce the spectrum of the solar radiation like no other. This gives a sense of summer day inside buildings at any time, and an impressive rendering of the indoor architecture.

REFERENCES

[1] CIE, International Commission on Illumination

[2] Opto.cal gmbh, accredited by Swiss Calibration Service SCS

[3] Osram, Philips, LG Electronics

[4] Osram, Philips, GE, LG Electronics

[5] Sergio Marques Dos Santos, Gilles Courret, Andreas Meyer, Remote sulphur lamp, Office Fédérale de l'Energie, N° du projet : 103152, Rapport final, décembre 2010.

STREAMLINING ACCESS TO INFORMATIVE PERFORMANCE METRICS FOR COMPLEX FENESTRATION SYSTEMS

S. Dave[1]; M. Andersen[2];

1: Building Technology Program, Massachusetts Institute of Technology, Cambridge, USA.

2: Interdisciplinary Laboratory of Performance-Integrated Design (LIPID), ENAC, Ecole Polytechnique Fédérale de Lausanne (EPFL), Lausanne , Switzerland.

ABSTRACT

A mechanism to accurately assess the performance of complex fenestration systems (CFS) is crucial for driving the appropriate adoption of these technologies to improve user comfort and energy use in both new construction and retrofit design. Typically, CFS are not provided sufficient consideration because user intuition is lacking: existing metrics, while valid for conventional systems, fail to reveal the dynamic nature of the performance of CFS. Conducting and reporting elaborate simulation results is neither feasible nor useful for manufacturers and users and thus a comprehensive rating system based on novel performance metrics has been identified as a means to describe CFS. This paper describes the methodology used to determine the simplified calculation procedure for three metrics defined in a previous paper, and the rational for the ultimate decision. The three metrics, the Relative Energy Impact (REI), the Extent of Comfortable Daylight (ECD), and the View-Through Potential (VTP) aim to provide context in three important areas of daylighting technology performance, namely energy efficiency, occupant visual comfort, and view through the facade respectively, such that the user can select systems to address his or her own priorities. Conducting and reporting full resolution calculations for all input conditions would be unfeasible and unwieldy because of the quantity of data that would have to be managed and the effort that would be spent on such en enterprise for every system. A method to eliminate redundancies and minimize the number of input parameters and calculations thus becomes necessary. This paper proposes an approach based on trends, sensitivity analysis, and error minimization techniques and presents the iterative simplifications required to produce the same relative ranking performance of the sample systems as a benchmark analysis would.

INTRODUCTION

Complex Fenestration Systems (CFS) are defined as daylighting facade systems that manipulate light in a variety of innovative ways in order to achieve improved performance objectives. When used appropriately, these advanced daylighting systems have the potential to reduce a building's energy use by up to 41% [1]. Buildings in the United States account for about 40% of the nation's energy use, 33% of which is attributed to heating and cooling and an additional 18% of which is associated with lighting energy use [2]. A building's facade system affects both these categories of total energy use as well as the visual comfort of occupants within the space. Broadly and qualitatively, occupants prefer well daylit spaces to spaces that are lit only with artificial light [3]. However, direct sunlight can present contrast problems, especially in spaces in which occupants use computer or television screens. Finally, windows are considered to be a channel by which occupants connect with the outdoors via the view to the outside. Ultimately, there are tradeoffs to performance in each of these categories as systems are typically optimized for a particular consideration.

The mathematical quantity which describes the angular behaviour of light through a facade is known as the Bi-Directional Transmission Distribution Function (BTDF). The BTDF is a relationship between the flux of light transmission and its angles of incidence and emergence, not a measure of system performance under actual facade conditions, which makes it difficult for anyone to relate the system to its contextual environment intuitively. The gap between BTDF values and system performance is complex enough to require a simulation workflow, which obviously renders the performance as being project-specific. Metrics that could relate BTDF quantities directly to at least relative performance (which would also make the information more generic) have the potential to fill this gap and provide context and intuition about a complex fenestration system to its users.

Existing metrics for conventional fenestration systems do describe aspects of each of the three categories presented previously, energy efficiency, occupant visual comfort, and view through the facade, for conventional systems. Reporting of fenestration specifications using these metrics is described in the United States by the National Fenestration Rating Council (NFRC), which mandates the calculation process and the labels that window manufacturers must provide on their windows upon sale to end users. The definition and calculation process of these metrics is adequate for simple window facades that do not exhibit significant angularly or spectrally changing properties. But because the existing approach is based on a single set of environmental conditions, it cannot be used as a reliable measure of annual performance for CFS, as these systems are often highly sensitive to solar position and climate conditions. Thus, there is a need for metrics that utilize the whole BTDF, rather than a single incident condition, and real climate data that changes with location and season in order to reveal the dynamics of complex fenestration systems.

THREE METRICS TO DESCRIBE CFS PERFORMANCE

In order to accomplish the needs described previously, three metrics have been defined to address the three most critical aspects of fenestration system performance mentioned previously, namely: energy efficiency, occupant visual comfort, and view through the facade.

Relative Energy Impact (REI)

The Relative Energy Impact or REI metric is defined as the effect on energy load that can be attributed to a particular fenestration system as compared to a base case scenario. The full resolution calculation of the REI metric uses climate data provided by the US Department of Energy and heat transfer and solar heat gain models in order to calculate the absolute value of energy that traverses the facade system [4, 5]. The net direction of energy flow is then identified as contributing to (increasing) or decreasing the energy load of the building's heating or cooling system. Lighting is accounted for using a simple algorithm that divides the test space into three zones, the perimeter, the middle, and the interior zones. Each zone is considered to have lights on unless all sensor locations within the zone exceed a given illuminance threshold chosen to be 200 lux, whereby the lights are dimmed. If all locations in the zone exceed 300 lux, the lights are turned off. But if the vertical illuminance produces a Daylight Glare Probability of more than 0.47, blinds are assumed to be drawn and lights are turned on, dimmed, again [4]. It is then possible to determine a value for the annual electricity required for the space for the base case window (double pane clear window) scenario and thus for each CFS as compared (normalized) to the base case.

Extent of Comfortable Daylight (ECD)

Meanwhile, although a subjective concept, occupant visual comfort can be described quantitatively using metrics that based on a virtual occupant's viewpoint in a space [6]. These

metrics are inherently disconnected from the fenestration system and rely on simulations, renderings, or measurements to calculate. The Extent of Comfortable Daylight or ECD has thus been defined to provide a reference of visual comfort as it relates to the particular facade system [4]. It is the percent of time and space which achieves comfortable daylighting conditions – exceeds a minimum illuminance threshold (similar to Daylight Autonomy [7]) and remains below a threshold of glare acceptability (based on Daylight Glare Probability thresholds [5]) – rather than relying on a particular field of view. Using a generic test space, values are calculated over the course of the year to provide a single value that describes the overall visual comfort, again with respect to a base case [4]. The ECD metric is calculated using vertical and horizontal illuminance readings for 300 sensors in the test module. The values for these illuminance sensors are calculated using the *genklemsamp* command that allows *Radiance* to use a Klem's basis BTDF and generate renderings and measurements with its ray-tracing engine [9]. (The same horizontal illuminance values are used to determine lighting loads in the REI metric.) This simulation provides values for each sample at 56 moments of the year, suggested as being representative of the year's lighting conditions [10].

As with the energy efficiency calculations, the ECD metric will be reported as a comparison to the base case window scenario. This provides a physical reference for how a complex fenestration is performing relative to a standard alternative.

View Through Potential (VTP)

Finally, the visible transmittance is a value that is widely accepted to describe facade systems and also available to users via the labels required by the NFRC. It can be calculated using BTDF values associated to normal incidence of sunlight penetration. Although this value does not change significantly for other incident light angles with conventional systems, angularly selective facades can exhibit large ranges of transmission values.

The View Through Potential addresses this property of a system by measuring its degree of scatter: because direct (undistorted) light, i.e. light that has not been bent or scattered, is required to produce a faithful image, direct light transmission can arguably be used as a proxy for the potential of clear view through a system. A fenestration system may provide a clear view from only one or a few selected view directions, unlike a standard clear window e.g. which would provide a clear view from most angles. In some cases, for example a bathroom window, a clear view may be unnecessary, or even undesirable. Ultimately, an occupant's most direct connection with a facade is how it looks and feels in a space, so the ability to view through is likely to be a critical performance argument in addition to energy and visual comfort performance.

The VTP metric approximates the capability of view through a façade by using the proportion of direct (undistorted) light transmission compared to non-direct (distorted) transmission as a basic proxy for an occupant's ability to view an undistorted image through it.

By using the transmission of a hole as a reference, it is possible to determine what portion of a system's BTDF can be considered as direct transmission: the BTDF of a sample is compared to the measured BTDF of a hole, where the hole represents a perfectly clear and undistorted view and, numerically, the "sharpest" peak in BTDF (Figure 1).

The amount of light that is transmitted in perfect transmission (a hole) is $BTDF_A$, $BTDF_C$, and $BTDF_F$. The ratios below refer to the drop off associated with ideal transmission.

$$r_C = \frac{BTDF_C}{BTDF_A}, \qquad r_F = \frac{BTDF_F}{BTDF_A} \tag{1}$$

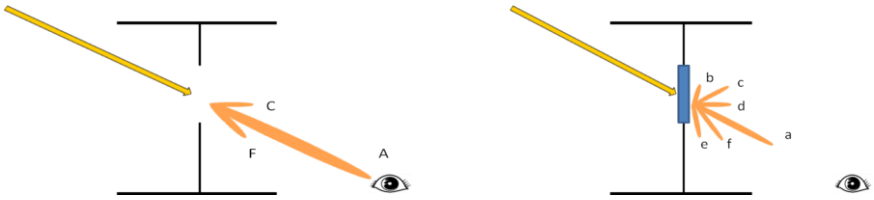

Figure 1: Visual representation of the BTDF of a hole (left) and a sample system (right) for a given view angle.

The amount of light that is transmitted directly due to the sample façade is *a*. The amount of light attributed to direct transmission in a given emerging direction is shown below, where $BTDF_a$ refers to the amount of light that is being transmitted in the view direction.

$$BTDF_{direct,c} = r_C * BTDF_a \tag{2}$$

Light that is being transmitted in directions along which it is modified or distorted – i.e. providing light but not view – is shown in Equation 3.

$$BTDF_{nondirect,c} = BTDF_c - BTDF_{direct,c} \tag{3}$$

The light transmitted in the b, d, and e directions is entirely non-direct. Once these fluxes have been separated into the direct and non-direct components (*BTDF* in Equation 4), the associated direct and non-direct integrated transmission is calculated [12].

$$flux(\theta_1, \theta_2, \emptyset_1, \emptyset_2) = \begin{cases} BTDF(\theta_1, \theta_2, \emptyset_1, \emptyset_2) * 2\pi * \left(1 - \cos\left(\frac{d\theta}{2}\right)\right) * \cos(\theta_2) & for\ \theta_2 = 0 \\ BTDF(\theta_1, \theta_2, \emptyset_1, \emptyset_2) * \sin(\theta_2) * \cos(\theta_2) * d\theta * d\emptyset & else \end{cases} \tag{4}$$

The degree of scatter, defined as *S* in Equation 5 below, is determined by calculating the ratio of direct transmission to scattered (everything but direct) transmission for a particular incident and emerging angle. τ represents the sum of fluxes for a given incident direction.

$$S = \frac{\tau_{direct}}{\tau_{diffuse}} \tag{5}$$

The degree of scatter is conducted for each view angle in the generic test space and consolidated into a single VTP value: the VTP metric is calculated using 300 sensor locations at eyelevel in the test module viewing 70 grid locations on the facade system so as to take into account that some view angles will be more relevant than others once the system is considered in a spatial context: while it may appear intuitive to disconnect the fenestration system from the space by identifying direct and diffuse transmission for each of the Klem's basis angles, integrating the test space in this analysis allows a weighting of view angles depending on their relevance to a user (view directions from a ceiling are typically irrelevant).

The averaging process applied to the room and window locations thus automatically weights the important angles more heavily than grazing angles that are unlikely occurrences for view. Again, normalization with the base case is important for comparison purposes since spaces are undeniably more complex than the test module.

RELATIVE RANKING AND DATA REDUCTION

Each of the metrics were evaluated for a generic space for 5 different systems using detailed hourly climate data and lighting simulation techniques. This full resolution dataset was then used as a benchmark for system performance ranking.

The systems covered a wide range of behaviours and included: a reflective, bi-colour fabric blind, a Holographic Optical Element, curved mirrored blinds, opalescent plexiglas and a prismatic panel, for which measured BTDFs were available [12]. The REI and ECD metrics were calculated using the highest resolution of input parameters for location, climate, and orientation, totalling 300 values for each, and about 120 hours of simulation processing time. The VTP metric was calculated independently of climate and location as it related to light transfer through a system but independently of sky conditions and sun position.

The data reduction procedure aims to reduce the quantity of input conditions by reducing the resolution of each input parameter, without affecting the ranking provided by the benchmark case. Beginning with the benchmark data set, the authors selected a number of reductions in resolution which simplify the process yet do not significantly affect the accuracy of the REI and ECD values. Each level of simplification was added to the previous and the percent difference in REI and ECD value with respect to the full resolution case was calculated and reviewed. If the simplifications caused unacceptable discrepancies compared to the full resolution data, they were revised or eliminated from the process.

Climate zones and heat transfer for REI

The simplification process to the REI metric was conducted in three steps. From the initial fifteen climate zones, cities that consistently produced the same ranking were grouped into a single zone. This initial simplification reduces the number climate zones to eight based on latitude, nearly a 50% reduction in the number of calculations required. The most representative climate zone was identified among those grouped by calculating the mean square variance of each climate zone and selecting the zone that provides the least total mean square variance across all the sample systems. The Maximum Variation column in Table 1 refer to a particular sample and climate location that is worst affected by the data reduction process, even if the ranking of systems remains constant.

Second, although the quantity of heat that passes over the facade varies greatly with climate zone due to indoor and outdoor temperatures, the U-factor remains fairly constant (variance of about 0.02 W/m^2 or less). Returning to the NFRC procedure to calculate the U-factor does not affect the overall accuracy of the REI metric substantially. Finally, condensing the solar heat gain factor to be a function of only time of day further increases the maximum variation.

REI simplification	Max variation	**ECD simplification**	Max variation
Four climate zones	22%	Four climate zones	5%
NFRC U-factor [8]	27%	Perez Intermediate sky [11]	18%
SHGF: time of day	35%	Direct/diffuse irradiance + sky clearness: time of day	25%

Table 1: Simplification process and maximum variation from benchmark calculation, south.

Latitude and sky conditions for ECD

Similarly, we applied a step by step simplification process to the full resolution calculation of the Extent of Comfortable Daylight (ECD) metric. The climate locations were reduced in the same manner; in this case, only one climate zone per orientation is necessary to produce the accurate ranking. Further simplifying the inputs to the *Radiance* simulation by defining all skies as Perez Intermediate skies increases the maximum variation to 18%. Finally, reducing the resolution of climate parameters to time of day affects the ECD metric less than the REI metric, but still increases the maximum variation.

Benchmark for VTP

The approach considered for the VTP metric was different. Since the ability to view through the facade is not related to solar position or climate conditions but rather on the degree of scatter of the system from a given view position, the quantitative calculation for VTP will be compared to a human opinion of overall view.

User studies will thus be conducted to validate the occupant ranking of view through by having Participants will be asked to observe various CFS samples and provide a ranking on view clearness going from perfectly clear to no view at all, with intermediate levels such as sense of contrast/distorted view, clear contrast/slightly distorted view, etc. We will then be able to evaluate calculated VTP values for these samples against perceived view through.

DISCUSSION

This paper proposed three performance metrics named Relative Energy Impact (REI), Extent of Comfortable Daylight (ECD) and View Through Potential (VTP) that are able to provide a link between optical properties – expressed as BTDFs – and relative benefits or limitations for an application as a façade element. It also proposes a way to reduce the overall complexity of the calculation procedure for determining the REI, ECD, and VTP metrics for CFS. Ultimately, the metrics described will be calculated using an analytical prediction that eliminates the need for annual simulation, such that they can be calculated using only climate data and BTDF values. The ultimate metric system is projected to be a ranking system that does not report absolute metric values but a system's relative performance (grade e.g.) for each of the input parameters.

The thermal performance that achieves a high ranking in a hot climate will not achieve the same degree of energy performance in a cold climate. The performance could potentially be reported on a specification sheet that accompanies the sale of a CFS, but this approach requires greater initiative from the user than the current metric structure does. In an effort to maintain the current metric reporting structure that is mandated for fenestration systems, the critical information must be represented in an easy-to-use manner at the scale of a label. Rather than being bound to the current value reporting approach, various mechanisms of representing different climate zones and orientations are being explored based on the results of this simplification procedure. Most notably, the reduction of the number of climate zones requires users to identify the location as being only one of four zones as opposed to fifteen.

ACKNOWLEDGEMENTS

The financial support for this research was provided by the MIT Energy Initiative Seed Grant (S. Dave) and through MIT and EPFL (Prof. M. Andersen).

REFERENCES

1. Arasteh, D., Apte, J., Huang, Y.J. "Future Advanced Windows for Zero-Energy Homes", ASHRAE Transactions, 109, 2 (2003).
2. Environmental Information Administration (2008). EIA Annual Energy Outlook.
3. Saxena, M., Heschong, L et. al., "61 Flavors of Daylight, American Council for an Energy Efficient Economy", ACEEE (2010).
4. Dave, S., Andersen, M. "A comprehensive method to determine performance metrics for complex fenestration systems." 27th Conference on Passive and Low Energy Architecture. *(forthcoming)*.
5. Karlsson, J., Karlsson, B., Roos, A., "A simple model for assessing the energy performance of windows," Energy&Buildgs, 33 (2001).
6. Wienold J. "Dynamic daylight glare evaluation." Proc. IBPSA Conference, Glasgow, July 27-30, pp. 944-951, (2009).
7. Reinhart, C.F., Walkenhorst, O., "Validation of dynamic RADIANCE-based daylight simulations for a test office with external blinds," Energy & Buildings, 33 (2001)
8. Saxena, M., Ward, G., Perry, T., Heschong, L., Higa, R. "Dynamic radiance – predicting annual daylighting with variable fenestration optics using BSDFs" SimBuild – forthcoming. (2010).
9. Kleindienst, S., Bodart, M., Andersen, M., "Graphical Representation of Climate-Based Daylight Performance to Support Architectural Design". LEUKOS - The Journal of the IESNA, 5, 1 (2008).
10. National Fenestration Rating Council. <www.nfrc.org> Accessed 14 October 2010
11. Perez, R., Seals, R., Michalsky, J "All-weather model for sky luminance distribution – preliminary configuration and validation" Solar Energy, 50, 3 (1993).
12. Andersen, M. "Validation of the performance of a new bidirectional video-goniophotometer" Light. Res. & Technology, 38(4) (2006).

ENERGY SAVING POTENTIAL AND STRATEGIES FOR ELECTRIC LIGHTING IN FUTURE LOW ENERGY OFFICE BUILDINGS: A LITERATURE REVIEW

M.-C. Dubois[1], M Arch PhD, Å. Blomsterberg[1], M Sc PhD

1: Div. Energy and Building Design, Dept of Architecture and Built Environment, Lund University, P.O. Box 118, SE-221 00 Lund, Sweden, marie-claude.dubois@ebd.lth.se

ABSTRACT

This paper presents a literature review carried out as part of a large Swedish research project entitled 'Energy-efficient office buildings with low internal heat gains: simulations and design guidelines'. This literature review specifically concerns energy saving potential and strategies for electric lighting in future very low energy office buildings. This review reveals that realistic energy saving figures of around 50% are achievable if the base line for comparison is the average office lighting energy intensity of around 21 kWh/m^{2}yr (valid for Sweden). Thus an electricity use of around 10 kWh/m^{2}yr for lighting office rooms is a realistic target in new low energy office buildings and building retrofits, assuming typical illuminance levels for office rooms.

This paper also discusses strategies for reducing lighting electricity use, which include: improvements in lamp, ballast and luminaire technology, use of task/ambient lighting, improvement in maintenance and utilization factor, reduction of maintained illuminance levels and total switch-on time, use of manual dimming, occupancy switch-off sensors and photoelectric dimming. Strategies based on daylight harvesting are also addressed and some design aspects such as window characteristics, reflectance of inner surfaces, ceiling and partition height are briefly discussed.

Overall, this review reveals that energy savings may be achieved by simply improving the electric lighting system i.e. by replacing or planning the electric lighting installation with energy-efficient luminaires fitted with T5 fluorescent lamps and CFL (or LED lamps) for task lighting and a combination of task/ambient lighting design, manual dimming, occupancy switch-off, etc. Daylight harvesting based on photoelectric dimming can provide additional energy savings even considering 'reasonable' glazing-to-wall ratios (GWR) of no more than 20-40%.

INTRODUCTION

Commercial buildings, and primarily office buildings, are classified among the buildings presenting the highest energy consumption. A recent inventory of energy use in 123 Swedish office buildings of different age revealed that office buildings have an energy intensity of 210 kWh/m^{2}yr in average, with a high electricity use by square meter (93 kWh/m^{2}yr excluding heating) [1]. However, office buildings also have a high potential for energy savings according to previous research in this field [2].

Electric lighting is one of the areas where energy savings are achievable at reasonable cost in new buildings as well as in retrofit projects. This article explores the potential for energy savings as well as strategies to reduce energy use in office lighting in the context of Northern Europe, with emphasis on the Swedish context. The article is based on a literature review

carried out as part of the Swedish research project 'Energy-efficient office buildings with low internal gains: simulations and design guidelines'.

METHOD

This review consisted of reading the literature from 1990 to 2011 related to electric lighting in office buildings for the Northern European or Nordic context. Around 150 scientific articles and reports were selected and summarised. Some information was also retrieved from websites of lighting organisations in Scandinavia.

RESULTS

1. Potential for energy savings in office lighting

An existing office uses around 21-23 kWh/m^{2}yr for electric lighting whereas a modern advanced installation may only use 11 kWh/m^{2}yr. If occupancy and daylight sensors are integrated in the installation, the annual energy consumption for lights may come down to as low as 5 kWh/m^{2}yr [3]. The potential for electricity savings is thus large. Besides direct electricity savings due to reduced use of electric lights, indirect energy savings can also be obtained in the warm season because of the reduced heat production and energy consumption for air conditioning. The following sections explore the strategies for reducing electricity use in office lighting.

2. Energy saving strategies related to the electric lighting system

2.1 Improvement in lamp technology

Although T5 fluorescent lamps have existed for 15 years, recent statistics (for Sweden) [1] indicate that the majority of existing lighting installations still use T8 or even, older T12 lamps, which have a much lower luminous efficacy (lm/W). Replacing T12 with T8 lamps can save up to 10% of the energy consumption while giving 10% more light [4]. Newer, T5 16 mm lamps have even higher efficacies (90-104 lm/W) achieving a 40% reduction in energy use (compared to T12 lamps of 60 lm/W with magnetic ballasts) but these lamps need different fittings [4].

According to current predictions, LEDs will provide the majority of light sources by 2035 [5]. The light efficacy of LEDs is increasing very quickly; it has nearly doubled every other year. In 2009, white LEDs with a light efficacy of 100 lm/W were available. However, it is expected that more traditional light sources will have a major role to play for some time yet [3]. This means that it will be developments in the design and control of the lighting installations that are likely to provide substantial energy saving opportunities in the immediate future [3].

2.2 Improvement in ballast technology

In order to improve efficiency, high-frequency (HF) ballasts have been developed in the course of the last decades, which have fewer losses. HF lighting has many advantages: an improved lighting quality, flicker-free lighting, and reduction in power demand, compatibility with occupation sensing and daylight control, better controllability and longer life. HF-ballasts are used in only 50% of today's lighting installations in spite of the fact that they have existed for more than 15 years and that conventional ballasts create negative effects both for energy-use and health [6, 7].

2.3 Improvement in luminaires

Lighting equipment essentially consists of a lamp, controls and control gear if needed, and a luminaire, each contributing to the overall efficiency [4]. New lighting fixtures reflect light in such a way that more light can be used where needed and less light gets lost in the light fixture itself [9]. Fittings with HF ballasts can result in savings of 20-25%, with a 20% longer life. Savings of up to 70% can be expected if HF is combined with other lighting improvements such as new luminaire designs and control [8].

2.4 Use of task/ambient lighting

A good general strategy used when integrating daylighting into a project is task/ambient electric lighting strategies, which use two levels of lighting to provide the illuminance requirements of the space; one providing an ambient level of lighting adequate for circulation and general tasks, and one providing higher illumination localized to the specific tasks that require it [8, 10]. Since daylighting is an effective method for providing the ambient needs of the space, but is not as effective in maintaining high localized illuminance requirements, a task/ambient lighting approach can better integrate with available daylight [11].

2.5 Maintenance factor

In offices, schools and shops, the lighting output can be reduced by up to 5% per year [12]. This reduction in light output depends on the fact that lighting fixtures, light sources, walls and ceiling, become dirtier and also some lamps get older or burn. A high maintenance factor (cleaning) together with an effective maintenance programme promotes energy efficient design and limits the installed lighting power requirements [13]. A high degree of installation maintenance involves cleaning of the luminaires every year, and of room surfaces every three years, as well as bulk lamp replacement every 10000 hours [8].

2.6 Utilance and utilization factor

As for lighting fixures (see 2.3), an important principle of energy efficient lighting is to make the most of any light sources available by directing light to where it is needed in the room [10]. Rea [14] introduced the term ‘application efficacy’ that is, first, based upon the lamp and luminaire combination rather than, as usually considered, solely on lamp luminous efficacy. The utilance U relates the luminous flux from the luminaires to the luminous flux on the target area. A target U for efficient interior lighting has been recently proposed [13]. One strategy in energy-efficient office lighting consists of placing light fixtures where they are needed. This should not be done, however, at the expense of acceptable contrast ratios.

2.7 Reduction of maintained illuminance levels

Recommended maintained illuminance levels are prescribed over the task area on the reference surface which may be horizontal, vertical or inclined. In many countries including Sweden, 500 lx on the work plane are often recommended for office work. Many studies indicate that office workers generally prefer illuminance levels which are lower than recommended by the standards [15-20]. However, several other studies [21-23] have indicated a preference for very high illuminance levels (including daylight) ranging from 0-3000 lx. Recently, Fotios & Cheal [24] demonstrated that the preferred illuminance is significantly influenced by the range of illuminances available to the research participant (the stimulus range), and that occupants tend to select the middle point of the range available. They concluded that studies with different stimulus range will lead to different estimates of preferred illuminance, with studies with large range resulting in higher preferred illuminance selected. Other research results have indicated that for a fixed output lighting installation, the

mean maintained illuminance to achieve the maximum percentage of people close to their preferred illuminance was 400 lx [16]. By using 400 lx as a design criterion, a 20% decrease in energy consumption could be gained together with a likely increase in the percentage of office workers who are within 100 lx of their preferred illuminance [16]. A universally preferred illuminance does not exist since the range of illuminance deemed acceptable is greater than the range considered as unacceptable [25]. Boyce [26] noted a lack of association between illuminances and their subjectively viewed suitability when subjects were carrying out realistic tasks, i.e. tasks for which visibility requirements were satisfied at relatively low levels of illuminance.

2.8 Duration of switch-on time

The total number of units of electricity consumed by the lighting installation will also obviously be affected by the length of time the lighting is switched on. The European standard EN 15193 [27] considers a total utilization time for electric lighting in offices of 2500 hours (2250 daytime hours + 250 nighttime hours). An annual time budget of 2500 hours corresponds to about 48 hours per week and thus 9.6 hours per day (5 days/week) of total switch-on time, which is feasible even taking into consideration flextime. Limiting the range of total switch-on time implies in practice that lighting systems must be switched-off after work hours, a practice which is unfortunately still not implemented in many countries. Also, even with a maximum switch-on time of 2500 hours and a lighting power density (LPD) of 10 W/m^2, the resulting annual energy use is 25 kWh/m^2yr. Therefore, in order to reach total energy intensity for lighting of around 10 kWh/m^2yr, it is necessary to either reduce the LPD to around $4W/m^2$ or to switch-off lights at least 60% of the time, by using control systems such as manual dimming, occupancy switch-off and/or daylight dimming.

2.9 Use of occupancy sensors and manual/automatic dimming

Several studies have generated promising results showing that electrical energy use can be substantially reduced by using lighting control systems such as manual dimming and occupancy sensors. For manual dimming, the electric lighting energy savings obtained range between 7-25% [15, 28, 29]. Moore, Carter & Slater [30] reported on a survey of user attitudes toward control systems and the luminous conditions they produce in 14 similar UK office buildings. They observed that controllable systems were typically operated at 50% of maximum output. For automatic switch-off occupancy sensors, lighting electricity savings in the range 20-35% have been reported [15, 31, 32].

2.10 Use of photoelectric dimming

Photoelectric dimming allows saving energy by replacing electric lights by daylight, which has also many positive effects because people generally prefer daylight [35]. Two studies [36, 37] achieved recently in Sweden with the simulation program DAYSIM have shown that perfectly commissioned photoelectric dimming allows saving at least 50% compared to a case with manual switch near the door with a mix of active and passive users. Also, several studies have shown that increasing window area does not necessarily lead to a reduction in energy use for lighting the building properly [36, 37, 38]. Glare problems that can be caused by the large amount of daylight entering a highly glazed working space often reduce the quality of visual comfort. Shading devices are used more frequently in highly glazed buildings often maintaining the same levels of daylight used in a building with a conventional facade [36]. It has been shown that for individual office rooms in Sweden, the optimal glazing-to-wall ratio lies in the range 20-40% depending on the orientation. The use of brighter colours for inner walls is necessary to maximize the reflection of natural light in the space and even the reflection of electric lights on walls and can have an effect of the same magnitude as a change

of orientation from south to north [37]. Another study in the USA showed that reducing partition reflectance seriously reduces the amount of daylight at 2nd row offices (for landscape office layouts) and should be avoided if daylighting is desired [39]. The ceiling is also a crucial design element since the majority of daylight that penetrates into a building beyond the 1st work station is reflected from the ceiling at least once. Increasing the ceiling reflectivity has a positive effect on energy savings and leads to a more uniform distribution of daylight throughout the space [39]. The same research showed that reducing the ceiling height from 9ft to 8ft cuts the energy savings in half for second row offices and that lowering partition heights from 64" (reference geometry) to 48" nearly doubled energy savings.

DISCUSSION

Key figures for energy consumption and energy saving potential for office lighting were presented based on a review of relevant literature, with a special emphasis on a North European context. The review reveals that the replacement of older lighting installations (T12 fluorescent lamps) with modern energy-efficient T5 lamps with HF ballasts and energy-efficient luminaires could provide up to 40% energy savings. An additional 40% energy savings could be obtained by using a combination of task/ambient lighting, occupancy switch-off and daylight dimming, making it possible to achieve totally 80% energy savings compared to older T12 fixed lighting installations. However, if the base line for comparison is the average office lighting energy intensity of 21 kWh/m^{2}yr (valid for Sweden), realistic energy saving figures using existing technology in combination with occupancy sensors, manual/automatic dimming, automatic switch-off and daylight dimmers are rather around 50%. Thus an energy intensity of around 10 kWh/m^{2}yr in office rooms is a realistic target for energy intensity in new low energy office buildings and retrofitting existing office buildings, assuming typical illuminance levels for office rooms (300 lx general space, 500 lx on task). This figure however varies according to room type (i.e. individual office rooms versus landscape rooms and common rooms). Lower energy intensities are even achievable by accepting lower installed illuminance levels and task/ambient lighting using very energy-efficient task lamps.

Strategies for reducing energy use for electric lighting were also presented and discussed, which include: improvements in lamp, ballast and luminaire technology, use of task/ambient lighting, improvement in maintenance and utilization factor, reduction of maintained illuminance levels and total switch-on time, use of manual dimming and occupancy sensors. Strategies based on daylight harvesting were also addressed and some design aspects such as window characteristics, reflectance of inner surfaces, ceiling and partition height were discussed. Daylight harvesting based on photoelectric dimming can provide additional energy savings. A number of studies have indicated that daylight harvesting can be achieved in peripheral spaces with ‘reasonable’ glazing-to-wall ratios (GWR) of no more than 20-40%. An increase in GWR does not provide substantial additional lighting energy savings and creates risks for overheating, glare and a consequent abusive use of shading devices, with associated reduced daylight benefits.

ACKNOWLEDGEMENTS

The authors thank SBUF (the development fund of the Swedish Building trade), CERBOF (Centre for energy and resource efficient construction and management of buildings) and NCC Construction Sweden for funding this research project.

REFERENCES

1. Statens energimyndighetenen, Energi i våra lokaler: Resultat från Energimyndighetens STIL2-projekt, Delrapport från Energimyndighetens projekt Förbättrad energistatistik i samhället, 2010.

2. H. Poirazis, Å. Blomsterberg, M. Wall, Energy simulations for glazed office buildings in Sweden, Energy and Buildings 40 (2008) 1161-1170.
3. N. Borg, Guidelines for integrating sustainable summer comfort into public procurement schemes for office equipment and lighting, Keep cool program, Deliverable 3.2, Swedish Energy Agency, October 2009.
4. Energy efficient lighting – guidance for installers and specifiers, CE61, Energy saving trust, London.
5. R. D. Carter, Good lighting with less energy: where next? Lighting Research and Technology 41 (2009) 285-286.
6. R. Küller, T. Laike, The impact of flicker from fluorescent lighting on well-being, performance and physiological arousal, Ergonomics, 41 (4) (1998) 433-447.
7. J. A. Veitch, G. R. Newsham, Lighting that Benefits People and the Environment. International Association for Energy-Efficient Lighting (IAEEL), Newsletter 1/99, 8 (22) (1999) 4-6.
8. D. Loe, Energy efficiency in lighting – an overview, Action Energy GIR092, Society of Light and Lighting, London, 2003.
9. Belysningsbranschen (2010). www.belysningsbranschen.se.
10. D. Loe, Energy efficiency in lighting – considerations and possibilities. Lighting Research and Technology 41 (2009) 209-218.
11. Z. Rogers, Daylight Metric Development Using Daylight Autonomy Calculations in the Sensor Placement Optimization Tool, Architectural Energy Corporation, Boulder, Colorado, 2006.
12. R. Svensson (ed.) Ljus och rum: Planeringsguide för belysning inomhus, Andra utgåvan, Ljuskultur, Stockholm (Sweden), 2010, ISBN 91-631-4675-4.
13. P. Hanselaer, C. Lootens, W. R. Ryckaert, G. Deconinck, P. Rombauts, Power density targets for efficient lighting of interior task areas, Lighting Research and Technology 39 (2) (2007) 171-184.
14. M. Rea, Energy-efficient lighting, Conference Energy efficient lighting in a human perspective, Ceebel (Centrum för energieffektiv belysning), 18-19 August 2010, Katrineholm (Sweden).
15. A.D. Galasiu, G. R. Newsham, C. Suvagau, D. M. Sander, Energy saving lighting control systems for open-plan offices: a field study, Report NRCC-49498, Institute for Research in Construction, National Research Council of Canada, Ottawa, 2007.
16. P. R. Boyce, J. A. Veitch, G. R. Newsham, C. C. Jones, J. M. Heerwagen, M. Myer, C. M. Hunter, Occupant use of switching and dimming controls in offices, Lighting Research and Technology 38(4) (2006) 358-378.
17. T. Moore, D. J. Carter, A. I. Slater, User attitude toward occupant controlled office lighting, Light Research and Technology 34 (3) (2002) 207-219.
18. T. Moore, D. J. Carter, A. I. Slater, A comparative study of user opinion in offices with and without individually controlled lighting, Proceedings of the 9th European Lighting Conference (Lux Europa), Reykjavik, Iceland, 2001, 234–241.
19. J.A. Veitch, G.R. Newsham, Preferred luminous conditions in open-plan offices: Research and practice recommendations, Lighting Research and Technology 32 (2000) 199-212.
20. G. R. Newsham, S. Mancini, R. G. Marchand, Detection and acceptance of demand-responsive lighting in offices with and without daylight, Report NRCC-50324, Institute for Research in Construction, National Research Council of Canada, Ottawa, also published in Leukos 4 (3) (2008) 139-156.
21. S. H. A. Begemann, G. J. van den Beld, A. D. Tenner, Daylight, artificial light and people in an office environment, overview of visual and biological responses. International Journal of Industrial Ergonomics (1997) 231-239.
22. A. Scholz, N. Farnum, A. R. Wilkes, M. A. Hampson, J. E. Hall, Minimum and optimum light output of Macintosh size 3 laryngoscopy blades: a manikin study, Anaesthesia 62 (2007) 163–168.
23. H. T. Juslén, M. C. H. M. Wouters, A. D. Tenner, Preferred task-lighting levels in an industrial work area without daylight, Lighting Research and Technology 37 (2005) 219–233.
24. S. A. Fotios, C. Cheal (2010). Stimulus range bias explains the outcome of preferred-illuminance adjustments, Lighting Research and Technology, 42 (2010) 433-447.
25. P. Tregenza, S. Romaya, S. Dawe, L. Heap, B. Tuck, Consistency and variation in preferences for office lighting, Lighting Research Technology, 6 (1974) 205–211.
26. P. R. Boyce. Age, illuminance, visual performance and preference. Lighting Research Technology 5 (1973)125–44.
27. European Committee for Standardization (CEN), Energy performance of buildings – Energy requirements for lighting, EN 15193:2007, Brussels, 2007.
28. G. R. Newsham, M. Aries, S. Mancini, G. Faye, Individual control of electric lighting in a daylit space, Report NRCC-49453. Institute for Research in Construction, National Research Council of Canada, Ottawa, also published in Lighting Research and Technology 40 (1) (2008) 25-41.
29. D. Maniccia, B. Rutledge, M. S. Rea, W. Morrow, Occupant use of manual lighting controls in private offices, Journal of the Illuminating Engineering Society 28 (2) (1999) 42–56.
30. T. Moore, D. J. Carter, A. I. Slater, Long-term patterns of use of occupant controlled office lighting, Lighting Research and Technology 35 (1) (2003) 43-59.
31. J. D. Jennings, F. M. Rubinstein, D. DiBartolomeo, S.L. Blanc, Comparison of control options in private offices in an advanced controls testbed. Journal of the Illuminating Engineering Society 29(2) (2000) 39-60.
32. M. G. Figueiro, Occupancy Sensors: Are there reliable estimates of the energy savings?, Lighting Design + Application (LD+A), January 2004.
33. X. Guo, D. K.Tiller, G. P. Henze, C. E. Waters, The performance of occupancy-based lighting control systems: A review, Lighting Research and Technology 42 (2010) 415-431.
34. X. Guo, D. K.Tiller, G. P. Henze, C. E. Waters, Validating the application of occupancy sensor networks for lighting control. Lighting Research and Technology 42 (2010) 399-414.
35. A.D. Galasiu, J. Veitch, Occupant preferences and satisfaction with the luminous environment and control systems in daylit offices: a literature review, Energy and Buildings 38 (7) (2006) 728-742.
36. H. Bülow-Hübe, Daylight in glazed office buildings: A comparative study of daylight availability, luminance and illuminance distribution for an office room with three different glass areas, Report EBD-R—08/17, Lund University, Department of Architecture and Built Environment, Division of Energy and Building Design, Lund (Sweden), 2008.
37. M.-C. Dubois, Å. Blomsterberg & K. Flodberg (2011). Towards zero energy office buildings in Northern Europe. Proc. of World Sustainable Buildings Conference. World Sustainable Building Conference, 18 - 21 October 2011 Helsinki, Finland.
38. A. Tzempelikos, A. K. Athienitis, The impact of shading design and control on buiding cooling and lighting demand, Solar Energy 81 (2007) 369-382.
39. C. F. Reinhart, Effects of interior design on the daylight availability in open plan offices, Proceedings of the ACEEE Summer study on energy efficient buildings, Pacific Grove, CA (USA), August 2002, 1-12.

NUMERICAL SIMULATION OF DAYLIGHTING USING THE SOFTWARE CODYRUN

A. H. Fakra[1]; M. Moosafeer[1]; H. Boyer[1]; F. Miranville[1].

1: Physics and Mathematical Engineering Laboratory for Energy and Environment (i.e PIMENTs), University of La Réunion, 117 rue du Général Aileret, 97430 Le Tampon.

ABSTRACT

Many different software applications exist to simulate indoor daylighting and/or electrical lighting. They are generally classified into two categories: software dedicated to research and commercial software (usually dedicated to consulting firms and individuals).

The first software category prefers to use computer codes and high performance physical models (which give very realistic values) while the second software category prefers to use more simplified tools that give very approximate values to describe reality.

In the case of indoor daylighting simulation, three software categories can be classified in relation with numerical, simplified and empirical (or experimental) models. .

All three different categories of models need to be improved, as. the numerical model requires a high calculation time the simplified models have limited conditions of use and finally, experimental models need major financial resources or perfect control of experimental devices (e.g. scale model) and climatic characteristics of the location (e.g. in situ experiment).

The PIMENT research Laboratory (located at the University of Reunion Island) has developed software capable of simulating lighting (artificial and natural) inside buildings called CODYRUN [1]. The software uses simplified models that were developed by the laboratory. Initially CODYRUN was dedicated to thermal building simulation; the natural lighting code was introduced in the software by Fakra for his PhD thesis work in 2009 [2]. Currently, the code is capable of describing the illuminance distribution of any point on a work plane, using a meteorological database. The software is also able to simulate the outdoor illuminance from the different values of irradiance given by the weather file [3]. This tool is very user-friendly both for physics researchers and designers or operators.

The daylighting model present in CODYRUN has been validated numerically, comparatively (comparison with other numerical simulation software) and experimentally.

Our remarks shall be illustrated with an application example on the optimization of visual comfort in natural illuminance. A method based on the percentage of glare inside the room shall also be denoted.

This paper equally presents a user guide and the different steps of a building description in CODYRUN.

INTRODUCTION

The description of the illuminance distribution is very important when attempting to study visual comfort within a building. Indeed, the sun is a potential source of discomfort, causing overhead and disability glare, both indoors.

Daylighting systems can produce discomfort glare. Increased interior electric lighting may be required to balance luminances and reduce glare produced by daylight, thus increasing energy use when daylighting is used. Direct glare is critically dependent on the luminance of the window. In fact, window brightness, due to direct glare, can be uncomfortable to view.

The degree of luminance control to be designed into a luminaire depends on its intended use and the luminous environment in which it is used.

Frequently, design compromises are required between visual comfort, use, and aesthetics.

Computational and measurement systems exist to evaluate the potential glare from daylighting. The established criteria were commonly used to guide luminaire designers and engineers in determining acceptable limits of maximum and average illuminances.

Many methods - predicting the presence of glare from large area sources - have been developed. This paper presents possibilities to simulate indoor daylighting and study glare with a new module of the software CODYRUN. The new module predicting daylighting (indoor and outdoor) was introduced in the software and validated by Fakra [3,4].

NUMERICAL SIMULATION

An example of application of the software CODYRUN to predict glare is presented in this paragraph. The aim of the study is to verify the areas where frequencies glare are observed during the year. This is a classroom (TD2) located at the University Institute of Technology at Saint – Pierre (Reunion Island).

Description of the building

TD2 classroom (see Figure 1 and 2) is located at Saint-Pierre (Latitude: 21°19’ South; Longitude: 55°28’ East; and Altitude: 68 m).

The climate is tropical and humid. It is between TD1 classroom (at the North) and TD3 (at the South) as mentioned in the scheme of Figure 3. Below is TD4 classroom.

The dimensions of TD2 classroom are: 7.2 m in length, 6.74 m in width and 3 m in height, that is to say an area of 145 m^2. Two large windows are located on the West side and three others on the East side (one small and two large openings).

The dimensions of the large openings are 1.10 m high by 1.50 m width each, whereas those of the small window are 1.1 m high by 1.2 m width.

The doors are 2.1 m high by 1 m width each. There are three doors and positioned respectively in the South, North and West side of the classroom.

The reflection coefficients of the walls, ceiling and floor are respectively estimated at 80%, 70% and 60%.

The transmission coefficients of each simple glass pane of the windows are 85% (given by the manufacturer). The reflection coefficients of each door are estimated at 70%.

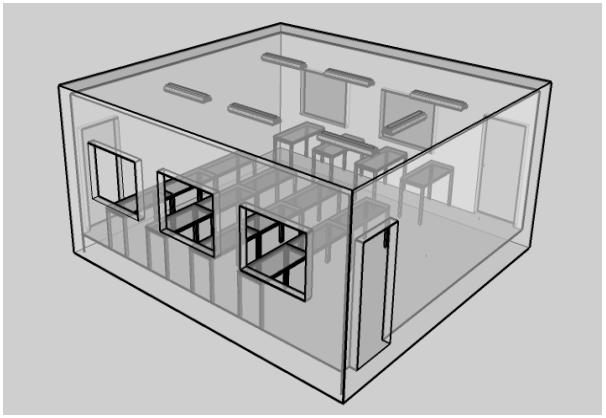

Figure 1. Perspective view of classroom TD2

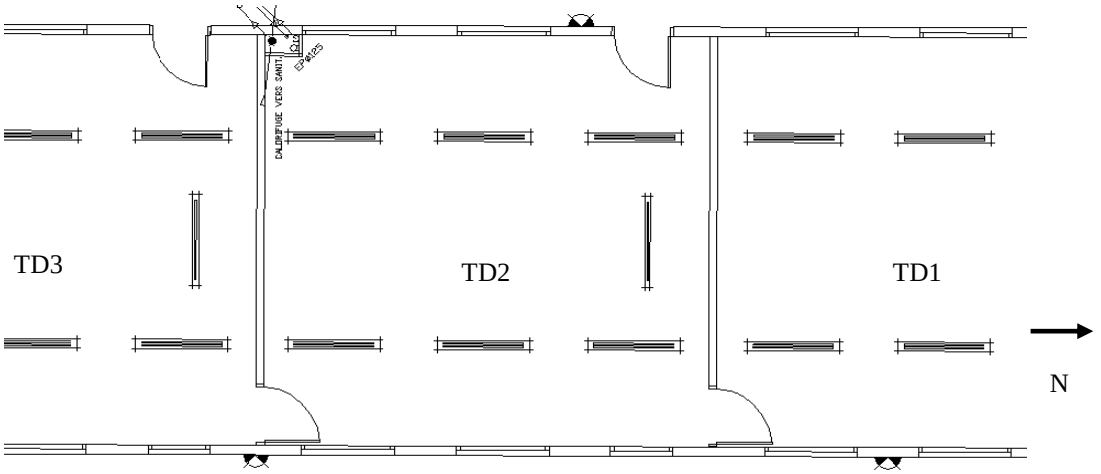

Figure 2. Ground plan of the classrooms at the IUT of Saint-Pierre (University of Reunion)

Hypothesis of the simulation

The description of the TD2 classroom and the meteorological database (provided by the weather forecast station of the Laboratory [3]) were introduced into the software.

The simulations conditions are:

- ✓ The building is described in the space (Cartesian coordinates);
- ✓ We consider the simulation of daylighting on a workplane (0.85 m in height) of 36x33 position points inside the room and for minutely time step during the year (Figure 3);
- ✓ The software is capable of dynamical studies;
- ✓ It does not consider overhangs in daylight simulations;
- ✓ No daylight calculations on vertical or inclined walls are considered;
- ✓ It does not consider obstructions inside the room (furniture, occupants, etc.), bidirectional transmissions (BRDF) and lightwell when simulating daylighting;
- ✓ All doors are considered closed;
- ✓ The openings should only be sidelight;

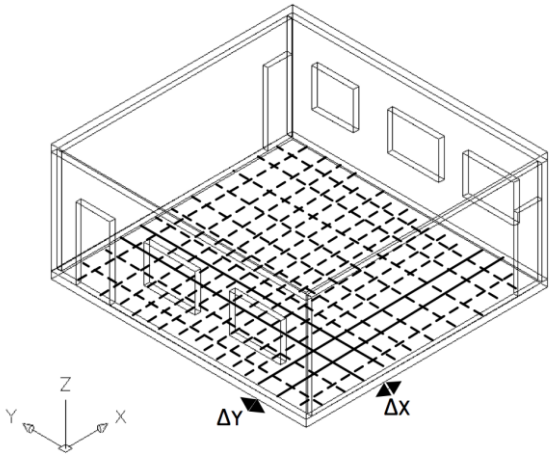

Figure 3. Grid surface plane (nodal points) for the calculation of the indoor illuminance

Percentage of discomfort glare study

The new method consists in determining and measuring the percentage of glare (hourly, daily, monthly or yearly) i.e G_{global} in a given room. To perform this study, CODYRUN uses the following report:

$$G_t = \frac{\sum_{i=1}^{p} S_{Glare,i,t}}{\sum_{j=1}^{n} S_{Floor,j}} \times 100 \quad (1)$$

$$G_{global} = Average(G_t) \quad (2)$$

When:

G_t : percentage of glare at the time t (in %)

$S_{Glare,j,t}$: Surface glare (or sunspot) number i inside the room at the time t (in m^2)

$S_{floor,i}$: Surface of the floor (at the building) number i (in m^2)

G_{global} : Global percentage of mean glare inside the room (in %)

Results of the simulation

Figure 4 gives the Daylight Factor (DF) coefficient in classroom TD2, which was simulated by CODYRUN. The mean DF value is 4.34% (minimum value is 0 % around the perimeter of the surface of the work plane and the maximum value is 15.62% near openings).

Figure 5 presents the yearly occurrence frequency of the surface glare at the workplane (0.85 m height) in classroom TD2. The occurrence frequency of the glare (OFG), coming directly from the sun, does not exceed 50% in the annual simulation, because the hypothesis simulation included the night (50% of the simulation does contain daylighting). The results show that there is only 0.74 % of the glare in the annual simulation (less than 1%). TD2 classroom has no major problems of natural glare all year along.

The occurrence frequency of the glare is more frequent on side openings. Solar shading systems should be installed near the top of the openings on the West side of the room.

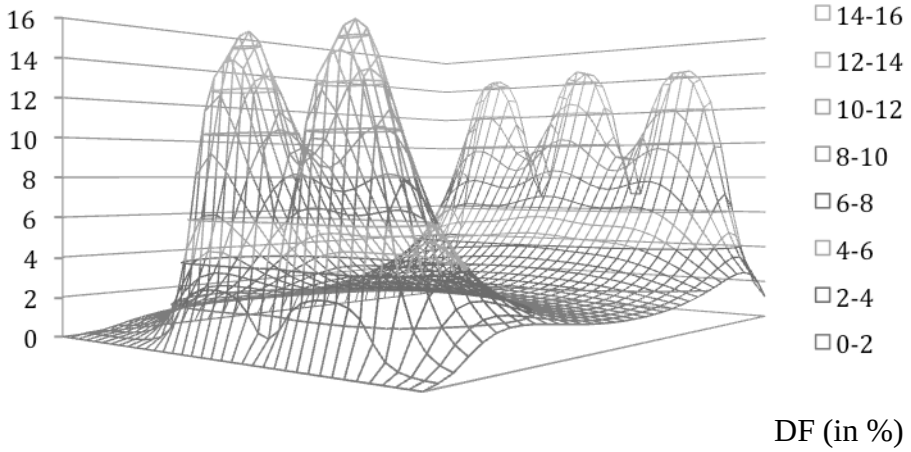

Figure 4: The distribution of Daylight Factor (DF) in classroom TD2

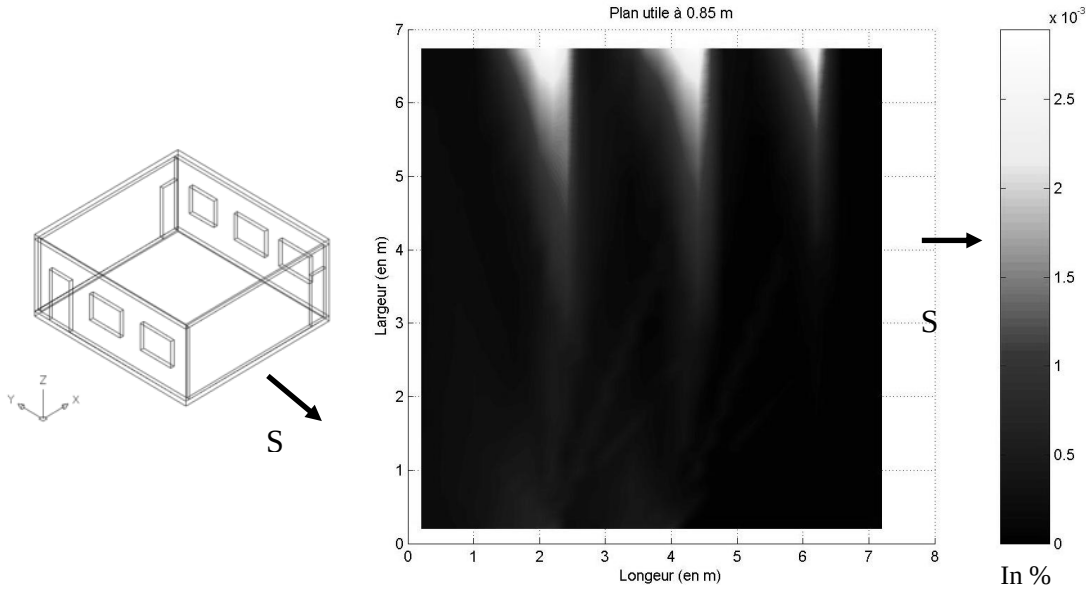

Figure 5: Yearly occurrence frequency of the glare in classroom TD2

Similarly, hypotheses were used to simulate global indoor daylighting on the work plane during the year.

The objective of the study is to represent the quantity of the light distribution on the work plane. Figure 6 shows this mean illuminance distribution on the work plane during the year. Global illuminance in the classroom is 1000 Klux in the year.

The maximal value is 111 Klux (in clear day) when direct light from the sun enters through the openings. This study shows that the openings are very well positioned to allow natural light into the room during the year. However, precautions must be taken at the located openings to prevent the light coming directly from the sun from entering the room.

CONCLUSION

Daylight can be an excellent source of ambient illumination. The potential for daylight utilization should be evaluated early in the design development of a space. Architectural features such as overhangs, light shelves, and window treatments may be incorporated into the design to enhance daylight utilization and control. The manner in which daylight is distributed in the space is important. The glare coming from the windows should be controlled. CODYRUN is able to predict these discomfort situations, as it allows simulating the occurrence frequency of surface glare within a room.

This new method permits to detect the problem of visual comfort. CODYRUN was used to view areas of glare and to provide technical or architectural solutions in order to remedy the uncomfortable situation.

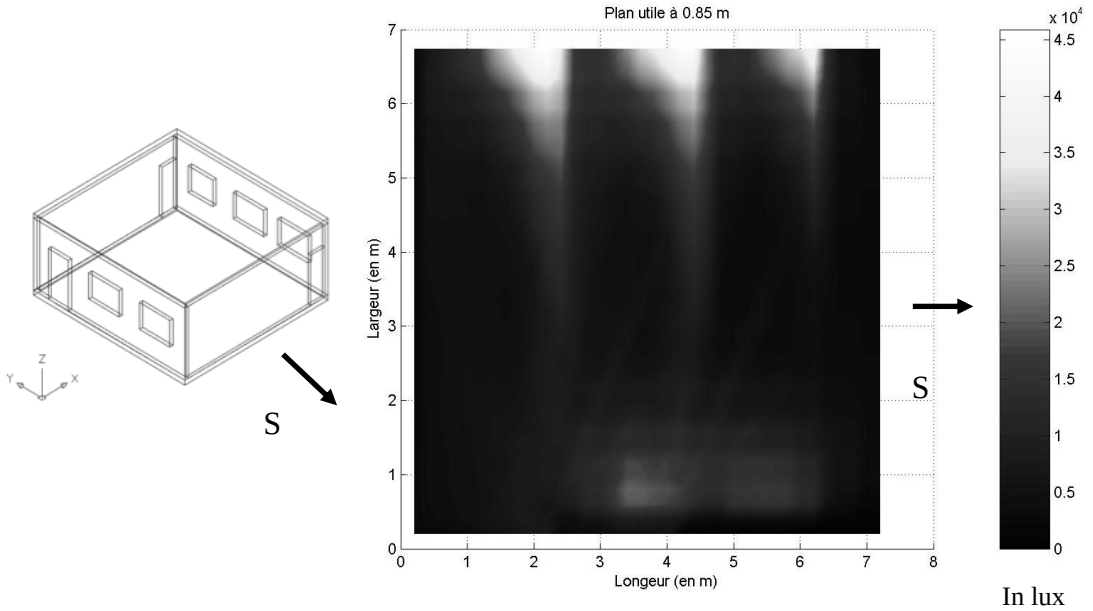

Figure 6: Average yearly global daylight in classroom TD2

REFERENCES

1. Boyer, H.; Garde, F.; Gatina, J., C.; Brau, J.; A multimodel approach to building thermal simulation for design and research purposes, Energy and Buildings, Vol. 28, Issue 1, pp. 77-78, 1998.
2. Fakra, A. H.: Intégration de modèles d'éclairage à un code de calcul en physique du bâtiment : modélisation, validation et applications, Université de La Réunion, Thèse de Doctorat, 2009.
3. Fakra, A. H.; Miranville, F.; Boyer, H.; Bigot, D.; A simple evaluation of global and diffuse luminous efficacy for all sky conditions in tropical and humid climate, Renewable Energy, Vol. 36, pp. 298-306, 2011.
4. Fakra, A. H.; Miranville, F.; Boyer, H.; Guichard, S.; Development of a new model to predict indoor daylighting: integration in CODYRUN and validation, Energy Conversion and Management, Vol. 52, pp. 2724-2734, 2011.

A STUDY ON DAYLIGHTING CONDITIONS IN CLASSROOMS OF IRANIAN SCHOOLS IN TEHRAN - MEASUREMENTS AND ANALYSIS OF ILLUMINANCE DISTRIBUTION

Rozita Farzam

Doctoral Course, In Graduate Department of Design & Architecture Kobe Design University, Gakuen-Nishimachi 8-1-1, Nishi-ku, Kobe, 651-2196 Japan, E-mail: rozfarzam@yahoo.com

ABSTRACT

Daylighting is one of the important environmental factors that affect the health, emotions and academic performance of students as well as the energy consumption of school buildings [1]. These days it is well known that daylighting systems in buildings should be considered from the view points of quantity and quality. The final aim of this research is to develop design methodologies to improve the lighting environment in school classrooms in Iran, utilizing daylight for lighting systems, with respect to Iranian culture. The purpose of this research is to improve the design of the windows and shading devices in order to obtain better daylight conditions by uniforming the daylight distribution on the working plane and creating ideal and light, in quantity and in quality. Coordinated by the "Tehran school Organization of renovation and development", some schools were selected as prototypes. In this paper we present a survey of observation, geometric assessment of devices and the results of measurements of daylight levels in selected classrooms in Tehran, focusing on hourly changes of illuminance distribution in different types of classrooms. Most classrooms in Tehran are either facing north or south. The selected case studies include two classrooms, one of them with a north-faced windows on the second floor and the second with south-faced windows, also on the second floor. We present the results of monitoring illuminance levels under overcast, sunny and intermediate sky. The location of the points of horizontal illuminance measurements in the classroom has been chosen to be in 12 different locations on the working plane, which corresponds to desk height, 70 cm above the floor. The illuminances were measured in this experiment by means of light meters in selected classrooms. In addition, some simulations were carried out in the selected samples using the simulation software "ECOTECT v 5.6". Finally, some unique aspects of Iranian classrooms and comparison results are discussed.

KEY WORDS: Daylight/ classroom / measurement /Analysis / Iran

INTRODUCTION

Classrooms are the places where students spend most of their time. The main purpose of schools is the promotion of learning and the educational level of students. For doing this, they have to create a suitable and attractive environment for students, especially in case of lighting. The design of schools can improve learning by providing appropriate lighting and air quality while simultaneously reducing energy consumption [2]. The research framework of this study is as follows;

- Surveys of the lighting environment of Iranian schools, through measuring daylight conditions such as illuminance values in selected classrooms. Identifying problems and analyzing the lighting environments in the Iranian schools of today.
- Finding and developing a simulation programs that can work as design tools and can support the design of lighting environment of the Iranian schools.

METHODOLOGY

The study area of this research includes schools of Tehran City located in the center of the Tehran province. These schools were selected in coordination with the "Tehran school organization of renovation and development". The classrooms in Tehran are either facing north or south. The

methodology of the present project is aimed at assessing the general daylighting performance of existing Iranian classrooms by evaluating the illuminances due to the daylighting strategy in the studied classrooms using physical model experiments. The illuminance was measured in this experiment by using two instruments: light meter and color analyzer. The experiment was conducted to represent the four seasons in Tehran. These seasons are the fall season (September 21), the winter season (December 21), the spring season (March21), and the summer season (June21). The measurements were recorded on 10 January, 2009, three times in a day. (10 AM, 13 PM, 16 PM). The sky conditions on the day of the experiment was intermediate sky (half-way between sunny and overcast state) [14]. The curtains were open and electric lights were off.

Objective Observations of the Case Studies

In order to distinguish the two types of classrooms, we use "MN" for the one with north-faced windows on the second floor and "KS" for the one with south-faced windows on the second floor. (Fig.2).

Fig 1: Satellite images showing location of case studies in Tehran; Left image is "Khalatbari" High School of Art" and right image is Motahari High School. Source: Google Earthpro4.

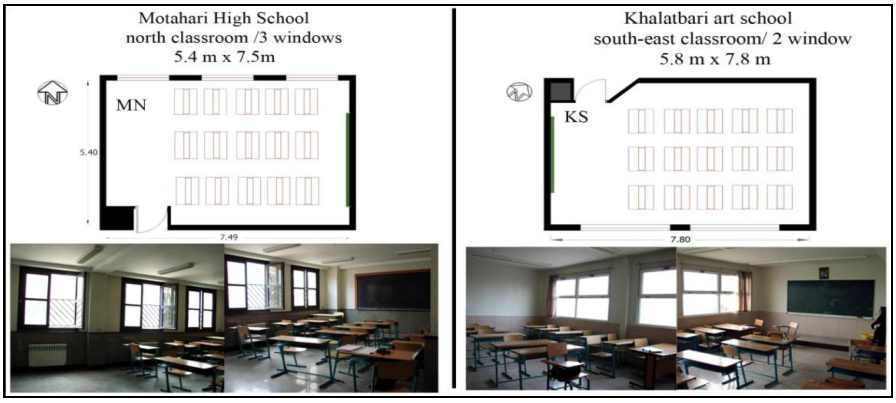

Fig 2: The selected classrooms.

Fig 3: The outside and inside in the classrooms under study

The overall picture was disappointing because there was no shading element used outside of the classrooms (i.e.in a country with so many hours of sunshine) and shading should have been seriously taken into consideration. Actually, the curtains were the only shading devices in the classrooms under study (Fig.3). The location of the points of horizontal illuminance measurements in the classrooms was chosen to be in 12 different locations on the working plane (i.e. 0.70 mm above the floor on desks level). These points inside the classroom were placed on the intersection points of a grid of about 2 m by 2 m (Fig.4).

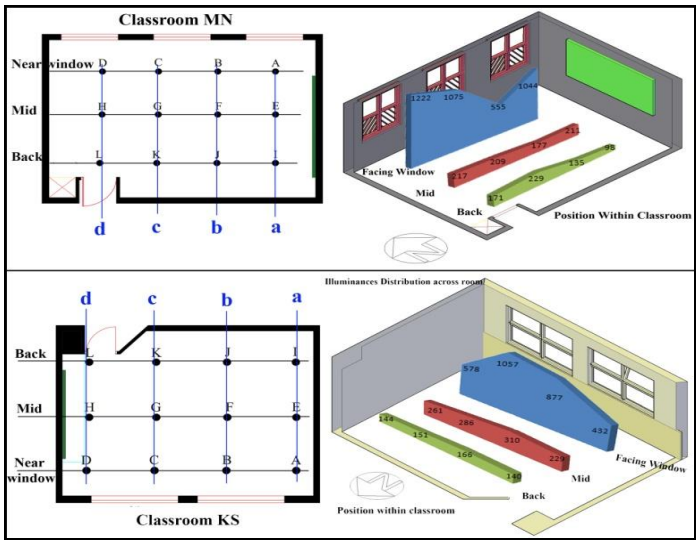

Fig 4: The comparison of illuminance values of the measurement points in "MN" &" KS".

Results of measurements

For both classrooms, daylight illuminances diminish rapidly with increasing distance from the windows. The average illuminance in the north orientated classroom (MN) (Ave: 445 lux) was higher than the illuminance in the south oriented classroom (KS) (Ave: 386 lux). For both of the classrooms, a seating position near a window was considered moderately comfortable for visual performance and was close to the local standard lighting requirement. In the north oriented classroom, the blackboard area did not receive enough daylight. The average illumination on the board was 222 Lx which was much lower than the recommended illuminance. In the south oriented classroom, the blackboard area had comfortable visual field, the average value was 504 lx, and the illuminance was in the range of 300-500 lx.

Calibration model in the simulation program (Ecotect v5.6)

To investigate the status of existing daylighting in the selected classrooms (photometry), we needed to simulate them on the same day and at the same sampled hour. To have more accurate and actual results, it was necessary to enter accurate materials and colors of walls, ceiling andfloor. Simulations were carried out in the selected samples by means of the simulation software "ECOTECT v 5.6". This program has an acceptable interface to define the geometry. Since color recognition and its reflection value cannot be measured by eyes, color analyzers were used to measure the rate of colors. After inputting R.G.B values in the simulation program, we calibrated models and compared illuminance values at measurement points (photometry). The measurement results were used to verify the adequacy of the simulation program (Fig.5).

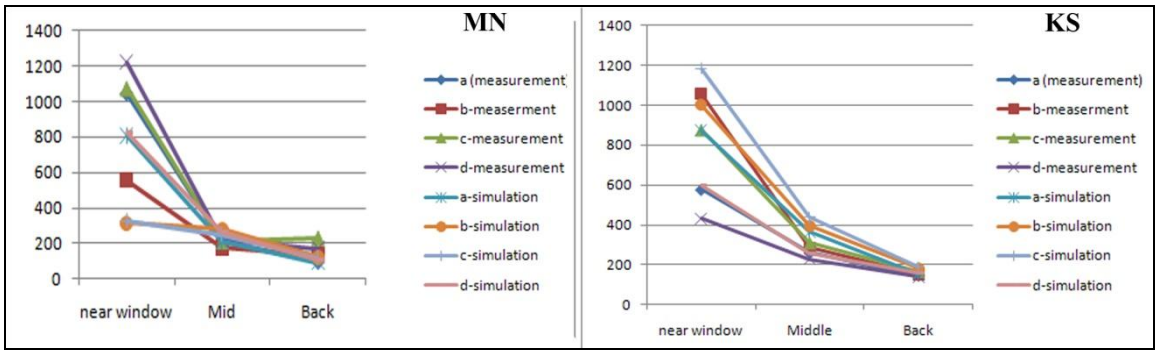

Fig 5: Illustrates the comparison of illuminaces between measurement and simulations in classroom "MN" and "KS". (Output from Microsoft Excel program)

Results and Analysis of Simulation

The case studies with existing materials were reproduced and calculated in the "Ecotect" program. These simulations predict the illuminance values (i.e. illuminance values in this simulation program show the amount of light falling on each surface) [14] over the measurement grid for 10 JAN at 10 under intermediate sky condition.

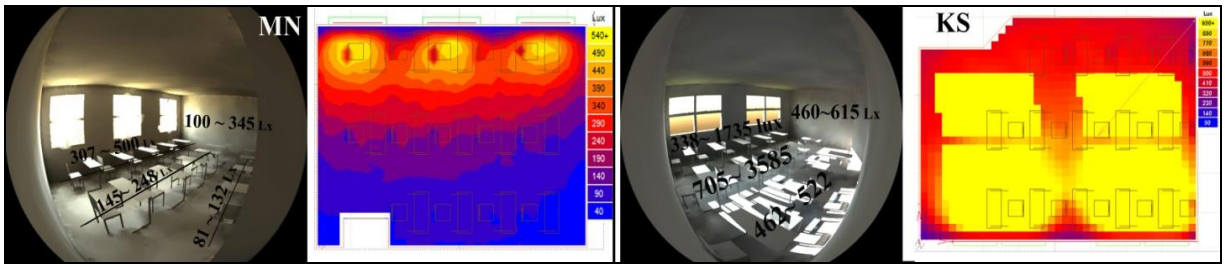

Fig 6: False color rendering image to study classroom "MN& KS".

The intention here is to compare the evaluative potential of the three different sky conditions. The simulations were recorded for the 15th of each of the 12 months of a year, at three different times in a day. (8 AM, 11 AM, 14 PM) and forthree different sky conditions: intermediate sky, sunny sky and overcast sky. Thus, The daylighting performance was evaluated for all 216 unique combinations of classroom type (x2), climate and sky condition (x3), for the 12 months of year and 3 times a day. A schematic showing the various parameters is given in Fig.7.

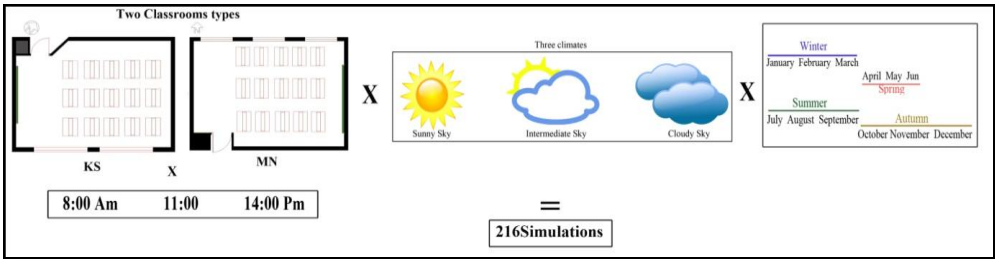

Fig 7: Parametric scheme

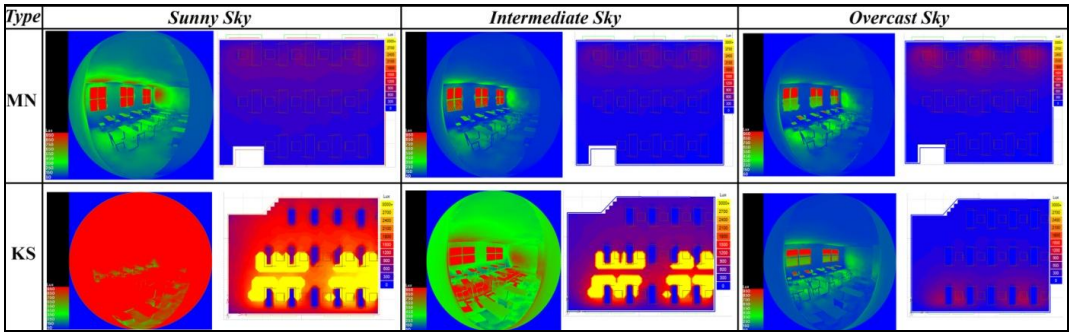

Fig 8: False-colored surface plots that show the illuminance values across the grid for classroom" KN" and "KS" on 15 JAN at time11.00 Am. (Output from Ecotect v5.6 program)

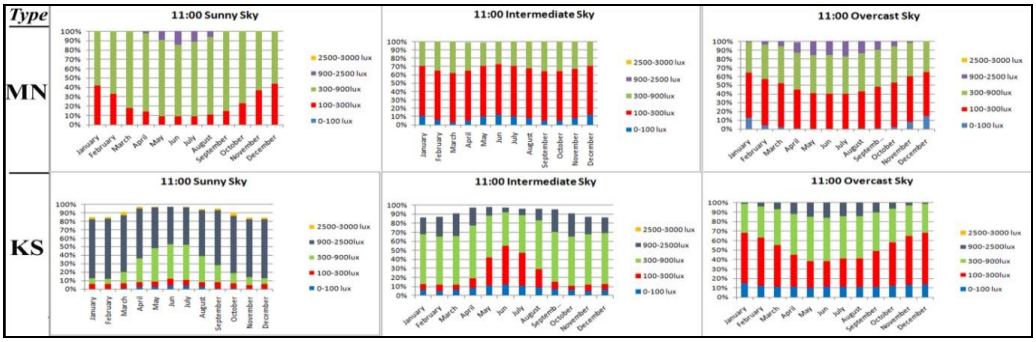

Fig9: Percentage of class level in terms of received illuminance during one year according to diagram

Class MN	Overcast	sunny	Intermediate	Class KS	Overcast	sunny	Intermediate
	11:00 AM	11:00 AM	11:00 AM		11:00 AM	11:00 AM	11:00 AM
0-100 lux	4%	0%	8%	0-100 lux	12%	2%	8%
100-300 lux	47%	22%	60%	100-300 lux	41%	6%	16%
300-900 lux	41%	75%	33%	300-900 lux	39%	21%	52%
900-2500 lux	9%	4%	0%	900-2500 lux	9%	60%	17%
2500-3000 lux	0%	0%	0%	2500-3000 lux	0%	2%	0%
100-2500 lux	96%	100%	92%	100-2500 lux	88%	88%	84%

Table 1: Percent of class level in terms of received illuminance during one year according to figures

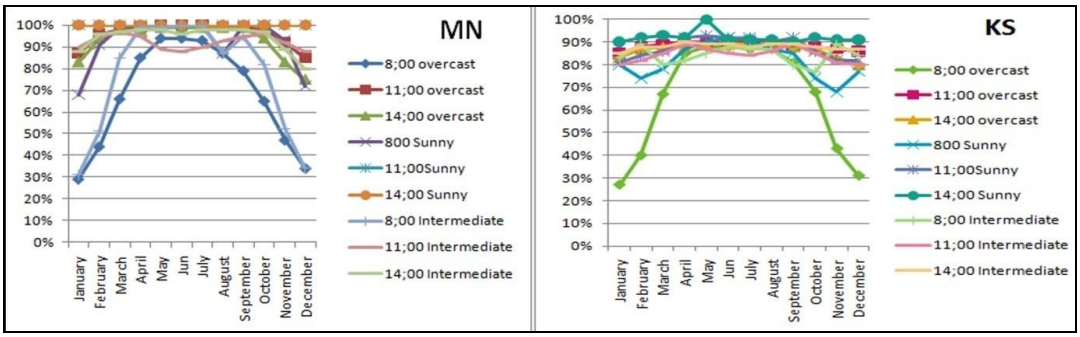

Fig 10: The percent of area had illumination amount of 100 to 2500 lux, in sunny, intermediate and overcast sky at 8AM, 11AM and14 PM.

Method of Analysis Results

The illuminance on the work surface was compared with the reference values given by the (CIBSE) [4], Lighting Guide, International Energy Agency (IEA) [12], (JIS) handbook [13], and (ISIRI) [11], the national lighting committee of standard and industrial organization of Iran. The reference value of illumination for classrooms is 300 ~ 500 lux. To achieve a comfortable brightness balance, it is desirable and practical to limit brightness ratios between areas of appreciable size (from normal view points) as follows(Moore, Fuller et.al.): [19] 10 to 1 between task and adjacent surroundingand 10 to 1 between task and more remote darker surface. On the other hand, (Dr. John Mardaljevic, et.al.) [15] applies the UDI scheme determining the occurrence of daylight illuminances as follows: 1. 100 lux to 2500 lux are within the range defined as useful.2. Less than 100 lux falls short of the useful range 3. Greater than 2500 lux exceeds the useful range.

RESULTS

Light categorization shown in Fig.9 was based on three factors found in the above mentioned reference books and papers (we suppose that in selected class rooms, room length and glazed surface are defined by standards and regarding the required illuminance in classrooms, the obtained results may complement former standards). According to the obtained results, the range of 0-100 lux is dark and the range of 100-300 lux (UDI supplement-tray) as well as a range of 300-900 lux are suitable light. A range of 900-2500 lux is excess light and may lead to discomfort glare, and the range of 2500-3000 lux will definitely cause disability glare or blind glare. According to moor Law [20], the ration of min lux to max lux must not exceed 1/3. For example, if light values for the entire room are between 900-2500 lux, this would be acceptable, but if they correspond to 300 lux by the window and 2500 lux on the blackboard, this would cause discomfort glare (i.e. light contrast).

CONCLUSION

Under overcast sky and in class rooms with south oriented windows, it is better to use light shelves to have even light, because light is much stronger by the window than further in the room. Under sunny sky, there is a glare problem and direct sunlight should be prevented because, according to results obtained in Fig 10, the light range of 2500-3000 lux leads to disability glare.

Under intermediate sky, everything is ok and there is no problem. Under sunny and intermediate sky and in class rooms with north oriented windows, there is no problem and we have the best situation. However, under overcast sky, light reflective tools such as light shelves are needed. In north facing class rooms, the wall opposite the window should be painted in a light colour so that a more even light is provided by more light reflection.

ACKNOWLEDGEMENTS

I am especially indebted to all the people who in one way or another have contributed to the PhD research briefly summarized through this paper. Special thanks to my family for their constant encouragement, and to the Supervisor Prof., Dr. Yuichiro Kodama "JIA, Department of Environmental Design of Kobe Design University", Japan, as well as to advisor Prof., Dr. Mansoore Tahbaz, Associate Professor of the "School of Architecture and Urban Planning,Shahid Beheshty University, Tehran", Iran, for their assistance.

REFERENCES

1. Antoniou K. and Meresi Aik., Analysis of different forms of classrooms in respect to Day lighting Performance, Proc. of the 22nd PLEA Conference on Passive and Low Energy Architecture,). November 13-16, pp93-97, Beirut, Lebanon, 2005.
2. Abdullah Al-Moraines and Omar Khattab, Green Classroom: Daylighting-conscius design for Kuwait Autism Center. Kuwait University.GBER vol.5 No.3, pp11-19.
3. Baharuddin, the use of computer simulation technique in the calculation of vertical daylight factor for heavily obstructed urban environments. Department of Architecture, the University of Hong Kong, China. PLEA 2007.
4. CIBSE Lighting Guide 5 Available, http://www.cibse.org/pdfs/lg5addendum.pdf [02-09-2008]
5. Cleo Axarli1, Aikaterini Meresi, Proc. of the 25th PLEA Conference on Passive and Low Energy Architecture, Dublin, Objective and Subjective Criteria Regarding the Effect of Sunlight and Daylight in Classrooms, Aristotle University of Thessaloniki, School of Civil Engineering, Laboratory of Construction and Building Physics, Greece. 2008.
6. Derek Philips, CIBSE. Day and Light. Natural Light in Architecture.
7. Evans, Benjamin H., Day light in Architecture, McGraw-Hill, New York. 2002.
8. Global Warming, Climate Change for Tehran-Mehrabad, Iran. 2007. http://www.climate-charts.com/Locations/i/IR40754.php
9. Guide for Day lighting in Schools Administered by Lighting research centre, Rensselaer Polytechnic Institute.
10. Heschong Mahone group. Re-Analysis Report, Day lighting in schools, For the California Energy Commission. 2001. www.newbuildings.org.
11. Institute of standards and industrial research of Iran ,(ISIRI) www.isiri.org
12. International Energy Agency (IEA), Daylight in Buildings: A Source Book on Day lighting Systems and Components, A report of IEA Task 21, 2000.
13. JIS-Z9110, JapaneseIndustrialStandardsCommittee, 2010. tttp://www.jisc.go.jp/app/jps/Jpso0020.html
14. Marsh A., Environmental Software Package, 'Square One' Research Group. (2000) www.squa1.com
15. Mardaljevic, Dr.John, Climate-Based Daylight Analysis for Residential Buildings, Institute of Energy and Sustainable Development, De Montfort University, the Gateway, Leicester, 2006, LE1 9BH, UK, p, 11
16. Nabil, A. and Mardaljevic.J. Useful daylight illuminate: A new paradigm for assessing, daylight in buildings. Lighting Research and Technology, 2005.p 37(1),
17. School's facilities office in Tehran .www.nosazimadares.ir
18. Tehran Climate. http://en.wikipedia.org/wiki/Tehran#Climate
19. Moore, Fuller, Concepts and Practice of Architectural Day lighting , Van Nostrand Reinhold, New York, 1991.

ENERGY EFFICIENT CONTROL OF DAYLIGHT IN AN OFFICE ROOM UNDER NORWEGIAN CLIMATE

M. Haase[1,2]

1: SINTEF Building and Infrastructure, Department Energy and Architecture, Alfred Getz vei 3, 7465 Trondheim, Norway

2: Norwegian University of Science and Technology (NTNU), Department of Architectural Design, History and Technology, Alfred Getz vei 3, 7491 Trondheim

ABSTRACT

This work is part of the project “Low energy commercial buildings” (LECO) run by SINTEF Building and Infrastructure. The project’s principal objectives are to develop more energy-efficient building solutions and new methods for the design of energy efficient commercial buildings. The project includes performance analyses of advanced building facades applied in different kinds of climates, different uses, and different construction methods.

Optimum control of daylight is a strategy with high energy savings potential in office and commercial buildings. Existing building regulations and tools suffer from several shortcomings in planning advanced facades for the maximum use of daylight.

In this context, the relation between solar control, lighting and energy consumption was investigated. The reason for this is that the sunshade often results in the use of electric lighting. In addition to the "unnecessary" use of electric energy, this leads also to the increase in temperature in the room and increased use of refrigeration. The purpose is to develop an energy efficient control strategies for the use of solar shading.

This paper presents results from work done on simulating the daylight performance of a room with backward ray tracing method. A rectangular room 4.8m x 7.2m with two windows on the south facing façade was modelled and different shading control strategies and different user types were simulated. In combination with four different user behaviours that has been used for both shading systems a comparison of the thermal performance of the office building was possible. The combination of daylight availability and user behaviours produced a schedule that was then linked to TRNSYS in order to calculate the thermal performance of different facade options. Results for total energy consumption of the office room were calculated, compared and performance differences assessed.

Results for annual net energy demand show total net energy demand for the options with external shading device are lower than for the options with internal shading device. The daylight control strategy provided a reduction in net energy demand for lighting which results in the lowest total net energy demand for both shading systems.

INTRODUCTION

This study is part of the research project "LECO, Low Energy Commercial buildings". Energy consumption related to non-residential buildings accounted for 36 TWh in 2007, which equals approximately 45% of energy consumption in buildings. The potential for energy efficiency of this part of the buildings through the use of existing technologies, assumed to be 6.5 TWh in 2020 (Low Energy Commission) [1].

LECO is intended to collect existing and developing new knowledge about energy efficient solutions to reduce energy consumption in commercial buildings. The goal is to create guidelines respectively. 50%, 75% and 90% reduction of energy consumption (4/2/10 factor) to a typical office of today (reference building = 300 kWh/(m^2 a) [2].

Energy for lighting accounts for a large portion the building's energy needs [3]. According to normative values in NS3031, this amounts to 25 kWh / (m2 year). This corresponds to 8 W/m^2 of installed power for lighting and 3120 hours annual operating hours in offices (12 hours per day, 5 days per week, 52 weeks per year). In addition to energy for lighting, this power is also considered in the calculations as additional internal heat gain [4].

The rules in NS3031 state that the heat contribution from lighting can be reduced by 20% if the management system for the utilization of daylight or management system based on presence sensors is used. Alternatively, other values for installed power for lighting can be used in the calculations and should be documented according to EN 15193 or equivalent [5].

In this context, the relation between solar control, lighting and energy consumption was investigated. The reason for this is that the sunshade often results in the use of electric lighting. In addition to the "unnecessary" use of electric energy, this leads also to the increase in temperature in the room and increased use of refrigeration. The purpose is to develop an energy efficient control strategies for the use of solar shading.

METHOD

Thermal simulation

A single room was modelled in TRNSYS, a dynamic building simulation software [6], with 4.8m width, 7.2m depth and 3.2m height. In Figure 1 the room geometry and technical details are given such as the following (according to models used in [2]):

- The model air-conditioned by a balanced mechanical ventilation system with airflow of the day V_{day} = 10m^3/(hm^2) which is lowered at night to V_{night} = 3m^3/(hm^2). The supply air temperature is assumed to be 19 °C and lowered to 16 °C in summer (May-August).
- The heating system consists of a local heating element that regulates the room temperature to 21 °C. A local cooling element is deactivated in this study. Cooling is only done by precooling ventilation air.
- Technical equipment is assumed to $P_{equipment}$ = 11 W/m^2 and internal heat gain from persons is set to P_{person} = 4 W/m^2. Light installation is assumed to $P_{lighting}$ = 8 W/m^2.
- South facing facade has two windows (U value 1.12 W / (m^2K)) consisting of 2-layer low emissivity glass with argon filling (U-value 1.1 W/(m^2K)), isolated frame with superspacer (U-value 0.09 W/(m^2K)).

Shading systems

The south facing windows were equipped with two different shading systems. The windows are fitted with either internal or external sunshade with the following specifications in relation to NS3031 and specified in Appendix A, Table A.2 [4].

- Internal sunshade consists of typical shading system with 28mm wide slats that together with glass (gt = 0.51) gives a transmission factor of T = 0.38.
- External sunshade consists of typical shading system with 80mm wide slats that together with glass (gt = 0.51), gives a transmission factor of 0.06.

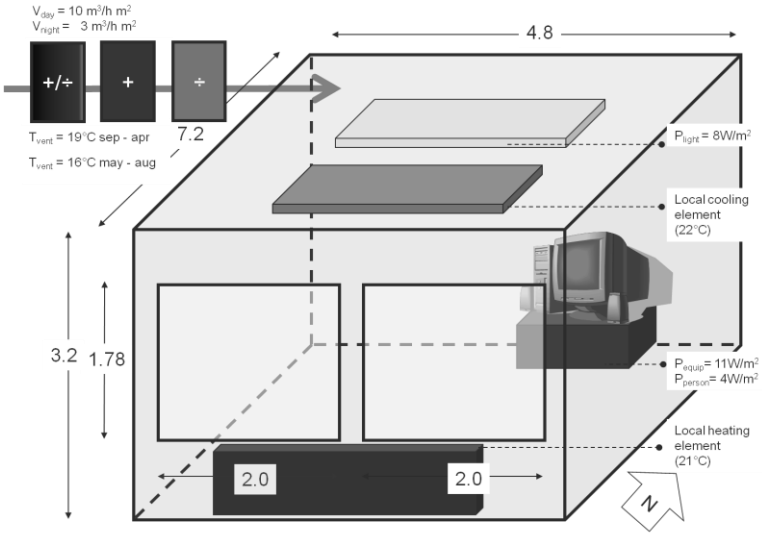

Figure 1 Model of office room

Shading control

The shading systems were equipped with two different control systems. One option closes the shading devices when radiation is above 200 W/m^2 (and opens again when radiation is below 150 W/m^2) (options (1) and (3)), the other option makes use of a daylight control which reduces the use of electric light according to daylight levels at the workplace.

The office user has a large influence on the thermal performance of office buildings if they are allowed to individually control lighting and blind systems. A key finding from field studies on manual lighting and blind control in commercial buildings is consciousness and consistency [7]. For different behaviours of occupants Lightswitch has been developed which approximates individual switching behaviours that have been observed in field studies [8]. In combination with the computerized user behaviours that has been used for both shading systems a comparison of the daylight autonomy of the office room was possible. Daylight autonomy is a measure of how often (e.g. percentage of the working year) a minimum work plane illuminance threshold of 500 lx can be maintained by daylight alone. Radiance was used for daylight simulations. Calculations for daylight autonomy were done using Daysim which uses daylight coefficients proposed by Tregenza and Waters [9, 10].

In order to find the sensitivity of their behaviour two extreme cases were analysed. In the first case the user is active, in the second case the user is passive. An active user is a user who operates the electric lighting in relation to ambient daylight conditions, opens the blinds in the morning, and partly closes them during the day to avoid direct sunlight. A passive user keeps the electric lighting on throughout the working day and keeps the blinds partly closed throughout the year to avoid direct sunlight.

Lighting and Blind Control

The electric lighting system has an installed lighting power density of 8.00 W/unit area and is controlled in three different ways:

- manually controlled with an on/off switch. The shading device is manually operated.
- automatically controlled via an on/off occupancy sensor with a delay time of 5 minutes. The shading device is automatically controlled. The automated control

lowers the shading device as soon as direct sunlight above 50W/m^2 hits the work pane. The device is automatically retracted otherwise.

- Without dimming
- With dimming: The dimming system has an ideally commissioned photocell control with a ballast loss factor of 20.00 percent.

The combination of daylight availability and user behaviours produced a schedule that was then linked to TRNSYS to calculate thermal performance of different shading options [7].

RESULTS

Results for daylight autonomy are shown in Figure 2 for two types of users. While an active user can increase daylight autonomy considerably in the whole depth of the office room the passive user shows less daylight autonomy and restricted to the facade perimeter (up til 3.7m).

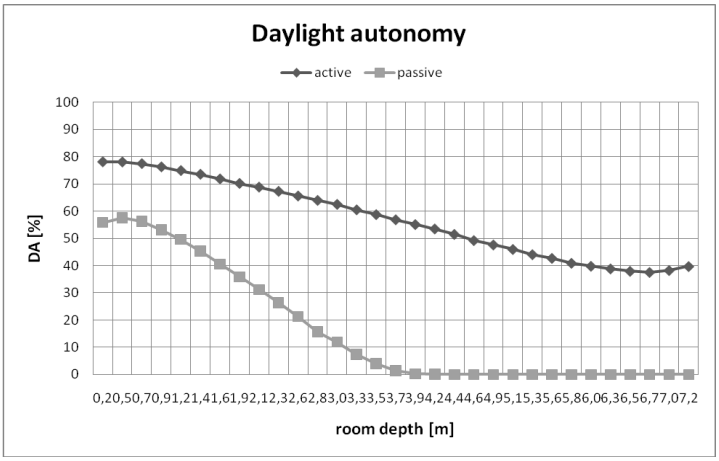

Figure 2: Results of calculated daylight autonomy for active and passive user profile.

Option	Ref.	basecase (0)	external shading (1)	(2)	internal shading (3)	(4)
kWh/(m^2 a)	TEK07	no shading	radiation control (150-200 W/m^2)	daylight control	radiation control (150-200 W/m^2)	daylight control
Room heating	54	27.9	29.6	30.7	28.2	22.6
Ventilation Preheating	incl.	27.7	28.1	28.4	27.7	27.0
DHW	5	5.0	5.0	5.0	5.0	5.0
Fans	22	16.8	8.5	13.6	14.7	15.5
Pumps	incl.	3.2	3.5	2.8	4.0	3.5
Lighting	25	25.1	25.1	10.1	25.1	10.1
Equipment	34	34.5	34.5	34.5	34.5	34.5
Ventilation precooling	25	35.0	19.5	14.5	31.4	25.9
Total	165	175.1	153.6	139.5	170.5	144.0

Table 1: Summary of results for net energy demand for different cases.

Results for annual net energy demand are presented in Table 1. It can be seen that total net energy demand for the options with external shading device (options (1) and (2)) are lower than for the options with internal shading device (options (3) and (4)). Also, a reduction in cooling energy demand (between 19.5 and 14.5 kWh/(m^2 a) for external shading compared with 31.4 and 25.9 kWh/(m^2 a) for internal shading) can be observed in addition to an increase in heating demand (between 29.6 and 30.7 kWh/(m^2 a) for external shading compared with 22.6 and 28.2 kWh/(m^2 a) for internal shading). The daylight control strategy provided a reduction in net energy demand for lighting (10.1 kWh/(m^2 a)) in both cases (2) and (4)).

Figures 3 and 4 show the results of TRNSYS calculations of operational temperatures during summer for different shading systems. While Figure 1 shows the results for external shading compared with the base case (0) (without shading device), figure 2 shows the results for internal shading compared with the base case (0) (without shading device).

Both control strategies provide a reduction of operational temperatures in the office room during the summer periods. From figure 3 it can be seen that an external shading system keep operational temperatures below 24°C with lower temperatures (below 23°C) for the daylight controlled system. The level of operational temperatures are higher in the cases with internal shading (Figure 4) and frequently exceed the 26 °C threshold [4].

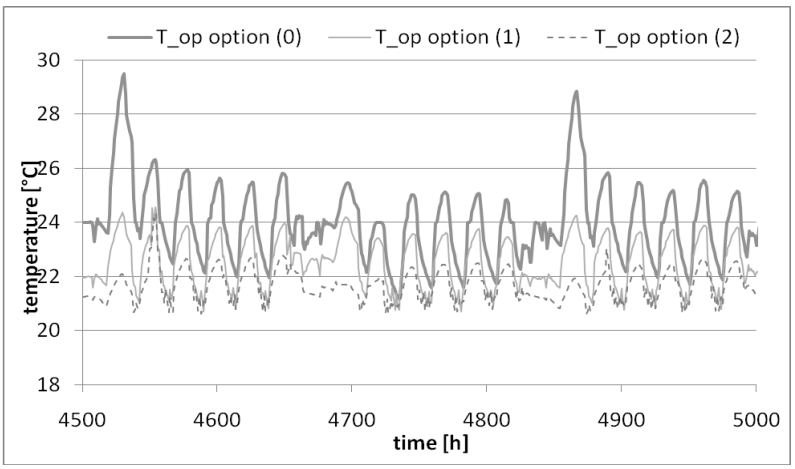

Figure 3: Results of calculated operational temperatures during summer in room with external shading.

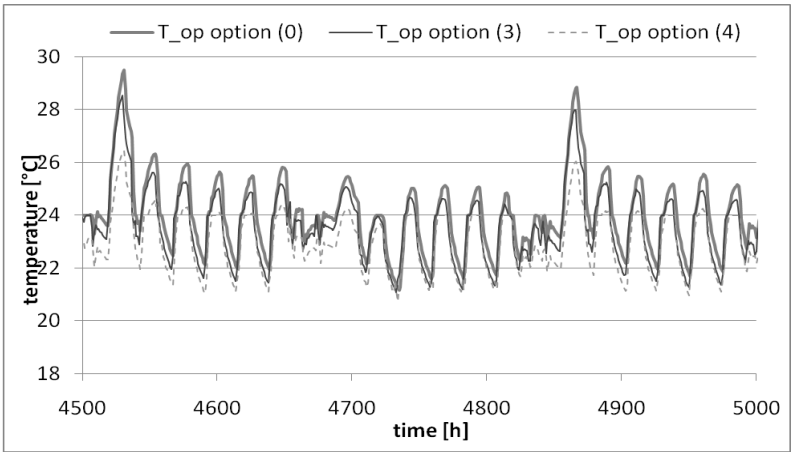

Figure 4: Results of calculated operational temperatures during summer in room with internal shading.

DISCUSSION

To quantify the potential of solar shading two different solar shading types were investigated with different control strategies. Integrated thermal and daylight simulations were carried out to demonstrate comparable results of the performances of the facades with respect to energy consumption and indoor environment. The performances of the facades were evaluated in terms of total energy demand, the individual energy demands for heating, cooling and artificial lighting, and also the amount of daylight in terms of daylight autonomy. Using external shading in Norwegian climate reduces the total energy demand in an office room in Norway. While an external shading device reduces cooling demand during summer, it increases heating demand during winter. The external shading device reduces the temperatures below 26°C for both control strategies. However, with daylight control the summer temperatures are below 23°C. The internal shading device shows higher temperatures and frequently exceeds the threshold of 26°C.

Each simulation was only performed on a single, but representative room in the south facing perimeter zone of a building, and the interaction with the rest of the building was considered. The actual performance of the entire building however depends on the control strategy for the entire building. More work is needed to investigate these issues.

ACKNOWLEDGEMENTS

This study is part of the research project "LECO, Low Energy Commercial buildings". The financial support from the Norwegian Research Council is highly acknowledged.

REFERENCES

1. Reinås, J., *Energieffektivisering*. 2009.
2. Wigenstad, T. and C. Grini, *Fra normbygg til faktor 4*, S. Byggforsk, Editor. 2010, SINTEF Building and Infrastructure: Oslo.
3. Dokka, T.H., et al., *Energibruk i bygninger. Nasjonal database og sammenligning av beregnet og målt energibruk.* , S.B.a. Infrastructure, Editor. 2011: Oslo.
4. NS3031, *Calculation of energy performance of buildings – Method and data*. 2007, Standard Norge.
5. NS-EN15193, *Energy performance of Buildings - Energy requirements for lighting*. 2007, Standard Norge.
6. TRNSYS. *Trnsys16 user manual*. [User manual] 2004 Oct 2006 [cited 2005 Jan 2005]; Available from: http://sel.me.wisc.edu/trnsys/.
7. Reinhardt, C.F., *Daysim 2.1 - Tutorial on the Use of Daysim Simulations for Sustainable Design*. 2006, National Research Council Canada: Ottawa, Canada.
8. Reinhardt, C.F., *Lightswitch 2002: A model for manual control of electric lighting and blinds.* Solar Energy, 2004. **77**(1): p. 15-28.
9. Tregenza, P.R. and I.M. Waters, *Daylight Coefficients.* Lighting Research & Technology, 1983. **15**(2): p. 65-71.
10. Reinhart, C.F. and O. Walkenhorst, *Validation of dynamic RADIANCE-based daylight simulations for a test office with external blinds.* Energy and Buildings, 2001. **33**(7): p. 683-697.

USING SATELLITE DATA TO PREDICT SKY CONDITIONS AND ZENITH LUMINANCE IN HONG KONG

Justin Z. He; Edward Ng.

School of Architecture, The Chinese University of Hong Kong, Shatin, NT, Hong Kong

ABSTRACT

This paper presents methods to predict sky conditions based on CIE standard general skies and hourly zenith luminance by cloud index n derived from visible channel data of geostationary satellite. Instantaneous cloud index averaged from nine pixels derived from satellite visible channel data was used to predict sky types. Two cut-off values of cloud index based on the cumulative frequency distribution under three sky conditions were determined to classify sky types. Three sky conditions based on CIE standard general skies can be classified by cloud index: $n > 0.38$, $0.13 \le n \le 0.38$ and $n < 0.13$, corresponding to overcast, partly cloudy and clear sky conditions, more specifically to sky 1, sky 8 and sky 13 of the "Hong Kong Representative Sky". Hourly zenith luminance can be derived as a function of the combination of relative standard overcast sky zenith luminance and relative standard clear sky zenith luminance determined by cloud index. The mean bias error and the root mean square error of hourly zenith luminance are 0.49 kcd/m^2 and 3.37 kcd/m^2 respectively.

The overall frequency of occurrences of three sky conditions predicted by satellite data can give a general understanding to architects and engineers about the local daylight climate. With the zenith luminance and the sky conditions predicted by cloud index, the absolute values of sky luminance distribution can be approximately estimated from CIE standard general sky model for daylight design. If one representative sky could be estimated by other climatic information under each sky condition (overcast, partly cloudy and clear skies) for a place; for example, sky type 1, 8 and 13 are "Hong Kong Representative Sky". The absolute values of sky luminance distribution might be better estimated with the zenith luminance and the frequency of occurrence of three sky conditions predicted by cloud index.

The accurate sky luminance distribution is essential for advanced daylight design. However, before obtaining detailed luminance records for the main climatic regions of the world, it is important to know the daylight climate to define regions that are with similar cloudiness and radiation condition and predictable by standard meteorological parameters. Satellite-based methods could be an effective approach to achieve this objective to some extend as satellite data can extend spatially the ground measurements over a large area.

INTRODUCTION

This study is to predict sky conditions based on the CIE standard general sky and zenith luminance from the cloud index derived from the visible channel data of a geostationary satellite. For ground measurement, sky data with 10-min intervals were collected from the International Daylight Monitoring Programme (IDMP) research class station in The Chinese University of Hong Kong (22˚25´N, 114˚12´E). For satellite data, the visible channel data of Geostationary Operational Environmental Satellite (GOES)-9 in the same period as the ground measurements from June 2003 to May 2005 were used in this study. Both data sets, including ground measurement and satellite data for sky classification and zenith luminance

prediction, were randomly separated into two groups respectively, 80% for fitting the models and 20% for accuracy assessment.

DERIVATION OF CLOUD INDEX

GOES-9 takes one or two images per hour in the visible channel. The gray-scale values of the GOES-9 visible channel range between 0-255 representing black to white. Our previous study used cloud index to predict global illuminance [1]. The procedure for deriving cloud index is similar in this study.

The cloud index n originally proposed by Cano et al. [2] was determined as follows:

$$n = \frac{C'_{nor} - C_{\min}}{C_{\max} - C_{\min}} \tag{1}$$

where C'_{nor} is the air mass corrected pixel value , $C_{\min}$, and $C_{\max}$ are corrected values of minimum and maximum satellite values, which are two horizontal lines determined by least squares fitting to the 2nd and 98th percentiles of air mass corrected pixel values in each 5-degree solar elevation bin. Here we adopted 2nd and 98th percentile pixel values instead of minimum and maximum values in each bin to avoid some outliers.

This study based the analysis on the average cloud index of 9×9 pixels surrounding the IDMP station in the Chinese University of Hong Kong.

CLASSIFICATION OF SKY CONDITIONS

Previous research shows that no single climatic parameter can classify all 15 CIE standard general sky types effectively [3]. So it could be impossible to classify 15 sky types by the single parameter of cloud index. In addition, some sky types, for example, sky type 15, are rare in Hong Kong [4]. It is difficult to analyze the relationship between the cloud index and a sky type with very low frequency of occurrence. Therefore, this study grouped the 15 CIE standard general sky types into three categories: overcast skies (sky nos. 1-5), partly cloudy skies (sky nos. 6-10) and clear skies (sky nos. 11-15).

Figure 1 shows the frequency distribution of cloud index n at 0.02 intervals. To classify the three conditions, two cut-off values of cloud index should be found taking into account the balance of the overlaps of three sky conditions. It is difficult to determine the two cut-off values of cloud index by eye. The two cut-off values can be estimated by the following expressions:

$$C1 = \min\{|\,(1 - FDO(n_i)) - FDP(n_i) - FDC(n_i)\,|\} \tag{2}$$

$$C2 = \min\{|\,FDC(n_i) - (1 - FDO(n_i)) - (1 - FDP(n_i))\,|\} \tag{3}$$

where $C1$ is the value of cloud index to separate overcast skies and partly cloudy skies; $C2$ is the value of cloud index to separate partly cloudy skies and clear skies; $FDO(n_i)$, $FDP(n_i)$ and $FDC(n_i)$ are frequency distributions at a given cloud index n_i ($i = 1, 2, 3, ..., N$) at 0.01 intervals for overcast skies, partly cloudy skies and clear skies respectively. Finally, $C1$ and $C2$ were determined to be 0.13 and 0.38 by Equation (2) and (3).

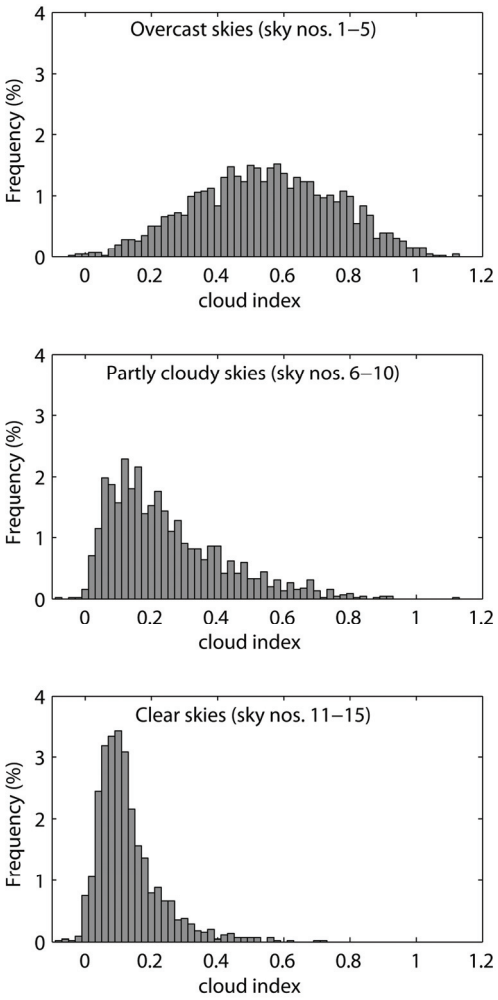

Figure 1: Frequency of occurrence of cloud index based on three sky conditions

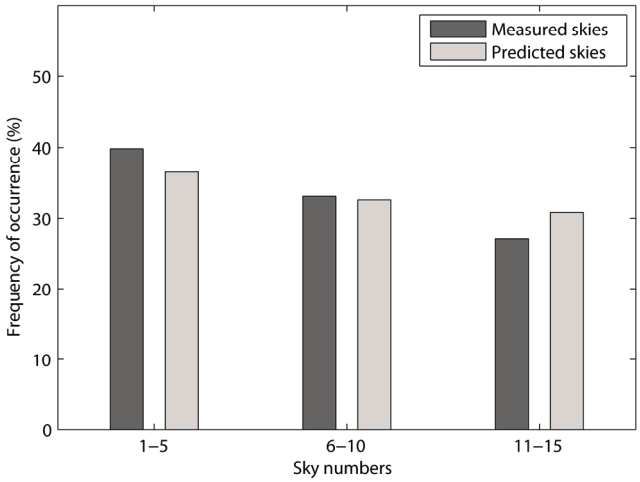

Figure 2: Comparison of frequency of occurrence between measured and predicted skies under three sky conditions

Figure 2 gives the frequency of occurrence of measured and predicted skies under the three sky conditions. It shows that the two cut-off values of cloud index, generally speaking, can classify the three sky conditions.

Our previous study proposed a reduced set of CIE general skies to represent the sky conditions of Hong Kong known as the "Hong Kong Representative Sky (HKRS)" [4]. Studies conducted by Tregenza [5] and Li et al. [6] suggested that eliminating some skies could simplify the sky model without a significant loss of overall accuracy. The subset of three sky types include sky types 1, 8 and 13, representing the overcast, partly cloudy and clear sky. Based on the cloud index categories mentioned above, the CIE general sky type can be predicted for further daylight analysis. Table 1 gives a summary of the relationship between cloud index categories and sky types.

Cloud index bins	**Sky conditions**	**HKRS**
$n < 0.13$	Clear skies	Sky 13
$0.13 \le n \le 0.38$	Partly cloudy skies	Sky 8
$n > 0.38$	Overcast skies	Sky 1

Table 1: Sky types classified by cloud index

PREDICTION OF ZENITH LUMINANCE

The hourly average of zenith luminance from June 2003 to May 2005 was used in this study to formulate a model taking into account the temporal resolution of the satellite which is around an hour most of the time. This study investigates the formulation of hourly zenith luminance (L_z) for all-sky conditions as a function of the combination of relative standard overcast sky zenith luminance (l_{zoc}) and relative standard clear sky zenith luminance (l_{zcl}) determined by cloud index as follows:

$$L_z = (Al_{zoc} + Bl_{zcl})E_v \tag{4}$$

where A and B are the coefficients; l_{zoc} and l_{zcl} are the relative zenith luminance for standard overcast sky and standard clear sky respectively, which can be defined from CIE standard general sky functions by choosing corresponding parameters [7]:

$$l_{zoc} = f(Z_s)\varphi(0) = 1 + 4e^{-0.7} = 2.986 \tag{5}$$

$$l_{zcl} = f(Z_s)\varphi(0) = 0.274(0.91 + 10e^{-3Z_s} + 0.45\cos^2 Z_s) \tag{6}$$

where Z_s is the solar zenith angle (rad).

E_v is the extraterrestrial horizontal illuminance[3]:

$$E_v = \varepsilon E_{vo} \sin\gamma_s \tag{7}$$

where ε is the eccentricity correction; the luminous solar constant $E_{vo} = 133.8$ klux; γ_s is the solar altitude (rad).

This data set of hourly zenith luminance was divided into ten bins for overcast skies ($n > 0.38$), ten bins for partly cloudy skies ($0.13 \le n \le 0.38$) and 5 bins for clear skies ($n < 0.13$) respectively, based on cloud index.

The total 25 regression equations in all the bins were then reduced to one equation by least square fitting the coefficients in all 25 bins as a function of cloud index.

The coefficients A, B were determined by the regression analysis mentioned above as follows:

$$A = -0.0682n^2 + 0.0757n \quad (8)$$

$$B = 0.1085n^2 - 0.2262 + 0.1177 \quad (9)$$

where n is the cloud index. When $n = 0$ (no cloud), coefficient $A = 0$, zenith luminance (L_z) is the function of CIE clear sky; while when $n = 1$ (cloudy), coefficient $B = 0$, zenith luminance (L_z) is the function of CIE overcast sky.

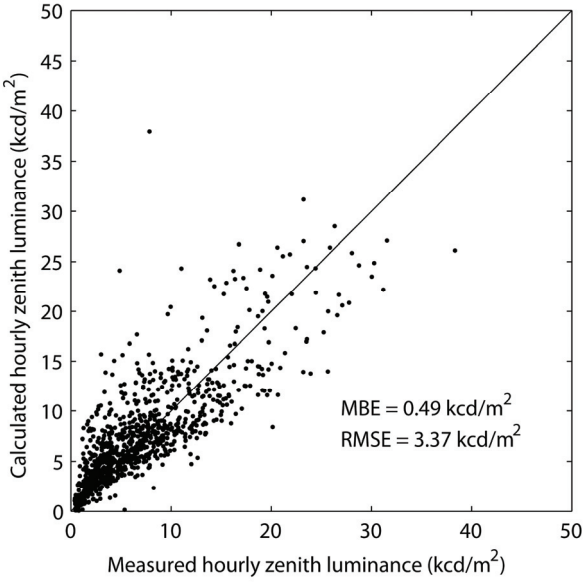

Figure 3: Calculated against measured hourly zenith luminance

The hourly calculated and measured zenith luminances are compared in Figure 3. The mean bias error (MBE) and the root mean square error (RMSE) are 0.49 kcd/m^2 and 3.37 kcd/m^2 respectively.

CONCLUSION

This study has presented simple methods to predict sky conditions and zenith luminance based on cloud index derived from satellite GOES-9 visible channel data. Three sky conditions based on CIE standard general skies can be classified by cloud index n: $n > 0.38$, $0.13 \le n \le 0.38$ and $n < 0.13$, corresponding to overcast, partly cloudy and clear sky conditions respectively, more specifically to sky 1, sky 8 and sky 13 of the "Hong Kong Representative Sky". In addition, this study has presented a model to predict hourly zenith luminance as a function of the combination of relative standard overcast sky zenith luminance (l_{zoc}) and relative standard clear sky zenith luminance (l_{zcl}) determined by cloud index. The

mean bias error (MBE) and the root mean square error (RMSE) are 0.49 kcd/m^2 and 3.37 kcd/m^2 respectively.

ACKNOWLEDGEMENTS

The work described in this paper was fully supported by a grant from the Research Grants Council of the Hong Kong Special Administrative Region, China. (Project no. CUHK 416109)

REFERENCES

1. He JZ, Ng E. Using satellite-based methods to predict daylight illuminance for subtropical Hong Kong. Lighting Research & Technology 2010; 42: 135-47.
2. Cano D, Monget JM, Albuisson M, Guillard H, Regas N, Wald L. A Method for the Determination of the Global Solar-Radiation from Meteorological Satellite Data. Solar Energy 1986; 37: 31-9.
3. Kittler R, Darula S. Parametric definition of the daylight climate. Renewable Energy 2002; 26: 177-87.
4. Ng E, Cheng V, Gadi A, Mu J, Lee M, Gadi A. Defining standard skies for Hong Kong. Building and Environment 2007; 42: 866-76.
5. Tregenza PR. Analysing sky luminance scans to obtain frequency distributions of CIE Standard General Skies. International Journal of Lighting Research and Technology 2004; 36: 271-81.
6. Li DHW, Lau CCS, Lam JC. A study of 15 sky luminance patterns against Hong Kong data. Architectural Science Review 2003; 46: 61-8.
7. Commission Internationale de l'Eclairage. Spatial Distribution of Daylight - CIE Standard General Sky. Vienna: CIE, 2003.

CODYRUN: ARTIFICIAL LIGHTING SIMULATION SOFTWARE FOR VISUAL COMFORT AND ENERGY SAVING OPTIMIZATION.

A.P. Jean[1]; A.H. Fakra[1]; H. Boyer[1] and F. Miranville[1];

1:University of La Reunion, Physics and Mathematical Engineering for Energy and Environment Laboratory, Reunion Island - France.

aurelien.jean@univ-reunion.fr, fakra@univ-reunion.fr

ABSTRACT

This paper reports a method about artificial lighting simulation. More precisely, we present a case study with software simulation. The software used is 'CODYRUN', a powerful tool developed by the PIMENT laboratory. This software has been developed by the building physics team of the PIMENT laboratory since 1993. It has been completed with a specific model dealing with artificial and natural lightning in 2009. The goal of this study is to analyse, with CODYRUN, the indoor artificial lighting repartition and optimization. In this way, we will be able to appreciate the quantity/quality of this repartition, and find a better solution if needed. Beyond this particular case, the method can be used in every other study configurations to find the artificial lighting repartition. Considering that, a succinct presentation of the newest CODYRUN lighting functionalities and applications is made. Moreover, we explain briefly how these are implemented.

The case study is a classroom located in a tropical island called 'La Réunion' (Indian ocean). The initial set-up is a classroom-typical light disposal. After simulation, mean artificial lighting values of 433 lux with an inadequate distribution is found. More precisely, it evolves between two hot spots of 794 lux in the centre of the room and 66 lux in the corners. This means, considering visual comfort, only 45% of the work plan is adequately lit. After correction, the distribution is much better. The new mean artificial lighting level has risen to 500 lux but with a better homogeneity. In this new configuration, there is no real hot spot, and the lighting level evolves between 550 lux and 250 lux, respectively at the centre of the room and in the corners. Considering visual comfort, 91% of the working plan surface is now adequately lit. So we improved the lighting quality by 46%.

Thus, this tool induces a good prediction of light distribution and allows optimising it, which means making a better choice considering economy and comfort of occupants (with good lighting, there will be no need for additional devices).

Key Words: CODYRUN, optimization, artificial lighting, simulation, comfort.

INTRODUCTION

Nowadays, in western countries, human beings spend most of their time in buildings. In order to provide quality lighting, leading to a good visual comfort in function of the activities, it is important to take care of the light intensity and distribution in the building. For this purpose, both natural and artificial light need to be taken into account and their evolutions all day/month/year long. These functions have been included in the software CODYRUN, which can thus be used to optimise natural and/or artificial light distribution.

CODYRUN is a research building-simulation software allowing to understand and predict complex configurations behaviour. Thus, it induces a good prediction of light distribution and allows optimizing it. The present paper presents the software and its application in an analysis and optimisation case study.

SOFTWARE PRESENTATION: CODYRUN

CODYRUN is a powerful building numerical simulation tool developed by the PIMENT laboratory. This software has been developed at the PIMENT laboratory building physics team by Harry BOYER [1] since 1993. Initially specialized on thermo-aerolic heat transfer, several models were implemented throughout the years improving the software capacities. Detailed elements of algorithm and validation of this software are presented in several papers [2,3]. CODYRUN philosophy is based on semi-detailed models, which allow to get precise results with low computational costs. Due to its numerous applications in the fields of thermal comfort and energy consumption, it is an appreciated research and predictive tool.

In 2009, a specific model dealing with artificial and natural lightning has been added. According to Fakra [4], this model is more precise than current software references such as RADIANCE, SUPERLITE or LESO-DIAL. It was validated following BESTEST procedures and successfully confronted to experimental data.

More precisely, considering the model, the light study is performed on a virtual horizontal surface called 'work plan'. This surface is located at a specified height from the floor. The work plan is simulated by a variable number of points specifically distributed in a plan, called grid. Each point corresponds to a location where the light intensity is researched, computed.

$$E_{glo,P} = \frac{I_{S,P}}{d_{SP}^2} \cdot \cos(\alpha) \cdot (1 + \rho()) \tag{1}$$

In artificial lighting, for one source, the direct and diffuse radiations are expressed and summarised by the equation (1). Where 'E' is the global artificial lighting at a position P (in lux), 'I' is the light intensity of the source S into P direction (in Cd), 'd' is the distance SP (in m), 'ρ' is the averaged walls reflection coefficients and 'α' is the angle between the work plan normal and the SP light segment.

CASE STUDY

The case study is a classroom located in a tropical island called 'La Réunion' (Indian ocean). The initial set-up is a classroom-typical light disposal (Fig. 1). The aim of this study is to appreciate the quantity/quality of the light distribution, and find a better solution if needed. This study focuses only on artificial light, but the same study could be done for natural light or a combination of both in function of the day time (etc.).

Nota: Beyond this particular case, the following method can be used in every other study configuration to find the artificial lighting distribution.

Hypothesis

Simulations are made on an work plan localised at 0.85 m from the floor. Artificial sources are considered Lambertian, punctual and isotropic. The grid discretisation has a regular pattern, the distance between two nodes is the same following x or y axes, $\Delta x = \Delta y = 0.2$m.

Description

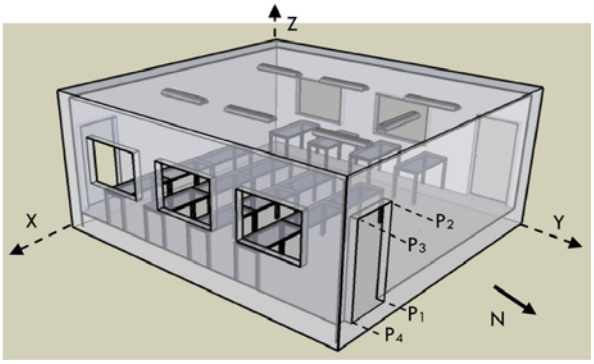

Figure 1: Classroom presentation and light disposal.

The classroom has seven neon lights. L1 to L6 are lighting the student desks (~1300 Cd) and L7 is lighting the blackboard (~950 Cd). The L1 to L7 intensities were found by measurement, they are expressed into Table 1, for localisation see Figure 2. After classroom description in CODYRUN, the simulation can be run.

Light Position	**L1**	**L2**	**L3**	**L4**	**L5**	**L6**	**L7**
Intensity (Cd)	1290	1370	1350	1148	1164	1372	955
Utilisation	Desk	Desk	Desk	Desk	Desk	Desk	Board

Table 1: Measured light intensities.

RESULTS AND DISCUSSION

Real set-up simulation

After simulation, a mean artificial lighting level of 433 lux with an inadequate distribution is found (Fig. 2). More precisely, it evolves between two hot spots of 794 lux in the centre of the room and 66 lux in the corners. Around 50% of the work plan is lit by more than 500 lux as imposed by the European norm (NF/EN 12464-1), whereas 5% shows a lighting level below 300 lux (next to the borders).

This light distribution implies a correct lighting distribution on 45% of the work plan leading globally to a bad visual comfort (both too much or not enough light).

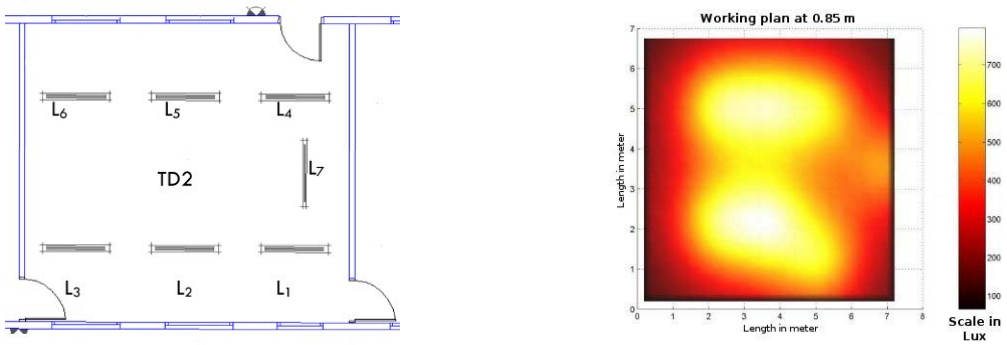

Figure 2: Classroom real light disposal and intensities distribution.

Optimization simulation

Considering the real light disposal intensities distribution and values, another light distribution was proposed in order to get a relatively homogeneous intensity throughout the classroom. Several methods could be used to get a new sizing. Here the main idea was a better distribution of the light, so the sizing is based on the global intensity conservation. In this case, nine identical lights of 1767 Cd (Fig. 3) were chosen.

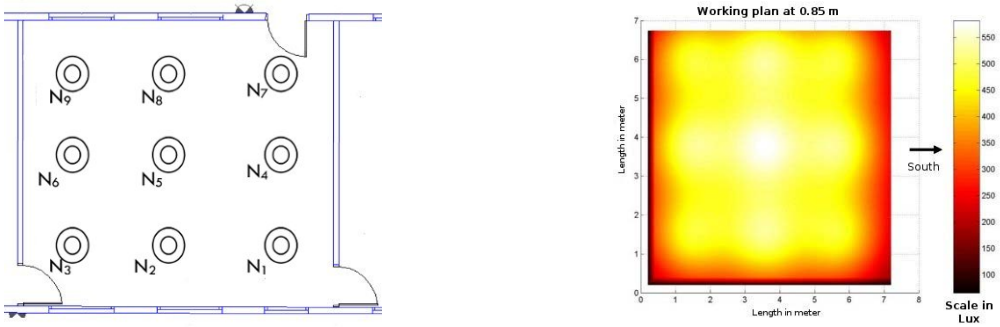

Figure 3: Optimized classroom light disposal and intensities distribution.

Corrected light disposal simulation gives a better distribution. The new artificial lighting mean rose from 433 to 500 lux but with a better homogeneity. In this distribution, there is no real hot spot, and the lighting evolve between 550 lux and 250 lux, respectively at the centre of the room and in the corners. Considering visual comfort, 91% of the working plan surface is adequately lit. So we improved the lightning quality by 46%.

CONCLUSION

CODYRUN allowed us to diagnose a classroom's artificial lighting in intensity and distribution. This predictive tool could also simulate another configuration to find a better light disposal, improving significantly visual comfort and lighting quality (+46%). Similar diagnostics could be performed for natural lighting or a time evolving mix of both natural and artificial lighting.

Considering the thermo-aerolic model implemented in CODYRUN, the light and thermal models can be coupled to get simultaneously an energy, thermal and visual study in the same simulation.

REFERENCES

1. Boyer, H.: Thermal building simulation and computer generation of nodal models, Building and Environment, Vol. 31, 207-214, 1996, ISSN 0360-1323.
2. Boyer H., Garde F., Gatina J.C., Brau J.: A multi model approach of thermal building simulation for design and research purposes, Energy and Buildings, Vol.28, 71-79, 1998, ISSN 0378-7788.
3. Boyer H., Miranville F., Bigot D., Guichard S., Jean A., Fakra A.H., Calogine D.:Heat transfer in buildings : application to air solar heating and Trombe wall design, 2011.
4. Fakra, A.H.: Intégration de modèles d'éclairage à un code de calcul en physique du bâtiment, modélisation, validation et applications, Ph.D. Thesis, University of La Reunion, France, 2009.

TOWARDS MICROSTRUCTURED GLAZING FOR DAYLIGHTING AND THERMAL CONTROL

Kostro A.[1], Geiger M.[1], Scartezzini J.-L.[1], Schüler A.[1]

1: Solar Energy and Building Physics Laboratory, Ecole Polytechnique Fédérale de Lausanne: LESO-PB, Station 18, Bâtiment LE, EPFL, 1015 Lausanne, Switzerland.

ABSTRACT

Glass is a central element to modern architecture and can cover up to 100% of a building façade. The main purpose of large glazed areas is to create bright, comfortable and healthy spaces. It was shown that increasing natural light in offices reduces sickness but high visual transmittance (τ_v) and excessive energetic transmittance (τ_e) can have opposite consequences: a high τ_v can cause glare and visual discomfort for occupants while a high τ_e induces overheating which has to be balanced with air conditioning in summer. The energetic and daylighting performances of a fenestration system are central and important issues for architects and the right compromise between good lighting levels, electrical savings, solar gains in winter and overheating in summer is not easy to find.

Over the past decades, progress was made and some solutions to these problems were found. Various types of blinds and shadings have been introduced to prevent glare, achieve a good daylight factor even far from the window and permit to adapt to conditions all along the year. Sun protection glazings on the other side are static systems with a selective coating to limit the transmitted part of the solar spectrum: traditionally a step function with maximum values in the visible range and minimal values in the infra-red and ultraviolet range cuts down excessive solar gains. Recent research show that the transmitted spectrum can be refined and applying a 'M' shaped transmittance distribution, a ratio of $\tau_e / \tau_v = 0.33$ can theoretically be reached [1]. A market study on complex fenestration systems integrating daylighting functions and thermal control shows that apart from blinds and coatings which can be found in many variations, few products exist. Cutting edge elements such as laser cut panel, prismatic sheets and other micro-structures were studied. The study showed that there is no existing static complex fenestration system (CFS) combining the advantages for both daylight and energetic aspects with a seasonal behaviour.

We are investigating a novel micro structure combining functions of daylighting, glare protection, overheating protection in summer and thermal insulation in winter. The optical performances of envisaged structures were evaluated with a simple two dimensional ray tracing program developed specially for the study of laminar structures. This tool permits to optimize parameters and search for new solutions.

INTRODUCTION

To provide modular daylighting, solar gains and solar protection, the traditional Venetian blinds, roller shades and screens have been introduced long ago. It is clear that a smart management of available energy is interesting: good lighting levels are comfortable, prevent 'sick building syndrome' [2] and lower the energy bill due to electrical lighting [3]. A good exploitation of solar radiation can reduce heating costs in winter and cooling loads in summer.

In the first part of this study, some of the most recent innovations with such goals are reviewed.

The development of new solutions requires modelling tools, ray tracing software are often used to calculate the Bidirectional Scattering Distribution Function (BSDF) of complex fenestration systems [4]. To the best of our knowledge, no dedicated tool or model exists for the characterisation of complex fenestration systems that are geometry and material dependent. Existing commercial tools provide complete and time consuming 3D characterisation, the resulting outputs are complex and make it hard to compare several solutions. In the second part of the present study, a simple and efficient ray tracing tool will be presented. Using this tool, a complex solution combining daylighting, solar gains and solar protection is pursued. This study presents preliminary results regarding the daylighting aspect.

RECENT INNOVATIONS FOR BETTER DAYLIGHTING AND SOLAR CONTROL

This section will introduce existing concepts and products for complex fenestration systems. It focuses on elements of the dimension of common windows and does not include large architectural elements such as light shelves, large integrated anidolic systems, light tunnels, heliostats and solar tubes.

Over the years, the profile and functionality of blinds and shadings was fine tuned to prevent glare and protect from overheating while keeping a sufficient daylight level and good energetic performance. Engineers have optimised blind shapes: *Retrolux* blinds by *RETROSolar* are an example of very interesting geometry *(see figure 1a)*. At high incidence most rays are reflected outwards, while the more horizontal rays are partially redirected towards the ceiling and deep into the room. Recently, split blinds with different inclination angles have been introduced and the upper and lower part of the blinds can be separately controlled. Automated control for blinds was introduced to optimize the position of shadings and adapt to changing conditions all along a day.

Figure 1: Photographs and schematic illustrations of existing products and application. a) Retrolux blinds [5] b) Solartran Lasercut Panels in a classroom [6] c) Lumitop [7].

Another approach uses static glazing with special angular properties. Laser cut acrylic panels, for example, use total internal refraction to redirect light upwards when it is incoming with a certain angle. The *Lumitop* glazing by *St-Gobain (see figure 1c)* traps light into banana shaped elements and guides it upwards. The S*erraglaze* sheets take advantage of the same concept and seek the same goals as laser cut panels but with a different fabrication scheme and slight different geometry (mainly differing by its smaller scale). Prismatic structures and holographic optical elements use geometric shapes and the index of refraction difference between air and glass or some acrylic to select rays from a certain angle.

For advanced thermal properties of transparent glazing, thin film coatings were introduced. For solar control, an interferometric coating composed of a succession of thin films "selects" a range of the spectrum for transmission. For low emissivity, a coating reduces heat losses through the window. Such coatings reduce lighting and cooling cost [8] but they don't have a seasonal behaviour, do not redirect light and can create too low light levels in winter.

Limitations of existing static solutions

Some CFSs are only partially transparent or distort the view and are thus often placed in the upper third of the window only in order to preserve a clear view in the bottom part. Others have the inconvenience that they only work for specific angles and therefore have to be mounted on tracking systems. It has been observed that the only existing product combining the advantages for both daylight and energetic aspects with a seasonal behaviour still are dynamic blinds systems with complex geometry. There is a strong interest for CFSs and they are used in public buildings and offices (see f*igure 1b*), but comparatively to the simplest blinds, they remain pricey. Beside the growing coated glazing market, split blinds are introduced in new buildings. They provide a dynamic control at a relatively low cost and a simple system to separately control daylight, view and thermal contributions. It would be ideal to have a static glazing achieving similar performances, with no mechanical parts subject to wear. Such a system does not exist.

RAY TRACING TOOLS

In order to investigate more complex systems, and because existing tools did not provide satisfaction, a custom ray tracing tool is developed. The goals are to make it simple to design new shapes and parameterize them; change and compare the effects of parameters; assess the propagation of light through the system rapidly and visually; compare multiple different systems regarding different criteria and finally produce usable BSDFs for rendering of daylighting in rooms with tools such as *Radiance*. Most blinds, redirecting glazings and structured systems are 2D profiles projected into the third dimension. A two dimensional approach was selected to simplify computation, programming and output. Neglecting the third dimension is exact in the plane that is perpendicular to the system and contains the normal vectors of all surfaces. Considering only variations of the elevation angle θ with a constant azimuth angle φ is sufficient to roughly and rapidly characterise systems.

Assessment of performances

The live visualisation of rays through the system at different incoming angles (*see figure 2*) give valuable indications about relevant parameters and approximate values. To get a quantification of the performance of a system, the ray tracing is performed for given incoming elevation angles θ_{in} on the outer side off the CFS. The intensity distribution of θ_{out} (transmitted and reflected) can then directly be displayed as a polar plot (*see figure 3*). The information given by this polar plot is not always sufficient since the incoming distribution in natural conditions is not uniform and changes with season, location and weather. For these reasons the transmission depending on the incoming angle is interesting and displayed in a second plot. But this ratio does not give sufficient information about daylighting and glare protection, we introduce the transmitted upward ratio indicating the proportion of light that is transmitted upward *(see figure 5)*. This representation is useful to assess behaviours dependent both on the solar elevation and the transmitted angle (potential daylight or glare contributing part). Because the amount of information is relatively limited in both representations, it is possible to compare two designs, eventually three. The angular distribution of outgoing angles

depending on incoming angles can also be exported as a angular matrix (BSDF) for other analysis or use in a program such as *Radiance*.

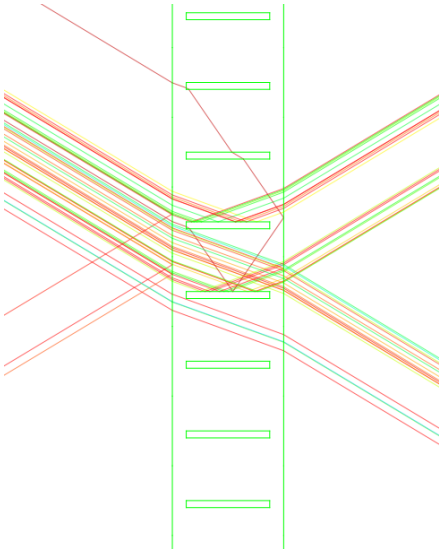

Figure 2: Simulated ray trajectories illustrating the Lasercut Panel principle.

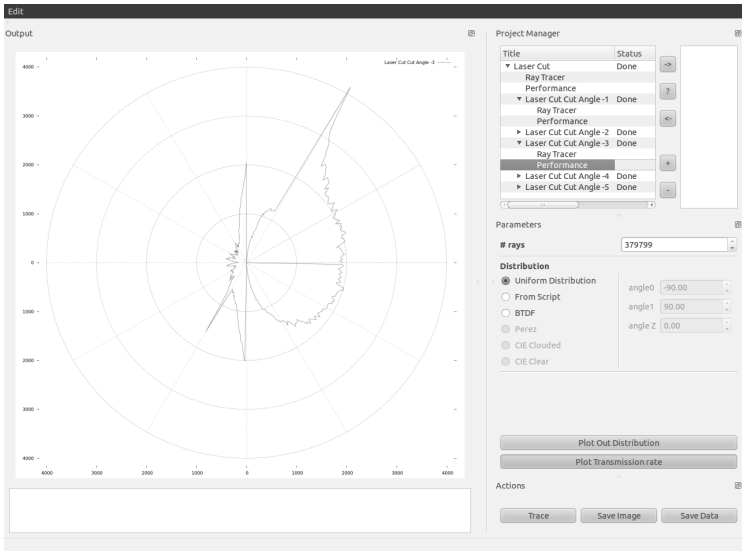

Figure 3: Screen-shot of the developed graphical Interface with a polar plot of output angle distribution for a laser cut panel with -90° < θ_{in} < 90°.

To complete the model and fully describe the desired systems, several improvements are in process and partially implemented. In order to be able to use selective coatings in the model, thin films will be introduced with wavelength dependent indices of refraction for more precision in interferometry and reflection / refraction. Diffuse reflection will be introduced to model diffusing interfaces and mirrors. The third dimension will be introduced to model the azimuth dependent behaviour. The characterisation will include plots for τ_e and τ_v.

RESULTS

On million rays being computed in less than a minute, the software allows rapid assessment of the designs. This section presents some results for optimisation of tilt angle in laser cut panels, then for optimisation of cut period. In the simulations, the CFS is vertical and rays are traced from left to right, uniformly distributed with 0° < θ_{in} < 90° where θ_{in} is the elevation from the horizon. *Figure 4a* shows how a laser cut panel (LC) and a clear glass (SG) transmit and reflect light. The SG transmits better towards the normal and reflects grazing light. The Laser cut panel partially redirects the light and creates a peak in the upper quadrant; this peak is due to the air-glass interval in the panel where light hitting with angles higher than 41° is reflected. As expected and shown in *figure 4b*, the tilt angle of the cuts directly influences the direction of the peak in the distribution of light. The steep step in the intensity (at 60° for example for the -3° tilted laser cut panel) is due to the inclination of the cuts, incoming rays are refracted at the air-glass interface into the panel: for 67° < θ_{in} < 90°, the first transmission cone is very narrow: 40° ± 2°. Due to the reflection at the cut, this angle is shifted by twice the tilt angle: 28° ± 2° for a 6° cut and light hits the exit interface with a much smaller angle than the initial transmitted angle. In this interval the transmission cone is much smaller: 41°-49° instead of 67°- 90° for direct transmission. The effect is a directional transmission at preferred angles where light is concentrated, and the overall transmission can also be slightly increased by this effect *(see table 1)*.

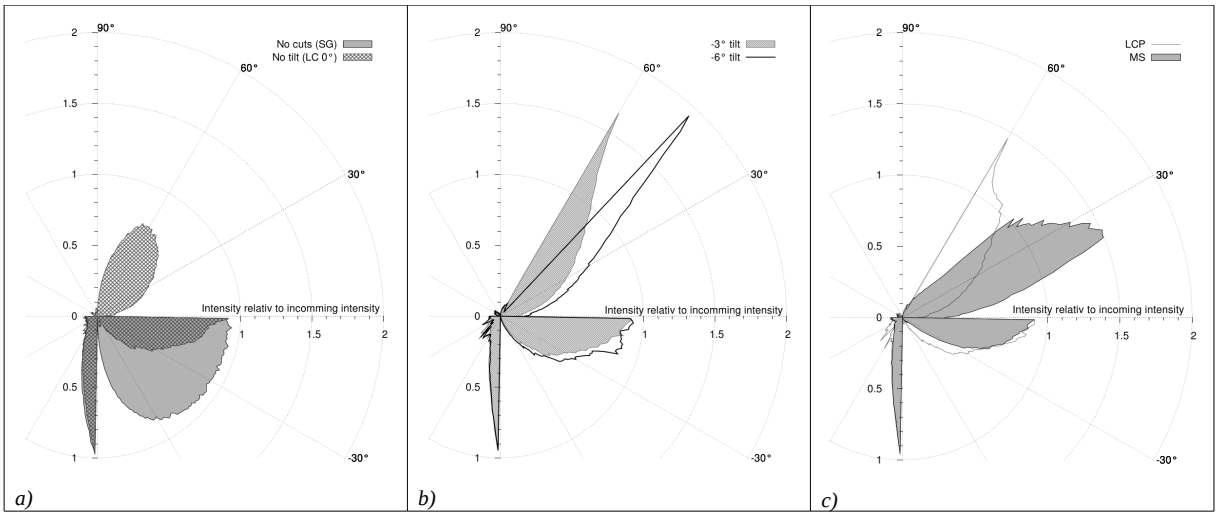

Figure 4: Polar plot of outgoing intensity distribution for 0° < θ_{in} < 90°. a) Clear glass (SG) and Laser cut panel (LC) . b) Laser cut panel at different tilt angles. c) Optimised Laser cut panel (LCP) and Microstructure (MS).

	SG	LC 0°	LC 1°	LC 2°	LC 3°	LC 5°	LC 2° 3.5mm	LC 2° 4mm	LC 2° 4.5mm	LC 3° 3.5mm	LC 3° 4mm	LC 3° 4.5 mm	MS
Mean Transmission	78.0	75.0	76.8	77.7	78.4	**78.8**	76.0	76.7	77.3	76.2	77.0	78.0	**81.7**
Mean T up Quadrant	0	41.7	42.9	42.9	42.2	39.7	42.0	44.3	**44.6**	42.3	44.4	44.4	**56.2**
Redirected 20° < θ_{in} < 70°	0	55.6	54.8	54.1	52.7	50.0	58.7	**59.9**	57.7	59.4	59.9	56.9	**74.7**
Redirected 50° < θ_{in} < 70°	0	68.5	69.2	69.5	68.7	67.5	57.8	70.8	73.5	62.6	73.7	**74.0**	**84.8**

Table 1: Mean percentages for different glasses and different laser cut panels. SG is a standard single glazing with BK7 glass. LC stands for laser cut with different tilts angles and a 5mm periodicity. The periodicity is specified when different. MS stands for micro structure, a custom microstructure developed using the ray tracing tool.

Lines 1 and 2 in *table 1* show the mean values for the total transmission and upward transmitted quarter. At angles of incidence corresponding to direct solar radiation in Lausanne in summer (50 to 70°) the 2° laser cut panel is the most efficient at redirecting the light with 68.7% transmitted upward. The influence of periodicity of the cuts for 2° and 3° tilts was studied next. We find that the best design is a 3° cut with a 4.5mm periodicity. As stated in *table 1* with a 4.5 mm period, 74.0% of light incoming between 50° and 70° is redirected against 68.7% with a 5mm period. A custom micro structure (MS) reaching 84.8% was developed, the transmission distribution for this MS is compared with the 3° 4.5mm laser cut panel in *figure 4c and 5b*. This design is also superior for overall transmission, overall redirection and most important, the "useful" redirection between 20 and 70°: the span of solar elevation during a year in Lausanne. The redirected light is distributed around 30° for the MS when it is centred around 50° for the laser cut panel. *Figure 5a and 5b* illustrate the difference in transmission and redirected light between different designs. The MS design is much superior for angles around 40° and at very low angles, around the normal, it does not redirect light.

CONCLUSION

There is no existing static system combining daylighting, solar protection and a seasonal behaviour for thermal control. To design an ideal CFS, a simulation tool was developed.

Preliminary results show that the daylighting goals can be reached and the parameters optimised. The resulting CFS outperforms existing structures in the simulations. The objectives differ depending on the type of building, the orientation of façades and the latitude on earth. A target function adapted to these conditions and evaluation simultaneously the visible light redirection for daylighting, the angular dependent energetic transmission, and a clear view factor needs to be developed.

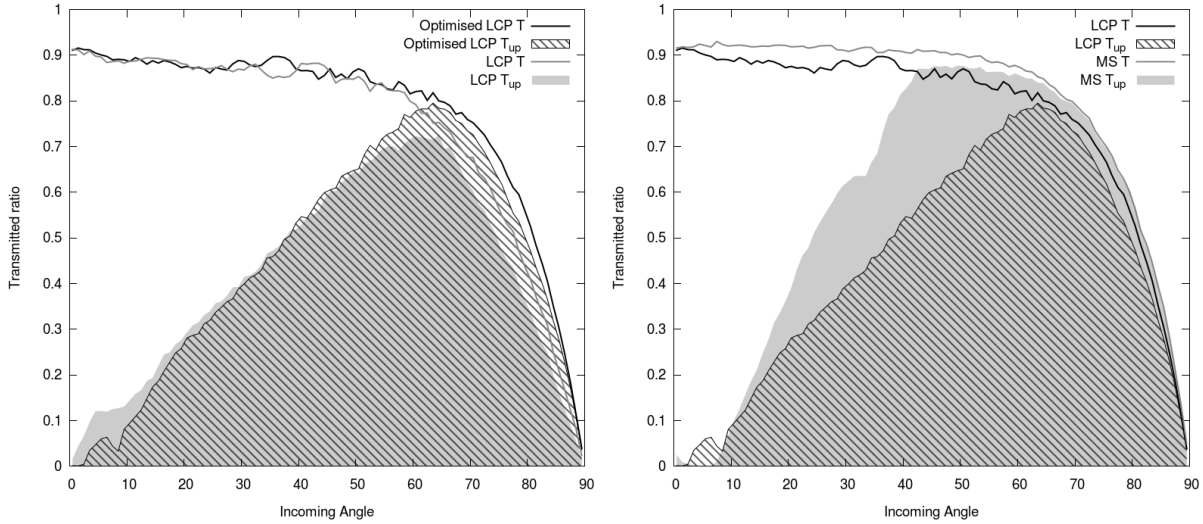

Figure 5: Comparing transmitted and redirected ratio in different CFS a) for Laser cut panel optimisation. b) For custom microstructured glass.

ACKNOWLEDGEMENT

The authors would like to thank the Swiss Federal Office for Energy for financial support and Jerôme Kaempf for his availability and inspiring discussions.

REFERENCES

1. P. Oelhafen. Optimized spectral transmittance of sun protection glasses, Solar Energy, Volume 81, Issue 9, pp 1191-1195, 2007.
2. S. H. A. Begemann et Al. Daylight, artificial light and people in an office environment, overview of visual and biological responses, International Journal of Industrial Ergonomics, Volume 20, pp 231-239, 1997.
3. Linhart F., Scartezzini J-L. Minimizing lighting power density in office rooms equipped with Anidolic Daylightin Systems, Solar Energy, Volume 84, pp 587-595, 2010.
4. Stephen Wittkopf et Al. Ray tracing study for non-imaging daylight collectors, Solar Energy, Volume 84, pp 986-996, 2010.
5. Retro Solar Retrolux http://www.retrosolar.de/flash/ani_rlux_e.html
6. Solartran Laser cut http://www.solartran.com.au/lasercutpanel.htm
7. St Gobain Lumitop http://uk.saint-gobain-glass.com/upload/files/sgg_lumitop_.pdf
8. Danny H.W. Li et Al. Lighting and cooling energy consumption in an open-plan office using solar film coating. Energy, Volume 33, pp 1288-1297, 2008.

LED LIGHTING IN MUSEUMS: THE NEW DIOCESAN MUSEUM IN PIOMBINO (ITALY)

F. Leccese, G. Salvadori, A. Colli

Dept. of Energy and Systems Engineering (DESE), University of Pisa
Faculty of Engineering, Largo L. Lazzarino, 56122 Pisa (Italy)

ABSTRACT
This study has been devoted by its authors to an examination of lighting conditions within the New Diocesan Museum based at the former St. Augustine's Convent (Piombino, Tuscany region, Italy). The lighting project has been developed with the aim of creating ideal conditions for conservation and enjoyment of the exhibited artworks, in an effort to ensure a significant energy saving while complying with adequate standards of interior comfort.

1. INTRODUCTION

The restoration of unused buildings is part of a wider strategy embraced by the Italian Government for many years with special care to preserving the rich architectural and building heritage to be found in the country. The majority of restored historical buildings are applied to public uses (such as offices, libraries, museums etc.) in compliance with specific requirements of interior comfort, particularly as far as lighting aspects are concerned [1-3].
In this paper, the study of lighting has focused on exhibition rooms at the New Diocesan Museum and forms part of a restoration and adaptive reuse project dealing with the former St. Augustine's Convent [4]. Along with the Convent itself, a large fourteenth century Church and its Cloister costitute the Monumental Complex of St. Antimo the Martyr's Co-cathedral (see figure 1). The Complex is placed in the oldest part of the Old Town in Piombino (Tuscany region, Italy). Having survived religious orders suppression decreed by Napoleon at the beginning of the nineteenth century, the Church is still being used for worship. In 1806, the remaining part of the Complex (consisting in both Convent and Cloister) was desecrated and heavily modified to become a barrack lodging. In 1998, the Convent (converted to house barracks for the command of the Financial Guard in Piombino) was declared unfit for use and abandoned.

2. THE ARCHITECTURAL DESIGN FOR THE NEW DIOCESAN MUSEUM

The Diocese of Massa Marittima and Piombino has recently announced its intention of using the former Convent to house the New Diocesan Museum, by widening the small existing museum. Accordingly, a planimetric and altimetric survey has been conducted on the Monumental Complex, carried out parallel to documentary investigations at the main historical archives in Tuscany [4]. These investigations have led to the discovery of a large amount of historical evidences, allowing to trace the interesting chronological background of the Monumental Complex as well as its architectural developments from the year 1377 (when the Church was founded) until now.
The proposed project includes a restoration of the existing exhibition rooms (110 m^2) located on the Convent's ground floor, along with new exhibition rooms to be placed on the first floor (190 m^2), see figure 2a. On the ground of a considerably expanded investigation range due to this increase in the museum's floor area, assumptions have been made as to the placement of more than 60 artworks, mainly represented by stone items and marble sculptures, in addition to vestments and religious ornaments (such as silver chalices, wooden crucifixes, manuscripts and paintings), partly stored in the ancient halls and partly disseminated in several buildings owned by the Diocese. The exhibition path goes from the first floor (housing the lapidarium),

proceeds to the ground floor and leads finally to a fresco from the fourteenth-fifteenth century, recently discovered on a wall in the last exhibition hall, which originally functioned as the Convent's chapterhouse [4].

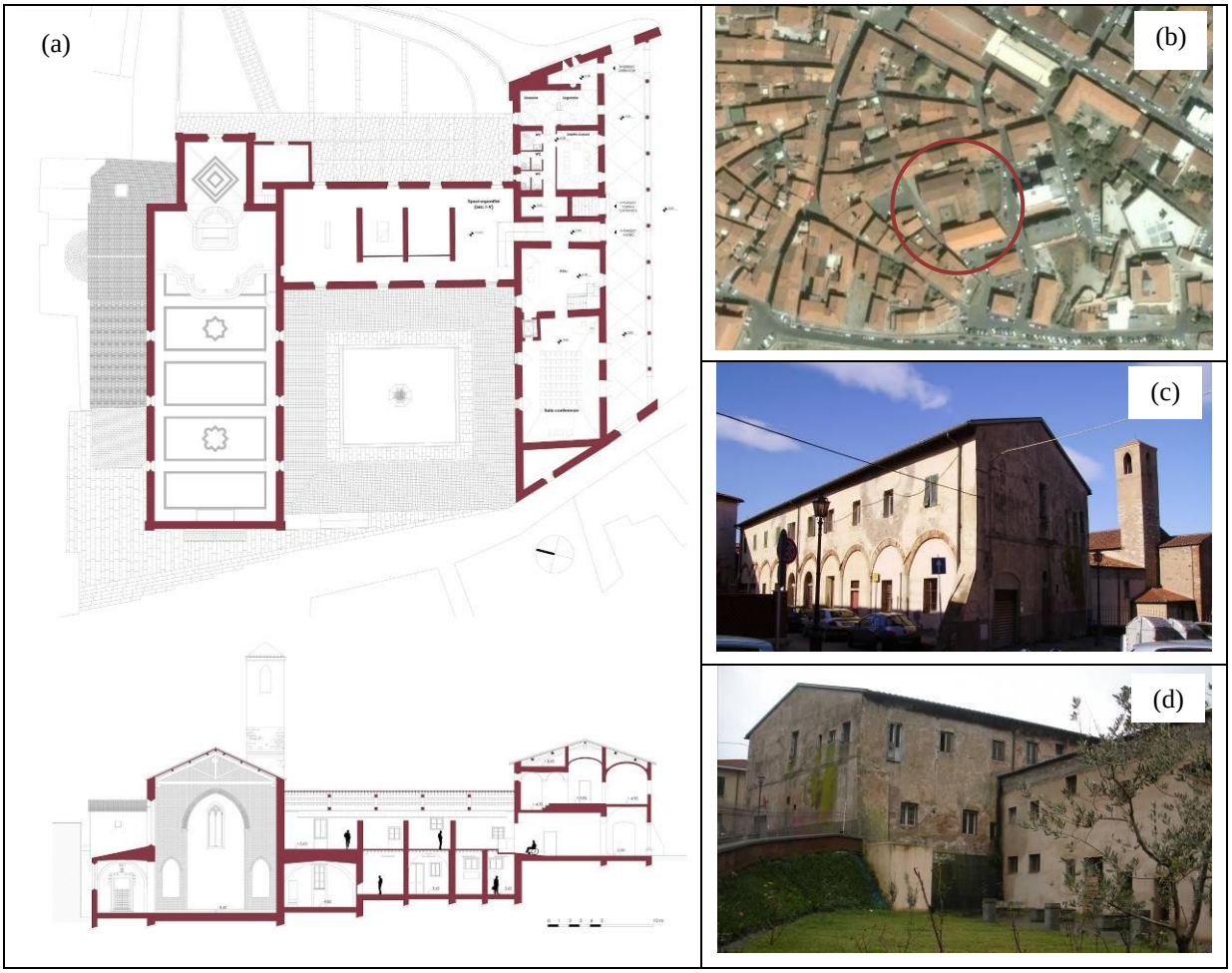

Figure 1: Complex of St. Antimo the Martyr's Co-cathedral, restoration project: (a-up) general plan, (a-down) section of the exhibition rooms, (b) aerial view. Photos of the current state: (c) north view, (d) east view.

3. THE LIGHTING DESIGN FOR THE EXHIBITION ROOMS

When conceived for a museum, lighting projects are usually very complex [5] as they imply compliance with different, occasionally conflicting requirements. On the one hand, care must be taken to safeguard respect for artworks by exposing them to a controlled lighting source (artificial light) at low illumination levels; on the other hand, attention must be paid to ensure their enjoyment by the public through a lighting system with high efficiency.

In the case examined, compliance with these requirements has been achieved by means of both a total shielding from direct sunlight (responsible for deteriorating light radiation sensitive materials) and the use of LED lights (i.e. particularly suitable sources in terms of energy savings, low damage rate and building adaptation). The overall lighting design for exhibition rooms has been based on the European standard EN 12464-1 [6], according to the following requirements: average illuminance E_m=300 lx, illuminance uniformity $U=E_{min}/E_m>0.5$, glare index UGR<22. As to the lighting of artworks, reference has been made to the Italian standard UNI 10829 [7] on indoor conditions for the preservation of artworks (see table 1). Equal account has also been taken of the following lighting quality parameters

[5]: lamp color rendering Ra>90, lamp color temperature 3100÷4200 K, on artworks U_{max}<5 (with U_{max} the ratio between maximum illuminance, E_{max}, and minimum illuminance, E_{min}).

Table 1: Lighting parameters for the conservation of artworks (UNI 10829).

Sensitive to light	**E_{max}** (lx)	**Q** (lx_ch/year)
low (e.g. marble and metal objects)	300	Over 500.000
medium (e.g. oil paintings and frescoes)	150	500.000
high (e.g. textiles and manuscripts)	50	50.000

Note – Q is the overall yearly energy exposure [7], expressed by hourly conventional lux per year (lx_ch/year).

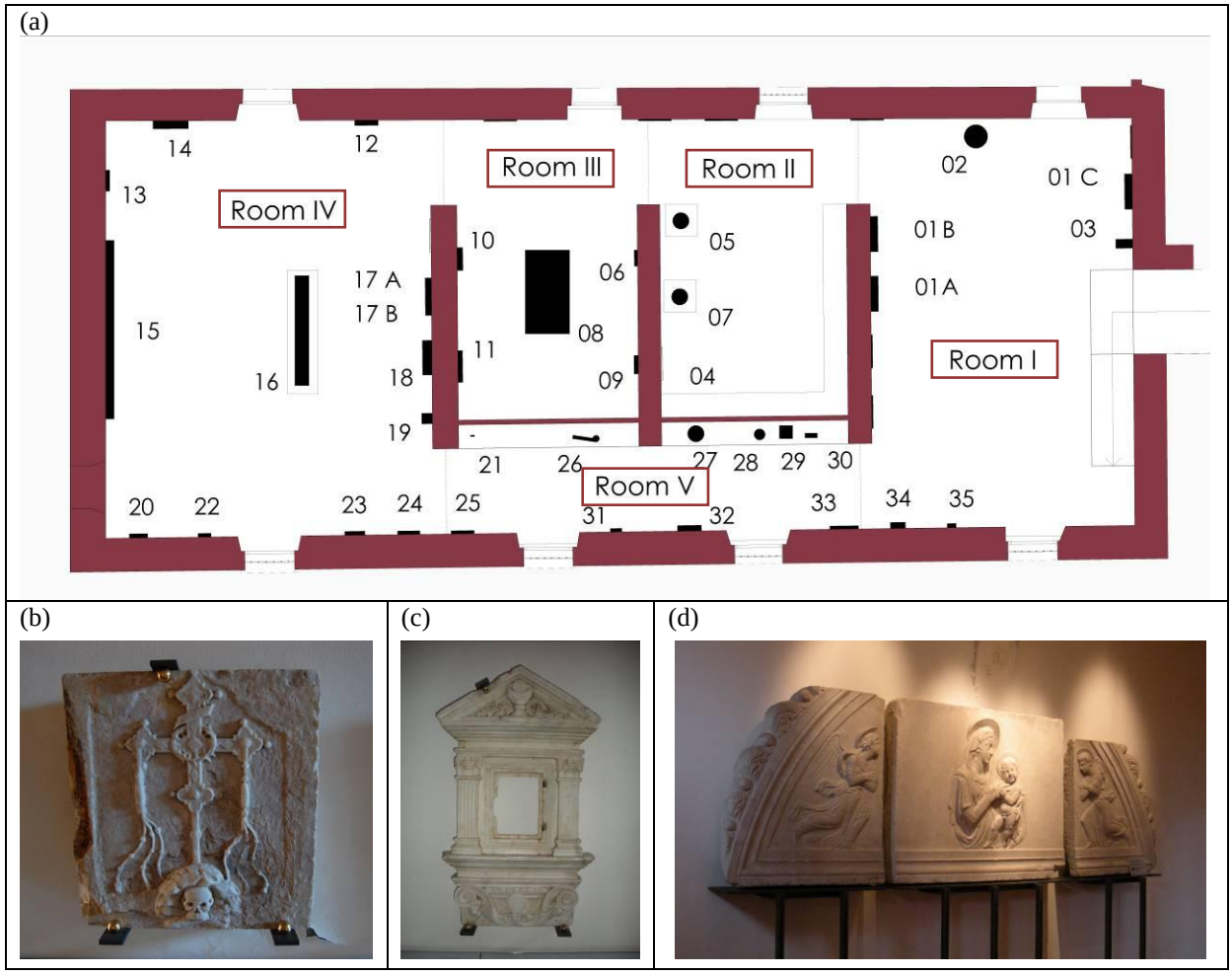

Figure 2: The New Diocesan Museum: (a) plan of exhibition rooms at the first floor (the numbers show exhibited artworks); (b) artwork n.12, Badge of the Confraternity of the Blessed Sacrament (1470-1480); (c) artwork n.13, Wall Tabernacle (1470-1480); (d) artwork n.15, The Holy Virgin with the Christ Child and Angels (1465-1470).

On the basis of a study of artworks placement along the exhibition path (extending from lapidarium to fresco's room), an artificial lighting system has been set out so as to allow a progressive lowering of illuminance levels in the halls, aimed at making spot lighting on all of the artworks stronger than overall lighting [8]. Therefore, E_m values for overall lighting in the exhibition rooms have accordingly been kept at around 50% of the E_m level determined by the standard [6].

The artificial lighting project for the exhibition rooms within the New Diocesan Museum has been software-aided by ReluxPro2010 (*www.relux.biz*). The use of this software has allowed a thorough geometric modeling of both exhibition rooms and artworks (see figure 3). The reflection coefficients (r) used in exhibition rooms are as follows: r=0.65 for vertical walls (white plaster); r=0.60 for the ceiling (white plasterboard panels); r=0.38 for the floor (brick tiles). As to artworks, reflection coefficients have been taken into account as factors related to whether material or finish type (in the case of matt white marble, they correspond, for instance, to 0.55). The following shows only the results obtained with regard to the first floor exhibition rooms (lapidarium), for further discussion on results see Refs. [4, 8].

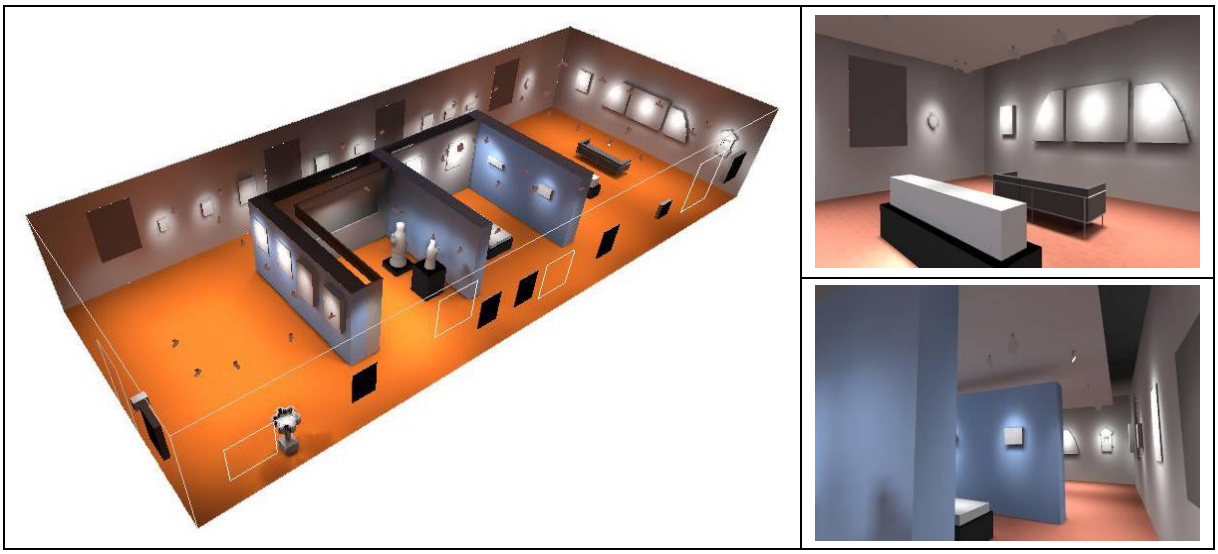

Figure 3: Modeling of the exhibition rooms of the New Diocesan Museum (first floor).

3a. Lamps and luminaires

According to the project, whilst recessed fixed luminaires have been used for the overall lighting, both artworks and didactic panels would be lit by relying on luminaires running on electrified tracks (adjustable spotlight), in a condition to provide a higher flexibility for the lighting system. The selected luminaires are installed in a way as to avoid surface reflection effects on artworks and minimize direct glare along the exhibition path.

The installation includes as many as 105 luminaires, supplied by LED lights (see table 2) and accommodated as follows: 30 luminaires in the ground floor and 75 in the first floor, of which, 29 luminaires devoted to overall lighting (recessed fixed luminaires) and 46 to artwork lighting (adjustable spotlight). The total installed electric power is equal to 1120 W, respectively distributed as follows: 331 W in the ground floor and 789 W in the first floor, of which, a 76% for overall lighting and a 24% for artworks lighting.

3b. Calculation results

Figures 5a-b show both isolux curves and isochromatic maps as related to overall lighting in the Museum's first floor. In particular, E_m values have been found to range from 160 lx (room I, see figure 2a) to 140 lx (room V, see figure 2a), along with U>0.5. It must be noted that the resulting rate has been established at UGR<21 with regard to all of the main sight directions in each room. Figures 5c-e show 3D images from isochromatic illuminance maps related to representatively selected artworks (see figures 2b-d).

Each exhibited artwork has been provided with a summary information sheet reporting its description, placement, luminaires in use as well as the main calculation results from a lighting point of view [8]. For instance, an examination on artwork n.12 (see figures 2b and

5c, Badge of the Confraternity of the Blessed Sacrament), gave the following results: E_{max}=224 lx, E_m=175 lx, U_{max}=1.7, Q=47.6 klx$_c$h/year. An examination on artwork n.13 (see figures 2c and 5d, Wall Tabernacle) gave: E_{max}=294 lx, E_m=197 lx, U_{max}=2.9, Q=53.6 klx$_c$h/year. An examination on artwork n.15 (see figures 2d and 5e, The Holy Virgin with the Christ Child and Angels), led to these results: E_{max}=290 lx, E_m=178 lx, U_{max}=3.2, Q=48.4 klx$_c$h/year. Q values relate to a lighting exposure of 1088 hours, being received on the basis of a weekly opening time of 34 hours, the same duration assumed to determine the LENI index.

Table 2. Characteristics of lamps and luminaires (exhibition rooms at the first floor).

Photos and dimensions	Photometric curves	Main characteristics	Qty.
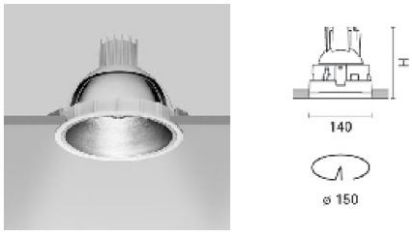	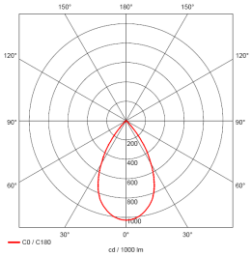	Name: iGuzzini **The Reflex professional** (Recessed fixed luminaire) Optical: professional optic for a LED lamp Luminaire efficiency: 0.91 • Lamp: LED (18W) Neutral White • Electric power: 18 W • Luminous flux: 1100 lm • Luminous efficacy: 61 lm/W • Color temperature: 4200 K	29
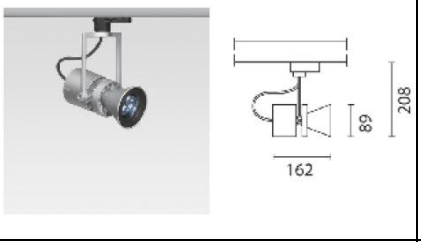	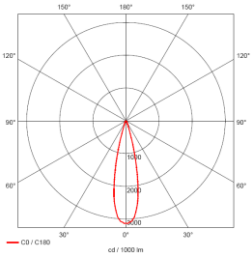	Name: iGuzzini **Le Perroquet Spot** (Adjustable spotlight) Optical: optics with plastic lenses and medium beam (25°) Luminaire efficiency: 0.65 • Lamp: LED (3x1W) Warm White • Electric power: 3.68 W • Luminous flux: 252 lm • Luminous efficacy: 68.5 lm/W • Color temperature: 3100 K	27
	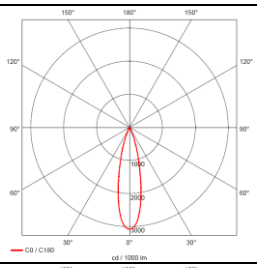	Name: iGuzzini **Faretto Parallel** (Adjustable spotlight) Optical: optics with plastic lenses and medium beam (25°) Luminaire efficiency: 0.69 • Lamp: LED (8x1W) Warm White • Electric power: 8.82 W • Luminous flux: 604,8 lm • Luminous efficacy: 68.5 lm/W • Color temperature: 3100 K	9
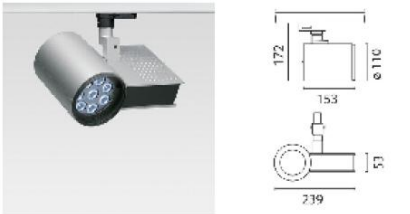	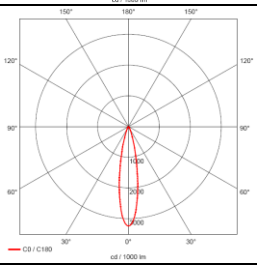	Name: iGuzzini **Express** (Adjustable spotlight) Optical: optics with plastic lenses and medium beam (25°) Luminaire efficiency: 0.61 • Lamp: LED (8x1W) Warm White • Electric power: 8,82 W • Luminous flux: 604.8 lm • Luminous efficacy: 68.5 lm/W • Color temperature: 3100 K	10

3c. Evaluation of the LENI index

The LENI index, calculated from the following equation [1, 9], refers to the yearly energy demand of a lighting system:

$$LENI = (W_L+W_P)/S \qquad (kWh/m^2year)$$

where: W_L energy demand needed by luminaires, in order for them to comply with the conditions set forth by the lighting project; W_P energy demand necessary to emergency luminaries; S floor area.

For this study's aims, the LENI index has been calculated with reference to the rooms located on the first floor, by using the comprehensive method specified in [9], which was implemented in software LUX R2.0 [1]. The obtained LENI values look as follows: in terms

of overall lighting, LENI=9.0 kWh/m^{2}year; in terms of lighting for the exhibited artworks (lapidarium), LENI=1.4 kWh/m^{2}year. In the first floor, the lighting system's total value gave a result of LENI=10.4 kWh/m^{2}year (lower than the smallest benchmark default value 24.8 kWh/m^{2}year, indicated in EN 15193 for the educational buildings).

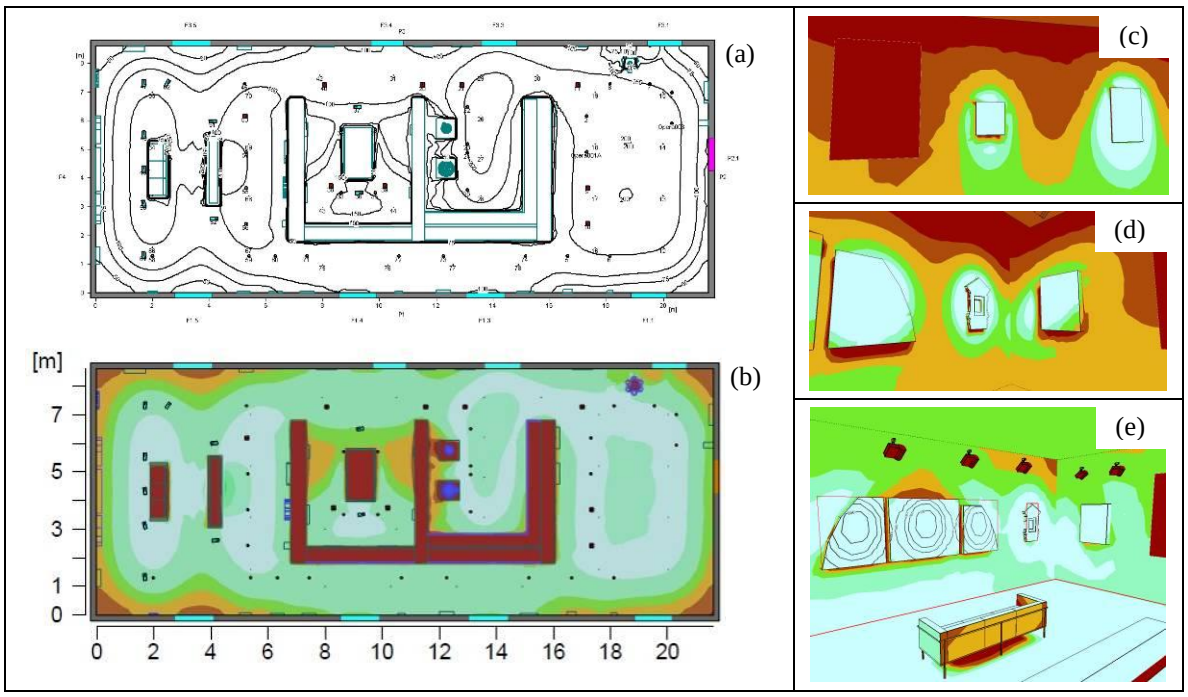

Figure 5: Overall lighting of the museum's first floor: (a) isolux curves, (b) isochromatic illuminance maps; 3D isochromatic illuminance maps: (c) artwork n.12, (d) artwork n.13, (e) artwork n.15 with isolux curves.

ACKNOWLEDGMENTS

The authors would like to thank Mr. Architect Giovanni Grassi from Piombino and Monsignor Pierluigi Castelli, parson of St. Antimo the Martyr's Co-cathedral.

REFERENCES

1. Leccese F., Salvadori G., Caruso G., Batistini E., Daylighting and lighting energy demand analysis of the new town library of Piombino (Italy). CISBAT 2009 – Renewables in a Changing Climate, EPFL, Lausanne (CH), 2009, CD-Rom, pp.249-254.
2. Leccese F., Salvadori G., Tuoni G., Casini M., Architectural lighting of the seventeenth-century building "Logge dei Banchi" (Pisa) for the retraining of the pedestrian axis Leaning Tower-Railway Station. LUX EUROPA 2009 - 11th European Lighting Conference, ATMK, Istanbul (Turkey), 2009, Vol. 2, ISBN: 978-975-561-352-9, pp. 1133-1140.
3. Angeli B., Leccese F., Tuoni G., Daylighting illuminance analysis of a new universitary library using ADELINE. LUX EUROPA 2005 – 10th European Lighting Conference, LiTG, Berlin (Germany), 2005, ISBN: 3-927787-27-2, pp. 205-208.
4. Colli A., Il nuovo Museo Diocesano nell'ex convento di S.Agostino di Piombino: elaborati preliminari ed aspetti illuminotecnici (*in Italian*). Master Degree (supervisors: Tuoni G., Maffei P.L., Leccese F., Munafò G., Cartei D.), University of Pisa, Faculty of Engineering, 2009.
5. AA.VV., Guida per l'illuminazione delle opere d'arte negli interni (*in Italian*). Italian Ass. of Lighting, Milan, 1996.
6. EN 12464-1/2002: Light and lighting – Lighting of work places – Part 1: Indoor work places (in Italy: UNI EN 12464-1, October 2004).
7. UNI 10829/1999: Beni di interesse storico e artistico – Condizioni ambientali di conservazione – Misurazione ed analisi (*in Italian*).
8. Leccese F., Salvadori G., Colli A., Il progetto illuminotecnico del Nuovo Museo Diocesano di Piombino (*in Italian*), to be published on "LUCE" (the Journal of the Italian Ass. of Lighting).
9. EN 15193/2007: Energy performance of buildings – Energy requirements for lighting (in Italy: UNI EN 15193, March 2008).

USING WIND-TOWERS SHAFT FOR DAYLIGHTING IN BRAZILIAN TERRACE HOUSES

T. A. L. Martins[1,2]; E. L. Didoné[3]; L. S. Bittencourt[4]; C. M. L. Barroso-Krause[2]

1: Laboratoire de Recherche en Architecture – LRA / ENSA Toulouse, France

2: Programa de Pós-graduação em Arquitetura – PROARQ / UFRJ, Rio de Janeiro, Brazil

3: Fachgebiet Bauphysik & Technischer Ausbau – FBTA / KIT, Karlsruhe, Germany

4: Dinâmicas do Espaço Habitado – DEHA / FAU / UFAL, Alagoas, Brazil

ABSTRACT

A type of terrace house is frequently found in Brazil, mainly as low income houses, under its diverse tropical climates, especially in the Northeastern region. Originally from the Brazilian colonial period, the terrace houses consist of a set of several single family units attached to each other on their sidewalls, forming a row of dwellings settled in narrow plots. This architectural typology presents bedrooms without openings for daylighting or natural ventilation. In tropical climates, natural ventilation associated with solar shading is the most efficient building design strategy to reach thermal comfort by passive means. One of the architectural techniques to provide efficient natural ventilation is the use of wind-towers. This device consists on shafts with openings located above the roof, designed to improve air circulation inside buildings. Recent qualitative studies concerning the use of wind-towers for natural ventilation in Brazilian terrace houses have been carried out. These studies showed that this device may constitute an efficient technique in promoting air changes as well as thermal comfort. In order to complement these studies, this paper presents the analysis of the potential use of the same wind-tower shafts to provide daylighting, considering the daylight coefficients obtained inside the enclosed rooms (alcoves) presented in the above mentioned typology. Parametric computational simulations using *Daysim* software to evaluate the dynamic daylight performance inside the alcoves were performed. Different geometries and opening characteristics of the component were analysed. Results indicate that the use of wind-towers shaft in enclosed environments, such as the Brazilian terrace houses alcoves shows a good potential to provide satisfactory interior daylighting, depending on its geometry and on characteristics of the opening located above de roof. Wind-tower models adopting an internal deflector conducted to more inter-reflections inside the examined rooms allowing a more uniform daylight distribution. The dynamic daylight simulation enabled to compare different models performance, identifying the configuration achieving best results which may be used to provide daylighting autonomy through a whole year.

INTRODUCTION

A traditional building pattern inherited from the Portuguese colonizers has still been widely applied either in warm-humid and hot-dry regions of Brazil, mainly as low-income houses. It can be described as a ground-floor house with a street facade generally composed by a single door and window (Figure 1). The terrace house is set on the alignment of public streets and presents its side walls straight on the limits of the building plot, without any setbacks or gardens. Its plan presents enclosed rooms (alcoves) lined up along an internal corridor, all

settled on a long and narrow plot. The building main facade can range from 3 to 5 m while the width of the plot can go up to 25m (REIS FILHO, 1973) (Figure 2).

Figure 1: Examples of terrace house commonly found in Brazil (After: Martins, 2008).

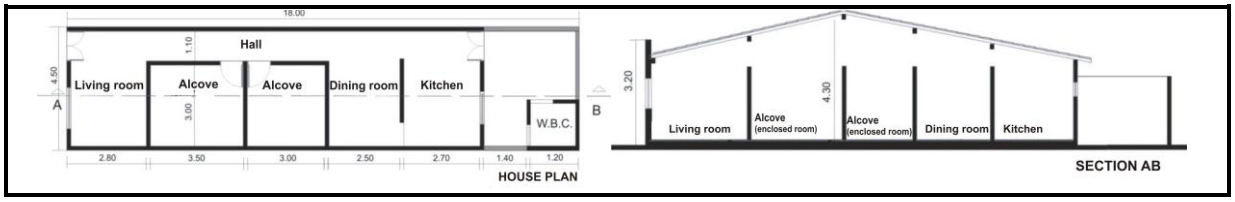

Figure 2: Plan and longitudinal section of the studied house.

Concerning the environmental performance of the building, this architectural typology does not provide solar shading on its front or back external walls, nor an effective natural ventilation or daylight inside most of its rooms especially due to the absence of building setbacks.

In tropical climates, however, natural ventilation associated with adequate solar shading is the most efficient building design strategies to reach thermal comfort by passive means. These strategies aim to reduce external heat gains, filter the high sky luminance while providing air movement (FATHY, 1986; BAHADORI, 1994; GIVONI, 1994).

Brazil, as many other equatorial countries, is a developing nation. This fact allied to the high costs of electricity generation, makes energy saving a national priority, including efforts toward low energy architecture. Most of its inhabitant´s household income cannot afford to neither buy air-conditioning devices (which can be founded in 7,5% of Brazilian households) nor pay for high electricity bills (IBGE, 2003).

On the other hand, concerning the Brazilian Northeast Atlantic coast, for example, the wind features have already been proved to be easily and widely exploited to provide thermal comfort by passive means, especially through the use of wind-catching devices (BITTENCOURT; LÔBO, 2003; MARTINS et al., 2010). Although barely considered in local architectural design, this kind of device may represent not only an important thermal performance strategy, but also a high potential to provide daylight autonomy, improving energy performance of buildings.

Objective

This paper aims to examine the potential use of wind-towers shafts to optimize daylighting in enclosed rooms of a typical Brazilian terrace house.

METHOD

Three main methodological steps were taken:

1. Selection and definition of the geometrical models to be studied;
2. Definition of the context and the parameters to be examined;
3. Computational parametric simulations over *Daysim* software.

Definition of the studied models

The research was developed considering three main geometrical models: the original house configuration and, two different variations of the model with a wind-tower shaft.

The two wind-tower shaft models can be distinguished from each other for the presence of an internal deflector placed at the shaft bottom. At previous study (MARTINS et al., 2010), this deflector performed efficiently regarding wind flow circulation inside the alcoves. Yet, at the external opening of the shaft, it was considered models without window glass, with double glass and solar factor of 90% and window glass with solar factor of 67% (Table 1).

Table 1: Simulation models.

Without shaft		**With wind-tower shaft**					
		Straight shaft			Shaft with internal deflector		
Door open	Door closed	Without glass	Glass 6mm FS = 90%	Glass 6mm FS = 67%	Without Glass	Glass 6mm FS = 90%	Glass 6mm FS = 67%
Model 1	**Model 2**	**Model 3**	**Model 4**	**Model 5**	**Model 6**	**Model 7**	**Model 8**
							

The Brazilian tropical climate – case-study

To carry on with the proposed study, one particular city situated at the Brazilian tropical semi-arid climate was selected; the selection followed the criteria of representation in terms of recurrence in which the studied typology is verified in the region.

The city of Pão de Açúcar, chosen as case-study in the present research, is located at 9 ° 44 ' 54 ' South latitude and 44 ° 26 ' 12 " longitude, located in West-Central portion of the Brazilian State of Alagoas, at an altitude of 29 m (IBGE, 2008), on the banks of the São Francisco River. This city is situated at the Brazilian tropical semi-arid climate.

This region climate can be defined predominantly by the occurrence of large daily and seasonal air temperature oscillations, low air humidity and intense solar radiation. The annual mean air temperature in the city is 36,5°C and the daily air temperature variation can reach up to 15,4°C during summer time. Though, air humidity can vary considerably throughout a typical climatic year. During winter it reaches up to 85% due mainly to the rain concentration in this season. However, during summer, it can reach 53,6% (INMET, 2008). Solar radiation levels and sky luminance measured for the city showed one of the highest in the state of Alagoas, Brazil (ATLAS SOLARIMÉTRICO DE ALAGOAS, 2008), showing good solar energy and daylighting potential.

The studied variables

Computational simulations were carried out using parametric analysis at the software *Daysim.* The dynamic daylight methodology was performed within the above presented models, through the analysis of the Daylight Autonomy distribution (DA)[1].

For each studied model, internal surfaces (wall and ceiling) and the shaft internal surfaces were considered with 80% of reflectance. The room floor had a reflectance of 20%. The shaft

1 *Daylight Autonomy* (DA) is defined as the percentage of occupied hours per year, in which a minimum level of illuminance can be maintained only provided by daylight (REINHART e MORRISON, 2003).

top opening was southeast-oriented (since it consists on the wind predominant orientation in the region), and the occupation period considered was from 8 am to 5 pm.

The minimum acceptable illuminance for the rooms was 150 lx (value required for this type of occupation according to the Brazilian Standards for Interior Illuminances - NBR 5413).

For the evaluation of Daylight Autonomy (DA), the room was divided into proportional areas, forming a mesh starting always in the center of each area. The mesh of points is a horizontal area situated 0,75 m from the floor plan (Figure 4).

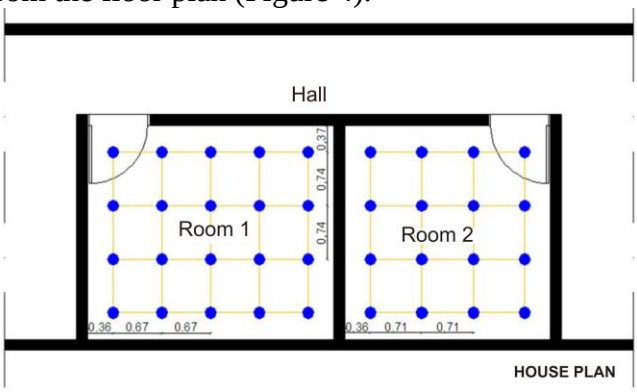

Figure 4- Analysis plan.

Computational parametric simulations – *Daysim* software

As already mentioned, the daylight simulations were performed over the *Daysim* software which provides data for de daylight autonomy calculation. To start the simulations, it was necessary to prepare the geometrical models over a software CAD. Then, configurations parameters were adjusted. As the software simulates daylighting through RADIANCE, its tutorial suggests that some of the input data files must be introduced according to the characteristics of the used model (see Table 2 and Table 3). The simulation parameters may be different according to the constructive features of the model which determines simulation accuracy and duration.

Table 2: Input data of the models (adapted from Reinhart, 2006)

Models	Ambient bounces	Ambient division	Ambient Sampling	Ambient accuracy	Ambient resolution	Direct threshold	Direct sampling
Without shading device	5	1000	20	0.1	300	0	0
With shading device	7	1500	100	0.1	300	0	0

The climatic data file

The simulations were performed using meteorological data file TRY (Test Reference Year). The climatic TRY files are based on a climatic database resulted from a reference year for the local climate, regarded as typical of each place.

RESULTS

As previously explained in this paper, the Daylight Autonomy indicates the percentage of occupied hours in which the minimum required amount of illuminance can be reached. Simulation results were presented with *isoDA* (Iso Daylight Autonomy) curves, represented by different shades of gray. Each shade representing the percentage value obtained in different zones of the studied room.

Results show that illuminance inside rooms of the original building typology (terrace house without wind-tower shaft, as displayed in Model 1 and 2) did not reach the minimum required

of 150 lx. The original model performance results were compared with results obtained with proposed models with different settings.

Figure 5 and Figure 6 present the other two groups of models: building models with the wind-tower straight shaft and models with the wind-tower provided with a deflector at the bottom of the shaft.

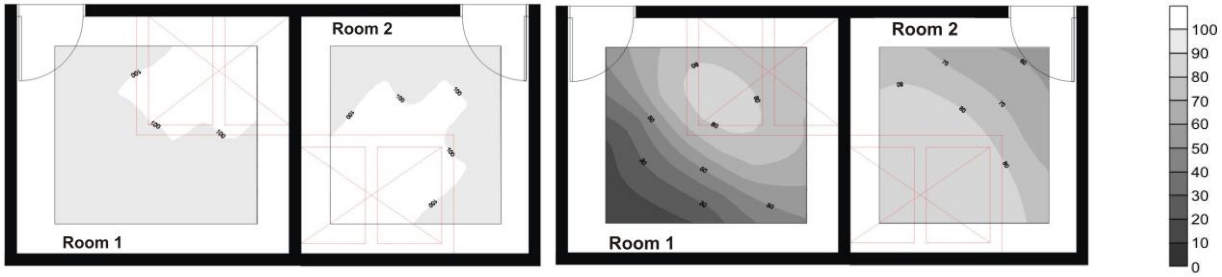

a) Model 3and 4: Wind-tower shaft openings without glass (left) and with glass solar factor of 90% (right)

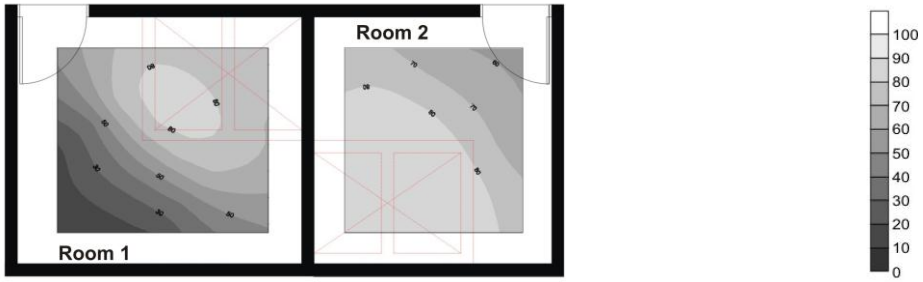

b) Model 5: Wind-tower shaft openings with glass solar factor of 67%.

Figure 5: Results for the rooms with wind-tower straight shaft

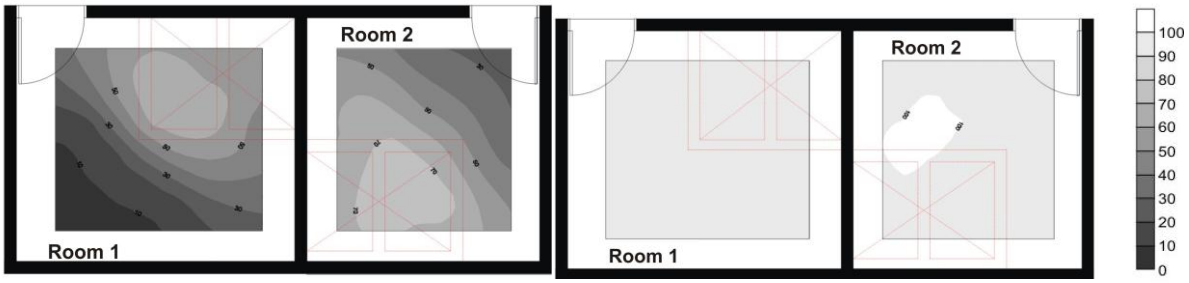

a) Model 6: Opening of the shaft without glass.

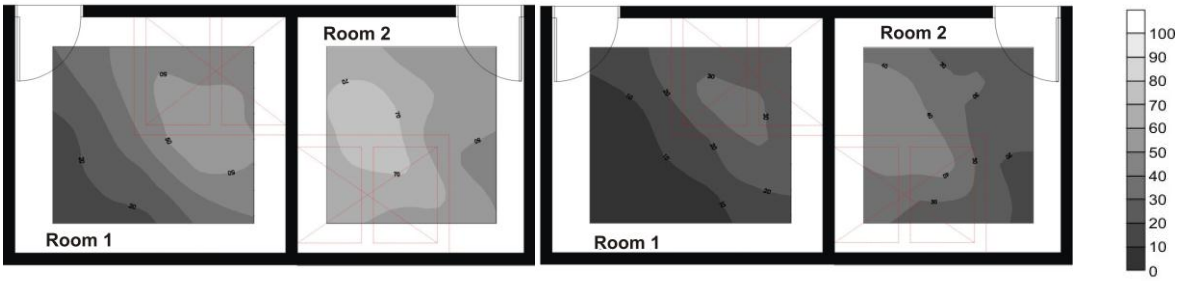

b) Model 7 and 8: Openings with glass solar factor of 90% (left) and 67% (right).

Figure 6 - Results for the rooms with wind-tower shaft and an internal deflector.

As it can be observed, the straight shaft without external window glass was the model presenting the greatest illuminance, featuring daylight autonomy for the time period examined of 100% in the area next to the shaft and of 90% in other areas of the room.

Regardless the changes in the shaft window glass features, the geometry of the wind-tower with straight shaft produces higher illuminance levels in the mesh points located right below

the shaft bottom-opening. But on one other hand if the solar factor of the glass decrease the heat gain from solar radiation, in the other hand, it may significantly diminish the percentage of daylight autonomy, reducing the illuminance levels especially over the points farther from the outlet shaft for up to 60% (Figure 5b).

For the shaft model with the deflector, the curves *isoDA* presented themselves more generously spaced, which means greater uniformity in the distribution of daylight, as can be seen in Figure 6. The simulation pointed out an autonomy of 90% on the entire room (room 1) for the period considered. This fact can be explained by the increase of inter-reflections inside the rooms. The deflector works similarly to a light-shelf, reflecting the sun rays towards the ceiling and thus re-distributing it more uniformly around the room. However, it was verified an illuminance reduction when adopting glass with higher solar factor.

DISCUSSION

The present work examined the daylight potential through the use of two models of wind-towers for a particular type of Brazilian terrace house. These models, previously examined for qualitative performance of wind flow distribution, were now investigated as daylighting shafts. Despite some limitations of the geometries analyzed, the results suggest that the use of wind towers may increase significantly daylighting potential depending on its sizing and configuration. The shaft models provided with a deflector allowed important internal reflections, hence better light distribution. The simulations carried out with the dynamic measure methodology, enabled the identification of the impact produced by different shaft configuration on illuminance levels and uniformity ratio considering daylight autonomy.

ACKNOWLEDGEMENTS

The authors would like to thank CAPES for the financial research support.

REFERENCES

1. ABNT: NBR-5413 Iluminância de Interiores. Associação Brasileira de Normas Técnicas. Rio de Janeiro, 13p., 1992.
2. Bahadori, M. N.: Viability of wind towers in achieving summer comfort in the hot arid regions of the Middle East. In: Proceedings of the third world renewable energy congress, Reading, UK, 11–16 September, 1994. p. 879–92.
3. Bittencourt, L., Lôbo, D. A influência dos captadores de vento na ventilação natural de habitações populares em clima quente e úmido. Ambientes Construídos. ANTAC, 2003.
4. Fathy, H.: Natural energy and vernacular architecture: Principles and examples with reference to hot arid climates. Londres: The Chicago University Press Ltd., 1986.
5. Givoni, B.: Passive and low energy cooling of buildings. New York: Van Nostrand Reinhold publishing company, 1994.
6. Martins, T. A. L.; Bittencourt, L. S.; Bastos, L. E. G.; Barroso-Krause, C.; Passos, I.: Wind-towers for natural ventilation in brazilian terrace houses. In: proceedings PALENC. Rhode Island – Greece, 2010.
7. Reinhart, C. F.; Morrison, M.: The lightswitch wizard – reliable daylight simulations forinitial design investigation. In: Buildings Simulation, 2003, Eindhoven, The Netherlands. Proceedings… Eindhoven: BS, 2003. Vol. III. p.1093-1100.
8. Reis Filho, Nestor G.: O Quadro da Arquitetura no Brasil. São Paulo: Perspectiva, 1973.

OPTICAL CHARACTERIZATION OF A TUBULAR DAYLIGHTING SYSTEM FOR EVALUATION OF ITS SUITABILITY FOR SWEDISH CLIMATES

A. M. Nilsson[1]; A. Roos[1]

1: Uppsala University, Department of Engineering Sciences, Box 534, SE-751 21 Uppsala, Sweden

ABSTRACT

This paper evaluates a tubular daylighting system using spectrophotometric measurements with both diffuse and direct illumination. The spectral transmittance of three scaled tubular systems is determined experimentally as a function of incident angle. The tubular systems have a length to diameter aspect ratio of 5, 7, and 9, and are lined with a flexible reflective foil. The spectrophotometric measurements are compared to ray tracing simulations of the same system, where the geometry of the pipe and the experimentally determined angle dependent spectral reflectance of the foil are used as input to the model. The measured hemispherical transmittance corresponds well to the integrated transmittance obtain from the ray tracing simulations. The ray tracing of the tubular system also provides the bi-directional scattering distribution of the system, which can be used for performance evaluation and daylight calculations.

INTRODUCTION

In Sweden, the building sector accounts for approximately 35% of the total energy use [1]. The goal of the European Union member states is to reduce the energy use in buildings with 20% (compared to 2005 year's level) by year 2020. To achieve this goal, significant upgrades of the existing building stock and implementation of energy efficient solutions in new construction are necessary. The Swedish Energy Agency has commissioned a detailed study of the energy use in buildings to provide a foundation for improved energy efficiency. The part of the study that investigated a selection of office buildings showed that electric lighting constitutes 21% of the building's total energy use [2]. This makes electric lighting the single most significant item and the potential for cost-effective savings is significant.

Multiple studies have shown that the implementation of daylighting systems can reduce electric energy use, while improving visual comfort and well-being of the building inhabitants. Only a handful of studies have, however, been conducted to establish the feasibility of daylighting systems in Scandinavian climates [3].

The transmittance of tubular daylighting systems have been studied by several authors. An early theoretical model was provided by Zastrow and Wittwer [4], which was refined by Swift and Smith [5] who also complemented the theoretical analyses with spectrophotometric measurements. Ray tracing simulations have also been employed [6, 7] for system evaluations and the collected knowledge regarding the systems were summarized in a CIE technical report published in 2006 [8].

The purpose of this paper is to validate a spectral ray tracing model using spectrophotometric measurements of three scaled tubular daylighting systems. Once the simulation procedure has

been validated the intention is to use the bi-directional scattering distribution data (BSDF) for performance evaluation of tubular daylighting systems in Swedish climates.

METHOD

Properties of tubular system

The measured and simulated tubes had length to diameter aspect ratios of 5, 7, and 9, and were lined with a thin highly reflective foil developed by 3M. The reflective material was laminated onto the diffuse side of an aluminum foil before positioned in a rigid plastic tube. The spectral reflectance of a plane surface of the reflective foil is presented in figure 1 as a function of incident angle. In the visible part of the spectrum the reflectance of the foil is between 96-99% and the variation for different incident angles is low. The reflective properties of the film are obtained by thin film interference and at longer wavelengths the reflectance drops abruptly as a function of incident angle.

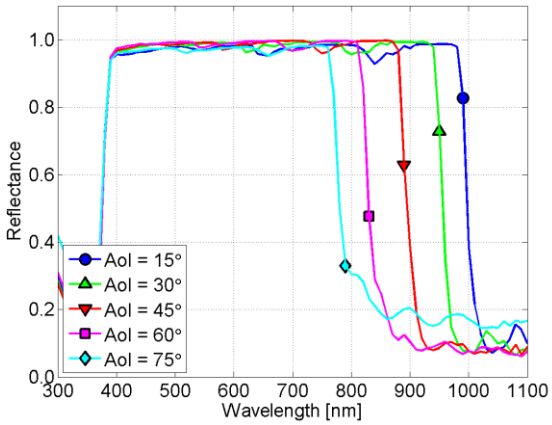

Figure 1: Reflectance spectra flexible foil as a function of incident angle. The angle dependent reflectance is used as input in the ray tracing simulations

Spectrophotometric measurements

The three scaled tubular daylighting systems were evaluated using a single beam spectrophotometer developed at Uppsala University [9]. The spectrophotometer is equipped with an integrating sphere detector and can be used for angle dependent measurements. For the characterization, the port of the integrating sphere was modified to the same size as the aperture of the tubular daylighting system. The instrument was set-up for characterization of the tubular system using both direct and diffuse illumination, as illustrated schematically in figure 2.

For the measurements with direct incident light, a thin light diffusing film was positioned across the sphere port to reduce errors due to nonuniform sphere response [10]. The spectral measurements were carried out in 10-degree steps for incident angles between 0 and 70 degrees. Different incident angles were obtained by rotating the tube and detector combination with the entrance port of the tube at the center of rotation. For the reference scans the tubular system was removed and the port of the integrating sphere positioned at the center of rotation. By moving the integrating sphere into the same center of rotation as for the system measurements the size and intensity distribution of the light spot is maintained between measurement and reference scan.

For characterization of the system with diffuse illumination an additional integrating sphere was attached to the entrance port of the tubular daylighting system. The incident light is scattered in the first integrating sphere, creating a diffuse light source with a nearly hemispherical distribution. Due to the intensity loss when two integrating spheres are connected in series the tubular system was only evaluated for white light for which higher intensities can be obtained.

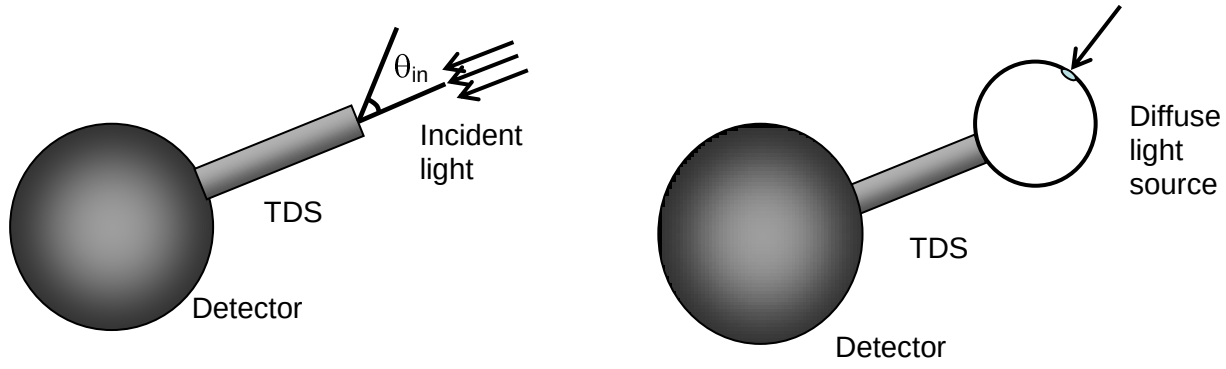

a) Direct illumination *b) Diffuse illumination*

Figure 2: Schematic illustration of the instrumental set-up for characterization of the tubular daylighting system (TDS). In a) for direct illumination and in b) for diffuse illumination.

Ray tracing simulations

The simulations were carried out using TracePro, a commercial ray tracing software developed by Lambda Research [11]. In the program a virtual sphere consisting of a source and a detector hemisphere iss constructed. Each hemisphere is divided into 145 patches according to Klems' coordinate system [12] and each patch functions as a detector or a light source. During the simulations the tubular daylighting system is positioned in the center of the sphere and rays are traced from each individual patch. The result of the simulation is a BSDF containing 145×145 values, one for each pair of incident and exiting direction.

Five tubular daylighting systems with different aspect ratios where simulated using TracePro. To be able to compare the simulations with the spectrophotometric measurements only the reflective duct of the tubular system was evaluated. The angle dependent spectral reflectance of the reflective foil (see figure 1) and the geometry of the tubular system were provided as input to the simulations.

RESULTS

Transmittance of direct light

Figure 3, shows the measured and simulated transmittance of direct light through a tubular daylighting system. The evaluated tubular system has an aspect ratio of 7 and the transmittance is presented for the incident angles of 10, 40, and 70 degrees. Overall, the simulated transmittance values correspond well to the measured transmittance of the system. The ray tracing simulations were carried out for 13 different wavelengths and were for the most part able to reproduce wavelength dependent properties caused by small absorption bands in the reflective foil.

The discrepancy between measured and simulated transmittance increases at wavelengths beyond the high reflectance cut-off. This is especially pronounced at low incident angles and is most likely caused by a measurement error that could be associated to the nonuniform light intensity across the light beam.

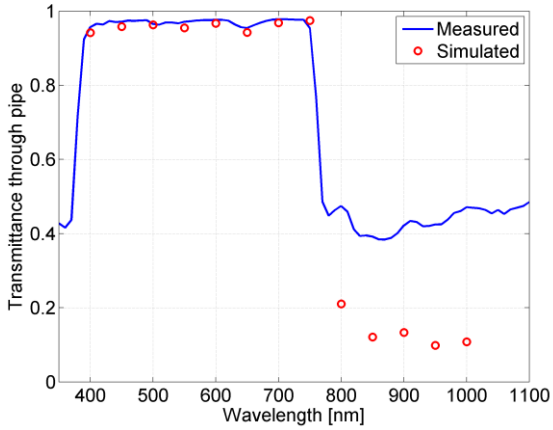

a) *Angle of incidence: 10°*

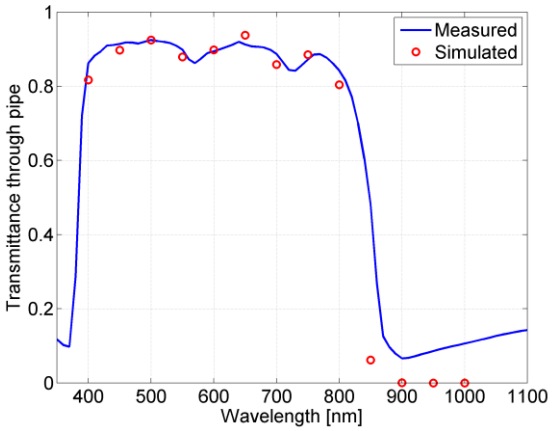

b) Angle of incidence: 40°

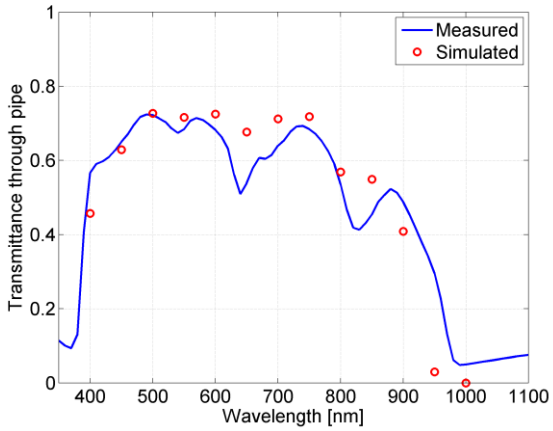

c) Angle of incidence: 70°

Figure 3: Comparison of the measured and ray traced transmittance of direct light through the tubular daylighting system. The aspect ratio (length/diameter) of the measured pipe is 7 and the results are presented for three angles of incidence a) 10°, b) 40°, and c) 70°.

The spectral transmittance of two tubular systems with length to diameter aspect ratios of 5 and 9 were also determined. Rather than presenting spectral data for these measurements the visible transmittance was calculated and in figure 4 compared to the ray tracing simulations. It can be noted that the measured and the simulated transmittance values correspond well, but that the discrepancy increases slightly for larger incident angles.

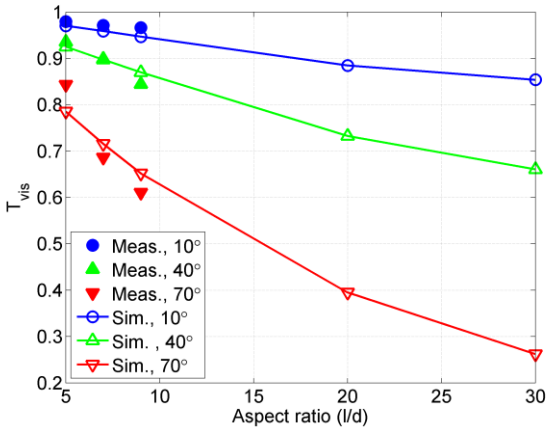

Figure 4. Visible transmittance for light with an incident angle of 10, 40, and 70 degrees. of tubular daylighting system as a function of aspect ratio.

Transmittance of diffuse light

The transmittance of diffuse light through the tubular daylighting system is presented in figure 5. The measurements were carried out using two integrating spheres connected in series. It can be noted that the transmittance is significantly lower for diffuse compared to direct illumination. However, it should be noted that losses around the port edge are more significant than for a system evaluated with direct incident light.

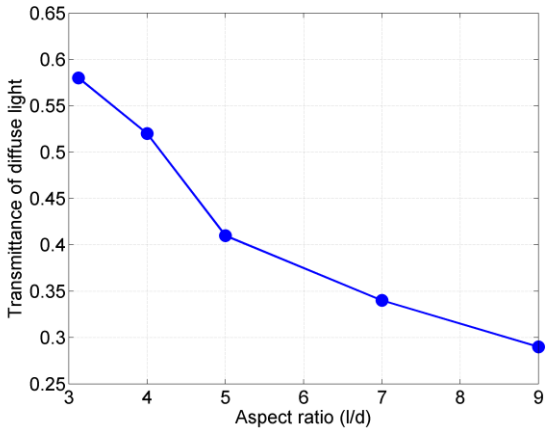

Figure 5. Transmittance of diffuse light as a function of the aspect ratio of the tubular daylighting system.

DISCUSSION

In this paper the transmittance of direct and diffuse light through a tubular daylighting system is determined using spectrophotometric measurements. The experimentally determined transmittance was used to validate the spectral and angle dependent properties of a ray tracing model. The advantages of ray tracing are that more complex systems can be evaluated and the scattering distribution for the system obtained. The intention is to use ray tracing to evaluate daylighting systems for a Swedish climate, which is characterized by low solar altitudes and mixed sky conditions. The BSDF obtained from the ray tracing simulations can also be used to evaluate the visual aspects of daylighting systems.

ACKNOWLEDGEMENTS

The authors would like to acknowledge Lambda Research Corporation for providing an educational license of TracePro, Jacob Jonsson for fruitful discussions, and LDT AB for providing material samples.

REFERENCES

1. Publication by the Swedish Energy Agency: Energiläget 2008 (in Swdish), 2008
2. Publication by the Swedish Energy Agency: Förbättrad energistatistik för lokaler – Stegvis STIL, Rapport för år 1 (in Swdish). 2007.
3. Sweitzer, G.: Three advanced daylighting technologies for offices. Energy, Vol. 19, No. 2, pp. 107-114, 1993
4. Zastrow A. and Wittwer V., Daylighting with mirror light pipes and with fluorescent planar concentrators. Proc. SPIE. Vol. 692, pp 227-234, 1986
5. Swift P.D. and Smith G.B. Cylindrical mirror light pipes. Solar Energy Materials and Solar Cells, Vol. 36, pp. 159-168, 1995
6. Dutton S. and Shao L. Raytracing simulation for predicting light pipe transmittance. International Journal of Low Carbon Technologies, 2/4, pp 339-358
7. Chirarattananon S. et al. Simulation of Transmission of Daylight through Cylindrical Light Pipes, Journal of Sustainable Energy & Environment, Vol. 1, pp. 97-103, 2010
8. CIE, Tubular Daylight Guidance Systems, CIE-173:2006, 2006
9. Nostell, P., Roos A., and Rönnow D.: Single-beam integrating sphere spectrophotometer for reflectance and transmittance measurements versus angle of incidence in the solar wavelength range of diffuse and specular samples. Review of Scientific Instruments, Vol 70, no 5, 1999.
10. Nilsson A.M et al. Method for more accurate transmittance measurements of low-angle scattering samples using an integrating sphere with an entry port beam diffuser. Appl. Opt. 50, 999-1006, 2011.
11. Lambda Research Corporation, http://www.lambdares.com, 2011
12. Klems J.H. A new method for predicting the solar heat gain of complex fenestration systems. I. Overview and derivation of the matrix layer calculation, ASHRAE Transactions V. 100, 1994

ASSESSMENT OF IRANIAN TRADITIONAL DOOR-WINDOWS, A PROPOSAL TO IMPROVE DAYLIGHTING SYSTEM IN CLASSROOMS

M. Tahbaz (PhD in Architecture)[1]; Sh. Djalilian (MArch.)[2]; F. Mousavi (MArch.)[1]

1: Assistant Professor, School of Architecture and Urban Planning, Shahid Beheshti University, Evin, 19834, Tehran, Iran 1

2: Master of Architecture, School of Architecture and Urban Planning, Shahid Beheshti University, Evin, 19834, Tehran, Iran 2

ABSTRACT

Door-window is one of the prevalent types of windows in Iranian traditional architecture. Among 20 different kinds of windows in 6 main lighting systems in Iranian architecture, it seems that door-window has a good potential to be used in classrooms. Ameriha Houses Complex in historical city of Kashan with 7 yards, is a good case study for examine this idea. Traditional houses in Kashan have their own regulations that are a sample of climatic design in hot-dry climate. Door-window rooms of these houses are placed in a context with some specific climatic solutions such as central yards with vegetation which modifies the microclimate, winter and summer places with appropriate solar income in different seasons, underground and pavilion spaces with pounds for controlling the temperature swing and humidity balance [4]. This article introduces the results of a field study research that has been done for 6 types of different rooms with door-windows in Ameriha house according to the illumination level and uniformity of its distribution in the room. Light level is divided to 5 groups according to the standards of lighting requirements in classroom. Door-windows have a specific detail for door design to control the heat exchange and daylight income through the glasses. Determining the role of these details on the success of door-window to improve the thermal condition and illumination demand in the room, is done by monitoring the climatic data using data logger and lux-meter in two days of observation in April 2011. Data of illumination, temperature, humidity and wind speed is gathered in the selected rooms, main yard and the roof of the building. Comparing indoor and outdoor temperature and light condition will show the positive or negative effect of door-windows. Isometric lines of illumination were drawn to show the distribution of light in the rooms. Analyzing these results and determining the efficiency of the daylight condition in these rooms for a classroom will show the ability of renewing door-windows for school design.

Keywords: daylighting system, door-window, glare, sun-patch, data logger, lux-meter,

INTRODUCTION

A glance at Iranian traditional architecture, with around six thousand years of history, shows the richness of this architecture in many aspects of design including the way it provides natural light for the building. 6 main types including 20 different kinds of windows are distinguished in a study research of Iranian traditional architecture [1]. Each type has its own discipline and modules and is used for a specific situation in the building. One of these types is a special wall window called "door-window". This kind of window has been used in the houses for living rooms (side rooms) and the main rooms that are placed in the main axis of the house, with the best view for a luxury usage. According to the size and shape of the room, door-windows are divided to three, five or seven modules. Door-windows have specific shape, size and dimension according to their related room.

The hypothesis of this article is that the lighting condition of door-window is one of the appropriate solutions that can be used in classrooms according to the light standards for educational spaces [2]. To examine this idea, door-windows and their related rooms are monitored in a complex traditional house in Kshan according to different aspects such as illumination distribution and glare problem. Other needs in the classroom such as thermal comfort, social or economic needs will be considered as the complementary studies. Determining the dimension, size and shape of the room related to its orientation and the number of door-windows will give a criterion for classroom's design.

FIELD STUDY RESEARCH

The monitoring has taken place in a traditional building complex in Kashan city called Ameriha House. Kashan is placed in the north part of Isfahan province in the edge of the central desert of Iran. It has hot and dry desert climate with very hot and dry summer and cold winter. Table 1 shows the average climatic information of this city for the period of 1966-2005 [5].

Comparing the gathered data in the field study research with the long term climatic data of meteorological station of Kashan [6] will show the condition of the chosen days in comparison with normal climatic condition. Climatic calendar of Kashan shows that there is a harsh condition in summer noon when the temperature goes over 35°C. In winter there is chill wind phenomenon when the temperature goes under 7°C (Fig 1 left). Most of the time in the year wind is in calm condition but in spring's noon and afternoon, fast winds may happen (Table 1 right). In the days of observation that was 25 and 26 of April 2011 weather was in moderate condition but stormy winds with some rain happened. It caused a lack of data for the information gathered of the roof illumination.

STATION KASHAN (40785) I.R OF IRAN METEOROLOGICAL ORGANIZATION (IRIMO)
LATITUDE 33 59 N
LONGITUDE 51 27 E DATA PROCESSING CENTER
ELEVATION 982.3 M
CLIMATOLOGICAL NORMALS FOR THE PERIOD 1966-2005

	JAN.	FEB.	MAR.	APR.	MAY	JUNE	JULY	AUG.	SEP.	OCT.	NOV.	DEC.	ANNUAL
AIR TEMPERATURE (C)	5	7.7	13.2	20	25.4	31.4	34	32.6	27.8	20.6	12.8	7	19.8
MINIMUN AIR TEMPERATURE (C)	-0.3	1.5	6.3	12.1	16.9	21.9	24.8	23.3	18.4	12.5	6.2	1.5	12.1
MAXIMUM AIR TEMPERATURE (C)	10.2	13.4	19	26.3	31.8	38.2	40.8	39.9	35.3	27.6	18.9	12.1	26.1
TEMPERATURE RECORDS LOWEST(C)	-12.5	-10	-5	-1	5.4	12	17	17	10	2	-3	-12	-12.5
TEMPERATURE RECORDS HIGHEST(C	22	27	32	36.4	42	48	48	47	43	39	31	24.5	48
RELATIVE HUMIDITY (MEAN% 03UT C)	76	71	64	57	51	39	35	36	40	52	66	75	55
RELATIVE HUMIDITY (MEAN% 09UT C)	52	44	37	30	27	20	19	20	21	28	39	49	32
AMOUNT OF PRECIPITATION MM.	26.3	19.6	26.1	17.5	13.3	1	0.5	0.5	0.2	4.3	12.2	16.9	138.4
DAYS WITH SKY CLEAR (0-2)/8	15.4	14.3	13.8	12.1	18.1	27.3	27.8	29.2	28.6	24.2	17.4	15.3	243.5
DAYS WITH P.CLOUDY (3-6)/8	9.3	8.9	10.9	13	10.1	2.5	3.1	1.7	1.1	5.6	9	9.3	84.5
DAYS WITH CLOUDY (7-8)/8	6.3	5.1	6.2	4.9	2.6	0.2	0.1	0.1	0	1.2	3.6	6.2	36.5

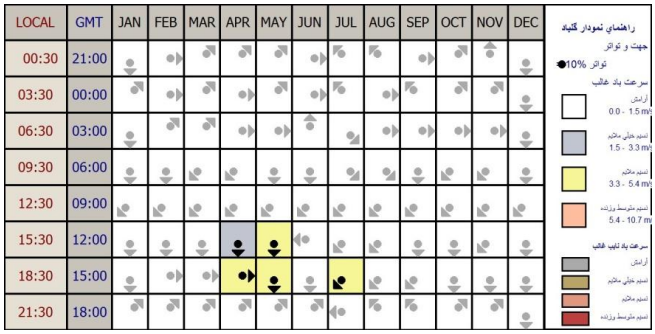

Table 1:above: climatic data of Kashan [5], *below: wind calendar of Kashan* [6]

Sky condition is sunny in 2/3 time of the year. In summer sunny sky has the most portions (over 80%) but in winter and spring it has the lowest portions (1/3). In the days of observation (25 and 26 April) cloudy and partly cloudy sky has the most portions (60%). Therefore overheating and glare problems are not in the worst condition for the interior spaces in the days of observation. (Fig 1 middle and right)

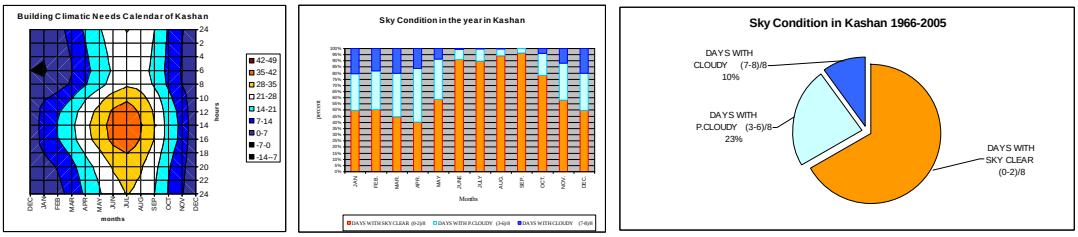

Figure 1: left: climatic needs calendar, middle and right: Sky condition in Kashan [6]

DATA GATHERING AND OBSERVATION

Ameriha house is placed in the traditional part of Kashan city. It has 7 big and small yards as a complex house [3] (Fig 2 left). To do the observation, data loggers where settled in different parts of the house. One Lux-meter and personal weather station were placed in the roof to collect the local climate data. One personal weather station was placed in the main yard to collect the data of microclimate in the yard. In the chosen rooms, data was gathered in a mesh of 60 cm and height level of 60 cm (Fig 2 right). Illuminations, temperature, relative humidity and wind speed are the gathered data in all places.

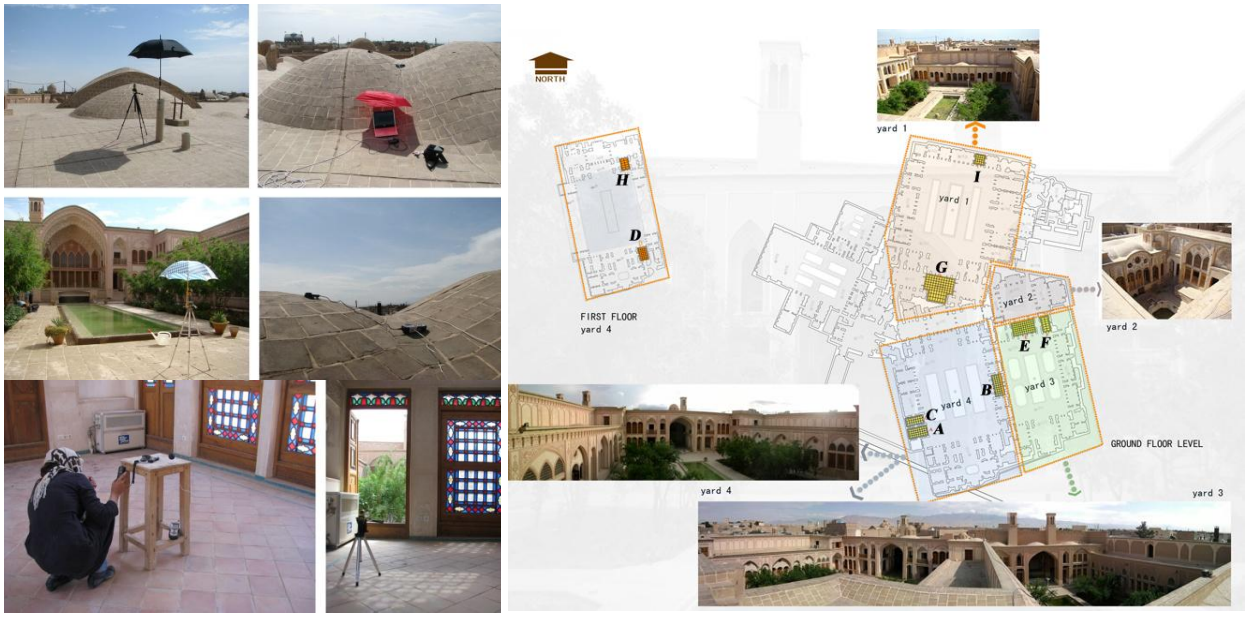

Figure 2: ameriha house (right) and data gathering in roof, yard and room (left)

ILLUMINATION ANALYSIS

In Ameriha house there are several rooms with door-windows. To clarify the effect of architectural design and details of rooms and windows on the level of illumination, distribution of light and darkness or glare problem, 9 rooms were selected in different yards. The rooms are located in different orientations and stories with different size and dimension of the room, height and shape of the ceiling, number of door-windows, shape and detail of the frame and glasses used in the door-windows. The data was gathered in 25th and 26th April 2011 form morning to the evening. According to the changeable condition of sky from overcast to partly cloudy and clear in the period of observation, the data of illumination on the roof is used as a reference for comparison. Figure 3 shows the illumination level in the roof and table 2 shows the information and analysis of the data gathered in 6 rooms among observation rooms according to illumination and distribution of light. To help the analysis of the illumination in the rooms, the legend of iso-lux diagrams in the plan and the section of the rooms are divided to some meaningful zones according to different illumination levels in classrooms [2, 7].

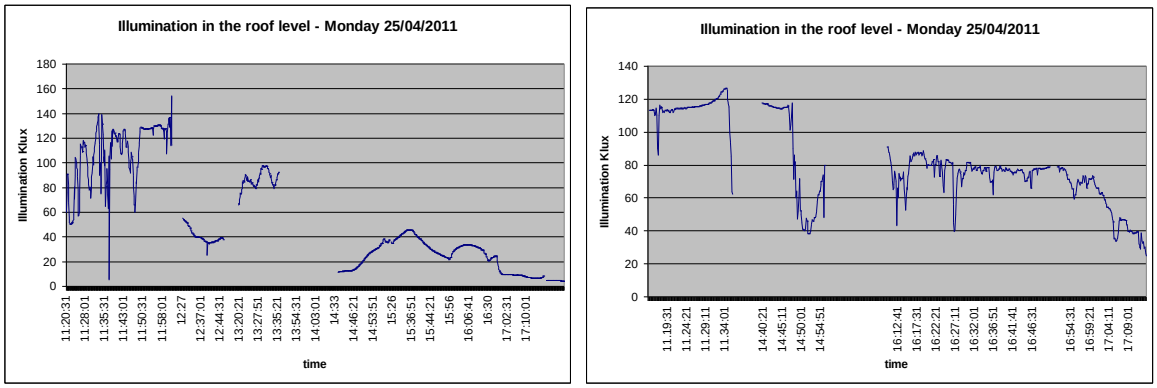

Figure 3: Illumination in the roof of Ameriha house Kashan in days of observation

Illumination legend (lux)	
0-100 very low 100-300 low acceptable 300-500 standard 500-900 slightly high acceptable 900-2100 medium high acceptable 2100-2500 high acceptable More than 2500 glare problem	0-100 100-200 200-300 300-400 400-500 500-600 600-700 700-800 800-900 900-1000 1000-1100 1100-1200 1200-1300 1300-1400 1400-1500 1500-1600 1600-1700 1700-1800 1800-1900 1900-2000 2000-2100 2100-2200 2200-2300 2300-2400 2400-2500 2500-2600 2600-2700 2700-2800 2800-2900 2900-3000 3000-3100

Room A 25/04/2011
Fixed Windows
at 11:20 to 12
Roof: 80-120 Klux

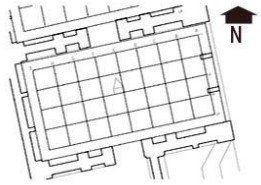

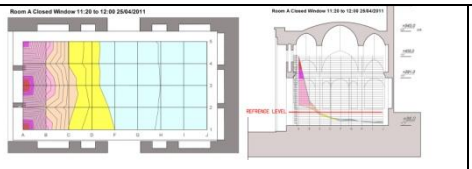

T = 27°C, RH=30%

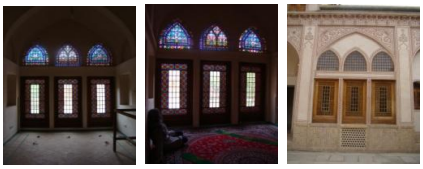

Fixed Windows
afternoon 13:50 to 14:00
Roof: 80 Klux ??

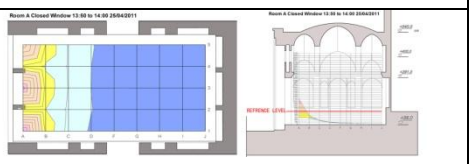

T = 24.7°C, RH=35%

Before noon and in partly cloudy and clear sky condition, all parts of the room have acceptable illumination except near the window that has glare in some small parts. In the afternoon only 1/3 part of the room has acceptable illumination. The long depth of the room is not appropriate for a good distribution of illumination.

Room B 25/04/2011
Close Windows 12:30 to 12:45
Roof: 35-50 Klux

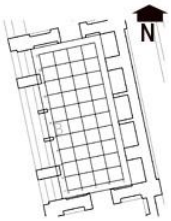

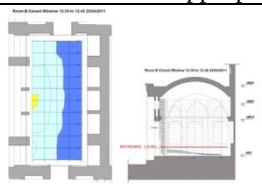

T = 25.7°C, RH=30%

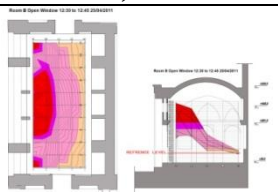

T = 23.6°C, RH=37.5%

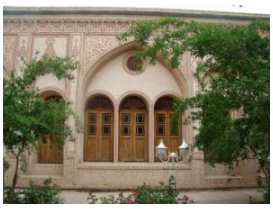

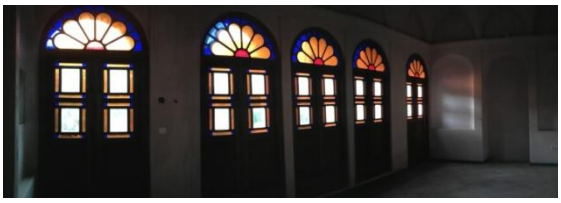

In the partly cloudy sky condition with close windows, 1/3 of the end part of the room has not acceptable illumination. In sunny sky with open windows, 2/3 parts of the room has enough illumination. 1/3 part of the room near the window (in sun patch condition) glare is happening. The short depth of the room is appropriate for a good distribution of illumination. By controlling the sun-patch, this room will have a good condition of illumination.

Room E 26/04/2011
Closed Window
12:15 to 12:35
Roof: 60 Klux ??

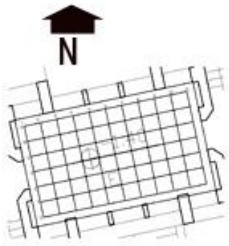

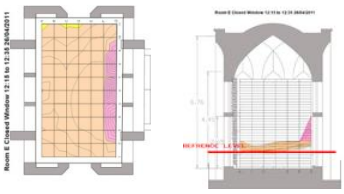

T = 24°C, RH=38%

In partly cloudy sky condition by close windows, the illumination in all parts of the room is very good. In clear sky by sun patch in the room, glare will happen near south windows. The dimensions of the room related to the two side windows, prepared the best distribution of illumination. Sun patch needs to be shaded in clear sky condition.

Room F
26/04/2011
Close Window
14:40 to 14:55
Roof: 60-110 Klux

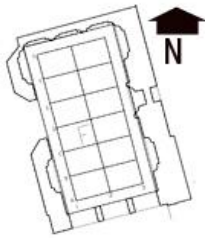

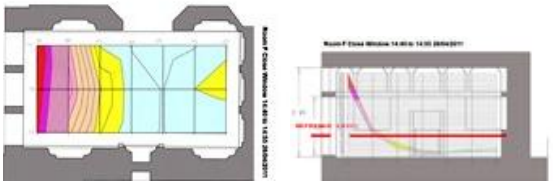

T = 24°C, RH=39%

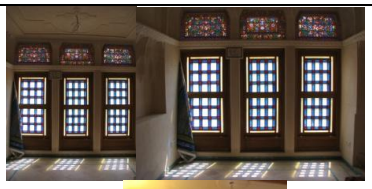

This south/east oriented room has a good illumination in all parts of the room even with close and fixed windows. Near the window because of sun-patch, there may be glare problem. The special windows frame has been a good solution to decrease the glare problem in the room. This room is a winter living room with low height ceiling.

Room G 26/04/2011
Close Window
16:10 to 16:50
Roof: 75-85 Klux

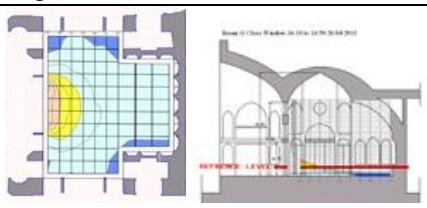

T = 22°C, RH=40%

This north oriented room with tall ceiling and several windows in three walls, has enough light with a very good distribution of illumination in the all parts of it. The luxury mirrors fixed in the ceiling and upper part of the walls, have increased the reflection of light and prepared more illumination in the end part of the room. Several doors in three walls of the room prepare a better uniformity of illumination and give it a good potential for natural ventilation. The semi open trace as a complementary space, make it a desirable place for rest in summer hot days.

Room I 26/04/2011
Close Window
16:50 to 17:10
Roof: 40-80 Klux

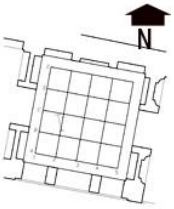

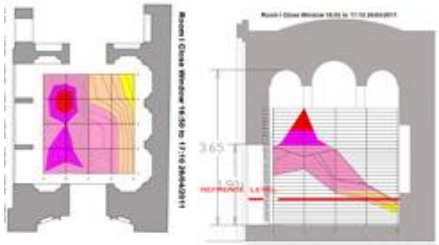

T = 23.5°C, RH=38.5%

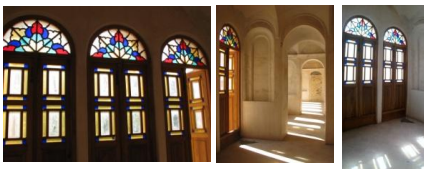

Small square shape room oriented toward south with three door-windows prepare a warm and illuminted space as a winter living room. It has glare in the evening with direct solar radiation that will increase the room's temperature. Small parts of glasing surfaces in the frame of door windows help to control the energy loose in cold periods. This room with close windows is not appropriate for Summer evenings, but it will become a semi open space with opening the door-windows.

Table 2: Different door-windows analysis according to classroom illumination requirement

CONCLUSION

This article presented a part of the research has been done in Ameriha house in Kashan. It shows the results of a field study that has been done in two days of April 2011 in some door-window rooms. The illumination, temperature, humidity and wind speed data were gathered in the roof and inside the rooms and the iso-lux diagrams were shown in plan and section of the rooms. Illumination data on the roof is used as a reference for comparison the results. According to the classroom illumination requirement the results can be concluded as follow: 1- The orientation of the room and the dept of the room according to the window position is one of the main factors to create uniform distribution of light in the room. Rooms toward north with less dept and more door-windows have the best potential for uniform distribution of light (room E). Rooms with long depth have the least potential (room A and F) 2- For the rooms toward south, east and west, direct sunshine and sun-patch is the cause of glare. Using appropriate shades or overhangs outside the room is one of the solutions for this problem. Using small colour glazing surfaces in window frame as a lattice is another solution. Otherwise these rooms (room A, F and I) are not appropriate for classroom but may be good for other activities with less sensitivity to glare. 3. Using lattice with colour glasses in door-windows in small size rooms will create more privacy and relaxation. These rooms are appropriate for private activities such as sleep, pray or private living (room F and I). 4- Using extra holes or windows in other walls or over the main door-window will help to get more reflected light from adjacent places. This strategy helps to modify the uniformity of inside light. Natural ventilation will modify as well (room D, E, G). 5- Large rooms with tall ceiling and more door-windows (or sash windows) have potential to get more illumination. To uniform the distribution of illumination, using extra windows in other walls or over the door-window is a kind of solution (room E). Using reflected surfaces such as mirror on the walls or ceiling is another solution (room G). To control the sun-patch in this condition, using external shades for rooms toward south, west or east is necessary. For rooms toward north there is not any glare problem (room G)

Other factors such as temperature, humidity and wind speed where gathered in this field study but are not analyzed here because of the moderate climatic condition in April. another observation in hot summer with more sunshine hours is needed.

ACKNOWLEDGMENT:

The authors like to give their appreciate to all kind responsible people of Ameriha House and Art Kashan University who prepared the condition of doing the field study in this historical building. Also we need to thank to Shahid Beheshti University as the sponsor of this research.

REFERENCES:

1- Tahbaz, Mansoureh and Fatemeh Moosavi, Daylighting Methods in Iranian Traditional Architecture (Green Lighting), CISBAT 2009, International Conference, EPFL Lausanne, Switzerland, 2-3 SEP 2009.
2- IEA**,** Task 21, **Daylight in Buildings,** International Energy Agency, July 2000.
3- Kashan Houses, Ganjnameh series, Documentation and Research Department, School of Architecture and Urban Planning, Shahid Beheshti University, Tehran, 1990.
4- Thabaz, Mansoureh and Shahrbanoo Djalilian, Principles of Climatic Design in Iran, Shahid Beheshti University, Tehran, 2009.
5- Institute of Meteorology of Iran, www.irimo.ir
6- Tahbaz, mansoureh, Analysis of Meteorological Data of Kashan in the Period of 1966-2005 by excel software, Tehran, 2011.
7- Moore, Fuller, Concepts and Practice of Architectural Daylighting Van Nostrand Reinhold, New York, 1991.

DIGITAL CAMERA FOR CONTINUOUS LUMINANCE MAPPING FOR DAYLIGHTING PERFORMANCE ASSESSMENT

A.Thanachareonkit; L.L. Fernandes[1] ; K. Papamichael.

California Lighting Technology Center (CLTC), University of California, Davis

ABSTRACT

Luminance maps for different view positions and directions within a luminous environment are most effective in evaluating luminous comfort, as they represent what the eye really sees. They also allow the determination of luminance ratios within the field of view, which can be used to determine potential for glare. Luminance distributions are either computed using lighting simulation software, or determined in real environments using High Dynamic Range (HDR) photography, an approach that has been long used by researchers and is now increasingly used in lighting practice.

Determination of luminance distributions using HDR photography requires use of a digital camera to capture the same view using a wide range of light exposures, from completely overexposed to completely underexposed, and software that can combine the multiple light exposure images into a luminance map.

Glare due to high luminance ratios is a common problem in window and skylight applications in buildings, when the exterior luminance values are significantly higher than interior luminance values. As daylight varies continuously through the day, effective daylight performance evaluation involves the acquisition of multiple luminance distributions for different times of the day and the year, which requires significant effort if the images are captured manually.

This paper presents an automatic approach for HDR time-lapse photography and the validation of the measured results using high accuracy calibrated luminance meters. The approach is based on the use of a Canon point-and -shoot digital camera with a Canon Hack Development Kit (CHDK), which allows use of UBASIC scripts that automatically set exposure to prescribed values and take photographs at prescribed time intervals. The photographs are automatically transferred to a remote computer using a wireless memory card. The photographs were combined into luminance distributions using the Photosphere software, which is available for free at www.anyhere.com.

Skylights are widely used in single story commercial and industrial buildings to save energy through the use of electric lighting controls. A common negative effect of this strategy is the increased brightness of the skylights after all electric lights are off or at minimum, especially during the middle of the day, when daylight reaches peak levels. Daylight luminance distributions can be used to evaluate skylight glare through time and to determine the effectiveness of automated light transmission modulation systems in reducing glare.

[1] L.L. Fernandes is currently with Lawrence Berkeley National Laboratory

Several tests were performed at the California Lighting Technology Center at the University of California, Davis, that involved HDR time-lapse photography during daylight hours. The accuracy of the approach was validated against simultaneous individual point luminance measurements using a Minolta LS-110 luminance meter. The results showed acceptable correlation between HDR luminance values and Minolta measurements.

INTRODUCTION

Daylight is a vital source of lighting in buildings. Windows, clerestories, and skylights are the most common daylight apertures in building walls and roofs. However, one of the most common problems in window and skylight applications is glare due to high luminance ratios between bright glazing and relatively dark interior wall and ceiling surfaces.

In an ongoing study aiming at reducing this contrast and associated glare and to improve the lighting quality, a number of advanced window and skylight systems are being developed to modulate the transmittance of the daylight aperture and possibly redirect some of the incoming daylight to illuminate walls and ceiling surfaces. The evaluation of the effectiveness of alternative systems is performed through measurement of luminance distributions (a.k.a. luminance maps) under real daylight conditions.

System	Tool	No. of exposure	Image	Luminance mapping
LDR	1. Digital camera	Single exposure 	One LDR image 	None
HDR	1. Digital camera 2. Tripod 3. Computer and HDR generator software	Multiple exposures 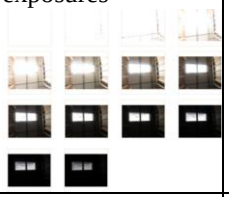	One HDR image  1	Single luminance mapping
Time lapse HDR	1. Canon digital point and shoot camera 2. Tripod 3. Computer and HDR generator software 4. CHDK software	Multiple exposures at interval 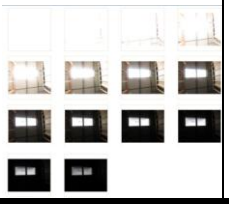	Multiple HDR images 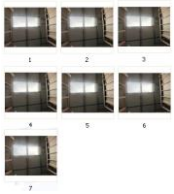	Continuous luminance mappings

Table 1: Low Dynamic Range (LDR), High Dynamic Range (HDR), and time lapse HDR photography for determining luminance distributions.

Luminance maps from viewpoints of interest are some of the most effective ways to assess visual comfort and glare potential. Using conventional luminance meters to determine luminance distributions is very expensive and impractical, and as a result, the use of luminance maps for evaluation of luminous comfort has been very limited. Digital photography has made it possible to determine luminous distributions using High Dynamic

Range (HDR) photography along with specialized software. HDR photography requires capturing a series of photographs of a luminous scene from the same viewpoint, varying the exposure for fully under-exposed to fully over-exposed images, which then are processed by specialized software to produce luminance maps [1].

Glare due to high luminance ratios is a common problem in window and skylight applications in buildings, when the exterior luminance values are significantly higher than interior luminance values. As daylight varies continuously through the day, effective daylight performance evaluation requires multiple luminance distributions for different times of the day and the year, which requires significant effort if the images are captured manually. Automation of HDR luminance mapping and time-lapse photography has also been very expensive, requiring sophisticated equipment and effort, such as a high-end single-lens-reflex digital camera and a computer program that controls the camera and stores the data [2]. As HDR imaging is becoming increasingly popular, several high-end digital cameras are now supporting it, mainly for enhanced photography, rather than determination of luminance maps. Canon has also introduced models that support easy automation of HDR time-lapse photography (Table 1).

This paper is focused on the measurement methodology and validation that has been developed for the study of skylight glare and the development of automated systems that modulate skylight transmittance to minimize potential for glare.

DETERMINATION OF LUMINANCE MAPS

System and Setting

The system used to automate the determination of luminance maps over time included the following:

- Canon point-and-shoot digital camera (Ixus or PowerShot series)
- Memory card and card reader
- Tripod (for most uses)
- Canon Hack Development Kit (CHDK) software and script for automated time-lapse photography
- Photosphere software

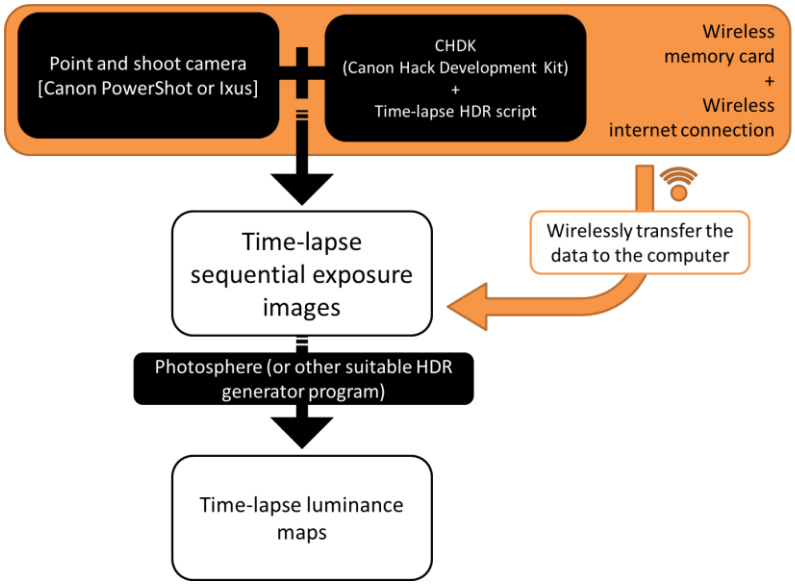

Figure 1: The process of determining luminance maps over time.

```
@Time-lapse HDR
set_av 18
for n=1 to 6
gosub "hdrseries"
for i=1 to 5
sleep 60000
press "shoot_half"
release "shoot_half"
next i
next n
end
:hdrseries
set_tv -9
shoot
set_tv -6
shoot

[...]

set_tv 27
shoot
set_tv 30
shoot
return
```

Figure 2: UBASIC script for time-lapse HDR image acquisition. Ellipsis in square brackets denotes part of routine omitted for compactness.

The CHDK is installed on the camera's memory card. CHDK [3] is free software that allows many models of Canon Ixus or PowerShot series to perform several special functions that are not supported by the camera's built-in firmware. Such functions are specified using scripts in simple scripting languages, such as UBASIC and Lua [4]. A custom script was developed to automate HDR time-lapse photography, i.e., the capturing of multiple consecutive photographs of the same scene varying exposure at desired settings, and repeating the process at desired time intervals.

To set up the system, the camera is installed with the memory card that contains CHDK and time-lapse HDR script, normally mounted on a tripod, and pointed at the scene of interest. The script is activated through the camera's user interface and the system is left to acquire images for the desired period of time. A wireless memory card [5] with wireless Internet connection was used to overcome memory card limitations and the Canon AC adapter was used to overcome battery life limitations. The determination of the luminance maps was performed using the Photospere software [6, 7], which supports many standard HDR image formats and removes lens flare and ghost effects (Figure 1).

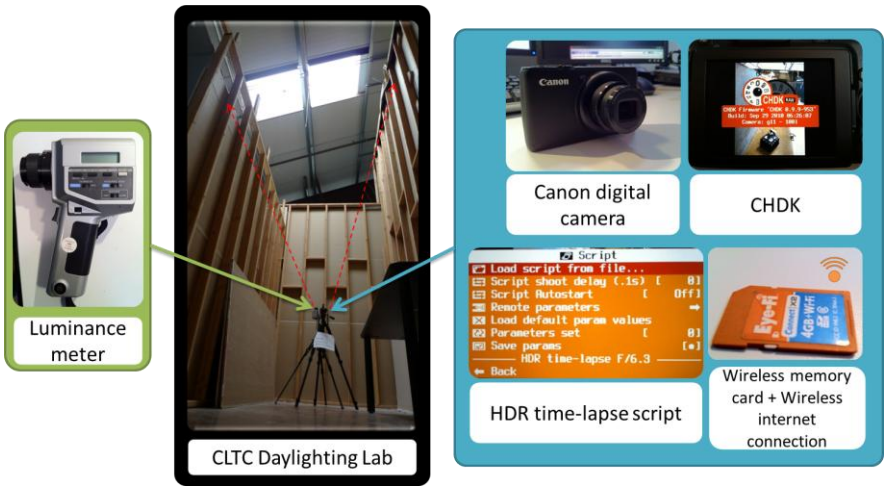

Figure 3: Time-lapse luminance mapping system.

System testing

In this study, a Canon PowerShot S90 and CHDK with a simple script (Figure 2) to activate the Time-lapse HDR imaging were used. The camera was initially calibrated with a reference light source, with luminance values from 600 to 22,000 cd/m^2, to ensure the reliability of the system. Later on, tests were conducted by monitoring the luminance of a skylight and ceiling at the California Lighting Technology Center's Daylighting Lab (Figure 3). A Minolta LS-110 luminance meter was used to validate the accuracy of the luminance maps' values. The images were processed using Photosphere into a series of time-lapse luminance maps.

RESULTS

To confirm the reliability of the results, the system calibration was done for different luminance values. Figure 4 provides the comparison of luminance measured using a luminance meter and luminance acquired from the HDR luminance mapping. Regression analysis confirmed the linearity of the HDR system's response, with R^2 higher than 0.99.

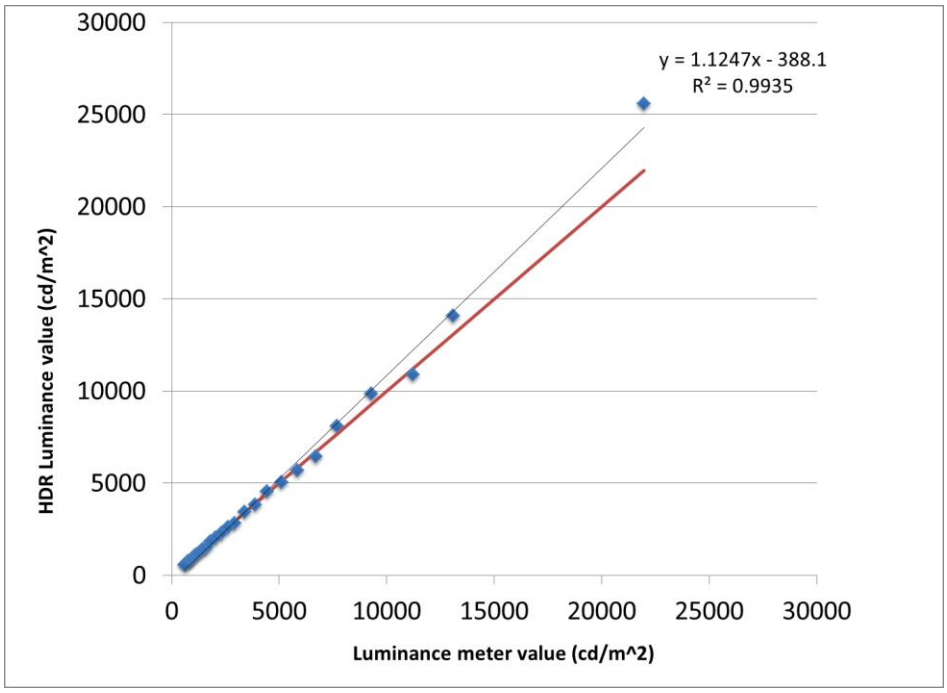

Figure 4: Comparison between luminance values acquired using HDR luminance mapping and the Minolta LS-110 luminance meter.

For the skylight testing, the comparisons of HDR luminance and the luminance measured using the luminance meter were done considering thirteen points of interest at the skylight glazing, frame, and ceiling. False color images were processed using Photosphere into a series of time-lapse luminance maps (Figure 5). These luminance values can be used for the prediction of glare potential. The same approach will be used to assess the effect of glare reduction using different automated transmittance modulation systems.

CONCLUSION

Digital photography combined with scripting for automated HDR time-lapse photography and use of free software for determination of luminance maps is a very effective way to determine luminance distributions for visual comfort evaluation. The luminance values acquired using

this technique are reasonably close to those gathered with a conventional spot luminance meter.

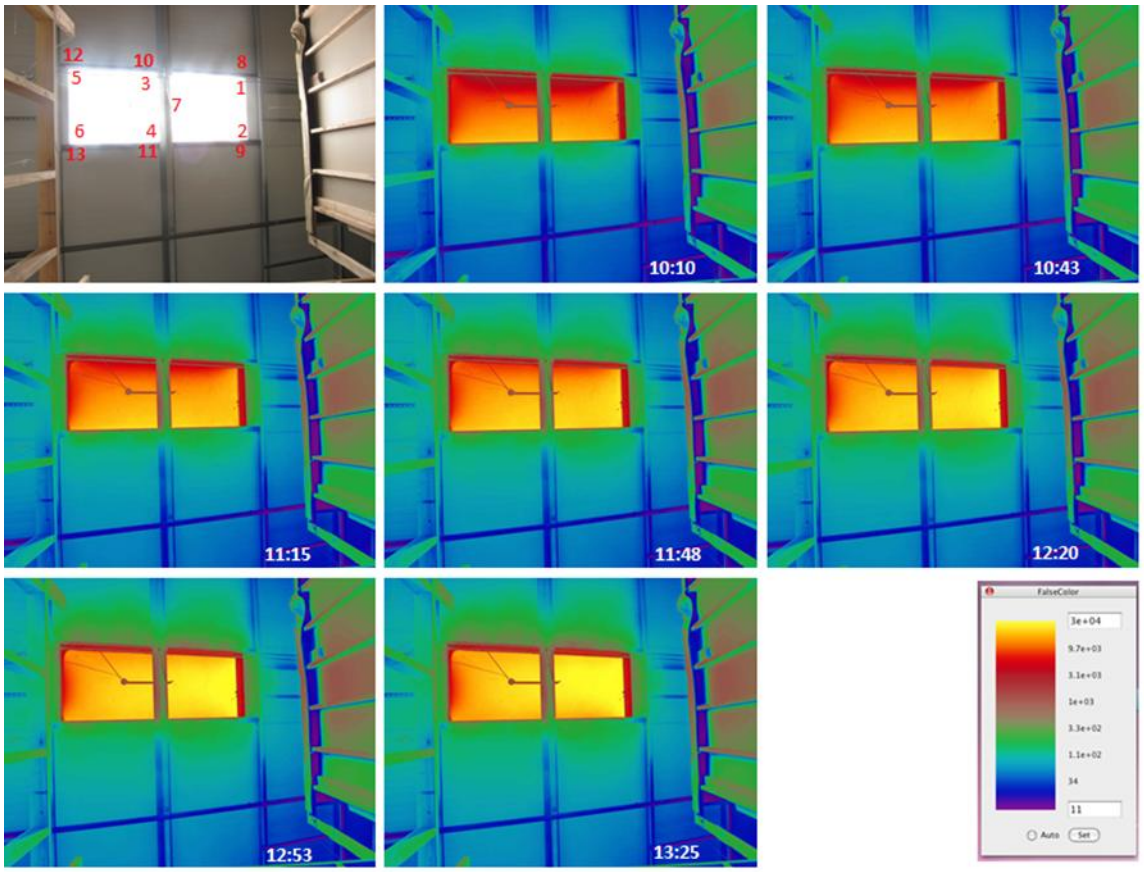

Figure 5: Time-lapse luminance maps. Luminance values in cd/m^2.

ACKNOWLEDGEMENTS

The work presented in this paper is supported by the Public Interest Energy Research (PIER) program of the California Energy Commission (CEC). The authors would like to thank Malvina Keller for her research assistance.

REFERENCES

1. Lee, E.S., Clear, R.D., Ward, G.J., Fernandes, L.L.: Commissioning and verification procedures for the automated roller shade system at the New York Times headquarters, New York, New York, Lawrence Berkeley National Laboratory, Berkeley, California, USA, 2007.
2. Reinhard, E., Ward, G., Pattanaik, S., Debevec, P.: High dynamic range imaging: acquisition, display and image-based lighting, Morgan Kaufmann, 2006.
3. Ward, G. : A Wide Field, High Dynamic Range, Stereographic Viewer, proc. Of PICS 20 (2) (2002), Portland, Oregon, USA, 2002.
4. Ward, G. Photosphere“.”Anyhere software. Web. 30 May 2011. <http://www.anyhere.com>
5. “CHDK.” Wikia. Wikia. Web. 16 Sep 2010. <http://chdk.wikia.com/wiki/CHDK>.
6. “Eye-Fi”. Eye-Fi. Web. 30 May 2011. <http://www.eye.fi>
7. DanielF. “uBASIC User Guide” CHDK Wikia. Web. 6 August 2010. <http://images2.wikia.nocookie.net/__cb20100806022158/chdk/images/e/e5/UBASIC_User_Guide_D0_5.pdf>.

SOLAR FIBRE OPTIC LIGHTS - DAYLIGHT TO OFFICE DESKS AND CORRIDORS

T T Volotinen[1]; N Nilsson[2]; D Johansson[2]; J Widen[1], Ph Kräuchi[3]

1: Solid State Physics, Dept. of Engineering Sciences, The Ångström Laboratory, Uppsala Univ., Box 534, 75121 Uppsala, Sweden

2: Parans Solar Lighting AB, Kämpegatan 4C, 41104 Göteborg, Sweden

3: Siemens Schweiz AG, Building Technologies Group, Inernational Headquarters, Gubelstrasse 22, I BT CPS GDT PR ICA, 6300 Zug, Switzerland

ABSTRACT

The illumination performance and light balancing behaviour of solar fibre optics light systems have been studied in office environment aiming to show that daylight through optical fibres can be used for illumination of indoor working environments supplement electric lights that are commonly used in daytime, resulting significant saving of electric energy. Even though the system studied here is an older version of this quickly advancing, very promising, illumination technology, the results show that solar fibre optic lights can be used to supplement successfully illumination for offices, corridors and other indoor environments to save energy. During direct sunlight in combination with daylight coming through the windows, the illuminance level exceeded 500 lux all over the office while the electric lights were switched off. In total 1000 – 3000 sunlight hours are available depending on the country and location. With solar fibre optic lights the energy consumption for lighting (now 10 - 12 W/m^2) can potentially be decreased down to 0.2 - 0.4 W/m^2 for offices and to 0.02 W/m^2 for corridors during fully sunny weather. For a country like Sweden with ca. 31 km^2 of heated office spaces the savings potential is in the order of 380 GWh per year (50 % of energy for electric light), estimated as a consumption for 1100 sunny hours when electric lights could be switched off. At Siemens tests were performed using fibre optic solar lights in combination with electric lights controlled to constant illumination and in combination with automated blinds. The decrease of electric energy depended on the weather and test configuration. Further tests are in progress to define the saving caused by the fibre optic lights. The tests on sunlight transmission for two types of optical fibres show that the coupling efficiency and transmitted daylight intensity can be further improved for this quickly advancing technology.

INTRODUCTION

The solar fibre optic light systems (Figs. 1 - 3) are currently tested for lighting of offices in daytime by the European research project Clear-up (www.clear-up.eu). They are aimed to supplement the electric lights and also decrease the electric cooling at offices, corridors and other parts of large buildings, where electric lights are used during daytime. The project aims to determine the illumination performance, energy saving capacity and increase of human comfort of these systems. The suitability for light balancing, i.e. for replacing the light loss caused by solar heat and radiation controlling window structures (such as blinds and electro-chromic windows), is also studied. -- Here we report the first results, showing the illumination provided by the solar optical fibre luminaires and the energy saving obtained in the test office in Zug, Switzerland during spring 2011.

One light collecting panel of a solar fibre optic light system (Figs. 1 - 3) can couple sunlight (which intensity is typically 110 000 lumens/m^2) into optical fibres altogether 2000 - 10000 lumens depending on the system construction and optical fibres. Theoretically estimated intensity coupled into a fibre can be as high as 1200 lumens. The fibres in optical cables transmit (guide) the light from the roof panel of a building to the luminaires installed in an office or other spaces of a building (Fig. 1). The intensity of the output light is dependent on the coupling efficiency and on the attenuation and length of the fibre cables. The lenses of a solar panel that couple the sunlight into the fibres, or the entire panel, track the sun position and follow its direction, thus providing all the time the high intensity of direct sunlight into the fibres. (Figs.1-3) Electric energy consumption of a whole system is 2 W.

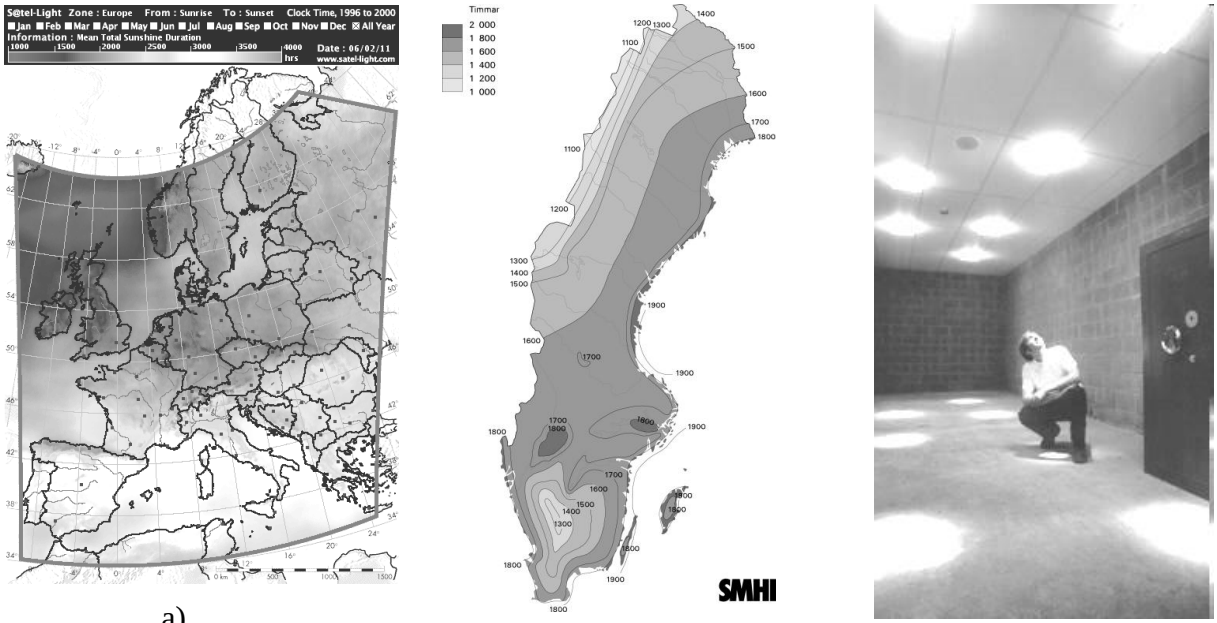

a) b) c)

Figure 1: a) Sunlight hours yearly in Europe [1] and b) in Sweden [2]. (The grey scales are opposite in these two maps.) c) A room illuminated by solar fibre optic luminaires.

Sunshine duration, which is the number of hours with direct solar radiation above a certain threshold, varies geographically and over time depending on the local climate and other insolation conditions such as horizon elevation. In Europe, sunshine duration varies from 1000 to 3000 hours per year between geographical regions [1] and there are large differences between sites within a country. For example, in Sweden, the sunshine duration is 1900 hours on the east coast and below 1100 hours only in the north-western mountainous areas [2].

The savings potential from an increased use of daylighting applications depends both on the number of available sunshine hours and on the current use of artificial lighting during these hours. It is hard to find any general statistics on the time variability of office lighting loads, but figures on annual totals are available in some cases. For example, in a Swedish monitoring study of 123 office and administration buildings, the average electricity use for lighting was 23 kWh per m^2 and year. The variability between buildings is considerable, ranging between 7 and 53 kWh per m^2 and year [3].

In the specific study cited above, the average installed lighting power (which was a mix of different light sources in different types of office spaces) was 10 W/m^2, giving an estimate of the average runtime of about 2300 hours per year. It is uncertain how many of these hours

with lighting coincide with sunshine hours. Assuming a perfect match and a lighting demand virtually independent of the outdoor daylight level, the artificial lighting demand could be reduced by 50 % (i.e. switched off for 1100 h), which corresponds to 11 kWh per m^2 and year. Noting that Sweden has around 31 km^2 of heated office spaces [4], the savings potential of lighting energy would be in the order of 380 GWh per year.

The standard requirement for working room illumination is 350 – 500 lux (lumens/m^2), dependent on the European country, and for corridors only 100 lux. Thus for a 10 m^2 area office in total 3500 – 5000 lumens are needed, if no other light is available at all. The fluorescent electric lights used in daytime in offices consume 10 - 12 W/m^2 of electric energy. When mechanical blinds or other heat controlling structures are shut down, the illuminance decreases below 200 lux in an office room, especially in the areas far from the window. The missing light, 150 - 300 lx, is needed from somewhere, and here especially we see an opportunity for the non-heating and extremely low energy solar fibre optic lights.

Figure 2: The Clear-up project test office at Siemens HVAC Lab in Zug. The components and layout for the equipment steered by an automatic building management system.

METHODS

Two kinds of test results are reported here. The automatic light balancing tests have been performed by using the building management system (Figs. 2 - 3): consisting of the outside weather station, illumination sensors, controller for venetian blinds and roller blinds (the roller blinds mimicking electro-chromic windows), solar fibre optic lights and dimmable fluorescent Waldmann lights.

Furthermore, in order to understand the potential for the light coupling efficiency of these systems, two kinds of plastic fibres have been tested for their sunlight transmission. The illuminance has been measured with a calibrated, V-filtered and cos-direction corrected Hagner E4-X lux-meter at 1 m distance from the fibre end inside a light transmission protected box (50 cm * 50 cm * 100 cm), by coupling direct sunlight into the fibres with a one lens containing sun tracker. The sunlight illuminance has also been measured with the same meter for the test system at Zug test office.

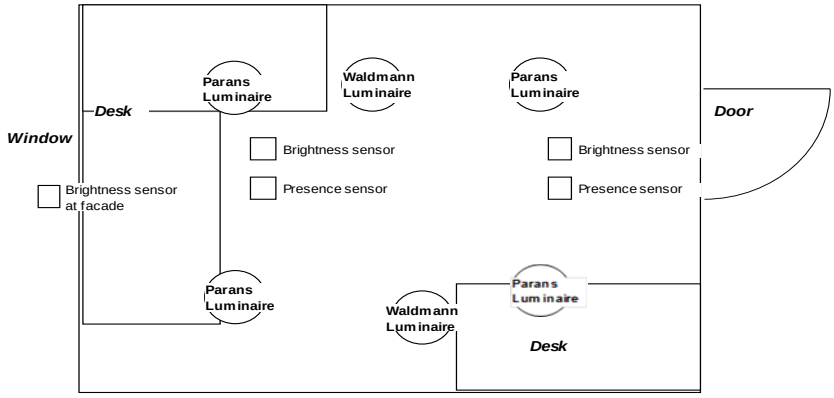

Figure 3: The locations of the sensors and luminaires for the test office.

RESULTS

The illuminances measured at the test office working desks under varies conditions were kept above 500 lux, by supplementing electric light by the dimmable Waldmann luminaires until the illuminance of 500 lux was achieved. By the window the illuminance exceeded 2000 lux, the upper limit of the sensor's measuring range (Table 1).

The energy consumed by the Waldman lamps depended on the weather, the shading device (roller blind or Ventian blind) and the supplement light provided by the fibre luminaires, and varied from 1155 Wh down to 342 Wh per day (Tables 1 - 2). These consumptions are slightly higher than they could have been at other location, because another building shaded the sunlight from both the window and the fibre light collector for a few afternoon hours. The electric lighting energy obtained was 18 to 60 % smaller during 5 of the 6 test days (150 Wh - 522 Wh/day less) when fibre lights were used together with the Waldmann lights that were dimmed, compared with the sunny day (Apr 28) without the fibre lights. It is unclear what share of the decrease is due the influencing factors (weather, type of shading device) and what share is due to the fibre luminaires. During two days (Apr 25 and 26) the electric lights were switched off and the full illuminance over 500 lux was achieved in the office during the morning hours up to mid-afternoon until a building shaded the access to the sunlight. To assess the electric energy savings by the fibre luminaries the most comparable test cases are the ones with Venetian blind control. Compared to the case with the fibre luminaries off, reductions of electric energy consumption of 37 % (Apr 21), 18% (Apr 24) or 28 % (May 1) were obtained, (322 Wh, 156 Wh or 238 Wh respectively). The diversity of these results shows the influence, that the weather has, even so the weather look comparable on these days. Therefore further tests are in progress. So far, saving of the order of 20 – 40 % is suggested.

The intensities of light, transmitted through the 20 m optical fibre bundles and measured by the lux meter at the working desks by the window and door of the test office, at the 1.8 m distance from the luminaire end surfaces were 1160 lux and 370 lux during the sunshine of 100 000 lux with blinds open (Table 3). When the roller and Venetian blinds were closed, the intensities decreased to 245 and 230 lux respectively which are in accordance with the automatic light balancing tests results (Table 1).

Date	Solar fibre lights	Waldmann lights	Roller blinds	Venetian blinds	Weather	Energy cons. Window/ Rear lights	Illuminance: By window/ By rear door
Apr 21	On	Const. light contr.	Open	Contr. by weather station	Almost Sunny	139 Wh / 403 Wh	600 – 2000 lux/ 500 – 650 lux
Apr 23	On	Const. light contr.	Contr. by weather station	Open	Half day sunny	94 Wh/ 248 Wh	600 – 2000 lux / 500 – 1000 lux
Apr 24	On	Const. light contr.	Open	Contr. by weather station	Sunny + clouds	199 Wh/ 509 Wh	500 – 2000 lux/ 500 – 700 lux (occasionally)
Apr 25 Apr 26	On	Off	Contr. by weather station	Open	Sunny, + glare, Clouds	-	>1000 lux 250 – 600 lux*
Apr 27	On	Const. light contr.	Contr. by weather station	Open	Cloudy + 2 h sunny	411 Wh/ 744 Wh	500 – 1000 lux/ 500 lux
Apr 28	Off	Const. light contr.	Open	Cont. by weather station	Half day sunny	131Wh/ 733 Wh	600 – 800 lux/ 500 lux
Apr 29	Off	Off	Down	Down	Cloudy, dark	0	0 lux/ 0 lux
Apr 30	On	Const. light contr.	Contr. by weather station	Open	Almost sunny	172 Wh/ 516 Wh	1000 – 1500 lux/ 500 – 700 lux
May 1	On	Const. light contr.	Open	Cont. by weather station	Sunny + clouds	170 Wh/ 465 Wh	>1000 lux/ 500 lux

Table 1: Summary of the light balancing test results in the test office (Fig. 3) at Siemens HVAC-Lab in Zug. For each test of 24 hours, the illuminance was continuously measured at the test points (Fig. 3) and the energy consumption by both Waldmann lights was recorded. The energy used for steering of the equipment is not included. The low energy tests are marked by the grey colour. Note: Below 500 lux by the rear door was obtained only late afternoons, when the blinds were shut and another building shaded first the window and later the fibre light collecting panel (Apr 25, Apr 26).*

Date, solar fibre lights	Energy, rear lamp, [Wh]	Energy, window lamp, [Wh]	Sum energy consumed, [Wh]	Energy consumed *, [%]	Energy consumed **, [%]
Apr 21, On	403	139	542	47	63
Apr 23, On	248	94	342	30	40
Apr 24, On	509	199	708	61	82
Apr 27, On	744	411	1155	100	134
Apr 28, Off	733	131	864	75	100
Apr 30, On	516	172	688	60	80
May 1, On	465	170	635	54	72

*: Compared with the cloudy day Apr 27, when the fibre lights did not give light
**: Compared with the sunny day Apr 28, when the fibre lights were off
Table 2: Analysis of the electric energy consumed by the electric Waldmann lights obtained by using the solar fibre optic light system together with roller or Venetian blinds (Table 1).

The wavelength spectrum, the colour, of the output light, is dependent on the fibres due to the intrinsic absorption spectrum of them. For the tested system the light colour is very white or slightly greenish. The total area that the four luminaires can illuminate at the level given above is obtained to be about 5 - 10 m^2 dependent on the office conditions, walls and furniture. This results in an electric energy consumption of the fibre system of 0.2 - 0.4 W/m^2 as the operation of this system consumes only 2 W.

In order to examine the light transmission properties of fibres, the sunlight intensity was also measured at "our standard" 1 m distance from the fibre luminaire end, inside a box of 0.5 m * 0.5 m * 1 m (Table 3). The output illuminances from the two luminaires were 900 and 950 lux. The output intensity of the 20 m fibres at 1 m distance for the SP2 system luminaires was obtained 62 ± 3 lux/fibre.

Luminaire	At 1.8 m, blinds open, [lux]	At 1.8 m, blinds closed, [lux]	At 1 m in box, [lux]	At 1 m in box, [lux/fibre]
By window desk, 16 fibres	1160 ± 6	245 ± 5	950 ± 10	59
By rear desk, 14 fibres	370 ± 10	230 ± 10	900 ± 10	64

Table 3. Illuminance values measured by Hagner E4-X for the SP2 system at Zug test lab under 100 000 ± 10 lux sunshine intensity, 10 March 2011.

Furthermore, we have checked at Uppsala lab the light transmission of the fibres used for Parans system SP2 and for the new generation system SP3 at 1 m in box. The transmitted intensities were 60 ± 5 lux/fibre for 2 m SP2 fibres, under 120000 lux sunshine. About double intensities, 116 ± 6 lux/fibre, were obtained for 14 m long SP3 fibres under the same coupling optics and sunshine conditions. These numbers are not directly comparable with the data of Table 3 or any installed system, because they are strongly dependent on the fibre end preparation and coupling optics used, but they show that at least double illumination intensity per fibre can be provided by the new fibres and SP3 system technology.

CONCLUSIONS

For offices and indoor environment the greatest saving can be reached having the fibre luminaires there where the light is mostly needed; at the working desks and far away from the windows. Full illumination, i.e. above 500 lux arriving from the window and solar fibre luminaires, was obtained in daytime for most of the light balancing tests in office with automated blinds and dimmable electric lights. On direct sunshine, the tested older type of solar fibre optic light system can supplement illuminate a total area of 5 - 10 m^2. A reliable quantification of the electric savings caused by the fibre system requires further data (the respective tests are currently running). It can be expected that new fibre systems can on sunshine fully cover the usual working illumination level. The tests on sunlight transmission for two optical fibres show that the coupling efficiency and transmitted daylight intensity will be greatly improved for this quickly advancing technology. Thus, the energy consumption of lighting (now 10 - 12 W/m^2 with fluorescent lights) could be decreased down to 0.2 - 0.4 W/m^2 for offices and to 0.02 W/m^2 for corridors during sunny hours by solar fibre optic lights. It is also significantly lower than 5 - 7 W/m^2 for LED lights. Further interesting is that the need for electric cooling is expected to decrease by another significant amount per square meter. This will be studied further by Clear-Up project.

REFERENCES

1. Map of mean total sunshine duration in Europe, Satel-Light – The European Database of Daylight and Solar Radiation. Available online: http://www.satel-light.com, 2011.
2. Map of normal sunshine duration for one year, Swedish Meteorological and Hydrological Institute (SMHI). Available online: http://www.smhi.se/klimatdata/meteorologi/stralning/normal-solskenstid-for-ett-ar-1.3052, 2011.
3. Swedish Energy Agency, Förbättrad energistatistik för lokaler, Report ER 2007:34. Eskilstuna, Sweden, 2007.
4. Swedish Energy Agency, Energy statistics for non-residential premises in 2009, Report ES 2011:03. Eskilstuna, Sweden, 2011.

RELIABLE DAYLIGHT SENSING FOR DAYLIGHT HARVESTING IN SIDE-LIT SPACES

J.Xu; K. Papamichael.

California Lighting Technology Center, University of California, Davis

ABSTRACT

Daylight harvesting is among the most promising strategies to save energy and reduce peak demand, and create a more desirable indoor environment. Interior daylight levels have been traditionally determined using a single photo sensor. The photo sensor placement and relationship to daylight and electric light sources has traditionally followed two main approaches: Open Loop and Closed Loop. However both approaches have their limitations. The single photosensor shortcomings are being resolved through use of two or more photo sensors, aimed at different areas in the space that are unlikely to be simultaneously affected by space changes at the same time. A "dual-loop" system, using a combination of open and closed loop sensors has been very successfully in increasing daylight sensing reliability and accuracy in skylight applications. Following the success of the dual-loop system, the multi-sensor approach is being explored for lighting control in side-lit spaces. This paper is focused on the options considered and the evaluation of their ability to accurately measure daylight changes in interior spaces considering long- and short-term changes in the geometry and reflectance of interior surfaces, as well as changes in the daylight transmittance of the window through use of operable shading systems. A number of experiments were carried out to find out the best combination of photo sensors, considering positions, directions, fields of view, directional sensitivities, people movement, window treatment changes, exterior changes, variations in sky conditions, weather, etc. Results so far indicate that the best location for the closed loop photo sensor is on the ceiling, looking at the space area where maintenance of lighting design levels is important. The open loop sensor needs to be carefully configured so that it only sees the window within its field of view, from a distance that is far enough from the Venetian blinds to eliminate effects of vertical placement relative the horizontal slats of the blinds. Properly configured, the system seems to handling daylight and space changes very effectively. Commercial prototypes are being considered for evaluation of the approach in real spaces.

INTRODUCTION

Photo-sensor based controls for daylight harvesting

Daylight harvesting can save significant electric lighting and cooling energy through use of photo sensor based controls that automatically adjust electric lighting levels based on available daylight. As daylight availability coincides with peak electricity demand, daylight harvesting is also a very effective strategy to significantly reducing peak electricity demand. The key to successful daylight harvesting for energy reduction is reliable sensing of available daylight for the control of electric lighting. While it seems simple and straightforward, reliable sensing of interior daylight levels is challenging.

Traditional daylight sensing approaches

Interior daylight levels have been traditionally determined using a single photo sensor. The photo sensor placement and relationship to daylight and electric light sources has traditionally followed two main approaches:

1. Open Loop, where the signal of the control photo sensor is NOT affected by the electric lighting being controlled, and

2. Closed Loop, where the signal of the control photo sensor IS affected by the electric lighting being controlled.

The placement of the photo sensor in open loop applications is usually outdoors, looking towards the sky dome, or indoors, looking at a daylight aperture, such as a window or a skylight. The placement of the photo sensor in closed loop applications is usually indoors, looking towards areas illuminated by both electric light and daylight. Both approaches, however, are limited in their effectiveness to provide reliable information about daylight changes through time.

The main limitation of open loop applications is the inability to sense daylight levels indoors, as indoor and outdoor light levels do not have the same rate of change, especially for lower solar altitudes, during the early and late hours of the day, as well as during large variations in daylight levels during partly cloudy days. In addition, open loop systems cannot respond to changes in the space, such as long term changes in the geometry and reflectance of interior surfaces (which requires recalibration) or when shading systems are deployed, significantly reducing indoor daylight levels, without corresponding changes to outdoor daylight levels.

The main limitation of closed loop applications is the inability to differentiate between true daylight changes and

1. Long-term changes in the geometry and reflectance of interior surfaces (which requires recalibration), and

2. Short-term changes due to people with different reflectance clothing moving within the field of view of the photo sensor.

Short-term changes have been traditionally addressed using time delays before adjusting electric lighting levels. These, however, also happen during true daylight changes, when electric lighting is expected to be pretty responsive, especially when the changes are significant, e.g., during partly cloudy days.

New and emerging multi-sensor daylight sensing

The single photosensor shortcomings are being resolved through use of two or more photo sensors, aimed at different areas in the space that are unlikely to be simultaneously affected by space changes at the same time.

A “dual-loop” system, using a combination of open and closed loop sensors has been very successfully in increasing daylight sensing reliability and accuracy in skylight applications. The dual-loop system controller is using the signals of both photo sensors to determine interior daylight changes. The algorithm used for the determination of daylight changes and the adjustment of the electric lighting is based on the closed loop photo sensor signal differences for different states of the electric lighting. This results in support for automatic, continuous calibration of the closed loop sensor, resolving the issue of changes in geometry and reflectance of interior surfaces [1]. A prototype installation in a big-box retail stores with skylights showed significant improvement in daylight sensing, offering 50% more electric

lighting savings than a single, open loop sensor approach [2]. The dual-loop approach is now available in commercial products.

MULTI-SENSOR LIGHTING CONTROL FOR SIDE-LIT SPACES

Following the success of the dual-loop system, the multi-sensor approach is being explored for window applications. This paper is focused on the options considered and the evaluation of their ability to accurately measure daylight changes in interior spaces considering long- and short-term changes in the geometry and reflectance of interior surfaces, as well as changes in the daylight transmittance of the window through use of operable shading systems.

Experiment setup

The side-daylighting laboratory is located at 633 Peña Drive in Davis, California. Outside the lab is a small parking lot with a few trees and plants. The interior space has a rectangular footprint. It is 4.87m deep, 5.49m wide and 2.74m tall, with two 1.83m wide by 1.5m tall windows on the North-facing wall. The windows are equipped with horizontal aluminium Venetian blinds. The electric lighting system is comprised of four 0.6m X 0.6m recessed Lithonia RT5 luminaires, using lamps powered by 0-10V Sylvania PowerSense dimming ballasts. (Figure 1, left)

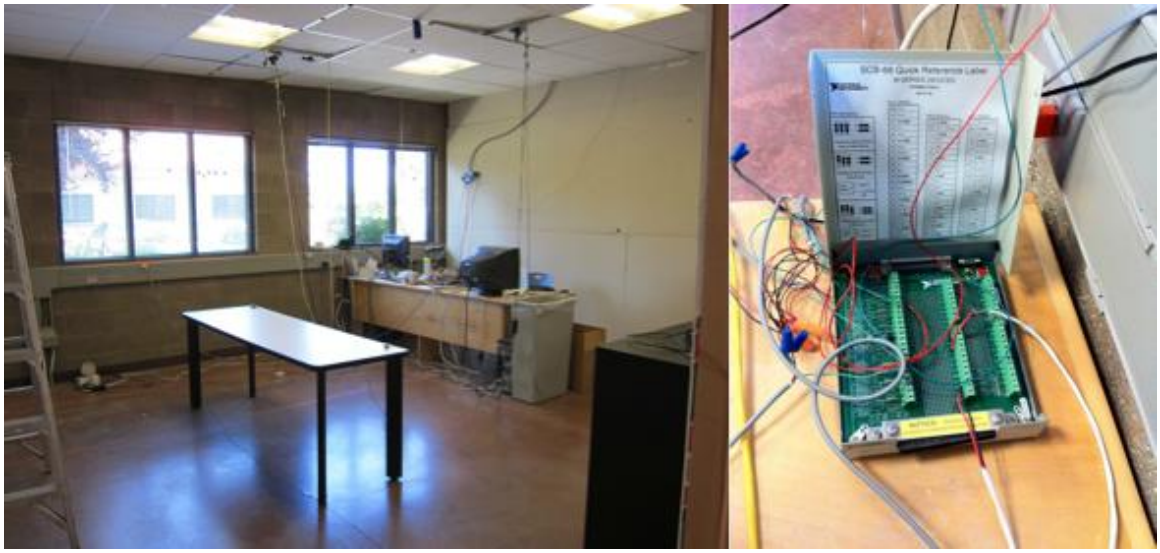

Figure 1: Side Daylighting Lab (left) and NI Data Acquisition Device (right)

Light levels are measured using an array of digital photo sensors, two of which measure work plane illuminance at different distances from the window wall and the rest light levels from various view points for electric lighting control consideration. An infrared occupancy sensor monitors occupancy status. The signals of the photo sensors are used as input to various control algorithms developed in LabVIEW on a personal computer. The LabVIEW program receives sensor signals, processes them and then sends 0-10V analog signals to the ballasts that control the electric lighting. The output signals of the system were sent through a National Instruments SCB68 M series data acquisition device. (Figure 1, right)

EXPERIMENTAL WORK AND RESULTS

Several combinations of photo sensors have been used to identify and evaluate combinations that could be used to reliably sense interior daylight changes. Efforts so far have been focused on the use of two photo sensors, similar to the “dual-loop” approach for the skylight

applications. A number of experiments were carried out to find out the best combination of photo sensors, considering positions, directions, fields of view, directional sensitivities, people movement, window treatment changes, exterior changes, variations in sky conditions, weather, etc.

Results so far indicate that the best location for the closed loop photo sensor is on the ceiling, looking at the space area where maintenance of lighting design levels is important. The open loop sensor needs to be carefully configured so that it only sees the window within its field of view, from a distance that is far enough from the Venetian blinds to eliminate effects of vertical placement relative the horizontal slats of the blinds. (Figure 2)

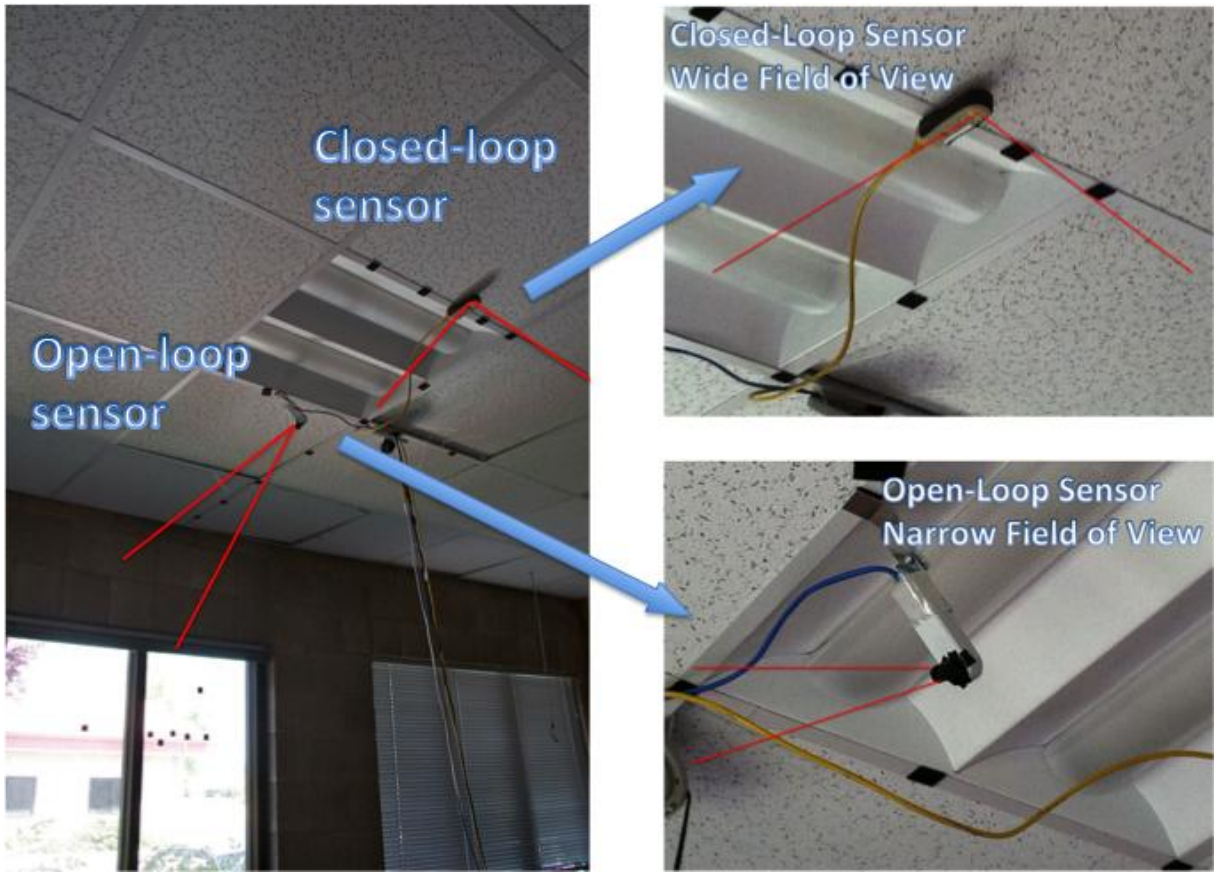

Figure 2: Closed- and Open-loop Sensor Placement

Several versions of the control algorithm were tested with various types of geometry and surface reflectance changes, as well as testing of occupants' movement and control of Venetian blinds.

Figure 3 shows the signals of the control photo sensors, as well as the electric lighting output during various changes in the space through time, during a cloudy day (March 16th, 2011). In morning, when the space was occupied and daylight was insufficient, electric lights were switched on with 20% electric light output. As daylight level increased and overall light level reached to set point, the electric lights dimmed and eventually switched off, around 10:45 am. At 12:30PM, after a period of occupant inactivity, the system performed re-calibration, which resulted at a slightly higher set point when the space was again occupied around 1:30 pm. Between 10AM and 3PM, despite the very cloudy day, daylight was sufficient to maintain electric lights off. After 3PM, as daylight decreased resulted in light level below the set point, electric lights were adjusted frequently as needed with significant variability in daylight levels

due to partly cloudy conditions. Daylight were reduced continuously after at 5PM resulting in dimming of the electric lights, which reached full light output around 6:30 pm. (Figure 3).

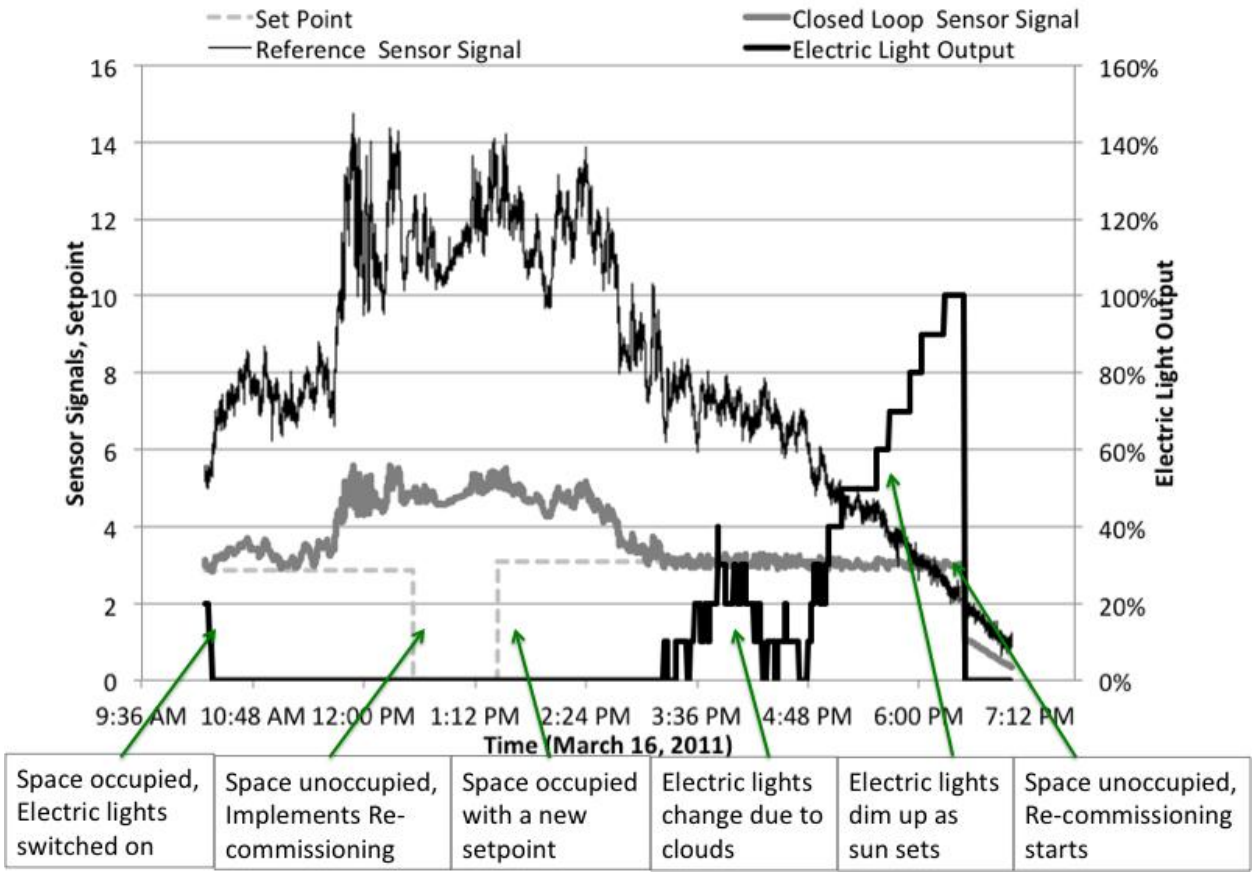

Figure 3: Dual-photo-sensor Lighting Control Operation for a Day

Figure 4 shows the signals of the control photo sensors, as well as the electric lighting output during a series of tests on April 26, 2011, which are also documented with photographs. The first photograph is the original state of the space. The set point of the lighting system was 2.6 fc and current ballast voltage was 2.6V. A black board was then placed on the white table to change the reflectance of the table within the view of the closed loop sensor. The control system updated the set point of the closed photo sensor to 2.3 fc, maintaining the ballast voltage at 2.6V. After half minute, the black board was then taken away, the set point was updated again back to its original value (2.6 fc) and the ballast voltage was again maintained at the same level. Later a white felt was placed on the floor, resulting in a set point adjustment of the closed loop signal to 3 fc, without changing the ballast voltage. Next, the Venetian blinds were closed, causing both open loop and closed loop sensor changes. The electric lighting output was increased to a ballast voltage of 6.8V. Then the window treatment was pulled up. Both sensors detected the light level change. The electric lights dimmed back to the previous voltage. Then the white felt was taken away, resulting in automatic change to the set point, which again fell to its original level (2.6), while the ballast voltage remained unchanged. (Figure 4)

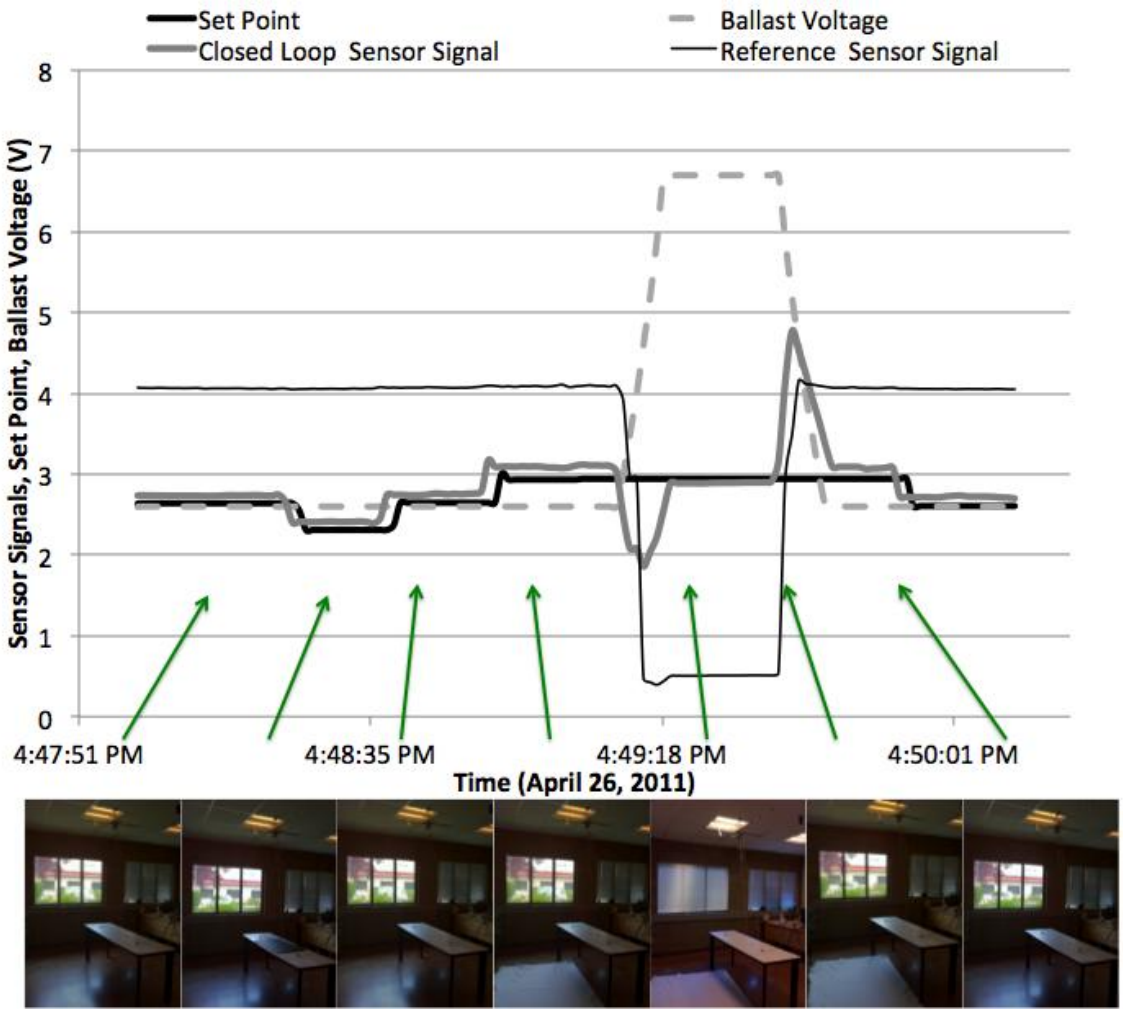

Figure 4: Experiment with Interior Change and Window Treatment Adjustment

CONCLUSION AND NEXT STEP

Dual sensor controls seem to be promising for reliable daylight sensing for window applications. They require careful design and placement of the "open loop" photo sensor to maximize the effect of the daylight introduced through the window. Properly configured, the system seems to handling daylight and space changes very effectively. Commercial prototypes are being considered for evaluation of the approach in real spaces.

ACKNOWLEDGEMENTS

The work presented in this paper is supported by the Public Interest Energy Research (PIER) program of the California Energy Commission (CEC).

REFERENCES

1. Pistochini, T. and K. Papamichael. : Self commissioning dual loop sensor dimming technology for daylight harvesting. California Lighting Technology Center, 2008.
2. Pistochini, T. and K. Papamichael.: Research matters. LD+A, 2009.

Indoor Environment Quality and Health

ADAPTIVE CONTROL STRATEGIES FOR SINGLE ROOM HEATING

M. Adolph[1], N. Kopmann[1], D. Müller[1], B. Böwer[2], J. Linden[2]
[1]*Institute for Energy Efficient Buildings and Indoor Climate*
E.ON Energy Research Center, RWTH Aachen University
Mathieustraße 6, 52074 Aachen, Germany
madolph@eonerc.rwth-aachen.de
[2] *ista International GmbH*
Grugaplatz 2
45131 Essen

ABSTRACT

The scope of the adaptive control strategies for single room heating is the reduction of energy demand by optimizing control strategies and thus decrease the waste of energy. To achieve this goal, the control system will adapt in two different ways.

First, the control system adapts to the user's demand profile. With a simple interface ("too cold" or "too warm") the user can provide feedback to the actual room temperature. The system calculates an usage profile for every single room and controls the room temperature according to this usage profile. This adaptation works without being noticed by the user and requires no more feedback than a thermostatic valve (i. e. feedback if "too cold" or "too warm"). This is necessary to keep the system useful for all levels of society.

The second adaptation of the control system is the adaptation to the system itself. By means of an iterative learning control, the behaviour of the room the day before will help to optimize the control strategy for the next day. Additionally it can be predicted, when the re-heating of a room has to start after it was left to cool down because the user was absent to ensure thermal comfort on the user's return.

The algorithm will be tested by simulations in Modelica, laboratory experiments and a field test to evaluate the ease of use and the thermal comfort for the user. In this paper simulation-only results will be discussed.

First simulative results show that an adaptation to the user profile yields energy savings around 18 %. Simultaneously, the mean room temperature is reduced and the predicted mean vote worsens. One main problem is that the room could not be re-heated fast enough because the temperature changes were too steep. With a second algorithm, limiting the temperature setpoint to values above 18 °C, energy savings up to 7 % are possible and the mean room temperature dips only slightly. When the user is present almost the same amount of energy is needed as in comparison to the base-case (constantly 20 °C) but the energy demand is reduced significantly when the user is absent.

It is concluded that the challenge of changes in the temperature demand profile has to be treated with a control algorithm which is aware of the upcoming changes in the profile and the thermal inertia of the building to ensure user satisfaction.

INTRODUCTION

Room heating accounts for approximately a third of the European primary energy consumption. Therefore optimizing the energy consumption of room heating can lead to high energy savings. One option of reducing the energy demand would be optimizing the control strategies for room heating which comes at relatively low costs compared to other measures (e. g. retrofitting). The E.ON Energy Research Center of RWTH Aachen University[1] develops an adaptive control system for single room heating.

Room heating is mainly controlled by thermostatic valves which ensure a constant room temperature. Normally, these thermostats are set to satisfy the user's thermal comfort. Especially from the point of energy efficiency it is sensible to provide this "comfort temperature" only if the user is present. If the user is absent, a reduction of the room temperature is possible. In case of a "normal" thermostatic valve, the user must actively reduce the room temperature and set it back on return. To avoid this, programmable thermostatic valves can be used. These valves allow programming of different schedules for heating. But as shown in Meier et al. [3] these programmable thermostatic valves are often not properly set up, the setup is not re-evaluated on a regular basis, or these valves are used as "normal" thermostatic valves. Besides existing misconceptions in the understanding of energy use and the way how thermostats work, one reason for the improper use are problems with the usage. Programming of different schedules is assumed to be too complicated for non experts [3].

The system under development adapts to the user's need in two different ways. First, an adaptation to a usage profile, secondly to the room's behaviour itself. To avoid problems with the setup, the user profile does not need any setup and will adapt to the user's need by using the most basic feedback options "too cold" and "'too warm". The second way of adaptation is implemented as an iterative learning control algorithm, improving the results from day to day.

ADAPTATION TO THE USAGE PROFILE

The main objective of the adaptive control system is to ensure the thermal comfort of the user. The secondary objective is the reduction of energy consumption. The system will start with a profile with equal values for every time-step. Depending on the user's feedback, the system will lower or rise the temperature-setpoint. To ensure low energy consumption the system will reduce the temperature setpoint randomly if no feedback is provided. The probability of this randomly reduction is correlated to the number of days without a feedback. If the "too cold" feedback was given just the day before, it is more unlikly that the temperature is reduced than if the last feedback was 10 days ago. The probability for a random temperature reduction is 50 % if no feedback was given for 20 days. In addition, no reduction will take place, if the real temperature is 2 K above the setpoint. If this is the case, the thermostatic valve will already be closed, so no additional energy saving can be expected. This situation can occur, for example, due to solar radiation or the thermal inertia of the building. Picture 1(a) shows a simplified flow-chart for the temperature profile.

ADAPTATION TO THE ROOM

Using an iterative learning control (ILC) algorithm, the quality of the control system is expected to improve. In particular, changes in the temperature profile can be anticipated, so that the

[1] www.eonerc.rwth-aachen.de

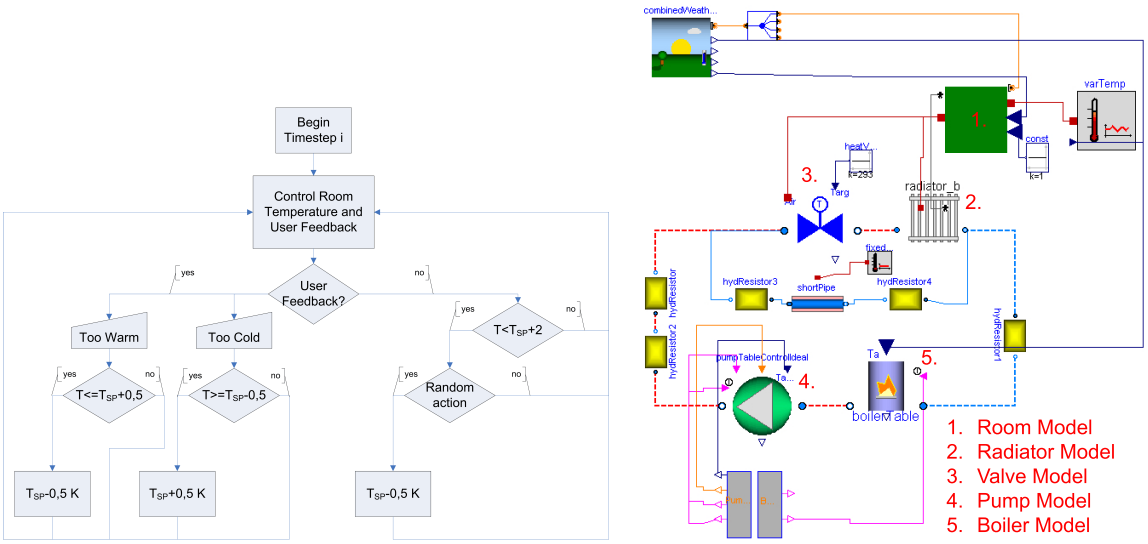

(a) Flow chart of adaptation to user profile

(b) Graphical representation of the simulations top-level

Figure 1: Flow-Chart for the user profile and simulations setup

user's "comfort temperature" is achieved when the user returns home and not 30 minutes after his arrival.

As many boundary conditions, especially the weather, can not be controlled, an underlying control algorithm is compulsory. For the ILC algorithm today's weather will be assumed to be tomorrow's weather as the most reasonable assumption without any additional data available. The final implementation of the ILC algorithm is still pending and thus results are not discussed in this paper.

METHOD

In a first step both algorithms are tested in a simulation-only environment. The algorithm for the usage profile is implemented in Python, the simulation is conducted in Modelica with Dymola as developer environment, employing the extensive building and HVAC library of the E.ON Energy Research Center.

The simulation features a room of $\approx 20\,\mathrm{m}^2$ with one outside wall and three inside walls. The inside walls are connected to a temperature source at a constant value of 20 °C, the outside temperature is taken from the german test reference year, zone 4 [1]. For the simulation one day is repeated, so the external weather is the same for every day. A window is included in the outside wall and solar radiation is accounted for. A thermostatic valve with no hysteresis is used to control the temperature of the room. Heat is brought into the room by means of a multi-layer radiator model. To close the hydraulic loop, a boiler, some pipes, hydraulic resistors and a pump are added. The simulative setup is shown in picture 1(b).

To model the user behaviour, the predicted mean vote (PMV) is calculated as described in DIN EN ISO 7730 [2]. The optimal value for the PMV is zero. At a PMV equal to zero, 5 % of the people would be statistically dissatisfied with the thermal comfort. At a value of 1.5 or -1.5, 50 % of the people would be dissatisfied. Negative values indicate a thermal sensation being too cold, positiv values indicate a thermal sensation as too warm.

Time	clothing factor	metabolic Rate	T with PMV≈0 in °C
7:00-7:30	0.4	0.8	28.0
7:30-8:00	1.0	1.0	23.0
8:00-17:00		absent	
17:00-19:00	1.0	1.6	18.0
19:00-22:30	1.0	1.0	23.0
22:30-23:00	0.4	0.8	28.0
23:00-07:00	3.1	0.8	18.0

Table 1: Parameters influencing the PMV-Vote of the user. Note: For people wearing normal clothing, the optimal temperature is above the normally suggested 20 °C

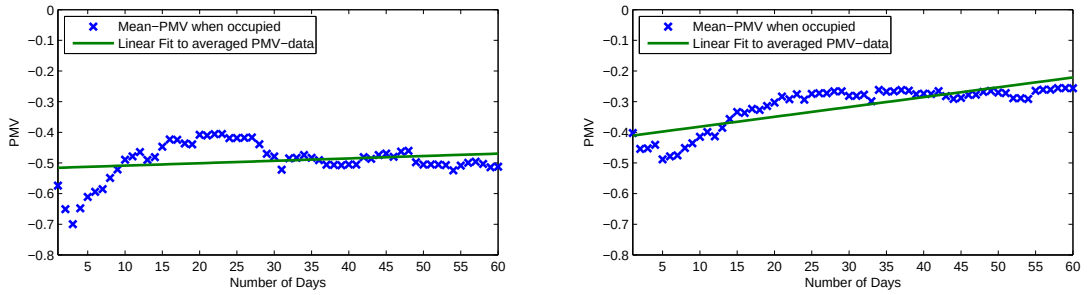

(a) Standard algorithm (b) Algorithm with minimal temperature set to 18 °C

Figure 2: Evolution of the daily mean PMVs

The simulation runs for 15 minutes then the mean PMV is calculated and a user feedback is assumed, depending on the PMV. If no feedback is given (i.e. user absent or satisfied) a decrease of 0.5 K of the temperature setpoint can occur on a random basis. The probability of this decrease depends on the time since the last user's feedback. User feedback will be ignored if the measured temperature is not equal to the temperature setpoint in a range of 1 K, because the feedback is then not related to the temperature setpoint but more to a problem in the control algorithm, which should be addressed using the iterative learning control.

To account for differences in user behaviour, the feedback of the user is not calculated by the theoretical PMV, but by the PMV plus a random number between -1 and 1, as differences in clothing, activity level or external heat can occur at any time. The range of -1 to 1 ensures that a good PMV between -0.5 and 0.5 will never lead to a negative feedback. PMVs lower than -1.5 or above 1.5 will lead to a negative feedback.

At this point, variations in the user's time schedule are neglected. Table 1 shows the assumed presence, clothing and metabolic rate of the user.

RESULTS

A first simulation of the adaptive control algorithm shows a constant increase of the PMV towards zero, stating that the algorithm continually improves the thermal comfort of the user.

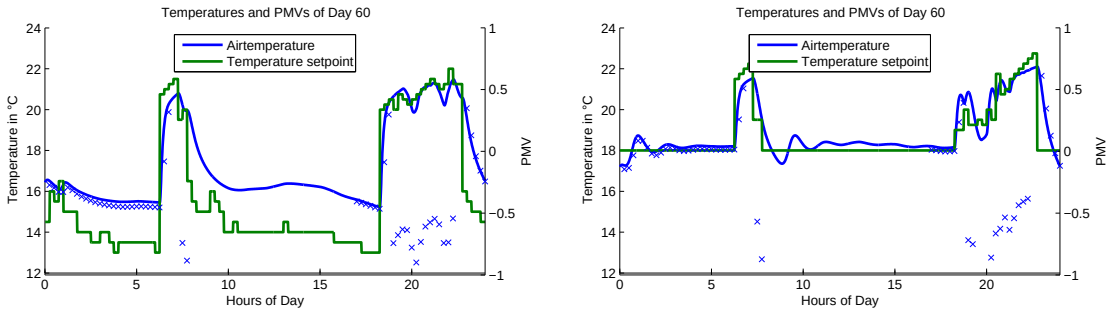

(a) Standard algorithm (b) Algorithm with minimal temperature set to 18 °C

Figure 3: Temperature setpoint vs. simulated temperature and the PMV

A graph of the development of the daily mean PMV can be found in figure 2(a). Analysis of the temperature data shows that the decrease in room-temperature while the user is absent leads to a cooling of the room, which eventually leads to a too cold temperature on the user's return. Thus an alternative algorithm was used where the minimal temperature was set to 18 °C. This increased the mean PMV (figure 2(b)), but especially in the morning the room temperature was too low. Figure 3 shows the temperature setpoint against the simulated temperature. It can be noticed that in both cases the match of temperature with the setpoint is not good enough. This is due to the steep changes in the temperature profile and the thermal inertia of the building. Table 2 shows the mean temperature at Day 60 of a base case ($T_{SP} = 20\,°\mathrm{C}$), and both algorithms. It also shows the mean PMV and the energy needed.

The energy demand can be reduced by up to 50 % with algorithm 1. This improvement in energy consumption is linked to a reduction of room temperature when the user is present by 2.2 K and by 3.4 K when the user is absent. The PMV worsens by the factor of three. Some of the energy savings can be accounted to the static boundary conditions for the inner walls. Thus the energy savings were corrected by adding respectively substracting the heat gains or losses to the total energy demand. This corrected Q_{demand} is shown in table 2. The energy savings are then $\approx 18\,\%$.

Algorithm 2 reduces the corrected energy demand by $\approx 7{,}5\,\%$, the room temperature is down 0.5 K when the user is present and 1.7 K when the user is absent. The PMV worsens slightly. The energy demand raises by 4.6 % when the user is present and decreases by 30 % when the user is absent. This shows that the energy is used when specifically needed by the user.

The standard deviation for all algorithms shows that, although the mean PMV values are acceptable for all three simulations, but several incidents with an unacceptable PMV per day are likely to occur. And although the mean PMV is best for the simulation with the constant temperature, the standard deviation is highest. This was to be expected as a constant temperature can not satisfy a user with varying activity rates. For both adaptive algorithms, the standard deviation of the PMV decreases as a sign of a successful adaptation process. For the first algorithm, the standard deviation is 0.93 on day one and 0.48 on day 60. For algorithm 2, the respective values are 0.90 and 0.53.

SUMMARY AND OUTLOOK

It was shown by simulation that the energy demand for heating can be reduced significantly by using a user dependent temperature profile. The applied algorithm did not need any setup and evolved over time by user feedback. Thus an ease of use close to that of a simple thermostatic

	T_{mean} when user present in °C	T_{mean} when user absent in °C	mean PMV		corrected Q_{demand} in kWh	corrected Q_{demand}, user present in kWh	corrected Q_{demand}, user absent, in kWh
Base case	19.9	20.0	−0.18	±0.76	10.76	7.18	3.58
Algorithm 1	17.7	16.6	−0.54	±0.48	8.85	7.16	1.69
Algorithm 2	19.3	18.3	−0.26	±0.53	9.99	7.51	2.48

Table 2: Results of the simulation day of base case (temperature setpoint constant at 20 °C) and two adaptive algorithms (standard algorithm and a minimal temperature setpoint of 18 °C). Day 60 of the simulation is analysed

valve can be achieved.

Still, the challenge remains that steep gradients between temperature settings when the user is present and when he's absent lead to uncomfortable temperatures at re-entering. This problem could be solved by a different setup (earlier increase of the temperature setpoint) or by an advanced control strategy. The idea of an iterative learning control is briefly mentioned but is not discussed in this paper.

Nonetheless, the results show that a room control system equipped only with a user profile can not fulfill the comfort requirements, because the thermal inertia of the building prevents fast temperature changes. Thus an advanced control strategy is needed, which is aware of upcoming changes and can ensure thermal comfort at any time.

In the next step, the iterative learning control will be included in the algorithm. After testing the algorithm in a simulation, tests in a laboratory and a field test will follow. The field test will be conducted in close cooperation with ista International GmbH.

ACKNOWLEDGEMENT

Grateful acknowledgement is made for financial support by BMWi (German Federal Ministry of Economics and Technology), promotional reference 0327387D.

REFERENCES

[1] Jürgen Christoffer, Thomas Deutschländer, and Monika Webs. *Testreferenzjahre von Deutschland für mittlere und extreme Witterungsverhältnisse TRY*. Selbstverlag des Deutschen Wetterdienstes, 2004.

[2] DIN EN ISO 7730. Ergonomie der thermischen Umgebung – Analytische Bestimmung und Interpretation der thermischen Behaglichkeit durch Berechnung des PMV- und des PPD-Indexes und Kriterien der lokalen thermischen Behaglichkeit, März 2006.

[3] Alan Meier, Cecilia Aragon, Becky Hurwitz, Daniel Perry, Therese Peffer, and Marco Pritoni. How people actually use thermostats. In *ACEEE Summer Study on Energy Efficiency in Buildings*, pages 193–206. ACEEE, 2010. http://eec.ucdavis.edu/ACEEE/2010/data/papers/1963.pdf.

AIR TEMPERATURE AND CO_2 VARIATION IN A UNIVERSITY OFFICE BUILDING WITH DOUBLE-SKIN

H. Altan[1]; M. Refaee[1]; J. Mohelnikova[2]

1: School of Architecture, The University of Sheffield, Sheffield, United Kingdom

2: Faculty of Civil Engineering, Brno University of Technology, Brno, Czech Republic

ABSTRACT

The design, construction and utilisation of low energy buildings have brought experiences that an excessive tendency towards energy savings could also lead into problematic indoor environments in buildings such as issues related to overheating and insufficient ventilation in order to achieve occupant satisfaction and environmental sustainability. Designing buildings for better indoor comfort and energy efficiency would therefore require consideration of optimisation during early design stages as well as at post occupancy phases.

The purpose of the paper is to present a post occupancy indoor environment evaluation of a newly built office building at the University of Sheffield campus in the UK, which is part of an ongoing investigation. The building accommodates three social sciences faculty departments at the same time holds the university administrative offices. It has fully glazed facades partly filled with non-transparent component positioned at window sills. The evaluation provided further information about thermal condition levels in several indoor work environments.

A long term monitoring of thermal regime in the investigated building will help determine indoor comfort conditions. The study consists of evaluating thermal profiles of both outdoor and indoor temperature and humidity levels using the same time intervals. HOBO monitoring apparatuses were used for indoor environment measurements. All locations of thermal sensors were determined to estimate overall indoor comfort conditions in the building during its occupancy and throughout one year period of monitoring.

The paper presents the analysis and results using the post occupancy monitoring data obtained after two weeks of measurements. Indoor air temperature, relative humidity (RH%), and carbon dioxide (CO_2) were monitored to investigate conditions within selected rooms and to compare them to accepted standard guidelines.

INTRODUCTION

The building envelope provides a separation between the interior and the exterior environments, and at the same time plays an important role in solar heat gain management, thermal load control, air infiltration and exfiltration, ventilation, noise control, design quality, and aesthetic definition. Traditional envelope design regarded the external skin as a barrier between the variable outdoor climate and the highly controlled interior environment [1].

Double-skin facades are an architectural concept that is gaining wider acceptance and application in Europe, North America and Japan. A double-skin facade is composed of two facade layers separated by a cavity. It came in vogue in Europe, followed by various claims of its superior ability to introduce natural ventilation while reducing noise propagation indoors. Transparent glazing is normally used on the exterior leaf to maintain a distinct transparent appearance to buildings. Double-skin facades are still under scientific scrutiny to optimise

their configuration to improve their thermal, light transmittance, acoustic properties. The methodologies used in research are mainly based on verifying simulation results by using experimental methods and there is limited research which has been done on actual buildings [2].

In January 2009, the Jessop West building with a double skin facade became the new home to the School of English Literature, Language and Linguistics, the Department of History and the School of Modern Languages and Linguistics for the University of Sheffield. The eco-friendly building is a model of sustainability with many features built into the design to maximise energy efficiency and make the best use of natural light. The building incorporates a number of environmental features both to preserve energy and to ensure comfort of staff and students based in the building [3]. These include:

- Natural ventilation so there is no need for energy or inefficient air conditioning.

- A design which makes the most of natural light.

- Green roofs to improve insulation, help with water run-off and encourage biodiversity.

- Heating provided from the energy-from-waste district heating network.

- Window design that reduces noise, increases natural ventilation and air circulation and allows room users to control their working environment.

Increasing the attention to indoor air quality has contributed to the awareness of poor health associated with a poor indoor environment. Two types of illnesses related to poor indoor air quality have been identified: Sick Building Syndrome (SBS) and Building Related Illness (BRI). While the definition of SBS varies slightly in the literature, SBS can be defined as the discomfort or sickness associated with poor indoor environments with no clear identification of the source substance. BRI is defined as a specific recognised disease entity caused by some known agents that can be identified clinically [4, 5].

The objective of this study is to monitor indoor air quality and to investigate conditions and performance within the newly built energy efficient office building with double-skin facade for the University of Sheffield, England, UK and to compare results to accepted standard guidelines.

METHOD

A measurement programme of internal environmental parameters was undertaken for a two weeks period (9th April – 21st April) in 2010.

Indoor air temperatures and relative humidity levels were measured at the six rooms of east wing using HOBO U10-003 data loggers. Indoor carbon dioxide levels were also recorded using Telaire 7001 CO_2 meters. Although CO_2 is not toxic, it is commonly used as an indicator of air quality. High levels of CO_2 indicate inadequate ventilation in a space.

All equipment was placed in the six rooms, specifically in the breathing zone of a person sitting on a chair (approximately 1.5 m above the floor) and away from open windows. In addition participants were requested to behave as normal within their office during the monitoring period in order to obtain realistic data.

RESULTS

The data were collected from the indoor monitoring equipment and statistically analysed to investigate the indoor thermal condition and air quality form April to August in six offices.

Temperature and relative humidity levels within an indoor environment will vary with the time of year and physical indoor environment. However, increased temperature within a confined space such as an indoor environment can create a more suitable environment for the growth of unwanted bacteria and fungi. In general, it would be reasonable to maintain a temperature of around 19°C to 20°C within an office [6].

Figure 1 shows the daily mean of indoor temperature in all rooms of east wing and concurrent outdoor temperature. It can be seen that level of indoor temperature in one office (R1.02) followed a pattern that to rise and fall with concurrent outdoor temperature for a period of two weeks. The main reason for this office to follow the pattern of outdoor temperature is because the space is an open plan and not enclosed. Table 1 show how the indoor and outdoor air temperatures varied over a ten day period from 9th of April to 21st of April 2010. The dashed line in Figure 1 is the internal air temperature of 20 °C recommended in office room. Average temperatures ranged from a low of 18.2 °C to a high of 23.5 °C.

If levels of humidity become too dry, below 40% this can have adverse effects, some people susceptible to sore throats due to the dryness of the air. The optimum level of humidity should be between 40-70% [6]. The average relative humidity ranged from 19 to 44 of RH% and does not agree with the standard guidelines for these six offices.

One office (Room 1.03) nearly complies with the standard guidelines as seen in figure 2 this is because the room has a humidifier in present. From figure 2, it can be seen that the rest of the five rooms has relative humidity levels which is lower than the recommended standard guidelines i.e. under 40%.

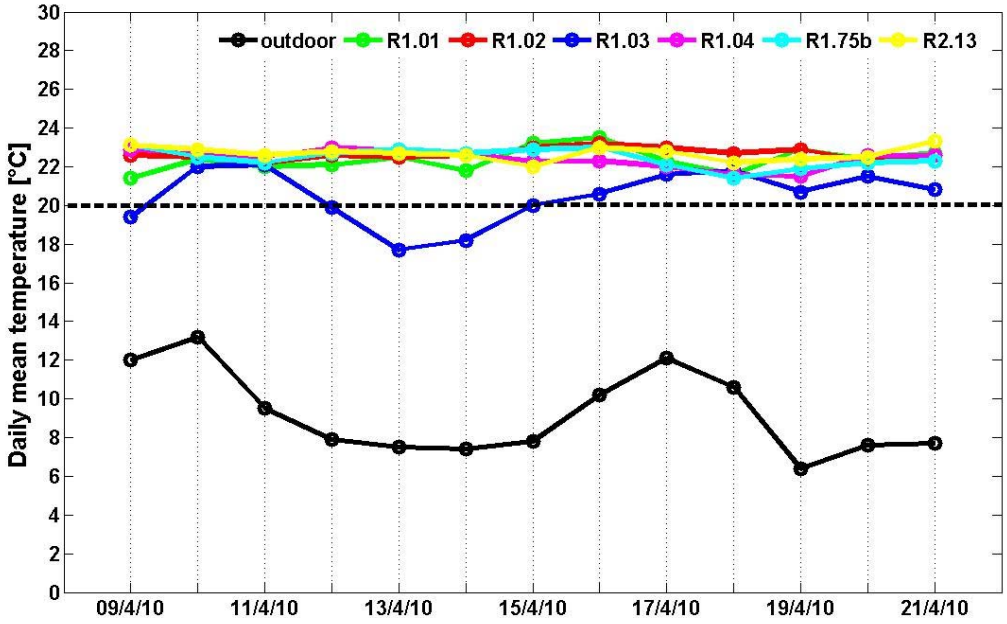

Figure1: Daily mean of indoor temperature in all rooms of east wing and concurrent outdoor temperature

Dates	Outdoor (°C)	Room 1.01 (°C)	Room 1.02 (°C)	Room 1.03 (°C)	Room 1.04 (°C)	Room 1.75b (°C)	Room 2.13 (°C)	Corridor East (°C)
9/4/10	12.0	21.4	22.6	19.4	22.9	23.1	23.1	23.6
10/4/10	13.2	22.4	22.5	22.0	22.8	22.5	22.9	23.2
11/4/10	9.5	22.0	22.2	22.1	22.5	22.2	22.6	23.1
12/4/10	7.9	22.1	22.6	19.9	23.0	22.7	22.8	23.4
13/4/10	7.5	22.5	22.5	17.7	22.8	22.9	22.7	23.4
14/4/10	7.4	21.8	22.6	18.2	22.7	22.7	22.6	23.3
15/4/10	7.8	23.2	23.0	20.0	22.3	22.9	22.0	23.3
16/4/10	10.2	23.5	23.2	20.6	22.3	23.0	23.0	23.3
17/4/10	12.1	22.3	23.0	21.6	22.0	22.1	22.8	22.7
18/4/10	10.6	21.6	22.7	21.8	21.6	21.4	22.2	22.3
19/4/10	6.4	22.9	22.9	20.7	21.5	21.9	22.4	22.4
20/4/10	7.6	22.4	22.3	21.5	22.6	22.2	22.5	22.7
21/4/10	7.7	22.7	22.6	20.8	22.6	22.3	23.3	22.4

Table 1: Summary of temperature data (daily mean) from six rooms in the east wing with the concurrent outdoor temperature

The relative humidity and ventilation should be kept at levels that prevent discomfort, dry throat or other problems. In addition, there were some of common complaints in the offices such as dry throat, itchy and sore eyes, and dry mouth which can be associated with low relative humidity. The use of plants and humidifier was recommended as they release steam and moisture into the air which is required in this office environment.

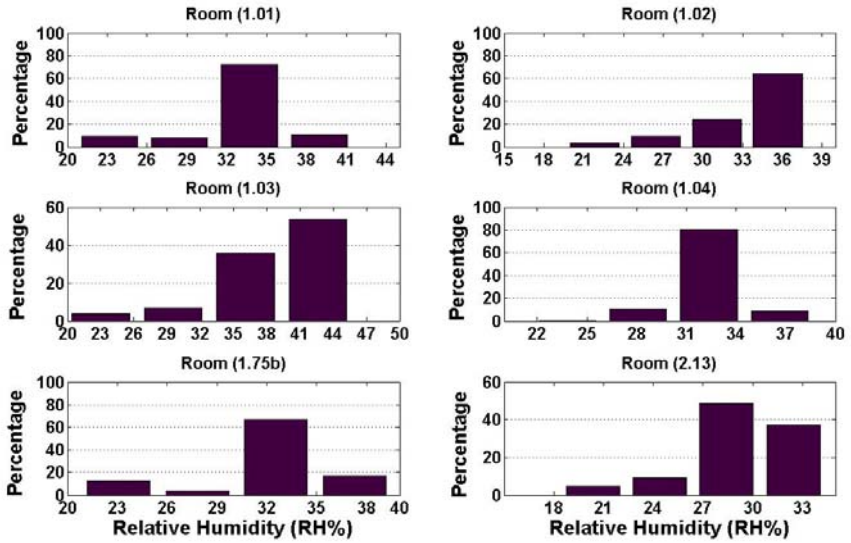

Figure 2: Percentage of indoor relative humidity for all rooms in the east wing

Carbon dioxide is present in the natural environment, being produced by combustion of biological processes. Carbon dioxide is present at typical levels of about 360 ppm in the

ambient urban environment though this can rise substantially inside occupied buildings. The American Society of Heating, Refrigerating and Air Conditioning Engineers (ASHRAE) recommend that carbon dioxide levels should not exceed 1000 ppm inside a space. However, carbon dioxide levels are often used as a guide to whether or not a space has a sufficient quantity of fresh air.

The indoor CO_2 levels in 6 rooms were around expected values of 1000 ppm which indicated the presence of fresh air supply. Only one room (1.04) has a CO_2 level higher than the expected value as seen in figure 2.

Room (1.04) exhibited a higher level of CO_2 than 1000 ppm and it was recommended to adjust the ventilation systems (i.e. open windows more often and/or regularly) to achieve the target values of carbon dioxide (see figure 4). Moreover, figure 4 indicates that the indoor CO_2 level followed a pattern in the six rooms. Levels were seen to rise during working days and drop at weekends, and rise again at working days.

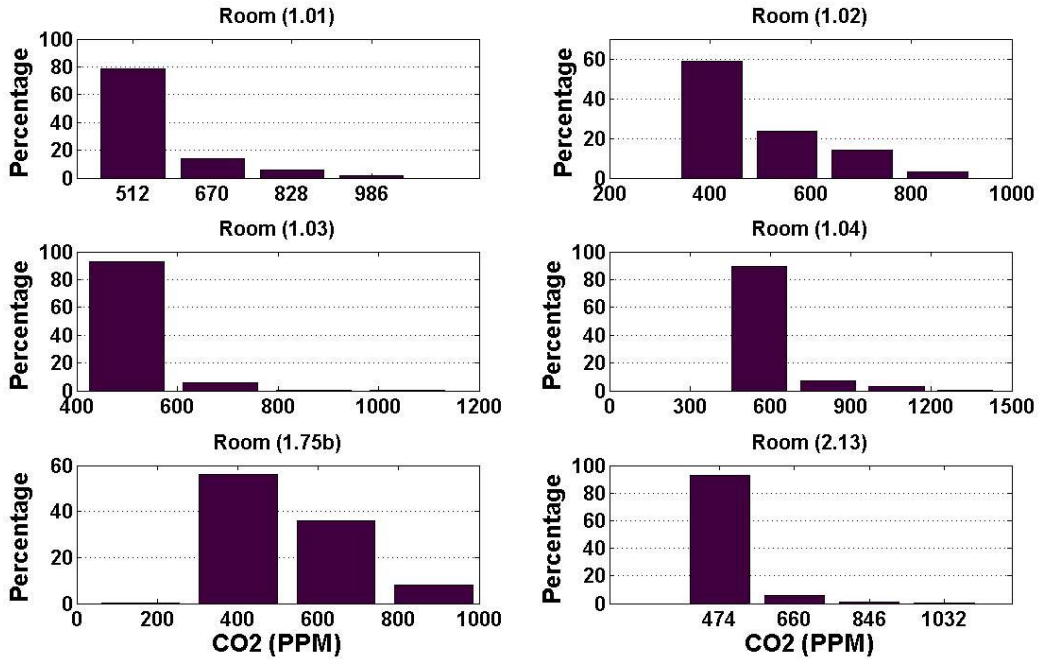

Figure 3: Percentage of indoor CO_2 for all rooms in the east wing

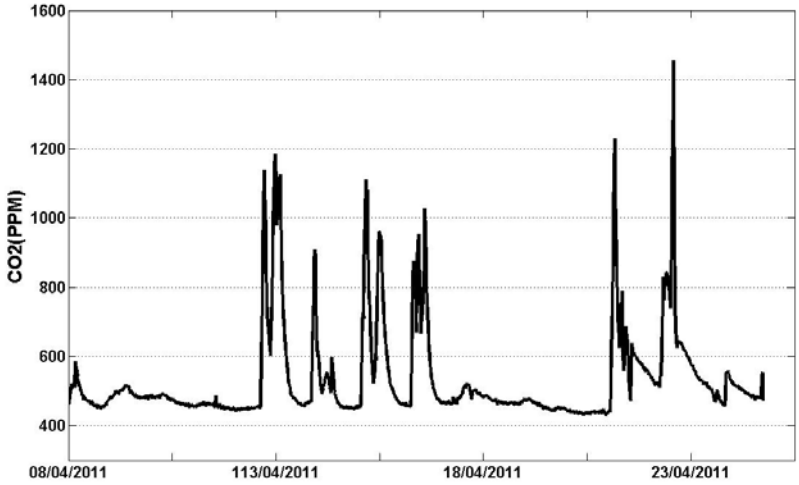

Figure 4: Level of CO_2 in room (1.04)

CONCLUSIONS

This study aimed to investigate air temperature, relative humidity and CO_2 levels in a university office building. In this case, a newly built energy efficient building with a double-skin facade were chosen at the University of Sheffield in England, UK and the study aimed to compare measured values to accepted standard of temperature, relative humidity, and CO_2 for its selected offices. The conclusions from this study are based on a limited number of samples (six offices). To further generalise the results, it would be necessary to do more sampling on a larger population which will be the future work. From this limited data, measured values in April 2010 of relative humidity have been found not to comply with standard guidelines. Levels were under 40% and as a result, it was recommended to use of plants and humidifier as they release steam and moisture into the air which is required in this office environment. The indoor CO_2 levels of one of the rooms have a CO_2 level higher than the expected value and therefore, it was recommended to adjust the ventilation systems by opening windows more often. The study shows that the rising pattern of CO_2 is in the working days which may be due to the increase of indoor human activity.

REFERENCES

[1] Yellamraju, V.: Evaluation and Design of Double-Skin Facades for Office Buildings in Hot Climates, Texas A&M University, Master thesis, 2004, pp. 1.

[2] Hamza, N.: Double versus Single Skin Facades in Hot Arid Areas, Energy and Buildings, 40, 2008, pp. 240–248

[3] http://www.shef.ac.uk/jessop/developmentandbuildings/jessopwest.html

[4] Carrer, P., Maroni, M., Alcini, D. and Cavallo, D.: Allegens in Indoor Air: Environmental Assessment and Health Effects. The Science of the Total Environment, 270, 33-42, 2001.

[5] Molhave, L.: The Sick Buildings – A Sub-population among the Problem Buildings, in Indoor Air ’87, Seifert B., Esdorn, H., and Fischer, M., eds., Proceedings of the IV International Conference on Indoor Air Quality and Climate, Vol. 2, Berlin, Institute for Water, Soil, and Air Hygiene, 469-473, 1987.

[6] Health and Safety Executive (1995). Sick Building Syndrome - Guidance for Employers, Building Owners and Building Managers London: HMSO.

ENVIRONMENTAL STUDY OF WATER-CISTERN AND ICE-HOUSE IN ARID REGIONS THROUGH CASE STUDIES IN YAZD, IRAN

Sadaf Jafari [1]; Dr. Nick Baker [2].

1: MPhil in Environmental Design, Architecture, University of Cambridge, Cambridge, UK, sadafjafari@yahoo.com

2: Department of Architecture, University of Cambridge, Cambridge, UK, NickVBaker@aol.com

ABSTRACT

Today sustainable development is a well-known approach to solve the crisis of the modern world including the damages that human has caused to the nature. On the other hand, environmental design for providing thermal comfort without using fossil fuel is one of the significant characteristics of Iranian historical architecture. Therefore, study and analysis of one of these valuable architectural features became the main subject of this research.

The buildings which are going to be studied in this article are water-cistern and ice-house. These building are brick buildings with large deep underground cisterns which have been respectively fulfilled the people's demand for potable water and ice during hot summers in arid regions of Iran in ancient time. Water-cisterns were filled with cold water in winters, and kept cool through the summer by providing a continuous and natural evaporation of water from their surfaces and being underground and ice-houses were filled with ice during winter and their low temperature were conserved by their underground cistern during summer. The use of cisterns has been diminishing rapidly in Iran because of the widespread use of piped water, household refrigerators and concerns about health issues. They are the valuable historical buildings in Iranian architecture worth of keeping which are fallen into ruin but still can be studied for their environmental lessons. In this article after brief introduction to the case studies and the city of Yazd, the data collected in a water-cistern and an ice-house in small duration of three seasons -winter 2008, spring and summer 2009- will be presented and their thermal behaviour will be analyzed. Then with comparison of their behaviour with each other and with the outside temperature and considering differences in their physical features the reasons of their performance and their efficiency will be described. Also their behaviour in the three different seasons will be compared.

Keywords: water-cistern – hot and arid climate – environmental design – ice-house

INTRODUCTION

The concept of using the ground for cooling the living spaces is not a new idea and has been used through the history and modern world by means of earth-sheltered buildings or ventilating the building by using the air that passed through one or several underground tunnels.

The examples of this technique which has been applied in Iran and its neighbouring countries for several centuries are water-cistern and ice-house.

By testing this idea as a cooling source, we can both keep these buildings safe and use the similar pattern for cooling more buildings.

THE CASE STUDIES

Climate of Yazd: Yazd is located beside the central mountains, far from the sea and adjacent to two deserts, and has an arid and semi-arid climate with the average annual rain fall of 60 millimetres. Its air temperature during summer frequently gets above 40 ° with blazing sunshine and no humidity. [1]

The case studies: The first objective of the data collecting was to compare an above-ground building with an underground building through an experiment. Four buildings with brick construction (heavy thermal mass) have been chosen: 1- Tomb (Boghe): a semi-open building above the ground, 2- Pigeon-house: an almost closed building above the ground, 3- Water-cistern: a semi-open building under the ground, 4- Ice-house: an almost closed building under the ground. The mentioned buildings were preserved and almost untouched except the water-cistern that an above ground building has been added over its entrance stairs (which will be called parent building in this paper) and is used as a small museum It is usually open to the public from 9am to 1pm and 3pm to 6pm. Figure 1 and 2 show pictures and possible air movement pattern of the selected buildings.

Temperature Monitoring: According to the fact that the deep ground temperature is relatively stable during a season, one whole day in every season was chosen for monitoring the buildings. Therefore, the temperatures for a day in December, March and June of 2008-09 were monitored by data loggers (called tinytags). The surface temperature was collected with the help of infrared thermometers (by hand) once or twice in every period of monitoring. Air velocity was measured by means of anemometer. The recording intervals of 5 minutes were chosen. Small circles in figure 1 and 2 are diagrammatic representation of the location of the data loggers in each building.

Ventilation in each season: In December and June, the only ventilation in the water-cistern was between the two wind-catchers as the openings of the above ground building connected to it were closed. However, should be noted that the wind speed during winter in Yazd is high. But, in March, the ventilation in the water-cistern consisted of normal ventilation between the two wind-catchers and from the wind-catchers toward the parent building. The openings on the two sides of the parent building were open during occupancy hours (9am-1pm and 3pm-6pm).Because of the high wind velocity inside the building above-ground, the air entering the water-cistern through the wind-catchers would pass the cistern and exit from the openings of the parent building, so the ventilation rate is also high in the cistern.

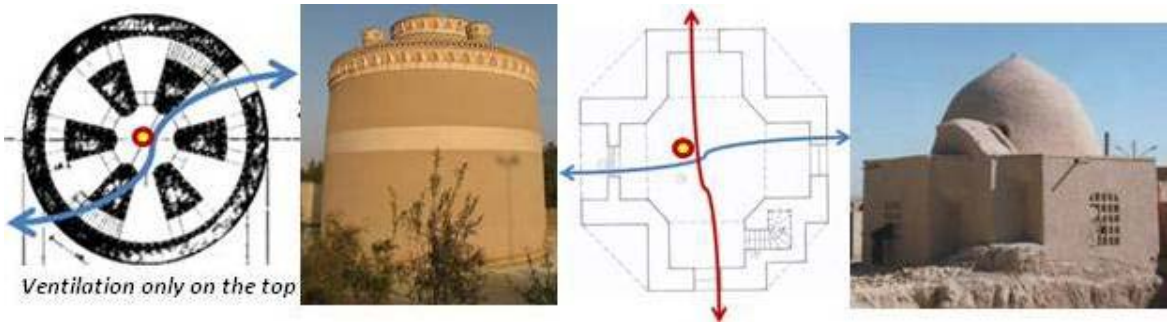

Figure 1: Picture and plan: The pigeon-house– On the left, the tomb – On the right

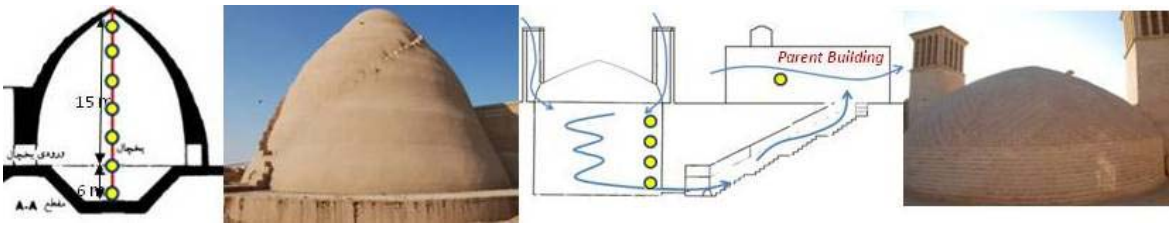

Figure 2: Picture and section: The ice-house – On the left, water-cistern which is restored as a museum and is connected to a building above the ground (called parent building) – On the right

MONITORING AND THE RESULTS

The data collected in the three different periods are presented in the form of graphs in the following figures and their results are analyzed.

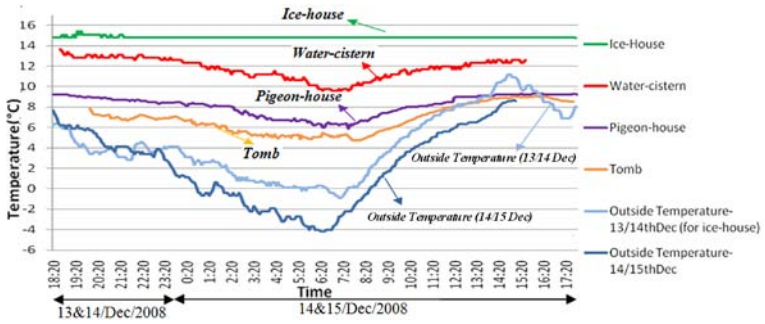

Figure 3: Thermal Performance of 4 buildings in December.

Observations: The average temperature and the temperature fluctuation for the inside and outside of the buildings are shown in the following table. It can be seen that the most stable temperature is in the ice-house which has the least ventilation and is underground and the most fluctuation happens in the tomb which is aboveground and has the most ventilation. The fluctuation in the water-cistern is more than the pigeon-house because of more ventilation. However, the mean temperature in the water-cistern is 3 to 4 °C more than the pigeon-house because of it being underground. This proves that the ground can have heating effect in winter (even with more ventilation relative to an above-ground building). Even though the pigeon-house has a heavy mass, it is not as effective as an underground building in moderating the interior temperature.

	Average temperature (°C)		**Temperature fluctuations (°C)**		**Average temperature (°C)**		**Temperature fluctuations (°C)**	
The ice-house	4.3	outside	0.5	outside	14.8	inside	0.9	inside
The water-cistern	2.3		2.7		11.7		4.1	
The Pigeon-house	2.3		3.5		8.1		3.4	
The Tomb	2.3		6.5		6.7		4.3	

Table 1: Average temperature and temperature fluctuation of the cases in December.

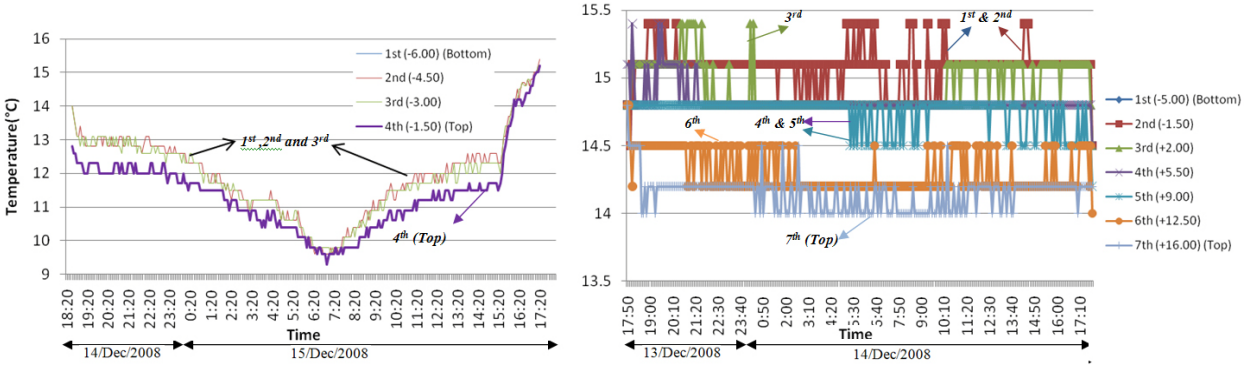

Figure 4: Thermal Performance of the cases in December: the water-cistern– On the left, the ice-house – On the right (to have a more detailed view of the internal temperature the outside temperature has not been presented here.)

Observations: In the water-cistern the temperatures collected by the three lower data loggers are almost the same (average temperature of 11.7 °C). However, the forth one which is on the top shows lower temperatures (average of 11.1 °C) due to direct contact with ambient air which circulates between two wind-catchers. In the ice-house approximately the higher it gets the lower the temperature becomes; (1st= 14.7, 2nd= 15, 3rd= 14.9, 4th= 14.8, 5th= 14.7, 6th= 14.3, 7th= 14.1 °C). The one at the top is the coldest as it is the closest to the hole in the apex of the dome. When the air next to the apex becomes colder and denser, it goes down and gradually become warmer again (even before reaching the bottom of the ice-house as the height is too much). In general however, there is no significant difference in temperature in the ice-house in different points from the bottom to the top and it remains almost stable during a whole day.

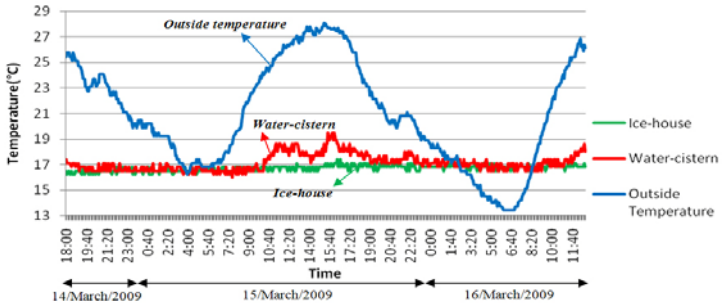

Figure 5: Comparison of Thermal Performance of the ice-house and the water-cistern in March

Observations: As expected, the temperature fluctuation in the water-cistern is higher than the ice-house. But at the time of no ventilation, water-cistern temperature is almost the same as the ice-house temperature. The small difference of 0.5 °C between the average temperature of the water-cistern and that of the ice-house is due to the temperature fluctuations when ventilation exists.

	Average temperature (°C)	Amplitude of fluctuation (°C)
The ice-house	16.6	1.2
The water-cistern	17.1	3.5
Outside	22.4	11.9

Table 2: Average temperature and temperature fluctuation of the cases in March.

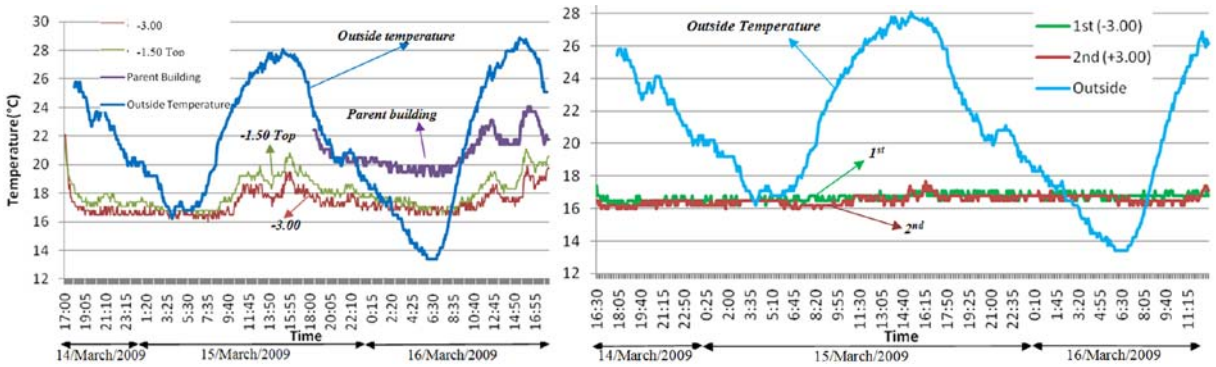

Figure 6: Thermal Performance of the cases in March: the water-cistern– On the left, the ice-house – On the right

Observations (the water-cistern): The average temperature at – 3.00 is 17.3 °C and at – 1.50 is 18 °C which show thermal stratification. Although the outside temperatures differ in the first and second day of monitoring, the interior temperature of the cistern does not change significantly from day 1 (average temperature of 17.5 °C) to day 2 (average temperature of 17.7 °C). Even this slight difference is due to the high ventilation rate in the occupancy hours and shows that, as expected, the inside temperature does not follow the outside temperature unless when the ventilation rate is so high. On the other hand, the amplitude of temperature fluctuation at – 3.00 is 3.4 °C compare to 4.9 °C in the parental building. It affirms that although the ventilation rate is the same, the temperature fluctuation in the underground is less than an over-ground heavy mass building.

Another observation is that the temperature of the cistern which is stable (about 16.5 °C) increases at occupancy hours (from 9am-1pm and from 3pm-6pm) that doors in the parental building are open and therefore the ventilation is higher. Additionally, the surface temperature (collected by the infrared thermometers) also shows increase after a time of high ventilation (compare 6pm on the 14th (about 15.3 °C) after 7 hours of high ventilation to 12pm on the 16th (about 13.7 °C) after 3 hours of high ventilation) and thus the underground cistern cannot have the same cooling effect after longer duration of high ventilation as it has for a lower ventilation rate. This is because the rate of ventilation is higher relative to the cooling capacity of the cistern. The conductivity of soil cannot compensate for this amount of ventilation rate and is less efficient in this situation.

Observations (the ice-house): Although the outside temperatures differ from day 1 to day 2 of monitoring, the interior temperature of the cistern with average of 16.6 °C does not differ. As expected, the inside temperature does not follow the outside temperature at all. Comparing the fluctuations at +3.00 (1.7 °C) and -3.00 (1.2 °C), which is under the ground, avers a higher amplitude of fluctuation for +3.00.

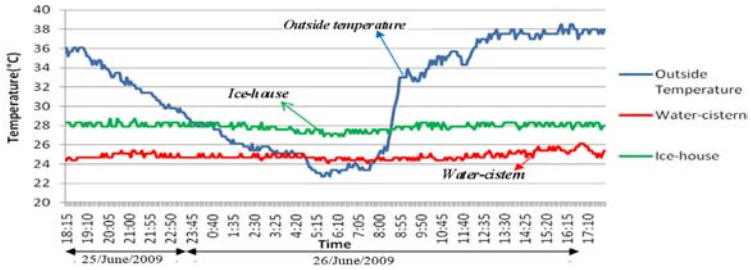

Figure 7: Thermal Performance of The ice-house and the water-cistern in June.

Observations: While the amplitude of fluctuation of outside temperature is 15.8 °C, both of the buildings temperatures remain stable. On the other hand, the average temperatures for the outside, the ice-house and the water-cistern are 31.2 °C, 27.9 °C and, 24.8 °C respectively. The ice-house average temperature is 3.3 °C higher than that of the water-cistern. This can be explained as follow: The roofs in both buildings gain heat from high solar radiation in Yazd which would consequently increase the thermal radiation heat exchange between the cisterns and the ceiling. However, there are two differences between the two buildings' conditions; first the high rate of ventilation under the dome in the water-cistern which according to [2] keeps the ceiling temperature of the dome at about the air temperature all the time; and second the bigger dome of the ice-house relative to the water-cistern would result in more heat gain from the sun and even the very hot ambient air.

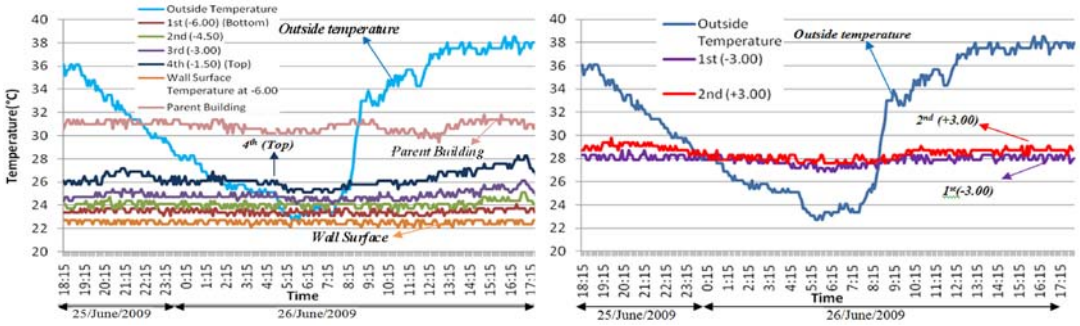

Figure 8: Thermal Performance of the cases in June: the water-cistern– On the left, the ice-house – On the right

Observations (the water-cistern): The average temperatures from the bottom to the top in the water-cistern were 23.5, 24.1, 24.9 and 26.3 °C respectively which show significant thermal stratification due to no air mixture and obvious heat source (ambient air). The process starts when the air becomes warm and goes up and as there is no source to cool it, the air partly remains under the dome and partly exits from the wind-catchers and since the air is not a good conductor the lower layers don't gain heat and so results in stratification.

The average surface temperature is 22.5 °C with 0.6 °C amplitude of fluctuation. This confirms that when the ventilation rate inside the cistern is not high (because the openings of the above building are closed and the only ventilation is between the two wind-catchers) the surface temperature does not change and it has the capacity to remain stable and also cools down the air inside it.

The temperature fluctuations in the water-cistern are 1, 1.7, 2 and 3.2 C from bottom to top. Comparing these numbers to the outside fluctuation of 15.8 again shows the stabilizing effect of being underground.

The average temperature inside the above building is 30.9 with amplitude of fluctuation of 2.4. By comparing this with the cistern temperature, it was concluded that when the ventilation rate is higher inside the cistern relative to the building (like the temperature at top of the cistern), even though the

amplitude of fluctuation would be higher (3.2 compare to 2.4 °C), but the general temperature would be lower. This confirms the cooling effect of the underground building in addition to its stabilizing effect (dampening the temperature fluctuation) compared to a heavy mass building.

Additionally,, the inside temperature of the cistern during the night in June ranges about 0.4 to 2.4 °C lower (from the bottom to the top) than the minimum outside temperature. This shows that at night, sometimes the air inside the cistern is warmer than outside. It can be argued that in these situations, the ambient air would have more cooling effect for the building than the air from the water-cistern and letting more ventilation to the cistern at night makes the cistern even cooler during the night to being more efficient for cooling during the following day.

Observations (the ice-house): The amplitude of fluctuation at +3.00 (2.2 °C) is higher compared to -3.00 (1.8 °C) which is under the ground. The average temperature of 28.5 °C at +3.00 and 27.9 °C at -3.00 show thermal stratification. Although there is not enough air ventilation as a heat source but the ice-house absorbs heat through its envelope which is a massive dome with the height of 15 meters.

DISCUSSION

In this article, we first compared the temperature of four heavy mass buildings (1-ventilated above the ground, 2- closed above the ground, 3- ventilated under the ground and 4- closed under the ground) and the results confirmed the conditioning and stabilizing effect of the underground construction.

Afterwards, we analysed the monitoring of an ice-house and a water-cistern in three seasons (winter, spring and summer), from which the following conclusions are drawn:

In none of the seasons, monitoring buildings showed any significant temperature variation in contrast with the variable outside temperature during a day which is of course one of the weather characteristics of desert areas. This again confirms the dampening effect of underground buildings which is the main reason for using this system as a ventilating and cooling system.

Temperature fluctuation in the ice-house was less than the water-cistern which is because of less ventilation and infiltration. This comparison along with different temperature of the water-cistern with different ventilation rates shows that ventilation at certain rates does not change the interior temperature of the cisterns while the high ventilation rate (as can be seen in the water-cistern in March) can have noticeable influences and even sometimes can be useful like it was seen at nights in June. Furthermore, ventilation can have more positive effects as it is seen in June which the warmer dome of the ice-house (without any ventilation) compare to the cooler dome of the water-cistern (with ventilation) can have negative effects. Another result is that the portion of the building above the ground compare to its portion inside the ground can have different influences on its cooling performance.

Table 3 show that the increase of the temperature from winter to summer which is 10.2 °C for inside the water-cistern compare to 28.8°C for outside temperature.

	Winter day	**Spring day**	**Summer day**	**Alteration**
Average outside temperature °C	2.4	17.1	31.2	28.8
Average water-cistern temperature °C	13.8	22.4	24	10.2

Table 3: Comparison of outside and the water-cistern average temperature from winter to summer

REFERENCES

1. Memarian, Gholamhosein. Going through Architecture of water cisterns in Yazd. Tehran : University of Elm va Sanat, 2004. written in Farsi.
2. Hagighat, M.N. Bahadori and F. Passive cooling in hot, arid regions in developing countreis by employing domed roofs and reducing the temperature of internal surfaces. Building and Environment. 1985, Vol. 20, pp. 103-113 .

OPTIMIZATION OF GLAZING AREA FOR HUMAN THERMAL COMFORT FOR COLD STATIONS OF INDIAN REGION

Ranjana Jha, Nikhil Jindal and Sarita Baghel
School of Applied Sciences, Netaji Subhas Institute of Technology, Dwarka, New Delhi 110078, India

ABSTRACT

This study is to optimize the glazing area to ensure the thermal comfort inside a building (i.e. room temperature 20 ± 2°C) for two different kinds of climatic zones i.e. cold-sunny (Leh, -14°C to -2.8°C) and cold-cloudy (Shillong, 3.6°C to 15.5°C). Single zone isolated house, having dimension 4m × 4m × 3m, has been analyzed in this study. The periodic solution of the heat conduction equation describing heat transmission through the different building components, floor, walls and roof has been adopted. Ambient temperature and total solar radiation intercepted by building envelope have been represented through Fourier series. Traditional construction with 22 cm thick brick wall, plastered 15 mm on both sides (U=2.0 W m^{-2} K^{-1}) and the other construction of same dimensions, but insulated with 10 cm of expanded polystyrene insulation on four walls and roof (U= 0.31 W m^{-2} K^{-1}) have been analyzed. It is observed that for the two stations considered, different glazed areas are not able to ensure thermal comfort if the building is traditional. If the building is insulated, 15% for Shillong and 40% for Leh is sufficient to ensure thermal comfort inside the building.

1. INTRODUCTION

In this study, with the help of the periodic solution of heat conduction equation, the explicit expressions for time variation of the room air temperature inside a building have been obtained. Glazing on the south wall has been taken to allow direct solar gain. As the expression completely depends on an exact energy balance, they can be used in any kind of climatic zone for any building. The calculations are performed for two types of climatic zones i.e. cold-sunny and cold-cloudy. The amount of glazing area is calculated to ensure the thermal comfort inside the building for each of two climates.

2. MATHEMATICAL MODELING

A single zone isolated house, having dimension 4m × 4m × 3m, has been analyzed in this study. The heat flows through fours walls, roof and ground by conduction. The inside room air exchanges the heat by convection with the internal surfaces of the room. There is a direct gain of heat via window i.e. glazed area. The heat exchange between the inside room air and the ambient air is in the form of ventilation and infiltration. The heat flux which contributes towards room temperature by each mode is calculated and summed over all the modes. The rate of increase in internal energy of the room air is equal to the sum over all the modes of heat gain. This results in an energy balance equation in terms of a Fourier series of harmonics for each variable.

The well known conduction equation for heat flow through a solid is given as

$$k \frac{\partial^2 T}{\partial x^2} = \rho c \frac{\partial T}{\partial t} \qquad (1)$$

The heat flux transmitted through the walls and roof can be expressed as

$$\dot{Q} = A\sum_{n=-\infty}^{+\infty} \frac{S_n\left(T_{rn} + \frac{\alpha_i I_{iwn}}{h_i}\right) - \left(T_{an} + \frac{\alpha_o I_{on}}{h_o}\right)}{Q_n} \times \exp(in\omega t) + A\sum_{n=-\infty}^{+\infty}(\alpha_i I_{iwn})\exp(in\omega t) \quad (2)$$

The floor has been treated as a semi-infinite medium, the energy flux through the floor is obtained as

$$\dot{Q} = A_F \sum_{n=-\infty}^{+\infty} \frac{S_n\left(T_{rn} + \frac{\alpha_i I_{ifn}}{h_i}\right)}{Q_n} \exp(in\omega t) \quad + A_F \sum_{n=-\infty}^{+\infty}(\alpha_i I_{ifn})\exp(in\omega t) \qquad (3)$$

Hourly calculations have been done for the direct gain through the glazing. The effect of direct gain has been found hourly by assuming that floor is absorbing 60% of radiation and 8% is absorbed by each of the four walls and ceiling.

The heat gain due to infiltration of air from ambient into room has been calculated from the expression

$$\dot{Q} = C_{inf}\sum_{n=-\infty}^{+\infty}(T_{an} - T_{rn})\exp(in\omega t) \qquad (4)$$

The expression for ventilation heat gain is given as

$$\dot{Q} = \sum_{n=-\infty}^{+\infty} C_v (T_{an} - T_{rn})\exp(in\omega t) = \sum_{m=-\infty}^{+\infty}\sum_{n=-\infty}^{+\infty} C_{vm}(T_{an} - T_{rn}) \times \exp\{i(n+m)\omega t\} \qquad (5)$$

Heat conduction through the glazing and the door has been expressed in terms of their respective U-values, i.e.

$$\dot{Q} = AU\sum_{n=-\infty}^{+\infty}(T_{an} - T_{rn})\exp(in\omega t) \qquad (6)$$

Room air temperature has been calculated by the net amount of heat gain/loss by the room air through all its components. It has been expressed in the form of energy balance equation as

$$M_r \frac{d}{dt}\left[\sum_{n=-\infty}^{+\infty} T_{rn}\exp(in\omega t)\right] = \sum_{j=2}^{6} Q_j \qquad (7)$$

The hourly variation of room temperature is expressed as

$$T(t) = \sum_{n=-6}^{+6} T_{rn}\exp(in\omega t) \qquad (8)$$

3. INPUT DATA

The structure of walls and roof used in this study has been given in Fig.1 and Fig.2 respectively. 10 cm of RCC has been considered on floor. And 10 cm of expanded polystyrene has been provided on the external surfaces of all walls and roof to account for the effect of insulation on the room temperature. Glazing area has been expressed as a percentage of floor area and it has been provided on the south wall only. Table 1 is showing the standard values of thermophysical properties of the materials used in this particular problem for simulation. Other related parameters used in the thermal analysis have been provided below.

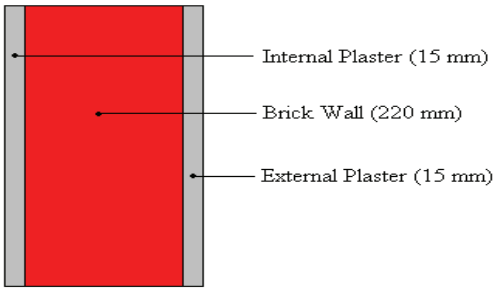

Fig. 1 Structure of the External Wall.

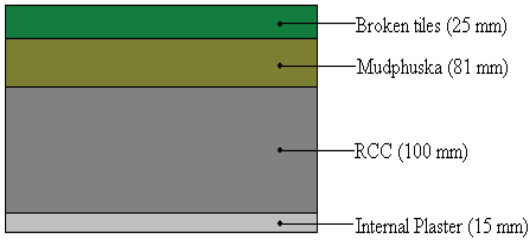

Fig. 2 Structure of the Roof.

Table 1. Thermo-physical properties of the building material used in this study

S. No.	Material	Specific Heat ($J\ kg^{-1}\ K^{-1}$)	Density ($kg\ m^{-3}$)	Conductivity ($W\ m^{-1}\ K^{-1}$)
1.	Brick	880	1820	0.81
2.	RCC	880	2280	1.58
3.	Plaster	840	1762	0.72
4.	Broken Tiles	880	1820	0.81
5.	Mudphuska	880	1622	0.52
6.	Insulation (Expanded Polystyrene)	1340	34	0.035

Table 2. Meteorological hourly data of the four stations used in this study

T: Ambient Temp. (°C); G: Global Radiation ($kWh\ m^{-2}$); D: Diffuse Radiation ($kWh\ m^{-2}$)

Time (hr)	Leh			Shillong		
	T	G	D	T	G	D
1	-12.5			5.1		
2	-13.1			4.6		
3	-13.6			4.1		
4	-13.9			3.7		
5	-14.0			3.6		
6	-13.8	0.100	0.100	3.8	0.100	0.100
7	-13.2	0.100	0.100	4.4	0.116	0.108
8	-12.2	0.207	0.129	5.5	0.284	0.139
9	-10.8	0.362	0.146	7.1	0.457	0.153
10	-9.1	0.485	0.156	8.8	0.595	0.163
11	-7.2	0.565	0.161	10.9	0.679	0.167
12	-5.4	0.592	0.163	12.8	0.708	0.168
13	-4.0	0.565	0.161	14.2	0.679	0.167
14	-3.1	0.485	0.156	15.1	0.595	0.163
15	-2.8	0.362	0.146	15.5	0.457	0.153
16	-3.1	0.207	0.129	15.1	0.284	0.139
17	-3.9	0.100	0.100	14.3	0.116	0.108
18	-5.2	0.100	0.100	13.0	0.100	0.100
19	-6.6			11.5		
20	-8.1			9.9		
21	-9.3			8.6		
22	-10.4			7.4		
23	-11.3			6.5		
24	-12.0			5.7		

1. *Heat transfer coefficients (W m^{-2} K^{-1})*
   Wall; External surface h_o: 20.00, Internal surface hi: 8.29
   Roof; External surface h_o: 23.00, Internal surface hi: 9.26
2. *Transmission of glazing, τ for single glazed (dimensionless) : 0.85*
   τ for double glazed (dimensionless) : 0.73
3. *Solar radiation absorption, α (dimensionless)*
   Wall; External surface α_o: 0.40, Internal surface αi: 0.08
   Roof; External surface α_o: 0.70, Internal surface αi: 0.08
   Floor α_i: 0.60

Leh (Latitude 34°09'N; Longitude 77°34'E; Altitude 3514m) and Shillong (Latitude 25°34'N; Longitude 91°53'E; Altitude 1500m), have been chosen for this study. Leh represents a cold and sunny climate while Shillong belongs to cold and cloudy climatic conditions. January, the coldest month of India has been chosen for simulation. The Table 2 is showing the monthly mean hourly temperature, global radiation and diffuse radiation [4].

3. RESULTS AND DISCUSSION

The results have been obtained in terms of hourly variation of room temperature for a typical winter day for Leh and Shillong. The effect of glazing area upon the room temperature, for different combinations of U-values of walls and roof has been determined.

3.1 Cold and sunny region; LEH

Leh is having cold and sunny climate where the ambient temperature varies from -14°C to -2.8°C in winter month (January). For this station, only well insulated building is considered. For the traditional building, no amount of glazed area can ensure the thermal comfort. In an insulated building, the inside room temperature has been calculated on hourly basis for the five different values of glazed area i.e. 10%, 20%, 30%, 35% and 40%.

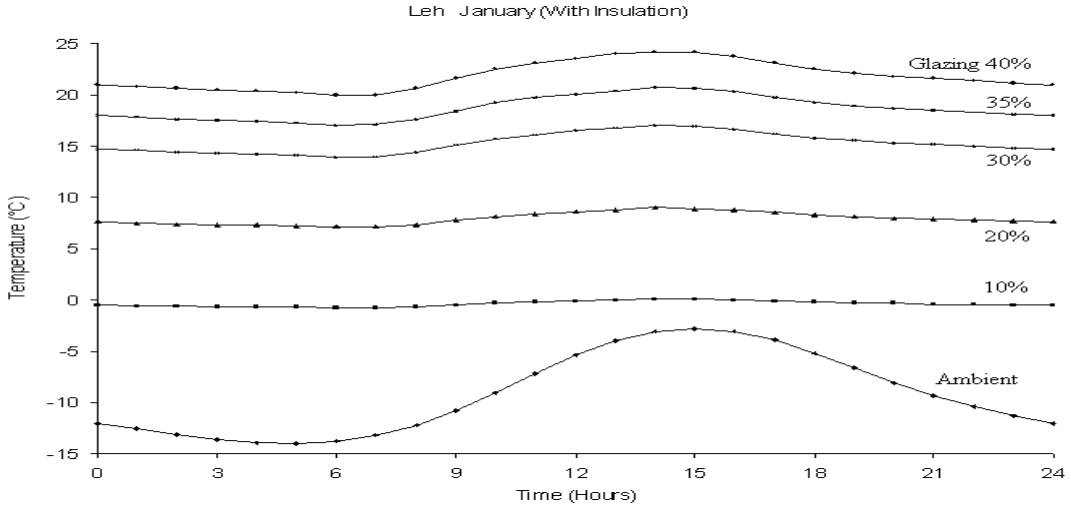

Fig. 3. Time variation of room air temperature in severe cold conditions at Leh, for different glazing areas (U= 1.5 W m^{-2} K^{-1} in day and 0.5 W m^{-2} K^{-1} in night); glazing, % of floor area, ACH=0.5;

3.2 Cold and cloudy region; Shillong

Shillong is having different climate than Leh i.e. cold and cloudy. Here the effect of glazed area has been optimized for insulated as well as non-insulated buildings. The results are shown in Fig. 4. It has been observed that glazing is beneficial for the insulated buildings only.

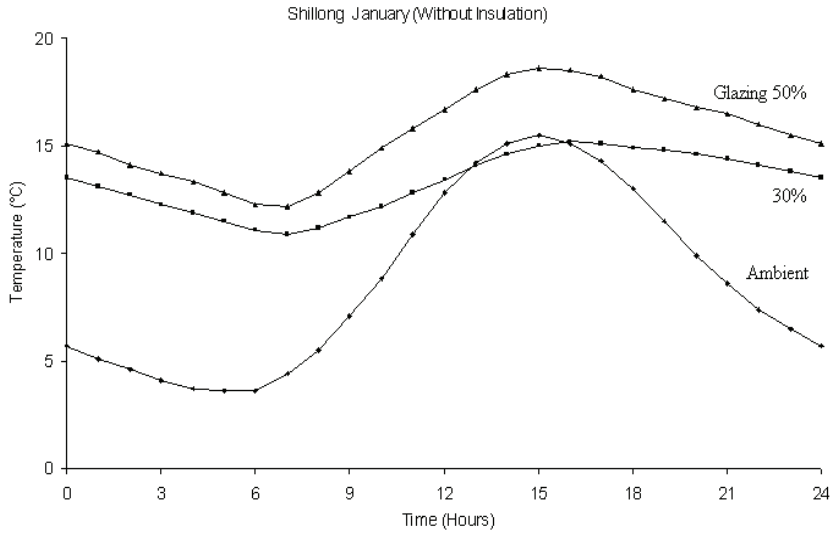

Fig. 4. Time variation of room air temperature for a non-insulated building at Shillong, for different glazing areas (U= 5.0 W m^{-2} K^{-1}); glazing, % of floor area, ACH=1.0;

For a well insulated building, four different values of glazed area have been used to decide the optimum area of glazed surface to get the comfortable room air temperature.

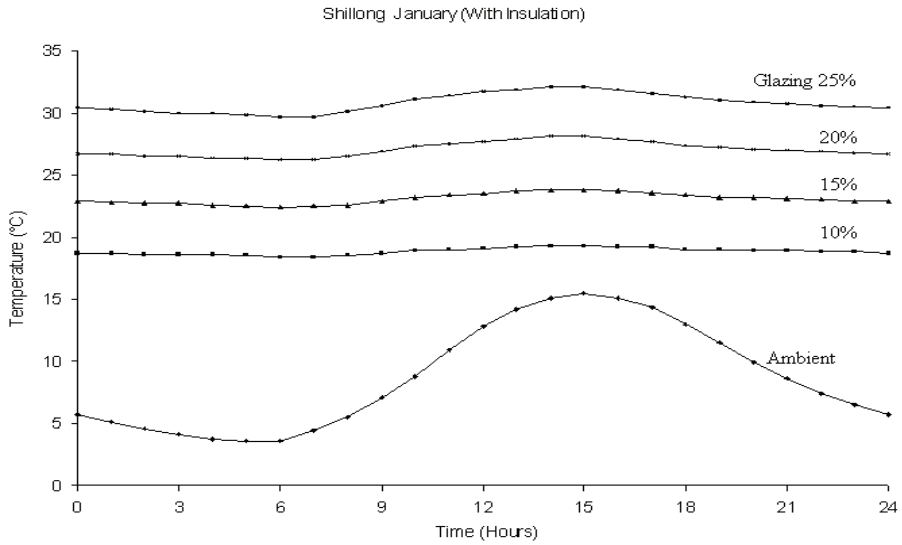

Fig. 5. Time variation of room air temperature for an insulated building at Shillong, for different glazing areas (U= 1.5 W m^{-2} K^{-1} in day and 0.5 W m^{-2} K^{-1} in night); glazing, % of floor area, ACH= 0.5;

4. CONCLUSIONS

1. The insulation on the outside surface of walls is having significant effect on room air temperature as well as on the swing of this temperature. The temperature swing is about 3°C to 4°C.
2. For the two stations considered here, if the building is non insulated, the amount of glazed area which ensures thermal comfort becomes too large and hence impracticable.
3. With insulation on the external surface of the building it has been observed that
    a) For Leh, 40% of the glazing area gives a comfortable room air temperature where the climatic condition is cold and sunny.
    b) For Shillong where the difference in max. and min. ambient temperature is about 10°C, 15% of the glazed area is advised to use for the building.

NOMENCLATURE

A area of the fabric (m^2); A_F area of the floor (m^2)
C heat transfer coefficient for air exchange ($W\ K^{-1}$)
C_{inf} infiltration coefficient; C_v ventilation coefficient
c specific heat ($J\ kg^{-1}\ K^{-1}$)
h convective heat transfer coefficient ($W\ m^{-2}\ K^{-1}$)
I radiation flux ($W\ m^{-2}$); L thickness (m)
k thermal conductivity ($W\ m^{-1}\ K^{-1}$); M thermal mass ($J\ K^{-1}$)
N number of air exchanges per hour
$\dot{Q}$ rate of heat flow across any fabric surface (W)
$\dot{q}$ rate of heat flow across any surface per unit area ($W\ m^{-2}$)
T temperature (°C); t time (sec)
ACH Air changes per hour
Q, S as defined by Eq (3) (see mathematical modeling)
U conduction transmittance ($W\ m^{-2}\ K^{-1}$)
V volume of room (m^3)
X coefficient matrix of order 13×13
Y column matrix of order 13×1

Greek letters

ρ density ($kg\ m^{-3}$); α absorptivity (dimensionless); ω angular frequency, $w = 2\pi/86{,}400$ rad s^{-1}

Subscripts

a air; d door; f floor; i inside surface; n nth harmonic; o outside surface;
r room; v ventilation; w wall; WN window;

REFERENCES

[1] Balcomb, J.D., Designing Passive Solar Buildings to Reduce Temperature Swings, Report Submitted to Arizona State University, Department of Architecture, Tempe, AZ, 1978.

[2] Wray, W.O., Design and Analysis of Direct Gain Solar Heated Buildings, Report No. LA-8885-MS, UC-59C, Los Alamos Scientific Laboratory, University of California, 1981.

[3] Bansal, N.K., Garg S.N., Lugani N. And Bhandari S.N., Determination of Glazing Area in Direct Gain Systems for Three Different Climatic Zones, Solar Energy 53 (1994) 81-90.

[4] Bansal, N.K. and G. Minke, Climatic Zones and Rural Housing in India, KFA, Jülich, 1988.

SUSTAINABILITY IN THE HISTORIC BUILT ENVIRONMENT - UPGRADE OF ENVIRONMENTAL PERFORMANCE OF LISTED STRUCTURES. THE HISTORIC CHURCHES IN THE UK.

M. Makrodimitri[1]; J.W.P. Campbell[2]; K. Steemers[3];

1, 2, 3: University of Cambridge, Department of Architecture, 1 – 5 Scroope Terrace, CB2 1PX, Cambridge, UK

ABSTRACT

The environmental management of listed buildings provides particularly difficult challenges, both because any necessary alterations have to avoid destroying the historic character of the building and because changes in the internal environment can easily have unexpected effects on sensitive historic fabric. This research focuses on a particular type of historic building: – the church. Managing churches in the UK environmentally is a great challenge as more than 2/3 of churches (16,000 in total) are listed buildings. Thus conservation of historic fabric needs to be carefully considered before adjustments are made. The paper suggests that the environmental performance of historic churches (and similar spaces) is highly dependent on the improvement of building services. The research looks specifically at the potential of adapting efficient heating systems and strategies to the historic church environment and is based on the results of a four case-study surveys undertaken in church buildings in Cambridge.

INTRODUCTION

Making an existing building more sustainable often means retrofitting environmental adaptation measures to the building envelope. In the modern structures this is achieved by insulating, sealing and draught-proofing the building envelope, which promises reduced heat losses via walls, ground floors, roofs and loose windows frames. However, historic structures are 'leaky', and much of the required ventilation is provided by this air leakage [1]. Sealing and draught-proofing can often cause deterioration of the internal fabric and have a detrimental impact on the overall Indoor Air Quality and the occupants' health. Reduced ventilation rates can result in damp indoor environments. Failure of excessive moisture to be removed can have adverse impacts on historic fabric and artefacts due to mould growth; and condensation of vapours on cold walls, ceilings, floors and glass surfaces. Moreover adequate air-movement is required to avoid dust and smoke from candles and open fires settling on the historic fabric and other elements.

In most cases, in listed buildings, improvements to the fabric cannot be implemented, especially those with important interiors, fixtures, fittings and details [2]. Special attention has to be given to ensuring that the building structure and elements are well understood, minimising any adverse impact on the existing fabric and only making changes to mechanical services which do not damage the internal fabric [3].

THE RISKS OF INTERVENTIONS

Listed buildings are often structures with solid walls, permeable materials and no damp-proof courses. Old buildings operate differently than modern structures and may require more ventilation to ensure their conservation and the comfort of their occupants [4].

Interventions on the historic fabric

A wide variety of interventions could theoretically be applied to elements of the fabric of historic structures but each carries risks:

- Windows: Draught stripping, secondary glazing and in some cases double glazing. There is an increased risk of condensation forming on other surfaces if windows are upgraded in this way.
- Floors: Insulation of suspended floors, insulation of solid ground floors and provision of underfloor ventilation and/or heating. Rarely possible because of the historical value of the floor and problems created with rising damp.
- Walls: Rarely possible either internally or externally for archaeological reasons and because of the increased risk of interstitial condensation.
- Roofs: Thermal insulation and ventilation provision of cold roofspaces, warm roof design. Usually possible but with risks of interstitial condensation.

Most interventions to the fabric aim at sealing the structure by limiting any heat losses by conduction, convection and air-infiltration, which often means limiting ventilation. However, older buildings allow moisture to move through the structure. The permeable materials of the historic structures allow the buildings to dry out in balance with any moisture ingress. Therefore any intervention to building envelope should respect the special requirements of historic structures as far as permeability; capillary action and hygroscopicity are concerned.

Heating

Sustainability of historic structures implies that Historic buildings should also be reasonably energy efficient, comfortable and provide healthy indoor conditions. In the case of old churches heating has been installed with the aim of providing thermal comfort for the occupants, with little consideration given to conservation of the building. Most churches use heating only during services. However, this intermittent operation of heating causes sharp fluctuations of relative humidity and major interruptions to the microclimatic conditions of historic buildings [5].

Given that the levels of humidity determine the adequacy of microclimatic conditions in terms of conservation particular care is required to ensure that heating does not cause major disruption to humidity equilibrium between building elements and the ambient indoor environment, which can cause evaporation of water, which is contained in the historic elements and condensation of vapours on cold surfaces. Water vapour condensation can then cause several types of fabric deterioration; **Salt Activity** due to hygroscopic salts dissolution and crystalisation due to humidity sharp fluctuations; **Bio-deterioration** can cause either physical disruption (the microorganisms colonise an area of the affected element), or chemical disruption, due to the by-products, which are produced by the life-cycle of the microorganism; **Dimensional Changes** - Expansion or contraction of different layers of materials, due to Relative Humidity fluctuations can cause flaking on the surfaces of multi layered elements, such as painted wood. [6]

Ventilation

Adequate ventilation strategies are very important for the maintenance of historic structures. Controlled natural or mechanical ventilation needs to ensure removal of excess humidity, dust and smoke from the interior. In the case of natural ventilation schemes, the risk lies on the fact that external air often contains more moisture than the internal; therefore excessive natural ventilation might increase the volume of moisture in the historic structure [6]. Mechanical ventilation usually offers the solution for the control of air movement and microclimate, but the air rates, movement patterns and speed need be carefully regulated and the sound may be a problem [7]. A characteristic example is a parish church in Geneva, which tried to reduce heating costs by adding insulation, in order to make heating system more efficient. Three years after the last renovations, it was observed that the internal surfaces of the naves had already become dusty because of the incense and candle combustion [8].

Energy use and Heating of historic churches

Heating is considered as the major factor that affects the three main axes of sustainability for historic churches: (1) occupants' satisfaction, (2) conservation of historic fabric and artefacts and (3) carbon footprint.

Heating systems and strategies were originally designed to serve economy and thermal comfort requirements, while conservation issues have been very rarely considered [9]. Each heating system has particular benefits and drawbacks in terms of thermal comfort and conservation provision, while it is generally accepted that the heating for historic churches and similar spaces should have the least possible impact on the internal microclimate, which should be maintained in rather stable thermal humidity conditions.

Moreover According to a report of CofE (Church of England) in 2008, space-heating accounts for the majority of carbon emissions from churches [10]. Therefore this study suggests that improving heating services is the most efficient way to enhance the sustainability of listed churches and similar structures and seeks to provide adequate guidance by investigating in depth the impact of different heating systems and strategies on the environmental performance of historic churches.

METHOD

The current study being conducted in Cambridge involves a sustained monitoring of internal environmental conditions coupled with carefully-designed questionnaires used to determine perceived levels of indoor air quality and comfort. Energy consumption of the case-studies is estimated by information collected by regular meter readings. Modelling is also intended to be included in the final project, using advanced simulation software to test possible alternative strategies for improving the indoor conditions. In this paper only part of data from monitoring and questionnaires is presented. The survey has been conducted in four representative churches with different types of heating strategies:

- Gt St Mary's church, Cambridge: Constant Central (Trench) heating
- St Botolph's church, Cambridge: Intermittent Local (Electric Panels on Pews) heating
- All Saints church, Cambridge: Constant Central heating, Thermostatically controlled to keep the church at conservation temperatures (11.5°C -12°C)

- Queens' College Chapel: Central heating with water pipes on windows level.

RESULTS ANALYSIS

The comparison of internal with external temperatures during a typical Sunday in Winter shows that the thermal mass of the churches help the structures maintain internal temperature that are higher than external conditions. (Figure 1a) Those with central heating systems have relatively stable thermal conditions throughout the day, even when services with large congregations take place, while the church with intermittent heating operation (St Botolph's) manages to provide quite high temperatures during services and afterwards maintain higher temperatures than at the beginning of the day. Therefore although historic churches are leaky structures due to high infiltration rates through doors and un-insulated fabric they provide a building envelope, which responds well in environmental terms.

However relative humidity is more problematic. Low comfort temperatures of 20°C and relative humidity 40% - 70% are likely to provide pleasant conditions but for conservation, RH needs be kept within the range of 30% – 60% [11], to ensure that conditions are neither too humid nor too dry. Regressing Temperature against Relative Humidity, offers a clear view of condition patterns in the case-studies [12]. The intermittent local heating in St Botolph's church produces dispersed results due to large fluctuations of Temperature (°C) and RH(%), which increases the risk of deterioration [9]. Apart from All Saints church, Central heating systems produce less scattered data and seem to offer more reasonable conservation and comfort conditions. (Figure 1b)

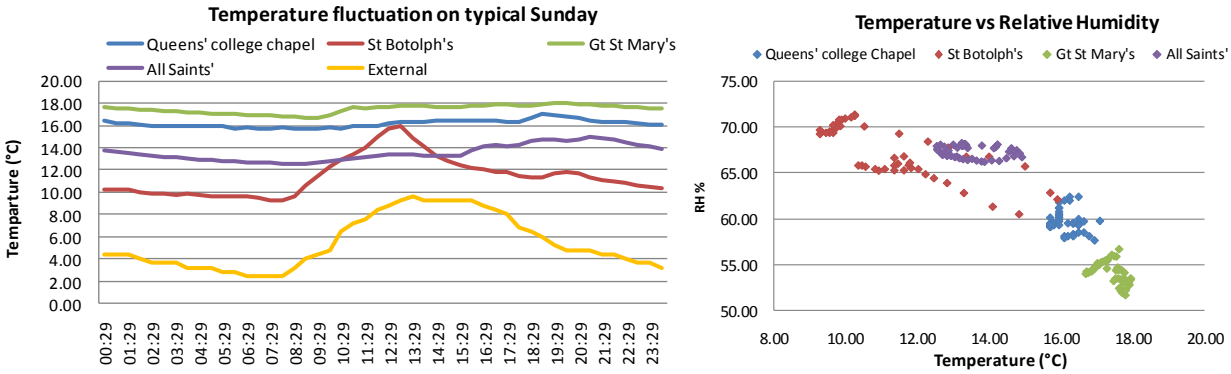

Figure 1: a). Left: Temperature fluctuations on a Typical Sunday (24/10/2010). b). Regression of temperature against Relative Humidity during a typical Sunday

In terms of thermal comfort provision, several factors can affect the thermal comfort perception by the occupants: (1) personal variables (Activity, Age, Clothing, Sex, etc.) and (2) physical variables (air temperature, humidity, surface temperatures, air movement), which were taken into account while conducting survey with Questionnaires.

The intermittent local heating system (St Botolph's church), provided the highest percentage of votes indicating that thermal conditions in the church during services are within the cold range of the thermal comfort scale. It is also interesting to notice that although the All Saints system was initially set to heat the church to low temperatures for conservation reasons, it achieved a higher percentage of temperatures which provided satisfactory. (Figure 2) Therefore heating the whole hall volume (regardless of whether to low or high temperatures), seems to be a more effective way of achieving comfort conditions, as it helps maintain the

radiant temperatures of the fabric at a relatively high level and thus enhance the feeling of warmth.

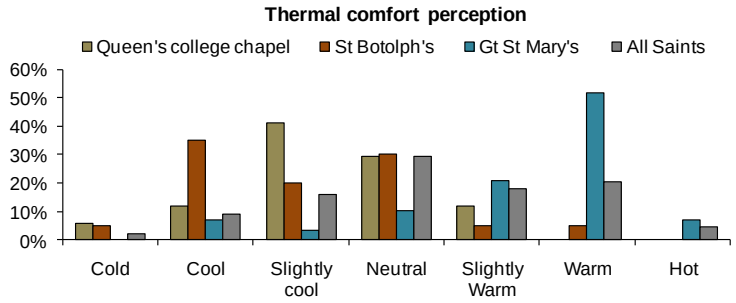

Figure 2: Thermal comfort levels in four case-studies in Cambridge

CONCLUSIONS AND SUGGESTIONS

Most historic churches are listed structures, which retain the historic fabric and host valuable artefacts (paintings, painted wooden ceilings, stained glass windows, historic furnishing, organs etc). Interventions to building envelopes are likely to cause adverse effects to the appearance of buildings and have major negative impacts on the indoor air quality. Therefore environmental adaptation of historic structures should mainly consider correct maintenance and adequate design of building services. In the case of historic churches, heating plays the most important role in total energy consumption, conservation and comfort provision. Therefore major carbon emission reduction, energy savings and improvements in the quality of indoor environment needs to be achieved by appropriate control and design of heating systems and strategies respectively.

The case-study survey has shown that low, constant heating helps to dispel damp and reduce the risk of condensation and keeps the internal conditions within low but acceptable levels of thermal comfort, as higher radiant temperatures occur due to constant heating loads. Therefore, it seems likely that the optimum heating strategy combines ambient warm conditions in low temperatures with a localised heating system acting as an additional source of heat during specific periods, when there is need for increased thermal comfort provision, e.g. Sunday services or other community events.

Time/switch controls with separate time channels can regulate various heating schedules, throughout a seven day period. Suitable heating schedules can then be formed according to the specific heating requirements, frequency of different activities and density of congregation that take place in the building and then major energy savings can be achieved.

Several factors now need to be studied in greater detail. In addition, and especially in connection with under-floor heating, the use of renewable energy sources such as ground heat source in combination with photovoltaics, could reduce or potentially eliminate carbon emissions.

For intermittently heated churches adequate ventilation needs to be provided to remove any excess moisture in the end of popular services. Indoor air movement needs to be adequately controlled by allowing acceptable levels of natural ventilation (occurring by the loose fitting of windows (i.e. infiltration), and opening windows when necessary) together with mechanical controls to regulate the air rates, movement patterns and speed and most of all the

moisture content of the incoming air, thus achieving conservation. Exactly how this is best achieved needs further research.

REFERENCES

1. English Heritage: Energy Conservation in Traditional Buildings, English Heritage, London, 2008
2. DETR (Department of the Environment, Transport and the Regions): The One Stop Shop Approach to Development Consents, London, 1998
3. English Heritage: Building Regulations and historic Buildings. Balancing the needs for energy conservation with those of building conservation: an Interim Guidance Note on the application of Part L, London, 2002
4. NIEA (Northern Ireland Environment Agency): historic Buildings & Energy Efficiency. A Guide to Part F of the Northern Ireland Building Regulations 2006, NIEA Built heritage Directorate, Belfast, 2006
5. Olstad, T.M., Haugen A.: Warm feet and cold art: is this the solution? Polychrome wooden ecclesiastical art - climate and dimensional changes, Contributions to the conference Museum Microclimates, pp 43-49, Copenhagen, 2007
6. Curteis, T.: Environmental Conditions In Historic Churches: Examining Their Effect On Wall Paintings And Polychrome Surfaces, Transactions of the Ecclesiastical Architects and Surveyors' Association, Vol 5, pp 36 – 46, Leeds, 2004
7. Park, S.C.: Heating, ventilation, and cooling historic buildings: problems and recommended approaches. Preservation Briefs, Vol 24, pp 1-14, Washington, D.C., 1991
8. Huynh, C. K., Savolainen, H., Vu-Duc, T., Guillemin, M., and Iselin, F.: Impact of thermal proofing of a church on its indoor air quality: The combustion of candles and incense as a source of pollution. Science of the Total Environment, Vol 102, pp 241–51, Elsevier science, 1991
9. Camuffo, D. and Della Valle, A.: Church Heating: A Balance between Conservation and Thermal Comfort, Contribution to the Experts, The Getty Conservation Institute, Roundtable on Sustainable Climate Management Strategies in Tenerife, Spain, 2007
10. CofE (Church of England): Shrinking the footprint, The Church of England's National Environmental Campaign, Guidance on Energy Efficient Operation and Replacement of Plant and Equipment, Deliverable D9 Carbon Management Programme, Church of England, London, 2008
11. Erhardt, D., Mecklenburg, M., Tumosa, C.S & McCormick-Goodhart, M.: The determination of appropriate museum environment. In: Bradley, S., ed., The Interface between Science and Conservation. British Museum, Occasional paper., Vol 116, pp 153 –163, London, 1997
12. Makrodimitri, M., Papavasileiou, S., Campbell, J.W.P., Steemers, K. 2011: Heating historic structures. A review of heating systems in historic church buildings and implications related to conservation and comfort. The case of four historic churches in Cambridge, Proceedings of Energy Management in Cultural Heritage conference, Dubrovnik, Croatia, 2011

ADAPTIVE ISSUES ON OUTDOOR THERMAL COMFORT

Leonardo Marques Monteiro, Marcia Peinado Alucci

Department of Technology, Faculty of Architecture and Urbanism, University of Sao Paulo, Rua do Lago, 876, Cidade Universitaria, 05508-080, Sao Paulo, Brazil, leo4mm@gmail.com

ABSTRACT

The research quantifies the correlations between the urban microclimatic variables air temperature, humidity and velocity and thermal radiation) and subjectivity variables (perception of thermal sensation variables), mediated by means of individual variables (clothing insulation and metabolic rate), allowing the prediction of the outdoor thermal environment adequacy to a population adapted to a given climatic condition. The objective is to verify the question of thermal adaptation in urban outdoor spaces. In order to achieve that, this paper verifying the influence of different metabolic rates (by means of commonly practiced physical activities in the open urban space) and of different clothing thermal insulation (also by means of commonly used clothing in urban open spaces) in the perception of thermal sensation. In order to do so, it also takes into account three factors: gender, acclimatization and adaptation. The methods applied were: experimental inductive (field research of microclimatic, individual and subjective variables), statistic (numeric regression), analytic (thermo-physiological model) and comparative (equivalent temperature). The results indicate that the outdoor thermal sensation prediction requires a model with aspecific empirical base for a given population adapted to certain climatic conditions, verifying yet the adaptation to the previous climatic conditions (considering the mean air temperature of a previous period of time), concluding with the proposition of an adaptive model in terms of adaptation to climate conditions.

INTRODUCTION

This research proposes an adaptive model for user behavior prediction in terms of clothing thermal insulation and different metabolic rates according to activities, regarding urban outdoor thermal comfort. The proposition allows the verification of the thermal adequacy of urban outdoor spaces in the subtropics and the adaptive opportunities in such areas. The method adopted is empirical, by means of field research of micro-climatic variables (air temperature, humidity, velocity, and mean radiant temperature), personal variables (clothing thermal insulation and metabolic rate according to activity) and subjective answers of thermal sensation and thermal comfort perception. Gender, acclimatization and previous climate adaptation (considering the mean air temperature of a previous period of time) were also considered aiming, together with the possibilities of adaptation through clothing and activities, to propose an adaptive model.

METHODS

The methods applied were: experimental inductive (field research of microclimatic, individual and subjective variables), statistic (numeric regression), analytic (thermo-physiological model) and comparative (equivalent temperature). The background for this paper can be seen in [1], in which is made a historical review of predictive models of thermal comfort. The same work presents the empirical research of 72 microclimatic situations and application of 2258 questionnaires, the procedures for the correlations between the variables air temperature, humidity and velocity and mean radiant temperature and the perception of thermal sensation gathered empirically and, finally, the different metabolic rates and clothing thermal insulation.

In the sequence will be considered: activities, clothing, and adaptation. It must be emphasized that the studies done until now, considering gender, did not bring any specific conclusion, in other words, the results tends to be the same for men and women. Considering the acclimatized and not acclimatized group of people, the differences were not so significant, and it was decided to wait for an increase in the data base. Until now there are only 476 questionnaires of non acclimatized people, who had come not randomly distributed by the country (Brazil), it is to say, they came more from hotter areas than colder areas, so it is not possible to deduce any tendency. Thus, only the questionnaires of acclimatized people (2258), who were living in the metropolitan area of Sao Paulo for over a year, were considered.

Activities

Different metabolic rates are considered, regarding the activities commonly performed in open spaces and the consequent results. Thus, the following models are considered for achieving not only thermo physiologic balance but also the prediction of the relative velocity between air and the individual. Following, there are the procedures for simulation.

Considering the most comprehensive set of data, seventy-two microclimate situations and 1750 questionnaires, it was found in [2] and [3] that the models that showed better results with the empirical counterparts were MENEX [4] *apud* [5] and [6], using index of thermal load [7] and Seville [8], using the rate of sweat required. The latter is based on the model of Vogt *et al.* [9], which also considers the rate of sweat required. This model showed satisfactory results, with correlation coefficients only slightly inferior to the two models mentioned. It should be noted that the model of Seville is only the beginning, the discovery of thermal heat situations. Thus, the thermophysiologic MENEX balance model proposed by Blazejczyk [4] is considered here, but with some modifications. Due to the characteristics of this model, which considers the solar radiation independently through empirical correlations, we chose to consider the radiative heat exchange of long wave according to Vogt *et al.* [9], using still gain from solar radiation was proposed by Dominguez *et al.* [7]. The work of these authors was presented in [10]. This is using a hybrid model based on the authors cited, considering as criteria for interpreting the thermal load index proposed by Blazejczyk *et al.* [8], for being among those derived from analytical models that consider thermal conditions of heat and cold, which showed the best correlation with empirical base in use. Considering the activities in open spaces, part of which involves shifts. In some cases the shift is what characterizes the activity, as occurs in traffic areas. Thus, in these cases, it is important to consider not only the speed of the air, but the relative velocity between air and the individual, since in many cases the speed of the individual is more significant than that of air. Therefore, it is necessary to know not only the magnitude of air velocity, but also its direction and meaning. In the fieldwork data were presented for wind direction. However, consideration of the sum vector implies also know the direction and sense in which people get around. Even in specific cases, determining the flow is not always accurate. In traffic areas, usually has the flow in one direction, but either way is possible. Thus, to evaluate a particular case, sometimes there is more than one answer, depending on the direction and sense of displacement of the individual, or a representative average value is reached. Since the goal here is to determine a general equation, it is preferred to reach a representative average value. The issue raised here pointed to the solution being used. It is, then the vector sum of the relative velocity between air and the individual, but assuming that the wind always relates laterally to the displacement of the individual. That is, the vectors are always perpendicular.

$$v_r = (v + v^2_{air\,i})^{2)\,1/2} \quad (1)$$

Therefore, it is not necessary to know the direction and sense of displacement of air, nor the individual. Imagine a typical situation in a place of passage, in which people move in the same direction and opposite directions, it has to be the vector sum to ninety degrees eventually because of possible underestimation of the relative velocity for one direction, but with consequent overestimation in the other direction. It is believed, therefore, to reach a representative average. Similarly, in a local residence, where the flows of people are not well defined, if the assumption that people are moving in random directions and senses, the incidence of side wind generates, once again, an average situation representative of the reality in question. Therefore, the vector sum to ninety degrees for the consideration of the relative velocity between air and individual is adopted here. To verify the change in metabolic rates, we used the temperature of equivalent perception, by Monteiro [15], presented also in [1], performing simulations using the model described above, adapting to the one proposed by Blazejczyk [4], Vogt *et al.* [9] and Dominguez *et al.* [7]. The full range of application of TEP index between its limit values for air temperature (T_{air} = 15 ~ 33 ° C), mean radiant temperature (T_{rm} = 15 ~ 66 ° C), humidity (RH = 30 ~ 95%), air velocity (v_{air} = 0.1 ~ 3.6 m / s) and thermal insulation of clothing (I_{cl} = 0.3 to 1.2 clo) were considered. Simulations were made in increments of t = 3 ° C $_{air,}$ t_{rm} = 6 ° C, RH = 15%, v_{air} = 0.5 m/s I_{cl} = 0.25 clo. The following adjustments were made: for t_{rm} considered until the value of 69 ° C for RH started at 35% $_{cl}$ and I started and finished at 0.25 clo to 1.25 clo, thereby ensuring the integrity of the intervals. It also ensures the coincidence with the values of $t_{air,}$ in the case of $_{rm,}$

and the values commonly used in the case of RH and $R_{cl.}$ All possible combinations of these variables (seven values of t_{air}, 10 $t_{rm,}$ 5 HR, 8 v_{air} and 5 R_{cl}) amounted to 14 000 simulations for each the metabolic rate, enabling the determination of perceived equivalent temperature values that provide the same thermal sensation in different activities.

Clothing

The procedures are presented here for the determination of a model to estimate the thermal insulation of clothing based on empirical data. The final model predicts the thermal insulation of clothing based on climatic data environment. We present here the regressions performed for the more limited set of microclimates. Considering that the air temperature and relative humidity have a high correlation, UR was not initially considered. The regression data led to the following equation, with statistical characterization in Table 1.

$$I_{cl} = 1.237 \text{ to } 0.0312 \cdot t_{air} - 0.0179 \cdot v_{air} + 0.00308 \cdot t_{rm} \quad (2)$$

with: $r = 0.844$, $r^2 = 0.712$, r^2 adj $= 0.707$ and $p = 0.064$, $p < 0.001$

Table 1 - Summary statistics and analysis of variance

	c	ep	t	p	VIF
Constant	1.237	0.0504	24.527	<0.001	
t_{air}	-0.031	0.0029	-10.77	<0.001	2.1
v_{air}	-0.018	0.022	-0.814	0.418	1.135
t_{rm}	0.0031	0.0011	2.854	0.006	1.915

	DF	SS	MS	F	p
Regression	3	0.75	0.25	61.01	<0.001
Residue	68	0.279	0.0041		
Total	71	1.028	0.0145		

As observed earlier, the air temperature is the only one to present very low p value ($p < 0.001$), and thus can possibly be able to individually predict the independent variable in question. The results for the linear regression of the variable air temperature are presented in sequence.

$$I_{cl} = 1.203 \text{ to } 0.0263 \cdot t_{air} \quad (3)$$

with: $r = 0.832$, $r^2 = 0.691$, r^2 adj $= 0.687$ and $p = 0.067$, $p < 0.001$

Table 2- Summary statistics and analysis of variance

	c	ep	t	p	VIF
Constant	1.203	0.0515	23.373	<0.001	
t_{air}	-0.026	0.0021	12.53	<0.001	-

	DF	SS	MS	F	p
Regression	1	0.711	0.711	156.87	<0.001
Residue	70	0.317	0.0045		
Total	71	1.028	0.0145		

As can be inferred from the results, the correlation shown only by the variable air temperature (0.83) is significant compared to the correlation with three dependent variables (0.84). Considering the F statistical test, there is a greater value for the regression with only the variable t_{air} in the more comprehensive data set (156.87 against 61.01), reiterating that this regression provides the best results.

Adaptation

This item is considered to adjust thermal sensation prediction depending on previous exposure to the weather, using the results of empirical surveys and climate data time series of meteorological stations. Below, we present climatic data for the years 2004, 2005 and 2006. It is noteworthy that in 2004 were performed only pre-tests, having been effectively used data collected between 2005 and 2006. However, all the climatic data for the period is considered to better characterize the climatic conditions prior to the survey. Finally, they are still considered the values of the climatic reference year for the city of São Paulo. Thus, the data, monthly and annual average, maximum and minimum air temperature were considered, the same data were taken into account for relative humidity and also data, monthly and annual average and maximum air speed recorded 10m from the ground. These data were recorded by the Meteorological Station of the Technical Section of the Meteorological Institute of Astronomy, Geophysics and Atmospheric Sciences, of University of São Paulo, registered with the World Meteorological Organisation under number 83004, located in the Parque Estadual das Fontes do Ipiranga, in the neighborhood Agua Funda, latitude 23 ° 39'S and longitude 46 ° 37'W [16]. The data, monthly and annual average and maximum incident solar radiation in the horizontal plane were recorded by the micrometeorological Platform

Lab of Micrometeorology, belonging to the Group of the Institute of Astronomy, Geophysics and Atmospheric Sciences, University of São Paulo, located on the campus of University City, in the district of Butantan, latitude 23 ° 24'S and longitude 46 ° 42'W [17]. The data for the reference climate (TRY: Test Reference Year) considered are shown by [18]. According to [19], the climatic reference year is made through the elimination of years for which data contain monthly mean temperatures high or low, until you get only one year of average data, thus becoming a reference climate situation in question.

RESULTS

The methodological description of the simulations indicated the use of perceived equivalent temperature (TEP) as a criterion for comparing the variation in metabolic rate. The index values of heat load (HL) were used for the determination of TEP, 'which is the new value of perceived equivalent temperature found for the different metabolic rates tested. The variation ("correction") is the difference between the values of TEP and TEP'. Table 10 shows the correction to be applied in the equation of TEP originally proposed for M = 1.3 met. Included also the limits within which the corrections were obtained and estimated error for each value.

Table 3: Summary of simulation results to determine the TEP for different metabolic rates

Activity	sitting	standing	walking	
speed of person (m/s)	-	-	0.9	1.1
speed of person (km/h)	-	-	3.2	4
metabolic rate (Met)	1	1.3	2.0	2.4
TEP considered (° C)	12~45	12~45	12~39	12~39
correction (° C)	-1.5	0.0	3.5	5.7
estimated error (° C)	± 0.0	± 0.0	± 0.1	± 0.5

As can be seen for metabolic rates of 1.0 and 2.0 Met, the results are quite accurate. To 2.4, the estimated error is around 0.5 ° C. In cases of higher metabolic rates, it appears that the estimated errors are increasing, even in the most restricted ranges of applicability. According to several authors, [4], [8] and [14], the average speed of walking down the street is 1.1 m/s. Thus, the metabolic activities of greatest interest for the assessment of open spaces can be summarized as three: 1.0 Met (occupant), Met 1.3 (a person standing with little activity) and 2.4 Met (person walking an average speed of 1.1 m/s). Thus, the corrections to be applied are between -1.5°C for seats and 5.7°C for people walking. Considering that for the metabolic activity of 2.4 Met the estimated error of 0.5°C is acceptable, it is proposed to follow a linearization of the values found for activity between 0.0 and 2.4 Met, giving up so an equation for application in activities commonly found in open spaces.

$$\Delta TEP = -6.648 + 5.118\ M \qquad (4)$$

where: ΔTEP = change in perceived equivalent temperature in °C. The above equation, for the range of values proposed, presents a correlation of r^2=1, r^2= adjusted 0.999. The standard error is 0.080 and the significance of p <0.001. In practical terms, the proposal maintains the linearization correction of values between 1.0 and 2.0 Met. For the value of 2.4 Met, the equation predicts a value of 5.6° C, while the correct would be 5.7°C. Since the estimated error for the results of the metabolic rate was already 0.5 ° C at worst, though unlikely, the accumulated error would be 0.6 ° C. It is important to mention that for greater than 2.4 Met, it is observed that the growth of the equivalent variation in temperature is no longer linear. So, if it is used for these cases, there will be an underestimation of the variance. Therefore, for M = 2.6 Met, the prediction would be 6.5° C, while the value was 7.5° C for M=3.0 and 3.5 Met, have respectively 8.5° C and 11.5° C versus 13.5 ° C and 20.5°C originally found. Thus, the use of the equation must be restricted to metabolic rates specified. It would be possible to determine a nonlinear model that embraces the entire fees considered. However, as seen in Table 3, these cases just mentioned have errors estimated considerable and still growing (respectively 0.8, 2.0 and 3.3). Therefore, as a linear equation includes activities commonly practiced in open spaces, we chose to keep it. It is emphasized that the corrections shown in Table 4 may be used, provided that the tracks to which they apply and their estimated errors are recognized. Moreover, it is believed that the newly proposed equation is justified by the possibility to be added to the equation originally proposed.

In Table 4, the maximum and minimum values observed among the mean values of the seventy-two cases considered regarding the individual surveys conducted are listed.

Table 4: Limit values for the variables of clothing insulation and air temperature

variable	minimum value observed	maximum value observed
$I_{cl\ absolute}$	0.26	1.17
$I_{cl\ mean}$	0.39	0.86
t_{air}	15.1	33.1

limit	t_{air}	I_{cl}
theoretical	> 45.5 ° C	0.00
for swimsuits	> 44.0 ° C	0.05
for garments used in urban spaces	> 30.0 ° C	0.40
for garments used in offices	> 26.5 ° C	0.50

These values are presented here to reaffirm the limits within which the above considerations are valid. Beyond these figures, the results are extrapolated verifiable. So, as determined along the explanation of methods, the proposed model to predict the thermal insulation of clothing according to environmental microclimatic variables occurs in fact only a function of air temperature, as follows.

$$I_{cl} = 1.203 \text{ to } 0.0263 \cdot t_{air} \quad (5)$$

For practical applications of the model, the establishment of reference values to limit the minimum value of insulation of clothing was suggested, since for physical issues that isolation will never be less than zero and for cultural reasons there are minimum values of even greater isolation. Table 10 shows schematically these limits.

Thus, if there were no cultural constraints, the limit could be adopted, even theoretical, at 45.5°C, in which I_{cl}=0.00 clo. Considering swimsuits for t_{air}> 44.0°C, we have I_{cl}=0.05 clo. However, roughly speaking, we can put that in general situations in open spaces for t_{air}>30.0 ° C, we have I_{cl}=0.40 clo. If one considers the restriction of clothing commonly used in office activities (social trousers, short-sleeved shirt, shoes, socks and underwear), it appears that for t_{air}>26.5° C, we have I_{cl} =0.50 clo. Considering the values of perceived equivalent temperature of neutrality (TEPn) for the days of summer and winter of two years in which surveys were conducted and the average temperatures of the thirty days prior to each day's survey, we obtain the following equation.

$$TEPn = 20{,}033 + 0{,}1742 \cdot t_m \quad (6)$$

It is noteworthy that due to the surveys having been conducted only in summer and winter days of two consecutive years, the equation presented is based on very sparse data. Thus, it is considered in order to present a possible approach that considers adaptation to prior climatic conditions. A greater amount of surveys conducted throughout the year and over several years is necessary for proper verification of the adaptive conditions of a given population in relation to climate variations. Recognizing the restrictions lifted, the following equation of the equivalent temperature is presented as a function of perceived neutrality of the average monthly temperatures (t_m), covering the limits contained in the reference climate years for Sao Paulo. Considering the role of activity, clothing and adaptation to prior weather conditions to the perceived equivalent temperature (PET) [1], one may come to the following equation.

$$PET = -29{,}877 + 0{,}4828 \cdot t_{air} + 0{,}5172 \cdot t_{rm} + 0{,}0802 \cdot UR - 2{,}322 \cdot v_{air} + \\ + 5{,}118 \cdot M + 38{,}023 \cdot I_{cl} - 0{,}1742 \cdot t_m \quad (7)$$

In order to use the equation without all the three adaptive terms, the reference values are M=1,3 met; I_{cl} = 0,6clo and t_m=19,3 ^oC

FINAL CONSIDERATION

The results indicate that the outdoor thermal sensation prediction requires a model with a specific empirical base for a given population adapted to certain cultural and climatic conditions, verifying yet the adaptation to the previous weather conditions (considering the mean air temperature of a previous period of time), concluding with the proposition of the adaptation of the perceived equivalent temperature (PET) in terms of an adaptive model considering activities, clothing and previous weather conditions.

ACKNOWLEDGEMENTS

The authors would like to thank the Fundacao de Amparo a Pesquisa do Estado de Sao Paulo (FAPESP) and the Conselho Nacional de Desenvolvimento Científico e Tecnológico (CNPq), for the financial support in this research.

REFERENCES

1. Monteiro, LM; Alucci, MP Proposal of an outdoor thermal comfort index: empirical verification in the subtropical climate. PLEA2011, Louvain-la-Neuve, Belgium
2. Monteiro, LM; Alucci, MP Conforto térmico em espaços abertos com diferentes abrangências microclimáticas. In: IX ENCAC, 2007, Ouro Preto. Anais ... Antac, 2007b.
3. Monteiro, LM; Alucci, MP Conforto térmico em espaços abertos com diferentes abrangências microclimáticas. Verificação experimental de modelos preditivos. In: IX ENCAC e V ELACAC, 2007, Ouro Preto. Anais... Antac, 2007a.
4. Blazejczyk, K. Climatological-and-physiological model of the human heat balance outdoor. Zeszyty IGiPZ PAN , v.28, p.27-58, 1996.
5. Blazejczyk, K. MENEX 2002. http://www.igipz. pan.pl/klimat/blaz/menex. 2002a. Accessed in 24/10/2008.
6. Blazejczyk, K. Man-environment heat exchange model http://www.igipz.pan.pl/ klimat/blaz/menex. ppt. 2002b. Accessed in 24/10/2008.
7. Dominguez et al. Control climatico en espacios abiertos : el proyecto Expo'92. Sevilla: Universidad de Sevilla, 1992.
8. Blazejczyk, K.. et al. Influence of the human heat balance on respiratory and circulatory diseases. In: Int Congress of Biomet, 15, 1999, Sydney. Geneva: WMO, p. 107-112, 2000.
9. Vogt et al. A thermal environment in physiologically significant terms. Arch. Meteor. Geophys. Bioclimatol. v.29, p. 313-326, 1981.
10. Monteiro, L.M.; Alucci, M.P. Outdoor thermal comfort: numerical modelling approaches and new perspectives. In: PLEA, 22, 2005, Beirut. Proceedings... 2005.
11. International Organization Standardization. ISO 7933. Hot environments: analytical determination of thermal stress using required sweat rate. Genève: ISO, 1989.
12. Blazejczyk, K. MENEX 2002. In: The Development of Heat Stress Watch Warning Systems for European Cities. Freiburg May 3, 2003. Proceedings of Conference…, Friburgo, 2003. In: http://www.gees.bham.ac.uk/research/ phewe/freiburg/.
13. Jendritzky, G. Klima-Michel-model . In: The Development of Heat Stress Watch Warning Systems for European Cities. Freiburg May 3, 2003.
14. Jendritzky, G. Selected questions of topical interest in human bioclimatology. International Journal of Biometeorology, 35 (3), p. 139-150, 1991.
15. Monteiro, L. M. Thermal comfort predictive models. 378p. Thesis (Doctoral). Faculdade de Arquitetura e Urbanismo, Universidade de São Paulo, São Paulo, 2008.
16. Instituto Astronômico e Geofísico da USP. Laboratório de Micrometeorologia. São Paulo: IAGUSP, 2007a. http://www.iag.usp.br. Accessed in 27/09/2009.
17. Instituto Astronômico e Geofísico da USP. Estação Meteorológica. São Paulo: IAGUSP, 2007b. http://www.dca.iag.usp.br/www/estacao/. Accessed in 27/07/2007.
18. Goulart, S. Dados Climáticos para Avaliação de Desempenho Térmico de Edificações. 1993. 111 f. Dissertação (Mestrado em Engenharia Civil). Florianópolis: UFSC, 1993.
19. Goulart, S., Lamberts, R., Firmino, S. Dados climáticos para projeto e avaliação energética de edificações para 14 cidades brasileiras. Florianópolis: UFSC, 1997.

LIGHT TRANSMITTANCE RANGE OF GLASS FOR VISUAL COMFORT IN AN OFFICE ENVIRONMENT

M.P.J. Aarts[1], S. Chraibi[1], M.B.C. Aries[1], E.J. van Loenen[1], R.A. Mangkuto[1], T.J.L. Wagenaar[2];

1: Eindhoven University of Technology, Unit Building Physics and Systems, VRT 6.11, P.O. Box 513, 5600 MB, Eindhoven, the Netherlands
2: Peer+ B.V., P.O. Box 2374, 5600 CJ, Eindhoven, the Netherlands

ABSTRACT

'Nothing is as variable as the weather' is a well-known Dutch expression demonstrating the instability of the Dutch climate and as a consequence the daylight availability. In rapidly changing climate conditions, a non-adjustable, structural shading device is unsuitable. Therefore a system that blocks the direct sunlight when necessary without obstructing the diffuse daylight next to keeping view intact would be the best solution, both for user comfort as for energy consumption. A glazing system with a rapidly adjustable transmittance might be a good solution for such climate. Smart Energy Glass (SEG), a glazing system being developed by Peer+ can quickly switch between two light transmittance values (max. range of 30%). The research question of this project was to determine, based on users comfort, these two values.

An experimental set-up was made in the laboratory of Building Physics and Systems group with five identical rooms. All rooms were equipped with an equal sized daylight opening; four rooms had a different light transmittance (0.08, 0.25, 0.52, and 0.70). The fifth was the reference room and had normal glass with a transmittance of 0.70. During summer, autumn, and winter, the same 24 healthy test-persons (age 23±4 years) participated in the tests. By filling out a questionnaire regarding comfort, preferred transmittances and lighting situation under different daylight conditions was determined.

The test people considered their working condition as comfortable with horizontal illuminance on the workplace of at least 267 lx. Regarding visual comfort, window luminance values of 6500 cd/m² were still accepted by the subjects, and glare was barely experienced or indicated. It could be concluded that during measurements with sunlight on the façade, the test space with a transmittance of 0.25 was mostly evaluated for its good lighting by daylight. During measurements without sun, the test spaces with a transmittance of 0.52 and 0.70 were mostly positively evaluated for their good lighting by daylight. In the summer period, transmittances of 0.25 and 0.52 were most preferred by the subjects. This also applies for sunny days in the autumn. During overcast days in the autumn and during winter, there was a desire for higher light transmission. Taken into account the maximum range of 30%, a transmittance range between 0.40 - 0.70 most users are satisfied with the lighting by daylight namely at least 71% of the time, up to 89% of the time.

INTRODUCTION

In the Dutch office environment, about 25% of the energy is used for lighting [1]. A better use of daylight could reduce the energy load. Since Dutch weather provides a rapidly changing sky condition, a daylight control system should be able to respond very quickly to these changes. Conventional daylight control systems are often noisy, partially or completely block the view, and prevent the use of daylight. Automated systems control for energy reduction and do not always take the users' preference into account, or actions of the system are too fuzzy for the user to understand and therefore often lead to sabotage. The energy saving of

manually-controlled systems largely depends on the user behaviour; a non-active user will close the shielding system when glare or heat is perceived but forgets to reopen it when the problem has disappeared. The ideal solution would be a system that quickly responds, leaves view intact, blocks only the disturbing light, and does not consume energy. Smart Energy Glass (SEG) under development by Peer+ [2] is a glazing system that instantly can be darkened or lightened for comfort improvement, and simultaneously generates enough energy, allowing for self sufficient switching. At the same time it guarantees an unblocked view due to a minimum of haze. The system is based on switchable luminescent solar concentrator technology as developed by Debije [3]. However, values for the darkest and lightest setting of the system in order to provide optimal comfort are not determined yet. In the literature, minimum transmittance values between 0.1% [4], <10% [5], and 25%-38% [6] were given to avoid visual discomfort under all weather conditions. Also, the appreciation of the room itself is positively correlated to the glass transmittance [7]. In this study, transmittance values of the glazing were investigated based on user perception and assessment in order to provide a visually comfortable environment.

METHOD

For this experiment a full scale study has been executed, to enable user evaluation alongside of measured values. In the laboratory of the Building Physics and Systems group of Eindhoven University of Technology, the Netherlands, a full-scale experiment set up was built, to accommodate five similar test rooms with a true West-facing window of 1.2 x 1.2 m^2. The rooms were 1.8 m wide, 3.9 m deep and 2.7 m high. Figure 1 (LTA means transmittance) shows a floor plan and a façade view of the built test spaces in the laboratory. The test facility is equipped with a full-glass façade with HR^{++}-glass (U=1.3 W/m^2K, transmittance=0.70). Four of the rooms were equipped for subjects; a fifth room functioned as a reference room.

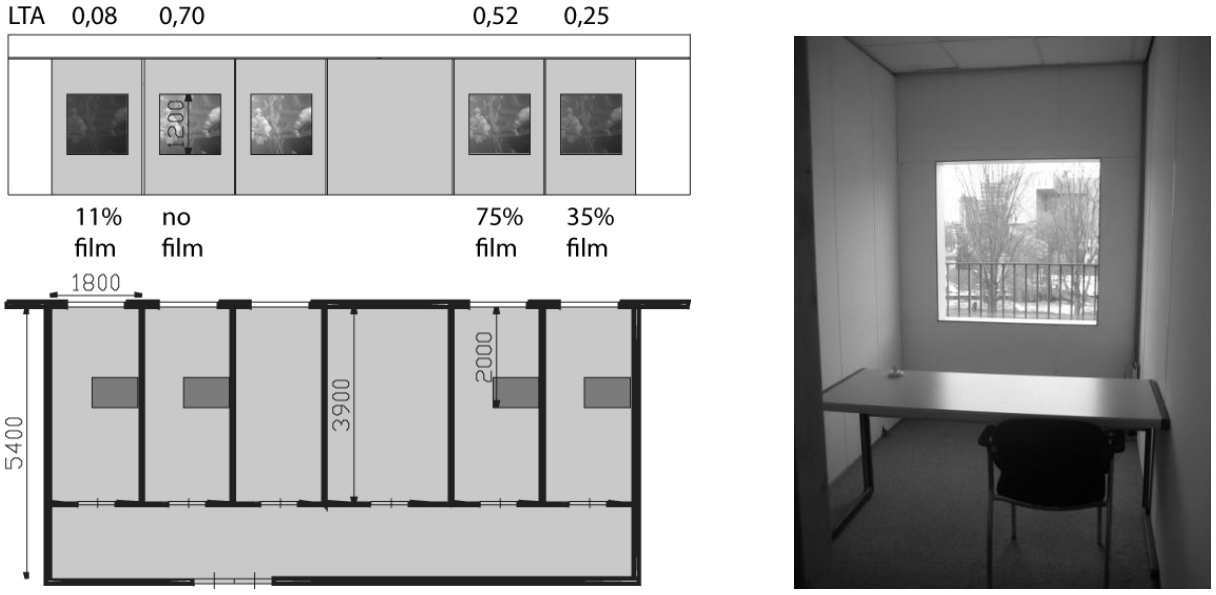

Figure 1: Floor plan and facade laboratory test spaces (left); photo of test room (right)

The four rooms had different combined glass properties due to the use of films with different light transmittances. The transmittance of the glass-film package was 0.08, 0.25, 0.52 and 0.70, determined by LBNL software Windows 5.0. The rooms were lit by daylight only with no additional electric lighting. To maintain a comfortable constant room temperature the rooms were equipped with heating and air conditioning.

Test subjects

In total, 18 male and 14 female subjects participated. Measurements with subjects were executed during three periods in 2010: summer, autumn, and winter. Each season about twenty-nine healthy subjects, all students (age 23±4 years old), evaluated the test spaces. Twenty-four healthy test subjects participated in all three periods, six subjects evaluated the rooms in only two periods, and two only participated once. The subjects were all students because of their flexible schedules. As a result of a tight schedule, measurements could be performed during office hours, two sessions per day, for two weeks. Subjects were paid for their participation in the experiment.

Procedure

As mentioned above, measurements with subjects were executed during three periods in 2010: summer from 20 August till 6 September, autumn from 11 October till 21 October, and winter from 13 December till 23 December. Three periods were chosen for their different sun elevations: a high sun during summer, middle high sun during autumn, and a low sun during winter. Measurements were executed in morning (start 10h00) and afternoon (start 14h00) sessions, of which 57% were morning measurements and 43% afternoon. The total experimental time took about 2 hours. The test subjects were asked to perform an office task: entering business card information in a database software program. After 10 minutes they had to fill in a questionnaire about visual comfort. This questionnaire has partially been adopted from Osterhaus [8]. The questionnaire took the general room evaluation into account, as well as the evaluation of daylight in the room, and well being and preferences of the office space users. For the current study, the questions about the workplace description were eliminated since these were constant and identical. Questions about the view were added, as well as questions about changes experienced by the subjects between the different rooms. After completing the questionnaire, the participants took place in a neutral 'waiting' room to adapt to a constant, low light level (avg. E_{hor} = 54lx), before they continued to the next room. This procedure was repeated until the subject had evaluated each of the four rooms. At the end of the sequence the subject repeated one randomly chosen room, serving as a validation of the evaluation.

Measuring equipment

Tests with subjects were performed in four different test spaces. During the test sessions the illuminance was logged continuously at four different positions in each room: vertically on the window, horizontally on the desk, vertically on the wall at eye level of the participant, and vertically on the rear wall of the room. Illuminance was logged in order to link the values to visual performance and visual comfort during the tests. On account of knowledge of the environment during user evaluation, room temperature and the relative humidity were continuously monitored in every room. The fifth room was used as a reference room, were a luminance picture was taken at the beginning and at the end of each session.

Data analyses

The data was analyzed using SPSS PASW 18.0. Evaluation results have been studied by means of a Factor Analysis in order to combine them into new variables. Hereafter a Reliability Test with a Cronbachs' alpha larger than 0.7 did point out whether a combination can be reliably made [9]. A Repeated Measures ANOVA and a one-way ANOVA test were used in order to find relations between the dependent variables as user comfort, transmittance values, and independent measured values as window luminance and the horizontal desktop illuminance. For a significant difference between variables, the probability level was set at

smaller than 5% with an F-value larger than 3. Post Hoc Tests were used to point out where the differences within groups are to be found. The data consisted of repeated evaluations of the different rooms in different seasons by the same participant. This is taken into account by the Repeated Measures ANOVA. The Partial Eta Squared **(**η_p^2) presents the contribution of each factor to the variable (effect size).

RESULTS

The average temperature during the 344 subject measurements in the test rooms was 21.6±1.3°C with an average relative humidity of 49.5±4.3%. There was no statistical significant difference in measured temperature and humidity between the different rooms. There were 15 sessions with direct sunlight in the room and 71 sessions with no direct sunlight present. The total average horizontal illuminance at the desk of all sessions ranged from 4 to 3191 lx and the maximum window luminance from 36 to 21800 cd/m².

Daylight comfort scale

The questionnaire used for evaluating the test spaces contained questions concerning the evaluation of the indoor environment and specifically the lighting by daylight. Several questions concerning daylight were distilled from the data by means of a Factor Analysis. These questions were: 1) *How do you evaluate the lighting by daylight on your desktop?;* 2) *How do you evaluate the lighting by daylight in the surrounding space?;* and 3) *How do you evaluate the lighting by daylight of the window surface?*All three questions had a 5-point rating scale; *too dark, a bit too dark, good, a bit too bright, and too bright.* The questions were re-coded from -2 till 2 and by summation combined into a new parameter *Daylight Comfort*, with a Cronbach's Alpha of 0.793. The *Daylight Comfort* parameter describes the overall evaluation of daylight in the test space. A score between -1 and 1 was considered as 'good' daylight comfort; scores over respectively -4 or 4 as 'too dark' and 'too bright'.

Illuminance and luminance

For insight in comfort of daylight in the test rooms and its relation to desktop lighting, the results of the Daylight Comfort parameter were plotted versus the measured average desktop illuminance, see Figure 2. Each dot represents one session.

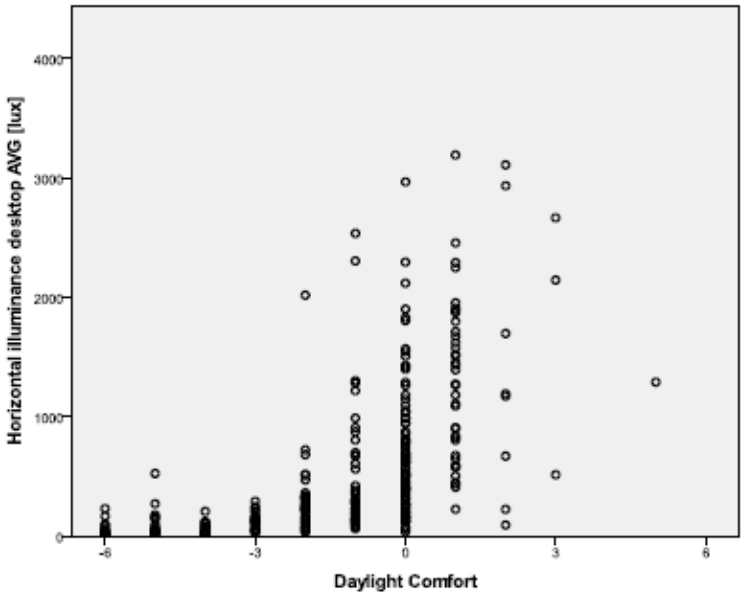

Figure 2: Scatter plot of Daylight Comfort and average horizontal illuminance workplace [lx]

Looking at the part from too dark (-6) till good (1), the figure shows a general increase of the horizontal illuminance at increasing daylight comfort. The test people considered their working condition as comfortable with horizontal illuminance on the workplace of at least 267 lx. Regarding visual comfort, window luminance values of 6500 cd/m² were still accepted by the subjects, and glare was barely experienced or indicated.

Preferred transmittance

Analysis of the Daylight Comfort parameter shows a statistically significant difference between the four different transmittances of the test rooms. Post-hoc tests showed the significant difference was present between all four of the rooms. Since there was a statistically significant effect for season, the difference between the rooms was analyzed per season (summer session $F=52.465$, $p=0.000$, $\eta_p^2=0.856$; autumn $F=68.434$, $p=0.000$, $\eta_p^2=0.888$; and winter $F=85.174$, $p=0.000$, $\eta_p^2=0.911$). Results show that the transmittance has a large effect (Partial Eta Squared) on the Daylight Comfort parameter. If the focus is on the situation where at least 75% of the time the perception 'good daylight' is obtained, a light transmittance in the range of 0.21 – 0.70 is desired for non-sunny summer days. At sunny days the range would be limited at transmittance=0.6 (only based on two measurements). During sunny autumn days a transmittance range between 0.21 - 0.70 falls in the 75-100% satisfaction area. For days without sun on the façade a transmittance of at least 0.65 is desired. During the winter period, the evaluation of daylight never reaches the 75-100% satisfaction area. Here, the highest transmittance value is desired; a transmittance of 0.7 provides a good lighting by daylight for 71% of the time.

In Figure 3 the results per season are combined in an overview for all three seasons. The results show that optimum satisfaction is reached when the light transmittance could change from 0.21 to 0.70.

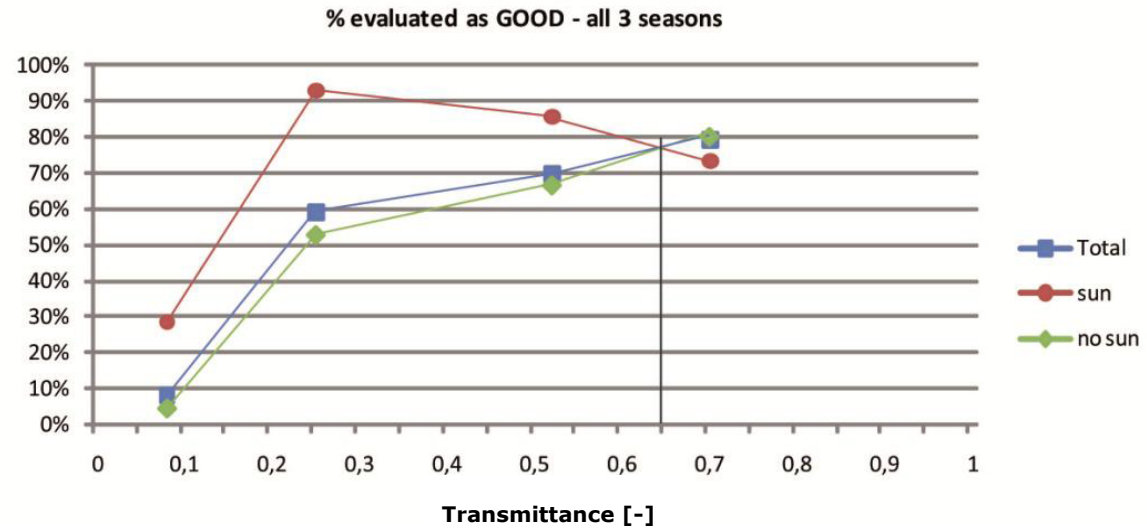

Figure 3: Positive daylight evaluations during measurements of all three seasons

DISCUSSION

According to this study, the optimal transmittance for every sky condition would be about 0.65 (see Figure 3). When taking the Peer+ requirement of switching with a maximum step of 0.30 into account, the transmittance should range from 0.35 to 0.65. In determination of this range the satisfaction percentages for sunny summer days were not taken into account because of the little number of measurements at this situation.

The conclusions of this experiment are based on a relatively young population of students, who are not used to working in an office environment. The assumption is that an older population might need more light for visual comfort. They also might encounter more glare issues due to the changed lens opacity.

In this study glass transmittance values for visual comfort in the Dutch climate have been examined. An optimal window design could also contribute to energy saving in an office building. However, this part is not examined in this study, the focus was visual comfort.

CONCLUSIONS AND RECOMMENDATIONS

When assuming a linear progress of the preferred transmittances and a maximum switching step of 30%, predictions can be made for the evaluation of the transmittance values located between the tested values. At a transmittance range of 0.4 – 0.7 the users are satisfied with the lighting by daylight at least 71% of the time, up to 89% of the time. At a transmittance range of 0.35 – 0.65 the users are at least 65% of the time satisfied, up to 90% of the time. A transmittance range of 0.4 to 0.7 is most sufficient for young (23±4 years) office users in the Dutch climate. When selecting a fixed range based on light comfort, the dominate parameter is the bright state instead of the dark state. Therefore the challenge for switchable glazing technologies (electrochrome, SPD, etc) is to get a bright state with a high light transmittance, although it will decrease the switching range.

The results are based on research with young participants (23±4 years old). For making statements concerning a larger group of office users, more research is necessary with an older population. This also counts for giving a transmittance advised for visual comfort in other climates. Here for more research is necessary. During the measuring sessions for this experiment the summer days did not include many sunny days. More experiments with a high direct sun are necessary for including those evaluations in the advised transmittance range.

ACKNOWLEDGEMENTS

Peer+ is greatly acknowledged for funding this research.

REFERENCES

1. Meijer Energie & Milieu-management B.V. Senternovem, 2008 (In Dutch)
2. Website Peer+ [www.peerplus.nl]
3. Debije MG. Solar energy collectors with tuneable transmission. Advanced Functional Materials, 2010; 20: 1498–1502
4. Piccolo A, Simone F. Effect of switchable glazing on discomfort glare from windows. Building and Environment, 2008; Volume 44(6): 1-10.
5. Selkowitz SE, Rubin M, Lee ES, Sullivan R, Finlayson E, Hopkins D. A review of Electrochromic Window Performance Factors. SPIE International Symposium, Germany, 1994.
6. Boyce PR. Human Factors in Lighting. 2de edition Lighting Research Center. Taylor and Francis group, London and New York, 2003, pages 107, and 162-192.
7. Dubois MC, Cantin F, Johnson K. The effect of coated glazing on visual perception: A pilot study using scale models. Lighting Research & Technology, 2007; Volume 39 (3): 283-304.
8. Osterhaus WKE. Discomfort glare assesment and prevention for daylight applications in office environments, Energy and Buildings, 2005; Volume 79 (2): 140-158.
9. Nunnally JC. Psychometric theory (2nd ed.). McGraw-Hill, New York, 1978.

POTENTIAL FOR ENERGY SAVING IN TRANSITIONAL SPACES IN COMMERCIAL BUILDINGS

Alonso, C.; Aguilar, A.; Coch, H.; Isalgué, A.

Universitat Politècnica de Catalunya / EtsaB, Edifici A, 7ª planta. Avda. Diagonal, 649. 08028 Barcelona, Spain. Tel: (0034) 93.401.08.68 / email: carlos.alonso-montolio@upc.edu

ABSTRACT

As it is known, the energy consumption of buildings is directly linked to their energy demand. Therefore, the most direct strategy to reduce the energy consumption of a building is to minimise its energy demand. This can be done in two ways. On the one hand, the energy demand can be reduced by minimising the size of some energy consuming spaces in the building. It can also be reduced by minimising the requirements of their comfort conditions. This second strategy is especially effective in transitional spaces, where the comfort requirements have wider limits than in normally occupied zones so energy savings are possible by allowing for a modest relaxation of the comfort standards. This paper reports on an analytical study into the energy-saving potential associated with modifications in thermal comfort limits in transitional spaces in commercial buildings. Such transitional spaces may not require the same high level and close control as more fully indoor or fully occupied areas, and thus a wider variation in conditions and interpretation of thermal comfort may be permitted. They also take up a significant fraction of the total volume of these kinds of buildings and give rise to significant energy use to provide comfort by means of heating or cooling systems. Initial trial calculations have been conducted using standardised commercial building layouts in order to determine the potential for energy savings. Commercial buildings have been chosen not only due to the extensive presence of this kind of building in almost all cities, but also because of the considerable percentage of transitional spaces that these buildings have in a standard floor plan. The relationship between these transitional spaces and the indoor areas will also be considered in this study. Estimates are made of the energy-saving potential based on different commercial buildings located in the climate of the Barcelona area in Spain.

INTRODUCTION

Transitional spaces

There are spaces in architecture that cannot be classified as either indoor or outdoor and whose existence cannot be explained in terms of any precise or specific use [1]. We can find this kind of space between the indoor environment and the outdoor environment, without defined limits between inside and outside. They are the transitional spaces and they have existed across different cultures throughout the history of architecture. Moreover, although transitional spaces may not have any specific use, they are required to fulfil a function of transition between the outdoors and the internal constructed environment, so this is why they are such adaptable and comfortable spaces, as well as why they are found in such a diverse array of places.

This paper deals with transitional spaces from an environmental point of view, due to the opportunity that such spaces provide for possibly modifying the comfort requirements.

Strategies to lower energy consumption

The energy consumption of buildings is directly related first to the efficiency of artificial energy systems and secondly to the energy demand of the buildings themselves. Due to the fact that the rise in the energy efficiency or performance of air conditioning and heating systems has its limits, and therefore there is little margin for reducing consumption, the challenge lies in reducing the energy demand without changing the users' perception of comfort.

From the standpoint of architectural design, this drop in the building's energy demand can be made both by minimising the size of some of the spaces inside the building that consume energy (which would have clear repercussions on the formal resolution of buildings and the consequent use and behaviour of the users), and by lowering the requirements in certain areas of the building, which would be more or less feasible depending on the kind of space in which we are acting. In this sense, the second strategy is particularly effective in transitional spaces, where we can allow greater variation in the thermal conditions and where the environmental needs have much broader limits than in the remaining spaces, leading to potentially quantifiable energy savings. Furthermore, in many cases transitional spaces bring added value to the architectural design regarding the users' perception of thermal comfort, as they dynamically adapt to environmental conditions halfway between indoor and outdoor and thus are not as static as the unvarying interior conditions.

Lowering the demand in transitional spaces

As a direct consequence, according to the typology of the building being studied, this reduction in consumption can be more or less important. This study concentrates on all the transitional spaces in public buildings. Despite the fact that they might also show private transitional elements (such as galleries, balconies, etc.), most of their functional demands require them to have large communal transitional spaces (such as entry lobbies, hallways, etc.).

Within these public buildings, we can find a series of examples (such as schools, museums, markets, airports and commercial buildings) that are based on the routes the users take through the building. That is, they all share the common feature of possessing large transitional spaces. In these cases, the hallway is one of the transitional elements between outdoors and indoors, and it is also the element that joins the different service-providing units (such as classrooms, works of art, market stalls, shops or products for sale, etc.).

By analysing the thermal needs of these transitional spaces, we reach the conclusion that they largely depend on the thermal needs of the different units to which the spaces lead, as well as on the relationships existing with these units. Furthermore, the thermal needs of transitional spaces also depend on the degree to which they are exposed to the outdoor environment (closely or loosely related) as well as on their own function, that is, how long the users are in them and these users' expectations, adaptation time, etc.

Therefore, this study focuses specifically on commercial buildings since a priori they seem to be clear examples of transitional spaces with a vast potential for energy savings, associated first with the wide margin of their levels and environmental control limits and secondly with the high percentage of the total volume they occupy in the standard floor of this kind of buildings. What is more, there are extensive examples of this building model throughout history as well as in the majority of cities in the world today: from the Mediterranean Greek and Roman agorae and stoas to the bazaars and souks of the warm Islamic climates, and even the porticoed galleries found in rainy climates and today's shopping malls.

METHOD

Existing environmental conditions

This study is based on real examples and was calculated for the city of Barcelona, which is located at a latitude of 41º 20' N and in a mild, humid Mediterranean climate which is hot in the summer (Csa), according to the Köpen-Geiger climate classification from the University of Melbourne. Regarding the temperatures, the winters are mild with average temperatures of 9º C to 11º C, while the summers are hot, with average temperatures ranging between 23º C and 24º C and a moderate thermal amplitude and average yearly rainfall of around 600 mm.

Study models

Based on an analysis of the contemporary casuistic of shopping centres in the city, we generated three basic calculation models. The first is the traditional shop model, usually on a local scale and relatively small in size, rectangular-shaped and attached to other shops on the side facades and with a relatively permeable facade facing the street outdoors through which customers enter (model A). On the other extreme is the mall-type building, which usually has a large interior volume and is shaped compactly and hermetically as a building. This model usually has a percentage of opaque facade and slightly lower percentage of glass-encased facade. Furthermore, the circulation to reach the goods for sale takes place inside the building, so in this case the goods for sale and the transitional space have the same environmental conditions (model C). Between model A and model C are commercial buildings which, like bazaars or ancient porticoed galleries, contain a series of independent shops connected to a transitional space with its own environmental conditions, halfway between the indoor conditions of the shops and the outdoor conditions. Therefore, these are rectangular-shaped shops attached to each other on their side facades with a highly permeable main facade leading towards a transitional space with environmental conditions between indoors and outdoors and an opaque rear facade facing outdoors (model B).

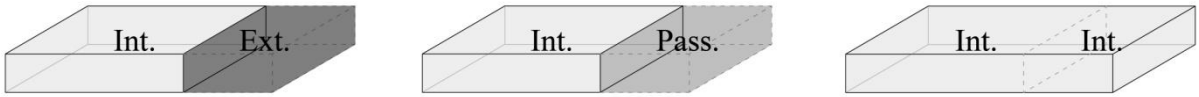

Figure 1: From right to left, model A, model B and model C of shops used in the simulation.

The top exponent of this kind of commercial building (model B) in Barcelona is Illa Diagonal, a building dating from 1993 designed by Rafael Moneo and Manuel de Solà-Morales. This building was taken as the reference for obtaining the initial values of volumes, surfaces, compactness, etc. Likewise, the shops near the city's commercial arteries, such as Sants Street, and the shops in Barcelona's Ensanche district were taken as references for model A. The El Corte Inglés department store in Francesc Macià Square was taken as a reference for model C.

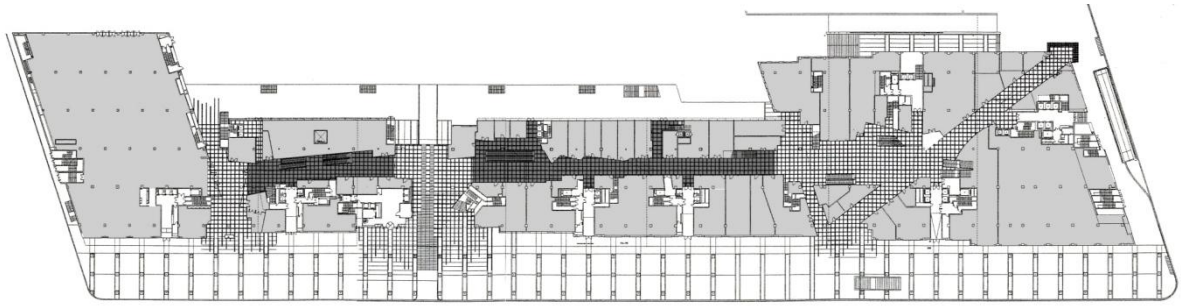

Figure 2: Ground floor of the Illa Diagona. Heated/air conditioned shops (gray), semi-h./a.c. transitional spaces (dark squares) and not h./a.c. transitional areas (light squares).

Calculations and simulation

A simulation was planned of the three basic models using the Archisun v3.0 software [2] developed by the Architecture and Energy research group at the U.P.C. This programme calculates the energy behaviour of buildings in a natural scheme and provides climatic and consumption results for 15 days in the four seasons. A variety of general parameters are taken into consideration in the calculations, including the building's location and its climatic data, those related to the definition of its immediate environment, as well as parameters related to the building's shape (such as the orientation, compactness and porosity), the volume, internal contributions and how it is used. Other more specific parameters are also taken into account, related to the interior design of the model and the definition of its skin (with variables on its placement, attachment to other buildings, the average coefficients of its skin thermal transmission, the hermeticity of its practicable surfaces, reflectances and transparencies, weights, protective and obstructive factors, and many others).

Therefore, a simulation was performed based on the three. In all three models, we assumed average outdoor temperatures of 26.6º C in the summer and 8.1º C in the winter.

Regarding model A, the standard volume was taken, and it was assumed that both the floor and ceiling and three of the four facades are attached to areas with the same environmental conditions (24º C in summer and 21º C in winter). To the contrary, the main facade, which is in contact with outdoor conditions, has a higher thermal transmission coefficient (U), since it is made of glass, and is also more permeable to the air.

Regarding model B, the same standard volume was taken, and it was assumed that the floor, ceiling and two of the four facades are attached to spaces with the same environmental conditions described above. Likewise, the rear facade has a low thermal transmission coefficient (of a standard opaque closure) in relation to the outdoor conditions. In contrast, the main facade has a greater thermal transmission coefficient since it is made of glass, plus it is more permeable to the air. However, the main facade does not exchange with an atmosphere in outdoor conditions; rather it exchanges with the naturally controlled atmosphere of the transitional space.

Since the Archisun software only allows one outdoor atmosphere to be presented, we introduced a coefficient "α" which relates the outdoor temperature conditions with the temperature conditions of the transitional area, such that in model B the exchanges of the rear facade are calculated by relating the indoor atmosphere with the outdoor atmosphere, and the exchanges of the main facade are calculated by relating the indoor atmosphere with the atmosphere in the transitional area (outdoor atmosphere times coefficient "α").

This coefficient "α" is obtained as follows:

- Assuming that the artificially heated or air conditioned shops will exchange energy primarily with the transitional space (due to the fact that the ground, ceiling and two facades in model B are attached to spaces with the same conditions and that the rear facade has a very small thermal transmission coefficient in relation to the large coefficient of the main facade and its extreme permeability to the passage of air).

- Assuming as well that the transitional space exchanges energy primarily with the outdoor atmosphere (due to its permeability to the air and the presence of large glass-encased spaces).

We conclude that the heat flow lost from the commercial spaces to the transitional space should be equal to the heat flow lost from the transitional space to the outdoor environment (bearing in mind in both cases the transmission, ventilation and internal contribution).

Thus, if the heat flow is equal to 0:

$$\sum Q = 0$$

Therefore:

$$Qin. \rightarrow trans. = Qtrans. \rightarrow out.$$

$$\boxed{Qtrans.in. + Qvent.in. + Qcont.in. = Qtrans.out. + Qvent.out. + Qcont.out.}$$

In which:

$$Qtrans. = \sum Si{\cdot}Ui{\cdot}\Delta T$$

$$Qvent. = Vi{\cdot}\delta{\cdot}Ce$$

$$Qcont. = in.contribution$$

With this, we obtain a function with three unknowns: the indoor temperature, the temperature of the transitional space and the outdoor temperature:

$$Tpas. = \frac{(k{\cdot}Tin.) + (k'{\cdot}Tex.) + k''}{k''''}$$

Assuming the outdoor and indoor conditions described above for the summer and winter, the result is:

$$\alpha = \frac{\Delta Tin.}{\Delta Tex.} = \frac{Tin. - Tpas.}{Tin. - Tex.}$$

Thus, we obtain the values: summer $\alpha = 0.4$; and winter $\alpha = 0.26$, in order to simulate with Archisun.

Regarding model C, the standard volume was once again taken, but adding the proportional part of the transitional area which is integrated into the inside of the shop and in the same environmental conditions. We also assumed that the floor is attached to a space with the same environmental conditions. To the contrary, we assumed the same kind of attachment for the ceiling, but with the percentage of roof proportional to the total volume of the building (since in this case there are neither homes nor offices above it). The four side facades were assumed to be open to spaces in the same environmental conditions, but also with the corresponding percentage of glass-encased or opaque facade corresponding to the volume of the model in relation to the total volume of the building.

RESULTS

The results of the simulations are as follows:

SUMMER	Model A	Model B	Model C
Outdoor temp. (ºC)	26.6	26.6	26.6
Transitional area temp. (ºC)	-	24.8	-
Natural indoor temp. (ºC)	27.1	27.1	27.6
Cooling energy consumption (kWh/m^3·year)	0.59	0.60	0.85

Table 1: List of outdoor temperature, temperature of the transitional area and natural indoor temperature as well as energy consumption for air conditioning in the summer scenario.

WINTER	Model A	Model B	Model C
Outdoor temp. (ºC)	8.1	8.1	8.1
Transitional area temp. (ºC)	-	17.6	-
Natural indoor temp. (ºC)	13.7	14.7	13.4
Heating energy consumption (kWh/m^3·year)	3.99	2.76	4.36

Table 2: List of outdoor temperature, temperature of the transitional area and natural indoor temperature as well as energy consumption for heating in the winter scenario.

DISCUSSION

Based on the simulations, we can see that the natural temperature results and therefore consumption are not significantly different. However, we can conclude that there are two variables that are particularly influential when calculating the results and which therefore must also be particularly influential when designing commercial spaces. First, we found that the parameter of the renewals per hour that the space experiences is particularly influential, that is, whether it is a very hermetically sealed place or, on the opposite extreme, highly ventilated (and therefore with high accessibility, but also with a higher energy exchange with the contiguous space). Secondly, we also noted that the parameter of internal contributions from the shop is also particularly influential, that is, the amount of heat dissipated inside it due to the activity of people, lighting points, computers, etc. Thus, we can see how the influence of the energy exchange due to the thermal transmission of the walls is not a priority parameter in the commercial spaces, and therefore when designing them a sound study of the ventilation and internal contributions from the commercial space will be much more decisive than the thermal insulation itself.

CONCLUSION

Finally, we should note that bearing in mind that the results of consumption are much more balanced than what might have been forecasted at first, model B does show an advantage regarding comfort, since it manages to achieve a more gradual thermal adaptation of the shop users with a higher adaptation time since they go from an outdoor to a fully heated and/or air conditioned indoor atmosphere through an intermediate atmosphere in environmental conditions that are halfway between indoors and outdoors.

ACKNOWLEDGEMENTS

This paper was supported by the Spanish MICINN under project ENE2009-11540.

REFERENCES

1. Coch, H.: La Utilitat dels Espais Inútils. Una aportació a l'avaluació del confort ambiental a l'arquitectura dels espais intermedis. PhD Thesis, Barcelona, 2003.
2. Rafael, S. and Roset, J.: Energy Conscious Design. World Renewable Energy Congress VI, 2000, p. 494-499.
3. Nicol, J. F. and Humphreys. M. A.: Adaptative thermal comfort and sustainable thermal standards for buildings. Energy and Buildings 34, p. 563-572.
4. Jentsch, M. F.; Bahaj, A. S. and James, P. A. B. Climate change future proofing of buildings – Generation and assessment of building simulation weather files. Energy and Buildings 40, p. 2148-2168.
5. Palme, M.; Coch, H.; Isalgué, A.; Marincic, I.; Fanchiotti, A. and Rafael, S: Dynamic sensation of comfort in buildings: the temperature changes effects. 2nd PALENC Conference Proceedings, Crete, Greece 27-29 September 2007, p. 13-18.
6. Palme, M.; Isalgué, A.; Coch, H. and Rafael, S: The possible impact of climatic change on the built environment: the importance of flexibility and energy robustness of the architecture. World Renewable Energy Congress XI, 2000, p. 544-549.

EXPERIMENTAL EVALUATION OF INDOOR VISUAL COMFORT CONDITIONS IN OFFICE BUILDINGS WITH THE INTEGRATION OF EXTERNAL BLINDS

Kleo Axarli[1]; Katerina Tsikaloudaki[1]; Charoula Ilioudi[1]

1: Laboratory of Building Construction and Physics, Department of Civil Engineering, Aristotle University of Thessaloniki, P.O. Box 429, 541 24 Thessaloniki, Greece.

ABSTRACT

The use of solar control devices contributes to the energy efficiency of buildings during the summer period and controls daylight levels throughout the year; however, it can result in increased heating loads in winter due to limited solar gains. Especially in modern office buildings with extensive glass surfaces, sun protection is essential and is often realized as unmovable blinds on the exterior of façades.

The objective of the proposed paper is to present the results of an experimental analysis regarding the impact of integrating external blinds on the transparent elements of the building envelope on the formation of indoor daylight conditions. The analysis is based on data derived from recording the illuminance on the working plane of two building models constructed for this purpose. The building cells are orientated due south and have identical geometrical and optical characteristics, with the exception of solar shading: one has no solar protection, while the other is shaded with unmovable horizontal blinds mounded on the external side of the window façade.

The evaluation parameters referred to both quantity and quality of daylighting. More especially, as regards daylight quantity, the distribution of illumination on characteristic points of the working surface of the two models is studied for two building cells for a period of one year. The quality of daylighting prevailing in the examined cells was approached by studying the uniformity of daylight distribution, as well as by conducting an in situ visual comfort survey among persons who used the space and filled in relative questionnaires.

The presentation of results for the two building cells, as well as their intercomparison, indicate the contribution of external blinds to the formation of daylight levels and visual comfort in office spaces.

INTRODUCTION

Nowadays, the bioclimatic building design regarding daylight is an important parameter, since it positively affects mental and physical health, workers' efficiency and environmental performance of buildings. However, careful study is required for the admittance and distribution of daylight in order to ensure its adequacy as well as its uniformity, so that glare occurrence is minimized.

At the same time, sun protection is necessary, especially in summer and particularly in the Mediterranean countries. The overall aim is to control the entry of direct solar radiation in buildings, which generally contributes to glare control and reduced cooling energy loads, without affecting the entry of diffuse radiation, leading thus to enhanced daylight levels and lower energy consumption for artificial lighting [1].

THE DESCRIPTION OF THE PROJECT

The effect of solar control devices on the optical behavior of spaces can be calculated theoretically or by measuring levels of daylight in an appropriate building [2]. For this reason, a special experimental building unit was constructed in Northern Greece (Thessaloniki, latitude 40°38'N, longitude 22°58'E), in order to investigate the optical behavior of external blinds. It was designed and developed in order to represent a typical module of an office building, with an aluminum and glass façade (curtain wall), which nowadays has wide application [3].

The building module is oriented due south and consists of two identical rooms, two separate "test cells" in contact (Figure 1). It is of rectangular shape, with external dimensions 7.10 m length in the direction east - west and 7.05 m width in the direction north - south. Its height is equal to 3.10 m and it covers a total area of 50.00 m^2. The cells are prefabricated, made of reinforced concrete and are fully insulated. Their entrance is placed on their northern side.

Each cell has a similar south-facing opening (2.90 m x 1.70 m), which acts as a passive solar direct gain system. In the west cell (cell A) a system with movable aluminium blinds extending from floor to ceiling has been mounted on the southern façade (Figure 1). The slats are 20 cm wide, gray-colored and the reflectivity of their surface was measured equal to 0.46. Their axis is placed at a distance of 15 cm from the south façade, while the distance between the slats is equal to 10.5 cm. The movement of the slats is achieved mechanically by an electrically driven mechanism, which allows their rotation of slats from 0^o (horizontal position, blinds completely open) up to 90^o (vertical position, blinds completely closed). Reverse rotation is not feasible.

The indoor conditions in both cells were recorded with a monitoring system. It includes 2 illuminance sensors placed horizontally in each cell at a height of 0,90 m above floor and at a distance of 1,75 m and 5,35 m respectively from the opening (Figure 2). Moreover, global solar radiation was also recorded for the simultaneous monitoring of ambient climatic conditions.

The experimental site and the monitoring system operated from August 2008 to July 2009. The blinds were regulated at 0^o, which means that they were placed in a horizontal position, except of the period of August and September 2008, during which the angle of the blinds was altered every 4 days, per 15^o.

Figure 1: The south side of the experimental cells [3]: Cell A with the integrated blinds on the left and cell B without solar protection on the right.

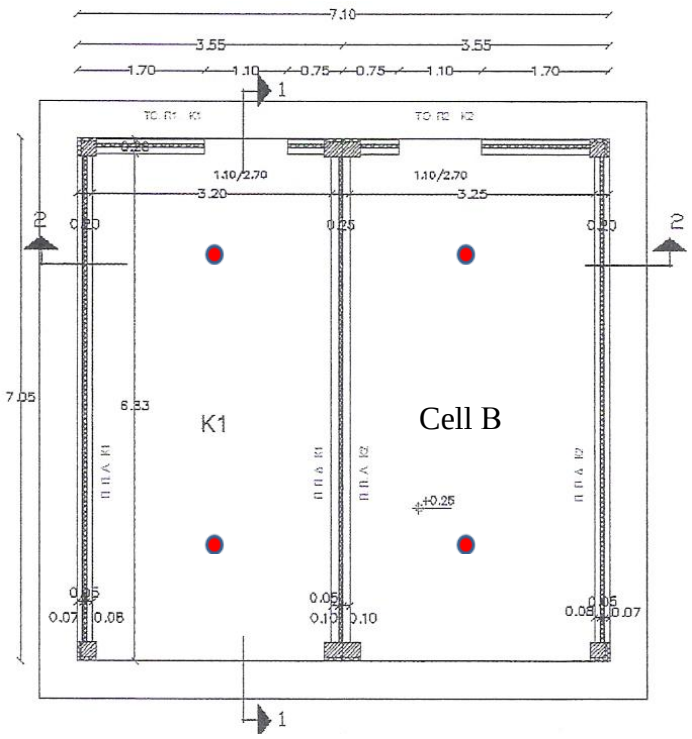

Figure 2: The mounting positions of sensors in relation to opening.

EXPERIMENTAL RESULTS OF MEASUREMENTS

The unmovable blinds on the exterior of façade of cell A is an integral element of the building, has an impact on the radiation that passes through the opening and participates in the configuration of visual comfort. The quantification of this impact, as well as the control of the efficiency of shading devices regarding daylight is the subject of this section. In general, visual comfort is defined from two aspects: the quantity and the quality of daylight in the interior of the building [4].

In order to study the influence of the blinds on both quantity and quality of daylight typical days representing cloudy and sunny sky conditions were selected on the basis of the intensity of global solar radiation [5], [6]. Two days were selected: the 21st of January 2009, as representative of a cloudy day and the 15th of July 2009, as representative of a sunny day.

Quantity of daylight

In Figures 3 and 4 the illuminance close to the opening and at the rear of the two cells is presented during the typical cloudy day respectively. Illumination levels in cell A is plotted on the left vertical axis (continuous line), while illumination in cell B (without solar protection) is plotted on the right vertical axis (dashed line). In general, the two lines follow the same distribution; maximum levels appear simultaneously, but their levels are significantly different. For example, the maximum illuminance recorded on the point near the opening in cell A is equal to approximately 1100lx, while the respective value for cell B reaches 115000lx. The difference becomes smaller at the rear of the building module; in cell A the illumination levels does not exceed 300lx, while in cell B it is almost six times higher. It must be mentioned that during the evening hours the illuminance in the interior of the cells is not equal to zero, due to external artificial lighting. The presence of blinds has led to reduced illumination levels on the horizontal plane near the window, which ranges from 82% to almost 90% of the levels recorded in the unshaded building module. The highest reduction of daylight levels is observed at noon, when the sun reaches its highest point in the sky vault.

At the rear of the room, the blinds reduce the illuminance at a rate ranging from 84% to 86% when compared to cell B.

The illuminance close to the openings of the two cells during a sunny day of July 2009 is presented in Figure 5. Again, illumination levels in cell A is plotted on the left vertical axis (continuous line), while illumination in cell B (without solar protection) is plotted on the right vertical axis (dashed line).

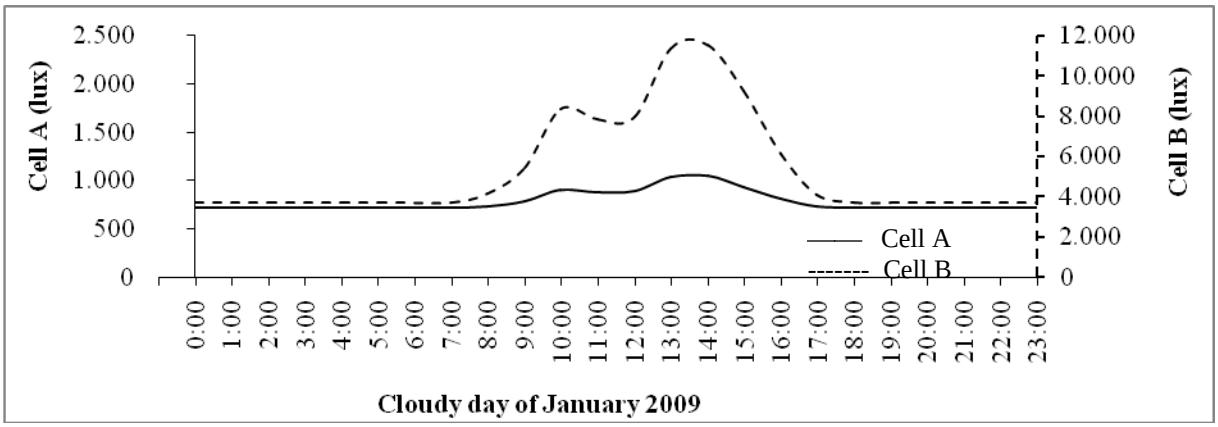

Figure 3: The illuminance close to the opening of cells (cloudy day of January 2009) [3].

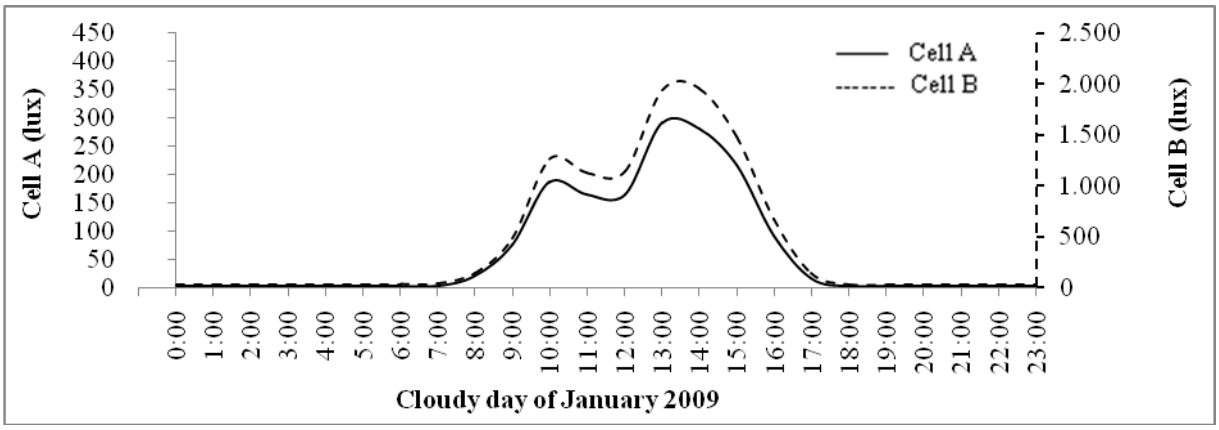

Figure 4: The illuminance away from the opening of cells (cloudy day of January 2009) [3].

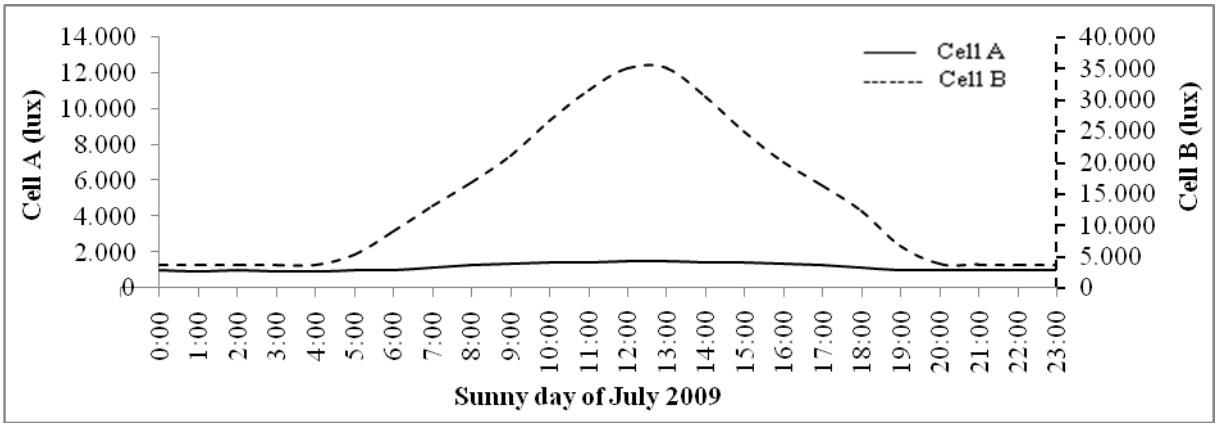

Figure 5: The illuminance close to the opening of the two test cells during the sunny day of July 2009[3].

Considering all the experimental results of measurements during one year, it is observed that the illuminance close to the opening of a building with integrated blinds is reduced from 75% to 98% when compared to an identical module without shading devices. Similarly, the illuminance away from the opening of the cell with integrated blinds is reduced from 80% to 94% compared to a module without shading devices. These rates depend on the prevailing weather conditions. It is obvious that external blinds influence the distribution and the levels of indoor illuminance at a great extent, since the transparency of the system "opening-shading device" alters significantly [7].

Quality of daylight

Quality of daylight can be assessed with qualitative characteristics, which interrelate the illuminance on the working plane with that of surrounding surfaces. A uniform distribution of light in the field of vision is required; otherwise, excessive contrasts can lead to visual comfort problems [8]. The illumination level on surrounding surfaces may be lower than the illuminance of the working plane, but it is recommended that both exceed threshold values. The uniformity of daylight can be expressed as the ratio of minimum to average value of illuminance in a space; ratio values greater than 0.7 contribute to visual comfort [9].

As has been already mentioned, the quantity of daylight is reduced at a great extent during both sunny and cloudy conditions. Due to the extremely high daylight levels prevailing under sunny skies, it is expected that the presence of the blinds and the consequent reduction of daylight levels at the front of the room would lead to a better lit environment. However, the question is whether the reduction of daylight under cloudy conditions would also contribute to the formation of visual comfort. The methodology described above was used in order to study the influence of external blinds on the formation of visual comfort in the building modules under cloudy conditions. For the most descriptive presentation of the results, it was assumed that the illuminance levels recorded close to the opening in cells A and B (named E_1 and E_3 respectively) represented the maximum values, while the illuminance recorded at the rear of the cells (named E_2 and E_4 respectively) represented the minimum values. The uniformity in the distribution of daylight in both cells was calculated for each hour of the selected cloudy day of January 2009 as the ratio of the minimum and average illuminance values (fractions $a=E_2/[(E_1+E_2)/2]$ and $b=E_4/[(E_3+E_4)/2)$. When *a* and *b*-values exceed 0.7, it can be regarded that the recommendation met in bibliography is satisfied. If *a*-value is greater than *b*-value, it is concluded that due to the presence of blinds the uniformity of daylight in cell A is enhanced in comparison to cell B.

Figure 6 shows the distribution of *a* and *b*-values during the selected cloudy day of January 2009. During the typical cloudy day, the *a* and *b*-values are significantly lower than 0.7. More

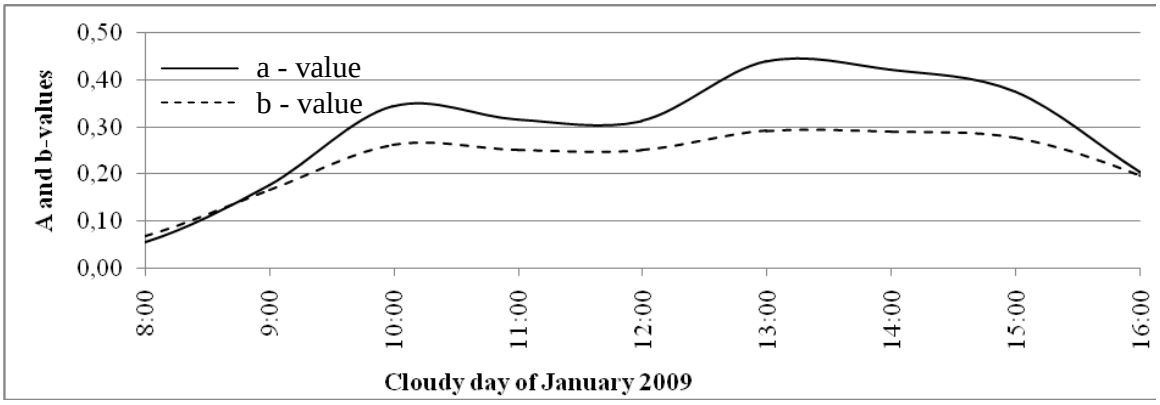

Figure 6: a and b-values for cells A and B respectively during a cloudy day in January 2009 [3].

specifically, *a*-value is greater than *b*-value from 09:00 to 16:00; that means that during the typical working hours the distribution of daylight in cell A is more uniform than the distribution of daylight in cell B, therefore the visual conditions in the interior of cell A are enhanced due to the presence of blinds.

CONCLUSIONS

The blinds in office buildings contribute to the formation of indoor daylight conditions by reducing illumination levels both in the front and at the rear of the room. The existence of horizontal blinds improves the distribution and uniformity of daylight, especially during working hours. The inclination of the blinds is responsible for the amount of daylight that is admitted indoors; the greater the inclination is (90^o corresponds to closed blinds), the lower the maximum illuminance becomes.

ACKNOWLEDGEMENTS

The project for the study of external blinds with regards to their influence on the formation of thermal and visual indoor conditions has been supported by ALUMIL S.A. which supplied the aluminum system-glazing and blinds.

REFERENCES

1 Baker, N., Steemers, K.: Daylight Design of Buildings. James & James, London, 2002.

2 Commission of the European Communities, Directotate-General XII for Science, Research and Development: Daylighting in Architecture, a European reference book. James & James, London, 1993.

3 Ilioudi, C.: Study of the impact of integrated external blinds on the estimation of daylight levels and visual comfort in office buildings. Thesis submitted in the Department of Civil Engineering, Aristotle University of Thessaloniki, Thessaloniki, 2010.

4 Argiriou, A., Asimakopoulos, D., Balaras, C.: Daylight Techniques in Buildings, reference handbook. European Commission, Directotate-General XVII for Energy, Altener Programme, Athens, 1997.

5 CIE: Spatial distribution of daylight-Luminance distributions of various reference skies. CIE 110.1, Austria, 1994.

6 Markou, M., Kambezidis, H., Katsoulis, B., Muneer, T. & Bartzokas, A.: Sky type classification in South England during the winter period. Building Res J 52 2004.

7 Axarli, K., Tsikaloudaki, K., & Vaitsi, Ch.: Assessing the solar transmittance of window blinds and their impact on the energy performance of office spaces. Proc. of 9th IHT conference, pp 117-124, Paphos, Cyprus, 2009.

8 Fuller, Moore: Concepts and Practice of Architectural Daylighting. Van Nostrand Reinhold, New York, 1991.

9 ISO 8995, CIE S 008/E, Lighting of indoor work places.

SIMULATING OCCUPANT BEHAVIOUR AND ENERGY PERFORMANCE OF DWELLINGS: A SENSITIVITY ANALYSIS OF PRESENCE PATTERNS IN DIFFERENT DWELLING TYPES

M. Bedir[1]; G. Ulukavak Harputlugil[1,2]

1: OTB Research Institute for Built Environment, TUDelft, Jaffalaan 9, 2628BX, Delft, the Netherlands

2: Safranbolu Fethi Toker Faculty of Fine Arts and Design, Karabük University, Karabük, Türkiye

ABSTRACT

Influence of occupant behaviour on the energy performance of dwellings is an emerging research topic: Not only the amount of studies is insufficient, but also they provide contradictory results. The aim of this study is to reveal the sensitivity of dwelling energy performance to the presence of occupants in different dwelling types, assuming that presence is the precondition of behaviour. Sensitivity of dwelling energy performance to occupant presence is analysed using Monte Carlo method, which is one of the most commonly used methods to investigate the approximate distribution of possible results (energy performance) on the basis of probabilistic inputs (presence). For this study, the hourly inputs of presence are derived from a database of 319 dwellings in the Netherlands. 4 different types of Dutch reference dwellings are selected for the simulation model: Row house, Corner/Semi-detached, Free standing, and Flat. Steps of the methodology are as follows: (1) Pre-processing behaviour data (the maximum and minimum values of the input parameters); (2) Gathering samples from SimLab pre-processor; (3) Simulating each sample by a dynamic simulation program to collect output data. (The simulations are made with 'one at a time' approach. Each input is perturbed in turn while keeping all other inputs constant at their nominal value); (4) Combination of inputs and outputs in post-processor of SimLab to run Monte-Carlo analyses. Results of this study showed that presence varies at the weekends more than it does during the weekdays. Corner/semi-detached dwelling is the dwelling type that presence is the most consistent during the weekdays, and row house at the weekend. Flat is the dwelling type that demands the least heating energy, and corner/semi-detached is the most. Weekdays are more influential on the heating energy demand than the weekends. Corner/semi-detached dwelling energy performance is the most sensitive to presence on weekdays, row house at the weekend.

INTRODUCTION

A building consumes energy depending on its envelope characteristics, the systems installed for its services (heating and ventilation systems, electricity production and hot water), the site and climate it is located in and the behaviour of its occupants. Presence and occupant behaviour is an aspect of building energy performance that has been studied for the last two decades. In this paper, assuming that presence is the precondition to occupant behaviour in a building, the sensitivity of dwelling energy performance to the presence of occupants in different dwelling types is studied.

Sensitivity analysis, the study of how the variation in the output of a model can be qualitatively or quantitatively apportioned to different sources of variation, is conducted based

on a mathematical model defined by a series of equations, input factors, parameters, and variables aimed to characterize the process being investigated. Input is subject to many sources of uncertainty including errors of measurement, absence of information and poor or partial understanding of the driving forces and mechanisms. This uncertainty imposes a limit on the confidence in the output of the model (e.g. Hamby et al, 1994; Helton et al, 2006)

One of the most common sensitivity analysis practice works is based on sampling (random, importance, Latin hypercube). In general, a sampling-based sensitivity analysis is one in which the model is executed repeatedly for combinations of values sampled from the distribution (assumed known) of the input factors. There are several examples of the application of sensitivity analysis in building thermal modelling (e.g. Spitler et al, 1989; Corson, 1992; Fülbringer and Roulet, 1999; McDonald, 2004; Harputlugil et al, 2009; Bedir et al, 2011). For sensitivity of energy simulation models, a set of input parameters and their values are defined and applied to a building model.

The simulated energy performance of the model is used as a base for comparison to determine how much the output (here measured in terms of heating energy demand in the heating season) changes due to particular increments of input values (here presence) (Corson, 1992). Consequently the results show which parameters can be classified as "sensitive" or "robust". Sensitive parameters are the parameters that by a change in their value cause effective changes on outputs (in this case heating energy demand). Contrarily, change of robust parameters causes negligible changes on outputs.

The aim of this study is to find how sensitive or robust the dwelling energy performance is to occupant presence, and presence only. Accordingly, the analysis looks for the thresholds that energy performance of a dwelling becomes sensitive to presence. The sensitivity analysis is conducted on 4 different types of Dutch reference dwellings from year 2010: Row house, Corner/Semi-detached, Free standing, and Flat, considering that the sensitivity of dwelling energy performance could be different in different dwelling types.

METHOD

Monte Carlo method is used for the sensitivity analysis. It is one of the most commonly used methods to analyse the approximate distribution of possible results on the basis of probabilistic inputs (Lomas and Eppel, 2007; Hopfe et al, 2007). In this research, the inputs (parameters) include presence at home, thus the internal heat gain resulting from presence.

The steps of the analysis are as follows (Figure-1):

- Pre-processing survey data (see next section) in statistical analysis program (the maximum and minimum values of the input parameters are determined)
- Gathering random samples which are uniformly distributed from max and min values from SimLab pre-processor (SimLab)
- Simulating each sample by a dynamic simulation program to collect output data. The simulations are made with 'one at a time' approach. Each input is perturbed in turn while keeping all other inputs constant at their nominal value.
- Combination of inputs and outputs in post-processor of Sim-Lab to get Monte-Carlo
- Interpretation of the results

Data

4 Dutch reference dwellings for row, corner/semi-detached, free standing, and flat (Referentie woning, 2010) are modelled using the simulation software. The characteristics of the

reference dwellings are explained below: Figure 1, the architectural drawings, and Table 1, the envelope properties.

Row house *freestanding house*

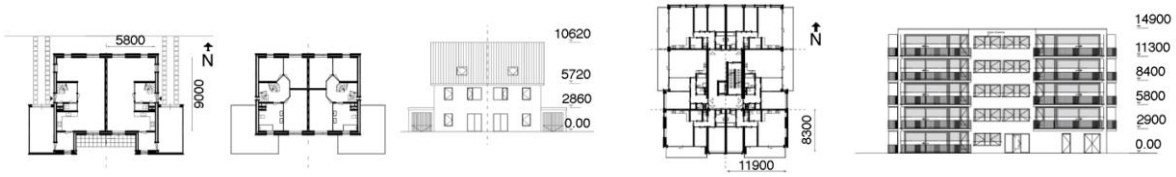

Semi-detached house *flat*

Figure 1: Plans and sections of the reference dwellings.

Characteristics of the reference dwelling	**Row**	**Corner/semi-detached**	**Free standing**	**Flat**
Width (m)	5,1	5,8	6,0	8,3
Depth (m)	8,9	9,0	10,2	11,9
Height (m)	2,6	2,6	2,6	2,6
Floor area (m^2)	45,4	52,2	61,2	98,8
Volume (m^3)	118,0	135,7	159,1	256,8
Rc façade (m^2K/W)	3,0	4,0	4,0	4,0
Rc roof (m^2K/W)	4,0	5,0	4,0	5,0
Rc ground floor (m^2K/W)	3,0	3,0	3,0	3,0
U window (W/m^2K)	1,8	1,7	1,7	1,7
U front door (W/m^2K)	2	2,0	2,0	2,0
EPC value (NEN5129)	0,78	0,80	0,80	0,80
Yearly energy use (MJ/m^2)	359	401	417	346

Table 1: Dimensions, envelope and energy use characteristics of the reference dwellings.

Data about presence is collected in two neighbourhoods that began to develop in 1996, in the Netherlands. The survey was conducted in Winter 2008, in 319 dwellings. Hourly presence patterns of these dwellings (based on the dwelling type) are converted to single daily presence values, and descriptive statistical analysis is applied to be able to obtain the maximum and minimum values of presence. These values are processed in SimLab pre-processor for gathering the generic presence patterns for 4 different dwelling types (see Pre-processing survey data step, in previous section).

Based on the 40 samples generated from pre-processor of SimLab, heating energy demand for each sample during the Dutch heating season (assumed as 01.October-01.April) is calculated with 'one at a time' approach (see previous section), using a dynamic building simulation program. Note that, semi-detached house is one of the two houses in the cluster, and the flat is one of the units that are located in one of the intermediary storeys of an apartment building.

The analysis of the results is conducted using the Monte Carlo statistical analysis method, in the post-processor of SimLab.

RESULTS AND DISCUSSION

The presence inputs generated from the survey sample for each dwelling type show that presence during weekdays in corner/semi-detached dwelling does not vary a lot (R^2:0.78). Second most constant is the weekdays presence for flat type (R^2:0.66). Weekdays presence for row houses (R^2:0.59) and free standing (R^2:0.09) follow the flat type. At the weekends, the variance of presence for different dwelling types is as such: Row house (R^2:0.28), flat (R^2:0.20), corner/semi-detached (R^2:0.13), and free standing (R^2:0.03).

	Minimum presence sample (w/day)			**Minimum presence sample (w/end)**			**Maximum presence sample (same w/day & w/end)**		
	W/day (person)	**W/end (person)**	**Heating Energy Demand (kWh)**	**W/day (person)**	**W/end (person)**	**Heating Energy Demand (kWh)**	**W/day (person)**	**W/end (person)**	**Heating Energy Demand (kWh)**
Row	1	2	43.56	2	1	41.80	4	5	31.89
Corner/ semi-detached	1	1	61.81	1	1	61.81	4	5	49.54
Free standing	1	2	51.30	2	1	50.45	3	3	47.53
Flat	0	1	9.10	1	0	8.47	3	3	5.41

Table 2: Minimum and maximum presence values for the weekdays and the weekend and the heating energy demands.

In addition, the samples of each dwelling type, with minimum and maximum presence for weekdays and weekends are compared (Table 2). The sample with minimum presence for weekday and the sample with minimum presence for weekend are considered separately for minimum presence samples. For the corner/semi-detached dwelling type, minimum presence for weekday and weekend is the same (1/1). Maximum presence for weekday and weekend are the same in all dwelling types. For flat, the minimum presence sample for weekday includes '0' person presence. The row and the corner/semi-detached dwelling have more presence than the flat and the free standing (4/5 to 3/3).

Presence has a negative influence on the heating energy demand of the dwelling, by means of the internal heat gain; and, flat is the least energy demanding dwelling type vs. corner/semi-detached dwelling type. Samples with minimum presence for weekend result in lower heating energy demand values than the ones with minimum presence for weekday. The minimum presence for weekday and weekend is the same for the row house and the free standing. The heating energy demand is higher in the latter, 15% for the minimum presence sample weekday (1/2), and 17% for the minimum presence sample weekend (2/1). The maximum presence values for weekday and weekend are the same for the row house and the semi-detached (4/5). The heating energy demand is 36% more in the latter. (Table 2 - Figure 2).

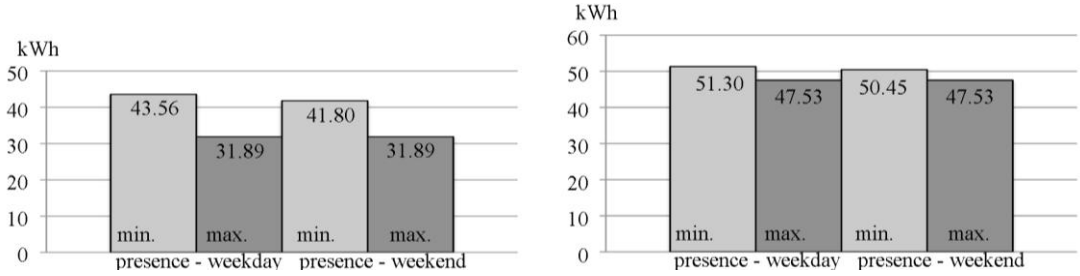

Row house *freestanding house*

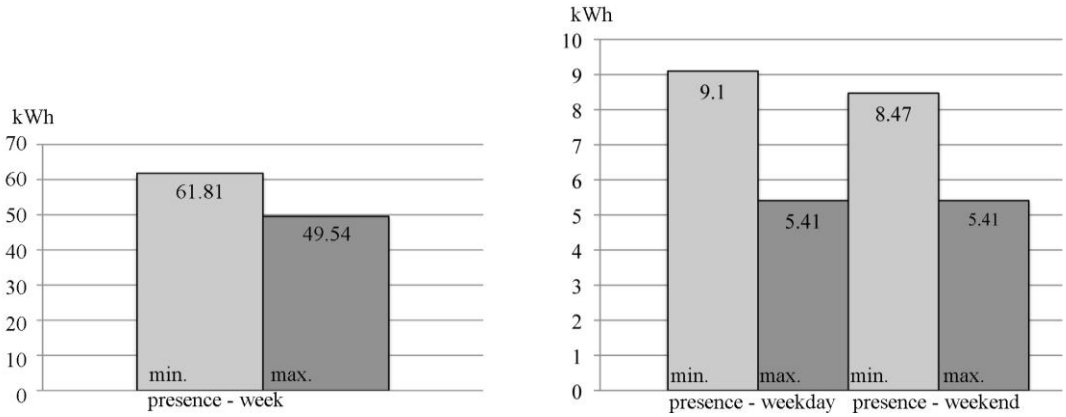

Semi-detached house *flat*

Figure 2: The heating energy demand values for minimum and maximum presence in weekday and weekend for different dwelling types.

When the pear values for different type of dwellings for the weekday and weekend presence values are compared, it could be seen that the most sensitive dwelling type to presence is the corner/semi-detached for the weekdays. The flat, the row and the freestanding dwelling types follow the corner/semi-detached dwelling type, from the most to the least sensitive, for the weekdays. When a similar comparison is made for the weekend, the row house is the most sensitive to presence. The flat, the corner/semi-detached, and the freestanding dwelling types follow the row house (Figure 3).

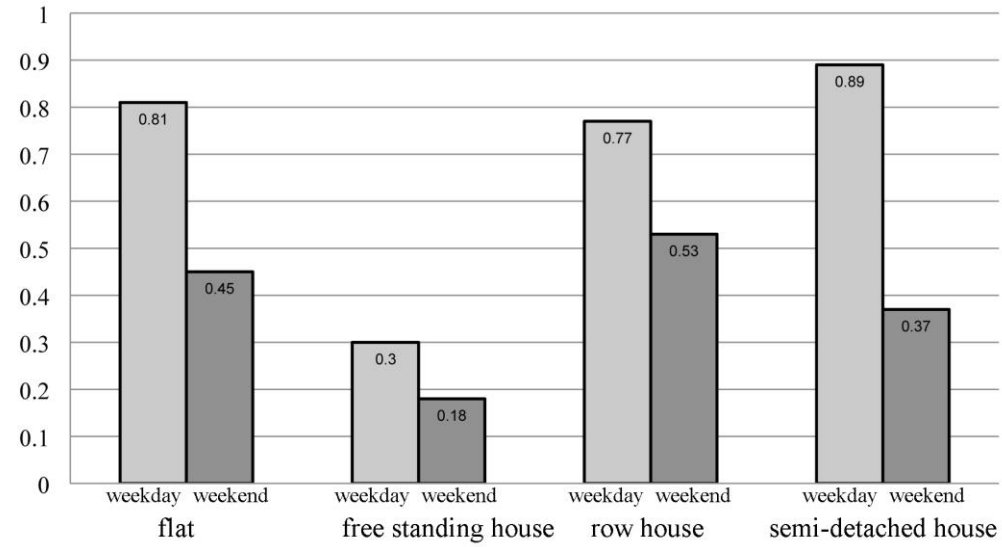

Figure 3: PEAR values for presence in weekday and weekend for different dwelling types.

CONCLUSION

In this paper, we focused on exploring the sensitivity of energy performance of a dwelling to presence, assuming that presence is the precondition of behaviour. Results of this study showed that weekdays are more influential on the heating energy demand than the weekends.

In addition, corner/semi-detached dwelling type is the most sensitive to presence in terms of the energy performance, during the weekdays, and row house is the most sensitive during the weekend.

Another result is that presence varies at the weekends more than it does during the weekdays. Also, corner/semi-detached dwelling is the dwelling type that presence is the most consistent during the weekdays, and row house at the weekend. Lastly, flat is the dwelling type that demands the least heating energy, and corner/semi-detached is the most.

This paper covers only presence, and it is necessary to include ventilation, and heating behaviour in further analysis. In order to reveal the interrelations among presence and different behavioural patterns, and their influence on the heating energy demand of dwellings, a further analysis is still under progress with 250 samples, and the factors of presence, ventilation, and thermostat settings.

ACKNOWLEDGEMENTS

This paper forms one part of Gülsu Ulukavak Harputlugil`s six months post-doc research in OTB Research Insititute for Built Environment/ Delft University of Technology, which is funded by Scientific and Technical Research Council of Turkey (TUBITAK).

REFERENCES

1. Bedir, M. and Harputlugil, G. U. 'Exploring Robustness of Energy Performance of Dwellings to Occupant Behaviour' The CIB International Conference – MISBE 2011
2. Corson G. C., Input-Output Sensitivity of Building Energy Simulations, *ASHRAE transactions, 98* (Part I), 618-626, 1992.
3. Fülbringer and Roulet, Confidence of Simulation Results: Put a Sensitivity Analysis Module in Your Model, *Energy and Buildings*, 30, 61-71, 1999.
4. Hamby, D. M., A Review of Techniques for Parameter Sensitivity Analysis of Environmental Models, *Enviromental Monitoring and Assessment*, 32, 135-154, 1994
5. Harputlugil, G.U., de Wilde, P.J.C.J, Hensen, J.L.M., Çelebi, G., Development of a thermally robust school outline design for the different climate regions of Turkiye, *Proceedings of 11th International IBPSA Conference*, Glasgow, United Kingdom, July 27-30, 1292-1298, 2009.
6. Helton, J. C., Johnson, J. D., Sallaberry, C. J., Storlie, C. B., Survey of Sampling Based Methods for Uncertainity and Sensitivity Analysis, *Reliability Engineering and System Safety*, 91, 1175-1209, 2006.
7. Hopfe, C., Hensen, J., Plokker, W., Uncertainity and Sensitivity Analysis for Detailed Design Support", *Proceedings of the 10th IBPSA Building Simulation Conference*, 3-5 September, Tsinghua University, Beijing, 1799-1804, 2007.
8. Lomas K.J., Eppel H., Sensitivity analysis techniques for building thermal simulation programs, *Energy and Buildings*, 19 (1), 21-44, 1992.
9. Mc Donald, Assessing the Significance of Design Changes when Simulating Building Performance Including the Effects of Uncertain Input Data, *Proceedings of e-Sim'04*.
10. NEN 5128, Energieprestatie van woonfuncties en woongebouwen - Bepalingsmethode
11. Referentiewoningen Nieuwbouw (as from 2010): www.senternovem.nl
12. SIMLAB, 2007, Simlab version 2.2 manual, http://simlab.jrc.ec.europa.eu/
13. Spitler, J. D., Fisher, D. E., Zietlow, D. C., A Primer on the Use of Influence Coefficients in Building *Simulation, Proceedings of Building Simulation '89 Conference*, IBPSA, Belgium, 299-304, 1989.

INDOOR ENVIRONMENT QUALITY – CASAS DE SANTO ANTÓNIO, BARREIRO

Carrapiço, I. [1], Amado, M.P. [2]

[1] *GEOTPU - Faculdade de Ciências e Tecnologia da Universidade Nova de Lisboa, Campus da Caparica, 2829-516 Caparica, Portugal. ic@fct.unl.pt*
[2] *Civil Engineering Department, Faculdade de Ciências e Tecnologia da Universidade Nova de Lisboa, Campus da Caparica, 2829-516 Caparica, Portugal. ma@fct.unl.pt*

ABSTRACT

In the context of a growing change in the way we inhabit and regarding the time spent indoors, the quality of indoor air and, more generally, all the factors related to the indoor environmental comfort such as air temperature, humidity and air movement, have become issues of major relevance. In this study we will analyze and pinpoint the relation between a set of physical factors that we present as contributing to the indoor environment quality, the bioclimatic and passive solar measures, together with other architectural solutions, and the quality of indoor environments; for that we referred to the case-study of urbanization of Casas de Santo António, which was developed in 2007 as a pioneering project for an eco-neighbourhood in Portugal. This way, we will begin by analyzing and systemizing which type of factors contribute in the process for obtaining indoor air quality and why; then we will analyze the case-study at the level of passive strategies, active and passive systems used to implement the project, such as the strategic importance of solar orientation of each volume housing, their places of permanence; and the relationship between them, given the emphasis attributed to exposure to direct sunlight in a continuous mode for all buildings. Therefore, we will also study a set of elements that have a direct impact on the quality of internal air, like the thermal insulation, the solar gains / losses, the natural ventilation, the ratio of glazed area in relation to its orientation and to the outside shade, materials and finishing, lighting, energy systems and solar thermal systems. It has also been considered interesting to assess the feedback from the residents of the urbanization, regarding their perception of indoor environment quality. In order to assess this relation, we will carry out a survey with residents designated A and B. This option is related to the belief that the quality of indoor environment, as well as thermal comfort levels, is largely influenced by users' behaviours.

INTRODUCTION

The analysis of the construction process regarding residential buildings, points out as relevant the fact that in its different constructive aspects it contributes for a better and more efficient environmental comfort and, simultaneously allows a reduction of the energy consumption from the project phase until its future use [5].

The relation between buildings and their users has been evolving in the last few decades; this evolution is reflected in the fact that individuals, particularly in urban spaces, spend 80 to 90% of their time indoors. The increasing concern to improve the environmental comfort inside buildings led to more frequent building envelop interventions and consequently to a growth of the energy consumption; indoor air quality has been left behind, leading the average concentrations of various pollutants in indoor air to increase substantially, with main consequences at the ecological and human level. The latter are already known to compromise

health and work performance in individuals. Such decrease in indoor air quality has come to be known as "Sick Building Syndrome" (SBS), which applies to situations where the poor quality of the air is at the origin of temporary unhealthy living conditions for the users. In this context, the quality of indoor air and, more generally, all the factors related to the internal environmental comfort such as air temperature, humidity and air movement, have become issues of major relevance in a number of countries.

In order to achieve an environmental comfort inside our buildings, minimize avoidable spending, rationalize natural resources, minimizing the environmental impacts, it becomes necessary to explore a methodology, converging to the operativeness of the sustainable building process [3]. This way, the present study aims to analyze the different factors that contribute to obtaining indoor environment quality and their role in it. Afterwards, we will relate those factors to what has been implemented on the case study, the urbanization of Casas de Santo António in Barreiro; we will analyze its architecture at the level of passive strategies; active and passive systems used to implement the project; the strategic importance of solar orientation of each volume housing, their places of permanence; and the relationship between them, given the emphasis attributed to exposure to direct sunlight in a continuous mode for all buildings. Therefore, we will also study a set of elements that have a direct impact on the quality of internal air, such as the thermal insulation, the solar gains / losses, the natural ventilation, the ratio of glazed area in relation to its orientation and to the outside shade, materials and finishing, lighting, energy systems and solar thermal systems.

Indoor Environmental Comfort

The factor of indoor comfort can be difficult to define, as a range of environmental and personal factors must be taken into consideration when deciding what makes people feel 'comfortable'. J. Fergus Nicol and Michael A. Humphrey (2002) defined thermal comfort though the parameters: temperature, humidity and wind velocity, where the activity and clothing are important [8]. Another concept of thermal comfort was defined in British Standard BS EN ISO 7730 as *"that condition of mind which expresses satisfaction with the thermal environment"*[12]. The Health and Safety Executive has stated that the "best that you can realistically hope to achieve is a thermal environment that satisfies the majority of people in the workplace". It considers 80% of occupants as a reasonable limit for the minimum number of people who should be thermally comfortable in an environment [12].

The efforts made towards the achievement of the desirable indoor environmental comfort during the different seasons, lead to important energy consumption through acclimatization solutions with mechanical equipment application, ventilation and air renewal. Even though the level of environmental comfort desired varies depending on the geographic location and is subjective from one person to another, some of its parameters can be standardized, through measures and procedures, making it possible to reach it with low levels of energy consumption. A division into two types of factors was considered: Physical and Sensitive factors (figure 1).

Since the sensitive factors are more difficult to standardize, given the aesthetics, sociological and cultural components they depend on, we opted to analyze the physical factors regarding its specific contribution to indoor environment quality.

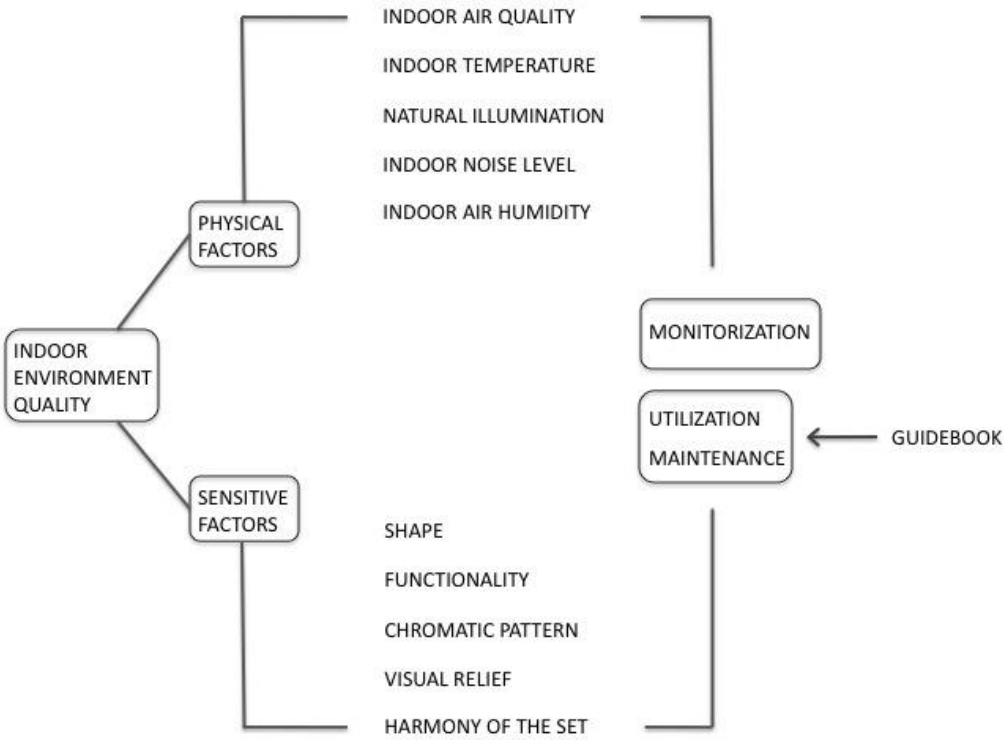

Figure 1: Factors contributing for Indoor Environment Quality

Method - Indoor Air Quality

Is variable according to the dimension and volume of the space, the speed and volume of the renewal of the air and the located sources of pollution inside the buildings [4]. Indoor air quality is a very important factor in the level of environmental comfort, and its improvement is associated with enhancing natural ventilation conditions. Various factors can influence the degradation of indoor air quality, such as the existence of dust and particles in suspension, odours, smoke and combustion gases and the gas release from products and materials used in the construction.

- Indoor Temperature

Temperature constitutes a highly determinative factor to the level of environmental comfort, being associated for this reason to the greatest energy consumptions of buildings use, throughout the different seasons of the year. The indoor temperature is conditioned by factors such as the inertia of the construction, the area of direct solar display, volume and air speed. [7]

- Natural Illumination

Is directly dependent of the solutions adopted in the conception of buildings, its form, dimension of glazed areas and solar protection systems. Natural light conditions should adapt to building functions, in order to prevent additional and permanent need of extra energy consumptions. [6]

- Indoor Noise Level

The level of noise depends essentially on two aspects: the space configuration and the constructive system adopted. We still verify that aerial noises and noises of percussion are, in a general way, inexistent or badly conceived in the project phase. Furthermore the acoustic insulation can prevent a level of noise that could be at the origin diseases of the users of the same buildings. [13]

- Indoor Air Humidity

A high level of indoor air humidity is in its great majority of times due to the lack of air renovation inside a building [4], and it is safe to say that in a general way the constructed residential buildings present a poor level of natural ventilation. The adoption of systems of general and permanent ventilation, incorrectly scaled and executed, without any control

possibility for the periods of summer and winter, leads to the use of mechanical equipment for humidity control, consuming a large amount of energy. Also, inadequate air moistness levels propitiate the appearance of building pathologies with negative effects in its users' health. Thus, building envelopes should guarantee adaptable natural ventilation systems and surface materials selection according to the hygrometric behaviour in the interior and exterior of the building [6].

RESULTS AND DISCUSSION

The chosen case-study for the analysis of these parameters and other architectural solutions contributing to the indoor environment quality is the urbanization of Casas de Santo António, a pioneering project for an eco-neighbourhood in Portugal; the project stemmed from a desire to combine sustainable urban planning and a bioclimatic architecture, embracing an ecological lifestyle. Its program is essentially residential, complemented with commercial and services areas. Within the residential area (253 dwellings) we have single and multi-family housing. The main goal was to develop a project with a bioclimatic basis, complemented with architectural systems and solutions that would allow the obtainance of a model of energetic efficiency and indoor environment quality. The intervention has prioritized factors such as the articulation between the set of the urbanization with the woods next to it, the solar orientation of each volume, its permanence spaces, with an emphasis regarding the natural light exposure in a continuous way to each dwelling. Also, the strategies of natural ventilation to obtain a good air quality, the proportion of glazed areas in relation with its solar orientation e respective solar protections, thermal insulation, solar thermal systems, the acoustic insulation and the guidance for the use and maintenance of each dwelling [10]. In the following table (Figure 2) we synthesize the referred measures according to the different intervention stages: Project, Construction, Utilization and Maintenance [2].

The results of the various bioclimatic features and architectural solutions contributing to the indoor environmental quality of the urbanization were verified on the one hand by a Class A+ [1] Energy Efficiency and indoor air quality Certificate, according to the new certification regulation, and on the other hand by the surveys made to residents A and B of the urbanization, the first one living in an apartment in a multifamily building and the second one occupying an isolated single family house.

As a complement to the bioclimatic strategies and systems, a building utilization and maintenance manual was made for each type of habitation, in order to obtain the highest level of comfort, in a sensitive, thermal, acoustic and functional level. The main topics are essentially the ventilation, the heating, the cooling, and the selective separation of trash and for the multifamily housing the use of the common spaces [11]. From the analysis of the surveys, it was understood that many of the procedures held on by the residents are very much the same as those expressed by the architects in the manual. Such procedures would be for example the utilization of equipments classified as A or superior, low-consumption illumination, water saving, among others. The general adherence to these "good procedures" can be explained by the fact that both residents A and B considered the opportunity to integrate a sustainable project as the most attractive factor in the urbanization. Globally, in terms of comfort the residents were satisfied; especially in terms of the crossed-ventilation system and the indoor air quality, the residents confirmed that humidity, condensations and odours were avoided, constituting a great improval regarding their previous houses. Regarding the thermal comfort, the solar orientations were referred as strategies for obtaining thermal comfort (Northeast Southwest and North/South for the single family houses and

INTERVENTION STAGE	ACTION	DESCRIPTION
PROJECT	Building setting, location, shape and solar orientation providing a high sun exposure level (energetic, thermal and light save)	. Exploitation of the gains comming from direct solar radiation . Orientation NorthEast - SouthWest - continuous direct sunlight in the SouthEast and SouthWest Facades during the majority of the day . Orientation North-South – continuous direct sunlight in the East, South and West Facade and ocasionally on the North facade . Natural daylight with appropriate intensity to the use within the building
	Orientation and glazed areas sizing, optimizing the Sun exposure	. Natural Illumination – natural light and relation with the internalspatial organization and the dimension and geometry of Windows . relation between spaces areas and glasses areas and solar orientation . Major surface at South/SouthWest . Thermic and luminic calculation to obtain the most efficient dimension and proportion assuring the solar gains necessary for the coldest periods of the year
	Building orientation and volume of the shape, according to the solar, winds and noise exposure (maximize the summer winds exposure)	. Spatial interior organization according to solar orientation – permanence areas at south and services areas at north . The volume of a house is a cube – ideal for prevention against thermic lossess and maintenance of solar gains
	Systems of shading and protection – passive and active systems	. Shading systems – fixed and removable and displacement of the concrete slab results in shadow during the Summer and solar penetration in the Winter
	Natural/natural ventilation for cooling and air renovation in the inside of the building	. Local main winds considered in the Project design. . Windows in opposite façades – passive crossed-ventilation for optimum thermal comfort and good air quality . Housings'shape allows the fluence of the air . Mixed Windows system – opening and tilting window allowing nocturn ventilation
	Constructive system that permits passive energetic save	. Thermal Insulation – System of exterior continuous thermal insulation . Thermal Inertia – Thermal break Windows with two – leaf glass and vacuum box . Stone Azul Valverde – material applied on the floor near the Windows facing south to the maintenance of solar gains
	Wind protection and orientation using vegetal species	. Vegetal species plantation as a way of assuring a good rate of air renewal indoors
	Utilization of systems and equipments that promote the energy savings	. System of water solar heating, thermodynamic, with solar panel . Selection of Water-saving and control of consumption equipment – with taps of pressure atomizer, thermostatically controlled taps and toilets with low-flow option, ensure efficiency in consumption and an improvement in the management of water resource . Also efficient lightening equipment. . Possibility of connecting the solar hot water to the washing machine
	Adeqiate building spaces and functional organization according to the number of users	
	Inclusive design of the building spaces improving mobility	. Conception of housing and public spaces in order to have total acessibility
	Systems of water re-utilization and rainfall water collection	. Naturalized system for the rainfall water collection . The dark waters produced in the housings are conveyed to the public network
CONSTRUCTION	Elaboration of workmanship quality and safety plan and manual of building construction	
	Rigorous control of workmanship plan implementation in the building phase	
	Workmanship's temporary consumptions reduction, reuse and recycle	
	Optimization of the technologic building process: minimize, modulate, adapt and computerize	
	Rigorous building execution control	
	Use of high-efficiency-low energy and water consumption equipments	
	Selection of certified materials: of high durability, minimum waste production and pollution, easy assemblage and maintenance	
	Energy consumption control automated systems (domotic's)	
	Thermal and acoustic exterior insulation	. Constructive materials ensure an effective thermal inertia, reducing the need of heating or cooling.
	Thermal isolated window components	
	Installation of wooden door blinds in Windows for improved thermal adaptation, with air space between glazed and blind surfaces	
	Exterior surface materials according to acoustic characteristics	
	Autonomous systems of air admission – natural ventilation	
	Execution of waterproofing emergency systems	
	Solar energy collector for sanitary waters in each dwelling	
	Water flow control and reduction devices	
UTILIZATION	Building utilization manual	
	Utilization of spaces according to the Project foreseen use	
	Natural/natural ventilation flow regulation according the year seasons (Winter/Summer)	
	Regulation of the solar protection systems according to the periods of major radiation	
	Daily opening of glazed surfaces	
	Utilization exclusively of equipment with a A classification or superior	
MAINTENANCE	Manual of building maintenance actions – the selection of building materials took into account their durability, in order to reduce its maintening. Procedures were created for the use of spaces regarding the ventilation and Sun protection aspects. A system of waste separation in the kitchen was also planned in order to encourage recycling and in the gardens a box for the compost of vegetable waste	
	Regular maintenance of solar protection, and natural ventilation systems	

Figure 2: Intervention stages and measures for Indoor Environment Quality

East/West for the multifamily houses); such as the exterior blinds, the displacement of the concrete slab facing south, the conduction of the main winds with the use of vegetation, the thermal break window with two leaf-glass and vacuum box, the type of materials near the window and the exterior thermal insulation, were referred in the surveys as efficient methods. However, it was pointed out that the houses would have a behaviour a little bit under the expect at this level, revealing colder than expected in the winter (for the multifamily houses) and just a bit hotter in the pick of the summer, and colder in the winter (for the single-family houses). Regarding the illumination, the residents enhance the natural light quality, in fact with an almost continuous presence for the entire day. The levels of internal illumination were determined in the Project phase, for each space and in function of the type of activities happening there. As the acoustics are concerned, both residents consider that the interior space is well isolated, with the windows with tow-leaf with acoustic insulation, and also the green space surrounding the urbanization.

To sum up, the case study was chosen for being a pioneer project in Portugal and for prioritizing sustainable measures leading to indoor environmental quality and energy saving; the project was developed in order to implement all the measures that we considered that contributed for indoor quality environment, and therefore the synthesis of those measures, confronted with the feedback of the residents, allowed us to conclude regarding their efficiency. Globally, it was possible to verify that the set of physical factors synthesized on Figure 1 actually permits us to obtain a satisfying indoor environment quality, especially regarding the ventilation strategy and consequent good air quality, the natural illumination constantly present for the entire day and in terms of the acoustics insulation. Only to what the thermal comfort was concerned, the residents pointed out that it hadn't reach their expectations, even thought it was enhanced that the house behaviour is still better than the average constructions. The fact that the residents of this urbanization choose it for its bioclimatic features is a positive contribution for sustainability in the society development.

REFERENCES

[1] ADENE – Agência para a Energia – *Certificação Energética e Ar Interior para Edifícios*

[2] AMADO, M. P. (2005), *Planeamento Urbano Sustentável*, Caleidoscópio Edição e Artes Gráficas, Casal de Cambra, 225p.

[3] AMADO, M.P. (2006), *Sustainable Building, Elsevier Editorial System(tm) for Energy and Buildings Manuscript Draft*

[4] ALLARD, F. et Al. (1998), *Natural Ventilation in Buildings*, James & James, Ltd, London

[5] ANINK, D. et Al. (1996), *Handbook of Sustainable Building*, James & James, Ltd,London

[6] BAKER, N. *et al* (1993), *Daylighting in Architecture*, James & James, Ltd

[7] GONÇALVES, H. (1999), *Conceitos Fundamentais de Térmica de Edifícios*, INETI

[8] HUMPHREYS, M.A., NICOL, F.J. (2002), *The validity of ISSO-PMV for predicting Comfort votes in every-day thermal environments*, Energy and Buildings, Volume 34, Issue 6, p.667-684

[9] KAMPF, J.H., MONTAVON, M., BUNYESC, J., BOLLIGER, R., ROBINSON, D.,(2009), *Optimisation of buildings' solar irradiation availability,* Lausanne, Switzerland

[10] PROGESTO (2007), Projecto de Licenciamento e Execução, Casas de Santo António, Barreiro

[11] PROGESTO (2007), Manual de Utilização e Manutenção da Habitação, Empreendimento Casas de Santo António – Barreiro, lote nº43

[12] *Thermal Comfort Guidance for Schools (2010)* , Ealing Schools Service

[13] *Actas do II Congresso Iberoamericano de acústica (2000),* Madrid

COUPLING THERMAL AND DAYLIGHTING DYNAMIC SIMULATIONS FOR AN OPTIMIZED SOLAR SCREEN CONTROL IN PASSIVE OFFICE BUILDINGS

O. Dartevelle[1] ; J. Deltour[1] ; M. Bodart [1]
1: Architecture et Climat, Catholic University of Louvain, Place du Levant1, 1348 Louvain-la-Neuve, Belgium.

ABSTRACT

In order to limit the risk of overheating and reduce therefore energy needs for cooling, passive standard office buildings often present external motorized shading devices. However, the frequent use of solar screens may deprive the occupants of visual contact with the environment and of the benefits of natural light. Moreover, the artificial lighting system must regularly compensate the lack of natural light, involving large variations of internal gains and increasing energy consumption. The choice of the control parameters for the closure of shading devices is therefore crucial.

Based on the case study of the research project BTP1000 whose main objective was to conceive a passive office building with a fixed cost of 1000 €/m², this paper describes an evaluation of control strategies for solar screens. It shows the impacts of the choice of control strategy on energy consumption for lighting, heating and cooling as well as on visual comfort. Several control strategies were tested: internal temperature, direct and global vertical radiation on façades, separately and combined. Energy consumptions are evaluated using iteratively two dynamic software: TRNsys for thermal assessments and DAYSIM for lighting assessments. In parallel, visual comfort is characterized by the evaluation of the Useful Daylight Illuminance and a view contact to exterior parameter. Control strategies are then discussed on base of these results describing visual and thermal comfort as well as energy consumption.

This analysis shows that an optimized global energy consumption cannot be obtained without considering precisely all energy consumption posts (including lighting). This paper also illustrates the importance of combining parameters (i.e. temperature and power radiation) for the control of motorized shading devices. In conclusion, this analysis shows that, for the case study, a control strategy based only on thermal parameters is not sufficient to preserve the occupants against the too high illuminance levels, pointing out the importance of considering together visual comfort and energy consumption in order to ensure an optimized screen control strategy.

INTRODUCTION

In Belgium, we are currently attending the application of passive house standard in commercial buildings. This construction standard promotes a building skin conception that minimizes thermal losses. Mainly, it requires a very high level of insulation and air tightness (n_{50}<0.6vol/hour) to reach an annual heating energy demand lower than 15kWh/m² [1].

If the concept seems to be appropriate for the residential sector, the thermal behavior of office buildings presents some specificities. Mainly due to high occupation rates, equipment and lighting, internal gains may reach high values in office buildings. In these conditions, rises in temperatures can appear quickly with the superposition of solar radiation (and/or heating in service in winter) [2]. To limit the risk and reduce energy needs for cooling, passive office buildings are often equipped with motorized shading devices.

The choice of the control strategy directly affects the view to exterior and the use of artificial lighting, modifying therefore internal gains which influence cooling and heating energy consumptions. This paper evaluates these impacts for different control strategies for motorized white screens.

CASE STUDY DESCRIPTION

This research is part of the BTP1000 project. The main objective of this project funded by the Walloon region is to improve the passive office building conception, with a fixed cost of 1000 €/m². It includes 4 levels of offices, meeting rooms and facilities. Each level has a gross area of around 1000m². Table 1 presents the data set up, the thermal properties of the building and the key hypothesis. Only the main façades of the building, oriented North and South, are glazed (around 30% of glazing).

U-values	Roof and façades : 0.17 W/m²K – Ground floor : 0.19 W/m²K
Windows	Triple glazing: 0.59 W/m²K; frame: 0.95W/m²K ; g factor : 0.58
Hygienic air flows	Determined according to EN 13779 Hygroscopic wheels with an 70 % heat recovery and bypass
Free cooling	Windows opened by occupant according to Humphrey's algorithm [3]
Internal gains	Between 4.5 and 5 W/m²: people, equipment and lighting.
Shading devices	External white screen with a 0.8 shading factor
Weather data	Brussels- IWEC [4]
Workings hours	From 8 am to 7 pm.

Table 1: Building properties.

METHOD

The study is made coupling two dynamic simulation software: DAYSIM for lighting assessment [5] and TRNsys17 [6] for thermal and energy simulations.
First of all, daylight simulations are run for two blinds positions: totally lowered or totally retracted. For both cases, illuminance levels and dimmed artificial lighting power are determined. Internal gains input in the thermal model are based on these results. Indeed, by a simple algorithm, taking into account the closure or the opening of the blinds, the lighting consumption from Daysim results is selected at each time step according to the screen position. TRNsys determines the energy consumptions for lighting, cooling and heating as well as hourly shading devices position. In total, 68 simulations were computed with a 30min time step, testing the following blind control strategies (Table 2):

Internal temperature	from 22 to 24.5 °C by an increment of 0.5°C
Direct vertical radiation[1] (DR)	from 50 to 250 W/m² by an increment of 50 W/m²
Global vertical radiation (GR)	from 100 to 300 W/m² by an increment of 50 W/m²
Internal temperature and beam radiation	from 50 to 200 W/m² by an increment of 50 W/m² and from 22.5 to 24.5 °C by an increment of 0.5°C
Internal temperature and global radiation	from 100 to 250 W/m² by an increment of 50 W/m² and from 22.5 to 24.5 °C by an increment of 0.5°C

Table 2: studied control strategies

This parametric analysis permits to determine for each control strategy the parameter(s) which minimize(s) the annual primary energy consumption of the building: internal temperature of

[1] *Radiations are calculated by orientation on each façade*

24.5°C; direct radiation (DR) of 100W/m²; global radiation (GR) of 300W/m²; combined internal temperature and direct radiation of 24°C and 50W/m²; combined internal temperature and global radiation of 24°C and 250W/m².

For these relevant cases, visual comfort is then evaluated by the Useful Daylight Illuminance and the view contact to exterior, taking into account the screen closure scheme. Only results for these five cases and the case without shading devices are presented below.

VARIABLES DESCRIPTION

Annual primary energy consumption

Heating and cooling loads are calculated by TRNsys to maintain respectively 21°C and 25°C during the presence time. The final energy consumption is then calculated taking into account machines efficiencies according to the Belgian Energy Performance Building calculation method. The annual performance of the centralized gas furnace is thus taken as 100% and the annual COP of the cooling unit is taken as 3. The ventilation network is used as heat and cold vector. Thermal control is made for each thermal zone.

The artificial lighting installation has a maximal power density of 7.5W/m² in the working spaces and a dimming possibility. Consumptions are calculated to maintain 500 lux on the working planes, as recommended by the norm EN 12464 for office buildings.

Conversion coefficients for primary energy are 1.1 for thermal energy and 2.995 for electric energy, according to the GEMIS4.4.2 database for Belgium. All the results are expressed in gross area for the entire building.

Useful Daylight Illuminance

In order to quantify the impact of natural light on visual comfort, the UDI was computed taking into account an occupancy pattern matching the work schedule for typical North and South offices. The UDI measures how often in the year daylight illuminances within some ranges are achieved [7]:

Illuminances	Less than 100 lux	100 lux to 2000 lux	More than 2000 lux
Sensation	Insufficient: too low	Useful: comfort	Discomfort: too high

Table 3: ranges of illuminances defined by UDI and associated sensation.

View contact to exterior/blinds obstruction

In order to quantify this parameter which strongly influences the visual comfort and the mood of occupants [8], the view contact to the outside is characterized taking into account the percentage of presence time when the blinds are lowered.

RESULTS

Annual primary energy consumption

As illustrated by Figure 1:

- The control strategy based on internal temperature of 24.5°C leads to the lowest energy consumption for cooling (5.14 kWh/m²), the half of the case without solar screen. Nevertheless, the lighting consumption of this control strategy leads to the highest total energy consumption (35.14 kWh/m²), which exceeds the case without screen.
- Control strategies based only on radiation increase the energy consumptions for heating (5.09 and 5.47 versus 3.85 kWh/m² for the case without solar screen).

- Control strategies based on internal temperature and radiation preserve a similar heating consumption respectively with the case without solar screen (3.91 and 3.94 kWh/m²). This strategy presents the best reduction of energy consumption: 7.5%.
- Controls strategies based on global radiation slightly decrease the energy consumption in comparison with those based on beam radiations.

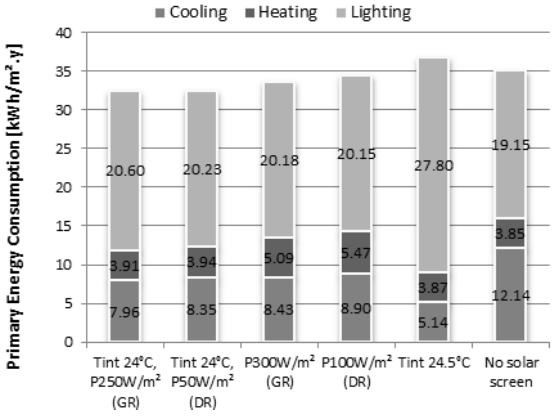

Figure 1: primary energy consumption for heating, cooling and lighting

Useful Daylight Illuminance

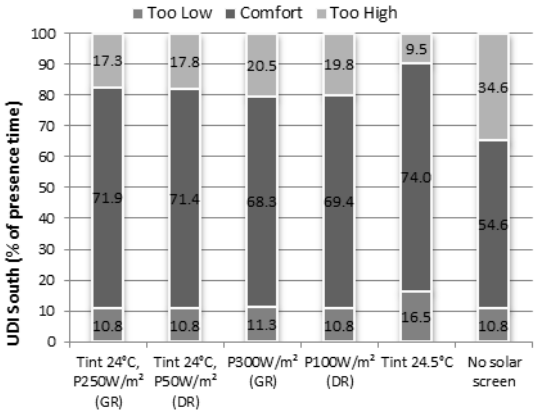

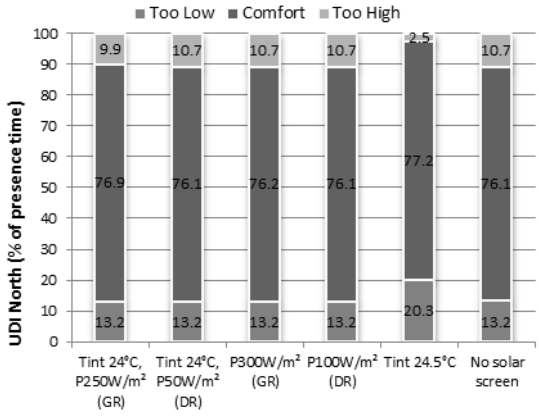

Figures 2, 3: UDI for typical South (left) and North (right) workspaces

Figures 2 and 3, illustrating the UDI obtained for the different control strategies, show that:

- Controlling screens on internal temperature increases the "comfort" category to 74%, compared to 54.6% for the case without screen for the South configuration. Moreover, it reduces the visual discomfort induced by too high illuminances (9.5% compared to 34.6% without screen). However, this control increases the "too low" range to 16.5% against 10.8% in the base case.
- Control based on temperature and global radiation leads to the best compromise for South, with a high comfort category obtained for 71.9% of the presence time, a "too low" category maintained to 10.8%, and a "too high" reduced to 17.3%. For North, the highest "comfort" category is achieved for the control strategy based on internal temperature with 77.2%. However, the "too low" category increases for this case significantly (20.3%).
- Comfort ranges are generally higher for North (76.1% versus 54.6% for South without solar protection), for a reduced "too high" category and a similar "too low" category. North spaces offer a better range of illuminance levels for offices.

View contact to exterior/blinds obstruction

Table 4 gives the percentage of working time during which the solar screens are lowered in the South and North offices for the different control strategies.

	Tint 24°C; P250W/m² (GR)	Tint 24°C; P50W/m² (DR)	P300W/m² (GR)	P100W/m² (DR)	Tint 24.5°C
South	23.92%	24.27%	21.35%	21.28%	58.55%
North	2.94%	0.03%	0.17%	0%	48.58%

Table 4: % of working time with screen closure for typical South and North offices.

For a shading control based on an internal temperature of 24.5°C, screens are lowered for 59% of the presence time for South local and 49% for North local. The other control strategies lead to lowering the solar screens during around 22% of the working time for the south office. In these cases, the use of screens is very limited for North offices (only a slightly increase is seen for controls based on global radiation).

DISCUSSION

As shown in Figure 5 presenting a summary of the relevant results, no solar screen leads to a non-optimal energy consumption (second highest) and the worst results regarding the comfort "category" of the UDI evaluation. However, the view contact to exterior is optimal.

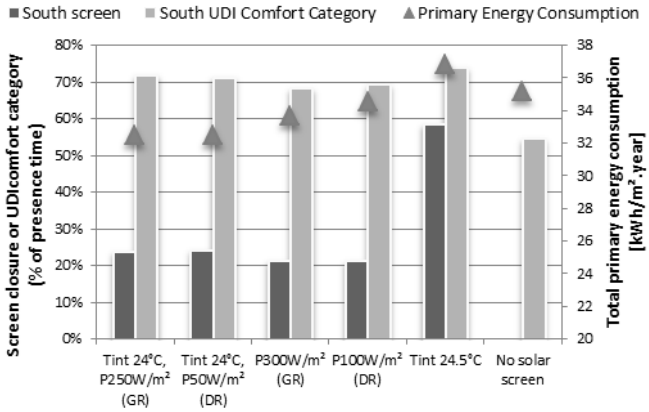

Figure 5: Total building primary energy consumptions, screen closure and UDI comfort category for typical South office of the case study.

The control strategy based on internal temperature reduces considerably the energy consumption for cooling. Nevertheless, it induces a too frequent use of solar screen (more than 50% of working time). Even if the UDI "too high" category is then reduced, the high frequency of too low illuminances increases lighting consumption. As a result, this strategy leads to a higher total energy consumption and not optimal visual comfort possibilities.

Control strategies based only on the value of radiation hitting the façade reduce the solar passive gains increasing thus the heating consumption. To avoid it, if the shading control strategy is based on only one parameter, the threshold value of this parameter should be differentiated according to the seasons, as already proposed by Bodart [9]. The best solution being to use a control strategy based on combined parameters, as it optimises the UDI as well.

Indeed, combining internal temperature and radiation control strategies offers better results in terms of energy consumptions and useful illuminance levels. On the other hand, view contact to exterior decreases compared to control strategies based on radiation. Basing the control strategy on global radiation permits a slightly reduction of the energy consumptions, reducing the time of screen closure for South offices and increasing a bit this closure time for North.

To conclude, basing the shading control strategy on a maximal internal temperature of 24° and a maximum global radiation of 250 W/m^2 is the optimal choice in the case of this highly insulated building. This strategy ensures low primary energy consumption while maintaining visual and thermal comfort in the offices during the whole year.

CONCLUSION

This study shows that in a commercial passive building, shading control strategies based on radiation present better performances than those based on interior temperature. Indeed, the latter do not consider the glare induced by the penetration of too much daylight. If the control strategy is based on internal temperature and if no additional interior blinds are present, it is thus necessary to offer the occupants the possibility to « by-pass » the automatic management system in order to allow them to protect themselves from too high quantities of daylight.

Another point is that for South façades, and in the case of control strategies based on interior temperatures, the shading devices will be closed during about half of the year. It is thus very important to choose shading devices that can still let a part of daylight (for example the diffuse part) penetrate the building. Otherwise, the electric light should be used to compensate a lack of daylight and the total building energy consumption will rise dramatically. This confirms the necessity of considering together all the energy consumptions posts in order to optimize blinds control in very high insulated buildings.

OUTCOME

This study has tested the influence of several control parameters on the global energy consumption of a high insulated commercial building. However, some parameters were not tested and should be analysed as well. Among them, we find:

- External temperatures, internal or external illuminance values.
- Type of shading devices and possibility of intermediate position.
- Differencing the control strategies by orientation and seasons.
- Analysing the impact of the choices in terms of HVAC, passive cooling.

The optimal shading strategy will be tested on the real building, and accurate measurements will allow a post-construction evaluation of the chosen strategy.

REFERENCES

1. Feist, W. ; Schniedersa, J. ; Dorer, V.; Haas, A.: Re-inventing air heating: Convenient and comfortable within the frame of the Passive House concept. Energy and Buildings, Vol 37, pp 1186-1203, Oxford, 2005.
2. Gratia, E. ; De Herde, A. : Design of low energy office buildings. Energy and buildings, Vol 35, pp. 473-491, Oxford, 2003.
3. Rijal, H.B.: Using results from field surveys to predict the effect of open windows on thermal comfort and energy use in buildings. Energy and Buildings, Vol 39, pp.823–836, Oxford, 2007.
4. Ashrae: International Weather for Energy Calculations, Atlanta, 2001.
5. Reinhart, C. F. ; Walkenhorst, O. : Validation of dynamic RADIANCE-based daylight simulations for a test office with external blinds. Energy and Buildings, Vol 33, pp. 683-697, Oxford, 2001.
6. Solar Energy Laboratory, TRNSYS: A Transient Simulation Program, University of Wisconsin, Madison, 2000.
7. Nabil, A.; Mardaljevic, J. : Useful daylight illuminances: a replacement for daylight factors. Energy and Buildings; Vol 38, pp. 905-913, Oxford, 2006.
8. Boyce, P. ; Hunter, C. ; Howlett, O..: The benefits of Daylight through windows. Lighting, Research Center, Renseselear Polytechnic Institute, Troy, New York, 2003.
9. Bodart M.; Creation of a design tool for the choice of glazing in office buildings, according to physic, ecologic and economic criteria, for better visual and thermal comfort», Université catholique de Louvain, PhD thesis, 2002.

INDOOR ENVIRONMENTAL QUALITY OF THE FIRST EUROPEAN MODELHOME 2020 : HOME FOR LIFE

Peter Foldbjerg[1]; Gitte Gylling Hammershøj[2+3]; Lone Feifer[1]; Ellen Katrine Hansen[2]

1: VELUX A/S, Ådalsvej 99, 2970 Hørsholm, Denmark

2: VKR Holding A/S, Breeltevej 18, 2970 Hørsholm, Denmark

3: Architecture & Design, Aalborg University, Østeraagade 6, 9000 Aalborg, Denmark

ABSTRACT

The Indoor Environmental Quality (IEQ) of our buildings is essential to our health. In developing sustainable residential buildings of the future there lie a great challenge in combining energy efficiency with healthy and good IEQ while creating beautiful buildings and environments that give more than they take. The Active House vision approached exactly this challenge by combining energy indoor climate and environment to develop ideas and knowledge of our future buildings. The ModelHome 2020 project grasps the Active House vision and materialises it by designing and constructing six buildings as suggestions on our future sustainable buildings. These buildings constitute a live scaled laboratory for exploration of every aspect possible. Real people move into these buildings to make it possible to explore not merely the technical performance of the buildings but especially also creating the possibility of exploring the qualities and experiential performance of the house. This paper focus on exploring the IEQ in the first of the ModelHome 2020 projects the residential single family house *Home for Life* in Denmark. The house is measured through one year while a test family live in the house – carrying out normal everyday-life-activities. Thereby both the technical performance of the house is measured and the occupants' experiences are measured. To be able to perform this holistic hybrid measurements methods from different scientific fields are applied. Natural and engineering science methods support measuring the quantitative performance of the buildings as temperature and CO_2-level. Methods from artistic and humanistic sciences are applied for measuring occupants experiences – and thereby the building's ability to perform in a more qualitative manner. These methods include observation, interviews and cultural probes. The paper describes results on the daylight environment, the thermal environment and the indoor air quality – presented through both quantitative and qualitative means. Lastly the paper discuss how the different results can challenge and support each other and support creating a wholesome evaluation of our future sustainable homes – based on a human centric perspective.

INTRODUCTION

In the Northern European countries we spend up to 90 percent of our time indoors – often in buildings with doubtful indoor environment [1]. Therefore, Indoor Environmental Quality (IEQ) of our residential buildings is a central subject that affects us all in our everyday lives – whether we are conscious of it or not. We wish to do something about these issues and aim at creating better and healthier environments for people with plenty of daylight and fresh air. Through the Active House vision we aim at developing buildings that give more than they take by uniting carbon neutral buildings with good IEQ adapted to the surrounding

environment [2]. The vision is realised in an extensive living laboratory through the ModelHome 2020 project [3]. The purpose of the project is to demonstrate different solutions and approaches to the challenge of combing a healthy and comfortable indoor environment with carbon neutrality. The project is unfolded through design and construction of six demonstration buildings. Architecture and energy systems are optimised to each of the six specific locations and seven criteria for both energy performance and IEQ are defined to realise the vision of the project [3]. When built, test families move into the houses for a one year period to test and experience these designs of a future generation of sustainable homes.

Fig. 1. "Home for Life". South facade (left). Daylight, ventilation and energy concept (right)

This paper studies the IEQ of the first realised ModelHome2020 through considerations and analysis of *both* quantitative *and* qualitative aspects. This first house, *Home for Life,* is constructed in Denmark and has been tested for a one year period by the Simonsen family.

The paper describes the methodology used for measuring the house – a mixed methods approach combining quantitative methods from natural and engineering science with qualitative methods from the artistic and humanistic sciences. The setup aim at exploring the IEQ from various sides by illuminating how the sciences can support each other when e.g. the measured optimum IEQ does not meet the occupants experiences. We wonder, should a good IEQ be determined through means of numbers solely – or can human experience be as good an indicator? Through presenting results on daylight, thermal environment and indoor air quality we illuminate how respectively quantitative and qualitative methods can provide data that tells the story from different perspectives. Lastly we discuss how the different results can challenge and support each other and support creating a wholesome evaluation of our future sustainable homes – based on a human centric perspective.

METHOD

In this paper the case study house is subject to explorations and analysis using both quantitative and qualitative methods with focus on the kitchen/dining room as it is the most used room in the house (also see fig. 2).

The Mixed Methods approach [4] combined methods from different sciences while considering all of them equally important. This approach illustrates that the aspects are inter-dependent and inter-connected – it is often possible to explain the quantitative aspects by studying the qualitative aspects and vice versa. Below, we summarise the quantitative and qualitative methods used for exploring and assessing the IEQ of Home for Life.

Methods for quantitative and qualitative evaluation

Results on daylight are based on calculated daylight factor levels as continuous measurements of daylight levels will require a permanent grid of sensors in the house during occupancy – an impossible setting in a family's everyday life. As the daylight factor is independent of actual

weather conditions, a calculation based on the actual geometry of the house provides a good indication of the actual conditions [5]. Indoor temperatures (^{o}C), CO_2 levels (ppm) and relative humidity (%) are continuously measured in 11 zones (rooms) and hourly values are recorded providing a detailed illustration of the indoor environment dynamics during both day and year. EN 15251 is used to evaluate the thermal comfort and indoor air quality categorizing a space from I to IV - where category IV indicates an unacceptable situation [6].

Methods for qualitative evaluation of IEQ are a rather un-explored field of research regarding sustainable homes – however a few examples have surfaced during the last couple of years (e.g. [7] [8]). The evaluation is approached in a holistic manner by using a triangulation of methods deriving from artistic and humanistic sciences. A triangulation implies a combination of methods making it possible to approach the problem of interest from several different angles [4]. Thereby the various methods can support or contradict each other in the quest for making an extensive exploration of the problem. The qualitative measurements include an anthropological study through participant observations of the families' experiences in the house [4], diaries written by the family following a Cultural Probes [4], semi-structured interviews carried out between researcher and occupants [4] and photo documentation.

Data registration and analysis are carried out through the same weaving approach where quantitative and qualitative aspects merge together to support and challenge each other.

RESULTS

Extensive qualitative and quantitative measurements have been performed on IEQ of *Home for Life* between July 1st 2009 and July 1st 2010. The results presented here are from that period through which the commissioning and adjustment of all systems also took place during this period which influenced the results.

Daylight Environment

The daylight factor calculations show an average daylight factor (DF) above 5% in the main rooms on the ground floor and in most of the bedrooms at the upper floor. Especially the kitchen/dining room at the ground floor receives high daylight levels. [5]

Fig. 2. Calculated daylight factor iso contours for ground floor (left) and upper floor (right).

Rooms with an average DF of 2% or more are considered daylit. A room will appear strongly daylit when the average DF is above 5% in which case electrical lighting will most likely not be used during daytime, according to CIBSE [9]. Through the semi-structure interviews the occupants verbalise the quality of having high daylight levels: *"The best thing about the new house compared to the old is the daylight. The daylight is better*" and *"What characterizes the house is the huge intake of daylight – and that is what I want!"*

The plenty amounts of daylight also bring side effects and the anthropologist observed that the daylight levels sometimes are too resulting in the occupants closing the curtains. When confronting the occupants with this they explain their frustration about this relation – because they are very much aware of the energy aspects knowing that the sunlight brings heat into the house which supports reducing the heat demand of the building. *"Yes, one doesn't really fell called upon to draw back the curtains – it is almost too much (the light)"*.

Fig. 3. The test family in the kitchen/dining room (left). Kitchen/dining room (middle + right).

The well-lit house influences the way the occupants use the electrical light and they experience using considerable less electrical light than in their previous house: *"It is very obvious! We actually don't switch on the electric light. Of course we do it at night. When it becomes dark outside it is necessary, but we actually don't switch on the electric light much."*

Thermal Environment

The family experiences large temperature swings relating to whether the sun falls directly into the house or not and express this experience as a deterioration of the indoor climate: "*So temperature fluctuations are much more dependent on whether the sun or not is outside."*

When evaluated against EN 15251 [6] the kitchen/dining room meets cat. III when both overheating and under heating is considered, while it meets cat. II when only overheating is considered. See Fig. 4. Underheating (uncomfortably low temperatures) is generally caused by airings performed by the occupants during winter and spring/autumn. Underheating is considered less problematic than overheating as the cause of underheating in this case is a matter of occupant preference rather than a consequence of the house design. The observations tell that the family is very aware of the indoor climate in the house. They use the information screen to follow the different levels but are not always satisfied with temperatures. Overheating occurs particularly during the spring period. This is to some extent due to the control system for the solar shading, which initially had two modes of operation; winter and summer. During the first year of operation those was changed. The family actively uses the sun screening and blinds to prevent overheating. This has resulted in an increasing awareness of the consequences of preventing e.g. view out: *"We can also look out over the bay [...] it's fantastic!"* Often the family has deactivated the automatic solar shading to be able to enjoy the view out; in this case they – subconsciously – accept mild overheating as the view is more important in the specific situation.

The use of solar shading illustrates a choice between different alternatives which the family often has to make; dependent on the actual situation, the family balanced indoor temperature against the nice view out and the visual connection to the outdoor. Often they prefer the view.

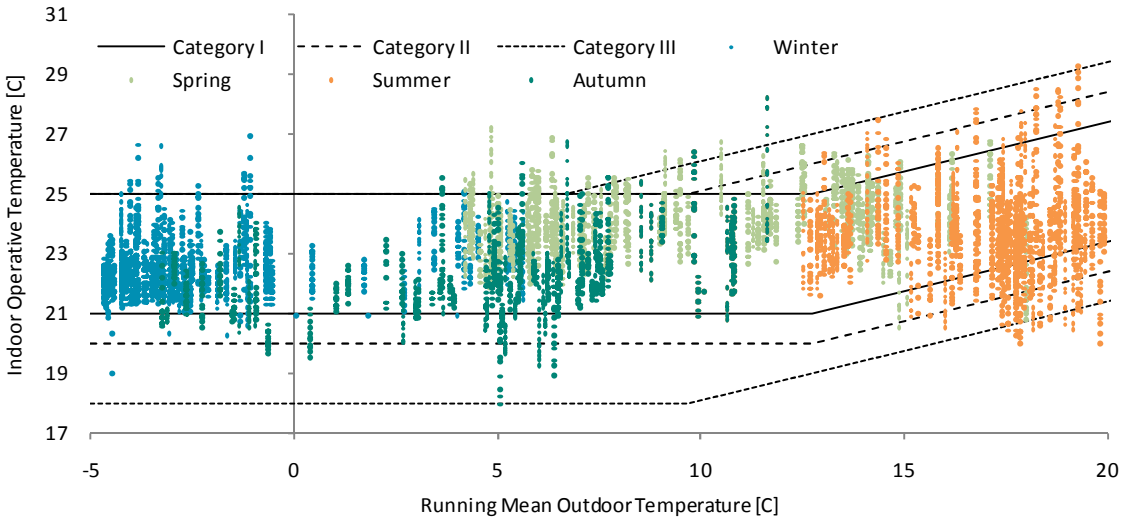

Fig. 4. Operative temperature in the kitchen/dining room depicted vs. outdoor temperature and comfort range limits according to the adaptive method of EN 15251.

Indoor Air Quality

The CO_2-level is used as indicator of air quality. The CO_2 concentration in the kitchen/dining room was above 1200 ppm for 210 hours during the measured year. The kitchen/dining room meets cat. III of EN 15251, see fig. 5.. The natural ventilation scheme during summertime provides low CO_2 levels, whereas the CO_2 levels during wintertime were higher.

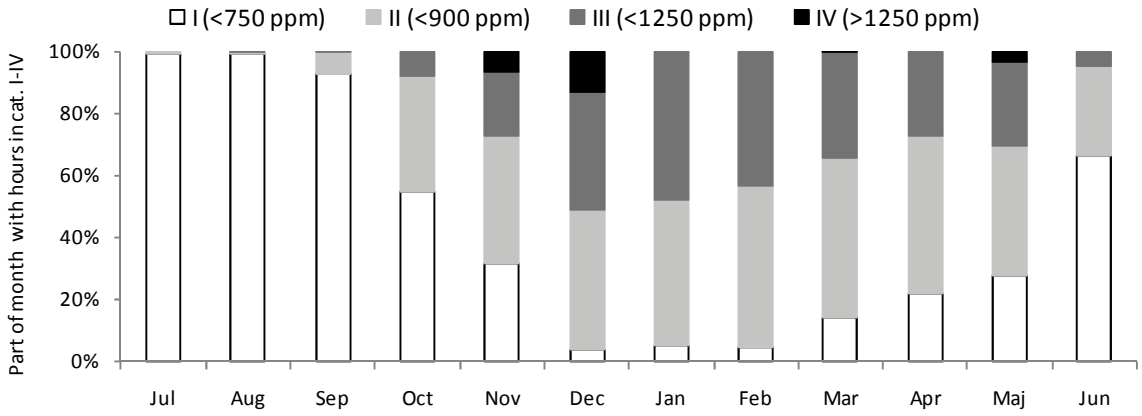

Fig. 5. Monthly CO_2-levels in the kitchen/dining categorised according to EN 15251.

"There is much more CO_2 since we do not get aired out automatically. And it is clear that when I've been here and open doors, typically so you can see that the CO_2-level goes down. It improves the CO_2 levels." The quote illustrates how the family has developed a dependency of the information screen – they have a firm belief that the quantitatively measured CO_2-levels solely determine their health, but they are not able to judge if a specific CO_2 level is too high; they often react on a rising trend. They air out for long periods even though the change of air is not needed and has no effect regarding health.

Discussion

The adaptive evaluation approach of EN 15251 of thermal environment seems in accordance with the family's experience of the thermal environment. The building is free running during

the summer time, as it is naturally ventilated, and the family could control solar shading and open windows on room level, giving them control over their environment, which generally contributed to increasing their satisfaction.

Results on thermal comfort show both some underheating and some overheating. The overheating occurred mainly in the spring period when the automatic external solar shading remained in "winter" mode, indicating that the family either trusted that the "system" was working correctly, or was unable to make efficient use of the shading. Another explanation could be that they simply enjoyed the elevated temperatures along with the light after a long Nordic winter, and preferred the view out. Their statements support the last explanation.

The calculations of daylight performance showed high daylight levels, and the occupants particularly expressed satisfaction with the daylight conditions in the house.

It is challenging to present the IEQ of a house through both quantitative and qualitative aspects due to the differences in their representation. Can a recorded quotation weigh as much as a measured number?

As de Dear [10] showed, the concept of thermal adaptation is better explained when a psychological angle is applied. Similarly, many nuances are added to a quantitative recording of e.g. temperature, when a structured analysis based on social sciences is applied. Qualitative recordings provide insight into what the family actually liked and disliked in their house.

ACKNOWLEDGEMENTS

Thank you for use of data and data reports to the MCHA project, the Aarhus School of Engineering with Arne Førland and the Alexandra Institute in Århus with Johanne Entwistle.

REFERENCES

1. European Commission, *NEST project; Innovative Sensor System for Measuring Perceived Air Quality and Brand Specific Odours*, Technical University of Berlin, 2007,
2. Eriksen, K.E., et al., *Active House Specification*, Hørsholm, Denmark, 2011
3. ModelHome 2020, http://www.velux.com/ ModelHome2020 (accessed May 2011)
4. Creswell, J.W., *Research design: qualitative, quantitative, and mixed methods approaches*, SAGE: London, 2009.
5. Daylight Visualizer, http://viz.velux.com/ (accessed May 2011).
6. CEN, *EN 15251:2007 Indoor environmental input parameters for design and assessment of energy performance of buildings addressing indoor air quality, thermal environment, lighting and acoustics*, European Committee for Standardisation, 2007
7. Brunsgaard, C., *Understanding of Danish Passive Houses based on Pilot Project Comfort Houses* DCE Thesis; 28. Aalborg: Aalborg University, Dpt. of Civil Engineering, 2010.
8. Entwistle, J.M., *Qualitative evaluation of Home for Life 2009/10,* Alexandra Institut, Århus, 2010.
9. CIBSE, *CIBSE, Code for Lighting*, Oxford: Chartered Institution of Building Services Engineers, 2002.
10. *de Dear, R., The Theory of Thermal Comfort in Naturally Ventilated Indoor Environments - "The Pleasure Principle"*, International Journal of Ventilation, Volume 8 No 3, 2009.

STUDY OF COMFORT CONDITION OF REHABILITATED AMIRCHAKHMAGH WATER-CISTERN IN YAZD, IRAN

Sadaf Jafari [1]; Dr. Nick Baker [2].

1: MPhil in Environmental Design, Architecture, University of Cambridge, Cambridge, UK, sadafjafari@yahoo.com

2: Department of Architecture, University of Cambridge, Cambridge, UK, NickVBaker@aol.com

ABSTRACT

Water-cisterns are valuable historical buildings in Iranian architecture which have fallen into ruin. These buildings should be preserved for both historical and aesthetic reasons. Also they have significant environmental potential because their architecture (containing wind-catchers and being underground) creates stable annual temperature and appropriate ventilation. One of the examples of these buildings which has been rehabilitated is Amirchakhmagh water-cistern in Yazd. This water-cistern is now used as an Iranian-traditional-sport-hall (zoorkhaneh).

This article will investigate actual conditions achieved in this selected example. First, its rehabilitated design features and strategies will be mentioned. Second, the observations made by the author via field research, data collecting, interviews and using questionnaire in March 2009 will be described with tables, graphs and pictures. These observations include Today's building condition; heating, cooling, air conditioning and other artificial facilities; temperature, humidity and ventilation measurement; airflow pattern; and occupants' conditions and behavior. Meanwhile, the above information will be analyzed thoroughly by considering human comfort conditions. The results show that the temperature is relatively stable throughout the year. Actually, not many steps have been taken to use the potential of the wind-catchers in different seasons. It is found that with the stable temperature of the underground building, proper ventilation for providing fresh air (and sometimes cooling in summer) could have removed the need for heating and cooling facilities. In this case, it could work properly as a zero carbon building if the wind-catchers and the ground cooling effect of it had been used correctly. On the other hand, even with the current design it is obvious that building underground makes it easier to deal with thermal comfort.

Keywords: Amirchakhmagh water-cistern – Yazd – thermal comfort – natural ventilation

INTRODUCTION

Seasonal storage of winter coolness in the forms of ice and chilled water in cisterns is centuries old. The use of cisterns in Iran has been diminishing rapidly due to the widespread use of piped water and household refrigerators. Most of the water-cisterns have: either given way to new developments; been remodeled as tourist attractions; or are in future plans to be rehabilitated. These buildings should be preserved for historical and aesthetic reasons and the fact that they have significant environmental potential because their architecture (containing wind-catchers and being underground) allows for stable annual temperature and appropriate ventilation. This article will investigate actual conditions achieved in a selected example.

CASE STUDY DESCRIPTION

The case study is a rehabilitated water-cistern called Amirchakhmagh (rehabiliated by Mohammad Hassan Khademzadeh) in one of the most populated urban areas (Amirchakhmagh square) in Yazd, Iran which its primitive shape is represented in figure 1.

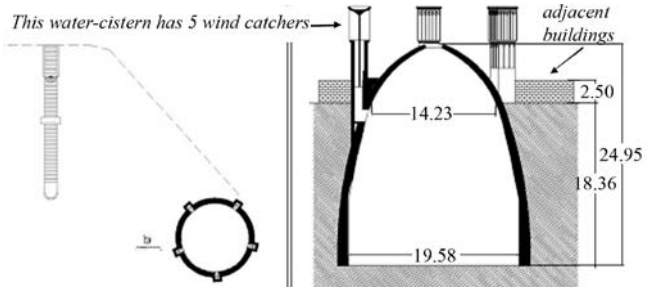

Figure 1: Section and plan of the water-cistern before rehabilitation (figure from the architect)

Rehabilitation: To rehabilitate this water-cistern a new structure (a 40 centimeter-thick wall placed next to the wall of the cistern and a new dome placed on top of it) was inserted into the main cistern to protect the existing fabric and divide the whole building into two spaces with different functions (over and below the new dome). Figure 3 shows the new spacial organization of the whole building.

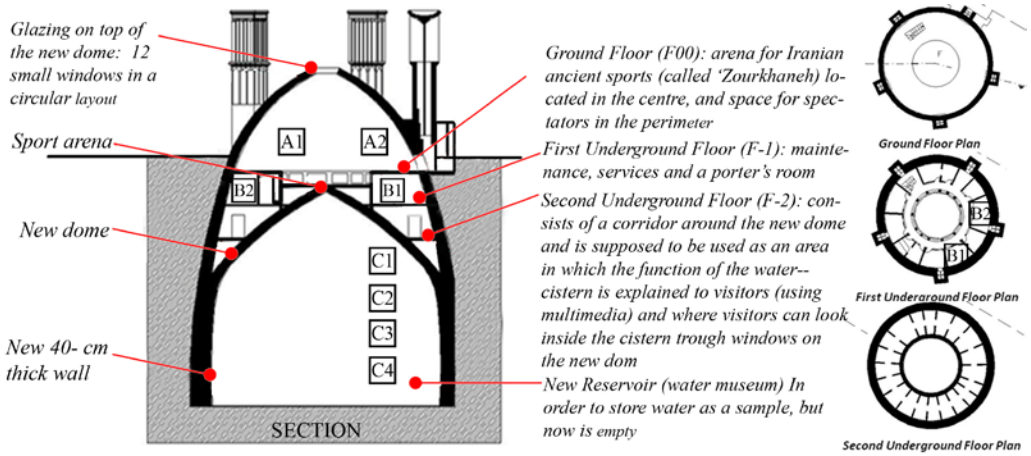

Figure 2: Amirchakhmagh water-cistern after rehabilitation (figure from the architect, amendments made by author), place of Data loggers is shown by letters in boxes.

All the spaces are almost related to each other which can be useful to: (1) Use the wind catchers for ventilation of the whole building; (2) Use the stable underground temperature. In this rehabilitation this characteristic has been achieved by employing three features: (1) leaving openings between different floors. This feature is accomplished by: First, locating the sport arena at 1 meter below the rest of the F00 while leaving the 1 meter descend open to the F-1; Second, by creating two big openings between the F-1 and the F-2 (a staircase and an opening in one of the sectors of the circle); Third, four openings on the top of the new dome are created which relate this floor to the inside of the cistern. (2) allowing the wind-catchers to ventilate both the F00 and the F-1 by placing the F00 in the middle of the inlet of the wind-catcher. (3) connecting rooms with wind-catcher inlets to adjacent rooms with no wind-catcher inlet on the same floor, to the F-2 and to the new cistern. (Visualized details available in figure 3)

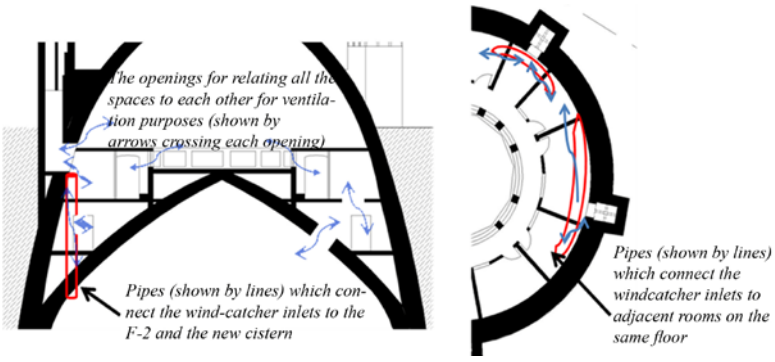

Figure 3: Strategies to connect all the spaces in the building (from author)

Today's building condition: The entrance door is opened every day from 5 30am to 10pm throughout the year. Inlets of some of the wind-catchers on the F00 are blocked by plastic to exclude dust. The inlets of the wind-catchers on the F-1 are blocked to some extent because the bottom of the wind-catchers has been used for putting maintenance materials. A small fan has been located by the owner in one of the 12 windows on top of the dome. The F-2 is a descriptive water gallery which is unused because of some official issues. Therefore, visitors are not staying very long. Furthermore, the new reservoir is empty because of the same dispute.

Heating, cooling, air conditioning and other artificial facilities: The only heating, cooling and ventilation facilities available are a small gas heater, an evaporative cooler and a fan. The only person responsible for the use them is the porter. He claimed that the gas heater works on the lowest level during whole winter and is only turned higher at dawn. The evaporative cooler (which cools down the air by adding water drops) works on medium level from the second month of spring until the end of fall when sport is on, while in June, July and August it works most of the day. The fan on top of the dome is used only during sport time in evenings due to smell. The heat gain from the lamps on the F00, F-1, F-2 and cistern are 120, 337, 576 and 120 watt respectively.

MONITORING THE BUILDING

The temperatures have been monitored by data loggers (called tinytags) from Friday 13/3/2009 8:00pm to Monday 16/3/2009 4:00pm. The place of data loggers are shown in figure 2.

Temperature measurements

Temperature was monitored in the cistern, the F00, and two rooms in the F-1 (one room with and one without a wind-catcher). Average temperature of the F-1 and the cistern is almost as same as the average of the outside temperature which both are almost the same as Yazd average annual temperature, but with clearly less fluctuation. This is one of the big advantages of being underground. The fluctuation on all floors (excluding the cistern) is around 2.5 degree centigrade because of the natural ventilation through wind-catchers. Both monitored rooms have similar temperature conditions (although the room with wind-catcher has a bit more fluctuation) because of the pipes that connect each wind-catcher to adjacent rooms. The cistern has no temperature fluctuation because it is underground and has no ventilation. The average temperature on the F00 is significantly more (6 degrees) than on the F-1 and outside which is caused by heat gains such as gas heaters, lights and people. Both, however, have the same fluctuation because they have the same ventilation rate.

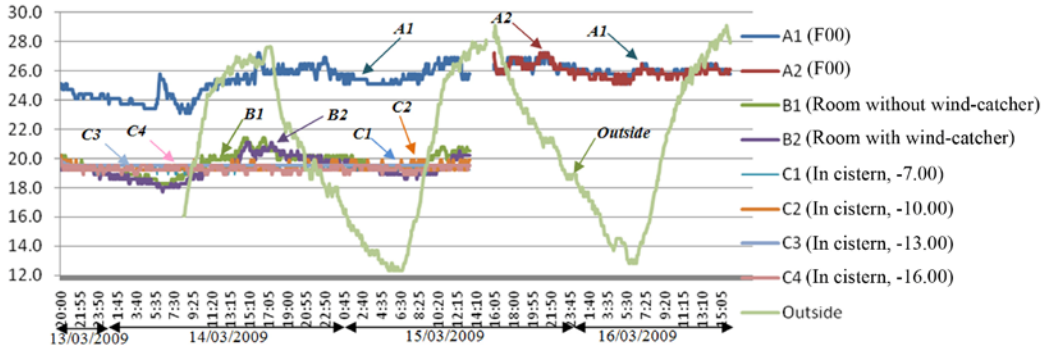

Figure 3: Results of the monitoring from Friday 13/3/2009 8:00pm to Monday 16/3/2009 4:00pm

	(A1)	(B1)	(B2)	(C1)	(C2)	(C3)	(C4)	Outside
Average Temperature °C	25.8	20.0	19.7	19.3	19.5	19.5	19.3	20.1
Min Temperature °C	25.1	19.3	18.6	18.9	19.2	19.5	18.9	12.3
Max Temperature °C	27.2	21.4	21.2	19.5	19.9	19.5	19.5	27.6
Temperature Fluctuation °C	2.1	2.2	2.5	0.6	0.7	0.0	0.6	15.3
Average RH %	30.4	24.5	26.6	72.1	74.4	64.0	59.9	20.5

Table 1: Results of the monitoring from 14/3/2009 1:00 pm to 15/3/2009 1:00 pm

Ventilation measurements and airflow pattern

Airflow was measured (with a thermo-anemometer) both in the afternoon and in the evening in the following locations: next to the wind-catcher inlets; in the middle of each floor; on the inlet and outlet of the pipes; and in the open area around the sport arena in the morning. Measured air velocities were around 0.2 to 0.5 and rarely got to 2 m/s next to the inlet of the wind-catchers. In other areas of the building the air velocity was about 0.2 to 0.3 m/s. All this time, the outside wind speed was about 0.5 to 8 m/s. During the sport time, the small fan was turned on by the porter.

The air flow (averaging around 0.2 m/s) was verified by a smoke test and observed in the whole building. The direction of airflow between the floors was always up, apart from next to the inlets of the wind-catchers where it was both towards the inside and towards the outside of the building. Direction of the air flow in the whole building was changing because of the effect of the wind catchers.

Occupants

Occupancy: This sport which is practiced in the sport arena is just played in certain hours of the day (6-7am, 5-6pm and 8-9pm on weekdays and 11-12am on holidays, in this case the Sunday was bank holiday). There are almost 10 men doing the sport in the morning and about 25 men in the evenings and weekends. Sport spectators in the mornings are usually less in number than in the evenings (sometimes about 30 visitors for each sport period). Visitors for the water-cistern come randomly throughout the day, averaging around 30 persons per day.

Occupants' responses: Visitors and participants' responses were gathered during five days using a questionnaire and doing interviews.

Visitors' opinion: In total 20 visitors have been interviewed. Visitors' opinions (15 men) are as follows: Morning visitors and evening visitors (not in sport times): 100%Comfortable

Evening visitors (more crowded with athletes and the visitors): (1) thermal Condition: 46% comfortable, 33% slightly uncomfortable and 20% uncomfortable (the last two groups preferred colder condition) (2) Ventilation: 6.6% comfortable, 40% slightly uncomfortable and 33% uncomfortable (because of the bad smell in the hall). Five women that were available were comfortable with the temperature but preferred more fresh air.

Visitors for the water-cistern during sport time: 90% comfortable with thermal conditions, 10% slightly uncomfortable. 90% of the total complained about bad smell upon entry.

Athletes' opinion: 30 athletes were interviewed by questionnaire. With regard to figure 4, it is obvious that most of the athletes are satisfied and the most problematic aspect is the ventilation. The condition of the moment of answering the questionnaire was neutral for 80% and slightly warm for 20% of the athletes. Clearly athletes were more comfortable than spectators (cf. visitors' opinion).

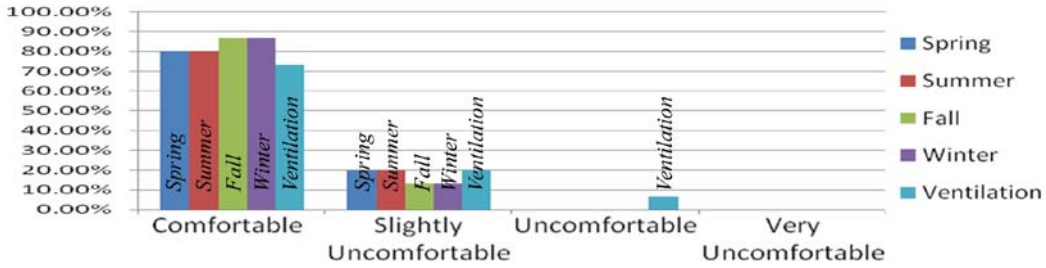

Figure 4: Result of athletes' questionnaire

The porter said that in spring and in fall, the temperature is comfortable both on the F00 and on the F-1. In summer, during days in which an evaporative cooler is on, the temperature is good, he prefers to sleep on the F-1 which is colder without any cooling facility. In winter he sleeps on the F00 because his room on the F-1 is too cold. During winter days the F00 temperature is comfortable with a small heater on the lowest level, while at dawn he prefers to turn the heater a bit higher.

Analysis

Thermal Satisfaction: Regarding the fact that the temperature of human comfort zone varies in different regions and seasons, the comfort zone calculated in Yazd in March is 19.5 to 24.5 °C.

Surprisingly, the main users of the building are satisfied with thermal conditions throughout time monitored, despite the temperature being above comfort zone in the sport hall which can be noticed in table 2. In order to explain this, we can refer to the fact that although temperature is usually the most important environmental variable affecting thermal comfort, a person's sensation of warmth is influenced by other physical parameters as well (environmental factors such as air temperature, mean radiant temperature, relative air speed and humidity; and personal factors such as metabolic heat production and clothing) [1].

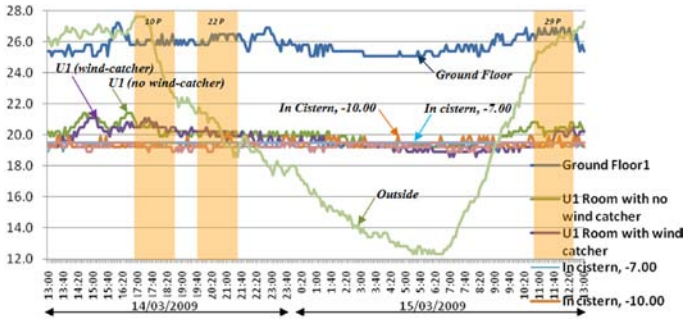

Figure 5: Results of the monitoring from 14/3/2009 1:00 pm to 15/3/2009 1:00 pm with specifying number of occupants during the sport time

	5-6pm-14/03/09 **10 Persons**	**8-9pm-**14/03/09 **22 Persons**	**11am-12pm-**15/03/09 **29 Persons**	**5 30am-10pm**	**10pm-5 30am**
Average Temperature	26.1	26.5	26.5	27.2	26.9
Min Temperature	25.8	25.8	26.9	25.1	25.1
Max Temperature	25.9	26.2	26.7	25.9	25.6

Table 2: temperature during occupancy hours from 14/3/2009 1:00 pm to 15/3/2009 1:00 pm with specifying number of occupants during the sport times

In this case, environmental and personal factors influence warmth sensation in three ways: (1) a change of three degrees according to the table of 'Thermal sensation scale' will change the response on the scale of subjective warmth by about one scale unit for sedentary persons, while more active persons are less sensitive to changes in room temperature. This reason explains why spectators are less satisfied. (2) the cooling effect of air movement is well known. Furthermore, regard to CIBSE [2] people are more tolerant of air movement if the direction of the air movement varies. As mentioned earlier, the function of the wind-catchers causes the air direction to vary. This makes the condition more satisfying. (3) according to CIBSE [2], where air speed in a room is greater than 0.15 m/s, the operative temperature should be increased from its 'still air' value to compensate for the cooling effect of the air movement. Furthermore, air speeds greater than about 0.3 m/s are probably unacceptable except in naturally ventilated buildings in summer when higher air speeds may be desirable for their cooling effect. In the case study, the air movement varied from 0.2 to 0.3 m/s. This range (more than 0.15 and less than 0.30 m/s) makes people feel cooler in high temperatures on the F00 while not being too high to annoy them.

Humidity Satisfaction: Humidity in the range of 40–70 % RH is generally acceptable. Consider CIBSE [2], Lower humidity is often acceptable for short periods of time. The average humidity on the F00 is 30% which is relatively low. However, during drier seasons (i.e. spring and summer) this has been compensated by the use of an evaporative cooler but, in cold seasons the air is very dry and some other techniques should be used to humidify the air. In the new cistern the humidity is strangely high.

Ventilation Satisfaction: Athletes and non-spectator visitors found the air freshness fine, but spectator visitors were not completely satisfied with the amount of fresh air. According to CIBSE [2] Guide, 10 l/s/person air supply rate is needed for sport halls. The calculated ventilation rate in the

building is 14 l/s/person (see calculation below). This rate is not completely used on the F00 because the inlets of the wind-catchers are partly inside the rooms on the F-2 instead of being completely exposed to the sport hall. Another fact is that the air flow rate in the sport arena is more than in the spectators' place because only the sport arena has a direct opening to the F-1 and the inlets of the wind-catchers around the spectators' place on the F00 have been blocked by the owner. So, when the small fan in the apex of the dome is working, it forces the air to flow from the wind-catchers directly to the outside via the opening around the sport arena. This is why athletes are satisfied with ventilation and spectators are not.

SUGGESTIONS AND CONCLUSIONS

Discussion and Suggestions

By mapping the occupants' responses onto temperature and airflow data, we would surprisingly see that occupants are satisfied while the temperature is not in the comfort zone. So, their impression of comfort does not relate to physical temperature. But, in the same time, the temperature is quite stable (fluctuation of at most 0.5 °C during occupancy) and the air velocity rate compensates the high temperature. It is concluded that occupants can be tolerant to high temperature if there is no fluctuation and there are some other elements like humidity, wind etc. to help the condition.

In theory, the temperature of an underground building should be the same as the average annual temperature which in Yazd, this is about 20 degrees centigrade). However, in reality, because of the ventilation, heating and cooling facilities and occupants, this is not what actually happens which can be seen also in the case study.

The environmental potentials of the building have been maximized by relating its different parts to each other which causes the usage of the stable underground temperature and the ventilation provided by the wind-catchers for the whole building. However, the issue here is the unreasonable usage of the heater for compensating the high air velocity during winter. This can be solved simply by controlling the ventilation during winter with modernization of the wind-catchers**.** On the other hand, during summer the evaporative cooler is in use while the F-2 is slightly cold. The evaporative cooler can be substituted by the colder air of the F-1 and the humidified air from the water-cistern. Furthermore, facilities with less heat emission should be used. As a result, wind-catchers should be modernized in order to solve the problem of dust and the impossibility of controlling the wind.

In Yazd, six months of the year are too dry while the rest of the year is not comfortably humid. Given that the new cistern is too humid, this humidity can also be used to humidify the dry air. One of the most effective techniques would be to try mixing the air of the whole building more by automatic sensors and fans.

CONCLUSION

This converted water-cistern is interesting because of mixture of wind cooled and underground spaces to provide comfort. The results show that the temperature is relatively stable, but it is obvious that it cannot be expected that the same amount of openings in different seasons work properly throughout the year. Actually, no steps have been taken to use the potential of the wind-catchers in different seasons. It is clear that with the stable temperature of the underground building, proper ventilation for providing fresh air (and sometimes cooling in summer) could have been done a lot better and may have even stopped the usage of heating and cooling facilities. In this case, it could work properly as a zero carbon building if the wind-catchers and the ground cooling effect of it had been used correctly. On the other hand, even with the current design it is obvious that building underground makes it easier to deal with thermal comfort issues because it has a naturally stable temperature. So, the most important fact in using the potential of underground sealed building is how to manage the ventilation.

REFERENCES

1. McMullan, Randall (1998) Environmental science in Building, Macmillan Press, London
2. Environmental Design, CIBSE Guide A (2006) The Chartered Institution of Building Services Engineers London

INTEGRATING VISUAL AND ENERGY CRITERIA FOR OPTIMAL WINDOW DESIGN IN TEMPERATE CLIMATES

C.E. Ochoa; M.B.C. Aries; M.P.J. Aarts; E.J. van Loenen; J.L.M. Hensen

Eindhoven University of Technology, Department of Architecture, Building and Planning, P.O. Box 513, 5600 MB, Eindhoven, The Netherlands

ABSTRACT

Building codes and certifications require maximal building performance in different aspects. However, focusing on achieving a single purpose can prevent obtaining additional ones. This work aims to help building designers balance energy and visual performance design criteria. Correct window size selection is part of early design stage decisions that influences total building performance. The study is based on temperate climates, but procedures can be applied to different locations.

Large numbers of techniques have been used to optimize building features for one objective. However, it is not common to find an integrative approach to visual and thermal aspects of window design. The difficulty to achieve many goals resides in high degrees of complexity introduced when many building features must be considered in an infinite number of possible design solutions. Multi-objective optimization techniques start to be applied in building science. Nevertheless, choosing adequate acceptance criteria presents additional dilemmas. Different assessment criteria applied to a single problem can lead to diverse valid solutions.

A brief review was made of commonly used energy consumption and visual comfort and performance criteria. The study was made through whole-building computer simulations of a standardized test room. The influence of window size variations on energy consumption, visual performance and visual comfort was examined. The window-to-wall-ratio (WWR) of the facade prototypes varied from 10% to 100% in 10% steps. Energy consumption and visual comfort criteria for acceptance were defined based on the review. A graphical optimization method was used to select a range of recommended window sizes for different orientations.

This provided a solution space with "compromise sizes" satisfying both energy and visual aspect objectives. However, unprotected windows cannot meet all these criteria. This makes the provision of sun-protecting elements necessary. A selection procedure based on design needs is detailed. When various related criteria are applied using adequate values, the variety of acceptable solutions is increased, but too many can limit it. Clear acceptance ranges and objectives that can be translated to decisions have to be conceptualized beforehand.

INTRODUCTION

Windows characterize energy consumption and visual comfort patterns in buildings. Choosing their size is among many fundamental early stage decisions. Therefore, determining optimal characteristics for building performance is essential. Multiple aspects must be considered at once in order to accomplish project objectives. Even though, most research efforts are dedicated to find optimal properties of a single element for one purpose only. Multi-objective optimization starts to be applied in building science, considering several variables at once. However, appropriate evaluation criteria must be considered beforehand.

Applying different assessment measures to a single aspect of the same problem can lead to diverse valid solutions. Additional new criteria are then needed to define a solution [1]. Daylighting systems have been evaluated through indicators involving illuminance and glare [2]. However, assigning importance values to each visual factor and their interaction with energy consumption requires further exploration.

Whole-building computer simulation was used to examine window size variations and their energy consumption, visual performance and visual comfort patterns for temperate climates. A solution space is defined, and results are examined different design criteria. A method is shown on how to use them in order to define a "compromise size" from the solution space.

AVAILABLE VISUAL AND ENERGY EVALUATION CRITERIA

Energy

Energy use can be measured on site and is of economic interest for building operation. It is usually expressed in terms of energy units (kWh or GJ) per unit area per time unit. It quantifies consumption of heating, cooling, lighting and ventilation. The goal is to select the least energy-consuming system. Other methods include evaluating adaptive thermal comfort [3] and the degree-days method [4].

Visual performance and comfort

Discomfort due to visual effects is reported more frequently than discomfort by thermal effects. This is due to the time delay in experiencing the latter [5]. Visual performance and comfort criteria will be divided into illuminance-based and glare-based criteria.

-Illuminance-based criteria serve to evaluate if a lighting setup provides the amount of light needed to carry out a task, usually in the horizontal plane. Examples include the daylight factor, range of useful illuminances, and illuminance uniformity (understood here as the ratio between maximum and minimum illuminance in a space) [6]. Suitable values for different activities are provided in various standards.

-Glare-based criteria are meant to assess visual comfort in a space. A comprehensive account of glare indexes and evaluation methods is detailed by [7]. Each measure is specific to a particular situation, such as luminance ratios [8]. Regarding natural light, a widely used measure is the Daylight Glare Index (DGI). A value of 22 is assigned to the evaluation "just acceptable". Other methods include the daylight glare probability (DGP) [9].

Dynamic evaluations involving the above criteria require statistical measures such as averages but these can mask severe occurrences of an indicator [10]. For yearly evaluations, it is usual to add the number of hours a certain condition (border, extreme or average) is met.

METHOD

Location and test room description

Computer simulations were made using EnergyPlus for a fictional office module located in Amsterdam, the Netherlands. The IEA Task 27 model [11] was used as basis. It consists of a hypothetical room (dimensions 3.5x5.3x2.7m) with a single external wall. The U-value at the opaque section of the external wall follows NEN 2916:2004 (0.32 W/m2K). Slabs and internal walls are assumed adiabatic. Visual properties and thermal load conditions follow the IEA Task 27 model. A single opening is placed on the centre of the external wall, providing view at all times. WWR of the opening varied from 10% to 100% in 10% steps. Glazing for

all window sizes was double pane clear (U-value at centre 1.7 W/m2-K), without any shading device. Evaluations were made for the four main orientations.

Mounted ceiling lamps provided a lighting density of 4x50W. They were controlled through a two-zoned dimmer. Lamps would supplement natural light if levels fell below 500lx at the working plane (0.8m from the floor). Daylight illuminance was measured at two sensor points, located at the centre of each lighting zone. P1 was the sensor closer to the window, while P2 closer to the back of the room. Glare was measured at P2, looking directly to the window.

Criteria used for optimization

The desired boundaries for the solution space are given below, detailing their yearly evaluation. Letters in italics refer to the notation used in equations (3.1) to (3.4).

a) Combined yearlong energy consumption (*En*) of heating, cooling, ventilation and artificial lighting had to be minimized.

b) Illuminance at P2 (*E*) had to be equal to or exceed 500lx for a minimum of 50% total occupancy hours. A value of 500lx is required in many standards to perform office tasks.

c) Illuminance uniformity, *U*, (Ep2/Ep1) had to be equal to or less than 3.5 for a minimum of 50% total occupancy hours. There is higher tolerance to daylight contrast than from artificial lighting.

d) Daylight glare when looking directly to the window from P2 (*G*), had to be equal to or less than DGI 22 [12] for a minimum of 50% total occupancy hours. Only this viewing direction was considered.

e) For this study, a solution was considered into the solution space if it accomplished illuminance criteria and at least one visual comfort criteria.

Compliance of a given criteria during all occupancy hours is unity. The above criteria can be stated as follows:

$$\text{Minimize} \quad En \tag{3.1}$$

$$\text{Subject to} \quad E \geq 0.5 \tag{3.2}$$

$$G \geq 0.5 \tag{3.3}$$

$$U \geq 0.5 \tag{3.4}$$

RESULTS

Figure 1 presents energy consumption and visual comfort for the analyzed cases. Stacked bars represent energy consumption detailed by heating, cooling, artificial lighting and ventilation. Curves represent percentage of occupancy hours for uniformity, glare and illuminance criteria. The graphical optimization method used is as follows: a shaded region covers the area below 50% occupancy hours. Curve points outside this area represents a given visual criteria being met. These results are valid for a single opening, placed in the centre of the facade.

In terms of energy consumption, larger window sizes for South increase cooling demand, while for North heating demand. East and West orientations have the highest overall energy consumption. Least energy use was observed at 30% WWR for North, and at 20% WWR for South, East and West orientations.

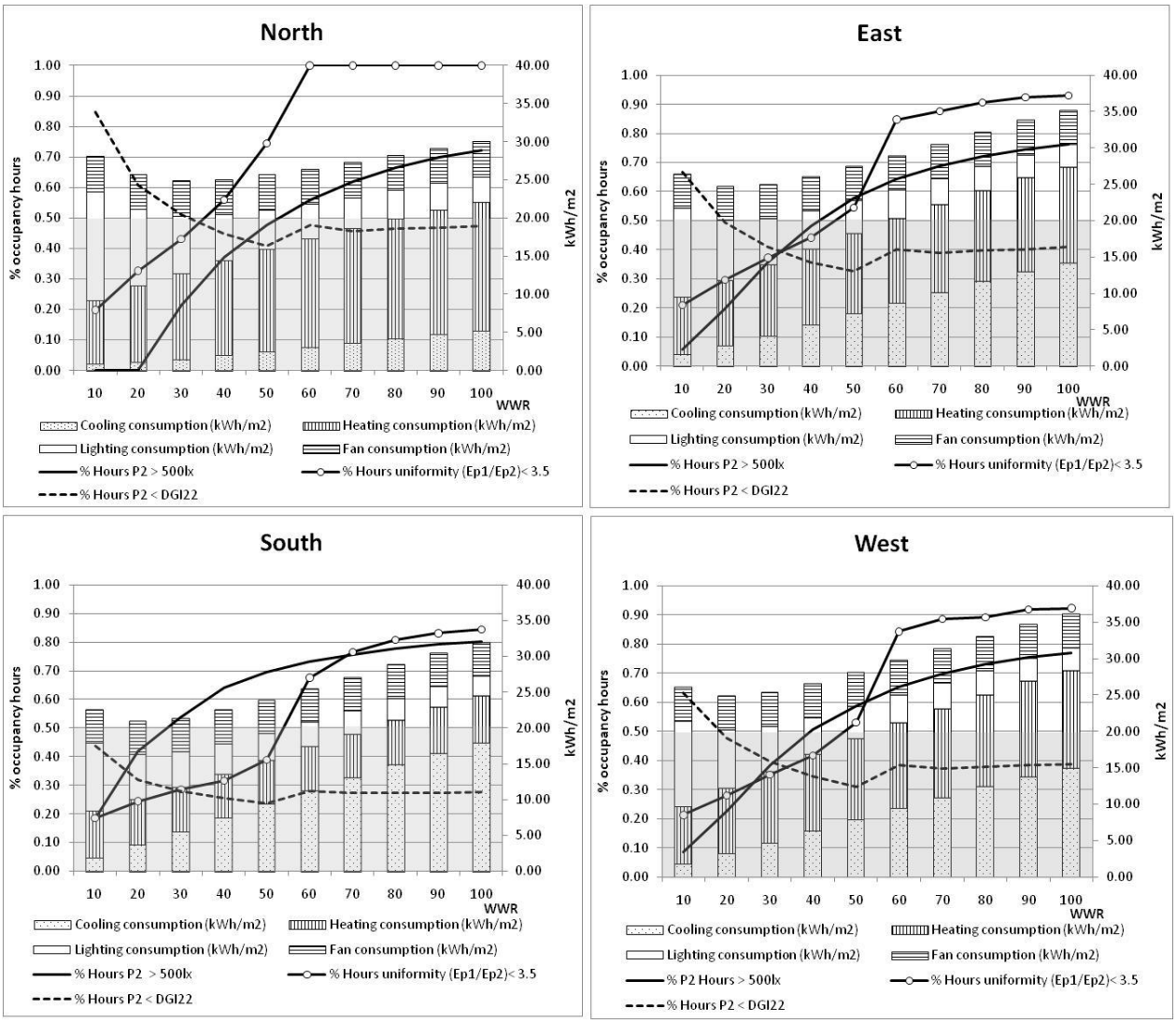

Figure 1: Energy consumption, visual performance and comfort for variable window-to-wall-ratio (WWR) of a hypothetical test room. Location: Amsterdam, the Netherlands. The four main orientations are shown. Unshaded areas on the graphs represent visual criteria being met.

However, window sizes with least total energy consumption are among the worst regarding visual aspects. Even though all visual criteria had equal importance values, illuminance performance at P2 was deemed a requisite to be met as it is stated in many standards. Window sizes achieving one of the two visual comfort criteria at P2 were found in the following window size range. For North: 50 to 100% WWR, for South: 60 to 100% WWR, for East and West: 50 to 100% WWR.

A "critical region" was observed for electric lighting consumption, occurring when reductions on electric lighting energy caused by daylight were less than 5% from the previous case. For North orientation, this was seen from 70% WWR. For South, East and West this was observed from 60% WWR.

The solution space is delimited by the intersection between compliance with at least one visual comfort criteria, compliance with illuminance criteria and start of the critical region.

The window size range is then for North: 50 to 70% WWR, for South: 60% WWR, for East and West: 50 to 60% WWR.

Higher-level information needs to be introduced to choose a single window size that also accomplishes other project objectives. If such additional objectives can be satisfied by a window size within the solution space, a "compromise" can be reached. For example, larger windows respond to improved views. Smaller windows respond to privacy, concerns on energy consumption, etc.

As an example, a designer wants to give the most views to the North, but keep energy consumption minimal. From the results, the solution space for that orientation comprises window sizes between 50 to 70% WWR. For most views, the designer can choose 70% WWR, as this is the upper limit in the solution space without wasting lighting energy.

DISCUSSION

Optimizing window size only for low energy consumption, results in an internal environment not meeting any visual acceptance criteria. This translates to an office environment dominated by high electric lighting usage. Window sizes optimized exclusively for visual comfort produce large heating or cooling energy consumption patterns. The inclusion of diverse visual comfort criteria enabled selecting more alternatives. For example, the glare acceptance criterion was not met by any alternative. However, including uniformity allowed other valid solutions to be accepted. It can also be discussed that measuring glare according to the accepted DGI formulas is not realistic, as it implies a user viewpoint directed towards the window year round.

It was also observed that the solution space, for this particular configuration and climate type, has limited window size options. The prototype already has high performance elements optimized for energy savings (insulation thickness, lighting control and luminaire zoning). Shading elements were not included in this study. This implies that adding too many criteria can limit excessively the solution space.

Differences in energy consumption between the window size using least total global energy and the smallest window size in the solution space are as follows: for North 3.25%, for South 21%, for East 11% and for West 13%. Except for South, this means that a relatively small increase in energy consumption can translate to a more acceptable space in terms of visual comfort, meeting illuminance requirements. Nevertheless, the increase in window size for South can be justified as an investment on visual comfort and views for higher acceptance and productivity from users. Shade elements can bring down this energy consumption.

The results also show that architectural propositions not providing visual control are problematic. Therefore, a careful design is needed that takes into account climatic elements such as glazing type and shade.

CONCLUSIONS

Window size is important in defining total energy consumption and overall visual comfort and performance. However, by itself is not enough to provide both low energy consumption and be an efficient visual system. More elements need to be taken into account from the earliest design stages. These include but are not limited to shading devices, adequate glazing types and adaptable personal visual comfort. Optimized building design requires that design teams set tolerance amounts to achieve compromise for each indicator. Multi-objective optimization methods can introduce additional complexity to the design process, but help reduce decision uncertainty.

From the results, it can be seen that optimizing window size for a single objective can hinder attaining additional ones, while failing to meet performance standards and comfort recommendations. Combining two suitable and clear objectives produces an acceptable environment in terms of visual comfort, performance and energy consumption.

The definition of "compromise sizes" includes a set of trade-off solutions found in the intersection of different criteria such as energy consumption, illuminance performance and visual comfort. Selecting a final size depends on additional project objectives set to meet user expectations. A larger variety of design elements can enrich options within the solution space. However, further research must be made to assign corresponding weight to visual performance and comfort criteria.

This paper presented an example of a trade-off selection procedure. It also presents a case where not all criteria can be met and a sample procedure on deciding acceptance for such cases. The solution space satisfies visual legal requirements, uniformity and is close to using the least energy. Objectives have to be clear in order to translate them to criteria, and in turn, show designers the range of solutions from which they can choose.

REFERENCES

1. De Antonellis, S., Joppolo, C.S., Molinaroli, L.: Simulation, performance analysis and optimization of desiccant wheels. Energy and Buildings, 42: 1386-1393, 2010.
2. Moeck, M., Selkowitz, S.E.: A computer-based daylight systems design tool. Automation in Construction, 5: 193-209, 1996.
3. Toftum, J., Andersen, R.V., Jensen, K.L.: Occupant performance and building energy consumption with different philosophies of determining acceptable thermal conditions. Building and Environment, 44: 2009-2016, 2009.
4. CIBSE: Degree-days: Theory and Application, Document TM41:2006. Available from: cibse.org (accessed October 2010).
5. Achard, G., Laforgue, P., Souyri, B.: Evaluation of Radiative Comfort in Office Buildings. Proc. CLIMA 2000 Session 1. Brussels, 1997.
6. Mardaljevic, J., Heschong, L., Lee, E.: Daylight metrics and energy savings. Lighting Research and Technology, 41: 261-283, 2009.
7. Osterhaus, W.K.E.: Discomfort glare assessment and prevention for daylight applications in office environments. Solar Energy, 79: 140-158, 2005.
8. Rhea, M. (ed.): Lighting Handbook-Reference and application, 9th Ed. IESNA. New York, 2000.
9. Wienold, J., Christoffersen, J.: Evaluation methods and development of a new glare prediction model for daylight environments with the use of CCD cameras. Energy and Buildings, 38: 743-757, 2006.
10. Lee, E.S., Tavil, A.: Energy and visual comfort performance of electrochromic windows with overhangs. Building and Environment, 42: 2439-2449, 2007.
11. Van Dijk, D.: Reference office for thermal, solar and lighting calculations. IEA Task 27, Performance of Solar Facade Components. TNO Building and Construction Research. Delft, 2001.
12. Nazzal, A.A.: A new evaluation method for daylight discomfort glare. International Journal of Industrial Ergonomics, 35: 295-306, 2005.

AN ANALYSIS OF SCHOOL BUILDING DESIGN EVALUATION TOOLS

Pereira, Paula R. P [1]; Kowaltowski, Doris C.C.K.[2]

1: Department of Architecture and Building, School of Civil Engineering, Architecture and Urban Design, State University of Campinas, UNICAMP
CP 6021, 13083-852, Campinas, SP, Brazil
paulapzr@hotmail.com

2: Department of Architecture and Building, School of Civil Engineering, Architecture and Urban Design, State University of Campinas, UNICAMP
CP 6021, 13083-852, Campinas, SP, Brazil
doris@fec.unicamp.br

ABSTRACT

Projects for school buildings in the State of São Paulo are managed by the Foundation for School Development (*Fundação para o Desenvolvimento Escolar* - FDE), which is also responsible for verifications and approvals. Results of post-occupancy evaluations have shown that these buildings present a less than satisfactory performance, mainly in environmental comfort issues and are not sufficiently stimulating to students and teachers, affecting the quality of education. The literature that argues the school environment issues evidences the aspects of sustainable and the relation of school environment and quality of education. Studies on the FDE design process show that professionals need support during the design process, especially to verify designs that are still being developed. This article has the objective to analyze design evaluation tools so as to verify the applicability of its elements for the construction of one that is specific to school buildings designs in the State of São Paulo. A survey was held and two tools were selected for analysis: *DQI for Schools* (*Design Quality Indicator*) and *Evaluation method for school building design with optimization of aspects of environmental comfort*. The sample is composed by FDE school building designs. Results show that both tools need to be adequate to a specific application. The final results highlight the necessities for a building design evaluation tool that includes specific instruments to analyze both objective and subjective data within its structure. The evaluation of projects requires objectivity both in the process of tool application and in the process of result visualization, alongside a quick return of information to support the architectural design process. It is essential to create a grid with design requirements specific to brazilian values.

INTRODUCTION

The international literature of schools design is large and emphasize the relevant works like Sanoff (2001), Nair & Fielding (2005), Dudek (2007) and Ford & Huton (2007). These works discuss the curriculum and architectural trends. They receive the support from researches that are concentrated in the quality of the architectural programming. In Brazil, the discussions about the school environment are, in most cases, about the results of post-occupancy evaluation (POE), (PIZARRO, 2005; ORNSTEIN & MOREIRA, 2008; RHEINGANTZ et al, 2008; ELALI & GONDIM, 2010; KOWALTOWSKI, 2011), it is not completely related to the design process or design evaluation.

The researches from POE are concentrated on the problems of the physical environment. The easy way to apply them allowed the development of own methods and concepts, even this presents a slow feedback to the projects, being, in such a way, more popular in the academy then in architecture offices. The professional design evaluation is informal, so this is the object of discussion for the architectural critics.

The results of POE in the Brazilian schools indicate that the environment comfort, the relation by curriculum and architecture and the integrate projects can be improved. The studies on these design process buildings can improve the quality of this aspect. In the State of São Paulo the Foundation for School Development (FDE) is responsible for verifications and approvals of projects developed by contracted offices. The FDE gives to the offices the design program defined by the Secretariat of the Education, the topographical issues and catalogues (constructive components and modulation), beyond a list of the norms that have to be consulted. Recently the FDE also introduced sustainability indicators into the catalogues to obtain the certification Environmental High Performance (AQUA) (FCAV, 2007).

It is notice that the design processes of high performance schools are integrated and have many evaluation phases. On this way, it is recommended the use of evaluation tools to guarantee good results and make possible the quickly design corrections.

This work compares the efficiency of two design evaluation tools. The tools *Design Quality Indicator* and *Evaluation method for school building design with optimization of aspects of environmental comfort* were selected because are specific to the schools buildings designs. Both had been applied in a sample of FDE design schools and its performances had been compared. This article is related to the first results of a thesis in progress named “New practical of school design evaluation for the school architecture in the State of São Paulo”, developed in the UNICAMP - State University of Campinas.

METHOD

The school design evaluation tools *DQI for Schools* and *Evaluation method for school building design with optimization of aspects of environmental comfort* are described, clarifying their concepts, morphology. The facilities and difficulties of the application are verified as positive and negative characteristics in each one. The results and the way as each one give a feedback of data to the design process. The sample is composed by 81 FDE school building designs (FDE, 2006). All the 81 designs had been evaluated by *Evaluation method for school building design with optimization of aspects of environmental* and one, by DQI *for Schools.*

ANALYSIS

Design Quality Indicator (DQI for Schools)

The Design Quality Indicator tool is composed by four structural elements: conceptual grid, data collection, weight and "questionnaire", which have four different versions for design and construction phases: Program, Project, Occupation and Post-Occupation Evaluation. The conceptual grid presents three main issues - functionality, construction quality and impact. The questionnaire that makes data collection presents ten indicators: use, access, space, performance, engineering systems, construction, form and materials, internal environment, social and urban integration, innovation and characteristics. The DQI tool evaluates every design, however a specific version for school building designs, called DQI for Schools, have being used successfully, mainly in the United Kingdom and some case studies are displayed in the DQI website (DQI, 2010).

The weight is presented through the notes, varying between "strong disagrees" to "strong agrees", and have the options "not applicable" and "I do not know", in a scale of seven degrees. The tool is friendly because each indicator has a dialogue box with a summarized explanation about the relation between the note and the design. In each issue the characteristics must be judged and, finally, each indicator also has its evaluation. It does not have pre-definition of importance. The tool is known by the format that stimulates the dialogue and the ideas exchange between the participants. Some authors already have presented critical about this tool (MARKUS, 2003; THOMSON et al., 2003; DEWULF & VAN MEEL, 2004), however none of them criticized the specific school design tool, therefore, this work apply it in a sample design and put together notes that had been already done with the results of the analysis.

In this paper DQI for Schools was applied in a design of the school EE Conjunto habitacional Campinas EB-1. It was noted that all the evaluated aspects have appeared in the three quality indicators (Functionality, Construction Quality and Impact) with different approaches. The subjective issues are complemented with indications of norms and regulations verification. It was noted that the subjective data collection encloses many activities as the need to establish a dialogue with all the participants of the process (what could not be done because this application involved only the author as an evaluator), 2D design observations (or even other representations of the design) and superposition about the future environment function. The nature of these activities is a deviation of the objective of data collection, which encloses the norms and regulations verifications. The scale with seven degrees is more appropriate for the objective issues. The subjective data collection does not need a point scale to be really evaluated.

It was used two perspectives and the design plants to evaluate the school design. The DQI does not indicate the type of material the respondent must have in hands during the analysis. To answer technician questions included in Construction Quality it was noted the need of more details about the design. 16.81% answers were annulled by the option "don't know". There was amount of "strong disagrees" answers presented in all the attributes. This result was related to the fact that DQI for Schools do not represents the reality of the Brazilian public schools, reinforcing the need to create a tool that has State of São Paulo specific values.

The final results were represented in a bar graphic that showed the difference between the true results and the goal results. The evaluation showed some difficulties; however, the

"questionnaire" application stimulated the reflection about the design situation. The results format characterizes much more a work summary then an instrument of design feedback. The professional can't use only the bar graphic to increase the design quality, he must need participate in all the design evaluation process. It was noted that DQI for Schools is a valuable tool for the architectural program, because stimulated the dialogue. To evaluate final design quality it would need more objective issues during the application and detailed results.

Evaluation method for school building design with optimization of aspects of environmental comfort

The optimization of multi-criteria takes into account a compromised solution in the analysis of interdependent variable because it's impossible to optimize all variable in a design. Thus, the design solutions are divided in two sets: not excellent set and excellent set. The main intention of the optimization theory is to help the designer to choose a design that has a set of viable solutions, giving the direction for the process of design decision through the comparison between the excellent set designs and those that presents the better alternatives.

The Evaluation method for school building design with optimization of aspects of environmental comfort developed by Graça (2002), can be divided in three phases. In the first one, it has the analysis of the school site dimensions; therefore many school designs suffer restrictions because the sites have small sizes. The second phase consists in a graphical analysis of typology variations done by environmental comfort experts. They evaluated the conditions of acoustic, thermal and luminous comfort in school designs. The criteria used to identify the compromise solutions, is: design solution that have, at least, one comfort variable evaluation superior in relation to another design.

Initially, 28 schools designs were eliminated because the site sizes, some in function of the width dimensions, others, of the length, others had presented reasons below of the recommended one. The number of schools in the sample was large, so the designs were drawing in the AutoCAD and it was created blocks that simulated each typology, to facilitate the analysis. It was found 10 compromise solutions in the sample.

The application of tools that work with indicators generally does not leave doubts about the data selection and analysis. However, this characteristic restricts the evaluation objective because considers only comfort issues. To develop a quality school design the architect needs a tool that analysis much more requisites, sometimes, subjective requisites. Although the typology have graphic express, the results present a scale. The architects not use to work with this kind of information.

RESULTS

The DQI for Schools is a special tool because presents the design language, that can improve the dialog between the participants of de design process. The application stimulated reflections about the design situation. These characteristics become the tool a rich support for the development of the program, however to evaluate final design quality it would need more objective issues during the application The results format characterizes much more a work summary then an instrument of design feedback.

The Evaluation method for school building design with optimization of aspects of environmental comfort showed needs of revisions. The method is not applied to the schools implanted in small sites; however, the analysis showed that some schools with good comfort performance were excluded in the site evaluation. It was necessary to create AutoCAD blocks

to evaluate a large number of designs. To develop a quality school design the architect needs a tool that analysis much more requisites, sometimes, subjective requisites, not only comfort issues. Although the typology have graphic express, the results present a scale. The architects not use to work with this kind of information. The use of drawings to evaluate the design is a positive aspect of this tool.

DISCUSSION

The final results highlight the necessities for a building design evaluation tool that includes specific instruments to analyze both objective and subjective data within its structure. The evaluation of projects requires objectivity both in the process of tool application and in the process of result visualization, alongside a quick return of information to support the architectural design process. It is essential to create a grid with design requirements specific to brazilian values.

ACKNOWLEDGEMENTS

The authors thanks FAPESP for the financial support received for the development of this research.

REFERENCES

1. Design Quality Indicator (DQI): Available http://www.dqi.org.uk, Dicember, 2010.
2. Dewful, G.; Van Meel, J.: Sense and nonsense of measuring design quality. Building Research and Information, v 32, n 3, pp 247-250, 2004.
3. Elali, G. V. M. A.; Gondim, L.: Avaliação Pós-ocupação como base para o projeto de intervenção no Núcleo de Educação da Infancia (NEI-UFRN) em Natal, Brasil. In: NUTAU 2010 - V Seminário Internacional Arquitetura, Urbanismo e Design - produtos e mensagens para ambientes sustentáveis. Anais do NUTAU 2010, v. 1. p. 1-16. São Paulo, 2010 (in portuguese).
4. Fundação Vanzolini (FCAV): Referencial técnico de certificação para edifícios do setor de serviços - Processo AQUA. Escritórios e edifícios escolares, 2007(in portuguese).
5. Fundação para o Desenvolvimento da Educação (FDE): Arquitetura escolar paulista - estruturas pré-fabricadas, 336 p. Diretoria de obras e serviços, São Paulo, 2006 (in portuguese).
6. Graça, V.A.Z. da.: Otimização de projetos arquitetônicos considerando parâmetros de conforto ambiental: o caso das escolas da rede estadual de Campinas. 139f. Dissertação (Mestrado em Engenharia Civil) – Universidade de Campinas, Campinas, 2002 (in portuguese).
7. Kowaltowski, D.C.C.K.: Arquitetura Escolar: o projeto do ambiente de ensino. Oficina de textos. São Paulo, 2011 (in portuguese).
8. Markus, T.A.: Lessons from the design quality indicator. Building Research and Information, v 31, n 5, pp 399-405, 2003.
9. Nair, P.; Fielding, R.: The language of school design. Design patterns for the 21th century school. 2ed. Nacional Clearinghouse for Educacional Facilities. Índia, 2005.

10. Ornstein, S.W.; MOREIRA, N.S: Evaluating School Facilities in Brazil. OECD/PEB – Program on Educational Building Department), 2008.
11. Pizarro, P.R: Estudo das variáveis do conforto térmico e luminoso em ambientes escolares. Dissertação (Mestrado em Desenho Industrial). UNESP - Universidade Estadual Paulista (Faculdade de Arquitetura, Artes e Comunicação). 155p. Bauru, São Paulo, 2005 (in portuguese).
12. Rheingantz, P.A.; Azevedo, G.A.N.; Brasileiro, A.; Alacantra,D.; Queiroz, M.: Observando a qualidade do lugar: procedimentos para a avaliação pós-ocupação. Editora FAPERJ Fundação Carlos Chagas Filho de Amparo à Pesquisa do Estado do Rio de Janeiro. Rio de janeiro, 2008 (in portuguese).
13. Sanoff, H.: School buildings assessment methods. Nacional Clearinghouse for Educacional facilities. Washington, DC., 2001.
14. Thomson, D.S.; Austin, S.A.; Devine-Wright, H. & Mills, G.R.: Managing value and quality in design. Building Research and Information, v 31, n 5, pp 334-345, 2003.

OCCUPANT SATISFACTION AS AN INDICATOR FOR THE SOCIO-CULTURAL DIMENSION OF SUSTAINABLE OFFICE BUILDINGS

Karin Schakib-Ekbatan[1], Andreas Wagner[1]

1: Building Science Group, Karlsruhe Institute of Technology (KIT), Englerstr. 7, 76131 Karlsruhe, Germany

ABSTRACT

Offices represent an important work environment and are a worthwhile challenge in the context of designing sustainable buildings with low energy consumption, high comfort and appropriate functionality for the employees. Against this background the main objective of the described project was the development of a method for the evaluation of building performance from the occupants' point of view and their day-to-day experiences with comfort at the workplace. The addressed comfort parameters thermal, visual and aural comfort, air quality as well as different workplace and building related aspects are compatible with the description of the socio-cultural dimension of the German `Sustainable Building´ Quality Label for office and administrative buildings.

Based on the statistical evaluation of surveys in 26 buildings in Germany an overall building index has been developed and calculated, which allows a quick evaluation of individual buildings or building stocks. By using different statistical procedures such as 'Factor Analyses', 'Principal Component Analysis' and 'Correspondence Analysis' it could be shown that a summed score of the above mentioned satisfaction parameters without weighting factors could be used as the overall index. Hence, benchmarks can be derived for the building performance as indicative information which then can be used for portfolio analysis by real estate managers. Beyond this index differentiated information on perceived comfort can be used for a comprehensive building assessment. By examining single comfort parameters information about strengths and weaknesses of a building from the occupants' perspective can be obtained. The outcome supports monitoring procedures, provides guidance for building performance improvement and contributes to evaluate interventions. As a further result from the project the instrument **INKA** (**I**nstrument für **N**utzerbefragungen zum **K**omfort am **A**rbeitsplatz) has emerged. It includes a questionnaire in paper and online version as well as a report sheet that shows the main survey results using Excel-based analysis routines. In an accompanying guideline information for the implementation and evaluation of surveys is given. With this systematic procedure a significant step towards a comprehensive building performance evaluation regarding sustainability is initiated. A useful application is thus given in two ways: in terms of a practical assessment procedure for the real estate market as well as of building up a substantial database for comparative scientific building analyses and discussion. In this paper results for the development of the index and practical implications of the survey instrument are reported.

INTRODUCTION

With approx. 40% of the German primary energy consumption, buildings are of special interest in the context of sustainability. Driven by policy guidelines and interest of the real estate market, building performance evaluation is becoming a growing marketing factor.

Offices represent an important work environment, thus building design should consider the needs of the occupants besides low energy strategies for heating, cooling, ventilation and lighting [1]. At present, little is known about approved criteria for the socio-cultural quality of buildings, whereas methods and tools for the monitoring of technical or economical characteristics are becoming more and more established. Particularly there is a lack of time- and cost-effective procedures with regard to evaluation of comfort at workplaces.

To meet targets Post-Occupancy Evaluation (POE) is a useful diagnostic tool and system which allows facility managers to identify and systematically evaluate critical aspects of building performance based on the employees' day-to-day experiences [2]. As complement to technical monitoring or lifecycle analyses, surveys have a great potential of gaining relevant feedback from the occupants as a basis for various improvements in energy efficiency regarding day-to-day operations. Experiences show that there is often a gap between the calculated and the metered energy consumption for a variety of reasons which can be assessed by continuous monitoring. This is expected as well in the wide field of comfort.

In Germany, a voluntary certification system for office and administration buildings has been launched recently. The Federal Ministry of Transport, Building and Urban Affairs (BMVBS) [3] in cooperation with the German Sustainability Buildings Society (DGNB) [4] developed a certification system for sustainable new office and administration buildings. Based on standards and calculated data topics such as ecology, economy, techniques, functionality and processes as well as the socio-cultural quality are considered. This topic includes comfort parameters like thermal, visual and aural comfort, air quality and options for occupants' control (e.g. operable windows) as well as safety and security aspects. Currently the certification system is expanded to existing buildings. It is intended to implement user surveys within a continuous monitoring procedure. The occupants' votes would allow a continuous check whether forecasted comfort parameters can be achieved in real building operation.

Main goals of the presented project were: (1) the development of an overall building index which allows the ranking of single buildings in comparison to a building stock on an aggregated level and (2) the development of a manageable (time- and cost-saving) and praxis-oriented instrument with focus on occupant satisfaction.

METHOD

Building Sample and Participants

The field studies were conducted from 2008 to 2011. The range of the assessed 26 buildings includes different types, such as new, certified, old or refurbished buildings. The occupants were employees from civil service and the private sector (total of 2,832 datasets; the response rate averaged 46%).

Measures

Participants were asked to fill in a questionnaire which was provided as paper-pencil version (2008 and 2009) as well as an online survey (2010 and 2011) where technical requirements were given. The questionnaire was developed in accordance to frameworks from environmental psychology, findings in the field of the sick-buildings-syndrome [5, 6] and the questionnaire of the Center for the Built Environment, University of California, Berkeley [7]. Besides demographic information (e.g. gender, age) and background information (e.g. orientation of the office, distance to window) the items focus the degree of satisfaction with the ambient comfort parameters in the workspace such as (1) temperature, (2) light (natural and artificial light, shades/blinds), (3) air quality, (4) acoustics/noise, (5) furniture/layout and

(6) spatial conditions (e.g. amount of space, privacy). Additionally, items were added which broach the issue of (7) the entire building (e.g. restrooms, conference rooms) and which coincide with the criteria for the German certificate (e.g. safety, security). Each of the 7 main comfort parameters includes a subset of items and the accordant concluding question `Overall, how satisfied are you with … in your workspace?´. Answers concerning the degree of satisfaction were coded continuously on a 5-point-Likert-scale from very dissatisfied (-2) to very satisfied (+2).

Statistical Analyses

The approach was to use different statistical procedures to prove if there is statistical evidence for an overall building index: (a) Factor Analysis, (b) Principal Component Analysis (PCA) with optimal scaling and (c) Correspondence Analysis. The aim was to prove if large sets of variables could be reduced to one factor by aggregating individual-level data to construct measures for units at a higher level. The applied software was PASW (Predictive Analysis SoftWare) and SPSS 18 (Statistical Package for the Social Sciences).

RESULTS

Statistical Analyses

After having tested that reliability for the 7 indicator subsets is given (Cronbachs alpha for winter survey = .84, Cronbachs alpha for summer survey = .81) all 7 concluding `Overall…´-questions were comprised in the analysis to test for the underlying dimensions in the data. The computations by PCA revealed a one-factor solution with high positive loadings for all seven indicators (> 0,7) and an eigenvalue greater 1 (3,856). The results were confirmed by correspondence analyses (for a more detailed description see [8, 9]). Table 1 shows results from the factor analysis.

Comfort parameter	**Winter Survey** *N* = 1,578	**Summer Survey** *N* = 1,254
Overall, how satisfied are you with **the building**?	.72	.77
Overall, how satisfied are you with **furniture/layout** in your workspace?	.70	.70
Overall, how satisfied are you with **spatial conditions** in your workspace?	.75	.81
Overall, how satisfied are you with **acoustics/noise** in your workspace?	.74	.77
Overall, how satisfied are you with **air quality** in your workspace?	.69	.71
Overall, how satisfied are you with **temperature** in your workspace?	.74	.73
Overall, how satisfied are you with **lighting conditions** in your workspace?	.70	.56

Table 1: Component loadings from factor analyses for comfort parameters. Component loadings: > 0, 7 = very high, 0, 5 - 0, 69 high, 0, 3-0, 49 poor, < 0, 3 very poor. Sample: 26 buildings.

All variables have very high or high loadings. A high value for the Kaiser-Meyer-Olkin-statistics (winter survey: KMO = .84, x^2 = 3318, p < .001, eigenvalue 3,614, other eigenvalues < 1; summer survey: KMO = .84, $x^{2 =}$ 1423, p < .001, eigenvalue 3,652, other eigenvalues < 1) shows that homogeneity in the data is given. An overall index could be developed (Figure 1)

which is applicable for the survey instrument **INKA** (**I**nstrument für **N**utzerbefragungen zum **K**omfort am **A**rbeitsplatz). The index results as the mean score of the 7 indicators (Figure 2).

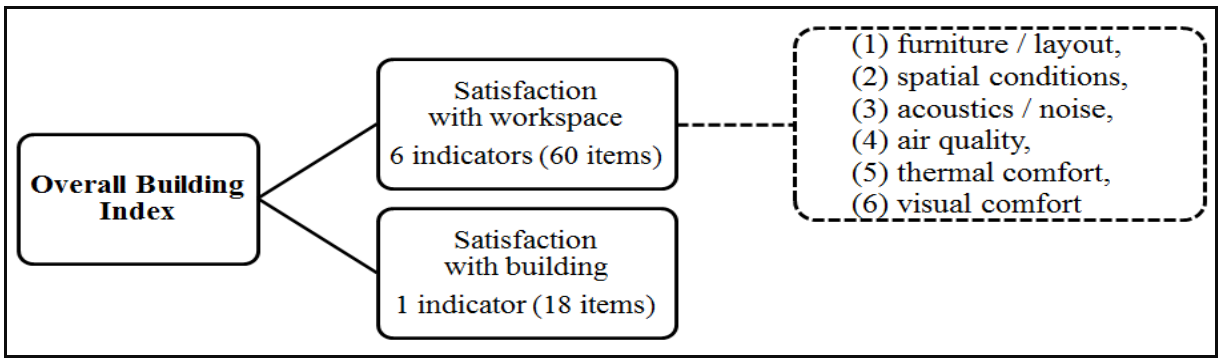

Figure 1: Facets of the final `Overall Building Index´

Instrument INKA

For wider application in practice we developed a time- and cost-effective survey instrument including a computer-based questionnaire and an easy to handle automatic evaluation procedure for the Facility Management staff respectively personnel from the real estate market. The given information includes a report sheet showing the index, mean values for comfort parameters (overall-questions) concerning the workspace and the building. Additionally, the frequency distribution for the comfort parameters is given based on three categories (very dissatisfied/dissatisfied, neutral and satisfied/very satisfied). On a general level, the overall building index and the mean scores for comfort parameters serve as benchmarks with respect to a comparison of larger building stocks and to screen monitoring processes regarding occupants' feedback in single buildings (Figure 2).

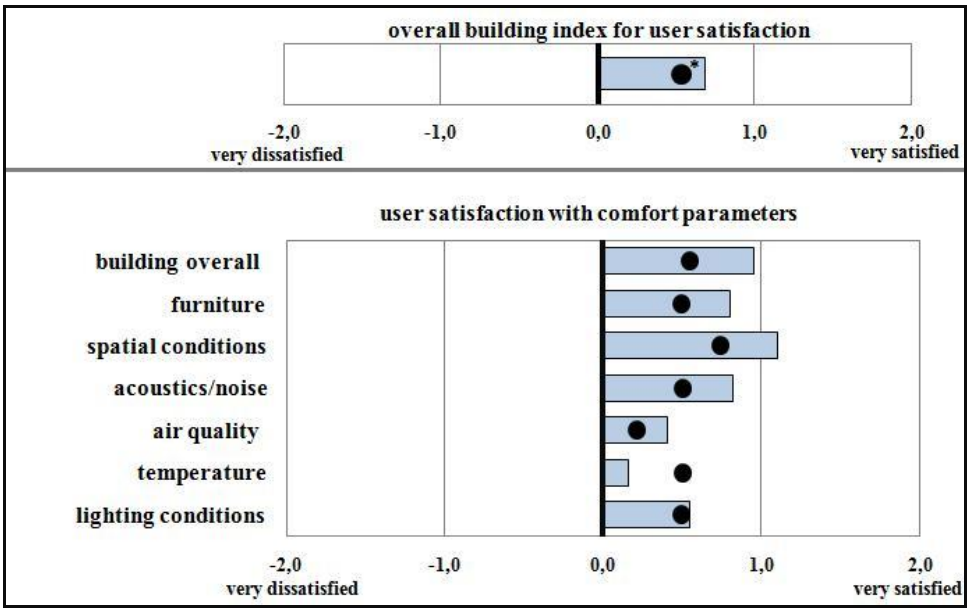

Figure 2: Results for a building with certificate in `gold´ (bars) in comparison to a sample of 26 buildings (● N =1,578) assessed in winter seasons 2008 to 2011.*

The graph shows results for a building with a certificate in `gold´ from the German certification system. In comparison to the scores of the sample most comfort parameters in this building are in line or even better, but obviously the occupants experienced less comfort

with temperature. This information is helpful for the Facility Management staff either for a portfolio analysis or for planning interventions. The benefit of occupant surveys as part of the new German certification system for existing buildings is to compare the results to the predicted outcome for the socio-cultural quality based on plans, standards and audits and to detect the potential for optimization (Table 2).

Comfort parameters	**Predicted comfort** from certification system	**Experienced comfort** based on occupant survey	
		satisfied/very satisfied	**dissatisfied/very dissatisfied**
thermal comfort in winter	100%	43%	31%
thermal comfort in summer[1]	100%	45%	26%
air quality	100%	50%	16%
acoustics/noise	100%	66%	6%
visual comfort	85%	73%	18%

Table 2: Ratings for the building with certificate in `gold´: predicted comfort from certification procedure (degree of compliance) and results from occupant surveys (N = 115) regarding comfort parameters ([1]survey in 2008, other comfort data derive from a survey in winter 2009.

Even if it is not realistic to obtain 100% satisfaction for comfort by subjective ratings, the outcome for this building shows an enormous gap between the predicted comfort and the results from the occupant surveys concerning the indoor environment conditions `temperature`, `air quality´ and `acoustics/noise´. Values for visual comfort are more congruent, maybe due to the fact that in the certification procedure the architectural feature `atrium´ was taken into account which resulted in a reduced degree of compliance.

DISCUSSION

The main scientific objective of the project was to develop an overall building index for comfort assessment. A result from statistical analysis was that general satisfaction with comfort at workspaces and in the building can be represented by one factor. The overall satisfaction can be expressed by an overall building index based on simply summed mean scores from the included comfort parameters. This score can be expressed comprehensible by the same codes used in the questionnaire (very dissatisfied (-2) to very satisfied (+2)) and therefore needs no further transformation into threshold values.

The high attractiveness of an `overall building index´ obtained from surveys expresses itself by the possibility of a quick ranking of buildings in terms of occupant satisfaction. With regard to portfolio analyses the index can be used as a first orientation in the sense of a screening instrument for investors or owners. An index has limitations as well. Buildings are complex due to e.g. architectural features, functionalities, and maintenance Thus an index should not replace an in-depth evaluation in buildings to detect the potential for optimization. Furthermore, when considering comfort as `a matter of culture and convention´ [10], changes in importance of comfort parameters over time respectively generations are expectable, and so instruments for measuring subjective issues should be well defined and adjusted for its scope. The discussed aspects illustrate the complexity of the social issues in the field of building performance and the challenge of translating social reality into scores. Another limitation to

the findings could be the sample size. The acquisition of buildings is often complicated and troublesome for a variety of reasons.

The database for occupant surveys in Germany is still too small to define threshold values or standards for the socio-cultural quality (presuming this is basically a realistic approach). For this a standardised sample would be required. Nevertheless, a continuous assessment of occupants' feedback seems to be a useful part for evaluating the sustainability of buildings in certification systems. With respect to the demand of energetic refurbishments, the huge number of existing office buildings is a crucial issue also in the field of comfort at workspaces. Besides energy efficiency and optimal building operation a great potential lies in occupants' behaviour. The development and evaluation of smart feedback-systems which enable occupants to understand and to react properly to the energy concept of a building are a future challenge in the field of post-occupancy evaluation as well as in the long run for updating certification systems.

ACKNOWLEDGEMENTS

The study was funded by the German Federal Ministry of Transport, Building and Urban Affairs (Research Initiative `Future Building´, Z 6 – 10.08.18.7-08.8/II 2 – F 20-08-09) and an industrial partner (bauperformance GmbH).

REFERENCES

[1] Voss, K., Löhnert, G., Herkel, S., Wagner, A., Wambsganß, M. (Hrsg.): Bürogebäude mit Zukunft. Konzepte, Analysen, Erfahrungen. solarpraxis, Berlin, 2006.

[2] Preiser, W. F. E., Schramm, U.: A conceptual framework for building performance evaluation. In W. F. Preiser, J. C. Vischer (Eds.) Assessing Building Performance, pp 15-26. Elsevier, Oxford, 2005.

[3] Bundesministerium für Bau-, Stadt- und Raumentwicklung: Leitfaden Nachhaltiges Bauen, 2. Auflage. BMVBS, Berlin, 2011.

[4] Deutsche Gesellschaft für Nachhaltiges Bauen e.V.: Excellence defined. Sustainable Building with a Systems Approach. DGNB, Stuttgart, 2010.

[5] Gifford, R.: Environmental Psychology: Principles and Practice (2th Ed.). Optimal books, Colville, WA. 2002.

[6] Bischof, W., Bullinger-Naber, M., Kruppa, B., Müller, H. B. Schwab, R.: Expositionen und gesundheitliche Beeinträchtigungen in Bürogebäuden - Ergebnisse des ProKlimA-Projektes. Fraunhofer IRB, Stuttgart, 2003.

[7] www.cbe.berkeley.edu

[8] Schakib-Ekbatan, K., Wagner, A., Lussac, C.: Occupant satisfaction as an indicator for the socio-cultural dimension of sustainable office buildings – Development of an overall building index. Proc. of Conference: Adapting to Change: New Thinking on Comfort, Windsor, 2010 [http://nceub.org.uk].

[9] Wagner, A., Schakib-Ekbatan, K.: Nutzerzufriedenheit als ein Indikator für die Beschreibung und Beurteilung der sozialen Dimension der Nachhaltigkeit. Fraunhofer IRB, Stuttgart, 2010.

[10] Chappells, H., Shove, E.: Debating the future of comfort: Environmental sustainability, energy consumption and the indoor environment. Building Research & Information, 33(1), pp 32-40, 2005.

RESPONSIVE ENVELOPES AND AIR DESIGN: THE STRATUS PROJECT

Geoffrey Thün[1]; Kathy Velikov[1]; Colin Ripley[2]; Mary O'Malley[1]

1 Taubman College of Architecture and Urban Planning, University of Michigan, 2000 Bonnisteel Blvd, Ann Arbor, MI 48109, USA

2. Ryerson University, Department of Architectural Science, 325 Church Street, Toronto, Ontario, Canada

ABSTRACT

The Stratus Project is an ongoing body of design research that investigates the potential for kinetic, sensing and environment-responsive interior envelope systems. The research emerges from a consideration of our attunement to the soft systems of architecture – light, thermal gradients, air quality and noise – to develop and prototype envelopes that not only perform to affect these atmospheres, but also to promote continual information and material exchange, and eventually dialogue, between occupant and atmosphere. The work aims to reclaim the environmentally performative elements of architecture – in this case, specifically, interior mechanical delivery and interface systems – to within the purview of the architectural discipline, as territories of material, formal, technological and experiential innovation, where performance and form are integrated conceptually, operationally and aesthetically. The physical research of the Stratus Project explores material fabrication, flexible systems, and integration of digital sensing and digital control, prioritizing a distributed approach to structural, mechanical and communications systems design and delivery, focusing on localized response to demand. The first constructed and installed prototype develops of a thick suspended ceiling that produces a light and air-based architectural environment. The work is being explored through the construction of prototype testbeds and is currently supported by institutional, industry and government funding.

From the perspective of building science, the Stratus Project is concerned with mediating indoor air quality and occupant comfort, and with providing live air quality information to the occupant in both analog and haptic ways. The research aims to advance the development of responsive, or adaptive architectures; architectures that include real-time sensing, kinetic climate-adaptive components, smart materials, automation and the ability not only for user-interactive characteristics such as computational algorithms which operate under the principles of second-order cybernetics, wherein both user and system are capable of shaping an unlimited set of performance outcomes so that both "learn" over time. It is anticipated that through this approach, inhabitants might develop more sensible and cognitive relationships between their own actions, the buildings they inhabit, and the larger environment. In this way, inhabitants might also be able to better understand their impact and agency within the air-based environment.

INTRODUCTION

The Stratus Project is concerned with mediating indoor air quality and occupant comfort, and with providing live air quality information to the occupant in both analog and haptic ways. In this pursuit, it prioritizes a distributed approach to sensing and actuation, air delivery and

environmental response. The project is conceived of as a layered system that extends from a raised floor assembly housing displacement ventilation, to a kinetic superstructure that provides distributed and personalized spatial and environmental adaptability. Through the gross movement of the ceiling, the volume of conditioned space is altered in response to occupation. Micro-fans respond to increases in temperature, altering perceptions of comfort and reducing the extent of cooling demand. LED lighting arrays pair illumination with the presence of the body. A distributed approach to the provision of air and light proposes to adjust in real time mechanical response to situational need. These strategies are aligned with ambitions to both minimize the energy consumption associated with air delivery, and provide a much more responsive and fine-grained approach to air quality provision driven by demand.

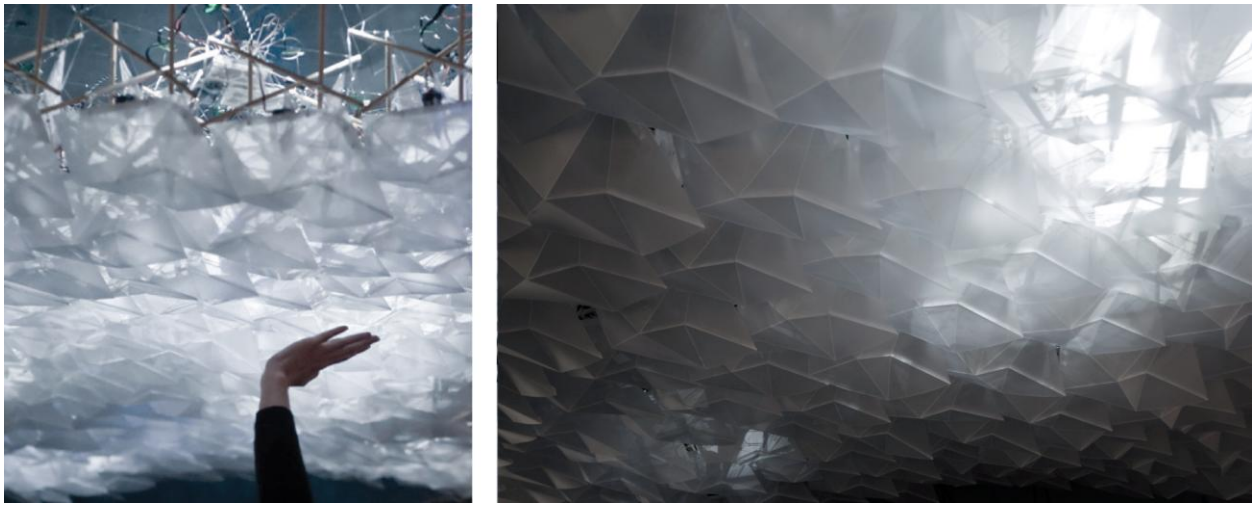

Figure 1: The Stratus Project v1.0 installed; light and air responding to individual occupancy.

METHOD

The method described will account for the approach and technologies deployed in the first generation prototype construction (Figure 1). The structural foundation of Stratus is a flexible tensegrity weave that organizes and supports the operational components. A tensegrity-based system was selected for its lightweight and stable properties, as well as for its potential capacity to deform as a textile without failing or disturbing the attached components. A cable strut system was adapted from a system developed by mathematicians Wang & Liu [1]. Each individual tensegrity unit is comprised of three rods connected with elastomer cord, selected to enhance overall flexibility. The individual units are woven together to create a 2.5m x 1.5m array. Woven into the tensegrity structure is a distributed array of sensors, actuators, lights, micro-fans and diffusing thermally absorptive fabric panels. On the underside of the structure are located the "breathing cells": individually actuated cells that form a translucent, light-diffusing skin and that open to allow thermal conditioning and air extraction. (Figure 2)

The breathing cells comprise the primary visible surface of the Stratus Project. Each cell is made from a single die-cut piece of translucent vinyl, folded and taped into form, and attached to a laser-cut acrylic substructure. Vinyl was chosen for its visual depth, high diffusion properties, and workable ease. In the next stage of the research, more environmentally benign materials will be explored for the cells. These cells are designed like scales, to provide a tight continuous surface across multiple formations of the ceiling plane when closed. The acrylic substructure consists of two main parts – the cell frame and the motor platform – and provides consistent details for support, mechanical motion, and mounting to the tensegrity fabric. A micro-servo motor is mounted into each motor platform

to open and close the cell. Like standard servos, these micro-servos will rotate to a specific angle based on electrical signals received from the control board. Each motor draws only 0.75 watts of power. Rotating the servo to 90° pulls the cell closed while rotating to 0° opens the cell. Motion is triggered by input from the temperature sensor; when the temperature threshold is exceeded, the cells open to create ventilation and airflow, closing them again when excessive heat is relieved.

A layer of elastic nylon fabric panels is woven into the tensegrity structure. In the first prototype, this layer contributes to light diffusion. In future explorations, these fabric panels will be impregnated with Phase Change Materials (PCMs) that will contribute to regulating the interior microclimate of the space. The fabric layer is designed to maximize its exposed surface area in order to provide as much absorptive PCM area as possible. Future tests will examine the ambient impact of PCM fabric coatings at varied densities.

A simple circuit consisting of a microprocessor, small servos, LED lights, sensors, and micro-fans forms the basic operational building block of the complete installation. One circuit controls a territory of six units, which is referred to as a module. The circuits are mounted to laser cut acrylic electronics platforms attached to the top of the tensegrity weave. Each circuit relies on an individual Arduino Uno prototyping board to read sensor inputs and generate the operations. Each Arduino reads input from one temperature sensor and one passive infrared (PIR) motion sensor; it also provides power and control signals to six micro-servos, and controls a group of six LED lights and one micro-fan. The lights and the fan each receive variable amperage signals from the Arduino through a transistor. This allows us to vary the intensity of the LED lights and the speed of the fan so that Stratus might not only respond to occupancy, but can tailor its output to individuals and specific conditions. A switching diode across the output and ground pins of the fan's transistor prevents reverse current from reaching the Arduino.

The distributed electronics platforms also house Celsius based, low-power temperature sensors with a -40°C - 150°C detection range that output analog voltage proportional to the ambient temperature. When the circuit is first powered up, the microcontroller takes 100 readings from the temperature sensor every 5 milliseconds and generates an average of these readings to determine the ambient air temperature. The control program for the Stratus Project was composed in the Arduino programming language (a Wiring based language similar to C++). It uses the baseline measurements to establish a temperature threshold, which governs the actuation of the cells and the operation of the fans. Once Stratus is in operation (ie in its "loop"), the program calls on a number of subset programs to control the separate systems of lighting, cooling, and cell activation. Custom Boolean logics generate feedback loops that inform Stratus when it is in an active cooling state or a passive state, and uses a similar structure to track light intensity levels in relation to occupancy. Tracking the operation of the servo actuators mitigates electrical interference that could disrupt the analog sensors. The program employs a modified Variable Speed Servo Library to choreograph the movements of the cells within each circuit and minimize conflict.

Passive Infrared (PIR) sensors distributed throughout the weave detect changes in infrared radiation levels across a 20' range. Using infrared insures that only motion created by occupancy will trigger operation. The sensors are nested in openings between the cells, and control the lighting in each module. This location permits a direct sight-line to movement in the space, but also brackets the detectable range to an area immediately below the module, in order to achieve personalized response. Working in conjunction with the breathing cells, distributed micro-fans provide localized, focused heat relief for occupants. Each fan requires 12V DC with a power draw of approximately 200 mA. The cooling fans are mounted via

wire stand-offs above the electronics platforms. They respond to input from the temperature sensors; when the ambient temperature exceeds the established threshold, the fans turn on at full power until the temperature is reduced. The fans are also outfitted with blue LED indicator lights that turn on when the fan is active, providing performance feedback to the occupants.

Low-energy high-brightness lights illuminate and track motion within the space. Each light contains one 0.5 watt 4000 K white LED module with a diffuse distribution and 30-lumen output. These LEDs require 3.5V forward voltage and draw 150mA each. The lights are wired in parallel in groups of six, one group for each module. The lights respond to the input from the PIR sensors: when activity is detected within the adjacent area, the lights begin to fade on. If activity continues, the lights continue to fade on until they reach full brightness, at which point they remain on until activity ceases. When no motion is detected in the immediate area, the lights begin to fade off at the same rate until they are completely off.

In addition to the modules that control lighting, cooling, and cell movement, additional circuits control an array of air extraction fans. These circuits consist of an Arduino microcontroller, a CO2 sensor, and six extraction fans. In the first prototype application, the CO2 sensor has been outfitted with a prefabricated circuit that allows the user to manually set a threshold level for CO2 concentration. When the threshold level is exceeded, the sensor outputs a digital signal to the micro-controller, triggering the bank extraction fans. These fans are intended to help displace stale air and permit the movement of fresh air into the space.

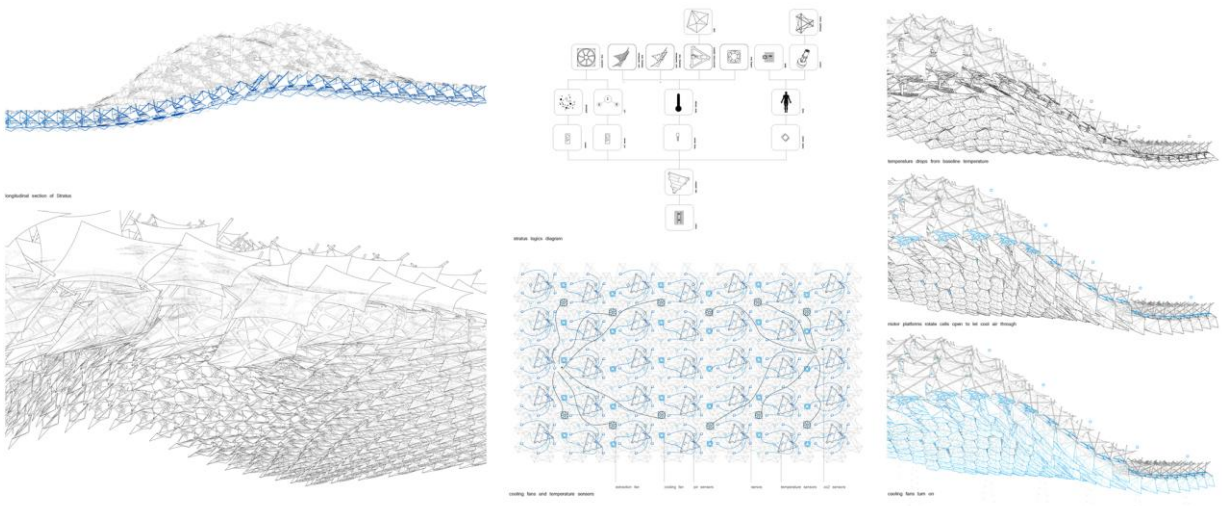

Figure 2: (left) The flexible tensegrity structure allows for the surface to undulate and respond to occupant presence and thermal requirements; (center) Sensing and response logics and connection diagrams of sensors, lighting, cooling and air extraction fans; (right) Deployment of breathing cells relative to sensed temperature fluctuation

RESULTS AND FURTHER DEVELOPMENTS

The current sensor and response regime for Stratus v 1.0 experimented with cooling and CO2 responses to air sensing. One of the goals of the project is to attune attention to the immediate air-based environment and to the physical conditions that produce it. Running concurrent to the operation of the air modifying apparatus, a custom graphing program provides visual feedback on atmospheric conditions to the occupant. This program also employs an Arduino platform to intake data readings, and interfaces it with a Processing-based animation. While

the visualization program could provide relatively accurate real time temperature readings, tracking of CO2, VOC, and humidity levels were presented more relatively than quantitatively, tracking variation over time rather than specific parts per million levels or percentage humidity. The next phase of research will include developing further ways to affect the 'design' of gaseous agents, especially in response to airborne pollutants and investigating further ways in which the structure itself might be able to register and communicate information, either biologically or electronically, providing to the breather a consciousness of their own agency within the air environment.

Further iterations of the project will deploy more robust generations of Micro Electromechanical Systems (MEMS) and Wireless Integrated Microsystems (WIMS). Specifically, the next generation will be developed to incorporate distributed wireless sensing networks utilizing the low power Narada wireless nodes capable of processing raw measurement data directly in the network, eliminating the need for a centralized server to process and aggregate data. Powering the wireless sensor and actuator network, could rely on energy harvested from thermal gradients at the building envelope via distributed thermal electric generators (TEGs), making the operation of Stratus a net-zero energy installation. Further exploration of Multi-Agent Systems (MAS) will enhance the intelligence and performance flexibility of Stratus. "Agents" are software abstractions that are capable of perceiving their environment through sensing, and then acting upon that perception through actuation based on a rational decision process of embedded intelligence. Multi-agent systems are particularly attractive for performing control for ubiquitous networked assemblies such as Stratus, as they represent a scalable control approach well suited for a decentralized sensor and actuator network.

The term "responsive" has often been used interchangeably with interactive and adaptive, and most simply can be described as "how natural and artificial systems can interact and adapt."[2] In a responsive milieu, user and system are able to shape an unlimited set of outcomes; rather than the designer predetermining appropriate responses to user inputs, the system measures reactions to its outputs and continually modifies its actions according to these responses. One of the goals of The Stratus Project is to develop a computational script with algorithms that allow the system to self-adjust and learn over time, both relative to environmental variable conditions and to occupancy patterns, preferences and habits, exploring how the system could become a second order cybernetic learning environment. [3]

CONCLUSION / PROJECTION

The Stratus Project anticipates applications across a range of spatial configurations and programs by providing dynamic, flexible, and responsive lighting, thermal, ventilation, and acoustic systems. Each system can be tailored and adjusted independently to provide optimum support for a range of activities while minimizing overall energy draw. The adjustable displacement of the soffit creates a stratification of thermal space, which reduces the amount of air to be conditioned when a space is unoccupied, limiting energy devoted to inactive spaces. Lighting levels can be calibrated from low ambient levels to high task requirements both through dimming controls and through adjusting the distance between the light source and the illuminated surface. This permits higher illumination levels where needed while keeping energy density well under 1 watt per square foot. Similarly, thermal comfort and ventilation systems could target individual bodies and occupation density. Central heating and cooling elements would condition the air to the appropriate temperature, while the breathing cells and micro-fans activate only in occupied zones to deliver the desired effect of cooling with air speeds as low as 0.1 m/s. Ventilation can also be improved by increasing air flow rates in response to increased occupation or decreased air qualities. Air

quality sensors distributed in the space, or attached to personal technology devices, could provide vital feedback to the operating system, allowing it to balance energy loads across multiple spaces and occupation types based on activity and pollutant levels. It is anticipated that the utilization of the distributed sensing network will simultaneously control localized response, and will be tied to building-wide controls, to permit coordinated interaction between Stratus and broader systems including the building envelope itself; for example, feedback balancing interior demand and exterior conditions tied to automated operable windows might prioritize passive ventilation over HVAC delivery when possible. When expanded to the full scale of a building Stratus promises a fully integrated interior interface and responsive lining that can be tuned locally to individual demand and desire.

ACKNOWLEDGEMENTS

The authors would like to acknowledge the following individuals for their contributions: Matt Peddie, Zain AbuSeir, F. Parke MacDowell, James Christian, Christopher Parker, Jason Prasad, Sara Dean, Jessica Mattson, Dan McTavish, Christopher Niswander, Lisa Sauve, Adam Smith. The Stratus Project is funded by the University of Michigan Taubman College of Architecture and Urban Planning *Research Through Making Grant*, the University of Michigan Office of the Vice President for Research Small Projects program, a Social Sciences and Humanities Research Council of Canada (SSHRC) Research/Creation Grant Program and a University of Michigan WIMS Institute Special Projects Grant.

REFERENCES

1. Bing, W.B. : Free-standing tension structures: from tensegrity systems to cable-strut systems, Oxford & New York: Spon Press, 2004, pp. 86-96.
2. Beesley, P., S. Hirosue, and J. Ruxton : Responsive Architectures. Subtle Technologies 06, Cambridge: Riverside Architectural Press, 2006, p.3.
3. Dubberly. H., P. Pangaro and U. Haque, "What is Interaction? Are there Different types?" in *Interactions Magazine*, Jan / Feb 2009 url:http://mags.acm.org/interactions/20090102/?pg=71#pg71 Accessed March 2011

AUTHOR INDEX

AUTHOR INDEX

Volume I: pp 1-612, Volume II: pp 613-1064

E

F

G

H

I

J

Q

R

S

T

V

W

X, Y

Z

ACKNOWLEDGEMENTS

CISBAT 2011 would not have been possible without the efficient contribution of the secretariat of the Solar Energy and Building Physics Laboratory as well as that of our scientific and technical staff. We would like to mention especially Barbara Smith who was responsible for the smooth running of the conference administration and Laurent Deschamps, the IT specialist and group leader. Our warm thanks to all staff involved.

Our scientific partners from Cambridge University and the Massachusetts Institute of Technology as well as the members of the international scientific committee and the session chairs have enthusiastically supported the conference and ensured its quality. We would like to express our sincere thanks for the time and effort they have spent to make it a success.

CISBAT can only exist thanks to the financial support of the Swiss Federal Office of Energy. We are grateful for their continuing support.

We also owe sincere thanks to the two private sponsors of this edition, Bank Julius Baer and Energie Romande, whose support was vital for the conference. Through their presence, they have not only allowed us to extend the programme, but have also shown their commitment for a more sustainable built environment.

Finally, we cordially thank all speakers, authors and participants who have brought CISBAT 2011 to life.

Prof. Dr J.-L. Scartezzini

Chairman of CISBAT 2011

Head of EPFL Solar Energy and Building Physics Laboratory